# Source to sink relations between the Qaidam basin (Tibet) and the surrounding mountains

Feng Cheng

**ANNÉE 2016**

**THÈSE / UNIVERSITÉ DE RENNES 1**
*sous le sceau de l'Université Européenne de Bretagne*

*En Cotutelle Internationale avec*

***L' Université de Pékin, Chine***

pour le grade de

**DOCTEUR DE L'UNIVERSITÉ DE RENNES 1**

*Mention : Sciences de la Terre*

**Ecole doctorale Sciences de la Matière**

présentée par


# Feng CHENG

Préparée à l'unité de recherche Géosciences Rennes
OSUR (Observatoire des Sciences de l'Univers) – UMR 6118
UFR Sciences et Propriétés de la Matière


---

# Relations érosion – sédimentation entre le bassin du Qaidam (Tibet) et les chaines associées.

# *Source to sink relations between the Qaidam basin (Tibet) and the surrounding mountains.*

**Thèse soutenue à Rennes**
**le 25 Mai 2016**
devant le jury composé de :

**Johan De Grave**
Professeur, Université de Ghent / *rapporteur*
**Jacques Malavieille**
Directeur de Recherche CNRS, Université de Montpellier / *rapporteur*
**Cécile Robin**
Maître de Conférence, Université de Rennes 1 / *examinateur*
**Marc Poujol**
Maître de Conférence, Université de Rennes 1 / *examinateur*
**Marc Jolivet**
Chargé de Recherche CNRS, Université de Rennes 1 / *directeur de thèse*
**Zhaojie Guo**
Professeur, Université de Pékin / *co-directeur de thèse.*

# Résumé en français

Le basin du Qaidam, situé sur la bordure nord du Plateau Tibétain est unique au monde en ce qu'il représente le bassin intracontinental le plus profond bien que situé sur le plus haut plateau et la plus épaisse croute continentale actuels (figure R1). Comprendre le développement et l'évolution de ce bassin en lien avec la collision Inde-Asie a des implications multiples pour la géologie du Tibet en particulier et la tectonique continentale dans les zones de convergence en général. De nombreuses études incluant de la thermochronologie, de la paléobotanique, du paléomagnétisme, de la paléoaltimétrie, de la sédimentologie et de la géologie structurale se sont intéressées à l'histoire tectonique et topographique de cette région. Toutefois la topographie initiale de la région actuellement représentée par le Plateau Tibétain ainsi que les premiers stades de développement du plateau restent méconnus et très débattus. Afin de mieux comprendre l'évolution cénozoïque du bassin du Qaidam et des régions environnantes (la chaine des Eastern Kunlun au sud, la chaine de l'Altyn Tagh au nord-ouest et la chaine des Qilian Shan au nord-east), quatre questions principales ont été abordées dans ce travail : 1) l'évolution cénozoïque conjointe du bassin du Qaidam et de la chaine des Eastern Kunlun ; 2) les relations entre la sédimentation dans le bassin du Qaidam et la tectonique le long de la faille de l'Altyn Tagh ; 3) une estimation quantitative de l'extrusion latérale du nord Tibet les long du système Altyn Tagh – Qilian Shan ; 4) la nature et la typologie du bassin du Qaidam.

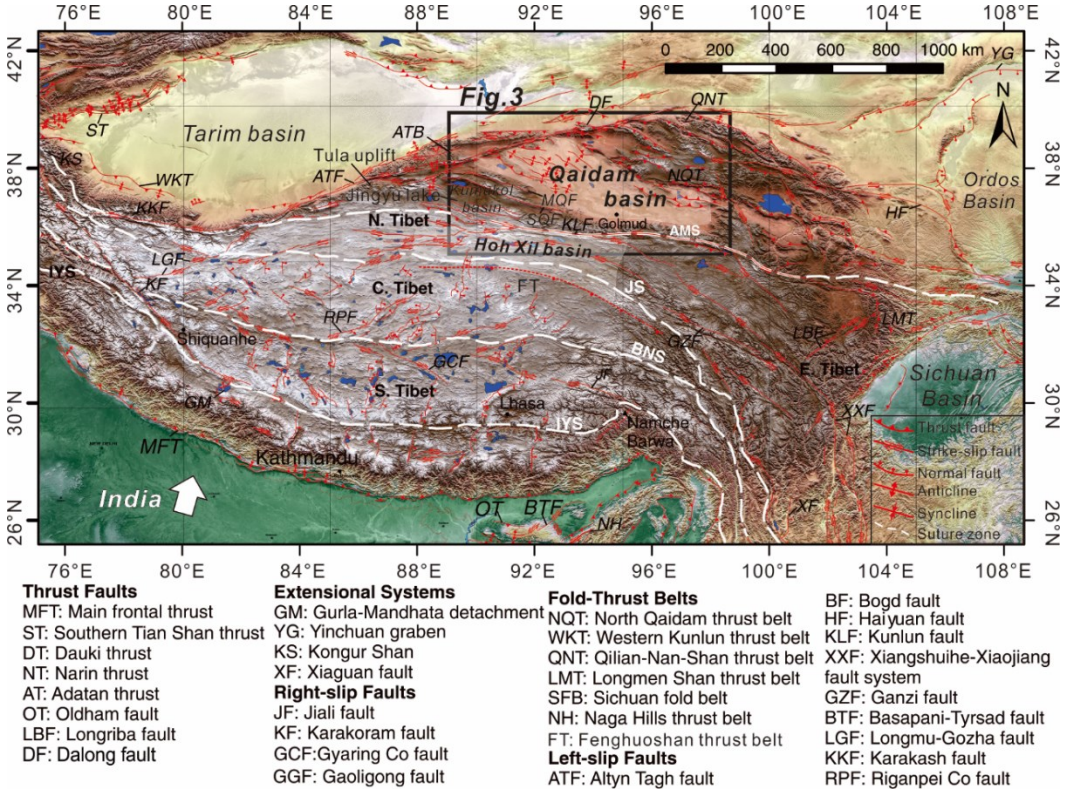


Figure R1 : Carte topographique du Plateau Tibétain montrant les principales structures tectoniques (d'après Yin et al. (2007), Taylor and Yin (2009) et Cheng et al. (2014, 2016).

Au cours des dernières décennies, de nombreux modèles ont été proposés pour rendre compte de l'évolution tectonique et sédimentaire du bassin du Qaidam. La majorité d'entre eux considèrent que la très forte subsidence du bassin au Cénozoïque est liée à la propagation vers le nord du prisme d'accrétion continental du Kunlun qui forme actuellement la bordure sud du bassin (figure R2). L'initiation de ce prisme est généralement datée de l'Oligocène ou du Miocène inférieur.

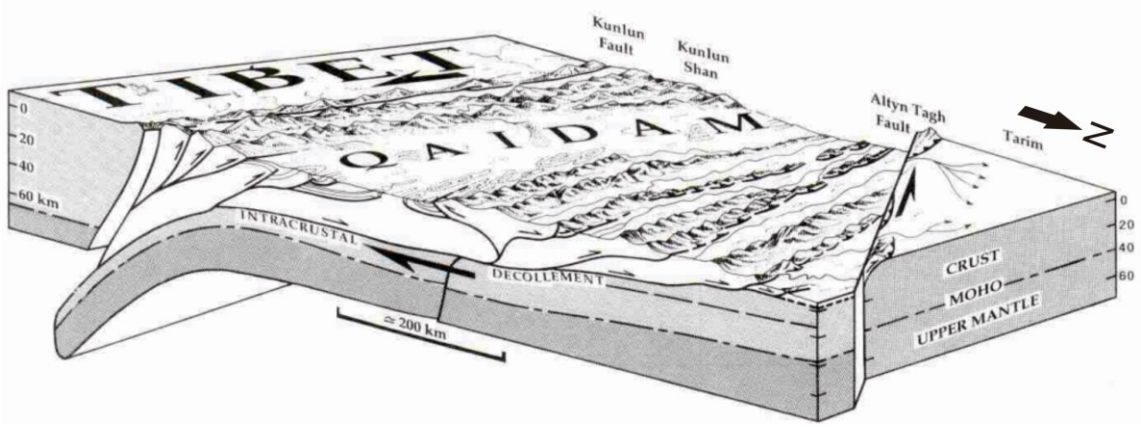


Figure R2 : Modèle de propagation vers le nord du prisme d'accrétion du Kunlun. D'après Meyer et al. (1998).

A partir de nouvelles observations et données de terrain, de l'interprétation de lignes sismiques nouvellement acquises dans le SO du bassin du Qaidam, d'images satellitaires et de données sismologiques, je suggère que le SO du bassin du Qaidam a été limité au sud par une série de failles décrochantes (constituant actuellement les chaînons du Qimantag) depuis le Miocène inférieur et non, comme initialement suggéré, par un système chevauchant vers le nord ou le sud. Les failles constituant ce système s'initient dans la continuité du système décrochant sénestre du Kunlun et sont progressivement déplacées vers le nord tout en subissant une rotation pour être enfin amenées dans leur position actuelle avec une cinématique transpressive. A ce titre le SO du bassin du Qaidam n'a pas été soumis à une compression et un raccourcissement important N-S avant le Miocène inférieur. D'autre part, à partir de l'analyse U-Pb par LA-ICP-MS de zircons détritiques obtenus dans 22 échantillons de grès (paléocène à holocène) provenant de 4 sections dans le SO du bassin du Qaidam, de l'analyse des provenances sédimentaires sur ces mêmes sections, et de profiles sismiques, je démontre que les sédiments paléocènes sont caractérisés par une source principale paléozoïque à protérozoïque supérieur. La présence de débris de carbonate à foraminifères paléozoïque dans les conglomérats paléocènes confirme ce résultat et suggère que la chaine des Esatern Kunlun était exhumée avant le Paléocène. De plus le recouvrement vers le sud des séries paléocènes à oligocènes, observé sur les profiles sismiques, et l'occurrence d'une composante mésozoïque dans les âges U-Pb sur zircon détritiques des séries éocènes à oligocène indiquent que le bassin du Qaidam s'élargissait vers le sud au début du Cénozoïque. Les strates de croissance post-oligocènes et l'augmentation des proportions des âges détritiques mésozoïques et paléozoïques à partir des séries du Néogène supérieur démontrent un accroissement du relief dans les Eastern Kunlun et l'Altyn Tagh, entrainant un isolement et un rétrécissement du bassin entre le Miocène et l'actuel (figure R3). Cette déformation par phases souligne la complexité de l'histoire tectonique du Plateau Tibétain.

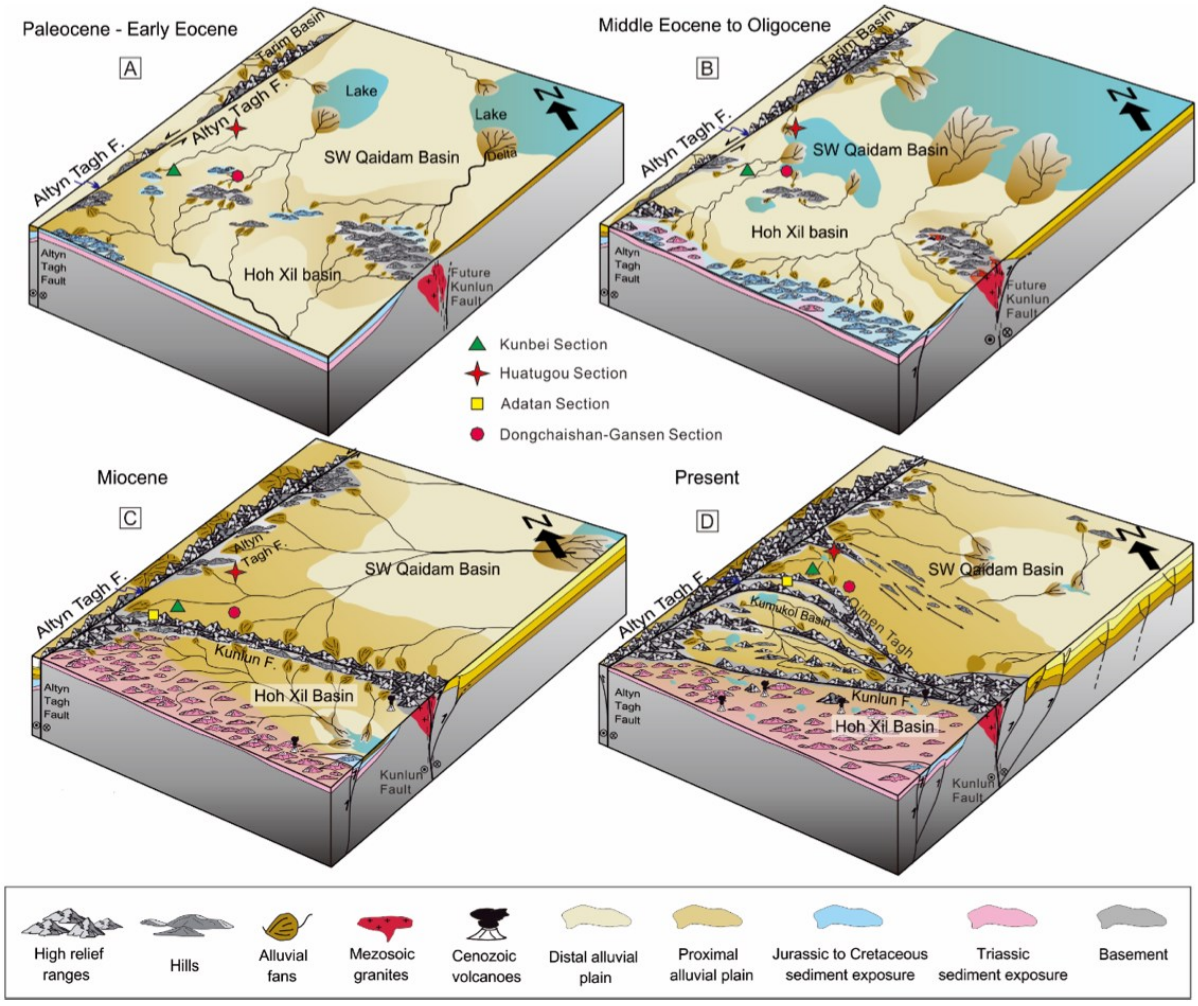


Figure R3 : Reconstitution de l'évolution tectonique et topographique de la bordure sud du bassin du Qaidam entre le Paleocene – Eocene inférieur (A) et le présent (D). Cheng et al., GSAB, 2015.

En combinant des données de sismique 3D, de stratigraphie et de géochronologie détritique sur les séries mésozoïques de l'ouest du bassin du Qaidam, j'ai identifié plusieurs sections comme étant des marqueurs du déplacement le long de la faille de l'Altyn Tagh. Ces données m'ont permis d'identifier les régions d'Anxi et de Tula à l'ouest du bassin, dans la zone où les systèmes tectoniques du Kunlun et de l'Altyn Tagh se rencontrent, comme faisant initialement partie intégrante du bassin du Qaidam (figure R4). Je suggère que la faille de l'Altyn Tagh a accommodé environs 360 km de déplacement depuis sont initiation au Miocène inférieur et que l'activité tectonique dans l'Altyn Tagh et le NO du Qaidam s'est accrue à partir du Miocène. Il est communément admis que le déplacement senestre le long de la faille de l'Altyn Tagh est accommodé pour une très faible partie par du raccourcissement dans le bloc lithosphérique du Qaidam mais surtout par le raccourcissement dans les systèmes d'accrétion contientale du Kunlun et des Qilian Shan. Je démontre toutefois que le bloc lithopshérique du Qaidam est très rigide et ne participe que d'une manière infime à l'accommodation de ce raccourcissement. En me basant sur les 360 km de migration vers le NE du bloc relativement rigide du Qaidam le long de la faille de l'Altyn Tagh, je démontre, à partir d'un bilan isovolumétrique 3D de la déformation crustale au sein du système Altyn Tagh – Qilian Shan,

l'existence d'un raccourcissement N20E de 250 ± 28 km (43.8 – 49.4 %) et de 250 à 370 km d'extrusion vers l'est de la croute des Qilian Shan. Cette déformation est prise en compte par du décrochement dans les Qilian Shan, de l'épaississement crustal dans les Qinling et de l'extension dans le système de grabens de Chine du Nord. Ce résultat remet en cause les calculs de vitesse et de taux de déformation au sein du système Kunlun – Altyn Tagh – Qilian Shan.

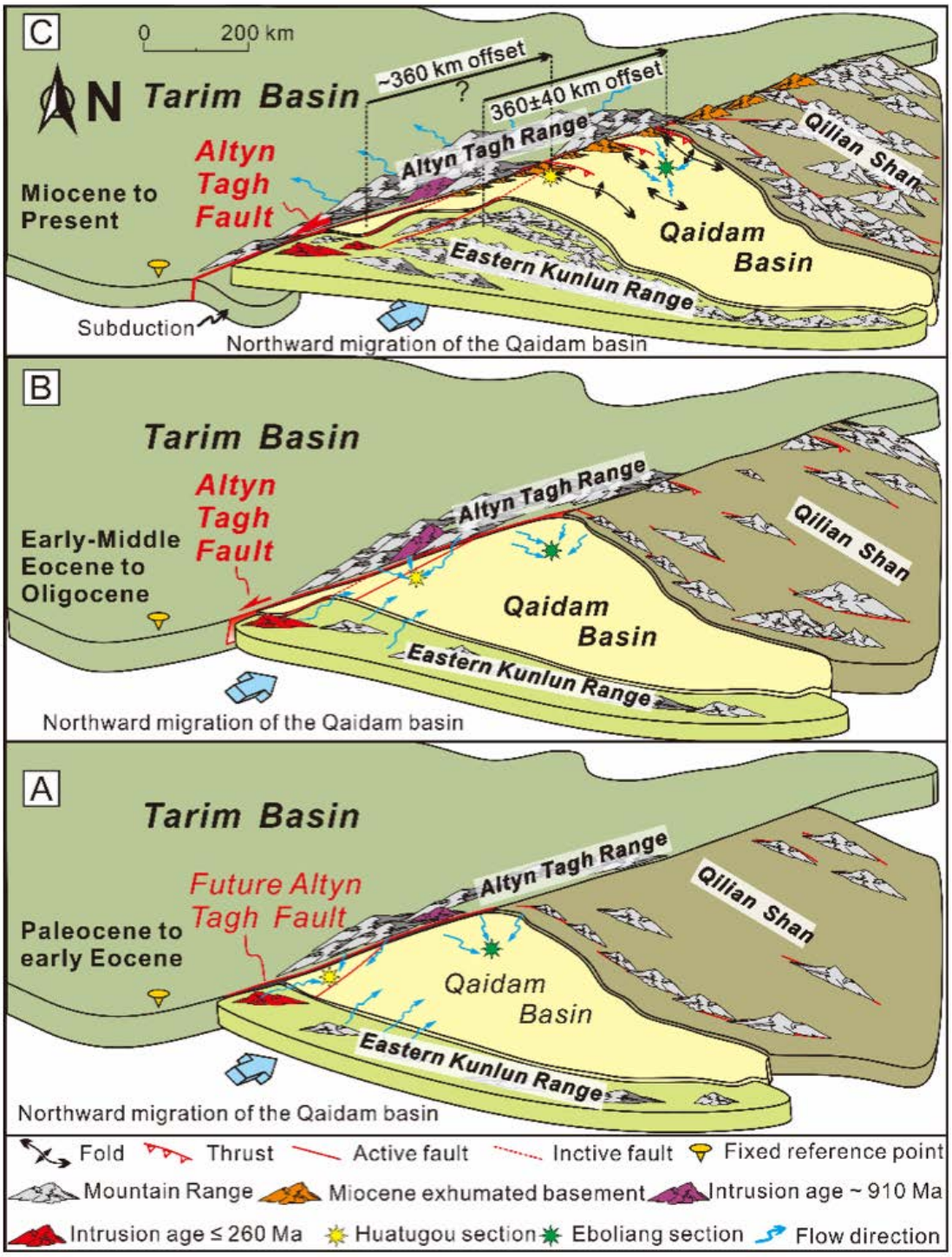


Figure R4 : Modèle cinématique de l'évolution cénozoïque de la faille de l'Altyn Tagh avec indication de l'évolution des principales zones d'apport de matériel sédimentaire dans le bassin du Qaidam. Cheng et al., Tectonophysics, 2016, accepté.

Enfin, à partir d'une analyse intégrée des données sur l'évolution cénozoïque du Qaidam, associée à des données récentes de géologie pétrolière (par exemple la distribution des roches mères dans le Qaidam), je conclu que le bassin du Qaidam est de type décrochant, contrôlé conjointement par les failles décrochantes de l'Altyn Tagh et du Kunlun Est. La faille de l'Altyn Tagh, au nord du bassin, contrôle l'essentiel de la structure sédimentaire du bassin, la faille du Kunlun au sud n'agissant que localement sur la bordure sud-ouest du bassin. La superposition dans le temps et l'espace des effets de ces deux décrochements majeurs durant le Cénozoïque a contrôlé l'évolution du bassin et la répartition des réserves d'huile et de gaz. Au cours du Paléogène, l'essentiel des roches mères se déposent dans des sous-bassins « sag » extensifs le long de la bordure sud-ouest du Qaidam. Les systèmes transpressif qui se met en place dans la région du Qimantag à partir du Miocène inférieur constitue des pièges majeurs pour les hydrocarbures (huile et gaz) (figure R5).

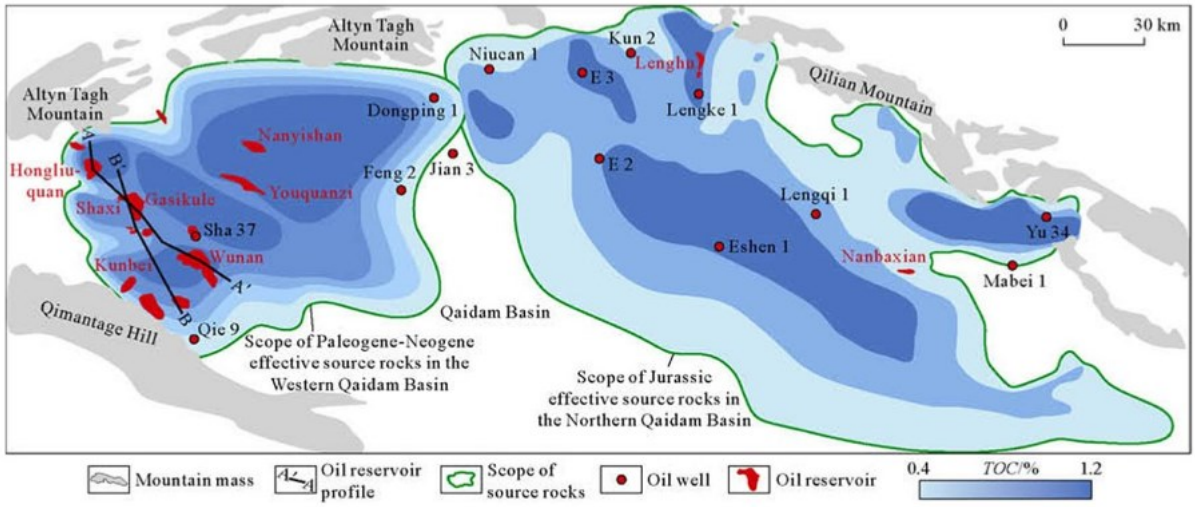


Figure R5 : Distribution des roches mères et des réservoir d'huile et de gaz dans le bassin du Qaidam. D'après Fu et al., Petroleum Exploration and Development, 2015.

**MOTS CLÉS :** Le basin du Qaidam, Plateau Tibétain, Détritique zircon géochronologie, l'interprétation de lignes sismiques, Relations érosion – sédimentation, décrochement, raccourcissement, extrusion

.

## Abstract

The Qaidam basin, located within the northern Tibetan plateau, is unique in the world in that it is the deepest intracontinental basin, yet located in the highest plateau with the thickest continental crust. Understanding how this peculiar basin developed during the India-Asia collision has broad implications for the Tibetan geology in particular and for continental tectonics in general. Though many approaches, including thermochronology, paleobotany, paleomagnetism, paleoaltimetry coupled with stratigraphic and tectonic analyses, have been used to decipher the tectonic and topographic history of that region, the initial topography of the area now represented by the northern Tibetan plateau, as well as the early stages of development of the present day topography remain poorly constrained and highly debated. In order to better understand the Cenozoic evolution of the Qaidam basin and its surrounding regions (including Eastern Kunlun Range to the south, Altyn Tagh Range to the northwest, and Qilian Shan to the northeast), four critical issues are addressed in this thesis: 1) the Cenozoic joint tectonic evolution of the Qaidam basin and the Eastern Kunlun Range; 2) the interplay between the sedimentation within the Qaidam basin and the active tectonics within the Altyn Tagh Range; 3) a quantitative estimate of the lateral extrusion along the Altyn Tagh Fault-Qilian Shan tectonic system; 4) the nature and classification of the Qaidam basin.

Based on new field observation and data, interpretation of newly acquired seismic reflection profiles within the southwestern Qaidam basin, remote sensing images, and earthquake focal mechanisms and epicenter distribution, I suggest that the SW Qaidam basin has been bordered by a series of strike-slip faults to the south since the Early Miocene, rather than, as previously suggested by a continuous northward or southward thrusting system. The SW Qaidam basin did not suffer major N–S compression and shortening before the Early Miocene. On the other hand, by conducting U-Pb dating (LA-ICP-MS) of detrital zircons from 22 sandstone samples (Paleocene to Holocene) collected from 4 sections within the southwestern Qaidam basin combined with provenance analysis and new seismic profile interpretation, I demonstrated that the U-Pb age distribution of detrital grains from Paleocene strata are characterized by a major component of Paleozoic to late Proterozoic ages, and recognized carbonate debris containing foraminifera in the Paleocene conglomerate sequences. These data suggest that the Eastern Kunlun Range was already exhumed prior to the Paleocene. In addition, the southward onlaps of Paleocene to Oligocene strata observed on seismic profiles and the appearance of a Mesozoic component in the detrital zircon age spectra of Eocene to Oligocene strata indicate that the Qaidam basin was widening southward during

that early Cenozoic period. Well-developed post-Oligocene growth strata and the increasing proportion of Mesozoic and Paleozoic U-Pb ages in detrital zircon grains from late Neogene strata demonstrate that the relief of the Eastern Kunlun and Altyn Tagh ranges had increased, leading to isolation and narrowing of the Qaidam basin from Miocene to the present. The inferred pulsed deformation in the Eastern Kunlun Range highlights the complex growth history of the Tibetan plateau.

By correlating stratigraphic contacts and lithologies, U-Pb age spectra of Mesozoic samples within the western Qaidam basin, and newly acquired 3D seismic reflection profiles interpretation, I identified the Tula-Huatugou and Anxi-Eboliang sections as piercing points along the western segment of Altyn Tagh Fault. I further defined the Tula and Anxi regions as residual parts of the original Qaidam basin. I thus suggest that the Altyn Tagh Fault has experienced a total of ~360 km of displacement since its Early Eocene initiation, whereas tectonic activity largely increased within the Altyn Tagh Range and northwestern Qaidam basin from Miocene time.

In addition, based on the ~360 km northeastward migration of the relatively rigid Qaidam block along the Altyn Tagh Fault and 3D isovolumetric balance of the crustal deformation within the Altyn Tagh Fault – Qilian Shan system, I demonstrate that 250 ± 28 km (43.8~49.4 %) of N20E directed crustal shortening and an additional ~250 to ~370 km of eastward motion of the Qilian Shan crust must be accounted for by strike-slip faulting in the Qilian Shan and crustal thickening in the Qinling area, as well as extension in the adjoining North China block graben systems.

Finally, based on a comprehensive analysis of the Cenozoic evolution of the Qaidam basin combined with recent petroleum exploration geological results (e.g. distribution of source rocks in the Qaidam basin), I conclude that the Qaidam Basin is a strike-slip superimposed basin jointly controlled by the left-lateral strike-slip Altyn Tagh and East Kunlun faults. The temporal and spatial superimposition of these two strike-slip faults during the Cenozoic controlled the evolution of the basin as well as the oil and gas accumulation.

**KEY WORDS**: Qaidam basin, Tibetan plateau, Detrital zircon geochronology, Seismic profile interpretation, Source to sink relation, Strike-slip tectonics, Compression, Extrusion.

## Acknowledgements

I would like to extend thanks to the many people, in many countries, who so generously contributed to the work presented in this thesis.

First and foremost I want to thank my two doctorial tutors Marc Jolivet, Université de Rennes 1 and Zhaojie Guo, Peking University. I thank Zhaojie wholeheartedly, not only for his tremendous academic guidance, but also for nurturing my enthusiasm for Tibetan geology and many wonderful opportunities. Not many PhDs involve field investigation throughout western China (including the Qaidam basin, Altyn Tagh and Eastern Kunlun ranges and Tian Shan) and a French-Chinese bilateral programme. His innovated ideas and fantastic geological thinking that linking the local geological information to regional or global scale tectonics inspired me to acquire critical thinking and overall four- dimensional perspective when doing Earth Science research. My gratitude is also extended to Marc, for his scientific advice and knowledge and many insightful discussions and advices during my PhD research. I cannot complete all the designed research in the framework of my PhD plan and pursue geologic research on the Tibetan plateau without his encouragement and suggestions. He not only taught me how the conduct the apatite fission track analysis, but also let me to know how to give the reasonable interpretation on the basic of scientific data in the rigorous and precise way. I am particularly indebted to Marc for his support when so generously hosting me in Rennes. I have very fond memories of my time in France and hope to revisit this land of exceptional beauty in the near future.

Heartfelt and special thanks are given to Chaodong Wu, Marc Jolivet and Guillaume Dupont-Nivet for their kindly assistance in applying the French-Chinese bilateral programme (Egide Cai Yuanpei program 2014). Special mention goes to China Scholarship Council who offered me the shcolarship these years. I would never have had a chance to enjoy the romantic and peaceful French life without the support of this international project.

I am grateful to members of my middle dissertation evaluation committee, Michel Ballevre, Sylvie Bourquin, Hervé Régnauld. Their kind jugement and valuable comments are greatly appreciated. Similarly, Zhicheng Zhang, JinjiangZhang, Baofu Han, Chaodong Wu, Bo Zhang, who provide logical and forethoughtful suggestions that strongly facilitated the scientific integrity of my dissertation, are acknowledged.

I am also hugely appreciative to Guillaume Dupont-Nivet, Hillary S. Jenkins, Kerry Gallagher for the excellent cooperation. Their insightful suggestions and polishing largely improved the quality of my manuscripts and helped me to develop my scientific analytical and

writing skills. I also thank Erwan Hallot and Wenzhe Fa for valuable discussion and generous help during data interpretation and drafting.

Profound gratitude goes to An Yin, Jean-Philippe Avouac, Jason Phipps Morgan, Shanaka de Silva, Christian Koeberl, Mian Liu, James A. Spotila, Todd A. LaMaskin, Franz Neubauer, and all the other anonymous referees, for their carefully reviewing my manuscripts and providing the constructive and insightful comments. The modification during the manuscript submitting process have left an indelible mark on my memory and will push me to present much higher quality contributions in my geology career.

I am very grateful to Suotang Fu, Dade Ma, Shuwei Guan, Yan Chen, Chuanwu Wang, Qiquan Zhang for giving me the opportunities to get involved to the incredible Qaidam basin. I would also like to commemorate Shihu Fang who gave me tremendous help during the first two years since I entered the Zhaojie's group. I must acknowledge with deep thanks Suping Zhou, Ruiying Chen, Qingyang Meng, Chuanming Zhou, Changhao Zhang, Yiquan Jiang, Wenjun Zhu, Peizhi Du, Anping Hou, Mingde Liu, Tailiang Jiang, Jihong Wang, and Xiangfeng Dai from Dunhuang, China, for their contribution to the field investigation and data collection.

Special mention also goes to those doctor and master students in Zhaojie's group, namely Yuanyuan Zhang, Shi Chen, Shufang Wang, Dongdong Liu, Wentao Huang, Wei Yang, Meng Li, Bei Zhu, Xiangjiang Yu, Ziya Zhang, Hanwen Hu, Xiang Cheng, Tuo Zhang, Runchao Liu, Wei Du, Xiaoru Tian, Zhendong Wang, Yang Zhang and Qing Bian.

Bo Zhang and Xiaoxian Wang are highly appreciated, for their help with cathodoluminescence (CL) imaging at Peking University, Beijing, while. Moreover, Li Su, Hongyu Zhang, Jiao Li, Linxi Zhong and Tong Liu are acknowledged for their help with detrital zircon U-Pb geochronology testing at China University of Geoscience, Beijing.

I also thank geologists from Université de Rennes 1, Marc Poujol, Cécile Robin, Thierry Nalpas, Jean-Noël Proust, for giving the outstanding lessons that highly impove my basic geologic skills. Dominique Bavay, Isabelle Dubigeon, Eddie Gaudin, Christian Le Carlier de Veslud, Michel Ballevre, Philippe Boulvais, François Guillocheau, Olivier Dauteuil, Aline Dia, Laura le Barzic and Marie-Anne Zeghers are highly appreciably for providing convenience for my daily life at Geoscience Rennes, Université de Rennes 1. In particular, I would like to appreciate those PhD. students, namely Christophe Ballouard, Youssef Nohra, Olivier Bochet, Benoît Quesnel, Duprat-Oualid Sylvia, De la Bernardie Jérôme Bondet, Roman Chelalou, Benjamin Corre, Gemma De Vicente I Bosch, Antoine Delaunay, Daniel Jara Heredia, Tamara Kolbe, Caroline Lotout. Thanks for their great assistance and accompany during my campus

life at Université de Rennes 1.

In addition, these acknowledgements would not be complete if I did not mention my forever friends, Qian Yuan, Yi Wei, Zhao Zhou, Sen Gu, and Pengfei Fan. Their assistance, patience, encouragement and enthusiastic help me pass through the hardship during my doctor study and shed a new light in my life. It is my honor to be your friend.

Through my PhD study, I have met many nice and compassionate individuals who did not hesitate to devote their valuable time to me when it was needed. I dare not risk missing to mention anyone's names, so I will simply say "Thank you ALL for being there for me.

Finally, but by no means least, I dedicate this thesis to my mum, dad, and my beloved fiancée for their unbelievable support and unconditional love. My parents have instilled many admirable qualities in me and given me a good foundation with which to meet life. My fiancée went through every excruciating step and mood change with me, and I could not have completed this journey without her by my side. I love you all dearly.

# Curriculum Vitae

**Feng Cheng**
Laboratoire Géosciences Rennes, Université de Rennes 1, Rennes, 35042, France
Phone: +33 (0)652766226; +86 18810523726
cfcf.chengfeng@gmail.com
https://www.researchgate.net/profile/Feng_Cheng10

## EDUCATION

Ph. D., Sciences de la Terre, Université de Rennes 1, **Advisor: Marc Jolivet,** 2013-2016 (expected)
*Thesis: Source to sink relations between the Qaidam basin and the surrounding mountains*
Ph. D., Structure geology, Peking University, **Advisor: Zhaojie Guo**, 2011-2016 (expected)
*Thesis: Cenozoic evolution of Qaidam basin, northern Tibetan Plateau: Implications for the plateau growth*
B. SC., Geology (Advance class), China University of Geoscience, Wuhan, **Advisor: Dewei Li** 2007-2011
*Thesis: Surface ruptures of the Eastern Kunlun, Wenchuan and Yushu earthquakes and their tectonic implications*

## PROFESSIONAL EXPERIENCE

Laboratory Assistant, SEM-EBSD-EDS-CL laboratory in the Key lab of Orogenic belts and crust evolution, Ministry of Education, Peking University, 2012-2013.

## FELLOWSHIPS & AWARDS

Chinese-French Egide Cai Yuanpei program scholarship, China Scholarship Council, 2014-2016
Dingdong Geology Scholarship, School of Earth and Space Science, Peking University, 2016
National Scholarship, Chinese Ministry of Education (Top prize for PhD candidates in China), 2015
National Scholarship, Chinese Ministry of Education (Top prize for PhD candidates in China), 2014
Innovation Award (Academic), Peking University, 2014
Excellent Learning Student of the Peking University, Peking University, 2013
Major and Minor Academic Scholarship, Peking University, 2011, 2012
Top Ten Pacesetter Students, China University of Geosciences (Wuhan)
Won the May 4th Youth Medal (Top prize for undergraduates in China University of Geosciences), 2011
First prize of the Science and Technology Papers Contest, China University of Geoscience (Wuhan), 2011
National Scholarship for Encouragement, Chinese Ministry of Education, 2009

## RESEARCH INTERESTS

Tectonics, Provenance analysis, Low-temperature thermochronology
My current research focuses on the Cenozoic kinematic evolution of the Tibetan Plateau. I am now targeting the Qaidam basin and seek to reconstruct the source to sink relations between the Qaidam basin and the surrounding regions, North Tibet (including Eastern Kunlun Range, Altyn Tagh Range as well as the Qilian Shan Range), and finally provide some constraints on the plateau growth process.
I conduct multi-faceted approach in my research, including field investigation, provenance analysis (detrital zircon U-Pb geochronology), thermochronology (AFT), seismic profile interpretation, remote sensing interpretation, ect.

**RESEARCH EXPERIENCE**

**Identifying the nature of the basement of the Qaidam basin, northern Tibetan Plateau, 2014-Present**

I collected granitoid basement rocks of the Qaidam basin from drill wells (Qinghai Petroleum Research Institute of PetroChina). I am conducting petrology, geochronology and geochemistry analysis to understand the origin of the Qaidam basin basement. In addition, Apatite Fission Track analysis is also used to constrain the Late Mesozoic to Cenozoic tectonics evolution of the basin.

**Quantitative estimation of the lateral extrusion along the Altyn Tagh Fault-Qilian Shan system, northern Tibetan Plateau, 2014-Present**

I propose a quantitative evaluation of the Cenozoic crustal shortening and lateral extrusion budget in the northern Tibetan Plateau, derived by both considering the northeastward migration of the relatively rigid Qaidam block along the ATF and restoring the 3D crustal deformation in the Qilian Shan.

**Source to sink relation between the Qaidam basin and the Eastern Kunlun Mountains, northern Tibetan Plateau, 2011-Present**

I conducted field investigation on several sections in the Qaidam basin and collected plenty of Cenozoic samples (outcrop and drill well samples). Then, U-Pb dating (LA-ICP-MS) of detrital zircons from 22 sandstone samples (Paleocene to Holocene) collected from four sections within the southwestern Qaidam basin is combined with provenance analysis and new seismic profile interpretation to investigate the mountain building of the Eastern Kunlun Range.
In addition, based on a new field observation and data, interpretation of newly acquired seismic reflection profiles within the SW Qaidam basin, remote sensing images, and earthquake focal mechanisms and epicenter distribution, I re-evaluated the tectonic pattern along the western portion of the Kunlun fault to decipher the Late Cenozoic interaction between the Eastern Kunlun Range and the SW Qaidam basin.

**Initial rupture and displacement on the Altyn Tagh Fault, northern Tibetan Plateau, 2011-Present**

I conducted an integrated analysis on several Mesozoic to Cenozoic stratigraphic sections in the western Qaidam basin, adjacent to the Altyn Tagh Fault. Detrital zircon U-Pb

geochronology data (outcrop and drill core samples) obtained from these sections are associated to high-quality newly acquired seismic profiles to better understand the kinematic history of the Altyn Tagh Fault.

**Surface rupture of the Eastern Kunlun, Wenchuan and Yushu earthquakes and their tectonic implications, 2008-2011**

After the Yushu earthquake (2010), I conducted fieldtrip in Yushu, Wenchuan and the Kunlun Mountains to investigate the surface rupture of these earthquakes to identify their features and explore potential connections among them in the context of the plateau growth.

## RECENT FIELD EXPERIENCE

**Northern Tibet: *Qaidam basin, Eastern Kunlun Range, Yushu***

Seismic profile interpretation and drill core samples collection (Mesozoic-Cenozoic and basement samples) in the PetroChina, Dunhuang, Gansu Province, China. Totaling 3 months 2012 to 2014.

Field investigation in the Qaidam basin and Eastern Kunlun Range to collect paleomagnetism and detrital zircon samples throughout the basin. Four weeks, 2011.

Field mapping in the Eastern Kunlun Range (to the west of Golmud). Six weeks, 2010.

Investigate the surface ruptures of the Kunlun earthquake. One week, 2010.

Investigate the surface ruptures of the Yushu earthquake. One week, 2010.

**Eastern Tibet: *Wenchuan***

Investigate the surface ruptures of the Eastern Kunlun earthquake, One week, 2010.

**Central Asian Orogenic Belt: *Tian Shan***

Investigate several Mesozoic sections along the northern and southern flanks of Tian Shan (Kuche, Shawan, Heiyingshan, etc.) and collect paleomagnetism and detrital zircon samples. Three weeks, 2010.

## ANALYTICAL TECHNIQUES UTILIZED

Structural mapping, Geochronology (U-Pb zircon LA-ICP-MS), Low-temperature thermochronology (Apatite Fission Track), Seismic profile interpretation (SMT), Remote sensing interpretation (ENVI, ArcGIS), Geochemistry (Major and trace elements, Sr-Nd isotope).

## PEER-REVIEWED PUBLICATIONS

***Papers in preparation:***

**Cheng F.**, Jolivet M., Fu S., Zhang C., Zhang, Q., Guo Z., Reconstructing the Cenozoic tectonics in the northern Tibetan plateau: insight from apatite fission track study of deep-drill-core samples from the basement of Qaidam basin. In Prep for Tectonics.

**Cheng F.**, Han B., Jolivet M., Fu S., Zhang C., Guo Z., Tectono-magmatic transformed Qaidam craton insight from the borehole core samples geochronological and geochemical constraints. In Prep for EPSL.

***Papers in review and revision:***

**Cheng F.,** Jolivet M., Fu S., Zhang C., Zhang, Q., Guo Z., Large-scale displacement along the Altyn Tagh Fault (North Tibet) since its Eocene initiation: insight from detrital zircon U-Pb

geochronology and subsurface data: ***Tectonophysics***, accepted with minor revision.

***Published, in press and accepted papers:***

***2016***

**Cheng, F.**, Fu, S., Jolivet, M., Zhang, C., and Guo, Z., 2016, Source to sink relation between the Eastern Kunlun Range and the Qaidam Basin, northern Tibetan Plateau, during the Cenozoic: ***Geological Society of America Bulletin***, v. 128, no. 1-2, p. 258-283, doi: 10.1130/B31260.1.

***2015***

**Cheng F.**, Jolivet M., Dupont-Nivet G., Wang L., Yu X., Guo Z., Lateral extrusion along the Altyn Tagh Fault, Qilian Shan (NE Tibet): insight from a 3D crustal budget: ***Terra Nova***, v. 27, no. 6, p. 416-425, doi: 10.1111/ter.12173.

Fu S., Ma D., Guo Z., **Cheng F.**, 2015. Strike-slip superimposed Qaidam basin and control on oil and gas accumulation: ***Petroleum Exploration and Development***, v. 42, no. 6, 712-722, doi: 10.11698/PED.2015.06.03.

**Cheng, F.,** Guo Z., Jenkins, H., Fu S., and Cheng X., 2015.Initial Rupture and Displacement on the strike-slip Altyn Tagh Fault, Northern Tibetan Plateau: Constraints based on residual Mesozoic to Cenozoic deposits in the western Qaidam Basin: ***Geosphere***, v. 11, no. 3, 921-942, doi: 10.1130/GES01070.1.

Liu, D., **Cheng, F.**, Guo, Z., Jolivet, M., Song, Y., 2015. Lahar facies of the Latest Paleozoic Arbasay Formation: Geomorphological characters and paleoenvironment reconstruction of Northern Tian Shan, NW China. ***Journal of Asian Earth Sciences***, v. 113, Part 1, p. 282-292, doi: 10.1016/j.jseaes.2015.01.024.

Wang L. and **Cheng F.**, 2015. DEM and GIS analysis of the stream gradient index for evaluating effects of active tectonics: Tula basin, north Tibet, China, Geoscience and Remote Sensing Symposium (IGARSS), 2015 IEEE International, Milan, 2015, 4680-4683, doi: 10.1109/IGARSS.2015.7326873.

Cheng, X., Fu, S., Wang, H., Yu, X., **Cheng, F.**, Liu, R., Du, W., Guo, Z., 2015. Geometry and kinematics of the Arlar strike-slip fault, SW Qaidam basin, China: New insights from 3-D seismic data. ***Journal of Asian Earth Sciences*** v. 98, 198-208, doi: 10.1016/j.jseaes.2014.09.039.

**2014**

**Cheng, F.,** Jolivet, M., Fu, S., Zhang, Q., Guan, S., Yu, X., and Guo, Z., 2014, Northward growth of the Qimen Tagh Range: A new model accounting for the Late Neogene strike-slip deformation of the SW Qaidam Basin: ***Tectonophysics***, v. 632, p. 32-47, doi: 10.1016/j.tecto.2014.05.034.

Liu, D., Guo, Z., Jolivet, M., **Cheng, F.**, Song, Y., Zhang, Z., 2014. Petrology and geochemistry of Early Permian volcanic rocks in South Tian Shan, NW China: implications for the tectonic evolution and Phanerozoic continental growth. ***International Journal of Earth Sciences*** 103, 737-756, doi: 10.1007/s00531-013-0994-1.

Zhu, B., Guo, Z., Zhang, Z., **Cheng, F.**, 2014. Peperites in the Permian Tarim large igneous province in Northwest China and their constraints on the local eruption environments. ***Science China Earth Sciences*** 57, 2914-2921. doi: 10.1007/s11430-014-4966-5.

Yu, X.J., Fu, S.T., Guan, S.W., Huang, B., **Cheng, F.**, Cheng, X., Zhang, T., Guo, Z.J., 2014. Paleomagnetism of Eocene and Miocene sediments from the Qaidam basin: Implication for

no integral rotation since the Eocene and a rigid Qaidam block. ***Geochemistry, Geophysics, Geosystems*** 15, 2109-2127., doi: 10.1002/2014GC005230.

Yu, X., Huang, B., Guan, S., Fu, S., **Cheng, F.**, Cheng, X., Zhang, T., Guo, Z., 2014. Anisotropy of magnetic susceptibility of Eocene and Miocene sediments in the Qaidam Basin, Northwest China: Implication for Cenozoic tectonic transition and depocenter migration. ***Geochemistry, Geophysics, Geosystems*** 15, 2095-2108, doi: 10.1002/2014GC005231.

**2013**

**Cheng F.,** and Guo Z., 2013. Northward Migration of the Western Segment of Eastern Kunlun Strike-slip Fault: Implications for Late Cenozoic Evolution of the Qimen Tagh Range and Southwestern Qaidam Basin, North Tibet, China. ***Acta Geologica Sinica (English Edition)***, v. 87(supp.), p. 205.

Zhang C., **Cheng F.**, Huang G., Huang Y., Xing C., Guan B., Zhang Q., Xu G.,. 2013. Sediment and reservoir characteristics with reservoir evaluation of Lunlehe Formation in Qie16 block of Kunlun oilfield in Qaidam Basin: ***Acta Petrologica Sinica***, v. 29, no. 8, p. 2883-2894 (in Chinese with English abstract).

Liu, D., Jolivet, M., Yang, W., Zhang, Z., **Cheng, F.**, Zhu, B., Guo, Z., 2013. Latest Paleozoic–Early Mesozoic basin–range interactions in South Tian Shan (northwest China) and their tectonic significance: Constraints from detrital zircon U–Pb ages. ***Tectonophysics*** 599, 197-213, doi: 10.1016/j.tecto.2013.04.018.

**2012**

**Cheng F.**, Li D., Luo W., Bartholomew J., 2012. Characteristics and Patterns of Surface Ruptures Caused by the Yushu Earthquake: ***Geotectonica Et Metallogenia***, v. 36, no.1, p. 69-75 (in Chinese with English abstract).

**CONFERENCES (1ST author only)**

**Cheng F.,** Jolivet M., Guo Z. 2016. Eastward extrusion of the North Tibetan plateau: insight from the Altyn Tagh fault offset and a 3D crustal budget in North Tibet. **The 5th International Geologica Belgica Meeting (GB2016), Oral**, Mons, Belgium.

**Cheng F.,** Jolivet M., Guo Z., 2015. Reconstruction of Cenozoic growth process in North Tibet: Source to sink relation between the Qaidam Basin and East Kunlun Mountains. **EGU General Assembly** 2015, **Poster**, Vienna, Austria.

**Cheng F.**, Guo Z., 2014, Initial rupture and displacement on the strike-slip Altyn Tagh fault, northern Tibetan plateau. **Seventh session of national tectonic geology and geodynamics academic seminar**, **Oral report**, Qingdao, China.

**Cheng F.,** Guo Z., 2013. Northward Migration of the Western Segment of Eastern Kunlun Strike-slip Fault: Implications for Late Cenozoic Evolution of the Qimen Tagh Range and Southwestern Qaidam Basin, North Tibet, China. **Roof of the World --- the First Joint Meeting of GSC and GSA, Oral report**, Chengdu, China.

**Cheng F.,** Li D., Bartholomew M., Luo W., 2011. Characteristics and mechanism of surface ruptures associated with the East Kunlun, Wenchuan and Yushu Earthquakes. **Fourth session of national tectonic geology and geodynamics academic seminar, Poster,** Nanjing, China.

**RESEARCH GRANTS**

China University of Geoscience Student Research Grant, 2009-2011 (1571 $)

# Table of contents

# Chapter 1 Preface

## 1.1 Introduction, Reginal Geology and Problems

Understanding the kinematics of the Asian tectonic system that contains one of the most diverse and complex patterns of active deformation on Earth not only has significant implications for deciphering the mechanisms of continental crust evolution or the interplay between lithospheric deformation and atmospheric circulation, but also contributes to exploring the crustal growth process of other planets within the solar system (Fig. 1; Molnar and Tapponnier, 1975; Tapponnier et al., 1982; England and Houseman,1986; Tapponnier et al., 1986; Cobbold and Davy, 1988; Davy and Cobbold, 1988; Molnar et al., 1993; Métivier et al., 1998; Meyer et al., 1998; Yin and Harrison, 2000; Tapponnier et al., 2001; Basilevsky and Head, 2007; Dupont-Nivet et al., 2007; Yin, 2010; Jolivet et al., 2015).

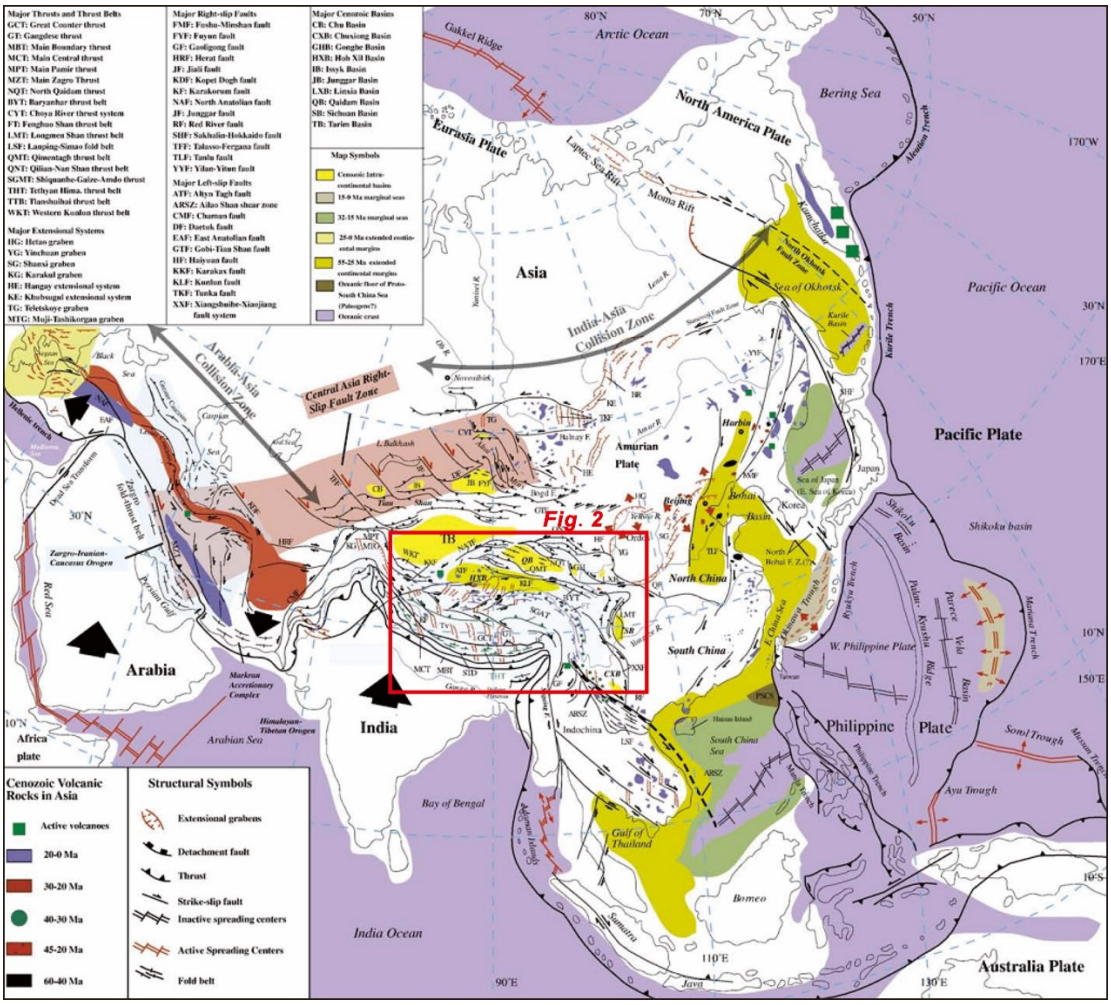


Fig.1 Cenozoic structures and distribution of volcanic rocks in Asia, modified from Yin, 2010.

Though it is widely acknowledged that the Cenozoic deformation of East Asia was associated with the India-Asia continental collision and the subsequent post-collision convergence, how this extensive area developed has long been a puzzling question. Resolving that question has implications on the understanding of the mechanical behavior of the continental lithosphere in convergent zones as well as climate evolution on regional and global scale (Molnar and Tapponnier, 1975; Métivier et al., 1998; Yin and Harrison, 2000; Tapponnier et al., 2001; Garzione et al., 2005; Dupont-Nivet et al., 2007; Yin, 2010; Jolivet et al., 2015). In particular, the initial topography of the area now represented by the Tibetan plateau and the early stages of development of the present-day topography remain poorly constrained and highly debated (e.g. England and Houseman,1986; Yin and Harrison, 2000; Tapponnier et al., 2001; Wang et al., 2006; Kapp et al., 2007; Yin et al., 2007, 2008a, 2008b; Wang et al., 2008; Wang et al., 2014).

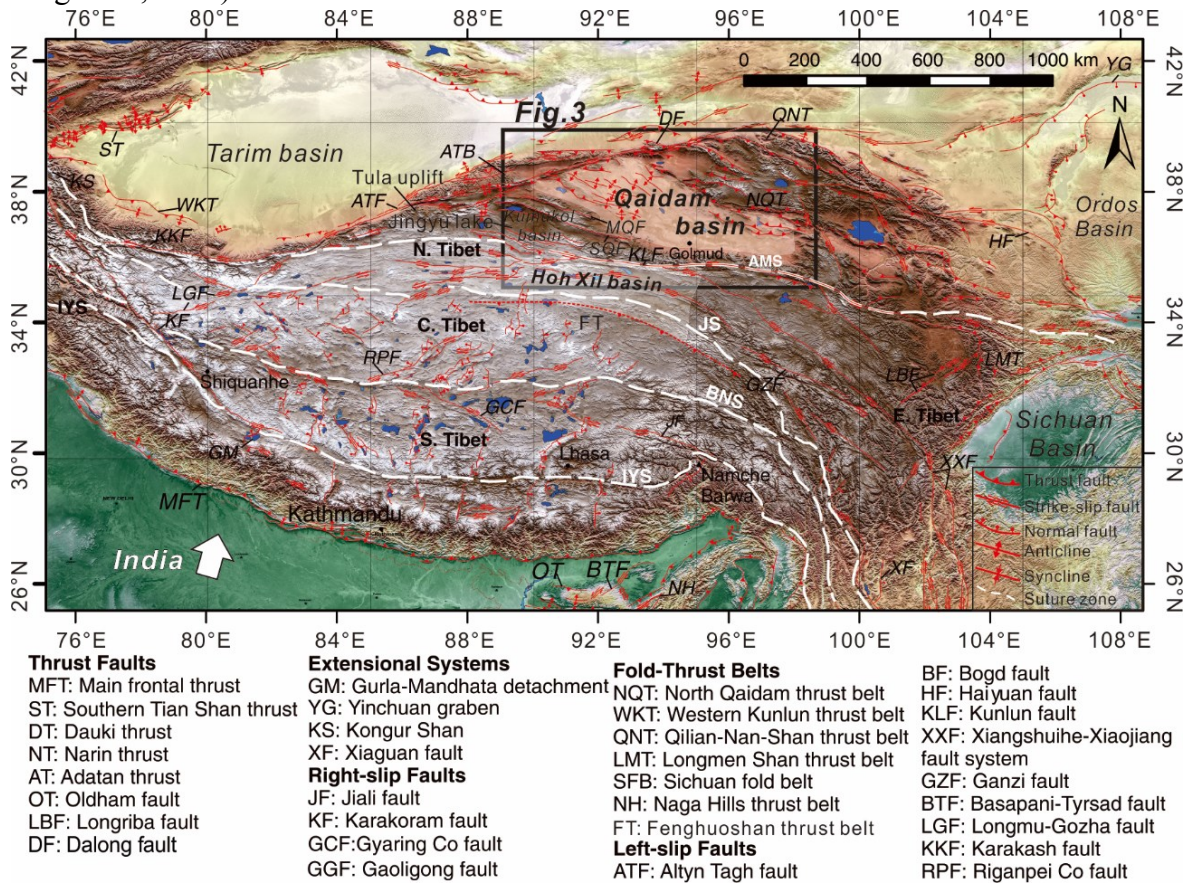


Fig.2 Digital topographic map of the Tibetan Plateau. Active fault kinematics and suture zones are mainly based on Yin et al. (2007), Taylor and Yin (2009), and Cheng et al. (2014, 2016).

The Qaidam basin is unique in the world in that it is the deepest intracontinental basin (>16 km thick of Cenozoic sediments alone), yet located in the highest plateau with the thickest continental crust. As the largest petroliferous basin on the Tibetan plateau, the triangular-shaped endorheic Qaidam basin is surrounded by the Altyn Tagh, the Qilian Shan,

and the Eastern Kunlun ranges, with ~2000 m of relief from the basin to the ranges (Figs. 2 and 3). The complete sequence of Cenozoic non-marine sedimentary rocks within the Qaidam basin as well as geological transects across the basin and ranges allow unraveling the formation mechanism and growth history of the Tibetan plateau, as well as the interplay between tectonics and climate. However, the Cenozoic evolution of the Qaidam basin and the Cenozoic kinematic evolution of the surrounding regions are highly debated, as briefly described below.

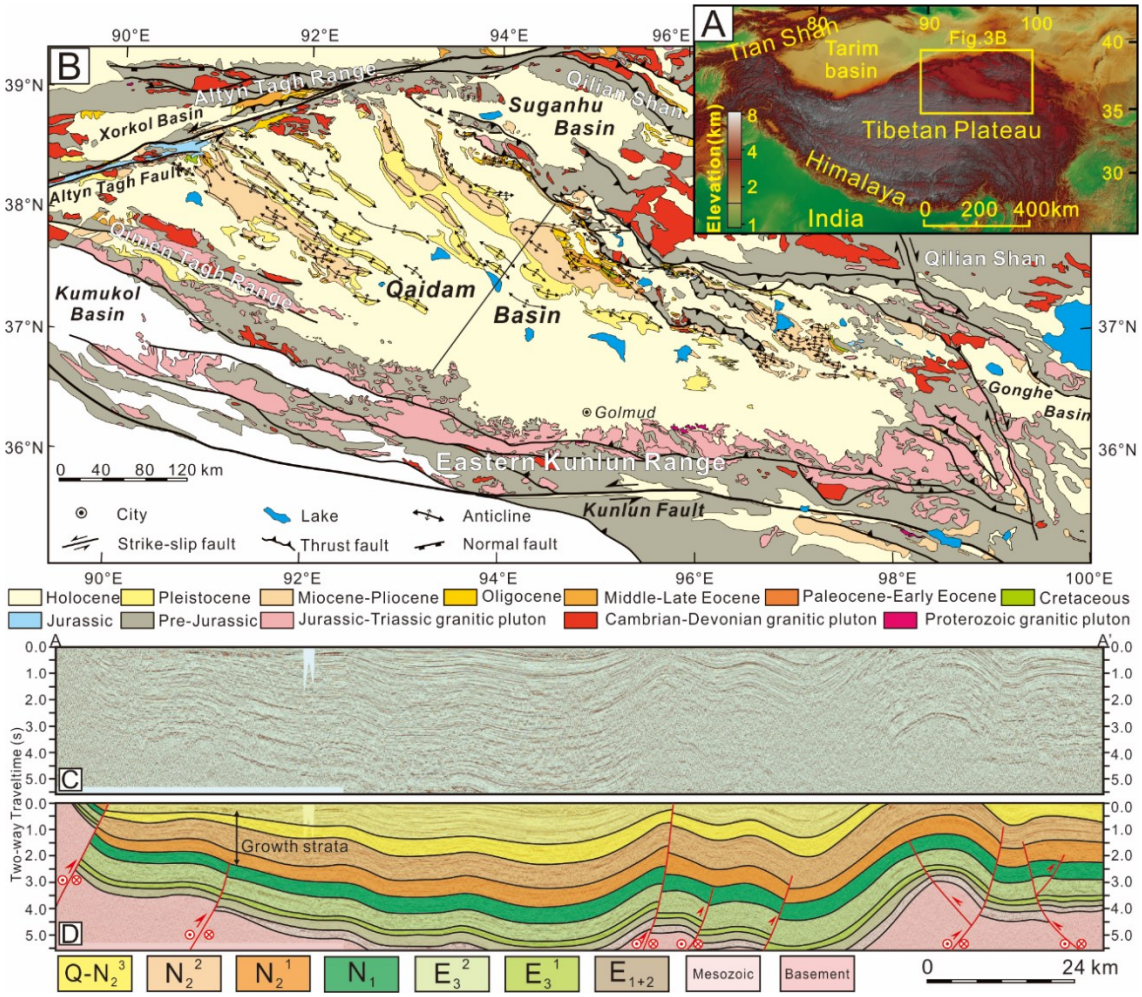


Fig.3 Geological map of the Qaidam basin, northern Tibetan plateau, modified from Chen et al. (2015). Seismic profile interpretations on the dip of the basement faults in the southwestern Qaidam basin are in dispute. Yin et al. (2007) proposed a series of south thrusting faults, whereas Cheng et al. (2014) and Wu et al. (2014) suggested those are south-dipping faults which are adopted in this study. Q-$N_2^3$—Quaternary to Late Miocene strata; $N_2^2$—Middle Miocene strata; $N_2^1$—Early Miocene strata; $N_1$—Oligocene strata; $E_3^2$—Late Eocene strata; $E_3^1$—Middle Eocene strata; $E_{1+2}$—Paleocene to Early Eocene strata.

In the past decades, several models have been proposed to explain the Cenozoic tectonic and sedimentary evolution of the Qaidam Basin. Most of those simply defined the tectonic pattern between the Eastern Kunlun Mountains and the Qaidam Basin through a northward or

southward thrusting model (Burchfiel et al., 1989; Meyer et al., 1998; Chen et al., 1999; Mock et al., 1999; Yin and Harrison, 2000; Jolivet et al., 2001; Tapponnier et al., 2001; Jolivet et al., 2003; Wang et al., 2006; Yin et al., 2007; Shi et al., 2009; Wang et al., 2011). The northward thrusting model prevailed during the last two decades, explaining the subsidence of the Qaidam Basin as a result of the basinward propagation of successive thrust sheets along the southern edge of the basin. Burchfiel et al. (1989) proposed that the southern edge of the Qaidam Basin is limited by a south-dipping thrust fault. Based on a synthesis of focal mechanisms and focal depth distribution combined with geological features, Chen et al. (1999) again speculated the existence of this south-dipping North Kunlun thrust fault along the northern margin of the East Kunlun belt. In addition, many authors indicated that northward basement thrusting across the Eastern Kunlun Mountains was associated to the northward propagation of a crustal-scale accretionary wedge initiating around ca. 30–20 Ma. (Fig. 4; Meyer et al., 1998; Mock et al., 1999; Jolivet et al., 2001; Tapponnier et al., 2001; Jolivet et al., 2003; Wang et al., 2006). These ideas suggest that the Eastern Kunlun Mountains consists in a large transpressional system limited to the south by the left-lateral strike slip Kunlun fault and to the north by a series of south-verging basement thrusts affecting the southern edge of the Qaidam Basin.

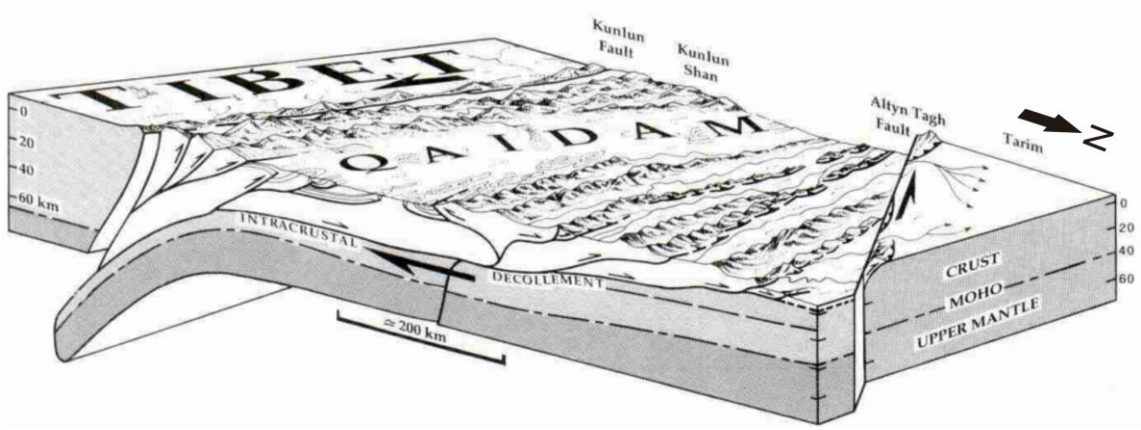


Fig.4 Northward propagation model, modified from Meyer et al. (1998). Note the south-dipping fault in the southern Qaidam basin.

The southward thrusting model has drawn much attention in recent years (Fig. 5; Yin et al., 2007; 2008; Shi et al., 2009; Wang et al., 2011). Yin and Harrison (2000) suggested that two major thrusts, the Qimen Tagh Thrust and the North Kunlun Thrust mark the southern boundary of the Qaidam Basin. Using seismic profiles within the Qaidam Basin as well as field observations, Yin et al. (2007) then proposed that the low altitude Qaidam Basin has been thrust onto the Eastern Kunlun Mountains along a major north dipping Cenozoic thrusts. Wang et al. (2011) later expanded this model based on a high-resolution deep seismic reflection

profile across this area. This model indicates that the Eastern Kunlun Mountains should not thrust northward onto the Qaidam Basin and that the initiation of compressive deformation along the southern margin of the Qaidam Basin is much younger than along the northern margin of the basin.

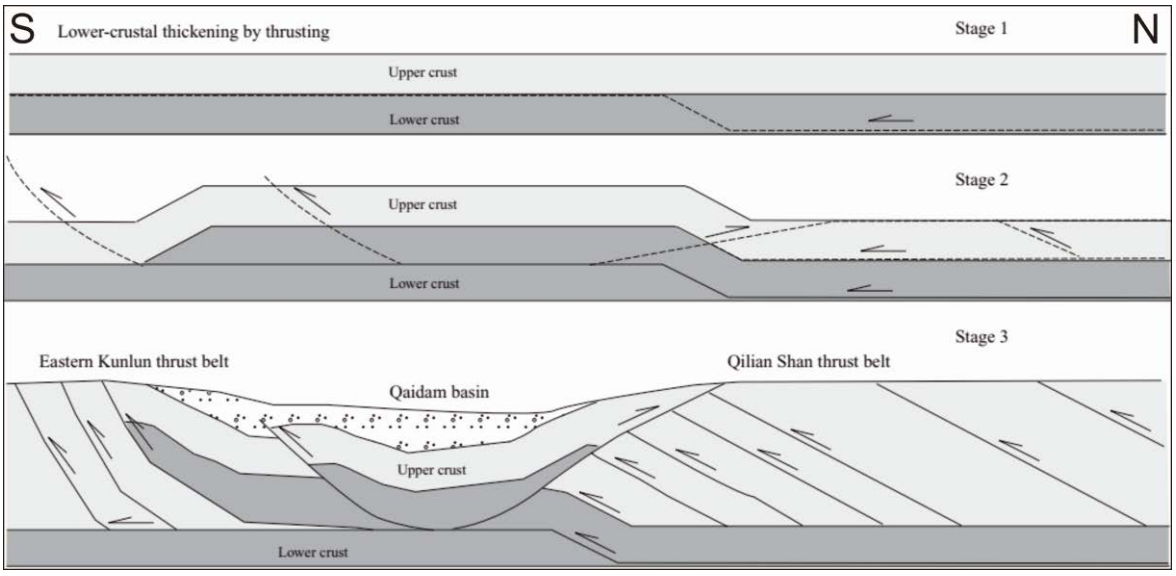


Fig.5 Southward propagation model, modified from Yin et al. (2008a). Note the south-thrusting fault in the southern Qaidam basin.

Other tectonic models have been proposed aside from the two main ones described above. Xia et al. (2001) proposed that the Qaidam Basin experienced a two stages evolution: an initial extension phase during the Early Tertiary was followed by a compressive phase leading to basin inversion. However, few seismic profiles in the western Qaidam Basin have revealed any extensional faults during the Early Tertiary. Meng and Fang (2008) suggested that the Cenozoic tectonic subsidence of the Qaidam Basin resulted from crustal folding or buckling in response to regional horizontal compression. However, the seismic profiles across the whole Qaidam Basin imply that the magnitude of Cenozoic upper crustal shortening decreases eastward across the basin from >48% in the west to <1% in the east (Yin et al., 2008a). In particular, the proposed onset time of uplift of the Eastern Kunlun Range mainly varies from Eocene to Miocene, depending on the approach used to estimate the onset of deformation (Mock et al., 1999; Jolivet et al., 2001; Yuan et al., 2006; Yin et al., 2007, 2008a; C. Wang et al., 2008; Clark et al., 2010; Dai et al., 2013; Duvall et al., 2013). Based on regional stratigraphic correlation between the Qaidam Basin and the Hoh Xil Basin to the south, Yin et al. (2008a) argued that they represented a single basin during the Paleogene, bounded to the north by the Altyn Tagh Range and the Qilian Shan, and to the south by the proto–Tibetan Plateau. This large structure was then partitioned by the tectonic uplift of the Eastern Kunlun

Range during the Neogene. This model questions the assumption of a progressive northward growth of the plateau through in-sequence propagation of thrust systems associated with filling of the intermediate basins (e.g., Métivier et al., 1998; Meyer et al., 1998; Tapponnier et al., 2001). This idea has motivated several attempts to reassess the tectonic processes affecting the northern edge of the Tibetan Plateau (e.g., Shi et al., 2009; Wang et al., 2011; Mao et al., 2014; Yu et al., 2014).

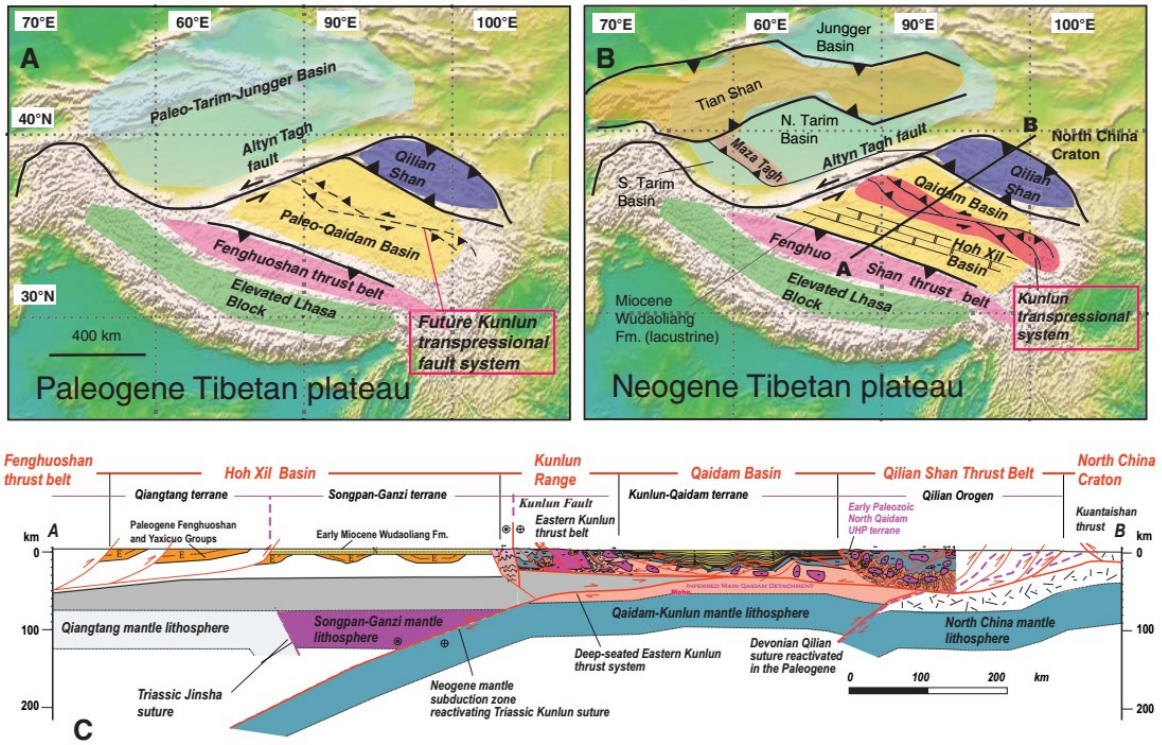


Fig.6 Paleo-Qaidam basin model, cited from Yin et al. (2008a). Note that during the Paleogene, the Paleo-Qaidam basin lies between the elevated Lhasa block and the Fenghuo Shan thrust belt in the south and the elevated Qilian Shan in the north. The region north of the Tibetan plateau was a large topographic depression that links Tarim and Junggar basins across the Tian Shan, as the Tian Shan was not uplifted until the early Miocene. The initiation of the Eastern Kunlun left-slip transpressional system caused the uplift of the Eastern Kunlun Range, which has partitioned the PaleoQaidam basin into the Hoh Xil basin to the south and the Qaidam basin to the north.

As the northwestern boundary of the Qaidam basin, the sinistral strike-slip Altyn Tagh fault plays a significant role in the Cenozoic deformation of northern Tibet (Fig. 7). Understanding the Cenozoic kinematic pattern of the Altyn Tagh fault holds important implications for unraveling the evolution of northern Tibet, deciphering the growth history of the entire Tibetan Plateau, and contributing to oil and gas exploration in the surrounding region (Fig. 2; Yue and Liou, 1999; Yin and Harrison, 2000; Tapponnier et al., 2001; Yin et al., 2002; Wang et al., 2014). Recent studies have revealed much about the large-scale geology of the Altyn Tagh Range and the surrounding region (Wang, 1997; Yue et al., 2001; Yin et al., 2002;

Chen et al., 2003; Cowgill et al., 2003; Dupont-Nivet et al., 2003, 2004; Ritts et al., 2004; Wu et al., 2012a, 2012b; Lu et al., 2014; Zhang et al., 2014). However, the immense size and extent of the Altyn Tagh Range make it difficult to locate ideal piercing points with which to estimate the initial timing of left-slip movement and total displacement along the Altyn Tagh fault. As a result, both the timing and amount of slip along the fault are vigorously debated (e.g., Yin et al., 2002; Cowgill et al., 2003; Gehrels et al., 2003a, 2003b; Ritts et al., 2004; Wu et al., 2012a, 2012b). Although some studies reference Mesozoic shearing in the Altyn Tagh Range (Arnaud et al., 2003; Wang et al., 2005; Li et al., 2006; Liu et al., 2007), the growth of the Tibetan Plateau is largely related to Cenozoic faulting along the Altyn Tagh fault rather than to any pre-Cenozoic shearing in the Altyn Tagh Range (Tapponnier et al., 2001). Various approaches have been used to constrain the initial timing of left-lateral slip movement along the Altyn Tagh fault, and the estimates vary greatly. Initial movement along the Altyn Tagh fault is estimated to have occurred broadly between the Eocene and Miocene epochs (Chen et al., 2001; Jolivet et al., 2001; Meng et al., 2001; Wan et al., 2001; Yue et al., 2001; Yin et al., 2002; Robinson et al., 2003; Wu et al., 2012a, 2012b), and estimates of the total displacement along the Altyn Tagh fault vary anywhere from ~1200 km to less than 90 km (Tapponnier et al., 1986; Wang, 1997; Yin and Harrison, 2000; Yang et al., 2001; Yin et al., 2002; Cowgill et al., 2003; Gehrels et al., 2003a, 2003b; Ritts et al., 2004). The wide variety of estimates regarding the initial timing and offset of the Altyn Tagh fault highlight the incomplete understanding of this remote region.

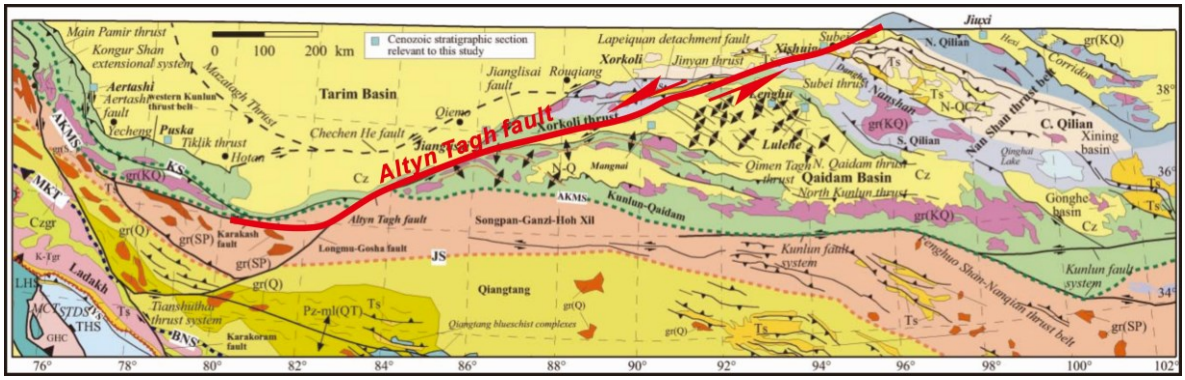


Fig.7 Simplified tectonic map of northern Tibet showing major tectonic terranes, sutures, and faults (modified from Yin et al., 2002). Cenozoic stratigraphic sections (locations shown by turquoise blue squares) were measured by this study at Aertashi, Puska, Jianglisai, and Xishuigou in the southern Tarim Basin. Other relevant stratigraphic sections are Mangnai, Lenghu, Lulehe, Xorkoli, and Jiuxi (Hexi Corridor). Map symbols: N-Q—Neogene–Quaternary sediments, Ts—Tert iary sedimentary rocks, THS—Tethyan Himalayan sequences (Proterozoic to Upper Cretaceous passive-continental-margin strata of northern India), GHC—Greater High Himalayan Crystalline Complex, LHS—Lesser Himalayan metasedimentary series. Major plutonic rocks: Czgr—Cenozoic granites, K-Tgr—plutonic rocks belongi ng to the Gangdese batholith, Ladakh batholith, and Kohistan arc, gr(Q)—plutonic rocks

in the Qiangtang terrane (mostly Jurassic–Cretaceous), gr(SP)—plutonic roc ks in the Songpan–Ganzi–Hoh Xil terrane (mostly Late Triassic), gr(KQ)—Ordovician–Silurian and Permian–Triassic plutonic rocks in the Kunlun and Qilian terranes. Major sutures: IYS—Indus-Yalu suture, BNS—Bangong-Nujiang suture, JS—Jinsha suture, AKMS—Ayimaqin-Kunlun-Mutztagh suture, KS—Kudi suture, MCT—Main Centra l thrust, MKT—Main Karakoram thrust, STDS—South Tibet detachment system.

Finally, with regard to the northeastern boundary of the Qaidam basin, the Qilian Shan separates the plateau from the Gobi-Alxa block to the northeast (Fig. 8). This crustal-scale wedge consists of massive NW-SE striking mountain ranges growing on folds, thrusts or strike-slip faults accommodating the northward motion and eastward extrusion of the Tibetan Plateau (Meyer et al., 1998; Yin and Harrison, 2000; Tapponnier et al., 2001; Bovet et al., 2009). The proposed Palaeocene to early Eocene initiation of the Cenozoic deformation and crustal shortening in the Qilian Shan (Jolivet et al. 2001; Yin et al., 2008; Clark et al., 2010; Duvall et al., 2011; Zhuang et al., 2011; Yuan et al., 2013) challenges the model of post-Pliocene initial deformation in the northern Tibetan plateau inferred from the hypothesis of northward progressive plateau growth (Métivier et al., 1998; Meyer et al., 1998; Tapponnier et al., 2001). Although large amounts of NE-SW directed shortening and eastward motion of the northern Tibetan crust have long been observed (e.g. Tapponnier and Molnar, 1977; Burchfiel et al., 1991; Dupont-Nivet et al., 2004; Zhang et al., 2004), the proposed amounts of Cenozoic crustal shortening vary widely from ~20% to ~60% (Bally et al., 1986; Meyer, et al., 1998; Yin et al., 2008a, 2008b; Zhang et al., 2014) and quantitative estimation of the amount of lateral extrusion in the northeastern Tibetan Plateau is deficient.

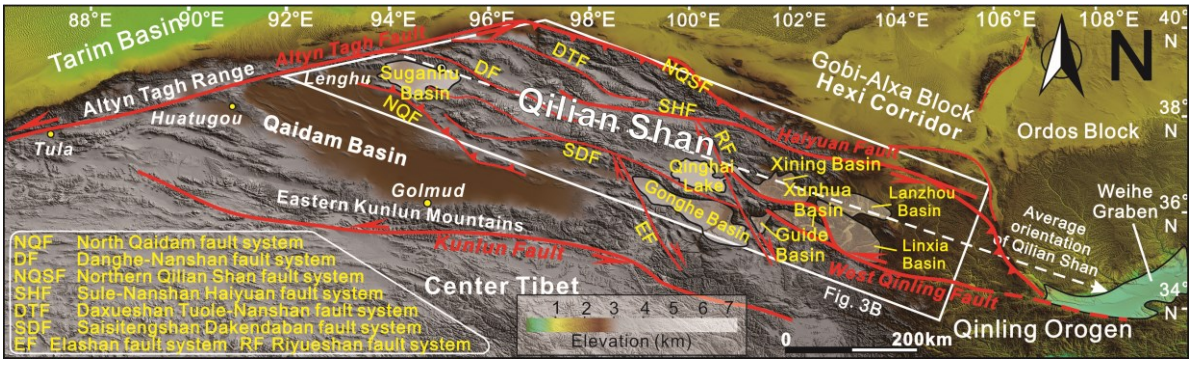


Fig.8 Topographic map of northern Tibet showing major tectonic terranes and faults within the Qilian Shan.

## 1.2 Research plan and framework of the dissertation

My PhD dissertation focuses on four key issues that contribute to understand the evolution of the Qaidam basin itself and kinematic history of the entire Tibetan plateau since the onset of the India-Asia collision: ***1) The Cenozoic tectonic evolution between the Qaidam***

***basin and the Eastern Kunlun Range; 2) The interplay between the sediments within the Qaidam basin and the active tectonic within the Altyn Tagh Range; 3) The quantitative estimate of the lateral extrusion along the Altyn Tagh Fault-Qilian Shan tectonic system; 4) The classification of the Qaidam basin: Foreland basin or Strike-slip superimposed basin*****?***

**Firstly**, I discuss the Cenozoic tectonic evolution between the Qaidam basin and the Eastern Kunlun Range in Chapter 2. I subdivided this issue into two parts: ***Chapter 2.1 Tectonic relationship between the Eastern Kunlun Range and the Qaidam basin***, and ***Chapter 2.2 Cenozoic source to sink relation between the Qaidam basin and the Eastern Kunlun Mountains***. In the first part, I analyze newly acquired 3D seismic-reflection profiles within the SW Qaidam basin, isopach maps of the Cenozoic strata in the SW Qaidam basin, remote sensing images in the Qimen Tagh Range, and earthquake focal mechanisms and epicenter distribution within the Qaidam basin, in order to re-evaluate the tectonic pattern along the western portion of the Kunlun fault and to decipher the Late Cenozoic interaction between the Eastern Kunlun Range and the SW Qaidam basin. I published this work in ***Tectonophysics*** as first author. Concerning the Cenozoic source to sink relation between the Qaidam basin and the Eastern Kunlun Mountains, I conducted field investigation, detrital zircon geochronology analysis combined with the seismic profile interpretation, in order to characterize the nature of the relation between the Eastern Kunlun Range and the Qaidam Basin, and present a clear image on the source to sink relation between these two regions. I published this contribution in ***Geological Society of American Bulletin*** as first author.

**Secondly**, in order to constrain ***the initial timing and kinematic pattern of movement along the Altyn Tagh fault***, I present a detailed analysis of the stratigraphy, sediment types, and detrital zircon U-Pb ages combined with seismic profile data along three sections (Tula, Anxi, and Caishiling sections) of the western segment of the Altyn Tagh fault in ***Chapter 3.1***. I also carried out a detailed analysis of the stratigraphy and detrital zircon geochronology of four key lithologic sections (Tula, Anxi, Caishiling and Eboliang) along the Altyn Tagh fault, presented in ***Chapter 3.2***. I published part of this work in ***Geosphere*** as first author (see ***Chapter 3.1***), while submitted the other part to ***Tectonophysics*** again as first author (see ***Chapter 3.2***). This last manuscript as been accepted with minor revision.

**Thirdly**, my work on ***the quantitative estimate of the lateral extrusion along the Altyn Tagh Fault-Qilian Shan system which*** is a follow-up research of issue 2 (i.e. ***the initial timing and kinematic patterns of movement along the Altyn Tagh fault***). The lithospheric strike-slip Altyn Tagh fault has accommodated hundreds of kilometers of displacement (~360 km) between the Qaidam and Tarim blocks since its Eocene reactivation. However, the way the

deformation is accommodated in the Qilian Shan and further east remains uncertain. I propose a new quantitative evaluation of the Cenozoic crustal shortening and lateral extrusion budget in the northern Tibetan plateau, based on my 360 km estimation of north-eastward migration of the relatively rigid Qaidam block along the Altyn Tagh fault, and 3D isovolumetric balancing of the crustal deformation within the Altyn Tagh fault–Qilian Shan system. I published this work in ***Terra Nova*** as first author, and present it in ***Chapter 4***.

**Finally**, in order to ***classify the peculiar Qaidam basin (Foreland basin or Strike-slip superimposed basin)***, I review the recent arguments on the Cenozoic evolution of the Qaidam baisn and summarize the kinematic features within the Qaidam basin and surrounding regions based on the abovementioned findings combined with recent petroleum exploration achievements in recent years (e.g. distribution of source rocks in the Qaidam basin). I conclude that the Qaidam basin is a strike-slip superimposed basin jointly controlled by the left-lateral strike-slip Altyn Tagh and East Kunlun faults. The temporal and spatial superimposition of these two strike-slip faults during the Cenozoic controlled the evolution of the basin as well as the oil and gas accumulation. This work is presented in ***Chapter 5***. I have published this contribution in ***Petroleum Exploration and Development*** as co-author.

# Chapter 2 Cenozoic tectonic evolution between the Qaidam basin and the Eastern Kunlun Range

## 2.1 Tectonic relationship between the Eastern Kunlun Range and the Qaidam basin

***Paper published in Tectonophysics, 2014, vol. 632, pp. 32-47***

**Northward growth of the Qimen Tagh Range: a new model accounting for the Late Neogene strike-slip deformation of the SW Qaidam Basin**

**Feng Cheng** [a], Marc Jolivet [b], Suotang Fu [c], Qiquan Zhang [c], Shuwei Guan [d], Xiangjiang Yu [a], Zhaojie Guo [a, *]

[a] Key Laboratory of Orogenic Belts and Crustal Evolution, Ministry of Education, School of Earth and Space Sciences, Peking University, Beijing, 100871, China

[b] Laboratoire Géosciences Rennes, CNRS-UMR6118, Université Rennes 1 - Observatoire des Sciences de L'Univers de Rennes, Rennes, France

[c] Qinghai Oilfield Company, PetroChina, Dunhuang, Gansu, 736202, China

[d] Research Institute of Petroleum Exploration and Development, PetroChina, Beijing, 100083, China

[*] Corresponding author. Tel.: + 86-10-62753545; fax: + 86-10-62758610. E-mail address: zjguo@pku.edu.cn

*Note: The online version of this contribution can be found as:* ***Cheng, F., Jolivet, M., Fu, S., Zhang, Q., Guan, S., Yu, X., Guo, Z., 2014. Northward growth of the Qimen Tagh Range: A new model accounting for the Late Neogene strike-slip deformation of the SW Qaidam Basin. Tectonophysics 632, 32-47, doi: 10.1016/j.tecto.2014.05.034***

### Abstract

Situated along the western termination of the Eastern Kunlun Mountains, the Qimen Tagh Range represents a key area to understand the Cenozoic basin-range interactions between the northeastern Tibetan Plateau and the Qaidam Basin. Within that region, several huge bow-like

fault systems such as the Kunbei and Qimen Tagh fault systems accommodate the transpressive deformation but their kinematic evolution is still highly debated. Newly acquired seismic profiles and isopach maps of the Late Eocene sediments strongly suggest that the Kunbei fault system (consisting of the Kunbei, Arlar and Hongliuquan faults) in the southwestern Qadaim Basin was initially a left-lateral strike-slip fault system rather than a thrusting system. Growth strata indicate an Early Miocene onset age for this strike-slip deformation. However, earthquakes focal mechanisms show that the present-day tectonic pattern of this fault system is dominated by NE-SW transpression. As for the Qimen Tagh fault system, numerous linear geomorphic features and fault scarps indicate that it was again a strike-slip fault system. Deformed sediments within the Adatan Valley prove that strike-slip motion prevailed during the Pleistocene, yet the present day deformation is marked by NE-SW transpression. Collectively, the Kunbei and Qimen Tagh fault systems were initially left-lateral strike-slip fault systems that formed during Early Miocene and Pleistocene respectively. Colligating with these southward younging left-lateral strike-slip faulting ages and the fact that these convex-northward structures converge to the center segment of active Kunlun Fault in the east, we thus considered the Kunbei and Qimen Tagh fault systems as former western segments of the Kunlun Fault once located further south in the present-day location of that fault. These faults gradually migrated northward since the Early Miocene while their kinematics changed from left-lateral strike-slip motion to NE-SW transpression.
Keywords: Cenozoic tectonics, North Tibet, Kunlun Fault, Qimen Tagh Range, southwestern Qaidam Basin.

### 2.1.1 Introduction

The Eastern Kunlun Mountains and adjacent Qaidam Basin present one of the strongest topographic gradients in Eurasia, similar to that of the Longmen Shan Range in East Tibet (Fig. 1). Within that region, the left-lateral strike-slip Kunlun Fault Zone represents one of the key tectonic features controlling the active deformation along the northern margin of the Tibetan Plateau (e.g. Avouac and Tapponnier, 1993; Meyer et al., 1998; Jolivet et al., 2001; Tapponnier et al., 2001; Xia et al., 2001 ;Yin et al., 2007). Most of the previous studies that dealt with the Tertiary deformation in the East Kunlun ranges focused on the central and eastern segment of the Kunlun Fault (Kirby et al., 2007; Harkins and Kirby, 2008) where the deformation is mostly localized along the major, unique strike-slip fault zone. However, only a limited number of studies describe the more structurally complex western termination of the

Kunlun Fault system (Jolivet et al., 2001, 2003).

Although the Cenozoic tectonic evolution of North Tibet has been largely studied, the relationship between the Qaidam Basin and the East Kunlun Range, as well as the tectonic pattern of the Kunlun Fault itself, remains controversial. For example, several contradicting models have been proposed to describe the tectonic structure of the southern edge of the Qaidam Basin: a crustal-scale south-dipping thrust system (Burchfiel et al., 1989); a large transpressional system including the left-lateral strike - slip Kunlun Fault to the south and a north - directed thrust system along the northern flank of the Eastern Kunlun Mountains (Meyer et al., 1998; Tapponnier et al., 2001; Jolivet et al., 2003); or a series of north - dipping thrusts carrying the Qaidam Basin southward onto the Qimen Tagh Range (Yin et al., 2007; Shi et al., 2009; Wang et al., 2011). Within most of those models, the large amount of Cenozoic strike-slip motion along the Kunlun Fault (Fu and Awata, 2007) is generally considered as secondary in controlling the overall structural setting of the SW Qaidam Basin and East Kunlun Range. However, if the boundary fault between the Qaidam Basin and the East Kunlun Range was indeed accommodating a large amount of lateral displacement, the southern Qaidam Basin should be largely decoupled from the Tibetan Plateau to the south and should not be affected by major N-S compression and shortening since the initiation of the strike-slip Kunlun Fault. Nonetheless, the Qimen Tagh Range, bordering the SW Qaidam Basin to the south forms a convex-northward bow-like tectonic prism clearly accommodating shortening along the southern margin of the basin while strike-slip motion occurs along the Kunlun Fault to the south.

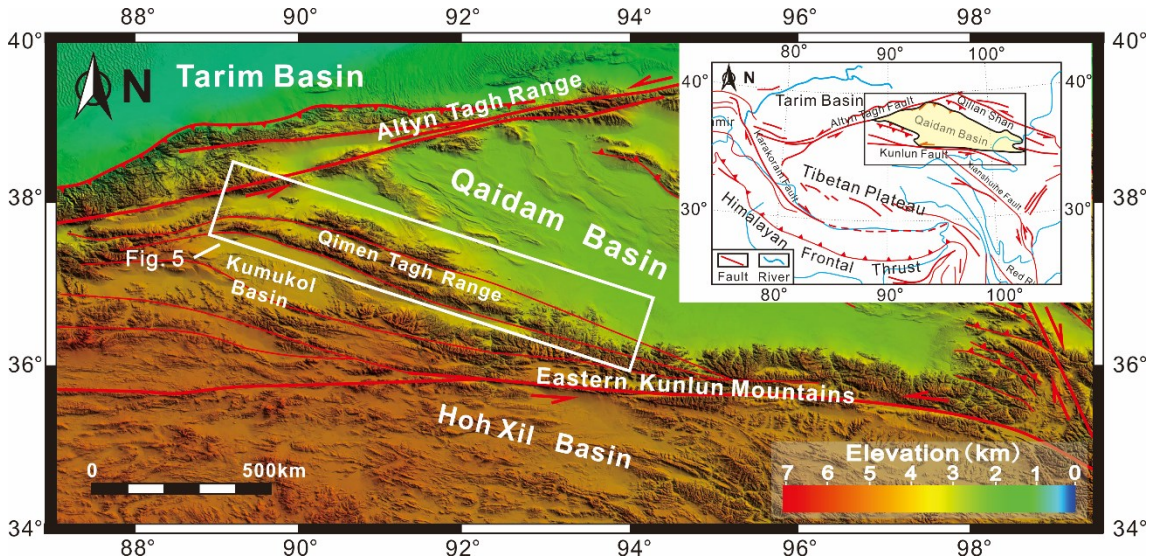


Fig.1 Digital topographic map of the western Qaidam Basin and surrounding area. Topography from SRTM data.

This paper aims to re-evaluate the tectonic pattern along the western portion of the Kunlun Fault and to decipher the Late Cenozoic interaction between the East Kunlun Range and the SW Qaidam Basin in the Qimen Tagh Range. This work is based on new field observation and data, interpretation of newly acquired seismic reflection profiles within the SW Qaidam Basin, remote sensing images, and earthquake focal mechanisms and epicenters distribution. Based on those data we propose that the Late Neogene northward growth of the convex-northward structures in the Qimen Tagh Range and SW Qaidam Basin is driven by left-lateral strike-slip motion along the Kunlun Fault. While migrating northward, the western segment of the Kunlun Fault gradually rotates through time. This northward rotation induces a progressive change from left-lateral strike-slip to NE-SW compressional motion. Continuous activity along the Kunlun Fault finally initiates a new strike-slip segment.

## 2.1.2 Regional Geology

### 2.1.2.1 Eastern Kunlun Mountains

The Eastern Kunlun Mountains, with an average altitude of ~4500m, separates the relatively low-relief Qaidam Basin to the north from the Hoh Xil Basin to the south. The Kunlun Fault Zone itself represents a major tectonic boundary between the Bayan Har-Songpan Garze terrane and the Kunlun-Qaidam basement (e.g. Meyer et al., 1996). The fault extends about 1600 km along-strike, initiating on the eastern margin of the Tibetan Plateau (Kirby et al., 2007; Lin and Guo, 2008) and ending in a splay structure with several curved faults in the west (Xu et al., 2002; Fu and Awata, 2007) (Fig. 1). Intense seismicity attests of the activity of this left-lateral strike-slip fault system (e.g., $M_w$ 7.8 Kunlunshan earthquake in 2001(Lin et al., 2002; Xu et al., 2002); $M_w$ 7.6 Manyi earthquake in 1997 (Peltzer et al., 1999); $M_w$ 7.5 Manyi earthquake in 1973 (Velasco et al., 2000); $M_w$ 7.5 Tuosu Lake earthquake in 1937 (Guo et al., 2007); $M_s$ 7.0 Alake Lake earthquake in 1963(Guo et al., 2007)). Both GPS and geological data suggest that the central segment of the Kunlun Fault has a uniform slip rate of ca.10 mm/yr (Kidd and Molnar, 1988; Van Der Woerd et al., 1998; Wang et al., 2001; Zhang et al., 2004; Fu et al., 2005; Kirby et al., 2007). This rate decreases to ~5 mm/yr along its eastern segment and finally dies out toward the eastern fault tip (Kirby et al., 2007; Harkins and Kirby, 2008). The total displacement along the fault since its initiation is approximately 100 ± 20 km according to the largest cumulative offset of basement rocks along the tectonic lineament (Fu and Awata, 2007).

The Cenozoic deformation and exhumation history of the Eastern Kunlun Mountains is

complex and still largely debated. For instance, the onset age of the Cenozoic cooling event in this area range from 35 to 10 Ma depending on the authors (Mock et al., 1999; Jolivet et al., 2001; Wang et al., 2004a; Liu et al., 2005; Yuan et al., 2006; Clark et al., 2010; Duvall et al., 2013). However, the onset age of left-lateral strike-slip motion along the Kunlun Fault has been estimated to be 15 Ma or earlier (Jolivet et al., 2003). Similarly, based on the growth strata records in the seismic profiles across the SW Qaidam Basin, Yin et al. (2008) asserted that the Cenozoic deformation across the Qimen Tagh Range and in the SW Qaidam Basin, directly related to the tectonic development of the Kunlun Fault Zone, initiated during or after Late Oligocene to Early Miocene times.

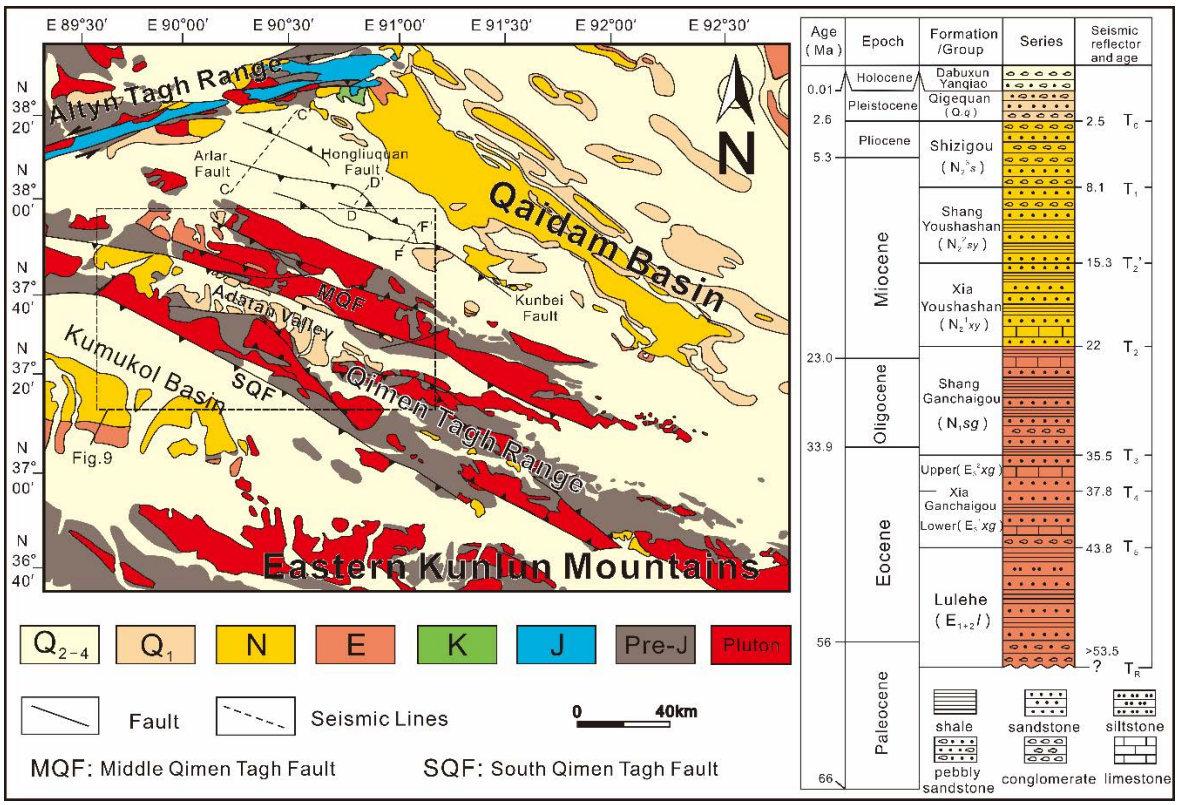


Fig.2 Geological map of the Qimen Tagh Range and SW Qaidam Basin. See Fig. 1 for location and the text for discussion. Modified after the Kulangmiqiti J46C003001 1:250,000 geological map (IGSQP, 2004).

### 2.1.2.2 SW Qaidam Basin and Kumukol Basin

The ~3500 m high (on average), low relief triangular Qaidam Basin is bounded by the Altyn Tagh Range to the northwest, the Eastern Kunlun Mountains to the south, and the Qilian Shan to the northeast (Fig. 1). Recent geological cross sections within the Qaidam Basin, mostly based on seismic profiles and drill cores data, demonstrate that the upper Cretaceous and Tertiary sediments rest unconformably on the Jurassic to Cretaceous strata. This

unconformity indicates that some deformation already took place within the basin during the Cretaceous (Xia et al., 2001; Fang et al., 2007). The Cenozoic sequences mainly consist of a series of continental clastic deposits (Fig. 2). The successive depocenters were consistently located along the long axis of the basin and gradually migrated eastward since the Eocene (Balley, 1986; Song and Wang, 1993; Qiu, 2002; Xia et al., 2001; Sun et al., 2005; Yin et al., 2008).

The chronology of the Cenozoic stratigraphic units has been precisely defined (Fig. 2) mostly using magnetostratigraphy, but also based on palynology and paleontology studies within the entire basin (QBGMR, 1991; Yang et al., 1992; Deng et al., 2004a, 2004b; Sun et al., 2005; Song et al., 2006; Zhang et al., 2006; Fang et al., 2007; Sun et al., 2007; Wang et al., 2007; Lu and Xiong, 2009; Ke et al., 2013). The series include: (1) the Lulehe Formation, $E_{1+2}l$, >53.5 - 43.8 Ma (Yang et al., 1992; Song et al., 2006; Zhang, 2006; Ke et al., 2013); (2) the lower Xiaganchaigou Formation, $E_3^1xg$, 43.8 - 37.8 Ma (Song et al., 2006; Zhang, 2006; Sun et al., 2007; Pei et al., 2009); (3) the upper Xiaganchaigou Formation, $E_3^2xg$, 37.8 - 35.5 Ma (Sun et al., 2005; Sun et al., 2007; Pei et al., 2009); (4) the Shangganchaigou Formation, $N_1sg$, 35.5 - 22.0 Ma (Sun et al., 2005; Lu and Xiong, 2009); (5) the lower Youshashan Formation, N21xy, 22.0 - 15.3 Ma (Fang et al., 2007; Lu and Xiong, 2009); (6) the upper Youshashan Formation, $N_2^2sy$, 15.3 - 8.1 Ma (Fang et al., 2007); (7) the Shizigou Formation, $N_2^3s$, 8.1 - 2.5 Ma (Fang et al., 2007); and finally, (8) the Quaternary sediments, including the Qigequan Formation (Q1q) and the Dabuxun - Yanqiao Formation, 2.5 - 0 Ma (Fang et al., 2007; Yin et al., 2008). The boundaries between these formations have been labeled $T_R$, $T_5$, $T_4$, $T_3$, $T_2$', $T_2$, $T_1$ and $T_0$ (from bottom to top) by petroleum geologists and will be used as it below (Fig. 2).

The Kumukol Basin (Figs. 1 and 2), with an average elevation of ~4000m, is located between the Qimen Tagh Range to the north and the western branches of the Eastern Kunlun Range to the south. Remote sensing image and field evidence indicate that the northern part of the Kumukol Basin is bordered by an active fault which controls the distribution of the present drainage system (IGSSP, 2003). The basin contains an Eocene to Pliocene sequence which has been deformed into a NW-SE oriented syncline (Meng and Fang, 2008). Based on fossils and stratigraphic correlation (Zhang et al., 1996), these Tertiary sequences can be divided into four units (from bottom to top) (Meng and Fang, 2008): the Huatiaoshan Formation (Eocene to Oligocene), the Hongshiliang Formation (Early Miocene), the Fengchenkou Formation (Middle Miocene), and the Jiantuliang Formation (Pliocene to Pleistocene). The Eocene to Oligocene series in the Kumukol Basin are dominated by

lacustrine deposits (IGSSP, 2003) displaying similar facies and depositional environments as the Eocene to Oligocene deposits in the SW Qaidam Basin and Hoh Xil Basin. This similarity of the deposits within the three basins suggests that they were largely connected during the Paleogene (Yin et al., 2008).

### 2.1.3 Active tectonic pattern in the western segment of the East Kunlun Range

The distribution and focal mechanisms of earthquakes reflect the occurrence and kinematics of active faults and allow describing the active tectonic pattern of the study area (e.g. Taylor and Yin, 2009; Jolivet et al., 2013). We analyzed the parameters of all earthquakes in an area between 89°E to 98°E and 35°N to 39°N, for which precisely determined hypocenter depths and focal mechanisms are available. The epicenters and depth - frequency distribution of seismicity used in this study are issued from the China Earthquakes Network Center (CENC). Only events with magnitude M > 3 that occurred between 1970 and 2011 have been considered (Fig. 3). Focal mechanisms were obtained from the U.S. Geological Survey and the Global Centroid Moment Tensor Project. The depth - frequency distribution of seismicity is presented along two profiles, A - A' (Fig. 4a) and B - B' (Fig. 4b) (See Fig. 3 for the location of the profiles). The epicenters of earthquakes situated between 89°E to 92°E and 35°N to 39°N are projected on profile A-A'; Those of the earthquakes situated between 90°E to 98°E and 35°N to 37°N are projected on profile B-B' .

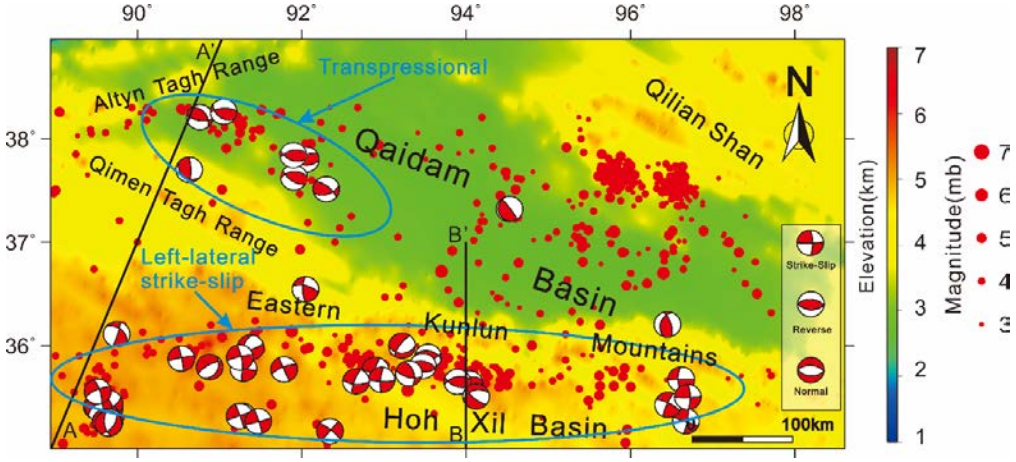


Fig.3. General topographic map of the Qaidam Basin and Eastern Kunlun Mountains with background seismicity from the China Earthquake Networks Center (CENC) from 1st January 1970 to 1st January 2011 (M>3).

Earthquakes magnitude ranges from M = 3 (the selected cut-off value) to M = 7. Strong tectonic activities (mean M between 5 and 6) are recorded along the Eastern Kunlun Mountains, on the southern edge of the Qaidam Basin. However, diffuse seismicity (mean M between 4 and 5) also occurs inside the basin (Fig. 3 and 4). Surprisingly, the Qimen Tagh

Range displays a relative lack of seismicity. Within the Eastern Kunlun Mountains, the distribution and focal mechanisms of the earthquakes are coherent with left-lateral, transpressive strike-slip movement on the Kunlun Fault. The existing few transtensive focal mechanisms can be explained by the occurrence of extensional relay-zones along the main Kunlun Fault (Jolivet et al., 2003). The focal mechanisms available inside the Qimen Tagh Range and the SW Qaidam Basin all correspond to reverse faults activity indicative of a general compressive stress field with no or extremely limited strike-slip motion.

The depth-frequency distribution of the earthquakes indicates that both in the Eastern Kunlun Mountains and in the Qaidam Basin, seismicity affects the upper 30 to 35 km of the crust (that is thought to be at least 50 km thick in that region (e.g. Jolivet et al., 2003; Zhang et al., 2011)) with most events occurring in the upper 10 to 15 km. This distribution pattern is similar to the depth-frequency distribution of seismicity over the entire Tibetan Plateau (Taylor and Yin, 2009), with exceptions where earthquakes might have occurred within the lower crust or upper lithospheric mantle (Chu et al., 2009). The observed seismicity is thus mostly indicative of the deformation of the upper to middle crust and can be reasonably compared to the fault pattern observed on the surface.

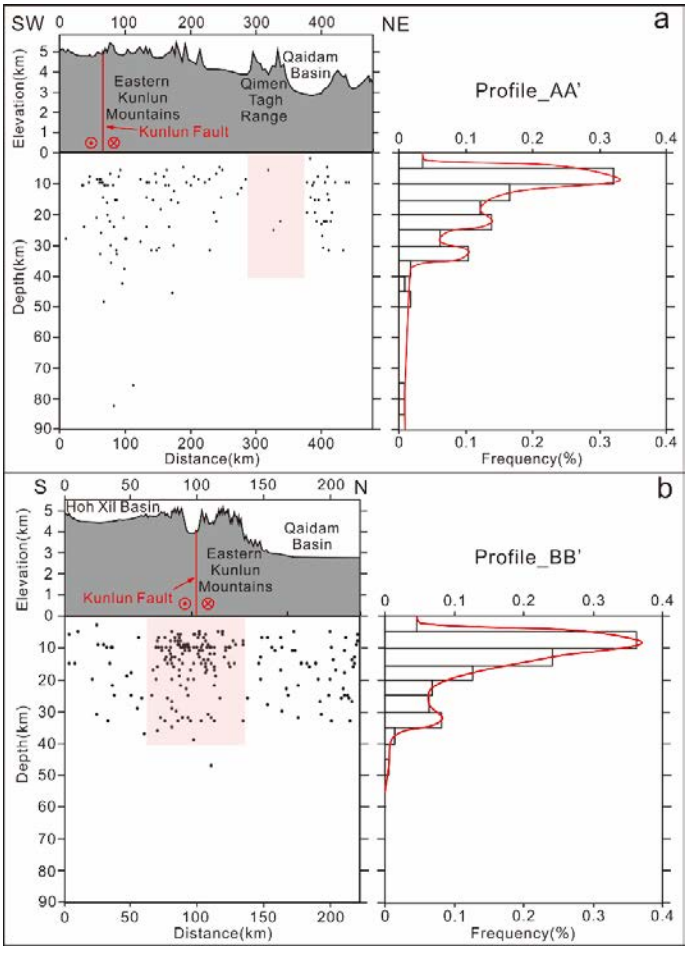

Fig.4. Depth-frequency distribution of earthquakes within the study area. Data from the China Earthquakes Networks Center (CENC), 1st January 1970 to 1st January 2011 with M>3. Two seismic profiles (AA' (a) and BB'. (b) (see location on Fig. 3)) are investigated with (left) depth distribution of earthquakes and (right) depth – frequency distribution of seismic events. See text for discussion.

### 2.1.4 Splay Fault System of the Kunlun Fault Zone

Different from the typical horse-tail structure, the western segment of the Kunlun Fault develops several asymmetric northward curved structures topographically characterized by a series of ridges and valleys (Fig. 1). These elongated linear geomorphic landforms are similar to those of the central segment of the Kunlun Fault, such as the Xidatan and Dongdatan valleys (Xu et al., 2002), and indicate the occurrence of left-lateral strike-slip faulting. Meanwhile, the valleys are largely filled with Cenozoic deposits that recorded the history of the strike-slip faulting and especially its onset time. In this study, taking the Qimen Tagh Range as an example, we aim at clarifying the tectonic pattern of the western segment of the Kunlun Fault through time.

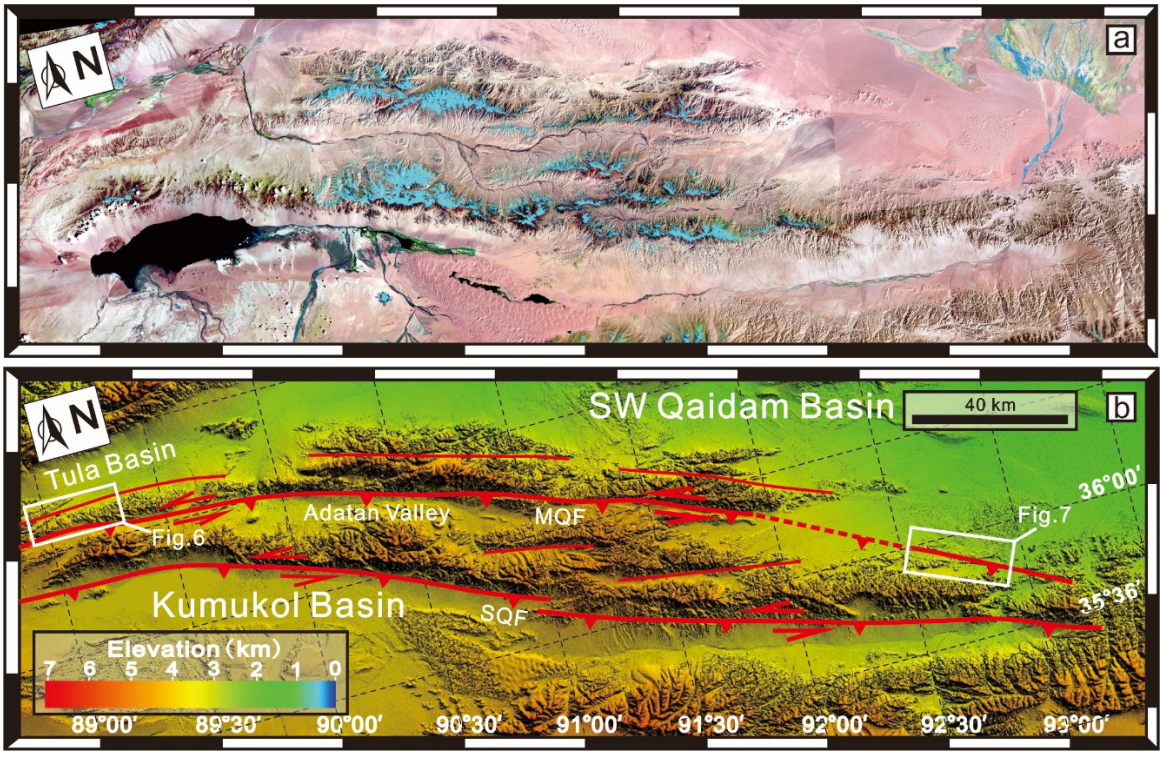


Fig.5. Remote sensing image from Landsat 5 on December 5, 2008 (USGS) (a) and SRTM digital topography map (b) of the Qimen Tagh Range. The red solid lines show the main tectonic structures. See the location in Fig. 1.

#### 2.1.4.1 Strike-slip faulting in the Qimen Tagh Range

The Qimen Tagh Range, located in the western part of the Eastern Kunlun Mountains, is

over ~4500 m high on average and marks the boundary between the Kumukol Basin to the south and the Qaidam Basin to the north (Fig. 1). The range has a general WNW-ESE elongated shape. To the NW, it bends sharply to a southwestward trend sub-parallel to the Altyn Tagh Range that lies directly to the north. To the SE, the Qimen Tagh Range converges with the Eastern Kunlun Mountains (Fig. 1 and 5). It is separated into two parallel NW-SE oriented sub-ranges by the Adatan Valley (Fig. 2).

To the north, the sharp contact between the Qaidam Basin and the Qimen Tagh Range has been interpreted as evidence for active north-directed thrusting (e.g., Meyer et al., 1998; Jolivet et al., 2003), whereas field examination suggests that this is a steeply north-dipping unconformity between bedrock in the south and north-dipping Cenozoic strata in the north (Yin et al., 2007). Detailed analysis of both SRTM digital elevation models (DEM) and Landsat 5 satellite images across the Qimen Tagh Range reveals abundant tectonic lineaments (Fig. 5). The extensive Qimen Tagh fault system consists of two major, sub-parallel tectonic lineaments: the Middle Qimen Tagh Fault (MQF) and the South Qimen Tagh Fault (SQF) (Fig. 5).

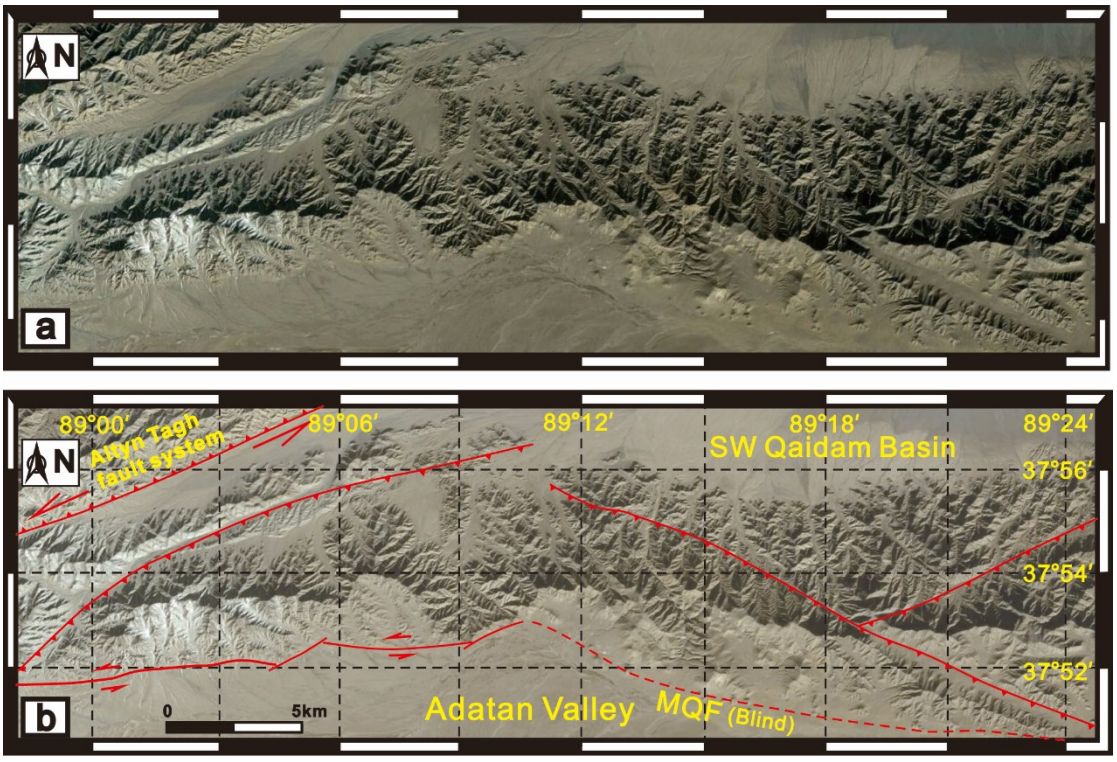


Fig.6. Un-interpreted (a) and interpreted SPOT-5 image (b) (Google Earth) centered on the western part of the Middle Qimen Tagh fault (MQF). See the location in Fig. 5. The red solid lines indicate the fault segments imaged by fault scarps on the surface. The dashed line represents the blind fault covered by the Quaternary sediments. The fault scarps in en-échelon arrangement indicates a left-lateral strike-slip movement on the MQF.

The MQF affects the northern edge of the Adatan Valley. Based on field measurements and on previous studies (Wang et al., 2007), the MQF dips about 55° to the south. The strike of the MQF changes from ENE in the western part of the range to WNW in the eastern part. The western segment shows a reverse motion associated to a slight left-lateral strike-slip component. Some of the scarps and branched faults are arranged in echelons (Fig. 6). In the eastern part of the MQF the main active fault is obliterated by Quaternary deposits. However, some linear structures are visible on the eastern end of the MQF and in the convergence zone with the Kunlun Fault system (Figs. 5 and 7). This however poorly exposed tectonic pattern suggests a very probable connection between the Qimen Tagh Fault system in the west and the Kunlun Fault system in the east.

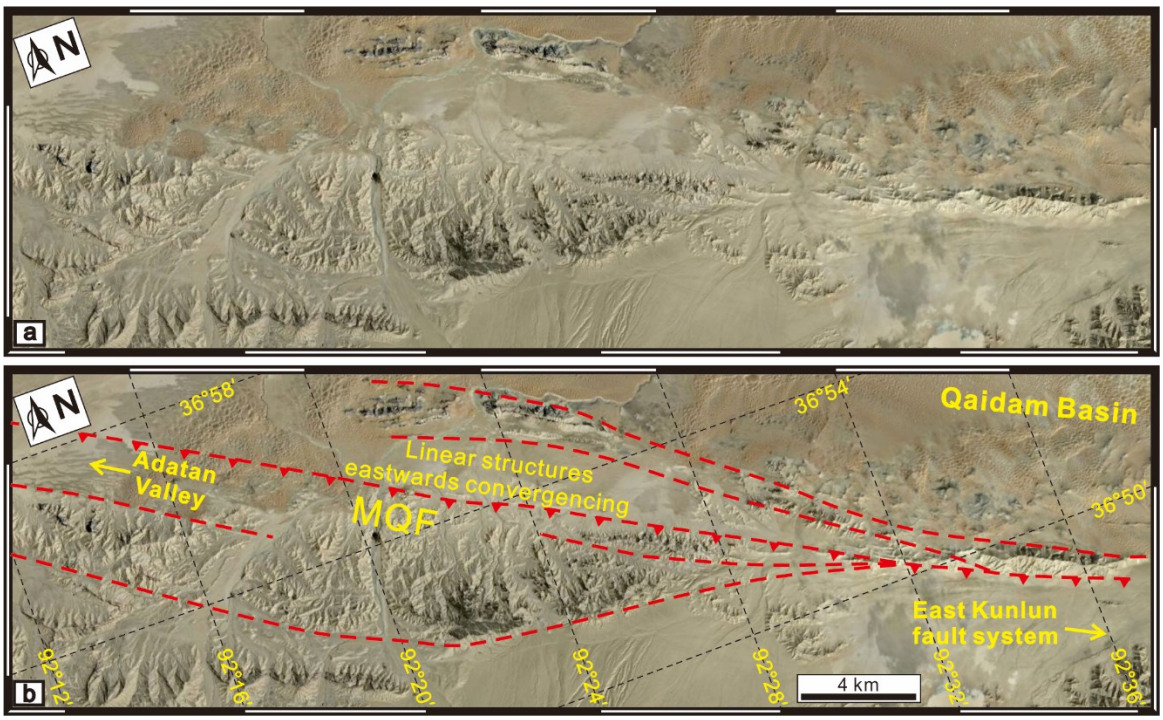


Fig.7. Un-interpreted (a) and interpreted SPOT-5 image (b) (Google Earth) centered on the eastern part of the Middle Qimen Tagh fault. See the location in Fig. 5. The red dashline indicates the linear fault linking the Qimen Tagh fault system in the west with the Eastern Kunlun fault system in the east.

The SQF separates the southern sub-range of the Qimen Tagh Range from the Kumukol Basin to the south (Fig. 5). The fault zone is marked by a series of distinctive fault scarps and structural lineaments which are inferred to be reverse faults striking approximately NE120° (Fig. 5). Furthermore, several evidences of recent activity such as river offsets and alluvial fan displacements indicate a left-lateral reverse movement on the fault.

Although the offset channels and geomorphic surfaces indicate a recent, probably still active general left-lateral shearing within the range, the focal mechanism solution mentioned

above suggest that this recent left-lateral strike-slip faulting is relatively slight compared to the NE-SW compressive component.

### 2.1.4.2 Pleistocene series within the Adatan valley

Fieldwork in the Adatan Valley was conducted to determine the timing of the strike-slip faulting in the south Qimen Tagh sub-range. Detailed analysis of the Cenozoic syntectonic deposits was conducted to provide a better understanding of the deformation in the Qimen Tagh Range (Fig. 8).

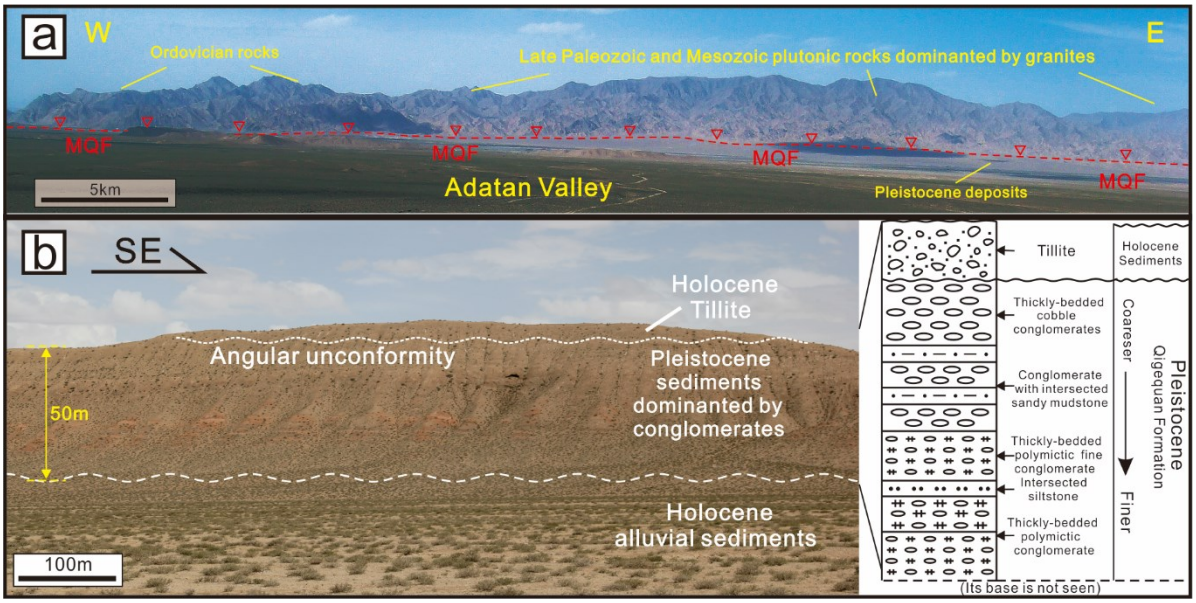


Fig.8. Cenozoic formations within the Adatan Valley. (a) General view of the Qimen Tagh Range. The picture, taken from ~10 km south of the Atantihan River checkpoint, shows the strong relief between the Adatan Valley and the mountains bordered by a series of triangular facets and fault scarps belonging to the MQF. The foothill domain is represented by Cenozoic strata which are deformed and pushed into gentle folds. See the location in Fig. 9. (b) Uplifted Pleistocene series covered by Holocene tillites (left) and general stratigraphic column (right). See the photographs' location in Fig. 9.

The morphology of the Adatan Valley is marked by a strong topographic relief between the valley and the mountains (Fig. 8a). Within the two sub-ranges, the series are mainly composed of Precambrian basement, Paleozoic metasediments and Paleozoic and Mesozoic igneous rocks. The Cenozoic series exposed within the Adatan Valley was assigned a Pleistocene age based on previous geology mapping and regional stratigraphic correlation (IGSSP, 2003; IGSQP, 2004; Wang et al., 2004b; Wang et al., 2007; Fu et al., 2008).

The deposits are deformed into several anticlines cut by modern rivers within the valley (Figs. 8a and 9). Along the northern edge of the valley, the Cenozoic series overlap northward on the Ordovician basement and are dominated by a sequence of conglomerates and sandstones. Along the southern edge of the valley, the Cenozoic series are deformed and

uncomformably covered by Holocene tillites and alluvial sediments. As in the north, these deposits are composed of coarse-grained conglomerates and sandstones in alluvial fans facies. The petrological composition of the conglomerates corresponds to the whole range of basement rocks exposed in the Qimen Tagh Range, including igneous, metamorphic rocks and marine limestones. Poor sphericity and poor sorting of the grains indicate very proximal deposits. The grain size generally increases upward (Fig. 8b). Similarly to the Quaternary sedimentary within the Xidatan Valley further east (Xu et al., 2002) that record the present active feature of the Kunlun Fault, the Pleistocene sequences exposed in the Adatan Valley record the topographic growth of both the north and south Qimen Tagh sub-ranges. They indicate a Pleistocene age for the onset of strike-slip faulting in the Qimen Tagh Range.

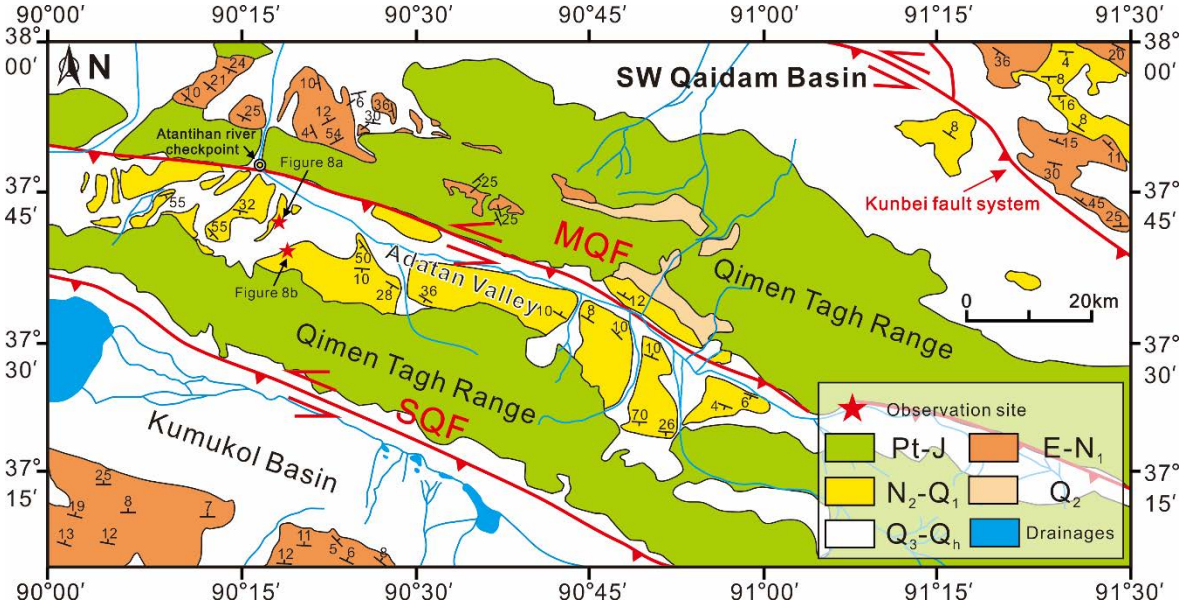


Fig.9. Geological sketch of the Qimen Tagh Range showing the distribution of the Cenozoic series. Modified after the Kulangmiqiti J46C003001 1:250,000 geological map (IGSQP, 2004) and the Ayakekumu J45C003004 1:250,000 geological map (IGSSP, 2003). See the location in Fig. 2.

As a consequence, the linear geomorphic features, occurrence of faults scarps in the Qimen Tagh Range as well as the deformed Pleistocene deposits in the Adatan Valley indicate that the reverse strike-slip deformation in the region has been active since the Pleistocene.

### 2.1.5 Strike-slip faulting in the SW Qaidam Basin

In order to decipher the Cenozoic strike-slip faulting pattern in the SW Qaidam Basin, we choose the isopach map of the upper Xiaganchaigou Fm. ($E_3^2xg$) as an example to analyze the impact of fault motion on the sediment distribution within the basin (Fig. 10). Data were obtained from the Qinghai Oilfield Company (China) who recently compiled information from thousands of drill holes and a dense network of seismic profiles.

The Kunbei fault system was composed of three major WNW trending faults, including the Kunbei Fault, the Arlar Fault and the Hongliuquan Fault. As reported on the isopach map based on seismic data, these three faults controls the general tectonic pattern of the SW Qaidam Basin. The Kunbei Fault and Arlar Fault have been previously interpreted as reverse faults active since the Paleogene (Wang et al., 2010). However, the three major faults mentioned above are arranged into a left-lateral right-step en-échelon pattern (Fig. 10), that does not correspond to the usual imbricated pattern of purely compressive thrust systems such as, for example, in the Appalachian thrust belt (Macedo and Marshak, 1999; Thomas, 2001) or in the Zagros fold and thrust belt (McQuarrie, 2004; Sepehr and Cosgrove, 2004). Meanwhile, the isopach lines of the Late Eocene Upper Xiaganchaigou Fm. are obviously offset across the faults reflecting a left-lateral strike-slip movement along these three faults. According to the well-expressed offset of the 400 meters isopach line, the left-lateral displacement of the Honglingquan Fault, the Arlar Fault and the Kunbei Fault increases from a few kilometers to tens of kilometers (Fig. 10). Therefore, the variations in thickness of the Late Eocene series across these three faults, as well as the en-échelon pattern of the faults, clearly demonstrates the occurrence of left-lateral strike-slip faulting in the SW Qaidam Basin after the Late Eocene.

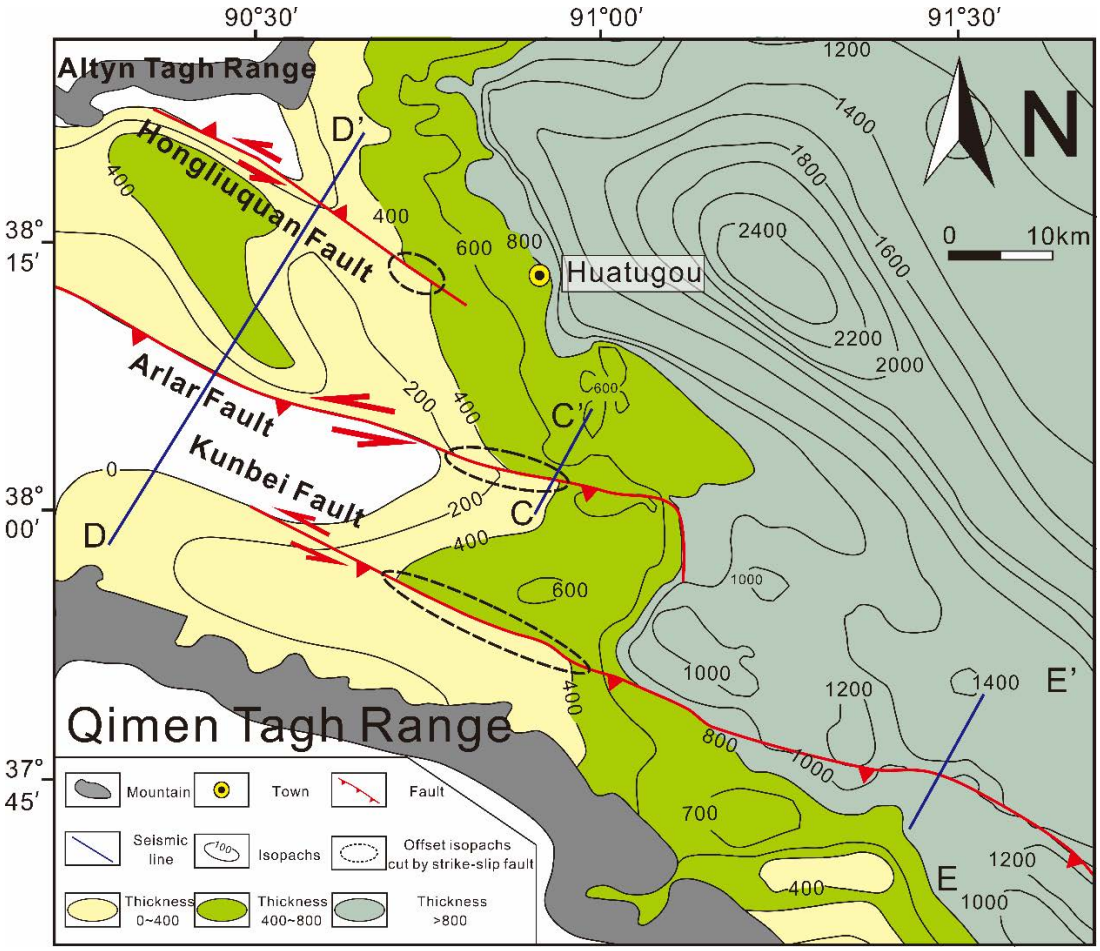

Fig.10. Isopach map of the Upper Xiaganchaigou Formation ($E_3^2$xg). Three major faults (the Kunbei fault, the Arlar fault and the Hongliuquan fault) are also marked on the isopach mapbased on seismic data. These data were acquired by the Qinghai Oilfield Company (China) who compiled information from thousands of drill holes and a dense network of seismic profiles in recent years. Note the offset of the 400 isopach line controlled by the faults and indicating the left-lateral strike-slip faulting of these faults.

To further explore the tectonic pattern of the SW Qadaim Basin and the timing of faulting, three seismic reflection profiles (C-C', D-D', E-E') recently acquired by the Qinghai Oilfield Company have been selected. These three NE-trending seismic lines extend from the northern front of the Qimen Tagh Range towards the center of the SW Qaidam Basin (See location on Figs. 2 and 10).

### 2.1.5.1 Seismic Section C-C'

The seismic section C-C' situated in the central part of the SW Qaidam Basin, intersects the Arlar Fault (Fig. 10 and 11). On that section the Arlar Fault is a south dipping high angle fault associated to a few branched faults. The Mesozoic series are not preserved on both sides of the Arlar Fault where only Cenozoic deposits can be identified. Although the strata on each side of the fault consist in the same Cenozoic series, the thickness of each formation is quite different showing obvious stratigraphic throw. This major stratigraphic throw corresponds to the offset

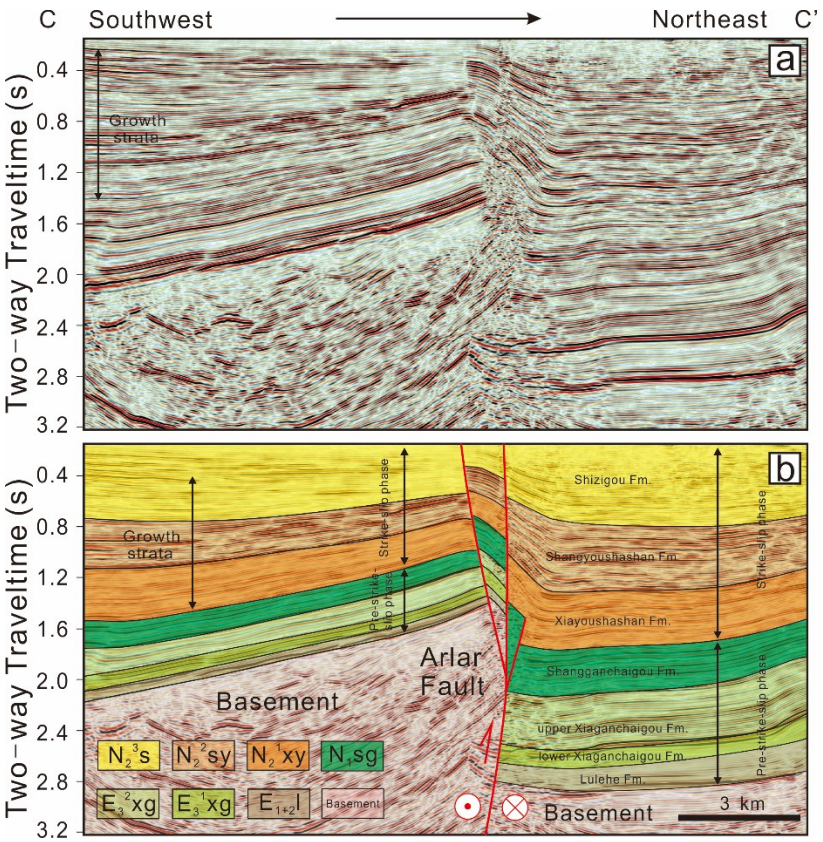


Fig.11. Seismic profile C-C'in the SW Qaidam Basin. See the location in Figs. 2 and 10. Note that the thickness of the Paleocene to Eocene strata shows a sharp difference between both sides of the Arlar fault. The growth strata associated to the positiveflower structure started to develop during the initial deposition of the Early Miocene unit ($N_2^1$xy), which suggests that the strike-slip movement on the Arlar fault initiated during the deposition of this unit.

observed in the isopach lines of the Late Eocene Upper Xiaganchaigou Fm. on both side of the Arlar Fault (Fig. 10). Combined together, these two sets of data demonstrate a left-lateral reverse motion along the Arlar Fault during the Tertiary.

The thickness of the strata younger than Neogene Xiayoushashan Fm. ($N_2^1$xy) decreases towards the Arlar Fault and growth strata develop on both sides of the fault. Based on these features, previous studies interpreted the Arlar Fault as a purely reverse fault that accommodated rapid uplift in the Eastern Kunlun Mountains since the Late Oligocene - Early Miocene (Song and Wang, 1993; Yin et al., 2007; Wang et al., 2010). Since it is very difficult to identify strike-slip faults on seismic profiles (Durand-Riard et al., 2012), these studies did not take into consideration the strike-slip component along the major faults within the SW Qaidam Basin. Growth strata are generally used to reveal the initiation time of a reverse fault (e.g. Suppe et al., 1992; Vergés et al., 2002), but strike-slip motion may also induce vertical offset of strata, such as in positive flower structure (e.g. Christophoul et al., 2002). Such motion can also generate growth strata which will then provide an accurate initiation time for the strike-slip faulting (e.g. Hinsch et al., 2005). Consequently, the growth strata associated to the positive flower structure in seismic profile C-C' presented above, as well as the northward thinning of the Early Miocene and younger series in the footwall of the Arlar Fault date the onset time of left-lateral strike-slip faulting along that fault (Fig. 10 and 11).

#### 2.1.5.2 Seismic Section D-D'

The tectonic pattern of section D-D' is characterized by several high angle faults defining a block-like structure (Fig. 12). The major faults are the Arlar Fault and the Hongliuquan Fault. The sediments within the section are Mesozoic to Cenozoic in age. The cover sequence in the hanging wall of the Arlar Fault is composed of Cenozoic sediments whereas the footwall is dominated by Late Mesozoic, Paleogene and Early Neogene deposits. The Mesozoic sediments are relatively thick within the footwall where the Tertiary series are also obviously thicker than that of the hanging wall. The basement and Cenozoic strata on both sides of the Arlar Fault display obvious stratigraphic throw. Further to the north, the Early to Middle Cenozoic and Late Mesozoic strata are cut by the north dipping high angle Hongliuquan Fault. In the hangingwall of the Hongliuquan Fault, the pre-Early Miocene strata were deformed in an anticline later cut and sealed by the Early Miocene sediments clearly indicating Early Miocene motion of this fault. Like in profile C-C', the thickness of the Cenozoic units is constant within each tectonic compartment but varies sharply between two adjacent blocks. Combined with the offset isopach lines of the Late Eocene deposits (Fig. 10), this pattern can

also be explained by lateral movements along the faults during the Tertiary. Again like in seismic profile C-C', the occurrence of growth strata initiating in the Early Miocene series north of the Arlar and Hongliuquan faults implies that left-lateral strike-slip deformation initiated during the Early Miocene in the SW Qaidam Basin.

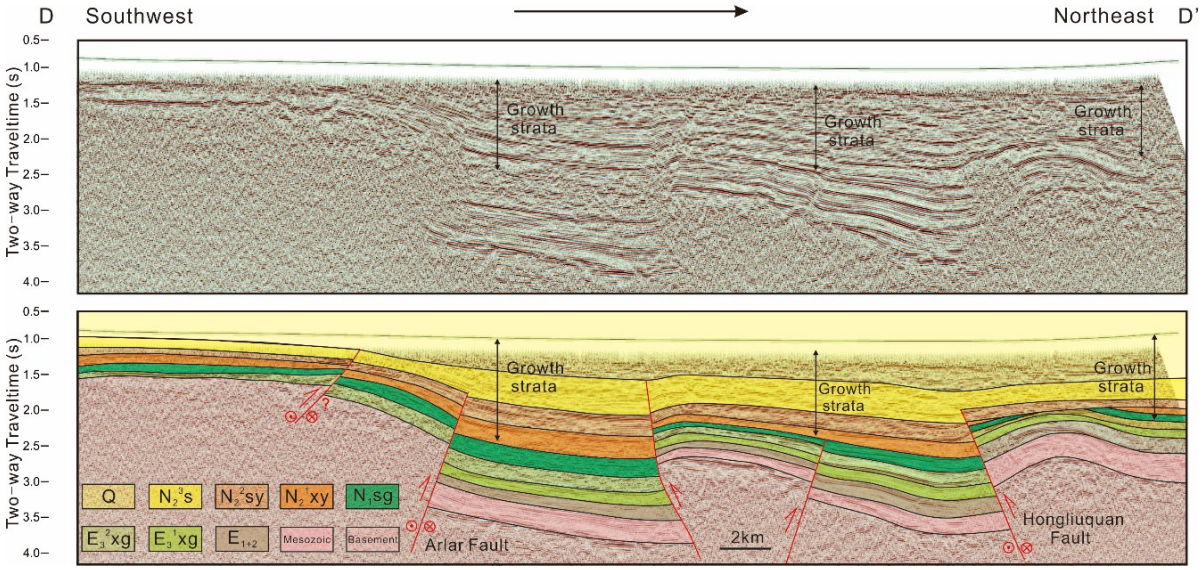


Fig.12. Seismic section D-D'in the SW Qaidam Basin. See Figs. 2 and 10 for location. Note that the strata below the Shangyoushashan Fm. ($N_2^1$xy) keep a constant thickness in the section, while the strata above it are thinning northward. The thickness of the Paleocene to Eocene strata shows a sharp difference between both sides of the Arlar fault. Meanwhile, Early Miocene growth strata above the Arlar and Hongliuquan faults indicate the onset of left-lateral strike-slip faulting during the Early Miocene.

### 2.1.5.3 Seismic Section E-E'

Seismic section E-E' is located about 20 km east of seismic section C-C' and again runs from the northern front of the Qimen Tagh Range to the western part of the central Qaidam Basin (Figs. 10 and 13). As in section D-D', the tectonic pattern is characterized by several high angle faults but the cover-sequence only consists in Cenozoic strata. To the south, the activity along the Kunbei Fault is marked in the hanging wall by the erosion of the Late Eocene and younger strata and probably by the non-deposition of some of the upper Tertiary and Quaternary series. This erosion also affects the footwall of the Kunbei Fault, though the Early Tertiary series are better preserved with some Late Eocene sediments still present. Like in section C-C' and D-D', the thickness of the Early Tertiary series vary across the fault showing obvious stratigraphic throw. To the north, the XIII fault dips to the north and cuts the Early to Middle Cenozoic sequence, while the large stratigraphic throw on both sides of the fault decreases from basement to Quaternary series. Like in the previous sections, the thickness of the Paleocene to Eocene strata varies sharply from both sides of the Kunbei and XIII faults,

again attesting of lateral movements on those structures during the Tertiary. Furthermore, the thickness of the strata younger than the Xiayoushashan Fm. ($N_2^1xy$) within the footwall of the Kunbei and XIII faults decreases towards the faults. Growth strata are again initiating in the footwall of both faults during Early Miocene times dating again the onset of deformation in that region.

From what has been discussed above, we conclude that the tectonic attribute of the Kunbei Fault during the Early Miocene is featured by a left-lateral transpressive system mainly composed of the Kunbei Fault, the Arlar Fault and the Hongliuquan Fault. Among these faults, the Kunbei and Arlar faults are the two major boundary faults separating the Cenozoic series within the SW Qaidam Basin from the Kunlun basement to the south.

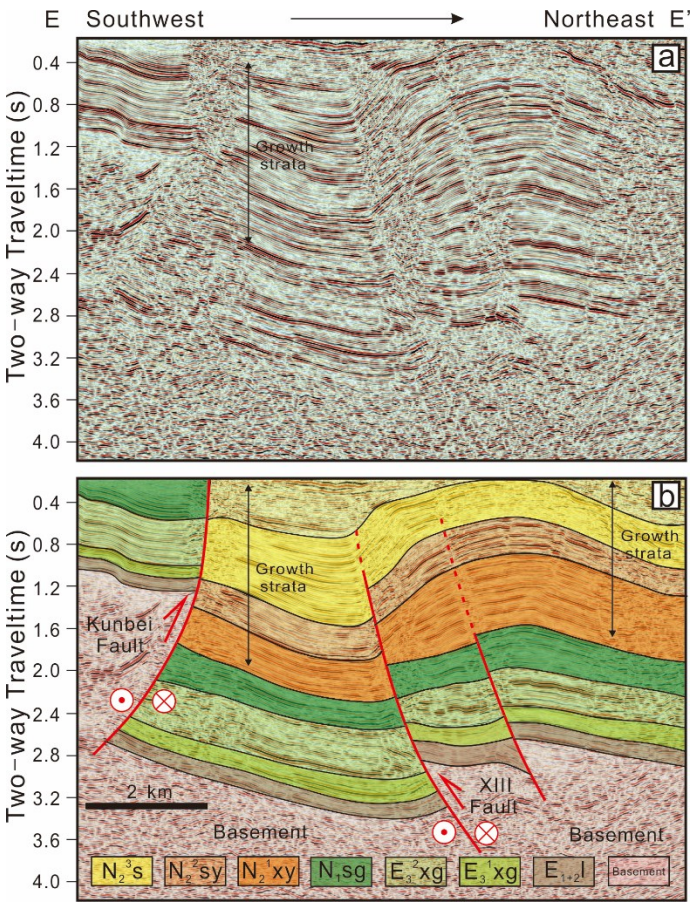


Fig.13. Seismic profile E-E' in the SW Qaidam Basin. See the location in Figs. 2 and 10. Note that the thickness of the Paleocene to Eocene strata shows a sharp difference between both sides of the Kunbei fault. Meanwhile, Early Miocene growth strata again indicate an onset of left-lateral strike-slip faulting during the Early Miocene.

## 2.1.6 Discussion

### 2.1.6.1 Available models for the Cenozoic evolution of the SW Qaidam Basin

In the past decades, several models have been proposed to explain the Cenozoic tectonic and sedimentary evolution of the Qaidam Basin. Most of those concentrated on the tectonic pattern displayed in the Qimen Tagh Range and SW Qaidam Basin, and simply defined the tectonic pattern between the Eastern Kunlun Mountains and the Qaidam Basin through a northward thrusting or southward thrusting model.

The northward thrusting model prevailed in the last two decades, explaining the subsidence of the Qaidam Basin as a result of the basinward propagation of successive thrust sheets along the southern edge of the basin. Burchfiel et al. (1989) proposed that the southern

edge of the Qaidam Basin is limited by a south-dipping thrust fault. However, field observation revealed that the contact between the Eastern Kunlun Mountains and the Qaidam Basin is defined by gentle north-dipping Pliocene strata overlapping north-dipping Carboniferous beds (Yin et al., 2007). Based on a synthesis of focal mechanisms and focal-depth distribution combined with geological features, Chen et al. (1999) again speculated the existence of this south-dipping North Kunlun thrust fault along the northern margin of the East Kunlun belt. However, their data projected on the single cross section were collected along the over 1000 km long Eastern Kunlun Mountains and Yin et al. (2007) showed that it was not possible to differentiate between the two possible fault planes solutions (N dipping or S dipping). In addition, many authors indicated that northward basement thrusting across the Eastern Kunlun Mountains was associated to the northward propagation of a crustal-scale accretionary wedge initiating around ca. 30-20 Ma. (Meyer et al., 1998; Mock et al., 1999; Jolivet et al., 2001; Tapponnier et al., 2001; Jolivet et al., 2003; Wang et al., 2006). These ideas suggest that the Eastern Kunlun Mountains consists in a large transpressional system limited to the south by the left-lateral strike-slip Kunlun Fault and to the north by a series of south-verging basement thrusts affecting the southern edge of the Qaidam Basin. Yet, the observed thickness pattern of the Cenozoic strata across the Qaidam Basin (Yin et al., 2008) seems poorly compatible with a major south-dipping range-bounding thrust along the northern margin of the Eastern Kunlun Mountains. All the individual Cenozoic units in the basin consistently thicken from the margins towards the center of the basin (Bally, 1986; Huang et al., 1996; Sobel et al., 2003; Wang et al., 2006; Yin et al., 2007, 2008). This isopach pattern contradicts the classic tectonically subsiding foreland-basin model that requires the maximum sediment thickness to be localized near the bounding thrust system (Jordan, 1981).

The southward thrusting model has drawn much attention in recent years (Yin et al., 2007; Shi et al., 2009; Wang et al., 2011). Yin and Harrison (2000) suggested that two major thrusts, the Qimen Tagh Thrust and the North Kunlun Thrust mark the southern boundary of the Qaidam Basin. Using seismic profiles within the Qaidam Basin and field observations, Yin et al. (2007) then proposed that the low altitude Qaidam Basin has been thrust onto the Eastern Kunlun Mountains along major north dipping Cenozoic thrusts. This model was later expanded by Wang et al., (2011) based on a high-resolution deep seismic reflection profile across this area. This model indicates that the Eastern Kunlun Mountains should not thrust northward onto the Qaidam Basin and that the initiation of compressive deformation along the southern margin of the Qaidam Basin is much younger than along the northern margin of basin. However, this model does not take any strike-slip component in the Qimen Tagh Range and

SW Qaidam Basin into account. In addition, the convex-northward bow-like tectonic structures in the Qimen Tagh Range are not consistent with southward thrusting of the basin onto the range. Such a deformation pattern would rather generate a southward inflexion of the structures.

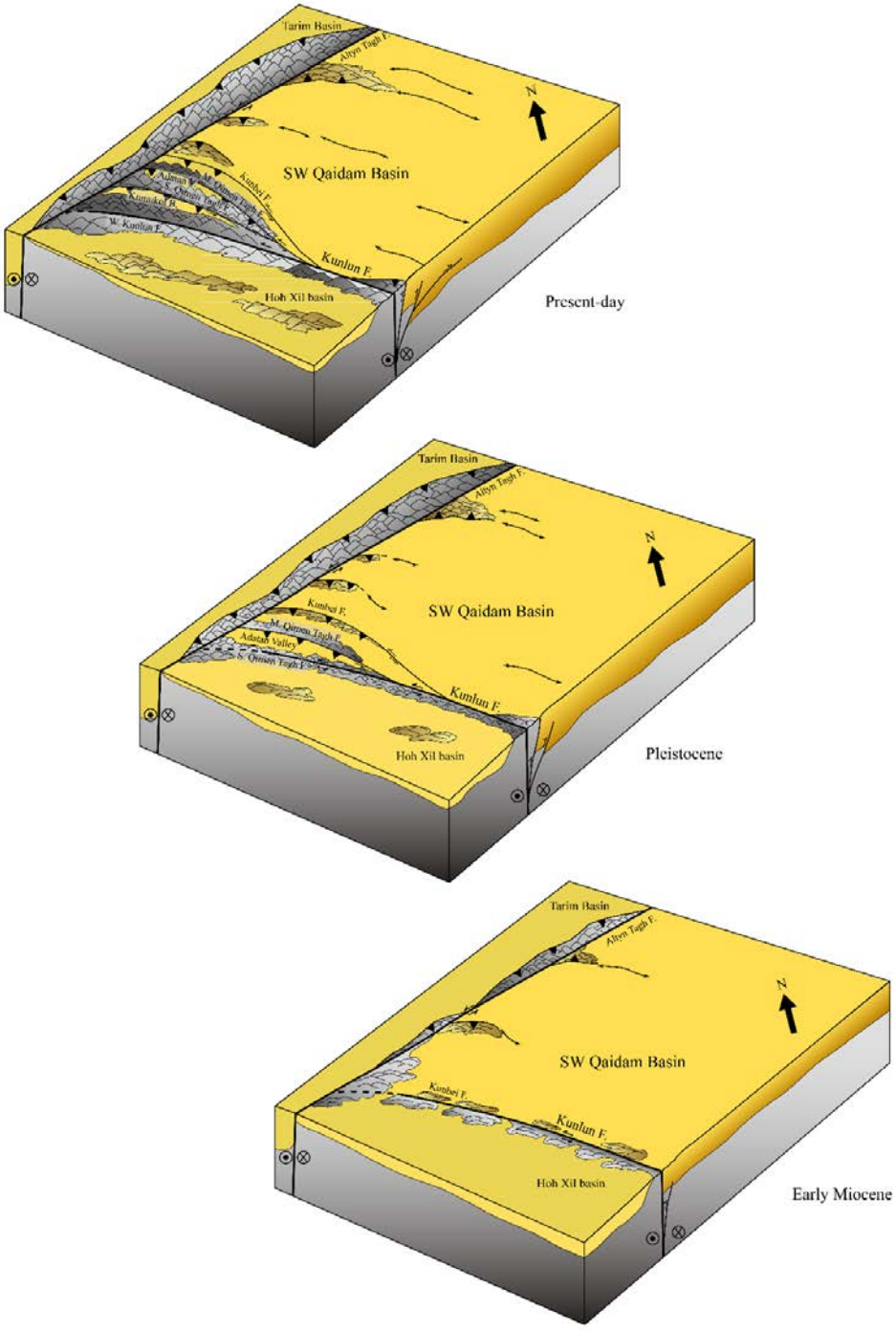


Fig.14. Tectonic evolution of the Qimen Tagh Range and the SW Qaidam Basin since the Early Neogene. See the text for discussion

Other tectonic models have been proposed aside from the two main ones described above. Xia et al. (2001) proposed that the Qaidam Basin experienced a two stages evolution: an initial extension phase during the Early Tertiary was followed by a compressive phase leading to basin inversion. However, few seismic profiles in the western Qaidam Basin have revealed any extensional faults during the Early Tertiary. Meng and Fang (2008) suggested that the Cenozoic tectonic subsidence of the Qaidam Basin resulted from crustal folding or buckling in response to regional horizontal compression. However, the seismic profiles across the whole Qaidam Basin imply that the magnitude of Cenozoic upper crustal shortening decreases eastward across the basin from >48% in the west to <1% in the east (Yin et al., 2008), whereas the present day basin is wider to the west and relatively narrow to the east. This phenomenon is difficult to explain only by crustal folding or buckling.

To summarize, despite the large number of models that have been proposed, few studies took the left-lateral strike-slip factor into account when considering the relationship between the Qaidam Basin and the Eastern Kunlun Mountains.

#### 2.1.6.2 Strike-slip tectonics and northward growth of western segment of Kunlun Fault

The Qaidam Basin is bordered to the northwest by the Altyn Tagh Fault which has been active since the Early or Middle Eocene (Jolivet et al., 1999, 2001; Yin et al., 2002). In addition, despite that Chen et al. (2002) concluded that the Qaidam Basin experienced an over 20° clockwise rotation during the Neogene resulting in differential shortening in the Nan Shan fold and thrust belt (Fig. 1), Dupont-Nivet et al. (2003, 2004) suggested that the Nan Shan fold and thrust belt and the Qaidam Basin did not experience any vertical axis rotation during the Neogene. As the limit between the thick, rigid Tarim block and the more deformable Qaidam Basin, the Altyn Tagh Fault is considered stable in time. Consequently, the deformation in the SW Qaidam Basin and the western segment of the Kunlun Fault should be bordered and limited to the NW by the Altyn Tagh Fault. When considering the geometric relation between the Altyn Tagh Fault and Kunlun Fault, the western Kunlun fault segment has to rotate northward: the left-lateral movement on the Altyn Tagh is progressively driving the connection point between that fault and the Kunlun fault towards the east. For the Kunlun Fault to be able to continuously act as a strike-slip fault, it would jump backwards towards its initial position creating a new strike-slip segment. As mentioned above, the distribution and focal mechanisms of earthquakes indicate that the active tectonic pattern along the Kunlun Fault is characterized by left-lateral strike-slip motion. However, in the SW Qaidam Basin and the Qimen Tagh Range the deformation is accommodated by NW-SE directed thrust faults

associated to a limited left-lateral strike-slip component (Fig. 3). In addition, the geomorphological WNW trending linear structures in the Qimen Tagh Range (Fig. 5) and deformed Pleistocene sequences in the Adatan Valley (Figs. 8 and 9) record the left-lateral strike-slip movements within the Qimen Tagh Range since the Pleistocene. Finally, the overall tectonic and structural architecture within the SW Qaidam Basin is dominated by a series of high angle faults. The sudden variation in sediment thickness marked by the offset of the isopachs on both side of the faults (Fig. 10) associated to the growth strata and the positive flower structures generated by movements on those faults (Figs. 11, 12 and 13), indicate Early Miocene left-lateral strike-slip faulting in SW Qaidam Basin. Synthesizes the above analysis, we thus propose that the Late Neogene northward growth of the convex-northward structures in the Qimen Tagh Range and SW Qaidam Basin (northern margin of the Tibetan Plateau) is driven by progressive northward migration of the left-lateral strike-slip Kunlun Fault (Fig. 14).

Around the Early Miocene, the left-lateral strike-slip faulting in the Kunlun Fault Zone initiated. This motion lead to E-W extension along the northern margin of the Tibetan Plateau and the deeply rooted strike-slip faults were acting as pathways for the shoshonitic magmas (Jolivet et al., 2003), leucogranites and rhyolites (Zhang et al., 2012) to reach the surface. During that period, the parallel Kunbei, Arlar and Hongliuquan faults (designated below as the Kunbei fault system) were forming the western segment of the Kunlun Fault, located in the same position as the present-day Kunlun Fault with a nearly E-W striking trend. The left-lateral movement between the Qiangtang-Bayan Har and Qaidam blocks caused the en-échelon arrangement of the faults and generated the growth strata recording the onset time (Early Miocene) of fault activation. Following this initial phase, the Kunbei fault system, progressively rotated clockwise and migrated northwards, forming the successive high-angle left-lateral compressional faults now observed in the SW Qaidam Basin. In order to maintain the strike-slip motion along the western segment of the Kunlun Fault, a new strike-slip fault system, the Qimen Tagh fault system (including the MQF and SQF) developed during the Pleistocene in place of the older western Kunlun Fault segment that migrated northward. This second phase is recorded by the deformed coarse-grain Pleistocene deposits in the Adatan Valley. This newly formed Qimen Tagh strike-slip fault segment again migrated northwards and progressively rotated clockwise forming the present-day Qimen Tagh prism. Another new strike-slip fault segment developed on the western end of the Kunlun Fault, replacing the previous one. During the process of northward migration of these left-lateral strike-slip faults (the Kunbei Fault, the Arlar Fault, the Hongliuquan Fault, the MQF and the SQF), their motion changed from left-lateral strike-slip to nearly NE-SW compressional motion. The

characteristic northward-convex bow-like shape of the Kubei fault system and of the Qimen Tagh prism is governed by the strike-slip motion along the Altyn Tagh Fault to the northwest. The northward migration of the western segment of the Kunlun Fault explains the lack of Early Miocene sediment records at the present day location of this western segment that would relate to the initiation of the Kunlun Fault.

The model proposed above is an evolution of the previously proposed transpressional model (Meyer et al., 1998; Jolivet et al., 2001; Tapponnier et al., 2001). It identifies the Kunbei fault system and Qimen Tagh fault systems as the western segment of the Kunlun Fault Zone and describes their progressive northward migration since Early Miocene. Their initiation as strike-slip faults explains the present-day steepness of the fault planes.

Based on the analysis of geological features in the Jingyu Basin (North Tibet) and the intrusion of Tertiary to Quaternary shoshonites along the western segment of the Eastern Kunlun Mountains, Meyer et al. (1998) and Jolivet et al. (2003) suggested that the strike-slip Kunlun Fault initated during the Early Neogene. Recently, after detailed geochemistry and geochronology studies on the Miocene leucogranites and rhyolites found in the Hoh Xil Lake area (north of the Kunlun Fault) (Fig. 1), Zhang et al. (2012) suggested that the dehydration melting in this area was probably triggered by localized E - W stretching decompression within the left-lateral strike-slip Kunlun Fault system around 15 Ma. Meanwhile, Duvall et al. (2013) and Yin (2010) also considered that the left-lateral East Kunlun transpressional system initiated around 30 to 20 Ma as a response to the collision between India and Asia. These ages of initial faulting in the Eastern Kunlun Mountains are roughly consistent with our results.

In addition, from the data described above, the boundary between the SW Qaidam Basin and the Eastern Kunlun Mountains is characterized, since the Early Miocene by a series of northward migrating and eastward rotating left-lateral strike-slip faults rather than by a continuous northward thrusting (e.g. Burchfiel et al., 1989; Meyer et al., 1998) or southward thrusting system (e.g. Yin et al., 2007; Wang et al., 2011). Consequently, the SW Qaidam Basin did not suffer a large amount of N-S compression and shortening before the Early Miocene. This observation is compatible with the Paleo-Qaidam model of Yin et al., (2008) which suggests the existence, during the Paleogene, of a large topographic depression encompassing the Hoh Xil Basin to the south and the Qaidam Basin to the north. This wide basin was partitioned by the uplift of the Eastern Kunlun Mountains during Late Oligocene - Early Miocene times.

### 2.1.7 Conclusions

The Eastern Kunlun Mountains and adjacent Qaidam Basin present one of the largest topographic gradients in the Tibetan Plateau. In that respect, determining the tectonic relations between the Qaidam Basin and the Eastern Kunlun Mountains and deciphering the complex tectonic architecture of the western segment of the Kunlun Fault has major implications in understanding the tectonic, sedimentary and geomorphic Cenozoic history of North Tibet.

The distribution and focal mechanisms of earthquakes presented in this study indicate that the active tectonic pattern in the SW Qaidam Basin and the Qimen Tagh Range is dominated by transpressional structures while that of the Eastern Kunlun Mountains is characterized by left-lateral strike-slip faulting. Geomorphological interpretation of remote sensing images shows that the Qimen Tagh Range is affected by obvious WNW trending linear structures which relate to left-lateral strike-slip motion. The deformed Pleistocene sediments within the Adatan Valley strongly suggest strike-slip faulting along those WNW trending faults during the Pleistocene. To the north, in the SW Qaidam Basin, the offset isopachs of the Late Eocene sediments and the en-échelon arrangement of Kunbei, Arlar and Hongliuquan faults again indicate left-lateral strike-slip faulting. This, associated to growth strata, implies an Early Miocene onset age for the left-lateral strike-slip deformation of the Kunbei fault system in the SW Qaidam Basin. This tectonic pattern and the southwards younging of the left-lateral strike-slip phases lead us to identify the Kunbei Fault system and the Qimen Tagh faults system as former western segments of the Kunlun Fault once located further south in the present-day location of that fault. These faults gradually migrated northward since the Early Miocene while their kinematics changed from left-lateral strike-slip motion to NE-SW compression.

We conclude that the SW Qaidam Basin has been bordered by a series of strike-slip faults to the south since the Early Miocene, rather than by a continuous northward thrusting or southward thrusting system. The SW Qaidam Basin did not suffer major N-S compression and shortening before the Early Miocene.

### Acknowlegements

This study was financially supported by grants from the National Science and Technology Major Project (2011E-03). Marc Jolivet was supported by the Darius Program, the French - Chinese Egide Cai Yuanpei Program and the French Centre National de la Recherche Scientifique (CNRS), Institut National des Sciences de l'Univers (INSU) Syster Program. We would like to thank Editor Mian Liu and anonymous reviewers who provided constructive and

thoughtful comments that helped improving the manuscript.

## Reference

Bally, A.W., Chou, I.-M., Clayton, R., Eugster, H.P., Kidwell, S., Meckel, L.D., Ryder, R.T., Watts, A.B., and Wilson, A.A., 1986. Notes on Sedimentary Basins in China-Report of the American Sedimentary Basins delegationto the People's Republic of China. U.S. Geological Survey Open-File Report, 108 pp. 86-327.

Burchfiel, B.C., Quidong, D., Molnar, P., Royden, L., Yipeng, W., Peizhen, Z., Weiqi, Z., 1989. Intracrustal detachment within zones of continental deformation. Geology 17, 748-752. doi: 10.1130/0091-7613(1989) 017<0448:IDWZOC>2.3.CO;2.

Chen, W., Chen, C., L Nábelek, J., 1999. Present-day deformation of the Qaidam basin with implications for intra-continental tectonics. Tectonophysics 305, 165-181, doi: 10.1016/S0040-1951(99)00006-2.

Christophoul, F., Baby, P., Dávila, C., 2002. Stratigraphic responses to a major tectonic event in a foreland basin: the Ecuadorian Oriente Basin from Eocene to Oligocene times. Tectonophysics 345, 281-298.

Chu, R., Zhu, L., Helmberger, D.V., 2009. Determination of earthquake focal depths and source time functions in central Asia using teleseismicPwaveforms. Geophysical Research Letters 36, doi: 10.1029/2009GL039494.

Clark, M.K., Farley, K.A., Zheng, D., Wang, Z., Duvall, A.R., 2010. Early Cenozoic faulting of the northern Tibetan Plateau margin from apatite (U–Th)/He ages. Earth and Planetary Science Letters 296, 78-88, doi:10.1016/j.epsl.2010.04.051.

Deng, T., Wang, X. M., 2004a. New material of the Neogene rhinocerotids from the Qaidam Basin in Qinghai, China, Vertebr. PalAsiat 42(3), 216-229.

Deng, T., Wang, X. M., 2004b. Late Miocene Hipparion (Equidae, Mammalia) of eastern Qaidam Basin in Qinghai, China, Vertebr. PalAsiat 42 (4), 316-333.

Dupont-Nivet, G., Butler, R.F., Yin, A., Chen, X., 2003. Paleomagnetism indicates no Neogene vertical axis rotations of the northeastern Tibetan Plateau. J. geophys. Res 108, 2386, doi: 10.1029/2003JB002399.

Dupont-Nivet, G., Robinson, D., Butler, R.F., Yin, A., Melosh, H.J., 2004. Concentration of crustal displacement along a weak Altyn Tagh fault: Evidence from paleomagnetism of the northern Tibetan Plateau. Tectonics 23, TC1020, doi: 10.1029/2002TC001397, 2004.

Durand-Riard, P., Shaw, J.H., Plesch, A., Lufadeju, G., 2013. Enabling 3D geomechanical restoration of strike-and oblique-slip faults using geological constraints, with applications to

the deep-water Niger Delta. Journal of Structural Geology, 48: 33-44, doi: 10.1016/j.jsg.2012.12.009.

Duvall, A.R., Clark, M.K., Kirby, E., Farley, K.A., Craddock, W.H., Li, C., Yuan, D.-Y., 2013. Low-temperature thermochronometry along the Kunlun and Haiyuan Faults, NE Tibetan Plateau: Evidence for kinematic change during late-stage orogenesis. Tectonics 32, 1190-1211, doi:10.1002/tect.20072.

Fang, X., Zhang, W., Meng, Q., Gao, J., Wang, X., King, J., Song, C., Dai, S., Miao, Y., 2007. High-resolution magnetostratigraphy of the Neogene Huaitoutala section in the eastern Qaidam Basin on the NE Tibetan Plateau, Qinghai Province, China and its implication on tectonic uplift of the NE Tibetan Plateau. Earth and Planetary Science Letters 258, 293-306, doi:10.1016/j.epsl.2007.03.042.

Fu, B.H., Awata, Y., Du, J.G., He, W.G., 2005. Late Quaternary systematic stream offsets caused by repeated large seismic events along the Kunlun fault, northern Tibet. Geomorphology 71, 278-292, doi:10.1016/j.geomorph.2005.03.001.

Fu, B. H., Awata, Y., 2007. Displacement and timing of left-lateral faulting in the Kunlun Fault Zone, northern Tibet, inferred from geologic and geomorphic features. Journal of Asian Earth Sciences 29, 253-265, doi:10.1016/j.jseaes.2006.03.004.

Fu J., 2008. Division of Quaternary sedimentary types in Adatan area, Xinjiang. World Nuclear Geoscience 25(2), 94-97(in Chinese with English abstract).

Gao, J., Li, S., Dai, S., Li, A., Peng, Y., 2009. Constraints of tectonic evolution in provenance from detrital zircon fission-track data of Cenozoic strata of Xichagou district in western Qaidam basin: Journal of Lanzhou University (Natural Sciences), 45 (3), 1-7, doi: 0455-2059(2009)03-0001-07 (in Chinese with English abstract).

Guo, J., Lin, A., Sun, G., Zheng, J., 2007. Surface ruptures associated with the 1937 M 7.5 Tuosuo Lake and the 1963 M 7.0 Alake Lake earthquakes and the paleoseismicity along the Tuosuo Lake Segment of the Kunlun Fault, Northern Tibet. Bulletin of the Seismological Society of America 97, 474-496, doi: 10.1785/0120050103.

Harkins, N., Kirby, E., 2008. Fluvial terrace riser degradation and determination of slip rates on strike-slip faults: An example from the Kunlun fault, China. Geophysical Research Letters 35, doi: 10.1029/2007GL033073.

Hinsch, R., Decker, K., Peresson, H., 2005. 3-D seismic interpretation and structural modeling in the Vienna Basin: implications for Miocene to recent kinematics. Austrian J. Earth Sci 97, 38-50.

Huang, H., Huang, Q., Ma, Y., 1996. Geology of Qaidam Basin and its petroleum prediction.

Geological Publishing House, Beijing pp. 1-257 (in Chinese with English abstract).
Huo, G.M., 1990. Petroleum geology of China: Oil fields in Qianghai and Xizang. Chinese Petroleum Industry Press, Beijing 14, pp. 1-483 (in Chinese with English abstract).
IGSSP (Insititute of Geological Survey of Shanxi Province), 2003. The Report of Regional Geological Survey at Scale 1:250000. P.R.C. China Industry Press, pp. 1-274 (in Chinese).
IGSQP (Insititute of Geological Survey of Qinhai Province), 2004. The Report of Regional Geological Survey at Scale 1:250000. P.R.C. China Industry Press, pp. 1-386 (in Chinese).
Jolivet, M., Roger, F., Arnaud, N., Brunel, M., Tapponnier, P., Seward, D., 1999. Histoire de l'exhumation de l'Altun Shan: indications sur l'âge de la subduction du bloc du Tarim sous le système de l'Altyn Tagh (Nord Tibet). C.R. Acad. Sci. Paris 329, 749-755, doi: 10.1016/S1251-8050(00)88495-5
Jolivet, M., Brunel, M., Seward, D., Xu, Z., Yang, J., Roger, F., Tapponnier, P., Malavieille, J., Arnaud, N., Wu, C., 2001. Mesozoic and Cenozoic tectonics of the northern edge of the Tibetan plateau: fission-track constraints. Tectonophysics 343, 111-134, doi: 10.1016/S0040-1951(01)00196-2.
Jolivet, M., Brunel, M., Seward, D., Xu, Z., Yang, J., Malavieille, J., Roger, F., Leyreloup, A., Arnaud, N., Wu, C., 2003. Neogene extension and volcanism in the Kunlun Fault Zone, northern Tibet: New constraints on the age of the Kunlun Fault. Tectonics 22, 1052, doi: 10.1029/2002TC001428.
Jolivet, M., Arzhannikov, S., Chauvet, A., Arzhannikova, A., Vassallo, R., Kulagina, N., Akulova, V., 2013. Accomodating large-scale intracontinental extension and compression in a single stress-field: A key example from the Baikal Rift System. Gondwana Research, 24(3), 918-935, doi:10.1016/j.gr.2012.07.017.
Jordan, T.E., 1981. Thrust loads and foreland basin evolution, Cretaceous, western United States. AAPG bulletin 65, 2506-2520.
Ke, X., Ji, J., Zhang, K., Kou, X., Song, B., Wang, C., 2013. Magnetostratigraphy and Anisotropy of Magnetic Susceptibility of the Lulehe Formation in the Northeastern Qaidam Basin. Acta Geologica Sinica-English Edition 87, 576-587, doi: 10.1111/1755-6724.12069.
Kidd, W.S.F., Molnar, P., 1988. Quaternary and active faulting observed on the 1985 Academia Sinica--Royal society geotraverse of Tibet. Philosophical Transactions of the Royal Society of London. Series A, Mathematical and Physical Sciences 327(1594), 337-363, doi: 10.1098/rsta.1988.0133.
Kirby, E., Harkins, N., Wang, E., Shi, X., Fan, C., Burbank, D., 2007. Slip rate gradients along the eastern Kunlun fault. Tectonics 26, doi: 10.1029/2006TC002033.

Lin, A., Fu, B., Guo, J., Zeng, Q., Dang, G., He, W., Zhao, Y., 2002. Co-seismic strike-slip and rupture length produced by the 2001 Ms 8.1 Central Kunlun earthquake. Science 296, 2015-2017, doi: 10.1126/science.107087.

Lin, A., Guo, J., 2008. Nonuniform Slip Rate and Millennial Recurrence Interval of Large Earthquakes along the Eastern Segment of the Kunlun Fault, Northern Tibet. Bulletin of the Seismological Society of America 98, 2866-2878, doi: 10.1785/0120070193.

Liu, Y.J., Genser, J., Neubauer, F., Jin, W., Ge, X.H., Handler, R., Takasu, A., 2005. $^{40}Ar/^{39}Ar$ mineral ages from basement rocks in the Eastern Kunlun Mountains, NW China, and their tectonic implications. Tectonophysics 398, 199-224, doi: 10.1016/j.tecto.2005.02.007.

Lu, H., Xiong, S., 2009. Magnetostratigraphy of the Dahonggou section, northern Qaidam Basin and its bearing on Cenozoic tectonic evolution of the Qilian Shan and Altyn Tagh Fault. Earth and Planetary Science Letters 288, 539-550, doi:10.1016/j.epsl.2009.10.016.

Macedo, J., Marshak, S., 1999. Controls on the geometry of fold-thrust belt salients. Geological Society of America Bulletin 111, 1808-1822, doi: 10.1130/0016-7606(1999)111<1808:COTGOF>2.3.CO;2.

McQuarrie, N., 2004. Crustal scale geometry of the Zagros fold–thrust belt, Iran. Journal of Structural Geology 26, 519-535, doi:10.1016/j.jsg.2003.08.009.

Meng, Q.R., Fang, X., 2008. Cenozoic tectonic development of the Qaidam Basin in the northeastern Tibetan Plateau. Geological Society of America Special Papers 444, 1-24, doi: 10.1130/2008.2444(01).

Meyer, B., Tapponnier, P., Bourjot, L., Metivier, F., Gaudemer, Y., Peltzer, G., Shunmin, G., Zhitai, C., 1998. Crustal thickening in Gansu-Qinghai, lithospheric mantle subduction, and oblique, strike‐slip controlled growth of the Tibet plateau. Geophysical Journal International 135, 1-47, doi: 10.1046/j.1365-246X.1998.00567.x.

Mock, C., Arnaud, N.O., Cantagrel, J.M., 1999. An early unroofing in northeastern Tibet? Constraints from $^{40}Ar/^{39}Ar$ thermochronology on granitoids from the Eastern Kunlun Mountains (Qianghai, NW China). Earth and Planetary Science Letters 171, 107-122, doi: 10.1016/S0012-821X(99)00133-8.

Pei, J., Sun, Z., Wang, X., Zhao, Y., Ge, X., Guo, X., Li, H., Si, J., 2009. Evidence for Tibetan plateau uplift in Qaidam Basin before Eocene-Oligocene boundary and its climatic implications. Journal of Earth Science 20, 430-437, doi: 10.1007/s12583-009-0035-y.

Peltzer, G., Crampé, F., King, G., 1999. Evidence of nonlinear elasticity of the crust from the Mw7. 6 Manyi (Tibet) earthquake. Science 286, 272-276, doi:10.1126/science.286.5438.272.

QBGMR (Qinhai Bureau of Geology Mineral Resources), 1991. Regional Geology of Qinghai

Province. Geological Publishing House, Beijing, pp. 1-662 (in Chinese).

Qiu, N., 2002. Tectono-thermal evolution of the Qaidam Basin, China: evidence from Ro and apatite fission track data. Petroleum Geoscience 8, 279-285, doi: 10.1144/petgeo.8.3.279.

Sepehr, M., Cosgrove, J., 2004. Structural framework of the Zagros fold–thrust belt, Iran. Marine and Petroleum Geology 21, 829-843, doi:10.1016/j.marpetgeo.2003.07.006.

Sobel, E.R., Hilley, G.E., Strecker, M.R., 2003. Formation of internally drained contractional basins by aridity-limited bedrock incision. J. Geophys. Res 108, 25, doi: 10.1029/2002JB001883.

Song, T., Wang, X., 1993. Structural styles and stratigraphic patterns of syndepositional faults in a contractional setting: Examples from Quaidam basin, northwestern China. AAPG bulletin 77, 102-117.

Song, C. H. 2006. Tectonic uplift and Cenozoic sedimentary evolution in the northern margin of the Tibetan Plateau. [Dissertation]. Lanzhou University, Lanzhou. 85-123 (in Chinese with English abstract).

Sun, Z.M., Yang, Z.Y., Pei, J.L., Ge, X.H., Wang, X.S., Yang, T.S., Li, W.M., Yuan, S.H., 2005. Magnetostratigraphy of Paleogene sediments from northern Qaidam Basin, China: implications for tectonic uplift and block rotation in northern Tibetan plateau. Earth and Planetary Science Letters 237, 635-646, doi: 10.1016/j.epsl.2005.07.007.

Sun, Z. C., Jing M. C., Sun, N. D., Lu Y.L., Cao, L., 2007. Discussion on boundary between the upper and lower members of Xiaganchaigou Formation of Paleogene in Well Kun-2, Qaidam Basin. Journal of Palaeogeography, 9(6), 611-618 (in Chinese with English abstract).

Suppe, J., Chou, G.T., Hook, S.C., 1992. Rates of folding and faulting determined from growth strata, Thrust tectonics. Springer, pp. 105-121.

Tapponnier, P., Zhiqin, X., Roger, F., Meyer, B., Arnaud, N., Wittlinger, G., Jingsui, Y., 2001. Oblique stepwise rise and growth of the Tibet Plateau. Science 294, 1671-1677, doi: 10.1126/science.105978.

Taylor, M., Yin, A., 2009. Active structures of the Himalayan-Tibetan orogen and their relationships to earthquake distribution, contemporary strain field, and Cenozoic volcanism. Geosphere 5, 199-214, doi: 10.1130/GES00217.1.

Van Der Woerd, J., Ryerson, F.J., Tapponnier, P., Gaudemer, Y., Finkel, R., Mériaux, A.S., Caffee, M., Guoguang, Z., Qunlu, H., 1998. Holocene left-slip rate determined by cosmogenic surface dating on the Xidatan segment of the Kunlun fault (Qinghai, China). Geology 26, 695-698, doi: 10.1130/GES00217.1.

Velasco, A.A., Ammon, C.J., Beck, S.L., 2000. Broadband source modeling of the November

8, 1997, Tibet (Mw=7.5) earthquake and its tectonic implications. Journal of Geophysical Research: Solid Earth (1978–2012) 105 (B12), 28065-28080, doi: 10.1029/2000JB900282.

Vergés, J., Marzo, M., Muñoz, J., 2002. Growth strata in foreland settings. Sedimentary Geology 146, 1-9, doi: 10.1016/S0037-0738(01)00162-2.

Wang, Q., Zhang, P.Z., Freymueller, J.T., Bilham, R., Larson, K.M., Lai, X., You, X., Niu, Z., Wu, J., Li, Y., 2001. Present-day crustal deformation in China constrained by global positioning system measurements. Science 294, 574-577, doi: 10.1126/science.1063647.

Wang, F., L., C. H., Li, Q., Yeh, M. W., Wan, J., Zheng, D., Wang, E., 2004a. Onset timing of significant unroofing around Qaidam basin, northern Tibet, China: constraints from $^{40}Ar/^{39}Ar$ and FT thermochronology on granitoids. Journal of Asian Earth Sciences 24, 59-69, doi: 10.1016/j.jseaes.2003.07.004.

Wang, S. J., Bai, Y. S., Hao, P., Chang, G. H., Bao, G. P., 2004b. Discovery of fresh water Gastropoda fossils in Ancient Neoteric period and its geological significance in Adatan basin. Northwestern Geology 37(3), 21-23 (in Chinese with English abstract).

Wang, E., Xu, F.Y., Zhou, J.X., Wan, J., Burchfiel, B.C., 2006. Eastward migration of the Qaidam basin and its implications for Cenozoic evolution of the Altyn Tagh fault and associated river systems. Geological Society of America Bulletin 118, 349-365, doi: 10.1130/B25778.1.

Wang, S. J., Bai, Y. S., Xu, Y. F., Zhang, K. C., Chang, G. H., 2007. Tectonic Evolution of the Adatan Basin in Late Paleogene. Northwestern Geology 40(4), 53-57 (in Chinese with English abstract).

Wang, Y.D., Nie, J.S., Zhang, T., Sun, G.Q., Yang, X., Liu, Y.H., Liu, X.W., 2010. Cenozoic tectonic evolution in the western Qaidam Basin inferred from subsurface data. Geosciences Journal 14, 335-344, doi: 10.1007/s12303-010-0033-1.

Wang, C.S., Gao, R., Yin, A., Wang, H., Zhang, Y.X., Guo, T.L., Li, Q.S., Li, Y.L., 2011. A mid-crustal strain-transfer model for continental deformation: A new perspective from high-resolution deep seismic-reflection profiling across NE Tibet. Earth and Planetary Science Letters 306, 279-288, doi: 10.1016/j.epsl.2011.04.010.

Xia, W.C., Zhang, N., Yuan, X.P., Fan, L.S., Zhang, B.S., 2001. Cenozoic Qaidam basin, China: A stronger tectonic inversed, extensional rifted basin. AAPG bulletin 85, 715-736.

Xu, X.W., Chen, W.B., Ma, W.T., Yu, G.H., Chen, G.H., 2002. Surface rupture of the Kunlunshan earthquake (Ms 8.1), northern Tibetan plateau, China. Seismological Research Letters 73, 884-892.

Yang, F., Ma, Z.Q., Xu, T.C., Ye, S.J., 1992. A Tertiary paleomagnetic stratigraphic profile in

Qaidam basin. Acta Petrolei Sinica 13(2), 97-101(in Chinese with English abstract).

Ye, D., 1997. Tertiary in Petroliferous Regions of China. Petroleum Inductry Press, Beijing, pp. 1-374 (in Chinese with English abstract).

Yin, A., Harrison, T.M., 2000. Geologic evolution of the Himalayan-Tibetan orogen. Annual Review of Earth and Planetary Sciences 28, 211-280, doi: 10.1146/annurev.earth.28.1.211.

Yin, A., Rumelhart, P.E., Cowgill, E., Butler, R., Harrison, T.M., Ingersoll, R.V., Cooper, K., Zhang, Q., and Wang, X. F., 2002. Tectonic history of the Altyn Tagh fault system in northern Tibet inferred from Cenozoic sedimentation. Geological Society of America Bulletin 114, 1257-1295, doi: 10.1130/0016-7606(2002)114<1257: THOTAT>2.0.CO;2.

Yin, A., Dang, Y.Q., Zhang, M., McRivette, M.W., Burgess, W.P., Chen, X.H., 2007. Cenozoic tectonic evolution of Qaidam basin and its surrounding regions (part 2): Wedge tectonics in southern Qaidam basin and the Eastern Kunlun Mountains. Geological Society of America Special Papers 433, 369-390, doi: 10.1130/2007.2433(18).

Yin, A., Dang, Y.Q., Zhang, M., Chen, X.H., McRivette, M.W., 2008. Cenozoic tectonic evolution of the Qaidam basin and its surrounding regions (Part 3): Structural geology, sedimentation, and regional tectonic reconstruction. Geological Society of America Bulletin 120, 847-876, doi: 10.1130/B26232.1.

Yin, A., 2010. Cenozoic tectonic evolution of Asia: A preliminary synthesis. Tectonophysics 488, 293-325, doi:10.1016/j.tecto.2009.06.002.

Yuan, W.M., Dong, J.Q., Wang, S.C., Carter, A., 2006. Apatite fission track evidence for Neogene uplift in the eastern Kunlun Mountains, northern Qinghai–Tibet Plateau, China. Journal of Asian Earth Sciences 27, 847-856, doi: 10.1016/j.jseaes.2005.09.002.

Zhang, Y.X., Che, Z.C., Liu, L., Luo, J.L., 1996. Tertiary in the Kumkol Basin, Xinjiang. Regional Geology of China 4, 311-316 (in Chinese with English abstract).

Zhang, P.Z., Shen, Z., Wang, M., Gan, W., Bürgmann, R., Molnar, P., Wang, Q., Niu, Z., Sun, J., Wu, J., 2004. Continuous deformation of the Tibetan Plateau from global positioning system data. Geology 32, 809-812, doi: 10.1130/G20554.1.

Zhang, W., 2006. The high precise Cenozoic magnetostratigraphy of the Qaidam Basin and uplift of the Northern Tibetan plateau. [Doctoral dissertation]. Lanzhou University, Lanzhou. 95-105 (in Chinese with English abstract).

Zhang, Z., Klemperer, S., Bai, Z., Chen, Y., Teng, J., 2011. Crustal structure of the Paleozoic Kunlun orogeny from an active-source seismic profile between Moba and Guide in East Tibet, China. Gondwana Research 19, 994-1007, doi: 10.1016/j.gr.2010.09.008.

Zhang, L.Y., Ding, L., Yang, D., Xu, Q., Cai, F.L., Liu, D.L., 2012. Origin of middle Miocene

leucogranites and rhyolites on the Tibetan Plateau: Constraints on the timing of crustal thickening and uplift of its northern boundary. Chinese Science Bulletin 57, 511-524, doi: 10.1007/s11434-011-4813-4.

Zhao, J., Mooney, W.D., Zhang, X., Li, Z., Jin, Z., Okaya, N., 2006. Crustal structure across the Altyn Tagh Range at the northern margin of the Tibetan plateau and tectonic implications. Earth and Planetary Science Letters 241, 804-814, doi:10.1016/j.epsl.2005.11.003.

## 2.2 Cenozoic source to sink relation between the Qaidam basin and the Eastern Kunlun Mountains

***Paper published in Geological Society of America Bulletin, 2016, vol. 128, pp. 258-283***

**Source to sink relation between the Eastern Kunlun Range and the Qaidam Basin, northern Tibetan Plateau, during the Cenozoic**

**Feng Cheng** [1, 2], Suotang Fu [3], Marc Jolivet [2], Changhao Zhang [3], Zhaojie Guo [1, *]

[1] Key Laboratory of Orogenic Belts and Crustal Evolution, Ministry of Education, School of Earth and Space Sciences, Peking University, Beijing, 100871, China

[2] Laboratoire Géosciences Rennes, CNRS-UMR6118, Université Rennes 1 - Observatoire des Sciences de l'Univers, Rennes, 35042, France

[3] Qinghai Oilfield Company, PetroChina, Dunhuang, Gansu, 736202, China

[*] Corresponding author. Tel.: + 86-10-62753545; fax: + 86-10-62758610. E-mail address: zjguo@pku.edu.cn

*Note: The online version of this contribution can be found as:* ***Cheng, F., Fu, S., Jolivet, M., Zhang, C., Guo, Z., 2016. Source to sink relation between the Eastern Kunlun Range and the Qaidam Basin, northern Tibetan Plateau, during the Cenozoic. Geological Society of America Bulletin 128, 258-283, doi: 10.1130/B31260.1.***

### Abstract

Understanding the source to sink relationship through time between the Eastern Kunlun Range, one of the major mountain belts in the northern Tibetan Plateau, and the actively deforming Qaidam Basin to the north has important implications for unravelling the growth history of the Tibetan plateau. In this study, U-Pb dating (LA-ICP-MS) of detrital zircons from

22 sandstone samples (Paleocene to Holocene) collected from 4 sections within the southwestern Qaidam basin is combined with provenance analysis and new seismic profile interpretation to investigate the mountain building of the Eastern Kunlun Range and its effects on the development of the Qaidam basin. The U-Pb age distributions of detrital grains from Paleocene strata are characterised by a major component of Paleozoic to late Proterozoic ages. Furthermore, carbonate debris containing foraminifera have been recognized in the Paleocene conglomerate sequences. We thus suggest that the Eastern Kunlun Range was already exhumed prior to the Paleocene. The southward onlaps of Paleocene to Oligocene strata observed on seismic profiles and the appearance of a Mesozoic component in the detrital zircon age spectra of Eocene to Oligocene strata indicate that the Qaidam basin was widening southward during that early Cenozoic period. Well-developed post-Oligocene growth strata and the increasing proportion of Mesozoic and Paleozoic U-Pb ages in detrital zircon grains from late Neogene strata demonstrate that the relief of the Eastern Kunlun and Altyn Tagh ranges had increased, leading to isolation and narrowing of the Qaidam basin from Miocene to the present. The inferred pulsed deformation in the Eastern Kunlun Range highlights the complex growth history of the Tibetan plateau.

Keywords: Cenozoic, North Tibet, Qaidam basin, Eastern Kunlun Range, Detrital U-Pb zircon geochronology, Source to sink

## 2.2.1 Introduction

The Tibetan plateau is the widest area of elevated topography on Earth (Fig. 1). Many approaches have been used to decipher the tectonic and topographic history of that region. These include thermochronology (e.g. Jolivet et al., 1999, 2001, 2003; Kapp et al., 2005), paleobotany (e.g. Spicer et al., 2003), paleomagnetism (e.g. Dupont-Nivet et al., 2010), paleoaltimetry (e.g. Graham et al., 2005; Rowley et al., 2006; Kent-Corson et al., 2009; Rieser et al., 2009; Quade et al., 2011; Hough et al., 2011) coupled with stratigraphic and tectonic analyses (e.g. Yin et al., 2008a, 2008b; C.Wang et al., 2008a, 2014; C.S.Wang et al., 2011). However, the initial topography of the area now represented by the Tibetan plateau, as well as the early stages of development of the present day topography remain poorly constrained and highly debated. Two competing models suggest that either the Tibetan lithosphere thickened as a thin viscous layer, with buoyancy driven uplift of the plateau (e.g. England and Houseman, 1989) or that the plateau grew stepwise by successive addition of large crustal thrust-wedges (e.g. Tapponnier et al., 2001). This last model is partly supported, for example, by the progressive decrease of initial deformation age from the center of the plateau towards its edges

(e.g. Métivier et al., 1998; Wang et al., 2008a, 2014). However, it has been recently suggested that an already elevated proto-plateau (similar to the present-dayAndean margin) surrounded by low-level basins already existed prior to the India – Asia collision (e.g. Kapp et al., 2003; Ding et al., 2013, Xu et al., 2013; Ding et al., 2014). In addition, the recent suggestion that the northern Tibetan plateau began to undergo horizontal shortening in the early Eocene, shortly after the India – Asia collision, also challenges the northward progressive plateau growth hypothesis (Yin et al., 2008b; Duvall et al., 2011; Zhuang et al., 2011; F. Cheng et al., 2015a).

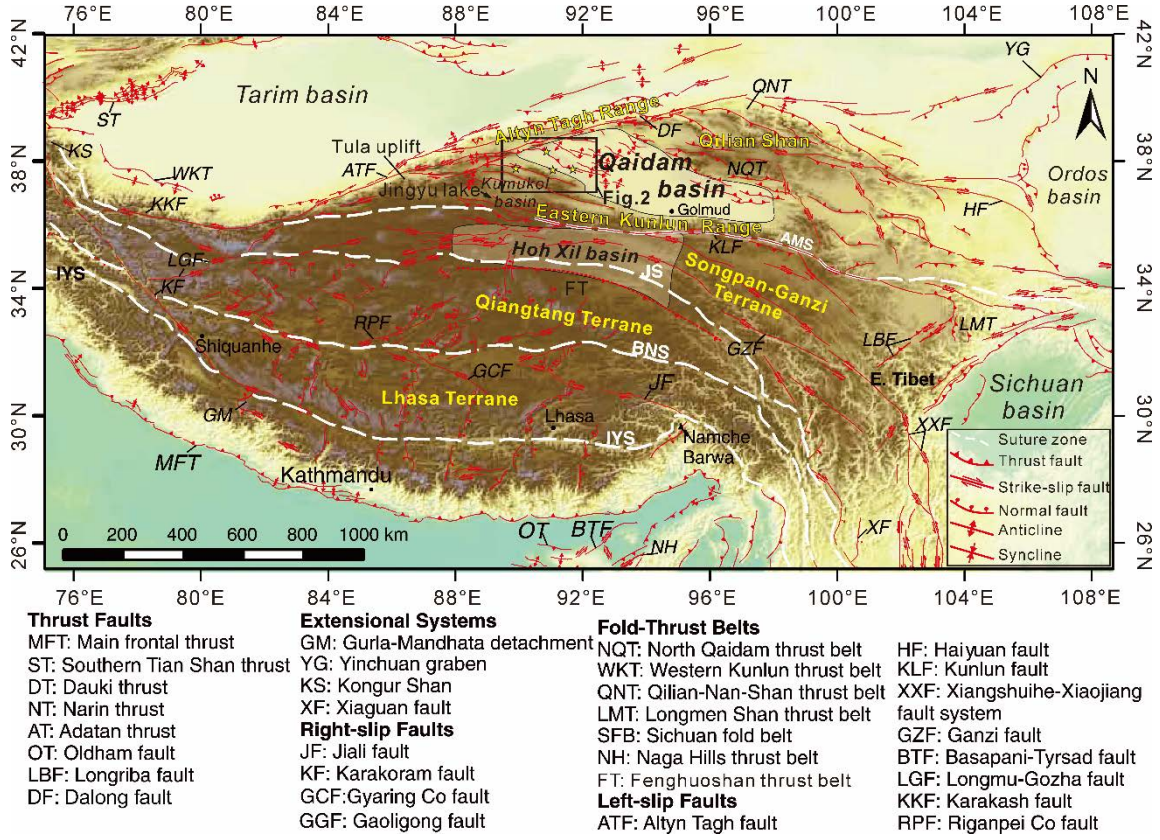


**Thrust Faults**
MFT: Main frontal thrust
ST: Southern Tian Shan thrust
DT: Dauki thrust
NT: Narin thrust
AT: Adatan thrust
OT: Oldham fault
LBF: Longriba fault
DF: Dalong fault

**Extensional Systems**
GM: Gurla-Mandhata detachment
YG: Yinchuan graben
KS: Kongur Shan
XF: Xiaguan fault

**Right-slip Faults**
JF: Jiali fault
KF: Karakoram fault
GCF:Gyaring Co fault
GGF: Gaoligong fault

**Fold-Thrust Belts**
NQT: North Qaidam thrust belt
WKT: Western Kunlun thrust belt
QNT: Qilian-Nan-Shan thrust belt
LMT: Longmen Shan thrust belt
SFB: Sichuan fold belt
NH: Naga Hills thrust belt
FT: Fenghuoshan thrust belt

**Left-slip Faults**
ATF: Altyn Tagh fault

HF: Haiyuan fault
KLF: Kunlun fault
XXF: Xiangshuihe-Xiaojiang fault system
GZF: Ganzi fault
BTF: Basapani-Tyrsad fault
LGF: Longmu-Gozha fault
KKF: Karakash fault
RPF: Riganpei Co fault

Figure 1. Digital topographic map of the Tibetan Plateau modified after Taylor and Yin (2009). Active fault kinematics and suture zones are based on Yin et al. (2007), Taylor and Yin (2009), and Cheng et al. (2014). Note that the Hoh Xil Basin has been diced up by the Neogene uplift phase. The yellow stars refer to the location of sampling sites. IYS—Indus Yalu suture zone; AMS—Anyimagen-Kunlun-Muztagh suture zone; JS—Jinsha suture zone; BNS—Bangong Nujiang suture zone.

The actively deforming northeastern and eastern edges of the Tibetan plateau are characterized by both a strong topographic gradient and a marked dichotomy between low relief basins (Qaidam and Sichuan basins) and highly dissected Alpine-style high ranges (Eastern Kunlun, Altyn Tagh, Qilian Shan and Longmen Shan ranges). Along the northeastern margin of the plateau, the ca. 3000 m high Qaidam basin is located between the ca. 5000 m high Eastern Kunlun Range, Altyn Tagh Range and Qilian Shan (Fig. 1). The late Mesozoic – Cenozoic evolution of the deformation pattern, sediment composition and depositional

environments in the basin are thus directly related to the tectonic and topographic growth of the surrounding ranges and represent key constraints on the tectonic and topographic evolution of the Tibetan plateau (e.g. Métivier et al., 1998; Rieser et al., 2006; Yin et al., 2007, 2008b; Fu et al., 2010; Zhuang et al., 2011; Song et al., 2013; F. Cheng et al., 2015a).

The proposed onset time of uplift of the Eastern Kunlun Range mainly varies from Eocene to Miocene depending on the approach used to estimate the onset of deformation (Mock et al., 1999; A. Wang et al., 2000; Jolivet et al., 2001; Yuan et al., 2003; Wang et al., 2006a; Yuan et al., 2006; Yin et al., 2007, 2008b; C. Wang et al., 2008a; Clark et al., 2010; Dai et al., 2013; Duvall et al., 2013). In particular, based on regional stratigraphic correlation between the Qaidam basin and the Hoh Xil basin to the south (Fig. 1), Yin et al. (2008b) argued that they represented a single basin during the Paleogene, bounded to the north by the Altyn Tagh Range and the Qilian Shan, and to the south by the proto-Tibetan plateau. This large structure was then partitioned by the tectonic uplift of the Eastern Kunlun Range during the Neogene. This model questions the assumption of a progressive northward growth of the plateau through in-sequence propagation of thrust systems associated with filling of the intermediate basins (e.g. Métivier et al., 1998, Meyer et al., 1998; Tapponnier et al., 2001). This idea has motivated several attempts to reassess the tectonic processes affecting the northern edge of the Tibetan plateau (e.g. Shi et al., 2009; Wang et al., 2011; Cheng et al., 2014; Mao et al., 2014; Yu et al., 2014).

In recent years, a number of studies have concentrated on the tectonic evolution of the southern margin of the Qaidam basin to describe the Cenozoic growth history of the Eastern Kunlun Range (Yin et al., 2007, 2008a, 2008b; Shi et al., 2009; Wang et al., 2011; Cheng et al., 2014). However, partially due to the remote, inaccessible geographical location of the late Mesozoic to Cenozoic sections in the South Qaidam basin (SQB) and northern flank of the Eastern Kunlun Range, little information is available on the temporal and spatial evolution of the sediment sources and depositional environments. Such source-sink information is of primary importance when trying to decipher the topographic growth of the Eastern Kunlun Range during the Cenozoic and to constrain the early Cenozoic topography of the northern edge of the Tibetan plateau (i.e. the pre-orogenic status).

In this study, twenty-two sandstone samples from Paleocene to Holocene strata (including six core samples from Paleogene strata) were collected along the Dongchaishan-Gansen, Kunbei, Huatugou and Adatan sections (Fig. 2) for U-Pb dating of detrital zircons using Laser Ablation Inductively Coupled-Plasma Mass Spectrometry (LA-ICP-MS). In order to characterize the nature of any relation between the Eastern Kunlun Range and the Qaidam

basin, this analysis was conducted together with sedimentology and petrography studies, as well as interpretation of newly-acquired seismic profiles in the SQB. Data are then interpreted in terms of Cenozoic topographic history of northern Tibet, and more precisely in terms of the influence of the Cenozoic topographic growth of the Eastern Kunlun Range on the sedimentary and topographic evolution of the SQB. Finally, this study provides a local framework for a better assessment of the Cenozoic spatial and temporal evolution of the entire Tibetan Plateau.

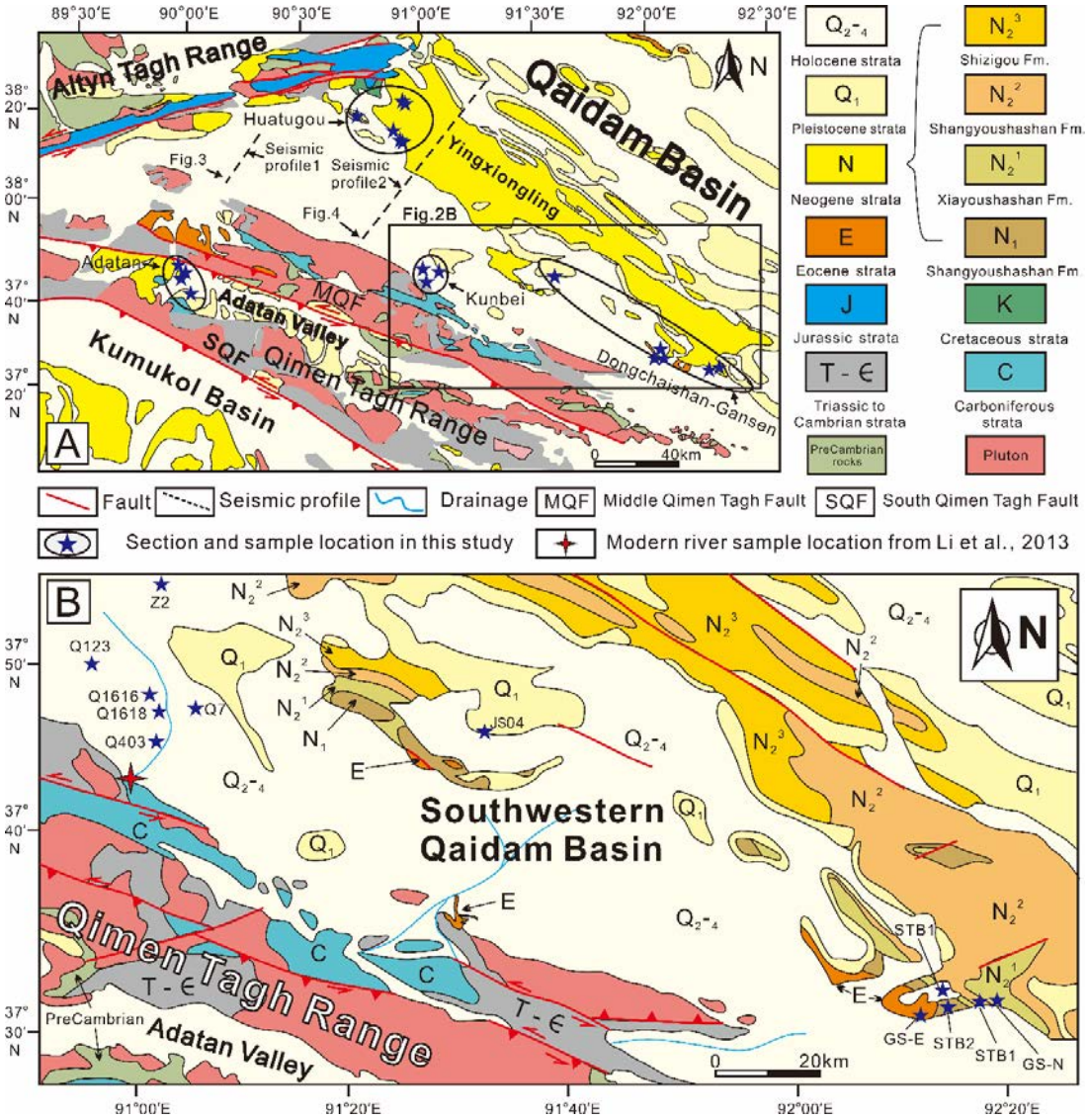


Figure 2. Geological map of the southwestern Qaidam Basin and surrounding area, modified after the 1:250,000 geologic map (SIGS, 2003; QIGS, 2004). See Figure 1 for location. Active fault kinematics are based on Cheng et al. (2014), SIGS (2003), and QIGS (2004).

## 2.2.2 Geological Setting

### 2.2.2.1 Eastern Kunlun Range

The Eastern Kunlun Range is oriented in a more or less east-west direction with an

average elevation of about 5000 m and has the largest topographic gradients within the Tibetan plateau. Both morphologically and tectonically, it separates the Hoh Xil basin to the south from the Qaidam basin to the north (Fig. 1). The sub-ranges that form the belt diverge westwards gradually forming a series of valleys and ranges such as the Qimen Tagh Range, the Adatan valley or the Kumukol basin (Figs.1 and 2). The basement of the Eastern Kunlun Range mainly consists of Proterozoic and Paleozoic metamorphic rocks overlaid by Paleozoic to Mesozoic strata. These were intruded by Paleozoic and Mesozoic (Permo – Triassic) igneous rocks and were then covered by Jurassic to Cenozoic continental deposits (Fig. 2; Mock et al., 1999; Cowgill et al., 2003; Robinson et al., 2003; Roger et al., 2003; QIGS, 2004; Yin et al., 2007). Finally, late Cenozoic to Quaternary volcanism crosscut the entire sequence (e.g. Jolivet et al., 2003).

Three ophiolite belts of Cambrian, Mississippian and Permo – Triassic ages are exposed within the Eastern Kunlun Range, indicating a long and complex history of oceanic closure within the area (Roger et al., 2008; Wang et al., 2011). Both the basement and sediment cover of the range are cut by a series of high angle faults, related to the major left-lateral strike-slip Kunlun Fault and forming ESE-WNW trending structures (e.g. Kirby et al., 2007; Duvall et al., 2013; Cheng et al., 2014). The Kunlun Fault initiates on the eastern margin of the Tibetan plateau (Lin and Guo, 2008), and terminates in the west with a splay structure composed of several curved thrust faults (Xu et al., 2002; Jolivet et al., 2003; Fu and Awata, 2007; Cheng et al., 2014). Initiation of the modern Kunlun Fault is dated around 30-20 Ma and the calculated total displacement is around 100 ± 20 km (Kidd and Molnar, 1988; Wang et al., 2001; van Der Woerd et al., 2002; Jolivet et al., 2003; Zhang et al., 2004; Yuan et al., 2006; Fu and Awata, 2007; Kirby et al., 2007; Duvall et al., 2013; Cheng et al., 2014). The Cenozoic deformation and exhumation patterns of the Eastern Kunlun Range are complex and remain controversial with estimated onset ages ranging from Eocene-Oligocene (Mock et al., 1999; Jolivet et al., 2001; Wang et al., 2004a; Clark et al., 2010; Duvall et al., 2013) to Miocene (Yuan et al., 2003; Yi et al., 2008) and even as young as Pliocene (A. Wang et al., 2006). Recent analyses of seismic profiles within the Qaidam basin also suggest that the Cenozoic deformation across the Eastern Kunlun Range and SQB initiated during or after the latest Oligocene – early Miocene (Yin et al., 2007; Y.D. Wang et al., 2010a). As the tectonic and topographic evolution of the Eastern Kunlun Range is assumed to control the northward growth of the Tibetan plateau (Yin et al., 2007; Wang et al., 2014), it is of primary importance to resolve the discrepancies in inferred timing.

### 2.2.2.2 Qaidam basin

As the largest petroliferous basin on the Tibetan plateau, the triangular shaped endorheic Qaidam basin is surrounded by the Altyn Tagh Range, the Qilian Shan and the Eastern Kunlun Range (Fig. 1), with about 2000 m of relief difference from the basin to the ranges. Numerous subsurface data (seismic profiles and drill cores) and sequence stratigraphy studies demonstrate that the Qaidam basin is filled with Jurassic, Cretaceous and Cenozoic continental clastic sediments (e.g. Xia et al., 2001; Fang et al., 2007; Yin et al., 2008b). The Cenozoic stratigraphy of the basin has been defined and dated in detail using magnetostratigraphy, and palynology data (Huo, 1990; QBGMR, 1991; Yang et al., 1992; Huang et al., 1996; Xia et al., 2001; Qiu, 2002; Z.M. Sun et al., 2005; Zhang, 2006; Zhao et al., 2006; Fang et al., 2007; Z.M. Sun et al., 2007; Yin et al., 2008b; Gao et al., 2009; Lu and Xiong, 2009; Pei et al., 2009; Ke et al., 2013). The Cenozoic sequences (Fig. 3) are composed of: 1) the Lulehe Formation, Paleocene to early Eocene, >53.5 - 43.8 Ma (Yang et al., 1992; Zhang, 2006; Ke et al., 2013); 2) the Lower Xiaganchaigou Formation, middle Eocene, 43.8 - 37.8 Ma (Zhang, 2006; Sun et al., 2007; Pei et al., 2009); 3) the Upper Xiaganchaigou Formation, late Eocene, 37.8 - 35.5 Ma (Z.M. Sun et al., 2005; Z.M. Sun, 2007; Pei et al., 2009); 4) the Shangganchaigou Formation, Oligocene, 35.5 - 22.0 Ma (Z.M. Sun et al., 2005; Lu and Xiong, 2009); 5) the Xiayoushashan Formation, early Miocene, 22.0 - 15.3 Ma (Fang et al., 2007; Lu and Xiong, 2009); 6) the Shangyoushashan Formation, middle to late Miocene, 15.3 - 8.1 Ma (Fang et al., 2007); 7) the Shizigou Formation, late Miocene to Pliocene, 8.1 - 2.5 Ma (Fang et al., 2007); and finally, 8) the Quaternary sediments, including the Qigequan Formation and the Dabuxun - Yanqiao Formation, Pleistocene to present, 2.5 - 0 Ma (Fang et al., 2007; Yin et al., 2008b).

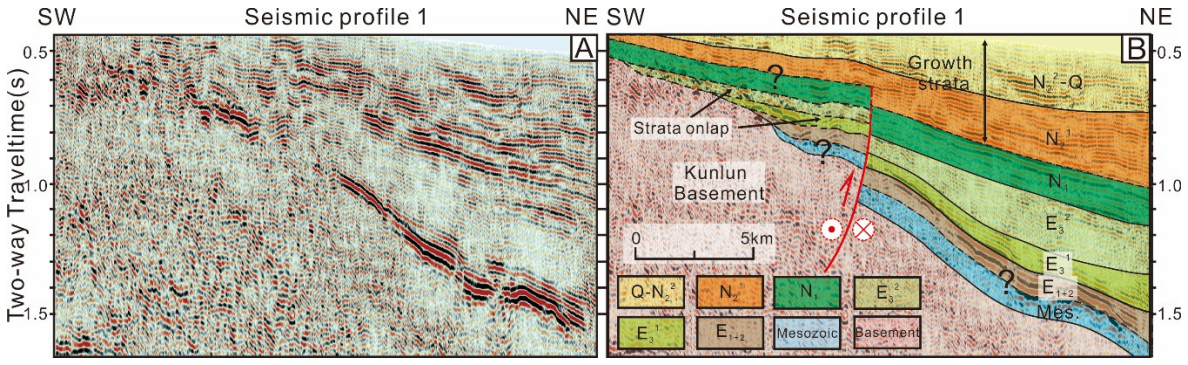


Figure 3. Original (A) and interpreted (B) NE-SW–oriented seismic profile 1 in SW Qaidam Basin. See the location in Figure 2. Note that stratigraphic overlaps between the Paleocene to early Eocene ($E_{1+2}$) and middle to late Eocene ($E_3$) strata, the middle to late Eocene ($E_3$) and Oligocene ($N_1$) strata, and the Oligocene ($N_1$) and early Miocene ($N_2^1$) strata, indicating the gradually enlarging basin from Paleocene to middle Miocene. The growth strata within the middle to late Miocene ($N_2^2$) strata, late Miocene to Pliocene ($N_2^3$) strata, and Pleistocene ($Q_1$) strata demonstrate the shrinking of the basin

since the Miocene.

Large-scale isopach maps, available for each Cenozoic stratigraphic unit in the Qaidam basin provide a clear image of the geometry of the Cenozoic strata (Meng and Fang, 2008; Yin et al., 2008b; Mao et al., 2014). From the Lulehe Formation up, all the formations are systematically thicker in the central part of the basin and thin toward the margins (Huang et al., 1996; E. Wang et al., 2006; Yin et al., 2008b). While the depocenter of the Qaidam basin migrated to the south and east during the Eocene (E. Wang et al., 2006; Yin et al., 2008b), the western Qaidam basin developed extensive saline oil accumulations dominated by two sets of major source rocks deposited in the early Eocene and Oligocene (Huang et al., 1996; Zhu et al., 2005). Newly acquired seismic profiles across the northern flank of the Qimen Tagh Range also show successive onlap of the Eocene and Oligocene Formations (Fig. 3). This geometry suggests a progressive widening of the Qaidam basin to the south from the Eocene to the Oligocene. Subsequently, from the early Miocene to Pliocene, the depocenter migrated northeastwards while the southern limit of the deposition area in the SQB gradually retreat northward, suggesting uplift along the southern edge of the basin (Yin et al., 2008a; Mao et al., 2014). Growth strata developed during this period (Figs. 3 and 4), which again implies tectonic activity (e.g. initiation of strike-slip faulting) in the Eastern Kunlun Range and the SQB (Clark et al., 2010; Duvall et al., 2013; Cheng et al., 2014).

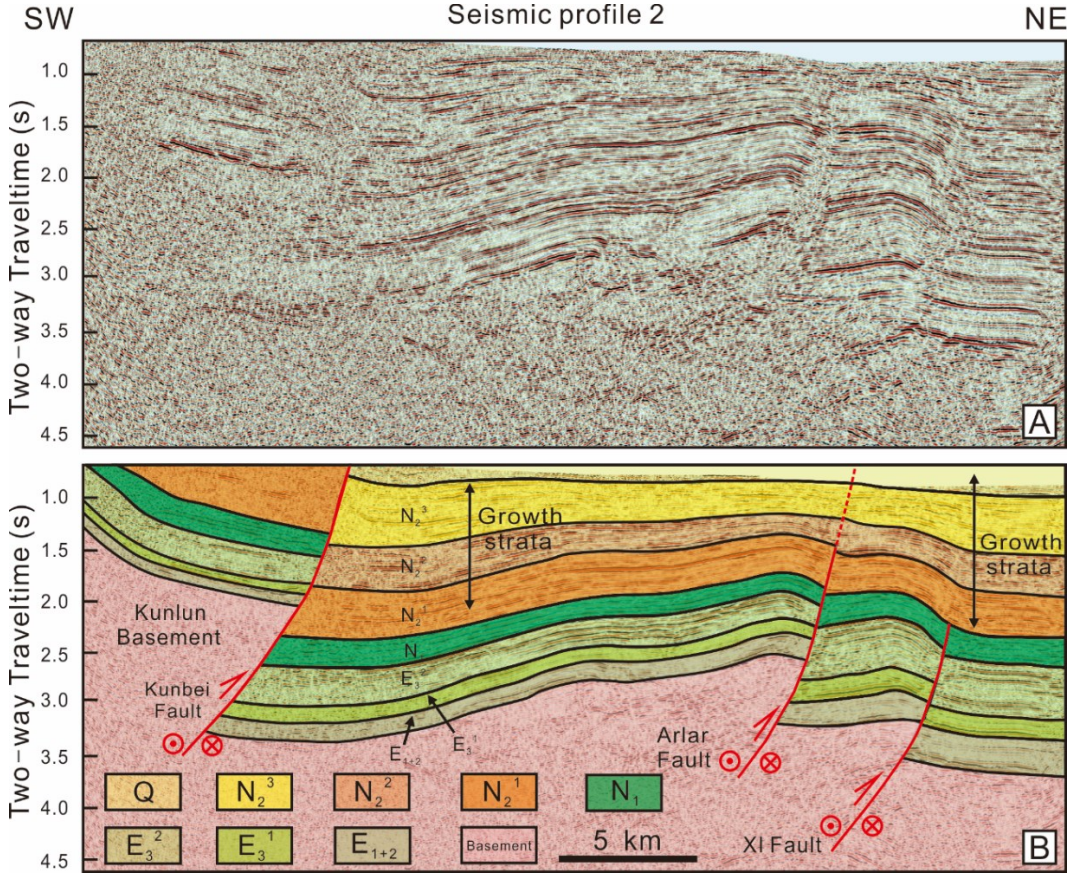

Figure 4. Original (A) and interpreted (B) NE-SW–oriented seismic profile 2 in the South Qaidam Basin. See the location in Figure 2. Note that growth strata near the Kunbei and Arlar faults indicate the uplifting of the Eastern Kunlun Range and shrinking of the basin since the Miocene.

The present-day structure of the SQB is dominated by a series of high angle north-dipping or south-dipping Cenozoic reverse faults accommodating the ongoing shortening generated by the India – Eurasia collision stress field (Wu et al., 2014). Some of these faults display an en echelon arrangement indicating transpressional deformation in local areas, such as the Kunbei and Arlar faults, (Fig. 4; F. Cheng et al., 2014, X. Cheng et al., 2015. Balanced cross-sections throughout the basin indicate that the Cenozoic shortening of the Qaidam Basin increased westward in response to several Eocene and younger shortening phases (Zhou et al., 2006; Yin et al., 2008b; Y.D. Wang et al., 2010).

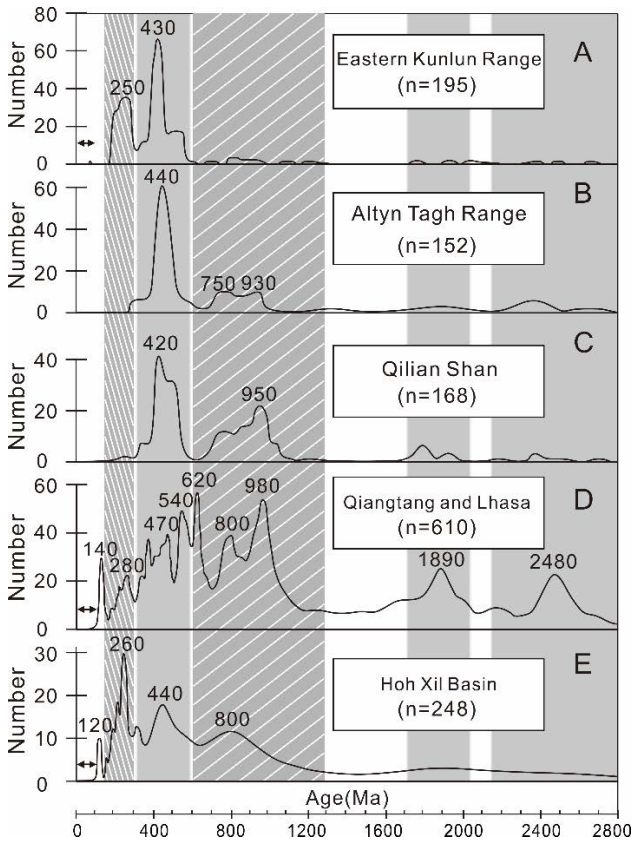


Figure 5. Relative probability plots of granitoid pluton ages in (A) the Eastern Kunlun Range, (B) the Altyn Tagh Range, (C) the Qilian Shan, and U-Pb ages of detrital zircons from (D) the Qiangtang and Lhasa blocks as well as (E) the Hoh Xil Basin. The age data were obtained from: J.S. Yang et al. (1996, 2002, 2006); J.X. Zhang et al. (1997, 2001, 2011); Chen et al. (2003); Gehrels et al. (2003a, 2003b); Yue et al. (2005); L. Liu et al. (2007, 2009); Lu et al. (2008); Chen et al. (2012); Dai et al. (2012); L. Liu et al. (2013b); C. Wang et al. (2013); Staisch et al. (2014); L.Y. Zhang et al. (2014). See also Figure DR1 and Table DR1 for more information on the data (see text footnote 1). Double-headed arrow within the figure refers to the few early Cenozoic and late Mesozoic $^{40}Ar/^{39}Ar$ and U-Pb zircon ages found with each range. Age distributions are marked by different shades according to age groups.

### 2.2.3 Synthesis of existing zircon U-Pb ages from basement

In order to identify the potential sediment source areas for the SQB, we compiled published zircon U-Pb ages on basement rocks from the surrounding Eastern Kunlun, Altyn Tagh and Qilian Shan ranges. A similar compilation was also made using the detrital zircon U-Pb ages available from the Qiangtang and Lhasa blocks as well as

from the Hoh Xil basin (Figs. 5 and DR1 [see footnote 1]; Table DR1 [see footnote 1[①]]).

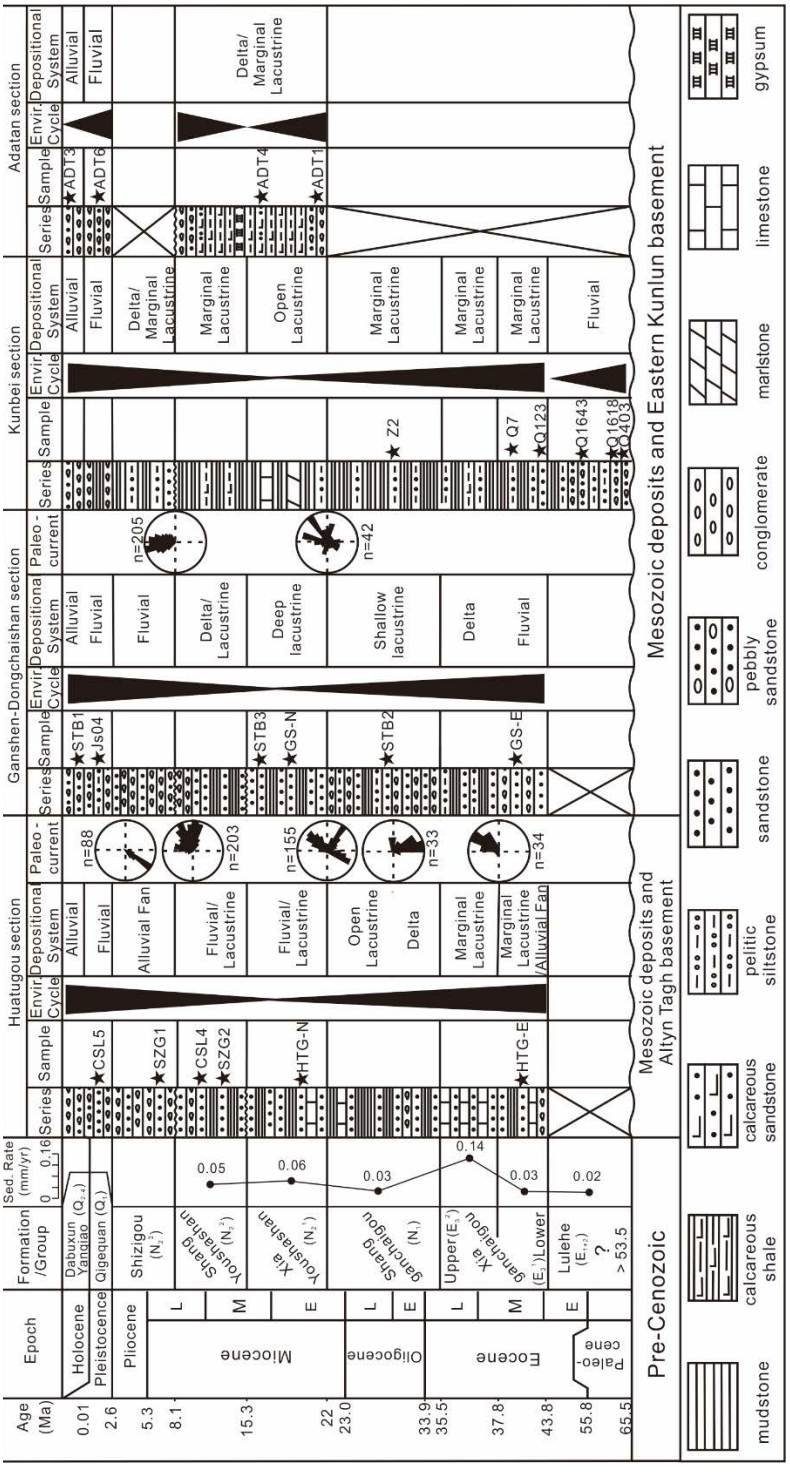


Figure 6. Generalized stratigraphic column of the studied Cenozoic series. Paleocurrent directions were obtained from Meng and Fang (2008) and Zhuang et al. (2011). Envir. Cycle and Sed. Rate in the figure refer to the environment cycle and average sedimentary rate in the South Qaidam Basin, respectively. The average sedimentary rate is generally calculated based on the Cenozoic sequence thickness data from three-dimensional seismic profiles (F. Cheng et al., 2014; X. Cheng et al., 2015) and the age ranges of each sequence (F. Yang et al., 1992; Fang et al., 2007; Zhang, 2006; Sun et al., 2005; Lu and Xiong, 2009; Pei et al., 2009; Ke et al., 2013).

Within the Eastern Kunlun Range, Archean and Proterozoic U-Pb zircon ages are very rare although three age groups can be inferred at 1300-600 Ma, 2100-1700 Ma and 2800-2200 Ma (Fig. 5A; QIGS, 2004; G.C. Wang et al., 2004). The late Proterozoic to Paleozoic age

[①] 1 GSA Data Repository item 2015256, Figure DR1 and Tables DR1–DR2, is available at http:// www.geosociety .org /pubs /ft2015 .htm or by request to editing@ geosociety .org.

group is well represented with a clear age peak around 430 Ma, derived from the early Paleozoic metamorphic rocks associated to the Ordovician – Silurian docking of the Kunlun and Tarim blocks (e.g. Cowgill et al., 2003; QIGS, 2004; Li et al. 2013). However, the Eastern Kunlun basement age distribution is mostly characterized by abundant late Paleozoic – early Mesozoic ages (ca. 300 Ma to ca. 200 Ma) (Fig. 5A). These ages correspond in timing to magmatism associated to the Permo – Triassic closure of the Paleo-Tethys Ocean and to the post-collision magmatism that followed the docking of the Qiangtang block (Roger et al., 2003; Liu et al., 2006; Roger et al., 2008, 2010; Li et al., 2013; Jolivet et al., 2015). Although a few similar Mesozoic ages are found in the Qilian Shan and Altyn Tagh Range, they do not represent such a well-defined component as in the Eastern Kunlun Range (Fig. 5). Finally, a few Cretaceous ages have been obtained from the Tula Uplift in the western reach of the Eastern Kunlun Range (Fig. 1; Robinson et al., 2003) and some Miocene to Quaternary volcanism is occurring in the southwestern part of the range (Jolivet et al., 2003).

The basement of the Altyn Tagh Range (Fig. 5B) displays a relatively large proportion of Archean and Proterozoic zircon U-Pb ages, with Archean ages ranging from ca. 3.6 Ga (Lu et al., 2008) to ca. 2.6 Ga (Lu and Yuan, 2003; Long et al., 2014) and Proterozoic ages ranging from ca. 2.4 Ga to ca. 650 Ma (Gehrels et al., 2003a, 2003b; C, Wang et al., 2006; Zhang et al., 2011). Among those Proterozoic ages, a clear age group can be inferred between ca. 1050 Ma and ca. 650 Ma (Fig. 5B; Wang et al., 2013). Large Paleozoic intrusions are mapped along the range with zircon U-Pb ages ranging from ca. 550 Ma to ca. 400 Ma, forming the major age group (~53 % of the total) within the age distribution pattern (Figs. 5B and DR1 [see footnote 1]; Sobel and Arnaud, 1999; Yue et al., 2004, 2005; J.X. Zhang et al., 2005; C. Wang et al., 2008; Liu et al., 2009; J. Zhang et al., 2014). Finally only a few isolated late Paleozoic igneous rocks are distributed along the central part of the range, with zircon U-Pb ages ranging between ca. 330 Ma and ca. 270 Ma (Cowgill et al., 2003; Gehrels et al., 2003a, 2003b). These ages only represent a small minority (~4% of the total) within the available data.

The age distribution observed in the Qilian Shan basement is largely similar to that of the Altyn Tagh Range (Fig. 5C). It consists of late Archean – early Proterozoic orthogneisses with zircon U-Pb ages ranging from ca. 2.6 Ga to 1.75 Ga (Lu et al., 2002); of late Proterozoic metamorphic rocks with zircon U-Pb ages of ca. 1.0 Ga (Guo and Li, 1999; Song, 2001; Wan et al., 2001); and finally of late Proterozoic ultramafic intrusions with zircon U-Pb ages of ca. 800 Ma (Li et al., 2005). Within the synthetic distribution of ages presented on Figure 5, the late Proterozoic ages form a distinct group between ca. 1050 Ma and 700 Ma. Early Paleozoic granitoid plutons, intruding the Proterozoic basement provide zircon U-Pb ages ranging

between 550 and 400 Ma (Yang et al., 2002; Cowgill et al., 2003; Gehrels et al., 2003a, 2003b; Shi et al., 2006; Bovet et al., 2009). Those ages represent a very distinctive component on the age spectrum (Fig. 5C). The northern part of the Qilian Shan was affected by an early to late Devonian (400 - 360 Ma) metamorphic phase (e.g. Wu et al.,1993; Zhang et al., 1997; Zuo and Wu, 1997), with peak metamorphism dated at 440 - 423 Ma within the north Qaidam ultrahigh pressure belt (Yang et al., 2001, 2002; Song et al., 2004, 2006; Yang et al., 2006). Finally Permian to Triassic igneous rocks are distributed sporadically within the range, with zircon U-Pb ages ranging between 270 Ma and 210 Ma (Fig. 5C; Menold, 2006; Wu et al., 2008). However, as in the Altyn Tagh Range, these Mesozoic ages are not a significant component of the Qilian Shan Range, which display predominantly Paleozoic and Precambrian ages.

The zircon U-Pb age spectrum of the Qiangtang and Lhasa terranes is extremely complex, with ages ranging from late Cenozoic to Archean and showing numerous distinctive peaks (Fig. 5D). In the Songpan – Ganzi and northern Qiangtang terranes, Mesozoic granitic intrusions cluster between 220 Ma and 200 Ma (e.g. Leier et al., 2007; Roger et al., 2010). In the southern part of the Qiangtang and to the south-east in Yidun, Mesozoic intrusion ages are

younger, between 150 Ma and 100 Ma (e.g. Reid et al., 2005). Finally, in the Lhasa terrane Mesozoic intrusions are dated between ~180 Ma and ~90 Ma (e.g. Kapp et al., 2005, 2007; Leier et al., 2007). In addition, sedimentary and meta-sedimentary rocks in both the Qiangtang and Lhasa terranes contain detrital zircons with U-Pb age populations of 2480 Ma, ~1890 Ma, ~980 Ma, ~800 Ma, ~620 Ma, ~540 Ma, and ~470 Ma (Fig. 5D; Kapp et al., 2005, Leier et al., 2007; Dai et al., 2012). Unlike in the other three areas mentioned above, the Paleoproterozoic and Archean populations are largely represented (over 75% of the total). Finally, Cenozoic volcanic activity is also widely distributed within those two blocks, with ages ranging between early Paleogene to late Miocene in the Lhasa block and early Paleocene to late Oligocene in the Qiangtang block (e.g. Ding et al., 2007; C. Wang et al., 2008; Xia et al., 2011).

The Hoh Xil basin contains a series of Mesozoic to Cenozoic stratigraphic sequences (Fig. 1; C. Wang et al., 2008a; Dai et al., 2012). Detrital zircon ages from the Cenozoic strata throughout the basin are dispersed between ~2800 Ma and ~60 Ma with major age peaks of ~800 Ma, ~440 Ma, ~260 Ma, and ~120 Ma (Dai et al., 2012). L. Y. Zhang et al. (2014) recently obtained eight sensitive high-resolution ion microprobe (SHRIMP) zircon U-Pb ages ranging from 225 Ma to 193 Ma from intrusives units. These are interpreted to be a consequence of the Mesozoic closure of the Paleo-Tethys Ocean. Late Oligocene to late Miocene volcanic rocks are also widespread in the central and eastern part of the Hoh Xil

basin and Pliocene ages have been reported from its western edge (e.g. Xia et al., 2011). Recently, Staisch et al. (2014) reported zircon U-Pb ages clustering around 60 Ma from a tuff layer interbedded within the sedimentary strata.

To summarize, the basement of the Eastern Kunlun Range displays a dominantly bimodal distribution of Mesozoic and Paleozoic ages, with some minor components (less than 10% of the total) of Proterozoic and Archean ages. The sediments of the Hoh Xil basin also contain those two age groups but they are associated to a much larger proportion of Proterozoic to Archean ages (over 30% of the total) and to late Mesozoic (mostly Cretaceous) ages, which are most probably derived from the Qiangtang and Lhasa terranes to the south. Finally, Cenozoic ages from volcanic rocks are widespread within the Lhasa and Qiangtang blocks, in the Hoh Xil basin, and to a more limited amount (less than 5% of the total) in the Eastern Kunlun Range.

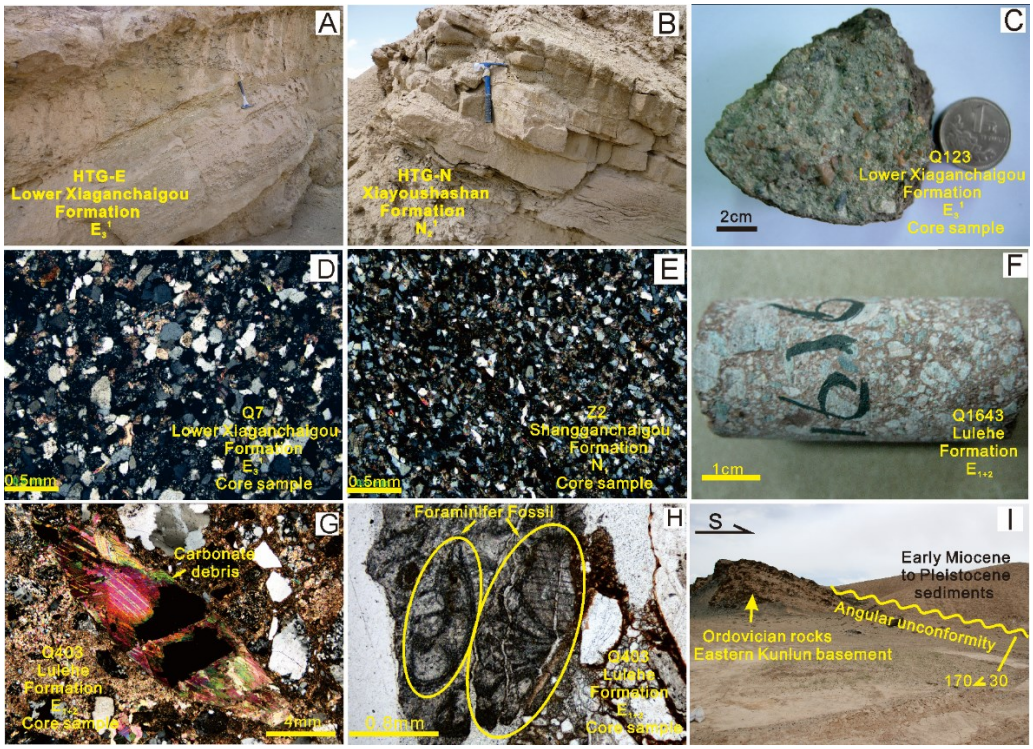


Figure 7. (A) Gray-yellow sandstones interbedded with conglomerates of the middle Eocene Lower Xiaganchaigou Formation ($E_3^1$) in the Huatugou section. (B) Gray-yellow sandstones interbedded with mudstones of the middle Miocene Xiayoushashan Formation (N21) in the Huatugou section. (C) Core sample of grayish white conglomerates of the middle Miocene Lower Xiaganchaigou Formation ($E_3^1$) in the Kunbei section. (D–E) Microscopic characteristics (crossed polarized light) of the middle Eocene to Oligocene sandstone core samples from the Kunbei section. Note the large number of lithic fragments, the fining of the grain size, and the increasing textural maturity from middle Eocene to Oligocene. (F) Core sample of conglomerates of the Paleocene Lulehe Formation ($E_{1+2}$) in the Kunbei section. (G) Carbonate debris included in conglomerates of the Paleocene Lulehe Formation ($E_{1+2}$) in the Kunbei section (core sample, crossed polarized light microphotograph). (H) Foraminifera in

carbonate debris within conglomerates of the Paleocene Lulehe Formation ($E_{1+2}$) in the Kunbei section (core sample, plane polarized light microphotograph). (I) Angular unconformity between the early Miocene to Pleistocene sediments and the Ordovician basement rocks of the Tanjianshan Group in the Adatan valley.

Table 1 Summary of major characteristics and the corresponding statistical data for of the samples

| Epoch | Formation | Sample number | GPS data/well number | Description | Detrital zircon age range (Ma) | Detrital zircon peaks (Ma) | Number of effective data points | Th/U ratios |
|---|---|---|---|---|---|---|---|---|
| Huatugou Section | | | | | | | | |
| Pleistocene | Qigequan Fm. | CSL5 | 38°20′40.5″ N; 90°41′20″ E | Gray-white fine-grained sandstones, well-sorted. | 211~2430 | ~260 ~420 ~860 | 98 | 0.04, 0.07, 0.09, 0.15~ 1.48 |
| Pliocene | Shizigou Fm. | SZG1 | 38°18′7″ N; 90°50′53.8″ E | Gray-yellow fine-grained sandstones, well-sorted. | 211~2430 | ~240 ~430 ~890 | 93 | 0.03, 0.09, 0.14~2.15 |
| Middle Miocene | Shangyou shashan Fm. | CSL4 | 38°22′5.4″ N; 90°48′10.6″ E | Brown fine-grained sandstones, well-sorted. | 202~2378 | ~220 ~430 ~880 | 95 | 0.03, 0.06, 0.08, 0.09, 0.11~2.00 |
| Middle Miocene | Shangyou shashan Fm. | SZG2 | 38°18′7″ N; 90°50′53.8″ E | Brown fine-grained sandstones, well-sorted. | 234~2019 | ~250 ~440 ~876 | 90 | 0.03, 0.04, 0.08, 0.10-1.20 |
| Early Miocene | Xiayousha shan Fm. | HTG-N | 38°25′53″ N; 90°53′15″ E | Gray-white fine-grained sandstones, well-sorted. | 235~2378 | ~260 ~400 | 95 | 0.12~1.56 |
| Middlc Eocene | Lower Xiagancha igou Fm. | HTG-E | 38°25′00″ N; 90°53′00″ E | Gray-white medium-grained sandstones, well-sorted. | 181~2662 | ~260 ~430 | 98 | 0.22~1.59 |
| Dongchaishan-Gansen Section | | | | | | | | |
| Holocene | Dabuxun-Yanqiao Fm. | STB1 | 37°31.6′ N; 92°11.2′ E | Gray-yellow coarse-grained sandy conglomerate, poorly sorted. | 109, 209~2573 | ~210 ~430 ~900 | 89 | 0.08, 0.10~2.15 |
| Pleistocence | Qigequan Fm. | JS04 | 37°47.9′ N; 91°33′ E | Gray-white fine-grained sandstones, well-sorted. | 56, 217~2430 | ~290 ~420 ~780 | 57 | 0.03, 0.07, 0.11~1.19 |
| Middle Miocene | Xiayousha shan Fm. | STB3 | 37°28′48″ N; 92°18′32.8″ E | Gray-yellow fine-grained sandstones, well-sorted. | 200~1350 | ~215 ~410 ~900 | 89 | 0.19~1.58 |
| Early Miocene | Xiayousha shan Fm. | GS-N | 37°28′53″ N; 92°19′27″ E | Brown medium-grained sandstones, well-sorted. | 128~2091 | ~220 ~400 ~890 | 97 | 0.13~1.57 |
| Oligocene | Shanggan chaigou | STB2 | 37°29′24.2″ N; 92°11′16.7″ E | Gray-yellow fine-grained | 200~1900 | ~220 ~390 | 93 | 0.12~1.03 |

| | | | | | | | | |
|---|---|---|---|---|---|---|---|---|
| | Fm. | | | sandstones, well-sorted. | | ~890 | | |
| Middlc Eocene | Lower Xiagancha igou Fm. | GS-E | 37°28′29.2″N; 92°8′39″ E | Gray- white fine-coarse-grained sandstones, well sorted. | 240~3000 | ~250 ~450 ~890 | 52 | 0.02~2.19 |
| Kunbei Section | | | | | | | | |
| Oligoc ene | Shanggan chaigou Fm. | Z2 | Zha 2 well | Gray-white fine-grained sandstones, well-sorted. | 173~1086 | ~230 ~400 ~ | 69 | 0.10~1.30 |
| Middlc Eocene | Lower Xiagancha igou Fm. | Q7 | Qie 7 well | Gray-white fine-grained sandstones, well-sorted. | 203~2621 | ~250 ~410 | 88 | 0.08, 0.10~2.25 |
| Middlc Eocene | Lower Xiagancha igou Fm. | Q123 | Qie 123 well | Gray coarse-grained sandstones, poorly sorted. | 276~472 | ~280 ~420 | 91 | 0.04, 0.32~1.51 |
| Early Eocene | Lulehe Formation | Q1643 | Qie 1616 well | Brownish red coarse-grained sandstone, poorly sorted. | 224~2026 | ~230 ~390 | 46 | 0.12~2.05 |
| Early Eocene | Lulehe Formation | Q1618 | Qie 1618 well | Brownish red coarse-grained sandstone, poorly sorted. | 219~1994 | ~430 | 96 | 0.17~0.99 |
| Early Eocene | Lulehe Formation | Q403 | Qie 403 well | Brownish red coarse-grained sandstone, poorly sorted. | 272~2459 | ~470 | 84 | 0.29~0.96 |
| Adatan Section | | | | | | | | |
| Holoce ne | Dabuxun-Yanqiao Fm. | ADT3 | 37°45′24.9″ N; 89°56′39.1″ E | Gray-white coarse-grained conglomerate, poorly sorted. | 226, 340~387 | ~360 | 98 | 0.39~1.11 |
| Pleisto cence | Qigequan Fm. | ADT6 | 37°41′19.9″ N; 89°55′10.5″ E | Brown fine-grained sandstones, well-sorted. | 222~2133 | ~230 ~380 | 83 | 0.14~1.00 |
| Early Mioce ne | Xiayousha shan Fm. | ADT4 | 37°44′31.7″ N; 89°55′28.5″ E | Gray-yellow grained sandstones, well-sorted. | 37, 177~1857 | ~220 ~410 ~447 ~776 ~890 | 51 | 0.02, 0.07, 0.18~2.45 |
| Early Mioce ne | Xiayousha shan Fm. | ADT1 | 37°47′50.9″ N; 89°55′19.9″ E | Gray-yellow coarse-grained sandy conglomerate, poorly sorted. | 206~1824 | ~220 ~380 | 73 | 0.06, 0.09, 0.22~2.09 |

### 2.2.4 Stratigraphy and sedimentary characteristics of the sections

The four selected sections are located in the southwestern Qaidam basin, close to the northern flank of the Qimen Tagh Range that belongs to the western part of the Eastern Kunlun Range (Figs. 1 and 2; Cheng et al., 2014). Within the Huatugou and Dongchaishan- Gansen

sections, all the Cenozoic formations described above in the geological setting are exposed except for the Lulehe Fm. The Kunbei section was constructed using well data that sample the complete Cenozoic sequences including the Lulehe Fm. Finally, the Adatan section from the Qimen Tagh Range is restricted to the late Upper Oligocene to present sequences (Fig. 4). A brief description of the lithologies, sediment facies and paleocurrents directions obtained from fieldwork and drill-core data in each section is given next.

The Huatugou section is located in the northernmost part of the prominent Yingxiongling uplift structure (Fig. 2). Except for the Lulehe Fm., the whole Cenozoic sequence is well exposed (Figs. 2 and 6). The over 180 m thick Lower Xiaganchaigou Fm. is composed mainly of grey green, green yellow sandstones and pebbly sandstones at the base, evolving upward towards brown red sandstones and siltstones. The sediment facies vary from fluvial to shallow lake deposits upward (Figs. 6 and 7A; Zhuang et al., 2011; Wu et al., 2012). The ~750 m thick Upper Xiaganchaigou Fm. rests conformably on the Lower Xiaganchaigou Fm. and consists mainly of earthy yellow, grey green sandstones, greyish-green silty mudstones and argillaceous siltstones intercalated with calcareous shales. The sediment facies vary upward from braided river to shallow lake deposits (Fig. 6; Wu et al., 2012). Paleocurrents are consistently directed towards the NE (Fig. 6; Meng and Fang, 2008). The over 800 m thick Shangganchaigou Fm. again rests conformably on the Upper Xiaganchaigou Fm. It is mainly composed of greyish-green carbonaceous mudstones and sandstones interbedded with grey-white mudstones. The sediment facies correspond to deltaic to shallow lake deposits (Fig. 6). Reported paleocurrent directions for this formation vary from SE (Fig. 6; Meng and Fang, 2008) to S-SSW (Wu et al., 2012) depending on the authors. The over 700 m thick Xiayoushashan Fm. conformable with the Shangganchaigou Fm., is mainly composed of yellowish-brown, purple red conglomerates, pebbly sandstones, sandstones and argillaceous siltstones with intercalations of thick-bedded limestones. The facies vary from shallow lake to fluvial deposits (Figs. 6 and 7B). Paleocurrent directions are variable but have three main orientations: towards the NE, SE and SW (Zhuang et al., 2011; Wu et al., 2012). The ~1000 m thick Shangyoushashan Fm. unconformably overlies the Xiayoushashan Fm. and consists of earthy yellow pebbly sandstones, sandstones and silty mudstones (Fig. 6). The sediment facies is characterized by shallow lake, alluvial plain and braided river deposits (Wu et al., 2012). Paleocurrents are mostly oriented towards the NE (Zhuang et al., 2011), although Wu et al. (2012) again report S to SSW paleocurrent directions probably due to local topography or to local effects of river meandering. The 190 m thick Shizigou Fm., again lying unconformably on the Shangyoushashan Fm., is mainly composed of earth-yellow sandstones and silty

mudstones corresponding to fluvial facies sediments (Fig. 6). Paleocurrent measurements indicate a S-SW flow direction (Fig. 6; Zhuang et al., 2011; Wu et al., 2012). The Qigequan and Dabuxun-Yanqiao Formations, resting unconformably on the Shizigou Fm., are mainly composed of grey and brown sandstones and conglomerates corresponding to flood plain and alluvial facies deposits (Fig. 6).

The Dongchaishan-Gansen section is situated within the southeastern part of the Yingxiongling structure (Fig. 2). The over 600 m thick Xiaganchaigou Fm. is composed of grey white conglomerates, grey brown sandstones and mudstones with intercalations of limestones and gypsum layers. The unit shows a distinct fining-upward sequence evolving from deltaic sediment facies at the base, to shore shallow lacustrine facies at the top (Fig. 6). The 700 m thick Shangganchaigou Fm., conformably resting on the Upper Xiaganchaigou Fm., consists of brownish green siltstones, grey sandstones, mudstones and limestones. This series is dominated by horizontally bedded deep lacustrine sediment facies (Fig. 6). The over 1000 m thick Xiayoushashan Fm., lying conformably on the Shangganchaigou Fm., is mainly composed of brownish red siltstones, brownish yellow mudstones and limestones successions corresponding to deep lacustrine facies deposits. The sedimentary sequence displays a generally retrograding cycle (Fig. 6) from its lower to its middle part (increasing frequency of limestone layers and horizontal beddings within the sandstones), followed by a prograding cycle from its middle to its upper part (increasing frequency of sandstones layers). Paleocurrent directions in that formation are N-NE (Fig. 6; Hertz et al., 2005; Zhuang et al., 2011). The 300 m thick Shangyoushashan Fm., lying unconformably on the Xiayoushashan Fm., is composed of grey mudstones, sandstones, siltstones with intercalations of limestones. The sedimentary sequence generally shows a progradation cycle characterized by shore to shallow lacustrine facies in the lower part and deltaic facies in the upper part of the section. The over 200 m thick Shizigou Fm., resting unconformably on the Shangyoushashan Fm., consists mainly of cross-bedded coarse grey white sandstones and grey brown conglomerates corresponding to fluvial deposits (Fig. 6). Paleocurrent directions in both the Shangyoushashan and Shizigou Formations are strongly unimodal towards N-NE (Fig. 6; Meng and Fang, 2008; Zhuang et al., 2011). As in the Huatugou section, the Qigequan and the Dabuxun-Yanqiao Formations (Yin et al., 2007) rest unconformably on the Shizigou Fm. They mainly consist of a succession of grey and brown sandstones and conglomerates corresponding to flood plains deposits (Fig. 6).

The Kunbei section, established on the basis of core data, is located along the northern flank of the Qimen Tagh Range (Fig. 2). Except for the occurrence of the Lulehe Fm., the

stratigraphy and sedimentary characteristics of both the Dongchaishan-Gansen and the Kunbei sections are similar (Figs. 6, 7C, 7D and 7E). In front of the Eastern Kunlun Range, the Altyn Tagh Range and the Qilian Shan, the Paleocene Lulehe Fm. is characterized by coarse-grained detrital sediments corresponding to braided river to deltaic sediment facies (Xia et al., 2001; Wu et al., 2012). The thickness of the formation generally increases towards the center of the Qaidam basin (Xia et al., 2001; Yin et al., 2008b). In the Kunbei section, the Mesozoic strata are missing and the Lulehe Fm. unconformably overlies the Eastern Kunlun crystalline basement (Paleozoic granitoid intrusions). Locally, the thickness of the formation may not exceed 200 m. The lithology is dominated by feldspathic litharenite and lithic arkoses. The strata show poor compositional and textural maturity, characterized by poorly sorted and poorly rounded clasts (Fig. 7F and 7G). The clasts are dominated by granitic grains, metamorphic fragments and some carbonate debris which are composed mainly of biosparite containing abundant foraminifera (Fig. 7G and 7H). The size of the carbonate debris is relatively large ranging from 5 to 30 mm. As carbonate is easily dissolved, it is assumed that carbonate fragments are generally not transported over long distances (Zuffa, 1980; Mack and Rasmussen, 1984), and thus the source area of the clasts preserved within the Lulehe Fm. must be relatively proximal. As a consequence of poor exposure, no paleocurrent data are available for the Paleocene series in the SQB. However, based on heavy mineral contents, calculated Zircon-Tourmaline-Rutile (ZTR) indices and the heavy mineral assemblages for the drill core samples from a large number of oil wells in the Kunbei section, Gong et al. (2012) and Fu et al. (2013) suggested that during the deposition of the Paleocene Lulehe Fm., the material deposited in the Kunbei area was derived from the south, probably from the Eastern Kunlun Range. In addition, the Carboniferous strata, largely exposed south of the Kunbei section (Fig. 2), consist mainly of biomicrite, biosparite, and bioclastic littoral to neritic limestones containing abundant brachiopods, coral, gastropods and foraminifera that could represent the source of the Lulehe Fm. carbonate clasts (QIGS, 2004).

The Adatan section is located within the Adatan valley between the two main sub-ranges forming the Qimen Tagh Range (Fig. 2). In this section, only the Xiayoushashan, Qigequan and Dabuxun-Yanqiao Formations are exposed, with the other formations being absent due to erosion. The Xiayoushashan Fm., unconformably resting on the Ordovician metamorphic basement (Fig. 7I), is composed of conglomerates, pebbly sandstones, siltstones and calcilutites. The sediment facies evolve upward from deltaic to shallow lake deposits (SIGS, 2003). The Qigequan Fm., unconformably overlying the Shizigou Fm., consists of conglomerates intercalated with sandstones and mudstones and mainly corresponds to alluvial

facies deposits (QIGS, 2004). Finally, the Dabuxun-Yanqiao Fm. is mainly composed of variegated gravels, erratic blocks, sandy soil and clay deposits of alluvial fan and fluvial facies (QIGS, 2004).

In general, from the Eocene to the Miocene, the sediments in the SQB are composed of lithic feldspar sandstones and lithic sandstones, with only a slight variation in composition (e.g. Fig. 7D). The lithic fragments are mainly of volcanic and magmatic origin, although a small proportion has a sedimentary origin, indicating that recycling of the Eocene to Miocene strata in the Qaidam basin is weak (Rieser et al., 2005, 2007; Xia et al., 2012). Material directly derived from the erosion of basement rocks in the source areas provides the largest contribution to the sediment deposited in the basin during that period.

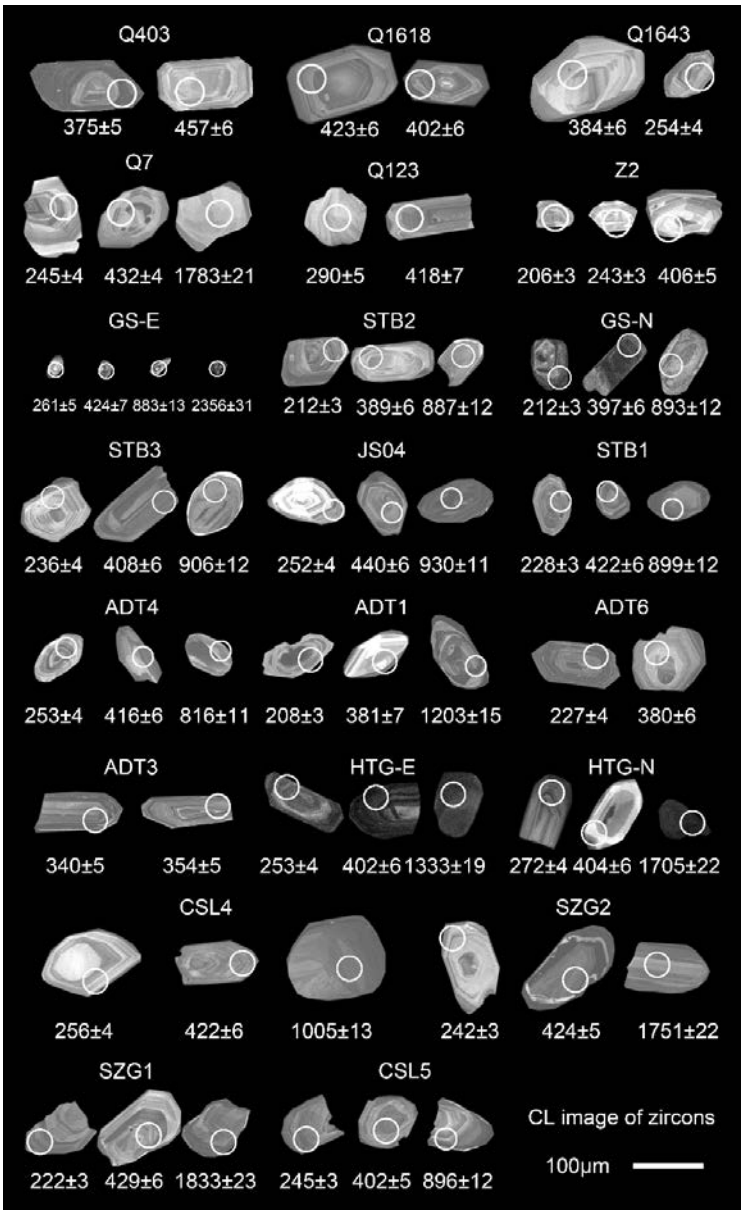


Figure 8. Representative cathodoluminescence (CL) images of detrital zircons from the 22 sandstone

samples. The white circles show the location of the U-Pb analysis spots. Numbers are U-Pb ages in Ma.

### 2.2.5 Sampling and analytical methods

Over the last decade or so, detrital zircon U-Pb geochronology has evolved into a very powerful provenance tool for reconstructing landscape evolution and tectonics. This is achieved by systematically relating detrital zircon age populations measured on sediments back to the potential source terranes ages (e.g., Fedo et al., 2003; Gehrels et al., 2011; D.D. Liu et al., 2013; Yang et al., 2013, 2014; Gehrels, 2014; F. Cheng et al., 2015). In this study, 22 samples, ranging in stratigraphic age from Paleocene to Quaternary, were collected from the four sections (Figs. 2, 6, and 7). Six samples from the Kunbei section were recovered from well cores. The major characteristics of the samples are briefly described in Table 1.Zircon grains were extracted from each sample following the standard procedures outlined in Yang et al. (2014). This work was conducted at the Chengxin Geology Service Co. Ltd., Langfang, Hebei Province, China. Individual zircon crystals (generally more than 200 grains) were mounted in epoxy resin without handpicking to avoid sampling bias. Samples were then polished to obtain a smooth flat internal surface. Reflected and transmitted light microscopy, as well as cathodoluminescence (CL) imagery, was undertaken to reveal internal heterogeneities and to select internal targets for isotopic dating. The U-Pb dating of zircon was performed on an Agilent 7500a ICP-MS connected to a 193 nm excimer laser-ablation system of an American New Wave UP 193 SS at the China University of Geosciences, Beijing, following the method described by Yang et al. (2014). All samples were analyzed using a laser spot size of 36 mm and a frequency of 10 Hz, except for GS-E, which was analyzed using a laser spot size of 25 mm and a frequency of 5 Hz due to the small grain size. To correct for instrument fluctuations and determine fractionation factors, two standards (Black et al., 2003; Qi et al., 2005) were analyzed every 10–20 grains. Zircons Qinghu and 91500 (Wiedenbeck et al., 1995) were the monitoring standards. For elemental concentration analysis, NIST610 was the external standard, and 29Si was the internal standard. NIST612 and NIST6 14 were used as monitoring standards. GLITTER 4.4 software was used to calculate the U-Pb isotope ratios and element contents (China University of Geosciences, laboratory of Y.S. Liu, Beijing, China). The U-Pb ages obtained were checked for discordance by plotting the analyses on concordia diagrams using the Isoplot 3.0 software (Ludwig, 2003). The common-Pb correction followed the method described by Andersen (2002). Ages younger than ca. 1000 Ma are based on common Pb–corrected $^{206}Pb/^{238}U$ ratios, whereas ages older than ca. 1000 Ma are based on

common Pb–corrected $^{207}Pb/^{206}Pb$ ratios. The U-Pb ages reported are those from analyses that range between 90% and 110% concordance, and reported errors are 1s. A more complete description of sample separation methods and analytical procedures is given in Yuan et al. (2004). Isotopic ages with errors and related raw data are listed in full in Table DR2 (see footnote 1). Representative CL images are provided in Figure 8.

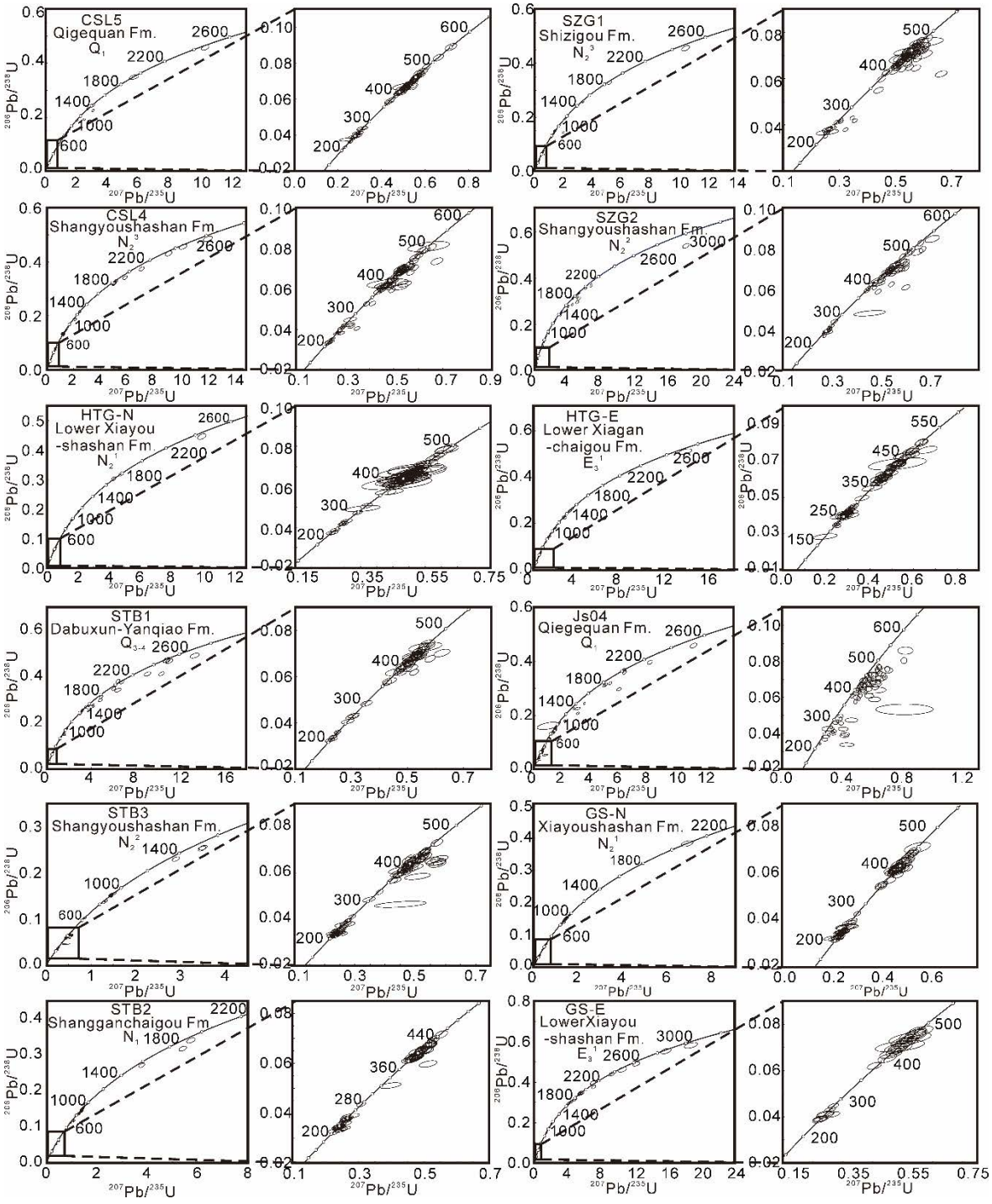


Figure 9. U-Pb concordia diagrams for zircon grains of the samples in the Huatugou and Dongchaishan-Gansen sections.

### 2.2.6 Results

The various zircon age ranges and the summary statistical data for each sample are shown in Table 1 (Figs. 9–15). Major age groups and their corresponding peak ages have been inferred by visual inspection of the detrital zircon U-Pb age probability plots for all 22 samples (Figs. 10, 11, 13, 14, and 15). A major peak refers to age populations including at least 50% of the total number of data, whereas a minor peak refers to those representing less than 20% of the total number of data.

#### 2.2.6.1 Huatugou section

Sample: HTG-E (Xiaganchaigou Fm., 43.8-37.8 Ma)

The zircon grains are generally large (50 μm ~ 150 μm) with well-preserved euhedral shapes. While a few grains show only faint zoning in CL suggesting a metamorphic origin, more than 90% of the crystals are characterized by relatively distinct oscillatory zoning (Fig. 8) indicating a magmatic origin. The Th/U ratios vary from 0.22 to 1.59, also indicative of a magmatic origin (Corfu et al., 2003; Hanchar and Rudnick, 1995; Hoskin and Black, 2000). Of 100 zircons analyzed, 98 ages have been obtained with discordance degree <10% (Fig. 9). U-Pb ages range from ~2662 Ma to ~181 Ma, with two peaks at ~430 Ma and ~260 Ma. A number of ages are spread between 2662 Ma and 500 Ma with 18% of the data clustering between 1500 Ma and 500 Ma (Fig. 10).

Sample: HTG-N (Xiayoushashan Fm., 22-15.3 Ma)

In this sample, zircon grains show euhedral to abraded shapes with an average size ranging between 80 μm and 200 μm. A large majority of crystals (about 90%) display distinct oscillatory zoning on CL images indicating a magmatic origin (Fig. 8). The Th/U ratios vary from 0.12 to 1.56 again indicating a magmatic origin. Among 100 analyses, 95 yield concordant ages (Fig. 9). U-Pb ages range from ~2378 Ma to ~235 Ma, with a small peak at ~260 Ma, a major peak at ~400 Ma and a possible sub-peak at ~960 Ma (Fig. 10).

Samples: SZG2 and CSL4 (Shangyoushashan Fm., 15.3-8.1 Ma)

Both samples were collected from the Shangyoushashan Fm. Zircon grains show euhedral to abraded shapes with an average size ranging between 50 μm and 250 μm. Most of the crystals (more than 90%) display distinct oscillatory zoning on CL images implying a magmatic origin (Fig. 8). However, like in the previous samples a few grains (less than 10%) show only faint zoning in CL suggesting a metamorphic origin.

For sample SZG2, 100 analyses were performed, providing 90 zircon ages with a discordance degree <10% (Fig. 9) and the Th/U ratios vary from 0.10 to 1.20, with three

exceptions of 0.03 (1473 Ma), 0.04 (637 Ma) and 0.08 (493 Ma), confirming the magmatic origin. U-Pb ages range from ~2019 Ma to ~234 Ma with two peaks at ~440 Ma and ~250 Ma. Some additional ages (less than 20%) are spread between ~1992 Ma and ~523 Ma with a potential sub-peak at ~870 Ma. The number of ages belonging to this last age group appears higher than in the previous samples. In sample CSL4, 95 ages were obtained from 100 analyzed zircon grains (Fig. 9). The Th/U ratios of the detrital zircons mainly vary from 0.11 to 2.00, with four exceptions of 0.03 (413 Ma), 0.06 (906 Ma), 0.08 (960 Ma) and 0.09 (947 Ma), reflecting the largely magmatic origin of the zircons. U-Pb ages range from ~2378 Ma to ~235 Ma, with three peaks at ~880 Ma, ~430 Ma and ~220 Ma. Some ages are again spread from 800 Ma to 1020 Ma (Fig. 10).

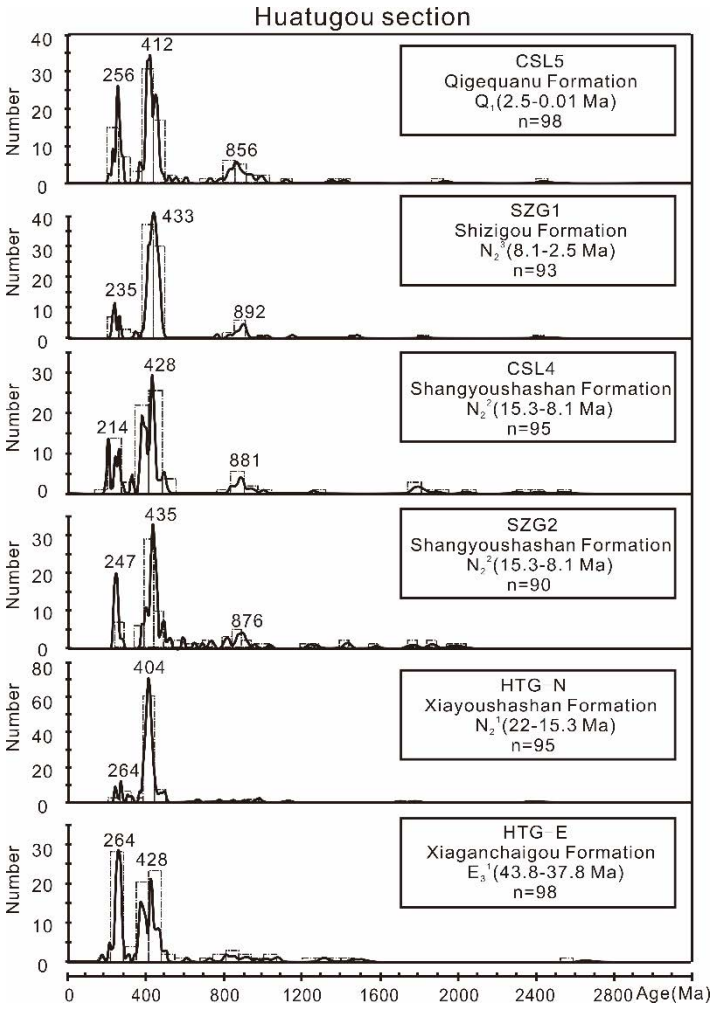


Figure 10. Relative probability plot histograms of U-Pb ages of detrital zircons from the Cenozoic samples in the Huatugou section. The number of zircons is given on the vertical axis (note the change in scale from one sample to the other); the ages, in Ma, are indicated on the horizontal axis.

Sample: SZG1 (Shizigou Fm., 8.1-2.5 Ma)

The zircon grains show euhedral to abraded shapes with an average size ranging between 80 μm and 200 μm. Again, most crystals (more than 90%) display a distinct oscillatory zoning on CL images indicating a magmatic origin. The Th/U ratios vary from 0.14 to 2.15, with two exceptions of 0.03 (440 Ma) and 0.09 (911 Ma), again suggesting a magmatic origin. 93 usable data points were obtained among 100 analyzed zircon grains (Fig. 9). U-Pb ages range from ~2421 Ma to ~222 Ma, with three peaks at ~890 Ma, ~430 Ma and ~240 Ma (Fig. 10).

Sample: CSL5 (Qigequan Fm., 2.5-0.01 Ma)

The zircon crystals are generally large (50 μm ~ 200 μm) with well-preserved euhedral shapes. Again, only a few grains (about 5%) show faint zoning in CL suggesting a metamorphic origin and most crystals display distinct oscillatory zoning characteristic of their magmatic origin (Fig. 8). The Th/U ratios vary from 0.15 to 1.48, with three exceptions of 0.04 (448 Ma), 0.07 (864 Ma) and 0.09 (462 Ma), confirming the predominant magmatic origin of the zircons. Among 100 analyzed zircons, 98 U-Pb ages with discordance degree <10% have been obtained (Fig. 9). U-Pb ages range from ~2430 Ma to ~211 Ma, with two major peaks at ~420 Ma and ~260 Ma and a minor peak at ~860 Ma (Fig. 10).

#### 2.2.6.2 Dongchaishan-Gansen section

Sample: GS-E (Xiaganchaigou Fm., 43.8-37.8 Ma)

The zircon grains morphologies vary from euhedral to abraded with an average size (25 μm ~ 70 μm) distinctly smaller than in any of the other samples. CL images (Fig. 8) show that most of these crystals (more than 90%) are characterized by relatively distinct oscillatory zoning indicating a magmatic origin. Only a few (less than 5%) show faint zoning suggesting a metamorphic origin. This is confirmed by the Th/U ratios that vary between 0.12 and 2.19, with three exception of 0.02 (437 Ma), 0.02 (965 Ma), and 0.05 (985 Ma), and are predominantly higher than 0.10, reflecting that magmatic zircons are in majority (Hoskin and Black, 2000).

Due to the small number of available grains, only 56 zircon crystals were analyzed providing 52 concordant ages (Fig. 9). U-Pb ages range from ~3000 Ma to ~240 Ma, with four distinctive age populations. Two major peaks are at ~450 Ma and ~250 Ma, while a smaller peak at ~890 Ma could be equivalent to the ~850 Ma - ~890 Ma peaks observed in the Huatugou section described above. Finally a number of Proterozoic ages are distributed between 3000 Ma and 1600 Ma (Fig. 11).

Sample: STB2 (Shangganchaigou Fm., 35.2-22 Ma)

In this sample, zircon crystals are large (80 μm ~ 200 μm) with well-preserved euhedral shapes. Most of the crystals (more than 95%) are characterized by a relatively distinct oscillatory zoning in CL images (Fig. 8) implying a magmatic origin. The Th/U ratios vary from 0.12 to 1.03, and are mostly higher than 0.10, confirming the predominantly magmatic origin of the zircons.

Among 100 analyzed crystals, 93 effective ages were obtained (Fig. 9). U-Pb ages range between ~1900 Ma and ~200 Ma, with two major peaks at ~390 Ma and ~220 Ma and one minor peak at ~890 Ma. The proportion of ages older than 1000 Ma is much smaller than in

sample GS-E (Fig. 11).

Sample: GS-N and STB3 (Xiayoushashan Fm., 22-15.3 Ma)

Both samples were collected from the Xiayoushashan Fm. In sample GS-N, the zircon grains have euhedral to abraded shapes and an average size between 40 μm and 100 μm. A large majority of (more than 95%) crystals show a distinct oscillatory zoning in CL images (Fig. 8) indicating a magmatic origin. The Th/U ratios vary from 0.13 to 1.57, again indicating a magmatic source. 100 crystals were analyzed and 97 ages having discordance degree <10% were obtained (Fig. 9). The U-Pb ages range from ~2091 Ma to ~128 Ma (Fig. 11), and can be divided into three populations with two major peaks at ~400 Ma and ~220 Ma, and a minor peak at ~890 Ma. The number of ages older than 1000 Ma is low (less than 5%). A single age at 128 Ma indicates the possibility of a Cretaceous zircon source.

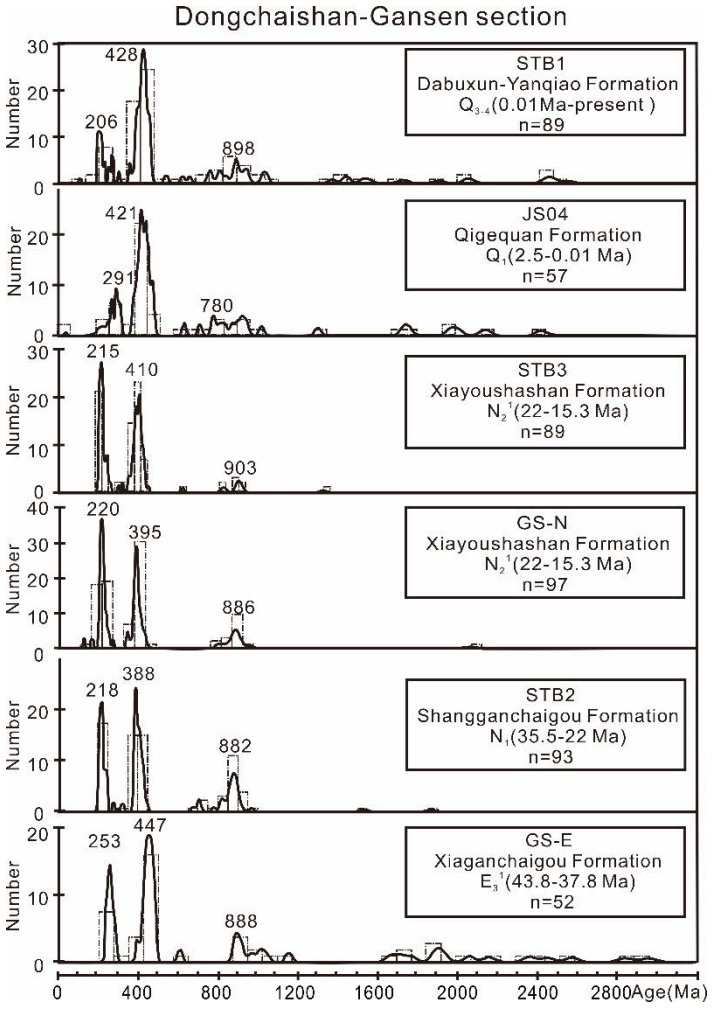


Figure 11. Relative probability plot histograms of U-Pb ages of detrital zircons from the Cenozoic samples in the DongchaishanGansen section (note the change in scale from one sample to the other); the ages, in Ma, are indicated on the horizontal axis.

In sample STB3, the zircon crystals again show euhedral to abraded shapes and an average size between 50 μm and 250 μm. Like in the previous samples most of the crystals (~95%) are of magmatic origin as indicated by distinct oscillatory zoning in CL images (Fig. 8). The Th/U ratios vary from 0.19 to 1.58, confirming the magmatic source. A hundred crystals have been analyzed and 89 yield concordant ages (Fig. 9). U-Pb ages range from ~1350 Ma to ~200 Ma (Fig. 11). The age populations are very similar to the ones observed in

the previous samples, with two major peaks at ~410 Ma and ~215 Ma and a possible minor peak at 900 Ma. Ages older than 1000 Ma are rare.

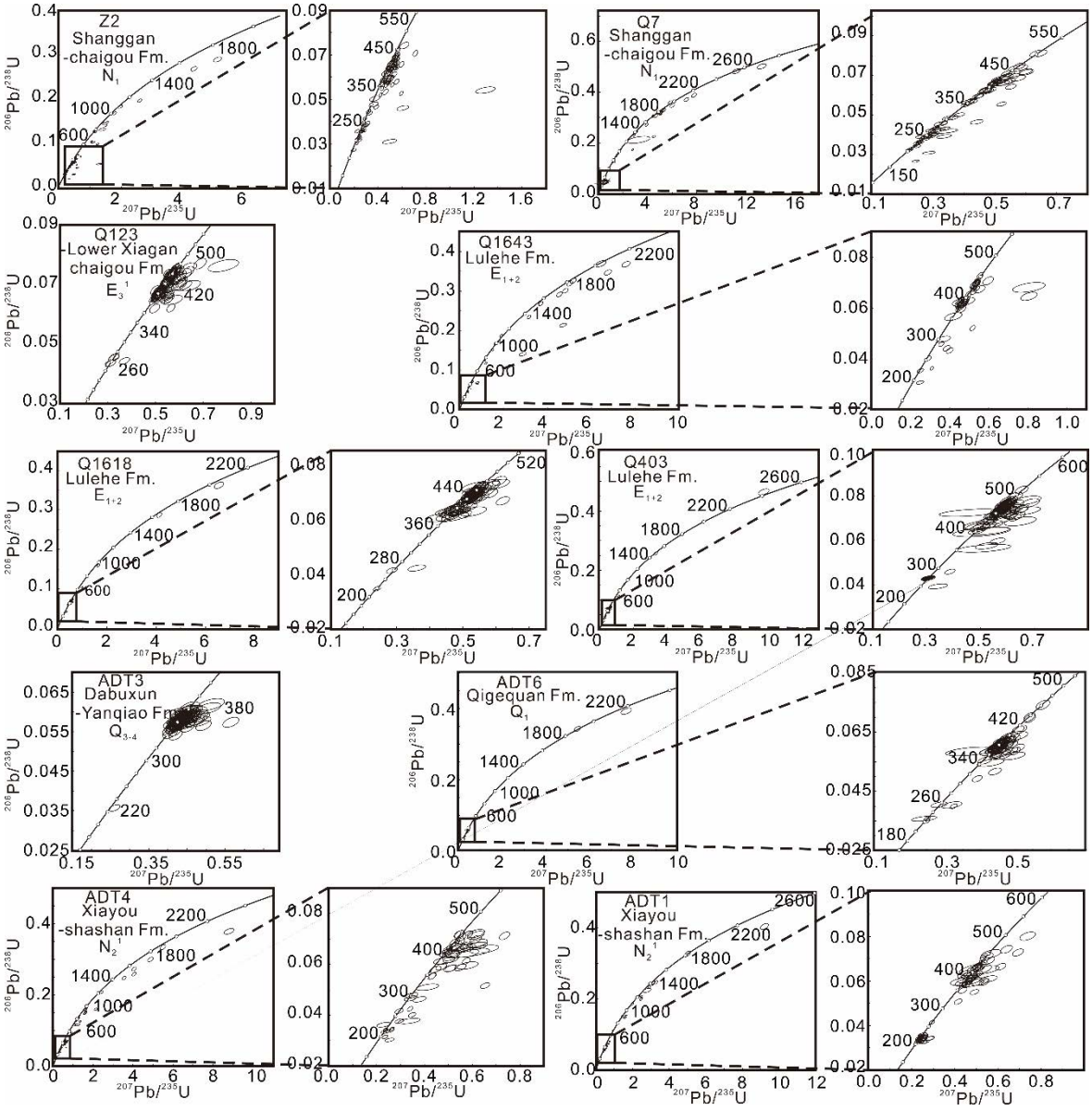


Figure 12. U-Pb concordia diagrams for zircon grains of the samples from the Kunbei and Adatan sections.

Sample: JS04 (Qigequan Fm., 2.5-0.01 Ma)

The zircon crystals display euhedral to abraded shapes for an average size ranging between 50 μm and 200 μm. The majority of the crystals (~95%) display distinct oscillatory zoning in CL images (Fig. 8) indicating a magmatic origin confirmed by Th/U ratios varying between 0.11 and 1.19, with two exceptions of 0.03 (385 Ma) and 0.07 (1828 Ma). Among 100 crystals analyzed, only 57 ages with discordance degree <10% were obtained (Fig. 9). The U-Pb ages range from ~2430 Ma to ~220 Ma (Fig. 11). The ages are distributed in four

groups with two major peaks at ~420 Ma and ~290 Ma, one more restricted peak at ~780 Ma corresponding to a more distributed population and finally a number of ages spread between 2430 Ma and 1200 Ma. A single age of 57 Ma indicates a possible Cenozoic source.

Sample: STB1 (Dabuxun-Yanqiao Fm., 0.01 Ma-present)

In this sample, zircon grains show euhedral to abraded shapes with an average size comprised between 50 μm and 200 μm. Most crystals (more than 90%) are again of magmatic origin as indicated by distinct oscillatory zoning in CL images (Fig. 8) and Th/U ratios varying from 0.10 to 2.15, with one exception of 0.08 (362 Ma). 100 grains were analyzed and 89 effective data points were obtained (Fig. 9). The U-Pb ages range from 2573 Ma to ~109 Ma (Fig. 11). The ages can be separated in four main populations with three peak ages at ~900 Ma, ~430Ma and ~210 Ma. Like in sample JS04 and GS-E a significant number of Proterozoic ages are distributed above 1000 Ma. Finally a single age at 109 Ma is obtained, probably reflecting recycling of a Cretaceous source.

#### 2.2.6.3 Kunbei section

Samples: Q403, Q1618 and Q1643 (Lulehe Fm., 53.5-43.8 Ma)

Three samples were collected from the Lulehe Fm. The zircon grains show euhedral to abraded shapes and an average size between 50 μm and 250 μm. Within all three samples, the majority of the zircons (more than 95%) show distinct oscillatory zoning in CL images indicating a magmatic origin (Fig. 8). Th/U ratios range from 0.29 to 0.96 in samples Q403, from 0.17 to 0.99 in sample Q1618 and from 0.12 to 2.05 in sample Q1643 confirming the magmatic source.

In sample Q403, 84 ages were obtained from 100 analyzed zircon grains (Fig. 12). The U-Pb ages range from ~2459 Ma to ~272 Ma with a single peak at ~470 Ma the few remaining ages being widely distributed (Fig. 13).

In sample Q1618, 96 ages were obtained among 100 analyzed zircon grains (Fig. 12). The U-Pb ages range from ~1994 Ma to ~219 Ma with a single peak at ~430 Ma and some few, widely distributed ages (Fig. 13).

In sample Q1643, due to the small amount of available zircons, only 46 ages were obtained among 62 analyzed grains (Fig. 12). The U-Pb ages range from ~2026 Ma to ~224 Ma with a major peak at ~390 Ma and a potential sub-peak at ~230 Ma (Fig. 13).

Samples: Q123 and Q7 (Xiaganchaigou Fm., 43.8-37.8 Ma)

In these two samples from the Lower Xiaganchaigou Fm., the zircon grains show euhedral to abraded shapes and an average size between 50 μm and 250 μm. Distinct

oscillatory zoning observed in CL images in the majority of the zircons (more than 95%) indicates again a largely magmatic origin (Fig. 8). The Th/U ratios vary from 0.32 to 1.51, with one exception at 0.04 (418 Ma), in sample Q123 and 0.10 to 2.25, with one exception at 0.08 (907 Ma), in sample Q7 confirming the magmatic origin of the crystals.

In sample Q123, 91 ages were obtained among 100 analyzed zircon grains (Fig. 12). This sample displays a narrow range in ages between 472 Ma and 276 Ma (Fig. 13). A major age peak at ~420 Ma is associated to a small sub-peak at ~280 Ma. No Proterozoic ages are observed although we cannot rule out a possible analytical bias (the Proterozoic zircons could be too small or simply badly preserved within the sample).

In sample Q7, 88 ages were obtained from 100 analyzed zircon grains (Fig. 12). The U-Pb ages ranges from ~2621 Ma to ~203 Ma with two major age peaks at ~410 Ma and ~250 Ma (Fig. 13). A sub-peak at ~1780 Ma might be individualized from the widely spread, well-represented Proterozoic age population.

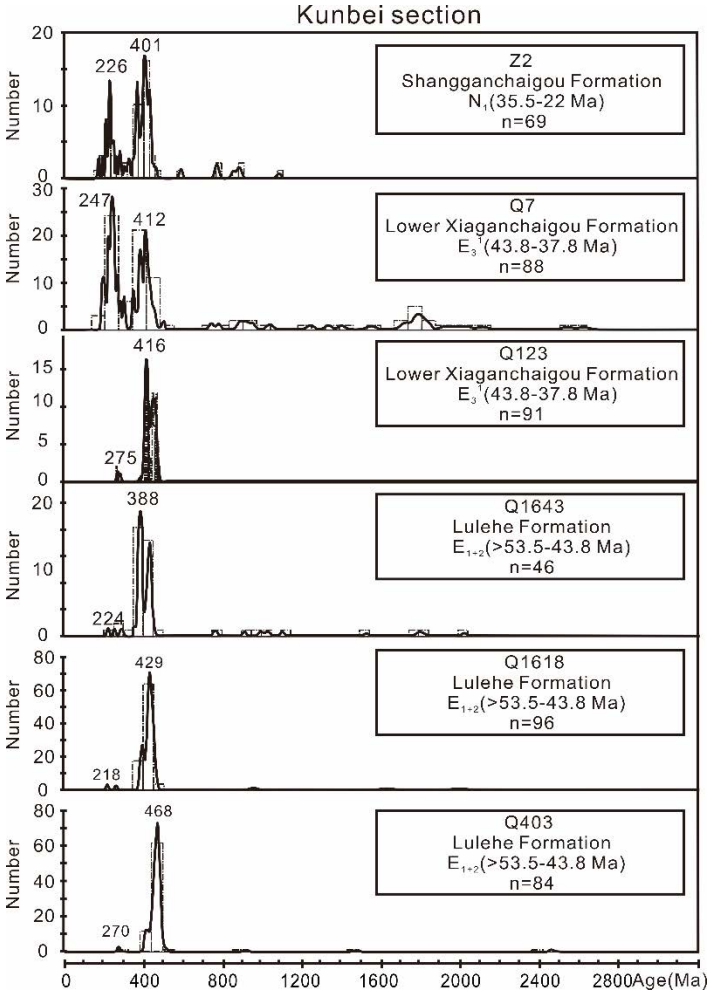


Figure 13. Relative probability plot histograms of U-Pb ages of detrital zircons from the Cenozoic samples in the Kunbei section. The number of zircons is given on the vertical axis (note the change in scale from one sample to the other); the ages, in Ma, are indicated on the horizontal axis

Sample: Z2 (Shangganchaigou Fm., 35.5-22 Ma)

In this sample, zircon grains show euhedral to abraded shapes and an average size between 50 μm and 150 μm. Distinct oscillatory zoning in CL images indicate a magmatic source for a large majority of (~95%) crystals (Fig. 8). The Th/U ratios vary from 0.10 to 1.30 confirming the magmatic source. Ninety-eight crystals have been analyzed and 69 yield

concordant ages (Fig. 12). The U-Pb ages range from ~1086 Ma to ~173 Ma with two major peaks at ~400 Ma and ~230 Ma associated to a potential minor age population around ~770 Ma (Fig. 13).

2.2.6.4 Adatan section

Samples: ADT1 and ADT4 (Xiayoushashan Fm., 22-15.3 Ma)

These two samples were collected from the Xiayoushashan Fm. The zircon grains show euhedral to abraded shapes and an average size between 50 μm and 150 μm. Again, distinct oscillatory zoning in CL images indicates the magmatic origin of most of the crystals (more than 90%) (Fig. 8). The Th/U ratios vary from 0.22 to 2.09, two exceptions of 0.06 (456 Ma) and 0.09 (397 Ma), in sample ADT1 and from 0.18 to 2.45, with two exceptions of 0.02 (442 Ma) and 0.07 (967 Ma), in sample ADT4 confirming the magmatic origin or the zircons.

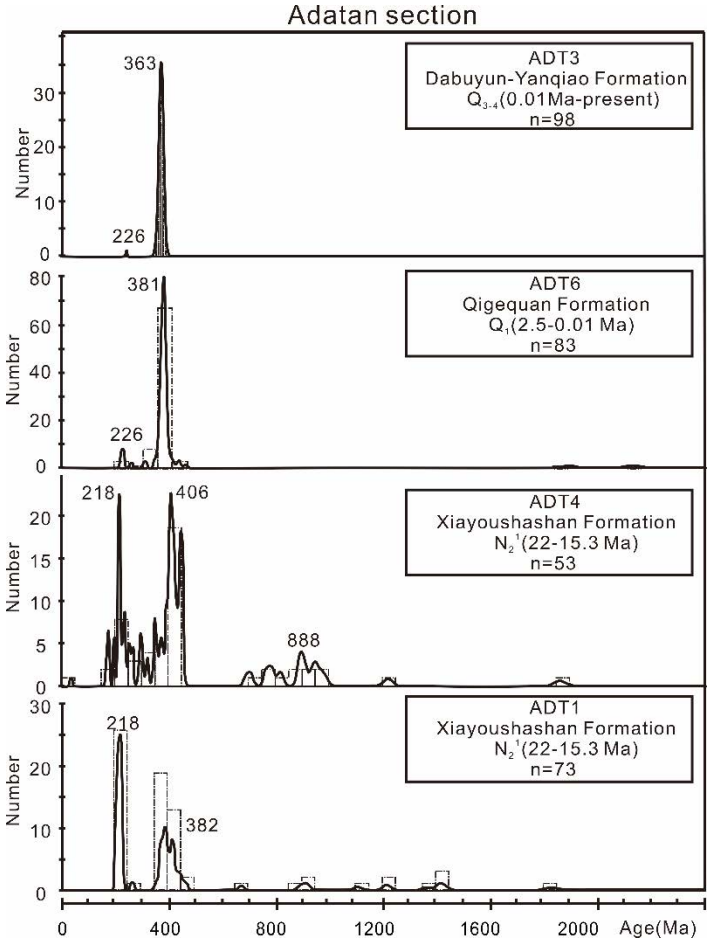


Figure 14. Relative probability plot histograms of U-Pb ages of detrital zircons from the Cenozoic samples in the Adatan section. The number of zircons is given on the vertical axis (note the change in scale from one sample to the other); the ages, in Ma, are indicated on the horizontal axis.

In sample ADT1, 100 crystals were analyzed and yield 73 concordant ages (Fig. 12). The U-Pb ages range from ~1824 Ma to ca. 206 Ma and two major age peaks are individualized at ~380 Ma and ~220 Ma (Fig. 14).

In sample ADT4, among 100 analyses, 51 yield concordant ages (Fig. 12). The U-Pb ages range between ~1857 Ma and ~37 Ma (Fig. 14). Two major peaks are displayed at ~410 Ma and ~220 Ma and a third distinctive small age population is centered around ~890 Ma. A single

age of 37 Ma seems to indicate a Cenozoic source similar to the one suggested by the 57 Ma age in sample JS04 (Dongchaishan-Gansen section).

Sample: ADT6 (Qigequan Fm., 2.5-0.01 Ma)

In this sample from the Qigequan Fm., zircon grains are large (80 μm ~ 250 μm) and show a well-preserved euhedral shape. The magmatic origin of most of the crystals (more than 95%) is indicated by distinct oscillatory zoning in CL images (Fig. 8) and Th/U ratios varying between 0.14 and 1.00. Among 100 analyzed zircons, 83 ages having discordance degree <10% were obtained (Fig. 12). The U-Pb ages ranges from 2133 Ma to 222 Ma, with a major age peak at ~380 Ma and a minor peak around 230 Ma (Fig. 14).

Sample: ADT3 (Dabuxun-Yanqiao Fm., 0.01 Ma-present)

In this sample, the zircon grains show euhedral to abraded shapes and an average size of 100 μm to 200 μm. As in all the other samples, the predominantly (more than 95%) magmatic origin of the crystals is attested by distinct oscillatory zoning in CL images (Fig. 8) and Th/U ratios varying between 0.39 and 1.11. Among 100 analyzed zircons, 98 ages showing discordance degree <10% were obtained (Fig. 12). The U-Pb ages vary from 387 Ma to 226 Ma with a major population around and age peak of ~360 Ma and a single age of 226 Ma (Fig. 14).

2.2.6.5 Summary

The data presented above show that the detrital zircons from the 22 sediment samples ranging in deposition age from Paleocene to Holocene are dominantly of magmatic origin (around 95%). On CL images, most of the Precambrian zircons are characterized by inner cores and outer rings or light zones on the surface (Fig. 8) indicating the occurrence of tectono-magmatic

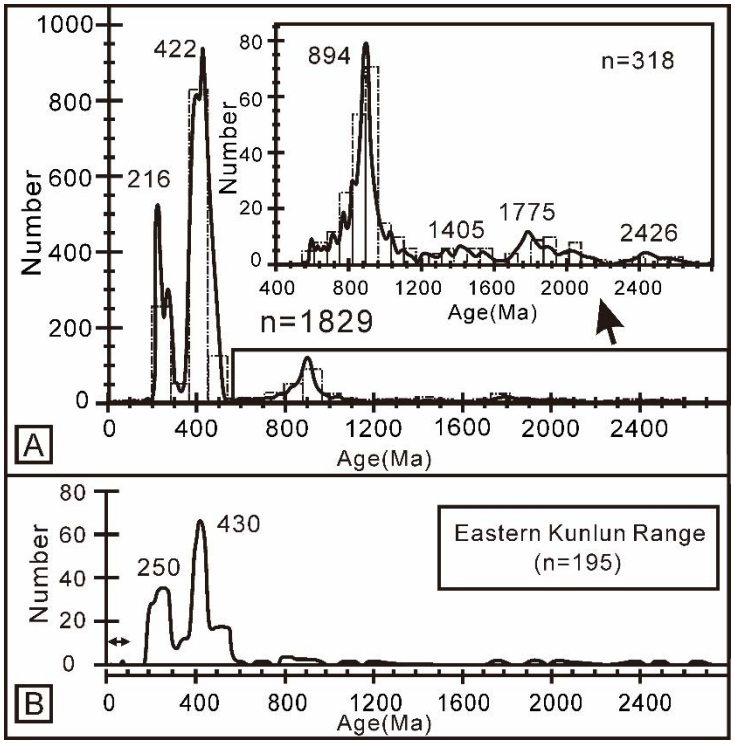


Figure 15. (A) Relative probability plot histograms of U-Pb ages of detrital zircons of the 22 samples. The insert diagram to the right corresponds to the black box in the first diagram. (B) Relative probability plots of granitoid pluton ages in the Eastern Kunlun Range.

hydrothermal events in their source areas. The U-Pb ages vary widely between 2956 Ma and 37 Ma (Fig. 15) and can be statistically divided into five main populations: a Cretaceous – Cenozoic group only represented by a few ages, a late Paleozoic – Mesozoic group, an early-middle Paleozoic group, a late Proterozoic group and finally an early Proterozoic – Archean group. Except for the occurrence of a few Cenozoic – Cretaceous ages and a distinctive late Proterozoic peak, the combined age distribution of the detrital zircons of the 22 samples appears similar to the basement age distribution of the Eastern Kunlun Range characterized by the late Paleozoic – Mesozoic and early-middle Paleozoic peaks (Figs. 3 and 15). However, the age distributions in each individual sample are variable. As the Eastern Kunlun Range, the Qilian Shan Range and the Altyn Tagh Range provided numerous Paleozoic basement zircon U-Pb ages, the early Paleozoic age peak observed in all the analyzed samples is not distinctive of a specific source area. In contrast, the Altyn Tagh and the Qilian Shan ranges display only a very small number of late Paleozoic – early Mesozoic ages that are characteristic of the Eastern Kunlun Range. Similarly, Cretaceous ages are only found in the Tula Uplift, in the western part of the Eastern Kunlun Range, in the Hoh Xil basin or further south in the Qiangtang and Lhasa terranes. Cenozoic and Quaternary volcanic rocks have been recognized and dated using $^{40}Ar/^{39}Ar$ and U-Pb zircon geochronology on rocks inside the Eastern Kunlun Range and to the south in the Hoh Xil basin and Qiangtang block (Pearce and Mei, 1988; Jolivet et al., 2003; Q. Wang et al., 2008; Xia et al., 2011; Staisch et al., 2014). However, no Cenozoic or Cretaceous zircon U-Pb ages have been reported from the Altyn Tagh Range or the Qilian Shan. Consequently, the distinctive late Paleozoic – early Mesozoic ages, as well as the limited number of Cretaceous and Cenozoic ages represented in the U-Pb age spectra can be used to fingerprint the source area of the Cenozoic sediments in order to explore the source to sink relations between the South Qaidam basin and the Eastern Kunlun Range.

## 2.2.7 Discussion

### 2.2.7.1 Pre-Paleocene exhumation of the Eastern Kunlun Range

Low temperature thermochronology studies suggested that the uplift of the Eastern Kunlun Range was initiated during late Eocene to early Oligocene times (Jolivet et al., 2001; Yuan et al., 2003, 2006; A. Wang et al., 2006; Clark et al., 2010; Dai et al., 2013; Duvall et al., 2013). This age is coeval with the age of initiation of crustal shortening along the southern margin of the Qaidam basin as inferred from published growth-strata analysis within the basin (Yin et al., 2008b; L. Wang et al., 2010). In addition, paleocurrent studies along the northern

margin of the Hoh Xil basin show that during the Eocene, paleorivers were flowing northward with a unidirectional dispersal pattern suggesting an absence of significant positive topography in the Eastern Kunlun Range area (Yi et al., 2008). This direction gradually switched eastwards during the Oligocene and Yi et al. (2008) interpreted this variation as due to the uplift of the Eastern Kunlun Range during the late Paleogene.

However, using detailed petrological analysis of core samples obtained from the Lulehe Fm. in the SQB, we have identified numerous angular carbonate fragments (containing abundant foraminifera) within the Paleocene strata (Fig. 7G and 7H). Foraminifera are generally found in marine environments (Rohling et al., 1998), although some have been found in salt lakes (Cann et al., 1981). However, while ostracoda, sporopollen and algae have been described in the Paleocene deposits of the Lulehe Fm., foraminifera have never been found within the Paleocene series of the southwestern Qaidam basin (QBGMR, 1991; QIGS, 2004; Xia et al., 2012; Ke et al., 2013). Paleocene strata in the southwestern Qaidam basin are characterized by coarse-grained detrital sediments corresponding to braided river to deltaic sediment facies (Xia et al., 2001; Meng and Fang, 2008; Yin et al., 2008b; Gong et al., 2012; Fu et al., 2013; C. Zhang et al., 2013) an environment that does not allow the development of foraminifera. These newly-identified foraminifera-bearing carbonate fragments found in the Paleocene Lulehe Fm. are therefore derived from a pre-Cenozoic source containing foraminifera. As they dissolve rapidly, carbonate fragments are generally not transported over long distances (Zuffa, 1980; Mack and Rasmussen, 1984). This then suggests a relatively proximal source area for the clasts preserved within the Lulehe Fm. In addition, the Carboniferous strata, exposed south of the Kunbei section (Fig. 2), consist mainly of biomicrite, biosparite, and bioclastic littoral to neritic limestones containing abundant brachiopods, coral, gastropods and foraminifera (QIGS, 2004). Thus, the carbonate fragments contained in the Paleocene Lulehe Fm. of the Kunbei section are most probably sourced from the foraminifera-rich Carboniferous sequences of the Qimen Tagh Range forming the western segment of the Eastern Kunlun Range (QIGS, 2004). This inference has the corollary that the basement of the Eastern Kunlun Range had already been exposed prior to the Paleocene, providing material for the Qaidam basin. Furthermore, a newly-acquired seismic profile in the northern flank of the Eastern Kunlun Range (Fig. 3) shows a discordance level separating the Mesozoic series from the Paleocene - Eocene deposits (Lulehe Fm.), possibly indicating a pre-Paleocene exhumation of the Eastern Kunlun Range as well.

Our new finding pushes back the onset time of the Eastern Kunlun Range uplift from Eocene/Oligocene (Jolivet et al., 2001; Yuan et al., 2003; A. Wang et al., 2006; Yuan et al.,

2006; Yin et al., 2007; Yin et al., 2008b; Clark et al., 2010; Dai et al., 2013; Duvall et al., 2013) to pre-Paleocene. With regard to the pre-Paleocene exhumation of the Eastern Kunlun Range, the northern Tibetan Plateau, over 1000 km away from the locus of the India – Eurasia collision front, had already been deformed or partially uplifted before the India – Eurasia collision occurred around ~50 Ma (e.g. Dupont-Nivet et al., 2010).

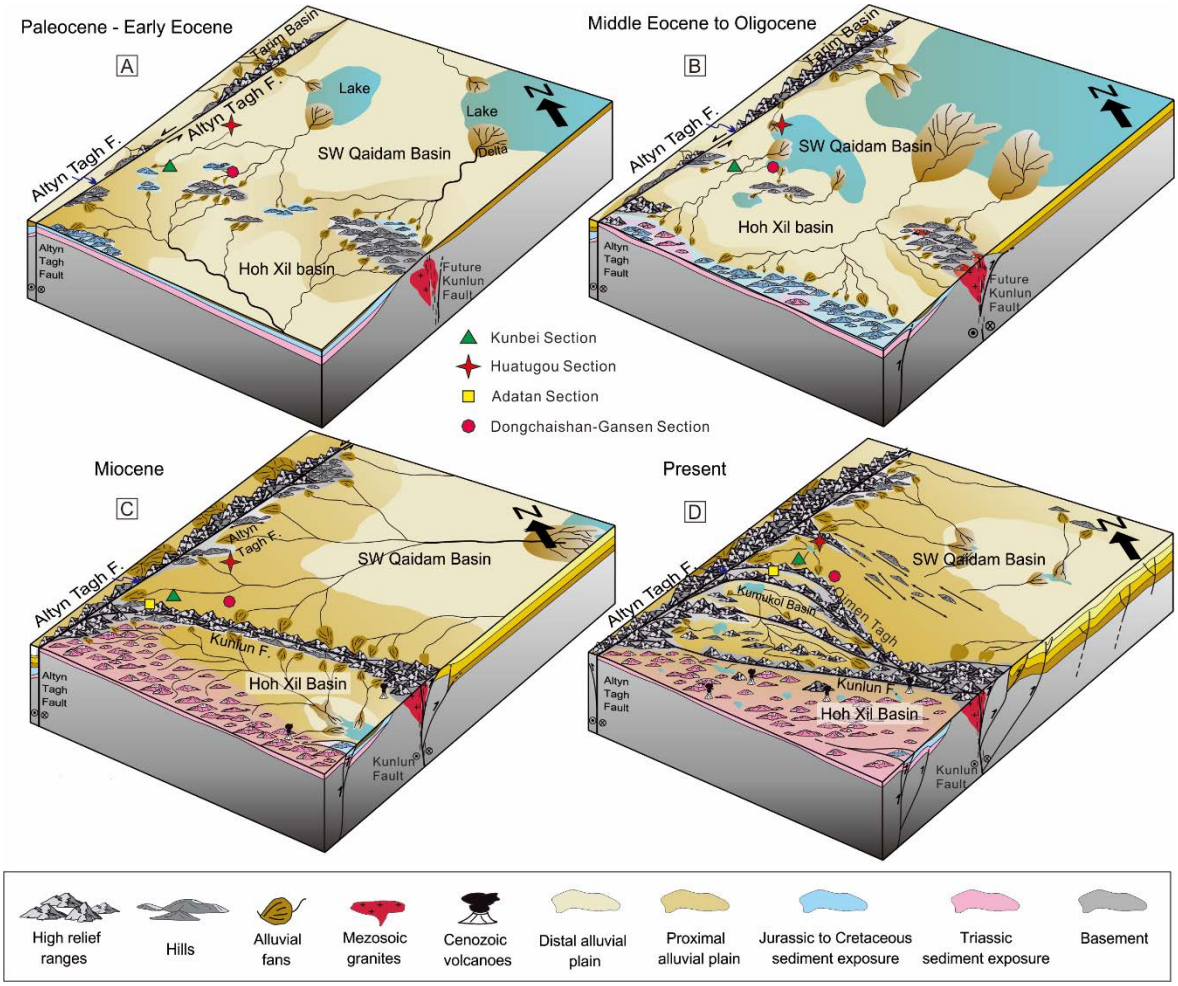


Figure 16. (A) Paleocene to early Eocene tectonic configuration of the Qaidam Basin. The Eastern Kunlun Range had already uplifted, separating the paleo–Qaidam Basin in the north from the North Qiangtang and Bayan Har terranes to the south. The Qaidam Basin is characterized by small lakes with limited extent during this period. (B) Middle Eocene to Oligocene tectonic configuration of the Qaidam Basin. During this period, the scope of the Qaidam Basin expanded southward with water getting deeper. The southward-expanding Qaidam Basin may have locally inundated the Eastern Kunlun Range and connected with the Kumukol Basin or even the Hoh Xil Basin to the south. (C–D) Miocene to present tectonic configuration of the Qaidam Basin. The scope of the basin narrowed, with water getting gradually shallower during this period. Note that intense Miocene uplifting of the Eastern Kunlun Range separated the Qaidam Basin and Hoh Xil Basin. The Eastern Kunlun Range and the Altyn Tagh Range had already been largely denudated, forming the major two provenance areas for the sediments deposited in the South Qaidam Basin.

#### 2.2.7.2 Cenozoic source to sink relationship between the South Qaidam basin and the Eastern Kunlun Range

##### 2.2.7.2.1 Paleocene - Early Eocene (Lulehe Fm.)

The fluvial deposits of the Lulehe Fm. are only exposed in the western Qaidam basin and pinch out eastward (Meng and Fang, 2008; Yin et al., 2008b). Sediment facies, sediment petrology and heavy minerals data obtained in the Kunbei area indicate that this formation most probably reflects rapid accumulation of clastic sediments along the front of a gradually uplifting topography in the Eastern Kunlun Range (this study; Xia et al., 2001; Gong et al., 2012; Wu et al., 2012; Fu et al., 2013). The zircon U-Pb age distributions in samples Q403, Q1618 and Q1643 are simple, mostly characterized by a major early Paleozoic age peak (Fig. 13). Only sample Q1643 shows a significant - although low - number (less than 5%) of Mesozoic and Proterozoic ages. The lack of Mesozoic ages in the spectra implies a source to the south either from the Mesozoic granites in the Eastern Kunlun and Qiangtang basement, or from recycled Mesozoic sediments in the Hoh Xil basin (Figs. 5 and DR1 [see footnote 1]). However, the effective absence of significant Proterozoic ages in the samples rules out a contribution from the Qiangtang – Lhasa and Hoh Xil sources. Similarly, no sediment seem to be derived from the Altyn Tagh or the Qilian Shan ranges, which is consistent with the occurrence of a depocenter in the central part of the basin (e.g. Meng and Fang, 2008; Yin et al., 2008b). Finally, the ZTR index variation from heavy mineral analysis (Gong et al., 2012; Fu et al., 2013), coupled with the occurrence of carbonate pebbles in the Lulehe Fm., suggests that the basement of the Eastern Kunlun Range was already acting as a significant sediment source feeding the SQB from the Paleocene (Fig. 16A). However, the lack of obvious growth strata in the Paleocene to early Eocene deposits of the SQB suggests that tectonic uplift in the Eastern Kunlun Range was limited at that time (Figs. 3, 4 and 16A).

Our new data contradict to some extent the Paleo-Qaidam model of Yin et al. (2008b) which suggests that, during the Paleocene, the Qaidam, Kumukol and Hoh Xil basins were forming a single, wide depression between the Qilian Shan to the north and the Fenghuo Shan to the south. This interpretation was based on the similarity of Paleocene to Eocene sedimentary features within these three basins (Fig. 1). This model prompted several attempts to reassess the tectonic processes affecting the northern edge of the Tibetan plateau (e.g. Jian et al., 2013; Cheng et al., 2014; Mao et al., 2014). However, the Paleo-Qaidam hypothesis is mostly based on the similarities between the Paleocene and Eocene depositional environments and sediment facies in the three basins. As proposed in Figure 16A, similar depositional

environments may have developed contemporaneously in the three basins without implying a unique drainage system between the SQB and the other two basins to the south. The slowly growing Eastern Kunlun Range was probably shedding sediments northward and southward but as suggested by the unimodal distribution of zircon ages in the Lulehe Fm. (Fig. 13), the SQB was not receiving sediments from the Qiangtang – Lhasa and Hoh Xil region.

2.2.7.2.2 Middle Eocene – Oligocene (Xiaganchaigou Fm. to Shangganchaigou Fm.)

Compared with the Paleocene – early Eocene Lulehe Fm., the middle Eocene Xiaganchaigou Fm. is largely distributed throughout the basin and source rocks are well-developed in the western Qaidam basin, indicating a general widening of the basin (Jin et al., 2002; Pang et al., 2004; Chen et al., 2008; Meng and Fang, 2008; Yin et al., 2008b; Mao et al., 2014). This is further attested by the southward migration of the depocenter in the SQB from the Paleocene to Oligocene (Meng and Fang, 2008; Yin et al., 2008b; Mao et al., 2014) and the southward successive onlaps of the Eocene and Oligocene deposits from our newly-acquired seismic profile (Fig. 3). A clear retrogradational trend is observed in the three sections (Kunbei, Huatugou and Dongchaishan-Gansen), from alluvial to shallow lake depositional environments in the middle Eocene Xiaganchaigou Fm. to the mostly lacustrine environments of the Oligocene Shangganchaigou Fm. (Fig. 6). Previous studies, using core and log analyses, revealed that the central part of the basin was occupied by widespread, probably deep lake environments characterized by dark mudstones and limestones (e.g. Xia et al., 2001).

In the Kunbei section, sample Q123 from the lowermost Xiaganchaigou Fm. (Fig. 13) shows a detrital zircon age distribution pattern identical to that of the lower part of the Lulehe Fm. (samples Q403 and Q1618). Proterozoic ages that were identified in sample Q1643 (upper Lulehe Fm.) are not found in sample Q123. Sample Q7 (Kunbei section), GS-E (Dongchaishan-Gansen section) and HTG-E (Huatugou section), collected slightly above sample Q123 in the Xiaganchaigou Fm. display a significant change in the age distribution pattern: the minor Mesozoic age peak that was nearly negligible in the previous samples becomes major and the proportion and number of Proterozoic to Archean ages increases significantly, especially in sample Q7 (Fig. 13). The appearance of a strong Mesozoic component (e.g. ~20% of the total amount of ages in sample Q7) in the sediments of the Lower Xiaganchaigou Fm. represents the main characteristic of the whole dataset. The occurrence of a large lake in the central part of the basin (e.g. Xia et al., 2001; Fig. 16B) most probably prevented sediments from coming from the Qilian Shan. Furthermore, the north-directed paleocurrents measured in the Eocene deposits of the Huatugou section implies that the source

region should be located south of the all four sections. The early Proterozoic and Archean zircons observed in the Eocene and Oligocene samples can then only be derived from the Eastern Kunlun Range, the Qiangtang – Lhasa region or the Hoh Xil basin. As recently shown by Dai et al. (2012), numerous potential sources for the early Proterozoic and Archean ages are exposed in the Qiangtang block to the south and were incorporated into the Mesozoic sediments (Fig. 5D). The southward progradation of the Eocene – Oligocene sediments (Fig. 3A) and the general widening of the Qaidam basin suggest that part of the slowly growing topography in the Eastern Kunlun Range was buried back during the Eocene. This sediment progradation might have allowed some connection between the Qaidam basin and the Hoh Xil and Kumukol basins to the south, providing routes for material eroded in the Qiangtang region to reach the SQB (Fig. 16B). Although limited early Proterozoic and Archean sources exist in the Eastern Kunlun Range, most of the Precambrian zircons observed in the Xiaganchaigou Fm. were thus probably derived from Triassic and Jurassic deposits eroded from the uplifting range or from the Hoh Xil basin to the south (Fig. 16B). Recycling of the Triassic series might explain the absence of the middle Mesozoic to early Cenozoic ages observed in the Qiangtang – Lhasa and Hoh Xil sediments.

Low temperature thermochronology studies suggested a late Eocene to Oligocene uplift and exhumation in the ranges surrounding the Qaidam basin. Paleocene – Eocene exhumation has been recorded by apatite fission track data and $^{40}Ar/^{39}Ar$ thermochronology data in the Altyn Tagh Range (e.g. Jolivet et al., 2001; Sobel et al., 2001) and in the Eastern Kunlun Range (e.g. Mock et al., 1999; Jolivet et al., 2001). On a larger scale, the uplift of the Tibetan plateau is assumed to have been initiated in the Eocene or late Paleocene (e.g. DeCelles et al., 2007; C. Wang et al., 2008; Dai et al., 2012). This is consistent with the Paleocene topographic barrier implied by our data between the Hoh Xil – Kumukol basins and the SQB during the Paleocene. However, the widening of the Qaidam basin and the re-establishment of connections between the three basins during the Eocene suggest that the relief in the Eastern Kunlun Range was still low enough to be occasionally buried back, possibly during periods of increased sedimentation rate (Fig. 16B).

The age distributions of samples Z2 (Kunbei section, Fig. 13) and STB2 (Dongchaishan-Gansen section, Fig. 11) from the Oligocene Shangganchaigou Fm. are similar to that of the Eocene Lower Xiaganchaigou Fm. However, the middle and early Proterozoic – Archean ages are absent, indicating a change in the source regions that most probably became restricted to the Eastern Kunlun Range basement (including the Mesozoic granites). This implies in turn that the Hoh Xil and Kumukol basins were again disconnected from the SQB during the

Oligocene. Uplift of the Eastern Kunlun Range during the Oligocene is also indicated by the clear increase in sedimentation rates observed on the seismic profiles (Figs. 3 and 4). In addition, published apatite (U-Th)/He and fission track basement ages in the Eastern Kunlun Range indicate rapid cooling and exhumation between 35 to 20 Ma (Jolivet et al., 2001, 2003; Liu et al., 2005; Clark et al., 2010; Duvall et al., 2013). Due to the poor exposure of the Shangganchaigou Fm. in the Kunbei and Dongchaishan-Gansen sections, no paleocurrent information is available for the southern sections. However, in the Huatugou section, the paleoflows direction from NNE to SSE, indicates relief building in the Altyn Tagh Range that became a significant sediment source at least for this northernmost section.

Our data thus confirm that the Oligocene is a key period in the tectonic evolution of North Tibet: the limited deformation that prevailed since at least the Paleocene, leading to a slowly growing topography in the Eastern Kunlun Range, was replaced by active exhumation and significant construction of topography. The connections that developed between the Qaidam, Kumukol and Hoh Xil basins during the Eocene had definitely ended in the late Oligocene.

#### 2.2.7.2.3 Miocene to Present phase (Xiayoushashan Fm. to Dabuxun-Yanqiao Fm.)

As seen in the Miocene Xiayoushashan Fm., the sediment coarsened upward, gradually changing from shallow lacustrine facies to alluvial and fluvial facies (Fig. 6). Miocene active tectonic deformation has been demonstrated around the Qaidam basin, both in the Qilian Shan, Eastern Kunlun and Altyn Tagh ranges (e.g. Jolivet et al., 2001, 2003; Yuan et al., 2003; C. Wang et al., 2006; Fu and Awata, 2007; Yin et al., 2007, 2008a, 2008b; Zhang et al., 2012). The basin progressively shrunk, its depocenter shifting eastwards, and its southern edge migrating northward due to intense tectonic deformation in the Eastern Kunlun Range (Meng and Fang, 2008; Yin et al., 2008b; Mao et al., 2014). Rapid uplift of the Eastern Kunlun Range is implied by the development of growth strata in the early Miocene Xiayoushashan Fm. (Figs. 3 and 4). Throughout the Miocene and up to the present, these growth strata are associated with a series of unconformities along the northern flank of the Eastern Kunlun Range and the southern flank of the Altyn Tagh Range (e.g. Yin et al., 2007, 2008b; Y.D. Wang et al., 2010, L. Wang et al., 2010; Cheng et al., 2014; Wu et al., 2014).

In the Dongchaishan-Gansen section, the early Miocene (Xiayoushashan Fm., GS-N, STB3) zircon age population pattern remains similar to the Oligocene pattern except for the relative increase in Mesozoic ages (e.g., the percentage of Mesozoic grains increases from ~7.7% in sample GS-E to 42.7% in sample GS-N) and the corresponding decrease in Proterozoic ages (e.g., the percentage of Precambrian grains decreases from ~42.3% in sample

GS-E to 19.1% in sample GS-N) (Fig. 11). The similar signal seen in the Adatan section (samples ADT1 and ADT4, Fig. 14) seems to indicate that, by the early Miocene, the source area for the whole SQB was largely homogeneous and situated within the Eastern Kunlun Range. The Miocene uplift of the Eastern Kunlun Range is also registered by changes in the paleocurrent directions both in the SQB and in the Hoh Xil basin (e.g. Hertz et al., 2005; Yi et al., 2008). The generally northward paleoflow directions in the early Miocene deposits of the Dongshaishan-Gansen section indicate that the Eastern Kunlun Range formed a positive topography at this time (Fig. 6). The single Cretaceous age observed in sample GS-N (Fig. 11) is difficult to interpret. It could either represent material from the Tula Uplift (Fig. 1), west of the Qaidam basin (Robinson et al., 2003), or more probably from recycling of pre-Miocene sediments that contain some late Mesozoic volcanic zircons derived from the Lhasa or Qiangtang blocks. Similarly, the Eocene zircon age observed in sample ADT4 from the Adatan section (Fig. 14) is likely to be derived from the Cenozoic volcanics exposed further south on the northern edge of the Qiangtang block (e.g. Jolivet et al., 2003; Ding et al., 2007). This indicates that while the Eastern Kunlun Range were being actively uplifted, the wide drainage system prevailing during the Eocene – Oligocene was not yet completely destroyed and that some rivers still connected the SQB to the south and west across the range. In the Huatugou section, the proportion of Mesozoic zircon ages largely decreases (from 32.7% in Eocene sample HTG-E to 8.4% in sample Miocene HTG-N) compared to the Paleozoic ages. This is consistent with an increased denudation in the Altyn Tagh Range (Jolivet et al., 1999, 2001) and southward-directed paleocurrents (Fig. 6) which would bring a higher proportion of Paleozoic ages with respect to the Mesozoic ones derived from the Eastern Kunlun Range.

The middle and upper Miocene series (Shangyoushashan and Shizigou Formations) have only been sampled in the Huatugou section. The Shangyoushashan Fm. corresponds to a second major tectonically driven change in the sedimentary environment of the SQB with the disappearance of major deep lakes and the eastward migration of the depocenters (e.g. Wang et al., 2006c; Yin et al., 2008b). Detrital zircon age distributions in samples SZG2, CSL4 and SZG1, with a minor but consistent Mesozoic age peak, indicate a mixed source between the Eastern Kunlun Range (most probably the growing Qimen Tagh Range) and the Altyn Tagh Range.

The Pliocene to Holocene detrital zircon U-Pb ages distributions in both the Huatugou and Dongchaishan-Gansen sections are complex and correspond in part to a mixture between sources in the basement of the Eastern Kunlun Range and the Altyn Tagh Range, but also to recycling of earlier Cenozoic or even Mesozoic sediments exhumed in the surrounding ranges

and inside the basin (Figs. 2, 10 and 11). This is demonstrated by the occurrence of Cretaceous and Paleocene ages in the Pleistocene and Holocene deposits of the Dongchaishan-Gansen section (Fig. 11). By that time, this section was isolated both from the Tula Uplift to the west and from the northern Qiangtang margin to the south by the topographically prominent Eastern Kunlun Range. The Pliocene rapid uplift and exhumation is recorded by magnetostratigraphy and sedimentology studies in the western Qaidam basin (e.g. W. Zhang et al., 2013) and the detrital zircon U-Pb age distributions registered in the Dongchaishan-Gansen (see samples JS04 and STB1 in the Fig. 11) is similar to that of modern river sands (Li et al., 2013) suggesting are similar drainage pattern from Pliocene to the present day. The unimodal zircon age distributions from the Pleistocene and the Holocene strata in the Adatan valley (samples ADT6 and ADT3) suggest that the valley-range landform in the Qimen Tagh Range formed around the Pleistocene isolating the Adatan valley from the Mesozoic zircon sources to the south. By that time, the extension of the drainage system became limited and sediment sources were limited to the locally exposed Paleozoic basement. Since the Miocene, the Qaidam basin narrowed with lake-water depth becoming gradually shallower. The Eastern Kunlun Range and the Altyn Tagh Range were being exhumed, forming the major two provenance areas for the sediments deposited in the SQB (Fig. 16C and 16D). The Qaidam basin and the depressions to the south (Kumukol and Hoh Xil basins) were no longer connected.

To summarize, the Cenozoic topographic evolution of the southern edge of the Qaidam basin can generally be separated in three main phases: 1) a pre-Paleocene exhumed Eastern Kunlun Range served as the source area for the SQB and separated the SQB from the Hoh Xil basin to the south from the Paleocene to the early Eocene; 2) southward widening of the SQB locally buried the Eastern Kunlun Range and connected the basin with the Hoh Xil basin to the south from the late Eocene to Oligocene; 3) intense uplift of the Eastern Kunlun Range since the Miocene limited the connection between the SQB and the Hoh Xil basin. The multiple-pulse growth of the Eastern Kunlun Range reflects a complex deformation history of the Tibetan plateau rather than a monotonous northwards stepwise growth process as previously proposed (e.g. Métivier et al., 1998; Tapponnier et al., 2001). Furthermore, although detrital zircons chronology has been proven to be an important tool for provenance and geodynamic studies (e.g. Fedo et a., 2003; Gehrels, 2014), our new interpretation on the pulsed growth process (multiple denudation and burial phases) for the Eastern Kunlun Range and the subtle variation of drainage connections between the Qaidam basin and Hoh Xil basin alert us to be cautious when dealing with the detrital zircon ages alone. A comprehensive integration of the detrital zircon age spectra, subsurface seismic profiles, petrographical

features, strata isopach maps, paleocurrents direction, as well as thermochronology data from the potential sources (e.g. fission track ages, $^{40}Ar/^{39}Ar$ ages, and (U-Th)/He ages) is critical when trying to decipher the nature of source to sink relations in regions with a complex growth history.

### 2.2.8 Conclusions

The twenty two detrital zircon U-Pb ages population spectra (including six core samples from Paleogene strata), the newly identified foraminifera-bearing carbonate debris from the Paleocene strata, and the newly-acquired seismic profiles in the SQB presented in this work bring important new constraints on the onset of uplift in the Eastern Kunlun Range and on the source to sink relations between the Qaidam basin and the Eastern Kunlun Range.

The carbonate debris which contains foraminifera in the Paleocene conglomerate sequences, the appearance of a wide population of Paleozoic to late Proterozoic U-Pb ages on detrital zircon from Paleocene strata, and the discordance level separating the Mesozoic series from the Paleocene – early Eocene deposits observed in the seismic profile strongly suggest that the Eastern Kunlun Range basement was locally exhumed prior to the Paleocene and that the Mesozoic sediment cover had been at least partially removed.

The topographic evolution of the southern edge of the Qaidam basin can be separated in three main phases: 1) the onset of exhumation in the Eastern Kunlun Range initiated during or possibly before the deposition of the Paleocene Lulehe Fm. Erosion only affected the existing Mesozoic cover and the Paleozoic basement without eroding the Mesozoic granitoids and the Precambrian basement. The South Qaidam basin was already separated from the Hoh Xil basin to the south; 2) during the middle Eocene to Oligocene, the Qaidam basin widened towards the south and east. However, during the widening of the basin, uplift and erosion in the Eastern Kunlun Range were still active and probably increased over time leading to the exhumation of the Mesozoic granitoids. The occurrence of numerous early Proterozoic and Archean zircon U-Pb ages suggests that at least local connections remained between the Qaidam basin and the Hoh Xil and Kumukol basins through the growing Eastern Kunlun Range; 3) from the Miocene to present, the topography of the Eastern Kunlun Range and the Altyn Tagh Range increased, progressively enclosing the Qaidam basin. The Eastern Kunlun Range formed the main source for the sediments deposited in the SQB while in the Huatugou area, materials were derived from both the Altyn Tagh and Eastern Kunlun ranges. During the Pliocene to Present, an increasing amount of sediment recycling occurred, leading to complex detrital zircon U-Pb age distributions. The present-day valley-range landform in the Qimen Tagh

Range developed around the Pleistocene. This multiple-pulsed growth history of the Eastern Kunlun Range and the SQB in turn reminds us to be cautious when dealing with detrital zircon ages. It is important to integrate all the available detrital zircon age spectra, subsurface seismic profiles, petrographic features, strata isopach maps, paleocurrents direction, and thermochronology data of potential source to try and decipher the sources to sink relation in regions with complex growth history.

## Acknolegdements

This work was supported by the National Science & Technology Major Project of China (Grant ZX05003) and the China Scholarship Council Chinese-French Egide Cai Yuanpei program (N° 32393WL, 2014). M. Jolivet was also supported by the Darius program, and the French Centre National de la Recherche Scientifique (CNRS), Institut National des Sciences de l'Univers (INSU) Syster program. We gratefully acknowledge the assistance of Dr. Ruiying Chen, Qinyang Meng, Suping Zhou, Xiangjiang Yu, Xiang Cheng and Tuo Zhang during field work. We particularly thank Li Su of the Geological Lab Center, China University of Geosciences (Beijing), for her help during detrital zircon analysis, and to Bo Zhang (Peking University) for his help with cathodoluminescence (CL) imaging. We gratefully acknowledge Yan Chen, Chuanwu Wang, Qiquan Zhang and Shihu Fang for their helpful suggestions on Cenozoic evolution of the Qaidam basin. Kerry Gallagher is thanked for his help with the English writing. We are grateful to the Science Editor Christian Koeberl, the Associate Editor An Yin, the referee Franz Neubauer and an anonymous reviewer, who provided constructive feedback that helped improving the manuscript.

## References Cited

Andersen, T., 2002, Correction of common lead in U-Pb analyses that do not report 204Pb: Chemical Geology, v. 192, no. 1, p. 59-79, doi: 10.1016/S0009-2541(02)00195-X.

Black, L. P., Kamo, S. L., Allen, C. M., Aleinikoff, J. N., Davis, D. W., Korsch, R. J., and Foudoulis, C., 2003, TEMORA 1: a new zircon standard for Phanerozoic U-Pb geochronology: Chemical Geology, v. 200, no. 1, p. 155-170, doi: 10.1016/S0009-2541(03)00165-7.

Bovet, P. M., Ritts, B. D., Gehrels, G., Abbink, A. O., Darby, B., and Hourigan, J., 2009, Evidence of Miocene crustal shortening in the north Qilian Shan from Cenozoic stratigraphy of the western Hexi Corridor, Gansu Province, China: American Journal of Science, v. 309, no. 4, p. 290-329, doi: 10.2475/00.4009.02.

Cann, J. H., and De Deckker, P., 1981, Fossil Quaternary and living foraminifera from

athalassic (non-marine) saline lakes, southern Australia: Journal of Paleontology, p. 660-670.

Chen, X. H., Yin, A., Gehrels, G. E., Cowgill, E. S., Grove, M., Harrison, T. M., and Wang, X. F., 2003, Two phases of Mesozoic north-south extension in the eastern Altyn Tagh range, northern Tibetan Plateau: Tectonics, v. 22, no. 5, p. 1053, doi: 10.1029/2001TC001336.

Chen, Z. H., Hu, S. Y., Jin, Z. J., Pang, X. Q., Jiang, Z. X., and Kirk, O. G., 2008, Exploration risk evaluation using object-based modeling, an example from the Tertiary fractured play, western Qaidam Basin of China: Petroleum Science, v. 5, no. 3, p. 195-202, doi: 10.1007/s12182-008-0031-3.

Chen, X., Gehrels, G., Yin, A., Li, L., and Jiang, R. B., 2012, Paleozoic and Mesozoic Basement Magmatisms of Eastern Qaidam Basin, Northern Qinghai-Tibet Plateau: LA-ICP-MS Zircon U-Pb Geochronology and its Geological Significance: Acta Geologica Sinica - English Edition, v. 86, no. 2, p. 350-369, doi: 10.1111/j.1755-6724.2012.00665.x.

Cheng, F., Jolivet, M., Fu, S., Zhang, Q., Guan, S., Yu, X., and Guo, Z., 2014, Northward growth of the Qimen Tagh Range: A new model accounting for the Late Neogene strike-slip deformation of the SW Qaidam Basin: Tectonophysics, v. 632, p. 32-47, doi: 10.1016/j.tecto.2014.05.034.

Cheng, F., Guo, Z., Jenkins, H.S., Fu, S., and Cheng, X., 2015a, Initial rupture and displacement on the Altyn Tagh fault, northern Tibetan Plateau: Constraints based on residual Mesozoic to Cenozoic strata in the western Qaidam Basin: Geosphere, v. 11, no. 3, doi: 10.1130 /GES01070.1.

Cheng, X., Fu, S., Wang, H., Yu, X., Cheng, F., Liu, R., Du, W., and Guo, Z., 2015b, Geometry and kinematics of the Arlar strike-slip fault, SW Qaidam basin, China: New insights from 3-D seismic data: Journal of Asian Earth Sciences, v. 98, no. 0, p. 198-208, doi: 10.1016/j.jseaes.2014.09.039.

Clark, M. K., Farley, K. A., Zheng, D., Wang, Z., and Duvall, A. R., 2010, Early Cenozoic faulting of the northern Tibetan Plateau margin from apatite (U-Th)/He ages: Earth and Planetary Science Letters, v. 296, no. 1, p. 78-88, doi:10.1016/j.epsl.2010.04.051.

Corfu, F., Hanchar, J. M., Hoskin, P. W., and Kinny, P., 2003, Atlas of zircon textures: Reviews in mineralogy and geochemistry, v. 53, no. 1, p. 469-500, doi: 10.2113/0530469.

Cowgill, E., Yin, A., Harrison, T. M., and Wang, X., 2003, Reconstruction of the Altyn Tagh fault based on U-Pb geochronology: Role of back thrusts, mantle sutures, and heterogeneous crustal strength in forming the Tibetan Plateau: Journal of Geophysical Research, v. 108, no. B7, p. 2346, doi: 10.1029/2002JB002080.

Dai, J. G., Zhao, X. X., Wang, C. S., Zhu, L. D., Li, Y. L., and Finn, D., 2012, The vast proto-

Tibetan Plateau: New constraints from Paleogene Hoh Xil Basin: Gondwana Research, v. 22, no. 2, p. 434-446, doi:10.1016/j.gr.2011.08.019.

Dai, J., Wang, C., Hourigan, J., and Santosh, M., 2013, Multi-stage tectono-magmatic events of the Eastern Kunlun Range, northern Tibet: Insights from U–Pb geochronology and (U–Th)/He thermochronology: Tectonophysics, v. 599, p. 97-106, doi: 10.1016/j.tecto.2013.04.005.

DeCelles, P. G., Quade, J., Kapp, P., Fan, M., Dettman, D. L., and Ding, L., 2007, High and dry in central Tibet during the late Oligocene: Earth and Planetary Science Letters, v. 253, no. 3, p. 389-401, doi: 10.1016/j.epsl.2006.11.001.

Ding, L., Kapp, P., Yue, Y., and Lai, Q., 2007, Postcollisional calc-alkaline lavas and xenoliths from the southern Qiangtang terrane, central Tibet: Earth and Planetary Science Letters, v. 254, no. 1, p. 28-38, doi:10.1016/j.epsl.2006.11.019.

Ding, L., Yang, D., Cai, F. L., Pullen, A., Kapp, P., Gehrels, G. E., Zhang, L. Y., Zhang, Q. H., Lai, Q. Z., Yue, Y. H., and Shi, R. D., 2013, Provenance analysis of the Mesozoic Hoh-Xil-Songpan-Ganzi turbidites in northern Tibet: Implications for the tectonic evolution of the eastern Paleo-Tethys Ocean: Tectonics, v. 32, no. 1, p. 34-48, doi: 10.1002/tect.20013.

Ding, L., Xu, Q., Yue, Y., Wang, H., Cai, F., and Li, S., 2014, The Andean-type Gangdese Mountains: Paleoelevation record from the Paleocene-Eocene Linzhou Basin: Earth and Planetary Science Letters, v. 392, p. 250-264, doi: 10.1016/j.epsl.2014.01.045.

Dupont-Nivet, G., Lippert, P. C., Van Hinsbergen, D. J. J., Meijers, M. J. M., and Kapp, P., 2010, Palaeolatitude and age of the Indo–Asia collision: palaeomagnetic constraints: Geophysical Journal International, v. 182, no. 3, p. 1189-1198, doi: 10.1111/j.1365-246X.2010.04697.x.

Duvall, A. R., Clark, M. K., van der Pluijm, B. A., and Li, C., 2011, Direct dating of Eocene reverse faulting in northeastern Tibet using Ar-dating of fault clays and low-temperature thermochronometry: Earth and Planetary Science Letters, v. 304, no. 3-4, p. 520-526, doi: 10.1016/j.epsl.2011.02.028.

Duvall, A. R., Clark, M. K., Kirby, E., Farley, K. A., Craddock, W. H., Li, C., and Yuan, D.Y., 2013, Low-temperature thermochronometry along the Kunlun and Haiyuan Faults, NE Tibetan Plateau: Evidence for kinematic change during late-stage orogenesis: Tectonics, v. 32, no. 5, p. 1190-1211, doi:10.1002/tect.20072, 2013.

England, P., and Houseman, G., 1989, Extension during continental convergence, with application to the Tibetan Plateau: Journal of Geophysical Research: Solid Earth (1978–2012), v. 94, no. B12, p. 17561-17579, doi: 10.1029/JB094iB12p17561.

Fang, X., Zhang, W., Meng, Q., Gao, J., Wang, X., King, J., Song, C., Dai, S., and Miao, Y., 2007, High-resolution magnetostratigraphy of the Neogene Huaitoutala section in the eastern Qaidam Basin on the NE Tibetan Plateau, Qinghai Province, China and its implication on tectonic uplift of the NE Tibetan Plateau: Earth and Planetary Science Letters, v. 258, no. 1-2, p. 293-306, doi:10.1016/j.epsl.2007.03.042.

Fedo, C. M., Sircombe, K. N., and Rainbird, R. H., 2003, Detrital zircon analysis of the sedimentary record: Reviews in mineralogy and geochemistry, v. 53, no. 1, p. 277-303, doi: 10.2113/0530277.

Fu, B. H., and Awata, Y., 2007, Displacement and timing of left-lateral faulting in the Kunlun Fault Zone, northern Tibet, inferred from geologic and geomorphic features: Journal of Asian Earth Sciences, v. 29, no. 2, p. 253-265, doi:10.1016/j.jseaes.2006.03.004.

Fu, S. T., Xu, L. G., Gong, Q. L., and Lv, Y. S., 2010, Petroleum Geologic Characteristics of Southwestern Qaidam Basin and Recommendations for Further Exploration and Study: Petroleum Geology, v. 1, p. 6-10 (in Chinese with English abstract).

Fu, L., Guan, P., Zhao, W. Y., Wang, M., Zhang, Y., Lu, J. W., 2013, Heavy mineral feature and provenance analysis of Paleogene Lulehe Formation in Qaidam Basin: Acta Petrologica Sinica, v. 29, no. 8, p 2867-2875 (in Chinese with English abstract).

Graham, S. A., Chamberlain, C. P., Yue, Y., Ritts, B. D., Hanson, A. D., Horton, T. W., Waldbauer, J. R., Poage, M. A., and Feng, X., 2005, Stable isotope records of Cenozoic climate and topography, Tibetan plateau and Tarim basin: American Journal of Science, v. 305, no. 2, p. 101-118, doi: 10.2475/ajs.305.2.101.

Gao, J., Li, S., Dai, S., Li, A., and Peng, Y., 2009, Constraints of tectonic evolution in provenance from detrital zircon fission-track data of Cenozoic strata of Xichagou district in western Qaidam basin: Journal of Lanzhou University (Natural Sciences), v. 3, p. 1-7 (in Chinese with English abstract).

Gehrels, G. E., Yin, A., and Wang, X. F., 2003a, Detrital-zircon geochronology of the northeastern Tibetan plateau: Geological Society of America Bulletin, v. 115, no. 7, p. 881-896, doi: 10.1130/0016-7606(2003)115<0881:DGOTNT>2.0.CO;2 .

Gehrels, G. E., Yin, A., and Wang, X. F., 2003b, Magmatic history of the northeastern Tibetan Plateau: Journal of Geophysical Research, v. 108, no. B9, p. 2423, doi: 10.1029/2002JB001876.

Gehrels, G., Kapp, P., DeCelles, P., Pullen, A., Blakey, R., Weislogel, A., Ding, L., Guynn, J., Martin, A., and McQuarrie, N., 2011, Detrital zircon geochronology of pre-Tertiary strata in the Tibetan-Himalayan orogen: Tectonics, v. 30, no. 5, p. TC5016,

doi:10.1029/2011TC002868.

Gehrels, G., 2014, Detrital Zircon U-Pb Geochronology Applied to Tectonics: Annual Review of Earth and Planetary Sciences, v. 42, no. 1, p. 127-149, doi: 10.1146/annurev-earth-050212-124012.

Gong, Q. S., Shou, J. F., Huang, G. P., Li, S. M., and Wang, Y. Q., 2012, Sedimentary characteristic of braided delta in Lulehe Formation of Kunbei oilfield in Qaidam Basin: Chinese Journal of Geology, v. 47, no. 1, p. 116-128 (in Chinese with English abstract).

Guo, J. J., and Li, H. K., 1999, Angular Unconformity between the Huashishan Group and Huangzhong Group in the Eastern Mid-Qilian Massif: Identification and Implications: Progress In Precambrian Research, v. 22, no. 2, p. 47-52 (in Chinese with English abstract).

Hanchar, J., and Rudnick, R., 1995, Revealing hidden structures: the application of cathodoluminescence and back-scattered electron imaging to dating zircons from lower crustal xenoliths: Lithos, v. 36, no. 3, p. 289-303, doi: 10.1016/0024-4937(95)00022-4.

Hertz, M., Ritts, B., Bovet, P., and Kent-Corson, M., 2005, Qimen Tagh Uplift Constrained From Tectonostratigraphy of Southwest Qaidam Basin, Northern Tibet Plateau, China: Eos Trans. AGU, 86(52), Fall Meet. Suppl., Abstract T41A-1276.

Hoskin, P., and Black, L., 2000, Metamorphic zircon formation by solid-state recrystallization of protolith igneous zircon: Journal of metamorphic Geology, v. 18, no. 4, p. 423-439, doi:10.1046/j.1525-1314.2000.00266.x.

Hough, B. G., Garzione, C. N., Wang, Z., Lease, R. O., Burbank, D. W., and Yuan, D., 2011, Stable isotope evidence for topographic growth and basin segmentation: Implications for the evolution of the NE Tibetan Plateau: Geological Society of America Bulletin, v. 123, no. 1-2, p. 168-185, doi: 10.1130/B30090.1.

Huang, H., Huang, Q., and Ma, Y., 1996, Geology of Qaidam Basin and its petroleum prediction, Beijing, Geological Publishing House, 257 p (in Chinese).

Huo, G. M., 1990, Petroleum geology of China: Oil fields in Qianghai and Xizang, Chinese Petroleum Industry Press, Beijing, 483 p (in Chinese with English abstract).

Jian, X., Guan, P., Zhang, W., and Feng, F., 2013, Geochemistry of Mesozoic and Cenozoic sediments in the northern Qaidam basin, northeastern Tibetan Plateau: Implications for provenance and weathering: Chemical Geology, v. 360, p. 74-88, doi: 0.1016/j.chemgeo.2013.10.011.

Jin, Q., Zha, M., Liu, Z., Gao, X. Z., Peng, D. H., and Lin, L. M., 2002, Geology and Geochemistry of source rocks in the Qaidam Basin, NW CHina: Journal of Petroleum Geology, v. 25, no. 2, p. 219-238, doi: 10.1111/j.1747-5457.2002.tb00005.x.

Jolivet, M., Roger, F., Arnaud, N., Brunel, M., Tapponnier, P., and Seward, D., 1999, Histoire de l'exhumation de l'Altun Shan: indications sur l'âge de la subduction du bloc du Tarim sous le système de l'Altyn Tagh (Nord Tibet): Comptes Rendus de l'Académie des Sciences-Series IIA-Earth and Planetary Science, v. 329, no. 10, p. 749-755, doi: 10.1016/S1251-8050(00)88495-5.

Jolivet, M., Brunel, M., Seward, D., Xu, Z., Yang, J., Roger, F., Tapponnier, P., Malavieille, J., Arnaud, N., and Wu, C., 2001, Mesozoic and Cenozoic tectonics of the northern edge of the Tibetan plateau: fission-track constraints: Tectonophysics, v. 343, no. 1-2, p. 111-134, doi: 10.1016/S0040-1951(01)00196-2.

Jolivet, M., Brunel, M., Seward, D., Xu, Z., Yang, J., Malavieille, J., Roger, F., Leyreloup, A., Arnaud, N., and Wu, C., 2003, Neogene extension and volcanism in the Kunlun Fault Zone, northern Tibet: New constraints on the age of the Kunlun Fault: Tectonics, v. 22, no. 5, p. 1052, doi: 10.1029/2002TC001428.

Jolivet, M., Roger, F., Xu, Z. Q., Paquette, J. L., and Cao, H., 2015, Mesozoic–Cenozoic evolution of the Danba dome (Songpan Garzê, East Tibet) as inferred from LA-ICPMS U–Pb and fission-track data: Journal of Asian Earth Sciences, v. 102, p. 180-204, doi: 10.1016/j.jseaes.2015.02.009.

Kapp, P., Yin, A., Manning, C. E., Harrison, T. M., Taylor, M. H., and Ding, L., 2003, Tectonic evolution of the early Mesozoic blueschist-bearing Qiangtang metamorphic belt, central Tibet: TECTONICS, v. 22, no. 4, p. 1043, doi: 10.1029/2002TC001383.

Kapp, P., Yin, A., Harrison, T. M., and Ding, L., 2005, Cretaceous-Tertiary shortening, basin development, and volcanism in central Tibet: Geological Society of America Bulletin, v. 117, no. 7-8, p. 865-878, 10.1130/B25595.1.

Kapp, P., DeCelles, P. G., Gehrels, G. E., Heizler, M., and Ding, L., 2007, Geological records of the Lhasa-Qiangtang and Indo-Asian collisions in the Nima area of central Tibet: Geological Society of America Bulletin, v. 119, no. 7-8, p. 917-933, doi: 10.1130/B26033.1.

Ke, X., Ji, J., Zhang, K., Kou, X., Song, B., and Wang, C., 2013, Magnetostratigraphy and Anisotropy of Magnetic Susceptibility of the Lulehe Formation in the Northeastern Qaidam Basin: Acta Geologica Sinica-English Edition, v. 87, no. 2, p. 576-587, doi: 10.1111/1755-6724.12069.

Kent-Corson, M. L., Ritts, B. D., Zhuang, G., Bovet, P. M., Graham, S. A., and Chamberlain, C. P., 2009, Stable isotopic constraints on the tectonic, topographic, and climatic evolution of the northern margin of the Tibetan Plateau: Earth and Planetary Science Letters, v. 282, no. 1, p. 158-166, doi: 10.1016/j.epsl.2009.03.011.

Kidd, W. S. F., and Molnar, P., 1988, Quaternary and active faulting observed on the 1985 Academia Sinica--Royal society geotraverse of Tibet: Philosophical Transactions of the Royal Society of London. Series A, Mathematical and Physical Sciences, v. 327, p. 337-363, doi: 10.1098/rsta.1988.0133.

Kirby, E., Harkins, N., Wang, E., Shi, X., Fan, C., and Burbank, D., 2007, Slip rate gradients along the eastern Kunlun fault: Tectonics, v. 26, no. 2, TC2010, doi: 10.1029/2006TC002033.

Leier, A. L., Kapp, P., Gehrels, G. E., and DeCelles, P. G., 2007, Detrital zircon geochronology of Carboniferous–Cretaceous strata in the Lhasa terrane, Southern Tibet: Basin Research, v. 19, no. 3, p. 361-378, doi: 10.1111/j.1365-2117.2007.00330.x.

Li, X. H., Su, L., Chung, S. L., Li, Z. X., Liu, Y., Song, B., and Liu, D. Y., 2005, Formation of the Jinchuan ultramafic intrusion and the world's third largest Ni-Cu sulfide deposit: Associated with the~825 Ma south China mantle plume?: Geochemistry, Geophysics, Geosystems, v. 6, no. 11, p. Q11004, doi:10.1029/2005GC001006.

Li, W., Neubauer, F., Liu, Y. J., Genser, J., Ren, S. M., Han, G. Q., and Liang, C. Y., 2013, Paleozoic evolution of the Qimantagh magmatic arcs, Eastern Kunlun Mountains: constraints from zircon dating of granitoids and modern river sands: Journal of Asian Earth Sciences, v.77, 183-202, doi: 10.1016/j.jseaes.2013.08.030.

Lin, A., and Guo, J., 2008, Nonuniform Slip Rate and Millennial Recurrence Interval of Large Earthquakes along the Eastern Segment of the Kunlun Fault, Northern Tibet: Bulletin of the Seismological Society of America, v. 98, no. 6, p. 2866-2878, doi: 10.1785/0120070193.

Liu, Y. J., Genser, J., Neubauer, F., Jin, W., Ge, X. H., Handler, R., and Takasu, A., 2005, $^{40}Ar/^{39}Ar$ mineral ages from basement rocks in the Eastern Kunlun Mountains, NW China, and their tectonic implications: Tectonophysics, v. 398, no. 3-4, p. 199-224, doi: 10.1016/j.tecto.2005.02.007.

Liu, Y. H., Mo, X. X., Yu, X. H., Zhang, X. T. and Xu, G. W., 2006. Zircon SHRIMP U-Pb dating of the Jingren granite, Yemaquan region of the east Kunlun and its geological significance: Acta Petrologica Sinica, v. 22, no. 10, doi: 10.3321/j.issn:1000-0569.2006.10.006 (in Chinese with English abstract).

Liu, L., Zhang, A., Chen, D., Yang, J., Luo, J., and Wang, C., 2007, Implications Based on LA-ICP-MS Zircon U-Pb Ages of Eclogite and Its Country Rock from Jianggalesayi Area, Altyn Tagh, China: Earth Science Frontiers, v. 14, no. 1, p. 98-107, doi: 10.1016/S1872-5791(07)60004-9.

Liu, L., Wang, C., Chen, D., Zhang, A., and Liou, J., 2009, Petrology and geochronology of HP-UHP rocks from the South Altyn Tagh, northwestern China: Journal of Asian Earth

Sciences, v. 35, no. 3, p. 232-244, doi: 10.1016/j.jseaes.2008.10.007.

Liu, D. D., Jolivet, M., Yang, W., Zhang, Z. Y., Feng, C., Zhu, B., and Guo, Z. J., 2013a, Latest Palaeozoic-Early Mesozoic basin-range interactions in South Tian Shan (Northwest China) and their tectonic significance: Constraints from detrital zircon U-Pb ages: Tectonophysics, v. 599, no. 25, p. 197-213, doi: 10.1016/j.tecto.2013.04.018.

Liu, L., Cao, Y. Y., Chen, D. L., Zhang, C. L., Yang, W. Q., Kang, L., and Liao, X. Y., 2013b, New progresses on the HP-UHP metamorphism in the South Altyn Tagh and the North Qinling: Chin Sci Bull, v. 58, p. 2113-2123 (in Chinese).

Long, X., Yuan, C., Sun, M., Kröner, A., and Zhao, G., 2014, New geochemical and combined zircon U–Pb and Lu–Hf isotopic data of orthogneisses in the northern Altyn Tagh, northern margin of the Tibetan plateau: Implication for Archean evolution of the Dunhuang Block and crust formation in NW China: Lithos, v. 200–201, p. 418-431, doi: 10.1016/j.lithos.2014.05.008.

Lu, H., and Xiong, S., 2009, Magnetostratigraphy of the Dahonggou section, northern Qaidam Basin and its bearing on Cenozoic tectonic evolution of the Qilian Shan and Altyn Tagh Fault: Earth and Planetary Science Letters, v. 288, no. 3, p. 539-550, doi:10.1016/j.epsl.2009.10.016.

Lu, S. N., Wang, H. C., Li, H. K., Yuan, G. B., Xin, H. T., and Zhen, J. K., 2002, Redefinition of the "Dakendaban Group" on the northern margin of the Qaidam Basin: Geological Bulletin of China, v. 21, no. 1, p. 19-23 (in Chinese with English abstract).

Lu, S. N., and Yuan, G. B., 2003, Geochronology of early Precambrian magmatic activities in Aketasdhtage, east Altyn Tagh: Journal of Acta Geologica Sinica, v. 77, no. 1, p. 61-68 (in Chinese with English abstract).

Lu, S. N., Li, H. K., Zhang, C. L., and Niu, G. H., 2008, Geological and geochronological evidence for the Precambrian evolution of the Tarim Craton and surrounding continental fragments: Precambrian Research, v. 160, no. 1, p. 94-107, doi:10.1016/j.precamres.2007.04.025.

Ludwig, K. R., 2003, User's manual for Isoplot 3.0: a geochronological toolkit for Microsoft Excel: Berkeley, California, Berkeley Geochronology Center. Center Special Publication no. 4, 70 p.

Mack, G. H., and Rasmussen, K. A., 1984, Alluvial-fan sedimentation of the Cutler Formation (Permo-Pennsylvanian) near Gateway, Colorado: Geological Society of America Bulletin, v. 95, no. 1, p. 109-116, doi: 10.1130/0016-7606(1984)95<109:ASOTCF>2.0.CO;2.

Mao, L. G., Xiao, A. C., Wu, L., Li, B. L., Wang, L. Q., Lou, Q. Q., Dong, Y. P., and Qin, S. H., 2014, Cenozoic tectonic and sedimentary evolution of southern Qaidam Basin, NE Tibetan

Plateau and its implication for the rejuvenation of Eastern Kunlun Mountains: Science China Earth Sciences, v.57, p.2726-2739, doi: 10.1007/s11430-014-4951-z.

Meng, Q. R., and Fang, X., 2008, Cenozoic tectonic development of the Qaidam Basin in the northeastern Tibetan Plateau: Geological Society of America Special Papers, v. 444, p. 1-24, doi: 10.1130/2008.2444(01).

Métivier, F., Gaudemer, Y., Tapponnier, P., and Meyer, B., 1998, Northeastward growth of the Tibet plateau deduced from balanced reconstruction of two depositional areas: The Qaidam and Hexi Corridor basins, China: Tectonics, v. 17, no. 6, p. 823-842, doi: 10.1029/98TC02764.

Menold, C. A., 2006, Tectonic and metamorphic evolution of the North Qaidam ultrahigh-pressure metamorphic terrane, Western China [Ph.D. thesis]: University of California, Los Angeles, 261 p.

Meyer, B., Tapponnier, P., Bourjot, L., Metivier, F., Gaudemer, Y., Peltzer, G., Shunmin, G., and Zhitai, C., 1998, Crustal thickening in Gansu‐Qinghai, lithospheric mantle subduction, and oblique, strike‐slip controlled growth of the Tibet plateau: Geophysical Journal International, v. 135, no. 1, p. 1-47, doi: 10.1046/j.1365-246X.1998.00567.x.

Mock, C., Arnaud, N. O., and Cantagrel, J. M., 1999, An early unroofing in northeastern Tibet? Constraints from 40 Ar/39 Ar thermochronology on granitoids from the eastern Kunlun range (Qianghai, NW China): Earth and Planetary Science Letters, v. 171, no. 1, p. 107-122, doi: 10.1016/S0012-821X(99)00133-8.

Pang, X. Q., Li, Y. X., and Jiang, Z. X., 2004, Key geological controls on migration and accumulation for hydrocarbons derived from mature source rocks in Qaidam Basin: Journal of Petroleum Science and Engineering, v. 41, no. 1–3, p. 79-95, doi: 10.1016/S0920-4105(03)00145-1.

Pearce, J. A., and Mei, H. J., 1988, Volcanic rocks of the 1985 Tibet geotraverse: Lhasa to Golmud: Philosophical Transactions of the Royal Society of London. Series A, Mathematical and Physical Sciences, v. 327, no. 1594, p. 169-201, doi: 10.1098/rsta.1988.0125.

Pei, J., Sun, Z., Wang, X., Zhao, Y., Ge, X., Guo, X., Li, H., and Si, J., 2009, Evidence for Tibetan plateau uplift in Qaidam basin before Eocene-Oligocene boundary and its climatic implications: Journal of Earth Science, v. 20, p. 430-437, doi: 10.1007/s12583-009-0035-y.

QBGMR, 1991, Regional Geology of Qinghai Province, Beijing, Geological Publishing House, 662 p (in Chinese).

Qi, C., Li, X., Liang, X., Liu, Y., and Tu, X., 2005, High-precision measurement of Hf isotopic reference values for the U-Pb geochronology standard zircons by multi-collector inductively coupled plasma-mass spectrometry: Journal of Chinese Mass Spectrometry Society, v. 26, no.

3, p. 149-154 (in Chinese with English abstract).

Qinghai Institude of Geological Surevey (QIGS), 2004, Introduction of geological map of Kulangmiqiti area: Qinghai Insititute of Geological Survey, Xining, scale 1:250000, 1 sheet (in Chinese).

Qiu, N. S., 2002, Tectono-thermal evolution of the Qaidam Basin, China: evidence from Ro and apatite fission track data: Petroleum Geoscience, v. 8, no. 3, p. 279-285, doi: 10.1144/petgeo.8.3.279.

Quade, J., Breecker, D. O., Daëron, M., and Eiler, J., 2011, The paleoaltimetry of Tibet: An isotopic perspective: American Journal of Science, v. 311, no. 2, p. 77-115, doi:10.2475/02.2011.01.

Reid, A. J., Wilson, C. J., and Liu, S., 2005, Structural evidence for the Permo-Triassic tectonic evolution of the Yidun Arc, eastern Tibetan Plateau: Journal of Structural Geology, v. 27, no. 1, p. 119-137, doi: 10.1016/j.jsg.2004.06.011.

Rieser, A. B., Neubauer, F., Liu, Y., and Ge, X., 2005, Sandstone provenance of north-western sectors of the intracontinental Cenozoic Qaidam Basin, western China: tectonic vs. climatic control: Sedimentary Geology, v. 177, no. 1, p. 1-18, doi: 10.1016/j.sedgeo.2005.01.012.

Rieser, A. B., Liu, Y., Genser, J., Neubauer, F., Handler, R., Friedl, G., and Ge, X. H., 2006, $^{40}Ar/^{39}Ar$ ages of detrital white mica constrain the Cenozoic development of the intracontinental Qaidam Basin, China: GSA Bulletin, v. 118, no. 11/12, p. 1522-1534, doi: 10.1130/B25962.1.

Rieser, A. B., Neubauer, F., Liu, Y., Genser, J., Handler, R., Ge, X.-H., and Friedl, G., 2007, $^{40}Ar/^{39}Ar$ Dating of Detrital White Mica as a Complementary Tool for Provenance Analysis: a Case Study from the Cenozoic Qaidam Basin (China), in Nichols, G., Williams, E., and Paola, C. eds.: Sedimentary Processes, Environments and Basins - A Tribute to Peter Friend: Special Publication-International Association of Sedimentologists 38, p. 301-325, doi: 10.1002/9781444304411.ch14.

Rieser, A. B., Bojar, A.-V., Neubauer, F., Genser, J., Liu, Y., Ge, X.-H., and Friedl, G., 2009, Monitoring Cenozoic climate evolution of northeastern Tibet: stable isotope constraints from the western Qaidam Basin, China: International Journal of Earth Sciences, v. 98, no. 5, p. 1063-1075, doi: 10.1007/s00531-008-0304-5.

Robinson, D. M., Dupont-Nivet, G., Gehrels, G. E., and Zhang, Y., 2003, The Tula uplift, northwestern China: Evidence for regional tectonism of the northern Tibetan Plateau during late Mesozoic-early Cenozoic time: Geological Society of America Bulletin: v. 115 no. 1 p. 35-47, doi: 10.1130/0016-7606(2003)115<0035:TTUNCE>2.0.CO;2.

Roger, F., Arnaud, N., Gilder, S., Tapponnier, P., Jolivet, M., Brunel, M., Malavieille, J., Xu, Z., and Yang, J., 2003, Geochronological and geochemical constraints on Mesozoic suturing in east central Tibet: Tectonics, v. 22, no. 4, p. 1037, doi:10.1029/2002TC001466.

Roger, F., Jolivet, M., and Malavieille, J., 2008, Tectonic evolution of the Triassic fold belts of Tibet: Comptes Rendus Geoscience, v. 340, no. 2, p. 180-189, doi:10.1016/j.crte.2007.10.014.

Roger, F., Jolivet, M., and Malavieille, J., 2010, The tectonic evolution of the Songpan-Garzê (North Tibet) and adjacent areas from Proterozoic to Present: A synthesis: Journal of Asian Earth Sciences, v. 39, no. 4, p. 254-269, doi:10.1016/j.jseaes.2010.03.008.

Rohling, E., Fenton, M., Jorissen, F., Bertrand, P., Ganssen, G., and Caulet, J., 1998, Magnitudes of sea-level lowstands of the past 500,000 years: Nature, v. 394, no. 6689, p. 162-165, doi: 10.1038/28134.

Rowley, D. B., and Currie, B. S., 2006, Palaeo-altimetry of the late Eocene to Miocene Lunpola basin, central Tibet: Nature, v. 439, no. 7077, p. 677-681, doi: 10.1038/nature04506.

Shi, R. D., Yang, J. S., Wu, C. L., Tsuyoshi, I., and Takafumi, H., 2006, Island arc volcanic rocks in the north Qaidam UHP belt, northern Tibet plateau: Evidence for ocean-continent subduction preceding continent-continent Subduction: Journal of Asian Earth Sciences, v. 28, no. 2, p. 151-159, doi:10.1016/j.jseaes.2005.09.019.

Shi, D. N., Shen, Y., Zhao, W. J., and Li, A. B., 2009, Seismic evidence for a Moho offset and south-directed thrust at the easternmost Qaidam-Kunlun boundary in the Northeast Tibetan plateau: Earth and Planetary Science Letters, v. 288, p. 329-334, doi:10.1016/j.epsl.2009.09.036.

Shanxi Insititute of Geological Survey (SIGS), 2003, Introduction of geological map of Ayakumu area: Shanxi Insititute of Geological Survey, Xi'an, scale 1:250000, 1 sheet (in Chinese).

Spicer, R. A., Harris, N. B., Widdowson, M., Herman, A. B., Guo, S., Valdes, P. J., Wolfe, J. A., and Kelley, S. P., 2003, Constant elevation of southern Tibet over the past 15 million years: Nature, v. 421, no. 6923, p. 622-624, doi:10.1038/nature01356.

Sobel, E. R., and Arnaud, N., 1999, A possible middle Paleozoic suture in the Altyn Tagh, NW China: Tectonics, v. 18, no. 1, p. 64-74, doi: 10.1029/1998TC900023.

Sobel, E. R., Arnaud, N., Jolivet, M., Ritts, B. D., and Brunei, M., 2001, Jurassic to Cenozoic exhumation history of the Altyn Tagh range, northwest China, constrained by $^{40}Ar/^{39}Ar$ and apatite fission track thermochronologym, In Hendrix, M.S., and Davis, G.A., eds., Paleozoic and Mesozoic Tectonic Evolution ofCentral and Eastern Asia: From Continental Assembly to

Intracontinental Deformation: Geological Society of America Memoir 194, p. 247.

Song, S. G., 2001, Petrology, Mineralogy and Metamorphic Evolution of the Dulan UHP Terrane in North Qaidam, NW China, and Its Tectonic Implications [PH.D. thesis]: Chinese Academy of Geological Sciences, Beijing, 96 p (in Chinese with English abstract).

Song, S. G., Zhang, L. F., Niu, Y. L., Song, B., Zhang, G. B., and Wang, Q. J., 2004, Zircon U-Pb SHRIMP ages of eclogites from the North Qilian Mountains in NW China and their tectonic implication: Chinese Science Bulletin, v. 49, no. 8, p. 848-852, doi : 10.1007/BF02889759.

Song, S. G., Zhang, L. F., Niu, Y. L., Su, L., Song, B., and Liu, D. Y., 2006, Evolution from oceanic subduction to continental collision: a case study from the Northern Tibetan Plateau based on geochemical and geochronological data: Journal of Petrology, v. 47, no. 3, p. 435-455, doi: 10.1093/petrology/egi080.

Song, B., Zhang, K., Lu, J., Wang, C., and Xu, Y., 2013, The middle Eocene to early Miocene integrated sedimentary record in the Qaidam Basin and its implications for paleoclimate and early Tibetan Plateau uplift: Canadian Journal of Earth Sciences, v. 50, no. 2, p. 183-196, doi: 10.1139/cjes-2012-0048.

Staisch, L. M., Niemi, N. A., Hong, C., Clark, M. K., Rowley, D. B., and Currie, B., 2014, A Cretaceous-Eocene depositional age for the Fenghuoshan Group, Hoh Xil Basin: Implications for the tectonic evolution of the northern Tibet Plateau: Tectonics, v. 33, no. 3, p. 281-301, doi: 10.1002/2013TC003367.

Sun, Z. M., Yang, Z. Y., Pei, J. L., Ge, X. H., Wang, X. S., Yang, T. S., Li, W. M., and Yuan, S. H., 2005, Magnetostratigraphy of Paleogene sediments from northern Qaidam Basin, China: implications for tectonic uplift and block rotation in northern Tibetan plateau: Earth and Planetary Science Letters, v. 237, no. 3, p. 635-646, doi: 10.1016/j.epsl.2005.07.007.

Sun, Z. C., Jing M. C., Sun, N. D., Lu Y.L., Cao, L., 2007. Discussion on boundary between the upper and lower members of Xiaganchaigou Formation of Paleogene in Well Kun-2, Qaidam Basin. Journal of Palaeogeography, v. 9, no. 6, 611-618 (in Chinese with English abstract).

Tapponnier, P., Xu, Z. Q., Roger, F., Meyer, B., Arnaud, N., Wittlinger, G., and Yang, J. S., 2001, Oblique stepwise rise and growth of the Tibet Plateau: Science, v. 294, no. 5547, p. 1671-1677, doi: 10.1126/science.105978.

Taylor, M., and Yin, A., 2009, Active structures of the Himalayan-Tibetan orogen and their relationships to earthquake distribution, contemporary strain field, and Cenozoic volcanism: Geosphere, v. 5, no. 3, p. 199-214, doi: 10.1130/GES00217.1.

van Der Woerd, J., Tapponnier, P., Ryerson, F. J., Meriaux, A. S., Meyer, B., Gaudemer, Y., Finkel, R. C., Caffee, M. W., Guoguang, Z., and Zhiqin, X., 2002, Uniform postglacial slip-rate along the central 600 km of the Kunlun Fault (Tibet), from 26Al, 10Be, and 14C dating of riser offsets, and climatic origin of the regional morphology: Geophysical Journal International, v. 148, no. 3, p. 356-388, doi: 10.1046/j.1365-246x.2002.01556.x.

Wan, Y. S., Xu, Z. Q., Yang, J. S., and Zhang, J. X., 2001, Ages and Compositions of the Precambrian High-grade Basement of the Qilian Terrane and Its Adjacent Areas: Acta Geologica Sinica-English Edition, v. 75, no. 4, p. 375-384, doi: 10.1111/j.1755-6724.2001.tb00055.x.

Wang, Q., Zhang, P. Z., Freymueller, J. T., Bilham, R., Larson, K. M., Lai, X., You, X., Niu, Z., Wu, J., and Li, Y., 2001, Present-day crustal deformation in China constrained by global positioning system measurements: Science, v. 294, no. 5542, p. 574-577, doi: 10.1126/science.1063647.

Wang, F., Lo, C. H., Li, Q., Yeh, M. W., Wang, J., Zheng, D., and Wang, E., 2004a, Onset timing of significant unroofing around Qaidam basin, northern Tibet, China: constraints from $^{40}Ar/^{39}Ar$ and FT thermochronology on granitoids: Journal of Asian Earth Sciences, v. 24, p. 59-69, doi: 10.1130/B25778.

Wang, G. C., Wang, Q. H., Jian P. and Zhu Y. H., 2004b, Zircon SHRIMP ages of Precambrian metamorphic basement rocks and their tectonic significance in the eastern Kunlun Mountains, Qinghai Province, China: Earth Science Frontiers, v.11, no. 4, p. 481-490 (in Chinese with English abstract).

Wang, A., Wang, G., Xie, D., and Liu, D., 2006a, Fission track geochronology of Xiaonanchuan Pluton and the morphotectonic evolution of eastern Kunlun since Late Miocene: Journal of China University of Geosciences, v. 17, no. 4, p. 302-309, doi: 10.1016/S1002-0705(07)60003-X.

Wang, E., Xu, F. Y., Zhou, J. X., Wan, J., and Burchfiel, B. C., 2006b, Eastward migration of the Qaidam basin and its implications for Cenozoic evolution of the Altyn Tagh fault and associated river systems: Geological Society of America Bulletin, v. 118, no. 3-4, p. 349-365, doi: 10.1130/B25778.

Wang, C., Liu, L., Che, Z. C., Chen, D. L., Zhang, A. D., and Luo, J. H., 2006c, U-Pb geochronology and tectonic setting of the granitic gneiss in Jianggaleisayi Eclogite Belt: Geological Journal of China Universities, v. 12, no. 1, p. 74-82 (in Chinese with English abstract).

Wang, C., Zhao, X., Liu, Z., Lippert, P. C., Graham, S. A., Coe, R. S., Yi, H., Zhu, L., Liu, S.,

and Li, Y., 2008a, Constraints on the early uplift history of the Tibetan Plateau: Proceedings of the National Academy of Sciences, v. 105, no. 13, p. 4987-4992, doi: 10.1073pnas.0703595105.

Wang, C., Liu, L., Zhang, A. D., Yang, W. Q., and Cao, Y. T., 2008b, Geochemistry and petrography of early Paleozoic Yusupuleke Tagh Rapakivi-textured Granite Complex, South Altyn - an example for magma mixing: Acta Petrolei Sinica, v. 24, no. 12, p. 2809-2819 (in Chinese with English abstract).

Wang, Q., Wyman, D. A., Xu, J. F., Dong, Y. H., Vasconcelos, P. M., Pearson, N., Wan, Y. S., Dong, H., Li, C. F., and Yu, Y. S., 2008c, Eocene melting of subducting continental crust and early uplifting of central Tibet: evidence from central-western Qiangtang high-K calc-alkaline andesites, dacites and rhyolites: Earth and Planetary Science Letters, v. 272, no. 1, p. 158-171, doi:10.1016/j.epsl.2008.04.034.

Wang, Y. D., Nie, J. S., Zhang, T., Sun, G. Q., Yang, X., Liu, Y. H., and Liu, X. W., 2010a, Cenozoic tectonic evolution in the western Qaidam Basin inferred from subsurface data: Geosciences Journal, v. 14, no. 4, p. 335-344, doi: 10.1007/s12303-010-0033-1.

Wang, L., Xiao, A. C., Gong, Q. L., Liu, D., Wu, L., Zhou, S. P., Shen, Z. Y., Lou, Q. Q., and Sun, X. W., 2010b, The unconformity in Miocene sequence of western Qaidam Basin and its tectonic significance: SCIENCE CHINA Earth Sciences, v. 53, no. 8, p. 1126-1133, doi: 10.1007_s11430-010-4006-z.

Wang, C. S., Gao, R., Yin, A., Wang, H., Zhang, Y. X., Guo, T. L., Li, Q. S., and Li, Y. L., 2011, A mid-crustal strain-transfer model for continental deformation: A new perspective from high-resolution deep seismic-reflection profiling across NE Tibet: Earth and Planetary Science Letters, v. 306, no. 3, p. 279-288, doi: 10.1016/j.epsl.2011.04.010.

Wang, C., Liu, L., Yang, W. Q., Zhu, X. H., Cao, Y. T., Kang, L., Chen, S. F., Li, R. S., and He, S. P., 2013, Provenance and ages of the Altyn Complex in Altyn Tagh: implications for the early Neoproterozoic evolution of northwestern China: Precambrian Research. v. 230, p. 193-208, doi: 10.1016/j.precamres.2013.02.003.

Wang, C., Dai, J., Zhao, X., Li, Y., Graham, S. A., He, D., Ran, B., and Meng, J., 2014, Outward-growth of the Tibetan Plateau during the Cenozoic: A review: Tectonophysics, v. 621, p. 1-43, doi: 10.1016/j.tecto.2014.01.036.

Wiedenbeck, M., Alle, P., Corfu, F., Griffin, W., Meier, M., Oberli, F., Quadt, A. v., Roddick, J., and Spiegel, W., 1995, Three natural zircon standards for U-Th-Pb, Lu-Hf, trace element and REE analyses: Geostandards Newsletter, v. 19, no. 1, p. 1-23, doi: 10.1111/j.1751-908X.1995.tb00147.x.

Wu, H., Feng, Y., and Song, S., 1993, Metamorphism and deformation of blueschist belts and their tectonic implications, North Qilian Mountains, China: Journal of metamorphic Geology, v. 11, p. 523-523, doi: 10.1111/j.1525-1314.1993.tb00169.x.

Wu, C. L., Gao, Y. H., Wu, S. P., Chen, Q. L., Wooden, J. L., Mazadab, F. K., and Mattinson, C., 2008, Zircon SHRIMP dating and geochemical characteristics of granite from the Westem Qaidam: Science in China (D), v. 38, no. 8, p. 930-949 (in Chinese).

Wu, L., Xiao, A., Yang, S., Wang, L., Mao, L., Dong, Y., and Xu, B., 2012, Two-stage evolution of the Altyn Tagh Fault during the Cenozoic: new insight from provenance analysis of a geological section in NW Qaidam Basin, NW China: Terra Nova, v. 24, no.5, p.387-395, doi: 10.1111/j.1365-3121.2012.01077.x.

Wu, L., Xiao, A. C., Ma, D. D., Li, H. G., Xu, B., Shen, Y., and Mao, L. G., 2014, Cenozoic fault systems in southwest Qaidam Basin, northeastern Tibetan Plateau: Geometry, temporal development, and significance for hydrocarbon accumulation: AAPG Bulletin, v. 98, no. 6, p. 1213-1234, doi: 10.1306/11131313087.

Xia, W. C., Zhang, N., Yuan, X. P., Fan, L. S., and Zhang, B. S., 2001, Cenozoic Qaidam basin, China: A stronger tectonic inversed, extensional rifted basin: AAPG bulletin, v. 85, no. 4, p. 715-736, doi: 10.1306/8626C98D-173B-11D7-8645000102C1865D.

Xia, L. Q., Li, X. M., Ma, Z. P., Xu, X. Y., and Xia, Z. C., 2011, Cenozoic volcanism and tectonic evolution of the Tibetan plateau: Gondwana Research, v. 19, no. 4, p. 850-866, doi: doi:10.1016/j.gr.2010.09.005.

Xia, G. Q., 2012, The sedimentary records of the tectonic uplift of the East Kunlun in the Cenozoic [Ph.D. thesis]: Chengdu University of Technology, Chengdu, 150 p. (in Chinese with English abstract).

Xu, X. W., Chen, W. B., Ma, W. T., Yu, G. H., and Chen, G. H., 2002, Surface rupture of the Kunlunshan earthquake (Ms 8.1), northern Tibetan plateau, China: Seismological Research Letters, v. 73, no. 6, p. 884-892, doi: 10.1785/gssrl.73.6.884.

Xu, Q., Ding, L., Zhang, L., Cai, F., Lai, Q., Yang, D., and Liu-Zeng, J., 2013, Paleogene high elevations in the Qiangtang Terrane, central Tibetan Plateau: Earth and Planetary Science Letters, v. 362, p. 31-42, doi: 10.1016/j.epsl.2012.11.05.

Yang, F., Ma, Z. Q., Xu, T. C., and Ye, S. J., 1992, A Tertiary paleomagnetic stratigraphic profile in Qaidam basin: Acta Petrolei Sinica, v. 13, no. 2, p. 97-101 (in Chinese).

Yang, J. S., Robinson, P., Jiang, C. F., and Xu, Z. Q., 1996, Ophiolites of the Kunlun Mountains, China and their tectonic implications: Tectonophysics, v. 258, no. 1-4, p. 215-231, doi: 10.1016/0040-1951(95)00199-9.

Yang, J. S., Xu, Z. Q., Zhang, J. X., Chu, C. Y., Zhang, R. Y., and Liou, J. G., 2001, Tectonic significance of early Paleozoic high-pressure rocks in Altun-Qaidam-Qilian Mountains, northwest China in Hendrix, M.S., and Davis, G.A., eds., Paleozoic and Mesozoic Tectonic Evolution of Central and Eastern Asia: From Continental Assembly to Intracontinental Deformation:Geological Society of America Memoir 194, p. 151–170.

Yang, J. S., Xu, Z. Q., Zhang, J. X., Song, S. G., Wu, C. L., Shi, R. D., Li, H. B., and Maurice, B., 2002, Early Palaeozoic North Qaidam UHP metamorphic belt on the north‐eastern Tibetan plateau and a paired subduction model: Terra Nova, v. 14, no. 5, p. 397-404, doi: 10.1046/j.1365-3121.2002.00438.x.

Yang, J. S., Wu, C. L., Zhang, J. X., Shi, R. D., Meng, F. C., Wooden, J. L., and Yang, H. Y., 2006, Protolith of eclogites in the north Qaidam and Altun UHP terrane, NW China: Earlier oceanic crust?: Journal of Asian Earth Sciences, v. 28, no. 2, p. 185-204, doi: 10.1016/j.jseaes.2005.09.020.

Yang, W., Jolivet, M., Dupont-Nivet, G., Guo, Z., Zhang, Z., and Wu, C., 2013, Source to sink relations between the Tian Shan and Junggar Basin (northwest China) from Late Palaeozoic to Quaternary: evidence from detrital U-Pb zircon geochronology: Basin Research, v. 25, no. 2, p. 219-240, doi: 10.1111/j.1365-2117.2012.00558.x.

Yang, W., Jolivet, M., Dupont-Nivet, G., and Guo, Z., 2014, Mesozoic - Cenozoic tectonic evolution of southwestern Tian Shan: Evidence from detrital zircon U/Pb and apatite fission track ages of the Ulugqat area, Northwest China: Gondwana Research, v. 26, no. 3–4, p. 986-1008, doi: 10.1016/j.gr.2013.07.020.

Yi, H. S., Wang, C. S., Shi, Z. Q., Lin, J. H., and Zhu, L. D., 2008, Early uplift history of the Tibetan plateau: Records from paleocurrents and paleodrainage in the Hoh Xil basin: Acta Geologica Sinica‐English Edition, v. 82, no. 1, p. 206-213, doi: 10.1111/j.1755-6724.2008.tb00339.x.

Yin, A., Dang, Y. Q., Zhang, M., McRivette, M. W., Burgess, W. P., and Chen, X. H., 2007, Cenozoic tectonic evolution of Qaidam basin and its surrounding regions (part 2): Wedge tectonics in southern Qaidam basin and the Eastern Kunlun Range, in Sears, J.W., Harms, T.A., and Evenchick, C.A., eds., Whence the Mountains? Inquiries into the Evolution of Orogenic Systems: A Volume in Honor or Raymond A. Price: Geological Society of America Special Paper 433, p. 369–390, doi:10.1130/2007.2433(18)

Yin, A., Dang, Y. Q., Wang, L. C., Jiang, W. M., Zhou, S. P., Chen, X. H., Gehrels, G. E., and McRivette, M. W., 2008a, Cenozoic tectonic evolution of Qaidam basin and its surrounding regions (Part 1): The southern Qilian Shan-Nan Shan thrust belt and northern Qaidam basin:

Geological Society of America Bulletin, v. 120, no. 7-8, p. 813-846, doi:10.1130.B26180.1.

Yin, A., Dang, Y. Q., Zhang, M., Chen, X. H., and McRivette, M. W., 2008b, Cenozoic tectonic evolution of the Qaidam basin and its surrounding regions (Part 3): Structural geology, sedimentation, and regional tectonic reconstruction: Geological Society of America Bulletin, v. 120, no. 7-8, p. 847-876, doi: 10.1130/B26232.1.

Yu, X., Huang, B., Guan, S., Fu, S., Cheng, F., Cheng, X., Zhang, T., and Guo, Z., 2014, Anisotropy of magnetic susceptibility of Eocene and Miocene sediments in the Qaidam Basin, Northwest China: Implication for Cenozoic tectonic transition and depocenter migration: Geochemistry, Geophysics, Geosystems, v. 15, no. 6, p. 2095-2108, doi: 10.1002/2014GC005231.

Yuan, W. M., Zhang, X. T., Dong, J. Q., Tang, Y. H., Yu, F. S., and Wang, S. C., 2003, A new vision of the intracontinental evolution of the eastern Kunlun Mountains, Northern Qinghai-Tibet plateau, China: Radiation Measurements, v. 36, no. 1-6, p. 357-362, doi:10.1016/S1350-4487(03)00151-3.

Yuan, H. L., Gao, S., Liu, X. M., Li, H. M., Günther, D., and Wu, F. Y., 2004, Accurate U-Pb age and trace element determinations of zircon by laser ablation-inductively coupled plasma-mass spectrometry: Geostandards and Geoanalytical Research, v. 28, no. 3, p. 353-370, doi: 10.1111/j.1751-908X.2004.tb00755.x.

Yuan, W. M., Dong, J. Q., Wang, S. C., and Carter, A., 2006, Apatite fission track evidence for Neogene uplift in the eastern Kunlun Mountains, northern Qinghai-Tibet Plateau, China: Journal of Asian Earth Sciences, v. 27, no. 6, p. 847-856, doi: 10.1016/j.jseaes.2005.09.002.

Yue, Y., Ritts, B. D., Graham, S. A., Wooden, J. L., Gehrels, G. E., and Zhang, Z., 2004, Slowing extrusion tectonics: lowered estimate of post-Early Miocene slip rate for the Altyn Tagh fault: Earth and Planetary Science Letters, v. 217, no. 1, p. 111-122, doi: 10.1016/S0012-821X(03)00544-2.

Yue, Y. J., Graham, S. A., Ritts, B. D., and Wooden, J. L., 2005, Detrital zircon provenance evidence for large-scale extrusion along the Altyn Tagh fault: Tectonophysics, v. 406, no. 3, p. 165-178, doi: 10.1016/j.tecto.2005.05.023.

Zhang, J. X., Xu, Z. Q., Chen, W., and Xu, H. F., 1997, A tentative discussion on the ages of the subduction-accretionary complex/volcanic arcs in the middle sector of North Qilian Mountain: Acta Petrologica et Mineralogica, v. 16, no. 2, p. 112-119 (in Chinese with English abstract).

Zhang, J. X., Zhang, Z. M., Xu, Z. Q., Yang, J. S., and Cui, J. W., 2001, Petrology and geochronology of eclogites from the western segment of the Altyn Tagh, northwestern China:

Lithos, v. 56, no. 2, p. 187-206, doi: 10.1016/S0024-4937(00)00052-9.

Zhang, P. Z., Shen, Z., Wang, M., Gan, W., Bürgmann, R., Molnar, P., Wang, Q., Niu, Z., Sun, J., and Wu, J., 2004, Continuous deformation of the Tibetan Plateau from global positioning system data: Geology, v. 32, no. 9, p. 809-812, doi: 10.1130/G20554.1.

Zhang, J. X., Mattinson, C. G., Meng, F. C., and Wan, Y. S., 2005, An Early Palaeozoic HP/HT granulite–garnet peridotite association in the south Altyn Tagh, NW China: P–T history and U-Pb geochronology: Journal of Metamorphic Geology, v. 23, no. 7, p. 491-510, doi: 10.1111/j.1525-1314.2005.00585.x.

Zhang, W. L., 2006, High-resolution Magnetostratigraphy of the Cenozoic Qaidam Basin, implications for the uplift of Tibetan Plateau [Ph.D. thesis]: LanZhou University, Lanzhou, 158 p. (in Chinese with English abstract).

Zhang, J. X., Li, H. K., Meng, F. C., Xiang, Z. Q., Yu, S. Y., and Li, J. P., 2011, Polyphase tectonothermal events recorded in metamorphic basement from the Altyn Tagh, the southeastern margin of the Tarim basin, western China: constraint from U-Pb zircon geochronology -Pb zircon geochronology: Acta Petrologica Sinica, v. 27, no. 1, p. 23-46 (in Chinese with English abstract).

Zhang, W., Appel, E., Fang, X., Song, C., and Cirpka, O., 2012, Magnetostratigraphy of deep drilling core SG-1 in the western Qaidam Basin (NE Tibetan Plateau) and its tectonic implications: Quaternary Research, v. 78, no. 1, p. 139-148, doi: 10.1016/j.yqres.2012.03.011.

Zhang, C., Cheng, F., Huang, G., Huang, Y., Xing, C., Guan, B., Zhang, Q. and Xu, F., 2013a, Sediment and reservoir characteristics with reservior evaluation of the Lulehe Formation in Qie 16 block of Kunbei oildfield in Qaidam Basin. Acta Petrologica Sinica, v. 20, no. 8, p. 2883-2894 (in Chinese with English abstract).

Zhang, W., Fang, X., Song, C., Appel, E., Yan, M., and Wang, Y., 2013b, Late Neogene magnetostratigraphy in the western Qaidam Basin (NE Tibetan Plateau) and its constraints on active tectonic uplift and progressive evolution of growth strata: Tectonophysics, v. 599, p. 107-116, doi: 10.1016/j.tecto.2013.04.010.

Zhang, J., Mattinson, C., Yu, S., and Li, Y., 2014a, Combined rutile–zircon thermometry and U–Pb geochronology: New constraints on Early Paleozoic HP/UHT granulite in the south Altyn Tagh, north Tibet, China: Lithos, v. 200, p. 241-257, doi: 10.1016/j.lithos.2014.05.006.

Zhang, L. Y., Ding, L., Pullen, A., Xu, Q., Liu, D. L., Cai, F. L., Yue, Y. H., Lai, Q. Z., Shi, R. D., and Ducea, M. N., 2014b, Age and geochemistry of western Hoh-Xil–Songpan-Ganzi granitoids, northern Tibet: Implications for the Mesozoic closure of the Paleo-Tethys ocean: Lithos, v. 190, p. 328-348, doi: 10.1016/j.lithos.2013.12.019.

Zhao, J., Mooney, W. D., Zhang, X., Li, Z., Jin, Z., and Okaya, N., 2006, Crustal structure across the Altyn Tagh Range at the northern margin of the Tibetan plateau and tectonic implications: Earth and Planetary Science Letters, v. 241, no. 3, p. 804-814, doi: 10.1016/j.epsl.2005.11.003.

Zhou, J. X., Xu, F. Y., Wang, T. C., Cao, A. F., and Yin, C. M., 2006, Cenozoic deformation history of the Qaidam Basin, NW China: Results from cross-section restoration and implications for Qinghai-Tibet Plateau tectonics: Earth and Planetary Science Letters, v. 243, no. 1-2, p. 195-210, doi:10.1016/j.epsl.2005.11.033.

Zhu, Y. M., Weng, H. X., Su, A. G., Liang, D. G., and Peng, D. H., 2005, Geochemical characteristics of Tertiary saline lacustrine oils in the Western Qaidam Basin, northwest China: Applied Geochemistry, v. 20, no. 10, p. 1875-1889, doi: 10.1016/j.apgeochem.2005.06.003.

Zhuang, G., Hourigan, J. K., Ritts, B. D., and Kent-Corson, M. L., 2011, Cenozoic multiple-phase tectonic evolution of the northern Tibetan Plateau: Constraints from sedimentary records from Qaidam basin, Hexi Corridor, and Subei basin, northwest China: American Journal of Science, v. 311, no. 2, p. 116-152, doi: 10.2475/02.2011.02.

Zuffa, G. G., 1980, Hybrid arenites: their composition and classification: Journal of Sedimentary Research, v. 50, no. 1, p.21-29, doi: 10.1306/212F7950-2B24-11D7-8648000102C1865D.

Zuo, G. C., and Wu, H. Q., 1997, A bisubduction collision orogenic model of Early Paleozoic in the middle part of North Qilian area: Advance in Earth Science, v. 12, no. 4, p. 315-323 (in Chinese with English abstract).

# Chapter 3 The interplay between the sediments within Qaidam basin and the active tectonic within Altyn Tagh Range

## 3.1 Initial rupture and displacement on the Altyn Tagh fault, northern Tibetan plateau: constraints based on residual Mesozoic to Cenozoic strata in the western Qaidam basin

***Paper published in Geosphere, 2015, vol. 11, pp. 921–942***

**Initial rupture and displacement on the Altyn Tagh fault, northern Tibetan plateau: constraints based on residual Mesozoic to Cenozoic strata in the western Qaidam basin**

**Feng Cheng**[1, 2], Zhaojie Guo[1, †], Hillary S. Jenkins[3], Suotang Fu[4], Xiang Cheng[1]

[1] Key Laboratory of Orogenic Belts and Crustal Evolution, Ministry of Education, School of Earth and Space Sciences, Peking University, Beijing, 100871, China

[2] Laboratoire Géosciences Rennes, CNRS-UMR6118, Université Rennes 1 - Observatoire des Sciences de l'Univers, Rennes, France

[3] Department of Environmental Studies, University of Redlands, Lewis Hall - 1200 E. Colton Avenue Redlands, CA 92373

[4] Qinghai Oilfield Company, PetroChina, Dunhuang, Gansu, 736202, China

[†] Corresponding author. E-mail address: cfcf.chengfeng@gmail.com

*Note: The online version of this contribution can be found as:* ***Cheng, F., Guo, Z., Jenkins, H.S., Fu, S., Cheng, X., 2015. Initial rupture and displacement on the Altyn Tagh fault, northern Tibetan Plateau: Constraints based on residual Mesozoic to Cenozoic strata in the western Qaidam Basin. Geosphere 11, 921-942, doi: 10.1130/GES01070.1.***

### Abstract

The Altyn Tagh fault (ATF), located in the northern Tibetan plateau, is a large left-lateral strike-slip fault heavily responsible for the growth and formation of the plateau during Cenozoic time. Despite its significance, the initial timing and kinematic patterns of movement along the ATF remain highly debated. Here we present a detailed analysis of the stratigraphy and geochronology of three key lithologic sections (the Tula, Anxi, and Caishiling) along the

ATF to better understand this kinematic history. By correlating stratigraphic contacts and lithology with the U-Pb age spectra of Mesozoic samples within the western Qaidam basin, we find the ATF has experienced a total of ~360 km of displacement during the Cenozoic. By combining seismic profile data with geologic observations, we divide the activity along this fault into two distinct stages of motion: 1) an initial stage which occurred between early Eocene (~49 Ma) and mid-Miocene time (~15 Ma) and resulted in ~170 km of offset, and 2) an early stage which began in the late Miocene epoch and continues into the present, resulting in ~190 km of offset along the fault. We identify the Tula and Anxi sections as piercing points along the western segment of ATF and define these regions as residual parts of the original Qaidam basin. These estimates suggest that motion along the ATF has accelerated from an average left-lateral strike-slip rate of ~5.0 mm/yr during initial stage faulting to a rate of ~12.6 mm/yr between the late Miocene epoch and present day.

Keywords: northern Tibetan plateau; Altyn Tagh fault; Qaidam basin; strike-slip fault; displacement

### 3.1.1 Introduction

As a major strike-slip fault on the Tibetan plateau, the Altyn Tagh fault (ATF) plays a significant role in the Cenozoic deformation of northern Tibet (Fig. 1). Understanding the Cenozoic kinematic patterns of the ATF holds important implications for unraveling the evolution of northern Tibet, deciphering the growth history of the entire Tibetan plateau, and contributing to oil and gas exploration in the surrounding region (Yue and Liou, 1999; Yin and Harrison, 2000; Tapponnier et al., 2001; Yin et al., 2002; Wang et al., 2014). Recent studies have revealed much about the basic geology of the Altyn Tagh Range and the surrounding region (Wang, 1997; Cowgill et al., 2000; Yue et al., 2001; Yin et al., 2002; Chen et al., 2003; Cowgill et al., 2003; Dupont-Nivet et al.,2003, 2004; Ritts et al., 2004; Yue et al., 2004a; Wu et al., 2012a, 2012b; Cheng et al., 2014; Lu et al., 2014; Zhang et al., 2014); however, the immense size and extent of the Altyn Tagh Range make it difficult to locate ideal piercing points to estimate the initial timing of left-slip movement and total displacement along the ATF. As a result, both the timing and amount of slip along the fault are vigorously debated (e.g. Yin et al., 2002; Cowgill et al., 2003; Gehrels et al., 2003a, 2003b; Ritts et al., 2004; Wu et al., 2012a, 2012b).

Although some studies reference Mesozoic shearing in the Altyn Tagh Range, the growth of the Tibetan plateau is largely related to Cenozoic faulting along the ATF rather than any pre-Cenozoic shearing in the Altyn Tagh Range (Tapponnier et al., 1986, 2001; Arnaud et al.,

2003; Wang et al., 2005; Li et al., 2006; Liu et al., 2007b). A variety of approaches have been used to constrain the initial timing of left-slip movement along the ATF, and the estimates vary greatly. Initial movement along the ATF is estimated to have occured broadly between the Eocene and Miocene epochs (Chen et al., 2001; Meng et al., 2001; Wan et al., 2001; Yue et al., 2001; Yin et al., 2002; Robinson et al., 2003; Wu et al., 2012a, 2012b), and estimates of the total displacement along the ATF vary anywhere from ~1200 km to less than 90 km (Tapponnier et al., 1986; CSBS, 1992; Wang, 1997; Yin and Harrison, 2000; Yang et al., 2001; Yin et al., 2002; Cowgill et al., 2003; Gehrels et al., 2003a, 2003b; Ritts et al., 2004). The wide variety of estimates regarding the initial timing and offset of the ATF highlight the incomplete understanding of this remote region.

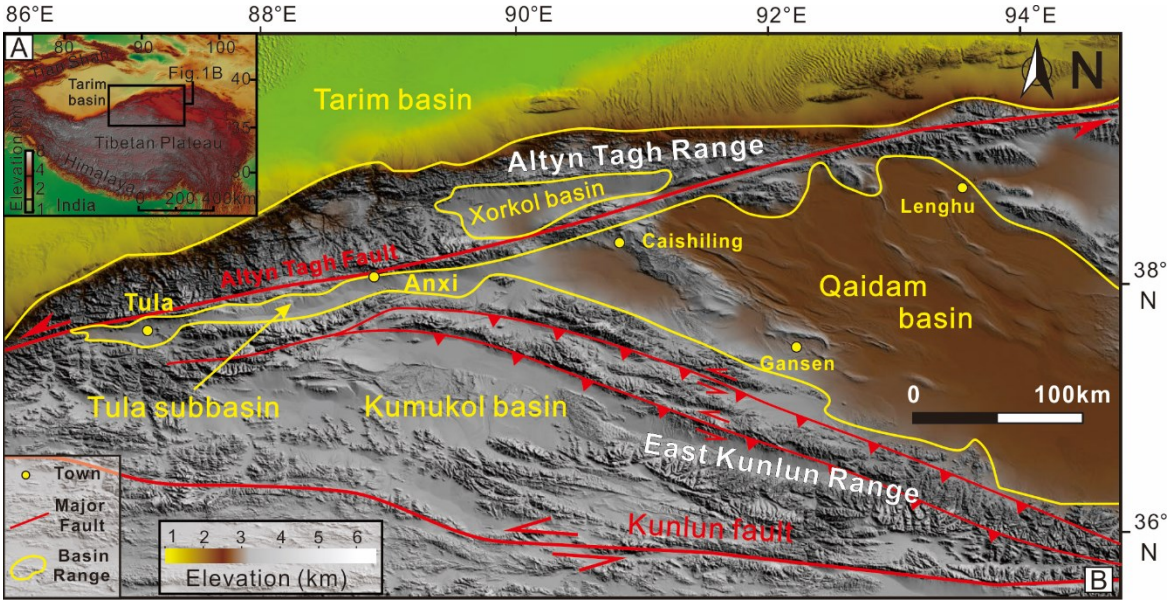


Figure 1. Digital topographic map of the center segment of the Altyn Tagh fault and surrounding area. Topography is from Shuttle Radar Topography Mission (SRTM) data.

In particular, Jurassic strata in both the southeast Tarim and northwest Qaidam basins across the ATF have been used as the geologic piercing point to constrain the total displacement along the ATF (e.g. Ritts and Biffi, 2000; Meng et al., 2001). However, Jurassic strata in western China are widespread and well developed in the foothills of several mountain belts (e.g. the Tian Shan, Altun Shan, Qilian Shan, and western Kunlun Mountains). These Jurassic strata are regionally similar, mainly characterized by a succession of terrestrial detrital rocks with coal-bearing deposits, locally intercalated with relatively few volcanic rocks (Hendrix et al., 1992, 2000; Li et al., 2004; Yue et al., 2004b; Yang et al., 2013; Liu et al., 2013a). While lithologically similar, these sedimentary features do not provide a distinct linear feature that can be matched across the ATF; thus Jurassic strata alone on either side of the ATF are inadequate and insufficient to document the total offset of the ATF.

In this paper, we present a detailed analysis of stratigraphy, sediment types, and detrital zircon U-Pb ages which enables us to establish stratigraphic correlations to source terranes and to constrain the amount of tectonic transport along the ATF (e.g. Gehrels, 2014). We present a synthesis of the stratigraphic and lithologic data along three sections (Tula, Anxi, and Caishiling sections) of the western segment of the ATF and the detrital zircon U-Pb geochronology for the Tula and Caishiling sections (Figs. 1 and 2). We use this information to constrain the timing of tectonic activity on the northern Tibetan plateau, to establish a more accurate estimate for the timing of initial movement along the ATF, and to provide a more accurate estimate of the total length of offset along the ATF during Cenozoic time.

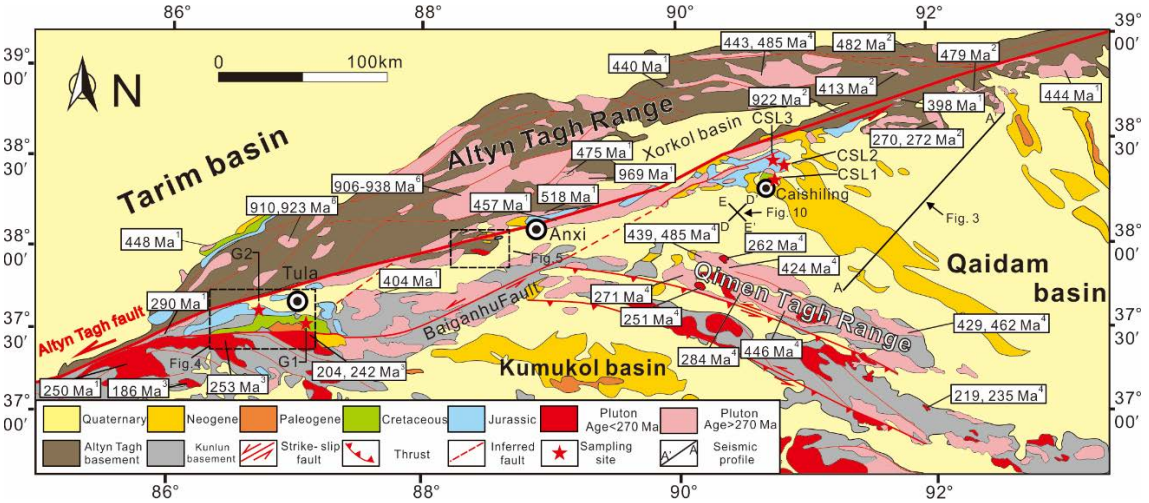


Figure 2. Geologic map of the center segment of the Altyn Tagh fault and the surrounding area, adapted from the Geologic Map of the Tibetan Plateau and Adjacent Areascompiled by Chengdu Institute of Geology and Mineral Resources and Chinese Geological Survey (map scale 1:1,500,000). Ages (zircon U-Pb) of plutons are mainly compiled from: 1—Cowgill et al. (2003); 2—Gehrels et al. (2003a); 3—HGSI (2003); 4—Chen et al. (2004); 5—Li et al. (2013); 6—Wang et al. (2013). See provenance analysis of Jurassic to Cretaceous strata sections for details.

## 3.1.2 Regional geology

### 3.1.2.1 Altyn Tagh Range

The Altyn Tagh Range is located at the northern edge of the Tibetan plateau, separating the Tarim basin to the northwest from the Qaidam basin to the southeast (Figs. 1 and 2). The bedrock of the Altyn Tagh Range is dominated by Precambrian igneous and metamorphic rocks and Paleozoic sedimentary rocks, whereas Mesozoic and Cenozoic strata are only sporadically represented (Wang, 1997; Sobel et al., 2001; Yin et al., 2002; Chen et al., 2003). Within the Altyn Tagh Range, the approximately 1600-km-long ENE-trending ATF starts in the western Kunlun Range in the southwest and terminates in the Qilian Shan Range in the

northeast, linking the Kunlun and Qilian Shan thrust belts (Burchfiel et al., 1989; Wang, 1997; Yue and Liou, 1999; Yin and Harrison, 2000; Yin et al., 2002). The origin of the ATF (Meyer et al., 1998; Chen et al., 2001; Meng et al., 2001; Wan et al., 2001; Yue et al., 2001; Yin et al., 2002; Ritts et al., 2004; Wu et al., 2012a, 2012b). The total displacement along the ATF fault remain heavily debated (CSBS, 1992; Ritts and Biffi, 2000; Yang et al., 2001; Cowgill et al., 2003; Gehrels et al., 2003a, 2003b). Quaternary slip rates of ~10 mm/yr on the ATF have been determined using field data, geodetic observations, and GPS measurements (Bendick et al., 2000; Shen et al., 2001; Yin et al., 2002; Zhang et al., 2004, 2007; Cowgill et al., 2009; Yin, 2010).

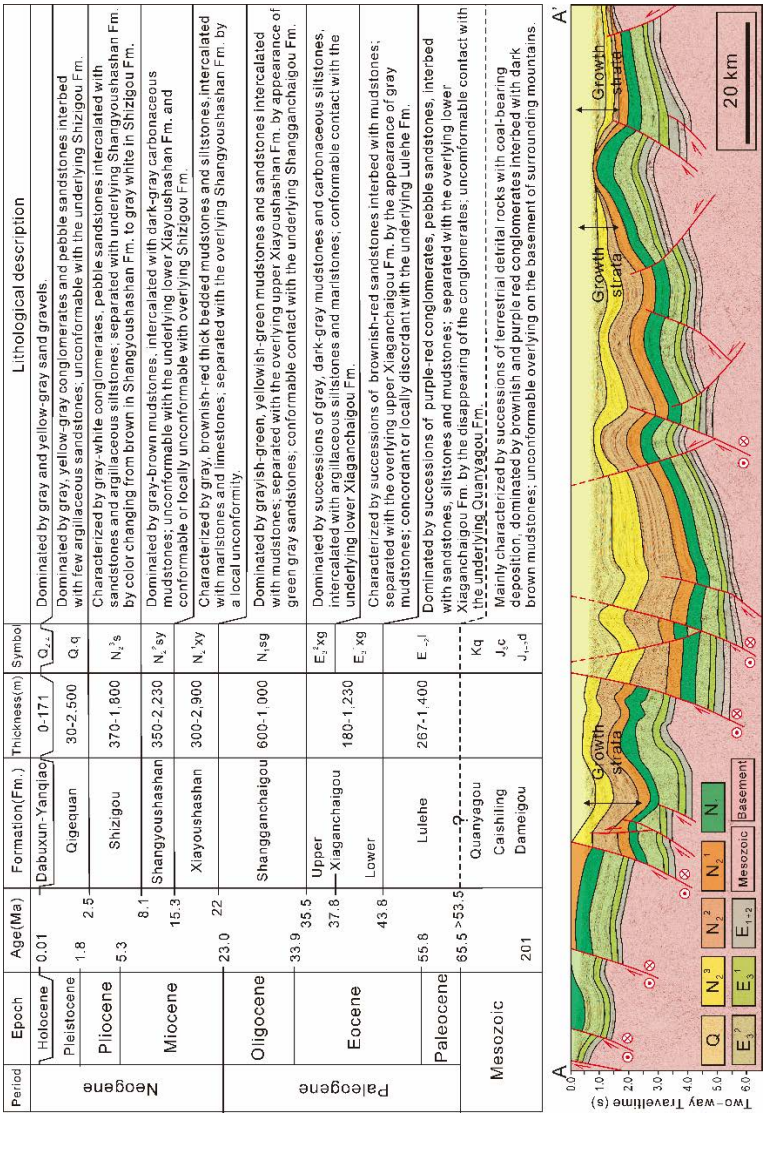


Figure 3. Stratigraphy and lithologic unit descriptions of the Qaidam Basin. The Cenozoic stratigraphy of the basin has been defined and dated in detail using magnetostratigraphy, palynology, and paleontology studies within the entire basin (Fang et al., 2007; Gao et al., 2009; Huang et al., 1996; Huo, 1990; Lu and Xiong, 2009; QBGMR, 1991; Qiu, 2002; Z.M. Sun et al., 2005; Xia et al., 2001; Yang et al., 1992; Zhao et al., 2006). See Figure 2 for seismic profile location. Note the growth strata above the Xiayoushashan Formation ($N_2^1$xy).

### 3.1.2.2 Qaidam basin

The triangular-shaped Qaidam basin, which lies on the southeastern side of the Altyn

Tagh Range, is the largest petroliferous basin within the northern Tibetan plateau (Figs. 1 and 2). The western Qaidam basin is bound by the Altyn Tagh Range to the northwest and the Qimen Tagh Range (western segment of the Eastern Kunlun Range) to the south. The westernmost part of the Qaidam basin is characterized by a unique NE-trending elongate landform known as the Tula trough (Wang et al., 2006a) or Tula subbasin (Guo et al., 1998) (Figs. 1 and 2). High-quality subsurface data have revealed that the southeastern Qaidam Basin is governed by a series of high-angle NW-trending reverse faults with considerable strike-slip component (Cheng et al., 2014, 2015) resulting in stratigraphic throw on either side of these faults in seismic profile (Fig. 3). The tectonic-sedimentary evolution of the Qaidam basin remains largely unknown though several hypotheses have been proposed (Métivier et al., 1996; Mock et al., 1999; Xia et al., 2001; Wang et al., 2006a; Yin et al., 2007; Meng and Fang, 2008; Yin et al., 2008a, 2008b; Wang et al., 2011). One hypothesis suggests that the western Qaidam basin experienced two Cenozoic structural phases: the first between the Paleocene and Eocene epochs and the second between the middle Miocene and Pleistocene epochs (Wang et al., 2010b). Growth strata and a regional angular unconformity between the early Miocene and late Miocene successions in the western Qaidam basin are identified as depositional responses to regional tectonic events in both the Altyn Tagh Range and the Eastern Kunlun Range during middle Miocene time (Song and Wang, 1993; Yin et al., 2007, 2008b; Wang et al., 2010a, 2010b; Wu et al., 2012a).

Geologic mapping and petroleum exploration have revealed that the Qaidam basin consists mainly of Cenozoic to Mesozoic nonmarine strata unconformably overlying an uncertain basement (Xia et al., 2001; Meng and Fang, 2008). The basement rock is too deep to be reached via drilling and its lithology therefore remains uncertain (Xia et al., 2001; Fang et al., 2007; Yin et al., 2008b). The Mesozoic strata are mainly located along the southern flank of the Altyn Tagh and the Qilian Shan ranges (Yin et al., 2008a; Wu et al., 2011). A succession of depo-centers of Cenozoic strata are present along the long axis of the basin and have gradually migrated eastward since the Eocene epoch (Song and Wang, 1993; Xia et al., 2001; Qiu, 2002; Sun et al., 2005a; Wang et al., 2006a; Yin et al., 2008b). Based on magnetostratigraphy, palynology and paleontology, the Mesozoic-Cenozoic strata of the Qaidam basin have been subdivided into 11 units and the chronostratigraphy of the Cenozoic units has been well constrained (Huo, 1990; QBGMR, 1991; Yang et al., 1992; Huang et al., 1996; Xia et al., 2001; Qiu, 2002; Sun et al., 2005a; Zhao et al., 2006; Fang et al., 2007; Yin et al., 2007; Gao et al., 2009; Lu and Xiong, 2009; Wu et al., 2011). These units are listed in order from oldest to youngest below, followed by the symbol for each unit, and the age range

capture of each unit, if available: (1) the Dameigou Fm., $J_{1+2}d$; (2) Caishiling Fm., $J_3c$; (3) Quanyagou Fm.., Kq; (4) the Lulehe Fm., $E_{1+2}l$, >53.5 - 43.8 Ma (Yang et al., 1992; Zhang, 2006; Ke et al., 2013); (5) the lower Xiaganchaigou Fm., $E_31xg$, 43.8 - 37.8 Ma (Zhang, 2006; Sun et al., 2007; Pei et al., 2009); (6) the upper Xiaganchaigou Fm., $E_3^2xg$, 37.8 - 35.5 Ma (Sun et al., 2005b, 2007; Pei et al., 2009); (7) the Shangganchaigou Fm., $N_1sg$, 35.5 - 22.0 Ma (Sun et al., 2005b; Lu and Xiong, 2009); (8) the lower Youshashan Fm., $N_2^1xy$, 22.0 - 15.3 Ma (Fang et al., 2007; Lu and Xiong, 2009); (9) the upper Youshashan Fm., $N_2^2sy$, 15.3 - 8.1 Ma (Fang et al., 2007); (10) the Shizigou Fm., $N_2^3s$, 8.1 - 2.5 Ma (Fang et al., 2007); (11) Quaternary deposits, including the Qigequan Fm. ($Q_1q$) and the Dabuxun-Yanqiao Fm. ($Q_{2-4}$), 2.5 - 0 Ma (Fang et al., 2007; Yin et al., 2008b). The lithologic features of each unit are summarized in detail Fig. 3.

### 3.1.3 Residual Mesozoic-Cenozoic stratigraphy along the Altyn Tagh Fault

#### 3.1.3.1 Mesozoic to Eocene strata in the Tula section

The Tula section is bounded by the ATF to the north and the Kunlun Precambrian and Paleozoic basement to the south (Figs. 2 and 4). A narrow valley runs through this region at the westernmost part of the Qaidam basin. Precambrian, Ordovician, and Carboniferous rocks comprise the basement rock which is unconformably overlain by Mesozoic to Cenozoic strata (Guo et al., 1998; HGSI, 2003; Ritts et al., 2004). Mesozoic strata in the Tula section are dominantly terrestrial clastic rocks. Several faults are present on the south side of the Tula basin (Fig. 2). The left-lateral NE-SW trending strike-slip Baiganhu Fault can be identified by a series of distinctive fault scarps and structural lineaments within the mountains, although the fault later becomes obscured by Quaternary deposits in the Tula basin (Fig. 2; Cowgill et al., 2003; HGIS, 2003; Wang et al., 2014).

Jurassic clastic coal-bearing strata rest unconformably on the Altyn Tagh basement (Fig. 4). Based on lithologic associations, sequence stratigraphy, and paleontology, these strata have been divided into two units: the Dameigou Fm. ($J_{1+2}d$), located in the lower part of the section and the Caishiling Fm. ($J_3c$), located in the upper part of the section (XBGRM, 1993; HGIS, 2003; Robinson et al., 2003; Dupont-Nivet et al., 2004). The lower part of the Dameigou Fm. ($J_{1+2}d$) is composed of fining-upward gray-brown conglomerate beds interbedded with greenish-gray sandstone and siltstone beds. The upper part of the Dameigou Fm. ($J_{1+2}d$) is characterized by a set of sandstone beds interbedded with conglomerate, siltstone and lithic sandstone (Fig 5A). Grain size increases upsection, indicating gradual shallowing and

subsiding of the basin. In the Caishiling section, thick-bedded lithic sandstone and conglomerate (Fig. 5B) are developed at the base of the Dameigou Fm. ($J_{1+2}$d), indicating that denudation of the source area began in Early Jurassic time (Robinson et al., 2003).

The Caishiling Fm. ($J_3$c) is composed of yellowish massive sandy conglomerate (Fig. 5C) intercalated with quartzolithic sandstone at the base, and is characterized by purple red, gray purple siltstone in the lower part of the section. These rocks transition to variegated sandstone and siltstone intercalated with conglomerate in the middle and upper parts of the section (Ritts and Biffi, 2000; Robinson et al., 2003). In the upper part of the Caishiling Fm. ($J_3$c), cross-bedding is well developed in the sandstone and imbrication can be found in the conglomerate (Fig. 5D). The uppermost part of the Caishiling Fm. ($J_3$c) contains thick-bedded oil sands (Fig. 5E) and natural asphalt (Fig. 5F), indicating the Tula unit was once a subsidence area characterized by a topographic low different from the narrow valley that exists at present (Fig. 1). Geochemical fingerprints (e.g. carbon isotopic composition) in the Jurassic oil-bearing sandstone of the Tula basin is similar to that of the geochemical fingerprints in the Jurassic oil-bearing sandstone oil in the Qaidam Basin (Guo et al., 1998).

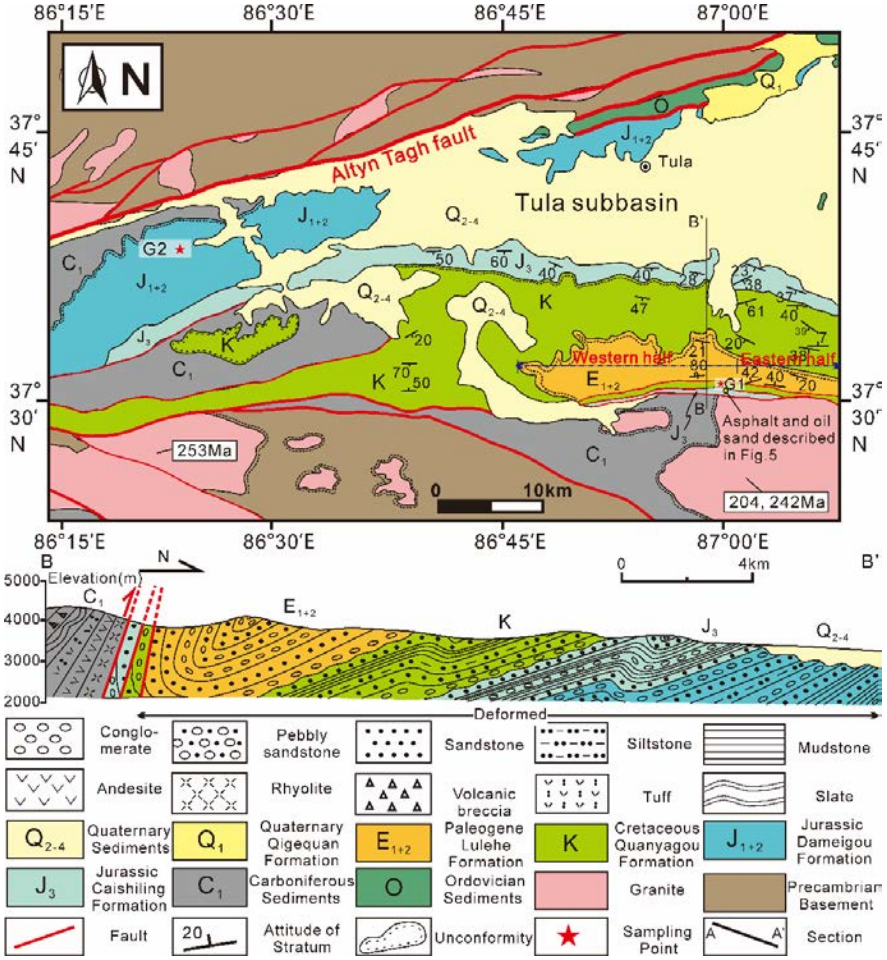


Figure 4. Geologic map (after Qiemo J45C003002 geologic map, scale 1:250,000) and geologic cross

section of the study area, compiled from HGSI (2003), Robinson et al. (2003), and XBGMR (1993). Red stars denote locations of U-Pb detrital zircon samples. Ages (zircon U-Pb) of plutons are mainly compiled from HGSI (2003). The western half and eastern half of the Eocene strata are based on the division of Dupont-Nivet et al. (2004).

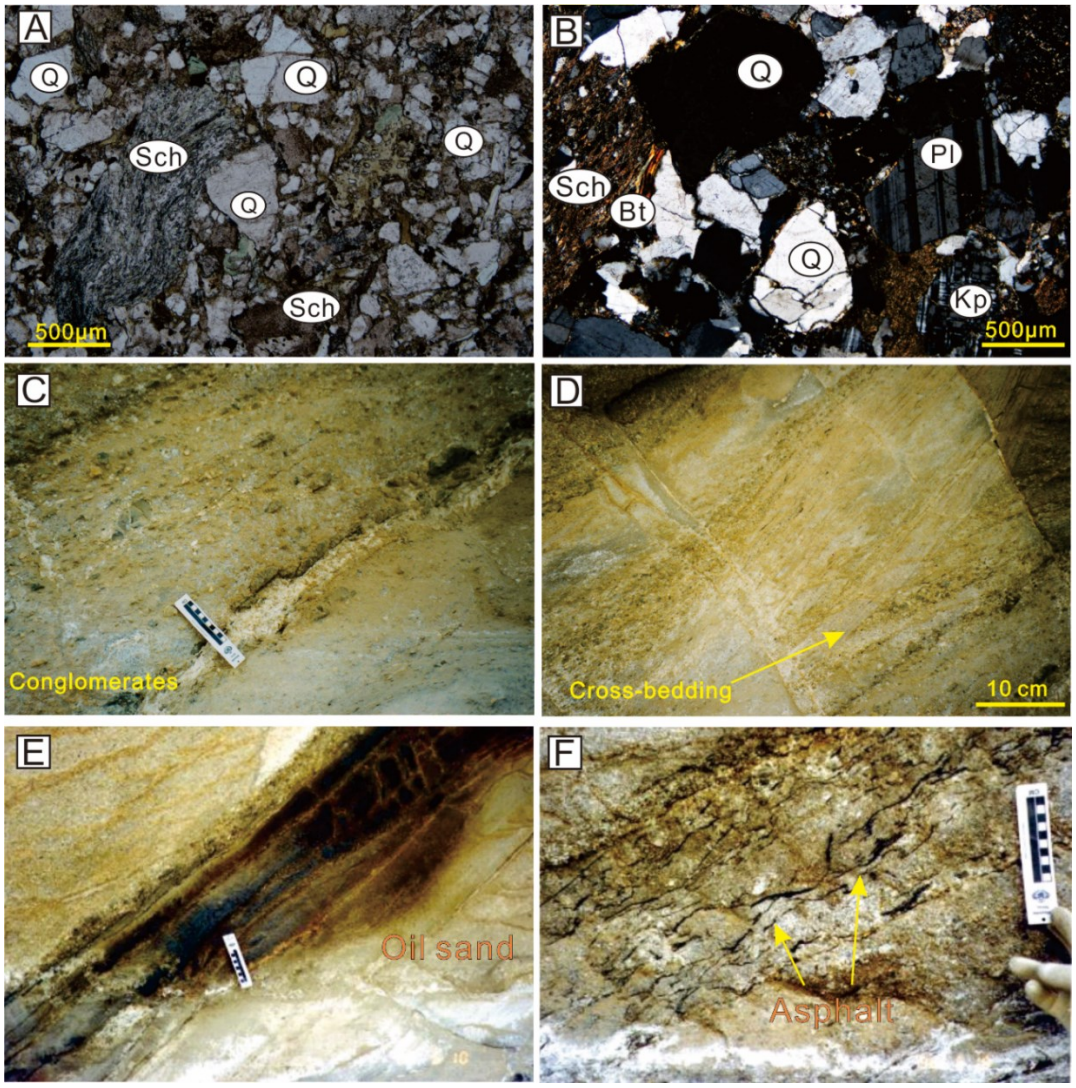


Figure 5. Typical photomicrographs and field photographs. (A) Lithic sandstone in early Jurassic strata ($J_{1+2}d$) of the Tula section, rich in lithic fragments, under plane polarized light. (B) Lithic sandstone in Early Jurassic strata ($J_{1+2}d$) of the Caishiling section, rich in various lithic fragments, under crossed polarized light. (C) Conglomerate and (D) cross-bedding in Late Jurassic ($J_3c$) strata of the Tula section. (E) Oil sand and (F) asphalt developed in Late Jurassic ($J_3c$) strata. Abbreviations: Sch—schist, Pl—plagioclase, Kp—potash feldspar, Q—quartz, Bt—biotite.

More than 2000 m of Cretaceous strata (Quanyagou Fm.) unconformably overlie the Late Jurassic strata Caishiling Fm. (XBGRM, 1993; Robinson et al., 2003). In the Tula section, Cretaceous plutons (~74 Ma) intrude Cretaceous strata, providing a minimum depositional age (XBGRM, 1993; Robinson et al., 2003). The lower part of the Cretaceous strata is dominated by purple-red conglomerate intercalated with sandstone, siltstone, and mudstone interpreted to represent lacustrine depositional environment. The upper part of Cretaceous strata consists

of purple red siltstone interbedded with silty mudstone interpreted to represent a lacustrine deltaic depositional environment (Ritts and Biffi, 2000; Robinson et al., 2003). The lacustrine to lacustrine delta deposits in the Tula unit reinforce the idea that the Tula unit was characterized by a topographic low during the Cretaceous, a setting very different from the narrow valley that exists at present (Fig. 1).

In the Tula unit, the well-exposed Paleocene to early Eocene Lulehe Fm. overlies the Mesozoic strata along a low-angle unconformity (XBGMR, 1993, HGSI, 2003; Robinson et al., 2003). The Lulehe Fm. consists mainly of purple red conglomerate interbedded with fine-grained sandstone at the base, which becomes coarser upsection with an increase in the abundance of conglomerate towards the top. The formation contains a high metamorphic lithic fraction and limestone clasts with coral fossils that suggest a proximal provenance and syntectonic deposits (Zuffa, 1980; Mack and Rasmussen, 1984; HGSI et al., 2003; Robinson et al., 2003). The distinctive purple red conglomerates found in the Lulehe Fm. are regionally similar to those found in the Qaidam basin. The Lulehe Fm. has been dated via magnetostratigraphy to between 65~53.5 and 43.8 Ma (Yang et al., 1992; Zhang et al., 2006; Ke et al., 2013). These dates further support a Paleocene to early Eocene age for the Lulehe Fm.

The Jurassic-early Eocene strata in the Tula section are heavily deformed, forming a major north-verging syncline with a steeply dipping south limb and a shallowly dipping north limb (Fig. 4). The Jurassic, Cretaceous, and Paleocene to early Eocene strata in the south limb of the syncline are inverted with a high dip angle (dipping mainly to the south from 180° to 200° at angles of 65°-80°). The contact between the Creteacous and Paleocene to early Eocene stata is characterized by a low-angle angular unconformity or a local fault boundary (XBGMR et al., 1993; HGSI et al., 2003; Robinson et al., 2003).

#### 3.1.3.2 Cenozoic strata in the Anxi section

The Anxi section, ~150 km northeast of the Tula section, is located in the ATF zone and is bounded by the Altyn Tagh basement to the north and the Kunlun Precambrian and Paleozoic basement to the south (Figs. 2 and 6). Precambrian and early Paleozoic metamorphic rocks with igneous intrusions comprise this basement which is overlain by Mesozoic and Cenozoic strata (Guo et al., 1998; Ritts and Biffi, 2000; GGSI, 2003). The Cenozoic units in the Anxi section have been identified based on the detailed field mapping of previous studies, and depositional ages are estimated by correlating these units with the well-constrained Cenozoic strata of the Qaidam basin (Fig. 7; Huo, 1990; QBGMR, 1991; Yang et al., 1992;

Huang et al., 1996; Xia et al., 2001; Qiu, 2002; GGSI, 2003; Sun et al., 2005a; Zhao et al., 2006; Fang et al., 2007; Yin et al., 2007; Gao et al., 2009; Lu and Xiong, 2009; Wu et al., 2011).

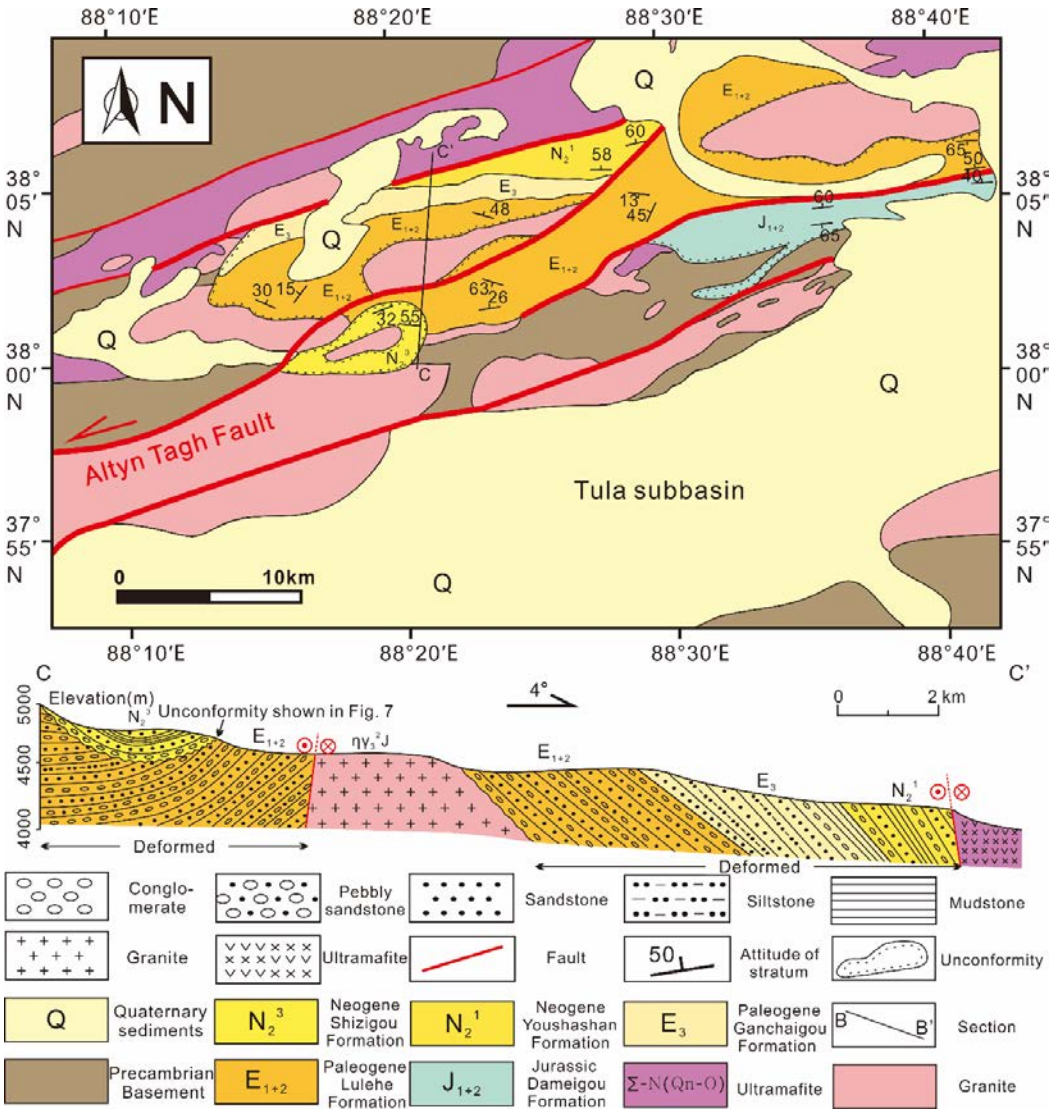


Figure 6. Geologic map (after the Washixia J45C002003 geologic map, scale 1:250,000) and geologic cross section of the study area, compiled from GGSI (2003) and XBGMR (1993).

Unlike the poorly preserved Cenozoic strata of the Tula section, the Anxi section contains a well-exposed Cenozoic stratigraphic succession that includes most of the Cenozoic units described above. The Anxi section includes the Paleocene to early Eocene Lulehe Fm., the Eocene to Oligocene Ganchaigou Fm., the Miocene Youshashan Fm. and the Pliocene Shizigou Fm. As visible in cross-sectional profile (Fig. 6), the Lulehe, Ganchaigou and Youshashan formations of the Anxi section are in conformable contact with one another and have been deformed synchronously after early Miocene time. However, in plan view, these

Paleocene to Miocene strata are cut by the left-lateral strike-slip ATF and separated from the overlying Pliocene strata of the Shizigou Fm. by an apparent angular unconformity (Fig. 6).

The Paleocene to early Eocene strata of the Lulehe Fm. crop out in the northern part of the valley and trend in a NE direction. These strata are characterized by brick-red conglomerates and pebble sandstones intercalated with sandstones and siltstones. This portion of the Lulehe Fm. is separated from the typically overlying Eocene strata of the Xiaganchaigou Fm. by the disappearance of the conglomerate layers (GGSI, 2003). The Eocene to Oligocene strata of the Ganchaigou Fm. only crop out in the northern part of the valley. The lack of paleomagnetic data in the Anxi section has thus far prevented a further division of these strata into two units as has been done in the western Qaidam basin (Fig. 3). The lower part of the Ganchaigou Fm. is dominated by grey to greyish-green sandstones intercalated with siltstones, biomicrites and mudstones. The upper part of the Ganchaigou Fm., however, is characterized by greyish-green calcareous shales and mudstones. The Gangchaigou Fm. is overlain by the Miocene Youshashan Fm., which contains brown granule conglomerate at its base (GGSI, 2003). Like the overlying Ganchaigou Fm., the Youshanshan Fm. crops out in the northern part of the valley. The Youghshanshan Fm. has not been subdivided into two units as has been done in the western Qaidam basin (Fig. 3; GGSI, 2003). The lower and middle sections of the Youshashan Fm. strata consist mainly of brown and maroon granule conglomerate interbedded with coarse sandstone while the upper part is characterized by purple and brown sandstone and pebble sandstone interbedded with conglomerate, siltstone and mudstone. These primarily brown strata distinguish the Youshashan Fm. from the overlying Pliocene strata of the Shizigou Fm., which is characterized by earthy yellow and grey pebble sandstone at its base (GGSI, 2003). The Pliocene strata are then overlain by Quaternary sand-gravel beds which lie atop an angular unconformity (Fig. 6). The lithology in the lower part of the Pliocene strata consists of sandstone interbedded with siltstone and mudstone while the middle and upper parts of the Pliocene strata are characterized by conglomerate and sandstone intercalated with siltstone (GGSI, 2003). These thickly-bedded conglomerates are interpreted to represent alluvial fan to fluvial facies (Ritts and Biffi, 2000).

### 3.1.4 Methods

#### 3.1.4.1 Field investigation and seismic profile interpretation

We used three sections (Tula, Anxi, and Caishiling) along the western segment of the ATF to study stratigraphic features of the Mesozoic-Cenozoic deposits (Fig. 2). We integrate

three high-quality seismic profiles of the western Qaidam basin with our surficial field observation to explain the tectonic history of this region. Two of the seismic profiles (A-A' and D-D') trend along strike (northeast) of the ATF while one of the profiles (E-E') trends perpendicular (northwest) to the ATF (Fig. 2). Seismic data were interpreted using SMT Kingdom software.

Table 1. Summary of the major characteristics and corresponding statistical data for each of the samples.

| Epoch | Formation (Fm.) | Sample number | Lithology | Detrital zircon age range (Ma) | Detrital zircon peaks (Ma) | Number of effective data points | Th/U ratios |
|---|---|---|---|---|---|---|---|
| Tula unit | | | | | | | |
| Cretaceous | Quanyagou Fm. | G1 | Gray-yellow pebbly sandstone | 218~2532 | ~238<br>~414<br>~904<br>~1737 | 89 | 0.13~1.51 |
| Early-Middle Jurassic | Dameigou Fm. | G2 | Gray-white sandstones | 254~2430 | ~250<br>~447<br>~1435<br>~2465 | 99 | 0.09, 0.10~ 1.98 |
| Caishiling unit | | | | | | | |
| Cretaceous | Quanyagou Fm. | CSL1 | Gray-white sandstone | 228~2915 | ~262<br>~456<br>~897 | 94 | 0.10~2.05 |
| Late Jurassic | Caishiling Fm. | CSL2 | Gray-white sandstones | 246~2661 | ~254<br>~445<br>~926 | 100 | 0.03, 0.06, 0.12~1.55 |
| Early-Middle Jurassic | Dameigou Fm. | CSL3 | Gray-yellow sandstones | 220~2480 | ~264<br>~433 | 97 | 0.25~3.82 |

3.1.4.2 Sampling and analytical process

Detrital zircon geochronology is rapidly developing into an essential tool for sediment provenance analysis and geodynamic study (e.g. Fedo et al., 2003; Thomas, 2011; Gehrels et al., 2011; Gehrels, 2014). U-Pb dating of detrital zircons from sediments is widely used to reconstruct the provenance of ancient sedimentary systems. To identify appropriate piercing points along the ATF, five sandstone samples ranging in age from Lower Jurassic to Cretaceous were collected from the Tula and Caishiling sections. In the Tula section, we collected two samples: G1 and G2. Sample G1 is gray-yellow pebbly sandstone from the Cretaceous Quanyagou Fm. (Kq). Sample G2 is gray-white sandstone from the lower Jurassic Dameigou Fm. ($J_{1+2}d$). In the Caishiling section, we took three samples: CSL1, CSL2 and CSL3. Sample CSL1 is a gray-white fine-grained sandstone from the Cretaceous Quanyagou Fm. (Kq). Sample CSL2 is a gray-white medium-grained sandstone from the Upper Jurassic

Caishiling Fm. ($J_3c$). Sample CSL3 is a gray-yellow coarse-grained sandstone from the Lower Jurassic Dameigou Fm. ($J_3c$) (Fig. 2). Detailed descriptions of the zircon separation and LA-ICP-MS U–Pb dating of zircon are provided in the GSA Data Repository (see footnote 1[①]).

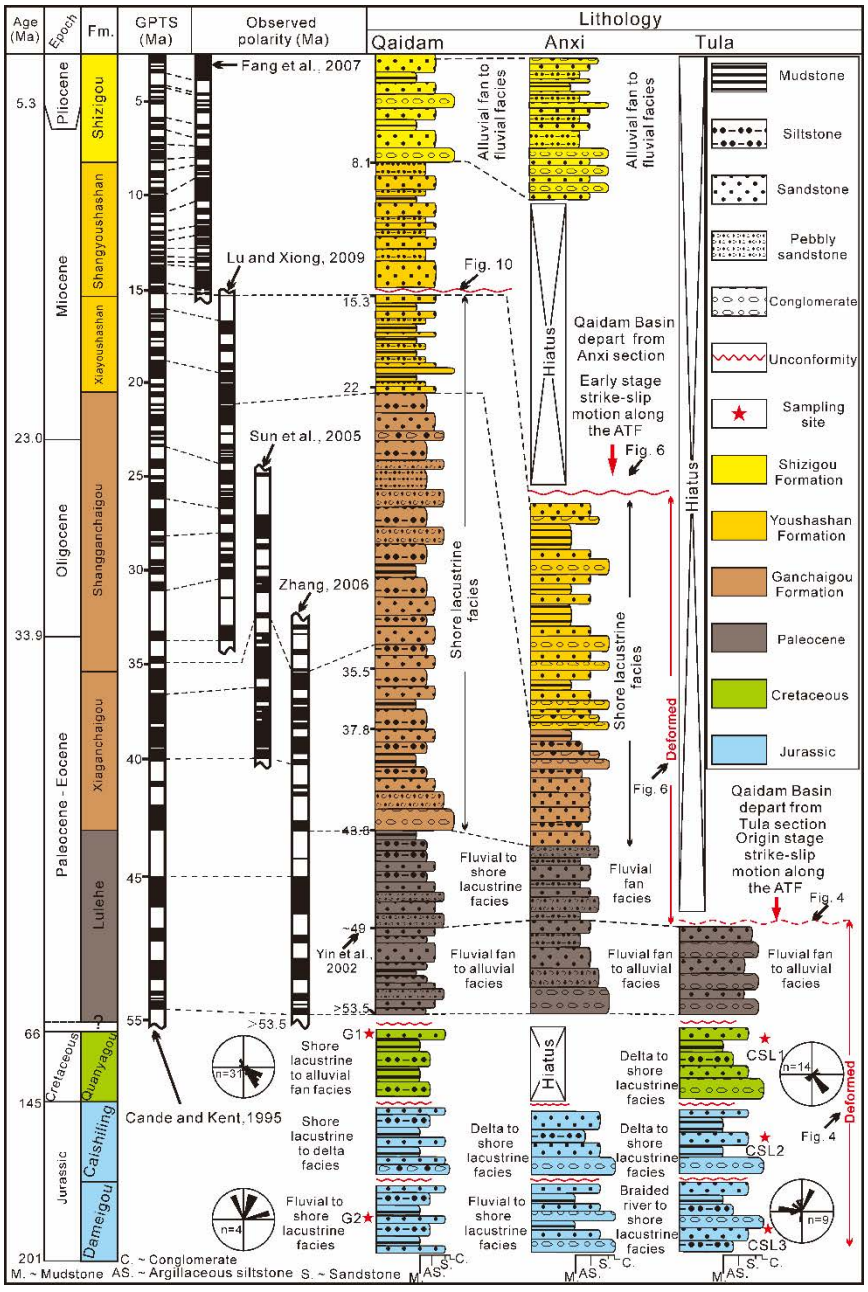


Figure 7. Chronostratigraphic correlation of the relic Mesozoic to Cenozoic strata along the Altyn Tagh fault. GPTS—geomagnetic polarity time scale of Cande and Kent (1995). Observed polarity was compiled from Yin et al. (2002), Z.M. Sun et al. (2005), Zhang (2006), Fang et al. (2007), and Lu and Xiong (2009). Paleocurrents are from Ritts and Biffi (2000). Chronostratigraphic correlation is based on field observation and previous studies (XBGMR, 1993; Guo et al., 1998; Ritts and Biffi, 2000; GGSI, 2003; HGSI, 2003; Robinson et al., 2003). ATF—Altyn Tagh fault.

[①] 1 Supplemental File. Description of zircon separation and LA-ICP-MS U-Pb dating of zircon, Figure DR1, and Tables DR1–DR2. Please visit http://dx .doi .org/10 .1130 /GES01070 .S1or the full-text article on www.gsapubs .org to view the Supplemental File

## 3.1.5 Results

### 3.1.5.1 U–Pb geochronology of detrital zircons

Isotopic ages with errors and related raw data are listed in full in Table DR1 (see footnote 1). The various zircon age groups and corresponding data for each sample are shown in Table 1. CL images of typical zircon grains are presented in Figure DR1 (see footnote 1).

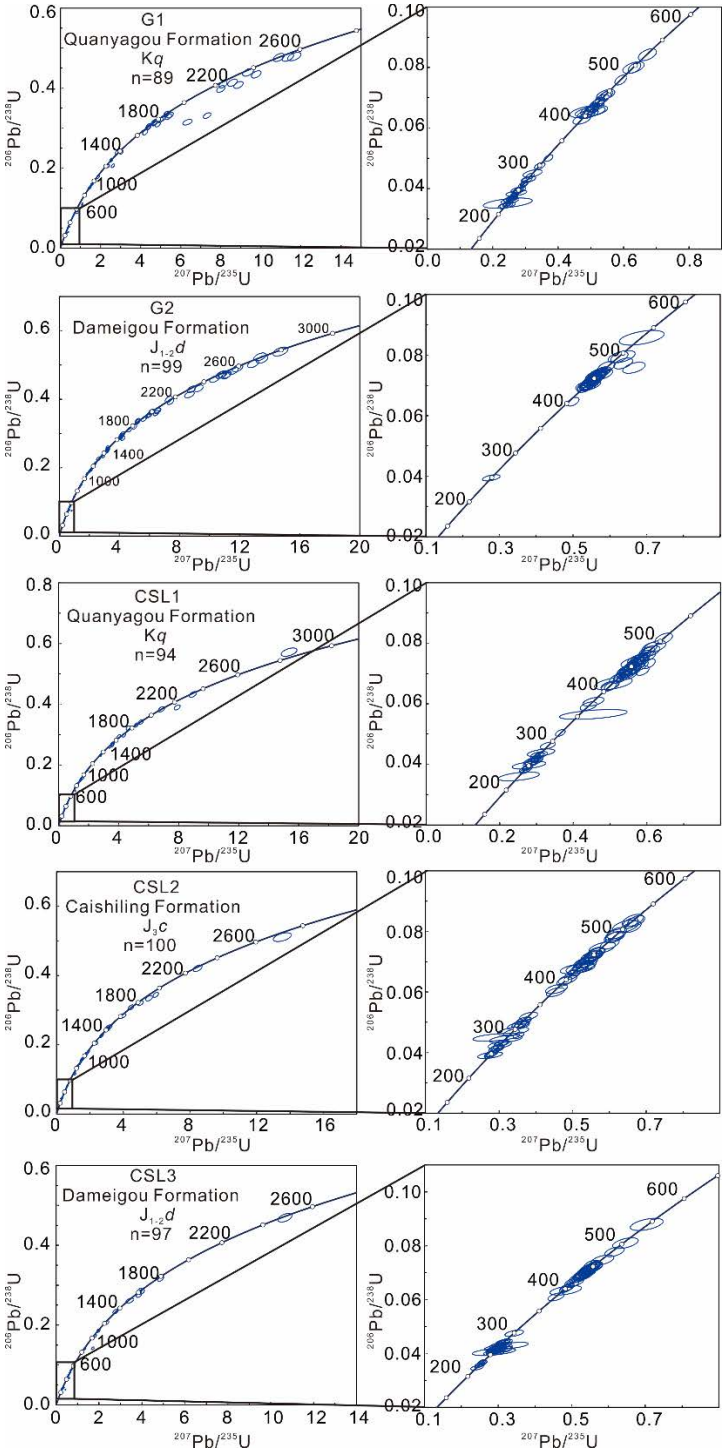


Figure 8. U-Pb concordia diagrams for zircon grains from the five sandstone samples

#### 3.1.5.1.1 Jurassic samples

The zircons from sample G2 (Dameigou Fm.) are ~50-200 μm long and mainly subhedral to subrounded. The grains are generally colorless and exhibit prominent oscillatory zoning. Th/U ratios typically clustered between 0.09 and 1.98. Forty-eight out of 99 dated grains yielded a 206Pb/238U range of 530 to 404 Ma with a single peak in the age spectrum at 447 Ma (Fig. 9A). Only one zircon with a Triassic age (250 Ma) was obtained. The ages of all other zircons range from 2781 to 696 Ma.

In sample CSL3 (Dameigou Fm.), zircon grain morphology ranges from euhedral to abraded with an average size ranging between 50 μm and 250 μm. CL images show that most of these zircon crystals are characterized by relatively distinct oscillatory zoning. Th/U ratios vary between 0.25 and 3.82. The U-Pb ages range from 2480 to 220 Ma (Fig. 9B). The ages can be separated in three main groups with two peak ages at 264 Ma, 433 Ma, and eleven ages between 2480 to 852 Ma.

In sample CSL2 (Caishiling Fm.), zircon crystals display euhedral to abraded shapes for an average size ranging between 50 μm and 250 μm. The majority of the crystals display distinct oscillatory zoning in CL images indicating a magmatic origin confirmed by Th/U ratios varying between 0.12 and 1.55 (with two exception of 0.03 and 0.06). Among the 100 crystals analyzed, all zircon ages with a discordance degree of <10% were used. The U-Pb ages range from ~2661 to ~246 Ma (Fig. 9C). The age distributions are divided into four groups with two major peaks at ~254 Ma and ~445 Ma, a distribution spanning from 1073 Ma to 701 Ma with a peak at 926 Ma, and finally seven ages clustered around 1416 Ma.

#### 3.1.5.1.2 Cretaceous samples

The zircons from sample G1 (Quanyagou Fm.) are predominantly colorless, euhedral to subhedral, and with a length of 50-150 μm. Most zircons show oscillatory zoning without inherited cores or overgrowths. All analyses have moderate U content, with variable Th/U from 0.13 to 1.51. In this study, 59 out of 89 dated grains yielded a 206Pb/238U range of 521 to 218 Ma with two age peaks at 414 Ma and 238 Ma (Fig. 9D). The age of the remaining zircons range from 2532 to 818 Ma with several subpeaks at 2502, 1737 and 904 Ma.

In sample CSL1 (Quanyagou Fm.), zircon grains show euhedral to abraded shapes with an average size between 50 μm and 200 μm. Most crystals show distinct oscillatory zoning. Th/U ratios vary from 0.10 to 2.05. 100 grains were analyzed and 94 effective data points were obtained. The U-Pb ages range from 2915 to 228 Ma. The ages can be separated in four main groups with three peaks at 897 Ma, 456 Ma and 262 Ma (Fig. 9E). In addition, fifteen

Proterozoic ages are given above 1000 Ma.

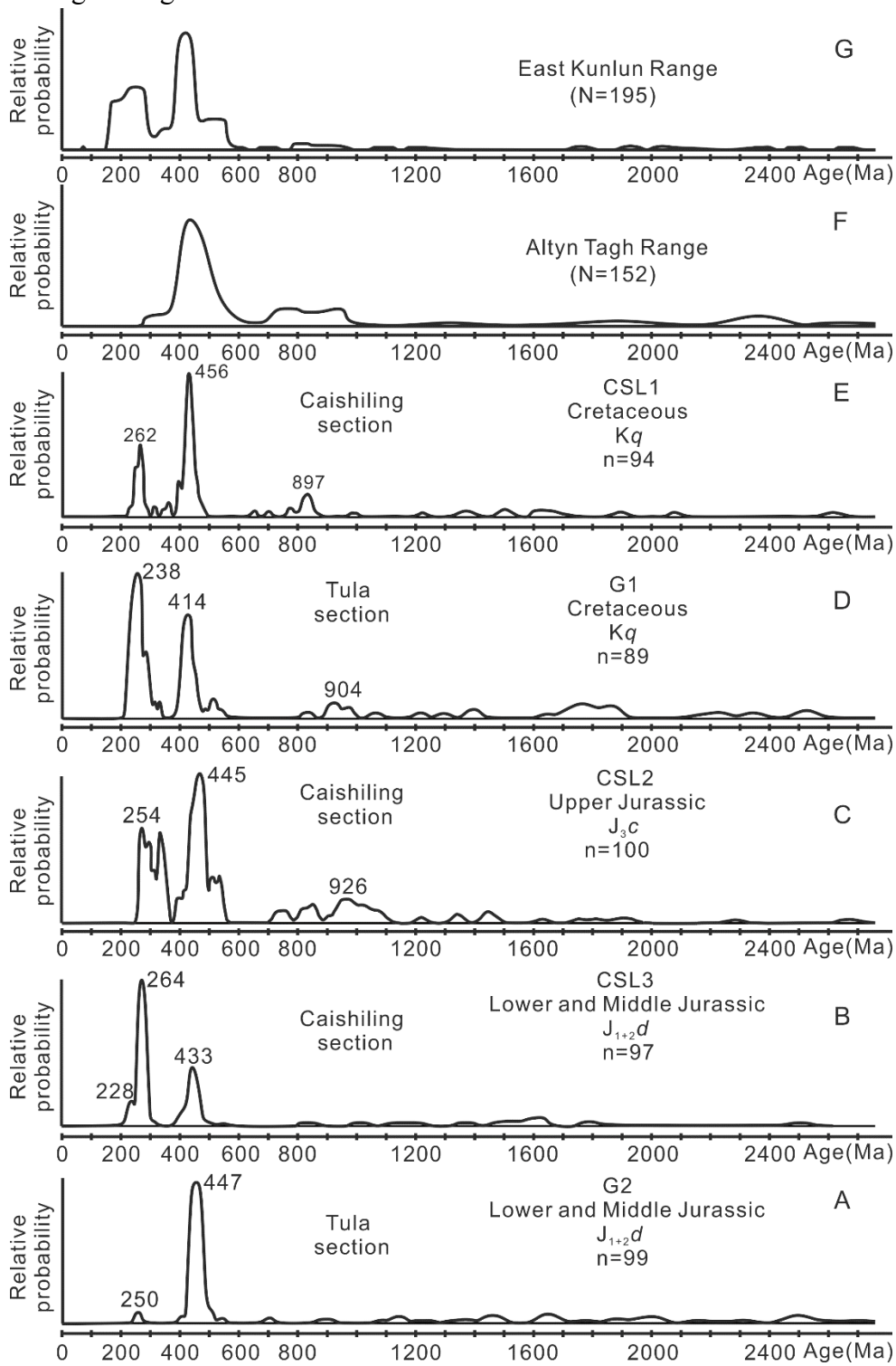


Figure 9. Relative probability histogram plots of U-Pb ages of detrital zircons from the five Jurassic and Cretaceous sandstone samples and relative probability histogram plots of pluton ages in the Altyn Tagh and Eastern Kunlun Ranges. Age data are from Yang et al. (2006), Zhang et al. (2001), Chen et al. (2003), Gehrels et al. (2003a, 2003b), Yue et al. (2005), Yang et al. (2006), L. Liu et al. (2007, 2013), Lu et al. (2008), Liu et al. (2009), Zhang et al. (2011), Li et al. (2013), and Wang et al. (2013). More information on dating and ages is provided in Table DR2 (see text footnote 1).

## 3.1.6 Discussion

### 3.1.6.1 New piercing points

Using lithologic and stratigraphic constraints, we conclude that both the Tula and Anxi sections were once regions of extensive subsidence characterized by topographic lows (Figs. 1 and 2). The dark mudstone, oil sands (Fig. 5E) and asphalt (Fig. 5F) found in the Upper Jurassic strata of the Tula section indicate Tula basin was once a depression during Late Jurassic time. In addition, matching geochemical fingerprints (e.g. carbon isotopic composition) between the Jurassic oil-bearing sandstone of the Tula basin and the Jurassic crude oil of Qaidam basin suggests that these two regions must have been parts of the same prototype basin (Guo et al., 1998). Recent studies confirm that the relatively rigid Qaidam basin was transported northeastward along the ATF during the Cenozoic, and has not undergone obvious basin-scale vertical axis rotation with respect to the Eurasian Plate since early Eocene time (Wang et al., 2006; Yu et al., 2014). Considering the large-scale left-lateral strike-slip displacement of the ATF during Cenozoic time, we suggest the Tula and Anxi sections were once part of the Qaidam basin but detached from the Qaidam during its northeasterward migration driven by faulting on the ATF. We propose the Qaidam basin may have actually been originally located much farther southwest along the ATF than its present position, likely located where the Tula and Anxi sections currently reside.

Stratigraphic successions are generally deposited during basin infilling processes, while periods of non-deposition or erosion are likely related to regional tectonic events (e.g. Wheeler, 1964; Allen and Allen, 1990; Boggs, 2006). In the Tula section, Paleocene strata correlate well with strata in the Caishiling section, however, post-Paleocene strata are missing (Figs. 4 and 7). In the Anxi section, Paleocene to early Miocene strata cross-correlate with comparable strata preserved in the Caishiling section, whereas the late Miocene are missing (Figs. 6 and 7). In the Qaidam basin, and particularly in the Caishiling section, the Paleocene to Quaternary strata are well developed (Figs. 2 and 7). If we consider a stepwise northeastward migration of the Qaidam basin along the ATF throughout the Cenozoic, the absence of post-Paleocene strata in the Tula section marks the detachment of the Qaidam basin from this section. Similarly, the absence of late Miocene strata in the Anxi section marks the detachment of the Qaidam basin from this section (Fig. 7). We therefore propose that the Paleocene strata in the Tula section and the Paleocene to early Miocene strata in the Anxi section represent the two piercing points to identify the initial position and early stages of Qaidam basin detachment and movement.

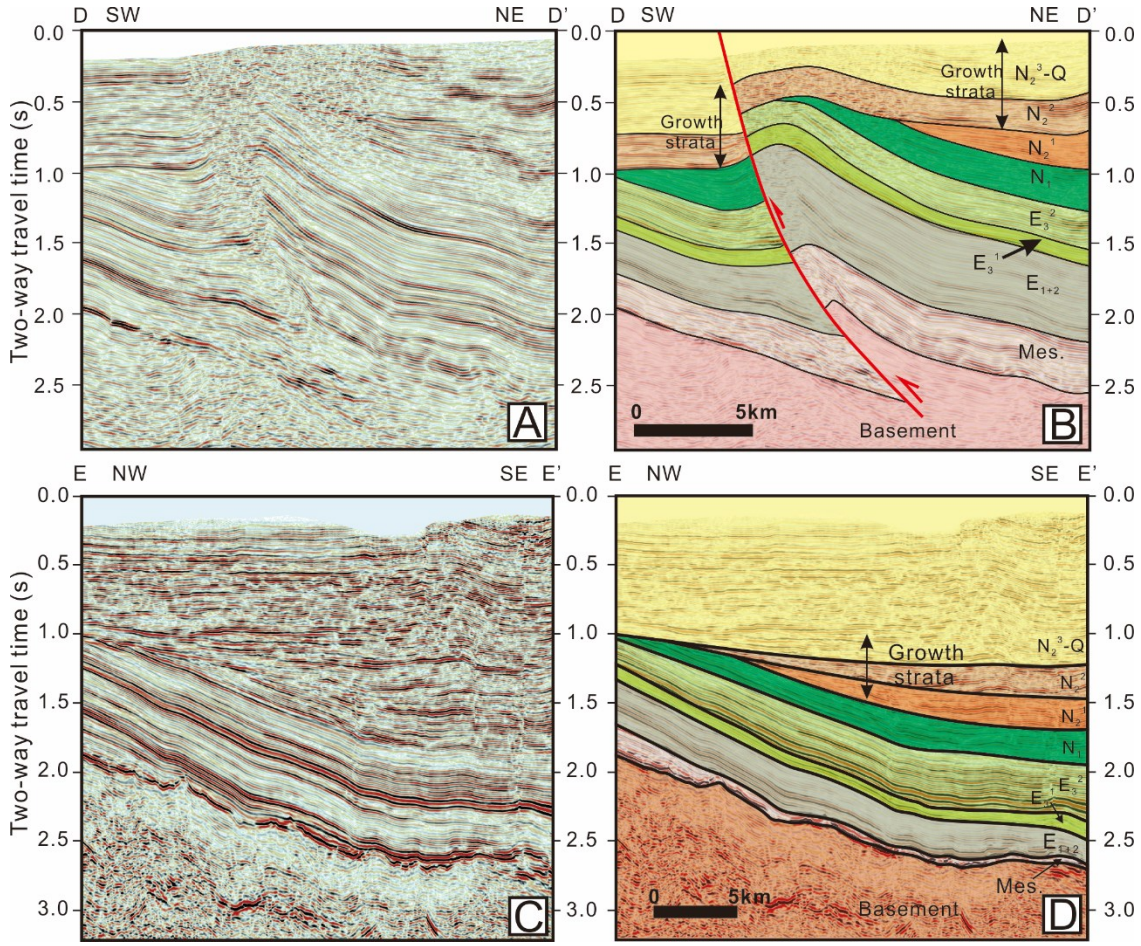


Figure 10. Seismic profiles in the southwestern Qaidam Basin; see Figure 2 for location. (A) Uninterpreted and (B) interpreted seismic profiles in the SW–NE direction; (C) uninterpreted and (D) interpreted seismic profiles in NW–SE direction. Note that the growth strata since the Xiayoushashan Formation ($N_2^1$xy) indicate the intense tectonic movement of the Altyn Tagh fault during middle Miocene time.

The Tula section contains consistently southward dipping strata on both sides of the low-angle (smaller than 10 degree) Jurassic-Cretaceous and Cretaceous-early Eocene unconformities (Fig. 4). These Jurassic-early Eocene sequences are heavily deformed, forming a major north-verging syncline with a steeply dipping south limb and a shallowly dipping north limb, indicating the deformation of these Jurassic-early Eocene sequences occurred during or after early Eocene time (Fig. 4). We therefore suggest that the topographic low in the Tula area became isolated during early Eocene time and the folding of the Tula syncline is related to motion on the fault to the south which was kinematically linked to the ATF during this time period. It is therefore likely that the Tula section was part of the Qaidam basin during early Eocene time and became isolated when the Qaidam basin migrated northward. This migration was induced by movement along the ATF, which is consistent with the initial timing of faulting along the ATF (ca. 49 Ma) as proposed by Yin et al. (2002). We therefore conclude that the

Tula section is an appropriate piercing point to constrain the initial stage (~49 Ma) of faulting along the ATF.

In Anxi section, the fine-grained deposits in the Oligocene to Miocene strata indicate that the Anxi unit was once a topographic low (HGSI, 2003). The lithofacies of the Pliocene Shizigou Fm. of the Anxi section are dominated by a succession of proximal fluvial deposits. In the western Qaidam basin, the Pliocene Shizigou Fm. is characterized by lacustrine facies (Yin et al., 2008b), suggesting that these two regions maintained different depositional systems during Pliocene time. The continuous sequences of Paleocene to early Miocene strata and the angular unconformity between the Youshanshan and Shizigou formations demonstrate that the Anxi section experienced a tectonic event between the early Miocene and Pliocene epochs, and this event in turn resulted in the deformation of the Paleocene to early Miocene strata (Figs. 6 and 7). Seismic profiles from the western Qaidam basin reveal that the Pliocene strata conformably overlie the Miocene strata and illustrate a distinctive unconformity between the Shangyoushashan and Xiayoushashan formations, both of which are Miocene in age. This unconformity becomes most prominent in the southern foothills of the Altyn Tagh Range, further indicating intense left-lateral strike-slip faulting along the ATF (Figs. 3 and 10; Meng and Fang, 2008; Wang et al., 2010a; Wu et al., 2012a). Within the western Qaidam basin, this unconformity is characterized by growth strata that started to develop after the initial deposition of Miocene strata. In profile DD' (Fig. 10), the deposits are cut by a branch fault of the ATF and the pre-Miocene strata are deformed by an anticline which was later cut and sealed by Miocene strata. Similarly, in profile EE' (Fig. 10), the growth strata are well developed and the thickness of the Eocene to Miocene pre-growth strata remains constant. The middle Miocene to Quaternary deposits thin northwestwards (toward the Altyn Tagh Range). Based on magnetostratigraphy, palynology and paleontology within the basin, the accurate timing of this regional unconformity has been constrained to ~15 Ma (Fang et al., 2007; Gao et al., 2009; Lu and Xiong, 2009; Wang et al., 2010a; Wu et al., 2012a). We thus suggest that the apparent unconformity between the Shangyoushashan and Xiayoushashan formations indicates middle Miocene (~15 Ma) motion of the Altyn Tagh fault system. Based on this, we propose that the deformed Paleocene to Miocene strata of the Anxi section represents another piercing point to constrain the historical position of the western Qaidam basin during mid-Miocene time. The initial stage of left-lateral strike-slip faulting along the ATF led to a gradual separation of the western Qaidam basin from the Anxi section. Tectonic movement precluded new deposition of strata, and the Anxi section became isolated from the Qaidam basin during late Miocene time. In addition to the ATF, we suggest the left-lateral strike-slip faulting of the

Baiganhu fault to the south of the basin also accommodated the northeastward motion of the Qaidam basin (Cowgill et al., 2003; HGIS, 2003; Wang et al., 2014). The Pliocene marginal conglomerate facies of the Anxi section formed via proximal accumulation sometime after initial stage left-lateral strike-slip faulting of the ATF.

#### 3.1.6.2 Provenance analysis of Jurassic to Cretaceous strata

If the Cenozoic strata in the Tula and Anxi sections represent the initial timing and early stages of motion along the ATF and the postulated historical position of the Qaidam basin is reasonable, the pre-faulting deposits (Mesozoic strata) in the Tula section and the western Qaidam basin (Caishiling section) should be lithologically similar and their provenance comparable.

Paleocurrents in the Jurassic strata of the Tula, Anxi, and Caishiling sections all suggest northward current movement while Cretaceous strata show southward moving paleocurrents (Fig. 7; Ritts and Biffi, 2000). In general, there is relatively little paleocurrent data for Tula, Anxi, and Caishiling sections (e.g. n = 4 in the Tula section), however, the generally consistent orientation of paleocurrents across all three sections reflects a similar topography for these regions (Tula, Anxi and Caishiling) between Jurassic and Cretaceous time. Relative probability histogram plots of pluton ages in the Altyn Tagh and Eastern Kunlun ranges are shown in Fig. 9. Based on the morphological characteristics, internal textures and Th/U ratio of zircons, magmatic zircons (about 80 %) appear to dominate the section while metamorphic zircons (about 20 %) comprise the remainder (Corfu et al., 2003; Hanchar and Rudnick, 1995; Hoskin and Black, 2000).

In the Altyn Tagh Range, Archean and Proterozoic basement rocks are widely exposed with Archean zircon U-Pb ages ranging from ~3.6 Ga (Lu et al., 2008) to ~2.6 Ga (Lu and Yuan, 2003) and Proterozoic zircon U-Pb ages ranging from ~2.4 Ga to ~650 Ma (Gehrels et al., 2003a; Gehrels et al., 2003b; Wang et al., 2006b; Zhang et al., 2011; Wang et al., 2013). Paleozoic intrusions within this range show zircon U-Pb ages ranging from ~550 Ma to ~400 Ma (Sobel and Arnaud, 1999; Zhang et al., 2001; Cowgill et al., 2003; Gehrels et al., 2003a; Chen et al., 2004; Yue et al., 2004a, 2005; Yang et al., 2006; Wang et al., 2008; Liu et al., 2009) (Fig. 2). Only a few isolated Permian igneous rocks are distributed along the center of this range, with zircon U-Pb ages ranging between ~300 Ma and ~270 Ma (Cowgill et al., 2003; Gehrels et al., 2003a, 2003b).

With regard to the Eastern Kunlun Range, the Proterozoic basement rocks are isolated and show zircon U-Pb ages ranging from 1900 to 800 Ma (e.g. HGSI, 2003; Wang et al., 2013).

The Paleozoic to late Proterozoic intrusions show a zircon U-Pb age peak around 430 Ma which is based on early Paleozoic metamorphic rocks which represent the Ordovician - Silurian docking of the Kunlun and Tarim blocks (e.g. Matte et al., 1996; Cowgill et al., 2003; Li et al. 2013). The Kunlun basement age distribution is characterized by the occurrence of late Paleozoic - early Mesozoic ages (~300 to ~200 Ma) which correspond to the Permo-Triassic closure of the Paleotethys Ocean and the docking of the Qiangtang Block (Roger et al., 2003, 2008; Roger et al.,2010; Dai et al., 2013; Li et al., 2013). Finally, a few Mesozoic ages (e.g. ~74 Ma) have been obtained from the Tula section (Robinson et al., 2003).

In order to better constrain the provenance of the five sandstone samples, the plutons of the Altyn Tagh and Eastern Kunlun ranges are simply divided into two groups: those plutons with an age older than 270 Ma and those whose age is younger than 270 Ma. Older plutons are widespread in both the Altyn Tagh and Eastern Kunlun ranges, whereas younger plutons are confined to the Eastern Kunlun Range just south of our sample sites (Fig. 2). This distinctive pluton distribution can be used as a provenance signature to identify the source of detrital zircon for our Mesozoic samples. In general, detrital zircon age clusters in all five samples are basically similar and characterized by two main groups of Permian-Triassic and Paleozoic ages along with a small number of Precambrian ages (Figs. 8 and 9). The appearance of the Permian-Triassic zircon ages (<270 Ma) in all five samples strongly suggests an East Kunlun Range provenance. We consider that the slightly different peak ages of sample CSL1, CSL2, CSL3, G1 and G2 result from contributions of plutonic debris with a variety of ages (Fig. 9; Tab. 1).

In the Caishiling section, the sampling sites of the three Jurassic-Cretaceous samples (CSL1, CSL2 and CSL3) are located at the southern piedmont of the Altyn Tagh Range, where the basement is mainly dominated by Paleozoic and Precambrian plutons with ages older than 270 Ma (Fig. 9). If the Caishiling section has been situated in roughly the same region that it occupies today (Fig. 2), the Altyn Tagh Range must serve as the ultimate provenance for the zircons from the Jurassic-Cretaceous samples. If this is the case, the U-Pb age spectrum of these samples should display a Paleozoic and Precambrian age peak (>270 Ma). In samples CSL1, CSL2 and CSL3, the detrital zircon age spectra are similar and characterized by two main groups of Permian-Triassic and Paleozoic ages along with a small number of Precambrian ages. The widespread distribution of the Paleozoic and Precambrian plutons in both the Altyn Tagh and Eastern Kunlun Ranges prevents the use of zircon age spectra to estimate the estimate the source area of these Cretaceous and Jurassic samples. Nevertheless, all three samples contain a host of late Permian to Triassic zircon ages (<270 Ma) which are

found only in the plutons of the Eastern Kunlun Range, particularly those in the south Tula section (Figs. 2 and 9). In addition, the angular grains in the Jurassic samples shows poor sphericity and poor sorting, indicating deposition from a proximal source terrain (Figs. 5A and 5B). Based on the proximal source feature and the particular age spectrum (containing a host of late Permian to Triassic zircons) of these three samples, we suggest the Caishiling section was situated far closer to the Tula section in the past as compared with its current position. Meanwhile, plutons in the Eastern Kunlun Range had already been unroofed during early Jurassic time, representing a main source to the Dameigou (J1+2d), Caishiling (J3c) and Quanyagou (Kq) formations since that time.

In the Tula section, two Jurassic and Cretaceous samples (G1 and G2) were selected from the narrow Tula subbasin. The G1 sample was selected near the East Kunlun Mountains while the G2 sample was selected near the Altyn Tagh Range (Figs. 2 and 4). The age cluster of sample G1 features two main groups of Permian-Triassic and Paleozoic ages along with minor Precambrian ages, a pattern similar to that found in the Cretaceous sample from the Caishiling section (Figs. 9D and 9E). We thus suggest that the late Permian to Triassic strata of the Eastern Kunlun Range, and the Paleozoic and Precambrian plutons in both Eastern Kunlun and the Altyn Tagh ranges are the source rocks for the Cretaceous strata (Figs. 2 and 4). In particular, the age spectrum in the early Jurassic sample (G2) is characterized by an exceptionally unimodal distribution of detrital zircon (age ranging from 404 to 493 Ma, peak at 447 Ma) with only one Triassic age (250 Ma), whereas all of the other samples (G1, CSL1, CSL2 and CSL3) are characterized by bimodal distributions (Permian-Triassic and Paleozoic groups), suggesting that G2 is a distinct sample. The site location for G2 is extremely close to the Altyn Tagh Range and the older plutons within the Altyn Tagh Range serve as a major source of debris for sample G2 (Figs. 2 and 4). Older plutons from the Altyn Tagh Range represent the dominant source material, resulting in relatively little contribution from the East Kunlun Range as evidenced by very few Permian to Triassic zircons in the age distribution of sample G2 (Fig. 9A). However, the one zircon grain with a Triassic age found in sample G2 and the northward paleocurrents do suggest some small contribution may have come from the Permian-Triassic rocks of the East Kunlun Range (Figs. 7 and 9A; Ritts and Biffi, 2000). Therefore, we suggest the most plausible explanation for the anomalous detrital zircon ages found in the G2 sample is a mixture of source material from both the Altyn Tagh and the East Kunlun ranges. If the plutons from both locations (Paleozoic and Precambrian in the Altyn Tagh Range and Permian to Triassic on the East Kunlun Range) were exhumed during Jurassic time, they would represent a mixed source for samples G2 and CSL3 during that time.

By reconciling the detrital zircon ages of the sediments from the Altyn Tagh and Eastern Kunlun Ranges and combining this data with the large-scale left-lateral strike-slip displacements measured along the ATF, we deduce that the Caishiling section must have been located much closer to the Eastern Kunlun Range between Jurassic and Cretaceous time. The Tula unit, on the other hand, likely has not moved since Jurassic time. The lithologic and stratigraphic contact features of the residual Mesozoic to Cenozoic strata along the ATF combined with U-Pb dating of the Jurassic and Cretaceous samples of the Tula and Caishiling sections enable us to establish the timing of movement along the ATF. We resolve the motion along the ATF into two distinct stages: initial movement occurring at ~49 Ma and a subsequent early stage movement occurring at ~15 Ma. Both stages promote strike-slip motion along the fault. The Tula and Anxi sections can be used as piercing points along the western segment of ATF and we identify these regions as residual components of the original Qaidam basin.

#### 3.1.6.3 Implications for the initial timing and total offset of the ATF

##### 3.1.6.3.1 A general review of previous estimates

In the past few decades, a number of approaches have been used to estimate the overall displacement along the ATF. By comparing Paleozoic suture zones in the western Kunlun range with those in the Qilian Shan, CSBS (1992) argued for ~ 1200 km of offset along the fault. By matching similar geological features, particularly Late Paleozoic magmatic belts in the western and eastern Kunlun Shan, ranges of 300~500 km, 475 ± 70 km and ~550 km of displacement have all been estimated (Tapponnier et al., 1986; Peltzer and Tapponnier, 1988; Cowgill et al., 2003). Comprehensive correlations of the geologic features with the magmatic histories in the Altyn Tagh Range, Qilian Shan and Nasn Shan enabled Gehrels et al. (2003a) to suggest offsets of ~370 km, 375 km and ~400 km along the ATF. By reconstructing the shortening of the Nan Shan thrust belt, Yin and Harrison (2000) inferred 360 ± 50 km of displacement. A comprehensive analysis of the geologic features along the north margin of the Tibetan plateau has yielded estimates of ~400 km of offset (Molnar and Tapponnier, 1975). Using the measured Pliocene-Quaternary slip rate over the inferred duration of faulting along the ATF, Burchfiel and Royden (1991) estimated a ~200 km fault displacement. By matching the Tertiary rocks along the northern and the central segments of the ATF, Wang (1997) ascertained 69-90 km of displacement. Chen et al. (2002) suggested an offset of 500 ± 130 km between 24 Ma and present based on paleomagmatic data from the Qaidam basin. Notably, 400 ± 60 km has also been suggested based on the reconstruction of a Jurassic facies boundary

across the ATF (Ritts and Biffi, 2000).

On the other hand, magnetostratigraphy and sedimentological analysis has led some to suggest the ATF has been active since ca. 49 Ma rather than simply 24 Ma (Yin et al., 2002). Thermochronological data from the Altyn Tagh Range in conjunction with sedimentological evidence suggests that left-lateral strike-slip faulting occurred from late Eocene to early Oligocene time (Chen et al., 2001; Meng et al., 2001; Yue et al., 2001; Ritts et al., 2004). Yet still others point to geologic evidence within the northern Tibetan plateau that shows the onset of this left-lateral faulting occurred sometime during Miocene epoch (Wan et al., 2001; Wu et al., 2012a, 2012b).

As is apparent, the tremendous discrepancies both in total displacement and the timing of initial left-lateral movement along the fault may be attributed partially to an incomplete understanding of the lithology and tectonic history of the Altyn Tagh Range. This also makes is particularly challenging to find an ideal piercing point. Some estimates on the displacement of the ATF use plutonic belts or suture zones as the offset markers, but these large tectonic features have poor spatial definition because of high uncertainties in their shape and the extent of their geologic margins (Yin and Harrison, 2000; Yin et al., 2002). The intense deformation and shortening of the eastern and western Kunlun Ranges throughout geologic history as well as the deformation along the Qilian Shan has served to profoundly complicate any measurement of the actual displacement of the ATF.

#### 3.1.6.3.2 Reassessing Cenozoic kinematic patterns on the ATF using new piercing points

The Qaidam and Tarim basins are both relatively rigid blocks when compared with the Altyn Tagh Range, which gives them relatively higher crustal strength (Wang et al., 2006a; Zhou et al., 2006). Paleomagnetic studies have revealed a 13.3°± 8.8° difference in paleomagnetic declination between the two halves of the arcuate structure outlined in the uplifted region of the Tula section (Fig. 4; see also Figure 3 in Dupont-Nivet et al., 2004) and suggest northwards transport along the ATF of this section, the western segment of the Eastern Kunlun Range (Qimen Tagh Range) and the Qaidam basin (Dupont-Nivet et al., 2004; Yu et al., 2014). The absence of a large vertical axis of rotation in the area adjacent to the ATF indicates that the left-lateral shear strain between the Tarim basin and the northern Tibetan plateau is concentrated on the relative weak ATF (Dupont-Nivet et al., 2002, 2003, 2004; Sun et al., 2005a). The relative movement of the Qaidam and Tarim basins is therefore representative of the actual displacement along the ATF. The distinctive sediment features that manifest along the ATF identify this displacement history can be used to locate appropriate

piercing points which can further be used to restrict the timing of this displacement (Yin and Harrison, 2000; Chen et al., 2003; Cowgill et al., 2003; Wang et al., 2006a; Yin et al., 2002, 2008b). In this paper, the residual Mesozoic to Cenozoic strata within the western Qaidam basin are documented as the piercing points that identify the Cenozoic kinematic pattern of the ATF. In order to account for the fact that the Qaidam basin and the relic Tula and Anxi units are situated south of the currently active ATF trace, two faults or major unconformities are required to act as boundaries between the detached Qaidam basin and relic Tula subbasin (Fig. 11).

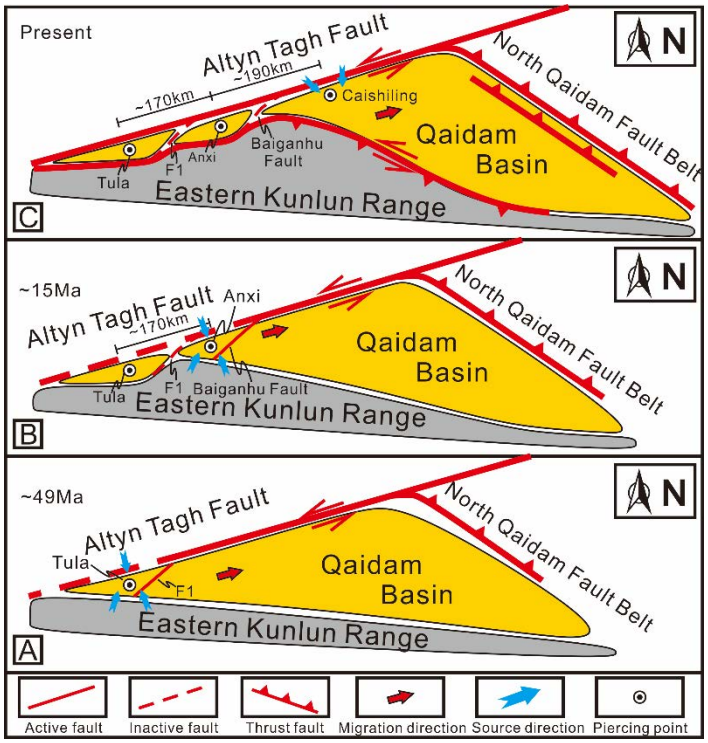


Figure 11. Proposed accelerated motion model for the Cenozoic Altyn Tagh fault (ATF). Note the piercing points along the Altyn Tagh fault. (A) Before early Eocene time, the Caishiling section was originally located where the Tula section is situated today. During early Eocene time (ca. 49 Ma), the left-lateral strike-slip faulting along the Altyn Tagh fault initiated, transporting the Qaidam Basin northeastward. Since then, the Tula unit remained stationary and was separated from the Qaidam Basin (B) during middle Miocene time (ca. 15 Ma), when the Caishiling section migrated northeastward to where the Anxi section is situated today. During this period, an intense left-lateral strike-slip faulting along the Altyn Tagh fault occurred and deformed the pre-Miocene strata in the Anxi section. Since then, the Anxi unit was left and separated from the Qaidam Basin (C) during continuous left-lateral strike-slip faulting along the Altyn Tagh fault that transported the Caishiling section to its present position. Consequently, ~360 km total Cenozoic offset is constrained along the Altyn Tagh fault, which is divided into ~170 km of offset between early Eocene and middle Miocene time and ~190 km of offset from the late Miocene until present.

Between the Jurassic and early Eocene, the westernmost part of the originally rigid Qaidam basin was located where the Tula section is situated today (Fig. 11A). Strike-slip movement along the ATF began shortly after the early Eocene. Faulting on the ATF induced the NE-SW trending branch fault (F1) in this region, now covered by Quaternary alluvium, deforming the Jurassic to early Eocene strata in the Tula section as it did so (Figs. 2 and 4). The initial strike-slip movement of the ATF also transported the original Qaidam basin northeastwards

and gradually separated the Qaidam basin from the Tula section. The depression in the Tula section then uplifted and was gradually isolated, leading to a pause in deposition during the Upper Paleogene to Neogene. This left-lateral faulting also lead to compression in the northern Qaidam basin, which began in the Paleocene to early Eocene as revealed by seismic profile data (Yin et al., 2008a; Fig. 11A). Systematic analysis of the Cenozoic stratigraphic sections along the ATF suggests that strike-slip movement along the western and central ATF was initiated at ca. 49 Ma (Yin et al., 2002), roughly consistent with the speculated sediment termination age of the Tula section. This onset age for large strike-slip faulting in the northern Tibetan plateau is also synchronous with the India-Asia collision as revealed by newly acquired palaeomagnetic evidence in southern Tibet (Dupont-Nivet et al., 2010; Huang et al., 2013; Lippert et al., 2014). This indicates that the deformation in northern Tibet may have begun as India and Eurasia began colliding. It is possible that the dominant cause of the large-scale strike-slip faults in the Asian interior (especially the ATF) is the India-Asia collision itself, the effects of which may still be felt on the northern Tibetan plateau today.

Between early Eocene and mid-Miocene time, movement of the ATF transported the westernmost part of the original Qaidam basin northeastwards to the position where the Anxi unit is at present. During the mid-Miocene, an intense left-lateral strike-slip motion occurred along the ATF and the originally rigid Qaidam separated from the Anxi unit and migrated northeastwards continuously (Fig. 11B). This fault motion tilted the Late Paleocene to early Miocene strata of the Anxi section and created a regional unconformity between the Shangyoushashan and Xiayoushashan formations. This unconformity matches the widespread unconformity within the western Qaidam basin (Figs. 3 and 7; Wang et al., 2010a, 2010b; Wu et al., 2012a, 2012b). The growth strata above this unconformity reveal a rapid tectonic event occurred just after the mid-Miocene epoch (~15 Ma). Based on the widespread potassic volcanism in northern Tibet, Yue and Liou (1999) also infer intense fault movement along the ATF ca. 13-16 Ma. This mid-Miocene faulting is recorded by the fission track present in both the Altyn Tagh Range and the north Qaidam basin (Jolivet et al., 2001; Wan et al., 2001). Overall, the tectonic events of the mid-Miocene are widespread and well developed in the Tibetan plateau (e.g. Yue and Liou, 1999; Kirby et al., 2002; Clark et al., 2004; Ding et al., 2004; Sun et al., 2005a; Wang et al., 2012), which may reflect a critical period in the process of Tibetan plateau growth. Following this, as seen in the Anxi section, the depression in the Anxi section becomes folded, uplifted and isolated gradually leading to a pause in deposition during the late Miocene (Figs. 6 and 7).

Since late Miocene epoch, the continuous left-lateral strike-slip faulting along the ATF

has gradually transported the Qaidam basin to its present position (Fig. 11C). Finally, recent left-lateral strike-slip faulting occurs along the entire ATF, reshaping the original faulting style. The Tula and Anxi units can be selected as piercing points to constrain the Cenozoic kinematic patterns of the ATF. Based on these offset markers, we estimate ~170 km of offset occurred between the mid-Eocene and mid-Miocene epochs, and ~190 km of offset occurred between the late Miocene epoch and the present, resulting in a total offset of ~360 km along the ATF during the Cenozoic (Fig. 11). This estimate suggests an average sinistral slip rate of ~5.0 mm/yr between the middle Eocene and the middle Miocene and an increase to ~12.6 mm/yr between the Miocene and the present. Our estimates for the overall displacement (~360 km) and average sinistral slip rate since the mid-Miocene are consistent with previous studies (Peltzer and Tapponnier, 1988; Ritts and Biffi, 2000; Yin and Harrison, 2000; Shen et al., 2001; Yin et al., 2002; Cowgill et al., 2003; Zhang et al., 2004, 2007; Cowgill et al., 2009). The accelerated strike-slip motion along the ATF between the mid-Miocene epoch and present day implies that the increased regional deformation of the northern Tibetan plateau may be related to the penetrative and far-reaching effects of the India-Asia collision.

### 3.1.7 Conclusions

As the major strike-slip fault on the northern Tibetan plateau, the ATF holds important implications for unraveling the Cenozoic growth history of the entire Tibetan plateau.

By correlating the lithology and sedimentary features of the Cenozoic strata along the ATF, and analyzing the detrital zircon U-Pb ages from Mesozoic strata in three sections along the fault, we find that these strata record the northward migration of the Qaidam basin and can be identified as the piercing points for defining the Cenozoic offset of the ATF. Specifically, the Tula section records the early Eocene position of the western Qaidam basin (e.g. Caishiling section), while the Anxi section documents its middle Miocene position. Based on this, we estimate ~170 km of offset occurred between the early Eocene (~49 Ma) to middle Miocene (~15 Ma) epochs and ~190 km of offset occurred between the late Miocene epoch and the present day, yielding ~360 km of total offset along the ATF during the Cenozoic period. This estimate implies that motion along the ATF has accelerated in recent time from an average sinistral slip rate of ~5.0 mm/yr between the early Eocene (~49 Ma) to middle Miocene (~15 Ma) epochs to an accelerated rate of ~12.6 mm/yr from the middle Miocene epoch to the present day.

## Acknolegdements

This work was supported by the National Oil and Gas Scientific and Technologic Major Programs of China (Grant ZX05003) and China Scholarship Council (Egide Cai Yuanpei program 2014). We gratefully acknowledge the assistance of Dr. Suping Zhou, and Xiangjiang Yu for their contributions in the field. We are very grateful to Prof. Li Su of the Geological Lab Center, China University of Geosciences (Beijing), for her help with detrital zircon analysis and to Dr. Bo Zhang for his help with cathodoluminescence (CL) imaging. We are particularly grateful to Dr. Dupont-Nivet Guillaume for his helpful suggestions. Communications with Dr. Marc Jolivet, Jianxun Zhou, Dr. Dewen Zheng and Dr. Jinjiang Zhang had sharpened the discussion on the appropriate piercing points. We would like to thank Dr. An Yin and an anonymous reviewer for reviewing the earlier version of this manuscript. We also would like to thank science editor Dr. Shanaka de Silva, associate editor Dr. Todd LaMaskin, and two anonymous reviewers, who provided constructive feedback that helped improve this manuscript.

## References Cited

Allen, P.A., and Allen, J.R., 1990, Basin analysis: Principles and applications: Cambridge, UK, Blackwell Scientific Publications, 451 p.

Arnaud, N., Tapponnier, P., Roger, F., Brunel, M., Scharer, U., Wen, C., and Zhiqin, X., 2003, Evidence for Mesozoic shear along the western Kunlun and Altyn‐Tagh fault, northern Tibet (China): Journal of Geophysical Research: Solid Earth (1978–2012), v. 108, no. B1, doi: 10.1029/2001JB000904.

Bendick, R., Bilham, R., Freymueller, J., Larson, K., and Yin, G., 2000, Geodetic evidence for a low slip rate in the Altyn Tagh fault system: Nature, v. 404, no. 6773, p. 69-72, doi: 10.1038/35003555.

Boggs, S., Jr., 2006, Principles of Sedimentology and Stratigraphy, 4th Edition: New Jersey, Pearson Prentice Hall, p. 326–333.

Burchfiel, B. C., Quidong, D., Molnar, P., Royden, L., Yipeng, W., Peizhen, Z., and Weiqi, Z., 1989, Intracrustal detachment within zones of continental deformation: Geology, v. 17, no. 8, p. 748-752., doi: 10.1130/0091-7613(1989)017<0448:IDWZOC>2.3.CO;2.

Burchfiel, B. C., and Royden, L. H., 1991, Tectonic of Asia 50 years after the death of Emile Argand: Eclogae Geologicae Helvetiae, v. 84, no. 3, p. 599-629.

Cande, S. C., and Kent, D. V., 1995, Revised calibration of the geomagnetic polarity timescale for the Late Cretaceous and Cenozoic: Journal of Geophysical Research: Solid Earth (1978–

2012), v. 100, no. B4, p. 6093-6095, doi: 10.1029/94JB03098.

Chen, Z. L., Zhang, Y. Q., Wang, X. F., and Chen, X. H., 2001, Fission Track Dating of Apatite Constrains on the Cenozoic Uplift of the Altyn Tagh Mountain: GEOSCIENTIA SINICA Acta Geoscientia Sinica, v. 22, no. 5, p. 413-418 (in Chinese with English).

Chen, Y., Gilder, S., Halim, N., Cogné, J. P., and Courtillot, V., 2002, New paleomagnetic constraints on central Asian kinematics: Displacement along the Altyn Tagh fault and rotation of the Qaidam Basin: Tectonics, v. 21, no. 5, p. 1042, doi: 10.1029/2001TC901030.

Chen, X. H., Yin, A., Gehrels, G. E., Cowgill, E. S., Grove, M., Harrison, T. M., and Wang, X. F., 2003, Two phases of Mesozoic north-south extension in the eastern Altyn Tagh range, northern Tibetan Plateau: Tectonics, v. 22, no. 5, p. 1053, doi: 10.1029/2001TC001336.

Chen, X. H., Wang, X. F., George, G. E., Yang, Y., Qin, H., Chen, Z. L., Yang, F., Chen, B. L., and Li, X. Z., 2004, Early Paleozoic Magmatism and Gold Mineralization in the Northern Altun, NW China: Acta Geologica Sinica-English Edition, v. 78, no. 2, p. 515-523, doi: 10.1111/j.1755-6724.2004.tb00161.x.

Cheng, F., Jolivet, M., Fu, S., Zhang, Q., Guan, S., Yu, X., and Guo, Z., 2014, Northward growth of the Qimen Tagh Range: A new model accounting for the Late Neogene strike-slip deformation of the SW Qaidam Basin: Tectonophysics, v. 632, p. 32-47, doi: 10.1016/j.tecto.2014.05.034.

Cheng, X., Fu, S., Wang, H., Yu, X., Cheng, F., Liu, R., Du, W., and Guo, Z., 2015, Geometry and kinematics of the Arlar strike-slip fault, SW Qaidam basin, China: New insights from 3-D seismic data: Journal of Asian Earth Sciences, v. 98, p. 198-208, doi: 10.1016/j.jseaes.2014.09.039.

Clark, M., Schoenbohm, L., Royden, L., Whipple, K., Burchfiel, B., Zhang, X., Tang, W., Wang, E., and Chen, L., 2004, Surface uplift, tectonics, and erosion of eastern Tibet from large-scale drainage patterns: Tectonics, v. 23, no. 1, p. TC1006, doi: 10.1029/2002TC001402.

Cowgill, E., Yin, A., Feng, W. X., and Qing, Z., 2000, Is the North Altyn fault part of a strike-slip duplex along the Altyn Tagh fault system?: Geology, v. 28, no. 3, p. 255-258, doi: 10.1130/0091-7613(2000)28<255:ITNAFP>2.0.CO;2.

Corfu, F., Hanchar, J. M., Hoskin, P. W., and Kinny, P., 2003, Atlas of zircon textures: Reviews in mineralogy and geochemistry, v. 53, no. 1, p. 469-500, doi: 10.2113/0530469.

Cowgill, E., Yin, A., Harrison, T. M., and Xiao-Feng, W., 2003, Reconstruction of the Altyn Tagh fault based on U-Pb geochronology: Role of back thrusts, mantle sutures, and heterogeneous crustal strength in forming the Tibetan Plateau: Journal of Geophysical Research, v. 108, no. B7, p. 2346, doi:10.1029/2002JB002080.

Cowgill, E., Gold, R. D., Xuanhua, C., Xiao-Feng, W., Arrowsmith, J. R., and Southon, J., 2009, Low Quaternary slip rate reconciles geodetic and geologic rates along the Altyn Tagh fault, northwestern Tibet: Geology, v. 37, no. 7, p. 647-650, doi: 10.1130/G25623A.1.

CSBS (Chinese Stata Bureau of Seismology), 1992. The Altyn Tagh Active Fault System. Seismology Publishing House, Beijing, pp. 319 (in Chinese).

Dai, J., Wang, C., Hourigan, J., and Santosh, M., 2013, Multi-stage tectono-magmatic events of the Eastern Kunlun Range, northern Tibet: Insights from U–Pb geochronology and (U–Th)/He thermochronology: Tectonophysics, v. 599, p. 97-106, doi: 10.1016/j.tecto.2013.04.005.

Ding, G., Chen, J., Tian, Q., Shen, X., Xing, C., and Wei, K., 2004, Active faults and magnitudes of left-lateral displacement along the northern margin of the Tibetan Plateau: Tectonophysics, v. 380, no. 3-4, p. 243-260, doi: 10.1016/j.tecto.2003.09.022.

Dupont-Nivet, G., Butler, R. F., Yin, A., and Chen, X., 2002, Paleomagnetism indicates no Neogene rotation of the Qaidam Basin in northern Tibet during Indo-Asian collision: Geology, v. 30, no. 3, p. 263, doi: 10.1130/0091-7613(2002)030<0263:PINNRO>2.0.CO;2.

Dupont-Nivet, G., Butler, R. F., Yin, A., and Chen, X., 2003, Paleomagnetism indicates no Neogene vertical axis rotations of the northeastern Tibetan Plateau: J. geophys. Res, v. 108, no. B8, p. 2386, doi: 10.1029/2003JB002399.

Dupont-Nivet, G., Robinson, D., Butler, R. F., Yin, A., and Melosh, H. J., 2004, Concentration of crustal displacement along a weak Altyn Tagh fault: Evidence from paleomagnetism of the northern Tibetan Plateau: Tectonics, v. 23, no. 1, p. TC1020, doi:10.1029/2002TC001397.

Dupont-Nivet, G., Lippert, P. C., Van Hinsbergen, D. J. J., Meijers, M. J. M., and Kapp, P., 2010, Palaeolatitude and age of the Indo–Asia collision: palaeomagnetic constraints: Geophysical Journal International, v. 182, no. 3, p. 1189-1198, doi: 10.1111/j.1365-246X.2010.04697.x.

Fang, X., Zhang, W., Meng, Q., Gao, J., Wang, X., King, J., Song, C., Dai, S., and Miao, Y., 2007, High-resolution magnetostratigraphy of the Neogene Huaitoutala section in the eastern Qaidam Basin on the NE Tibetan Plateau, Qinghai Province, China and its implication on tectonic uplift of the NE Tibetan Plateau: Earth and Planetary Science Letters, v. 258, no. 1-2, p. 293-306, doi:10.1016/j.epsl.2007.03.042.

Fedo, C. M., Sircombe, K. N., and Rainbird, R. H., 2003, Detrital zircon analysis of the sedimentary record: Reviews in mineralogy and geochemistry, v. 53, no. 1, p. 277-303, doi: 10.2113/0530277.

Gao, J., Li, S., Dai, S., Li, A., and Peng, Y., 2009. Constraints of tectonic evolution in

provenance from detrital zircon fission-track data of Cenozoic strata of Xichagou district in western Qaidam basin. Journal of Lanzhou University (Natural Sciences), v. 45, no. 3, p. 639-643 (in Chinese with English abstract).

Gehrels, G. E., Yin, A., and Wang, X. F., 2003a, Detrital-zircon geochronology of the northeastern Tibetan plateau: Geological Society of America Bulletin, v. 115, no. 7, p. 881-896, doi: 10.1130/0016-7606(2003)115<0881:DGOTNT>2.0.CO;2.

Gehrels, G. E., Yin, A., and Wang, X. F., 2003b, Magmatic history of the northeastern Tibetan Plateau: Journal of Geophysical Research, v. 108, no. B9, p. 2423, doi: 10.1029/2002JB001876.

Gehrels, G., 2014, Detrital Zircon U-Pb Geochronology Applied to Tectonics: Annual Review of Earth and Planetary Sciences, v. 42, no. 1, p. 127-149, doi: 10.1146/annurev-earth-050212-124012.

GGSI (Guangxi Geological Survey Institute), 2003. The Report of Regional Geological Survey of Washixia at Scale 1:250000. P.R.C.: Beijing, China Industry Press, 261 p. (in Chinese).

Guo, Z. J., Zhang, Z. C., and Zeng, F. G., 1998, Discovery of mega-thick oil sandstone and asphalt in the Jurassic System in the Tula Basin and its significance: Chinese Science Bulletin, v. 43, no. 22, p. 1898-1901, doi: 10.1007/BF02883468.

Hanchar, J., and Rudnick, R., 1995, Revealing hidden structures: the application of cathodoluminescence and back-scattered electron imaging to dating zircons from lower crustal xenoliths: Lithos, v. 36, no. 3, p. 289-303, doi: 10.1016/0024-4937(95)00022-4.

Hoskin, P., and Black, L., 2000, Metamorphic zircon formation by solid-state recrystallization of protolith igneous zircon: Journal of metamorphic Geology, v. 18, no. 4, p. 423-439, doi:10.1046/j.1525-1314.2000.00266.x.

Hendrix, M. S., Graham, S. A., Carroll, A. R., Sobel, E. R., McKNIGHT, C. L., Schulein, B. J., and Wang, Z., 1992, Sedimentary record and climatic implications of recurrent deformation in the Tian Shan: Evidence from Mesozoic strata of the north Tarim, south Junggar, and Turpan basins, northwest China: Geological Society of America Bulletin, v. 104, no. 1, p. 53-79, doi: 10.1130/0016-7606(1992)104<0053:SRACIO>2.3.CO;2.

Hendrix, M. S., 2000, Evolution of Mesozoic Sandstone Compositions, Southern Junggar, Northern Tarim, and Western Turpan Basins, Northwest China: A Detrital Record of the Ancestral Tian Shan: Journal of Sedimentary Research, v. 70, no. 3, p. 520-532, doi: 10.1306/2DC40924-0E47-11D7-8643000102C1865D.

HGSI (Hunan Geological Survey Institute), 2003, The Report of Regional Geological Survey

of Qiemo at Scale 1:250000. P.R.C.: Beijing, China Industry Press, 281 p. (in Chinese).

Huang, H., Huang, Q., and Ma, Y., 1996, Geology of Qaidam Basin and its petroleum prediction. Geological Publishing House, Beijing, 257 p. (in Chinese).

Huang, W., Dupont-Nivet, G., Lippert, P. C., van Hinsbergen, D. J., and Hallot, E., 2013, Inclination shallowing in Eocene Linzizong sedimentary rocks from Southern Tibet: correction, possible causes and implications for reconstructing the India-Asia collision: Geophysical Journal International, v. 1, p. 309, doi: 10.1093/gji/ggt188.

Huo, G. M., 1990, Petroleum geology of China: Oil fields in Qianghai and Xizang. Chinese Petroleum Industry Press, Beijing, 483 p. (in Chinese with English abstract).

Jolivet, M., Brunel, M., Seward, D., Xu, Z., Yang, J., Roger, F., Tapponnier, P., Malavieille, J., Arnaud, N., and Wu, C., 2001, Mesozoic and Cenozoic tectonics of the northern edge of the Tibetan plateau: fission-track constraints: Tectonophysics, v. 343, no. 1-2, p. 111-134, doi: 10.1016/S0040-1951(01)00196-2.

Ke, X., Ji, J., Zhang, K., Kou, X., Song, B., and Wang, C., 2013, Magnetostratigraphy and Anisotropy of Magnetic Susceptibility of the Lulehe Formation in the Northeastern Qaidam Basin: Acta Geologica Sinica-English Edition, v. 87, no. 2, p. 576-587, doi: 10.1111/1755-6724.12069.

Kirby, E., Reiners, P. W., Krol, M. A., Whipple, K. X., Hodges, K. V., Farley, K. A., Tang, W., and Chen, Z., 2002, Late Cenozoic evolution of the eastern margin of the Tibetan Plateau: Inferences from $^{40}Ar/^{39}Ar$ and (U-Th)/He thermochronology: Tectonics, v. 21, no. 1, p. 1-1-1-20, doi: 10.1029/2000TC001246.

Li, Z., Song, W. J., Peng, S. T., Wang, D. X., and Zhang, Z. P., 2004, Mesozoic-Cenozoic tectonic relationships between the Kuqa subbasin and Tian Shan, northwest China: constraints from depositional records: Sedimentary Geology, v. 172, no. 3, p. 223-249, doi: 10.1016/j.sedgeo.2004.09.002.

Li, H.B., Yang, J.S., Xu, Z.Q., Sun, Z.M., Tapponnier, P., van der Woerd, J., and Meriaux, A. S., 2006. The constraint of the Altyn Tagh fault system to the growth and rise of the northern Tibetan Plateau: Earth Science Frontiers, v. 13, no. 4, 59-79 (in Chinese with English abstract).

Li, W., Neubauer, F., Liu, Y. J., Genser, J., Ren, S. M., Han, G. Q., and Liang, C. Y., 2013, Paleozoic evolution of the Qimantagh magmatic arcs, Eastern Kunlun Mountains: constraints from zircon dating of granitoids and modern river sands: Journal of Asian Earth Sciences, v. 77, p. 183-202, doi: 10.1016/j.jseaes.2013.08.030.

Lippert, P., van Hinsbergen, D., and Dupont-Nivet, G., 2014, The Early Cretaceous to present 31 latitude of the central Lhasa-plano (Tibet): A paleomagnetic synthesis with implications for

Cenozoic 32 tectonics, paleogeography, and climate of Asia: Nie, JS, Hoke, GD, and Horton, BK, editors, v. 33, p. 2, doi: 10.1130/2014.2507(01).

Liu, L., Zhang, A., Chen, D., Yang, J., Luo, J., and Wang, C., 2007a, Implications Based on LA-ICP-MS Zircon U-Pb Ages of Eclogite and Its Country Rock from Jianggalesayi Area, Altyn Tagh, China: Earth Science Frontiers, v. 14, no. 1, p. 98-107, doi: 10.1016/S1872-5791(07)60004-9.

Liu, Y. J., Neubauer, F., Genser, J., Ge, X. H., Takasu, A., Yuan, S. H., Chang, L. H., and Li, W. M., 2007b, Geochronology of the initiation and displacement of the Altyn Strike-Slip Fault, western China: Journal of Asian Earth Sciences, v. 29, no. 2, p. 243-252, doi:10.1016/j.jseaes.2006.03.002.

Liu, L., Wang, C., Chen, D., Zhang, A., and Liou, J., 2009, Petrology and geochronology of HP–UHP rocks from the South Altyn Tagh, northwestern China: Journal of Asian Earth Sciences, v. 35, no. 3, p. 232-244, doi: 10.1016/j.jseaes.2008.10.007.

Liu, D. D., Jolivet, M., Yang, W., Zhang, Z. Y., Feng, C., Zhu, B., and Guo, Z. J., 2013a, Latest Palaeozoic-Early Mesozoic basin-range interactions in South Tian Shan (Northwest China) and their tectonic significance: Constraints from detrital zircon U-Pb ages: Tectonophysics v. 599, 197-213, 10.1016/j.tecto.2013.04.018.

Liu, L., Cao, Y. Y., Chen, D. L., Zhang, C. L., Yang, W. Q., Kang, L., and Liao, X. Y., 2013b, New progresses on the HP-UHP metamorphism in the South Altyn Tagh and the North Qinling: Chin Sci Bull, v. 58, p. 2113-2123 (in Chinese).

Lu, S. N., and Yuan, G. B., 2003, Geochronology of early Precambrian magmatic activities in Aketasdhtage, east Altyn Tagh: Journal of Acta Geologica Sinica, v. 77, no. 1, p. 61-68 (in Chinese with English abstract).

Lu, S. N., Li, H. K., Zhang, C. L., and Niu, G. H., 2008, Geological and geochronological evidence for the Precambrian evolution of the Tarim Craton and surrounding continental fragments: Precambrian Research, v. 160, no. 1, p. 94-107, doi: 10.1016/j.precamres.2007.04.025.

Lu, H., and Xiong, S., 2009, Magnetostratigraphy of the Dahonggou section, northern Qaidam Basin and its bearing on Cenozoic tectonic evolution of the Qilian Shan and Altyn Tagh Fault: Earth and Planetary Science Letters, v. 288, no. 3, p. 539-550, doi: 10.1016/j.epsl.2009.10.016.

Lu, H., Wang, E., and Meng, K., 2014, Paleomagnetism and anisotropy of magnetic susceptibility of the Tertiary Janggalsay section (southeast Tarim basin): Implications for Miocene tectonic evolution of the Altyn Tagh Range: Tectonophysics, v. 618, p. 67-78, doi: 10.1016/j.tecto.2014.01.031.

Mack, G. H., and Rasmussen, K. A., 1984, Alluvial-fan sedimentation of the Cutler Formation (Permo-Pennsylvanian) near Gateway, Colorado: Geological Society of America Bulletin, v. 95, no. 1, p. 109-116, doi: 10.1130/0016-7606(1984)95<109:ASOTCF>2.0.CO;2.

Matte, P., Tapponnier, P., Arnaud, N., Bourjot, L., Avouac, J., Vidal, P., Qing, L., Yusheng, P., and Yi, W., 1996, Tectonics of Western Tibet, between the Tarim and the Indus: Earth and Planetary Science Letters, v. 142, no. 3, p. 311-330, doi: 10.1016/0012-821X(96)00086-6.

Meng, Q. R., Hu, J. M., and Yang, F. Z., 2001, Timing and magnitude of displacement on the Altyn Tagh fault: constraints from stratigraphic correlation of adjoining Tarim and Qaidam basins, NW China: Terra Nova, v. 13, no. 2, p. 86-91, doi: 10.1046/j.1365-3121.2001.00320.x.

Meng, Q. R., and Fang, X., 2008, Cenozoic tectonic development of the Qaidam Basin in the northeastern Tibetan Plateau: Geological Society of America Special Papers, v. 444, p. 1-24, doi: 10.1130/2008.2444(01).

Métivier, F., Gaudemer, Y., Tapponnier, P., and Meyer, B., 1998, Northeastward growth of the Tibet plateau deduced from balanced reconstruction of two depositional areas: The Qaidam and Hexi Corridor basins, China: Tectonics, v. 17, no. 6, p. 823-842, doi: 10.1029/98TC02764.

Meyer, B., Tapponnier, P., Bourjot, L., Metivier, F., Gaudemer, Y., Peltzer, G., Shunmin, G., and Zhitai, C., 1998, Crustal thickening in Gansu‐Qinghai, lithospheric mantle subduction, and oblique, strike‐slip controlled growth of the Tibet plateau: Geophysical Journal International, v. 135, no. 1, p. 1-47, doi: 10.1046/j.1365-246X.1998.00567.x.

Mock, C., Arnaud, N. O., and Cantagrel, J. M., 1999, An early unroofing in northeastern Tibet? Constraints from $^{40}Ar/^{39}Ar$ thermochronology on granitoids from the eastern Kunlun range (Qianghai, NW China): Earth and Planetary Science Letters, v. 171, no. 1, p. 107-122, doi: 10.1016/S0012-821X(99)00133-8.

Molnar, P., and Tapponnier, P., 1975, Cenozoic tectonics of Asia: Effects of a continental collision: Science, v. 189, no. 4201, p. 419-426, doi: 10.1126/science.189.4201.419.

Pei, J., Sun, Z., Wang, X., Zhao, Y., Ge, X., Guo, X., Li, H., and Si, J., 2009, Evidence for Tibetan plateau uplift in Qaidam basin before Eocene-Oligocene boundary and its climatic implications: Journal of Earth Science, v. 20, p. 430-437, doi: 10.1007/s12583-009-0035-y.

Peltzer, G., and Tapponnier, P., 1988, Formation and evolution of strike-slip faults, rifts, and basins during the India-Asia collision: An experimental approach: Journal of Geophysical Research: Solid Earth (1978–2012), v. 93, no. B12, p. 15085-15117, doi: 10.1029/JB093iB12p15085.

QBGMR, 1991, Regional Geology of Qinghai Province. Geological Publishing House, Beijing, 662 p. (in Chinese).

Qiu, N. S., 2002, Tectono-thermal evolution of the Qaidam Basin, China: evidence from Ro and apatite fission track data: Petroleum Geoscience, v. 8, no. 3, p. 279-285, doi: 10.1144/petgeo.8.3.279.

Ritts, B. D., and Biffi, U., 2000, Magnitude of post-Middle Jurassic (Bajocian) displacement on the central Altyn Tagh fault system, northwest China: Geological Society of America Bulletin, v. 112, no. 1, p. 61-74, doi: 10.1130/0016-7606(2000)112<61:MOPJBD>2.0.CO;2.

Ritts, B. D., Yue, Y., and Graham, S. A., 2004, Oligocene–Miocene Tectonics and Sedimentation along the Altyn Tagh Fault, Northern Tibetan Plateau: Analysis of the Xorkol, Subei, and Aksay Basins: The Journal of geology, v. 112, no. 2, p. 207-229, doi: 10.1086/381658.

Robinson, D. M., Dupont-Nivet, G., Gehrels, G. E., and Zhang, Y., 2003, The Tula uplift, northwestern China: Evidence for regional tectonism of the northern Tibetan Plateau during late Mesozoic–early Cenozoic time: Geological Society of America Bulletin, v. 115, no. 1, p. 35-47, doi: 10.1130/0016-7606(2003)115<0035:TTUNCE>2.0.CO;2.

Roger, F., Arnaud, N., Gilder, S., Tapponnier, P., Jolivet, M., Brunel, M., Malavieille, J., Xu, Z., and Yang, J., 2003, Geochronological and geochemical constraints on Mesozoic suturing in east central Tibet: Tectonics, v. 22, no. 4, p. 1037, doi:10.1029/2002TC001466.

Roger, F., Jolivet, M., and Malavieille, J., 2008, Tectonic evolution of the Triassic fold belts of Tibet: Comptes Rendus Geoscience, v. 340, no. 2, p. 180-189, doi:10.1016/j.crte.2007.10.014.

Roger, 2010, The tectonic evolution of the Songpan-Garzê (North Tibet) and adjacent areas from Proterozoic to Present: A synthesis: Journal of Asian Earth Sciences, v. 39, no. 4, p. 254-269, doi:10.1016/j.jseaes.2010.03.008.

Shen, Z. K., Wang, M., Li, Y. X., Jackson, D. D., Yin, A., Dong, D. N., and Fang, P., 2001, Crustal deformation along the Altyn Tagh fault system, western China, from GPS: Journal of Geophysical Research: Solid Earth (1978–2012), v. 106, no. B12, p. 30607-30621, doi: 10.1029/2001JB000349.

Sobel, E. R., and Arnaud, N., 1999, A possible middle Paleozoic suture in the Altyn Tagh, NW China: Tectonics, v. 18, no. 1, p. 64-74, doi: 10.1029/1998TC900023.

Sobel, E. R., Arnaud, N., Jolivet, M., Ritts, B. D., and Brunei, M., 2001, Jurassic to Cenozoic exhumation history of the Altyn Tagh range, northwest China, constrained by $^{40}Ar/^{39}Ar$ and apatite fission track thermochronology: Paleozoic and Mesozoic tectonic evolution of central and eastern Asia, v. 194, p. 247-267, doi: doi: 10.1130/0-8137-1194-0.247.

Song, T., and Wang, X., 1993, Structural styles and stratigraphic patterns of syndepositional

faults in a contractional setting: Examples from Quaidam basin, northwestern China: AAPG bulletin, v. 77, no. 1, p. 102-117.

Sun, J. M., Zhu, R. X., and An, Z. S., 2005a, Tectonic uplift in the northern Tibetan Plateau since 13.7 Ma ago inferred from molasse deposits along the Altyn Tagh Fault: Earth and Planetary Science Letters, v. 235, no. 3, p. 641-653, doi: doi:10.1016/j.epsl.2005.04.034.

Sun, Z. M., Yang, Z. Y., Pei, J. L., Ge, X. H., Wang, X. S., Yang, T. S., Li, W. M., and Yuan, S. H., 2005b, Magnetostratigraphy of Paleogene sediments from northern Qaidam Basin, China: implications for tectonic uplift and block rotation in northern Tibetan plateau: Earth and Planetary Science Letters, v. 237, no. 3, p. 635-646, doi: 10.1016/j.epsl.2005.07.007.

Sun, Z. C., Jing M. C., Sun, N. D., Lu Y.L., Cao, L., 2007. Discussion on boundary between the upper and lower members of Xiaganchaigou Formation of Paleogene in Well Kun-2, Qaidam Basin. Journal of Palaeogeography, 9(6), 611-618 (in Chinese with English abstract).

Tapponnier, P., Peltzer, G., and Armijo, R., 1986, On the mechanics of the collision between India and Asia: Geological Society, London, Special Publications, v. 19, no. 1, p. 113-157, doi: 10.1144/GSL.SP.1986.019.01.07.

Tapponnier, P., Xu, Z. Q., Roger, F., Meyer, B., Arnaud, N., Wittlinger, G., and Yang, J. S., 2001, Oblique stepwise rise and growth of the Tibet Plateau: Science, v. 294, no. 5547, p. 1671-1677, doi: 10.1126/science.105978.

Thomas, W. A., 2011, Detrital-zircon geochronology and sedimentary provenance: Lithosphere, v. 3, no. 4, p. 304-308, doi: 10.1130/RF.L001.1.

Wan, J. L., Wang, Y., Li, Q., Wang, F., and Wang, E., 2001, FT Evidence of Northern Altyn Uplift in Late-Cenozoic: Bulletin of Mineralogy, Petrology and Geochemistry, v. 20, no. 4, p. 222-224 (in Chinese with English abstract).

Wang, E., 1997, Displacement and timing along the northern strand of the Altyn Tagh fault zone, northern Tibet: Earth and Planetary Science Letters, v. 150, no. 1, p. 55-64, doi: 10.1016/S0012-821X(97)00085-X.

Wang, X. F., Metcalfe, I., Jian, P., He, L. Q., and Wang, C. S., 2000, The Jinshajiang-Ailaoshan suture zone, China: tectonostratigraphy, age and evolution: Journal of Asian Earth Sciences, v. 18, no. 6, p. 675-690, doi: 10.1016/S1367-9120(00)00039-0.

Wang, Y., Zhang, X., Wang, E., Zhang, J., Li, Q., and Sun, G., 2005, $^{40}Ar/^{39}Ar$ thermochronological evidence for formation and Mesozoic evolution of the northern-central segment of the Altyn Tagh fault system in the northern Tibetan Plateau: Geological Society of America Bulletin, v. 117, no. 9-10, p. 1336-1346, doi: 10.1130/B25685.

Wang, E., Xu, F. Y., Zhou, J. X., Wan, J., and Burchfiel, B. C., 2006a, Eastward migration of

the Qaidam basin and its implications for Cenozoic evolution of the Altyn Tagh fault and associated river systems: Geological Society of America Bulletin, v. 118, no. 3-4, p. 349-365, doi: 10.1130/b25778.1.

Wang, C., Liu, L., Che, Z. C., Chen, D. L., Zhang, A. D., and Luo, J. H., 2006b, U-Pb geochronology and tectonic setting of the granitic gneiss in Jianggaleisayi Eclogite Belt: Geological Journal of China Universities, v. 12, no. 1, p. 74-82 (in Chinese with English abstract).

Wang, C., Liu, L., Zhang, A. D., Yang, W. Q., and Cao, Y. T., 2008, Geochemistry and petrography of early Paleozoic Yusupuleke Tagh Rapakivi-textured Granite Complex, South Altyn - an example for magma mixing: Acta Petrolei Sinica, v. 24, no. 12, p. 2809-2819 (in Chinese with English abstract).

Wang, L., Xiao, A. C., Gong, Q. L., Liu, D., Wu, L., Zhou, S. P., Shen, Z. Y., Lou, Q. Q., and Sun, X. W., 2010a, The unconformity in Miocene sequence of western Qaidam Basin and its tectonic significance: SCIENCE CHINA Earth Sciences, v. 53, no. 8, p. 1126-1133, doi: 10.1007/s11430-010-4006-z.

Wang, Y. D., Nie, J. S., Zhang, T., Sun, G. Q., Yang, X., Liu, Y. H., and Liu, X. W., 2010b, Cenozoic tectonic evolution in the western Qaidam Basin inferred from subsurface data: Geosciences Journal, v. 14, no. 4, p. 335-344, doi: 10.1007/s12303-010-0033-1.

Wang, C. S., Gao, R., Yin, A., Wang, H., Zhang, Y. X., Guo, T. L., Li, Q. S., and Li, Y. L., 2011, A mid-crustal strain-transfer model for continental deformation: A new perspective from high-resolution deep seismic-reflection profiling across NE Tibet: Earth and Planetary Science Letters, v. 306, no. 3, p. 279-288, doi: 10.1016/j.epsl.2011.04.010.

Wang, C., Dai, J., Zhao, X., Li, Y., Graham, S. A., He, D., Ran, B., and Meng, J., 2014, Outward-growth of the Tibetan Plateau during the Cenozoic: A review: Tectonophysics, v. 621, p. 1-43, doi: 10.1016/j.tecto.2014.01.036.

Wang, E., Kirby, E., Furlong, K. P., van Soest, M., Xu, G. Q., Shi, X., Kamp, P. J. J., and Hodges, K. V., 2012, Two-phase growth of high topography in eastern Tibet during the Cenozoic: Nature Geoscience, v. 5, no. 9, p. 640-645, doi: 10.1038/NGEO1538.

Wang, C., Liu, L., Yang, W. Q., Zhu, X. H., Cao, Y. T., Kang, L., Chen, S. F., Li, R. S., and He, S. P., 2013, Provenance and ages of the Altyn Complex in Altyn Tagh: implications for the early Neoproterozoic evolution of northwestern China: Precambrian Research, v. 230, p. 193-208, doi: 10.1016/j.precamres.2013.02.003.

Wang, Z. Z., Han B. F., Feng C. Y. and Li, G. C., 2009.Geochronology, geochemistry and tectonic significance of granites in Baiganhu area, Xinjiang. Acta Petrologica et Mineralogica,

v. 33, no. 4, p. 597-616 (in Chinese with English abstract).

Wheeler, H. E., 1964, Baselevel, lithosphere surface, and time-stratigraphy: Geological Society of America Bulletin, v. 75, no. 7, p. 599-610, doi: 10.1130/0016-7606(1964)75[599:BLSAT]2.0.CO;2.

Wu, L., Xiao, A., Wang, L., Shen, Z., Zhou, S., Chen, Y., Wang, L., Liu, D., and Guan, J., 2011, Late Jurassic–Early Cretaceous Northern Qaidam Basin, NW China: Implications for the earliest Cretaceous intracontinental tectonism: Cretaceous Research, v. 32, no. 4, p. 552-564, doi: 10.1016/j.cretres.2011.04.002.

Wu, L., Xiao, A., Wang, L., Mao, L., Wang, L., Dong, Y., and Xu, B., 2012a, EW-trending uplifts along the southern side of the central segment of the Altyn Tagh Fault, NW China: Insight into the rising mechanism of the Altyn Mountain during the Cenozoic: SCIENCE CHINA Earth Sciences, v. 55, no. 6, p. 926-939, doi: 10.1007/s11430-012-4402-7.

Wu, L., Xiao, A. C., Yang, S. F., Wang, L. Q., Mao, L. G., Wang, L., Dong, Y. P., and Xu, B., 2012b, Two-stage evolution of the Altyn Tagh Fault during the Cenozoic: new insight from provenance analysis of a geological section in NW Qaidam Basin, NW China: Terra Nova, v. 24, no. 5, p. 387-395, doi: 10.1111/j.1365-3121.2012.01077.x.

XBGMR (Xinjiang Bureau of Geology and Mineral Resources), 1993, Regional Geology of Xinjiang Uygur Autonomous Region: Beijing, Geological Publishing House, 841 p. (in Chinese with English summary).

Xia, W. C., Zhang, N., Yuan, X. P., Fan, L. S., and Zhang, B. S., 2001, Cenozoic Qaidam basin, China: A stronger tectonic inversed, extensional rifted basin: AAPG bulletin, v. 85, no. 4, p. 715-736, doi: 10.1306/8626C98D-173B-11D7-8645000102C1865D.

Yang, F., Ma, Z. Q., Xu, T. C., and Ye, S. J., 1992, A Tertiary paleomagnetic stratigraphic profile in Qaidam basin. Acta Petrolei Sinica, v. 13, no. 2, 97-101 (in Chinese).

Yang, J. S., Xu, Z. Q., Zhang, J. X., Chu, C. Y., Zhang, R. Y., and Liou, J. G., 2001, Tectonic significance of early Paleozoic high-pressure rocks in Altun-Qaidam-Qilian Mountains, northwest China: MEMOIRS-GEOLOGICAL SOCIETY OF AMERICA, p. 151-170.

Yang, J. S., Wu, C. L., Zhang, J. X., Shi, R. D., Meng, F. C., Wooden, J. L., and Yang, H. Y., 2006, Protolith of eclogites in the north Qaidam and Altun UHP terrane, NW China: Earlier oceanic crust?: Journal of Asian Earth Sciences, v. 28, no. 2, p. 185-204, doi: 10.1016/j.jseaes.2005.09.020.

Yang, W., Jolivet, M., Dupont‐Nivet, G., Guo, Z., Zhang, Z., and Wu, C., 2013, Source to sink relations between the Tian Shan and Junggar Basin (northwest China) from Late Palaeozoic to Quaternary: evidence from detrital U‐Pb zircon geochronology: Basin

Research, v. 25, no. 2, p. 219-240, doi: 10.1111/j.1365-2117.2012.00558.x.

Yin, A., and Harrison, T. M., 2000, Geologic evolution of the Himalayan-Tibetan orogen: Annual Review of Earth and Planetary Sciences, v. 28, no. 1, p. 211-280, doi: 10.1146/annurev.earth.28.1.211.

Yin, A., Rumelhart, P., Butler, R., Cowgill, E., Harrison, T., Foster, D., Ingersoll, R., Qing, Z., Xian-Qiang, Z., and Xiao-Feng, W., 2002, Tectonic history of the Altyn Tagh fault system in northern Tibet inferred from Cenozoic sedimentation: Geological Society of America Bulletin, v. 114, no. 10, p. 1257-1295, doi: 10.1130/0016-7606(2002)114<1257:THOTAT>2.0.CO;2.

Yin, A., Dang, Y. Q., Zhang, M., McRivette, M. W., Burgess, W. P., and Chen, X. H., 2007, Cenozoic tectonic evolution of Qaidam basin and its surrounding regions (part 2): Wedge tectonics in southern Qaidam basin and the Eastern Kunlun Range: Geological Society of America Special Papers, v. 433, p. 369-390, doi: 10.1130/2007.2433(18).

Yin, A., Dang, Y.Q., Wang, L.C., Jiang, W.M., Zhou, S.P., Chen, X.H., Gehrels, G.E., and McRivette, M.W., 2008a. Cenozoic tectonic evolution of Qaidam basin and its surrounding regions (Part 1): The southern Qilian Shan-Nan Shan thrust belt and northern Qaidam basin. Geological Society of America Bulletin 120, 813-846, doi:10.1130.B26180.1.

Yin, A., Dang, Y. Q., Zhang, M., Chen, X. H., and McRivette, M. W., 2008b, Cenozoic tectonic evolution of the Qaidam basin and its surrounding regions (Part 3): Structural geology, sedimentation, and regional tectonic reconstruction: Geological Society of America Bulletin, v. 120, no. 7-8, p. 847-876, doi: 10.1130/B26232.1.

Yin, A., 2010, Cenozoic tectonic evolution of Asia: A preliminary synthesis: Tectonophysics, v. 488, no. 1, p. 293-325, doi:10.1016/j.tecto.2009.06.002.

Yu, X. J., Fu, S. T., Guan, S. W., Huang, B., Cheng, F., Cheng, X., Zhang, T., and Guo, Z. J., 2014, Paleomagnetism of Eocene and Miocene sediments from the Qaidam basin: Implication for no integral rotation since the Eocene and a rigid Qaidam block: Geochemistry, Geophysics, Geosystems, v. 15, no. 6, p. 2109-2127, doi: 10.1002/2014GC005230.

Yue, Y. J., and Liou, J. G., 1999, Two-stage evolution model for the Altyn Tagh fault, China: Geology, v. 27, no. 3, p. 227-230, doi: 10.1130/0091-7613(1999)027<0227:TSEMFT>2.3.CO;2.

Yue, Y. J., Ritts, B. D., and Graham, S. A., 2001, Initiation and long-term slip history of the Altyn Tagh Fault, v. 43, no. 12, p. 1087-1093, doi: 10.1080/00206810109465062.

Yue, Y., Ritts, B. D., Graham, S. A., Wooden, J. L., Gehrels, G. E., and Zhang, Z., 2004a, Slowing extrusion tectonics: lowered estimate of post-Early Miocene slip rate for the Altyn Tagh fault: Earth and Planetary Science Letters, v. 217, no. 1, p. 111-122, doi:10.1016/S0012-

821X(03)00544-2.

Yue, Y. J., Ritts, B. D., Hanson, A. D., and Graham, S. A., 2004b, Sedimentary evidence against large strike-slip translation on the Northern Altyn Tagh fault, NW China: Earth and Planetary Science Letters, v. 228, no. 3, p. 311-323, doi: doi:10.1016/j.epsl.2004.10.008.

Yue, Y. J., Graham, S. A., Ritts, B. D., and Wooden, J. L., 2005, Detrital zircon provenance evidence for large-scale extrusion along the Altyn Tagh fault: Tectonophysics, v. 406, no. 3, p. 165-178, doi: 10.1016/j.tecto.2005.05.023.

Zhang, J. X., Zhang, Z. M., Xu, Z. Q., Yang, J. S., and Cui, J. W., 2001, Petrology and geochronology of eclogites from the western segment of the Altyn Tagh, northwestern China: Lithos, v. 56, no. 2, p. 187-206, doi: 10.1016/S0024-4937(00)00052-9.

Zhang, P. Z., Shen, Z., Wang, M., Gan, W., Bürgmann, R., Molnar, P., Wang, Q., Niu, Z., Sun, J., and Wu, J., 2004, Continuous deformation of the Tibetan Plateau from global positioning system data: Geology, v. 32, no. 9, p. 809-812, doi: 10.1130/G20554.1.

Zhang, W. L., 2006, High-resolution megnetostratigraphy of the Cenozoic Qaidam Basin, implications for the uplift of Tibetan Plateau [Ph.D. thesis]: LanZhou University, 158p. (in Chinese).

Zhang, P. Z., Molnar, P., and Xu, X. W., 2007, Late Quaternary and present-day rates of slip along the Altyn Tagh Fault, northern margin of the Tibetan Plateau: Tectonics, v. 26, no. 5, doi: 10.1029/2006TC002014.

Zhang, J. X., Li, H. K., Meng, F. C., Xiang, Z. Q., Yu, S. Y., and Li, J. P., 2011, Polyphase tectonothermal events recorded in “metamorphic basement” from the Altyn Tagh, the southeastern margin of the Tarim basin, western China: Constraint from U-Pb zircon geochronology: Acta Petrologica Sinica, v. 27, no. 1, p. 23-46 (in Chinese with English abstract).

Zhang, H. P., Zhang, P. Z., Zheng, D. W., Zheng, W. J., Chen, Z. W., and Wang, W. T., 2014, Transforming the Miocene Altyn Tagh fault slip into shortening of the north-western Qilian Shan: insights from the drainage basin geometry: Terra Nova, v. 26, no. 3, p. 216-221, doi: 10.1111/ter.12089.

Zhao, J. M., Mooney, W. D., Zhang, X. K., Li, Z. C., Jin, Z. J., and Okaya, N., 2006, Crustal structure across the Altyn Tagh Range at the northern margin of the Tibetan plateau and tectonic implications: Earth and Planetary Science Letters, v. 241, no. 3, p. 804-814, doi: 10.1016/j.epsl.2005.11.003.

Zhou, J. X., Xu, F. Y., Wang, T. C., Cao, A. F., and Yin, C. M., 2006, Cenozoic deformation history of the Qaidam Basin, NW China: Results from cross-section restoration and

implications for Qinghai–Tibet Plateau tectonics: Earth and Planetary Science Letters, v. 243, no. 1-2, p. 195-210, doi: 10.1016/j.epsl.2005.11.033.

Zuffa, G.G., 1980. Hybrid arenites: their composition and classification. Journal of Sedimentary Research 50, 21-29, doi: 10.1306/212F7950-2B24-11D7-8648000102C1865D.

## 3.2 Large-scale displacement along the Altyn Tagh Fault (North Tibet) since its Eocene initiation: insight from detrital zircon U-Pb geochronology and subsurface data

***Paper published in Tectonophysics, 2016(Accepted with minor revision)***

**Large-scale displacement along the Altyn Tagh Fault (North Tibet) since its Eocene initiation: insight from detrital zircon U-Pb geochronology and subsurface data**

**Feng Cheng** [1, 2], Marc Jolivet [2], Suotang Fu [3], Changhao Zhang [3], Qiquan Zhang [3], Zhaojie Guo [1, †]

[1] Key Laboratory of Orogenic Belts and Crustal Evolution, Ministry of Education, School of Earth and Space Sciences, Peking University, Beijing, 100871, China

[2] Laboratoire Géosciences Rennes, CNRS-UMR6118, Université Rennes 1 - Observatoire des Sciences de l'Univers, Rennes, 35042, France

[3] Qinghai Oilfield Company, PetroChina, Dunhuang, Gansu, 736202, China

[†] Corresponding author. Tel.: + 86-10-62753545; fax: + 86-10-62758610. E-mail address: zjguo@pku.edu.cn (Z.J. Guo)

*Note: This work is submitted to the Tectonophysics and is undergoing peer-review process.*

### Abstract

Marking the northern boundary of the Tibetan plateau, the Altyn Tagh fault plays a crucial role in accommodating the Cenozoic crustal deformation affecting the plateau. However, its initiation time and amount of offset are still controversial despite being key information for the understanding of Tibet evolution. In this study, we present 1122 single LA-ICP-MS detrital zircon U-Pb ages obtained from 11 Mesozoic and Cenozoic sandstone samples, collected along two sections in the northwestern Qaidam basin (Eboliang and Huatugou). These data which are associated with new 3D seismic reflection profiles to demonstrate: (1) From the Paleocene to early Eocene, the Eboliang section was approximately located near the present

position of Anxi, ca. 360 ± 40 km southwest to its current location along the Altyn Tagh fault, and sediments were mainly derived from the Altyn Tagh Range. At the same period, the Huatugou section was approximately located near the present position of Tula, ca. 360 km southwest to its current location along the Altyn Tagh fault, and the Eastern Kunlun Range represented the significant sediment source. (2) Left-lateral strike-slip movement along the Altyn Tagh fault initiated during the early to middle Eocene, resulting in northeastward displacement of the two sections. (3) By the early Miocene, the intensive deformation within the Altyn Tagh Range and northwestern Qaidam basin strongly modified the drainage system, preventing the materials derived from the Altyn Tagh Range to reach the Eboliang and the Huatugou sections. The post-Oligocene clastic material in the western Qaidam basin is generally derived from local sources and recycling of the deformed Paleocene to Oligocene strata. From these data, we suggest enhanced tectonic activity within the Altyn Tagh Range and northwestern Qaidam basin since Miocene time, and propose an early to middle Eocene initiation of left-lateral strike-slip faulting and a 360 ± 40 km offset along the Altyn Tagh fault.
Keywords：Detrital zircon U-Pb geochronology, Cenozoic tectonics, North Tibet, Altyn Tagh fault, Qaidam basin.

### 3.2.1 Introduction

Two competing end-member mechanisms have been proposed to explain the accommodation of the ongoing convergence between India and Eurasia since the early Eocene collision: (1) a homogeneous crustal thickening of the Tibetan plateau (e.g. England and Houseman, 1989; Searle, 1996); and (2) an eastward extrusion of the Tibetan plateau and southeast Asia away from the indenting Indian plate (Molnar and Tapponnier, 1975; Peltzer and Tapponnier, 1988; Avouac and Tapponnier, 1993; Tapponnier, et al., 2001). The second model requires large-scale displacement along lithospheric strike-slip fault zones to allow extrusion of the Tibetan crust. (e.g. Searle, 1996; Tapponnier, et al., 2001). Marking the northern boundary of the Tibetan plateau (Fig. 1), the lithospheric-scale left-lateral strike-slip Altyn Tagh fault (ATF) plays a crucial role in accommodating the crustal deformation and appears to be an ideal field laboratory for ascertaining the dynamics of plateau formation (Molnar and Tapponnier, 1975; Wittlinger et al., 1998; Jolivet et al., 1999, 2001; Yin and Harrison, 2000; Yin et al., 2002; Searle et al., 2011). Understanding the kinematic pattern of the ATF, especially the exact Cenozoic initiation time and the amount of Cenozoic offset, is of major importance for unraveling the crustal accommodation processes within the plateau since the India-Eurasian collision and for deciphering the growth history of the entire Tibetan

plateau.

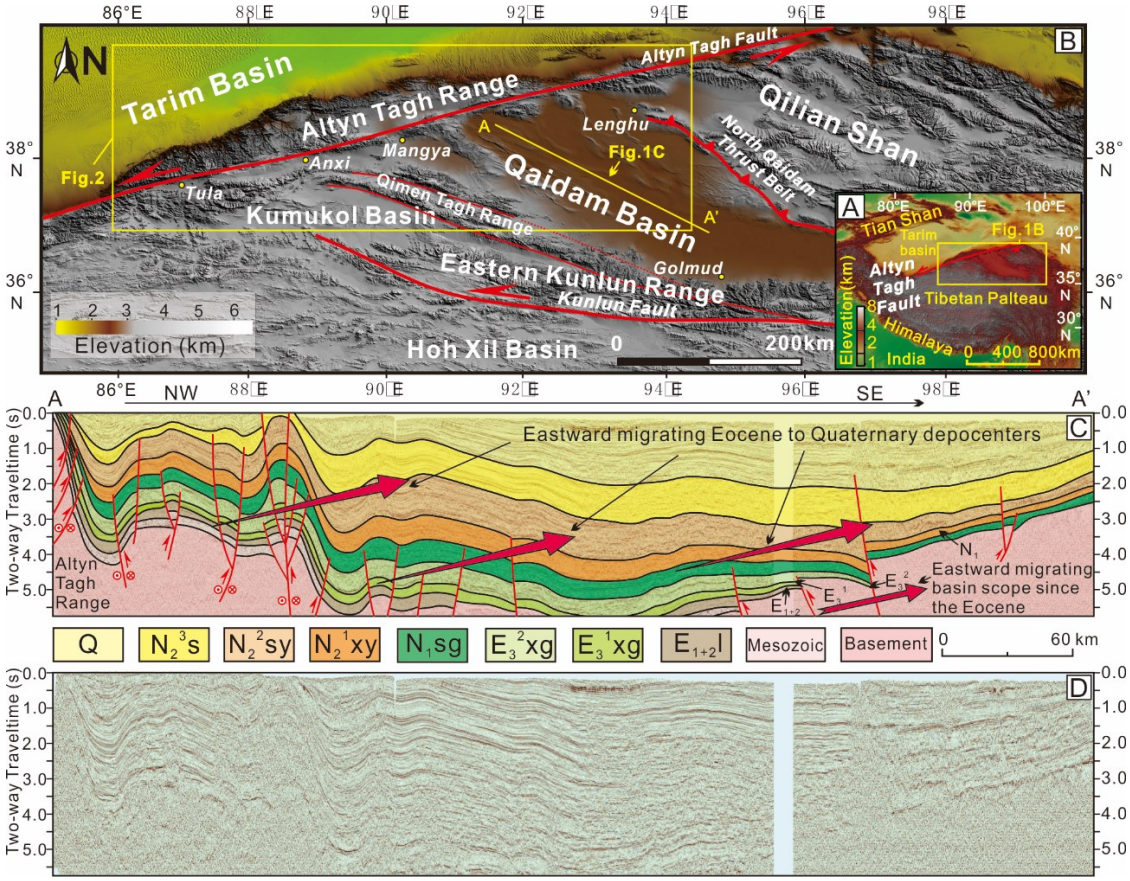


Fig. 1 (A) SRTM based digital topographic map of the Tibetan plateau. (B) Digital elevation model (DEM) and major tectonic elements of the Altyn Tagh Range, the Qaidam basin and the surrounding regions. The location of Fig. 2 is identified by the solid box. The DEM map was generated from the 90 m SRTM data. Note that the yellow solid line refers to the location of seismic profile AA'. (C) Interpreted and (D) non-interpreted seismic profile AA'. Note that the succession of Cenozoic depo-centers is marked along the long axis of the basin. These depo-centers gradually migrated eastward since the Eocene.

In spite of its widely recognized significance, the Cenozoic initial rupture and displacement on the ATF are still controversial and highly debated. Several authors proposed that a large scale Jurassic basement cooling event associated to tectonic exhumation affected a corridor along the ATF (e.g. Delville et al., 2001; Sobel et al., 2001; Wang et al., 2005). In addition, many researchers consider that deformation along the ATF initiated after the late Mesozoic, during the early Cenozoic, or even not before Neogene (e.g. Tapponnier et al., 1986; Jolivet et al., 1999; Chen et al., 2001; Jolivet et al., 2001; Yin et al., 2002; Wang et al., 2006a; Wu et al., 2012a, 2012b; Zhang et al., 2012, 2014a). Similarly, estimations of the total displacement along the ATF vary widely from ~1200 km to less than 90 km (e.g. Tapponnier et al., 1986; Wang, 1997; CSBS, 1992; Ritts and Biffi, 2000; Yin and Harrison, 2000; Yang et al., 2001; Yue et al., 2001; Chen et al., 2002; Yin et al., 2002; Cowgill et al., 2003; Gehrels et

al., 2003a, 2003b; Darby et al., 2005; Yue et al., 2005; Searle et al., 2011; Cheng et al., 2015a). These tremendous discrepancies may be partially attributed to the immense size and extent of the Altyn Tagh Range, making it difficult to locate ideal piercing points to estimate the total displacement along the ATF. Furthermore, due to strong Cenozoic deformation, continuous Mesozoic to Cenozoic stratigraphic sections useful to estimate the time of initiation of left-slip movement are seldom preserved (e.g. Yin and Harrison, 2000; Cheng et al., 2015a).

Detrital zircon analysis of a continuous, well dated stratigraphic succession has become a powerful tool for unraveling source to sink relationships and constraining the tectonic and topographic evolution of an area (e.g. Fedo et al., 2003; Thomas, 2011; Gehrels, 2014). To bring more constraints on the kinematic evolution of the ATF, we conducted an integrated analysis on two Jurassic to Pleistocene sedimentary sections in the western part of the Qaidam basin, adjacent to the ATF (Fig. 2). Detrital zircon U-Pb geochronology data obtained from these sections are associated to high-quality subsurface data, including newly acquired seismic profiles and drill core sandstone samples.

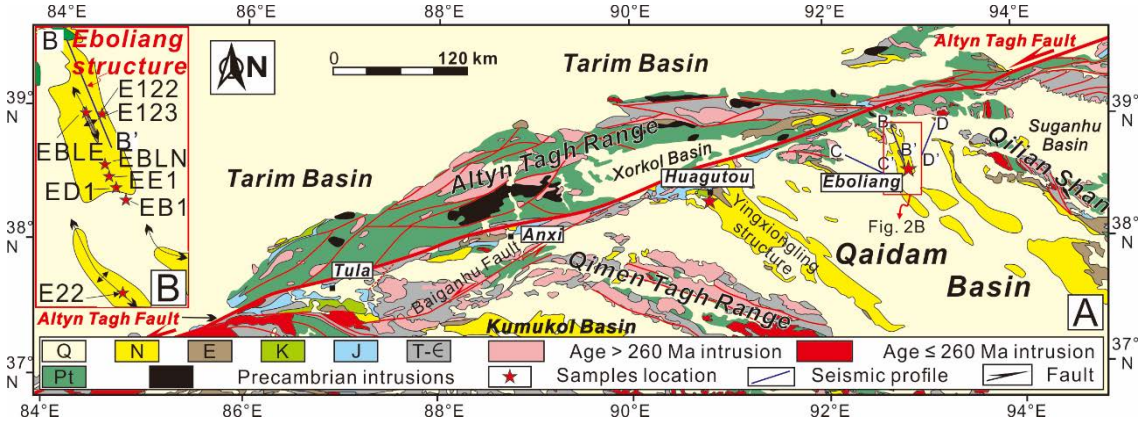


Fig. 2 Simplified geological map of the northwestern Qaidam basin and eastern segment of the Altyn Tagh Range, adapted from the Geologic Map of the Tibetan plateau and adjacent areas compiled by the Chengdu Institute of Geology and Mineral Resources and Chinese Geological Survey (map scale, 1:1,500,000).

## 3.2.2 Geological Background

### 3.2.2.1 Altyn Tagh Range

The Altyn Tagh Range is located along the northern edge of the Tibetan plateau, separating the Tarim basin to the northwest from the Tibetan plateau and the Qaidam basin to the south (Figs. 1 and 2). The bedrock of the Altyn Tagh Range mainly consists of Precambrian igneous and metamorphic rocks and Paleozoic igneous and sedimentary rocks (e.g. Sobel and Arnaud, 1999; Yin et al., 2002). It has been shown that the Altyn Tagh Range experienced

multiple-stage deformation and tectonic exhumation from the Jurassic to the Holocene (Tapponnier et al., 1986; Jolivet et al., 1999; Yue and Liou, 1999; Chen et al., 2001; Delville et al., 2001; Jolivet et al., 2001; Sobel et al., 2001; Yin et al., 2002; Wang et al., 2005, 2006a; Zhang et al., 2012). Within this range, the over 1600 km long ENE-trending ATF links the western Kunlun thrust belt in the southwest and the Qilian Shan thrust belt in the northeast (Fig. 1; Burchfiel et al., 1989; Wang, 1997; Yue and Liou, 1999; Yin and Harrison, 2000; Yin et al., 2002). Although Mesozoic shearing occurred in the Altyn Tagh Range, the northern Tibetan plateau growth is largely influenced by Cenozoic sinistral strike-slip faulting along the ATF (Tapponnier et al., 1986, 2001; Arnaud et al., 2003; Wang et al., 2005; Li et al., 2006; Liu et al., 2007). As previously mentioned, the estimation of the total displacement along the fault remains heavily debated, varying from about 1200 km to less than 90 km (e.g. CSBS, 1992; Ritts and Biffi, 2000; Yang et al., 2001; Chen et al., 2002; Cowgill et al., 2003; Gehrels et al., 2003a, 2003b; Yue et al., 2005; Cheng et al., 2015a).

#### 3.2.2.2 Qaidam basin

The rhomb-shaped Qaidam basin, is the largest petroliferous basin within the entire Tibetan plateau (Figs. 1 and 2). Geomorphologically, the basin is surrounded by the Altyn Tagh Range to the northwest, the Qilian Shan to the northeast and the Eastern Kunlun Range to the south. Geological mapping and petroleum exploration revealed that the Qaidam basin is filled with Mesozoic to Cenozoic clastic sediment series unconformably overlying an uncertain basement (Xia et al., 2001; Meng and Fang, 2008; Yin et al., 2008a, 2008b). The Mesozoic strata, especially the Jurassic and lower Cretaceous sequences, are mainly distributed along the foreland of both the Altyn Tagh Range and the Qilian Shan (Ritts et al., 1999; Wu et al., 2011), while the Cenozoic series are generally deposited within the entire basin (Yin et al., 2008b). The Cenozoic sedimentation pattern is largely controlled by a succession of depocenters consistently located along the long axis of the basin and gradually migrating eastward since Eocene times, indicating the gradual uplift of the Altyn Tagh Range (Fig. 1; Song and Wang, 1993; Qiu, 2002; Sun et al., 2005; Wang et al., 2006a; Yin et al., 2008b). Using magnetostratigraphy, palynology and paleontology, the Mesozoic-Cenozoic strata have been precisely subdivided into 11 chronostratigraphically constrained units (Fig. 3; Huo, 1990; QBGMR, 1991; Yang et al., 1992; Huang et al., 1996; Xia et al., 2001; Qiu, 2002; Deng et al., 2004a, 2004b; Sun et al., 2005; Zhang, 2006; Zhao et al., 2006; Fang et al., 2007; Sun et al., 2007; Yin et al., 2008b; Gao et al., 2009; Pei et al., 2009; Lu and Xiong, 2009; Ke et al., 2013). These units are: (1) the Dameigou Formation, $_{J1+2}$d; (2) the Caishiling Formation,

$J_3c$; (3) the Quanyagou Formation, Kq; (4) the Lulehe Formation, $E_{1+2}l$, >53.5 - 43.8 Ma (Yang et al., 1992; Zhang, 2006; Ke et al., 2013); (5) the lower Xiaganchaigou Formation, $E_3^1xg$, 43.8 - 37.8 Ma (Zhang, 2006; Sun et al., 2007; Pei et al., 2009); (6) the upper Xiaganchaigou Formation, $E_3^2xg$, 37.8 - 35.5 Ma (Sun et al., 2005; Sun, 2007; Pei et al., 2009); (7) the Shangganchaigou Formation, $N_1sg$, 35.5 - 22.0 Ma (Sun et al., 2005; Lu and Xiong, 2009); (8) the Xiayoushashan Formation, $N_2^1xy$, 22.0 - 15.3 Ma (Fang et al., 2007; Lu and Xiong, 2009); (9) the Shangyoushashan Formation, $N_2^2sy$, 15.3 - 8.1 Ma (Fang et al., 2007); (10) the Shizigou Formation, $N_2^3s$, 8.1 - 2.5 Ma (Fang et al., 2007); (11) the Quaternary deposits, including the Qigequan Formation ($Q_1q$) and the Dabuxun-Yanqiao Formation ($Q_2d$), 2.5 - 0.01 Ma (Fang et al., 2007; Yin et al., 2008b). Effective elastic thickness calculation implies that the mechanical strength of the Qaidam crust is exceptionally strong compared to the rest of the Tibetan plateau (Braitenberg et al., 2003). Based on balanced cross section results, Zhou et al. (2006) proposed that the Qaidam basin experienced an average of 10% of NE-SW shortening during the Cenozoic, whereas Yin et al. (2008b) suggested that the shortening strain across the basin decreases systematically eastward from ca. 48% in the west, to ca. 11% in the center, and <1% in the east.

### 3.2.3 Stratigraphy and sedimentary characteristics of the studied sections

In this study, the Eboliang and Huatugou sections, situated along the eastern and central segments of the ATF, have been chosen for their exceptional preservation and exposure of the Jurassic to Pleistocene sedimentary series (Figs. 2 and 3). In order to give a continuous description of the Jurassic to Quaternary sediment evolution of the northwestern Qaidam basin, we constructed the Eboliang and Huatugou sections based on the lithologies, sediment facies and paleocurrent directions obtained from fieldwork, drill-core and literature data as summarized in the Figure 3 and in the text below. The strata in Huatugou and Eboliang sections have already been established by previous field geological studies which give age constraint based on fossil assemblages, distinctive lithology feature, magnetostratigraphy, palynology and paleontology (e.g. XBGRM, 1993; HGSI, 2003; IGSQP, 2004). Consequently, we follow the previous division of formations.

#### 3.2.3.1 Eboliang section

The Eboliang section is located along the southern flank of the Altyn Tagh Range (Fig. 2). The upper Jurassic-Cretaceous strata are missing, and the Paleogene deposits rest unconformably on lower - middle Jurassic series. Except for the absence of the Paleocene

Lulehe Formation, the Cenozoic sequence is complete and exceptionally well exposed.

High-quality seismic profiles and drill core data reveal that the base of the Eboliang section is formed by the lower to middle Jurassic Dameigou Formation ($J_{1+2}$d), resting unconformably on the basement rocks (Yin et al., 2008). This Jurassic sequence generally contains a succession of three well-developed fining upward cycles. Each cycle characteristically begins with medium- to coarse-grained sandstone deposits (Fig. 4A), fining upwards to silty mudstone. The sequence, as in general for the Qaidam basin, is considered to represent shore shallow lacustrine facies at the base, evolving into flood plain sediments upward (Ritts et al., 1999; Ritts and Biffi, 2000; Wu et al., 2011; Jian et al., 2013). Trough and planar cross-stratification and clast imbrication from those fluvial strata indicates northward paleoflows during the Jurassic (Fig. 3; Ritts and Biffi, 2000).

The entire upper Jurassic and Cretaceous sequence is missing and the Paleocene Lulehe Formation ($E_{1+2}$l,) unconformably overlies the lower and middle Jurassic series (Wu et al., 2011). The strata are composed of dark brown mudstone (Fig. 4B) and sandy mudstone intercalated with gray siltstone at the base, evolving towards brown pebbly sandstone intercalated with conglomerates and gypsum-salt layers in the middle and upper parts of the section. The Lulehe Formation is generally interpreted as braided river and alluvial fan depositional environments (Zhuang et al., 2011; Jian et al., 2013; Song et al., 2013). Based on heavy mineral contents, calculated zircon-tourmaline-rutile (ZTR) indices, and the heavy mineral assemblages from drill-core samples from a large number of oil wells in the Eboliang section, Fu et al. (2013) suggested that during the deposition of the Paleocene-early Eocene Lulehe Formation, the material deposited in the Eboliang area was derived from the north, probably from the Altyn Tagh Range.

The Eocene to Oligocene strata of the Xiaganchaigou Formation unconformably rest on the Lulehe Formation. The strata are mainly composed of grey and brown sandstone (Fig. 4C) and conglomerate at the bottom corresponding to alluvial facies deposits (Zhuang et al., 2011; Jian et al., 2013; Wang et al., 2013) and contain a succession of fining upward cycles. The middle part of the Xiaganchaigou Formation is dominated by brownish red mudstone and sandy mudstone intercalated with gray calcareous mudstone and marlstone. The upper part of the Xiaganchaigou Formation, however, is dominated by variegated mudstone intercalated with thin-layers of sandy conglomerate, sandstone and limestone, generally associated to a lacustrine depositional environment (Zhuang et al., 2011; Jian et al., 2013; Wang et al., 2013). Conglomerate fabrics in the Eboliang area show north-directed or south-directed bilateral paleoflows, suggesting a low-energy lacustrine-offshore environment at the time (Fig. 3; Wu

et al., 2012b).

The Oligocene Shangganchaigou Formation (N1sg), conformably rests on the Xiaganchaigou Formation. It consists of brownish red, gray siltstone, grey mudstone, sandy mudstone and siltstone, intercalated with gray sandstone and marlstone (Fig. 4D) mostly corresponding to lacustrine sediment facies (Zhuang et al., 2011; Jian et al., 2013; Wang et al., 2013). Paleocurrents measured from the conglomerate fabrics become dominantly south-directed away from the Altyn Tagh Range (Fig. 3; Wu et al., 2012b).

The early Miocene Xiayoushashan Formation ($N_2^1$xy) conformably lies on the Shangganchaigou Formation. The lower part of the formation is composed of gray and brownish red mudstone and sandy mudstone intercalated with gray siltstone, grayish yellow sandstone and grayish brown marlstone. It evolves upwards to gray mudstone, argillaceous sandstone and argillaceous siltstone intercalated with grey siltstone, brownish red mudstone and gray marlstone (Fig. 4E). The early Miocene sequence in the north Qaidam basin is generally considered as deposited in a fluvial to marginal lacustrine environment (Zhuang et al., 2011; Jian et al., 2013; Wang et al., 2013). Conglomerate fabrics in the section suggest south-directed paleocurrents during the early Miocene (Fig. 3; Wu et al., 2012b).

The late Miocene Shangyoushashan Formation ($N_2^2$sy) conformably rests on the Xiayoushashan Formation. The deposits are mainly composed of grey mudstone and sandy mudstone intercalated with grey argillaceous sandstone, argillaceous siltstone, grayish yellow marlstone and some limited gray sandy limestone corresponding again to a fluvial to marginal lacustrine environment (Zhuang et al., 2011; Jian et al., 2013; Wang et al., 2013). Paleocurrent measurements from the sandstone layers around the Eboliang area indicate southwest-directed paleoflows (Fig. 3; Wu et al., 2012b).

The Pliocene Shizigou Formation ($N_2^3$s) generally conformably and locally unconformably rests on the Shangyoushashan Formation. The series are composed of gray mudstone and silty mudstone intercalated with brown siltstone, pebbly sandstone and gypsum-salt layers. It is generally interpreted as marginal lacustrine to alluvial fan environment (Fig. 4F; Zhuang et al., 2011; Heermance et al., 2013; Jian et al., 2013; Wang et al., 2013). Trough cross-bedding within the strata suggests generally southwestward paleoflows during the Pliocene (Fig. 3; Heermance et al., 2013).

Finally, the Pleistocene sequence, dominated by the Qigequan Formation ($Q_1$q), unconformably overlies the Shizigou Formation. The sediments are characterized by brown sandstone, pebbly sandstone and conglomerate intercalated with gypsum layers, corresponding to fluvial to evaporatic lacustrine facies (Heermance et al., 2013; Jian et al.,

2013). Well-developed cross-bedding within the strata shows primarily unidirectional paleocurrents toward the south (Fig. 3; Heermance et al., 2013).

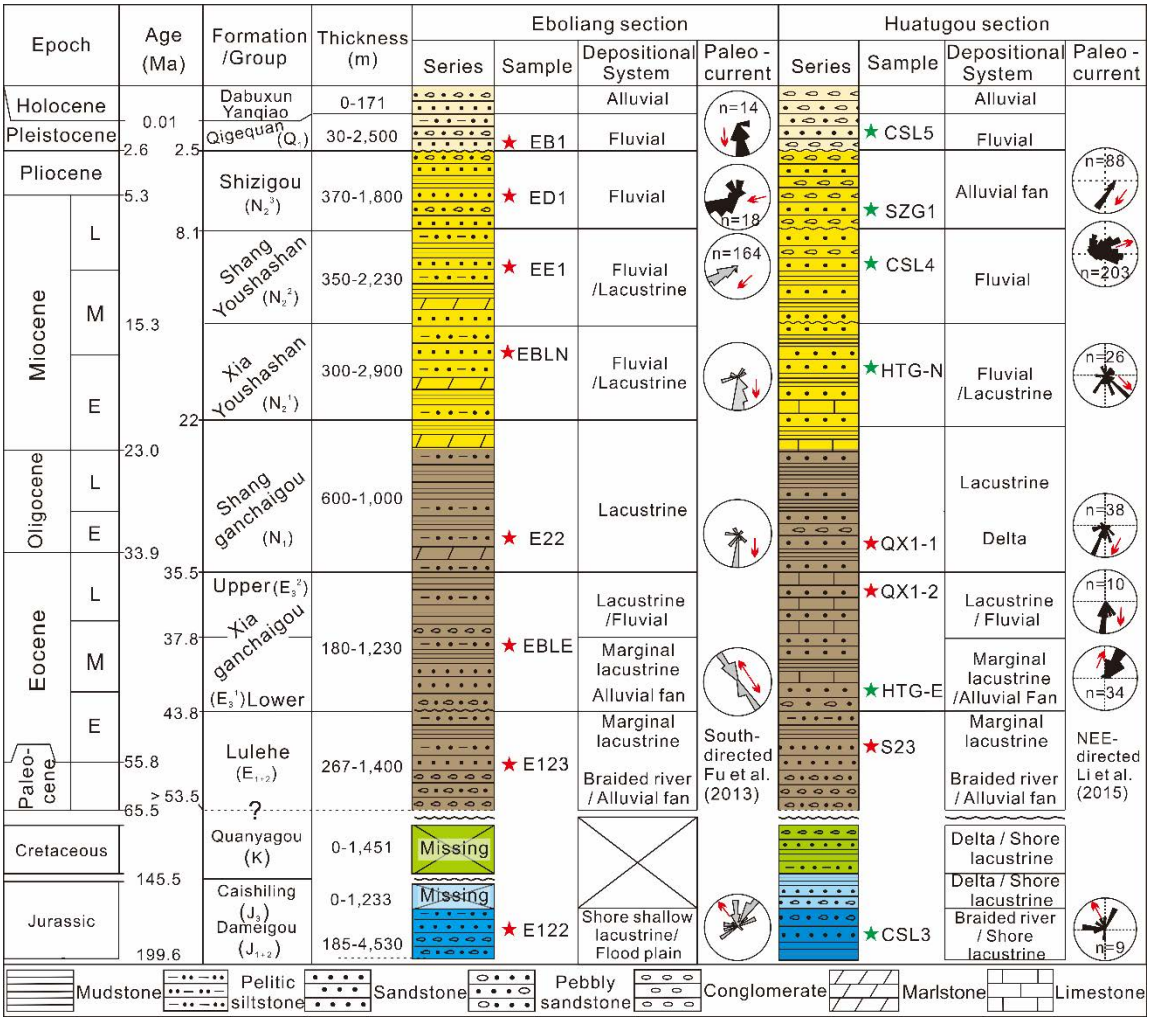


Fig. 3 Generalized stratigraphic column of the studied Mesozoic to Cenozoic series. Paleocurrent directions in the Huatugou section were obtained from Meng and Fang, (2008), Wu et al. (2012b) and Zhuang, et al. (2011). Paleocurrent directions in the Eboliang section were obtained from Zhuang, et al. (2011), Wu et al. (2012b) and Heermance et al. (2013). Note that sample CSL3 is cited from Cheng et al. (2015a), and samples HTG-E, HTG-N, CSL4, SZG1 and CSL5 are cited from Cheng et al. (2016). Red arrows refer to the general paleocurrent directions.

### 3.2.3.2 Huatugou section

The Huatugou section is located in the northernmost part of the prominent Yingxiongling uplift structure (Fig. 2). Except again for the Paleocene Lulehe Fm., the whole Mesozoic-Cenozoic sequence is well exposed (Figs. 2 and 3).

Subsurface data reveal that the Jurassic clastic coal-bearing strata rest unconformably on the Altyn Tagh Range basement (Xia et al., 2001; Yin et al., 2008). The Dameigou Formation ($J_{1+2}d$) is dominated by a set of sandstone beds interbedded with conglomerate, siltstone and

mudstone (Ritts et al., 1999; Ritts and Biffi, 2000). The sediment facies vary from fluvial to shallow lake deposits (Ritts and Biffi, 2000). Trough and planar cross-stratification as well as clast imbrication within the strata indicate northward paleoflows during the Jurassic (Fig. 3; Ritts and Biffi, 2000).

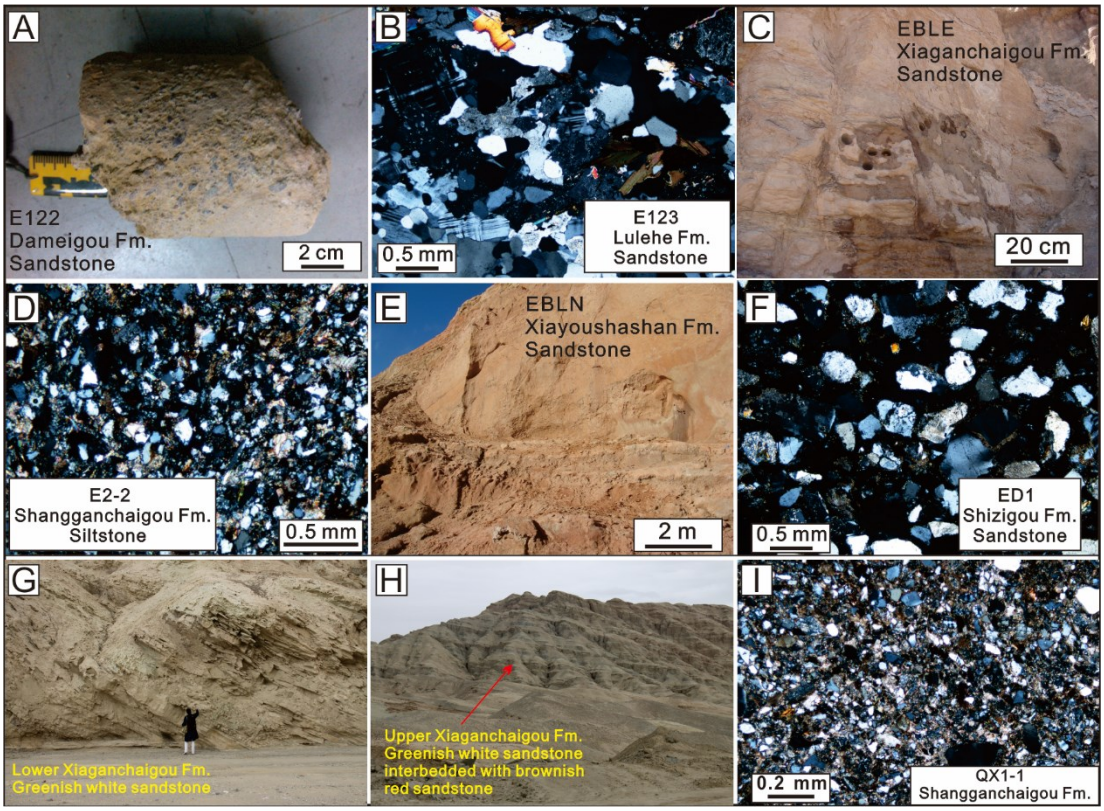


Fig. 4 Typical photomicrographs and field photographs of the various analyzed sediments. (A) Drill core sample of early to middle Jurassic ($J_{1+2}$) lithic sandstone obtained from drill well in the Eboliang section; (B) Thin section image of lithic sandstone from the Paleocene to early Eocene strata ($E_{1+2}$) in the Eboliang section, under crossed polarized light. (C) Horizontally stratified sandstone interbedded with mudstones of the Xiaganchaigou Formation ($E_3^1$) in the Eboliang section. (D) Thin section image of siltstone from the Oligocene strata ($N_1$), under crossed polarized light, obtained from drill well in the Eboliang section. (E) Thick-bedded sandstone in the early Miocene strata, Xiayoushashan Formation ($N_2^1$), Eboliang section. (F) Thin section image of siltstone from the Pliocene strata ($N_2^3$), in the Eboliang section, under crossed polarized light. (G) Greenish white sandstone intercalated with mudstone in the middle Eocene strata ($E_3^1$), Huatugou section. (H) Greenish white sandstone intercalated with brownish red mudstone in the late Eocene strata ($E_3^1$), Huatugou section. (I) Thin section image of sandstone in the Oligocene strata ($N_1$), Huatugou section, under crossed polarized light.

Based on the subsurface data (core and seismic profile data), the Paleocene to early Eocene Lulehe Formation ($E_{1+2}$l) is dominated by successions of purple-red conglomerate interbedded with sandstone at the base, evolving upward towards grey sandstone, siltstone and sandy mudstone. The sediment facies vary from fluvial to shallow lake deposits upward and

basinward (Fu et al., 2013; Li et al., 2015). Heavy mineral contents in surface samples, calculated zircon-tourmaline-rutile (ZTR) indices, and the heavy mineral assemblages from the drill-core samples from a large number of oil wells in the Huatugou area suggest that during the deposition of the Paleocene-early Eocene Lulehe Formation, the material deposited in the Huatugou area was mainly derived from the southwest, probably from the Eastern Kunlun Range (Fu et al., 2013; Li et al., 2015).

The middle Eocene lower Xiaganchaigou Formation ($E_3^1$xg) is mainly composed of grey-green, brownish-red sandstone and pebbly sandstone at the base, evolving upward towards brown red sandstone and siltstone (Fig. 4G). The sediment facies vary from fluvial to shallow lacustrine deposits upward (Zhuang et al., 2011; Wu et al., 2012a, 2012b). Paleocurrents from the pebble imbrication and cross-stratification in the fluvial sandstone layers are directed towards the NE (Fig. 3; Meng and Fang, 2008).

The late Eocene upper Xiaganchaigou Formation ($E_3^2$xg) rests conformably on the lower Xiaganchaigou Formation. This sequence is dominated by successions of grey-green, brownish-red mudstone and carbonaceous siltstone, intercalated with argillaceous siltstone and marlstone (Fig. 4H). The sediment facies vary upward from braided river to shallow lake deposits (Wu et al., 2012a, 2012b). Clast imbrications within the fluvial strata suggest that paleocurrents were directed towards the south during the deposition of the upper Xiaganchaigou Formation. (Fig. 3; Wu et al., 2012a).

The Oligocene Shangganchaigou Formation ($N_1$sg), conformably resting on the upper Xiaganchaigou Formation, is mainly composed of greyish-green carbonaceous mudstone and sandstone interbedded with grey-white mudstone. This series is dominated by deltaic to shallow lake facies deposits (Wu et al., 2012a, 2012b). Reported paleocurrents from clast imbrications are generally directed towards the south (Fig. 3; Wu et al., 2012a).

The Xiayoushashan Formation ($N_2^1$xy), conformable with the Shangganchaigou Formation, is mainly composed of yellowish-brown, pebbly sandstone, sandstone and argillaceous siltstone with intercalations of limestone. The facies vary from shallow lake to fluvial deposits (Wu et al., 2012a, 2012b). Clast imbrications within the sequences suggest generally southwestward paleoflows during the early Miocene.

The Shangyoushashan Formation ($N_2^2$sy), resting unconformably on the Xiayoushashan Formation (Wang et al., 2010), mainly consists of yellow pebbly sandstone, sandstone and silty mudstone. The sediment facies is dominated by shallow lake, alluvial plain and braided river deposits (Wu et al., 2012a, 2012b). Clast imbrication as well as trough (and lesser planar) cross-stratification within the layers in the section suggest generally northwestward

paleoflows (Zhuang et al., 2011).

The Shizigou Formation ($N_2^3s$), again lying unconformably on the Shangyoushashan Formation, is mainly composed of earth-yellow sandstone and silty mudstone corresponding to fluvial facies sediments (Wu et al., 2012a, 2012b). Paleocurrents from clast imbrications indicate generally south-directed paleoflows away from the Altyn Tagh Range during the deposition of the Shizigou Formation (Fig. 3; Zhuang et al., 2011).

The Qigequan ($Q_1q$) and Dabuxun-Yanqiao ($Q_2$) formations, unconformably overly the Shizigou Formation, and mainly consists of grey and brown sandstone and conglomerate corresponding to flood plain and alluvial facies deposits.

### 3.2.4 Methods and analytical procedures

#### 3.2.4.1 Detrital zircon geochronology

Detrital zircon U-Pb geochronology has rapidly developed into a very powerful tool for determining sediment provenances (e.g. Fedo, et al., 2003; Thomas, 2011; Liu et al., 2013; Yang et al., 2013; Gehrels et al., 2014; Cheng et al., 2015a). By systematically comparing the detrital zircon U-Pb age spectrum obtained from sedimentary sequences in basins with the known ages of potential source terranes, it is possible to describe the source to sink relations through time within a given area and to reconstruct the landscape evolution of the region (e.g. Fedo, et al., 2003; Gehrels et al., 2011; Thomas, 2011; Liu et al., 2013; Yang et al., 2013; Gehrels et al., 2014; Yang et al., 2014; Cheng et al., 2015a). In the Eboliang section, eight samples were collected, ranging in age from Jurassic to Pleistocene (Fig. 2), and including three samples from drill cores. In the Huatugou section, three core samples were obtained from drill wells, ranging in age from Paleocene to Oligocene. In order to derive a continuous Jurassic to Pleistocene source to sink relation between the Altyn Tagh Range and the western Qaidam basin, we also integrated six published detrital zircon U-Pb dating results obtained on samples collected from the Huatugou section (Cheng et al., 2015a, 2016). The major petrological characteristics of all the samples are described in Table 1.

Zircon grains for U-Pb age dating were concentrated from each sample following the standard procedures outlined in Liu et al. (2013). This work was conducted at the Chengxin Geology Service Co. Ltd, Langfang, Hebei Province, China. Individual zircon crystals (generally more than 200 grains) were mounted in epoxy resin without handpicking to avoid sampling bias. Samples were then polished to obtain a smooth flat internal surface. Reflected and transmitted light as well as cathodoluminescence (CL) images were made to reveal

internal heterogeneities and allow choosing potential internal targets for isotopic dating. U-Pb analysis was performed on an Agilent 7500a ICP-MS connected to an American New Wave UP 193 SS 193 nm Excimer laser ablation system at the China University of Geosciences, Beijing. All samples were analyzed using a laser spot size of 36 μm and a frequency of 10 Hz. Two standards (Black et al., 2003; Qi et al., 2005) were analyzed every 10 to 20 grains, to correct for instrument fluctuations and determine fractionation factors. Zircons Qinghu and 91500 (Wiedenbeck et al., 1995) were the monitoring standards. For elemental concentration analysis, NIST610 was the external standard, and 29Si was the internal standard. Meanwhile, NIST612 and NIST614 were used as monitoring standards. The GLITTER 4.4 software was used to calculate the U-Pb isotope ratios and element contents (China University of Geosciences, Lab. of Prof. Y.S. Liu, Beijing, China). The U-Pb ages obtained were checked for discordance by plotting the analyses on concordia diagrams using the Isoplot 3.0 software (Ludwig, 2003). The common-Pb correction followed the method described by Andersen (2002). Ages younger than ca. 1000 Ma are based on common Pb-corrected 206Pb/238U ratios, whereas ages older than ca. 1000 Ma are based on common Pb-corrected 207Pb/206Pb ratios. For ICP-MS analyses, those ages with discordance degree >10% were excluded from analysis (e.g. Gehrels et al., 2003a; Yang et al., 2013; Liu et al., 2015). A more complete description of the sample separation methods and analytical procedures is given in Yuan et al. (2004).

#### 3.2.4.2 Seismic profile

Extensive petroleum exploration of the Qaidam basin in recent years has provided abundant subsurface data, including high-quality seismic profiles and drill core data. In this study, we integrated two 3D and two 2D seismic profiles (A-A', B-B', CC' and DD', see locations in Figs. 1 and 2) from the western Qaidam basin with our surface field investigation to describe the tectonic history of the western Qaidam basin. Seismic data were interpreted using the SMT Kingdom software.

### 3.2.5 U–Pb geochronology results of detrital zircons

Representative CL images of typical zircon grains are presented in Figure 5. U-Pb isotopic ages with errors and related raw data are listed in full as Appendix S1. Concordia plots for the eleven samples are shown in Figure 6. The zircon age spectrum of the samples from the Eboliang and Huatugou sections are shown in Figs. 7 and 8, respectively. In the following, age peaks are considered major when corresponding to an age group including at least 50% of the total number of data, whereas a minor peak refers to those representing less

than 20% of the total number of data.

Table 1. Summary of the major characteristics and corresponding U-Pb age data for each sample

| Epoch | Formation (Fm.) | Sample number | Lithology | Detrital zircon age range (Ma) | Detrital zircon peaks (Ma) | Number of effective data points | Th/U ratios |
|---|---|---|---|---|---|---|---|
| *Eboliang section* | | | | | | | |
| Pleistocence | Qigequan Fm. ($Q_1q$) | EB1 | Greyish green sandstone | 232~1053 | ~253 ~417 | 100 | 0.08, 0.09, 0.14~2.19 |
| Pliocene | Shizigou Fm. ($N_2^3s$) | ED1 | Gray-white sandstone | 234~1252 | ~242 ~401 | 94 | 0.10~2.43 |
| Late Miocene | Shangyoushashan Fm. ($N_2^2sy$) | EE1 | Greyish green sandstone | 232~2114 | ~253 ~424 | 87 | 0.03, 0.04, 0.05, 0.07, 0.11~1.52 |
| Early Miocene | Xiayoushashan Fm. ($N_2^1xy$) | EBLN | Gray-white sandstone | 231~1746 | ~258 ~444 | 100 | 0.01, 0.08, 0.14~1.46 |
| Oligocene | Shangganchaigou Fm. ($N_1sg$) | E22 | Gray-white sandstone | 212~2608 | ~246 ~414 | 84 | 0.13~3.28 |
| Eocene | Xiaganchaigou Fm. ($E_3^1xg$) | EBLE | Greyish green sandstone | 57~2513 | ~255 ~461 | 95 | 0.02, 0.06, 0.08, 0.09, 0.15~4.04 |
| Paleocene | Lulehe Fm. ($E_{1+2}l$) | E123 | Gray-white sandstone | 221~1429 | ~246 ~426 ~911 | 93 | 0.09, 0.10~1.66 |
| Jurassic | Dameigou Fm. ($J_{1+2}d$) | E122 | Gray-white sandstone | 241~1871 | ~253 ~422 | 87 | 0.09, 0.12~2.51 |
| *Huatugou section* | | | | | | | |
| Pleistocene | Qigequan Fm. ($Q_1q$) | CSL5* | Gray-white fine-grained sandstones, well- sorted. | 211~2430 | ~260 ~420 ~860 | 98 | 0.04, 0.07, 0.09, 0.15~ 1.48 |
| Pliocene | Shizigou Fm. ($N_2^3s$) | SZG1* | Gray-yellow fine-grained sandstones, well- sorted. | 211~2430 | ~240 ~430 ~890 | 93 | 0.03, 0.09, 0.14~2.15 |
| Middle Miocene | Shangyoushashan Fm. ($N_2^2sy$) | CSL4* | Brown fine-grained sandstones, well-sorted. | 202~2378 | ~220 ~430 ~880 | 95 | 0.03, 0.06, 0.08, 0.09, 0.11~2.00 |
| Early Miocene | Xiayoushashan Fm. ($N_2^1xy$) | HTG-N* | Gray-white fine-grained sandstones, well- sorted. | 235~2378 | ~260 ~400 | 95 | 0.12~1.56 |
| Oligocene | Shangganchaigou Fm. ($N_1sg$) | QX1-1 | Gray-yellow pebbly sandstone | 193~3188 | ~268 ~422 ~926 | 93 | 0.001, 0.08, 0.14~1.53 |
| Late Eocene | Upper Xiaganchaigou Fm. ($E_3^2xg$) | QX1-2 | Gray-white pebbly sandstone | 215~2513 | ~285 ~461 ~920 | 98 | 0.08, 0.12~ 4.95 |
| Middle Eocene | Lower Xiaganchaigou Fm. ($E_3^1xg$) | HTG-E* | Gray-white medium - grained sandstones, well- sorted. | 181~2662 | ~260 ~430 | 98 | 0.22~1.59 |
| Paleocene to Early Eocene | Lulehe Fm. ($E_{1+2}l$) | S23 | Gray-white sandstone | 188~1804 | ~247 ~412 | 59 | 0.14~1.84 |

| | | | | | | | |
|---|---|---|---|---|---|---|---|
| Early-Middle Jurassic | Dameigou Fm. ($J_{1+2}$d) | CSL3[#] | Gray-yellow sandstones | 220~248<br>0 | ~264<br>~433 | 97 | 0.25~3.82 |

Note: [*] Samples cited from Cheng et al. (in press); [#] Sample cited from Cheng et al. (2015a).

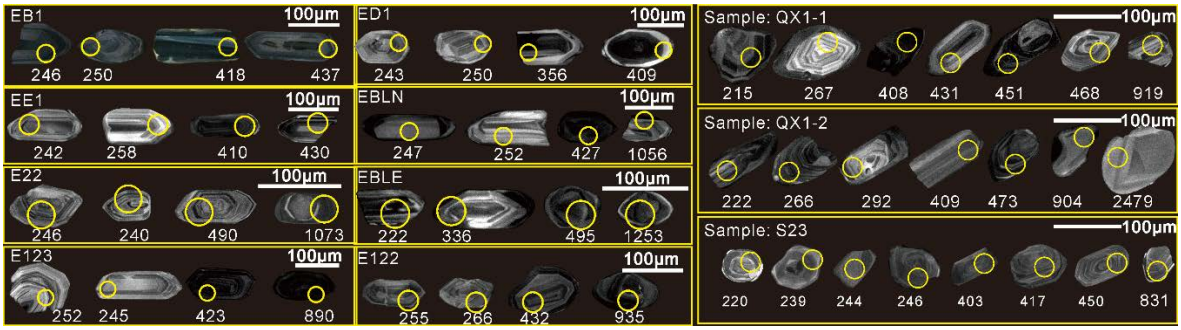


Fig. 5 Representative CL images of zircons from the 11 sandstone samples. The yellow circles show the location of the U-Pb analysis. Numbers are U-Pb ages in Ma.

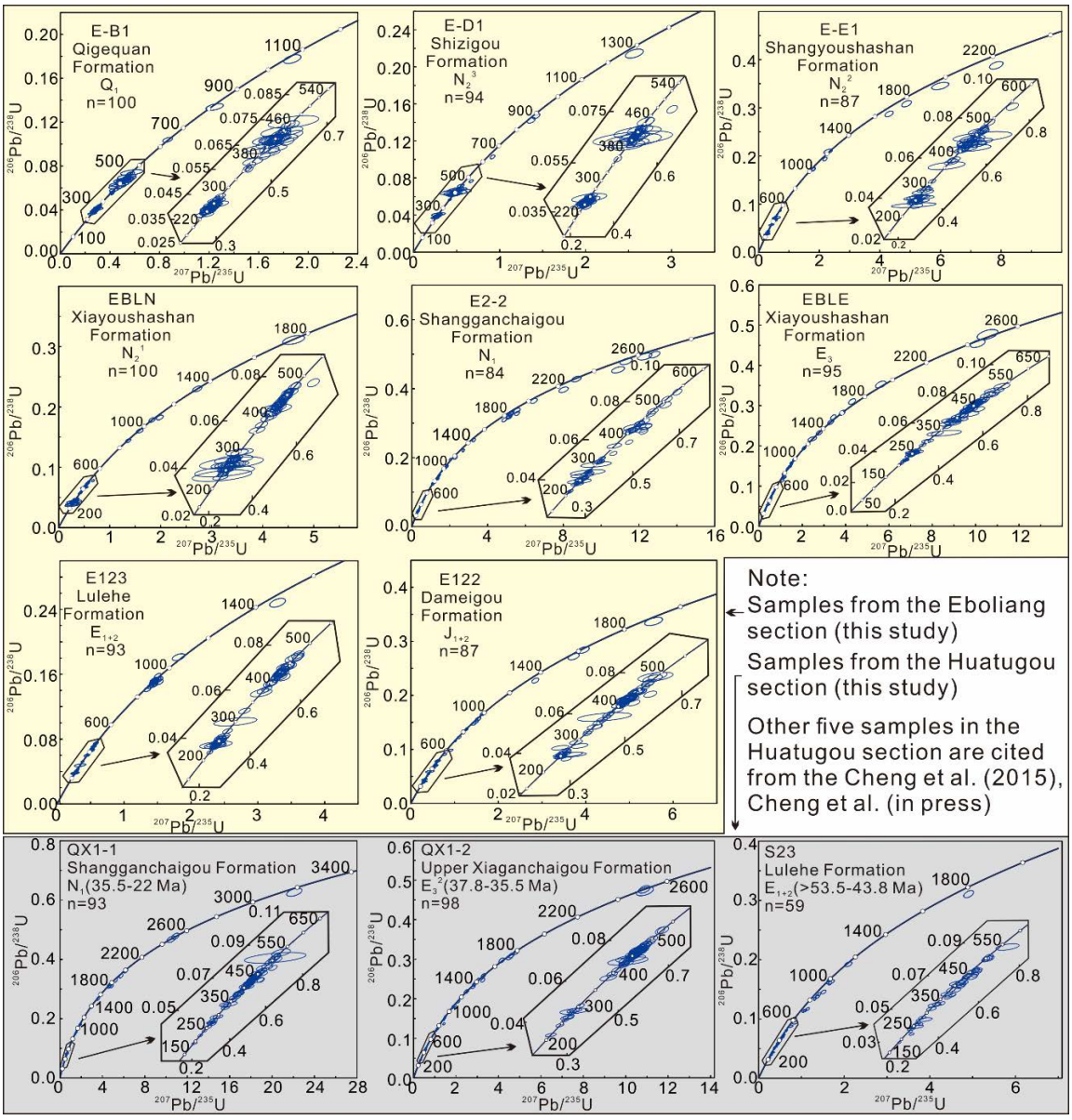


Fig. 6 U-Pb concordia diagrams for zircon grains of the 11 sandstone samples.

#### 3.2.5.1 Eboliang section

Sample E122 (Dameigou Fm., early to middle Jurassic)

In sample E122, zircon grain morphologies range from subhedral to subrounded with an average size of 80 - 200 μm. The grains are generally colorless and exhibit obvious oscillatory zoning, with a few ones showing inherited cores and rims. Except for one grain with a Th/U ratio of 0.09, all the crystals show high Th/U ratios from 0.12 to 2.51, indicative of a magmatic origin (Corfu et al., 2003; Hanchar and Rudnick, 1995; Hoskin and Black, 2000). 87 out of 105 dated grains yielded a 206Pb/238U age ranging between 1871 to 241 Ma with two major peaks at ~422 Ma and ~253 Ma (Fig. 7A).

Sample E123 (Lulehe Fm., 53.5-43.8 Ma)

In sample E123, zircon crystals display subhedral to abraded shapes and an average size ranging between 50 μm and 350 μm. The majority of crystals (~90% of the total) display distinct oscillatory zoning in CL images indicating a magmatic origin, confirmed by Th/U ratios varying between 0.1 and 1.66 with only one grain having a slightly lower value of 0.09. Among 100 crystals analyzed, 93 concordant analyses yielded ages ranging from 1429 Ma to 221 Ma (Fig. 7B). The zircon age population is distributed in four groups with two major peaks at ~426 Ma and ~246 Ma, and one more restricted peak at ~911 Ma. Finally, two outlying ages of 1429 Ma and 1073 Ma were also obtained.

Sample EBLE (Lower Xiaganchaigou Fm., 43.8-37.8 Ma)

In sample EBLE, zircon grain morphologies range from subhedral to subrounded with an average size of 50 - 150 μm. CL images show that most zircon crystals (over 90% of the total) are characterized by relatively distinct oscillatory zoning suggesting a magmatic origin. Except for four grains with Th/U ratio of 0.02, 0.06, 0.08 and 0.09, all zircons show high Th/U ratios from 0.15 to 4.04, confirming the magmatic origin (Tab. 1). Among 100 crystals analyzed, 95 analyses are concordant and yielded ages mainly ranging from 2513 Ma to 207 Ma, with two peak ages at 461 Ma and 255 Ma (Fig. 7C). The age of the remaining zircons are evenly distributed from 2469 Ma to 690 Ma. One outlying grain yielded a much younger age of 57 Ma.

Sample E22 (Upper Xiaganchaigou Fm., 37.8-35.5 Ma)

Zircons from sample E22 are predominantly colorless, euhedral to abraded, with a length of 50 - 150 μm. Over 90% of the crystals show oscillatory zoning and some of them show inherited cores or overgrowths (Fig. 5). All analyses show high Th/U ratios ranging from 0.13 to 3.28 indicating a magmatic origin. 53 out of 105 dated grains yielded a 206Pb/238U age of

530 Ma to 212 Ma with two age peaks at 414 Ma and 246 Ma (Fig. 7D). The age of the remaining zircons are evenly distributed from 2608 Ma to 742 Ma.

Sample EBLN (Xiayoushashan Fm., 22.0-15.3 Ma)

In sample EBLN, zircon grains show euhedral to subhedral shapes with an average size ranging between 100 μm and 300 μm. Over 80% of crystals show distinct oscillatory zoning suggesting a magmatic origin, with a few showing inherited cores and rims. Except for two grains with Th/U ratio of 0.01 and 0.08, all the zircons show high Th/U ratios ranging from 0.14 to 1.46, indicative of their magmatic origin. The 100 crystals analyzed have a discordance degree of <10% and provided U-Pb ages ranging from 2114 Ma to 231 Ma (Fig. 7E). The ages can be separated in two main populations with two peak ages at 424 Ma and 253 Ma. In addition, 4 isolated grains have Proterozoic ages.

Sample EE1 (Shangyoushashan Fm., 15.3-8.1 Ma)

Zircons from sample EE1 are predominantly colorless, euhedral to abraded, with a length of 50 μm to 200 μm. CL images show that 90% of these grains are characterized by relatively distinct oscillatory zoning and some of them exhibit inherited cores or overgrowths. Except for four grains with Th/U ratio of 0.03, 0.04, 0.05 and 0.07, all zircons show high Th/U ratios ranging from 0.15 to 4.04, typical of a magmatic origin. All 105 U-Pb analyses are concordant and yielded ages mainly ranging from 2114 Ma to 232 Ma. The large majority of those ages can be divided in two groups with peak ages at 424 Ma (47 % of total) and 253 Ma (39 % of total), respectively (Fig. 7F). Eight zircons yielded single Proterozoic ages of 2114, 1912, 1732, 1627, 1226, 1140, 1026 and 1023 Ma.

Sample ED1 (Shizigou Fm., 8.1-2.5Ma)

In sample ED1, the majority of zircon grains (90 % of the total) are subhedral to subrounded, ranging from 100 to 250 μm in length. Most zircon crystals (~80 % of the total) exhibit oscillatory growth zoning, with some (~20 % of the total) showing inherited cores and rims. All zircons give high Th/U ratios from 0.10 to 2.43, indicating their magmatic origin. Among a total of 105 analyses, 94 concordant analyses yielded ages ranging from 1252 Ma to 234 Ma, falling into two main age population with peaks at 401 Ma (50 % of total) and 242 Ma (45 % of total) respectively (Fig. 7G). Five zircons yielded outlying ages of 1461, 1252, 883, 857 and 631 Ma.

Sample EB1 (Qigequan Fm., 2.5-0.01 Ma)

Zircons from sample EB1 are 80 - 250 μm long and mainly subhedral to subrounded. Over 90% of the zircons show oscillatory zoning and some of them show inherited cores or overgrowths. Except for two grains with Th/U ratio of 0.08 and 0.09, all the zircons have high

Th/U ratios ranging from 0.14 to 2.19, indicating their magmatic origin. All the 100 analyses have age discordance degree of <10%, and span from 1053 Ma to 232 Ma (Fig. 7H). The data group into two age populations with peaks at 417 Ma (48 % of total) and 253 Ma (46 % of total) respectively. Three zircons yielded ages of 1053, 809 and 637 Ma.

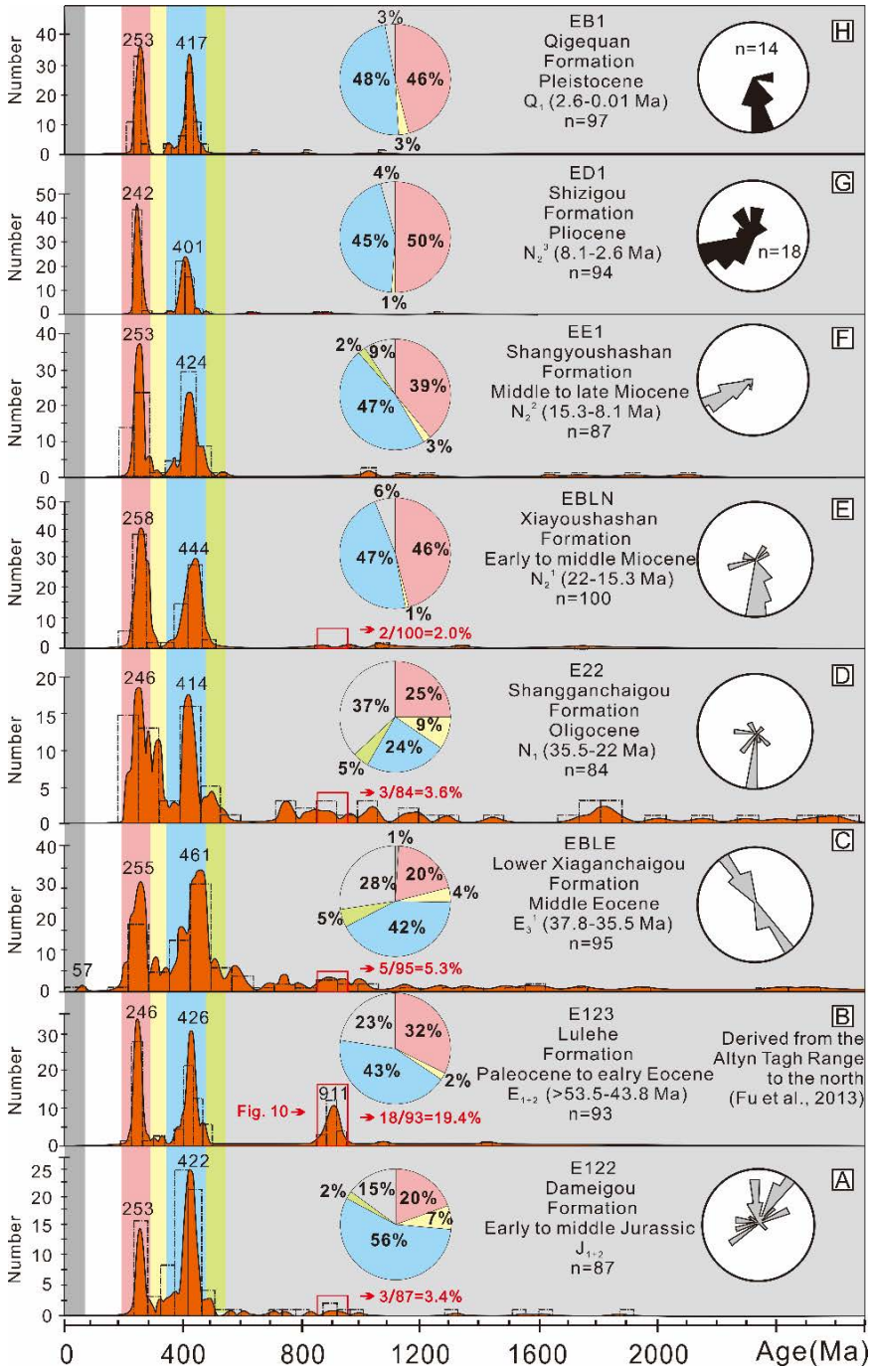


Fig. 7 Combined probability density functions (lines) and histogram plots (bars) depicting detrital zircon U-Pb ages of samples from the Eboliang section, arranged in stratigraphic order. Age distributions are colored according to age groups, and the pie diagrams show percentages of grains in those age categories. Paleocurrents rose diagrams in black are compiled from Heermance et al. (2013) and rose diagrams in gray are compiled from Wu et al. (2012b) and Ritts and Biffi (2000).

Overall, the U-Pb ages of detrital zircons from the 9 Jurassic to Pleistocene samples range from 2608 Ma to 57 Ma. Based on their morphological characteristics, internal textures and Th/U ratio, magmatic zircons appear to dominate (about 90 %) the section while the remaining ones are metamorphic zircons (about 10 %).

#### 3.2.5.2 Huatugou section

Sample CSL3 (Dameigou Fm., early to middle Jurassic)

Zircons from sample CSL3 are predominantly euhedral to abraded, with a length of 50-250 μm. CL images show that most zircon crystals (90% of the total) are characterized by relatively distinct oscillatory zoning. Th/U ratios vary between 0.25 and 3.82. Among 100 zircons analyzed, 97 concordant analyses yielded ages ranging from 2480 to 220 Ma (Fig. 8A; Cheng et al., 2015a). The ages can be separated in three main groups with two peak ages at 433 Ma and 264 Ma, and some isolated ages between 2480 to 852 Ma (Fig. 8A).

Sample S23 (Lulehe Fm., 53.5-43.8 Ma)

In sample S23, zircon crystals display subhedral to abraded shapes for an average size ranging between 50 μm and 100 μm. The majority of crystals (90% of the total) display distinct oscillatory zoning in CL images indicating a magmatic origin, confirmed by Th/U ratios varying between 0.14 and 1.84. 59 usable data points were obtained among 102 analyzed zircon grains. U-Pb ages range from ~1804 Ma to ~188 Ma, with two peaks at ~412 Ma and ~247 Ma. Finally, a few isolated ages range from 1200 Ma to 600 Ma (Fig. 8B).

Sample HTG-E (Lower Xiaganchaigou Fm., 43.8-37.8 Ma)

In sample HTG-E, zircon grains show well-preserved euhedral shapes with an average size ranging between 50 μm and 150 μm. Over 90% of the crystals are characterized by relatively distinct oscillatory zoning indicating a magmatic origin confirmed by Th/U ratios varying from 0.22 to 1.59. Among 100 zircons analyzed, 98 concordant analyses yielded ages ranging from ~2662 Ma to ~181 Ma, with two peaks at ~430 Ma and ~260 Ma. A number of ages are spread between 2662 Ma and 500 Ma with 18% of the data clustering between 1500 Ma and 500 Ma (Fig. 8C; Cheng et al., 2016).

Sample QX1-2 (Upper Xiaganchaigou Fm., 37.8-35.5 Ma)

In sample QX1-2, zircon grain morphologies range from euhedral to subhedral with an average size of 100 ~ 200 μm. CL images show that most of these zircon crystals (~90% of the total) display relatively distinct oscillatory zoning suggesting a magmatic origin. Except for one grain with Th/U ratio of 0.08, all zircons show high Th/U ratios from 0.12 to 4.95, confirming the magmatic origin. Among a total of 105 analyses, 98 concordant analyses

yielded ages ranging from 2513 Ma to 215 Ma with two peak ages at 461 Ma and 285 Ma, and a potential sub-peak at 920 Ma (Fig. 8D).

Sample QX1-1(Shangganchaigou Fm., 35.5-22 Ma)

Zircons from sample QX1-1 are predominantly colorless, euhedral to abraded, with a length of 50-200 μm. Over 90 percent of the crystals show oscillatory zoning. Except for two grains with Th/U ratio of 0.001 and 0.08, all zircons show high Th/U ratios ranging from 0.14 to 1.53 indicating a magmatic origin. Among 100 crystals analyzed, 93 concordant analyses yielded ages ranging from 3188 Ma to 193 Ma, with a major age peak at ~422 Ma, a minor age peak at ~268 Ma, and a potential sub-peak at ~926 Ma (Fig. 8E).

Sample HTG-N (Xiayoushashan Fm., 22-15.3 Ma)

In sample HTG-N, zircon grain morphologies range from euhedral to abraded with an average size ranging between 80 μm and 200 μm. A large majority of zircon crystals (about 90%) display distinct oscillatory zoning on CL images indicating a magmatic source, which is also confirmed by Th/U ratios varying from 0.12 to 1.56. Among a total of 100 analyses, 95 concordant analyses yielded ages ranging from 2378 Ma to 235 Ma with two peak ages at 400 Ma and 260 Ma, and a number of ages clustering between 1200 Ma and 700 Ma (Fig. 8F; Cheng et al., 2016).

Sample CSL4 (Shangyoushashan Fm., 15.3-8.1 Ma)

Zircons from sample CSL4 are predominantly euhedral to abraded, with a length of 50 - 250 μm. More than 90% of the crystals display distinct oscillatory zoning on CL images implying a magmatic origin as attested by Th/U ratios varying from 0.11 to 2.00. Among 100 crystals analyzed, 95 concordant analyses yielded U-Pb ages ranging from ~2378 Ma to ~235 Ma, with three peaks at ~880 Ma, ~430 Ma and ~220 Ma. Finally, some ages are again spread from 1020 Ma to 800 Ma (Fig. 8G; Cheng et al., 2016).

Sample SZG1 (Shizigou Fm., 8.1-2.5Ma)

In sample SZG1, zircon grain morphologies range from euhedral to abraded with an average size of 80 - 200 μm. Most crystals (more than 90%) display a distinct oscillatory zoning on CL images indicating a magmatic origin. The Th/U ratios vary from 0.14 to 2.15, with two exceptions of 0.03 and 0.09, confirming a generally magmatic origin. 93 usable data points were obtained among 100 analyzed zircon grains. U-Pb ages range from ~2421 Ma to ~222 Ma, with three peaks at ~890 Ma, ~430 Ma and ~240 Ma (Fig. 8H; Cheng et al., 2016).

Sample CSL5 (Qigequan Fm., 2.5-0.01 Ma)

Zircons from sample CSL5 are predominantly well-preserved euhedral, with a length of 50-200 μm. Only a few grains (about 5%) show faint zoning in CL suggesting a metamorphic

origin. Most crystals display distinct oscillatory zoning characteristic of their magmatic origin. This is confirmed by Th/U ratios varying from 0.15 to 1.48, with three exceptions of 0.04, 0.07 and 0.09. Among 100 analyzed zircons, 98 U-Pb ages with discordance degree <10% obtained, ranging from ~2430 Ma to ~211 Ma, with two major peaks at ~420 Ma and ~260 Ma and a minor peak at ~860 Ma (Fig. 8I; Cheng et al., 2016).

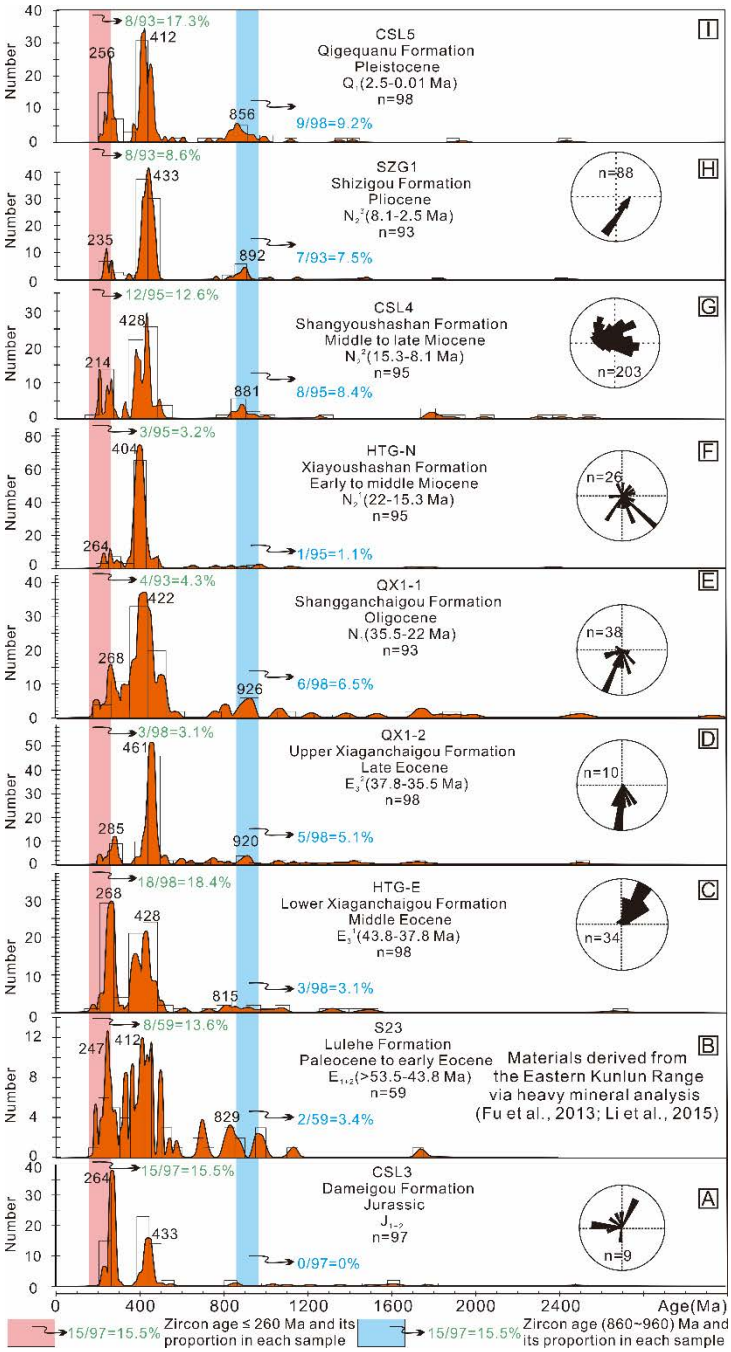


Fig. 8 Combined probability density functions (lines) and histogram plots (bars) depicting detrital zircon U-Pb ages of samples from the Huatugou section, arranged in stratigraphic order. Two distinctive age groups, indicative of separate sources, are colored. Paleocurrents rose diagrams are compiled from Meng and Fang, (2008), Wu et al. (2012b) and Zhuang, et al. (2011).

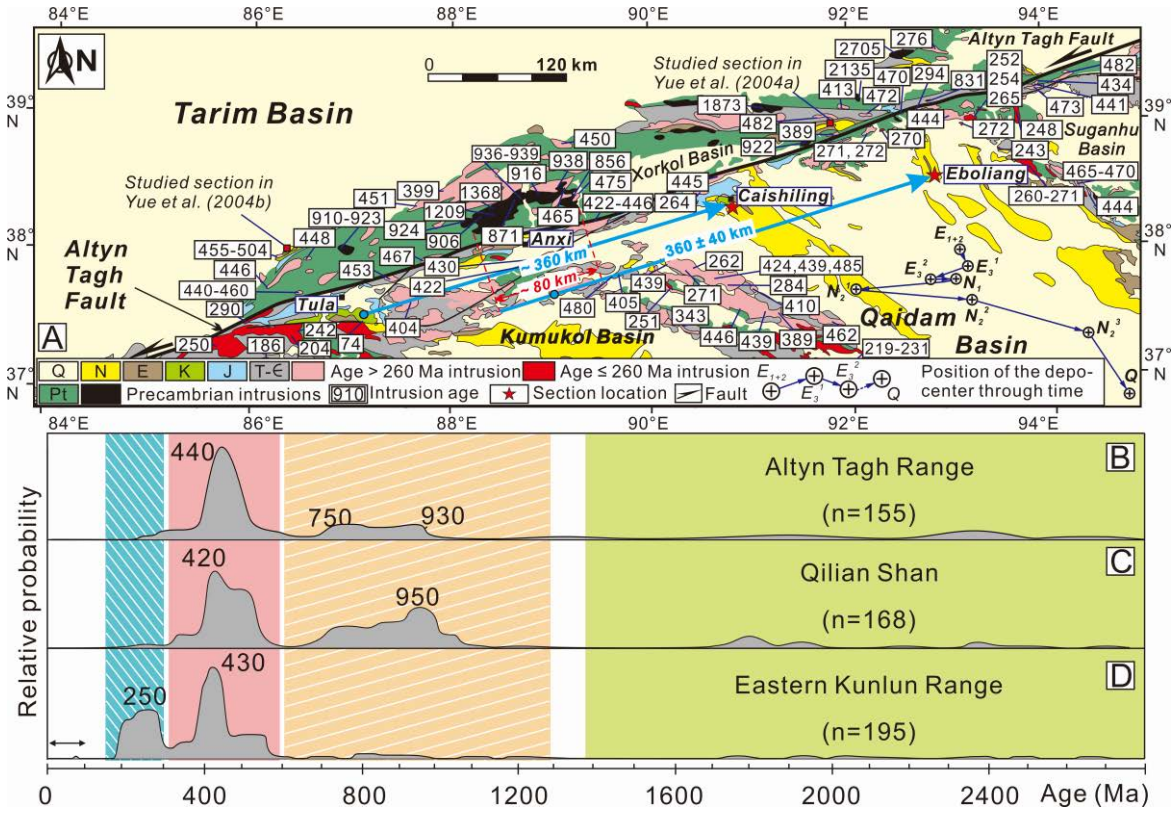


Fig. 9 (A) Sketched geological map of the Altyn Tagh Range and surrounding areas, showing the distribution of zircon U–Pb ages for granitoids. The numbers denote ages in Ma. Relative probability plots of zircon U-Pb ages from basement rocks and intrusives in: (B) the Altyn Tagh Range, (C) the Qilian Shan, and (D) the Eastern Kunlun Range. Age data are mainly cited from: Guo and Li, (1999), Sobel and Arnaud, (1999), Yang et al. (2001), Zhang et al. (2001), Yang and Song, (2002), Cowgill et al. (2003), Gehrels et al. (2003a, 2003b), Jolivet et al. (2003), Lu and Yuan, (2003), Robinson et al. 2003, Roger et al. (2003), Chen et al. (2004), IGSQP, (2004), Yue et al. (2004, 2005), Liu et al. (2006), Shi et al. (2006), Song et al. (2006), Wang et al. (2006b), Yang et al. (2006), Lu et al. (2008), Roger et al. (2008), Bovet et al. (2009), Liu et al. (2009), Wu et al. (2009), Xiao et al. (2009), Roger et al. (2010), Zhang et al. (2011), Dai et al. (2013), Li et al. (2013), Wang et al. (2013), Long et al. (2014), Song et al (2014), Wang et al.(2014b) , Zhang et al. (2014a), Dong et al. (2014, 2015), Chen et al. (2015) and references therein. The blue arrow refers to the northeastward migration of the Huatugou and Eboliang sections from their origins.

## 3.2.6 Discussion

### 3.2.6.1 Geochronological characteristics of potential sources for the sedimentary rocks in the western Qaidam basin

Highlands surrounding the basin is the priori potential source for the deposited clastic material (e.g. Bruguier et al., 1997; Allen and Allen, 2005). The Altyn Tagh Range, the Qilian Shan, as well as the Eastern Kunlun Range are all potential source regions likely to provide zircons to the Qaidam basin (e.g. Métivier et al., 1998; Xia et al., 2001; Meng and Fang, 2008;

Yin et al., 2007, 2008a, 2008b). In order to better constrain the provenance area of the samples collected in the western Qaidam basin (Fig. 9A), we compiled the zircon U-Pb ages available on basement rocks of the Altyn Tagh Range (Fig. 9B), the Qilian Shan (Fig. 9C) and the Eastern Kunlun Range (Fig. 8D).

In the Altyn Tagh Range, the basement mainly consists of Archean and Proterozoic rocks with Archean zircon U-Pb ages ranging from ~3.6 Ga to ~2.6 Ga (Lu and Yuan, 2003; Lu et al., 2008; Long et al., 2014; Zhang et al., 2014b and references therein), and Proterozoic zircon U-Pb ages ranging from ~2.4 Ga to ~650 Ma (Gehrels et al., 2003a, 2003b; Wang et al., 2006b; Lu et al., 2008 and references therein; Zhang et al., 2011; Wang et al., 2013). A few scattered Neoproterozoic intrusions are exposed, with a large, distinctive early Neoproterozoic intrusion (ca. 850 Ma to ca. 1000 Ma in age) exposed west of the Xorkol basin (Fig. 9A). Wang et al. (2013) recently reported a mean crystallization age of ~910 Ma for the basement rocks near the Anxi area, in the western part of the Altyn Tagh Range (Fig. 9A). Paleozoic intrusions with ages spanning from ~550 Ma to ~400 Ma are widely distributed (Jolivet et al., 1999; Sobel and Arnaud, 1999; Zhang et al., 2001; Cowgill et al., 2003; Gehrels et al., 2003a; Chen et al., 2004; Yue et al., 2004a, 2005; Yang et al., 2006; Wang et al., 2014b and references therein). Finally a few Permian igneous rocks are sporadically distributed along the central part of the Altyn Tagh Range, with zircon U-Pb ages ranging between ~300 Ma and ~260 Ma (Fig. 9A; Cowgill et al., 2003; Gehrels et al., 2003a; Gehrels et al., 2003b; Wu et al., 2014).

Zircon age from the North Qaidam and South Qilian Shan terranes mainly group between 2700 to 1100 Ma, 550 to 400 Ma, and 300 to 200 Ma (Fig. 9B; Yang and Song, 2002; Cowgill et al., 2003; Gehrels et al., 2003a, 2003b; Yue et al., 2005; Shi et al., 2006; Song et al., 2014 and references therein). The North Qilian Shan basement mainly consists of early Paleozoic marine strata associated with a series of Ordovician volcanics and Silurian granitic plutons (Bovet et al., 2009; Xiao et al., 2009; Song et al., 2014 and references therein). These granitoid intrusions yielded U-Pb zircon ages ranging from ca. 550 to ca. 440 Ma (Wu et al., 2001; Gehrels et al., 2003a, 2003b; Yue et al., 2005; Song et al., 2014 and references therein). Finally, the central Qilian Shan basement is composed of Mesoproterozoic to Neoproterozoic marine sequences intruded by early Paleozoic plutons, with detrital and plutonic zircon ages comprised between 2333 to 874 Ma and 442 to 424 Ma respectively (Guo and Li, 1999; Lu, 2002; Yue et al., 2005; Bovet et al., 2009; Song et al., 2014 and references therein). The Qilian Shan basement was affected by a Devonian phase of metamorphism (400-360 Ma), with a metamorphic peak at 440-423 Ma within the north Qaidam ultrahigh pressure belt (Yang et al., 2001, Yang and Song, 2002; Song et al., 2006; Yang et al., 2006; Song et al., 2014 and

references therein). Finally, sporadically distributed late Permian to early Triassic granitoids are exposed along the western edge of the South Qilian Shan terrane, yielding zircon U-Pb ages ranging from ca. 270 Ma to ca. 230 Ma (Fig. 9A and 9C; Yang and Song, 2002; Wu et al., 2009; Dong et al., 2014, 2015).

Within the Eastern Kunlun Range, Proterozoic ages are rare (Fig. 9A and 9D). Several early Paleozoic intrusions with U-Pb zircon ages ranging from ca. 500 Ma to 400 Ma have been reported by previous studies (Fig. 9C; Cowgill et al., 2003; IGSQP, 2004; Dai et al., 2013; Li et al. 2013). Late Paleozoic - early Mesozoic granitoids (ca. 300 Ma to ca. 200 Ma), corresponding to the magmatism associated to the Permo-Triassic closure of the Paleo-Tethys Ocean and to the post-collision magmatism that followed the docking of the Qiangtang Block, are extensively distributed (Fig. 9A; e.g. Roger et al., 2003, 2008, 2010; Liu et al., 2006; Li et al., 2013; Jolivet et al., 2015; Chen et al., 2015). Finally, a few Cretaceous ages have been obtained from the Tula Uplift in the western reach of the Eastern Kunlun Range (Figs. 2A and 9A; Robinson et al., 2003; Cheng et al., 2015a) and some Miocene to Quaternary volcanism was occurring in the southwestern part of the range (Jolivet et al., 2003).

#### 3.2.6.2 Provenance analyses of the Mesozoic-Cenozoic strata in the western Qaidam basin

##### 3.2.6.2.1 Eboliang section

On a first order analysis, the detrital zircon U-Pb age spectrum obtained from the eight samples collected on the Eboliang section are largely similar (Fig. 7), suggesting that the provenance area was largely homogeneous through time. However, second-order variations in age cluster proportions among those samples record source changes during basin filling. In general, the detrital zircons U-Pb ages can be statistically subdivided into three major groups of Precambrian (spanning from ca. 2.8 Ga to 550 Ma), early to middle Paleozoic (peaks at 460~400 Ma) and late Paleozoic to Mesozoic (peaks at ca. 260~240 Ma) (Fig. 7). Aside from these major groups, the restricted early Neoproterozoic age group spanning from ca. 850 to ca. 1100 Ma with a peak age around 911 Ma (for example in sample E123, Lulehe Formation) represents the contribution from a distinctive source in the Altyn Tagh Range that will be discussed in details below.

Based on isopachs distribution, the Jurassic depocenter was situated farther south of the Eboliang section, which rules out any contribution from the Eastern Kunlun Range in the Jurassic sediments from that section (Fig. 9A; also see Fig. 3b in Meng et al., 2001). We thus consider that the paleocurrents in the northwestern Qaidam basin (Ritts and Biffi, 2000)

probably provided sediments from mixed sources both in the Qilian Shan and Altyn Tagh Range. Based on $^{40}Ar/^{39}Ar$ thermochronology as well as zircon and apatite fission track analysis, previous researches have reported Jurassic exhumation in the Altyn Tagh Range (Delville et al., 2001; Jolivet et al., 2001; Sobel et al., 2001; Wang et al., 2005). The detrital zircon age distribution of the Jurassic sediments in the Eboliang section (sample E122, Fig. 7D), is very similar to those of the Cenozoic samples, including early to middle Paleozoic zircons (peaks at 422 Ma; 56 % of total), late Paleozoic to Mesozoic zircons (peaks at ca. 253 Ma; 20 % of total) and a few Precambrian zircon (15 % of total). This similarity suggests that the source of the material deposited in the Eboliang region has been largely stable since the early Jurassic including both Permian granitoids and Ordovician to Devonian basement from either or both the Altyn Tagh Range and the Qilian Shan (Figs. 7A and 9).

The Paleogene depocenters of the Qaidam basin were consistently located south of the Eboliang section (see Fig. 12A in Yin et al., 2008b), again excluding material contribution from the Eastern Kunlun Range (Fig. 9A; Meng and Fang, 2008; Yin et al., 2008b; Mao et al., 2014). Paleocurrent directions obtained from conglomerate fabrics (clast imbrications) as well as heavy mineral assemblages suggest that the Paleogene clastic materials deposited in the northwestern Qaidam basin mainly derived from the Qilian Shan to the northeast and the Altyn Tagh Range to the north (Fig. 7; Wu et al., 2011; Fu et al., 2013; Jian et al., 2013). The age spectrum obtained from the three Paleogene samples (E123, EBLE, and E22) are characterized by early to middle Paleozoic zircons (peaks at ca. 414 to ca. 461 Ma; 20 % ~ 43 % of total), late Paleozoic to early Mesozoic zircons (peaks at ca. 246 Ma to ca. 255 Ma; 20 % ~ 23 % of total), and a progressively increasing proportion of Precambrian zircons (from 23 % to 37 %).

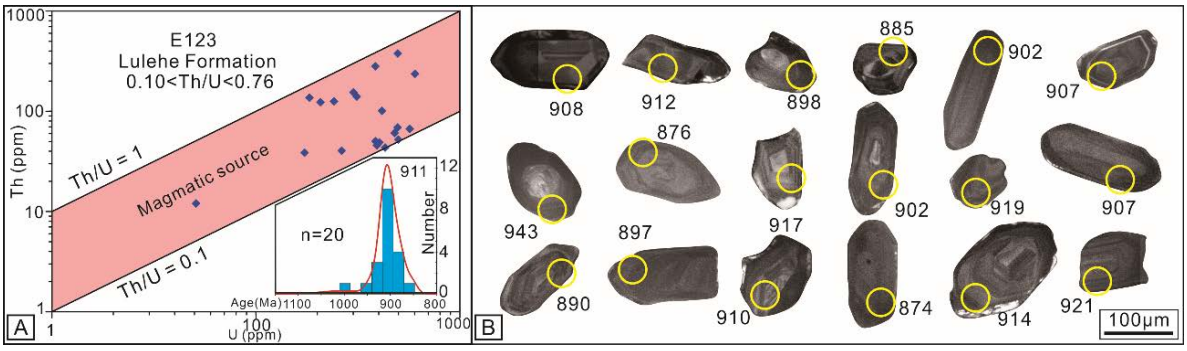


Fig. 10 (A) Frequency histograms for restricted early Neoproterzoic ages groups of detrital zircons from the Paleocene to early Eocene Lulehe Fm. ($E_{1+2}$) and the Th/U ratio for those zircon ages. (B) CL images of zircons for all early Neoproterzoic ages zircons from the Paleocene to early Eocene Lulehe Fm. The yellow circles show the location of the U-Pb analysis. Numbers are U-Pb ages in Ma. Note that the ~911 Ma peak age for the Neoproterozoic ages groups coincides with the mean crystallization age of ~910 Ma for the basement rocks in the western segment of the Altyn Tagh Range (Fig. 9A;

Wang et al., 2013). The distinctive Th/U ratio and oscillatory zones for those zircons indicate magmatic sources.

The age spectrum of sample E123 displays a distinctive early Neoproterozoic age group (Fig. 7B; 1100 Ma to 850 Ma; peak at 911 Ma). The oscillatory zoning in CL images and the relatively high Th/U ratios (over 0.1, average value 0.3) of those early Neoproterozoic zircons in sample E123 indicate a clear magmatic origin (Fig. 10; Hanchar and Rudnick, 1995; Hoskin and Black, 2000; Corfu et al., 2003). As shown in Figure 9A, the early Neoproterozoic sources are few and small in the Altyn Tagh Range and Qilian Shan, but for a large magmatic complex north of the Anxi area. Wang et al. (2013) recently reported a mean zircon U-Pb crystallization age of ~910 Ma for these intrusives, consistent with the 911 Ma peak age in the Paleocene to early Eocene sample E123 (Fig. 9A). The enriched early Neoproterozoic zircon age groups (ca. 1100 to ca. 850 Ma) in sample E123 that accounts for over 20% of the total analysis represents a major difference from the age spectrum of the Jurassic and post-Paleocene samples. We suggest that this group indicates that the extensive early Neoprotozoic intrusive north of Anxi area (Fig. 9A) formed a potential source area for the Paleocene to early Eocene strata in the Eboliang section. According to the isopach map of the Paleocene to early Eocene Lulehe Formation provided by Yin et al. (2008b), the main depocenter was located south of the Eboliang section and the strata in the Eboliang section generally thicken southwards and westwards (Fig. 8). In addition, a sub-depocenter developed in the western Qaidam basin close to the early Neoproterozoic basement rocks in the Altyn Tagh Range (see Fig. 12A in Yin et al., 2008b). If the Eboliang section had been continuously situated in roughly the same region as it occupies today (Fig. 2), the clastic materials derived from the early Neoproterozoic basement would thus not have been transported to the northwestern Qaidam basin. In addition, the few Neoproterozoic intrusions in the central and northern Qilian Shan region are not only far away from the Eboliang section, but also completely obstructed by the Paleocene uplift of the northern Qaidam thrust belt, clearly revealed by the seismic profiles in the southwestern flank of the Qilian Shan (Yin et al., 2008a). Based on these results combined with the generally southward paleoflows data reported from the northern Qaidam basin (e.g. Fu et al., 2013; Jian et al., 2013) and the largely accepted hundreds of kilometers of Cenozoic offset along the lithospheric ATF (e.g. Wittlinger et al., 1998; Wang et al., 2006a; Yu et al., 2014; Cheng et al., 2015a, 2015b), we conclude that the Eboliang section must have been located much closer to the present day position of Anxi (Figs. 1 and 2). The single Paleogene age observed in sample EBLE (Fig. 7C) is difficult to interpret since no Cenozoic magmatism has been reported in the Qaidam basin, Altyn Tagh Range or Qilian Shan. Our preferred interpretation is that the single

Paleocene zircon (57 Ma) was derived from the Cenozoic volcanic ash emitted from the volcanic centers along the northern edge of the Qiangtang Block (e.g. Jolivet et al., 2003; Ding et al., 2007; Staisch et al., 2015).

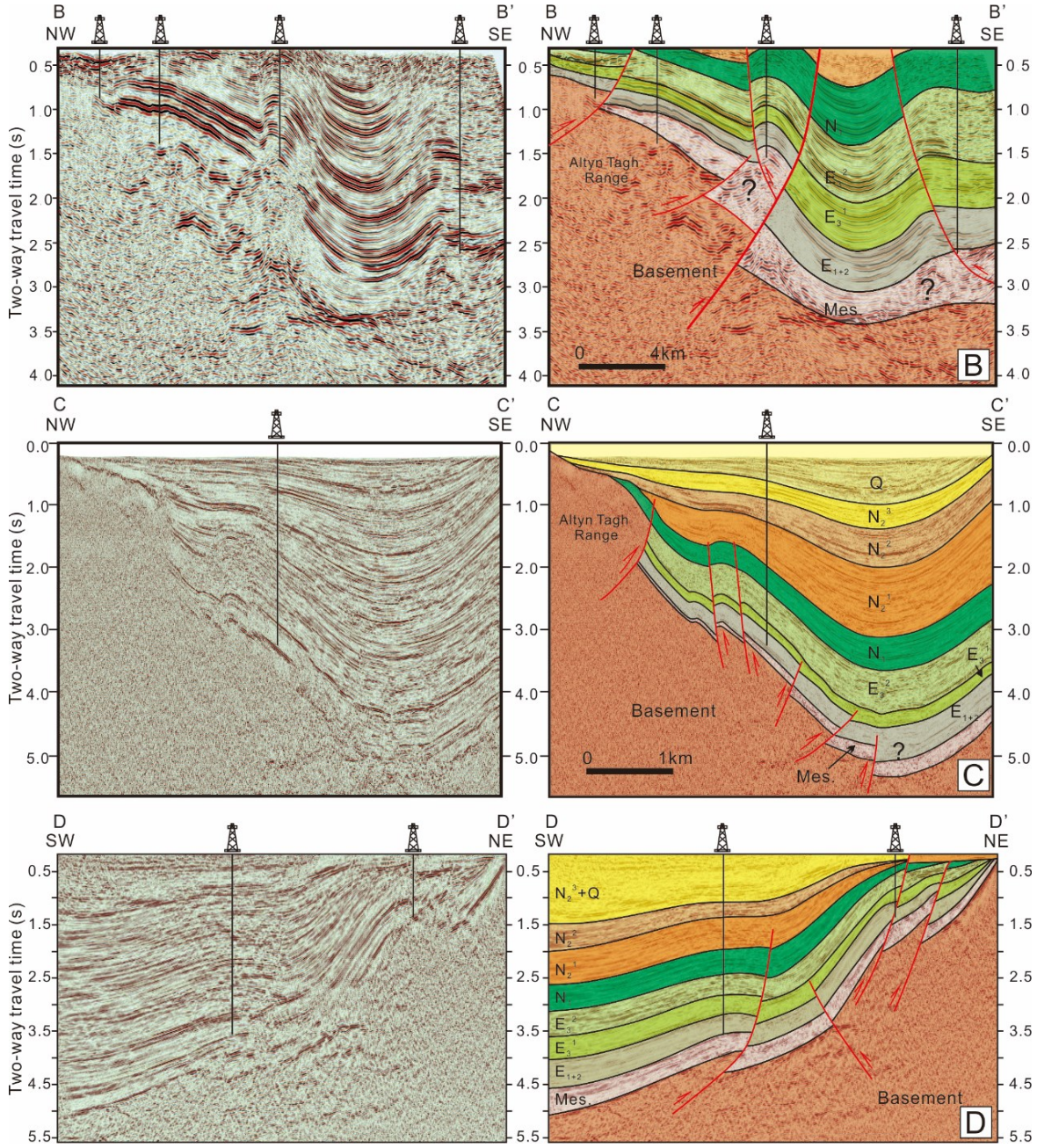


Fig. 11 Seismic profiles in the southwestern Qaidam basin. See Fig. 2A for location. Note the fold and thrusts in seismic profile BB', indicating the deformation in the northwestern Qaidam basin since the early Miocene. Offset of the Paleogene strata in seismic profiles CC' and DD' indicates the Eocene to Oligocene deformation in the northwestern Qaidam basin which would be associated with deformation along the ATF. Growth strata of the post-Oligocene strata in seismic profiles BB' and CC' indicate intense tectonic movements along the ATF since the Miocene.

The post-Oligocene depocenters are all located in the center of the Qaidam basin, south

of the Eboliang section (Fig. 8; Meng and Fang, 2008; Yin et al., 2008b; Mao et al., 2014). This again excludes the possibility that the Neogene Eboliang sediments issued from the Eastern Kunlun Range to the south. Consistently, the generally south-directed paleocurrents indicate that the sources of the post-Oligocene sediments in the Eboliang section were to the north, probably in the Altyn Tagh Range and the Qilian Shan (Wu et al., 2012b). However, the paleoflows changed from south-directed during the early Miocene, to generally southwest-directed during the Pliocene (Fig. 7). Unidirectional, south-directed paleocurrents are dominating during the Quaternary (Fig. 7). Although Miocene to Quaternary strata are still dominated by early to middle Paleozoic zircons (peaks at ca. 444 Ma to ca. 401 Ma; 45 % ~ 48 % of total) and late Paleozoic to Mesozoic zircons (peaks at ca. 258 Ma to ca. 242 Ma; 39 % ~ 50 % of total), Precambrian zircons become scarce (3% ~ 9 % of total), especially in Pliocene and Quaternary strata (Fig. 7F, 7G and 7H). As shown in the 3D seismic profile (Fig. 11), growth strata that developed during the deposition of the early Miocene series most probably indicate intense tectonic deformation along the adjacent ATF. Based on sediment facies studies and provenance analysis of the Oligocene to Miocene strata in the Xorkol basin, Ritts et al. (2004) concluded that the Oligocene to early Miocene sequence coarsens upwards from low-energy playa and alluvial mudflat deposits to proximal alluvial fan deposits, again supporting early Miocene deformation within the Altyn Tagh Range. A similar transition has been observed in the Oligocene to Miocene strata along the northern flank of the Altyn Tagh Range (Yue et al., 2004a). In addition, Miocene deformation within the Altyn Tagh Range has been clearly registered by thermochronology and paleomagnetism data (e.g. Jolivet et al., 1999; Chen et al., 2001; Jolivet et al., 2001; Wang et al., 2006; Liu et al., 2007; Lu et al., 2014). We thus propose that the disappearance of the Precambrian zircon in the post-Oligocene strata is linked to a major change in drainage pattern within the Altyn Tagh Range. The early Miocene deformation along the ATF led to the growth of a prominent topographic barrier, cutting off the link between the Precambrian source rocks in the Altyn Tagh Range and the Eboliang section area. Furthermore, the post-Oligocene samples (EBLN, EB1, ED1 and EE1) were collected in the south of the Eboliang fold structure that formed during or after the early Miocene (Figs. 2 and 11 A; e.g. Shang, 2001). Similarly to that produced in the Altyn Tagh Range, material sourced from the Qilian Shan was thus blocked east of the elevated growing structure and was not able to reach the deposition area to the south (Figs. 2, 9 and 11A). These results imply that the post-Oligocene clastic material deposited in the northwestern Qaidam basin was mainly derived from restricted local sources and/or recycling of the deformed pre-Oligocene strata.

3.2.6.2.2 Huatugou section

Along this section the detrital zircons U-Pb ages are again statistically subdivided into three major populations of Precambrian (spanning from ca. 3.2 Ga to 600 Ma), early to middle Paleozoic (peaks at 460~400 Ma) and late Paleozoic to Mesozoic (peaks at ca. 290~210 Ma) (Fig. 8). The Jurassic to Pleistocene basin depocenters were consistently situated farther southeast to Huatugou section, which rules out any material contribution from the Qilian Shan to the Huatugou section (Fig. 9A; Meng and Fang, 2008; Yin et al., 2008b; Mao et al., 2014).

Late Paleozoic - early Mesozoic granitic intrusions are widespread in the Altyn Tagh and Eastern Kunlun ranges, however, most of the early Mesozoic intrusions (younger than ca. 260 Ma) are confined to the Eastern Kunlun Range just south of our sample sites (Fig. 9A). This distinctive pluton distribution, together with the early Neoproterozoic zircons (1100~850 Ma) issued from the remarkably large intrusion in the Altyn Tagh Range (Fig. 9A; Wang et al., 2013; Cheng et al., 2015a) can be used as provenance signatures to identify the source of detrital zircons within our nine sandstone samples.

The poorly sorted, angular grains in the Jurassic samples suggest deposition from a proximal source terrain (see Figs. 5A and 5B in Cheng et al., 2015a). The zircon ages spectrum of the Jurassic sample (CSL3, Fig. 8A) is characterized by an exceptionally bimodal distribution (Permian-Triassic and Paleozoic groups). The zircons with ages younger than 260 Ma accounts for 15.5 % of the total number of analysis, suggesting that the Eastern Kunlun Range was a significant source of material for the Jurassic strata in the Huatugou section. This result is consistent with the general north- to west- directed paleoflows (Fig. 8A). The few Precambrian zircons (no early Neoproterozoic zircons) as well as the few south-directed paleocurrents might indicate limited contribution from the Altyn Tagh Range to the north, which suggests a limited topographic relief within that range, locally exposing basement rocks (Delville et al., 2001; Sobel et al., 2001; Ritts and Biffi, 2000).

In the Paleocene-early Eocene sample (S23) and the middle Eocene sample (HTG-E), the age spectrums from both samples are still largely bimodal, with about 15% of < 260 Ma zircons, suggesting that the Eastern Kunlun Range was still a significant material source for these samples. This assumption is consistent with the N-NE-directed paleoflows observed in the Paleocene to middle Eocene series (Fig. 8B and 8C; Meng and Fang, 2008; Fu et al., 2013; Li et al., 2015). On the other hand, the increasing proportion of Precambrian zircons (over 3% of early Neoproterozoic zircons in both samples) indicates that the Altyn Tagh Range was gradually becoming a significant source of clastic material for the Paleocene to middle Eocene

strata in the Huatugou section.

The late Eocene to Oligocene sample (QX1-2) displays a significant change in the detrital zircon age distribution pattern (Fig. 8C, 8D and 8E): the major Mesozoic age peak observed in the previous samples becomes nearly negligible with the proportion of < 260 Ma zircons decreasing dramatically (from 13.6% in sample S23 and 18.4% in sample HTG-E to 3.1% in sample QX1-2). In addition, the paleocurrent directions changed abruptly from generally north-directed in the Paleocene to middle Eocene strata to south-directed in the late Eocene strata (Fig. 8C and 8D). This implies major shift in the source region from the Eastern Kunlun Range to the Altyn Tagh Range during the middle to late Eocene time. The proportion of early Neoproterozoic zircons gradually increased (e.g. from 3.1% in sample HTG-E to 5.1% in sample QX1-2) further attesting that basement rocks in the Altyn Tagh Range served as a significant source for the sediments in the Huatugou section.

Recent sedimentology and paleomagnetic studies demonstrated that the relatively rigid Qaidam basin, together with the western segment of the Eastern Kunlun Range, have been transported northeastward along the ATF during the Cenozoic (Wang et al., 2006a; Yu et al., 2014; Cheng et al., 2015a, 2015b). This translation occurred without obvious basin-scale vertical axis rotation with respect to the Eurasia Plate since the early Eocene (Dupont-Nivet et al., 2002; Yu et al., 2014). We suggest that this sharp change in the detrital zircon age distribution pattern was directly related to the onset of large-scale left-lateral strike-slip displacement along the ATF. Except for the still slightly increasing proportion of Precambrian ages, the detrital zircon U-Pb age distributions registered in the Oligocene sample (QX1-1) is similar to those in the late Eocene sample (QX1-2), suggesting a relatively stable drainage pattern from the late Eocene to the Oligocene (Fig. 8D and 8E).

The age spectrum of the early Miocene sample (HTG-N) is again characterized by a major Paleozoic age peak and a minor Mesozoic age sub-peak (Fig. 8F). However, the amount of Precambrian zircons decreased significantly (early Neoproterozoic ages only represent 1.1% of the total analysis). A similar decrease in the proportion of Precambrian zircons was also registered in the early Miocene sample of the Eboliang section (sample EBLN in Fig. 7E), indicating of a regional change in source area and/or drainage pattern throughout the Altyn Tagh Range. As already mentioned in the provenance analysis of samples from the Eboliang section, we suggest that the regional early Miocene deformation within the Altyn Tagh Range cut off the link between the Precambrian source rocks in the Altyn Tagh and Qilian Shan ranges and the depositional area in the Huatugou and Eboliang sections. The early Miocene clastic material in these two sections was mainly derived from more restricted local source

regions and recycling of the deformed Paleocene to Oligocene strata.

Detrital zircon age distributions in the middle Miocene to Pleistocene samples (CSL4, SZG1 and CSL5) are similar, characterized by a major middle Paleozoic age peak, a minor but consistent Mesozoic age peak as well as few Precambrian zircons (Fig. 8G, 8H and 8I). Based on seismic profile interpretation, the fold structures developing perpendicular to the Altyn Tagh fault trend (e.g. the Yingxiongling structure, Fig. 2) initiated during or after the Oligocene (Yin et al., 2007; Yin et al., 2008a; Wu et al., 2014). After the Oligocene onset of deformation, the Huatugou section, located in the northernmost part of the prominent Yingxiongling uplift structure, was gradually isolated from the main Qaidam basin. A complex, local drainage pattern developed while recycling of the deformed Paleocene to Oligocene strata served as a major material source (Fig. 8).

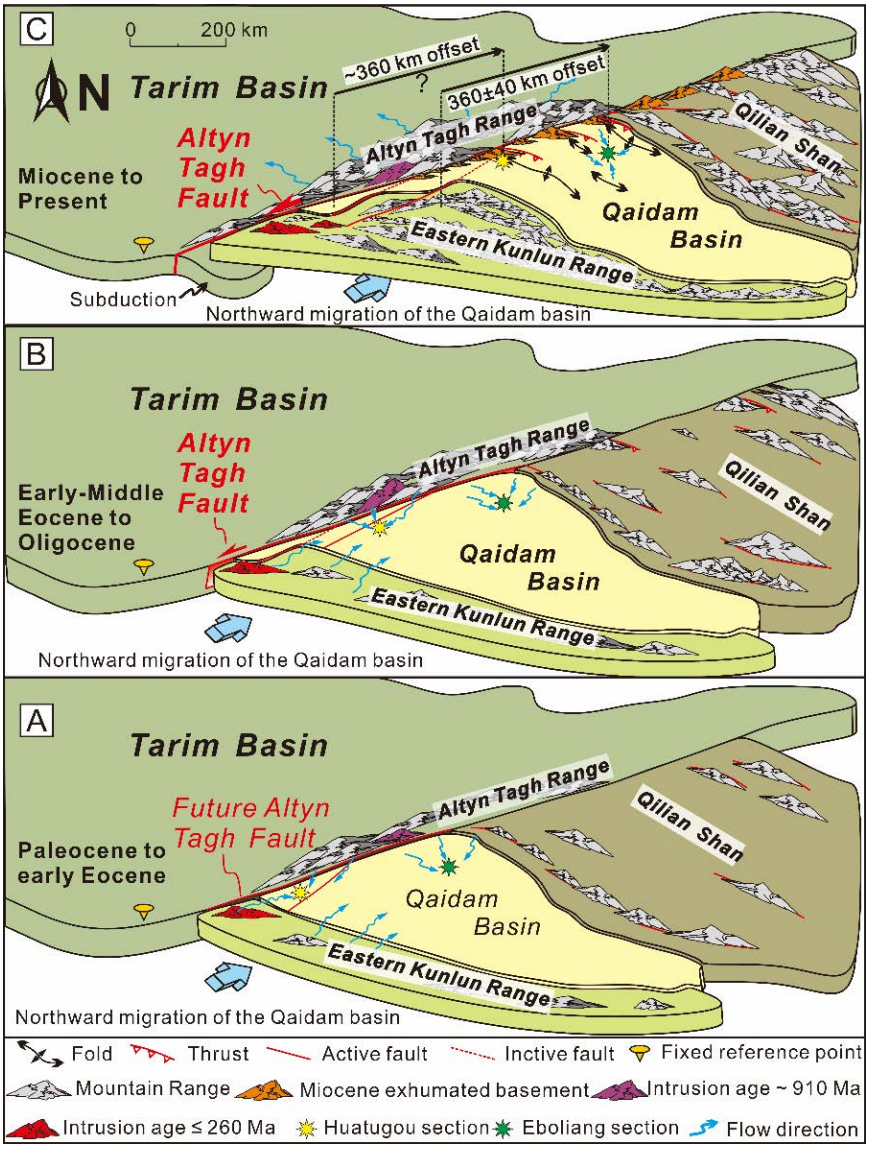


Fig. 12 Cenozoic kinematic model of the Altyn Tagh Fault and source to sink relation between the

western Qaidam basin and the surrounding regions. (A) during the Paleocene to early Eocene, the basement rocks in the Altyn Tagh Range served as the major source for the clastic material deposited in the Eboliang section, while sediments in the Huatugou section were derived from the Eastern Kunlun Range; (B) during the early Eocene to the Oligocene, the Qaidam basin migrated northeastward due to left-lateral strike-slip faulting along the ATF; (3) since the Miocene, intense left-lateral faulting along the ATF continuously offset the Qaidam basin towards the northeast and triggered post-Oligocene crustal deformation within the Altyn Tagh Range and western Qaidam basin. See text for detailed discussion.

#### 3.2.6.3 Tectonics implications

##### 3.2.6.3.1 Source to sink relation between the Qaidam basin and the Altyn Tagh Range

Provenance analysis results obtained from the two studied sections along the ATF reveal that the source to sink relation between the Qaidam basin and the Altyn Tagh Range underwent a three stages evolution:

During the Paleocene and early Eocene, the Eboliang and Huatugou sections were respectively located near the present day position of Anxi, and Tula (Figs. 2A and 12A). The basement rocks in the Altyn Tagh Range (including the early Neoproterozoic intrusive north of Anxi area) served as the major source area for the Eboliang section while a number of materials deposited in the Huatugou section derived from the Eastern Kunlun Range.

By early to middle Eocene, left-lateral strike-slip movement along the ATF initiated, resulting in gradually northeastward migration of the Qaidam basin (including the Eboliang and Huatugou sections). This migration ultimately disconnected the Eboliang section from the early Neoproterozoic source north of Anxi area (Fig. 12B), as attested by the decreasing proportion of early Neoprotozoic zircons (from 19.4% in Paleocene to early Eocene sample E123, to 5.3% in middle-late Eocene sample EBLE and 3.6% in the Oligocene sample E22). Similarly, the Huatugou section gradually moved away from the Tula area towards Anxi (Fig. 12B). This led to a decreasing proportion of < 260 Ma zircons (from ca. 15% in the Paleocene to middle Eocene samples S23 and HTG-E to ca. 3% in the late Eocene sample QX1-2; Fig. 8B, 8C and 8D) and an abrupt change in paleocurrent directions (Fig. 8C and 8D). In parallel, the gradual increase in early Neoproterozoic zircons (from ca. 3% in middle Eocene sample HTG-E to 6.5% in Oligocene sample QX1-1; Fig. 8C, 8D and 8E) suggests that the Huatugou section might be close to the early Neoproterozoic intrusives north of Anxi area during the middle Eocene to Oligocene.

On seimic profiles BB’ and CC’ (trending perpendicular to the Altyn Tagh Range; Figs. 2, 11A and 11B), several basement-involved thrust faults offset the Mesozoic strata and die

out in the Eocene and Oligocene strata. In addition, the Eocene to Oligocene strata slightly thicken towards the depocenter exhibiting a growth-strata structure (Fig. 11B). The oldest unit affected by growth strata is the middle Eocene lower Xiaganchaigou Fm., suggesting that the deformation along the ATF initiated around that time. Paleocurrents measurements and provenance analysis of conglomerates in the Xorkol basin (Fig. 2) and western Qaidam basin indicate that uplift along the central segment of ATF occurred prior to the Oligocene (Yue et al., 2001; Ritts et al., 2004; Wu et al., 2012a, 2012b), probably during the early to middle Eocene.

Since the early Miocene, the Eboliang and Huatugou sections continuously migrated northeastwards along the left-lateral strike-slip ATF. However, the scarcity of the Precambrain zircons, especially the early Neoproterozoic zircons, in the post-Oligocene sediments (e.g. sample EBLN in the Eboliang section and sample HTG-N in the Huatugou section) indicates a major change in the drainage pattern leading to disruption of the source to sink relation between the Altyn Tagh Range and the western Qaidam basin. On seimic profiles BB' and CC' (Fig. 11A and 11B), generally northward-tapering growth strata within the Miocene to Pliocene deposits are well-developed, likely associated with the left-lateral faulting along the ATF and deformation within the Altyn Tagh Range since the early Miocene. The post-Oligocene deformation and uplift within the Altyn Tagh Range and northwestern Qaidam basin largely modified the regional drainage pattern. Most of the material derived from the erosion of the Altyn Tagh Range was directed towards the Tarim basin to the north (Fig. 12C; Yue et al., 2004b). The post-Oligocene clastic materials deposited in the western Qaidam basin was derived from local sources including recycling of the deformed Paleocene to Oligocene strata.

#### 3.2.6.3.2 Implications for the Miocene deformation within the Altyn Tagh Range

In this study, the disappearance of an early Neophrotozoic component in the detrital zircon age spectra of the Miocene strata both in the Eboliang and Huatugou sections as well as the Mioecene initiation of growth strata within the northwestern Qaidam basin are indicative of enhanced tectonic activity within the Altyn Tagh Range and Qaidam basin since the Miocene. This finding is consistent with the results of several previous multi-faceted studies including: thermochronology on the basement rocks within the Altyn Tagh Range (e.g. Chen et al., 2001; Jolivet et al., 1999, 2001; Sobel et al., 2001; Zhang et al., 2012); paleomagnetism studies on the Cenozoic strata within the northwestern Qaidam basin (e.g. Zhang et al., 2013; Lu et al., 2014; Chang et al., 2015); basin-scale seismic profile interpretation (Meng and Fang,

2008; Yin et al., 2008a, 2008b; Wang et al., 2010; Cheng et al., 2015a); provenance analyses along the Altyn Tagh Range (e.g. Yue et al., 2001; Yin et al., 2002; Wu et al., 2012a, 2012b) and synthetized tectonic analysis (e.g. Burchfiel et al.,1989; Meyer et al., 1998; Fu et al., 2015). In addition, the Miocene deformation has been widely recognized in the northern and eastern Tibetan plateau, including the Eastern Kunlun Range, the Altyn Tagh Range, the Longmen Shan and the Qilian Shan (e.g., Kirby et al., 2002; Clark et al., 2004; Ding et al., 2004; Ritts et al., 2004; Sun et al., 2005; Duvall et al., 2013; Yuan et al., 2013; Cheng et al., 2014, 2015a, 2016; Lease, 2014; Chang et al., 2015; Jolivet et al., 2015), which may reflect a critical period in the growth process of the Tibetan plateau.

#### 3.2.6.3.3 Implications for the Cenozoic offset of the ATF

The Eboliang and Huatugou sections record the northward migration of the Qaidam basin and can be used as two piercing points for defining the Cenozoic offset of the ATF. A 360 ± 40 km offset can be estimated by corelating the Eboliang section to the early Neoprotozoic intrusive north of Anxi. Similarly, a ~360 km offset is obtained by corelating the Huatugou section to the Mesozoic plutons south of Tula area. We concede that, from analyzing detrital zircon spectra of Mesozoic to Cenozoic strata, the Eboliang-Anxi piercing point is much more convicing than the Tula-Huatugou piercing. However, by correlating the lithology and sedimentary features of the Cenozoic strata and analyzing the detrital zircon U-Pb ages from Mesozoic strata in both Tula and Huatugou sections, we previously found potential links between the Tula and Huatugou sections (Cheng et al., 2015a). We thus considered that the Tula section used to be a part of the Qaidam basin and was left behind due to the northeastward migration of the Qaidam basin. Two faults which have been indentified by previous research (Figs. 1, 2 and 12; e.g. Cowgill, et al., 2003) are acting as boundaries between the detached Qaidam basin and the relic Tula sub-basin (Cheng et al., 2015a). Since the early Eocene, faulting on the ATF induced these NE-SW–trending branch faults, now covered by Quaternary deposits. Northwards migration of the rigid Qaidam basin left the Tula section and parts of the Kunlun basement behind (Cheng et al., 2015a). Moreover, considering the strong mechanical behaviour of the rigid Qaidam basin, the Huatugou section should be approximately located near the present-day position of the Tula section if we restore the horizontal offset along the AFT based on the convincing Eboliang-Anxi piercing point. Consequently, we suggest a 360 ± 40 km offset along the ATF, which contradicts the extraordinary ~1200 km offset estimation (CSBS, 1992), but is in excellent agreement with independent, albeit indirect piercing points suggesting 300 to 400 km of displacement along the Altyn Tagh Range: (1) 400 ± 60 km offset

based on Jurassic lacustrine shorelines along the northern and southern sides of the Altyn Tagh fault (Ritts and Biffi, 2000), (2) ~375 km offset of the Cambrian magmatic arc in the Qilian Shan and the Altyn Tagh Range (Gehrels et al., 2003a), (3) ~375 ± 25 km offset of pre-Oligocene strata between the Qaidam and Xorkol basins (Yue et al., 2001), (4) ~360 ± 40 km offset estimation based on source to sink relation between the Xorkol basin and the North Qilian Shan (Yue et al., 2005), (5) 350~400 km offset based on eclogite, ophiolite and blueschist facies units in the Altyn Tagh Range and Qilian Shan (Yang et al., 2001; Zhang et al., 2001), (6) ~350 km offset based on similar early to middle Jurassic cooling zones on both side of the Altyn Tagh fault (Sobel et al., 2001). This large-scale lithospheric offset along the ATF would be totally accomodated by crustal deformation within the terrane to the east, especially by the NE-SW shortening and eastward extrusion along the faults within the Qilian Shan (e.g. Yin et al., 2002, 2008a; Cheng et al., 2015b). The confirmation of the hundreds of kilometers of displacement along the strike-slip ATF again supports the eastward extrusion of the Tibetan plateau driven by the India-Asia collision.

### 3.2.7 Conclusions

Detrital zircon U-Pb age patterns evolution from two Jurassic to Pleistocene stratigraphic sections in the northwestern Qaidam basin associated to high-quality seismic-reflection profiles revealed that: a) During the Paleocene to early Eocene, the Eboliang and Huatugou sections were respectively located near the present-day position of Anxi area and Tula area. The basement rocks in Altyn Tagh Range served as the significant source for the sediments to the Eboliang section, while the material deposited in the Huatugou section mostly derived from the Eastern Kunlun Range; b) Left-lateral strike-slip movement along the ATF initiated during the early-middle Eocene, resulting in gradually northeastward migration of the Qaidam basin; c) The post-Oligocene deformation within the Altyn Tagh Range and northwestern Qaidam basin strongly modified the regional drainage pattern. By Oligocene times, most of the material issued from the erosion of the Altyn Tagh Range was directed towards the Tarim basin to the north. The post-Oligocene clastic materials in the western Qaidam basin was mainly derived from local sources largely including recycling of the deformed Paleocene to Oligocene strata. Using the Eboliang and Huatugou sections as piercing points, we estimate a 360 ± 40 km offset along the ATF.

## Acknolegdements

This work was supported by the Oil and Gas Scientific and Technologic Major Programs

of China (Grant ZX05003) and the China Scholarship Council – Campus France Egide Cai Yuanpei program N° 32393WL (2014). We gratefully acknowledge the assistance of Shuwei Guan, Qinyang Meng, Ruiying Chen, Chuanmin Zhou, Suping Zhou, Xiangjiang Yu, Xiang Cheng, Wei Du, Runchao Liu and Tuo Zhang during field work. We thank Li Su of the Geological Lab Center, China University of Geosciences (Beijing), for her help during detrital zircon analysis and to Prof. Chaodong Wu, Chuanwu Wang, Yan Chen for their helpful suggestions on the Cenozoic evolution of the Qaidam basin. Communications with Michel Ballevre, Sylvie Bourquin, Hervé Régnauld, Baofu Han and Zhicheng Zhang had sharpened the discussion on the appropriate piercing points. We particularly thank Science Editor Jean-Philippe Avouac and two anonymous reviewers for careful and insightful comments.

## References

Allen, P.A., Allen, J.R., 2005. Basin Analysis: Principles and Applications. Blackwell Publishing Company, Oxford. 549 pp.

Andersen, T., 2002. Correction of common lead in U-Pb analyses that do not report 204Pb. Chemical Geology 192, 59-79.

Arnaud, N., Tapponnier, P., Roger, F., Brunel, M., Scharer, U., Chen, W., Xu, Z., 2003. Evidence for Mesozoic shear along the western Kunlun and Altyn-Tagh fault, northern Tibet (China). Journal of Geophysical Research: Solid Earth (1978-2012) 108.

Avouac, J.P., Tapponnier, P., 1993. Kinematic model of active deformation in central Asia. Geophysical Research Letters 20, 895-898.

Black, L.P., Kamo, S.L., Allen, C.M., Aleinikoff, J.N., Davis, D.W., Korsch, R.J., Foudoulis, C., 2003. TEMORA 1: a new zircon standard for Phanerozoic U–Pb geochronology. Chemical Geology 200, 155-170.

Bovet, P.M., Ritts, B.D., Gehrels, G., Abbink, A.O., Darby, B., Hourigan, J., 2009. Evidence of Miocene crustal shortening in the north Qilian Shan from Cenozoic stratigraphy of the western Hexi Corridor, Gansu Province, China. American Journal of Science 309, 290-329.

Braitenberg, C., Wang, Y., Fang, J., Hsu, H., 2003. Spatial variations of flexure parameters over the Tibet–Quinghai plateau. Earth and Planetary Science Letters 205, 211-224.

Bruguier, O., Lancelot, J., Malavieille, J., 1997. U–Pb dating on single detrital zircon grains from the Triassic Songpan–Ganze flysch (Central China): provenance and tectonic correlations. Earth and Planetary Science Letters 152, 217-231.

Burchfiel, B.C., Quidong, D., Molnar, P., Royden, L., Yipeng, W., Peizhen, Z., Weiqi, Z., 1989. Intracrustal detachment within zones of continental deformation. Geology 17, 748-752.

Chang, H., Li, L., Qiang, X., Garzione, C.N., Pullen, A., An, Z., 2015. Magnetostratigraphy of Cenozoic deposits in the western Qaidam Basin and its implication for the surface uplift of the northeastern margin of the Tibetan Plateau. Earth and Planetary Science Letters 430, 271-283.

Chen, Z.L., Zhang, Y.Q., Wang, X.F., Chen, X.H., 2001. Fission Track Dating of Apatite Constrains on the Cenozoic Uplift of the Altyn Tagh Mountain. Acta Geoscientia Sinica 22, 413-418 (in Chinese with English abstract).

Chen, X.H., Wang, X.F., E. George, G., Yang, Y., Qin, H., Chen, Z.L., Yang, F., Chen, B.L., Li, X.Z., 2004. Early Paleozoic Magmatism and Gold Mineralization in the Northern Altun, NW China. Acta Geologica Sinica-English Edition 78, 515-523.

Chen, Y., Gilder, S., Halim, N., Cogné, J.P., Courtillot, V., 2002. New paleomagnetic constraints on central Asian kinematics: Displacement along the Altyn Tagh fault and rotation of the Qaidam Basin. Tectonics 21, 1042.

Chen, X., Gehrels, G., Yin, A., Zhou, Q., Huang, P., 2015. Geochemical and Nd–Sr–Pb–O isotopic constrains on Permo–Triassic magmatism in eastern Qaidam Basin, northern Qinghai-Tibetan plateau: Implications for the evolution of the Paleo-Tethys. Journal of Asian Earth Sciences 114, Part 4, 674-692.

Cheng, F., Jolivet, M., Fu, S., Zhang, Q., Guan, S., Yu, X., Guo, Z., 2014. Northward growth of the Qimen Tagh Range: A new model accounting for the Late Neogene strike-slip deformation of the SW Qaidam Basin. Tectonophysics 632, 32-47.

Cheng, F., Guo, Z., Jenkins, H.S., Fu, S., Cheng, X., 2015a. Initial rupture and displacement on the Altyn Tagh fault, northern Tibetan Plateau: Constraints based on residual Mesozoic to Cenozoic strata in the western Qaidam Basin. Geosphere 11, 921-942.

Cheng, F., Jolivet, M., Dupont-Nivet, G., Wang, L., Yu, X., Guo, Z., 2015b. Lateral extrusion along the Altyn Tagh Fault, Qilian Shan (NE Tibet): insight from a 3D crustal budget. Terra Nova 27, 416-425.

Cheng, F., Fu, S., Jolivet, M., Zhang, C., Guo, Z., 2016. Source to sink relation between the Eastern Kunlun Range and the Qaidam Basin, northern Tibetan Plateau, during the Cenozoic. Geological Society of America Bulletin 128, 258-283, doi: 10.1130/B31260.1.

Clark, M., Schoenbohm, L., Royden, L., Whipple, K., Burchfiel, B., Zhang, X., Tang, W., Wang, E., Chen, L., 2004. Surface uplift, tectonics, and erosion of eastern Tibet from large-scale drainage patterns. Tectonics 23, TC1006.

Corfu, F., Hanchar, J.M., Hoskin, P.W., Kinny, P., 2003. Atlas of zircon textures. Reviews in mineralogy and geochemistry 53, 469-500.

Cowgill, E., Yin, A., Harrison, T.M., Xiao-Feng, W., 2003. Reconstruction of the Altyn Tagh fault based on U-Pb geochronology: Role of back thrusts, mantle sutures, and heterogeneous crustal strength in forming the Tibetan Plateau. Journal of Geophysical Research 108, 2346.

CSBS (Chinese Stata Bureau of Seismology), 1992. The Altyn Tagh Active Fault System. Seismology Publishing House, Beijing, pp. 1-319 (in Chinese).

Dai, J., Wang, C., Hourigan, J., Santosh, M., 2013. Multi-stage tectono-magmatic events of the Eastern Kunlun Range, northern Tibet: Insights from U–Pb geochronology and (U–Th)/He thermochronology. Tectonophysics 599, 97-106.

Darby, B.J., Ritts, B.D., Yue, Y., Meng, Q., 2005. Did the Altyn Tagh fault extend beyond the Tibetan Plateau? Earth and Planetary Science Letters 240, 425-435.

Delville, N., Arnaud, N., Montel, J.-M., Roger, F., Brunel, M., Tapponnier, P., Sobel, E., 2001. Paleozoic to Cenozoic deformation along the Altyn Tagh fault in the Altun Shan massif area, eastern Qilian Shan, northeastern Tibet, China. Geological Society of America Memoirs 194, 269-292.

Deng, T., Wang, X.M., 2004a. New material of the Neogene rhinocerotids from the Qaidam Basin in Qinghai, China. Vert. PalAsiat. 42 (3), 216–229.

Deng, T., Wang, X.M., 2004b. Late Miocene Hipparion (Equidae, Mammalia) of eastern Qaidam Basin in Qinghai, China. Vert. PalAsiat. 42 (4), 316–333.

Ding, G., Chen, J., Tian, Q., Shen, X., Xing, C., Wei, K., 2004. Active faults and magnitudes of left-lateral displacement along the northern margin of the Tibetan Plateau. Tectonophysics 380, 243-260.

Ding, L., Kapp, P., Yue, Y., Lai, Q., 2007. Postcollisional calc-alkaline lavas and xenoliths from the southern Qiangtang terrane, central Tibet. Earth and Planetary Science Letters 254, 28-38.

Dong, Z., Pei, X., Gu, P., Zhang, H., Chen, R., Zhang, X., 2014. Geochronology, Geochemistry, and Hf Isoplot of Yanchangbeishan Granodiorite of Lenghu Area in Qinghai. Nonwestern Geology 47 (4), 141-155 (in Chinese with English abstract).

Dong, Z., Gu, P., Chen, R., Zhang, X., Zhang, H., 2015. Geochronology, Geochemistry, and Hf Isoplot of Yanchangbeishan Adamellite of Lenghu Area in Qinghai. Earth Science-Journal of China University of Geosciences 40 (1), 130-144 (in Chinese with English abstract).

Duvall, A.R., Clark, M.K., Kirby, E., Farley, K.A., Craddock, W.H., Li, C., Yuan, D.-Y., 2013. Low-temperature thermochronometry along the Kunlun and Haiyuan Faults, NE Tibetan Plateau: Evidence for kinematic change during late-stage orogenesis. Tectonics 32, 1190-1211.

Dupont-Nivet, G., Butler, R.F., Yin, A., Chen, X., 2002. Paleomagnetism indicates no

Neogene rotation of the Qaidam Basin in northern Tibet during Indo-Asian collision. Geology 30, 263.

Dupont-Nivet, G., Lippert, P.C., Van Hinsbergen, D.J.J., Meijers, M.J.M., Kapp, P., 2010. Palaeolatitude and age of the Indo–Asia collision: palaeomagnetic constraints. Geophysical Journal International 182, 1189-1198.

England, P., Houseman, G., 1989. Extension during continental convergence, with application to the Tibetan Plateau. Journal of Geophysical Research: Solid Earth (1978–2012) 94, 17561-17579.

Fang, X., Zhang, W., Meng, Q., Gao, J., Wang, X., King, J., Song, C., Dai, S., Miao, Y., 2007. High-resolution magnetostratigraphy of the Neogene Huaitoutala section in the eastern Qaidam Basin on the NE Tibetan Plateau, Qinghai Province, China and its implication on tectonic uplift of the NE Tibetan Plateau. Earth and Planetary Science Letters 258, 293-306.

Fedo, C.M., Sircombe, K.N., Rainbird, R.H., 2003. Detrital zircon analysis of the sedimentary record. Reviews in mineralogy and geochemistry 53, 277-303.

Fu, L., Guan, P., Zhao, W. Y., Wang, M., Zhang, Y., Lu, J. W., 2013. Heavy mineral feature and provenance analysis of Paleogene Lulehe Formation in Qaidam Basin. Acta Petrologica Sinica, 29, 2867-2875 (in Chinese with English abstract).

Gao, J., Li, S., Dai, S., Li, A., Peng, Y., 2009. Constraints of tectonic evolution in provenance from detrital zircon fission-track data of Cenozoic strata of Xichagou district in western Qaidam basin. Journal of Lanzhou University (Natural Sciences) 45, 1-7 (in Chinese with English abstract).

Gehrels, G.E., Yin, A., Wang, X.F., 2003a. Magmatic history of the northeastern Tibetan Plateau. Journal of Geophysical Research 108, 2423.

Gehrels, G.E., Yin, A., Wang, X.F., 2003b. Detrital-zircon geochronology of the northeastern Tibetan plateau. Geological Society of America Bulletin 115, 881-896.

Gehrels, G., Kapp, P., DeCelles, P., Pullen, A., Blakey, R., Weislogel, A., Ding, L., Guynn, J., Martin, A., McQuarrie, N., 2011. Detrital zircon geochronology of pre-Tertiary strata in the Tibetan-Himalayan orogen. Tectonics 30, TC5016.

Gehrels, G., 2014. Detrital Zircon U-Pb Geochronology Applied to Tectonics. Annual Review of Earth and Planetary Sciences 42, 127-149.

Guo, J.J., Li, H.K., 1999. Angular Unconformity between the Huashishan Group and Huangzhong Group in the Eastern Mid-Qilian Massif: Identification and Implications. Progress In Precambrian Research 22, 47-52.

Hanchar, J., Rudnick, R., 1995. Revealing hidden structures: the application of

cathodoluminescence and back-scattered electron imaging to dating zircons from lower crustal xenoliths. Lithos 36, 289-303.

Hoskin, P., Black, L., 2000. Metamorphic zircon formation by solid-state recrystallization of protolith igneous zircon. Journal of metamorphic Geology 18, 423-439.

Heermance, R.V., Pullen, A., Kapp, P., Garzione, C.N., Bogue, S., Ding, L., Song, P., 2013. Climatic and tectonic controls on sedimentation and erosion during the Pliocene–Quaternary in the Qaidam Basin (China). Geological Society of America Bulletin 125, 833-856.

Huang, H., Huang, Q., Ma, Y., 1996. Geology of Qaidam Basin and its Petroleum Prediction. Geological Publishing House, Beijing, pp. 1–257 (in Chinese with English abstract).

Huo, G.M., 1990. Petroleum Geology of China: Oil Fields in Qianghai and Xizang, 14. Chinese Petroleum Industry Press, Beijing, pp. 1-483 (in Chinese with English abstract).

IGSQP (Institute of Geological Survey of Qinhai Province), 2004. The Report of Regional Geological Survey at Scale 1:250000. P.R.C. China Industry Press, pp. 1–386 (in Chinese).

Jian, X., Guan, P., Zhang, D.W., Zhang, W., Feng, F., Liu, R.J., Lin, S.D., 2013. Provenance of Tertiary sandstone in the northern Qaidam basin, northeastern Tibetan Plateau: Integration of framework petrography, heavy mineral analysis and mineral chemistry. Sedimentary Geology 290, 109-125.

Jolivet, M., Roger, F., Arnaud, N., Brunel, M., Tapponnier, P., Seward, D., 1999. Histoire de l'exhumation de l'Altun Shan: indications sur l'âge de la subduction du bloc du Tarim sous le système de l'Altyn Tagh (Nord Tibet). Comptes Rendus de l'Académie des Sciences-Series IIA-Earth and Planetary Science 329, 749-755.

Jolivet, M., Brunel, M., Seward, D., Xu, Z., Yang, J., Roger, F., Tapponnier, P., Malavieille, J., Arnaud, N., Wu, C., 2001. Mesozoic and Cenozoic tectonics of the northern edge of the Tibetan plateau: fission-track constraints. Tectonophysics 343, 111-134.

Jolivet, M., Brunel, M., Seward, D., Xu, Z., Yang, J., Malavieille, J., Roger, F., Leyreloup, A., Arnaud, N., Wu, C., 2003. Neogene extension and volcanism in the Kunlun Fault Zone, northern Tibet: New constraints on the age of the Kunlun Fault. Tectonics 22, 1052.

Jolivet, M., Roger, F., Xu, Z.Q., Paquette, J.L., Cao, H., 2015. Mesozoic–Cenozoic evolution of the Danba dome (Songpan Garzê, East Tibet) as inferred from LA-ICPMS U–Pb and fission-track data. Journal of Asian Earth Sciences 102, 180-204.

Ke, X., Ji, J., Zhang, K., Kou, X., Song, B., Wang, C., 2013. Magnetostratigraphy and Anisotropy of Magnetic Susceptibility of the Lulehe Formation in the Northeastern Qaidam Basin. Acta Geologica Sinica-English Edition 87, 576-587.

Kirby, E., Reiners, P.W., Krol, M.A., Whipple, K.X., Hodges, K.V., Farley, K.A., Tang, W.Q.,

Chen, Z.L., 2002. Late Cenozoic evolution of the eastern margin of the Tibetan Plateau: Inferences from $^{40}Ar/^{39}Ar$ and (U-Th)/He thermochronology. Tectonics 21, 1001.

Lease, R.O., 2014. Cenozoic mountain building on the northeastern Tibetan Plateau. Geological Society of America Special Papers 507, 115-127.

Li, H.B., Yang, J.S., Xu, Z.Q., Sun, Z.M., Tapponnier, P., van der Woerd, J., Meriaux, A.-S., 2006. The constraint of the Altyn Tagh fault system to the growth and rise of the northern Tibetan Plateau. Earth Science Frontiers 13, 59-79 (in Chinese with English abstract).

Li, W., Neubauer, F., Liu, Y.J., Genser, J., Ren, S.M., Han, G.Q., Liang, C.Y., 2013. Paleozoic evolution of the Qimantagh magmatic arcs, Eastern Kunlun Mountains: constraints from zircon dating of granitoids and modern river sands. Journal of Asian Earth Sciences 77, 183-202.

Li, L., Guo, Z., Guan, S., Zhou, S., Wang, M., Fang, Y., Zhang, C., 2015. Heavy mineral assemblage characteristics and the Cenozoic paleogeographic evolution in southwestern Qaidam Basin. Science China Earth Sciences, 1-17.

Liu, Y. H., Mo, X. X., Yu, X. H., Zhang, X. T. and Xu, G. W., 2006. Zircon SHRIMP U-Pb dating of the Jingren granite, Yemaquan region of the east Kunlun and its geological significance: Acta Petrologica Sinica 22, 2457-2463 (in Chinese with English abstract).

Liu, Y.J., Neubauer, F., Genser, J., Ge, X.H., Takasu, A., Yuan, S.H., Chang, L.H., Li, W.M., 2007. Geochronology of the initiation and displacement of the Altyn Strike-Slip Fault, western China. Journal of Asian Earth Sciences 29, 243-252.

Liu, D., Jolivet, M., Yang, W., Zhang, Z., Cheng, F., Zhu, B., Guo, Z., 2013. Latest Paleozoic–Early Mesozoic basin–range interactions in South Tian Shan (northwest China) and their tectonic significance: Constraints from detrital zircon U–Pb ages. Tectonophysics 599, 197-213.

Liu, D., Cheng, F., Guo, Z., Jolivet, M., Song, Y., 2015. Lahar facies of the Latest Paleozoic Arbasay Formation: Geomorphological characters and paleoenvironment reconstruction of Northern Tian Shan, NW China. Journal of Asian Earth Sciences 113, Part 1, 282-292.

Long, X., Yuan, C., Sun, M., Kröner, A., Zhao, G., 2014. New geochemical and combined zircon U–Pb and Lu–Hf isotopic data of orthogneisses in the northern Altyn Tagh, northern margin of the Tibetan plateau: Implication for Archean evolution of the Dunhuang Block and crust formation in NW China. Lithos 200–201, 418-431.

Lu, S.N., 2002. Preliminary Study of Precambrian Geology in the North Tibet–Qinghai Plateau. Geological Publishing House, Beijing, pp. 1-125 (in Chinese).

Lu, S.N., Yuan, G.B., 2003. Geochronology of early Precambrian magmatic activities in

Aketasdhtage, East Altyn Tagh. Acta Geological Sinica 77, 61–68 (in Chinese with English abstract).

Lu, S.N., Li, H.K., Zhang, C.L., Niu, G.H., 2008. Geological and geochronological evidence for the Precambrian evolution of the Tarim Craton and surrounding continental fragments. Precambrian Research 160, 94-107.

Lu, H., Xiong, S., 2009. Magnetostratigraphy of the Dahonggou section, northern Qaidam Basin and its bearing on Cenozoic tectonic evolution of the Qilian Shan and Altyn Tagh Fault. Earth and Planetary Science Letters 288, 539-550.

Lu, H., Wang, E., Meng, K., 2014. Paleomagnetism and anisotropy of magnetic susceptibility of the Tertiary Janggalsay section (southeast Tarim basin): Implications for Miocene tectonic evolution of the Altyn Tagh Range. Tectonophysics 618, 67-78.

Ludwig, K.R., 2003. User's manual for Isoplot 3.0: a geochronological toolkit for Microsoft Excel. Berkeley Geochronology Center. Spec. Pub., 4, pp. 1-71.

Mao, L.G., Xiao, A.C., Wu, L., Li, B.L., Wang, L.Q., Lou, Q.Q., Dong, Y.P., Qin, S.H., 2014. Cenozoic tectonic and sedimentary evolution of southern Qaidam Basin, NE Tibetan Plateau and its implication for the rejuvenation of Eastern Kunlun Mountains. Science China Earth Sciences, 1-14 (in Chinese).

Meng, Q.R., Hu, J.M., Yang, F.Z., 2001. Timing and magnitude of displacement on the Altyn Tagh fault: constraints from stratigraphic correlation of adjoining Tarim and Qaidam basins, NW China. Terra Nova 13, 86-91.

Meng, Q.R., Fang, X., 2008. Cenozoic tectonic development of the Qaidam Basin in the northeastern Tibetan Plateau. Geological Society of America Special Papers 444, 1-24.

Métivier, F., Gaudemer, Y., Tapponnier, P., Meyer, B., 1998. Northeastward growth of the Tibet plateau deduced from balanced reconstruction of two depositional areas: The Qaidam and Hexi Corridor basins, China. Tectonics 17, 823-842.

Meyer, B., Tapponnier, P., Bourjot, L., Metivier, F., Gaudemer, Y., Peltzer, G., Shunmin, G., Zhitai, C., 1998. Crustal thickening in Gansu‐Qinghai, lithospheric mantle subduction, and oblique, strike-slip controlled growth of the Tibet plateau. Geophysical Journal International 135, 1-47.

Molnar, P., Tapponnier, P., 1975. Cenozoic tectonics of Asia: Effects of a continental collision. Science 189, 419-426.

Pei, J., Sun, Z., Wang, X., Zhao, Y., Ge, X., Guo, X., Li, H., Si, J., 2009. Evidence for Tibetan plateau uplift in Qaidam basin before Eocene-Oligocene boundary and its climatic implications. Journal of Earth Science 20, 430-437.

Peltzer, G., Tapponnier, P., 1988. Formation and evolution of strike-slip faults, rifts, and basins during the India-Asia collision: An experimental approach. Journal of Geophysical Research: Solid Earth (1978–2012) 93, 15085-15117.

QBGMR (Qinhai Bureau of Geology Mineral Resources), 1991. Regional Geology of Qinghai Province. Geological Publishing House, Beijing, pp. 1–662 (in Chinese).

Qi, C., Li, X., Liang, X., Liu, Y., Tu, X., 2005. High-precision measurement of Hf isotopic reference values for the U-Pb geochronology standard zircons by multi-collector inductively coupled plasma-mass spectrometry. J. Chin. Mass Spectrom. Soc 26, 149-154.

Qiu, N.S., 2002. Tectono-thermal evolution of the Qaidam Basin, China: evidence from Ro and apatite fission track data. Petroleum Geoscience 8, 279-285.

Ritts, B.D., Hanson, A.D., Zinniker, D., Moldowan, J.M., 1999. Lower-Middle Jurassic nonmarine source rocks and petroleum systems of the northern Qaidam basin, northwest China. AAPG bulletin 83, 1980-2005.

Ritts, B.D., Biffi, U., 2000. Magnitude of post-Middle Jurassic (Bajocian) displacement on the central Altyn Tagh fault system, northwest China. Geological Society of America Bulletin 112, 61-74.

Ritts, B.D., Yue, Y., Graham, S.A., 2004. Oligocene-Miocene Tectonics and Sedimentation along the Altyn Tagh Fault, Northern Tibetan Plateau: Analysis of the Xorkol, Subei, and Aksay Basins. The Journal of geology 112, 207-229.

Roger, F., Arnaud, N., Gilder, S., Tapponnier, P., Jolivet, M., Brunel, M., Malavieille, J., Xu, Z., Yang, J., 2003. Geochronological and geochemical constraints on Mesozoic suturing in east central Tibet. Tectonics 22, 1037.

Roger, F., Jolivet, M., Malavieille, J., 2008. Tectonic evolution of the Triassic fold belts of Tibet. Comptes Rendus Geoscience 340, 180-189.

Roger, F., Jolivet, M., Malavieille, J., 2010. The tectonic evolution of the Songpan-Garzê (North Tibet) and adjacent areas from Proterozoic to Present: A synthesis. Journal of Asian Earth Sciences 39, 254-269.

Robinson, D.M., Dupont-Nivet, G., Gehrels, G.E., Zhang, Y., 2003. The Tula uplift, northwestern China: Evidence for regional tectonism of the northern Tibetan Plateau during late Mesozoic–early Cenozoic time. Geological Society of America Bulletin 115, 35-47.

Searle, M., 1996. Geological evidence against large-scale pre-Holocene offsets along the Karakoram Fault: Implications for the limited extrusion of the Tibetan plateau. Tectonics 15, 171-186.

Searle, M., Elliott, J., Phillips, R., Chung, S. L., 2011. Crustal–lithospheric structure and

continental extrusion of Tibet. Journal of the Geological Society 168, 633-672.

Shang Erjie, 2001. Basic structural style of tertiary in the western part of the northern area in the Qaidam basin and its petroleum significance. Geoscience 12, 422-424 (in Chinese with English abstract).

Shi, R.D., Yang, J.S., Wu, C.L., Tsuyoshi, I., Takafumi, H., 2006. Island arc volcanic rocks in the north Qaidam UHP belt, northern Tibet plateau: Evidence for ocean–continent subduction preceding continent–continent Subduction. Journal of Asian Earth Sciences 28, 151-159.

Sobel, E.R., Arnaud, N., 1999. A possible middle Paleozoic suture in the Altyn Tagh, NW China. Tectonics 18, 64-74.

Sobel, E.R., Arnaud, N., Jolivet, M., Ritts, B.D., Brunel, M., 2001. Jurassic to Cenozoic exhumation history of the Altyn Tagh range, northwest China, constrained by $^{40}Ar/^{39}Ar$ and apatite fission track thermochronology. Geological Society of America Memoirs 194, 247-267.

Song, T., Wang, X., 1993. Structural styles and stratigraphic patterns of syndepositional faults in a contractional setting: Examples from Quaidam basin, northwestern China. AAPG bulletin 77, 102-117.

Song, S.G., Zhang, L.F., Niu, Y.L., Su, L., Song, B., Liu, D.Y., 2006. Evolution from oceanic subduction to continental collision: a case study from the Northern Tibetan Plateau based on geochemical and geochronological data. Journal of Petrology 47, 435-455.

Song, S., Niu, Y., Su, L., Zhang, C., Zhang, L., 2014. Continental orogenesis from ocean subduction, continent collision/subduction, to orogen collapse, and orogen recycling: The example of the North Qaidam UHPM belt, NW China. Earth-Science Reviews 129, 59-84.

Staisch, L.M., Niemi, N.A., Hong, C., Clark, M.K., Rowley, D.B., Currie, B., 2014. A Cretaceous‐Eocene depositional age for the Fenghuoshan Group, Hoh Xil Basin: Implications for the tectonic evolution of the northern Tibet Plateau. Tectonics 33, 281-301.

Sun, Z.M., Yang, Z.Y., Pei, J.L., Ge, X.H., Wang, X.S., Yang, T.S., Li, W.M., Yuan, S.H., 2005. Magnetostratigraphy of Paleogene sediments from northern Qaidam Basin, China: implications for tectonic uplift and block rotation in northern Tibetan plateau. Earth and Planetary Science Letters 237, 635-646.

Sun, Z.C., Jing, M.C., Sun, N.D., Lu, Y.L., Cao, L., 2007. Discussion on boundary between the upper and lower members of Xiaganchaigou Formation of Paleogene in Well Kun-2, Qaidam Basin. J. Palaeogeogr. 9 (6), 611–618 (in Chinese with English abstract).

Sun, Y., Chen, Z., Chen, B., Han F., Zhou, Y., Hao, R. and Li, S., 2014. Cenozoic Uplift and Denudation of the EW-trending Range of Northern Altun Mountains: Evidence from Apatite Fission Track Data. Acta Geoscientica Sinica, 37 (1), 67-75 (in Chinese with English abstract).

Tapponnier, P., Peltzer, G., Armijo, R., 1986. On the mechanics of the collision between India and Asia. Geological Society, London, Special Publications 19, 113-157.

Tapponnier, P., Xu, Z.Q., Roger, F., Meyer, B., Arnaud, N., Wittlinger, G., Yang, J.S., 2001. Oblique stepwise rise and growth of the Tibet Plateau. Science 294, 1671-1677.

Thomas, W.A., 2011. Detrital-zircon geochronology and sedimentary provenance. Lithosphere 3, 304-308.

Wang, E., 1997. Displacement and timing along the northern strand of the Altyn Tagh fault zone, northern Tibet. Earth and Planetary Science Letters 150, 55-64.

Wang, Y., Zhang, X., Wang, E., Zhang, J., Li, Q., Sun, G., 2005. $^{40}Ar/^{39}Ar$ thermochronological evidence for formation and Mesozoic evolution of the northern-central segment of the Altyn Tagh fault system in the northern Tibetan Plateau. Geological Society of America Bulletin 117, 1336-1346.

Wang, E., Xu, F.Y., Zhou, J.X., Wan, J., Burchfiel, B.C., 2006a. Eastward migration of the Qaidam basin and its implications for Cenozoic evolution of the Altyn Tagh fault and associated river systems. Geological Society of America Bulletin 118, 349-365.

Wang, C., Liu, L., Che, Z.C., Chen, D.L., Zhang, A.D., Luo, J.H., 2006b. U–Pb geochronology and tectonic setting of the granitic gneiss in Jianggaleisayi Eclogite Belt. Geological Journal of China Universities 12, 74-82.

Wang, L., Xiao, A.C., Gong, Q.L., Liu, D., Wu, L., Zhou, S.P., Shen, Z.Y., Lou, Q.Q., Sun, X.W., 2010. The unconformity in Miocene sequence of western Qaidam Basin and its tectonic significance. Science China Earth Sciences 53, 1126-1133 (in Chinese).

Wang, C., Liu, L., Yang, W.Q., Zhu, X.H., Cao, Y.T., Kang, L., Chen, S.F., Li, R.S., He, S.P., 2013. Provenance and ages of the Altyn Complex in Altyn Tagh: implications for the early Neoproterozoic evolution of northwestern China. Precambrian Research 230, 193-208.

Wang, C., Dai, J., Zhao, X., Li, Y., Graham, S.A., He, D., Ran, B., Meng, J., 2014a. Outward-growth of the Tibetan Plateau during the Cenozoic: A review. Tectonophysics 621, 1-43.

Wang, C., Liu, L., Xiao, P.X., Cao, Y.T., Yu, H.Y., Meert, J.G., Liang, W.T., 2014b. Geochemical and geochronologic constraints for Paleozoic magmatism related to the orogenic collapse in the Qimantagh–South Altyn region, northwestern China. Lithos 202–203, 1-20.

Wiedenbeck, M., Alle, P., Corfu, F., Griffin, W., Meier, M., Oberli, F., Quadt, A.v., Roddick, J., Spiegel, W., 1995. Three natural zircon standards for U‐Th‐Pb, Lu‐Hf, trace element and REE analyses. Geostandards Newsletter 19, 1-23.

Wittlinger, G., Tapponnier, P., Poupinet, G., Mei, J., Danian, S., Herquel, G., Masson, F., 1998. Tomographic evidence for localized lithospheric shear along the Altyn Tagh fault. Science 282,

74-76.

Wu, C.L., Yang, J.S., Ireland, T., Wooden, J.L., Li, H.B., Wan, Y.S., Shi, R.D., 2001. Zircon SHRIMP ages of Aolaoshan granite from the south margin of Qilianshan and its geological significance. Acta Petrologica Sinica 17, 215–221 (in Chinese with English abstract).

Wu, C.L., Wooden, J.L., Robinson, P.T., Gao, Y.H., Wu, S.P., Chen, Q.L., Mazdab, F.K., Mattinson, C., 2009. Geochemistry and zircon SHRIMP U–Pb dating of granitoids from the west segment of the North Qaidam. Sci. China, Ser. D Earth Sci. 52 (11), 1771–1790 (in Chinese).

Wu C. L., Gao Y. H., Lei M., Qin H. P., Liu C. H., Li M. Z., Frost. B. R., Wooden J. L., 2014. Zircon SHRIMP U-Pb dating, Lu-Hf isotopic characteristics and petrogenesis of the Palaeozoic granites in Mangya area, south Altun, NW China. Acta Petrologica Sinica, 30(8), 2297-2323 (in Chinese with English abstract).

Wu, L., Xiao, A., Wang, L., Shen, Z., Zhou, S., Chen, Y., Wang, L., Liu, D., Guan, J., 2011. Late Jurassic–Early Cretaceous Northern Qaidam Basin, NW China: Implications for the earliest Cretaceous intracontinental tectonism. Cretaceous Research 32, 552-564.

Wu, L., Xiao, A.C., Yang, S.F., Wang, L.Q., Mao, L.G., Wang, L., Dong, Y.P., Xu, B., 2012a. Two-stage evolution of the Altyn Tagh Fault during the Cenozoic: new insight from provenance analysis of a geological section in NW Qaidam Basin, NW China. Terra Nova 24, 387-395.

Wu, L., Xiao, A., Wang, L., Mao, L., Wang, L., Dong, Y., Xu, B., 2012b. EW-trending uplifts along the southern side of the central segment of the Altyn Tagh Fault, NW China: Insight into the rising mechanism of the Altyn Mountain during the Cenozoic. Science China Earth Sciences 55, 926-939 (in Chinese).

Wu, L., Xiao, A., Ma, D., Li, H., Xu, B., Shen, Y., Mao, L., 2014. Cenozoic fault systems in southwest Qaidam Basin, northeastern Tibetan Plateau: Geometry, temporal development, and significance for hydrocarbon accumulation. AAPG bulletin 98, 1213-1234.

Xia, W.C., Zhang, N., Yuan, X.P., Fan, L.S., Zhang, B.S., 2001. Cenozoic Qaidam basin, China: A stronger tectonic inversed, extensional rifted basin. AAPG bulletin 85, 715-736.

Xiao, W., Windley, B.F., Yong, Y., Yan, Z., Yuan, C., Liu, C., Li, J., 2009. Early Paleozoic to Devonian multiple-accretionary model for the Qilian Shan, NW China. Journal of Asian Earth Sciences 35, 323-333.

Xiao, Q., Shao, G., Liu-Zeng, J., Oskin, M.E., Zhang, J., Zhao, G., Wang, J., 2015. Eastern termination of the Altyn Tagh Fault, western China: Constraints from a magnetotelluric survey. Journal of Geophysical Research: Solid Earth 120, 2838-2858.

Yang, F., Ma, Z.Q., Xu, T.C., Ye, S.J., 1992. A Tertiary paleomagnetic stratigraphic profile in Qaidam basin. Acta Petrolei Sinica 13, 97-101 (in Chinese with English abstract).

Yang, J., Xu, Z., Song, S., Wu, C., Shi, R., Zhang, J., Wan, Y., Li, H., Jin, X., Jolivet, M., 2000. Discovery of eclogite in Dulan, Qinghai Province and its significance for studying the HP-UHP metamorphic belt along the central orogenic belt of China. Acta Geologica Sinica 74, 156-168 (in Chinese with English abstract).

Yang, J., Xu, Z., Zhang, J., Chu, C. Y., Zhang, R., Liou, J. G., 2001. Tectonic significance of early Paleozoic high-pressure rocks in Altun-Qaidam-Qilian Mountains, northwest China. Geological Society of America Memoirs 194, 151-170.

Yang, M.H., Song, J.J., 2002. Petrology of the Lenghu granite mass, northwestern Qaidam basin, China. Northwestern Geol. 35, 94-98 (in Chinese with English abstract).

Yang, J.S., Wu, C.L., Zhang, J.X., Shi, R.D., Meng, F.C., Wooden, J.L., Yang, H.Y., 2006. Protolith of eclogites in the north Qaidam and Altun UHP terrane, NW China: Earlier oceanic crust? Journal of Asian Earth Sciences 28, 185-204.

Yang, W., Jolivet, M., Dupont-Nivet, G., Guo, Z., Zhang, Z., Wu, C., 2013. Source to sink relations between the Tian Shan and Junggar Basin (northwest China) from Late Palaeozoic to Quaternary: evidence from detrital U-Pb zircon geochronology. Basin Research 25, 219-240.

Yang, W., Jolivet, M., Dupont-Nivet, G., Guo, Z., 2014. Mesozoic - Cenozoic tectonic evolution of southwestern Tian Shan: Evidence from detrital zircon U/Pb and apatite fission track ages of the Ulugqat area, Northwest China. Gondwana Research 26, 986-1008.

Yin, A., Harrison, T.M., 2000. Geologic evolution of the Himalayan-Tibetan orogen. Annual Review of Earth and Planetary Sciences 28, 211-280.

Yin, A., Rumelhart, P., Butler, R., Cowgill, E., Harrison, T., Foster, D., Ingersoll, R., Qing, Z., Xian-Qiang, Z., Xiao-Feng, W., 2002. Tectonic history of the Altyn Tagh fault system in northern Tibet inferred from Cenozoic sedimentation. Geological Society of America Bulletin 114, 1257-1295.

Yin, A., Dang, Y.Q., Zhang, M., McRivette, M.W., Burgess, W.P., Chen, X.H., 2007. Cenozoic tectonic evolution of Qaidam basin and its surrounding regions (part 2): Wedge tectonics in southern Qaidam basin and the Eastern Kunlun Range. Geological Society of America Special Papers 433, 369-390.

Yin, A., Dang, Y.Q., Wang, L.C., Jiang, W.M., Zhou, S.P., Chen, X.H., Gehrels, G.E., McRivette, M.W., 2008a. Cenozoic tectonic evolution of Qaidam basin and its surrounding regions (Part 1): The southern Qilian Shan-Nan Shan thrust belt and northern Qaidam basin.

Geological Society of America Bulletin 120, 813-846.

Yin, A., Dang, Y.Q., Zhang, M., Chen, X.H., McRivette, M.W., 2008b. Cenozoic tectonic evolution of the Qaidam basin and its surrounding regions (Part 3): Structural geology, sedimentation, and regional tectonic reconstruction. Geological Society of America Bulletin 120, 847-876.

Yu, X.J., Fu, S.T., Guan, S.W., Huang, B., Cheng, F., Cheng, X., Zhang, T., Guo, Z.J., 2014. Paleomagnetism of Eocene and Miocene sediments from the Qaidam basin: Implication for no integral rotation since the Eocene and a rigid Qaidam block. Geochemistry, Geophysics, Geosystems 15, 2109-2127.

Yuan, H.L., Gao, S., Liu, X.M., Li, H.M., Günther, D., Wu, F.Y., 2004. Accurate U-Pb age and trace element determinations of zircon by laser ablation‐inductively coupled plasma-mass spectrometry. Geostandards and Geoanalytical Research 28, 353-370.

Yuan, D.Y., Ge, W.P., Chen, Z.W., Li, C.Y., Wang, Z.C., Zhang, H.P., Zhang, P.Z., Zheng, D.W., Zheng, W.J., Craddock, W.H., Dayem, K.E., Duvall, A.R., Hough, B.G., Lease, R.O., Champagnac, J.-D., Burbank, D.W., Clark, M.K., Farley, K.A., Garzione, C.N., Kirby, E., Molnar, P., Roe, G.H., 2013. The growth of northeastern Tibet and its relevance to large-scale continental geodynamics: A review of recent studies. Tectonics 32, 2013TC003348.

Yue, Y.J., Liou, J.G., 1999. Two-stage evolution model for the Altyn Tagh fault, China. Geology 27, 227-230.

Yue, Y.J., Ritts, B.D., Graham, S.A., 2001. Initiation and long-term slip history of the Altyn Tagh Fault. International Geology Review 43, 1087-1093.

Yue, Y., Ritts, B.D., Graham, S.A., Wooden, J.L., Gehrels, G.E., Zhang, Z., 2004a. Slowing extrusion tectonics: lowered estimate of post-Early Miocene slip rate for the Altyn Tagh fault. Earth and Planetary Science Letters 217, 111-122.

Yue, Y.J., Ritts, B.D., Hanson, A.D., Graham, S.A., 2004b. Sedimentary evidence against large strike-slip translation on the Northern Altyn Tagh fault, NW China. Earth and Planetary Science Letters 228, 311-323.

Yue, Y.J., Graham, S.A., Ritts, B.D., Wooden, J.L., 2005. Detrital zircon provenance evidence for large-scale extrusion along the Altyn Tagh fault. Tectonophysics 406, 165-178.

Zhang, J.X., Zhang, Z.M., Xu, Z.Q., Yang, J.S., Cui, J.W., 2001. Petrology and geochronology of eclogites from the western segment of the Altyn Tagh, northwestern China. Lithos 56, 187-206.

Zhang, W., 2006. The High precise Cenozoic magnetostratigraphy of the Qaidam basin and uplift of the northern Tibetan Plateau. (Doctoral dissertation) Lanzhou University, Lanzhou,

pp. 1–105 (in Chinese with English abstract).

Zhang, J.X., Li, H.K., Meng, F.C., Xiang, Z.Q., Yu, S.Y., Li, J.P., 2011. Polyphase tectonothermal events recorded in metamorphic basement from the Altyn Tagh, the southeastern margin of the Tarim basin, western China: constraint from U-Pb zircon geochronology –Pb zircon geochronology. Acta Petrol. Sin. 27, 23-46.

Zhang, Z.C., Guo, Z.J., Li, J.F., Tang, W.H., 2012. Mesozoic and Cenozoic uplift-denudation along the Altyn Tagh fault, northwestern china: constraints from apatite fission track data. Quaternary Sciences, 32(3): 499-509 (in Chinese with English abstract).

Zhang, W., Fang, X., Song, C., Appel, E., Yan, M., Wang, Y., 2013. Late Neogene magnetostratigraphy in the western Qaidam Basin (NE Tibetan Plateau) and its constraints on active tectonic uplift and progressive evolution of growth strata. Tectonophysics 599, 107-116.

Zhang, J., Mattinson, C., Yu, S., Li, Y., 2014a. Combined rutile–zircon thermometry and U-Pb geochronology: New constraints on Early Paleozoic HP/UHT granulite in the south Altyn Tagh, north Tibet, China. Lithos 200, 241-257.

Zhang, H.P., Zhang, P.Z., Zheng, D.W., Zheng, W.., Chen, Z.W., Wang, W.T., 2014b. Transforming the Miocene Altyn Tagh fault slip into shortening of the north-western Qilian Shan: insights from the drainage basin geometry. Terra Nova 26, 216-221.

Zhao, J.M., Mooney, W.D., Zhang, X.K., Li, Z.C., Jin, Z.J., Okaya, N., 2006. Crustal structure across the Altyn Tagh Range at the northern margin of the Tibetan plateau and tectonic implications. Earth and Planetary Science Letters 241, 804-814.

Zhou, J.X., Xu, F.Y., Wang, T.C., Cao, A.F., Yin, C.M., 2006. Cenozoic deformation history of the Qaidam Basin, NW China: Results from cross-section restoration and implications for Qinghai–Tibet Plateau tectonics. Earth and Planetary Science Letters 243, 195-210.

Zhuang, G., Hourigan, J.K., Ritts, B.D., Kent-Corson, M.L., 2011. Cenozoic multiple-phase tectonic evolution of the northern Tibetan Plateau: Constraints from sedimentary records from Qaidam basin, Hexi Corridor, and Subei basin, northwest China. American Journal of Science 311, 116-152.

# Chapter 4 Quantitative estimate of the lateral extrusion along the Altyn Tagh Fault-Qilian Shan tectonic system

***Paper published in Terra Nova, 2015, vol. 27, pp. 416-425***

**Lateral extrusion along the Altyn Tagh Fault – Qilian Shan (NE Tibet): insight from a 3D crustal budget**

**Feng Cheng**[1, 2], Marc Jolivet[2], Guillaume Dupont-Nivet[1, 2, 3], Lin Wang[4], Xiangjiang Yu[1], Zhaojie Guo[1, †]

[1] Key Laboratory of Orogenic Belts and Crustal Evolution, Ministry of Education, School of Earth and Space Sciences, Peking University, Beijing, 100871, China

[2] Laboratoire Géosciences Rennes, CNRS-UMR6118, Université Rennes 1, Rennes, 35042, France

[3] Institute of Earth and Environmental Science, University of Potsdam, Potsdam, 14476, Germany

[4] Institute of Remote Sensing and Geographic Information System, Peking University, Beijing, 100871, China

[†] Corresponding author. Tel.: + 86-10-62753545; fax: + 86-10-62758610. E-mail address: zjguo@pku.edu.cn (Z.J. Guo)

*Note: The online version of this contribution can be found as:* ***Cheng, F., Jolivet, M., Dupont-Nivet, G., Wang, L., Yu, X., Guo, Z., 2015. Lateral extrusion along the Altyn Tagh Fault, Qilian Shan (NE Tibet): insight from a 3D crustal budget. Terra Nova 27, 416-425, doi: 10.1111/ter.12173.***

## Abstract

The lithospheric strike-slip Altyn Tagh Fault accommodated hundreds of kilometers of displacement between the Qaidam and Tarim blocks since its Eocene reactivation. However, the way the deformation is accommodated in the Qilian Shan and further east remains to be clarified. Based on the 360 km northeastward migration of the relatively rigid Qaidam block along the Altyn Tagh Fault and 3D isovolumetric balance of the crustal deformation within the

Altyn Tagh Fault – Qilian Shan system, we demonstrate that 250 ± 28 km (43.8~49.4 %) of N20E directed crustal shortening and an additional ~250 to ~370 km of eastward motion of the Qilian Shan crust that must be accounted for by strike-slip faulting in the Qilian Shan and crustal thickening in the Qinling area, as well as extension in the adjoining North China block graben systems.

Keywords: Tibetan Plateau; Altyn Tagh Fault; Qilian Shan; Extrusion; Qaidam Basin

## 4.1 Introduction

As one of the major strike-slip fault system on the Tibetan Plateau, the Altyn Tagh Fault (ATF) accommodates a significant amount of post-collisional convergence between India and Eurasia through left-lateral strike-slip faulting (Molnar and Tapponnier, 1975). The kinematics of the ATF itself has been studied in details and around 360 km Cenozoic offset has been confirmed (Jolivet et al., 1999; Ritts and Biffi, 2000; Sobel et al., 2001; Gehrels et al., 2003; Yue et al., 2005; Searle et al., 2011; Cheng et al., 2015). Nonetheless, the accommodation of the strike-slip motion along the fault within the Qilian Shan wedge that forms its eastern termination remains highly debated (Fig. 1; Meyer et al., 1998; Yue and Liou, 1999; Yin and Harrison, 2000; Yin et al., 2002; Darby et al., 2005; Yin et al., 2008a; Xiao et al., 2015).

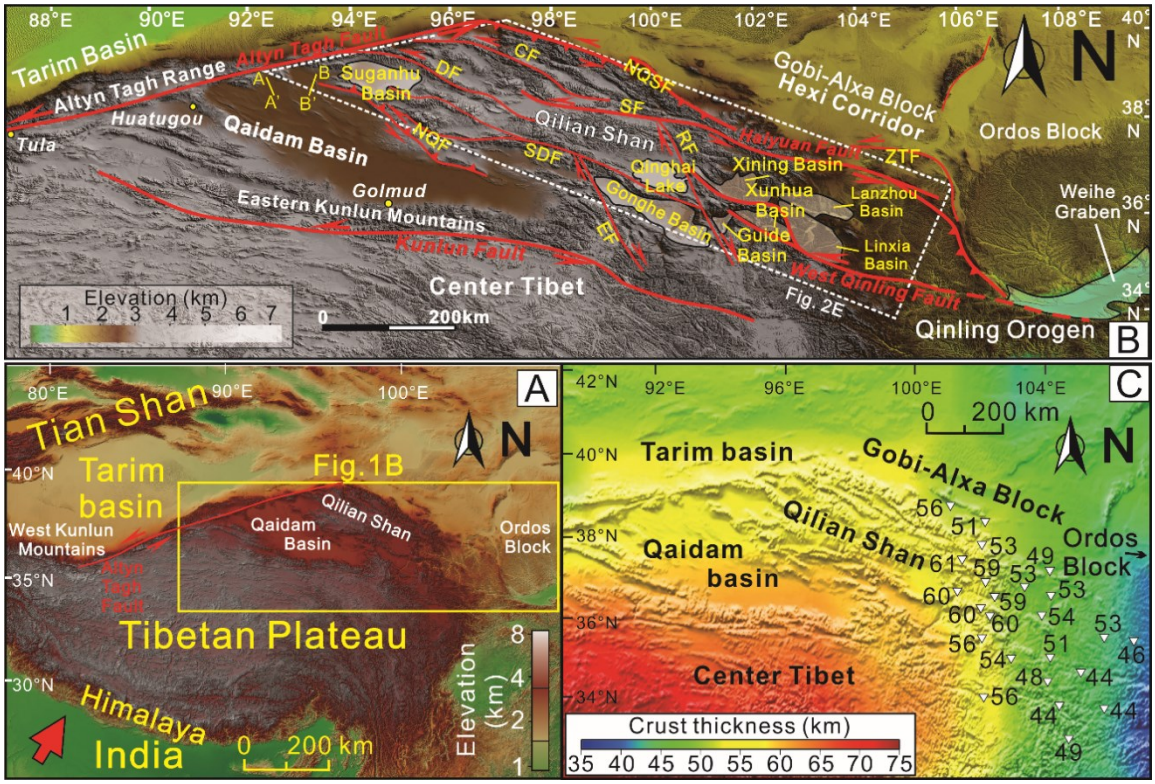


Fig.1 (A) SRTM-based digital topographic map of the Tibetan Plateau and the surrounding region. (B) SRTM-based digital topographic map of the northern Tibetan Plateau. NQSF, Northern Qilian Shan

Fault system; NQF, Northern Qaidam Fault; SDF, Saisitengshang-Dakendaban Fault; DF, Danghe-Nanshan Fault; DTF, Daxueshan Yuole-Nanshan Fault; SF, ShuleNanshan Fault; EF, Elashan Fault; RF, Riyueshan Fault; CF, Changma Fault; ZTF, Zhongwei-Tongxing Fault. Solid lines A–A' and B–B' represent the locations of the seismic profiles presented in Appendix S1. Dash-lined right trapezoid represents the studied Qilian Shan region. (C) SRTM-based present-day crustal-thickness map of the northern Tibetan Plateau and the surrounding region, modified from Li et al. (2014). The white solid triangles represent the locations of seismic stations, and numbers refer to the corresponding crustal thickness.

To understand lateral extrusion in the northern Tibetan Plateau, one major issue that remains to be explored within the kinematic pattern of the ATF – Qilian Shan system is whether the hundreds of kilometers of displacement along the ATF are totally absorbed by NE-SW crustal shortening within the Qilian Shan (Burchfiel et al., 1989; Yin and Harrision, 2000), or if they are transferred farther east in the Qinling region and possibly farther in North China (Fig. 1; Yue and Liou, 1999; Darby et al., 2005). Although large amounts of NE-SW directed shortening and eastward motion of the northern Tibetan crust has long been observed (e.g. Tapponnier and Molnar, 1977; Burchfiel et al., 1991; Dupont-Nivet et al., 2004; Zhang et al., 2004), proposed amounts of Cenozoic crustal shortening vary widely from ~20 % to ~60 % (Bally et al., 1986; Meyer, et al., 1998; Yin et al., 2008a; Zhang et al., 2014) and quantitative estimation of the amount of lateral extrusion in the northeastern Tibetan Plateau is deficient. More importantly, the large variation in crustal shortening estimation lead in turn to diverse understandings of the crustal deformation mechanism in the northern Tibetan Plateau, such as distributed or diffuse deformation (England and Seale, 1986; Burchfiel et al., 1991; Ratschbacher et al., 1994; Meyer et al., 1998), or lower crustal flow (Zhao and Morgan, 1987; Royden et al., 1997; Clark and Royden, 2000; Lease et al., 2012).

In this study, we propose a new quantitative evaluation of the Cenozoic crustal shortening and lateral extrusion budget in the northern Tibetan Plateau by considering both the northeastward migration of the relatively rigid Qaidam block along the ATF and restoring the 3D crustal deformation in the Qilian Shan.

## 4.2 Geological setting

The northern Tibetan Plateau is characterized by three key tectonic units: the left-lateral strike-slip lithospheric ATF, the Qilian Shan crustal wedge, and the near-rigid Qaidam block (Fig. 1; Wittlinger et al., 1998). The ATF bounds the northern part of the thickened Tibetan crust, and runs for over 1,600 km from the West Kunlun Mountains to the northwestern end of the Qilian Shan (Fig. 1; Cowgill et al., 2003). Proposed Cenozoic initiation of the ATF

generally varies from Eocene to Miocene and estimation on the offset between 300 and 400 km (Ritts and Biffi, 2000; Jolivet et al., 2001; Gehrels et al., 2003; Yue et al., 2005; Yin et al., 2008b; Wu et al., 2012; Cheng et al., 2015). The Qilian Shan separates the plateau from the Gobi-Alxa block to the northeast (Fig. 1B). This crustal-scale wedge consists of massive NW-SE striking mountain ranges growing on folds, thrusts or strike-slip faults accommodating the northward motion and eastward extrusion of the Tibetan Plateau (Meyer et al., 1998; Yin and Harrison, 2000; Tapponnier et al., 2001; Bovet et al., 2009). The proposed Paleocene to early Eocene initiation of the Cenozoic deformation and crustal shortening in the Qilian Shan (Métivier et al., 1998; Tapponnier et al., 2001; Jolivet et al. 2001; Yin et al., 2008a; Clark et al., 2010; Duvall et al., 2011; Zhuang et al., 2011; Yuan et al., 2013) challenges the model of post-Pliocene initial deformation in the northern Tibetan plateau inferred from northward progressive plateau growth hypothesis. The Qaidam block is bordered by the ATF to the northwest and the Qilian Shan to the northeast (Fig. 1B). Effective elastic thickness calculations indicate that the mechanical strength of the Qaidam crust is exceptionally high compared to that of the Qilian Shan (Braitenberg et al., 2003). Zhou et al. (2006) proposed that the Qaidam Basin experienced an average of 10 % of NE-SW shortening during the Cenozoic.

## 4.3 Methods

To estimate the amount of movement transferred from the ATF into the Qilian Shan, we followed the previously proposed 2D large-scale crustal deformation analyses of post-collision convergence between India and Eurasia (van Hinsbergen et al., 2011), to which we added the vertical component of crustal thickening. Recent studies demonstrated that the relatively rigid Qaidam block (Braitenberg et al., 2003; Zhou et al., 2006; Le Pape et al., 2012) has been transported northeastward along the ATF during the Cenozoic (Wang et al., 2006), without obvious post-Eocene basin-scale vertical axis rotation with respect to Eurasia (Dupont-Nivet et al., 2002; Yu et al., 2014). We thus consider that crustal shortening and vertical axis rotation of the Qaidam block have been minimal. The amount of northeastward migration of that block along the ATF must have been largely transferred into the Qilian Shan where it can be vertically partitioned into NE-SW directed crustal shortening and eastward extrusion (Fig. 2).

In the following analysis, we define the extent of the Qilian Shan to be the region comprised between the ATF, the Gobi-Alxa and the Qaidam blocks with an open boundary to the east. The general relations between the offset of the ATF, the amount of crustal shortening

and the shortening strain in the Qilian Shan are given by:

$$L_S = L_d \sin\alpha, \quad (1)$$

and

$$R_S = \frac{L_d \sin\alpha}{L_0 \sin\alpha} = \frac{L_d \sin\alpha}{(L_d + L_1)\sin\alpha} = \frac{L_d}{L_d + L_1}, \quad (2)$$

where α is the constant angle between the strike direction of the ATF and the average orientation of the Qilian Shan long-axis in plane view (Fig. 2E); $L_d$ is the amount of offset along the ATF since its initiation; $L_0$ and $L_1$ are the average limb length of the Qilian Shan along the ATF before its initiation and at present day respectively; *Ls* is the average amount of crustal shortening since ATF initiation; finally *Rs* is the crustal shortening strain in the Qilian Shan since ATF initiation.

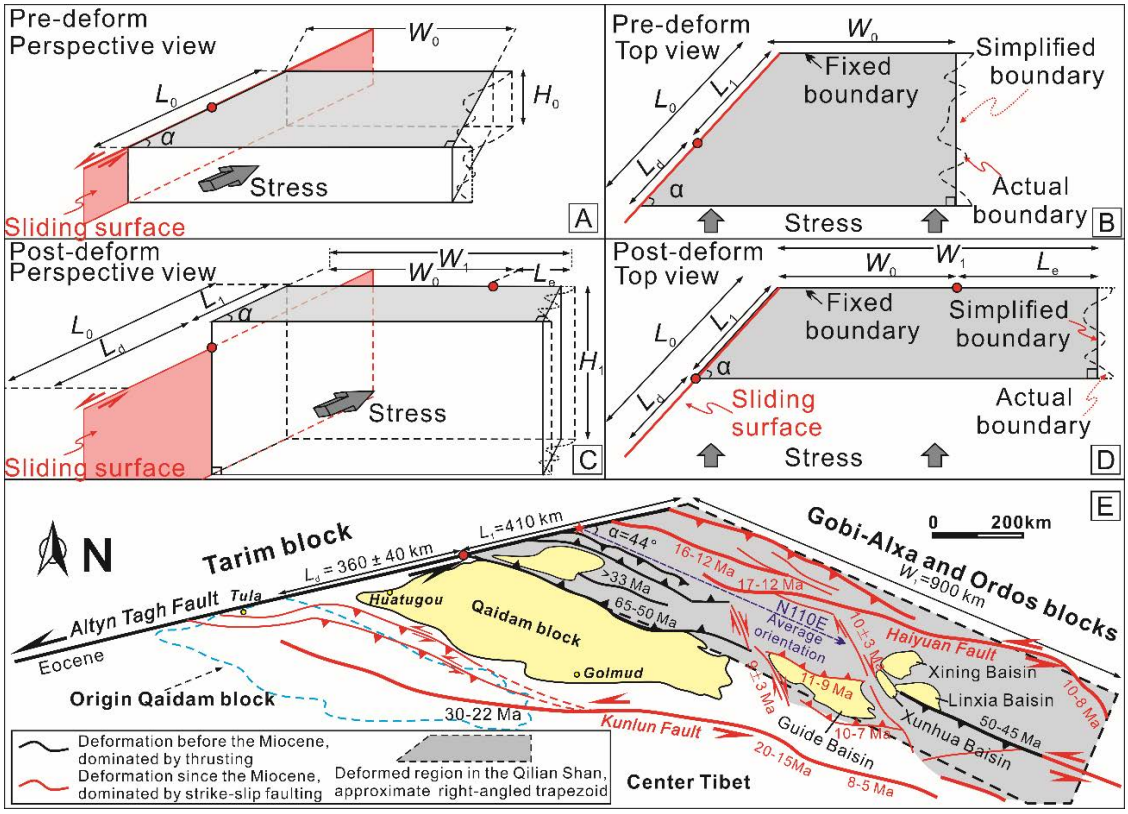


Fig.2 General model for balanced 3D crustal deformation in the Qilian Shan during the Cenozoic. (A) Perspective view of the Qilian Shan region before deformation. (B) Top view of the Qilian Shan region before deformation. (C) Perspective view of the Qilian Shan region after deformation. (D) Top view of the Qilian Shan region after deformation. (E) Sketch of the main active structures in the northern Tibetan plateau, modified from Duvallet al. (2013). To simplify the model, we consider the shape of the Qilian Shan to be an approximately right-angled trapezoid in plan view. The initiation ages are mainly compiled from previous work (e.g. Mocket al., 1999; Yin et al., 2002, 2007, 2008a,b; Jolivet et al., 2003; Lease et al., 2007; Bovet et al., 2009;Clarket al., 2010; Zheng et al., 2010; Craddock et al., 2011; Duvall et al., 2011, 2013; Hough et al., 2011; Yuan et al., 2011).

As shown by Yakovlev and Clark (2014), neglecting the density contrast between the upper and lower crust hardly changes the estimates of the modern orogenic mass. The occurrence of lower crustal flow in the northeastern Tibetan Plateau has recently been rejected (e.g. Lease et al., 2012; Li et al., 2014). From this conclusion and the lack of Cenozoic magmatism in the Qaidam Basin and Qilian Shan (Yin and Harrison, 2000), we consider the Cenozoic crust-mantle interaction and transition as sufficiently weak to be neglected in our model, and simplify the mass balance to volume balance.

Considering that both the Qaidam and Gobi-Alxa boundaries of the Qilian Shan are nearly parallel to the average orientation of the long-axis of the range during the deformation (Fig. 1B), we simplified the plane view geometry of the Qilian Shan into a right-angled trapezoid (Fig. 2). Based on isovolumetric balancing before and after crustal deformation in the Qilian Shan, the relations between the average amount of lateral crustal movement in the range, the initial crustal thickness, the present-day crustal thickness and the offset along the ATF, are described by:

$$V_0 = \frac{1}{2}\left[2\left(W_1 - L_e\right) + \left(L_d + L_1\right)\cos\alpha\right]\left(L_d + L_1\right)H_0\sin\alpha = V_1 = \frac{1}{2}\left(2W_1 + L_1\cos\alpha\right)L_1H_1\sin\alpha \quad (3)$$

where $V_0$ and $V_1$ are the constant crustal volumes of the Qilian Shan before the initiation of the ATF and at present, respectively; $W_0$ and $W_1$ are the widths of the northeastern front of the Qilian Shan before the initiation of the ATF and at present, respectively; $H_0$ and $H_1$ are the average crustal thicknesses of the Qilian Shan before the initiation of the ATF and at present, respectively; $L_e$ is the average amount of lateral crustal movement in the Qilian Shan.

We define the Cenozoic offset along the ATF to be 360 ± 40 km based both on newly identified piercing points along the ATF (Cheng et al., 2015) and as synthesis of previous estimates (Fig. 3A). The limited crustal shortening (<20 km) within the near-rigid Qaidam block (Zhou et al., 2006) is obviously insufficient to accommodate the enormous sinistral displacement along the ATF. $W_1$, $L_1$ and α are respectively estimated to about 900 km, 410 km and 44° from Google Earth measurements (Fig. 2). The present-day crustal thickness ($H_1$) in the Qilian Shan was calculated adding the average crustal thickness below sea-level (~60 km) (Fig. 1C; Tian et al., 2013; Li et al., 2014), the average amount of Cenozoic exhumation (~6 km) estimated from fission-track analysis (Jolivet et al., 2001), and the average elevation of the range (~4 km) measured on Google Earth. The obtained value for $H_1$ is ~70 km. The estimated initial crustal thickness ($H_0$) of the Qilian Shan is generally ranging from 40 to 55 km (Tian et al., 2013), with a probable value around 45 km (Meyer et al., 1998; Lease et al., 2012). In order to account for this uncertainty we calculated solutions for multiple values of H0 (35, 40, 45, 50 and 55 km). Relevant parameter constraints in this study are listed in Table

1. Darby et al. (2005) favor the hypothesis that the ATF bypasses the northern margin of Qilian Shan. However, we feel that results from a recent magnetotelluric survey (Xiao et al., 2015) are opposed to the hypothesis of Darby et al. (2005), and favor the scenario that the ATF has its eastward termination within the Qilian Shan. Further details and discussion are given in Appendix S1.

Table 1. Relevant parameter estimates used in this study

| Parameters | Estimation | Source |
|---|---|---|
| Cenozoic offset along the ATF ($L_d$) | 300~400 km, mean offset of 360 ± 40 km | Yue and Liou, 1999; Ritts and Biffi, 2000; Yin and Harrison, 2000; Soble et al., 2001; Yue et al., 2001; Yue et al., 2005; Gehrels et al., 2003; Searle et al., 2011; Cheng et al., 2015 |
| Average limb length of the Qilian Shan along the ATF at present day ($L_1$) | 410 km | Measured on Google Earth |
| Width of the northeastern front of the Qilian Shan at present ($W_1$) | 900 km | Measured on Google Earth |
| The average amount of Cenozoic exhumation since Eocene initiation ($H_e$) | ~6 km | Jolivet et al., 2001; Yin et al., 2002; Zheng et al., 2010 |
| Average elevation of the Qilian Shan range ($H_a$) | ~4 km | Measured on Google Earth |
| Average crustal thickness of the Qilian Shan range below sea-level ($H_b$) | ~60 km | Tian et al., 2011, 2013, 2014; Li et al., 2015 |
| Average crustal thickness at present ($H_1$) | ~70 km | $H_1 = H_e + H_a + H_b$ |
| Initial crustal thickness of the Qilian Shan ($H_0$) | 40~55 km<br>Probable 45 km | Meyer et al., 1998; Tian et al., 2011; Lease et al., 2012; Tian et al., 2013, 2014 |
| Constant angle between the strike direction of the ATF and the average orientation of the Qilian Shan long-axis in plane view (α) | 44° | Measured on Google Earth |
| N110E directed crustal lateral (extrusion) movement ($L_e$) | $L_e = W_1 + 1/2(L_1 + L_d)\cos\alpha - 1/2(2W_1 + L_1\cos\alpha)[L_1/(L_1 + L_d)](H_1/H_0)$ | |
| Crustal shortening within the Qilian Shan (N20E directed) ($L_s$) | $L_s = L_1\sin\alpha$ | |

Note: The Altyn Tagh Fault was defined as terminating at the northern margin of the Qilian Shan;

The Qaidam basin as a nearly-rigid block, which is based on the estimation by Braitenberg et al. (2003); Zhou et al. (2006), Pape et al. (2012). Detailed principles are given in Appendix S1.

## 4.4 Results

Considering a 360 ± 40 km offset along the ATF and a 45 km initial crustal thickness for the Qilian Shan, the calculated average N20E directed crustal shortening within the Qilian Shan is 250 ± 28 km, corresponding to a mean shortening strain of 43.8~49.4 %. From equation 3, using the previous values and the present-day crustal thickness of 70 km calculated above for the Qilian Shan, we obtain a value of ~250 to ~370 km of eastward crustal extrusion in the Qilian Shan during the Cenozoic. Detailed estimations of the crustal shortening and lateral extrusion are given in Figures 2-3, Tables 1-2 and Appendix S1.

Table. 2 N20E crustal shortening, shortening strain, and eastward extrusion estimates

| Initial crust thickness $H_0$ (km) | | ATF offsets $L_d > 0$ (km) | | Eastward extrusion $L_e > 0$ (km) | Shortening $L_s > 0$ (km) | Shortening Rate $Rs$ (%) |
|---|---|---|---|---|---|---|
| Total present crust thickness (including erosion) $H_1$ =70 km | | | | | | |
| 35 | | Max. | 400 | 131 | 278 | 49.4 |
| | | Min. | 320 | -14 | 222 | 43.8 |
| 40 | | Max. | 400 | 263 | 278 | 49.4 |
| | | Min. | 320 | 133 | 222 | 43.8 |
| 45 | | Max. | 400 | 367 | 278 | 49.4 |
| | | Min. | 320 | 247 | 222 | 43.8 |
| 50 | | Max. | 400 | 449 | 278 | 49.4 |
| | | Min. | 320 | 339 | 222 | 43.8 |
| 55 | | Max. | 400 | 517 | 278 | 49.4 |
| | | Min. | 320 | 413 | 222 | 43.8 |
| Probable | 45 | Probable | 360 | 309 | 250 | 46.8 |

Note: In order to account for this uncertainty we calculated solutions for multiple values of $H_0$ (35, 40, 45, 50 and 55 km). Further considering a mean offset of 360 km along the ATF ($L_d$), the Qilian Shan would have accommodated as much as 309 km of lateral deformation since the Eocene activation of the ATF. Detailed parameter estimates are given in Table 1 and Appendix S1.

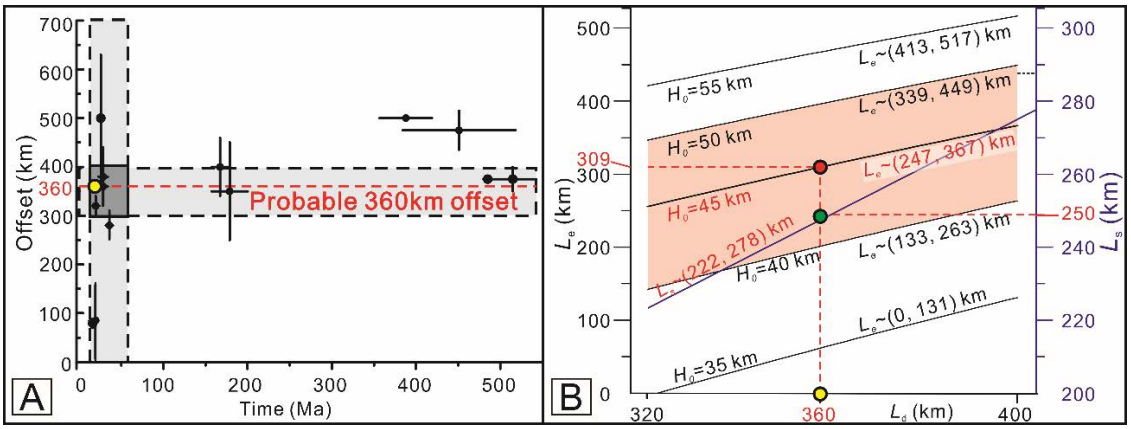


Fig.3 (A) Offset estimation along the Altyn Tagh Fault. Data were mainly compiled from Ritts and Biffi (2000), Yin et al. (2002), Gehrels et al. (2003), Yue et al. (2005); Searle et al. (2011) and Cheng et al. (2015). The grey rectangle represents the probable offset along the ATF and its probable time of initiation. In this study, we consider an offset of 360 ± 40 km along the ATF since its Eocene initiation based both on newly found piercing points in the western Qaidam Basin (Cheng et al., 2015) and on a summary of previous estimates, which is represented by the yellow circle. (B) Balanced calculation results. The black lines relate the amount of extrusion within the Qilian Shan ($L_e$) to the amount of offset along the ATF ($L_d$), while the blue line relates the amount of N20E directed crustal shortening within the Qilian Shan ($L_s$) to the amount of offset along the ATF ($L_d$). Considering the probable 360 km offset along the ATF (represented by the yellow circle in the figure) and an initial crustal thickness of 45 km in the Qilian Shan, there has been 309 km of eastward extrusion and 250 km of N20E directed crustal shortening in the Qilian Shan range, represented by the red circle and the green circle respectively. The pink region represents the possible range of $L_e$ and $L_s$. In this study, we define the N110E-directed elongation of the Qilian Shan as the eastward extrusion.

## 4.5 Discussion and Conclusions

The dramatic decrease in GPS-measured velocities across the Qilian Shan implies large-scale N20E directed crustal shortening, accommodated along the major SE-NW thrust faults that structure the range (Fig. 4; Zhang et al., 2004; Duvall and Clark et al., 2010). The calculated 250 ± 28 km crustal shortening corresponding to a shortening strain of 47 ± 3 % are in good agreement with independent, albeit indirect evidence suggesting that the shortening strain in the Qilian Shan range between 30 % and 50 %: (1) geomorphological and geological features in the Qilian Shan as well as available subsurface data from the Qaidam Basin and the Hexi Corridor suggest a ~30-50 % of post-Neogene crustal shortening across the area (Bally et al.,1986; Meyer et al.,1998), (2) modeling of crustal deformation using the geometry of the drainage system within the Qilian Shan results in an estimate of ~39 % of shortening strain across the range (Zhang et al., 2014), (3) integration of receiver function analysis and wide-angle reflection/refraction profiles across the Qilian Shan indicate 250 to

350 km of N30E directed crustal shortening through the range (Tian et al., 2014).

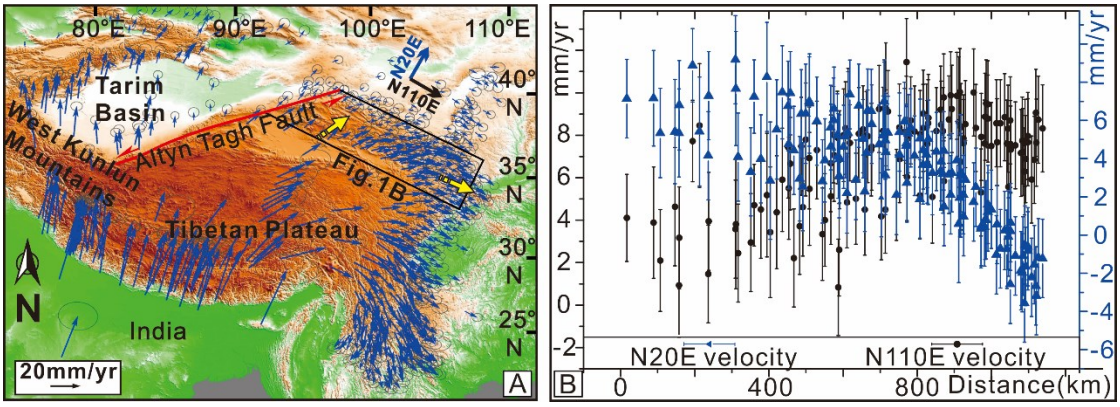


Fig.4 (A) Global Positioning System (GPS) velocities relative to stable Eurasia, modified from Zhang et al. (2004). The yellow arrows show the changes in orientation of the displacement vectors, clearly implying ongoing eastward crustal extrusion within the Qilian Shan region. (B) Strike-parallel and strike-perpendicular velocity (N110E) vs. distance. Solid-lined right trapezoid in the Fig. 4A represents the studied Qilian Shan region. GPS data from Gan et al. (2007). Details of the analytical method of geodetic velocities are given in Appendix S2. The sharp decrease in N20E directed GPS velocities from the northern Qaidam Basin to the Hexi Corridor and the large increase in N110E directed GPS velocities from the Altyn Tagh Range to the eastern Qilian Shan imply large amounts of crustal shortening and eastward extrusion within the Qilian Shan region at present.

Moreover, based on 3D isovolumetric deformation reconstruction, the Qilian Shan tectonic system accommodates between ~250 and ~370 km of eastward extrusion of the northeastern Tibetan Plateau crust (Fig. 3A). Although this eastward extrusion had already been evidenced by the N110E directed increase and N20E directed decrease of GPS velocities in the Qilian Shan (Fig. 4; Zhang et al., 2004), by strong earthquakes associated with sinistral faulting along strike-slip faults in the Qilian Shan (e.g. Haiyuan Fault; Lasserre et al., 1999), or by the occurrence of WNW–ESE and NW–SE oriented crustal and the upper mantle structures beneath the northeastern Tibetan Plateau (e.g. Li et al., 2011), few quantitative estimates of the total amount of Cenozoic displacement had been established up to now. Our estimate for crustal eastward extrusion in the Qilian Shan range provides one of the first quantitative budgets in the northeastern Tibetan Plateau.

We suggest that the >250 km eastward crustal extrusion is mainly accommodated by transcurrent motion on the main strike-slip faults that developed in the Qilian Shan (Fig. 1; Tab. 3). Since the eastward GPS velocities die out in the eastern margin of the plateau (Fig. 4; Zhang et al., 2004), this eastward crustal material flowing from the northeastern Tibetan Plateau should be partly absorbed by crustal thickening in the Qinling Orogen which initiated at 9~4 Ma slightly after the onset time of strike-slip faulting in the Qilian Shan (Fig. 5; Enkelmann et al., 2006). Finally, eastward crustal extrusion of the Qilian Shan would be a

possible driving mechanism for sinistral strike-slip faulting along the Haiyuan and West Qinling faults (Burchfiel et al., 1991; Duvall et al., 2011) and counter-clockwise rotation of the Ordos block (Zhang et al., 1998) leading to extension in the adjoining North China block graben systems, such as the Weihe Graben (Fig. 5B; Mercier et al., 2013).

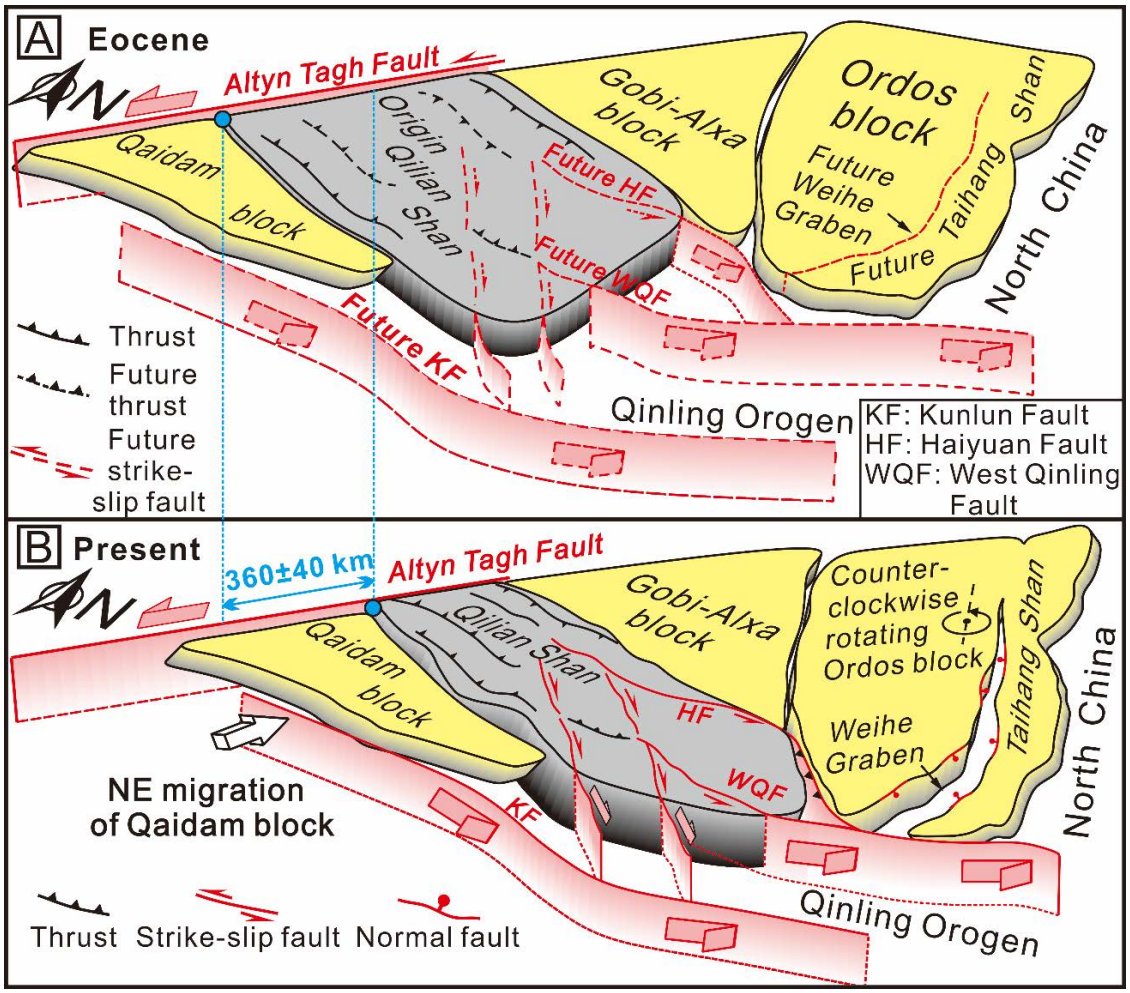


Fig.5 North-eastward migration model of the Qaidam block, corresponding to crustal shortening and eastward extrusion inthe Qilian Shan. (A) Pre-deformation phase. (B) Post-deformation phase. Note that hundreds of kilometres of offset along theATF have been absorbed within the Qilian Shan region and partly accommodated by N20E directed crustal shortening (250 ± 18 km). A large amount of this displacement was transferred further east through crustal transpression within the Qilian Shan. This eastward extrusion (~250–370 km) of crustal material from the north-eastern Tibetan Plateau is responsible for strike-slip faulting in the Qilian Shan region, crustal thickening in the Qinling region, anticlockwise rotation of the Ordos block, and extension in the Weihe Graben.

The lithospheric strike-slip Altyn Tagh Fault accommodated hundreds of kilometers of displacement between the Qaidam and Tarim blocks since its Eocene reactivation. However, the way the deformation is accommodated in the Qilian Shan and further east remains to be clarified. Based on the 360 km northeastward migration of the relatively rigid Qaidam block along the Altyn Tagh Fault and 3D isovolumetric balance of the crustal deformation within the

Altyn Tagh Fault – Qilian Shan system, we demonstrate that 250 ± 28 km (43.8~49.4 %) of N20E directed crustal shortening and an additional ~250 to ~370 km of eastward motion of the Qilian Shan crust that must be accounted for by strike-slip faulting in the Qilian Shan and crustal thickening in the Qinling area, as well as extension in the adjoining North China block graben systems.

Table.3 Potential structures that accommodate the eastward crustal extrusion in the Qilian Shan

| Name of structure | Strike-slip faulting Initiation (Ma) | Slip rate (mm/yr) | Offset (km) |
|---|---|---|---|
| Haiyuan fault | 17~12 (Duvall et al., 2013) | 4~6 (Zhang et al., 1988; Gaudemer et al., 1995; Li et al., 2009; Zheng et al., 2012) | 60~90 (Gaudemer et al., 1995;Ding et al., 2004) |
| Shulenanshan fault | 23 (Ding et al., 2004) | 6.5 (Ding et al., 2004) | ~150 (Ding et al., 2004) |
| Zhongwei-Tongxing fault | 5.3-3.4 (Ding et al., 2004) | 4–7 (Ding et al., 2004) | 20-25 (Ding et al., 2004) |
| West Qinling fault | 16 (Wang et al., 2012) | 2 (Li et al., 2005) | ≥ 25 (Ratschbacher et al., 2003) |
| Northern Qilian fault | 10 (Zheng et al., 2010) | ~1 (Zheng et al., 2010) | ~10 (Zheng et al., 2010) |
| Elashan fault | 9 ± 3 (Yuan et al., 2011) | 1.1 ± 0.3 mm/yr (Yuan et al., 2013) | 9~12 (Yuan et al., 2011) |
| Riyueshan fault | 10 ± 3 (Yuan et al., 2011) | 1.2 ± 0.4 (Yuan et al., 2013) | 6-12 (Yuan et al., 2011) |
| Changma fault | ≤ 23 Oligocene (Kang et al., 1986) | 1~5 (Peltzer et al., 1988; Zheng et al., 2012) | 20~120 |

## Acknowledgements

We thank Science Editor Jason Phipps Morgan for providing constructive feedback. This work was funded by the National S&T Major Project of China (No. 2011ZX05009-001) and the China Scholarship Council - Campus France Egide Cai Yuanpei program (201404490136; N° 32393WL(2014)).

## Reference

Bally, A.W., Chou, I.M., Clayton, R., Heugster, H.P., Kidwell, S., Meckel, L.D., Ryder, R.T.,

Watts, A.B. and Wilson, A.A., 1986. Notes on Sedimentary Basins in China, Report of the American Sedimentary Basins Delegation to the People's Republic of China, August 17–September 8, open file report 86–327, USGS.

Bovet, P.M., Ritts, B.D., Gehrels, G., et al., 2009. Evidence of Miocene crustal shortening in the north Qilian Shan from Cenozoic stratigraphy of the western Hexi Corridor, Gansu Province, China. American Journal of Science, 309, 290-329.

Braitenberg, C., Wang, Y., Fang, J. and Hsu, H., 2003. Spatial variations of flexure parameters over the Tibet–Quinghai plateau. Earth and Planetary Science Letters, 205, 211-224.

Burchfiel, B.C., Quidong, D., Molnar, P., et al., 1989. Intracrustal detachment within zones of continental deformation. Geology, 17, 748-752.

Burchfiel, B., Zhang, P., Wang, Y., et al., 1991. Geology of the Haiyuan fault zone, Ningxia-Hui Autonomous Region, China, and its relation to the evolution of the northeastern margin of the Tibetan Plateau. Tectonics, 10, 1091-1110.

Cheng, F., Guo, Z., Jenkins, H.S., et al., 2015. Initial rupture and displacement on the Altyn Tagh fault, northern Tibetan Plateau: Constraints based on residual Mesozoic to Cenozoic strata in the western Qaidam Basin. Geosphere, 11, 921-942.

Clark, M.K. and Royden, L.H., 2000. Topographic ooze: Building the eastern margin of Tibet by lower crustal flow. Geology, 28, 703-706.

Clark, M.K., Farley, K.A., Zheng, D., et al., 2010. Early Cenozoic faulting of the northern Tibetan Plateau margin from apatite (U–Th)/He ages. Earth and Planetary Science Letters, 296, 78-88.

Cowgill, E., Yin, A., Harrison, T.M. and Xiao-Feng, W., 2003. Reconstruction of the Altyn Tagh fault based on U-Pb geochronology: Role of back thrusts, mantle sutures, and heterogeneous crustal strength in forming the Tibetan Plateau. Journal of Geophysical Research, 108, 2346.

Craddock, W., Kirby, E. and Zhang, H., 2011. Late Miocene-Pliocene range growth in the interior of the northeastern Tibetan Plateau. Lithosphere, 3, 420-438.

Darby, B.J., Ritts, B.D., Yue, Y. and Meng, Q., 2005. Did the Altyn Tagh fault extend beyond the Tibetan Plateau? Earth and Planetary Science Letters, 240, 425-435.

Ding, G., Chen, J., Tian, Q., et al., 2004. Active faults and magnitudes of left-lateral displacement along the northern margin of the Tibetan Plateau. Tectonophysics, 380, 243-260.

Dupont-Nivet, G., Butler, R.F., Yin, A. and Chen, X., 2002. Paleomagnetism indicates no Neogene rotation of the Qaidam Basin in northern Tibet during Indo-Asian collision. Geology, 30, 263-266.

Dupont-Nivet, G., Horton, B., Butler, R., et al., 2004. Paleogene clockwise tectonic rotation of the Xining-Lanzhou region, northeastern Tibetan Plateau. J. Geophys. Res, 109, B04401.

Duvall, A.R. and Clark, M.K., 2010. Dissipation of fast strike-slip faulting within and beyond northeastern Tibet. Geology, 38, 223-226.

Duvall, A.R., Clark, M.K., van der Pluijm, B.A. and Li, C., 2011. Direct dating of Eocene reverse faulting in northeastern Tibet using Ar-dating of fault clays and low-temperature thermochronometry. Earth and Planetary Science Letters, 304, 520-526.

Duvall, A.R., Clark, M.K., Kirby, E., et al., 2013. Low-temperature thermochronometry along the Kunlun and Haiyuan Faults, NE Tibetan Plateau: Evidence for kinematic change during late-stage orogenesis. Tectonics, 32, 1190-1211.

England, P. and Houseman, G., 1986. Finite strain calculations of continental deformation: 2. Comparison with the India-Asia collision zone. Journal of Geophysical Research: Solid Earth (1978–2012), 91, 3664-3676.

Enkelmann, E., Ratschbacher, L., Jonckheere, R., et al., 2006. Cenozoic exhumation and deformation of northeastern Tibet and the Qinling: Is Tibetan lower crustal flow diverging around the Sichuan Basin? Geological Society of America Bulletin, 118, 651-671.

Gaudemer, Y., Tapponnier, P., Meyer, B., et al., 1995. Partitioning of crustal slip between linked, active faults in the eastern Qilian Shan, and evidence for a major seismic gap, the 'Tianzhu gap', on the western Haiyuan Fault, Gansu (China). Geophysical Journal International, 120, 599-645.

Gehrels, G.E., Yin, A. and Wang, X.F., 2003. Magmatic history of the northeastern Tibetan Plateau. Journal of Geophysical Research, 108, 2423.

Hough, B.G., Garzione, C.N., Wang, Z., et al., 2011. Stable isotope evidence for topographic growth and basin segmentation: Implications for the evolution of the NE Tibetan Plateau. Geological Society of America Bulletin, 123, 168-185.

Jolivet, M., Roger, F., Arnaud, N., et al., 1999. Histoire de l'exhumation de l'Altun Shan: indications sur l'âge de la subduction du bloc du Tarim sous le système de l'Altyn Tagh (Nord Tibet). Comptes Rendus de l'Académie des Sciences-Series IIA-Earth and Planetary Science, 329, 749-755.

Jolivet, M., Brunel, M., Seward, D., et al., 2001. Mesozoic and Cenozoic tectonics of the northern edge of the Tibetan plateau: fission-track constraints. Tectonophysics, 343, 111-134.

Jolivet, M., Brunel, M., Seward, D., et al., 2003. Neogene extension and volcanism in the Kunlun Fault Zone, northern Tibet: New constraints on the age of the Kunlun Fault. Tectonics, 22, 1052.

Kang, L., 1986. Study of paleo-earthquakes in Changma Fault zone. Journal of seismology, 12, 16-22 (in Chinese with English abstract).

Lasserre, C., Morel, P.H., Gaudemer, Y., et al., 1999. Postglacial left slip rate and past occurrence of M≥ 8 earthquakes on the western Haiyuan fault, Gansu, China. Journal of Geophysical Research: Solid Earth (1978–2012), 104, 17633-17651.

Lease, R.O., Burbank, D.W., Gehrels, G.E., et al., 2007. Signatures of mountain building: Detrital zircon U/Pb ages from northeastern Tibet. Geology, 35, 239-242.

Lease, R.O., Burbank, D.W., Clark, M.K., et al., 2011. Middle Miocene reorganization of deformation along the northeastern Tibetan Plateau. Geology, 39, 359-362.

Lease, R.O., Burbank, D.W., Zhang, H., et al., 2012. Cenozoic shortening budget for the northeastern edge of the Tibetan Plateau: Is lower crustal flow necessary? Tectonics, 31, TC3011.

Le Pape, F., Jones, A.G., Vozar, J. and Wenbo, W., 2012. Penetration of crustal melt beyond the Kunlun Fault into northern Tibet. Nature Geoscience, 5, 330-335.

Li, C., 2005. Quantitative researches on several prominent faults in the NE Margin of the Tibetan plateau. Doctoral dissertation, China Earthquake Administration, Beijing, 230 pp (in Chinese with English abstract).

Li, C., Zhang, P.Z., Yin, J. and Min, W., 2009. Late Quaternary left-lateral slip rate of the Haiyuan fault, northeastern margin of the Tibetan Plateau. Tectonics, 28.

Li, J., Wang, X. and Niu, F., 2011. Seismic anisotropy and implications for mantle deformation beneath the NE margin of the Tibet plateau and Ordos plateau. Physics of the Earth and Planetary Interiors, 189, 157-170.

Li, X., Li, H., Shen, Y., et al., 2014. Crustal Velocity Structure of the Northeastern Tibetan Plateau from Ambient Noise Surface-Wave Tomography and Its Tectonic Implications. Bulletin of the Seismological Society of America, 104, 1045-1055.

Mercier, J.L., Vergely, P., Zhang, Y.Q., et al., 2013. Structural records of the Late Cretaceous–Cenozoic extension in Eastern China and the kinematics of the Southern Tan-Lu and Qinling Fault Zone (Anhui and Shaanxi provinces, PR China). Tectonophysics, 582, 50-75.

Métivier, F., Gaudemer, Y., Tapponnier, P. and Meyer, B., 1998. Northeastward growth of the Tibet plateau deduced from balanced reconstruction of two depositional areas: The Qaidam and Hexi Corridor basins, China. Tectonics, 17, 823-842.

Meyer, B., Tapponnier, P., Bourjot, L., et al., 1998. Crustal thickening in Gansu-Qinghai, lithospheric mantle subduction, and oblique, strike-slip controlled growth of the Tibet plateau. Geophysical Journal International, 135, 1-47.

Mock, C., Arnaud, N.O. and Cantagrel, J.M., 1999. An early unroofing in northeastern Tibet? Constraints from $^{40}Ar/^{39}Ar$ thermochronology on granitoids from the eastern Kunlun range (Qianghai, NW China). Earth and Planetary Science Letters, 171, 107-122.

Molnar, P. and Tapponnier, P., 1975. Cenozoic tectonics of Asia: Effects of a continental collision. Science, 189, 419-426.

Peltzer, G., Tapponnier, P., Gaudemer, Y., et al., 1988. Offsets of late Quaternary morphology, rate of slip, and recurrence of large earthquakes on the Chang Ma fault (Gansu, China). Journal of Geophysical Research: Solid Earth (1978–2012), 93, 7793-7812.

Ratschbacher, L., Frisch, W., Liu, G. and Chen, C., 1994. Distributed deformation in southern and western Tibet during and after the India-Asia collision. Journal of Geophysical Research: Solid Earth (1978–2012), 99, 19917-19945.

Ratschbacher, L., Hacker, B.R., Calvert, A., et al., 2003. Tectonics of the Qinling (Central China): tectonostratigraphy, geochronology, and deformation history. Tectonophysics, 366, 1-53.

Ritts, B.D. and Biffi, U., 2000. Magnitude of post-Middle Jurassic (Bajocian) displacement on the central Altyn Tagh fault system, northwest China. Geological Society of America Bulletin, 112, 61-74.

Royden, L.H., Burchfiel, B.C., King, R.W., et al., 1997. Surface deformation and lower crustal flow in eastern Tibet. Science, 276, 788-790.

Searle, M., Elliott, J., Phillips, R. and Chung, S.-L., 2011. Crustal–lithospheric structure and continental extrusion of Tibet. Journal of the Geological Society, 168, 633-672.

Sobel, E.R., Arnaud, N., Jolivet, M., et al., 2001. Jurassic to Cenozoic exhumation history of the Altyn Tagh range, northwest China, constrained by $^{40}Ar/^{39}Ar$ and apatite fission track thermochronology. Geological Society of America Memoirs, 194, 247-267.

Tapponnier, P. and Molnar, P., 1977. Active faulting and tectonics in China. Journal of Geophysical Research, 82, 2905-2930.

Tapponnier, P., Xu, Z.Q., Roger, F., et al., 2001. Oblique stepwise rise and growth of the Tibet Plateau. Science, 294, 1671-1677.

Tian, X., Teng, J., Zhang, H., et al., 2011. Structure of crust and upper mantle beneath the Ordos Block and the Yinshan Mountains revealed by receiver function analysis. Physics of the Earth and Planetary Interiors, 184, 186-193.

Tian, X. and Zhang, Z., 2013. Bulk crustal properties in NE Tibet and their implications for deformation model. Gondwana Research, 24, 548-559.

Tian, X., Liu, Z., Si, S. and Zhang, Z., 2014. The crustal thickness of NE Tibet and its

implication for crustal shortening. Tectonophysics, 634, 198-207.

van Hinsbergen, D.J., Kapp, P., Dupont-Nivet, G., et al., 2011. Restoration of Cenozoic deformation in Asia and the size of Greater India. Tectonics, 30, TC5003.

Wang, E., 1996. Early Tertiary Strike Slip Displacement AlongQilian Mountain Range And Associated Sedimentation And Deformation in the Lanzhou Basin, 30th International Geological Congress, Beijing, Abstracts, 1, 268.

Wang, E., Xu, F.Y., Zhou, J.X., et al., 2006. Eastward migration of the Qaidam basin and its implications for Cenozoic evolution of the Altyn Tagh fault and associated river systems. Geological Society of America Bulletin, 118, 349-365.

Wang, Z., Zhang, P., Garzione, C.N., et al., 2012. Magnetostratigraphy and depositional history of the Miocene Wushan basin on the NE Tibetan plateau, China: implications for middle Miocene tectonics of the West Qinling fault zone. Journal of Asian Earth Sciences, 44, 189-202.

Wittlinger, G., Tapponnier, P., Poupinet, G., et al., 1998. Tomographic evidence for localized lithospheric shear along the Altyn Tagh fault. Science, 282, 74-76.

Wu, L., Xiao, A.C., Yang, S.F., et al., 2012. Two-stage evolution of the Altyn Tagh Fault during the Cenozoic: new insight from provenance analysis of a geological section in NW Qaidam Basin, NW China. Terra Nova, 24, 387-395.

Xiao, Q., Shao G., Liu-Zeng J., et al., 2015. Eastern termination of the Altyn Tagh Fault, western China: Constraints from a magnetotelluric survey, J. Geophys. Res. Solid Earth, 120, doi: 10.1002/2014JB011363.

Yakovlev, P.V. and Clark, M.K., 2014. Conservation and redistribution of crust during the Indo-Asian collision .Tectonics, 33, 1016-1027.

Yin, A. and Harrison, T.M., 2000. Geologic evolution of the Himalayan-Tibetan orogen. Annual Review of Earth and Planetary Sciences, 28, 211-280.

Yin, A., Rumelhart, P., Butler, R., et al., 2002. Tectonic history of the Altyn Tagh fault system in northern Tibet inferred from Cenozoic sedimentation. Geological Society of America Bulletin, 114, 1257-1295.

Yin, A., Dang, Y.Q., Zhang, M., et al., 2007. Cenozoic tectonic evolution of Qaidam basin and its surrounding regions (part 2): Wedge tectonics in southern Qaidam basin and the Eastern Kunlun Range. Geological Society of America Special Papers, 433, 369-390.

Yin, A., Dang, Y.Q., Wang, L.C., et al., 2008a. Cenozoic tectonic evolution of Qaidam basin and its surrounding regions (Part 1): The southern Qilian Shan-Nan Shan thrust belt and northern Qaidam basin. Geological Society of America Bulletin, 120, 813-846.

Yin, A., Dang, Y.Q., Zhang, M., et al., 2008b. Cenozoic tectonic evolution of the Qaidam basin and its surrounding regions (Part 3): Structural geology, sedimentation, and regional tectonic reconstruction. Geological Society of America Bulletin, 120, 847-876.

Yu, X.J., Fu, S.T., Guan, S.W., et al., 2014. Paleomagnetism of Eocene and Miocene sediments from the Qaidam basin: Implication for no integral rotation since the Eocene and a rigid Qaidam block. Geochemistry, Geophysics, Geosystems, 15, 2109-2127.

Yuan, D.Y., Champagnac, J.D., Ge, W.P., et al., 2011. Late Quaternary right-lateral slip rates of faults adjacent to the lake Qinghai, northeastern margin of the Tibetan Plateau. Geological Society of America Bulletin, 123, 2016-2030.

Yuan, D.Y., Ge, W.P., Chen, Z.W., et al., 2013. The growth of northeastern Tibet and its relevance to large-scale continental geodynamics: A review of recent studies. Tectonics, 32, 2013TC003348.

Yue, Y.J. and Liou, J.G., 1999. Two-stage evolution model for the Altyn Tagh fault, China. Geology, 27, 227-230.

Yue, Y.J., Ritts, B.D. and Graham, S.A., 2001. Initiation and long-term slip history of the Altyn Tagh Fault. International Geology Review, 43, 1087-1093.

Yue, Y.J., Graham, S.A., Ritts, B.D. and Wooden, J.L., 2005. Detrital zircon provenance evidence for large-scale extrusion along the Altyn Tagh fault. Tectonophysics, 406, 165-178.

Zhang, P., Molnar, P., Burchfiel, B., et al., 1988. Bounds on the Holocene slip rate of the Haiyuan fault, north-central China. Quaternary Research, 30, 151-164.

Zhang, Y.Q., Mercier, J.L. and Vergély, P., 1998. Extension in the graben systems around the Ordos (China), and its contribution to the extrusion tectonics of south China with respect to Gobi-Mongolia. Tectonophysics, 285, 41-75.

Zhang, P.Z., Shen, Z., Wang, M., et al., 2004. Continuous deformation of the Tibetan Plateau from global positioning system data. Geology, 32, 809-812.

Zhang, H.P., Zhang, P.Z., Zheng, D.W., et al., 2014. Transforming the Miocene Altyn Tagh fault slip into shortening of the north-western Qilian Shan: insights from the drainage basin geometry. Terra Nova, 26, 216-221.

Zhao, W.L. and Morgan, W.J., 1987. Injection of Indian crust into Tibetan lower crust: A two-dimensional finite element model study. Tectonics, 6, 489-504.

Zheng, D., Clark, M.K., Zhang, P., et al., 2010. Erosion, fault initiation and topographic growth of the North Qilian Shan (northern Tibetan Plateau). Geosphere, 6, 937-941.

Zheng, W., Zhang, P., He, W., et al., 2013. Transformation of displacement between strike-slip and crustal shortening in the northern margin of the Tibetan Plateau: Evidence from decadal

GPS measurements and late Quaternary slip rates on faults. Tectonophysics, 584, 267-280.
Zhou, J.X., Xu, F.Y., Wang, T.C., et al., 2006. Cenozoic deformation history of the Qaidam Basin, NW China: Results from cross-section restoration and implications for Qinghai–Tibet Plateau tectonics. Earth and Planetary Science Letters, 243, 195-210.
Zhuang, G., Hourigan, J.K., Ritts, B.D. and Kent-Corson, M.L., 2011. Cenozoic multiple-phase tectonic evolution of the northern Tibetan Plateau: Constraints from sedimentary records from Qaidam basin, Hexi Corridor, and Subei basin, northwest China. American Journal of Science, 311, 116-152.

## 4.6 Chapter summary

The lithospheric strike-slip Altyn Tagh Fault accommodated hundreds of kilometers of displacement between the Qaidam and Tarim blocks since its Eocene reactivation. However, the way the deformation is accommodated in the Qilian Shan and further east remains to be clarified. Based on the 360 km northeastward migration of the relatively rigid Qaidam block along the Altyn Tagh Fault and 3D isovolumetric balance of the crustal deformation within the Altyn Tagh Fault – Qilian Shan system, we demonstrate that 250 ± 28 km (43.8~49.4 %) of N20E directed crustal shortening and an additional ~250 to ~370 km of eastward motion of the Qilian Shan crust that must be accounted for by strike-slip faulting in the Qilian Shan and crustal thickening in the Qinling area, as well as extension in the adjoining North China block graben systems.

# Chapter 5 Strike-slip superimposed Qaidam Basin and its control on oil and gas accumulation

***Paper published in Petroleum Exploration and Development, 2015, vol. 42, pp. 778-789***

**Strike-slip superimposed Qaidam Basin and its control on oil and gas accumulation, NW China**

FU Suotang[1], MA Dade[1], GUO Zhaojie[2,†], **CHENG Feng**[2]

[1] Qinghai Oilfield Company, PetroChina, Dunhuang, Gansu 736202, China;
[2] Key Laboratory of Orogenic Belts and Crustal Evolution, Ministry of Education, School of Earth and Space Sciences, Peking University, Beijing 100871, China
[†] Corresponding author. Tel.: + 86-10-62753545; fax: + 86-10-62758610. E-mail address: zjguo@pku.edu.cn (Z.J. Guo)

Note: *This English version is translated from a Chinese version by the editorial office of the journal* ***Petroleum Exploration and Development***. The online version of this contribution can be found as: ***Fu, S., Ma, D., Guo, Z., Cheng, F., 2015. Strike-slip superimposed Qaidam Basin and its control on oil and gas accumulation, NW China. Petroleum Exploration and Development 42, 778-789, doi: 10.1016/S1876-3804(15)30074-4.***

## Abstract

Based on detailed field survey in the western Qaidam Basin, combined with petroleum exploration practices in recent years, this study suggests that the Qaidam Basin is a strike-slip superimposed basin jointly controlled by the left-lateral strike-slip Altyn Tagh and East Kunlun faults. The Altyn Tagh fault acts as the major controlling boundary, while the East Kunlun fault only controls the local evolution of the southern edge of the basin. To the east, the northern Qaidam-Qilian Shan thrust-fold belt passively accommodates the northeastward displacement along the Altyn Tagh fault through NE-SW directed shortening. In the India-Asia collision background, the left-lateral strike-slip faulting along the Altyn Tagh fault initiated from the early Eocene, forcing the Qaidam Basin to move northeastward, causing the

thrust and slip deformation of the NW-SE faults in northern Qaidam margin-Qilian Mountain area, and the deposition of the Cenozoic since the Paleogene Lulehe Formation. During the Paleogene, the northern Qaidam Basin developed coarse-grained sediments like that in a foreland basin, forming poor quality source rocks; while the southwestern Qaidam Basin was an extensional sag basin where good quality source rocks deposited. By the early Miocene, left-lateral faulting along the Kunlun fault became active, leading to the formation of a series of en-echelon faults (e.g. the Kunbei fault, the Arlar fault and the Hongliuquan fault). These faults gradually migrated northward, their kinematics changing from left-lateral strike-slip motion to NE-SW transpression. Strike-slip-related structures controlled by those faults (e.g. the Yingxiongling structure) are ideal places for oil and gas accumulation from Paleogene source rocks. To sum up, the Qaidam Basin is a strike-slip superimposedbasin jointly controlled by the left-lateral strike-slip AltynTagh and East Kunlun faults. The temporal and spatial superimposition of these two strike-slip faults during the Cenozoic controlled theevolution of the basin as well as the oil and gas accumulation.

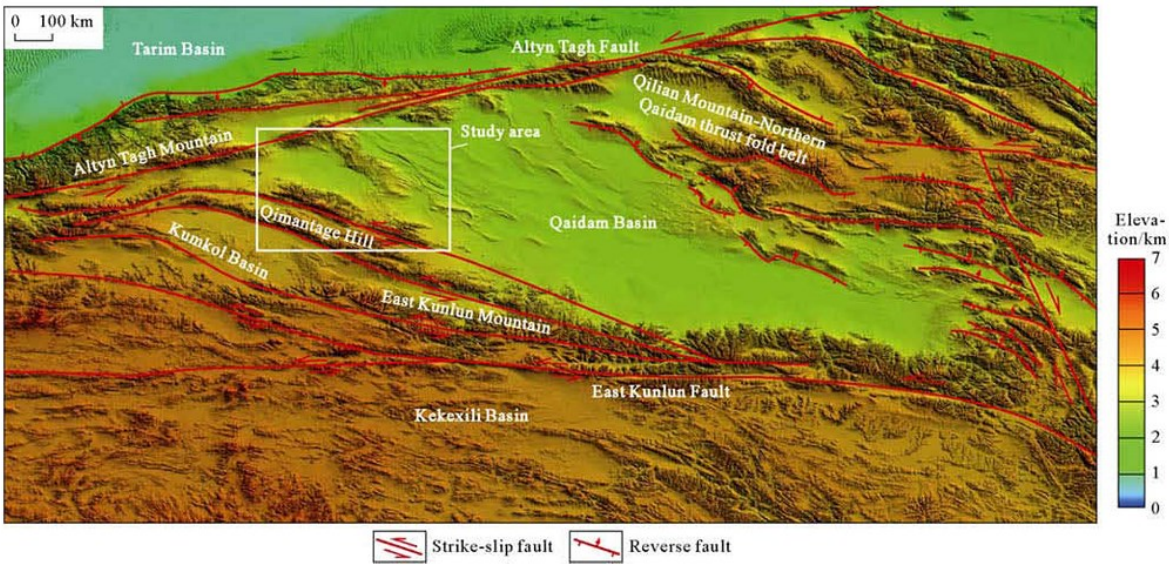


Fig. 1. Topography and distribution of the main faults of the Qaidam Basin and its periphery (Topographic data adopts the SRTMdata in 90 m resolution[17]).

## 5.1 Introduction

The Qaidam Basin in triangular shape is located in the northern margin of the Tibetan Plateau and held in between Altyn Tagh, East Kunlun and Qilian Mountain. It is the largest oil and gas basin in the Tibetan Plateau. Since Well Qie 6 drilled in the southwestern Qaidam Basin obtained high-yield industrial oil flow in 2007, a series of large oil and gas fields have been successively discovered in the Qiekelike, Yingdong, Dongping and Yingxi regions,

opening a new page of oil and gas exploration in plateau basins. The Qaidam Basin has not only unique tectonic setting and attributes, but also unique hydrocarbon accumulation process and pattern, since (1) it is the only basin held by two large strike-slip faults (Altyn Tagh and East Kunlun strike-slip faults) in the world; (2) it is the only large oil and gas-bearing basin in the interior Tibetan Plateau; (3) it is the only large oil and gas-bearing basin that develops Cenozoic continental reservoirs in western China. Therefore, the Qaidam Basin must have unique tectonic and hydrocarbon accumulation theory as it has different characteristics and petroleum exploration practice from other basins.

## 5.2 Similarities, differences and key points of the cognition

The genesis and attributes of the Qaidam Basin is a subject of intense debate for a long time. Previous petroleum geologists believed that the Qaidam Basin had experienced three tectonic evolution stages during the Mesozoic and Cenozoic, Jurassic to Cretaceous rifting stage, Paleogene depression stage and Neogene inversion stage[1]. With the deepening of exploration, some researchers advanced the Qaidam Basin experienced two tectonic evolution stages, Cretaceous to Paleogene extensional stage and Neogene compressional stage[2]. In recent years, some researchers put forward a new finding that the Qaidam Basin was a superimposed basin, which means it was an analogous foreland basin superimposed on the Jurassic to Paleogene fold basement pull-apart basin since the Neogene[3-4]. In addition, some researchers considered the Qaidam Basin had experienced four evolution stages based on the latest oil and gas exploration results, Jurassic rifting stage, Cretaceous compressional stage, Paleogene stable and wide basin/transpression stage and Neogene compressional and intracontinential depression stage[5]. The different recognitions on the tectonic evolution and attributes of the Qaidam Basin are ascribed to the different recognitions on the relationship between the Qaidam Basin and its peripheral orogenic belts (Fig. 1). Most studies in early stage reached the conclusion that the formation of the Qaidam Basin was related to the northward overthrust of the East Kunlun Mountain[6-9], which means the Qaidam Basin is the foreland basin of the East Kunlun Mountain which continues obducting northwards along a series south-dipping faults or converted transpression system in the southern Qaidam Basin[10-11]. However, based on the seismic profile collected from the interior basin, Yin et al.[12]put forward an opposite view point that a large set of wedge structure developed beneath the Qaidam Basin obducted the Qaidam Basin to the East Kunlun Mountain southwards from Qilian piedmont, indicating the Qaidam Basin was not only a foreland basin of the Qilian

Mountain, but also a piggyback basin of the East Kunlun Mountain[12-14]. In addition, some researchers believed the Qaidam Basin was part of the Tarim Basin before the Oligocene based on the stratigraphic correlation results between the southwestern margin of the Tarim Basin and the western Qaidam Basin, the left-lateral strike-slip of Altyn Tagh fault initiated from the Oligocene resulted in the separation of Qaidam Basin from the Tarim Basin, after that, the Qaidam Basin gradually evolved into a large inter-mountain compressional basin.

Moreover, they further pointed out that the flexural folding occurred in the upper crust of the northern Tibetan Plateau was the major cause of the formation of the Qaidam Basin[15-16]. Although there is controversy over the genesis and attributes of the Qaidam Basin, with the promotion of seismic exploration in recent years, the basic geological features of the Qaidam Basin have been gradually revealed. Based on the major breakthroughs in magnetic stratigraphy, paleobotany and seismic exploration, the Cenozoic stratigraphic sequence and age of the entire basin have been established and accurately constrained, in which eight sets of rock stratigraphic units are identified from bottom to top[18-24], including Lulehe Formation, Lower Member of Lower Ganchaigou Formation, Upper Member of Lower Ganchaigou Formation, Upper Ganchaigou Formation, Lower Youshashan Formation, Upper Youshashan Formation, Shizigou Formation and Qigequan Formation (Fig. 2). Moreover, the Cenozoic stratigraphic distribution across the entire basin reflects the depocenter of the Qaidam Basin has been located in the axis center of the basin since Lulehe Period, and gradually migrated eastwards[20-22].At the same time, controlled by the left-lateral strike-slip of Altyn Tagh faults, the entire Qaidam Basin migrated

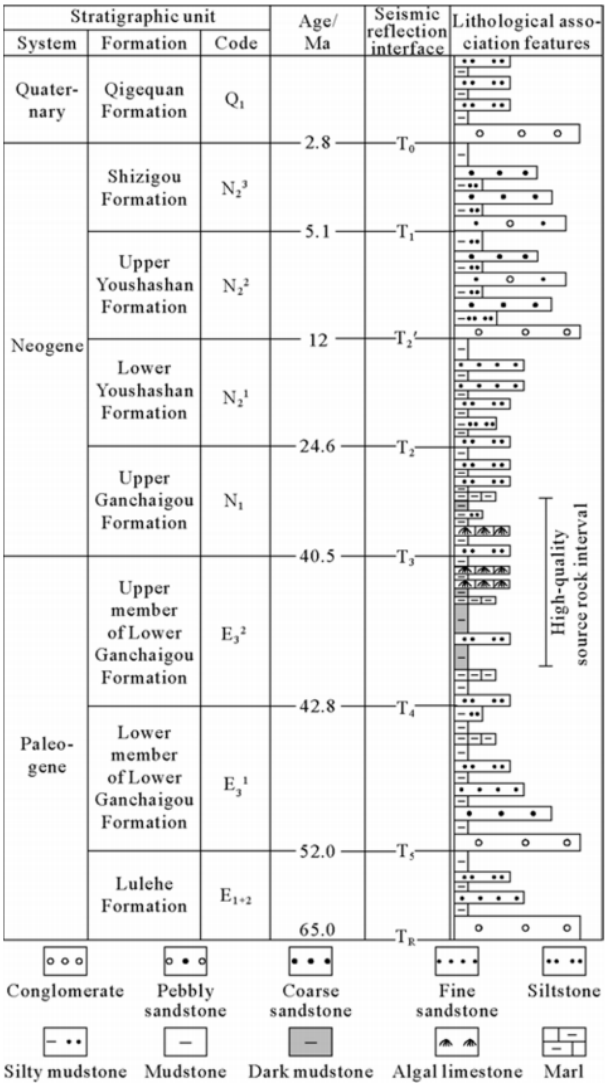

Fig. 2. Composite stratigraphic column of the Cenozoic strata in the western Qaidam Basin.

northeastwards as a rigid block[25-26]. Numerous high-resolution 2D and 3D seismic profiles reveal the crust deformation in northern margin of the Qaidam Basin started in the Eocene[12-13], but the Miocene growth strata developing in Altyn Tagh and East Kunlun piedmont in the western part of the Qaidam Basin indicate the crustal deformation of the East Kunlun Mountain occurred in the Miocene[12-13]. In addition, a set of fine-grained salty lacustrine deposits have been discovered in the Paleogene-Neogene strata in the western Qaidam Basin during oil and gas exploration, which are the major high-quality source rocks in the upper member of Lower Ganchaigou Formation and Upper Ganchaigou Formation (Fig. 2), while the Paleogene in the northern margin of the Qaidam Basin is a set of coarse clastic deposits of foreland basin without source rocks[27]. The geological features and exploration results have provided good foundation for further study of the Qaidam Basin. It can be seen that finding out the tectonic relationship between the Qaidam Basin and its peripheral orogenic belts is the key to revealing the Cenozoic evolution, clarifying the genesis and attributes and the hydrocarbon accumulation theory of the Qaidam Basin.

## 5.3 Structural features of peripheral Qaidam Basin

### 5.3.1 Altyn Tagh left-lateral strike-slip fault – North Qaidam thrust system

Altyn Tagh fault, a large left-lateral strike-slip fault at the margin of the Tibetan Plateau, defines the western boundary of the Qaidam Basin (Fig. 1), and its movement controlled the evolution of the Qaidam Basin during the Cenozoic, thereby, exploring the active regularity and tectonic evolution history of the Altyn Tagh fault during the Cenozoic is of great significance for recognizing the Cenozoic evolution of the Qaidam Basin[28-31]. Two key issues need to be clarified in studying the Cenozoic tectonic activity of Altyn Tagh strike-slip fault, the initial duration and displacement of the left-lateral strike-slip movement of Altyn Tagh fault during the Cenozoic. There is controversy over the time when Altyn Tagh fault began to move since India-Eurasia collision, but most researchers consider it is from the Eocene to Miocene[29,32-38](Table 1). For the left-lateral strike-slip displacement of Altyn Tagh fault during the Cenozoic, although different reference points were taken by previous researchers (suture zone, magmatic rock or Jurassic coal line), it is generally estimated at 300~400 km[15,38-48]. The latest paleomagnetic study shows the Qaidam Basin has migrated along Altyn Tagh fault northeastwards since the Eocene, during the course, large-scale vertical rotation doesn't occur[26]. Based on the above understandings, Cheng et al.[38]identified the syntectonic sedimentation related to the left-lateral strike-slip of Altyn Tagh fault during the Cenozoic

through correlating the stratigraphic depositional features between the Qaidam Basin and Tula Basin, and further pointed out that the left-lateral strike-slip movement of Altyn Tagh fault began in Lulehe Period, then sped up after the Miocene, that indicates the Eocene is the initial active time limit for the Altyn Tagh fault and its left-lateral strike-slip displacement is about 360 km.

Table 1. Summary of the initial strike-slip time limit of Altyn Tagh fault.

| Number | Initial strike-slip time limit | Study method | Reference |
|---|---|---|---|
| 1 | About 49 Ma ago | Comprehensive analysis of the Cenozoic profile along Altyn Tagh Mountain | [29] |
| 2 | Eocene | Comparative analysis of the Cenozoic strata along Altyn Tagh fault | [38] |
| 3 | 35.5 Ma ago | Studying the low temperature geochronology of Altyn Tagh basement (fission track) | [36] |
| 4 | Oligocene | Comparative analysis of the Oligocene strata between Tarim Basin and Qaidam Basin | [15] |
| 5 | Miocene | Analysis of the Cenozoic provenance along Altyn Tagh fault | [33-34] |
| 6 | Oligocene to early Miocene | Analysis of the Cenozoic strata along Altyn Tagh fault | [37] |
| 7 | Middle Miocene | Studying the low temperature geochronology of Altyn Tagh basement (fission track) | [32] |

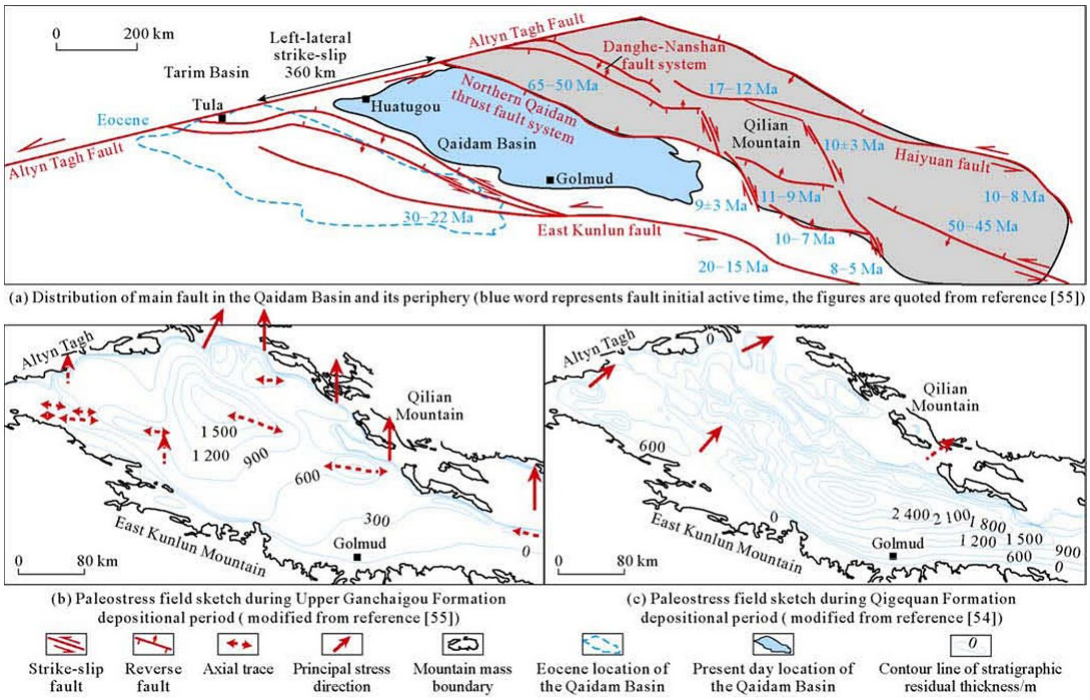


Fig. 3. Main fault distribution and the Paleogene and Neogene principal stress orientation in the Qaidam

Basin and its periphery.

There develop a series of NWW-trending thrust systems in North Qaidam – Qilian South Mountain, the northeastern boundary of the Qaidam Basin, such as the North Qaidam thrust system and Danghe-Nanshan fault system (Figs.1 and 3), among which, North Qaidam thrust system is NWW-SEE trending in plane and northward-dipping in vertical. The faults in this system generally obduct from Qilian Mountain to the basin, some faults have strike-slip component[14,49-50]. The seismic profiles of North Qaidam region reveal that these overthrust faults began to move in the Eocene and has lasted to present day[13-14]. According to field sedimentary record, it is generally believed the North Qaidam-Qilian Mountain began to deform in Eocene Lulehe Period since the collision between India and Eurasia plate[14,51], along with 20%~50% crustal shortening in NE-SW direction[13-14,52-53]. Based on the study on the magnetic fabric of the Cenozoic strata basinwide, Yu et al.[54]found that since the Paleogene, the North Qaidam began to experience compressional stress from north to south, while the southwestern Qaidam Basin was in extensional state, however, since the Neogene, the northern Qaidam Basin began to experience NE-SW compressional stress, the western Qaidam Basin also was affected by NE-SW compressional stress (Fig. 3). The overthrust and strike-slip events of the North Qaidam fault system have reformed the Mesozoic stratigraphic distribution pattern of the northern margin of the Qaidam Basin since Lulehe Period, and the transpression faults and related fold traps formed at the same time provide effective sealing conditions for Jurassic reservoirs[50].

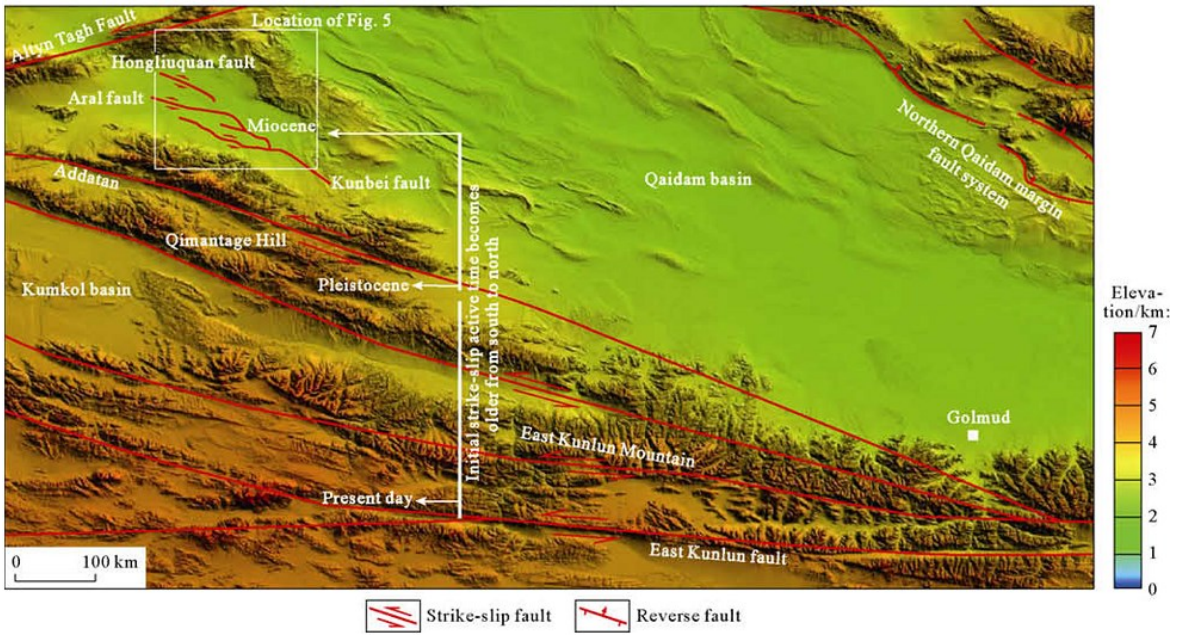


Fig. 4. Northward migration model of the strike-slip fault in the west segment of East Kunlun Mountain, Southwest Qaidam (topographic data adopts the SRTM data with 90 m resolution[17]).

The authors think that the left-lateral strike-slip faulting of the Altyn Tagh fault and the overthrust faulting of the North Qaidam might initiate from the Eocene. In other words, the Altyn Tagh left-lateral strike-slip faults and North Qadam fault system are in the same tectonic system: the Altyn Tagh left-lateral strike-slip initiating in the Paleocene-Eocene resulted in the NW-trending thrust activities of North Qaidam, at the same time the Qaidam began to subside in large scale as a whole. According to the evaluation that the left-lateral strike-slip displacement of Altyn Tagh fault is about 360 km, the Qaidam Basin with a relatively rigid basement has migrated 360 km northeastwards along Altyn Tagh fault as a whole since the Eocene, however, the displacement is adjusted by the NE-SW trending shortening and SE trending extrusion of the crust of North Qaidam-Qilian region. Thus, the Altyn Tagh strike-slip fault has been an important boundary for the Qaidam Basin since the Eocene and the North Qaidam-Qilian overthrust fold fault belt has been a passive adjustment boundary for the Qaidam Basin.

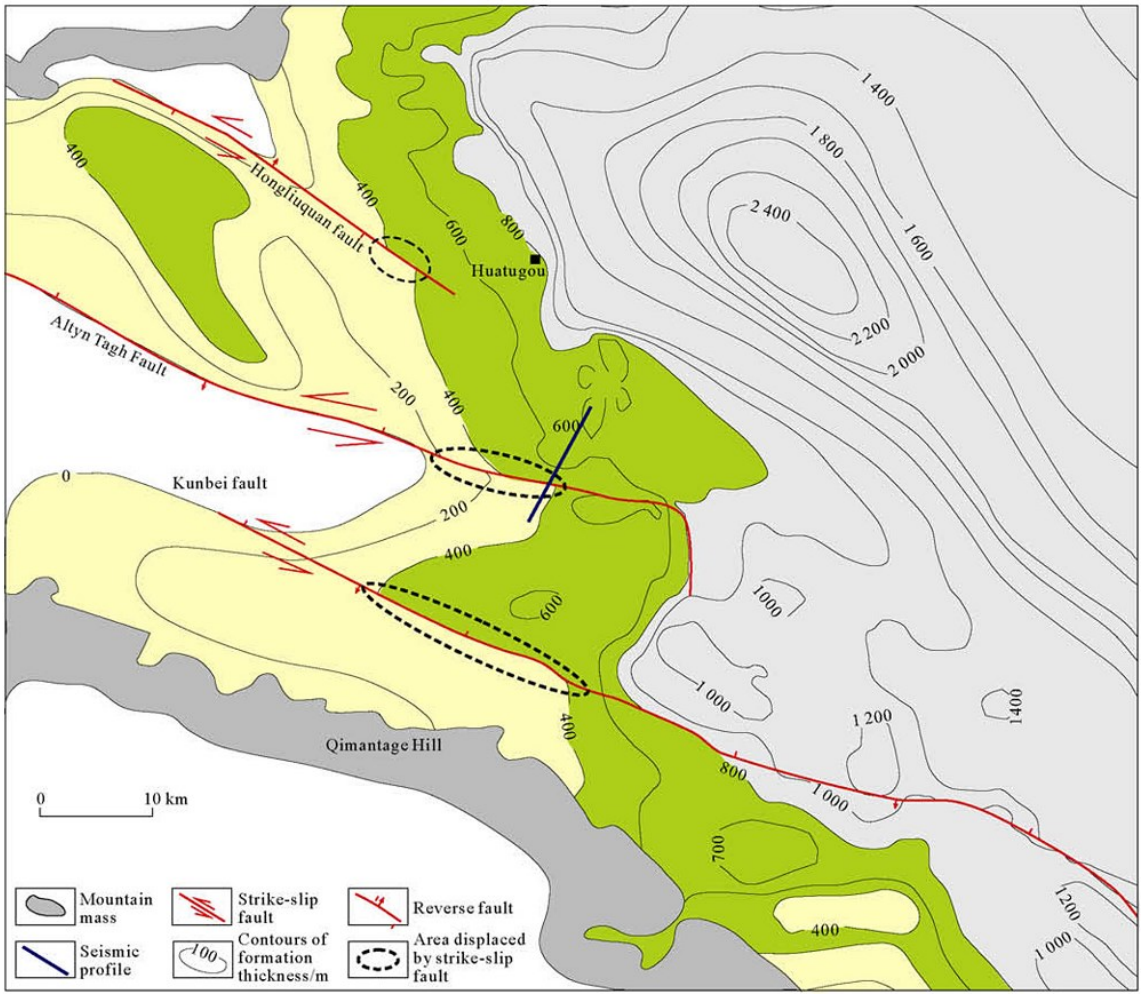


Fig. 5. Formation thickness and fault distribution of the upper member of Lower Ganchaigou Formation in Southwestern Qaidam Basin (Modified from reference [58]).

### 5.3.2 Left-lateral strike-slip of East Kunlun fault and its superimposed regulation on the basin since the Miocene

Located in the southern margin of the Qaidam Basin, and in W-E trend, the East Kunlun left-lateral strike-slip fault extends westwards through Kunlun Pass, giving rise to a series of arcuate structures composed of linear faults in Qimantage region in the west part[56-59](Figs. 1 and 4). The study on the fission track and $^{40}Ar/^{39}Ar$ low temperature thermochronology of the East Kunlun basement show several rapid cooling events happened to in the East Kunlun Mountain from the Oligocene to Early Miocene, which may be related to the large-scale tectonic movement of the East Kunlun Mountain occurred in the same period[10-11]. Based on the study on the fission track and (U-Th)/He low temperature thermochronology of the East Kunlun basement, Cheng et al.[58]and Duvall et al.[55]concluded the East Kunlun left-lateral strike-slip faulting might initiate from the Oligocene to Miocene, but Yin et al.[12]thought the East Kunlun left-lateral strike-slip faulting initiated in the Oligocene based on the Cenozoic growth strata identified in East Kunlun piedmont and the southern margin of the Qaidam Basin.

There are different opinions about the structural relationship between the East Kunlun Mountain and the Qaidam Basin[6-13]. Previous study reached the finding that there developed a large-scale transpressive system in East Kunlun region, with East Kunlun left-lateral strike-slip fault as southern boundary, and a series of south-dipping faults in the north which control the Cenozoic evolution of the southwestern margin of the Qaidam Basin[6-8,10-11]. But since this model can't reasonably explain the feature that the depocenter of the Qaidam Basin is not closed to East Kunlun Piedmont, Yin et al.[13] proposed an opposite point of view that a large wedge-shaped structure developed in the southern margin of the Qaidam Basin, which obducted the Qaidam Basin onto East Kunlun orogenic belt southwards, leading to the obduction of Qaidam Basin with low altitude onto the Qimantage Hill with relatively high altitude along a series of north-dipp ing Cenozoic faults southwards. This point of view is supported by some geophysical data collected from deep crust[60-61]. Although the southward thrust model can reasonably explain the dish distribution of the Cenozoic strata of the Qaidam Basin, but can't reasonably interpret the genesis of the arcuate structure of the Qimantage Hill in the west segment of the East Kunlun Mountain in plane[57].

Latest study on the distribution and mechanism of natural earthquake sources show the structures of the Southwest Qaidam and Qimantage Hill represent thrust and left-lateral strike-slip features[58] (Fig. 4). Remote sensing image and field geological survey show Qimantage mountain area has the Pleistocene sedimentary record of strike-slip tectonic deformation[58].

In addition, the tectonic and depositional framework of the Southwest Qaidam Basin represents a structural pattern of uplifts and depressions separated by a series of high-angle strike-slip faults, where the major faults include Kunbei Fault, Alar Fault and Hongliuquan Fault, their echelon shape and Eocene displaced by faults are signs of left-lateral strike-slip (Fig. 5). The growth strata identified in the seismic profiles of the southwestern Qaidam Basin indicate left-lateral strike-slip movement began in early Miocene (Fig. 6). In plane, the initial active time of the western branch fault of East Kunlun left-lateral strike-slip fault gradually becomes older from south (present East Kunlun left-lateral active fault) to north ( Kunbei fault zone in the Southwest Qaidam Basin) (Fig. 4).

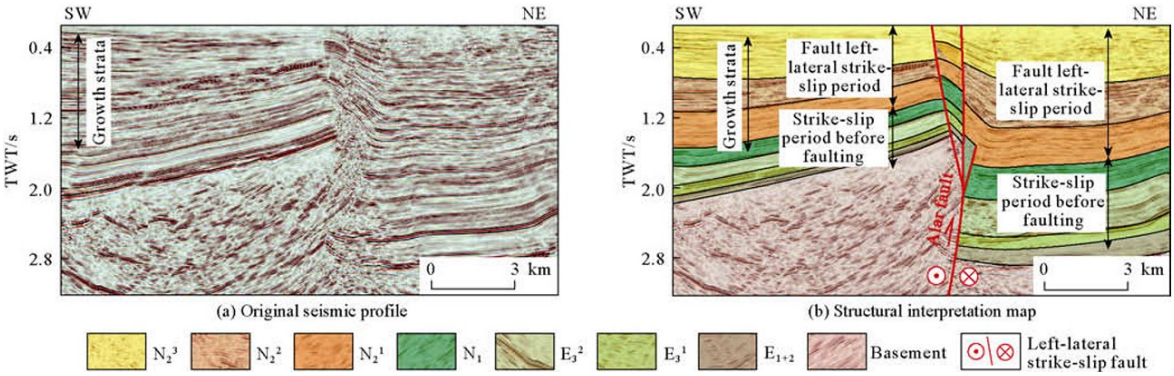


Fig. 6. Alar fault structural profile in Southwestern Qaidam Basin (Profile location is shown in Fig. 5).

Based on the analysis above, the author conclude that the boundary between the East Kunlun Mountain and the Qaidam Basin is neither southward thrust nor simple overthrust, but a strike-slip fault boundary, which is represented by Kunlun left-lateral strike-slip fault. Based on the fact that the initial time of the East Kunlun left-lateral strike-slip faulting in Qimantage region becomes younger from north to south, we think East Kunlun left-lateral strike-slip fault gradually has migrated northwards under the control of Altun Tagh left- lateral strike-slip faulting since early Miocene, during this process, left-lateral strike-slip attribute has gradually transited into northward thrust and left-lateral strike-slip attribute (Fig. 7), that means the East Kunlun left-lateral strike-slip fault has been an important strike-slip adjustment boundary since Neogene.

## 5.4 Structural control of the strike-slip superimposed Qaidam Basin on oil and gas accumulation

### 5.4.1 Distribution of sourcerocks in the Qaidam Basin

Exploration results reveal that there are three sets of important petroleum systems in the Qaidam Basin, including Jurassic, Paleogene-Neogene and Quaternary petroleum systems [62-

[63], among which, Jurassic petroleum system mainly occurs in the northern margin of the Qaidam basin, and its source rocks are predominantly composed of Lower Jurassic ($J_{1+2}$) dark coal measure mudstone (Fig. 8).

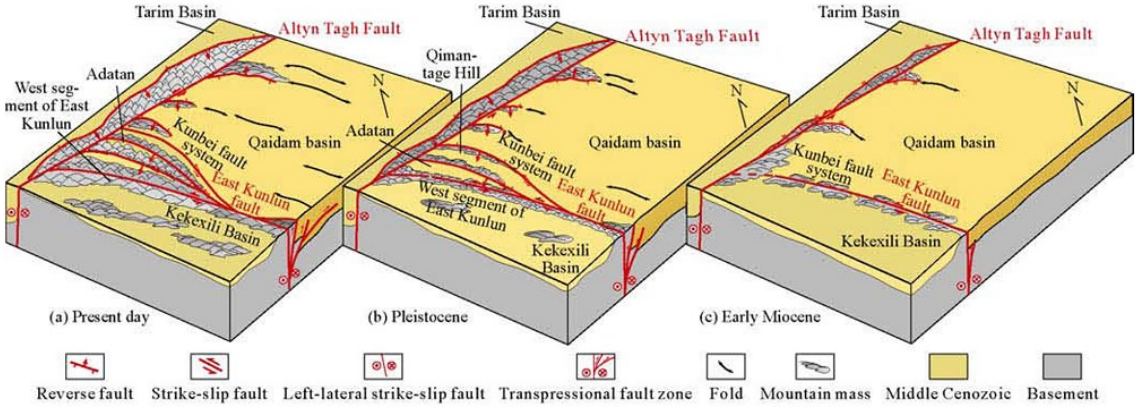


Fig. 7. Northward migration model of strike-slip fault in Southwestern Qaidam Basin (Modified from reference [58]).

Not developed in the northern margin of the Qaidam Basin, but developed in the Western Qaidam Basin, Paleogene-Neogene effective source rocks have features of typical salt lake source rocks [27,63]. The source rocks in the Western Qaidam Basin are characterized by low abundance of organic matter, high conversion rate and large hydrocarbon generation potential, leading to the occurrence of oil and gas rich sags in the Western Qaidam Basin (Fig. 8). Occurring in multiple series, wide in distribution and large in thickness, the Paleogene-Neogene source rocks in the Western Qaidam Basin predominantly are distributed in Upper Lulehe Formation ($E_{1+2}$), Lower Ganchaigou Formation ($E_3$), Upper Ganchaigou Formation ($N_1$), Lower Youshashan Formation ($N_2^1$) and Upper Youshashan Formation ($N_2^2$) in Mangya Sag, among which, the major source rocks in the upper member of Eocene Lower Ganchaigou Formation ($E_3^2$) and Oligocene Upper Ganchaigou Formation ($N_1$), are characterized by high carbonate content, low organic matter abundance and high hydrocarbon conversion rate, and give rise to various types of reservoirs, such as structural and stratigraphic-lithological reservoirs[27]. Previous researchers concluded the oil and gas reservoirs in the Western Qaidam Basin were mainly formed in middle-late Himalayan Period, especially in late $N_2^1$ and $N_2^3$-Q Period through dissecting the typical oilfield structures, such as Gasi, Wunan, Hongliuyan, Qie6, Nanyishan and Youquanzi in the Western Qaidam Basin and comprehensive regional geologic analysis[27]. The hydrocarbon accumulation features and time indicate the oil and gas reservoirs in the Western Qaidam Basin are closely related to the tectonic movement of late stage, the hydrocarbon accumulation phase and time correspond to the activity of East Kunlun strike-slip fault and its control on basin very well, especially for the reservoirs formed in 15-8

Ma ago (about late $N_2^1$) and the reservoirs formed in 4 Ma ago[27].

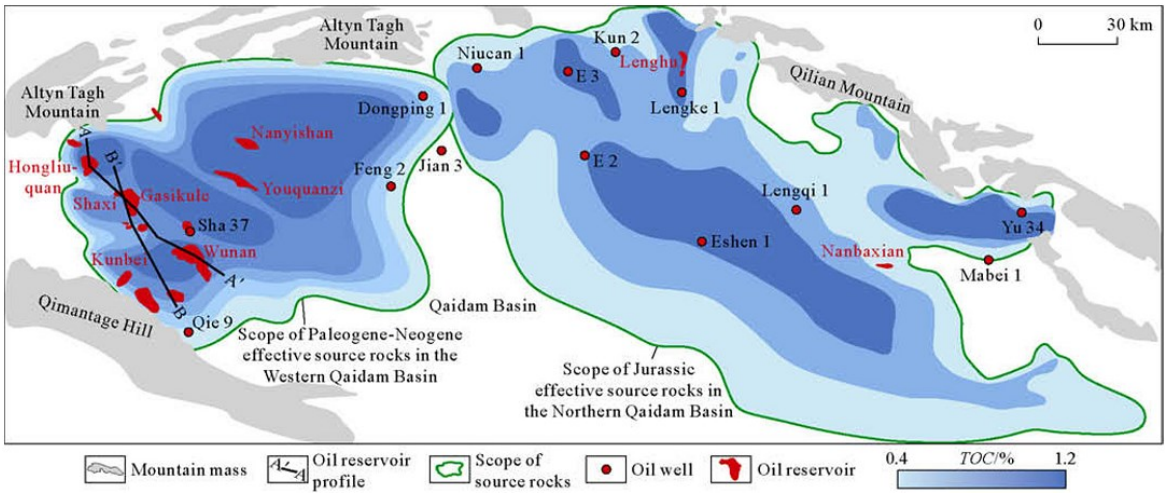


Fig. 8. Distribution of source rocks and oil and gasin Qaidam Basin (Modified from reference [27]).

Under the jointly effect of Qimantage Mountain thrust fault system and Altyn Tagh left-lateral strike-slip faults, a large number of NW-NWW trending, NE trending and nearly N-S trending faults develop in the Western Qaidam Basin[57,64].

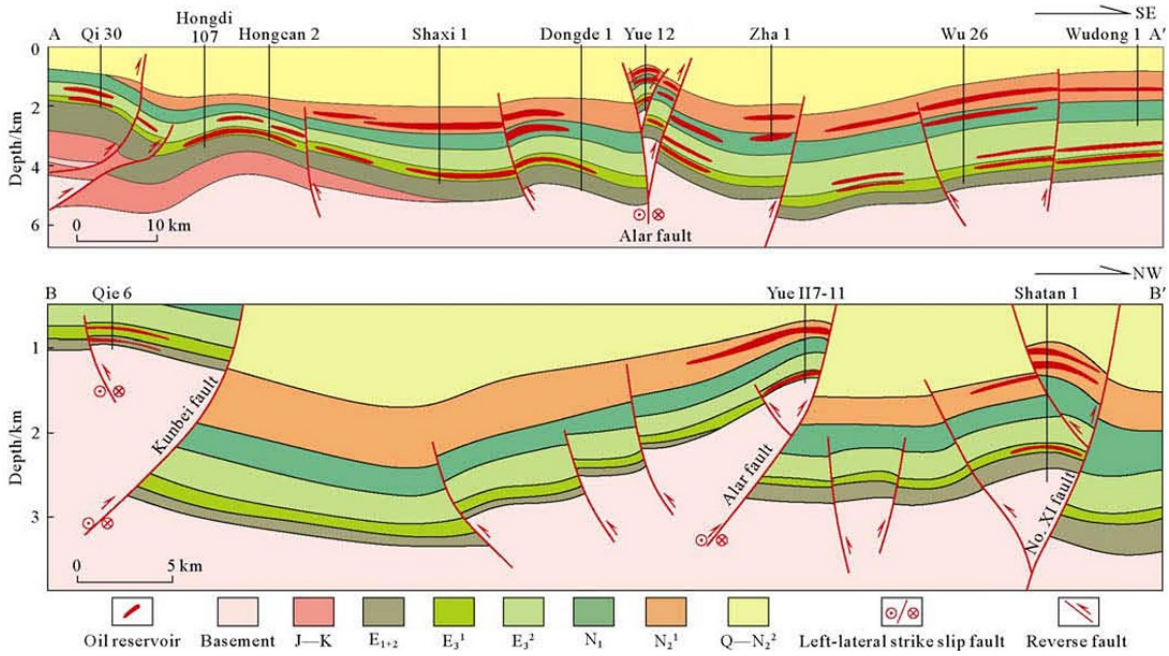


Fig. 9. Typical oil reservoir profile in Southwestern Qaidam Basin (Profile locatin is shown in Fig. 8).

The reservoirs in the Western Qaidam Basin are generally associated with fault structures[65]. Shaxi-Gasikule oil and gas accumulation zones distributing along Alar, No.XI fault (Figs. 8 and 9), the large oil and gas reservoirs discovered in Yingxi, Youshashan and Yingdong structure along the southern margin of Yingxiong Ridge are all closely related to the late Cenozoic fault belt; structural-stratigraphic-lithologic composite reservoirs distributing along Hongliuquan fault in Altyn Tagh piedmont zone, are controlled by fault nose

structure. In addition, structural-fractured reservoirs are distributed along Nanyishan fault and Jiandingshan fault (Figs. 8 and 9). Therefore, the strike-slip related faults developed since Neogene are of great significance for the trap formation and hydrocarbon accumulation in the western Qaidam Basin[64-65].

### 5.4.2 Control of strike-slip superimposed basin on oil and gas accumulation

A new theoretical model that the Qaidam Basin is a strike-slip superimposed basin jointly controlled by the left-lateral strike-slip Altyn Tagh and East Kunlun faults is proposed through systematically analyzing the structural relationship between the Qaidam Basin and its periphery orogenic belts.

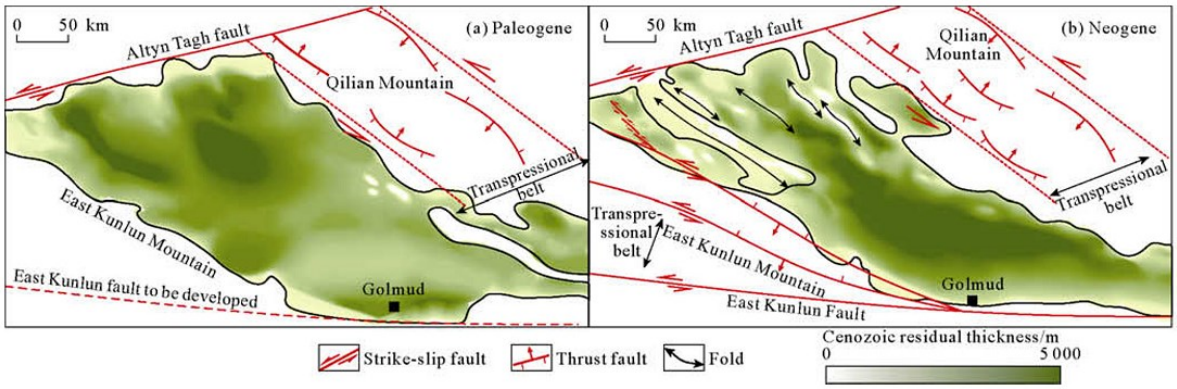


Fig. 10. Cenozoic tectonic - sedimentary evolution schematic of the Qaidam Basin and its periphery.

Since the Eocene (Fig. 10a), Altyn Tagh began left-lateral strike-slip movement, affected by which, the Qaidam Basin with a relatively rigid basement gradually has migrated northeastwards along Altyn Tagh left-lateral strike-slip fault, resulting in the shortening of crust in the northern Qaidam Basin-Qilian region in NE-SW direction since the Eocene, thereby, the northern Qaidam Basin seems a foreland basin of Qilian Mountain. There deposited a set of coarse-grained clastic strata but no high-quality source rocks in the northern Qaidam Basin during the Paleogene. At the same time, the southwestern Qaidam Basin was in extensional stress field, representing as a depression in tenso-shear context, thereby, a set of fine-grained strata deposited, acting as high-quality source rocks.

Since the Miocene (Fig. 10b), the East Kunlun fault system started left-lateral strike-slip movement, along with the northeastward migration of the Qaidam Basin, the west segment of the East Kunlun left-lateral strike-slip fault gradually migrated southwards, forming a series of en echelon faults (such as Kunbei fault, Alar fault, Qimantage Hill fault ). The formation of these strike-slip fault systems and their continuous northward migration as well as the rapid uplifting of East Kunlun Mountain and Qimantage Mountain resulted in the transition from

extensional background into compressional background under the compressional stress of NE-NW trending in western Qaidam Basin since Miocene, thus, the Neogene strata in the western Qaidam Basin are composed of the clastic sediments with grain size gradually increasing from bottom to top. The strike-slip related structures formed during Miocene (Kunbei fault, No. XI fault, Alar fault, Hongliuquan fault and Yingxiong Ridge) are ideal places for oil and gas accumulation and the fracture systems developed along fault zone are one of the important factor to improve reservoir petrophysical properties.

Altyn Tagh strike-slip fault is an important controlling boundary of the Qaidam Basin, which controlled the development and migration of different Cenozoic depocenters since Eocene; North Qaidam-Qilian thrust fold fault zone is the passive adjustment boundary of Qaidam Basin, which has suffered compression and deformation in NE-SW direction since the Eocene; East Kunlun left-lateral strike-slip fault is the positive superimposed adjustment boundary of the basin, its left-lateral strike-slip movement and migration lay foundation for the tectonic style of the Western Qaidam Basin and has become an important oil and gas accumulation controlling factor. The temporal and spatial superimposition of Altyn Tagh and East Kunlun strike-slip faults as well as North Qaidam-Qilian fold thrust fault zone give rise to the unique tectonic features of strike-slip superimposed basin and has controlled the oil and gas accumulation of the Qaidam Basin since Cenozoic.

In recent years, along with thinking innovation and technical progress, major exploration breakthroughs have been successively achieved in Qiekelike, Yingdong, Dongping, Niudong and Yingxi regions, indicating the Qaidam Basin is a plateau basin with great exploration potential. The gradual maturation of the new concept of Qaidam “strike-slip superimposed basin” and the continuous improvement in the hydrocarbon accumulation theory with strike-slip superimposed basin characteristics will create a new phase for the oil and gas exploration of the Qaidam Basin and provide solid theoretical support for accelerating construction of a plateau oil and gas field of ten million tons order.

## Reference

[1] Compiling Group of Petroleum Geology in Tibet Oil and Gas Area. Petroleum geology of China: Vol. 14. Beijing: Petroleum Industry Press, 1990: 331–482.

[2] Xia Wenchen, Zhang Ning, Yuan Xiaoping, et al. Cenozoic Qaidam Basin, China: A stronger tectonic inversed, extensional rifted basin. AAPG Bulletin, 2001, 85(4): 715–736.

[3] Zhao Wenzhi, Zhang Guangya, Wang Hongjun, et al. Basic features of petroleum geology in the superimposed petroliferous basins of China and their research methodologies.

Petroleum Exploration and Development, 2003, 30(2): 1–8.

[4] He Dengfa, Jia Chengzao, Tong Xiaoguang, et al. Discussion and analysis of superimposed sedimentary basins. Petroleum Exploration and Development, 2004, 31(1): 1–7.

[5] Jin Zhijun, Zhang Mingli, TangLiangjie, et al. Evolution of Meso-Cenozoic Qaidam Basin and its control on oil and gas. Oil & Gas Geology, 2004, 25(6): 603–608.

[6] Burchfiel B C, Deng Q D, Molnar P, et al. Intracrustal detachment within zones of continental deformation. Geology, 1989, 17(8): 748–752.

[7] Meyer B, Tapponnier P, Bourjot L, et al. Crustal thickening in Gansu-Qinghai, lithospheric mantle subduction, and oblique, strike-slip controlled growth ofthe Tibet Plateau. Geophysical Journal International, 1998, 135(1): 1–47.

[8] Tapponnier P, Xu Z Q, Roger F,et al. Oblique stepwise rise and growth of the Tibet Plateau. Science, 2001, 294: 1671–1677.

[9] Chen W P, Chen C Y, Nábelek J L. Present-day deformation of the Qaidam Basin with implications for intra-continental tectonics. Tectonophysics, 1999, 305(1/2/3): 165–181.

[10] Mock C, Arnaud N O, Cantagrel J M. An early unroofing in northeastern Tibet constraints from $^{40}Ar/^{39}Ar$ thermochronology on granitoids from the eastern Kunlun range (Qianghai, NW China). Earth and Planetary Science Letters, 1999, 171(1): 107–122.

[11] Jolivet M, Brunel M, Seward D, et al. Mesozoic and Cenozoic tectonics of the northern edge of the Tibetan Plateau: Fission-track constraints. Tectonophysics, 2001, 343(1/2): 111–134.

[12] Yin A, Dang Y Q, Zhang M,et al. Cenozoic tectonic evolution of Qaidam Basin and its surrounding regions (part 2): Wedge tectonics in southern Qaidam Basin and the Eastern Kunlun range. Geological Society of America, Special Papers, 2007, 433: 369–390.

[13] Yin A, Dang Y Q, Zhang M,et al. Cenozoic tectonic evolution of the Qaidam Basin and its surrounding regions (Part 3): Structural geology, sedimentation, and regional tectonic reconstruction. Geological Society of America Bulletin, 2008, 120(7/8): 847–876.

[14] Yin A, Dang Y Q, Wang L C, et al. Cenozoic tectonic evolution of Qaidam Basin and its surrounding regions (Part 1): The southern Qilian Shan-Nan Shan thrust belt and northern Qaidam Basin. Geological Society of America Bulletin, 2008, 120(7/8): 813–846.

[15] Meng Q R, Hu J M, Yang F Z. Timing and magnitude of displacement on the Altyn Tagh fault: Constraints from stratigraphic correlation of adjoining Tarim and Qaidam Basins, NW China. Terra Nova, 2001, 13(2): 86–91.

[16] Meng Q R, Fang X. Cenozoic tectonic development of the Qaidam Basin in the

northeastern Tibetan Plateau. Geological Society of America, Special Papers, 2008, 444: 1–24.

[17] CGIAR. SRTM 90m digital elevation data. (2008-08-19) [2015-05-20]. http://srtm.csi.cgiar.org.

[18] Fang Xiaoming, Zhang Weilin, Meng Qingquan, et al. High-resolution magnetostratigraphy of the Neogene Huaitoutala section in the eastern Qaidam Basin on the NE Tibetan Plateau, Qinghai Province, China and its implication on tectonic uplift of the NE Tibetan Plateau. Earth and Planetary Science Letters, 2007, 258(1/2): 293–306.

[19] Lu Haijian, Xiong Shangfa. Magnetostratigraphy of the Dahonggou Section, northern Qaidam Basin and its bearing on Cenozoic tectonic evolution ofthe Qilian Shan and Altyn Tagh fault. Earth and Planetary Science Letters, 2009, 288(3): 539–550.

[20] Huang Hanchun, Huang Qinghua, Ma Yongsheng. Geology of Qaidam Basin and its petroleum prediction. Beijing: Geological Publishing House, 1996.

[21] Yang Fan, Ma Zhiqiang, Xu Tongchun, et al. A Tertiary paleomagnetic stratigraphic profile in Qaidam Basin. Acta Petrolei Sinica, 1992, 13(2): 97–101.

[22] Sun Jimin, Zhu Rixiang, An Zhishen. Tectonic uplift in the northern Tibetan Plateau since 13.7 Ma ago inferred from molasse deposits along the Altyn Tagh fault. Earth and Planetary Science Letters, 2005, 235(3): 641–653.

[23] Ke Xue, Ji Junliang, Zhang Kexin, et al. Magnetostratigraphy and anisotropy of magnetic susceptibility of the Lulehe Formation in the Northeastern Qaidam Basin. Acta Geologica Sinica: English Edition, 2013, 87(2): 576–587.

[24] Rieser A B, Liu Yongjiang, Genser J, et al. $^{40}Ar/^{39}Ar$ ages of detrital white mica constrain the Cenozoic development of the intracontinental Qaidam Basin, China. GSA Bulletin, 2006, 118(11/12): 1522–1534.

[25] Yu Xiangjiang, Fu Suotang, Guan Shuwei, et al. Paleomagnetism of Eocene and Miocene sediments from the Qaidam Basin: Implication for no integral rotation since the Eocene and a rigid Qaidam Block. Geochemistry, Geophysics, Geosystems, 2014, 15(6): 2109–2127.

[26] Wang Erchie, Xu Fengyin, Zhou Jianxun, et al. Eastward migration of the Qaidam Basin and its implications for Cenozoic evolution of the Altyn Tagh fault and associated river systems. Geological Society of America Bulletin, 2006, 118(3/4): 349–365.

[27] Fu Suotang. Key controlling factors of oil and gas accumulation in the western Qaidam Basin and its implications for favorable exploration direction.Acta Sedimentologica Sinica, 2010, 28(2): 373–379.

[28] Molnar P, Tapponnier P. Cenozoic tectonics of Asia: Effects of a continental collision. Science, 1975, 189: 419–426.

[29] Yin An, Rumelhart P, Butler R, et al. Tectonic history of the Altyn Tagh fault system in northern Tibet inferred from Cenozoic sedimentation. GeologicalSociety of America Bulletin, 2002, 114(10): 1257–1295.

[30] Robinson D M, Dupont-Nivet G,Gehrels G E, et al. The Tula uplift, northwestern China: Evidence for regional tectonism of the northern Tibetan Plateau during late Mesozoic–early Cenozoic time. Geological Society of America Bulletin, 2003, 115(1): 35–47.

[31] Peltzer G, Tapponnier P. Formation and evolution of strike-slip faults, rifts, and basins during the India-Asia collision: An experimental approach. Journal of Geophysical Research: Solid Earth(1978-2012), 1988, 93(B12): 15085–15117.

[32] Wan Jinglin, Wang Yu, Li Qi, et al. FT evidence of northern Altyn uplift in Late-Cenozoic. Bulletin of Mineralogy, Petrology and Geochemistry, 2001, 20(4): 222–224.

[33] Wu Lei, Xiao Ancheng, Yang Shufeng, et al. Two-stage evolution of the Altyn Tagh fault during the Cenozoic: New insight from provenance analysis of a geological section in NW Qaidam Basin, NW China. Terra Nova, 2012, 24(5): 387–395.

[34] Wu Lei, Xiao Ancheng, Wang Liang, et al. EW-trending uplifts along the southern side of the central segment of the Altyn Tagh fault, NW China: Insight into the rising mechanism of the Altyn Mountain during the Cenozoic. SCIENCE CHINA Earth Sciences, 2012, 55(6): 926–939.

[35] Wang Liang, Xiao Ancheng,Gong Qinglin, et al. The unconformity in Miocene sequence of western Qaidam Basin and its tectonic significance. SCIENCE CHINA Earth Sciences, 2010, 53(8): 1126–1133.

[36] Chen Zhengle, Zhang Yueqiao, Wang Xiaofeng, et al. Fission track dating of apatite constrainson the Cenozoic uplift of the Altyn Tagh Mountain. Acta Geoscientia Sinica, 2001, 22(5): 413–418.

[37] Yue Yongjun, Ritts B D, Graham S A. Initiation and long-term slip history of the Altyn Tagh fault. International Geology Review, 2001, 43(12): 1087–1093.

[38] Cheng Feng, Guo Zhaojie, Jenkins H S, et al. Initial rupture and displacement on the Altyn Tagh fault, northern Tibetan Plateau: Constraints based on residual Mesozoic to Cenozoic strata in the western Qaidam Basin. Geosphere, 2015, 11(3): 921–942.

[39] Cowgill E, Yin An, Harrison T M, et al. Reconstruction of the Altyn Tagh fault based on U-Pb geochronology: Role of back thrusts, mantle sutures, and heterogeneous crustal

strength in forming the Tibetan Plateau. Journal of Geophysical Research, 2003, 108(B7): 2346.

[40] Che Zicheng, Liu Liang, Liu Hongfu, et al. The constituents of the Altun fault system and genetic characteristics of related Meso-Cenozoic petroleum-bearing basin. Regional Geology of China, 1998, 17(4): 377–384.

[41] Ge Xiaohong, Liu Junlai. Formation and tectonic background of the northern Qilian orogenic belt. Earth Science Frontiers, 1999, 6(4): 223–230.

[42] Yue Yongjun, Liou J G. Two-stage evolution model for the Altyn Tagh fault, China. Geology, 1999, 27(3): 227–230.

[43] Gehrels G E, Yin An, Wang Xiaofeng. Magmatic history of the northeastern Tibetan Plateau. Journal of Geophysical Research, 2003, 108(B9): 2423.

[44] Yang Jinsui, Xu Zhiqin, Zhang Jianxin, et al. Tectonic significance of early Paleozoic high-pressure rocks in Altun-Qaidam-Qilian Mountains, northwest China. Geological Society of America Memoirs, 2001, 194: 151–170.

[45] Zhang Jianxin, Zhang Zeming, Xu Zhiqin, et al. Petrology and geochronology of eclogites from the western segment of the Altyn Tagh, northwestern China. Lithos, 2001, 56(2): 187–206.

[46] Gehrels G, Yin A, Chen X, etal. Constraints on the offset of the eastern Altyn Tagh fault, western China. EOS: Transactions of the American Geophysical Union, 2000, 81: F1093.

[47] Sobel E R, Arnaud N, JolivetM, et al. Jurassic to Cenozoic exhumation history of the Altyn Tagh range, northwest China, constrained by $^{40}Ar/^{39}Ar$ and apatite fission track thermochronology. In: Paleozoic and Mesozoic tectonic evolution of central Asia: From continental assembly to intracontinental deformation. Boulder, CO: Geological Society of America, 2001, 194: 247–267.

[48] Ritts B D, Biffi U. Magnitude of post-Middle Jurassic (Bajocian) displacement on the central Altyn Tagh fault system, northwest China. Geological Society of America Bulletin, 2000, 112(1): 61–74.

[49] Wang Guihong, Ma Dade, Zhou Chuanmin, et al. The seismic profile interpretation and development mechanism of strike-slip faults in northern Qaidam Basin. Acta Geoscientica Sinica, 2011, 32(2): 204–210.

[50] Wei Guoqi, Li Benliang, XiaoAncheng, et al. Strike-thrust structures and petroleum exploration in northern Qaidam Basin. Earth Science Frontiers, 2005, 12(4): 397–402.

[51] Zhuang Guangsheng, Hourigan J K, Ritts B D, et al. Cenozoic multiple-phase tectonic

evolution of the northern Tibetan Plateau: Constraints from sedimentary records from Qaidam Basin, Hexi Corridor, and Subei Basin, northwest China. American Journal of Science, 2011, 311(2): 116–152.

[52] Bally A W, Chou I M, Clayton R, et al. Notes on sedimentary basins in China, report of the American sedimentary basins delegation to the People's Republic of China. Washington: US Geological Survey, 1986.

[53] Zhang Huiping, Zhang Peizheng, Zheng Dewen, et al. Transforming the Miocene Altyn Tagh fault slip into shortening of the north-western Qilian Shan: Insights from the drainage basin geometry. Terra Nova, 2014, 26(3): 216–221.

[54] Yu Xiangjiang, Huang Baochun, Guan Shuwei, et al. Anisotropy of magnetic susceptibility of Eocene and Miocene sediments in the Qaidam Basin, northwest China: Implication for Cenozoic tectonic transition and depocenter migration. Geochemistry, Geophysics, Geosystems, 2014, 15(6): 2095–2108.

[55] Duvall A R, Clark M K, Kirby E, et al. Low-temperature thermochronometry along the Kunlun and Haiyuan faults, NE Tibetan Plateau: Evidence for kinematic change during late-stage orogenesis. Tectonics, 2013, 32(5): 1190–1211.

[56] Kirby E, Reiners P W, Krol M A, et al. Late Cenozoic evolution of the eastern margin of the Tibetan Plateau: Inferences from $^{40}Ar/^{39}Ar$ and (U-Th)/He thermochronology. Tectonics, 2002, 21(1): 1–20.

[57] Fu Bihong, Awata Y. Displacement and timing of left-lateral faulting in the Kunlun fault zone, northern Tibet, inferred from geologic and geomorphic features. Journal of Asian Earth Sciences, 2007, 29(2): 253–265.

[58] Cheng Feng, Jolivet M, Fu Suotang, et al. Northward growth of the Qimen Tagh range: A new model accounting for the Late Neogene strike-slip deformation of the SW Qaidam Basin. Tectonophysics, 2014, 632: 32–47.

[59] Jolivet M, Brunel M, Seward D, et al. Neogene extension and volcanism in the Kunlun fault zone, northern Tibet: New constraints on the age of the Kunlun fault. Tectonics, 2003, 22(5): 1052.

[60] Shi Danian, Shen Yang, Zhao Wenjin, et al. Seismic evidence for a Moho offset and south-directed thrust at the easternmost Qaidam–Kunlun boundary in the Northeast Tibetan Plateau. Earth and Planetary Science Letters, 2009, 288(1/2): 329–334.

[61] Wang Chengshan, Gao Rui, Yin An, et al. A mid-crustal strain-transfer model for continental deformation: A new perspective from high-resolution deep seismic-reflection profiling across NE Tibet. Earth and Planetary Science Letters, 2011, 306(3): 279–288.

[62] Zhao Fan, Sun Deqiang, Yan Cunfeng, et al. Meso-Cenozoic evolution of the Qaidam Basin and its relationship with oil and gas accumulation. Natural Gas and Geoscience, 2013, 24(5): 940–947.

[63] Xu Fengyin, Peng Dehua, Hou Enke. Hydrocarbon accumulation and exploration potential in Qaidam Basin. Acta Petrolei Sinica, 2003, 24(4): 1–6.

[64] Fang Xiang, Jiang Bo, Zhang Yongshu. Faulted structure and hydrocarbon accumulation in western Qaidam Basin. Oil & Gas Geology, 2006, 27(1): 56–61.

[65] Chen Shaojun, Luo Qun, Wang Tiecheng, et al. Faulting characteristics and effects on the hydrocarbon distribution in Qaidam Basin. Xinjiang Petroleum Geology, 2004, 25(1): 22–25.

# Chapter 6 Conclusions and Follow-up research

## 6.1 General Conclusions

The main objective of my PhD dissertation is to understand the Cenozoic evolution of the Qaidam basin and its surrounding regions, North Tibet (including Eastern Kunlun Range, Altyn Tagh Range, and Qilian Shan). The major contributions from this thesis are that:

A. The SW Qaidam Basin has been bordered by a series of strike-slip faults to the south since the Early Miocene, rather than by a continuous northward or southward thrusting system. The SW Qaidam Basin did not suffer a major N–S compression and shortening before the Early Miocene.

B. The Eastern Kunlun Range was already exhumed prior to the Paleocene. From the Late Eocene to Oligocene, the southward expanding Qaidam basin may locally inundate the eastern Kunlun Range and connect with the Kumukol basin or even the Hoh Xil basin to the south. Since the Miocene, the intense uplifting of the Eastern Kunlun Range separated the Qaidam basin and Hoh Xil basin.

C. An early-middle Eocene initiation of left-lateral strike-slip faulting is determined and a 360 ± 40 km offset along the Altyn Tagh fault since its Cenozoic reactivation is estimated. The enhanced tectonic activity within the Altyn Tagh Range and northwestern Qaidam basin from Miocene time is also suggested.

D. Based on the 360 km northeastward migration of the relatively rigid Qaidam block along the Altyn Tagh Fault and 3D isovolumetric balance of the crustal deformation within the Altyn Tagh Fault – Qilian Shan system, I demonstrate that 250 ± 28 km (43.8~49.4 %) of N20E directed crustal shortening and an additional ~250 to ~370 km of eastward motion of the Qilian Shan crust must be accounted for by strike-slip faulting in the Qilian Shan and crustal thickening in the Qinling area, as well as extension in the adjoining North China block graben systems.

E. Collectively, the Qaidam Basin is not a foreland basin nor an extensional basin, but a strike-slip superimposed basin jointly controlled by the left-lateral strike-slip Altyn Tagh and East Kunlun faults. The Altyn Tagh fault acts as the major controlling boundary, while the East Kunlun fault only controls the local evolution of the southern edge of the basin. The temporal and spatial superimposition of these two strike-slip faults during the Cenozoic controlled the evolution of the basin as well as the oil and gas accumulation.

## 6.2 Follow-up research

Based on my recent research on the Cenozoic tectonic evolution of the northern Tibetan plateau, I would like to address three issues:

A. The early stage (Paleocene-Eocene, Lulehe Fm.) of the northern Tibetan plateau since the India-Asian collision is still poorly constrained. In my thesis (Chapter 2.2), I suggest that the Eastern Kunlun Range was already exhumed prior to the Paleocene. In order to obtain better constraints on the early stage of the plateau, I would like to employ O isotopes and clumped isotopes to study the paleoelevation and paleoclimate. In addition, magnetostratigraphy study on well-exposed, continuous outcrops of Paleocene-Eocene strata (Lulehe Fm.) within the Qaidam basin would also provide a useful, detailed calendar for the deposition of that formation and the corresponding paleoenvironment evolution.

B. In recent years, the Miocene deformation phase (~15 Ma) has been widely studied in the northern Tibetan plateau. In particular, a middle Miocene reorganization of the deformation has been recognized. This reorganization can be summarized as: prior to the Miocene, the north-northeastern margin of the Tibetan Plateau was characterized primarily by compressive structures accommodating N or NE convergence beginning roughly at the onset of the India-Eurasia collision (Eocene); These compressive structures were gradually overprinted by the Miocene-Pliocene initiation of near E-W or NWW-SEE strike-slip faults, such as the Kunlun and Haiyuan faults. Identifying how the regional climate responded to this intense Miocene deformation in the northern Tibetan plateau would be a significant attempt for exploiting the interplay between tectonics and climate.

# Reference

Arnaud, N., Tapponnier, P., Roger, F., Brunel, M., Scharer, U., Chen, W., Xu, Z., 2003. Evidence for Mesozoic shear along the western Kunlun and Altyn‐Tagh fault, northern Tibet (China). Journal of Geophysical Research: Solid Earth (1978–2012) 108.

Bally, A.W., Chou, I.-M., Clayton, R., Eugster, H.P., Kidwell, S., Meckel, L.D., Ryder, R.T., Watts, A.B., Wilson, A.A., 1986.Notes on sedimentary basins in China—report of the American Sedimentary Basins delegation to the People's Republic of China. U.S. Geological Survey Open-File Report, 108, pp. 86–327.

Basilevsky, A.T., Head, J.W., 2007. Beta Regio, Venus: Evidence for uplift, rifting, and volcanism due to a mantle plume. Icarus 192, 167-186.

Bovet, P.M., Ritts, B.D., Gehrels, G., Abbink, A.O., Darby, B., Hourigan, J., 2009. Evidence of Miocene crustal shortening in the north Qilian Shan from Cenozoic stratigraphy of the western Hexi Corridor, Gansu Province, China. American Journal of Science 309, 290-329.

Burchfiel, B.C., Quidong, D., Molnar, P., Royden, L., Yipeng, W., Peizhen, Z., Weiqi, Z., 1989. Intracrustal detachment within zones of continental deformation. Geology 17, 748-752.

Burchfiel, B., Zhang, P., Wang, Y., Zhang, W., Song, F., Deng, Q., Molnar, P., Royden, L., 1991. Geology of the Haiyuan fault zone, Ningxia‐Hui Autonomous Region, China, and its relation to the evolution of the northeastern margin of the Tibetan Plateau. Tectonics 10, 1091-1110.

Chen, W.P., Chen, C.Y., L Nábelek, J., 1999. Present-day deformation of the Qaidam basin with implications for intra-continental tectonics. Tectonophysics 305, 165-181.

Chen, Z.L., Zhang, Y.Q., Wang , X.F., Chen, X.H., 2001. Fission Track Dating of Apatite Constrains on the Cenozoic Uplift of the Altyn Tagh Mountain. GEOSCIENTIA SINICA Acta Geoscientia Sinica 22, 413-418 (in Chinese with English abstract).

Chen, X.H., Yin, A., Gehrels, G.E., Cowgill, E.S., Grove, M., Harrison, T.M., Wang, X.F., 2003. Two phases of Mesozoic north-south extension in the eastern Altyn Tagh range, northern Tibetan Plateau. Tectonics 22, 1053.

Chen, X., Gehrels, G., Yin, A., Zhou, Q., Huang, P., 2015. Geochemical and Nd–Sr–Pb–O isotopic constrains on Permo–Triassic magmatism in eastern Qaidam Basin, northern Qinghai-Tibetan plateau: Implications for the evolution of the Paleo-Tethys. Journal of Asian Earth Sciences 114, Part 4, 674-692.

Clark, M.K., Farley, K.A., Zheng, D., Wang, Z., Duvall, A.R., 2010. Early Cenozoic faulting of the northern Tibetan Plateau margin from apatite (U–Th)/He ages. Earth and Planetary Science Letters 296, 78-88.

Cheng, F., Jolivet, M., Fu, S., Zhang, Q., Guan, S., Yu, X., Guo, Z., 2014. Northward growth of the Qimen Tagh Range: A new model accounting for the Late Neogene strike-slip deformation of the SW Qaidam Basin. Tectonophysics 632, 32-47.

Cheng, F., Fu, S., Jolivet, M., Zhang, C., Guo, Z., 2016. Source to sink relation between the Eastern Kunlun Range and the Qaidam Basin, northern Tibetan Plateau, during the Cenozoic. Geological Society of America Bulletin 128, 258-283.

Cobbold, P., Davy, P., 1988. Indentation tectonics in nature and experiment. 2. Central Asia, Bull. Geol. Inst. Univ. Uppsala 14, 143-162.

Cowgill, E., Yin, A., Harrison, T.M., Xiao-Feng, W., 2003. Reconstruction of the Altyn Tagh fault based on U-Pb geochronology: Role of back thrusts, mantle sutures, and heterogeneous crustal strength in forming the Tibetan Plateau. Journal of Geophysical Research 108, 2346.

Davy, P., Cobbold, P., 1988. Indentation tectonics in nature and experiment. 1. Experiments scaled for gravity. Bull. Geol. Inst. Univ. Uppsala 14, 129-141.

Dai, J., Wang, C., Hourigan, J., Santosh, M., 2013. Multi-stage tectono-magmatic events of the Eastern Kunlun Range, northern Tibet: Insights from U–Pb geochronology and (U–Th)/He thermochronology. Tectonophysics 599, 97-106.

Dupont-Nivet, G., Butler, R.F., Yin, A., Chen, X., 2003. Paleomagnetism indicates no Neogene vertical axis rotations of the northeastern Tibetan Plateau. J. geophys. Res 108, 2386.

Dupont-Nivet, G., Robinson, D., Butler, R.F., Yin, A., Melosh, H.J., 2004. Concentration of crustal displacement along a weak Altyn Tagh fault: Evidence from paleomagnetism of

the northern Tibetan Plateau. Tectonics 23, TC1020.

Dupont-Nivet, G., Krijgsman, W., Langereis, C.G., Abels, H.A., Dai, S., Fang, X., 2007. Tibetan plateau aridification linked to global cooling at the Eocene–Oligocene transition. Nature 445, 635-638.

Duvall, A.R., Clark, M.K., 2010. Dissipation of fast strike-slip faulting within and beyond northeastern Tibet. Geology 38, 223-226.

Duvall, A.R., Clark, M.K., Kirby, E., Farley, K.A., Craddock, W.H., Li, C., Yuan, D.-Y., 2013. Low-temperature thermochronometry along the Kunlun and Haiyuan Faults, NE Tibetan Plateau: Evidence for kinematic change during late-stage orogenesis. Tectonics 32, 1190-1211.

England, P., Houseman, G., 1986. Finite strain calculations of continental deformation: 2. Comparison with the India‐Asia collision zone. Journal of Geophysical Research: Solid Earth (1978–2012) 91, 3664-3676.

Garzione, C.N., Ikari, M.J., Basu, A.R., 2005. Source of Oligocene to Pliocene sedimentary rocks in the Linxia basin in northeastern Tibet from Nd isotopes: Implications for tectonic forcing of climate. Geological Society of America Bulletin 117, 1156-1166.

Gehrels, G.E., Yin, A., Wang, X.F., 2003a. Magmatic history of the northeastern Tibetan Plateau. Journal of Geophysical Research 108, 2423.

Gehrels, G.E., Yin, A., Wang, X.F., 2003b. Detrital-zircon geochronology of the northeastern Tibetan plateau. Geological Society of America Bulletin 115, 881-896.

Kapp, P., DeCelles, P.G., Gehrels, G.E., Heizler, M., Ding, L., 2007. Geological records of the Lhasa-Qiangtang and Indo-Asian collisions in the Nima area of central Tibet. Geological Society of America Bulletin 119, 917-933.

Jolivet, M., Brunel, M., Seward, D., Xu, Z., Yang, J., Roger, F., Tapponnier, P., Malavieille, J., Arnaud, N., Wu, C., 2001. Mesozoic and Cenozoic tectonics of the northern edge of the Tibetan plateau: fission-track constraints. Tectonophysics 343, 111-134.

Jolivet, M., Brunel, M., Seward, D., Xu, Z., Yang, J., Malavieille, J., Roger, F., Leyreloup, A., Arnaud, N., Wu, C., 2003. Neogene extension and volcanism in the Kunlun Fault Zone, northern Tibet: New constraints on the age of the Kunlun Fault. Tectonics 22, 1052.

Jolivet, M., Roger, F., Xu, Z.Q., Paquette, J.L., Cao, H., 2015. Mesozoic–Cenozoic evolution of the Danba dome (Songpan Garzê, East Tibet) as inferred from LA-ICPMS U–Pb and fission-track data. Journal of Asian Earth Sciences 102, 180-204.

Li, H.B., Yang, J.S., Xu, Z.Q., Sun, Z.M., Tapponnier, P., van der Woerd, J., Meriaux, A.-S., 2006. The constraint of the Altyn Tagh fault system to the growth and rise of the northern Tibetan Plateau. Earth Science Frontiers 13, 59-79 (in Chinese with English abstract).

Liu, Y.J., Neubauer, F., Genser, J., Ge, X.H., Takasu, A., Yuan, S.H., Chang, L.H., Li, W.M., 2007. Geochronology of the initiation and displacement of the Altyn Strike-Slip Fault, western China. Journal of Asian Earth Sciences 29, 243-252.

Lu, H., Wang, E., Meng, K., 2014. Paleomagnetism and anisotropy of magnetic susceptibility of the Tertiary Janggalsay section (southeast Tarim basin): Implications for Miocene tectonic evolution of the Altyn Tagh Range. Tectonophysics 618, 67-78.

Mao, L., Xiao, A., Wu, L., Li, B., Wang, L., Lou, Q., Dong, Y., Qin, S., 2014. Cenozoic tectonic and sedimentary evolution of southern Qaidam Basin, NE Tibetan Plateau and its implication for the rejuvenation of Eastern Kunlun Mountains. Science China Earth Sciences 57, 2726-2739.

Meng, Q.R., Hu, J.M., Yang, F.Z., 2001. Timing and magnitude of displacement on the Altyn Tagh fault: constraints from stratigraphic correlation of adjoining Tarim and Qaidam basins, NW China. Terra Nova 13, 86-91.

Meng, Q.R., Fang, X., 2008. Cenozoic tectonic development of the Qaidam Basin in the northeastern Tibetan Plateau. Geological Society of America Special Papers 444, 1-24.

Métivier, F., Gaudemer, Y., Tapponnier, P., Meyer, B., 1998. Northeastward growth of the Tibet plateau deduced from balanced reconstruction of two depositional areas: The Qaidam and Hexi Corridor basins, China. Tectonics 17, 823-842.

Meyer, B., Tapponnier, P., Bourjot, L., Metivier, F., Gaudemer, Y., Peltzer, G., Shunmin, G., Zhitai, C., 1998. Crustal thickening in Gansu-Qinghai, lithospheric mantle subduction, and oblique, strike-slip controlled growth of the Tibet plateau. Geophysical Journal International 135, 1-47.

Mock, C., Arnaud, N.O., Cantagrel, J.M., 1999. An early unroofing in northeastern Tibet?

Constraints from $^{40}Ar/^{39}Ar$ thermochronology on granitoids from the eastern Kunlun range (Qianghai, NW China). Earth and Planetary Science Letters 171, 107-122.

Molnar, P., Tapponnier, P., 1975. Cenozoic tectonics of Asia: Effects of a continental collision. Science 189, 419-426.

Molnar, P., England, P., Martinod, J., 1993. Mantle dynamics, uplift of the Tibetan Plateau, and the Indian monsoon. Reviews of Geophysics 31, 357-396.

Ritts, B.D., Yue, Y., Graham, S.A., 2004. Oligocene–Miocene Tectonics and Sedimentation along the Altyn Tagh Fault, Northern Tibetan Plateau: Analysis of the Xorkol, Subei, and Aksay Basins. The Journal of geology 112, 207-229.

Robinson, D.M., Dupont-Nivet, G., Gehrels, G.E., Zhang, Y., 2003. The Tula uplift, northwestern China: Evidence for regional tectonism of the northern Tibetan Plateau during late Mesozoic–early Cenozoic time. Geological Society of America Bulletin 115, 35-47.

Shi, D.N., Shen, Y., Zhao, W.J., Li, A.B., 2009. Seismic evidence for a Moho offset and south-directed thrust at the easternmost Qaidam–Kunlun boundary in the Northeast Tibetan plateau. Earth and Planetary Science Letters 288, 329-334.

Tapponnier, P., Molnar, P., 1977. Active faulting and tectonics in China. Journal of Geophysical Research 82, 2905-2930.

Tapponnier, P., Peltzer, G., Armijo, R., Cobbold, P., 1982. Propagating extrusion tectonics in Asia; new insights from simple experiments with plasticine. Geology 10, 611-616.

Tapponnier, P., Peltzer, G., Armijo, R., 1986. On the mechanics of the collision between India and Asia. Geological Society, London, Special Publications 19, 113-157.

Tapponnier, P., Xu, Z.Q., Roger, F., Meyer, B., Arnaud, N., Wittlinger, G., Yang, J.S., 2001. Oblique stepwise rise and growth of the Tibet Plateau. Science 294, 1671-1677.

Taylor, M., Yin, A., 2009. Active structures of the Himalayan-Tibetan orogen and their relationships to earthquake distribution, contemporary strain field, and Cenozoic volcanism. Geosphere 5, 199-214.

Wan, J.L., Wang, Y., Li, Q., Wang, F., Wang, E., 2001. FT Evidence of Northern Altyn Uplift in Late-Cenozoic. Bulletin of Mineralogy, Petrology and Geochemistry 20, 222-224 (in

Chinese with English abstract).

Wang, E., 1997. Displacement and timing along the northern strand of the Altyn Tagh fault zone, northern Tibet. Earth and Planetary Science Letters 150, 55-64.

Wang, Y., Zhang, X., Wang, E., Zhang, J., Li, Q., Sun, G., 2005. $^{40}Ar/^{39}Ar$ thermochronological evidence for formation and Mesozoic evolution of the northern-central segment of the Altyn Tagh fault system in the northern Tibetan Plateau. Geological Society of America Bulletin 117, 1336-1346.

Wang, E., Xu, F.-Y., Zhou, J.-X., Wan, J., Burchfiel, B.C., 2006. Eastward migration of the Qaidam basin and its implications for Cenozoic evolution of the Altyn Tagh fault and associated river systems. Geological Society of America Bulletin 118, 349-365.

Wang, C., Zhao, X., Liu, Z., Lippert, P.C., Graham, S.A., Coe, R.S., Yi, H., Zhu, L., Liu, S., Li, Y., 2008. Constraints on the early uplift history of the Tibetan Plateau. Proceedings of the National Academy of Sciences 105, 4987-4992.

Wang, C.S., Gao, R., Yin, A., Wang, H., Zhang, Y.X., Guo, T.L., Li, Q.S., Li, Y.L., 2011. A mid-crustal strain-transfer model for continental deformation: A new perspective from high-resolution deep seismic-reflection profiling across NE Tibet. Earth and Planetary Science Letters 306, 279-288.

Wang, C., Dai, J., Zhao, X., Li, Y., Graham, S.A., He, D., Ran, B., Meng, J., 2014. Outward-growth of the Tibetan Plateau during the Cenozoic: A review. Tectonophysics.

Wu, L., Xiao, A., Wang, L., Mao, L., Wang, L., Dong, Y., Xu, B., 2012a. EW-trending uplifts along the southern side of the central segment of the Altyn Tagh Fault, NW China: Insight into the rising mechanism of the Altyn Mountain during the Cenozoic. SCIENCE CHINA Earth Sciences 55, 926-939.

Wu, L., Xiao, A.C., Yang, S.F., Wang, L.Q., Mao, L.G., Wang, L., Dong, Y.P., Xu, B., 2012b. Two-stage evolution of the Altyn Tagh Fault during the Cenozoic: new insight from provenance analysis of a geological section in NW Qaidam Basin, NW China. Terra Nova 24, 387-395.

Wu, L., Xiao, A.C., Ma, D.D., Li, H.G., Xu, B., Shen, Y., Mao, L.G., 2014. Cenozoic fault systems in southwest Qaidam Basin, northeastern Tibetan Plateau: Geometry, temporal

development, and significance for hydrocarbon accumulation. AAPG Bulletin 98, 1213-1234.

Xia, W.C., Zhang, N., Yuan, X.P., Fan, L.S., Zhang, B.S., 2001. Cenozoic Qaidam basin, China: A stronger tectonic inversed, extensional rifted basin. AAPG bulletin 85, 715-736.

Yang, J., Xu, Z., Zhang, J., Chu, C.-Y., Zhang, R., Liou, J.-G., 2001. Tectonic significance of early Paleozoic high-pressure rocks in Altun-Qaidam-Qilian Mountains, northwest China. Geological Society of America Memoirs 194, 151-170.

Yin, A., Harrison, T.M., 2000. Geologic evolution of the Himalayan-Tibetan orogen. Annual Review of Earth and Planetary Sciences 28, 211-280.

Yin, A., Rumelhart, P., Butler, R., Cowgill, E., Harrison, T., Foster, D., Ingersoll, R., Qing, Z., Xian-Qiang, Z., Xiao-Feng, W., 2002. Tectonic history of the Altyn Tagh fault system in northern Tibet inferred from Cenozoic sedimentation. Geological Society of America Bulletin 114, 1257-1295.

Yin, A., Dang, Y.Q., Zhang, M., McRivette, M.W., Burgess, W.P., Chen, X.H., 2007. Cenozoic tectonic evolution of Qaidam basin and its surrounding regions (part 2): Wedge tectonics in southern Qaidam basin and the Eastern Kunlun Range. Geological Society of America Special Papers 433, 369-390.

Yin, A., Dang, Y.Q., Zhang, M., Chen, X.H., McRivette, M.W., 2008a. Cenozoic tectonic evolution of the Qaidam basin and its surrounding regions (Part 3): Structural geology, sedimentation, and regional tectonic reconstruction. Geological Society of America Bulletin 120, 847-876.

Yin, A., Dang, Y.Q., Wang, L.C., Jiang, W.M., Zhou, S.P., Chen, X.H., Gehrels, G.E., McRivette, M.W., 2008b. Cenozoic tectonic evolution of Qaidam basin and its surrounding regions (Part 1): The southern Qilian Shan-Nan Shan thrust belt and northern Qaidam basin. Geological Society of America Bulletin 120, 813-846.

Yin, A., 2010. Cenozoic tectonic evolution of Asia: A preliminary synthesis. Tectonophysics 488, 293-325.

Yu, X., Huang, B., Guan, S., Fu, S., Cheng, F., Cheng, X., Zhang, T., Guo, Z., 2014. Anisotropy of magnetic susceptibility of Eocene and Miocene sediments in the Qaidam Basin,

Northwest China: Implication for Cenozoic tectonic transition and depocenter migration. Geochemistry, Geophysics, Geosystems 15, 2095-2108.

Yuan, W.M., Dong, J.Q., Wang, S.C., Carter, A., 2006. Apatite fission track evidence for Neogene uplift in the eastern Kunlun Mountains, northern Qinghai–Tibet Plateau, China. Journal of Asian Earth Sciences 27, 847-856.

Yuan, D.Y., Ge, W.P., Chen, Z.W., Li, C.Y., Wang, Z.C., Zhang, H.P., Zhang, P.Z., Zheng, D.W., Zheng, W.J., Craddock, W.H., Dayem, K.E., Duvall, A.R., Hough, B.G., Lease, R.O., Champagnac, J.-D., Burbank, D.W., Clark, M.K., Farley, K.A., Garzione, C.N., Kirby, E., Molnar, P., Roe, G.H., 2013. The growth of northeastern Tibet and its relevance to large-scale continental geodynamics: A review of recent studies. Tectonics 32, 2013TC003348.

Yue, Y.J., Liou, J.G., 1999. Two-stage evolution model for the Altyn Tagh fault, China. Geology 27, 227-230.

Yue, Y.J., Ritts, B.D., Graham, S.A., 2001. Initiation and long-term slip history of the Altyn Tagh Fault. International Geology Review 43, 1087-1093.

Zhang, P.Z., Shen, Z., Wang, M., Gan, W., Bürgmann, R., Molnar, P., Wang, Q., Niu, Z., Sun, J., Wu, J., 2004. Continuous deformation of the Tibetan Plateau from global positioning system data. Geology 32, 809-812.

Zhang, H.-p., Zhang, P.-z., Zheng, D.-W., Zheng, W.-J., Chen, Z.-W., Wang, W.-T., 2014. Transforming the Miocene Altyn Tagh fault slip into shortening of the north-western Qilian Shan: insights from the drainage basin geometry. Terra Nova 26, 216-221.

Zhuang, G., Hourigan, J.K., Ritts, B.D., Kent-Corson, M.L., 2011. Cenozoic multiple-phase tectonic evolution of the northern Tibetan Plateau: Constraints from sedimentary records from Qaidam basin, Hexi Corridor, and Subei basin, northwest China. American Journal of Science 311, 116-152.

# Appendix

Appendix to Chapter 2.2

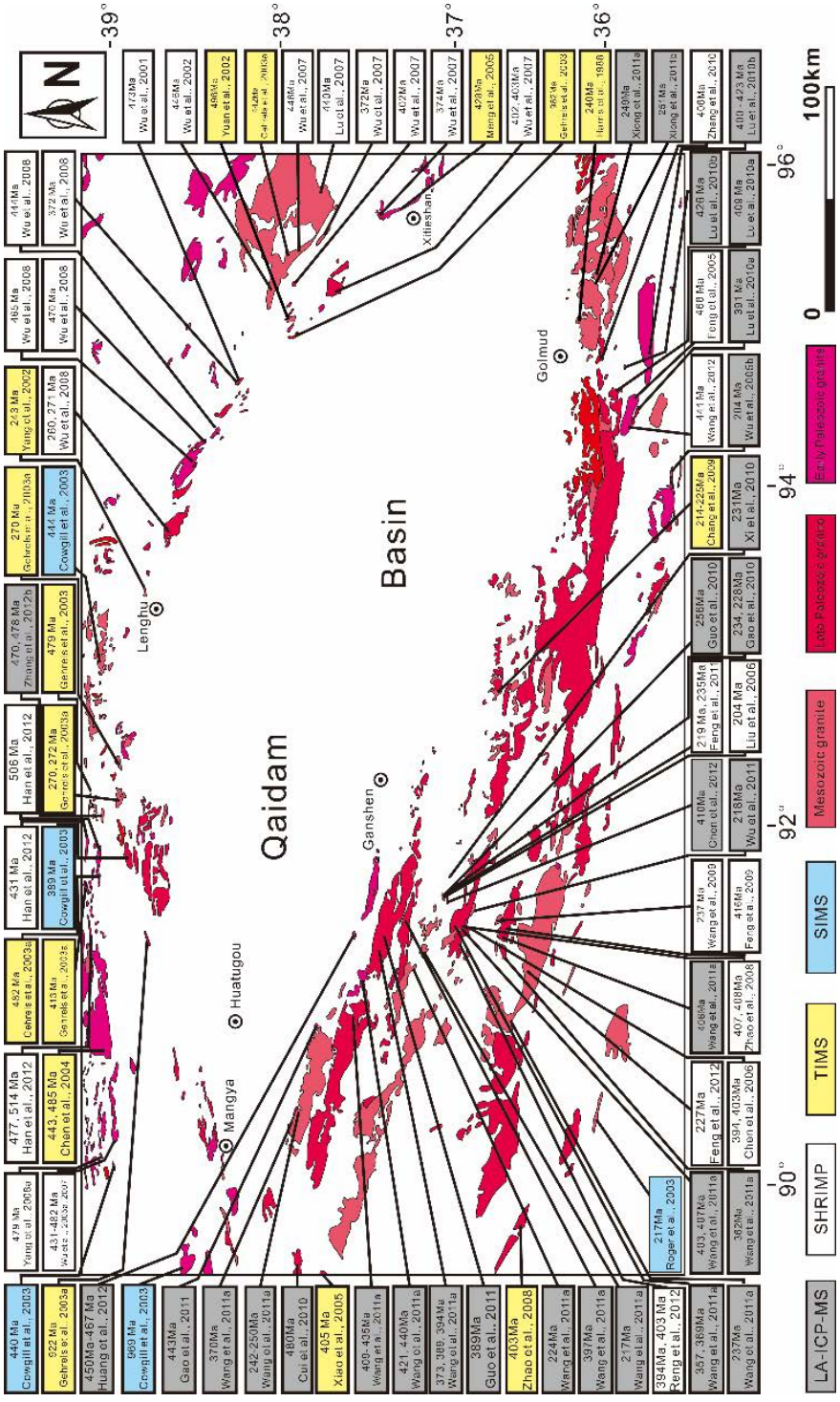


gure DR1 Distribution of magmatic rocks in the surrounding area of Qaidam basin and statistics of the zircon U-Pb ages. The statistics of the zircon U-Pb ages are mainly collected from references in Table DR1

Table DR1. Zircon U-Pb ages from plutons of the Eastern Kunlun Range, Altyn Tagh Range and Qilian Shan.

| Altyn Tagh Range | | | Qilian Shan | | | East Kunlun Range | | |
|---|---|---|---|---|---|---|---|---|
| Source | Year | Age(Ma) | Source | Year | Age(Ma) | Source | Year | Age(Ma) |
| Yue Yongjun et al., | 2005 | 413 | Yue Yongjun et al., | 2005 | 1728 | She Hongquan et al., | 2007 | 215 |
| Yue Yongjun et al., | 2005 | 482 | Yue Yongjun et al., | 2005 | 482 | Li Shijin et al., | 2008 | 224 |
| Yue Yongjun et al., | 2005 | 1870 | Yue Yongjun et al., | 2005 | 424 | Wang Song et al., | 2009 | 237 |
| Yue Yongjun et al., | 2005 | 1877 | Yue Yongjun et al., | 2005 | 472 | Li Dongsheng et al., | 2009 | 206 |
| Yue Yongjun et al., | 2005 | 479 | Yue Yongjun et al., | 2005 | 480 | Li Dongsheng et al., | 2009 | 223 |
| Gehrels et al., | 2003 | 270 | Yue Yongjun et al., | 2005 | 423 | Feng Chengyou et al., | 2009 | 237 |
| Gehrels et al., | 2003 | 272 | Yue Yongjun et al., | 2005 | 406 | Huang Limei et al., | 2012 | 459 |
| Gehrels et al., | 2003 | 270 | Yue Yongjun et al., | 2005 | 425 | Guo Lei et al., | 2010 | 256 |
| Gehrels et al., | 2003 | 440 | Yue Yongjun et al., | 2005 | 366 | Gao Yongbao et al., | 2012 | 228 |
| Cowgill et al., | 2003 | 922 | Yue Yongjun et al., | 2005 | 248 | Gao Yongbao et al., | 2012 | 234 |
| Cowgill et al., | 2003 | 389 | Yue Yongjun et al., | 2005 | 434 | Liu Chengdong et al., | 2003 | 242 |
| Cowgill et al., | 2003 | 2720 | Yue Yongjun et al., | 2005 | 441 | Liu Yunhua et al., | 2006 | 204 |
| Cowgill et al., | 2003 | 442 | Yue Yongjun et al., | 2005 | 473 | Wu Xiangke et al., | 2011 | 218 |
| Cowgill et al., | 2003 | 290 | Yue Yongjun et al., | 2005 | 430 | Feng Chengyou et al., | 2011 | 219 |
| Cowgill et al., | 2003 | 404 | Gehrels et al., | 2003 | 461 | Feng Chengyou et al., | 2011 | 235 |
| Cowgill et al., | 2003 | 457 | Cowgill et al., | 2003 | 459 | Chen Danling et al., | 2011 | 212 |
| Cowgill et al., | 2003 | 518 | Cowgill et al., | 2003 | 922 | Ren Erfeng et al., | 2012 | 403 |
| Cowgill et al., | 2003 | 475 | Cowgill et al., | 2003 | 928 | Ren Erfeng et al., | 2012 | 394 |
| Cowgill et al., | 2003 | 969 | Cowgill et al., | 2003 | 442 | Feng Chengyou et al., | 2010 | 227 |
| Cowgill et al., | 2003 | 444 | Cowgill et al., | 2003 | 422 | Feng Chengyou et al., | 2010 | 220 |
| Cowgill et al., | 2003 | 2396 | Lu Songnian et al., | 2008 | 2366 | Gao Yongbao et al., | 2011 | 430 |
| Lu Songnian et al., | 2008 | 2582 | Lu Songnian et al., | 2008 | 2412 | Gao Yongbao et al., | 2011 | 431 |
| Lu Songnian et al., | 2008 | 2604 | Lu Songnian et al., | 2008 | 1939 | Feng Chengyou et al., | 2009 | 417 |
| Lu Songnian et al., | 2008 | 2830 | Lu Songnian et al., | 2008 | 2348 | Feng Chengyou et al., | 2009 | 468 |
| Lu Songnian et al., | 2008 | 3574 | Lu Songnian et al., | 2008 | 1852 | Chen Junlu et al., | 2004 | 405 |

| | | | | | | | | |
|---|---|---|---|---|---|---|---|---|
| Lu Songnian et al., | 2008 | 3665 | Lu Songnian et al., | 2008 | 1763 | Chen Junlu et al., | 2004 | 2380 |
| Lu Songnian et al., | 2008 | 2396 | Lu Songnian et al., | 2008 | 844 | Chen Junlu et al., | 2004 | 816 |
| Lu Songnian et al., | 2008 | 1978 | Lu Songnian et al., | 2008 | 740 | Chen Junlu et al., | 2004 | 401 |
| Lu Songnian et al., | 2008 | 2670 | Lu Songnian et al., | 2008 | 1050 | Cui Meihui et al., | 2011 | 480 |
| Lu Songnian et al., | 2008 | 2830 | Lu Songnian et al., | 2008 | 1020 | Wang Bingzhang et al., | 2009 | 271 |
| Lu Songnian et al., | 2008 | 1986 | Lu Songnian et al., | 2008 | 1020 | Wang Bingzhang et al., | 2009 | 284 |
| Lu Songnian et al., | 2008 | 2374 | Lu Songnian et al., | 2008 | 1020 | Wang Bingzhang et al., | 2009 | 251 |
| Lu Songnian et al., | 2008 | 2351 | Lu Songnian et al., | 2008 | 987 | Mo xuanxue et al., | 2005 | 212 |
| Lu Songnian et al., | 2008 | 2358 | Lu Songnian et al., | 2008 | 928 | Qinghai Geology investigation institute | 2008 | 214 |
| Lu Songnian et al., | 2008 | 2366 | Lu Songnian et al., | 2008 | 917 | Qinghai Geology investigation institute | 2008 | 225 |
| Lu Songnian et al., | 2008 | 2412 | Lu Songnian et al., | 2008 | 917 | Xiao Aifang et al., | 2005 | 405 |
| Lu Songnian et al., | 2008 | 2426 | Lu Songnian et al., | 2008 | 878 | Wang Xiangli et al., | 2010 | 1090 |
| Lu Songnian et al., | 2008 | 1900 | Lu Songnian et al., | 2008 | 953 | Wang Xiangli et al., | 2010 | 312 |
| Lu Songnian et al., | 2008 | 930 | Lu Songnian et al., | 2008 | 875 | Gao Yongbao et al., | 2010 | 430 |
| Wu Cailai et al., | 2005 | 474 | Lu Songnian et al., | 2008 | 878 | Gao Yongbao et al., | 2010 | 430 |
| Wu Cailai et al., | 2005 | 446 | Lu Songnian et al., | 2008 | 864 | Gao Yongbao et al., | 2010 | 430 |
| Wu Cailai et al., | 2005 | 435 | Lu Songnian et al., | 2008 | 855 | Qinghai Geology investigation institute | 2003 | 410 |
| Wu Cailai et al., | 2005 | 431 | Lu Songnian et al., | 2008 | 844 | Qinghai Geology investigation institute | 2003 | 419 |
| Yang Jingsui et al., | 2008 | 479 | Lu Songnian et al., | 2008 | 821 | Ma Yongshou et al., | 2010 | 550 |
| Yang Wenqiang et al., | 2012 | 453 | Lu Songnian et al., | 2008 | 1776 | Ma Yongshou et al., | 2010 | 2046 |
| Hao Jie et al., | 2006 | 467 | Lu Songnian et al., | 2008 | 740 | Wu Shaofeng et al., | 2012 | 429 |
| Sun Jiming et al., | 2012 | 497 | Lu Songnian et al., | 2008 | 1793 | Tan Shengxiang et al., | 2004 | 831 |
| Wang Chao et al., | 2013 | 923 | Lu Songnian et al., | 2008 | 1800 | Cao Shitai et al., | 2011 | 429 |
| Wang Chao et al., | 2013 | 910 | Wang Chao et al., | 2013 | 976 | Cao Shitai et al., | 2011 | 430 |

| | | | | | | | | |
|---|---|---|---|---|---|---|---|---|
| Wang Chao et al., | 2013 | 927 | Wang Chao et al., | 2013 | 952 | Wang Binzhang | 2012 | 440 |
| Wang Chao et al., | 2013 | 924 | Wang Chao et al., | 2013 | 941 | Wang Binzhang | 2012 | 450 |
| Wang Chao et al., | 2013 | 906 | Wang Chao et al., | 2013 | 935 | Feng Chengyou et al., | 2010 | 219 |
| Wang Chao et al., | 2013 | 916 | Wang Chao et al., | 2013 | 953 | Xi Rengang et al., | 2011 | 231 |
| Wang Chao et al., | 2013 | 938 | Wang Chao et al., | 2013 | 915 | Guo Tongzhen et al., | 2011 | 389 |
| Wang Chao et al., | 2013 | 907 | Wang Chao et al., | 2013 | 907 | Qinghai Geology investigation institute | 2010 | 224 |
| Xiu Qunye et al., | 2007 | 449 | Wang Chao et al., | 2013 | 932 | Feng Chengyou et al., | 2012 | 227 |
| Han Dengbin et al., | 2012 | 446 | Wang Chao et al., | 2013 | 918 | Feng Chengyou et al., | 2012 | 220 |
| Han Dengbin et al., | 2012 | 477 | Wang Chao et al., | 2013 | 930 | Chang Youying et al., | 2009 | 223 |
| Han Dengbin et al., | 2012 | 477 | Liu Liang et al., | 2013 | 783 | Chang Youying et al., | 2009 | 214 |
| Han Dengbin et al., | 2012 | 514 | Liu Liang et al., | 2013 | 748 | Chang Youying et al., | 2009 | 225 |
| Han Dengbin et al., | 2012 | 417 | Liu Liang et al., | 2013 | 847 | Liu Xiaokang et al., | 2011 | 419 |
| Han Dengbin et al., | 2012 | 488 | Liu Liang et al., | 2013 | 847 | Chen Bo et al., | 2012 | 410 |
| Han Dengbin et al., | 2012 | 479 | Liu Liang et al., | 2013 | 457 | Gao Xiaofeng et al., | 2011 | 443 |
| Han Dengbin et al., | 2012 | 506 | Liu Liang et al., | 2013 | 446 | Luo Zhaohua et al., | 2002 | 212 |
| Han Dengbin et al., | 2012 | 431 | Liu Liang et al., | 2013 | 909 | Mo xuanxue et al., | 2007 | 471 |
| Han Dengbin et al., | 2012 | 443 | Liu Liang et al., | 2013 | 1005 | Mo xuanxue et al., | 2007 | 485 |
| Han Dengbin et al., | 2012 | 417 | Liu Liang et al., | 2013 | 891 | Mo xuanxue et al., | 2005 | 387 |
| Han Dengbin et al., | 2012 | 431 | Liu Liang et al., | 2013 | 890 | Mo xuanxue et al., | 2005 | 386 |
| Han Dengbin et al., | 2012 | 440 | Liu Liang et al., | 2013 | 516 | Mo xuanxue et al., | 2005 | 408 |
| Wu Cailai et al., | 2007 | 435 | Shi Rendeng et al., | 2004 | 550 | Mo xuanxue et al., | 2005 | 408 |
| Wu Cailai et al., | 2007 | 433 | Meng Fancong et al., | 2010 | 505 | Mo xuanxue et al., | 2005 | 401 |
| Wu Cailai et al., | 2007 | 435 | Zeng Jianyuan et al., | 2007 | 497 | Chen Hongwei et al., | 2006 | 403 |
| Wu Cailai et al., | 2007 | 431 | Wu Cailai et al., | 2010 | 501 | Chen Hongwei et al., | 2006 | 394 |
| Liu Han et al., | 2012 | 750 | Wu Cailai et al., | 2010 | 512 | Lu Songnian et al., | 2002 | 522 |
| Liu Han et al., | 2012 | 763 | Wu Cailai et al., | 2010 | 508 | Lu Songnian et al., | 2002 | 2468 |
| Liu Han et al., | 2012 | 754 | Wu Cailai et al., | 2010 | 477 | Lu Songnian et al., | 2002 | 1955 |

| | | | | | | | | |
|---|---|---|---|---|---|---|---|---|
| Liu Liang et al., | 1999 | 524 | Wu Cailai et al., | 2010 | 463 | Yang Jinsui et al., | 1996 | 518 |
| Zeng Jianyuan et al., | 2006 | 776 | Wu Cailai et al., | 2010 | 424 | Feng Jianyun et al., | 2010 | 509 |
| Zeng Jianyuan et al., | 2006 | 774 | Wu Cailai et al., | 2010 | 435 | Wang Binzhang | 2012 | 509 |
| Lu Songnian et al., | 2009 | 757 | Wu Cailai et al., | 2010 | 429 | Wang Binzhang | 2012 | 434 |
| Lu Songnian et al., | 2009 | 438 | Song Zhongbao et al., | 2004 | 482 | Wang Binzhang | 2012 | 435 |
| Lu Songnian et al., | 2009 | 425 | Song Zhongbao et al., | 2007 | 458 | Wang Binzhang | 2012 | 419 |
| | 2009 | 2679 | Huang Chuanjian et | 1995 | 486 | Wang Binzhang | 2012 | 421 |
| Wu Yuezhong et al., | | | al., | | | | | |
| Wu Yuezhong et al., | 2009 | 856 | Wu Cailai et al., | 2007 | 477 | Wang Binzhang | 2012 | 413 |
| Wu Yuezhong et al., | 2009 | 1312 | Wu Cailai et al., | 2007 | 463 | Wang Binzhang | 2012 | 409 |
| Wu Yuezhong et al., | 2009 | 1209 | Wang Yusheng et al., | 2001 | 940 | Wang Binzhang | 2012 | 1782 |
| Wu Yuezhong et al., | 2009 | 871 | Wang Yusheng et al., | 2001 | 1030 | Wang Binzhang | 2012 | 2642 |
| Wu Yuezhong et al., | 2009 | 1311 | Wang Yusheng et al., | 2001 | 1020 | Wang Binzhang | 2012 | 881 |
| Wu Yuezhong et al., | 2009 | 450 | Wang Yusheng et al., | 2000 | 930 | Wang Binzhang | 2012 | 923 |
| Wu Yuezhong et al., | 2009 | 465 | Wang Yusheng et al., | 2000 | 930 | Wang Binzhang | 2012 | 427 |
| Wu Yuezhong et al., | 2009 | 445 | Wang Yusheng et al., | 2000 | 750 | Wang Binzhang | 2012 | 451 |
| Wu Yuezhong et al., | 2009 | 452 | Guo Jinjing et al., | 1999 | 920 | Wang Binzhang | 2012 | 189 |
| Wu Yuezhong et al., | 2009 | 448 | Guo Jinjing et al., | 1999 | 910 | Wang Binzhang | 2012 | 290 |
| Wu Yuezhong et al., | 2009 | 327 | Mei Hualin et al., | 1998 | 2670 | Wang Binzhang | 2012 | 397 |
| Wu Yuezhong et al., | 2009 | 313 | Mei Hualin et al., | 1999 | 880 | Wang Binzhang | 2012 | 683 |
| Wu Yuezhong et al., | 2009 | 397 | Xu Wanchun et al., | 2007 | 891 | Wang Binzhang | 2012 | 373 |
| | 2003 | 495 | Wang Christina Yan | 2005 | 445 | Wang Binzhang | 2012 | 394 |
| Xiao Peixi et al., | | | et al., | | | | | |
| Song Zhongbao et al., | 2004 | 482 | Xu Wangchun et al., | 2007 | 776 | Wang Binzhang | 2012 | 373 |
| Liu Han et al., | 2011 | 462 | Xu Wangchun et al., | 2007 | 774 | Wang Binzhang | 2012 | 369 |
| Liu Han et al., | 2011 | 437 | Li Xianhua et al., | 2004 | 827 | Wang Binzhang | 2012 | 370 |
| Zhang Zhicheng et al., | 2008 | 521 | Ayers et al., | 2002 | 1921 | Wang Binzhang | 2012 | 397 |
| Kang Lei et al., | 2011 | 500 | Mattinson et al., | 2006 | 433 | Wang Binzhang | 2012 | 395 |

| | | | | | | | | |
|---|---|---|---|---|---|---|---|---|
| Gherels et al., | 1999 | 480 | Xia Xiaohong et al., | 2009 | 490 | Wang Binzhang | 2012 | 370 |
| Chen Xuanhua et al., | 2003 | 443 | He Shiping et al., | 2007 | 443 | Wang Binzhang | 2012 | 357 |
| Dong Shunli et al., | 2013 | 450 | He Shiping et al., | 2007 | 1782 | Wang Binzhang | 2012 | 284 |
| Dong Shunli et al., | 2013 | 465 | He Shiping et al., | 2007 | 385 | Wang Binzhang | 2012 | 241 |
| Zhang Zhanwu et al., | 2012 | 478 | He Shiping et al., | 2007 | 471 | Wang Binzhang | 2012 | 250 |
| Zhang Zhanwu et al., | 2012 | 470 | Li Shuguang et al., | 2004 | 447 | Wang Binzhang | 2012 | 217 |
| Dong Zengchan et al., | 2011 | 445 | Zhang Zhaowei et al., | 2012 | 441 | Wang Binzhang | 2012 | 224 |
| Liu Han et al., | 2012 | 2007 | Wei Fanghui et al., | 2012 | 441 | Ma Shengchao et al., | 2012 | 219 |
| Ma Zhongping et al., | 2012 | 467 | Zhang Zhaowei et al., | 2012 | 443 | Ma Shengchao et al., | 2012 | 235 |
| Ma Zhongping et al., | 2012 | 462 | Mao Jingwen et al., | 2000 | 460 | Cui Meihui et al., | 2012 | 480 |
| Ma Zhongping et al., | 2012 | 470 | Xiong Ziliang et al., | 2012 | 424 | Zhang Dequan et al., | 2001 | 438 |
| Ma Zhongping et al., | 2012 | 464 | Xiong Ziliang et al., | 2012 | 402 | Cheng Nengsong et al., | 2008 | 517 |
| Yang Qi et al., | 2004 | 443 | Su Jianping et al., | 2004 | 444 | Cheng Nengsong et al., | 2008 | 516 |
| Yang Qi et al., | 2004 | 485 | Yu Jiyuan et al., | 2012 | 455 | Cheng Nengsong et al., | 2008 | 559 |
| Liu Liang et al., | 2007 | 750 | Wu Cailai et al., | 2006 | 476 | Cheng Nengsong et al., | 2008 | 482 |
| | 2005 | 846 | Wu Cailai et al., | 2006 | 463 | Cheng Nengsong et al., | 2008 | 516 |
| Zhang Jianxin | abc | | | | | | | |
| | 2005 | 844 | Wang Yinchuan et al., | 2012 | 1765 | Cheng Nengsong et al., | 2008 | 549 |
| Zhang Jianxin | abc | | | | | | | |
| Zhang Jianxin | 2004 | 842 | Wu Cailai et al., | 2004 | 383 | Yang Jingsui et al., | 1995 | 518 |
| Liu Liang | 2009 | 1800 | Chen Junlu et al., | 2006 | 440 | Lu Songnian et al., | 2002 | 522 |
| | 2009 | 821 | Wang Hongliang et | 2007 | 1192 | Yang Jingsui et al., | 1996 | 579 |
| Liu Liang | | | al., | | | | | |
| Qi Xuexiang | 2005 | 482 | Qi Ruirong et al., | 2012 | 463 | Li Huaikun et al., | 2006 | 506 |
| | 2005 | 404 | Huang Zengbao et al., | 2010 | 414 | Guangxi Geology | 2003 | 1209 |
| Qi Xuexiang | | | | | | investigation institute | | |
| | 2013 | 754 | Xiang Zengqun et al., | 2007 | 504 | Guangxi Geology | 2003 | 871 |
| Liu Liang | | | | | | investigation institute | | |

| | | | | | | | | |
|---|---|---|---|---|---|---|---|---|
| | 2013 | 752 | Yang Jinsui et al., | 2008 | 479 | Guangxi Geology investigation institute | 2003 | 550 |
| Liu Liang | | | | | | | | |
| | 2013 | 647 | Xiao Lin et al., | 1997 | 2152 | Guangxi Geology investigation institute | 2003 | 408 |
| Liu Liang | | | | | | | | |
| | 2013 | 730 | Yong Yong et al., | 2008 | 454 | Guangxi Geology investigation institute | 2003 | 397 |
| Liu Liang | | | | | | | | |
| | 2013 | 857 | Yong Yong et al., | 2008 | 846 | Guangxi Geology investigation institute | 2003 | 320 |
| Liu Liang | | | | | | | | |
| | 2013 | 719 | Yong Yong et al., | 2008 | 756 | Guangxi Geology investigation institute | 2003 | 381 |
| Liu Liang | | | | | | | | |
| | 2013 | 867 | Yong Yong et al., | 2008 | 853 | Guangxi Geology investigation institute | 2003 | 271 |
| Liu Liang | | | | | | | | |
| | 2013 | 563 | Xu Xueyi et al., | 2008 | 723 | Qinghai Geology investigation institute | 2003 | 831 |
| Liu Liang | | | | | | | | |
| Wu Cailai et al., | 2001 | 446 | Zeng Jianyuan et al., | 2006 | 776 | Yang Jinsui et al., | 2005 | 417 |
| Chen Xuanhua et al., | 2003 | 2926 | Zeng Jianyuan et al., | 2006 | 774 | Yang Jinsui et al., | 2005 | 421 |
| Chen Xuanhua et al., | 2003 | 1728 | Chen Junlu et al., | 2008 | 445 | Yang Jinsui et al., | 2005 | 250 |
| Chen Xuanhua et al., | 2003 | 405 | Xia Xiaohong et al., | 2010 | 490 | Yang Jinsui et al., | 2005 | 308 |
| Wu Suoping et al., | 2007 | 385 | He Yanhong et al., | 2005 | 447 | Bian Qiantao et al., | 1999 | 402 |
| Li Weidong et al., | 2012 | 462 | Guo Jinjing et al., | 1999 | 917 | Cheng Nengsong et al., | 2000 | 447 |
| Cao Yuting et al., | 2013 | 579 | Pei Xianzhi et al., | 2007 | 440 | Gao Xiaofeng et al., | 2010 | 458 |
| | 2010 | 410 | Pei Xianzhi et al., | 2007 | 450 | Shanxi Geology investigation institute | 2003 | 432 |
| Liu Feng et al., | | | | | | | | |
| Liu Han et al., | 2013 | 457 | He Yanhong et al., | 2005 | 1900 | Feng Jianyun et al., | 2010 | 509 |
| Liu Han et al., | 2013 | 419 | He Yanhong et al., | 2005 | 2350 | Zhang Yafeng et al., | 2010 | 515 |
| Liu Han et al., | 2013 | 411 | He Yanhong et al., | 2005 | 2500 | Sun Yu et al., | 2009 | 255 |
| Liu Han et al., | 2013 | 503 | Wu Cailai et al., | 2008 | 465 | Liu Chengdong et al., | 2004 | 239 |
| Liu Han et al., | 2013 | 420 | Wu Cailai et al., | 2008 | 470 | Liu Chengdong et al., | 2004 | 242 |

| | | | | | | | | |
|---|---|---|---|---|---|---|---|---|
| Liu Han et al., | 2013 | 419 | Wu Cailai et al., | 2008 | 444 | Liu Chengdong et al., | 2000 | 236 |
| Liu Han et al., | 2013 | 411 | Wu Cailai et al., | 2008 | 372 | Liu Chengdong et al., | 2000 | 235 |
| Liu Han et al., | 2013 | 420 | Wu Cailai et al., | 2008 | 271 | Long Xiaoping et al., | 2006 | 411 |
| Liu Han et al., | 2013 | 405 | Wu Cailai et al., | 2008 | 260 | Long Xiaoping et al., | 2006 | 396 |
| Chen Xuanhua et al., | 2003 | 418 | Li Jianfeng et al., | 2010 | 415 | Zhang Jianxin et al., | 2003 | 402 |
| Chen Xuanhua et al., | 2003 | 413 | Li Jianfeng et al., | 2010 | 435 | Liu Zhanqing et al., | 2011 | 516 |
| Chen Xuanhua et al., | 2003 | 413 | Dong Guoan et al., | 2007 | 930 | Liu Zhanqing et al., | 2011 | 332 |
| | | | Dong Guoan et al., | 2007 | 918 | Liu Zhanqing et al., | 2011 | 441 |
| | | | Dong Guoan et al., | 2007 | 790 | Li Wangye et al., | 2007 | 493 |
| | | | Wu Cailai et al., | 2007 | 446 | Lu Lu et al., | 2010 | 423 |
| | | | Wu Cailai et al., | 2007 | 409 | Zhang Yaoling et al., | 2010 | 406 |
| | | | Wu Cailai et al., | 2007 | 403 | Sun Yu et al., | 2009 | 254 |
| | | | Wu Cailai et al., | 2007 | 375 | China University of Geosciences (Wuhan) | 2003 | 205 |
| | | | Wu Cailai et al., | 2007 | 372 | Ren Junhu et al., | 2009 | 436 |
| | | | Wu Peng et al., | 2012 | 499 | Ren Junhu et al., | 2009 | 413 |
| | | | Yu Jiyuan et al., | 2012 | 910 | Ren Junhu et al., | 2009 | 403 |
| | | | Xue Ning et al., | 2009 | 829 | Xiong Fuhao et al., | 2011 | 249 |
| | | | Xue Ning et al., | 2009 | 842 | Liu Bin et al., | 2012 | 407 |
| | | | Su Jianping et al., | 2004 | 751 | Liu Bin et al., | 2012 | 406 |
| | | | Lu Xinxiang et al., | 2007 | 440 | Liu et al., | 2004 | 242 |
| | | | Xia Xiaohong et al., | 2012 | 501 | Liu et al., | 2004 | 239 |
| | | | Xia Xiaohong et al., | 2012 | 495 | Cheng Nengsong et al., | 2002 | 448 |
| | | | Dang Jinhua et al., | 2011 | 345 | Cheng Nengsong et al., | 2002 | 427 |
| | | | | | | Cheng Nengsong et al., | 2002 | 920 |
| | | | | | | Zhang Jianxin et al., | 2003 | 460 |
| | | | | | | Cheng Nengsong et al., | 1999 | 500 |
| | | | | | | Li Huaikun et al., | 2006 | 500 |

| | | |
|---|---|---|
| China University of Geosciences (Wuhan) | 2003 | 438 |
| Zhu Yunhai et al., | 2005 | 419 |
| Zhu Yunhai et al., | 2005 | 401 |
| Li Fudong et al., | 1993 | 222 |
| Li Fudong et al., | 1993 | 206 |
| Li Fudong et al., | 1993 | 223 |
| Zhan fayu et al., | 2007 | 230 |
| Zhan fayu et al., | 2007 | 222 |
| Zhan fayu et al., | 2007 | 215 |
| Zhan fayu et al., | 2007 | 228 |
| Zhan fayu et al., | 2007 | 219 |
| Zhang Hongfei et al., | 2006 | 218 |
| Bian Qiantao et al., | 2007 | 402 |
| Lu Lu et al., | 2010 | 409 |
| Lu Lu et al., | 2010 | 391 |
| Robbinson et al., | 2003 | 74 |
| Li Wei et al., | 2013 | 485 |
| Li Wei et al., | 2013 | 439 |
| Li Wei et al., | 2013 | 424 |
| Li Wei et al., | 2013 | 262 |
| Li Wei et al., | 2013 | 462 |
| Li Wei et al., | 2013 | 428 |
| Li Wei et al., | 2013 | 446 |

Table DR2. LA-ICP-MS U-Pb data of detrital zircons from the 22 sandstone samples.

| Analysis number | Th/U | Isotopic ratios and errors | | | | | | Ages and errors (Ma) | | | | | | Disc.% |
|---|---|---|---|---|---|---|---|---|---|---|---|---|---|---|
| | | $^{207}Pb/^{206}Pb$ | 1σ | $^{207}Pb/^{235}U$ | 1σ | $^{206}Pb/^{238}U$ | 1σ | $^{207}Pb/^{206}Pb$ | 1σ | $^{207}Pb/^{235}U$ | 1σ | $^{206}Pb/^{238}U$ | 1σ | |
| **HTG-E** | | | | | | | | | | | | | | |
| HTG-01 | 1.14 | 0.05583 | 0.00138 | 0.53192 | 0.0133 | 0.06909 | 0.00099 | 446 | 31 | 433 | 9 | 431 | 6 | 0.5 |
| HTG-02 | 0.72 | 0.05142 | 0.0026 | 0.2838 | 0.01417 | 0.04002 | 0.00069 | 260 | 83 | 254 | 11 | 253 | 4 | 0.4 |
| HTG-03 | 0.45 | 0.05474 | 0.00138 | 0.48562 | 0.01239 | 0.06433 | 0.00093 | 402 | 32 | 402 | 8 | 402 | 6 | 0 |
| HTG-04 | 0.57 | 0.06984 | 0.00157 | 1.48928 | 0.03402 | 0.15464 | 0.00222 | 924 | 25 | 926 | 14 | 927 | 12 | -0.1 |
| HTG-05 | 0.61 | 0.05156 | 0.00179 | 0.30118 | 0.01037 | 0.04236 | 0.00067 | 266 | 50 | 267 | 8 | 267 | 4 | 0 |
| HTG-06 | 0.98 | 0.05133 | 0.00371 | 0.29057 | 0.02058 | 0.04105 | 0.00087 | 256 | 123 | 259 | 16 | 259 | 5 | 0 |
| HTG-07 | 0.54 | 0.05248 | 0.00142 | 0.28769 | 0.00786 | 0.03975 | 0.00058 | 306 | 36 | 257 | 6 | 251 | 4 | 2.4 |
| HTG-08 | 0.49 | 0.05171 | 0.0016 | 0.30426 | 0.00936 | 0.04266 | 0.00065 | 273 | 43 | 270 | 7 | 269 | 4 | 0.4 |
| HTG-09 | 1.08 | 0.05122 | 0.0019 | 0.28264 | 0.01042 | 0.04002 | 0.00063 | 251 | 56 | 253 | 8 | 253 | 4 | 0 |
| HTG-10 | 1.55 | 0.09464 | 0.00214 | 3.45538 | 0.07954 | 0.26474 | 0.00386 | 1521 | 23 | 1517 | 18 | 1514 | 20 | 0.5 |
| HTG-11 | 0.38 | 0.08592 | 0.00275 | 2.72175 | 0.08636 | 0.2297 | 0.0037 | 1336 | 37 | 1334 | 24 | 1333 | 19 | 0.2 |
| HTG-12 | 1.59 | 0.06724 | 0.00205 | 1.30861 | 0.03942 | 0.14113 | 0.00224 | 845 | 37 | 850 | 17 | 851 | 13 | -0.1 |
| HTG-13 | 0.53 | 0.05514 | 0.00322 | 0.44021 | 0.02469 | 0.0579 | 0.00093 | 418 | 134 | 370 | 17 | 363 | 6 | 1.9 |
| ~~HTG-14~~ | ~~0.05~~ | ~~0.16236~~ | ~~0.00339~~ | ~~9.02601~~ | ~~0.19329~~ | ~~0.4031~~ | ~~0.00578~~ | ~~2480~~ | ~~18~~ | ~~2341~~ | ~~20~~ | ~~2183~~ | ~~27~~ | ~~13.6~~ |
| HTG-15 | 0.53 | 0.05168 | 0.0021 | 0.30648 | 0.01237 | 0.043 | 0.00067 | 271 | 64 | 271 | 10 | 271 | 4 | 0 |
| HTG-16 | 0.22 | 0.05626 | 0.00133 | 0.57136 | 0.01369 | 0.07365 | 0.00106 | 463 | 29 | 459 | 9 | 458 | 6 | 0.2 |
| HTG-17 | 1.00 | 0.05085 | 0.00241 | 0.26975 | 0.01267 | 0.03847 | 0.00064 | 234 | 78 | 242 | 10 | 243 | 4 | -0.4 |
| HTG-18 | 1.06 | 0.05176 | 0.00203 | 0.30631 | 0.01185 | 0.04291 | 0.0007 | 275 | 59 | 271 | 9 | 271 | 4 | 0 |
| HTG-19 | 0.69 | 0.05463 | 0.00393 | 0.47712 | 0.0338 | 0.06333 | 0.00126 | 397 | 124 | 396 | 23 | 396 | 8 | 0 |
| HTG-20 | 1.06 | 0.05119 | 0.00492 | 0.28202 | 0.02671 | 0.03995 | 0.00092 | 249 | 171 | 252 | 21 | 253 | 6 | -0.4 |
| HTG-21 | 0.52 | 0.07792 | 0.00331 | 1.9669 | 0.07795 | 0.18309 | 0.0028 | 1145 | 87 | 1104 | 27 | 1084 | 15 | 5.6 |
| HTG-22 | 0.91 | 0.07544 | 0.00267 | 1.86739 | 0.06482 | 0.17949 | 0.00311 | 1080 | 42 | 1070 | 23 | 1064 | 17 | 1.5 |

| | | | | | | | | | | | | | | |
|---|---|---|---|---|---|---|---|---|---|---|---|---|---|---|
| HTG-23 | 0.93 | 0.05701 | 0.0016 | 0.63664 | 0.01791 | 0.08098 | 0.00122 | 492 | 36 | 500 | 11 | 502 | 7 | -0.4 |
| HTG-24 | 0.42 | 0.05563 | 0.00194 | 0.52888 | 0.01823 | 0.06894 | 0.00111 | 438 | 48 | 431 | 12 | 430 | 7 | 0.2 |
| HTG-25 | 0.73 | 0.07017 | 0.00475 | 1.38465 | 0.09204 | 0.14309 | 0.00296 | 933 | 102 | 882 | 39 | 862 | 17 | 2.3 |
| HTG-26 | 0.54 | 0.04962 | 0.00947 | 0.19482 | 0.03663 | 0.02847 | 0.00103 | 177 | 315 | 181 | 31 | 181 | 6 | 0 |
| HTG-27 | 0.65 | 0.05141 | 0.00806 | 0.28292 | 0.04384 | 0.03991 | 0.00114 | 259 | 287 | 253 | 35 | 252 | 7 | 0.4 |
| HTG-28 | 0.78 | 0.05468 | 0.00183 | 0.47955 | 0.0159 | 0.0636 | 0.00101 | 399 | 46 | 398 | 11 | 397 | 6 | 0.3 |
| HTG-29 | 0.40 | 0.05352 | 0.00287 | 0.28534 | 0.01512 | 0.03866 | 0.00067 | 351 | 88 | 255 | 12 | 245 | 4 | 4.1 |
| HTG-30 | 0.62 | 0.05195 | 0.00188 | 0.32112 | 0.01154 | 0.04482 | 0.0007 | 283 | 54 | 283 | 9 | 283 | 4 | 0 |
| HTG-31 | 0.63 | 0.05571 | 0.00279 | 0.52718 | 0.02613 | 0.06862 | 0.00116 | 441 | 80 | 430 | 17 | 428 | 7 | 0.5 |
| HTG-32 | 0.56 | 0.05478 | 0.00211 | 0.48393 | 0.0183 | 0.06406 | 0.00109 | 403 | 54 | 401 | 13 | 400 | 7 | 0.2 |
| HTG-33 | 0.33 | 0.06604 | 0.00205 | 1.22579 | 0.03787 | 0.1346 | 0.0021 | 808 | 39 | 812 | 17 | 814 | 12 | -0.2 |
| HTG-34 | 0.56 | 0.05158 | 0.00242 | 0.29437 | 0.01362 | 0.04138 | 0.00072 | 267 | 74 | 262 | 11 | 261 | 4 | 0.4 |
| HTG-35 | 1.06 | 0.05136 | 0.00388 | 0.28391 | 0.02108 | 0.04008 | 0.00083 | 257 | 131 | 254 | 17 | 253 | 5 | 0.4 |
| HTG-36 | 0.59 | 0.05392 | 0.00179 | 0.25385 | 0.0084 | 0.03413 | 0.00053 | 368 | 47 | 230 | 7 | 216 | 3 | 6.5 |
| HTG-37 | 1.15 | 0.07332 | 0.002 | 1.73243 | 0.04735 | 0.17133 | 0.00261 | 1023 | 31 | 1021 | 18 | 1019 | 14 | 0.4 |
| HTG-38 | 0.71 | 0.05173 | 0.00203 | 0.30579 | 0.01181 | 0.04286 | 0.00071 | 273 | 58 | 271 | 9 | 271 | 4 | 0 |
| HTG-39 | 0.78 | 0.05354 | 0.004 | 0.40882 | 0.0301 | 0.05537 | 0.00111 | 352 | 131 | 348 | 22 | 347 | 7 | 0.3 |
| HTG-40 | 0.99 | 0.05535 | 0.00333 | 0.55771 | 0.03316 | 0.07306 | 0.00133 | 426 | 100 | 450 | 22 | 455 | 8 | -1.1 |
| HTG-41 | 0.30 | 0.06283 | 0.00282 | 0.66466 | 0.02941 | 0.07671 | 0.0013 | 702 | 65 | 517 | 18 | 476 | 8 | 8.6 |
| HTG-42 | 0.89 | 0.05179 | 0.00553 | 0.29852 | 0.03158 | 0.04179 | 0.00088 | 276 | 200 | 265 | 25 | 264 | 5 | 0.4 |
| HTG-43 | 1.21 | 0.05586 | 0.00164 | 0.55139 | 0.01613 | 0.07158 | 0.00109 | 447 | 38 | 446 | 11 | 446 | 7 | 0 |
| HTG-44 | 0.85 | 0.05555 | 0.00303 | 0.52298 | 0.02794 | 0.06826 | 0.00131 | 434 | 85 | 427 | 19 | 426 | 8 | 0.2 |
| HTG-45 | 0.53 | 0.05412 | 0.00194 | 0.44413 | 0.01567 | 0.05951 | 0.00098 | 376 | 50 | 373 | 11 | 373 | 6 | 0 |
| HTG-46 | 0.94 | 0.05621 | 0.00192 | 0.56264 | 0.01898 | 0.07258 | 0.00118 | 461 | 46 | 453 | 12 | 452 | 7 | 0.2 |
| HTG-47 | 0.46 | 0.05137 | 0.0016 | 0.30107 | 0.00931 | 0.0425 | 0.00066 | 257 | 43 | 267 | 7 | 268 | 4 | -0.4 |
| HTG-48 | 0.58 | 0.05618 | 0.00161 | 0.58709 | 0.01675 | 0.07578 | 0.00116 | 459 | 37 | 469 | 11 | 471 | 7 | -0.4 |
| HTG-49 | 0.74 | 0.05167 | 0.00277 | 0.29782 | 0.0158 | 0.0418 | 0.00072 | 271 | 90 | 265 | 12 | 264 | 4 | 0.4 |
| HTG-50 | 0.54 | 0.05082 | 0.00225 | 0.25119 | 0.01094 | 0.03584 | 0.00061 | 233 | 69 | 228 | 9 | 227 | 4 | 0.4 |

| | | | | | | | | | | | | | | |
|---|---|---|---|---|---|---|---|---|---|---|---|---|---|---|
| HTG-51 | 0.52 | 0.0553 | 0.00231 | 0.52488 | 0.02155 | 0.06882 | 0.00118 | 424 | 61 | 428 | 14 | 429 | 7 | -0.2 |
| HTG-52 | 0.42 | 0.09013 | 0.00358 | 2.79364 | 0.10182 | 0.2248 | 0.00353 | 1428 | 78 | 1354 | 27 | 1307 | 19 | 9.3 |
| HTG-53 | 1.12 | 0.05286 | 0.00318 | 0.36331 | 0.02142 | 0.04984 | 0.00098 | 323 | 98 | 315 | 16 | 314 | 6 | 0.3 |
| HTG-54 | 0.48 | 0.05524 | 0.00325 | 0.51835 | 0.03001 | 0.06804 | 0.00126 | 422 | 96 | 424 | 20 | 424 | 8 | 0 |
| HTG-55 | 0.75 | 0.05183 | 0.00295 | 0.31339 | 0.0174 | 0.04385 | 0.00086 | 278 | 91 | 277 | 13 | 277 | 5 | 0 |
| HTG-56 | 1.09 | 0.05133 | 0.00361 | 0.29415 | 0.02029 | 0.04155 | 0.00087 | 256 | 120 | 262 | 16 | 262 | 5 | 0 |
| HTG-57 | 0.58 | 0.05376 | 0.00229 | 0.43579 | 0.01823 | 0.05878 | 0.00102 | 361 | 63 | 367 | 13 | 368 | 6 | -0.3 |
| HTG-58 | 0.52 | 0.05563 | 0.00228 | 0.53272 | 0.02144 | 0.06944 | 0.00119 | 438 | 59 | 434 | 14 | 433 | 7 | 0.2 |
| HTG-59 | 0.58 | 0.05487 | 0.00179 | 0.49359 | 0.01597 | 0.06523 | 0.00103 | 407 | 44 | 407 | 11 | 407 | 6 | 0 |
| HTG-60 | 0.62 | 0.06888 | 0.00191 | 1.42808 | 0.03958 | 0.15034 | 0.00233 | 895 | 32 | 901 | 17 | 903 | 13 | -0.2 |
| HTG-61 | 0.82 | 0.05432 | 0.00218 | 0.45526 | 0.01797 | 0.06077 | 0.00104 | 384 | 58 | 381 | 13 | 380 | 6 | 0.3 |
| HTG-62 | 0.73 | 0.05492 | 0.00204 | 0.49022 | 0.01794 | 0.06472 | 0.00108 | 409 | 52 | 405 | 12 | 404 | 7 | 0.2 |
| HTG-63 | 0.90 | 0.05445 | 0.00283 | 0.45999 | 0.0234 | 0.06125 | 0.00117 | 390 | 80 | 384 | 16 | 383 | 7 | 0.3 |
| HTG-64 | 0.58 | 0.05656 | 0.00171 | 0.59192 | 0.01775 | 0.07588 | 0.00119 | 474 | 39 | 472 | 11 | 471 | 7 | 0.2 |
| HTG-65 | 0.46 | 0.05727 | 0.00185 | 0.63645 | 0.0203 | 0.08059 | 0.0013 | 502 | 42 | 500 | 13 | 500 | 8 | 0 |
| HTG-66 | 0.42 | 0.0549 | 0.00196 | 0.45753 | 0.01621 | 0.06043 | 0.00098 | 408 | 50 | 383 | 11 | 378 | 6 | 1.3 |
| HTG-67 | 0.61 | 0.05161 | 0.00245 | 0.30802 | 0.01437 | 0.04328 | 0.00077 | 268 | 74 | 273 | 11 | 273 | 5 | 0 |
| HTG-68 | 0.47 | 0.05632 | 0.00364 | 0.57228 | 0.03629 | 0.07368 | 0.00151 | 465 | 104 | 459 | 23 | 458 | 9 | 0.2 |
| HTG-69 | 0.58 | 0.05438 | 0.00259 | 0.46854 | 0.02178 | 0.06248 | 0.00117 | 387 | 71 | 390 | 15 | 391 | 7 | -0.3 |
| HTG-70 | 0.38 | 0.09241 | 0.00301 | 3.25629 | 0.10488 | 0.25551 | 0.00425 | 1476 | 36 | 1471 | 25 | 1467 | 22 | 0.6 |
| HTG-71 | 0.47 | 0.05474 | 0.00193 | 0.47067 | 0.01639 | 0.06235 | 0.00102 | 402 | 49 | 392 | 11 | 390 | 6 | 0.5 |
| HTG-72 | 0.43 | 0.05077 | 0.00239 | 0.24517 | 0.01134 | 0.03502 | 0.00062 | 230 | 74 | 223 | 9 | 222 | 4 | 0.5 |
| HTG-73 | 0.66 | 0.0544 | 0.0031 | 0.46269 | 0.02586 | 0.06168 | 0.00119 | 388 | 91 | 386 | 18 | 386 | 7 | 0 |
| HTG-74 | 1.43 | 0.05412 | 0.00263 | 0.45702 | 0.0217 | 0.06123 | 0.00114 | 376 | 73 | 382 | 15 | 383 | 7 | -0.3 |
| HTG-75 | 0.77 | 0.05529 | 0.00186 | 0.52349 | 0.01742 | 0.06866 | 0.00112 | 424 | 45 | 427 | 12 | 428 | 7 | -0.2 |
| HTG-76 | 0.54 | 0.0554 | 0.00939 | 0.52627 | 0.08804 | 0.06888 | 0.00225 | 428 | 313 | 429 | 59 | 429 | 14 | 0 |
| HTG-77 | 0.82 | 0.06618 | 0.00283 | 1.22955 | 0.05134 | 0.13472 | 0.00247 | 812 | 57 | 814 | 23 | 815 | 14 | -0.1 |
| HTG-78 | 0.69 | 0.05127 | 0.00273 | 0.29021 | 0.01512 | 0.04104 | 0.00079 | 253 | 84 | 259 | 12 | 259 | 5 | 0 |

| | | | | | | | | | | | | | | |
|---|---|---|---|---|---|---|---|---|---|---|---|---|---|---|
| HTG-79 | 0.59 | 0.05406 | 0.00407 | 0.45214 | 0.03325 | 0.06065 | 0.00141 | 374 | 124 | 379 | 23 | 380 | 9 | -0.3 |
| HTG-80 | 0.51 | 0.05518 | 0.00158 | 0.51989 | 0.01489 | 0.06832 | 0.00106 | 420 | 37 | 425 | 10 | 426 | 6 | -0.2 |
| HTG-81 | 0.56 | 0.05434 | 0.00272 | 0.44887 | 0.02218 | 0.0599 | 0.00107 | 385 | 79 | 376 | 16 | 375 | 7 | 0.3 |
| HTG-82 | 0.59 | 0.05538 | 0.00221 | 0.52724 | 0.0207 | 0.06903 | 0.00118 | 428 | 57 | 430 | 14 | 430 | 7 | 0 |
| HTG-83 | 0.60 | 0.05128 | 0.0021 | 0.28825 | 0.01155 | 0.04076 | 0.00071 | 253 | 60 | 257 | 9 | 258 | 4 | -0.4 |
| HTG-84 | 0.46 | 0.05165 | 0.00193 | 0.30158 | 0.01109 | 0.04234 | 0.00072 | 270 | 53 | 268 | 9 | 267 | 4 | 0.4 |
| HTG-85 | 0.69 | 0.0563 | 0.00178 | 0.59529 | 0.01864 | 0.07667 | 0.00123 | 464 | 41 | 474 | 12 | 476 | 7 | -0.4 |
| HTG-86 | 0.29 | 0.05526 | 0.00203 | 0.53191 | 0.01923 | 0.0698 | 0.00118 | 423 | 51 | 433 | 13 | 435 | 7 | -0.5 |
| HTG-87 | 0.78 | 0.06486 | 0.00283 | 1.07174 | 0.04564 | 0.11982 | 0.00222 | 770 | 58 | 740 | 22 | 730 | 13 | 1.4 |
| HTG-88 | 0.74 | 0.05406 | 0.00216 | 0.44507 | 0.01748 | 0.0597 | 0.00103 | 374 | 57 | 374 | 12 | 374 | 6 | 0 |
| HTG-89 | 0.03 | 0.05631 | 0.00245 | 0.58798 | 0.02521 | 0.07572 | 0.00132 | 465 | 64 | 470 | 16 | 471 | 8 | -0.2 |
| HTG-90 | 1.07 | 0.05356 | 0.00255 | 0.43177 | 0.02026 | 0.05846 | 0.00104 | 353 | 74 | 364 | 14 | 366 | 6 | -0.5 |
| HTG-91 | 0.58 | 0.07473 | 0.0032 | 1.67484 | 0.06999 | 0.16251 | 0.00306 | 1061 | 54 | 999 | 27 | 971 | 17 | 2.9 |
| HTG-92 | 0.34 | 0.06174 | 0.00324 | 0.84897 | 0.04384 | 0.09971 | 0.00182 | 665 | 79 | 624 | 24 | 613 | 11 | 1.8 |
| HTG-93 | 0.63 | 0.05174 | 0.00232 | 0.29968 | 0.01321 | 0.042 | 0.00075 | 274 | 68 | 266 | 10 | 265 | 5 | 0.4 |
| HTG-94 | 0.44 | 0.05574 | 0.00184 | 0.5427 | 0.01771 | 0.0706 | 0.00115 | 442 | 44 | 440 | 12 | 440 | 7 | 0 |
| HTG-95 | 0.31 | 0.19336 | 0.00549 | 13.63387 | 0.38682 | 0.51131 | 0.00807 | 2771 | 26 | 2725 | 27 | 2662 | 34 | 4.1 |
| HTG-96 | 0.57 | 0.0516 | 0.00204 | 0.29104 | 0.01131 | 0.0409 | 0.00071 | 268 | 57 | 259 | 9 | 258 | 4 | 0.4 |
| HTG-97 | 0.30 | 0.05508 | 0.00231 | 0.5048 | 0.02076 | 0.06645 | 0.00119 | 415 | 60 | 415 | 14 | 415 | 7 | 0 |
| ~~HTG-98~~ | ~~0.70~~ | ~~0.08382~~ | ~~0.00303~~ | ~~1.99761~~ | ~~0.0706~~ | ~~0.17282~~ | ~~0.00307~~ | ~~1288~~ | ~~42~~ | ~~1115~~ | ~~24~~ | ~~1028~~ | ~~17~~ | ~~25.3~~ |
| HTG-99 | 0.73 | 0.05563 | 0.00206 | 0.53124 | 0.01935 | 0.06925 | 0.00119 | 438 | 51 | 433 | 13 | 432 | 7 | 0.2 |
| HTG-100 | 0.29 | 0.05194 | 0.00239 | 0.3252 | 0.0148 | 0.0454 | 0.00079 | 283 | 72 | 286 | 11 | 286 | 5 | 0 |
| | | | | | | | | | | | | | | |
| **HTG-N** | | | | | | | | | | | | | | |
| HTG-01 | 0.42 | 0.05483 | 0.00228 | 0.45594 | 0.01891 | 0.0603 | 0.00097 | 405 | 64 | 381 | 13 | 377 | 6 | 1.1 |
| HTG-02 | 1.07 | 0.05535 | 0.00145 | 0.51807 | 0.01383 | 0.06787 | 0.00103 | 426 | 33 | 424 | 9 | 423 | 6 | 0.2 |
| HTG-03 | 0.64 | 0.05492 | 0.0021 | 0.49752 | 0.01909 | 0.06569 | 0.00102 | 409 | 58 | 410 | 13 | 410 | 6 | 0 |

| | | | | | | | | | | | | | | |
|---|---|---|---|---|---|---|---|---|---|---|---|---|---|---|
| HTG-04 | 0.44 | 0.05526 | 0.00141 | 0.50457 | 0.0131 | 0.06621 | 0.001 | 423 | 32 | 415 | 9 | 413 | 6 | 0.5 |
| HTG-05 | 0.97 | 0.16334 | 0.00267 | 10.04928 | 0.181 | 0.44612 | 0.00625 | 2491 | 14 | 2439 | 17 | 2378 | 28 | 4.8 |
| HTG-06 | 0.87 | 0.05181 | 0.00196 | 0.3077 | 0.0117 | 0.04307 | 0.00067 | 277 | 59 | 272 | 9 | 272 | 4 | 0 |
| HTG-07 | 0.55 | 0.05517 | 0.00186 | 0.51483 | 0.01752 | 0.06767 | 0.00104 | 419 | 49 | 422 | 12 | 422 | 6 | 0 |
| HTG-08 | 0.85 | 0.05483 | 0.00193 | 0.48262 | 0.01701 | 0.06382 | 0.00101 | 405 | 51 | 400 | 12 | 399 | 6 | 0.3 |
| HTG-09 | 0.18 | 0.05689 | 0.00188 | 0.51447 | 0.01535 | 0.06558 | 0.00094 | 487 | 75 | 421 | 10 | 409 | 6 | 2.9 |
| HTG-10 | 0.45 | 0.05713 | 0.00121 | 0.62606 | 0.01385 | 0.07947 | 0.00115 | 497 | 25 | 494 | 9 | 493 | 7 | 0.2 |
| HTG-11 | 1.15 | 0.05669 | 0.00123 | 0.59684 | 0.01354 | 0.07635 | 0.0011 | 479 | 26 | 475 | 9 | 474 | 7 | 0.2 |
| HTG-12 | 0.67 | 0.05548 | 0.00198 | 0.49205 | 0.01758 | 0.06431 | 0.00102 | 432 | 51 | 406 | 12 | 402 | 6 | 1 |
| HTG-13 | 0.98 | 0.05143 | 0.00132 | 0.29634 | 0.00777 | 0.04178 | 0.00062 | 260 | 34 | 264 | 6 | 264 | 4 | 0 |
| HTG-14 | 0.58 | 0.05462 | 0.00153 | 0.47635 | 0.0136 | 0.06324 | 0.00095 | 397 | 38 | 396 | 9 | 395 | 6 | 0.3 |
| HTG-15 | 0.75 | 0.06008 | 0.00214 | 0.53638 | 0.01894 | 0.06474 | 0.00107 | 606 | 48 | 436 | 13 | 404 | 6 | 7.9 |
| HTG-16 | 0.43 | 0.05468 | 0.00147 | 0.48626 | 0.01335 | 0.06448 | 0.00096 | 399 | 35 | 402 | 9 | 403 | 6 | -0.2 |
| HTG-17 | 0.64 | 0.05434 | 0.00127 | 0.46186 | 0.01116 | 0.06164 | 0.0009 | 385 | 29 | 386 | 8 | 386 | 5 | 0 |
| ~~HTG-18~~ | ~~0.69~~ | ~~0.06824~~ | ~~0.00175~~ | ~~0.5988~~ | ~~0.01567~~ | ~~0.06363~~ | ~~0.00095~~ | ~~876~~ | ~~30~~ | ~~476~~ | ~~10~~ | ~~398~~ | ~~6~~ | ~~19.6~~ |
| ~~HTG-19~~ | ~~0.74~~ | ~~0.08731~~ | ~~0.00303~~ | ~~0.59889~~ | ~~0.0206~~ | ~~0.04974~~ | ~~0.00082~~ | ~~1367~~ | ~~41~~ | ~~477~~ | ~~13~~ | ~~313~~ | ~~5~~ | ~~52.4~~ |
| HTG-20 | 0.51 | 0.054 | 0.00181 | 0.45848 | 0.01542 | 0.06157 | 0.00097 | 371 | 48 | 383 | 11 | 385 | 6 | -0.5 |
| HTG-21 | 0.51 | 0.0769 | 0.00135 | 2.02718 | 0.0385 | 0.19116 | 0.00269 | 1119 | 18 | 1125 | 13 | 1128 | 15 | -0.8 |
| HTG-22 | 0.57 | 0.05487 | 0.00308 | 0.48245 | 0.02679 | 0.06376 | 0.00114 | 407 | 92 | 400 | 18 | 398 | 7 | 0.5 |
| HTG-23 | 0.90 | 0.05471 | 0.00266 | 0.48406 | 0.02342 | 0.06416 | 0.00106 | 400 | 79 | 401 | 16 | 401 | 6 | 0 |
| HTG-24 | 0.74 | 0.05571 | 0.00643 | 0.52488 | 0.05985 | 0.06832 | 0.00167 | 441 | 212 | 428 | 40 | 426 | 10 | 0.5 |
| ~~HTG-25~~ | ~~0.44~~ | ~~0.07525~~ | ~~0.00334~~ | ~~0.51288~~ | ~~0.02253~~ | ~~0.04942~~ | ~~0.00085~~ | ~~1075~~ | ~~60~~ | ~~420~~ | ~~15~~ | ~~311~~ | ~~5~~ | ~~35~~ |
| HTG-26 | 0.82 | 0.05646 | 0.00147 | 0.58541 | 0.01539 | 0.07519 | 0.00114 | 471 | 32 | 468 | 10 | 467 | 7 | 0.2 |
| HTG-27 | 0.43 | 0.05103 | 0.00178 | 0.27306 | 0.00948 | 0.0388 | 0.00061 | 242 | 51 | 245 | 8 | 245 | 4 | 0 |
| HTG-28 | 0.55 | 0.05513 | 0.00317 | 0.50519 | 0.02859 | 0.06645 | 0.00128 | 417 | 92 | 415 | 19 | 415 | 8 | 0 |
| HTG-29 | 0.52 | 0.05533 | 0.00373 | 0.43892 | 0.02861 | 0.05753 | 0.00099 | 426 | 155 | 369 | 20 | 361 | 6 | 2.2 |
| HTG-30 | 0.50 | 0.05488 | 0.00748 | 0.50918 | 0.06852 | 0.06727 | 0.00186 | 407 | 252 | 418 | 46 | 420 | 11 | -0.5 |
| HTG-31 | 0.67 | 0.05452 | 0.00166 | 0.48416 | 0.0149 | 0.06439 | 0.00097 | 393 | 42 | 401 | 10 | 402 | 6 | -0.2 |

| | | | | | | | | | | | | | | |
|---|---|---|---|---|---|---|---|---|---|---|---|---|---|---|
| HTG-32 | 0.32 | 0.05499 | 0.00222 | 0.5103 | 0.02056 | 0.06729 | 0.00108 | 412 | 61 | 419 | 14 | 420 | 7 | -0.2 |
| HTG-33 | 0.58 | 0.05488 | 0.00132 | 0.50346 | 0.01248 | 0.06652 | 0.00098 | 407 | 30 | 414 | 8 | 415 | 6 | -0.2 |
| HTG-34 | 1.05 | 0.05468 | 0.00345 | 0.47932 | 0.02981 | 0.06356 | 0.00125 | 399 | 104 | 398 | 20 | 397 | 8 | 0.3 |
| HTG-35 | 0.88 | 0.05838 | 0.0014 | 0.5194 | 0.0128 | 0.06451 | 0.00095 | 544 | 29 | 425 | 9 | 403 | 6 | 5.5 |
| HTG-36 | 1.07 | 0.05531 | 0.00151 | 0.48646 | 0.01355 | 0.06377 | 0.00095 | 425 | 36 | 402 | 9 | 399 | 6 | 0.8 |
| HTG-37 | 0.55 | 0.05432 | 0.00854 | 0.46228 | 0.07146 | 0.06171 | 0.00207 | 384 | 287 | 386 | 50 | 386 | 13 | 0 |
| HTG-38 | 0.12 | 0.05687 | 0.00225 | 0.61621 | 0.02418 | 0.07857 | 0.00133 | 486 | 57 | 487 | 15 | 488 | 8 | -0.2 |
| HTG-39 | 0.36 | 0.05618 | 0.00236 | 0.49847 | 0.01951 | 0.06435 | 0.00097 | 459 | 95 | 411 | 13 | 402 | 6 | 2.2 |
| HTG-40 | 0.67 | 0.06582 | 0.00187 | 1.1536 | 0.0332 | 0.12709 | 0.00195 | 801 | 35 | 779 | 16 | 771 | 11 | 1 |
| HTG-41 | 0.70 | 0.05261 | 0.0052 | 0.3578 | 0.03505 | 0.04931 | 0.00103 | 312 | 183 | 311 | 26 | 310 | 6 | 0.3 |
| HTG-42 | 0.49 | 0.05481 | 0.00617 | 0.52101 | 0.05774 | 0.06892 | 0.0018 | 404 | 202 | 426 | 39 | 430 | 11 | -0.9 |
| HTG-43 | 0.47 | 0.05449 | 0.00358 | 0.46222 | 0.0301 | 0.06151 | 0.00111 | 391 | 114 | 386 | 21 | 385 | 7 | 0.3 |
| HTG-44 | 0.53 | 0.05277 | 0.00179 | 0.36874 | 0.01249 | 0.05067 | 0.00081 | 319 | 48 | 319 | 9 | 319 | 5 | 0 |
| HTG-45 | 0.77 | 0.05471 | 0.00179 | 0.48887 | 0.01605 | 0.0648 | 0.00101 | 400 | 46 | 404 | 11 | 405 | 6 | -0.2 |
| HTG-46 | 0.78 | 0.05472 | 0.00634 | 0.48458 | 0.05571 | 0.06421 | 0.0014 | 401 | 219 | 401 | 38 | 401 | 8 | 0 |
| HTG-47 | 0.35 | 0.05636 | 0.00182 | 0.53117 | 0.01725 | 0.06834 | 0.00105 | 467 | 45 | 433 | 11 | 426 | 6 | 1.6 |
| HTG-48 | 0.91 | 0.0549 | 0.0042 | 0.49953 | 0.03781 | 0.06598 | 0.00128 | 408 | 135 | 411 | 26 | 412 | 8 | -0.2 |
| HTG-49 | 0.49 | 0.05466 | 0.00265 | 0.49752 | 0.02384 | 0.066 | 0.00116 | 398 | 76 | 410 | 16 | 412 | 7 | -0.5 |
| HTG-50 | 0.57 | 0.05559 | 0.00106 | 0.47923 | 0.00969 | 0.06251 | 0.00088 | 436 | 22 | 398 | 7 | 391 | 5 | 1.8 |
| HTG-51 | 1.09 | 0.05436 | 0.00564 | 0.46863 | 0.04817 | 0.06251 | 0.00133 | 386 | 193 | 390 | 33 | 391 | 8 | -0.3 |
| HTG-52 | 0.44 | 0.05502 | 0.002 | 0.49708 | 0.01793 | 0.06551 | 0.00107 | 413 | 52 | 410 | 12 | 409 | 6 | 0.2 |
| HTG-53 | 0.15 | 0.07015 | 0.00129 | 1.58152 | 0.03115 | 0.16348 | 0.0023 | 933 | 20 | 963 | 12 | 976 | 13 | -1.3 |
| HTG-54 | 0.57 | 0.05536 | 0.00261 | 0.50629 | 0.02353 | 0.06631 | 0.00118 | 427 | 72 | 416 | 16 | 414 | 7 | 0.5 |
| HTG-55 | 1.56 | 0.05495 | 0.00157 | 0.4969 | 0.01438 | 0.06557 | 0.001 | 410 | 38 | 410 | 10 | 409 | 6 | 0.2 |
| HTG-56 | 0.87 | 0.05552 | 0.00379 | 0.51616 | 0.03492 | 0.06741 | 0.00126 | 433 | 118 | 423 | 23 | 421 | 8 | 0.5 |
| HTG-57 | 0.27 | 0.05491 | 0.00172 | 0.49223 | 0.01545 | 0.06501 | 0.00102 | 409 | 43 | 406 | 11 | 406 | 6 | 0 |
| HTG-58 | 0.29 | 0.05531 | 0.00147 | 0.5111 | 0.01383 | 0.067 | 0.001 | 425 | 34 | 419 | 9 | 418 | 6 | 0.2 |
| HTG-59 | 0.87 | 0.05492 | 0.0013 | 0.48769 | 0.0119 | 0.06439 | 0.00093 | 409 | 30 | 403 | 8 | 402 | 6 | 0.2 |

| | | | | | | | | | | | | | | |
|---|---|---|---|---|---|---|---|---|---|---|---|---|---|---|
| HTG-60 | 1.15 | 0.05535 | 0.00235 | 0.53347 | 0.02245 | 0.06988 | 0.00117 | 426 | 64 | 434 | 15 | 435 | 7 | -0.2 |
| HTG-61 | 0.23 | 0.07007 | 0.00162 | 1.45321 | 0.03459 | 0.15039 | 0.00221 | 930 | 26 | 911 | 14 | 903 | 12 | 0.9 |
| HTG-62 | 0.14 | 0.05622 | 0.00138 | 0.57296 | 0.01444 | 0.0739 | 0.00107 | 461 | 31 | 460 | 9 | 460 | 6 | 0 |
| HTG-63 | 0.70 | 0.05599 | 0.00259 | 0.55147 | 0.02525 | 0.07142 | 0.00125 | 452 | 70 | 446 | 17 | 445 | 8 | 0.2 |
| HTG-64 | 0.62 | 0.05562 | 0.00268 | 0.50381 | 0.02404 | 0.06569 | 0.00114 | 437 | 75 | 414 | 16 | 410 | 7 | 1 |
| HTG-65 | 0.84 | 0.0549 | 0.00224 | 0.50223 | 0.02034 | 0.06633 | 0.0011 | 408 | 61 | 413 | 14 | 414 | 7 | -0.2 |
| HTG-66 | 0.68 | 0.05442 | 0.00188 | 0.47132 | 0.01624 | 0.0628 | 0.001 | 388 | 49 | 392 | 11 | 393 | 6 | -0.3 |
| HTG-67 | 1.33 | 0.05486 | 0.00376 | 0.49758 | 0.0337 | 0.06576 | 0.00126 | 407 | 118 | 410 | 23 | 411 | 8 | -0.2 |
| HTG-68 | 0.82 | 0.05514 | 0.00591 | 0.48278 | 0.0511 | 0.06349 | 0.00152 | 418 | 194 | 400 | 35 | 397 | 9 | 0.8 |
| HTG-69 | 0.34 | 0.05562 | 0.00156 | 0.53587 | 0.01511 | 0.06987 | 0.00107 | 437 | 36 | 436 | 10 | 435 | 6 | 0.2 |
| HTG-70 | 0.37 | 0.05549 | 0.0016 | 0.50319 | 0.01466 | 0.06575 | 0.001 | 432 | 38 | 414 | 10 | 410 | 6 | 1 |
| HTG-71 | 1.30 | 0.05503 | 0.00188 | 0.5013 | 0.01701 | 0.06606 | 0.00109 | 413 | 47 | 413 | 12 | 412 | 7 | 0.2 |
| HTG-72 | 0.95 | 0.0554 | 0.00254 | 0.51848 | 0.02355 | 0.06787 | 0.00114 | 428 | 71 | 424 | 16 | 423 | 7 | 0.2 |
| HTG-73 | 0.56 | 0.05515 | 0.00134 | 0.50784 | 0.01269 | 0.06677 | 0.00098 | 418 | 31 | 417 | 9 | 417 | 6 | 0 |
| HTG-74 | 0.34 | 0.07267 | 0.00262 | 1.64201 | 0.0591 | 0.16385 | 0.00266 | 1005 | 47 | 986 | 23 | 978 | 15 | 0.8 |
| HTG-75 | 0.83 | 0.0516 | 0.00183 | 0.29721 | 0.01054 | 0.04177 | 0.00065 | 268 | 53 | 264 | 8 | 264 | 4 | 0 |
| HTG-76 | 0.65 | 0.05571 | 0.00159 | 0.54565 | 0.01564 | 0.07102 | 0.00109 | 441 | 37 | 442 | 10 | 442 | 7 | 0 |
| HTG-77 | 0.92 | 0.05481 | 0.00133 | 0.48169 | 0.01189 | 0.06373 | 0.00095 | 404 | 30 | 399 | 8 | 398 | 6 | 0.3 |
| HTG-78 | 1.27 | 0.05106 | 0.00237 | 0.26332 | 0.01211 | 0.03739 | 0.00064 | 244 | 74 | 237 | 10 | 237 | 4 | 0 |
| HTG-79 | 0.91 | 0.05457 | 0.00205 | 0.47846 | 0.01794 | 0.06358 | 0.00102 | 395 | 55 | 397 | 12 | 397 | 6 | 0 |
| HTG-80 | 0.51 | 0.05521 | 0.00227 | 0.51026 | 0.02088 | 0.06702 | 0.00107 | 421 | 63 | 419 | 14 | 418 | 6 | 0.2 |
| HTG-81 | 0.41 | 0.05228 | 0.00148 | 0.34119 | 0.00977 | 0.04733 | 0.00072 | 298 | 38 | 298 | 7 | 298 | 4 | 0 |
| ~~HTG-82~~ | ~~0.47~~ | ~~0.04619~~ | ~~0.00738~~ | ~~0.39454~~ | ~~0.06265~~ | ~~0.06194~~ | ~~0.0011~~ | ~~8~~ | ~~285~~ | ~~338~~ | ~~46~~ | ~~387~~ | ~~7~~ | ~~-12.7~~ |
| ~~HTG-83~~ | ~~13.32~~ | ~~0.05628~~ | ~~0.00107~~ | ~~0.44693~~ | ~~0.00899~~ | ~~0.05759~~ | ~~0.00081~~ | ~~463~~ | ~~22~~ | ~~375~~ | ~~6~~ | ~~361~~ | ~~5~~ | ~~3.9~~ |
| HTG-84 | 0.88 | 0.05126 | 0.00127 | 0.26253 | 0.00664 | 0.03714 | 0.00054 | 253 | 32 | 237 | 5 | 235 | 3 | 0.9 |
| HTG-85 | 1.05 | 0.0565 | 0.0018 | 0.60989 | 0.01944 | 0.07828 | 0.00123 | 472 | 43 | 483 | 12 | 486 | 7 | -0.6 |
| HTG-86 | 0.88 | 0.1092 | 0.00217 | 4.80437 | 0.09995 | 0.31903 | 0.00458 | 1786 | 19 | 1786 | 17 | 1785 | 22 | 0.1 |
| HTG-87 | 0.15 | 0.06813 | 0.00144 | 1.31211 | 0.02877 | 0.13965 | 0.00201 | 873 | 23 | 851 | 13 | 843 | 11 | 0.9 |

| | | | | | | | | | | | | | | |
|---|---|---|---|---|---|---|---|---|---|---|---|---|---|---|
| HTG-88 | 0.66 | 0.0553 | 0.00158 | 0.52529 | 0.01515 | 0.06888 | 0.00105 | 424 | 38 | 429 | 10 | 429 | 6 | 0 |
| HTG-89 | 0.60 | 0.05465 | 0.00352 | 0.4649 | 0.02931 | 0.06169 | 0.00128 | 398 | 104 | 388 | 20 | 386 | 8 | 0.5 |
| HTG-90 | 0.74 | 0.0549 | 0.00113 | 0.49643 | 0.01068 | 0.06557 | 0.00094 | 408 | 24 | 409 | 7 | 409 | 6 | 0 |
| HTG-91 | 1.12 | 0.05452 | 0.00387 | 0.46714 | 0.03279 | 0.06213 | 0.00118 | 393 | 124 | 389 | 23 | 389 | 7 | 0 |
| HTG-92 | 1.36 | 0.05756 | 0.00131 | 0.49573 | 0.0116 | 0.06245 | 0.00091 | 513 | 27 | 409 | 8 | 391 | 6 | 4.6 |
| HTG-93 | 0.54 | 0.0549 | 0.00475 | 0.49215 | 0.04229 | 0.06501 | 0.00126 | 408 | 159 | 406 | 29 | 406 | 8 | 0 |
| HTG-94 | 0.40 | 0.05552 | 0.00161 | 0.51548 | 0.01501 | 0.06732 | 0.00103 | 433 | 38 | 422 | 10 | 420 | 6 | 0.5 |
| HTG-95 | 1.11 | 0.05577 | 0.00164 | 0.54206 | 0.01593 | 0.07048 | 0.00109 | 443 | 38 | 440 | 10 | 439 | 7 | 0.2 |
| HTG-96 | 0.57 | 0.05413 | 0.00172 | 0.45384 | 0.01451 | 0.0608 | 0.00093 | 376 | 45 | 380 | 10 | 380 | 6 | 0 |
| HTG-97 | 0.37 | 0.06249 | 0.00188 | 0.92879 | 0.02798 | 0.10778 | 0.00167 | 691 | 38 | 667 | 15 | 660 | 10 | 1.1 |
| HTG-98 | 0.77 | 0.05493 | 0.00144 | 0.49966 | 0.01324 | 0.06596 | 0.00099 | 409 | 33 | 411 | 9 | 412 | 6 | -0.2 |
| HTG-99 | 0.77 | 0.05119 | 0.00129 | 0.2972 | 0.0076 | 0.0421 | 0.00063 | 249 | 32 | 264 | 6 | 266 | 4 | -0.8 |
| HTG-100 | 0.40 | 0.10343 | 0.00223 | 4.31811 | 0.09611 | 0.30274 | 0.00445 | 1687 | 21 | 1697 | 18 | 1705 | 22 | -1.1 |
| **SZG2** | | | | | | | | | | | | | | |
| SZG2-01 | 1.04 | 0.05166 | 0.0012 | 0.27265 | 0.00652 | 0.03827 | 0.00053 | 270 | 30 | 245 | 5 | 242 | 3 | 1.2 |
| SZG2-02 | 0.24 | 0.09542 | 0.00206 | 3.2949 | 0.05673 | 0.25045 | 0.00327 | 1536 | 42 | 1480 | 13 | 1441 | 17 | 6.6 |
| SZG2-03 | 0.12 | 0.11663 | 0.00123 | 5.44527 | 0.07158 | 0.33856 | 0.00437 | 1905 | 11 | 1892 | 11 | 1880 | 21 | 1.3 |
| SZG2-04 | 0.37 | 0.05858 | 0.00078 | 0.59574 | 0.00908 | 0.07374 | 0.00097 | 552 | 15 | 475 | 6 | 459 | 6 | 3.5 |
| SZG2-05 | 1 | 0.0566 | 0.00069 | 0.47699 | 0.00683 | 0.06111 | 0.0008 | 476 | 14 | 396 | 5 | 382 | 5 | 3.7 |
| SZG2-06 | 0.43 | 0.056 | 0.00064 | 0.53683 | 0.0074 | 0.06951 | 0.0009 | 452 | 14 | 436 | 5 | 433 | 5 | 0.7 |
| SZG2-07 | 0.26 | 0.05874 | 0.00142 | 0.55076 | 0.01121 | 0.068 | 0.00089 | 558 | 54 | 445 | 7 | 424 | 5 | 5 |
| SZG2-08 | 0.32 | 0.05802 | 0.00063 | 0.66478 | 0.00892 | 0.08309 | 0.00108 | 531 | 13 | 518 | 5 | 515 | 6 | 0.6 |
| SZG2-09 | 0.04 | 0.0657 | 0.00141 | 0.8723 | 0.01495 | 0.09629 | 0.00124 | 797 | 46 | 637 | 8 | 593 | 7 | 7.4 |
| ~~SZG2-10~~ | ~~0.83~~ | ~~0.06851~~ | ~~0.00655~~ | ~~0.45635~~ | ~~0.04277~~ | ~~0.04831~~ | ~~0.00092~~ | ~~884~~ | ~~205~~ | ~~382~~ | ~~30~~ | ~~304~~ | ~~6~~ | ~~25.7~~ |
| SZG2-11 | 0.48 | 0.0555 | 0.00078 | 0.54847 | 0.00867 | 0.07165 | 0.00095 | 432 | 16 | 444 | 6 | 446 | 6 | -0.4 |
| ~~SZG2-12~~ | ~~0.31~~ | ~~0.07484~~ | ~~0.00178~~ | ~~1.09644~~ | ~~0.02164~~ | ~~0.10625~~ | ~~0.0014~~ | ~~1064~~ | ~~49~~ | ~~752~~ | ~~10~~ | ~~651~~ | ~~8~~ | ~~15.5~~ |

| | | | | | | | | | | | | | | |
|---|---|---|---|---|---|---|---|---|---|---|---|---|---|---|
| SZG2-13 | 0.69 | 0.05602 | 0.0008 | 0.53375 | 0.00853 | 0.06908 | 0.00092 | 453 | 16 | 434 | 6 | 431 | 6 | 0.7 |
| SZG2-14 | 0.39 | 0.07054 | 0.00082 | 1.45263 | 0.02023 | 0.14933 | 0.00195 | 944 | 13 | 911 | 8 | 897 | 11 | 1.6 |
| SZG2-15 | 0.23 | 0.06068 | 0.00186 | 0.71153 | 0.0196 | 0.08505 | 0.00116 | 628 | 68 | 546 | 12 | 526 | 7 | 3.8 |
| SZG2-16 | 0.41 | 0.05651 | 0.00065 | 0.57094 | 0.00789 | 0.07326 | 0.00095 | 472 | 14 | 459 | 5 | 456 | 6 | 0.7 |
| SZG2-17 | 0.59 | 0.05601 | 0.00267 | 0.48669 | 0.02206 | 0.06303 | 0.00093 | 453 | 109 | 403 | 15 | 394 | 6 | 2.3 |
| SZG2-18 | 0.03 | 0.09545 | 0.00101 | 3.26743 | 0.0432 | 0.24823 | 0.00321 | 1537 | 11 | 1473 | 10 | 1429 | 17 | 7.6 |
| SZG2-19 | 1.15 | 0.05297 | 0.00083 | 0.2961 | 0.00511 | 0.04053 | 0.00054 | 328 | 18 | 263 | 4 | 256 | 3 | 2.7 |
| SZG2-20 | 0.38 | 0.08432 | 0.00109 | 2.54203 | 0.03797 | 0.21861 | 0.00292 | 1300 | 13 | 1284 | 11 | 1275 | 15 | 2 |
| SZG2-21 | 0.4 | 0.05931 | 0.0017 | 0.57604 | 0.01458 | 0.07045 | 0.00095 | 578 | 64 | 462 | 9 | 439 | 6 | 5.2 |
| SZG2-22 | 0.46 | 0.05257 | 0.00073 | 0.28943 | 0.00458 | 0.03993 | 0.00053 | 310 | 16 | 258 | 4 | 252 | 3 | 2.4 |
| SZG2-23 | 0.34 | 0.05675 | 0.00068 | 0.54767 | 0.00778 | 0.06998 | 0.00092 | 482 | 14 | 443 | 5 | 436 | 6 | 1.6 |
| SZG2-24 | 0.48 | 0.05667 | 0.00067 | 0.5009 | 0.00706 | 0.06409 | 0.00084 | 479 | 14 | 412 | 5 | 400 | 5 | 3 |
| SZG2-25 | 0.31 | 0.06002 | 0.00163 | 0.59686 | 0.0141 | 0.07213 | 0.00097 | 604 | 60 | 475 | 9 | 449 | 6 | 5.8 |
| SZG2-26 | 0.22 | 0.06887 | 0.00079 | 1.38199 | 0.01918 | 0.14551 | 0.0019 | 895 | 13 | 881 | 8 | 876 | 11 | 0.6 |
| SZG2-27 | 0.53 | 0.061 | 0.00068 | 0.67197 | 0.00912 | 0.07987 | 0.00104 | 639 | 13 | 522 | 6 | 495 | 6 | 5.5 |
| ~~SZG2-28~~ | ~~0.35~~ | ~~0.09522~~ | ~~0.00214~~ | ~~3.14908~~ | ~~0.05722~~ | ~~0.23986~~ | ~~0.00318~~ | ~~1532~~ | ~~43~~ | ~~1445~~ | ~~14~~ | ~~1386~~ | ~~17~~ | ~~10.5~~ |
| SZG2-29 | 0.15 | 0.07031 | 0.00082 | 1.48543 | 0.02077 | 0.1532 | 0.00201 | 937 | 13 | 924 | 8 | 919 | 11 | 0.5 |
| SZG2-30 | 0.37 | 0.05421 | 0.00205 | 0.29153 | 0.01026 | 0.03901 | 0.00055 | 380 | 87 | 260 | 8 | 247 | 3 | 5.3 |
| SZG2-31 | 0.11 | 0.0698 | 0.00078 | 1.44376 | 0.01968 | 0.14998 | 0.00196 | 922 | 13 | 907 | 8 | 901 | 11 | 0.7 |
| SZG2-32 | 0.31 | 0.05694 | 0.0016 | 0.56408 | 0.01391 | 0.07185 | 0.00097 | 489 | 63 | 454 | 9 | 447 | 6 | 1.6 |
| SZG2-33 | 0.41 | 0.116 | 0.00128 | 5.11693 | 0.06929 | 0.31986 | 0.00418 | 1895 | 11 | 1839 | 12 | 1789 | 20 | 5.9 |
| SZG2-34 | 0.33 | 0.06822 | 0.00195 | 1.26953 | 0.03203 | 0.13498 | 0.00183 | 875 | 61 | 832 | 14 | 816 | 10 | 2 |
| SZG2-35 | 0.56 | 0.10643 | 0.00119 | 4.08699 | 0.05568 | 0.27845 | 0.00365 | 1739 | 11 | 1652 | 11 | 1584 | 18 | 9.8 |
| SZG2-36 | 0.15 | 0.06563 | 0.00144 | 0.95848 | 0.01699 | 0.10592 | 0.00138 | 795 | 47 | 683 | 9 | 649 | 8 | 5.2 |
| SZG2-37 | 1.13 | 0.05982 | 0.00072 | 0.60553 | 0.00865 | 0.0734 | 0.00097 | 597 | 14 | 481 | 5 | 457 | 6 | 5.3 |
| SZG2-38 | 0.46 | 0.05719 | 0.00075 | 0.61505 | 0.0093 | 0.07798 | 0.00103 | 499 | 15 | 487 | 6 | 484 | 6 | 0.6 |
| SZG2-39 | 0.48 | 0.05913 | 0.00186 | 0.56549 | 0.01598 | 0.06936 | 0.00095 | 572 | 70 | 455 | 10 | 432 | 6 | 5.3 |
| SZG2-40 | 0.76 | 0.07137 | 0.00101 | 1.20034 | 0.01917 | 0.12196 | 0.00164 | 968 | 15 | 801 | 9 | 742 | 9 | 8 |

| | | | | | | | | | | | | | | |
|---|---|---|---|---|---|---|---|---|---|---|---|---|---|---|
| SZG2-41 | 0.62 | 0.05657 | 0.00088 | 0.5301 | 0.0091 | 0.06794 | 0.00091 | 475 | 18 | 432 | 6 | 424 | 5 | 1.9 |
| SZG2-42 | 0.36 | 0.07492 | 0.00084 | 1.79853 | 0.02456 | 0.17408 | 0.00228 | 1066 | 12 | 1045 | 9 | 1035 | 13 | 3 |
| SZG2-43 | 0.53 | 0.05675 | 0.00071 | 0.56798 | 0.00831 | 0.07257 | 0.00096 | 482 | 14 | 457 | 5 | 452 | 6 | 1.1 |
| ~~SZG2-44~~ | ~~0.94~~ | ~~0.06312~~ | ~~0.00077~~ | ~~0.54552~~ | ~~0.00785~~ | ~~0.06266~~ | ~~0.00083~~ | ~~712~~ | ~~14~~ | ~~442~~ | ~~5~~ | ~~392~~ | ~~5~~ | ~~12.8~~ |
| SZG2-45 | 0.98 | 0.06185 | 0.00083 | 0.60239 | 0.00921 | 0.07062 | 0.00094 | 669 | 15 | 479 | 6 | 440 | 6 | 8.9 |
| SZG2-46 | 1.2 | 0.05306 | 0.00111 | 0.28271 | 0.0062 | 0.03864 | 0.00054 | 331 | 26 | 253 | 5 | 244 | 3 | 3.7 |
| SZG2-47 | 0.88 | 0.13459 | 0.00148 | 6.82656 | 0.09253 | 0.36779 | 0.00482 | 2159 | 11 | 2089 | 12 | 2019 | 23 | 6.9 |
| SZG2-48 | 0.21 | 0.06698 | 0.0008 | 1.04012 | 0.01483 | 0.1126 | 0.00149 | 837 | 13 | 724 | 7 | 688 | 9 | 5.2 |
| SZG2-49 | 0.81 | 0.06072 | 0.00078 | 0.58752 | 0.00874 | 0.07017 | 0.00093 | 629 | 14 | 469 | 6 | 437 | 6 | 7.3 |
| SZG2-50 | 0.52 | 0.05404 | 0.00082 | 0.44511 | 0.00749 | 0.05972 | 0.00081 | 373 | 17 | 374 | 5 | 374 | 5 | 0 |
| SZG2-51 | 0.19 | 0.06957 | 0.0015 | 1.39332 | 0.02394 | 0.14525 | 0.0019 | 916 | 45 | 886 | 10 | 874 | 11 | 1.4 |
| SZG2-52 | 0.81 | 0.05617 | 0.00082 | 0.54119 | 0.00883 | 0.06987 | 0.00094 | 459 | 16 | 439 | 6 | 435 | 6 | 0.9 |
| SZG2-53 | 0.43 | 0.05416 | 0.00069 | 0.45266 | 0.00673 | 0.06061 | 0.0008 | 378 | 15 | 379 | 5 | 379 | 5 | 0 |
| SZG2-54 | 0.5 | 0.05703 | 0.00068 | 0.54709 | 0.00782 | 0.06956 | 0.00092 | 493 | 14 | 443 | 5 | 434 | 6 | 2.1 |
| SZG2-55 | 0.59 | 0.05593 | 0.00199 | 0.53054 | 0.01736 | 0.06879 | 0.00095 | 450 | 81 | 432 | 12 | 429 | 6 | 0.7 |
| ~~SZG2-56~~ | ~~0.96~~ | ~~0.06041~~ | ~~0.00088~~ | ~~0.49136~~ | ~~0.00804~~ | ~~0.05898~~ | ~~0.00079~~ | ~~618~~ | ~~16~~ | ~~406~~ | ~~5~~ | ~~369~~ | ~~5~~ | ~~10~~ |
| SZG2-57 | 0.33 | 0.0554 | 0.0023 | 0.4927 | 0.01916 | 0.0645 | 0.00095 | 428 | 95 | 407 | 13 | 403 | 6 | 1 |
| SZG2-58 | 0.72 | 0.05346 | 0.00082 | 0.27293 | 0.00462 | 0.03702 | 0.0005 | 348 | 18 | 245 | 4 | 234 | 3 | 4.7 |
| SZG2-59 | 0.44 | 0.0518 | 0.00137 | 0.30043 | 0.00809 | 0.04206 | 0.00061 | 277 | 36 | 267 | 6 | 266 | 4 | 0.4 |
| SZG2-60 | 0.1 | 0.11535 | 0.00128 | 5.32413 | 0.07252 | 0.3347 | 0.00439 | 1885 | 11 | 1873 | 12 | 1861 | 21 | 1.3 |
| SZG2-61 | 0.2 | 0.05176 | 0.00075 | 0.2758 | 0.0045 | 0.03864 | 0.00052 | 275 | 17 | 247 | 4 | 244 | 3 | 1.2 |
| SZG2-62 | 0.91 | 0.12554 | 0.00152 | 6.18972 | 0.08865 | 0.35753 | 0.00479 | 2036 | 11 | 2003 | 13 | 1970 | 23 | 3.4 |
| SZG2-63 | 0.92 | 0.0626 | 0.00274 | 1.02874 | 0.04246 | 0.11918 | 0.00175 | 695 | 96 | 718 | 21 | 726 | 10 | -1.1 |
| SZG2-64 | 0.98 | 0.05849 | 0.00073 | 0.55858 | 0.00822 | 0.06926 | 0.00092 | 548 | 14 | 451 | 5 | 432 | 6 | 4.4 |
| SZG2-65 | 0.45 | 0.05682 | 0.00069 | 0.53543 | 0.0077 | 0.06833 | 0.0009 | 485 | 14 | 435 | 5 | 426 | 5 | 2.1 |
| SZG2-66 | 0.44 | 0.05086 | 0.00084 | 0.27193 | 0.00489 | 0.03877 | 0.00053 | 234 | 19 | 244 | 4 | 245 | 3 | -0.4 |
| SZG2-67 | 0.64 | 0.05517 | 0.00069 | 0.4797 | 0.00706 | 0.06304 | 0.00084 | 419 | 15 | 398 | 5 | 394 | 5 | 1 |
| SZG2-68 | 0.55 | 0.05175 | 0.00113 | 0.28566 | 0.00651 | 0.04002 | 0.00056 | 274 | 28 | 255 | 5 | 253 | 3 | 0.8 |

| | | | | | | | | | | | | | | |
|---|---|---|---|---|---|---|---|---|---|---|---|---|---|---|
| SZG2-69 | 0.1 | 0.05505 | 0.00115 | 0.47995 | 0.00785 | 0.06324 | 0.00083 | 414 | 48 | 398 | 5 | 395 | 5 | 0.8 |
| SZG2-70 | 0.88 | 0.05629 | 0.00076 | 0.56422 | 0.00877 | 0.07268 | 0.00097 | 464 | 15 | 454 | 6 | 452 | 6 | 0.4 |
| ~~SZG2-71~~ | ~~0.17~~ | ~~0.11596~~ | ~~0.00233~~ | ~~4.57494~~ | ~~0.06956~~ | ~~0.28615~~ | ~~0.00375~~ | ~~1895~~ | ~~37~~ | ~~1745~~ | ~~13~~ | ~~1622~~ | ~~19~~ | ~~16.8~~ |
| SZG2-72 | 0.33 | 0.0555 | 0.00075 | 0.51512 | 0.00801 | 0.06731 | 0.0009 | 432 | 16 | 422 | 5 | 420 | 5 | 0.5 |
| SZG2-73 | 0.54 | 0.0558 | 0.00073 | 0.51289 | 0.0078 | 0.06665 | 0.00089 | 444 | 15 | 420 | 5 | 416 | 5 | 1 |
| SZG2-74 | 0.73 | 0.05116 | 0.00149 | 0.31248 | 0.00921 | 0.04429 | 0.00065 | 248 | 41 | 276 | 7 | 279 | 4 | -1.1 |
| SZG2-75 | 0.97 | 0.08404 | 0.00101 | 2.45192 | 0.03519 | 0.21155 | 0.00282 | 1293 | 12 | 1258 | 10 | 1237 | 15 | 4.5 |
| SZG2-76 | 0.56 | 0.05623 | 0.00067 | 0.59128 | 0.00841 | 0.07625 | 0.00101 | 461 | 14 | 472 | 5 | 474 | 6 | -0.4 |
| SZG2-77 | 0.95 | 0.05621 | 0.00076 | 0.50207 | 0.0078 | 0.06477 | 0.00087 | 461 | 15 | 413 | 5 | 405 | 5 | 2 |
| SZG2-78 | 0.27 | 0.06992 | 0.00083 | 1.43413 | 0.02036 | 0.14874 | 0.00197 | 926 | 13 | 903 | 8 | 894 | 11 | 1 |
| SZG2-79 | 0.53 | 0.1072 | 0.00145 | 4.6272 | 0.07142 | 0.313 | 0.00429 | 1752 | 13 | 1754 | 13 | 1755 | 21 | -0.2 |
| SZG2-80 | 0.36 | 0.0569 | 0.00068 | 0.56003 | 0.00804 | 0.07136 | 0.00095 | 488 | 14 | 452 | 5 | 444 | 6 | 1.8 |
| SZG2-81 | 0.58 | 0.05166 | 0.00103 | 0.29257 | 0.00614 | 0.04107 | 0.00057 | 270 | 24 | 261 | 5 | 259 | 4 | 0.8 |
| SZG2-82 | 0.28 | 0.05703 | 0.00069 | 0.55784 | 0.00807 | 0.07093 | 0.00094 | 493 | 14 | 450 | 5 | 442 | 6 | 1.8 |
| ~~SZG2-83~~ | ~~0.83~~ | ~~0.12455~~ | ~~0.00371~~ | ~~5.35921~~ | ~~0.13901~~ | ~~0.31208~~ | ~~0.00457~~ | ~~2022~~ | ~~54~~ | ~~1878~~ | ~~22~~ | ~~1751~~ | ~~22~~ | ~~15.5~~ |
| SZG2-84 | 0.13 | 0.06722 | 0.00142 | 1.26539 | 0.02105 | 0.13654 | 0.00179 | 844 | 45 | 830 | 9 | 825 | 10 | 0.6 |
| SZG2-85 | 0.24 | 0.06932 | 0.00187 | 1.2658 | 0.02953 | 0.13243 | 0.0018 | 908 | 57 | 831 | 13 | 802 | 10 | 3.6 |
| SZG2-86 | 0.69 | 0.05543 | 0.00073 | 0.53214 | 0.00815 | 0.06961 | 0.00093 | 430 | 15 | 433 | 5 | 434 | 6 | -0.2 |
| SZG2-87 | 0.38 | 0.0801 | 0.00106 | 1.76899 | 0.02709 | 0.16015 | 0.00215 | 1199 | 13 | 1034 | 10 | 958 | 12 | 7.9 |
| ~~SZG2-88~~ | ~~0.16~~ | ~~0.24466~~ | ~~0.00469~~ | ~~18.20403~~ | ~~0.25457~~ | ~~0.53965~~ | ~~0.00707~~ | ~~3151~~ | ~~31~~ | ~~3001~~ | ~~13~~ | ~~2782~~ | ~~30~~ | ~~13.3~~ |
| ~~SZG2-89~~ | ~~0.6~~ | ~~0.12638~~ | ~~0.00364~~ | ~~5.16357~~ | ~~0.12723~~ | ~~0.29633~~ | ~~0.0044~~ | ~~2048~~ | ~~52~~ | ~~1847~~ | ~~21~~ | ~~1673~~ | ~~22~~ | ~~22.4~~ |
| SZG2-90 | 0.38 | 0.06005 | 0.00169 | 0.6508 | 0.01609 | 0.0786 | 0.00107 | 605 | 62 | 509 | 10 | 488 | 6 | 4.3 |
| SZG2-91 | 0.2 | 0.05599 | 0.00069 | 0.54817 | 0.00798 | 0.07099 | 0.00095 | 452 | 14 | 444 | 5 | 442 | 6 | 0.5 |
| SZG2-92 | 0.43 | 0.05747 | 0.00078 | 0.5696 | 0.0089 | 0.07187 | 0.00097 | 510 | 15 | 458 | 6 | 447 | 6 | 2.5 |
| SZG2-93 | 0.93 | 0.05172 | 0.00204 | 0.28214 | 0.01111 | 0.03956 | 0.00063 | 273 | 61 | 252 | 9 | 250 | 4 | 0.8 |
| SZG2-94 | 0.8 | 0.0553 | 0.00073 | 0.50487 | 0.00769 | 0.06621 | 0.00089 | 424 | 15 | 415 | 5 | 413 | 5 | 0.5 |
| SZG2-95 | 0.27 | 0.06089 | 0.00102 | 0.80018 | 0.01451 | 0.09529 | 0.00132 | 635 | 18 | 597 | 8 | 587 | 8 | 1.7 |
| SZG2-96 | 0.08 | 0.05744 | 0.00079 | 0.62551 | 0.00987 | 0.07897 | 0.00107 | 508 | 16 | 493 | 6 | 490 | 6 | 0.6 |

| | | | | | | | | | | | | | | |
|---|---|---|---|---|---|---|---|---|---|---|---|---|---|---|
| SZG2-97 | 0.44 | 0.05707 | 0.00083 | 0.53608 | 0.00875 | 0.06812 | 0.00092 | 494 | 16 | 436 | 6 | 425 | 6 | 2.6 |
| ~~SZG2-98~~ | ~~0.85~~ | ~~0.0717~~ | ~~0.00122~~ | ~~0.60443~~ | ~~0.01111~~ | ~~0.06113~~ | ~~0.00085~~ | ~~977~~ | ~~18~~ | ~~480~~ | ~~7~~ | ~~382~~ | ~~5~~ | ~~25.7~~ |
| SZG2-99 | 0.46 | 0.06944 | 0.00082 | 1.37194 | 0.01957 | 0.14326 | 0.0019 | 912 | 13 | 877 | 8 | 863 | 11 | 1.6 |
| SZG2-100 | 0.32 | 0.05537 | 0.00081 | 0.5333 | 0.00877 | 0.06984 | 0.00095 | 427 | 17 | 434 | 6 | 435 | 6 | -0.2 |
| **CSL4** | | | | | | | | | | | | | | |
| ~~CSL4-01~~ | ~~0.75~~ | ~~0.06661~~ | ~~0.00149~~ | ~~0.67635~~ | ~~0.01605~~ | ~~0.07363~~ | ~~0.00111~~ | ~~826~~ | ~~26~~ | ~~525~~ | ~~10~~ | ~~458~~ | ~~7~~ | ~~14.6~~ |
| CSL4-02 | 0.06 | 0.0701 | 0.00188 | 1.44133 | 0.03253 | 0.14912 | 0.00217 | 931 | 56 | 906 | 14 | 896 | 12 | 1.1 |
| CSL4-03 | 0.7 | 0.05104 | 0.00159 | 0.28476 | 0.00907 | 0.04046 | 0.00064 | 243 | 45 | 254 | 7 | 256 | 4 | -0.8 |
| CSL4-04 | 0.08 | 0.07149 | 0.00196 | 1.57285 | 0.03653 | 0.15957 | 0.00233 | 971 | 57 | 960 | 14 | 954 | 13 | 0.6 |
| CSL4-05 | 0.35 | 0.05498 | 0.00135 | 0.53496 | 0.01376 | 0.07055 | 0.00108 | 411 | 31 | 435 | 9 | 439 | 7 | -0.9 |
| CSL4-06 | 0.62 | 0.05567 | 0.00145 | 0.49032 | 0.0133 | 0.06387 | 0.00099 | 439 | 34 | 405 | 9 | 399 | 6 | 1.5 |
| CSL4-07 | 0.7 | 0.05072 | 0.00148 | 0.24417 | 0.00727 | 0.03491 | 0.00056 | 228 | 40 | 222 | 6 | 221 | 3 | 0.5 |
| CSL4-08 | 0.63 | 0.15355 | 0.0025 | 9.12499 | 0.16046 | 0.43093 | 0.006 | 2386 | 14 | 2351 | 16 | 2310 | 27 | 3.3 |
| CSL4-09 | 0.84 | 0.06049 | 0.00106 | 0.56835 | 0.01065 | 0.06813 | 0.00093 | 621 | 19 | 457 | 7 | 425 | 6 | 7.5 |
| CSL4-10 | 1.04 | 0.06007 | 0.00094 | 0.49181 | 0.00845 | 0.05937 | 0.0008 | 606 | 17 | 406 | 6 | 372 | 5 | 9.1 |
| CSL4-11 | 0.28 | 0.07364 | 0.00126 | 1.71318 | 0.03153 | 0.16869 | 0.00232 | 1032 | 18 | 1013 | 12 | 1005 | 13 | 2.7 |
| CSL4-12 | 0.11 | 0.06982 | 0.00107 | 1.4347 | 0.02429 | 0.14899 | 0.00201 | 923 | 16 | 904 | 10 | 895 | 11 | 1 |
| CSL4-13 | 0.78 | 0.05769 | 0.00099 | 0.4829 | 0.00889 | 0.0607 | 0.00083 | 518 | 19 | 400 | 6 | 380 | 5 | 5.3 |
| CSL4-14 | 0.72 | 0.05424 | 0.00104 | 0.448 | 0.00908 | 0.05989 | 0.00083 | 381 | 23 | 376 | 6 | 375 | 5 | 0.3 |
| CSL4-15 | 0.4 | 0.05538 | 0.00132 | 0.5355 | 0.01313 | 0.07012 | 0.00099 | 428 | 30 | 435 | 9 | 437 | 6 | -0.5 |
| CSL4-16 | 0.4 | 0.05699 | 0.00112 | 0.62277 | 0.01282 | 0.07925 | 0.00111 | 491 | 23 | 492 | 8 | 492 | 7 | 0 |
| CSL4-17 | 1.75 | 0.0556 | 0.00105 | 0.53325 | 0.01068 | 0.06955 | 0.00096 | 436 | 22 | 434 | 7 | 433 | 6 | 0.2 |
| CSL4-18 | 0.44 | 0.05034 | 0.0009 | 0.22084 | 0.00422 | 0.03181 | 0.00044 | 211 | 21 | 203 | 4 | 202 | 3 | 0.5 |
| CSL4-19 | 0.63 | 0.05476 | 0.00137 | 0.46215 | 0.01189 | 0.0612 | 0.00087 | 402 | 33 | 386 | 8 | 383 | 5 | 0.8 |
| CSL4-20 | 0.22 | 0.05592 | 0.00097 | 0.53339 | 0.00995 | 0.06917 | 0.00095 | 449 | 20 | 434 | 7 | 431 | 6 | 0.7 |
| CSL4-21 | 0.67 | 0.05571 | 0.00094 | 0.52308 | 0.00953 | 0.06808 | 0.00093 | 441 | 19 | 427 | 6 | 425 | 6 | 0.5 |

| | | | | | | | | | | | | | | |
|---|---|---|---|---|---|---|---|---|---|---|---|---|---|---|
| CSL4-22 | 0.9 | 0.05685 | 0.00104 | 0.54372 | 0.01058 | 0.06935 | 0.00096 | 486 | 21 | 441 | 7 | 432 | 6 | 2.1 |
| CSL4-23 | 0.5 | 0.05148 | 0.00121 | 0.29352 | 0.00713 | 0.04134 | 0.00059 | 262 | 31 | 261 | 6 | 261 | 4 | 0 |
| CSL4-24 | 0.86 | 0.05268 | 0.003 | 0.27652 | 0.01516 | 0.03807 | 0.00058 | 315 | 133 | 248 | 12 | 241 | 4 | 2.9 |
| CSL4-25 | 1.23 | 0.05625 | 0.00091 | 0.50521 | 0.00895 | 0.06513 | 0.00089 | 462 | 18 | 415 | 6 | 407 | 5 | 2 |
| CSL4-26 | 0.59 | 0.05473 | 0.00237 | 0.46138 | 0.01985 | 0.06113 | 0.00101 | 401 | 67 | 385 | 14 | 382 | 6 | 0.8 |
| CSL4-27 | 0.39 | 0.05539 | 0.00104 | 0.53299 | 0.01065 | 0.06978 | 0.00097 | 428 | 22 | 434 | 7 | 435 | 6 | -0.2 |
| CSL4-28 | 0.75 | 0.05692 | 0.00153 | 0.3255 | 0.00893 | 0.04146 | 0.0006 | 488 | 36 | 286 | 7 | 262 | 4 | 9.2 |
| CSL4-29 | 0.49 | 0.11291 | 0.00167 | 5.02692 | 0.08315 | 0.32285 | 0.00437 | 1847 | 14 | 1824 | 14 | 1804 | 21 | 2.4 |
| CSL4-30 | 0.64 | 0.0571 | 0.00106 | 0.54286 | 0.0107 | 0.06894 | 0.00095 | 495 | 21 | 440 | 7 | 430 | 6 | 2.3 |
| CSL4-31 | 0.88 | 0.05124 | 0.00116 | 0.25021 | 0.00585 | 0.03541 | 0.0005 | 252 | 29 | 227 | 5 | 224 | 3 | 1.3 |
| CSL4-32 | 0.61 | 0.05453 | 0.00336 | 0.46407 | 0.02848 | 0.06171 | 0.00104 | 393 | 108 | 387 | 20 | 386 | 6 | 0.3 |
| CSL4-33 | 0.93 | 0.0551 | 0.00184 | 0.49158 | 0.01634 | 0.06469 | 0.00104 | 416 | 46 | 406 | 11 | 404 | 6 | 0.5 |
| CSL4-34 | 0.44 | 0.05559 | 0.00108 | 0.52376 | 0.01077 | 0.06833 | 0.00095 | 436 | 23 | 428 | 7 | 426 | 6 | 0.5 |
| CSL4-35 | 1.42 | 0.06015 | 0.00102 | 0.58382 | 0.01076 | 0.07038 | 0.00097 | 609 | 19 | 467 | 7 | 438 | 6 | 6.6 |
| CSL4-36 | 0.03 | 0.05504 | 0.00104 | 0.50182 | 0.01006 | 0.06611 | 0.00092 | 414 | 22 | 413 | 7 | 413 | 6 | 0 |
| CSL4-37 | 0.2 | 0.0551 | 0.00088 | 0.48671 | 0.00855 | 0.06405 | 0.00087 | 416 | 18 | 403 | 6 | 400 | 5 | 0.8 |
| CSL4-38 | 0.89 | 0.05671 | 0.00112 | 0.53487 | 0.01121 | 0.06839 | 0.00095 | 480 | 24 | 435 | 7 | 426 | 6 | 2.1 |
| CSL4-39 | 0.09 | 0.07199 | 0.00159 | 1.5408 | 0.02714 | 0.15523 | 0.00207 | 986 | 46 | 947 | 11 | 930 | 12 | 1.8 |
| CSL4-40 | 0.81 | 0.05556 | 0.00236 | 0.53383 | 0.0225 | 0.06968 | 0.00114 | 435 | 65 | 434 | 15 | 434 | 7 | 0 |
| CSL4-41 | 0.58 | 0.05502 | 0.00148 | 0.49155 | 0.01347 | 0.06479 | 0.00095 | 413 | 36 | 406 | 9 | 405 | 6 | 0.2 |
| CSL4-42 | 0.5 | 0.05407 | 0.00153 | 0.45069 | 0.01303 | 0.06044 | 0.00088 | 374 | 39 | 378 | 9 | 378 | 5 | 0 |
| CSL4-43 | 0.59 | 0.05403 | 0.0015 | 0.43669 | 0.0124 | 0.05861 | 0.00084 | 372 | 38 | 368 | 9 | 367 | 5 | 0.3 |
| CSL4-44 | 0.57 | 0.05525 | 0.00106 | 0.46991 | 0.0096 | 0.06168 | 0.00086 | 422 | 23 | 391 | 7 | 386 | 5 | 1.3 |
| CSL4-45 | 0.08 | 0.05895 | 0.00101 | 0.65507 | 0.01221 | 0.08057 | 0.00111 | 565 | 19 | 512 | 7 | 500 | 7 | 2.4 |
| CSL4-46 | 0.39 | 0.06619 | 0.00216 | 1.26537 | 0.03714 | 0.13865 | 0.00197 | 812 | 70 | 830 | 17 | 837 | 11 | -0.8 |
| CSL4-47 | 0.37 | 0.05595 | 0.00093 | 0.48462 | 0.00879 | 0.06281 | 0.00087 | 450 | 19 | 401 | 6 | 393 | 5 | 2 |
| CSL4-48 | 1 | 0.05782 | 0.00122 | 0.4925 | 0.01092 | 0.06176 | 0.00088 | 523 | 25 | 407 | 7 | 386 | 5 | 5.4 |
| CSL4-49 | 0.38 | 0.08264 | 0.00263 | 2.46524 | 0.06965 | 0.21635 | 0.00314 | 1261 | 64 | 1262 | 20 | 1263 | 17 | -0.2 |

| | | | | | | | | | | | | | | |
|---|---|---|---|---|---|---|---|---|---|---|---|---|---|---|
| CSL4-50 | 0.42 | 0.1141 | 0.00187 | 5.17229 | 0.09296 | 0.32871 | 0.00459 | 1866 | 15 | 1848 | 15 | 1832 | 22 | 1.9 |
| CSL4-51 | 1.3 | 0.05637 | 0.00132 | 0.58571 | 0.0142 | 0.07535 | 0.00108 | 467 | 29 | 468 | 9 | 468 | 6 | 0 |
| CSL4-52 | 1.28 | 0.05114 | 0.00105 | 0.27415 | 0.00593 | 0.03887 | 0.00055 | 247 | 26 | 246 | 5 | 246 | 3 | 0 |
| CSL4-53 | 0.72 | 0.13755 | 0.00218 | 7.09205 | 0.12433 | 0.37388 | 0.00518 | 2197 | 14 | 2123 | 16 | 2048 | 24 | 7.3 |
| CSL4-54 | 0.46 | 0.05204 | 0.00286 | 0.3215 | 0.01758 | 0.04479 | 0.00074 | 287 | 95 | 283 | 14 | 282 | 5 | 0.4 |
| CSL4-55 | 0.3 | 0.05676 | 0.00106 | 0.56289 | 0.01121 | 0.07192 | 0.00101 | 482 | 21 | 453 | 7 | 448 | 6 | 1.1 |
| CSL4-56 | 0.3 | 0.05767 | 0.00177 | 0.5607 | 0.01527 | 0.07051 | 0.00099 | 517 | 69 | 452 | 10 | 439 | 6 | 3 |
| CSL4-57 | ~~0.37~~ | 0.05451 | 0.00101 | 0.46422 | 0.0092 | 0.06175 | 0.00087 | 392 | 22 | 387 | 6 | 386 | 5 | 0.3 |
| ~~CSL4-58~~ | 0.56 | ~~0.08232~~ | ~~0.00294~~ | ~~2.11361~~ | ~~0.06872~~ | ~~0.18621~~ | ~~0.00273~~ | ~~1253~~ | ~~71~~ | ~~1153~~ | ~~22~~ | ~~1101~~ | ~~15~~ | ~~13.8~~ |
| CSL4-59 | 0.28 | 0.05705 | 0.00209 | 0.55942 | 0.01885 | 0.07112 | 0.00103 | 493 | 83 | 451 | 12 | 443 | 6 | 1.8 |
| CSL4-60 | 0.29 | 0.05155 | 0.00107 | 0.23511 | 0.00513 | 0.03307 | 0.00047 | 266 | 26 | 214 | 4 | 210 | 3 | 1.9 |
| CSL4-61 | 0.96 | 0.05177 | 0.00123 | 0.27988 | 0.0069 | 0.0392 | 0.00057 | 275 | 31 | 251 | 5 | 248 | 4 | 1.2 |
| CSL4-62 | 2 | 0.11371 | 0.00225 | 5.04151 | 0.10521 | 0.32149 | 0.00472 | 1860 | 18 | 1826 | 18 | 1797 | 23 | 3.5 |
| CSL4-63 | 0.84 | 0.05486 | 0.0065 | 0.47453 | 0.05577 | 0.06272 | 0.00143 | 407 | 223 | 394 | 38 | 392 | 9 | 0.5 |
| CSL4-64 | 0.78 | 0.05515 | 0.00118 | 0.51491 | 0.01159 | 0.06771 | 0.00097 | 418 | 26 | 422 | 8 | 422 | 6 | 0 |
| CSL4-65 | 0.47 | 0.05706 | 0.00098 | 0.60295 | 0.01131 | 0.07662 | 0.00107 | 494 | 20 | 479 | 7 | 476 | 6 | 0.6 |
| CSL4-66 | 0.54 | 0.05183 | 0.00143 | 0.23891 | 0.00673 | 0.03343 | 0.0005 | 278 | 38 | 218 | 6 | 212 | 3 | 2.8 |
| CSL4-67 | 0.7 | 0.0564 | 0.00109 | 0.52662 | 0.01088 | 0.0677 | 0.00096 | 468 | 23 | 430 | 7 | 422 | 6 | 1.9 |
| CSL4-68 | 1.42 | 0.05162 | 0.00124 | 0.27326 | 0.00682 | 0.03839 | 0.00056 | 269 | 32 | 245 | 5 | 243 | 3 | 0.8 |
| CSL4-69 | 0.46 | 0.05612 | 0.00103 | 0.52516 | 0.01038 | 0.06785 | 0.00096 | 457 | 21 | 429 | 7 | 423 | 6 | 1.4 |
| CSL4-70 | 0.28 | 0.05347 | 0.00108 | 0.38775 | 0.00833 | 0.05259 | 0.00075 | 349 | 25 | 333 | 6 | 330 | 5 | 0.9 |
| CSL4-71 | 0.26 | 0.11397 | 0.00283 | 5.01459 | 0.10304 | 0.31911 | 0.00446 | 1864 | 46 | 1822 | 17 | 1785 | 22 | 4.4 |
| CSL4-72 | ~~0.55~~ | 0.05703 | 0.00131 | 0.5796 | 0.01376 | 0.0737 | 0.00109 | 493 | 28 | 464 | 9 | 458 | 7 | 1.3 |
| CSL4-73 | 0.57 | 0.05483 | 0.00132 | 0.45158 | 0.01125 | 0.05972 | 0.00087 | 405 | 31 | 378 | 8 | 374 | 5 | 1.1 |
| CSL4-74 | 0.31 | 0.05655 | 0.001 | 0.54547 | 0.01049 | 0.06995 | 0.00098 | 474 | 20 | 442 | 7 | 436 | 6 | 1.4 |
| CSL4-75 | 0.63 | 0.05162 | 0.00156 | 0.30013 | 0.00925 | 0.04216 | 0.00063 | 269 | 44 | 267 | 7 | 266 | 4 | 0.4 |
| CSL4-76 | ~~0.54~~ | 0.05488 | 0.00116 | 0.51526 | 0.01152 | 0.06808 | 0.00098 | 407 | 26 | 422 | 8 | 425 | 6 | -0.7 |
| CSL4-77 | 1.16 | 0.18018 | 0.00302 | 12.05815 | 0.22267 | 0.48527 | 0.00684 | 2655 | 14 | 2609 | 17 | 2550 | 30 | 4.1 |

| | | | | | | | | | | | | | | |
|---|---|---|---|---|---|---|---|---|---|---|---|---|---|---|
| CSL4-78 | 0.14 | 0.0548 | 0.00103 | 0.48859 | 0.00987 | 0.06466 | 0.00092 | 404 | 22 | 404 | 7 | 404 | 6 | 0 |
| CSL4-79 | 0.67 | 0.05429 | 0.00153 | 0.45714 | 0.0132 | 0.06106 | 0.00091 | 383 | 39 | 382 | 9 | 382 | 6 | 0 |
| CSL4-80 | 0.37 | 0.05025 | 0.00207 | 0.23283 | 0.00963 | 0.03359 | 0.00053 | 207 | 67 | 213 | 8 | 213 | 3 | 0 |
| CSL4-81 | 0.47 | 0.05655 | 0.00132 | 0.54124 | 0.01319 | 0.06941 | 0.00101 | 474 | 29 | 439 | 9 | 433 | 6 | 1.4 |
| CSL4-82 | 0.17 | 0.06929 | 0.00124 | 1.34381 | 0.02619 | 0.14063 | 0.002 | 907 | 19 | 865 | 11 | 848 | 11 | 2 |
| CSL4-83 | 0.56 | 0.05691 | 0.00164 | 0.62053 | 0.01817 | 0.07906 | 0.0012 | 488 | 38 | 490 | 11 | 491 | 7 | -0.2 |
| CSL4-84 | 0.56 | 0.05603 | 0.00187 | 0.49409 | 0.01657 | 0.06394 | 0.00103 | 454 | 46 | 408 | 11 | 400 | 6 | 2 |
| CSL4-85 | 0.67 | 0.05741 | 0.00115 | 0.56127 | 0.01198 | 0.0709 | 0.00102 | 507 | 24 | 452 | 8 | 442 | 6 | 2.3 |
| CSL4-86 | 0.37 | 0.05752 | 0.00509 | 0.64173 | 0.05631 | 0.0809 | 0.00165 | 512 | 159 | 503 | 35 | 501 | 10 | 0.4 |
| CSL4-87 | 0.7 | 0.12415 | 0.00215 | 5.8487 | 0.11113 | 0.3416 | 0.00484 | 2017 | 16 | 1954 | 16 | 1894 | 23 | 6.5 |
| CSL4-88 | 0.29 | 0.07054 | 0.00129 | 1.43026 | 0.02843 | 0.14702 | 0.0021 | 944 | 20 | 902 | 12 | 884 | 12 | 2 |
| ~~CSL4-89~~ | 0.59 | ~~0.06245~~ | ~~0.00254~~ | ~~0.52486~~ | ~~0.02141~~ | ~~0.06094~~ | ~~0.00098~~ | ~~690~~ | ~~59~~ | ~~428~~ | ~~14~~ | ~~381~~ | ~~6~~ | ~~12.3~~ |
| CSL4-90 | 0.82 | 0.16199 | 0.00279 | 10.194 | 0.19322 | 0.45633 | 0.00645 | 2477 | 15 | 2453 | 18 | 2423 | 29 | 2.2 |
| CSL4-91 | 0.58 | 0.05082 | 0.00273 | 0.23788 | 0.01219 | 0.03395 | 0.00054 | 232 | 125 | 217 | 10 | 215 | 3 | 0.9 |
| ~~CSL4-92~~ | 0.71 | ~~0.06308~~ | ~~0.00219~~ | ~~0.54332~~ | ~~0.01894~~ | ~~0.06246~~ | ~~0.001~~ | ~~711~~ | ~~47~~ | ~~441~~ | ~~12~~ | ~~391~~ | ~~6~~ | ~~12.8~~ |
| CSL4-93 | 0.82 | 0.05602 | 0.00127 | 0.49195 | 0.01168 | 0.06367 | 0.00094 | 453 | 28 | 406 | 8 | 398 | 6 | 2 |
| CSL4-94 | 1.11 | 0.05547 | 0.0013 | 0.53882 | 0.01315 | 0.07044 | 0.00104 | 431 | 29 | 438 | 9 | 439 | 6 | -0.2 |
| ~~CSL4-95~~ | 0.75 | ~~0.06274~~ | ~~0.00136~~ | ~~0.34994~~ | ~~0.008~~ | ~~0.04045~~ | ~~0.00059~~ | ~~699~~ | ~~25~~ | ~~305~~ | ~~6~~ | ~~256~~ | ~~4~~ | ~~19.1~~ |
| CSL4-96 | 0.21 | 0.06964 | 0.0013 | 1.41985 | 0.02864 | 0.14785 | 0.00212 | 918 | 20 | 897 | 12 | 889 | 12 | 0.9 |
| CSL4-97 | 0.16 | 0.06966 | 0.00187 | 1.38716 | 0.03152 | 0.14442 | 0.00205 | 918 | 56 | 883 | 13 | 870 | 12 | 1.5 |
| CSL4-98 | 0.53 | 0.05512 | 0.00117 | 0.52034 | 0.01167 | 0.06845 | 0.001 | 417 | 26 | 425 | 8 | 427 | 6 | -0.5 |
| CSL4-99 | 0.46 | 0.05672 | 0.00111 | 0.41268 | 0.00866 | 0.05276 | 0.00076 | 481 | 23 | 351 | 6 | 331 | 5 | 6 |
| CSL4-100 | 0.67 | 0.05523 | 0.00202 | 0.32164 | 0.01181 | 0.04223 | 0.00067 | 422 | 54 | 283 | 9 | 267 | 4 | 6 |
| | | | | | | | | | | | | | | |
| **SZG1** | | | | | | | | | | | | | | |
| SZG1-01 | 0.65 | 0.05588 | 0.0009 | 0.53076 | 0.0094 | 0.06888 | 0.00095 | 448 | 18 | 432 | 6 | 429 | 6 | 0.7 |
| SZG1-02 | 2.15 | 0.05625 | 0.0008 | 0.5744 | 0.00924 | 0.07405 | 0.001 | 462 | 16 | 461 | 6 | 461 | 6 | 0 |

| | | | | | | | | | | | | | | |
|---|---|---|---|---|---|---|---|---|---|---|---|---|---|---|
| ~~SZG1-03~~ | ~~0.66~~ | ~~0.05823~~ | ~~0.00079~~ | ~~0.34527~~ | ~~0.00539~~ | ~~0.043~~ | ~~0.00058~~ | ~~538~~ | ~~15~~ | ~~301~~ | ~~4~~ | ~~271~~ | ~~4~~ | ~~11.1~~ |
| SZG1-04 | 0.54 | 0.05559 | 0.00082 | 0.54161 | 0.00899 | 0.07065 | 0.00096 | 436 | 17 | 439 | 6 | 440 | 6 | -0.2 |
| SZG1-05 | 0.4 | 0.06859 | 0.00086 | 1.19076 | 0.01764 | 0.12587 | 0.00168 | 886 | 14 | 796 | 8 | 764 | 10 | 4.2 |
| SZG1-06 | 0.61 | 0.05934 | 0.00077 | 0.52475 | 0.00796 | 0.06412 | 0.00086 | 580 | 15 | 428 | 5 | 401 | 5 | 6.7 |
| SZG1-07 | 0.21 | 0.05625 | 0.00074 | 0.57964 | 0.00886 | 0.07473 | 0.00101 | 462 | 15 | 464 | 6 | 465 | 6 | -0.2 |
| SZG1-08 | 0.41 | 0.06597 | 0.00106 | 1.36305 | 0.02391 | 0.14981 | 0.00208 | 805 | 17 | 873 | 10 | 900 | 12 | -3 |
| SZG1-09 | 0.47 | 0.0549 | 0.00073 | 0.49679 | 0.00766 | 0.06561 | 0.00088 | 408 | 15 | 410 | 5 | 410 | 5 | 0 |
| SZG1-10 | 0.93 | 0.05793 | 0.00078 | 0.58728 | 0.00911 | 0.07351 | 0.00099 | 527 | 15 | 469 | 6 | 457 | 6 | 2.6 |
| SZG1-11 | 0.37 | 0.05586 | 0.00086 | 0.5513 | 0.00946 | 0.07157 | 0.00098 | 447 | 17 | 446 | 6 | 446 | 6 | 0 |
| SZG1-12 | 0.35 | 0.0599 | 0.00078 | 0.54695 | 0.00832 | 0.06621 | 0.00089 | 600 | 15 | 443 | 5 | 413 | 5 | 7.3 |
| SZG1-13 | 0.47 | 0.06152 | 0.00086 | 0.55101 | 0.00876 | 0.06494 | 0.00088 | 657 | 15 | 446 | 6 | 406 | 5 | 9.9 |
| ~~SZG1-14~~ | ~~1.24~~ | ~~0.06143~~ | ~~0.00092~~ | ~~0.35486~~ | ~~0.00592~~ | ~~0.04188~~ | ~~0.00057~~ | ~~654~~ | ~~16~~ | ~~308~~ | ~~4~~ | ~~264~~ | ~~4~~ | ~~16.7~~ |
| SZG1-15 | 1 | 0.05919 | 0.00083 | 0.6048 | 0.00969 | 0.07409 | 0.00101 | 574 | 16 | 480 | 6 | 461 | 6 | 4.1 |
| ~~SZG1-16~~ | ~~0.85~~ | ~~0.07747~~ | ~~0.00158~~ | ~~0.66341~~ | ~~0.01408~~ | ~~0.06209~~ | ~~0.0009~~ | ~~1133~~ | ~~21~~ | ~~517~~ | ~~9~~ | ~~388~~ | ~~5~~ | ~~33.2~~ |
| ~~SZG1-17~~ | ~~1.34~~ | ~~0.06433~~ | ~~0.00114~~ | ~~0.57329~~ | ~~0.01092~~ | ~~0.06462~~ | ~~0.00091~~ | ~~752~~ | ~~19~~ | ~~460~~ | ~~7~~ | ~~404~~ | ~~6~~ | ~~13.9~~ |
| SZG1-18 | 0.72 | 0.05242 | 0.00088 | 0.30433 | 0.00558 | 0.0421 | 0.00058 | 304 | 20 | 270 | 4 | 266 | 4 | 1.5 |
| SZG1-19 | 0.77 | 0.05117 | 0.00124 | 0.29065 | 0.00727 | 0.04118 | 0.00059 | 248 | 32 | 259 | 6 | 260 | 4 | -0.4 |
| SZG1-20 | 0.24 | 0.05632 | 0.00074 | 0.53707 | 0.00823 | 0.06915 | 0.00093 | 465 | 15 | 436 | 5 | 431 | 6 | 1.2 |
| SZG1-21 | 0.3 | 0.0797 | 0.00104 | 2.15135 | 0.03283 | 0.19573 | 0.00265 | 1190 | 13 | 1165 | 11 | 1152 | 14 | 3.3 |
| SZG1-22 | 0.57 | 0.0555 | 0.00078 | 0.56501 | 0.00908 | 0.07381 | 0.00101 | 432 | 16 | 455 | 6 | 459 | 6 | -0.9 |
| SZG1-23 | 0.45 | 0.0562 | 0.00085 | 0.51628 | 0.0087 | 0.06661 | 0.00091 | 460 | 17 | 423 | 6 | 416 | 5 | 1.7 |
| SZG1-24 | 0.51 | 0.05587 | 0.00106 | 0.53713 | 0.01084 | 0.0697 | 0.00098 | 447 | 22 | 437 | 7 | 434 | 6 | 0.7 |
| SZG1-25 | 0.77 | 0.05548 | 0.00126 | 0.52681 | 0.01248 | 0.06885 | 0.00099 | 432 | 28 | 430 | 8 | 429 | 6 | 0.2 |
| SZG1-26 | 1.44 | 0.05719 | 0.00084 | 0.56945 | 0.00941 | 0.0722 | 0.00099 | 499 | 16 | 458 | 6 | 449 | 6 | 2 |
| SZG1-27 | 0.17 | 0.06986 | 0.00085 | 1.4282 | 0.02082 | 0.14825 | 0.00198 | 924 | 13 | 901 | 9 | 891 | 11 | 1.1 |
| SZG1-28 | 0.49 | 0.05637 | 0.00071 | 0.57296 | 0.00854 | 0.0737 | 0.00099 | 467 | 15 | 460 | 6 | 458 | 6 | 0.4 |
| SZG1-29 | 0.39 | 0.05599 | 0.00076 | 0.5899 | 0.00922 | 0.0764 | 0.00103 | 452 | 16 | 471 | 6 | 475 | 6 | -0.8 |
| SZG1-30 | 1.81 | 0.05535 | 0.00077 | 0.54808 | 0.00869 | 0.0718 | 0.00097 | 426 | 16 | 444 | 6 | 447 | 6 | -0.7 |

| | | | | | | | | | | | | | | |
|---|---|---|---|---|---|---|---|---|---|---|---|---|---|---|
| SZG1-31 | 0.2 | 0.05528 | 0.00072 | 0.57489 | 0.00871 | 0.07541 | 0.00101 | 424 | 15 | 461 | 6 | 469 | 6 | -1.7 |
| SZG1-32 | 1.3 | 0.05606 | 0.00082 | 0.50832 | 0.00834 | 0.06575 | 0.0009 | 455 | 16 | 417 | 6 | 410 | 5 | 1.7 |
| SZG1-33 | 0.46 | 0.09484 | 0.00115 | 3.39229 | 0.04921 | 0.25938 | 0.00347 | 1525 | 12 | 1503 | 11 | 1487 | 18 | 2.6 |
| SZG1-34 | 0.48 | 0.0565 | 0.00076 | 0.58355 | 0.00904 | 0.07489 | 0.00101 | 472 | 15 | 467 | 6 | 466 | 6 | 0.2 |
| SZG1-35 | 0.54 | 0.05678 | 0.00072 | 0.57755 | 0.00865 | 0.07375 | 0.00099 | 483 | 15 | 463 | 6 | 459 | 6 | 0.9 |
| ~~SZG1-36~~ | ~~1.03~~ | ~~0.0615~~ | ~~0.00105~~ | ~~0.32217~~ | ~~0.00594~~ | ~~0.03799~~ | ~~0.00053~~ | ~~657~~ | ~~19~~ | ~~284~~ | ~~5~~ | ~~240~~ | ~~3~~ | ~~18.3~~ |
| SZG1-37 | 0.71 | 0.05329 | 0.00094 | 0.30556 | 0.0058 | 0.04157 | 0.00058 | 341 | 20 | 271 | 5 | 263 | 4 | 3 |
| SZG1-38 | 0.09 | 0.06929 | 0.00085 | 1.45179 | 0.02129 | 0.15193 | 0.00204 | 907 | 13 | 911 | 9 | 912 | 11 | -0.1 |
| SZG1-39 | 0.18 | 0.05496 | 0.00135 | 0.53531 | 0.01103 | 0.07064 | 0.00095 | 411 | 56 | 435 | 7 | 440 | 6 | -1.1 |
| SZG1-40 | 1.17 | 0.05887 | 0.00125 | 0.5706 | 0.01266 | 0.07029 | 0.00101 | 562 | 25 | 458 | 8 | 438 | 6 | 4.6 |
| SZG1-41 | 0.16 | 0.06835 | 0.00153 | 1.3596 | 0.0244 | 0.14427 | 0.00192 | 879 | 47 | 872 | 11 | 869 | 11 | 0.3 |
| ~~SZG1-42~~ | ~~0.18~~ | ~~0.10095~~ | ~~0.00289~~ | ~~1.9977~~ | ~~0.04911~~ | ~~0.14352~~ | ~~0.00212~~ | ~~1642~~ | ~~54~~ | ~~1115~~ | ~~17~~ | ~~865~~ | ~~12~~ | ~~28.9~~ |
| SZG1-43 | 0.92 | 0.05607 | 0.00077 | 0.52981 | 0.00837 | 0.06851 | 0.00093 | 455 | 16 | 432 | 6 | 427 | 6 | 1.2 |
| SZG1-44 | 1.18 | 0.05767 | 0.0008 | 0.54584 | 0.00865 | 0.06863 | 0.00093 | 517 | 16 | 442 | 6 | 428 | 6 | 3.3 |
| SZG1-45 | 0.48 | 0.06105 | 0.00096 | 0.57864 | 0.01002 | 0.06873 | 0.00095 | 641 | 17 | 464 | 6 | 428 | 6 | 8.4 |
| SZG1-46 | 0.95 | 0.05666 | 0.0012 | 0.49478 | 0.011 | 0.06333 | 0.0009 | 478 | 26 | 408 | 7 | 396 | 5 | 3 |
| SZG1-47 | 0.4 | 0.05594 | 0.00119 | 0.50853 | 0.0113 | 0.06591 | 0.00094 | 450 | 26 | 417 | 8 | 411 | 6 | 1.5 |
| SZG1-48 | 0.69 | 0.05384 | 0.00074 | 0.46317 | 0.00731 | 0.06238 | 0.00085 | 364 | 16 | 386 | 5 | 390 | 5 | -1 |
| SZG1-49 | 0.19 | 0.05524 | 0.0008 | 0.49859 | 0.00817 | 0.06545 | 0.00089 | 422 | 17 | 411 | 6 | 409 | 5 | 0.5 |
| SZG1-50 | 0.45 | 0.05557 | 0.00104 | 0.50585 | 0.01014 | 0.06601 | 0.00093 | 435 | 22 | 416 | 7 | 412 | 6 | 1 |
| SZG1-51 | 0.32 | 0.05608 | 0.00114 | 0.52362 | 0.01126 | 0.06772 | 0.00099 | 456 | 24 | 428 | 8 | 422 | 6 | 1.4 |
| SZG1-52 | 0.21 | 0.05429 | 0.0015 | 0.47056 | 0.0112 | 0.06287 | 0.00088 | 383 | 63 | 392 | 8 | 393 | 5 | -0.3 |
| SZG1-53 | 0.73 | 0.05507 | 0.00318 | 0.52263 | 0.02966 | 0.06882 | 0.00138 | 415 | 91 | 427 | 20 | 429 | 8 | -0.5 |
| SZG1-54 | 0.63 | 0.05541 | 0.00121 | 0.53331 | 0.01218 | 0.0698 | 0.00103 | 429 | 26 | 434 | 8 | 435 | 6 | -0.2 |
| SZG1-55 | 0.22 | 0.06947 | 0.00182 | 1.36166 | 0.03007 | 0.14216 | 0.00199 | 913 | 55 | 873 | 13 | 857 | 11 | 1.9 |
| SZG1-56 | 0.45 | 0.05478 | 0.00206 | 0.5191 | 0.01795 | 0.06873 | 0.00102 | 403 | 86 | 425 | 12 | 428 | 6 | -0.7 |
| SZG1-57 | 0.46 | 0.05679 | 0.00102 | 0.55204 | 0.01076 | 0.07049 | 0.00101 | 483 | 21 | 446 | 7 | 439 | 6 | 1.6 |
| SZG1-58 | 0.84 | 0.05812 | 0.00202 | 0.57752 | 0.01996 | 0.07206 | 0.00121 | 534 | 47 | 463 | 13 | 449 | 7 | 3.1 |

| | | | | | | | | | | | | | | |
|---|---|---|---|---|---|---|---|---|---|---|---|---|---|---|
| SZG1-59 | 0.58 | 0.06138 | 0.00247 | 0.59599 | 0.0236 | 0.07042 | 0.00127 | 653 | 54 | 475 | 15 | 439 | 8 | 8.2 |
| SZG1-60 | 0.66 | 0.05181 | 0.00102 | 0.25061 | 0.00527 | 0.03508 | 0.00051 | 277 | 24 | 227 | 4 | 222 | 3 | 2.3 |
| SZG1-61 | 1.24 | 0.05051 | 0.00531 | 0.25674 | 0.02641 | 0.03686 | 0.00079 | 219 | 240 | 232 | 21 | 233 | 5 | -0.4 |
| SZG1-62 | 0.72 | 0.05977 | 0.00153 | 0.59523 | 0.01556 | 0.07221 | 0.00111 | 595 | 31 | 474 | 10 | 449 | 7 | 5.6 |
| SZG1-63 | 0.51 | 0.0568 | 0.00105 | 0.50817 | 0.01012 | 0.06488 | 0.00093 | 484 | 21 | 417 | 7 | 405 | 6 | 3 |
| SZG1-64 | 0.51 | 0.05632 | 0.00088 | 0.5228 | 0.00924 | 0.06732 | 0.00094 | 465 | 18 | 427 | 6 | 420 | 6 | 1.7 |
| SZG1-65 | 0.67 | 0.05084 | 0.00236 | 0.27026 | 0.01237 | 0.03855 | 0.0007 | 234 | 72 | 243 | 10 | 244 | 4 | -0.4 |
| SZG1-66 | 0.65 | 0.05744 | 0.00117 | 0.54794 | 0.01182 | 0.06918 | 0.00101 | 508 | 24 | 444 | 8 | 431 | 6 | 3 |
| SZG1-67 | 1.4 | 0.05753 | 0.00119 | 0.54781 | 0.012 | 0.06906 | 0.00101 | 512 | 24 | 444 | 8 | 430 | 6 | 3.3 |
| SZG1-68 | 0.41 | 0.05771 | 0.00105 | 0.6149 | 0.01214 | 0.07727 | 0.00111 | 519 | 21 | 487 | 8 | 480 | 7 | 1.5 |
| SZG1-69 | 1.05 | 0.05766 | 0.00125 | 0.56148 | 0.01273 | 0.07061 | 0.00105 | 517 | 25 | 452 | 8 | 440 | 6 | 2.7 |
| SZG1-70 | 0.33 | 0.05801 | 0.00131 | 0.57613 | 0.01349 | 0.07202 | 0.00108 | 530 | 27 | 462 | 9 | 448 | 6 | 3.1 |
| SZG1-71 | 0.38 | 0.05596 | 0.00128 | 0.51598 | 0.01228 | 0.06687 | 0.001 | 451 | 28 | 422 | 8 | 417 | 6 | 1.2 |
| SZG1-72 | 1.13 | 0.05632 | 0.00097 | 0.55038 | 0.01039 | 0.07087 | 0.00101 | 465 | 20 | 445 | 7 | 441 | 6 | 0.9 |
| SZG1-73 | 0.53 | 0.07498 | 0.00122 | 1.77203 | 0.03202 | 0.17138 | 0.00243 | 1068 | 17 | 1035 | 12 | 1020 | 13 | 4.7 |
| SZG1-74 | 1.41 | 0.05076 | 0.00107 | 0.25576 | 0.00569 | 0.03654 | 0.00053 | 230 | 26 | 231 | 5 | 231 | 3 | 0 |
| SZG1-75 | 0.23 | 0.05578 | 0.00126 | 0.51792 | 0.01221 | 0.06734 | 0.00101 | 444 | 27 | 424 | 8 | 420 | 6 | 1 |
| SZG1-76 | 0.71 | 0.05578 | 0.00109 | 0.51357 | 0.01072 | 0.06677 | 0.00097 | 444 | 23 | 421 | 7 | 417 | 6 | 1 |
| ~~SZG1-77~~ | ~~0.21~~ | ~~0.10062~~ | ~~0.00328~~ | ~~1.90619~~ | ~~0.05542~~ | ~~0.1374~~ | ~~0.00203~~ | ~~1636~~ | ~~62~~ | ~~1083~~ | ~~19~~ | ~~830~~ | ~~11~~ | ~~30.5~~ |
| SZG1-78 | 1.35 | 0.05627 | 0.00118 | 0.54406 | 0.01203 | 0.07012 | 0.00103 | 463 | 25 | 441 | 8 | 437 | 6 | 0.9 |
| SZG1-79 | 0.63 | 0.05447 | 0.00121 | 0.45007 | 0.01047 | 0.05992 | 0.00089 | 391 | 27 | 377 | 7 | 375 | 5 | 0.5 |
| SZG1-80 | 0.35 | 0.05664 | 0.00123 | 0.57195 | 0.01305 | 0.07322 | 0.00109 | 478 | 26 | 459 | 8 | 456 | 7 | 0.7 |
| SZG1-81 | 0.74 | 0.16803 | 0.00257 | 10.56279 | 0.18308 | 0.45586 | 0.00647 | 2538 | 13 | 2485 | 16 | 2421 | 29 | 0 |
| SZG1-82 | 0.64 | 0.05479 | 0.00126 | 0.5434 | 0.01304 | 0.07192 | 0.00108 | 404 | 28 | 441 | 9 | 448 | 6 | -1.6 |
| SZG1-83 | 2.07 | 0.05764 | 0.00099 | 0.54685 | 0.01035 | 0.0688 | 0.00098 | 516 | 20 | 443 | 7 | 429 | 6 | 3.3 |
| SZG1-84 | 0.47 | 0.0549 | 0.00102 | 0.54351 | 0.01091 | 0.0718 | 0.00103 | 408 | 22 | 441 | 7 | 447 | 6 | -1.3 |
| SZG1-85 | 0.91 | 0.05045 | 0.00148 | 0.25552 | 0.00758 | 0.03673 | 0.00058 | 216 | 40 | 231 | 6 | 233 | 4 | -0.9 |
| SZG1-86 | 1.14 | 0.05844 | 0.00392 | 0.61089 | 0.03962 | 0.07581 | 0.00129 | 546 | 151 | 484 | 25 | 471 | 8 | 2.8 |

| | | | | | | | | | | | | | | |
|---|---|---|---|---|---|---|---|---|---|---|---|---|---|---|
| SZG1-87 | 0.58 | 0.05802 | 0.00149 | 0.44026 | 0.01156 | 0.05503 | 0.00085 | 531 | 32 | 370 | 8 | 345 | 5 | 7.2 |
| SZG1-88 | 0.83 | 0.05576 | 0.00146 | 0.49949 | 0.01336 | 0.06496 | 0.00101 | 443 | 33 | 411 | 9 | 406 | 6 | 1.2 |
| SZG1-89 | 1.59 | 0.05627 | 0.00136 | 0.55844 | 0.01393 | 0.07197 | 0.0011 | 463 | 30 | 451 | 9 | 448 | 7 | 0.7 |
| SZG1-90 | 0.27 | 0.05601 | 0.00412 | 0.55412 | 0.03962 | 0.07175 | 0.00121 | 453 | 168 | 448 | 26 | 447 | 7 | 0.2 |
| SZG1-91 | 0.97 | 0.05021 | 0.00196 | 0.26187 | 0.01014 | 0.03782 | 0.00065 | 205 | 58 | 236 | 8 | 239 | 4 | -1.3 |
| SZG1-92 | 0.44 | 0.07082 | 0.00124 | 1.45347 | 0.02781 | 0.14884 | 0.00214 | 952 | 18 | 911 | 12 | 894 | 12 | 1.9 |
| SZG1-93 | 0.38 | 0.05716 | 0.00135 | 0.59523 | 0.01458 | 0.07551 | 0.00115 | 498 | 29 | 474 | 9 | 469 | 7 | 1.1 |
| SZG1-94 | 0.4 | 0.05746 | 0.0027 | 0.58618 | 0.0259 | 0.07398 | 0.00117 | 509 | 106 | 468 | 17 | 460 | 7 | 1.7 |
| SZG1-95 | 1.59 | 0.0575 | 0.00121 | 0.56055 | 0.01243 | 0.0707 | 0.00105 | 511 | 25 | 452 | 8 | 440 | 6 | 2.7 |
| SZG1-96 | 0.14 | 0.07083 | 0.00119 | 1.48002 | 0.0275 | 0.15154 | 0.00216 | 953 | 18 | 922 | 11 | 910 | 12 | 1.3 |
| SZG1-97 | 0.97 | 0.11551 | 0.00183 | 5.23981 | 0.09359 | 0.32896 | 0.00468 | 1888 | 15 | 1859 | 15 | 1833 | 23 | 3 |
| SZG1-98 | 0.03 | 0.0587 | 0.00143 | 0.54239 | 0.01081 | 0.06701 | 0.00094 | 556 | 54 | 440 | 7 | 418 | 6 | 5.3 |
| SZG1-99 | 0.17 | 0.0682 | 0.00183 | 1.28441 | 0.0291 | 0.1366 | 0.00195 | 875 | 57 | 839 | 13 | 825 | 11 | 1.7 |
| SZG1-100 | 0.75 | 0.04971 | 0.00283 | 0.26029 | 0.01457 | 0.03797 | 0.00074 | 181 | 93 | 235 | 12 | 240 | 5 | -2.1 |
| **CSL5** | | | | | | | | | | | | | | |
| CSL5-01 | 0.53 | 0.05616 | 0.00115 | 0.56648 | 0.01232 | 0.07314 | 0.00103 | 459 | 25 | 456 | 8 | 455 | 6 | 0.2 |
| CSL5-02 | 0.43 | 0.05187 | 0.00077 | 0.27698 | 0.00465 | 0.03872 | 0.00053 | 280 | 17 | 248 | 4 | 245 | 3 | 1.2 |
| CSL5-03 | 0.38 | 0.06803 | 0.00095 | 1.32025 | 0.02122 | 0.14073 | 0.00192 | 869 | 15 | 855 | 9 | 849 | 11 | 0.7 |
| CSL5-04 | 0.55 | 0.05155 | 0.001 | 0.29626 | 0.00612 | 0.04167 | 0.00058 | 266 | 24 | 263 | 5 | 263 | 4 | 0 |
| CSL5-05 | 0.39 | 0.05737 | 0.00114 | 0.58271 | 0.01235 | 0.07365 | 0.00103 | 506 | 24 | 466 | 8 | 458 | 6 | 1.7 |
| CSL5-06 | 0.8 | 0.05569 | 0.00082 | 0.49368 | 0.00823 | 0.06428 | 0.00087 | 440 | 17 | 407 | 6 | 402 | 5 | 1.2 |
| CSL5-07 | 0.69 | 0.0547 | 0.00101 | 0.5078 | 0.01005 | 0.06732 | 0.00094 | 400 | 22 | 417 | 7 | 420 | 6 | -0.7 |
| CSL5-08 | 0.85 | 0.05593 | 0.00096 | 0.54454 | 0.01021 | 0.0706 | 0.00099 | 450 | 20 | 441 | 7 | 440 | 6 | 0.2 |
| CSL5-09 | 0.36 | 0.07085 | 0.00095 | 1.40496 | 0.02205 | 0.14378 | 0.00195 | 953 | 14 | 891 | 9 | 866 | 11 | 2.9 |
| CSL5-10 | 0.65 | 0.0509 | 0.00159 | 0.27486 | 0.0087 | 0.03916 | 0.00058 | 236 | 46 | 247 | 7 | 248 | 4 | -0.4 |
| CSL5-11 | 0.68 | 0.05375 | 0.00177 | 0.43662 | 0.01445 | 0.0589 | 0.00092 | 361 | 47 | 368 | 10 | 369 | 6 | -0.3 |

| | | | | | | | | | | | | | | |
|---|---|---|---|---|---|---|---|---|---|---|---|---|---|---|
| CSL5-12 | 0.36 | 0.05638 | 0.00088 | 0.51831 | 0.00906 | 0.06667 | 0.00092 | 467 | 18 | 424 | 6 | 416 | 6 | 1.9 |
| CSL5-13 | 0.46 | 0.05588 | 0.00118 | 0.55057 | 0.01228 | 0.07145 | 0.00101 | 448 | 26 | 445 | 8 | 445 | 6 | 0 |
| CSL5-14 | 1.35 | 0.05853 | 0.00135 | 0.71908 | 0.01724 | 0.08908 | 0.00128 | 550 | 28 | 550 | 10 | 550 | 8 | 0 |
| CSL5-15 | 1.48 | 0.04609 | 0.00412 | 0.23903 | 0.02099 | 0.03761 | 0.00062 | 2 | 195 | 218 | 17 | 238 | 4 | -8.4 |
| CSL5-16 | 0.31 | 0.16406 | 0.00346 | 10.35702 | 0.16753 | 0.45786 | 0.00621 | 2498 | 36 | 2467 | 15 | 2430 | 27 | 2.8 |
| CSL5-17 | 0.36 | 0.05647 | 0.00112 | 0.60673 | 0.01286 | 0.0779 | 0.0011 | 471 | 24 | 481 | 8 | 484 | 7 | -0.6 |
| CSL5-18 | 0.65 | 0.05153 | 0.00126 | 0.30319 | 0.00768 | 0.04267 | 0.00062 | 265 | 32 | 269 | 6 | 269 | 4 | 0 |
| CSL5-19 | 0.7 | 0.05453 | 0.00078 | 0.47941 | 0.00786 | 0.06375 | 0.00087 | 393 | 17 | 398 | 5 | 398 | 5 | 0 |
| CSL5-20 | 0.15 | 0.06955 | 0.00153 | 1.38151 | 0.02401 | 0.14407 | 0.00193 | 915 | 46 | 881 | 10 | 868 | 11 | 1.5 |
| CSL5-21 | 0.3 | 0.07085 | 0.00102 | 1.45701 | 0.02405 | 0.14912 | 0.00205 | 953 | 15 | 913 | 10 | 896 | 12 | 1.9 |
| CSL5-22 | 0.39 | 0.05609 | 0.00123 | 0.54832 | 0.01264 | 0.07089 | 0.00101 | 456 | 27 | 444 | 8 | 442 | 6 | 0.5 |
| CSL5-23 | 0.59 | 0.05097 | 0.00335 | 0.27532 | 0.01801 | 0.03917 | 0.00067 | 239 | 119 | 247 | 14 | 248 | 4 | -0.4 |
| CSL5-24 | 0.92 | 0.05635 | 0.00126 | 0.54878 | 0.01279 | 0.07062 | 0.00101 | 466 | 28 | 444 | 8 | 440 | 6 | 0.9 |
| CSL5-25 | 0.47 | 0.05578 | 0.00101 | 0.55808 | 0.01095 | 0.07255 | 0.00101 | 444 | 21 | 450 | 7 | 452 | 6 | -0.4 |
| CSL5-26 | 0.44 | 0.07836 | 0.00111 | 2.0417 | 0.03319 | 0.18894 | 0.0026 | 1156 | 14 | 1130 | 11 | 1116 | 14 | 3.6 |
| CSL5-27 | 0.81 | 0.0566 | 0.00094 | 0.56015 | 0.01023 | 0.07176 | 0.00099 | 476 | 19 | 452 | 7 | 447 | 6 | 1.1 |
| CSL5-28 | 0.22 | 0.05106 | 0.00094 | 0.27732 | 0.00549 | 0.03938 | 0.00055 | 244 | 22 | 249 | 4 | 249 | 3 | 0 |
| CSL5-29 | 0.45 | 0.05151 | 0.00124 | 0.28808 | 0.00726 | 0.04056 | 0.00057 | 264 | 33 | 257 | 6 | 256 | 4 | 0.4 |
| CSL5-30 | 0.47 | 0.05051 | 0.0013 | 0.23159 | 0.00612 | 0.03325 | 0.00048 | 219 | 35 | 212 | 5 | 211 | 3 | 0.5 |
| CSL5-31 | 0.5 | 0.07197 | 0.00097 | 1.56049 | 0.02454 | 0.15723 | 0.00214 | 985 | 14 | 955 | 10 | 941 | 12 | 1.5 |
| CSL5-32 | 0.67 | 0.05648 | 0.0015 | 0.58891 | 0.01597 | 0.0756 | 0.00113 | 471 | 34 | 470 | 10 | 470 | 7 | 0 |
| CSL5-33 | 1.01 | 0.07166 | 0.00108 | 1.53535 | 0.02608 | 0.15536 | 0.00215 | 976 | 16 | 945 | 10 | 931 | 12 | 1.5 |
| CSL5-34 | 0.6 | 0.09182 | 0.00134 | 3.09862 | 0.05129 | 0.2447 | 0.0034 | 1464 | 14 | 1432 | 13 | 1411 | 18 | 3.8 |
| CSL5-35 | 1.33 | 0.05461 | 0.00075 | 0.4676 | 0.00745 | 0.06208 | 0.00084 | 396 | 16 | 390 | 5 | 388 | 5 | 0.5 |
| CSL5-36 | 0.71 | 0.05577 | 0.00106 | 0.5515 | 0.01125 | 0.0717 | 0.00101 | 443 | 22 | 446 | 7 | 446 | 6 | 0 |
| CSL5-37 | 0.22 | 0.05459 | 0.00152 | 0.48417 | 0.01173 | 0.06433 | 0.00089 | 395 | 64 | 401 | 8 | 402 | 5 | -0.2 |
| CSL5-38 | 0.23 | 0.0657 | 0.0016 | 1.217 | 0.02464 | 0.13434 | 0.00183 | 797 | 52 | 808 | 11 | 813 | 10 | -0.6 |
| CSL5-39 | 0.56 | 0.0564 | 0.00117 | 0.54295 | 0.01192 | 0.06981 | 0.00099 | 468 | 25 | 440 | 8 | 435 | 6 | 1.1 |

| | | | | | | | | | | | | | | |
|---|---|---|---|---|---|---|---|---|---|---|---|---|---|---|
| CSL5-40 | 0.88 | 0.05554 | 0.00172 | 0.52436 | 0.0164 | 0.06847 | 0.00105 | 434 | 43 | 428 | 11 | 427 | 6 | 0.2 |
| CSL5-41 | 1.2 | 0.11908 | 0.00457 | 5.73027 | 0.19984 | 0.349 | 0.0056 | 1942 | 70 | 1936 | 30 | 1930 | 27 | 0.6 |
| CSL5-42 | 0.83 | 0.05152 | 0.00136 | 0.25797 | 0.007 | 0.03631 | 0.00053 | 264 | 36 | 233 | 6 | 230 | 3 | 1.3 |
| CSL5-43 | 0.85 | 0.05645 | 0.00081 | 0.52431 | 0.00863 | 0.06735 | 0.00092 | 470 | 16 | 428 | 6 | 420 | 6 | 1.9 |
| CSL5-44 | 0.49 | 0.05764 | 0.00128 | 0.66151 | 0.01543 | 0.08322 | 0.00119 | 516 | 27 | 516 | 9 | 515 | 7 | 0.2 |
| CSL5-45 | 0.45 | 0.05564 | 0.00084 | 0.51702 | 0.00881 | 0.06738 | 0.00092 | 438 | 17 | 423 | 6 | 420 | 6 | 0.7 |
| CSL5-46 | 0.58 | 0.0565 | 0.00114 | 0.5639 | 0.01211 | 0.07237 | 0.00102 | 472 | 24 | 454 | 8 | 450 | 6 | 0.9 |
| CSL5-47 | 0.58 | 0.05467 | 0.00166 | 0.47872 | 0.01485 | 0.0635 | 0.00095 | 399 | 43 | 397 | 10 | 397 | 6 | 0 |
| CSL5-48 | 0.61 | 0.05135 | 0.00185 | 0.28583 | 0.01036 | 0.04037 | 0.00062 | 257 | 55 | 255 | 8 | 255 | 4 | 0 |
| CSL5-49 | 0.66 | 0.05588 | 0.00082 | 0.51544 | 0.00865 | 0.06689 | 0.00092 | 448 | 17 | 422 | 6 | 417 | 6 | 1.2 |
| CSL5-50 | 0.63 | 0.05623 | 0.001 | 0.57696 | 0.01115 | 0.0744 | 0.00104 | 461 | 21 | 463 | 7 | 463 | 6 | 0 |
| CSL5-51 | 0.04 | 0.05738 | 0.00085 | 0.55515 | 0.00934 | 0.07016 | 0.00096 | 506 | 17 | 448 | 6 | 437 | 6 | 2.5 |
| CSL5-52 | 0.5 | 0.05572 | 0.00083 | 0.50319 | 0.00856 | 0.06548 | 0.0009 | 441 | 17 | 414 | 6 | 409 | 5 | 1.2 |
| CSL5-53 | 1.08 | 0.05564 | 0.00075 | 0.49459 | 0.00782 | 0.06446 | 0.00088 | 438 | 16 | 408 | 5 | 403 | 5 | 1.2 |
| CSL5-54 | 0.47 | 0.07125 | 0.00101 | 1.4438 | 0.02359 | 0.14695 | 0.00202 | 965 | 15 | 907 | 10 | 884 | 11 | 2.6 |
| CSL5-55 | 0.37 | 0.0552 | 0.00087 | 0.5137 | 0.00903 | 0.06748 | 0.00093 | 420 | 18 | 421 | 6 | 421 | 6 | 0 |
| CSL5-56 | 0.25 | 0.05471 | 0.00094 | 0.4926 | 0.00928 | 0.06529 | 0.00091 | 400 | 20 | 407 | 6 | 408 | 6 | -0.2 |
| CSL5-57 | 0.47 | 0.05582 | 0.00136 | 0.52153 | 0.01317 | 0.06775 | 0.00098 | 445 | 31 | 426 | 9 | 423 | 6 | 0.7 |
| CSL5-58 | 0.62 | 0.05073 | 0.00075 | 0.25318 | 0.00425 | 0.03619 | 0.0005 | 229 | 18 | 229 | 3 | 229 | 3 | 0 |
| CSL5-59 | 0.07 | 0.06874 | 0.0009 | 1.34217 | 0.02079 | 0.1416 | 0.00193 | 891 | 14 | 864 | 9 | 854 | 11 | 1.2 |
| CSL5-60 | 0.47 | 0.05553 | 0.00106 | 0.51573 | 0.0106 | 0.06735 | 0.00095 | 434 | 23 | 422 | 7 | 420 | 6 | 0.5 |
| CSL5-61 | 0.62 | 0.05128 | 0.00107 | 0.29122 | 0.00642 | 0.04118 | 0.00059 | 253 | 26 | 260 | 5 | 260 | 4 | 0 |
| CSL5-62 | 0.69 | 0.05119 | 0.00156 | 0.28494 | 0.0088 | 0.04037 | 0.00061 | 249 | 44 | 255 | 7 | 255 | 4 | 0 |
| ~~CSL5-63~~ | ~~0.49~~ | ~~0.0945~~ | ~~0.00289~~ | ~~2.49045~~ | ~~0.06714~~ | ~~0.19113~~ | ~~0.00278~~ | ~~1518~~ | ~~59~~ | ~~1269~~ | ~~20~~ | ~~1128~~ | ~~15~~ | ~~34.6~~ |
| CSL5-64 | 0.71 | 0.05671 | 0.00092 | 0.50792 | 0.00914 | 0.06495 | 0.0009 | 480 | 19 | 417 | 6 | 406 | 5 | 2.7 |
| CSL5-65 | 0.65 | 0.05174 | 0.00275 | 0.31247 | 0.01654 | 0.04379 | 0.00073 | 274 | 91 | 276 | 13 | 276 | 5 | 0 |
| CSL5-66 | 0.44 | 0.05506 | 0.00254 | 0.49912 | 0.02298 | 0.06573 | 0.0011 | 415 | 73 | 411 | 16 | 410 | 7 | 0.2 |
| CSL5-67 | 0.51 | 0.0551 | 0.00089 | 0.51769 | 0.00928 | 0.06813 | 0.00095 | 416 | 19 | 424 | 6 | 425 | 6 | -0.2 |

| | | | | | | | | | | | | | | |
|---|---|---|---|---|---|---|---|---|---|---|---|---|---|---|
| CSL5-68 | 1.04 | 0.05586 | 0.00091 | 0.50255 | 0.00912 | 0.06524 | 0.0009 | 447 | 19 | 413 | 6 | 407 | 5 | 1.5 |
| CSL5-69 | 0.74 | 0.05143 | 0.00293 | 0.2918 | 0.0165 | 0.04114 | 0.00071 | 260 | 98 | 260 | 13 | 260 | 4 | 0 |
| CSL5-70 | 0.79 | 0.07028 | 0.00094 | 1.37501 | 0.02162 | 0.14188 | 0.00194 | 937 | 14 | 878 | 9 | 855 | 11 | 2.7 |
| CSL5-71 | 0.31 | 0.0553 | 0.00086 | 0.52189 | 0.00916 | 0.06844 | 0.00095 | 424 | 18 | 426 | 6 | 427 | 6 | -0.2 |
| CSL5-72 | 0.54 | 0.08539 | 0.00143 | 2.72967 | 0.05026 | 0.23182 | 0.00331 | 1324 | 17 | 1337 | 14 | 1344 | 17 | -1.5 |
| CSL5-73 | 0.28 | 0.07351 | 0.00109 | 1.6933 | 0.02853 | 0.16705 | 0.00232 | 1028 | 15 | 1006 | 11 | 996 | 13 | 1 |
| CSL5-74 | 1.44 | 0.05432 | 0.00123 | 0.29978 | 0.00711 | 0.04002 | 0.00057 | 384 | 29 | 266 | 6 | 253 | 4 | 5.1 |
| CSL5-75 | 0.53 | 0.06817 | 0.00119 | 1.28128 | 0.02442 | 0.1363 | 0.00193 | 874 | 19 | 837 | 11 | 824 | 11 | 1.6 |
| CSL5-76 | 0.75 | 0.05457 | 0.00108 | 0.48333 | 0.0102 | 0.06422 | 0.00091 | 395 | 24 | 400 | 7 | 401 | 6 | -0.2 |
| CSL5-77 | 0.75 | 0.05145 | 0.0012 | 0.2699 | 0.00658 | 0.03804 | 0.00054 | 261 | 31 | 243 | 5 | 241 | 3 | 0.8 |
| CSL5-78 | 0.87 | 0.05476 | 0.00123 | 0.49538 | 0.01167 | 0.06561 | 0.00095 | 402 | 28 | 409 | 8 | 410 | 6 | -0.2 |
| CSL5-79 | 0.18 | 0.0707 | 0.00097 | 1.34168 | 0.02156 | 0.13762 | 0.00189 | 949 | 15 | 864 | 9 | 831 | 11 | 4 |
| CSL5-80 | 0.27 | 0.05523 | 0.00086 | 0.515 | 0.00906 | 0.06762 | 0.00094 | 422 | 18 | 422 | 6 | 422 | 6 | 0 |
| CSL5-81 | 0.19 | 0.05141 | 0.00103 | 0.29391 | 0.00626 | 0.04146 | 0.00059 | 259 | 25 | 262 | 5 | 262 | 4 | 0 |
| CSL5-82 | 0.68 | 0.05118 | 0.00176 | 0.27367 | 0.00952 | 0.03878 | 0.0006 | 249 | 52 | 246 | 8 | 245 | 4 | 0.4 |
| CSL5-83 | 0.09 | 0.05694 | 0.00089 | 0.57554 | 0.01008 | 0.0733 | 0.00102 | 489 | 18 | 462 | 6 | 456 | 6 | 1.3 |
| CSL5-84 | 0.53 | 0.06495 | 0.00107 | 1.06917 | 0.01955 | 0.11937 | 0.00168 | 773 | 18 | 738 | 10 | 727 | 10 | 1.5 |
| CSL5-85 | 0.35 | 0.05501 | 0.00093 | 0.49455 | 0.0092 | 0.06519 | 0.00091 | 413 | 20 | 408 | 6 | 407 | 6 | 0.2 |
| CSL5-86 | 0.19 | 0.05611 | 0.00085 | 0.56453 | 0.0097 | 0.07296 | 0.00101 | 457 | 17 | 454 | 6 | 454 | 6 | 0 |
| CSL5-87 | 0.2 | 0.06972 | 0.00175 | 1.45679 | 0.03042 | 0.15155 | 0.0021 | 920 | 53 | 913 | 13 | 910 | 12 | 0.3 |
| CSL5-88 | 0.91 | 0.05502 | 0.00413 | 0.50933 | 0.03793 | 0.06713 | 0.00129 | 413 | 133 | 418 | 26 | 419 | 8 | -0.2 |
| CSL5-89 | 0.6 | 0.05558 | 0.00218 | 0.48639 | 0.0177 | 0.06347 | 0.00092 | 436 | 89 | 402 | 12 | 397 | 6 | 1.3 |
| CSL5-90 | 0.68 | 0.05124 | 0.00114 | 0.28524 | 0.00666 | 0.04037 | 0.00059 | 252 | 28 | 255 | 5 | 255 | 4 | 0 |
| CSL5-91 | 0.9 | 0.05418 | 0.00108 | 0.44756 | 0.0095 | 0.0599 | 0.00086 | 379 | 24 | 376 | 7 | 375 | 5 | 0.3 |
| CSL5-92 | 1.15 | 0.05517 | 0.00107 | 0.56565 | 0.01171 | 0.07435 | 0.00107 | 419 | 23 | 455 | 8 | 462 | 6 | -1.5 |
| CSL5-93 | 0.63 | 0.0538 | 0.00112 | 0.43081 | 0.00946 | 0.05807 | 0.00085 | 363 | 25 | 364 | 7 | 364 | 5 | 0 |
| CSL5-94 | 0.48 | 0.06389 | 0.00149 | 1.12979 | 0.02716 | 0.12824 | 0.00194 | 738 | 27 | 768 | 13 | 778 | 11 | -1.3 |
| CSL5-95 | 0.41 | 0.05679 | 0.00095 | 0.55781 | 0.01029 | 0.07123 | 0.001 | 483 | 19 | 450 | 7 | 444 | 6 | 1.4 |

| | | | | | | | | | | | | | | |
|---|---|---|---|---|---|---|---|---|---|---|---|---|---|---|
| ~~CSL5-96~~ | ~~0.42~~ | ~~0.09896~~ | ~~0.00135~~ | ~~3.07143~~ | ~~0.04911~~ | ~~0.22508~~ | ~~0.0031~~ | ~~1605~~ | ~~13~~ | ~~1426~~ | ~~12~~ | ~~1309~~ | ~~16~~ | ~~22.6~~ |
| CSL5-97 | 0.58 | 0.07101 | 0.00103 | 1.6102 | 0.02689 | 0.16443 | 0.00228 | 958 | 15 | 974 | 10 | 981 | 13 | -0.7 |
| CSL5-98 | 0.7 | 0.05945 | 0.00109 | 0.54633 | 0.01083 | 0.06664 | 0.00096 | 584 | 21 | 443 | 7 | 416 | 6 | 6.5 |
| CSL5-99 | 0.47 | 0.05978 | 0.00211 | 0.80654 | 0.02588 | 0.09785 | 0.00142 | 596 | 78 | 601 | 15 | 602 | 8 | -0.2 |
| CSL5-100 | 0.67 | 0.05265 | 0.00109 | 0.32001 | 0.00699 | 0.04408 | 0.00064 | 314 | 25 | 282 | 5 | 278 | 4 | 1.4 |
| | | | | | | | | | | | | | | |
| **GS-E** | | | | | | | | | | | | | | |
| GSE-01 | 0.46 | 0.0554 | 0.00182 | 0.51894 | 0.01656 | 0.06792 | 0.00112 | 428 | 42 | 424 | 11 | 424 | 7 | 0 |
| GSE-02 | 0.57 | 0.13755 | 0.00312 | 7.12679 | 0.1611 | 0.37568 | 0.00548 | 2197 | 20 | 2127 | 20 | 2056 | 26 | 6.9 |
| GSE-03 | 0.34 | 0.0776 | 0.00305 | 2.09061 | 0.07583 | 0.1954 | 0.00299 | 1137 | 80 | 1146 | 25 | 1151 | 16 | -1.2 |
| GSE-04 | 0.52 | 0.05179 | 0.00212 | 0.30864 | 0.01239 | 0.04321 | 0.00071 | 276 | 62 | 273 | 10 | 273 | 4 | 0 |
| GSE-05 | 0.96 | 0.05605 | 0.00192 | 0.56976 | 0.01901 | 0.07371 | 0.00121 | 454 | 45 | 458 | 12 | 458 | 7 | 0 |
| GSE-06 | 0.47 | 0.05652 | 0.00188 | 0.57846 | 0.01879 | 0.07421 | 0.00121 | 473 | 43 | 463 | 12 | 461 | 7 | 0.4 |
| GSE-07 | 0.57 | 0.05111 | 0.00311 | 0.27488 | 0.01644 | 0.039 | 0.00072 | 246 | 103 | 247 | 13 | 247 | 4 | 0 |
| GSE-08 | 2.19 | 0.05143 | 0.00337 | 0.29312 | 0.01879 | 0.04133 | 0.00082 | 260 | 111 | 261 | 15 | 261 | 5 | 0 |
| GSE-09 | 0.69 | 0.18101 | 0.00417 | 12.23168 | 0.28122 | 0.48998 | 0.00721 | 2662 | 20 | 2622 | 22 | 2571 | 31 | 3.5 |
| ~~GSE-10~~ | ~~1.12~~ | ~~0.06867~~ | ~~0.00594~~ | ~~0.65556~~ | ~~0.05539~~ | ~~0.06923~~ | ~~0.00167~~ | ~~889~~ | ~~135~~ | ~~512~~ | ~~34~~ | ~~432~~ | ~~10~~ | ~~18.5~~ |
| GSE-11 | 0.43 | 0.05505 | 0.00278 | 0.50966 | 0.02516 | 0.06713 | 0.00123 | 414 | 77 | 418 | 17 | 419 | 7 | -0.2 |
| GSE-12 | 0.3 | 0.05547 | 0.00226 | 0.53388 | 0.02114 | 0.06979 | 0.00123 | 431 | 57 | 434 | 14 | 435 | 7 | -0.2 |
| GSE-13 | 0.5 | 0.05583 | 0.00318 | 0.55756 | 0.03102 | 0.07242 | 0.00139 | 446 | 89 | 450 | 20 | 451 | 8 | -0.2 |
| GSE-14 | 1.11 | 0.05328 | 0.00186 | 0.45561 | 0.0155 | 0.06201 | 0.00102 | 341 | 48 | 381 | 11 | 388 | 6 | -1.8 |
| GSE-15 | 1.49 | 0.06058 | 0.0033 | 0.81885 | 0.04374 | 0.09801 | 0.00184 | 624 | 83 | 607 | 24 | 603 | 11 | 0.7 |
| GSE-16 | 0.21 | 0.11511 | 0.00304 | 5.39927 | 0.14019 | 0.34012 | 0.00536 | 1882 | 25 | 1885 | 22 | 1887 | 26 | -0.3 |
| GSE-17 | 0.3 | 0.15323 | 0.0039 | 9.32284 | 0.23446 | 0.4412 | 0.00684 | 2382 | 23 | 2370 | 23 | 2356 | 31 | 1.1 |
| GSE-18 | 0.39 | 0.06964 | 0.0019 | 1.46593 | 0.0393 | 0.15265 | 0.00237 | 918 | 31 | 916 | 16 | 916 | 13 | 0 |
| GSE-19 | 0.77 | 0.05087 | 0.00306 | 0.27405 | 0.01614 | 0.03906 | 0.00075 | 235 | 100 | 246 | 13 | 247 | 5 | -0.4 |
| GSE-20 | 0.74 | 0.05559 | 0.00564 | 0.54104 | 0.05412 | 0.07057 | 0.00165 | 436 | 183 | 439 | 36 | 440 | 10 | -0.2 |
| GSE-21 | 1.56 | 0.20685 | 0.00548 | 15.79196 | 0.41246 | 0.55361 | 0.00886 | 2881 | 23 | 2864 | 25 | 2840 | 37 | 1.4 |

| | | | | | | | | | | | | | | |
|---|---|---|---|---|---|---|---|---|---|---|---|---|---|---|
| GSE-22 | 0.2 | 0.06894 | 0.00192 | 1.39497 | 0.0382 | 0.14673 | 0.00229 | 897 | 32 | 887 | 16 | 883 | 13 | 0.5 |
| GSE-23 | 1 | 0.05601 | 0.00208 | 0.55042 | 0.0199 | 0.07126 | 0.00124 | 453 | 50 | 445 | 13 | 444 | 7 | 0.2 |
| GSE-24 | 0.61 | 0.05569 | 0.00326 | 0.53598 | 0.03052 | 0.06979 | 0.00144 | 440 | 90 | 436 | 20 | 435 | 9 | 0.2 |
| GSE-25 | 0.36 | 0.23417 | 0.0076 | 18.7828 | 0.52856 | 0.58173 | 0.00941 | 3081 | 53 | 3031 | 27 | 2956 | 38 | 4.2 |
| GSE-26 | 0.05 | 0.07028 | 0.00206 | 1.63752 | 0.04709 | 0.16895 | 0.00273 | 937 | 33 | 985 | 18 | 1006 | 15 | -6.9 |
| GSE-27 | 0.44 | 0.06944 | 0.00259 | 1.40525 | 0.05071 | 0.14674 | 0.00264 | 912 | 45 | 891 | 21 | 883 | 15 | 0.9 |
| GSE-28 | 0.14 | 0.10615 | 0.00308 | 4.43759 | 0.12639 | 0.30315 | 0.00494 | 1734 | 29 | 1719 | 24 | 1707 | 24 | 1.6 |
| GSE-29 | 0.02 | 0.0556 | 0.00229 | 0.53839 | 0.02162 | 0.07021 | 0.00125 | 436 | 58 | 437 | 14 | 437 | 8 | 0 |
| ~~GSE-30~~ | ~~1.47~~ | ~~0.07381~~ | ~~0.00313~~ | ~~0.5377~~ | ~~0.02208~~ | ~~0.05283~~ | ~~0.00098~~ | ~~1036~~ | ~~53~~ | ~~437~~ | ~~15~~ | ~~332~~ | ~~6~~ | ~~31.6~~ |
| GSE-31 | 0.44 | 0.12816 | 0.00384 | 7.0095 | 0.20608 | 0.39662 | 0.0066 | 2073 | 29 | 2113 | 26 | 2153 | 30 | -3.7 |
| GSE-32 | 0.69 | 0.05582 | 0.00214 | 0.55226 | 0.02051 | 0.07174 | 0.00129 | 445 | 51 | 446 | 13 | 447 | 8 | -0.2 |
| GSE-33 | 0.58 | 0.0564 | 0.00196 | 0.59787 | 0.02027 | 0.07687 | 0.00132 | 468 | 45 | 476 | 13 | 477 | 8 | -0.2 |
| GSE-34 | 0.59 | 0.10047 | 0.00325 | 4.06593 | 0.12814 | 0.29346 | 0.00511 | 1633 | 33 | 1647 | 26 | 1659 | 25 | -1.6 |
| GSE-35 | 0.85 | 0.05179 | 0.00193 | 0.31882 | 0.01158 | 0.04464 | 0.00079 | 276 | 51 | 281 | 9 | 282 | 5 | -0.4 |
| GSE-36 | 0.23 | 0.05822 | 0.00198 | 0.62031 | 0.02056 | 0.07726 | 0.00132 | 538 | 43 | 490 | 13 | 480 | 8 | 2.1 |
| GSE-37 | 0.63 | 0.05619 | 0.00263 | 0.31815 | 0.01447 | 0.04105 | 0.00078 | 460 | 67 | 280 | 11 | 259 | 5 | 8.1 |
| GSE-38 | 0.9 | 0.05142 | 0.00317 | 0.27843 | 0.01672 | 0.03927 | 0.00083 | 260 | 99 | 249 | 13 | 248 | 5 | 0.4 |
| GSE-39 | 0.12 | 0.11218 | 0.00356 | 4.86847 | 0.15153 | 0.3147 | 0.0053 | 1835 | 33 | 1797 | 26 | 1764 | 26 | 4 |
| GSE-40 | 0.3 | 0.07331 | 0.00274 | 1.76356 | 0.06414 | 0.17444 | 0.00317 | 1023 | 45 | 1032 | 24 | 1037 | 17 | -1.4 |
| GSE-41 | 0.59 | 0.05609 | 0.00235 | 0.55924 | 0.0228 | 0.07229 | 0.00133 | 456 | 58 | 451 | 15 | 450 | 8 | 0.2 |
| GSE-42 | 0.32 | 0.07014 | 0.00254 | 1.44329 | 0.0508 | 0.14922 | 0.00269 | 932 | 43 | 907 | 21 | 897 | 15 | 1.1 |
| GSE-43 | 0.95 | 0.16586 | 0.00558 | 10.56064 | 0.34751 | 0.46169 | 0.00808 | 2516 | 32 | 2485 | 31 | 2447 | 36 | 2.8 |
| GSE-44 | 0.68 | 0.05682 | 0.00235 | 0.59547 | 0.02401 | 0.07599 | 0.00141 | 485 | 56 | 474 | 15 | 472 | 8 | 0.4 |
| GSE-45 | 1.78 | 0.05699 | 0.00213 | 0.59498 | 0.02164 | 0.0757 | 0.00137 | 491 | 49 | 474 | 14 | 470 | 8 | 0.9 |
| GSE-46 | 0.02 | 0.07132 | 0.00274 | 1.58745 | 0.0593 | 0.16139 | 0.003 | 967 | 46 | 965 | 23 | 964 | 17 | 0.1 |
| GSE-47 | 0.24 | 0.05582 | 0.00219 | 0.53115 | 0.02024 | 0.069 | 0.00128 | 445 | 52 | 433 | 13 | 430 | 8 | 0.7 |
| ~~GSE-48~~ | ~~0.39~~ | ~~0.06999~~ | ~~0.00323~~ | ~~0.89749~~ | ~~0.04022~~ | ~~0.09298~~ | ~~0.00185~~ | ~~928~~ | ~~59~~ | ~~650~~ | ~~22~~ | ~~573~~ | ~~11~~ | ~~13.4~~ |
| GSE-49 | 0.29 | 0.11537 | 0.00426 | 5.48605 | 0.19701 | 0.34481 | 0.00642 | 1886 | 38 | 1898 | 31 | 1910 | 31 | -1.3 |

| | | | | | | | | | | | | | | |
|---|---|---|---|---|---|---|---|---|---|---|---|---|---|---|
| GSE-50 | 0.87 | 0.05646 | 0.00295 | 0.58369 | 0.02971 | 0.07496 | 0.00153 | 471 | 76 | 467 | 19 | 466 | 9 | 0.2 |
| GSE-51 | 0.34 | 0.05524 | 0.00235 | 0.49804 | 0.0206 | 0.06537 | 0.00125 | 422 | 58 | 410 | 14 | 408 | 8 | 0.5 |
| GSE-52 | 0.71 | 0.05631 | 0.00463 | 0.57437 | 0.04637 | 0.07395 | 0.00172 | 465 | 138 | 461 | 30 | 460 | 10 | 0.2 |
| GSE-53 | 0.58 | 0.05099 | 0.00288 | 0.27157 | 0.01494 | 0.03862 | 0.00081 | 240 | 88 | 244 | 12 | 244 | 5 | 0 |
| GSE-54 | 0.2 | 0.11851 | 0.00445 | 5.65569 | 0.20719 | 0.34604 | 0.0064 | 1934 | 39 | 1925 | 32 | 1916 | 31 | 0.9 |
| GSE-55 | 1.38 | 0.05173 | 0.00348 | 0.29077 | 0.01908 | 0.04076 | 0.00091 | 273 | 109 | 259 | 15 | 258 | 6 | 0.4 |
| ~~GSE-56~~ | ~~0.74~~ | ~~0.13276~~ | ~~0.00509~~ | ~~6.40543~~ | ~~0.23956~~ | ~~0.34985~~ | ~~0.00658~~ | ~~2135~~ | ~~39~~ | ~~2033~~ | ~~33~~ | ~~1934~~ | ~~31~~ | ~~10.4~~ |
| **STB2** | | | | | | | | | | | | | | |
| STB2-01 | 0.74 | 0.05108 | 0.00203 | 0.26568 | 0.01065 | 0.03772 | 0.00057 | 244 | 64 | 239 | 9 | 239 | 4 | 0 |
| STB2-02 | 0.39 | 0.05186 | 0.00116 | 0.22909 | 0.00536 | 0.03203 | 0.00045 | 279 | 29 | 209 | 4 | 203 | 3 | 3 |
| STB2-03 | 0.57 | 0.05555 | 0.00109 | 0.48745 | 0.01016 | 0.06363 | 0.00089 | 434 | 23 | 403 | 7 | 398 | 5 | 1.3 |
| STB2-04 | 0.26 | 0.06829 | 0.00116 | 1.30465 | 0.02417 | 0.13853 | 0.00192 | 877 | 18 | 848 | 11 | 836 | 11 | 1.4 |
| STB2-05 | 0.27 | 0.07074 | 0.00125 | 1.42152 | 0.02721 | 0.14571 | 0.00204 | 950 | 19 | 898 | 11 | 877 | 11 | 2.4 |
| STB2-06 | 0.4 | 0.05383 | 0.0011 | 0.45872 | 0.00989 | 0.06179 | 0.00087 | 364 | 25 | 383 | 7 | 387 | 5 | -1 |
| STB2-07 | 0.79 | 0.05499 | 0.00126 | 0.48093 | 0.01146 | 0.06342 | 0.00091 | 412 | 29 | 399 | 8 | 396 | 6 | 0.8 |
| STB2-08 | 0.6 | 0.05513 | 0.00151 | 0.47581 | 0.01337 | 0.06259 | 0.00092 | 417 | 37 | 395 | 9 | 391 | 6 | 1 |
| STB2-09 | 0.41 | 0.06769 | 0.00138 | 1.27863 | 0.02759 | 0.13696 | 0.00196 | 859 | 23 | 836 | 12 | 827 | 11 | 1.1 |
| STB2-10 | 0.42 | 0.0539 | 0.00104 | 0.46264 | 0.00954 | 0.06224 | 0.00087 | 367 | 23 | 386 | 7 | 389 | 5 | -0.8 |
| STB2-11 | 0.23 | 0.07038 | 0.00122 | 1.43096 | 0.02702 | 0.14744 | 0.00206 | 939 | 18 | 902 | 11 | 887 | 12 | 1.7 |
| STB2-12 | 0.38 | 0.05661 | 0.00099 | 0.526 | 0.00997 | 0.06738 | 0.00093 | 476 | 20 | 429 | 7 | 420 | 6 | 2.1 |
| STB2-13 | 0.65 | 0.0553 | 0.00183 | 0.47447 | 0.01588 | 0.06221 | 0.00093 | 424 | 48 | 394 | 11 | 389 | 6 | 1.3 |
| STB2-14 | 0.62 | 0.05409 | 0.00107 | 0.46618 | 0.00983 | 0.0625 | 0.00088 | 375 | 24 | 389 | 7 | 391 | 5 | -0.5 |
| STB2-15 | 0.67 | 0.06864 | 0.00136 | 1.09883 | 0.02317 | 0.11608 | 0.00164 | 888 | 22 | 753 | 11 | 708 | 9 | 6.4 |
| STB2-16 | 0.26 | 0.06801 | 0.0013 | 1.37557 | 0.02816 | 0.14666 | 0.00207 | 869 | 21 | 879 | 12 | 882 | 12 | -0.3 |
| ~~STB2-17~~ | ~~0.51~~ | ~~0.0926~~ | ~~0.0027~~ | ~~2.71415~~ | ~~0.06922~~ | ~~0.21259~~ | ~~0.00302~~ | ~~1480~~ | ~~57~~ | ~~1332~~ | ~~19~~ | ~~1243~~ | ~~16~~ | ~~19.1~~ |
| STB2-18 | 0.17 | 0.06949 | 0.00107 | 1.38493 | 0.02389 | 0.14452 | 0.00199 | 913 | 16 | 883 | 10 | 870 | 11 | 1.5 |

| | | | | | | | | | | | | | | |
|---|---|---|---|---|---|---|---|---|---|---|---|---|---|---|
| STB2-19 | 0.34 | 0.05507 | 0.00122 | 0.46813 | 0.01082 | 0.06164 | 0.00088 | 415 | 27 | 390 | 7 | 386 | 5 | 1 |
| STB2-20 | 0.96 | 0.05625 | 0.00114 | 0.52233 | 0.01125 | 0.06733 | 0.00095 | 462 | 24 | 427 | 8 | 420 | 6 | 1.7 |
| STB2-21 | 0.73 | 0.0545 | 0.00189 | 0.46393 | 0.01627 | 0.06173 | 0.00093 | 392 | 52 | 387 | 11 | 386 | 6 | 0.3 |
| STB2-22 | 0.76 | 0.05051 | 0.0025 | 0.26465 | 0.01308 | 0.03799 | 0.00061 | 219 | 85 | 238 | 11 | 240 | 4 | -0.8 |
| STB2-23 | 0.34 | 0.06996 | 0.00155 | 1.45226 | 0.03366 | 0.15052 | 0.00217 | 927 | 25 | 911 | 14 | 904 | 12 | 0.8 |
| STB2-24 | 0.29 | 0.05432 | 0.00118 | 0.46105 | 0.01055 | 0.06154 | 0.00087 | 384 | 27 | 385 | 7 | 385 | 5 | 0 |
| ~~STB2-25~~ | ~~0.36~~ | ~~0.12371~~ | ~~0.00207~~ | ~~5.41064~~ | ~~0.09887~~ | ~~0.31713~~ | ~~0.00451~~ | ~~2010~~ | ~~15~~ | ~~1887~~ | ~~16~~ | ~~1776~~ | ~~22~~ | ~~13.2~~ |
| STB2-26 | 0.74 | 0.05111 | 0.00224 | 0.25851 | 0.01135 | 0.03668 | 0.00058 | 246 | 72 | 233 | 9 | 232 | 4 | 0.4 |
| STB2-27 | 0.46 | 0.05405 | 0.00233 | 0.24654 | 0.01065 | 0.03307 | 0.00053 | 373 | 68 | 224 | 9 | 210 | 3 | 6.7 |
| ~~STB2-28~~ | ~~0.46~~ | ~~0.06242~~ | ~~0.00236~~ | ~~0.51364~~ | ~~0.01792~~ | ~~0.05968~~ | ~~0.00087~~ | ~~689~~ | ~~83~~ | ~~421~~ | ~~12~~ | ~~374~~ | ~~5~~ | ~~12.6~~ |
| STB2-29 | 0.42 | 0.05588 | 0.00105 | 0.48131 | 0.0097 | 0.06246 | 0.00088 | 448 | 22 | 399 | 7 | 391 | 5 | 2 |
| STB2-30 | 0.7 | 0.05175 | 0.00337 | 0.27661 | 0.01794 | 0.03876 | 0.00065 | 274 | 118 | 248 | 14 | 245 | 4 | 1.2 |
| STB2-31 | 0.54 | 0.05489 | 0.0012 | 0.49135 | 0.01128 | 0.06491 | 0.00093 | 408 | 27 | 406 | 8 | 405 | 6 | 0.2 |
| STB2-32 | 0.44 | 0.05011 | 0.00254 | 0.23658 | 0.012 | 0.03423 | 0.00054 | 200 | 88 | 216 | 10 | 217 | 3 | -0.5 |
| STB2-33 | 0.31 | 0.07017 | 0.0013 | 1.43515 | 0.02854 | 0.14831 | 0.00209 | 933 | 20 | 904 | 12 | 891 | 12 | 1.5 |
| STB2-34 | 0.38 | 0.06305 | 0.0019 | 0.96753 | 0.02949 | 0.11128 | 0.00172 | 710 | 39 | 687 | 15 | 680 | 10 | 1 |
| STB2-35 | 0.26 | 0.07097 | 0.00122 | 1.39414 | 0.02619 | 0.14245 | 0.00199 | 957 | 18 | 886 | 11 | 859 | 11 | 3.1 |
| STB2-36 | 0.4 | 0.06545 | 0.00146 | 1.05187 | 0.02449 | 0.11654 | 0.00169 | 789 | 26 | 730 | 12 | 711 | 10 | 2.7 |
| STB2-37 | 0.8 | 0.05474 | 0.00143 | 0.49225 | 0.01315 | 0.06521 | 0.00096 | 402 | 34 | 406 | 9 | 407 | 6 | -0.2 |
| STB2-38 | 0.78 | 0.05518 | 0.00144 | 0.48514 | 0.01305 | 0.06375 | 0.00092 | 420 | 35 | 402 | 9 | 398 | 6 | 1 |
| STB2-39 | 0.52 | 0.05528 | 0.00123 | 0.53005 | 0.01232 | 0.06952 | 0.00099 | 424 | 28 | 432 | 8 | 433 | 6 | -0.2 |
| STB2-40 | 0.38 | 0.07056 | 0.00116 | 1.45888 | 0.02639 | 0.14994 | 0.00208 | 945 | 17 | 914 | 11 | 901 | 12 | 1.4 |
| STB2-41 | 0.43 | 0.07034 | 0.00235 | 1.58597 | 0.04781 | 0.16352 | 0.00236 | 938 | 70 | 965 | 19 | 976 | 13 | -1.1 |
| STB2-42 | 0.92 | 0.05533 | 0.00109 | 0.51841 | 0.01087 | 0.06794 | 0.00096 | 426 | 23 | 424 | 7 | 424 | 6 | 0 |
| STB2-43 | 0.42 | 0.05078 | 0.00267 | 0.24083 | 0.01264 | 0.03439 | 0.00056 | 231 | 91 | 219 | 10 | 218 | 3 | 0.5 |
| STB2-44 | 0.12 | 0.05594 | 0.00161 | 0.48186 | 0.01214 | 0.06247 | 0.00086 | 450 | 65 | 399 | 8 | 391 | 5 | 2 |
| STB2-45 | 0.2 | 0.06919 | 0.00119 | 1.41662 | 0.02664 | 0.14848 | 0.00207 | 904 | 18 | 896 | 11 | 892 | 12 | 0.4 |
| STB2-46 | 0.87 | 0.05089 | 0.00196 | 0.23634 | 0.00918 | 0.03368 | 0.00051 | 236 | 62 | 215 | 8 | 214 | 3 | 0.5 |

| | | | | | | | | | | | | | | |
|---|---|---|---|---|---|---|---|---|---|---|---|---|---|---|
| STB2-47 | 0.61 | 0.06822 | 0.00186 | 1.29267 | 0.03605 | 0.1374 | 0.00204 | 875 | 34 | 842 | 16 | 830 | 12 | 1.4 |
| STB2-48 | 0.42 | 0.0564 | 0.00182 | 0.50507 | 0.01656 | 0.06494 | 0.00097 | 468 | 46 | 415 | 11 | 406 | 6 | 2.2 |
| STB2-49 | 0.59 | 0.05614 | 0.00129 | 0.55358 | 0.01321 | 0.0715 | 0.00103 | 458 | 29 | 447 | 9 | 445 | 6 | 0.4 |
| STB2-50 | 0.66 | 0.05462 | 0.00138 | 0.49391 | 0.01282 | 0.06558 | 0.00096 | 397 | 33 | 408 | 9 | 409 | 6 | -0.2 |
| STB2-51 | 0.68 | 0.0537 | 0.00171 | 0.26627 | 0.00862 | 0.03596 | 0.00054 | 358 | 46 | 240 | 7 | 228 | 3 | 5.3 |
| STB2-52 | 0.62 | 0.05492 | 0.00288 | 0.25629 | 0.01341 | 0.03384 | 0.00055 | 409 | 88 | 232 | 11 | 215 | 3 | 7.9 |
| STB2-53 | 0.45 | 0.05485 | 0.0014 | 0.49394 | 0.01298 | 0.06531 | 0.00095 | 406 | 34 | 408 | 9 | 408 | 6 | 0 |
| STB2-54 | 0.22 | 0.07053 | 0.0012 | 1.39886 | 0.02596 | 0.14383 | 0.00201 | 944 | 18 | 888 | 11 | 866 | 11 | 2.5 |
| STB2-55 | 0.5 | 0.05519 | 0.00113 | 0.50883 | 0.01104 | 0.06685 | 0.00095 | 420 | 25 | 418 | 7 | 417 | 6 | 0.2 |
| STB2-56 | 0.36 | 0.07002 | 0.00129 | 1.42923 | 0.0283 | 0.14801 | 0.00209 | 929 | 20 | 901 | 12 | 890 | 12 | 1.2 |
| STB2-57 | 0.46 | 0.05426 | 0.00204 | 0.48288 | 0.01829 | 0.06453 | 0.00099 | 382 | 57 | 400 | 13 | 403 | 6 | -0.7 |
| STB2-58 | 0.49 | 0.05036 | 0.00264 | 0.23994 | 0.01259 | 0.03455 | 0.00055 | 212 | 92 | 218 | 10 | 219 | 3 | -0.5 |
| STB2-59 | 0.93 | 0.05562 | 0.00116 | 0.475 | 0.01042 | 0.06193 | 0.00088 | 437 | 25 | 395 | 7 | 387 | 5 | 2.1 |
| STB2-60 | 0.56 | 0.05574 | 0.00125 | 0.51992 | 0.01221 | 0.06763 | 0.00097 | 442 | 28 | 425 | 8 | 422 | 6 | 0.7 |
| STB2-61 | 0.48 | 0.0506 | 0.00204 | 0.25002 | 0.01011 | 0.03583 | 0.00056 | 223 | 64 | 227 | 8 | 227 | 3 | 0 |
| STB2-62 | 0.16 | 0.06526 | 0.00171 | 1.16384 | 0.02583 | 0.12934 | 0.0018 | 783 | 56 | 784 | 12 | 784 | 10 | 0 |
| STB2-63 | 0.88 | 0.05093 | 0.00165 | 0.24897 | 0.00814 | 0.03545 | 0.00053 | 238 | 48 | 226 | 7 | 225 | 3 | 0.4 |
| STB2-64 | 0.7 | 0.05153 | 0.00148 | 0.30867 | 0.00907 | 0.04344 | 0.00064 | 265 | 41 | 273 | 7 | 274 | 4 | -0.4 |
| STB2-65 | 1.03 | 0.06831 | 0.00153 | 1.40148 | 0.03277 | 0.14878 | 0.00216 | 878 | 26 | 890 | 14 | 894 | 12 | -0.4 |
| STB2-66 | 0.54 | 0.05522 | 0.00116 | 0.49909 | 0.01102 | 0.06553 | 0.00094 | 421 | 25 | 411 | 7 | 409 | 6 | 0.5 |
| STB2-67 | 0.44 | 0.05223 | 0.00232 | 0.24632 | 0.0103 | 0.0342 | 0.00051 | 295 | 104 | 224 | 8 | 217 | 3 | 3.2 |
| STB2-68 | 0.42 | 0.05013 | 0.0014 | 0.23331 | 0.00664 | 0.03375 | 0.0005 | 201 | 39 | 213 | 5 | 214 | 3 | -0.5 |
| STB2-69 | 0.69 | 0.05097 | 0.00238 | 0.26343 | 0.01232 | 0.03748 | 0.0006 | 239 | 78 | 237 | 10 | 237 | 4 | 0 |
| STB2-70 | 0.5 | 0.05055 | 0.00229 | 0.23588 | 0.01071 | 0.03384 | 0.00053 | 220 | 76 | 215 | 9 | 215 | 3 | 0 |
| ~~STB2-71~~ | ~~0.7~~ | ~~0.07549~~ | ~~0.00516~~ | ~~0.33641~~ | ~~0.02225~~ | ~~0.03232~~ | ~~0.00056~~ | ~~1082~~ | ~~141~~ | ~~294~~ | ~~17~~ | ~~205~~ | ~~3~~ | ~~43.4~~ |
| STB2-72 | 0.35 | 0.07011 | 0.00153 | 1.45202 | 0.03327 | 0.15017 | 0.00217 | 932 | 25 | 911 | 14 | 902 | 12 | 1 |
| STB2-73 | 0.79 | 0.055 | 0.00134 | 0.47823 | 0.01209 | 0.06306 | 0.00091 | 412 | 32 | 397 | 8 | 394 | 6 | 0.8 |
| STB2-74 | 0.3 | 0.07061 | 0.0013 | 1.39053 | 0.02747 | 0.14281 | 0.00202 | 946 | 20 | 885 | 12 | 861 | 11 | 2.8 |

| | | | | | | | | | | | | | | |
|---|---|---|---|---|---|---|---|---|---|---|---|---|---|---|
| STB2-75 | 0.45 | 0.05556 | 0.00143 | 0.2566 | 0.00681 | 0.03349 | 0.00049 | 435 | 34 | 232 | 6 | 212 | 3 | 9.4 |
| STB2-76 | 0.51 | 0.0544 | 0.0013 | 0.46397 | 0.0115 | 0.06185 | 0.0009 | 388 | 31 | 387 | 8 | 387 | 5 | 0 |
| STB2-77 | 0.48 | 0.05557 | 0.0019 | 0.49954 | 0.01722 | 0.06518 | 0.001 | 435 | 49 | 411 | 12 | 407 | 6 | 1 |
| STB2-78 | 0.93 | 0.12231 | 0.0022 | 5.73487 | 0.11133 | 0.34002 | 0.00486 | 1990 | 16 | 1937 | 17 | 1887 | 23 | 5.5 |
| STB2-79 | 0.63 | 0.10153 | 0.00183 | 3.78764 | 0.07348 | 0.27052 | 0.00385 | 1652 | 17 | 1590 | 16 | 1543 | 20 | 7.1 |
| STB2-80 | 0.51 | 0.05548 | 0.00118 | 0.52408 | 0.01175 | 0.0685 | 0.00098 | 432 | 26 | 428 | 8 | 427 | 6 | 0.2 |
| STB2-81 | 0.53 | 0.05038 | 0.00309 | 0.22811 | 0.01394 | 0.03283 | 0.00056 | 213 | 109 | 209 | 12 | 208 | 3 | 0.5 |
| STB2-82 | 0.7 | 0.05098 | 0.00228 | 0.26181 | 0.01171 | 0.03724 | 0.0006 | 240 | 73 | 236 | 9 | 236 | 4 | 0 |
| STB2-83 | 0.63 | 0.05424 | 0.00207 | 0.45925 | 0.01765 | 0.0614 | 0.00095 | 381 | 58 | 384 | 12 | 384 | 6 | 0 |
| STB2-84 | 0.45 | 0.05463 | 0.00113 | 0.48562 | 0.01064 | 0.06446 | 0.00092 | 397 | 25 | 402 | 7 | 403 | 6 | -0.2 |
| STB2-85 | 0.37 | 0.06696 | 0.00242 | 1.07991 | 0.0356 | 0.11696 | 0.00173 | 837 | 77 | 744 | 17 | 713 | 10 | 4.3 |
| STB2-86 | 0.19 | 0.06944 | 0.00141 | 1.41837 | 0.03052 | 0.14811 | 0.00213 | 912 | 22 | 897 | 13 | 890 | 12 | 0.8 |
| STB2-87 | 0.25 | 0.06966 | 0.00127 | 1.30208 | 0.02567 | 0.13554 | 0.00192 | 918 | 20 | 847 | 11 | 819 | 11 | 3.4 |
| STB2-88 | 0.41 | 0.05079 | 0.00257 | 0.2421 | 0.01222 | 0.03456 | 0.00057 | 231 | 86 | 220 | 10 | 219 | 4 | 0.5 |
| ~~STB2-89~~ | ~~0.6~~ | ~~0.07907~~ | ~~0.00145~~ | ~~1.32055~~ | ~~0.0261~~ | ~~0.12111~~ | ~~0.00172~~ | ~~1174~~ | ~~19~~ | ~~855~~ | ~~11~~ | ~~737~~ | ~~10~~ | ~~16~~ |
| STB2-90 | 0.67 | 0.05436 | 0.00202 | 0.46987 | 0.01755 | 0.06268 | 0.00097 | 386 | 56 | 391 | 12 | 392 | 6 | -0.3 |
| STB2-91 | 0.45 | 0.0542 | 0.00114 | 0.46971 | 0.0104 | 0.06284 | 0.0009 | 379 | 26 | 391 | 7 | 393 | 5 | -0.5 |
| STB2-92 | 0.24 | 0.0566 | 0.00321 | 0.39808 | 0.02177 | 0.05101 | 0.00077 | 476 | 129 | 340 | 16 | 321 | 5 | 5.9 |
| ~~STB2-93~~ | ~~0.62~~ | ~~0.05834~~ | ~~0.00377~~ | ~~0.28534~~ | ~~0.01834~~ | ~~0.03546~~ | ~~0.00061~~ | ~~543~~ | ~~111~~ | ~~255~~ | ~~14~~ | ~~225~~ | ~~4~~ | ~~13.3~~ |
| STB2-94 | 0.24 | 0.07045 | 0.00136 | 1.41271 | 0.02904 | 0.14541 | 0.00207 | 941 | 21 | 894 | 12 | 875 | 12 | 2.2 |
| ~~STB2-95~~ | ~~0.38~~ | ~~0.29843~~ | ~~0.00514~~ | ~~24.98591~~ | ~~0.47004~~ | ~~0.60712~~ | ~~0.00851~~ | ~~3462~~ | ~~14~~ | ~~3308~~ | ~~18~~ | ~~3058~~ | ~~34~~ | ~~13.2~~ |
| STB2-96 | 0.34 | 0.07115 | 0.00153 | 1.42721 | 0.03208 | 0.14546 | 0.00212 | 962 | 24 | 900 | 13 | 875 | 12 | 2.9 |
| STB2-97 | 0.48 | 0.06953 | 0.00146 | 1.48241 | 0.0327 | 0.15461 | 0.00224 | 915 | 23 | 923 | 13 | 927 | 13 | -0.4 |
| STB2-98 | 0.39 | 0.05633 | 0.00129 | 0.50549 | 0.01208 | 0.06507 | 0.00095 | 465 | 28 | 415 | 8 | 406 | 6 | 2.2 |
| STB2-99 | 0.41 | 0.0694 | 0.00153 | 1.4494 | 0.03346 | 0.15144 | 0.0022 | 911 | 25 | 910 | 14 | 909 | 12 | 0.1 |
| STB2-100 | 0.5 | 0.05583 | 0.00132 | 0.51712 | 0.0127 | 0.06716 | 0.00098 | 446 | 30 | 423 | 8 | 419 | 6 | 1 |

| | | | | | | | | | | | | | | |
|---|---|---|---|---|---|---|---|---|---|---|---|---|---|---|
| **GS-N** | | | | | | | | | | | | | | |
| GS-N-001 | 0.43 | 0.06771 | 0.00174 | 1.33474 | 0.0343 | 0.14295 | 0.00211 | 860 | 30 | 861 | 15 | 861 | 12 | 0 |
| GS-N-002 | 0.67 | 0.0546 | 0.00235 | 0.47878 | 0.02037 | 0.06358 | 0.00103 | 396 | 66 | 397 | 14 | 397 | 6 | 0 |
| GS-N-003 | 0.73 | 0.05168 | 0.00161 | 0.30874 | 0.00949 | 0.04332 | 0.00067 | 271 | 42 | 273 | 7 | 273 | 4 | 0 |
| GS-N-004 | 0.26 | 0.06882 | 0.00164 | 1.40977 | 0.03371 | 0.14854 | 0.00217 | 893 | 26 | 893 | 14 | 893 | 12 | 0 |
| GS-N-005 | 0.63 | 0.05021 | 0.00139 | 0.23105 | 0.00639 | 0.03337 | 0.0005 | 205 | 37 | 211 | 5 | 212 | 3 | -0.5 |
| GS-N-006 | 0.63 | 0.05039 | 0.00265 | 0.2202 | 0.01144 | 0.03169 | 0.00054 | 213 | 89 | 202 | 10 | 201 | 3 | 0.5 |
| GS-N-007 | 0.7 | 0.05047 | 0.00145 | 0.23765 | 0.00679 | 0.03414 | 0.00051 | 217 | 39 | 216 | 6 | 216 | 3 | 0 |
| GS-N-008 | 0.44 | 0.05401 | 0.00132 | 0.45837 | 0.01125 | 0.06154 | 0.00089 | 371 | 30 | 383 | 8 | 385 | 5 | -0.5 |
| GS-N-009 | 0.68 | 0.05071 | 0.00234 | 0.24963 | 0.01143 | 0.0357 | 0.00058 | 228 | 76 | 226 | 9 | 226 | 4 | 0 |
| GS-N-010 | 0.44 | 0.05747 | 0.00164 | 0.47596 | 0.01353 | 0.06006 | 0.0009 | 510 | 37 | 395 | 9 | 376 | 5 | 5.1 |
| GS-N-011 | 0.55 | 0.0507 | 0.00172 | 0.24636 | 0.00823 | 0.03523 | 0.00056 | 227 | 48 | 224 | 7 | 223 | 3 | 0.4 |
| GS-N-012 | 0.47 | 0.05033 | 0.00175 | 0.2366 | 0.00815 | 0.03409 | 0.00053 | 210 | 51 | 216 | 7 | 216 | 3 | 0 |
| GS-N-013 | 0.64 | 0.05058 | 0.00189 | 0.24467 | 0.00896 | 0.03508 | 0.00057 | 222 | 55 | 222 | 7 | 222 | 4 | 0 |
| GS-N-014 | 0.35 | 0.05448 | 0.00173 | 0.47326 | 0.01496 | 0.06299 | 0.00096 | 391 | 44 | 393 | 10 | 394 | 6 | -0.3 |
| GS-N-015 | 0.73 | 0.0535 | 0.00177 | 0.41365 | 0.01351 | 0.05607 | 0.00089 | 350 | 45 | 352 | 10 | 352 | 5 | 0 |
| ~~GS-N-016~~ | ~~0.48~~ | ~~0.06536~~ | ~~0.00186~~ | ~~0.58815~~ | ~~0.0167~~ | ~~0.06525~~ | ~~0.00098~~ | ~~786~~ | ~~35~~ | ~~470~~ | ~~11~~ | ~~407~~ | ~~6~~ | ~~15.5~~ |
| GS-N-017 | 0.73 | 0.05456 | 0.00224 | 0.46926 | 0.01884 | 0.06237 | 0.00108 | 394 | 59 | 391 | 13 | 390 | 7 | 0.3 |
| GS-N-018 | 0.53 | 0.0541 | 0.00161 | 0.45267 | 0.01342 | 0.06067 | 0.00091 | 375 | 40 | 379 | 9 | 380 | 6 | -0.3 |
| GS-N-019 | 0.52 | 0.05038 | 0.00156 | 0.23154 | 0.00713 | 0.03333 | 0.00051 | 213 | 43 | 211 | 6 | 211 | 3 | 0 |
| GS-N-020 | 0.85 | 0.05432 | 0.00157 | 0.47118 | 0.01348 | 0.0629 | 0.00096 | 384 | 37 | 392 | 9 | 393 | 6 | -0.3 |
| GS-N-021 | 0.35 | 0.05351 | 0.00204 | 0.40509 | 0.01525 | 0.0549 | 0.00088 | 350 | 56 | 345 | 11 | 345 | 5 | 0 |
| GS-N-022 | 0.4 | 0.05512 | 0.00197 | 0.51422 | 0.01803 | 0.06765 | 0.0011 | 417 | 49 | 421 | 12 | 422 | 7 | -0.2 |
| GS-N-023 | 0.49 | 0.05072 | 0.00161 | 0.24393 | 0.00765 | 0.03487 | 0.00054 | 228 | 44 | 222 | 6 | 221 | 3 | 0.5 |
| GS-N-024 | 1.09 | 0.05497 | 0.00183 | 0.50162 | 0.01648 | 0.06617 | 0.00106 | 411 | 45 | 413 | 11 | 413 | 6 | 0 |
| GS-N-025 | 0.61 | 0.05437 | 0.00209 | 0.46418 | 0.01765 | 0.06191 | 0.00099 | 386 | 57 | 387 | 12 | 387 | 6 | 0 |
| GS-N-026 | 0.59 | 0.05064 | 0.00303 | 0.24374 | 0.01423 | 0.03491 | 0.00069 | 224 | 98 | 221 | 12 | 221 | 4 | 0 |
| GS-N-027 | 0.39 | 0.06628 | 0.00214 | 1.23622 | 0.03946 | 0.13525 | 0.00214 | 815 | 41 | 817 | 18 | 818 | 12 | -0.1 |

| | | | | | | | | | | | | | | |
|---|---|---|---|---|---|---|---|---|---|---|---|---|---|---|
| GS-N-028 | 0.63 | 0.05472 | 0.00326 | 0.48912 | 0.02847 | 0.06481 | 0.00129 | 401 | 95 | 404 | 19 | 405 | 8 | -0.2 |
| GS-N-029 | 0.43 | 0.07174 | 0.00185 | 1.61467 | 0.04173 | 0.16322 | 0.00242 | 979 | 29 | 976 | 16 | 975 | 13 | 0.1 |
| GS-N-030 | 0.59 | 0.04948 | 0.00496 | 0.22173 | 0.02178 | 0.0325 | 0.00065 | 171 | 224 | 203 | 18 | 206 | 4 | -1.5 |
| GS-N-031 | 0.33 | 0.05901 | 0.00172 | 0.51218 | 0.01483 | 0.06293 | 0.00095 | 567 | 37 | 420 | 10 | 393 | 6 | 6.9 |
| GS-N-032 | 0.99 | 0.05119 | 0.00354 | 0.27777 | 0.01896 | 0.03935 | 0.00073 | 249 | 122 | 249 | 15 | 249 | 5 | 0 |
| GS-N-033 | 0.82 | 0.05534 | 0.00273 | 0.5056 | 0.02457 | 0.06625 | 0.00115 | 426 | 77 | 415 | 17 | 414 | 7 | 0.2 |
| GS-N-034 | 0.82 | 0.05077 | 0.00563 | 0.26395 | 0.02886 | 0.0377 | 0.00089 | 230 | 203 | 238 | 23 | 239 | 6 | -0.4 |
| ~~GS-N-035~~ | ~~0.29~~ | ~~0.07187~~ | ~~0.00193~~ | ~~0.53729~~ | ~~0.0144~~ | ~~0.05421~~ | ~~0.00081~~ | ~~982~~ | ~~31~~ | ~~437~~ | ~~10~~ | ~~340~~ | ~~5~~ | ~~28.5~~ |
| GS-N-036 | 0.34 | 0.07101 | 0.00266 | 1.36298 | 0.04688 | 0.13921 | 0.00209 | 958 | 79 | 873 | 20 | 840 | 12 | 3.9 |
| GS-N-037 | 0.61 | 0.0504 | 0.00159 | 0.23974 | 0.00747 | 0.03449 | 0.00053 | 213 | 44 | 218 | 6 | 219 | 3 | -0.5 |
| GS-N-038 | 0.2 | 0.04842 | 0.00517 | 0.13402 | 0.01419 | 0.02007 | 0.00041 | 120 | 199 | 128 | 13 | 128 | 3 | 0 |
| GS-N-039 | 0.6 | 0.12976 | 0.00337 | 6.85457 | 0.17724 | 0.38306 | 0.00603 | 2095 | 24 | 2093 | 23 | 2091 | 28 | 0.2 |
| GS-N-040 | 0.45 | 0.06958 | 0.00203 | 1.49217 | 0.04308 | 0.1555 | 0.00245 | 916 | 34 | 927 | 18 | 932 | 14 | -0.5 |
| GS-N-041 | 0.75 | 0.05487 | 0.00225 | 0.47804 | 0.01916 | 0.06318 | 0.00109 | 407 | 59 | 397 | 13 | 395 | 7 | 0.5 |
| GS-N-042 | 0.4 | 0.05556 | 0.00175 | 0.52959 | 0.01646 | 0.06911 | 0.00109 | 435 | 42 | 432 | 11 | 431 | 7 | 0.2 |
| GS-N-043 | 0.53 | 0.05555 | 0.00198 | 0.531 | 0.01858 | 0.06932 | 0.00116 | 434 | 48 | 432 | 12 | 432 | 7 | 0 |
| GS-N-044 | 0.65 | 0.05054 | 0.00408 | 0.24769 | 0.01966 | 0.03554 | 0.00077 | 220 | 140 | 225 | 16 | 225 | 5 | 0 |
| GS-N-045 | 0.5 | 0.05081 | 0.0024 | 0.25312 | 0.01172 | 0.03613 | 0.00065 | 232 | 74 | 229 | 9 | 229 | 4 | 0 |
| GS-N-046 | 0.64 | 0.05409 | 0.0023 | 0.47182 | 0.01961 | 0.06325 | 0.00111 | 375 | 62 | 392 | 14 | 395 | 7 | -0.8 |
| GS-N-047 | 0.88 | 0.05053 | 0.00292 | 0.23992 | 0.01369 | 0.03443 | 0.00061 | 219 | 99 | 218 | 11 | 218 | 4 | 0 |
| GS-N-048 | 0.94 | 0.05028 | 0.00255 | 0.23057 | 0.01146 | 0.03325 | 0.0006 | 208 | 82 | 211 | 9 | 211 | 4 | 0 |
| GS-N-049 | 0.13 | 0.06793 | 0.00194 | 1.37126 | 0.03906 | 0.14637 | 0.00223 | 866 | 34 | 877 | 17 | 881 | 13 | -0.5 |
| GS-N-050 | 0.57 | 0.05037 | 0.00231 | 0.23812 | 0.01071 | 0.03428 | 0.0006 | 212 | 72 | 217 | 9 | 217 | 4 | 0 |
| GS-N-051 | 0.51 | 0.05073 | 0.00255 | 0.23546 | 0.01165 | 0.03366 | 0.00059 | 229 | 82 | 215 | 10 | 213 | 4 | 0.9 |
| GS-N-052 | 0.33 | 0.06898 | 0.00215 | 1.42453 | 0.04373 | 0.14975 | 0.0024 | 898 | 37 | 899 | 18 | 900 | 13 | -0.1 |
| GS-N-053 | 0.4 | 0.05081 | 0.00165 | 0.2607 | 0.00836 | 0.0372 | 0.00058 | 232 | 46 | 235 | 7 | 235 | 4 | 0 |
| GS-N-054 | 0.53 | 0.06972 | 0.00211 | 1.46291 | 0.04394 | 0.15215 | 0.00238 | 920 | 37 | 915 | 18 | 913 | 13 | 0.2 |
| GS-N-055 | 0.73 | 0.05161 | 0.00262 | 0.28639 | 0.01434 | 0.04023 | 0.0007 | 268 | 83 | 256 | 11 | 254 | 4 | 0.8 |

| | | | | | | | | | | | | | | |
|---|---|---|---|---|---|---|---|---|---|---|---|---|---|---|
| GS-N-056 | 0.44 | 0.05435 | 0.00194 | 0.46245 | 0.01624 | 0.0617 | 0.00101 | 386 | 50 | 386 | 11 | 386 | 6 | 0 |
| GS-N-057 | 0.16 | 0.06913 | 0.00194 | 1.4149 | 0.0396 | 0.14842 | 0.00227 | 903 | 33 | 895 | 17 | 892 | 13 | 0.3 |
| GS-N-058 | 0.67 | 0.06963 | 0.00222 | 1.44638 | 0.04569 | 0.15063 | 0.00239 | 917 | 39 | 908 | 19 | 904 | 13 | 0.4 |
| GS-N-059 | 0.62 | 0.05565 | 0.00188 | 0.53988 | 0.01792 | 0.07035 | 0.00115 | 438 | 45 | 438 | 12 | 438 | 7 | 0 |
| GS-N-060 | 0.46 | 0.05554 | 0.00204 | 0.44256 | 0.01598 | 0.05778 | 0.00095 | 434 | 51 | 372 | 11 | 362 | 6 | 2.8 |
| GS-N-061 | 0.21 | 0.05485 | 0.00173 | 0.49744 | 0.01549 | 0.06577 | 0.00104 | 406 | 42 | 410 | 11 | 411 | 6 | -0.2 |
| GS-N-062 | 0.67 | 0.05054 | 0.00357 | 0.24643 | 0.01715 | 0.03536 | 0.00069 | 220 | 123 | 224 | 14 | 224 | 4 | 0 |
| GS-N-063 | 0.44 | 0.05054 | 0.00186 | 0.24039 | 0.00869 | 0.03449 | 0.00058 | 220 | 53 | 219 | 7 | 219 | 4 | 0 |
| GS-N-064 | 0.64 | 0.05075 | 0.00257 | 0.24675 | 0.01232 | 0.03525 | 0.00062 | 229 | 83 | 224 | 10 | 223 | 4 | 0.4 |
| GS-N-065 | 0.42 | 0.05436 | 0.00172 | 0.46527 | 0.01461 | 0.06207 | 0.00097 | 386 | 43 | 388 | 10 | 388 | 6 | 0 |
| GS-N-066 | 0.67 | 0.05303 | 0.00216 | 0.40693 | 0.01625 | 0.05565 | 0.00097 | 330 | 59 | 347 | 12 | 349 | 6 | -0.6 |
| GS-N-067 | 0.87 | 0.05114 | 0.0024 | 0.27023 | 0.0124 | 0.03832 | 0.0007 | 247 | 72 | 243 | 10 | 242 | 4 | 0.4 |
| GS-N-068 | 0.24 | 0.06813 | 0.00214 | 1.364 | 0.0423 | 0.14518 | 0.00234 | 873 | 38 | 874 | 18 | 874 | 13 | 0 |
| GS-N-069 | 0.63 | 0.06904 | 0.00241 | 1.40568 | 0.04832 | 0.14765 | 0.00245 | 900 | 44 | 891 | 20 | 888 | 14 | 0.3 |
| GS-N-070 | 1.17 | 0.052 | 0.00591 | 0.26834 | 0.03003 | 0.03743 | 0.00073 | 285 | 260 | 241 | 24 | 237 | 5 | 1.7 |
| GS-N-071 | 0.57 | 0.05453 | 0.00322 | 0.46203 | 0.02684 | 0.06144 | 0.00113 | 393 | 97 | 386 | 19 | 384 | 7 | 0.5 |
| GS-N-072 | 1.06 | 0.05036 | 0.00462 | 0.24545 | 0.02216 | 0.03534 | 0.00079 | 212 | 162 | 223 | 18 | 224 | 5 | -0.4 |
| GS-N-073 | 0.37 | 0.04932 | 0.00239 | 0.18197 | 0.00862 | 0.02675 | 0.00049 | 163 | 76 | 170 | 7 | 170 | 3 | 0 |
| GS-N-074 | 0.57 | 0.05449 | 0.00218 | 0.47349 | 0.01858 | 0.06301 | 0.00109 | 391 | 57 | 394 | 13 | 394 | 7 | 0 |
| GS-N-075 | 0.5 | 0.0548 | 0.00314 | 0.47976 | 0.02707 | 0.06349 | 0.00118 | 404 | 93 | 398 | 19 | 397 | 7 | 0.3 |
| GS-N-076 | 0.34 | 0.0545 | 0.00206 | 0.48326 | 0.01799 | 0.0643 | 0.00107 | 392 | 54 | 400 | 12 | 402 | 6 | -0.5 |
| GS-N-077 | 0.75 | 0.05045 | 0.00378 | 0.22907 | 0.01689 | 0.03292 | 0.00067 | 216 | 130 | 209 | 14 | 209 | 4 | 0 |
| GS-N-078 | 0.25 | 0.05466 | 0.00221 | 0.47897 | 0.01893 | 0.06354 | 0.0011 | 398 | 58 | 397 | 13 | 397 | 7 | 0 |
| GS-N-079 | 0.45 | 0.05433 | 0.00239 | 0.46546 | 0.01999 | 0.06212 | 0.00113 | 385 | 64 | 388 | 14 | 389 | 7 | -0.3 |
| GS-N-080 | 0.49 | 0.05455 | 0.00269 | 0.47303 | 0.02277 | 0.06288 | 0.0012 | 394 | 74 | 393 | 16 | 393 | 7 | 0 |
| ~~GS-N-081~~ | ~~0.5~~ | ~~0.06815~~ | ~~0.00265~~ | ~~0.8139~~ | ~~0.03104~~ | ~~0.0866~~ | ~~0.00148~~ | ~~873~~ | ~~51~~ | ~~605~~ | ~~17~~ | ~~535~~ | ~~9~~ | ~~13.1~~ |
| GS-N-082 | 0.31 | 0.05445 | 0.00199 | 0.46848 | 0.01685 | 0.06239 | 0.00104 | 390 | 51 | 390 | 12 | 390 | 6 | 0 |
| GS-N-083 | 0.19 | 0.06643 | 0.00237 | 1.21456 | 0.04257 | 0.13258 | 0.00223 | 820 | 45 | 807 | 20 | 803 | 13 | 0.5 |

| | | | | | | | | | | | | | | |
|---|---|---|---|---|---|---|---|---|---|---|---|---|---|---|
| GS-N-084 | 0.22 | 0.06826 | 0.00217 | 1.41246 | 0.04416 | 0.15005 | 0.00244 | 876 | 38 | 894 | 19 | 901 | 14 | -0.8 |
| GS-N-085 | 0.46 | 0.05052 | 0.00269 | 0.24395 | 0.01275 | 0.03502 | 0.00064 | 219 | 87 | 222 | 10 | 222 | 4 | 0 |
| GS-N-086 | 0.44 | 0.0503 | 0.00219 | 0.23794 | 0.01012 | 0.0343 | 0.00062 | 209 | 65 | 217 | 8 | 217 | 4 | 0 |
| GS-N-087 | 0.7 | 0.0545 | 0.00231 | 0.47901 | 0.01985 | 0.06373 | 0.00114 | 392 | 61 | 397 | 14 | 398 | 7 | -0.3 |
| GS-N-088 | 0.68 | 0.05002 | 0.00282 | 0.23052 | 0.01269 | 0.03342 | 0.00067 | 196 | 90 | 211 | 10 | 212 | 4 | -0.5 |
| GS-N-089 | 0.28 | 0.05456 | 0.00198 | 0.49475 | 0.01756 | 0.06576 | 0.00112 | 394 | 49 | 408 | 12 | 411 | 7 | -0.7 |
| GS-N-090 | 0.82 | 0.05063 | 0.00459 | 0.26172 | 0.02335 | 0.03749 | 0.00085 | 224 | 159 | 236 | 19 | 237 | 5 | -0.4 |
| GS-N-091 | 0.56 | 0.05044 | 0.004 | 0.2312 | 0.01804 | 0.03324 | 0.0007 | 215 | 138 | 211 | 15 | 211 | 4 | 0 |
| GS-N-092 | 0.51 | 0.05056 | 0.00211 | 0.23563 | 0.00961 | 0.03379 | 0.0006 | 221 | 62 | 215 | 8 | 214 | 4 | 0.5 |
| GS-N-093 | 0.7 | 0.05459 | 0.00401 | 0.46956 | 0.03394 | 0.06238 | 0.00128 | 395 | 126 | 391 | 23 | 390 | 8 | 0.3 |
| GS-N-094 | 0.71 | 0.0506 | 0.00249 | 0.25044 | 0.01199 | 0.03589 | 0.0007 | 223 | 75 | 227 | 10 | 227 | 4 | 0 |
| GS-N-095 | 0.42 | 0.04605 | 0.0053 | 0.2079 | 0.02353 | 0.03275 | 0.00068 | | 228 | 192 | 20 | 208 | 4 | -7.7 |
| GS-N-096 | 0.42 | 0.05434 | 0.00265 | 0.46666 | 0.02226 | 0.06227 | 0.00115 | 385 | 74 | 389 | 15 | 389 | 7 | 0 |
| GS-N-097 | 0.42 | 0.0544 | 0.00221 | 0.47427 | 0.01881 | 0.06322 | 0.00113 | 388 | 57 | 394 | 13 | 395 | 7 | -0.3 |
| GS-N-098 | 0.42 | 0.05561 | 0.0022 | 0.51248 | 0.01985 | 0.06683 | 0.00117 | 437 | 55 | 420 | 13 | 417 | 7 | 0.7 |
| GS-N-099 | 1.57 | 0.05592 | 0.00369 | 0.55416 | 0.03574 | 0.07186 | 0.00153 | 449 | 105 | 448 | 23 | 447 | 9 | 0.2 |
| GS-N-100 | 0.18 | 0.06988 | 0.00264 | 1.48617 | 0.05497 | 0.15422 | 0.00269 | 925 | 48 | 925 | 22 | 925 | 15 | 0 |
| **STB3** | | | | | | | | | | | | | | |
| STB3-01 | 0.31 | 0.05588 | 0.00133 | 0.52794 | 0.01294 | 0.06852 | 0.001 | 448 | 30 | 430 | 9 | 427 | 6 | 0.7 |
| STB3-02 | 0.45 | 0.05466 | 0.00167 | 0.46421 | 0.01429 | 0.06159 | 0.00094 | 398 | 42 | 387 | 10 | 385 | 6 | 0.5 |
| STB3-03 | 0.68 | 0.05129 | 0.0014 | 0.29061 | 0.00804 | 0.04109 | 0.00061 | 254 | 37 | 259 | 6 | 260 | 4 | -0.4 |
| STB3-04 | 0.78 | 0.07001 | 0.00153 | 1.44159 | 0.03258 | 0.14933 | 0.00215 | 929 | 24 | 906 | 14 | 897 | 12 | 1 |
| STB3-05 | 0.65 | 0.05069 | 0.00312 | 0.2472 | 0.01513 | 0.03537 | 0.0006 | 227 | 110 | 224 | 12 | 224 | 4 | 0 |
| STB3-06 | 0.43 | 0.05542 | 0.00139 | 0.47572 | 0.0122 | 0.06225 | 0.00091 | 429 | 32 | 395 | 8 | 389 | 6 | 1.5 |
| STB3-07 | 0.54 | 0.05598 | 0.00146 | 0.53009 | 0.01409 | 0.06867 | 0.00101 | 452 | 34 | 432 | 9 | 428 | 6 | 0.9 |
| STB3-08 | 0.36 | 0.05574 | 0.00223 | 0.48391 | 0.01801 | 0.06296 | 0.00092 | 442 | 91 | 401 | 12 | 394 | 6 | 1.8 |

| | | | | | | | | | | | | | | |
|---|---|---|---|---|---|---|---|---|---|---|---|---|---|---|
| STB3-09 | 0.48 | 0.05708 | 0.00279 | 0.49186 | 0.02287 | 0.0625 | 0.00095 | 495 | 111 | 406 | 16 | 391 | 6 | 3.8 |
| STB3-10 | 0.55 | 0.05122 | 0.00264 | 0.24587 | 0.01255 | 0.03481 | 0.00059 | 251 | 86 | 223 | 10 | 221 | 4 | 0.9 |
| STB3-11 | 0.69 | 0.05138 | 0.00187 | 0.26475 | 0.00964 | 0.03736 | 0.00058 | 258 | 55 | 238 | 8 | 236 | 4 | 0.8 |
| STB3-12 | 0.32 | 0.0568 | 0.00218 | 0.48239 | 0.0171 | 0.0616 | 0.0009 | 484 | 87 | 400 | 12 | 385 | 5 | 3.9 |
| STB3-13 | 0.62 | 0.05453 | 0.00138 | 0.47709 | 0.01228 | 0.06345 | 0.00093 | 393 | 32 | 396 | 8 | 397 | 6 | -0.3 |
| STB3-14 | 0.71 | 0.05031 | 0.00294 | 0.23568 | 0.01368 | 0.03397 | 0.00057 | 209 | 103 | 215 | 11 | 215 | 4 | 0 |
| STB3-15 | 0.62 | 0.0509 | 0.0014 | 0.2742 | 0.00763 | 0.03907 | 0.00058 | 236 | 37 | 246 | 6 | 247 | 4 | -0.4 |
| STB3-16 | 0.76 | 0.05358 | 0.00187 | 0.44007 | 0.01536 | 0.05956 | 0.00092 | 353 | 51 | 370 | 11 | 373 | 6 | -0.8 |
| STB3-17 | 0.63 | 0.05069 | 0.00465 | 0.23755 | 0.02164 | 0.03398 | 0.00063 | 227 | 171 | 216 | 18 | 215 | 4 | 0.5 |
| STB3-18 | 0.48 | 0.0501 | 0.00148 | 0.22089 | 0.00653 | 0.03197 | 0.00048 | 200 | 41 | 203 | 5 | 203 | 3 | 0 |
| STB3-19 | 0.5 | 0.0549 | 0.00136 | 0.49249 | 0.01242 | 0.06505 | 0.00095 | 408 | 31 | 407 | 8 | 406 | 6 | 0.2 |
| STB3-20 | 0.44 | 0.05675 | 0.00126 | 0.52642 | 0.01202 | 0.06727 | 0.00097 | 482 | 26 | 429 | 8 | 420 | 6 | 2.1 |
| STB3-21 | 0.49 | 0.05414 | 0.00141 | 0.45818 | 0.01204 | 0.06137 | 0.0009 | 377 | 34 | 383 | 8 | 384 | 5 | -0.3 |
| ~~STB3-22~~ | ~~1.29~~ | ~~0.05674~~ | ~~0.0016~~ | ~~0.26388~~ | ~~0.00749~~ | ~~0.03372~~ | ~~0.00051~~ | ~~481~~ | ~~37~~ | ~~238~~ | ~~6~~ | ~~214~~ | ~~3~~ | ~~11.2~~ |
| STB3-23 | 0.69 | 0.05447 | 0.00184 | 0.48705 | 0.01643 | 0.06484 | 0.00101 | 391 | 48 | 403 | 11 | 405 | 6 | -0.5 |
| STB3-24 | 0.44 | 0.05065 | 0.00343 | 0.23063 | 0.01548 | 0.03302 | 0.00058 | 225 | 121 | 211 | 13 | 209 | 4 | 1 |
| STB3-25 | 0.46 | 0.05513 | 0.00148 | 0.47164 | 0.0128 | 0.06203 | 0.00091 | 417 | 35 | 392 | 9 | 388 | 6 | 1 |
| STB3-26 | 0.29 | 0.05504 | 0.00207 | 0.43098 | 0.01495 | 0.05679 | 0.00081 | 414 | 86 | 364 | 11 | 356 | 5 | 2.2 |
| STB3-27 | 0.55 | 0.05442 | 0.00108 | 0.44112 | 0.00922 | 0.05878 | 0.00084 | 388 | 23 | 371 | 6 | 368 | 5 | 0.8 |
| STB3-28 | 0.64 | 0.05674 | 0.00123 | 0.57199 | 0.0129 | 0.0731 | 0.00106 | 481 | 26 | 459 | 8 | 455 | 6 | 0.9 |
| STB3-29 | 0.8 | 0.05131 | 0.00165 | 0.25503 | 0.00821 | 0.03604 | 0.00057 | 255 | 45 | 231 | 7 | 228 | 4 | 1.3 |
| STB3-30 | 0.38 | 0.06922 | 0.00131 | 1.46392 | 0.02935 | 0.15336 | 0.00219 | 905 | 20 | 916 | 12 | 920 | 12 | -0.4 |
| ~~STB3-31~~ | ~~0.06~~ | ~~0.09972~~ | ~~0.00153~~ | ~~3.50166~~ | ~~0.05963~~ | ~~0.25462~~ | ~~0.0035~~ | ~~1619~~ | ~~14~~ | ~~1528~~ | ~~13~~ | ~~1462~~ | ~~18~~ | ~~10.7~~ |
| STB3-32 | 0.54 | 0.05507 | 0.00104 | 0.47377 | 0.00952 | 0.06238 | 0.00088 | 415 | 22 | 394 | 7 | 390 | 5 | 1 |
| STB3-33 | 0.47 | 0.05227 | 0.00185 | 0.23547 | 0.00828 | 0.03267 | 0.00053 | 297 | 51 | 215 | 7 | 207 | 3 | 3.9 |
| STB3-34 | 0.82 | 0.05527 | 0.00112 | 0.45776 | 0.00974 | 0.06006 | 0.00086 | 423 | 24 | 383 | 7 | 376 | 5 | 1.9 |
| STB3-35 | 0.63 | 0.05298 | 0.00115 | 0.25262 | 0.00567 | 0.03458 | 0.0005 | 328 | 26 | 229 | 5 | 219 | 3 | 4.6 |
| STB3-36 | 0.43 | 0.05352 | 0.00098 | 0.38226 | 0.00749 | 0.05179 | 0.00073 | 351 | 21 | 329 | 6 | 326 | 4 | 0.9 |

| | | | | | | | | | | | | | | |
|---|---|---|---|---|---|---|---|---|---|---|---|---|---|---|
| STB3-37 | 0.93 | 0.05676 | 0.00117 | 0.47449 | 0.0102 | 0.06062 | 0.00087 | 482 | 24 | 394 | 7 | 379 | 5 | 4 |
| STB3-38 | 0.41 | 0.0569 | 0.00144 | 0.51961 | 0.01335 | 0.06621 | 0.001 | 488 | 31 | 425 | 9 | 413 | 6 | 2.9 |
| STB3-39 | 0.88 | 0.04895 | 0.00156 | 0.23507 | 0.00751 | 0.03482 | 0.00055 | 145 | 46 | 214 | 6 | 221 | 3 | -3.2 |
| STB3-40 | 0.22 | 0.07093 | 0.00114 | 1.52149 | 0.02688 | 0.15555 | 0.00215 | 955 | 17 | 939 | 11 | 932 | 12 | 0.8 |
| STB3-41 | 0.91 | 0.09126 | 0.00163 | 2.8967 | 0.05529 | 0.23015 | 0.00327 | 1452 | 17 | 1381 | 14 | 1335 | 17 | 8.8 |
| ~~STB3-42~~ | ~~0.32~~ | ~~0.06294~~ | ~~0.00361~~ | ~~0.50732~~ | ~~0.02806~~ | ~~0.05846~~ | ~~0.0009~~ | ~~706~~ | ~~126~~ | ~~417~~ | ~~19~~ | ~~366~~ | ~~5~~ | ~~13.9~~ |
| STB3-43 | 0.65 | 0.05683 | 0.00112 | 0.51571 | 0.01072 | 0.06581 | 0.00094 | 485 | 23 | 422 | 7 | 411 | 6 | 2.7 |
| STB3-44 | 0.5 | 0.05418 | 0.00137 | 0.48377 | 0.01244 | 0.06475 | 0.00097 | 379 | 32 | 401 | 9 | 404 | 6 | -0.7 |
| STB3-45 | 0.54 | 0.05269 | 0.00135 | 0.47544 | 0.01242 | 0.06543 | 0.00098 | 315 | 33 | 395 | 9 | 409 | 6 | -3.4 |
| STB3-46 | 0.46 | 0.05587 | 0.00113 | 0.50333 | 0.01069 | 0.06533 | 0.00093 | 447 | 24 | 414 | 7 | 408 | 6 | 1.5 |
| STB3-47 | 0.46 | 0.05149 | 0.00116 | 0.24859 | 0.00578 | 0.035 | 0.00051 | 263 | 28 | 225 | 5 | 222 | 3 | 1.4 |
| STB3-48 | 0.21 | 0.0545 | 0.00117 | 0.50139 | 0.0112 | 0.0667 | 0.00096 | 392 | 26 | 413 | 8 | 416 | 6 | -0.7 |
| STB3-49 | 0.22 | 0.05285 | 0.00118 | 0.48478 | 0.01117 | 0.06651 | 0.00097 | 322 | 27 | 401 | 8 | 415 | 6 | -3.4 |
| ~~STB3-50~~ | ~~0.9~~ | ~~0.08548~~ | ~~0.01049~~ | ~~0.76555~~ | ~~0.09241~~ | ~~0.06495~~ | ~~0.00144~~ | ~~1327~~ | ~~249~~ | ~~577~~ | ~~53~~ | ~~406~~ | ~~9~~ | ~~42.1~~ |
| STB3-51 | 0.61 | 0.05124 | 0.0023 | 0.26965 | 0.01212 | 0.03816 | 0.0006 | 252 | 74 | 242 | 10 | 241 | 4 | 0.4 |
| ~~STB3-52~~ | ~~1.58~~ | ~~0.09967~~ | ~~0.00144~~ | ~~3.47455~~ | ~~0.05698~~ | ~~0.25278~~ | ~~0.00347~~ | ~~1618~~ | ~~14~~ | ~~1521~~ | ~~13~~ | ~~1453~~ | ~~18~~ | ~~11.4~~ |
| ~~STB3-53~~ | ~~0.28~~ | ~~0.06505~~ | ~~0.00136~~ | ~~0.57929~~ | ~~0.01272~~ | ~~0.06457~~ | ~~0.00091~~ | ~~776~~ | ~~24~~ | ~~464~~ | ~~8~~ | ~~403~~ | ~~6~~ | ~~15.1~~ |
| STB3-54 | 0.57 | 0.05443 | 0.0015 | 0.44557 | 0.01261 | 0.05936 | 0.00086 | 389 | 38 | 374 | 9 | 372 | 5 | 0.5 |
| ~~STB3-55~~ | ~~0.63~~ | ~~0.06174~~ | ~~0.00176~~ | ~~0.55735~~ | ~~0.01624~~ | ~~0.06545~~ | ~~0.00096~~ | ~~665~~ | ~~38~~ | ~~450~~ | ~~11~~ | ~~409~~ | ~~6~~ | ~~10~~ |
| STB3-56 | 0.45 | 0.06826 | 0.00148 | 1.28491 | 0.02912 | 0.1365 | 0.00196 | 876 | 25 | 839 | 13 | 825 | 11 | 1.7 |
| STB3-57 | 0.48 | 0.05433 | 0.00107 | 0.46878 | 0.00984 | 0.06257 | 0.00087 | 385 | 24 | 390 | 7 | 391 | 5 | -0.3 |
| ~~STB3-58~~ | ~~0.69~~ | ~~0.06513~~ | ~~0.00207~~ | ~~0.57378~~ | ~~0.01842~~ | ~~0.06388~~ | ~~0.00096~~ | ~~779~~ | ~~42~~ | ~~460~~ | ~~12~~ | ~~399~~ | ~~6~~ | ~~15.3~~ |
| STB3-59 | 1.19 | 0.05575 | 0.00107 | 0.5353 | 0.01095 | 0.06962 | 0.00097 | 442 | 23 | 435 | 7 | 434 | 6 | 0.2 |
| STB3-60 | 0.41 | 0.05044 | 0.00166 | 0.23402 | 0.00783 | 0.03364 | 0.0005 | 215 | 50 | 214 | 6 | 213 | 3 | 0.5 |
| STB3-61 | 0.54 | 0.05255 | 0.0025 | 0.24486 | 0.01108 | 0.0338 | 0.00051 | 309 | 111 | 222 | 9 | 214 | 3 | 3.7 |
| STB3-62 | 0.5 | 0.0546 | 0.00133 | 0.49611 | 0.01247 | 0.06589 | 0.00095 | 396 | 31 | 409 | 8 | 411 | 6 | -0.5 |
| STB3-63 | 0.95 | 0.05599 | 0.00088 | 0.52043 | 0.00909 | 0.0674 | 0.00092 | 452 | 18 | 425 | 6 | 420 | 6 | 1.2 |
| STB3-64 | 0.56 | 0.05573 | 0.00133 | 0.52872 | 0.01305 | 0.0688 | 0.00098 | 442 | 30 | 431 | 9 | 429 | 6 | 0.5 |

| | | | | | | | | | | | | | | |
|---|---|---|---|---|---|---|---|---|---|---|---|---|---|---|
| STB3-65 | 0.31 | 0.06121 | 0.00159 | 0.86497 | 0.02297 | 0.10247 | 0.00151 | 647 | 32 | 633 | 13 | 629 | 9 | 0.6 |
| STB3-66 | 0.76 | 0.05096 | 0.00133 | 0.2776 | 0.00745 | 0.0395 | 0.00057 | 239 | 36 | 249 | 6 | 250 | 4 | -0.4 |
| STB3-67 | 0.92 | 0.05359 | 0.00317 | 0.45208 | 0.02658 | 0.06117 | 0.00106 | 354 | 102 | 379 | 19 | 383 | 6 | -1 |
| STB3-68 | 0.57 | 0.05672 | 0.0013 | 0.51363 | 0.01227 | 0.06566 | 0.00093 | 481 | 29 | 421 | 8 | 410 | 6 | 2.7 |
| STB3-69 | 0.51 | 0.05189 | 0.00199 | 0.34699 | 0.0134 | 0.04849 | 0.00074 | 281 | 60 | 302 | 10 | 305 | 5 | -1 |
| STB3-70 | 0.31 | 0.05472 | 0.00096 | 0.47349 | 0.00903 | 0.06275 | 0.00087 | 401 | 21 | 394 | 6 | 392 | 5 | 0.5 |
| STB3-71 | 0.89 | 0.05161 | 0.00324 | 0.23815 | 0.01448 | 0.03347 | 0.00053 | 268 | 145 | 217 | 12 | 212 | 3 | 2.4 |
| STB3-72 | 0.78 | 0.05576 | 0.00131 | 0.50004 | 0.01217 | 0.06502 | 0.00093 | 443 | 30 | 412 | 8 | 406 | 6 | 1.5 |
| STB3-73 | 0.24 | 0.06933 | 0.00106 | 1.33744 | 0.02286 | 0.13988 | 0.00192 | 909 | 16 | 862 | 10 | 844 | 11 | 2.1 |
| STB3-74 | 0.33 | 0.0508 | 0.00093 | 0.2426 | 0.00478 | 0.03463 | 0.00048 | 232 | 22 | 221 | 4 | 219 | 3 | 0.9 |
| STB3-75 | 1.07 | 0.05058 | 0.00137 | 0.23105 | 0.00643 | 0.03312 | 0.00048 | 222 | 38 | 211 | 5 | 210 | 3 | 0.5 |
| STB3-76 | 0.39 | 0.05099 | 0.00109 | 0.24068 | 0.00544 | 0.03423 | 0.00048 | 240 | 28 | 219 | 4 | 217 | 3 | 0.9 |
| STB3-77 | 0.43 | 0.05718 | 0.00088 | 0.51934 | 0.00901 | 0.06586 | 0.0009 | 498 | 18 | 425 | 6 | 411 | 5 | 3.4 |
| STB3-78 | 0.59 | 0.05174 | 0.00188 | 0.24254 | 0.0089 | 0.03399 | 0.00051 | 274 | 57 | 220 | 7 | 215 | 3 | 2.3 |
| STB3-79 | 0.55 | 0.05571 | 0.00113 | 0.53265 | 0.01148 | 0.06933 | 0.00098 | 441 | 25 | 434 | 8 | 432 | 6 | 0.5 |
| STB3-80 | 0.62 | 0.05129 | 0.00199 | 0.25039 | 0.00976 | 0.0354 | 0.00055 | 254 | 61 | 227 | 8 | 224 | 3 | 1.3 |
| STB3-81 | 0.28 | 0.05481 | 0.0009 | 0.48468 | 0.00882 | 0.06412 | 0.00088 | 404 | 19 | 401 | 6 | 401 | 5 | 0 |
| STB3-82 | 0.43 | 0.05435 | 0.00139 | 0.42518 | 0.01121 | 0.05673 | 0.00082 | 386 | 34 | 360 | 8 | 356 | 5 | 1.1 |
| ~~STB3-83~~ | ~~1.11~~ | ~~0.06361~~ | ~~0.0021~~ | ~~0.57959~~ | ~~0.01934~~ | ~~0.06607~~ | ~~0.00099~~ | ~~729~~ | ~~45~~ | ~~464~~ | ~~12~~ | ~~412~~ | ~~6~~ | ~~12.6~~ |
| STB3-84 | 0.45 | 0.05014 | 0.00125 | 0.23241 | 0.00599 | 0.03361 | 0.00049 | 201 | 34 | 212 | 5 | 213 | 3 | -0.5 |
| STB3-85 | 0.82 | 0.05065 | 0.00116 | 0.26872 | 0.00644 | 0.03847 | 0.00055 | 225 | 30 | 242 | 5 | 243 | 3 | -0.4 |
| STB3-86 | 0.37 | 0.0555 | 0.00087 | 0.53262 | 0.00932 | 0.06959 | 0.00095 | 432 | 18 | 434 | 6 | 434 | 6 | 0 |
| STB3-87 | 0.73 | 0.05136 | 0.00429 | 0.26694 | 0.022 | 0.03769 | 0.0008 | 257 | 148 | 240 | 18 | 238 | 5 | 0.8 |
| STB3-88 | 0.61 | 0.05005 | 0.00188 | 0.23806 | 0.00899 | 0.03449 | 0.00052 | 197 | 60 | 217 | 7 | 219 | 3 | -0.9 |
| STB3-89 | 0.58 | 0.05489 | 0.00201 | 0.48183 | 0.01779 | 0.06365 | 0.00097 | 408 | 55 | 399 | 12 | 398 | 6 | 0.3 |
| STB3-90 | 0.31 | 0.06882 | 0.00112 | 1.44129 | 0.02589 | 0.15185 | 0.00211 | 893 | 17 | 906 | 11 | 911 | 12 | -0.5 |
| STB3-91 | 0.29 | 0.05462 | 0.00095 | 0.47525 | 0.00902 | 0.06309 | 0.00087 | 397 | 20 | 395 | 6 | 394 | 5 | 0.3 |
| STB3-92 | 0.19 | 0.06968 | 0.00112 | 1.44979 | 0.02596 | 0.15088 | 0.00209 | 919 | 17 | 910 | 11 | 906 | 12 | 0.4 |

| | | | | | | | | | | | | | | |
|---|---|---|---|---|---|---|---|---|---|---|---|---|---|---|
| ~~STB3-93~~ | ~~0.45~~ | ~~0.07046~~ | ~~0.00898~~ | ~~0.4508~~ | ~~0.05681~~ | ~~0.0464~~ | ~~0.0009~~ | ~~942~~ | ~~275~~ | ~~378~~ | ~~40~~ | ~~292~~ | ~~6~~ | ~~29.5~~ |
| STB3-94 | 0.42 | 0.05425 | 0.00107 | 0.48945 | 0.01027 | 0.06542 | 0.00092 | 381 | 24 | 405 | 7 | 409 | 6 | -1 |
| STB3-95 | 0.47 | 0.05469 | 0.00143 | 0.4751 | 0.01282 | 0.06299 | 0.00091 | 400 | 35 | 395 | 9 | 394 | 6 | 0.3 |
| STB3-96 | 0.58 | 0.05787 | 0.0012 | 0.53695 | 0.01178 | 0.06729 | 0.00095 | 525 | 25 | 436 | 8 | 420 | 6 | 3.8 |
| STB3-97 | 0.63 | 0.05718 | 0.00125 | 0.51731 | 0.0119 | 0.0656 | 0.00093 | 498 | 27 | 423 | 8 | 410 | 6 | 3.2 |
| STB3-98 | 0.5 | 0.05074 | 0.00114 | 0.23927 | 0.00562 | 0.0342 | 0.00049 | 229 | 29 | 218 | 5 | 217 | 3 | 0.5 |
| STB3-99 | 0.64 | 0.05164 | 0.00192 | 0.26011 | 0.00976 | 0.03652 | 0.00055 | 270 | 58 | 235 | 8 | 231 | 3 | 1.7 |
| ~~STB3-100~~ | ~~0.48~~ | ~~0.06376~~ | ~~0.00261~~ | ~~0.56916~~ | ~~0.02173~~ | ~~0.06474~~ | ~~0.00096~~ | ~~734~~ | ~~89~~ | ~~457~~ | ~~14~~ | ~~404~~ | ~~6~~ | ~~13.1~~ |
| **JS04** | | | | | | | | | | | | | | |
| ~~JS04-01~~ | ~~1.16~~ | ~~0.11028~~ | ~~0.01751~~ | ~~0.81104~~ | ~~0.12536~~ | ~~0.05334~~ | ~~0.00194~~ | ~~1804~~ | ~~308~~ | ~~603~~ | ~~70~~ | ~~335~~ | ~~12~~ | ~~80~~ |
| JS04-02 | 0.03 | 0.05488 | 0.0012 | 0.46044 | 0.0081 | 0.06085 | 0.00079 | 408 | 50 | 385 | 6 | 381 | 5 | 1 |
| ~~JS04-03~~ | ~~0.64~~ | ~~0.06921~~ | ~~0.00093~~ | ~~0.6797~~ | ~~0.01021~~ | ~~0.07121~~ | ~~0.00094~~ | ~~905~~ | ~~14~~ | ~~527~~ | ~~6~~ | ~~443~~ | ~~6~~ | ~~19~~ |
| ~~JS04-04~~ | ~~0.09~~ | ~~0.07424~~ | ~~0.00152~~ | ~~1.1668~~ | ~~0.01872~~ | ~~0.11399~~ | ~~0.00146~~ | ~~1048~~ | ~~42~~ | ~~785~~ | ~~9~~ | ~~696~~ | ~~8~~ | ~~12.8~~ |
| ~~JS04-05~~ | ~~0.67~~ | ~~0.10581~~ | ~~0.00127~~ | ~~3.56702~~ | ~~0.04992~~ | ~~0.24444~~ | ~~0.00319~~ | ~~1728~~ | ~~11~~ | ~~1542~~ | ~~11~~ | ~~1410~~ | ~~17~~ | ~~22.6~~ |
| JS04-06 | 1.06 | 0.12834 | 0.00143 | 6.361 | 0.08493 | 0.3594 | 0.00461 | 2075 | 11 | 2027 | 12 | 1979 | 22 | 4.9 |
| ~~JS04-07~~ | ~~0.82~~ | ~~0.04605~~ | ~~0.02332~~ | ~~1.02319~~ | ~~0.51506~~ | ~~0.16116~~ | ~~0.00907~~ | | ~~847~~ | ~~716~~ | ~~258~~ | ~~963~~ | ~~50~~ | ~~-25.6~~ |
| ~~JS04-08~~ | ~~0.62~~ | ~~0.06886~~ | ~~0.00305~~ | ~~0.8167~~ | ~~0.03383~~ | ~~0.08602~~ | ~~0.00135~~ | ~~895~~ | ~~94~~ | ~~606~~ | ~~19~~ | ~~532~~ | ~~8~~ | ~~13.9~~ |
| ~~JS04-09~~ | ~~0.9~~ | ~~0.07048~~ | ~~0.00442~~ | ~~0.46015~~ | ~~0.0278~~ | ~~0.04735~~ | ~~0.0008~~ | ~~942~~ | ~~132~~ | ~~384~~ | ~~19~~ | ~~298~~ | ~~5~~ | ~~28.9~~ |
| JS04-10 | 0.96 | 0.06058 | 0.00074 | 0.63032 | 0.00893 | 0.07545 | 0.00098 | 624 | 14 | 496 | 6 | 469 | 6 | 5.8 |
| ~~JS04-11~~ | ~~0.42~~ | ~~0.14592~~ | ~~0.0032~~ | ~~5.97631~~ | ~~0.10423~~ | ~~0.29703~~ | ~~0.00394~~ | ~~2299~~ | ~~39~~ | ~~1972~~ | ~~15~~ | ~~1677~~ | ~~20~~ | ~~37.1~~ |
| ~~JS04-12~~ | ~~0.21~~ | ~~0.07882~~ | ~~0.00168~~ | ~~1.57504~~ | ~~0.02667~~ | ~~0.14494~~ | ~~0.00186~~ | ~~1168~~ | ~~43~~ | ~~960~~ | ~~11~~ | ~~873~~ | ~~10~~ | ~~10~~ |
| ~~JS04-13~~ | ~~0.93~~ | ~~0.07275~~ | ~~0.0011~~ | ~~0.80744~~ | ~~0.0133~~ | ~~0.08048~~ | ~~0.00108~~ | ~~1007~~ | ~~15~~ | ~~601~~ | ~~7~~ | ~~499~~ | ~~6~~ | ~~20.4~~ |
| ~~JS04-14~~ | ~~0.37~~ | ~~0.0622~~ | ~~0.00191~~ | ~~0.39126~~ | ~~0.01076~~ | ~~0.04562~~ | ~~0.00062~~ | ~~681~~ | ~~67~~ | ~~335~~ | ~~8~~ | ~~288~~ | 4 | ~~16.3~~ |
| JS04-15 | 0.36 | 0.06861 | 0.00181 | 1.10829 | 0.02526 | 0.11716 | 0.00155 | 887 | 56 | 757 | 12 | 714 | 9 | 6 |
| JS04-16 | 0.47 | 0.06114 | 0.0008 | 0.64586 | 0.00962 | 0.07659 | 0.001 | 644 | 14 | 506 | 6 | 476 | 6 | 6.3 |
| ~~JS04-17~~ | ~~0.63~~ | ~~0.06696~~ | ~~0.00229~~ | ~~0.65212~~ | ~~0.02038~~ | ~~0.07064~~ | ~~0.00099~~ | ~~836~~ | ~~73~~ | ~~510~~ | ~~13~~ | ~~440~~ | ~~6~~ | ~~15.9~~ |

| | | | | | | | | | | | | | | |
|---|---|---|---|---|---|---|---|---|---|---|---|---|---|---|
| JS04-18 | 0.46 | 0.05965 | 0.00179 | 0.49307 | 0.01323 | 0.05995 | 0.0008 | 591 | 67 | 407 | 9 | 375 | 5 | 8.5 |
| ~~JS04-19~~ | ~~0.86~~ | ~~0.06906~~ | ~~0.00398~~ | ~~0.40424~~ | ~~0.02244~~ | ~~0.04245~~ | ~~0.00066~~ | ~~901~~ | ~~122~~ | ~~345~~ | ~~16~~ | ~~268~~ | ~~4~~ | ~~28.7~~ |
| JS04-20 | 0.11 | 0.07017 | 0.00079 | 1.53849 | 0.02077 | 0.15898 | 0.00205 | 933 | 12 | 946 | 8 | 951 | 11 | -0.5 |
| ~~JS04-21~~ | ~~0.39~~ | ~~0.06378~~ | ~~0.00085~~ | ~~0.64474~~ | ~~0.00969~~ | ~~0.0733~~ | ~~0.00096~~ | ~~734~~ | ~~14~~ | ~~505~~ | ~~6~~ | ~~456~~ | ~~6~~ | ~~10.7~~ |
| JS04-22 | 0.63 | 0.06018 | 0.00081 | 0.5486 | 0.00834 | 0.0661 | 0.00087 | 610 | 15 | 444 | 5 | 413 | 5 | 7.5 |
| ~~JS04-23~~ | ~~1.37~~ | ~~0.09236~~ | ~~0.00713~~ | ~~0.42867~~ | ~~0.03187~~ | ~~0.03366~~ | ~~0.00069~~ | ~~1475~~ | ~~151~~ | ~~362~~ | ~~23~~ | ~~213~~ | 4 | ~~70~~ |
| JS04-24 | 0.33 | 0.05311 | 0.00069 | 0.25075 | 0.00372 | 0.03423 | 0.00045 | 333 | 15 | 227 | 3 | 217 | 3 | 4.6 |
| JS04-25 | 0.34 | 0.05688 | 0.00154 | 0.49062 | 0.01161 | 0.06256 | 0.00083 | 487 | 61 | 405 | 8 | 391 | 5 | 3.6 |
| ~~JS04-26~~ | ~~0.67~~ | ~~0.06045~~ | ~~0.00191~~ | ~~0.3433~~ | ~~0.01082~~ | ~~0.04118~~ | ~~0.00063~~ | ~~620~~ | ~~42~~ | ~~300~~ | ~~8~~ | ~~260~~ | 4 | ~~15.4~~ |
| JS04-27 | 0.68 | 0.07669 | 0.00092 | 1.82141 | 0.02561 | 0.17222 | 0.00224 | 1113 | 13 | 1053 | 9 | 1024 | 12 | 8.7 |
| JS04-28 | 0.53 | 0.05686 | 0.00075 | 0.56556 | 0.00848 | 0.07213 | 0.00094 | 486 | 15 | 455 | 5 | 449 | 6 | 1.3 |
| JS04-29 | 1.05 | 0.05843 | 0.00113 | 0.38742 | 0.0078 | 0.04807 | 0.00067 | 546 | 22 | 332 | 6 | 303 | 4 | 9.6 |
| JS04-30 | 0.48 | 0.11557 | 0.00129 | 4.94541 | 0.06659 | 0.31029 | 0.004 | 1889 | 11 | 1810 | 11 | 1742 | 20 | 8.4 |
| JS04-31 | 0.92 | 0.0579 | 0.00081 | 0.52039 | 0.00819 | 0.06518 | 0.00086 | 526 | 16 | 425 | 5 | 407 | 5 | 4.4 |
| JS04-32 | 0.41 | 0.05849 | 0.00171 | 0.54179 | 0.01407 | 0.06718 | 0.0009 | 548 | 65 | 440 | 9 | 419 | 5 | 5 |
| ~~JS04-33~~ | ~~0.79~~ | ~~0.07527~~ | ~~0.00346~~ | ~~0.61146~~ | ~~0.02646~~ | ~~0.05892~~ | ~~0.00091~~ | ~~1076~~ | ~~95~~ | ~~484~~ | ~~17~~ | ~~369~~ | ~~6~~ | ~~31.2~~ |
| ~~JS04-34~~ | ~~0.81~~ | ~~0.06106~~ | ~~0.00261~~ | ~~0.33602~~ | ~~0.01351~~ | ~~0.03991~~ | ~~0.00058~~ | ~~641~~ | ~~94~~ | ~~294~~ | ~~10~~ | ~~252~~ | 4 | ~~16.7~~ |
| ~~JS04-35~~ | ~~0.47~~ | ~~0.06295~~ | ~~0.00211~~ | ~~0.59817~~ | ~~0.01822~~ | ~~0.06892~~ | ~~0.00096~~ | ~~706~~ | ~~73~~ | ~~476~~ | ~~12~~ | ~~430~~ | ~~6~~ | ~~10.7~~ |
| JS04-36 | 0.94 | 0.0673 | 0.00316 | 0.96035 | 0.04273 | 0.1035 | 0.00156 | 847 | 100 | 683 | 22 | 635 | 9 | 7.6 |
| JS04-37 | 0.54 | 0.05648 | 0.00189 | 0.54025 | 0.01653 | 0.06937 | 0.00095 | 471 | 76 | 439 | 11 | 432 | 6 | 1.6 |
| JS04-38 | 0.68 | 0.06233 | 0.00102 | 0.60551 | 0.01069 | 0.07044 | 0.00095 | 685 | 18 | 481 | 7 | 439 | 6 | 9.6 |
| JS04-39 | 1.03 | 0.05475 | 0.0033 | 0.28836 | 0.01681 | 0.0382 | 0.00059 | 402 | 139 | 257 | 13 | 242 | 4 | 6.2 |
| ~~JS04-40~~ | ~~0.88~~ | ~~0.06117~~ | ~~0.00084~~ | ~~0.48558~~ | ~~0.00752~~ | ~~0.05756~~ | ~~0.00076~~ | ~~645~~ | ~~15~~ | ~~402~~ | ~~5~~ | ~~361~~ | ~~5~~ | ~~11.4~~ |
| ~~JS04-41~~ | ~~0.59~~ | ~~0.0688~~ | ~~0.0025~~ | ~~0.57686~~ | ~~0.01923~~ | ~~0.06081~~ | ~~0.00088~~ | ~~893~~ | ~~77~~ | ~~462~~ | ~~12~~ | ~~381~~ | ~~5~~ | ~~21.3~~ |
| JS04-42 | 0.83 | 0.07109 | 0.00086 | 1.27288 | 0.01805 | 0.12983 | 0.0017 | 960 | 13 | 834 | 8 | 787 | 10 | 6 |
| JS04-43 | 0.88 | 0.05628 | 0.00081 | 0.53938 | 0.00864 | 0.0695 | 0.00092 | 463 | 16 | 438 | 6 | 433 | 6 | 1.2 |
| JS04-44 | 0.32 | 0.07241 | 0.00084 | 1.55002 | 0.02147 | 0.15522 | 0.00202 | 997 | 13 | 951 | 9 | 930 | 11 | 2.3 |
| JS04-45 | 0.31 | 0.07565 | 0.00091 | 1.40505 | 0.0199 | 0.13468 | 0.00176 | 1086 | 13 | 891 | 8 | 815 | 10 | 9.3 |

| | | | | | | | | | | | | | | |
|---|---|---|---|---|---|---|---|---|---|---|---|---|---|---|
| ~~JS04-46~~ | ~~0.28~~ | ~~0.12182~~ | ~~0.00137~~ | ~~5.36985~~ | ~~0.07301~~ | ~~0.31965~~ | ~~0.00414~~ | ~~1983~~ | ~~11~~ | ~~1880~~ | ~~12~~ | ~~1788~~ | ~~20~~ | ~~10.9~~ |
| JS04-47 | 0.53 | 0.06097 | 0.00081 | 0.60822 | 0.0092 | 0.07234 | 0.00095 | 638 | 15 | 482 | 6 | 450 | 6 | 7.1 |
| ~~JS04-48~~ | ~~0.55~~ | ~~0.06745~~ | ~~0.00083~~ | ~~0.63841~~ | ~~0.00916~~ | ~~0.06864~~ | ~~0.0009~~ | ~~852~~ | ~~13~~ | ~~501~~ | ~~6~~ | ~~428~~ | ~~5~~ | ~~17.1~~ |
| ~~JS04-49~~ | ~~1.16~~ | ~~0.0654~~ | ~~0.00093~~ | ~~0.63835~~ | ~~0.0101~~ | ~~0.07078~~ | ~~0.00094~~ | ~~787~~ | ~~15~~ | ~~501~~ | ~~6~~ | ~~441~~ | ~~6~~ | ~~13.6~~ |
| JS04-50 | 0.12 | 0.09046 | 0.00103 | 2.81139 | 0.03843 | 0.22537 | 0.00293 | 1435 | 12 | 1359 | 10 | 1310 | 15 | 9.5 |
| JS04-51 | 0.61 | 0.05796 | 0.00073 | 0.58105 | 0.00847 | 0.07269 | 0.00095 | 528 | 14 | 465 | 5 | 452 | 6 | 2.9 |
| ~~JS04-52~~ | ~~1.08~~ | ~~0.06128~~ | ~~0.00086~~ | ~~0.51695~~ | ~~0.0081~~ | ~~0.06117~~ | ~~0.00082~~ | ~~649~~ | ~~15~~ | ~~423~~ | ~~5~~ | ~~383~~ | ~~5~~ | ~~10.4~~ |
| JS04-53 | 0.07 | 0.11647 | 0.00132 | 5.05021 | 0.06905 | 0.31441 | 0.00409 | 1903 | 11 | 1828 | 12 | 1762 | 20 | 8 |
| JS04-54 | 0.42 | 0.05578 | 0.00201 | 0.35303 | 0.01172 | 0.0459 | 0.00064 | 444 | 82 | 307 | 9 | 289 | 4 | 6.2 |
| JS04-55 | 0.62 | 0.0572 | 0.00075 | 0.55096 | 0.0083 | 0.06984 | 0.00092 | 499 | 15 | 446 | 5 | 435 | 6 | 2.5 |
| JS04-56 | 0.46 | 0.05957 | 0.00087 | 0.54445 | 0.00883 | 0.06628 | 0.00088 | 588 | 16 | 441 | 6 | 414 | 5 | 6.5 |
| JS04-57 | 0.54 | 0.05618 | 0.00271 | 0.28298 | 0.01304 | 0.03653 | 0.00053 | 459 | 110 | 253 | 10 | 231 | 3 | 9.5 |
| ~~JS04-58~~ | ~~0.77~~ | ~~0.06714~~ | ~~0.00257~~ | ~~0.69507~~ | ~~0.02466~~ | ~~0.07509~~ | ~~0.00108~~ | ~~842~~ | ~~82~~ | ~~536~~ | ~~15~~ | ~~467~~ | ~~6~~ | ~~14.8~~ |
| JS04-59 | 0.72 | 0.06034 | 0.00228 | 0.60273 | 0.02117 | 0.07245 | 0.00102 | 616 | 84 | 479 | 13 | 451 | 6 | 6.2 |
| JS04-60 | 0.2 | 0.07247 | 0.00087 | 1.49129 | 0.02118 | 0.14922 | 0.00196 | 999 | 13 | 927 | 9 | 897 | 11 | 3.3 |
| JS04-61 | 0.28 | 0.05647 | 0.00067 | 0.52675 | 0.00745 | 0.06764 | 0.00088 | 471 | 14 | 430 | 5 | 422 | 5 | 1.9 |
| ~~JS04-62~~ | ~~0.25~~ | ~~0.08713~~ | ~~0.00195~~ | ~~2.16661~~ | ~~0.039~~ | ~~0.18036~~ | ~~0.00238~~ | ~~1363~~ | ~~44~~ | ~~1170~~ | ~~13~~ | ~~1069~~ | ~~13~~ | ~~27.5~~ |
| ~~JS04-63~~ | ~~0.5~~ | ~~0.05718~~ | ~~0.00228~~ | ~~0.05528~~ | ~~0.00204~~ | ~~0.00701~~ | ~~0.0001~~ | ~~499~~ | ~~90~~ | ~~55~~ | ~~2~~ | ~~45~~ | ~~0.7~~ | ~~22.2~~ |
| JS04-64 | 0.19 | 0.0716 | 0.00082 | 1.37233 | 0.01902 | 0.13898 | 0.00181 | 975 | 13 | 877 | 8 | 839 | 10 | 4.5 |
| ~~JS04-65~~ | ~~0.27~~ | ~~0.10795~~ | ~~0.00274~~ | ~~3.09204~~ | ~~0.06561~~ | ~~0.20775~~ | ~~0.00291~~ | ~~1765~~ | ~~48~~ | ~~1431~~ | ~~16~~ | ~~1217~~ | ~~16~~ | ~~45~~ |
| ~~JS04-66~~ | ~~1~~ | ~~0.05976~~ | ~~0.00105~~ | ~~0.33483~~ | ~~0.0063~~ | ~~0.04063~~ | ~~0.00055~~ | ~~595~~ | ~~20~~ | ~~293~~ | ~~5~~ | ~~257~~ | ~~3~~ | ~~14~~ |
| ~~JS04-67~~ | ~~0.38~~ | ~~0.06407~~ | ~~0.00094~~ | ~~0.60241~~ | ~~0.00979~~ | ~~0.06818~~ | ~~0.00092~~ | ~~744~~ | ~~16~~ | ~~479~~ | ~~6~~ | ~~425~~ | ~~6~~ | ~~12.7~~ |
| ~~JS04-68~~ | ~~0.76~~ | ~~0.05714~~ | ~~0.00093~~ | ~~0.30922~~ | ~~0.00547~~ | ~~0.03924~~ | ~~0.00053~~ | ~~497~~ | ~~18~~ | ~~274~~ | ~~4~~ | ~~248~~ | ~~3~~ | ~~10.5~~ |
| ~~JS04-69~~ | ~~1.24~~ | ~~0.09873~~ | ~~0.00404~~ | ~~3.06853~~ | ~~0.11622~~ | ~~0.22542~~ | ~~0.00346~~ | ~~1600~~ | ~~78~~ | ~~1425~~ | ~~29~~ | ~~1310~~ | ~~18~~ | ~~22.1~~ |
| JS04-70 | 0.48 | 0.05669 | 0.0019 | 0.38743 | 0.01182 | 0.04956 | 0.00068 | 480 | 76 | 332 | 9 | 312 | 4 | 6.4 |
| ~~JS04-71~~ | ~~0.86~~ | ~~0.0772~~ | ~~0.004~~ | ~~0.4117~~ | ~~0.02031~~ | ~~0.03868~~ | ~~0.00062~~ | ~~1126~~ | ~~106~~ | ~~350~~ | ~~15~~ | ~~245~~ | ~~4~~ | ~~42.9~~ |
| ~~JS04-72~~ | ~~0.43~~ | ~~0.06787~~ | ~~0.00211~~ | ~~0.61453~~ | ~~0.01714~~ | ~~0.06567~~ | ~~0.0009~~ | ~~865~~ | ~~66~~ | ~~486~~ | ~~11~~ | ~~410~~ | ~~5~~ | ~~18.5~~ |
| JS04-73 | 0.57 | 0.05964 | 0.00076 | 0.57965 | 0.0086 | 0.07047 | 0.00093 | 591 | 14 | 464 | 6 | 439 | 6 | 5.7 |

| | | | | | | | | | | | | | | |
|---|---|---|---|---|---|---|---|---|---|---|---|---|---|---|
| JS04-74 | 0.75 | 0.05617 | 0.00072 | 0.52159 | 0.00775 | 0.06733 | 0.00089 | 459 | 15 | 426 | 5 | 420 | 5 | 1.4 |
| ~~JS04-75~~ | ~~0.57~~ | ~~0.07744~~ | ~~0.00093~~ | ~~1.46043~~ | ~~0.02073~~ | ~~0.13674~~ | ~~0.0018~~ | ~~1133~~ | ~~13~~ | ~~914~~ | ~~9~~ | ~~826~~ | ~~10~~ | ~~10.7~~ |
| ~~JS04-76~~ | ~~0.34~~ | ~~0.10216~~ | ~~0.00133~~ | ~~1.53308~~ | ~~0.02285~~ | ~~0.10882~~ | ~~0.00146~~ | ~~1664~~ | ~~12~~ | ~~944~~ | ~~9~~ | ~~666~~ | ~~8~~ | ~~41.7~~ |
| JS04-77 | 0.71 | 0.06034 | 0.0008 | 0.64075 | 0.00975 | 0.077 | 0.00103 | 616 | 15 | 503 | 6 | 478 | 6 | 5.2 |
| ~~JS04-78~~ | ~~0.93~~ | ~~0.06676~~ | ~~0.00095~~ | ~~0.69728~~ | ~~0.01112~~ | ~~0.07574~~ | ~~0.00102~~ | ~~830~~ | ~~15~~ | ~~537~~ | ~~7~~ | ~~471~~ | ~~6~~ | ~~14~~ |
| JS04-79 | 0.41 | 0.07472 | 0.00202 | 1.57932 | 0.03687 | 0.15329 | 0.00209 | 1061 | 56 | 962 | 15 | 919 | 12 | 4.7 |
| ~~JS04-80~~ | ~~1.03~~ | ~~0.06733~~ | ~~0.00712~~ | ~~0.59542~~ | ~~0.06195~~ | ~~0.06414~~ | ~~0.0012~~ | ~~848~~ | ~~229~~ | ~~474~~ | ~~39~~ | ~~401~~ | ~~7~~ | ~~18.2~~ |
| JS04-81 | 0.63 | 0.05191 | 0.00471 | 0.30411 | 0.02696 | 0.04249 | 0.00082 | 281 | 208 | 270 | 21 | 268 | 5 | 0.7 |
| ~~JS04-82~~ | ~~0.77~~ | ~~0.06405~~ | ~~0.00174~~ | ~~0.57325~~ | ~~0.01574~~ | ~~0.0649~~ | ~~0.00096~~ | ~~743~~ | ~~34~~ | ~~460~~ | ~~10~~ | ~~405~~ | ~~6~~ | ~~13.6~~ |
| JS04-83 | 0.17 | 0.05596 | 0.00166 | 0.49291 | 0.01299 | 0.06388 | 0.00087 | 451 | 67 | 407 | 9 | 399 | 5 | 2 |
| JS04-84 | 1.19 | 0.06064 | 0.00089 | 0.56634 | 0.00931 | 0.06773 | 0.00091 | 626 | 16 | 456 | 6 | 422 | 5 | 8.1 |
| JS04-85 | 0.28 | 0.04605 | 0.00147 | 0.05629 | 0.00161 | 0.00887 | 0.00013 | | 66 | 56 | 2 | 56.9 | 0.8 | -1.6 |
| JS04-86 | 0.96 | 0.05996 | 0.00093 | 0.57525 | 0.00982 | 0.06957 | 0.00094 | 602 | 17 | 461 | 6 | 434 | 6 | 6.2 |
| ~~JS04-87~~ | ~~0.91~~ | ~~0.06727~~ | ~~0.00094~~ | ~~0.67131~~ | ~~0.01058~~ | ~~0.07236~~ | ~~0.00097~~ | ~~846~~ | ~~15~~ | ~~522~~ | ~~6~~ | ~~450~~ | ~~6~~ | ~~16~~ |
| JS04-88 | 0.46 | 0.0545 | 0.00086 | 0.32585 | 0.00562 | 0.04336 | 0.00059 | 392 | 18 | 286 | 4 | 274 | 4 | 4.4 |
| JS04-89 | 0.39 | 0.12466 | 0.00152 | 6.29824 | 0.09089 | 0.36637 | 0.00487 | 2024 | 11 | 2018 | 13 | 2012 | 23 | 0.6 |
| JS04-90 | 0.71 | 0.06123 | 0.00253 | 0.53103 | 0.02058 | 0.0629 | 0.00091 | 647 | 91 | 432 | 14 | 393 | 6 | 9.9 |
| JS04-91 | 0.4 | 0.05697 | 0.00078 | 0.36648 | 0.00573 | 0.04665 | 0.00062 | 490 | 15 | 317 | 4 | 294 | 4 | 7.8 |
| ~~JS04-92~~ | ~~1.17~~ | ~~0.07668~~ | ~~0.00391~~ | ~~0.41797~~ | ~~0.02025~~ | ~~0.03953~~ | ~~0.00063~~ | ~~1113~~ | ~~104~~ | ~~355~~ | ~~15~~ | ~~250~~ | ~~4~~ | ~~42~~ |
| JS04-93 | 0.22 | 0.0567 | 0.00156 | 0.5158 | 0.01241 | 0.06597 | 0.00089 | 480 | 62 | 422 | 8 | 412 | 5 | 2.4 |
| ~~JS04-94~~ | ~~0.68~~ | ~~0.06672~~ | ~~0.00288~~ | ~~0.62134~~ | ~~0.02508~~ | ~~0.06754~~ | ~~0.00102~~ | ~~829~~ | ~~92~~ | ~~491~~ | ~~16~~ | ~~421~~ | ~~6~~ | ~~16.6~~ |
| JS04-95 | 0.96 | 0.07181 | 0.00095 | 1.26947 | 0.01929 | 0.12819 | 0.00172 | 981 | 14 | 832 | 9 | 778 | 10 | 6.9 |
| JS04-96 | 0.58 | 0.14869 | 0.00183 | 8.13718 | 0.11828 | 0.39683 | 0.0053 | 2331 | 11 | 2246 | 13 | 2154 | 24 | 8.2 |
| JS04-97 | 0.45 | 0.06001 | 0.00201 | 0.53405 | 0.0163 | 0.06455 | 0.0009 | 604 | 74 | 434 | 11 | 403 | 5 | 7.7 |
| JS04-98 | 0.18 | 0.06166 | 0.00083 | 0.63411 | 0.00978 | 0.07458 | 0.001 | 662 | 15 | 499 | 6 | 464 | 6 | 7.5 |
| JS04-99 | 0.24 | 0.17678 | 0.00212 | 11.18255 | 0.16013 | 0.45869 | 0.00608 | 2623 | 11 | 2538 | 13 | 2434 | 27 | 7.8 |
| ~~JS04-100~~ | ~~0.74~~ | ~~0.06187~~ | ~~0.00085~~ | ~~0.50636~~ | ~~0.00788~~ | ~~0.05935~~ | ~~0.0008~~ | ~~670~~ | ~~15~~ | ~~416~~ | ~~5~~ | ~~372~~ | ~~5~~ | ~~11.8~~ |

| | | | | | | | | | | | | | | |
|---|---|---|---|---|---|---|---|---|---|---|---|---|---|---|
| **STB1** | | | | | | | | | | | | | | |
| STB1-01 | 0.41 | 0.0547 | 0.00085 | 0.50449 | 0.00883 | 0.06688 | 0.00092 | 400 | 18 | 415 | 6 | 417 | 6 | -0.5 |
| ~~STB1-02~~ | ~~1.24~~ | ~~0.10971~~ | ~~0.00176~~ | ~~4.18093~~ | ~~0.07438~~ | ~~0.27633~~ | ~~0.00388~~ | ~~1795~~ | ~~15~~ | ~~1670~~ | ~~15~~ | 109 | ~~20~~ | ~~14.1~~ |
| STB1-03 | 1.13 | 0.05582 | 0.00175 | 0.57047 | 0.0182 | 0.07411 | 0.00111 | 445 | 44 | 458 | 12 | ~~204~~ | 7 | -0.7 |
| ~~STB1-04~~ | ~~0.41~~ | ~~0.1817~~ | ~~0.00251~~ | ~~10.3301~~ | ~~0.16572~~ | ~~0.41225~~ | ~~0.00563~~ | ~~2668~~ | ~~12~~ | ~~2465~~ | ~~15~~ | 206 | ~~26~~ | ~~19.9~~ |
| STB1-05 | 0.43 | 0.05161 | 0.00261 | 0.30329 | 0.01532 | 0.04261 | 0.00069 | 268 | 86 | 269 | 12 | 206 | 4 | 0 |
| STB1-06 | 0.43 | 0.05619 | 0.00394 | 0.56368 | 0.03924 | 0.07275 | 0.00133 | 460 | 122 | 454 | 25 | 210 | 8 | 0.2 |
| STB1-07 | 0.6 | 0.05536 | 0.00101 | 0.51852 | 0.01023 | 0.06791 | 0.00095 | 427 | 21 | 424 | 7 | 214 | 6 | 0 |
| STB1-08 | 0.4 | 0.05548 | 0.00119 | 0.55537 | 0.01259 | 0.07259 | 0.00104 | 432 | 26 | 449 | 8 | 215 | 6 | -0.7 |
| STB1-09 | 0.55 | 0.0619 | 0.00102 | 0.92233 | 0.01681 | 0.10805 | 0.0015 | 671 | 18 | 664 | 9 | 226 | 9 | 0.5 |
| STB1-10 | 0.69 | 0.05477 | 0.00136 | 0.5092 | 0.01306 | 0.06742 | 0.00099 | 403 | 32 | 418 | 9 | 228 | 6 | -0.7 |
| STB1-11 | 0.31 | 0.05545 | 0.00147 | 0.52944 | 0.01439 | 0.06923 | 0.00102 | 430 | 35 | 431 | 10 | 256 | 6 | -0.2 |
| ~~STB1-12~~ | ~~0.25~~ | ~~0.06148~~ | ~~0.0011~~ | ~~0.52425~~ | ~~0.0102~~ | ~~0.06183~~ | ~~0.00087~~ | ~~656~~ | ~~20~~ | ~~428~~ | ~~7~~ | 269 | ~~5~~ | ~~10.6~~ |
| STB1-13 | 0.51 | 0.05508 | 0.00102 | 0.51941 | 0.01043 | 0.06839 | 0.00096 | 415 | 22 | 425 | 7 | 272 | 6 | -0.2 |
| STB1-14 | 0.2 | 0.12219 | 0.00183 | 6.40892 | 0.10873 | 0.38032 | 0.00528 | 1988 | 14 | 2033 | 15 | 304 | 25 | -4.3 |
| STB1-15 | 1.5 | 0.09438 | 0.00145 | 3.49578 | 0.06039 | 0.26857 | 0.00373 | 1516 | 15 | 1526 | 14 | 359 | 19 | -1.2 |
| STB1-16 | 0.45 | 0.05555 | 0.00134 | 0.50431 | 0.01264 | 0.06584 | 0.00095 | 434 | 31 | 415 | 9 | 364 | 6 | 1 |
| STB1-17 | 0.46 | 0.05523 | 0.00096 | 0.52588 | 0.01001 | 0.06905 | 0.00097 | 422 | 20 | 429 | 7 | 386 | 6 | -0.2 |
| STB1-18 | 0.29 | 0.05559 | 0.00108 | 0.50365 | 0.01051 | 0.0657 | 0.00093 | 436 | 23 | 414 | 7 | 386 | 6 | 1 |
| STB1-19 | 0.76 | 0.05565 | 0.00117 | 0.53467 | 0.01188 | 0.06967 | 0.001 | 438 | 26 | 435 | 8 | ~~387~~ | 6 | 0.2 |
| STB1-20 | 0.49 | 0.05698 | 0.00126 | 0.49851 | 0.01161 | 0.06344 | 0.00091 | 491 | 27 | 411 | 8 | 387 | 6 | 3.5 |
| STB1-21 | 0.88 | 0.0552 | 0.00247 | 0.4933 | 0.02212 | 0.0648 | 0.00104 | 420 | 71 | 407 | 15 | 393 | 6 | 0.5 |
| ~~STB1-22~~ | ~~0.62~~ | ~~0.06748~~ | ~~0.00364~~ | ~~0.29894~~ | ~~0.01545~~ | ~~0.03213~~ | ~~0.0005~~ | ~~853~~ | ~~115~~ | ~~266~~ | ~~12~~ | 397 | ~~3~~ | ~~30.4~~ |
| STB1-23 | 0.73 | 0.05327 | 0.0026 | 0.45492 | 0.02221 | 0.06192 | 0.00101 | 340 | 81 | 381 | 16 | 397 | 6 | -1.6 |
| STB1-24 | 0.46 | 0.05581 | 0.00196 | 0.54879 | 0.01942 | 0.07131 | 0.00111 | 445 | 51 | 444 | 13 | 397 | 7 | 0 |
| STB1-25 | 0.14 | 0.05004 | 0.00104 | 0.22414 | 0.00494 | 0.03248 | 0.00046 | 197 | 27 | 205 | 4 | 398 | 3 | -0.5 |
| STB1-26 | 0.49 | 0.05433 | 0.00123 | 0.47064 | 0.01117 | 0.06282 | 0.0009 | 385 | 29 | 392 | 8 | 403 | 5 | -0.3 |

| | | | | | | | | | | | | | | |
|---|---|---|---|---|---|---|---|---|---|---|---|---|---|---|
| STB1-27 | 0.44 | 0.05593 | 0.00103 | 0.53594 | 0.01066 | 0.06949 | 0.00098 | 450 | 22 | 436 | 7 | 405 | 6 | 0.7 |
| STB1-28 | 0.49 | 0.06068 | 0.00158 | 0.85437 | 0.02287 | 0.1021 | 0.00152 | 628 | 33 | 627 | 13 | 408 | 9 | 0 |
| STB1-29 | 1.35 | 0.05134 | 0.00268 | 0.28726 | 0.01495 | 0.04057 | 0.00068 | 256 | 89 | 256 | 12 | 410 | 4 | 0 |
| STB1-30 | 0.33 | 0.05568 | 0.00097 | 0.54703 | 0.01044 | 0.07124 | 0.001 | 440 | 20 | 443 | 7 | 410 | 6 | -0.2 |
| STB1-31 | 0.8 | 0.05012 | 0.00205 | 0.2343 | 0.00959 | 0.0339 | 0.00054 | 201 | 65 | 214 | 8 | 411 | 3 | -0.5 |
| STB1-32 | 0.5 | 0.05656 | 0.001 | 0.56948 | 0.01101 | 0.07301 | 0.00102 | 474 | 21 | 458 | 7 | 417 | 6 | 0.9 |
| STB1-33 | 0.48 | 0.07024 | 0.00122 | 1.44897 | 0.0276 | 0.14958 | 0.0021 | 935 | 19 | 909 | 11 | 421 | 12 | 1.1 |
| STB1-34 | 0.97 | 0.09148 | 0.00218 | 3.20456 | 0.0787 | 0.25402 | 0.00387 | 1457 | 25 | 1458 | 19 | ~~422~~ | 20 | -0.1 |
| STB1-35 | 0.1 | 0.05449 | 0.00101 | 0.46428 | 0.00931 | 0.06178 | 0.00087 | 391 | 22 | 387 | 6 | 423 | 5 | 0.3 |
| STB1-36 | 0.47 | 0.05533 | 0.00162 | 0.5406 | 0.0162 | 0.07084 | 0.00106 | 426 | 40 | 439 | 11 | 424 | 6 | -0.5 |
| STB1-37 | 0.38 | 0.09245 | 0.00164 | 3.21879 | 0.06225 | 0.25247 | 0.00359 | 1477 | 17 | 1462 | 15 | 426 | 18 | 1.8 |
| ~~STB1-38~~ | ~~1.24~~ | ~~0.06439~~ | ~~0.00192~~ | ~~0.62347~~ | ~~0.01884~~ | ~~0.07021~~ | ~~0.00107~~ | ~~754~~ | ~~38~~ | ~~492~~ | ~~12~~ | 426 | ~~6~~ | ~~12.6~~ |
| STB1-39 | 0.46 | 0.05453 | 0.00131 | 0.47798 | 0.01193 | 0.06356 | 0.00093 | 393 | 31 | 397 | 8 | 427 | 6 | 0 |
| STB1-40 | 0.43 | 0.05518 | 0.00317 | 0.52488 | 0.02897 | 0.06899 | 0.00109 | 420 | 132 | 428 | 19 | 429 | 7 | -0.5 |
| STB1-41 | 2.15 | 0.05948 | 0.00126 | 0.72158 | 0.01611 | 0.08797 | 0.00127 | 585 | 25 | 552 | 10 | 430 | 8 | 1.5 |
| STB1-42 | 0.24 | 0.05507 | 0.00109 | 0.49666 | 0.01048 | 0.06539 | 0.00093 | 415 | 24 | 409 | 7 | 430 | 6 | 0.2 |
| STB1-43 | 0.39 | 0.06999 | 0.00119 | 1.51548 | 0.02842 | 0.15701 | 0.0022 | 928 | 18 | 937 | 11 | 430 | 12 | -0.3 |
| STB1-44 | 1.08 | 0.12595 | 0.00216 | 6.03621 | 0.11346 | 0.34753 | 0.00494 | 2042 | 16 | 1981 | 16 | 432 | 24 | 6.2 |
| STB1-45 | 0.7 | 0.05703 | 0.00142 | 0.57489 | 0.01481 | 0.07309 | 0.00106 | 493 | 32 | 461 | 10 | 432 | 6 | 1.3 |
| STB1-46 | 0.66 | 0.05599 | 0.00135 | 0.54661 | 0.01372 | 0.07079 | 0.00103 | 452 | 31 | 443 | 9 | 433 | 6 | 0.5 |
| STB1-47 | 0.58 | 0.13022 | 0.0022 | 6.76647 | 0.12588 | 0.37679 | 0.00532 | 2101 | 15 | 2081 | 16 | 434 | 25 | 1.9 |
| STB1-48 | 0.64 | 0.06585 | 0.00162 | 1.2206 | 0.03115 | 0.1344 | 0.00198 | 802 | 30 | 810 | 14 | ~~437~~ | 11 | -0.4 |
| STB1-49 | 1.55 | 0.16565 | 0.00283 | 10.78044 | 0.20205 | 0.47191 | 0.00671 | 2514 | 15 | 2504 | 17 | 437 | 29 | 0.9 |
| STB1-50 | 0.13 | 0.07125 | 0.00128 | 1.56916 | 0.0307 | 0.15969 | 0.00226 | 965 | 19 | 958 | 12 | 441 | 13 | 0.3 |
| ~~STB1-51~~ | ~~0.77~~ | ~~0.1361~~ | ~~0.0046~~ | ~~6.40577~~ | ~~0.19248~~ | ~~0.34136~~ | ~~0.00526~~ | ~~2178~~ | ~~60~~ | ~~2033~~ | ~~26~~ | 441 | ~~25~~ | ~~15.1~~ |
| STB1-52 | 0.25 | 0.07623 | 0.00218 | 1.82383 | 0.04506 | 0.17352 | 0.00248 | 1101 | 58 | 1054 | 16 | 444 | 14 | 6.8 |
| STB1-53 | 0.64 | 0.04848 | 0.00369 | 0.1138 | 0.00862 | 0.01702 | 0.0003 | 123 | 136 | 109 | 8 | 444 | 2 | 0 |
| STB1-54 | 0.54 | 0.05095 | 0.00116 | 0.25012 | 0.00596 | 0.0356 | 0.00052 | 239 | 29 | 227 | 5 | 452 | 3 | 0.4 |

| | | | | | | | | | | | | | | |
|---|---|---|---|---|---|---|---|---|---|---|---|---|---|---|
| STB1-55 | 0.33 | 0.16697 | 0.00286 | 10.78672 | 0.20321 | 0.46843 | 0.00662 | 2527 | 15 | 2505 | 18 | 453 | 29 | 2 |
| ~~STB1-56~~ | ~~0.1~~ | ~~0.08148~~ | ~~0.00149~~ | ~~1.67286~~ | ~~0.03315~~ | ~~0.14888~~ | ~~0.00212~~ | ~~1233~~ | ~~19~~ | ~~998~~ | ~~13~~ | 454 | ~~12~~ | ~~11.5~~ |
| STB1-57 | 1.08 | 0.05566 | 0.00146 | 0.5315 | 0.01431 | 0.06924 | 0.00104 | 439 | 34 | 433 | 9 | 455 | 6 | 0.2 |
| STB1-58 | 0.5 | 0.05068 | 0.00148 | 0.23614 | 0.00707 | 0.03379 | 0.0005 | 226 | 42 | 215 | 6 | 455 | 3 | 0.5 |
| STB1-59 | 0.49 | 0.05548 | 0.0028 | 0.52282 | 0.02635 | 0.06833 | 0.00114 | 432 | 82 | 427 | 18 | 461 | 7 | 0.2 |
| STB1-60 | 0.52 | 0.05529 | 0.00158 | 0.4918 | 0.01437 | 0.06449 | 0.00097 | 424 | 39 | 406 | 10 | 544 | 6 | 0.7 |
| ~~STB1-61~~ | ~~0.5~~ | ~~0.06225~~ | ~~0.00124~~ | ~~0.58098~~ | ~~0.01236~~ | ~~0.06768~~ | ~~0.00097~~ | ~~683~~ | ~~23~~ | ~~465~~ | ~~8~~ | 627 | ~~6~~ | ~~10.2~~ |
| STB1-62 | 0.53 | 0.05647 | 0.00137 | 0.5357 | 0.01352 | 0.06879 | 0.00101 | 471 | 31 | 436 | 9 | 661 | 6 | 1.6 |
| STB1-63 | 0.59 | 0.17121 | 0.00315 | 11.01587 | 0.21934 | 0.46653 | 0.00676 | 2570 | 16 | 2524 | 19 | 763 | 30 | 4.1 |
| STB1-64 | 0.68 | 0.07084 | 0.00162 | 1.45359 | 0.03467 | 0.14878 | 0.00219 | 953 | 26 | 911 | 14 | 764 | 12 | 1.9 |
| STB1-65 | 0.3 | 0.07625 | 0.00234 | 1.55853 | 0.04218 | 0.14824 | 0.00214 | 1102 | 63 | 954 | 17 | 807 | 12 | 7.1 |
| STB1-66 | 0.27 | 0.07266 | 0.00136 | 1.58547 | 0.03205 | 0.15822 | 0.00226 | 1004 | 20 | 965 | 13 | 813 | 13 | 1.9 |
| STB1-67 | 0.24 | 0.06843 | 0.00132 | 1.3333 | 0.02756 | 0.14128 | 0.00202 | 882 | 21 | 860 | 12 | 829 | 11 | 0.9 |
| STB1-68 | 0.15 | 0.05564 | 0.00117 | 0.56088 | 0.01251 | 0.07309 | 0.00106 | 438 | 26 | 452 | 8 | 852 | 6 | -0.7 |
| STB1-69 | 0.34 | 0.11395 | 0.00209 | 4.89113 | 0.09739 | 0.31125 | 0.00444 | 1863 | 17 | 1801 | 17 | 889 | 22 | 6.6 |
| STB1-70 | 0.87 | 0.05442 | 0.00207 | 0.43599 | 0.01666 | 0.05809 | 0.00092 | 388 | 57 | 367 | 12 | 891 | 6 | 0.8 |
| STB1-71 | 0.33 | 0.05048 | 0.00152 | 0.25081 | 0.00767 | 0.03603 | 0.00054 | 217 | 43 | 227 | 6 | 894 | 3 | -0.4 |
| STB1-72 | 0.44 | 0.05264 | 0.00145 | 0.24033 | 0.00678 | 0.03311 | 0.00049 | 313 | 38 | 219 | 6 | ~~895~~ | 3 | 4.3 |
| STB1-73 | 0.32 | 0.07472 | 0.00151 | 1.82576 | 0.03938 | 0.17718 | 0.00257 | 1061 | 22 | 1055 | 14 | 899 | 14 | 0.9 |
| STB1-74 | 0.6 | 0.05554 | 0.00124 | 0.51896 | 0.01218 | 0.06775 | 0.00099 | 434 | 28 | 424 | 8 | 902 | 6 | 0.2 |
| STB1-75 | 1.91 | 0.06593 | 0.00256 | 1.24721 | 0.04852 | 0.13716 | 0.00225 | 804 | 54 | 822 | 22 | 922 | 13 | -0.8 |
| STB1-76 | 0.24 | 0.06983 | 0.0016 | 1.44633 | 0.03457 | 0.15018 | 0.00222 | 923 | 26 | 908 | 14 | 940 | 12 | 0.7 |
| STB1-77 | 0.39 | 0.04979 | 0.00238 | 0.22277 | 0.01064 | 0.03244 | 0.00054 | 185 | 80 | 204 | 9 | 947 | 3 | -1 |
| STB1-78 | 0.08 | 0.05421 | 0.00125 | 0.42855 | 0.01035 | 0.05732 | 0.00084 | 380 | 29 | 362 | 7 | 955 | 5 | 0.8 |
| STB1-79 | 0.59 | 0.05181 | 0.00233 | 0.30845 | 0.01391 | 0.04316 | 0.00069 | 277 | 74 | 273 | 11 | 1031 | 4 | 0.4 |
| STB1-80 | 0.35 | 0.05535 | 0.00204 | 0.50143 | 0.01865 | 0.06569 | 0.00103 | 426 | 55 | 413 | 13 | 1042 | 6 | 0.7 |
| STB1-81 | 0.55 | 0.07416 | 0.00158 | 1.79384 | 0.04043 | 0.17539 | 0.00257 | 1046 | 23 | 1043 | 15 | 1052 | 14 | 0.4 |
| ~~STB1-82~~ | ~~1.49~~ | ~~0.10555~~ | ~~0.00732~~ | ~~3.9133~~ | ~~0.26147~~ | ~~0.26888~~ | ~~0.00503~~ | ~~1724~~ | ~~131~~ | ~~1616~~ | ~~54~~ | 1384 | ~~26~~ | ~~12.3~~ |

| | | | | | | | | | | | | | | |
|---|---|---|---|---|---|---|---|---|---|---|---|---|---|---|
| STB1-83 | 0.31 | 0.19677 | 0.00376 | 13.31079 | 0.27393 | 0.4905 | 0.00704 | 2800 | 17 | 2702 | 19 | 1451 | 30 | 8.8 |
| STB1-84 | 0.92 | 0.06687 | 0.00177 | 1.1607 | 0.03152 | 0.12586 | 0.0019 | 834 | 32 | 782 | 15 | 1459 | 11 | 2.4 |
| STB1-85 | 0.57 | 0.05702 | 0.00208 | 0.53851 | 0.01982 | 0.06848 | 0.00108 | 492 | 53 | 437 | 13 | 1534 | 7 | 2.3 |
| STB1-86 | 0.18 | 0.07131 | 0.0015 | 1.45433 | 0.03239 | 0.14788 | 0.00216 | 966 | 23 | 912 | 13 | ~~1535~~ | 12 | 2.6 |
| STB1-87 | 0.62 | 0.05843 | 0.00177 | 0.5129 | 0.0158 | 0.06365 | 0.00098 | 546 | 41 | 420 | 11 | 1569 | 6 | 5.5 |
| STB1-88 | 0.59 | 0.05643 | 0.00131 | 0.48084 | 0.01166 | 0.06178 | 0.00091 | 469 | 29 | 399 | 8 | ~~1573~~ | 6 | 3.4 |
| STB1-89 | 0.83 | 0.0554 | 0.00201 | 0.51021 | 0.0187 | 0.06678 | 0.00105 | 428 | 54 | 419 | 13 | ~~1680~~ | 6 | 0.5 |
| STB1-90 | 0.31 | 0.06638 | 0.00174 | 1.14987 | 0.0309 | 0.1256 | 0.00191 | 818 | 32 | 777 | 15 | 1747 | 11 | 1.8 |
| ~~STB1-91~~ | ~~1.16~~ | ~~0.15979~~ | ~~0.00322~~ | ~~9.06795~~ | ~~0.19497~~ | ~~0.41147~~ | ~~0.006~~ | ~~2453~~ | ~~18~~ | ~~2345~~ | ~~20~~ | ~~1893~~ | ~~27~~ | ~~10.4~~ |
| STB1-92 | 0.13 | 0.10057 | 0.00272 | 3.82211 | 0.08752 | 0.27562 | 0.00396 | 1635 | 51 | 1597 | 18 | 1923 | 20 | 4.2 |
| STB1-93 | 0.48 | 0.07149 | 0.00173 | 1.51524 | 0.03803 | 0.15367 | 0.0023 | 971 | 28 | 937 | 15 | 2061 | 13 | 1.6 |
| STB1-94 | 0.71 | 0.06735 | 0.00226 | 1.23843 | 0.04202 | 0.13333 | 0.00211 | 849 | 44 | 818 | 19 | 2078 | 12 | 1.4 |
| STB1-95 | 0.44 | 0.0547 | 0.00162 | 0.47926 | 0.01448 | 0.06353 | 0.00097 | 400 | 41 | 398 | 10 | ~~2222~~ | 6 | 0.3 |
| STB1-96 | 0.67 | 0.05307 | 0.00202 | 0.35394 | 0.01355 | 0.04836 | 0.00077 | 332 | 58 | 308 | 10 | ~~2225~~ | 5 | 1.3 |
| STB1-97 | 0.51 | 0.09188 | 0.00194 | 3.03522 | 0.06773 | 0.23953 | 0.00351 | 1465 | 22 | 1417 | 17 | 2468 | 18 | 5.9 |
| ~~STB1-98~~ | ~~0.21~~ | ~~0.1174~~ | ~~0.00248~~ | ~~4.82143~~ | ~~0.10774~~ | ~~0.29777~~ | ~~0.00439~~ | ~~1917~~ | ~~20~~ | ~~1789~~ | ~~19~~ | 2477 | ~~22~~ | ~~14.1~~ |
| STB1-99 | 0.5 | 0.05644 | 0.00197 | 0.54593 | 0.01927 | 0.07013 | 0.0011 | 470 | 50 | 442 | 13 | 2492 | 7 | 1.1 |
| STB1-100 | 1.03 | 0.05622 | 0.00127 | 0.53473 | 0.01263 | 0.06896 | 0.00102 | 461 | 28 | 435 | 8 | 2573 | 6 | 1.2 |
| | | | | | | | | | | | | | | |
| **Q403** | | | | | | | | | | | | | | |
| ~~Q403-01~~ | ~~0.49~~ | ~~0.06843~~ | ~~0.00434~~ | ~~0.64807~~ | ~~0.03914~~ | ~~0.06869~~ | ~~0.00132~~ | ~~882~~ | ~~135~~ | ~~507~~ | ~~24~~ | ~~428~~ | ~~8~~ | ~~18.5~~ |
| Q403-02 | 0.55 | 0.05685 | 0.00175 | 0.60512 | 0.01894 | 0.07718 | 0.00122 | 486 | 42 | 480 | 12 | 479 | 7 | 0.2 |
| ~~Q403-03~~ | ~~0.52~~ | ~~0.06584~~ | ~~0.00384~~ | ~~0.66653~~ | ~~0.03726~~ | ~~0.07343~~ | ~~0.00122~~ | ~~801~~ | ~~126~~ | ~~519~~ | ~~23~~ | ~~457~~ | ~~7~~ | ~~13.6~~ |
| Q403-04 | 0.87 | 0.0579 | 0.00191 | 0.56907 | 0.01904 | 0.07127 | 0.00114 | 526 | 46 | 457 | 12 | 444 | 7 | 2.9 |
| Q403-05 | 0.57 | 0.06187 | 0.00203 | 0.61208 | 0.02022 | 0.07173 | 0.00117 | 670 | 43 | 485 | 13 | 447 | 7 | 8.5 |
| Q403-06 | 0.6 | 0.06037 | 0.0017 | 0.60268 | 0.01728 | 0.07239 | 0.00114 | 617 | 35 | 479 | 11 | 451 | 7 | 6.2 |
| ~~Q403-07~~ | ~~1.37~~ | ~~0.06285~~ | ~~0.00437~~ | ~~0.34196~~ | ~~0.02355~~ | ~~0.03945~~ | ~~0.00077~~ | ~~703~~ | ~~114~~ | ~~299~~ | ~~18~~ | ~~249~~ | ~~5~~ | ~~20.1~~ |
| Q403-08 | 0.61 | 0.05629 | 0.00159 | 0.59724 | 0.01723 | 0.07694 | 0.00121 | 464 | 37 | 475 | 11 | 478 | 7 | -0.6 |

| | | | | | | | | | | | | | | |
|---|---|---|---|---|---|---|---|---|---|---|---|---|---|---|
| ~~Q403-09~~ | ~~0.44~~ | ~~0.06453~~ | ~~0.00216~~ | ~~0.68501~~ | ~~0.02301~~ | ~~0.07698~~ | ~~0.00127~~ | ~~759~~ | ~~43~~ | ~~530~~ | ~~14~~ | ~~478~~ | ~~8~~ | ~~10.9~~ |
| ~~Q403-10~~ | ~~0.49~~ | ~~0.08273~~ | ~~0.00211~~ | ~~0.66928~~ | ~~0.01757~~ | ~~0.05866~~ | ~~0.00092~~ | ~~1263~~ | ~~28~~ | ~~520~~ | ~~11~~ | ~~367~~ | ~~6~~ | ~~41.7~~ |
| Q403-11 | 0.83 | 0.05725 | 0.0081 | 0.50473 | 0.07052 | 0.06394 | 0.00142 | 501 | 318 | 415 | 48 | 400 | 9 | 3.8 |
| ~~Q403-12~~ | ~~0.75~~ | ~~0.06093~~ | ~~0.00197~~ | ~~0.38698~~ | ~~0.01264~~ | ~~0.04606~~ | ~~0.00075~~ | ~~637~~ | ~~43~~ | ~~332~~ | ~~9~~ | ~~290~~ | ~~5~~ | ~~14.5~~ |
| Q403-13 | 0.58 | 0.06126 | 0.00171 | 0.61988 | 0.01774 | 0.07338 | 0.00116 | 648 | 35 | 490 | 11 | 456 | 7 | 7.5 |
| Q403-14 | 0.41 | 0.05686 | 0.00161 | 0.59418 | 0.01715 | 0.07578 | 0.0012 | 486 | 36 | 474 | 11 | 471 | 7 | 0.6 |
| ~~Q403-15~~ | ~~0.54~~ | ~~0.06358~~ | ~~0.00167~~ | ~~0.64869~~ | ~~0.01754~~ | ~~0.07399~~ | ~~0.00116~~ | ~~728~~ | ~~32~~ | ~~508~~ | ~~11~~ | ~~460~~ | ~~7~~ | ~~10.4~~ |
| Q403-16 | 0.5 | 0.05496 | 0.00275 | 0.49856 | 0.0249 | 0.06578 | 0.00115 | 411 | 80 | 411 | 17 | 411 | 7 | 0 |
| ~~Q403-17~~ | ~~0.77~~ | ~~0.06835~~ | ~~0.00328~~ | ~~0.37156~~ | ~~0.01766~~ | ~~0.03942~~ | ~~0.00071~~ | ~~879~~ | ~~68~~ | ~~321~~ | ~~13~~ | ~~249~~ | 4 | ~~28.9~~ |
| Q403-18 | 0.55 | 0.05656 | 0.00174 | 0.58757 | 0.01841 | 0.07533 | 0.00121 | 474 | 41 | 469 | 12 | 468 | 7 | 0.2 |
| Q403-19 | 0.82 | 0.05622 | 0.00231 | 0.55279 | 0.02278 | 0.07129 | 0.00121 | 461 | 61 | 447 | 15 | 444 | 7 | 0.7 |
| Q403-20 | 0.5 | 0.06249 | 0.00336 | 0.67328 | 0.03436 | 0.07814 | 0.00131 | 691 | 118 | 523 | 21 | 485 | 8 | 7.8 |
| ~~Q403-21~~ | ~~0.47~~ | ~~0.06478~~ | ~~0.002~~ | ~~0.63625~~ | ~~0.01986~~ | ~~0.07122~~ | ~~0.00116~~ | ~~767~~ | ~~39~~ | ~~500~~ | ~~12~~ | ~~444~~ | ~~7~~ | ~~12.6~~ |
| Q403-22 | 0.61 | 0.06153 | 0.00173 | 0.63293 | 0.01821 | 0.07459 | 0.00119 | 658 | 35 | 498 | 11 | 464 | 7 | 7.3 |
| Q403-23 | 0.48 | 0.06577 | 0.00366 | 0.52305 | 0.0277 | 0.05768 | 0.00098 | 799 | 120 | 427 | 18 | 362 | 6 | 18 |
| Q403-24 | 0.57 | 0.05682 | 0.00154 | 0.59405 | 0.01656 | 0.07582 | 0.0012 | 485 | 35 | 473 | 11 | 471 | 7 | 0.4 |
| ~~Q403-25~~ | ~~0.73~~ | ~~0.06584~~ | ~~0.00862~~ | ~~0.51336~~ | ~~0.06636~~ | ~~0.05655~~ | ~~0.00118~~ | ~~801~~ | ~~290~~ | ~~421~~ | ~~45~~ | ~~355~~ | ~~7~~ | ~~18.6~~ |
| Q403-26 | 0.55 | 0.0565 | 0.00171 | 0.58668 | 0.01803 | 0.0753 | 0.00122 | 472 | 40 | 469 | 12 | 468 | 7 | 0.2 |
| Q403-27 | 0.45 | 0.05635 | 0.0015 | 0.58977 | 0.01623 | 0.07589 | 0.00111 | 466 | 36 | 471 | 10 | 472 | 7 | -0.2 |
| Q403-28 | 0.62 | 0.06266 | 0.00137 | 0.61509 | 0.0141 | 0.07118 | 0.00104 | 697 | 25 | 487 | 9 | 443 | 6 | 9.9 |
| ~~Q403-29~~ | ~~0.58~~ | ~~0.06469~~ | ~~0.00146~~ | ~~0.62845~~ | ~~0.01483~~ | ~~0.07045~~ | ~~0.00103~~ | ~~764~~ | ~~26~~ | ~~495~~ | ~~9~~ | ~~439~~ | ~~6~~ | ~~12.8~~ |
| Q403-30 | 0.53 | 0.05706 | 0.00118 | 0.56547 | 0.01244 | 0.07186 | 0.00103 | 494 | 25 | 455 | 8 | 447 | 6 | 1.8 |
| Q403-31 | 0.49 | 0.05645 | 0.00144 | 0.56835 | 0.01494 | 0.07301 | 0.00108 | 470 | 33 | 457 | 10 | 454 | 6 | 0.7 |
| ~~Q403-32~~ | ~~0.43~~ | ~~0.06836~~ | ~~0.00242~~ | ~~0.56449~~ | ~~0.01822~~ | ~~0.05989~~ | ~~0.00087~~ | ~~879~~ | ~~75~~ | ~~454~~ | ~~12~~ | ~~375~~ | ~~5~~ | ~~21.1~~ |
| Q403-33 | 0.57 | 0.05893 | 0.00134 | 0.58816 | 0.01395 | 0.07236 | 0.00106 | 565 | 27 | 470 | 9 | 450 | 6 | 4.4 |
| Q403-34 | 0.51 | 0.0571 | 0.00106 | 0.58914 | 0.01184 | 0.07481 | 0.00106 | 495 | 22 | 470 | 8 | 465 | 6 | 1.1 |
| Q403-35 | 0.96 | 0.06064 | 0.00456 | 0.20597 | 0.01505 | 0.02464 | 0.00043 | 626 | 167 | 190 | 13 | 157 | 3 | 21 |
| ~~Q403-36~~ | ~~0.24~~ | ~~0.07433~~ | ~~0.00258~~ | ~~1.1498~~ | ~~0.04003~~ | ~~0.11216~~ | ~~0.00182~~ | ~~1050~~ | ~~44~~ | ~~777~~ | ~~19~~ | ~~685~~ | ~~11~~ | ~~13.4~~ |

| | | | | | | | | | | | | | | |
|---|---|---|---|---|---|---|---|---|---|---|---|---|---|---|
| Q403-37 | 0.75 | 0.05794 | 0.00409 | 0.55212 | 0.03891 | 0.06909 | 0.00118 | 527 | 125 | 446 | 25 | 431 | 7 | 3.5 |
| Q403-38 | 0.65 | 0.05815 | 0.00128 | 0.53778 | 0.01241 | 0.06706 | 0.00098 | 535 | 26 | 437 | 8 | 418 | 6 | 4.5 |
| Q403-39 | 0.52 | 0.05645 | 0.00141 | 0.5714 | 0.01482 | 0.07339 | 0.00108 | 470 | 32 | 459 | 10 | 457 | 6 | 0.4 |
| Q403-40 | 0.45 | 0.05756 | 0.0018 | 0.59396 | 0.01891 | 0.07482 | 0.00114 | 513 | 43 | 473 | 12 | 465 | 7 | 1.7 |
| Q403-41 | 0.48 | 0.05597 | 0.00141 | 0.5781 | 0.01507 | 0.0749 | 0.0011 | 451 | 33 | 463 | 10 | 466 | 7 | -0.6 |
| Q403-42 | 0.4 | 0.05564 | 0.00126 | 0.56477 | 0.01336 | 0.0736 | 0.00107 | 438 | 28 | 455 | 9 | 458 | 6 | -0.7 |
| Q403-43 | 0.41 | 0.0562 | 0.00148 | 0.57617 | 0.01561 | 0.07434 | 0.00111 | 460 | 34 | 462 | 10 | 462 | 7 | 0 |
| Q403-44 | 0.45 | 0.05602 | 0.00141 | 0.57964 | 0.01508 | 0.07503 | 0.00111 | 453 | 32 | 464 | 10 | 466 | 7 | -0.4 |
| Q403-45 | 0.51 | 0.05633 | 0.00147 | 0.57414 | 0.01544 | 0.07391 | 0.0011 | 465 | 34 | 461 | 10 | 460 | 7 | 0.2 |
| Q403-46 | 0.38 | 0.05725 | 0.00132 | 0.65318 | 0.01578 | 0.08274 | 0.00121 | 501 | 29 | 510 | 10 | 512 | 7 | -0.4 |
| Q403-47 | 0.44 | 0.05666 | 0.00192 | 0.57899 | 0.01985 | 0.07409 | 0.00115 | 478 | 48 | 464 | 13 | 461 | 7 | 0.7 |
| Q403-48 | 0.5 | 0.05545 | 0.00256 | 0.52398 | 0.02416 | 0.06852 | 0.00112 | 430 | 73 | 428 | 16 | 427 | 7 | 0.2 |
| Q403-49 | 0.51 | 0.05647 | 0.00162 | 0.58504 | 0.01724 | 0.07512 | 0.00112 | 471 | 39 | 468 | 11 | 467 | 7 | 0.2 |
| Q403-50 | 0.41 | 0.0567 | 0.00127 | 0.59285 | 0.01399 | 0.07582 | 0.0011 | 480 | 28 | 473 | 9 | 471 | 7 | 0.4 |
| ~~Q403-51~~ | ~~0.56~~ | ~~0.06394~~ | ~~0.0015~~ | ~~0.65575~~ | ~~0.01594~~ | ~~0.07437~~ | ~~0.00111~~ | ~~740~~ | ~~27~~ | ~~512~~ | ~~10~~ | ~~462~~ | ~~7~~ | ~~10.8~~ |
| Q403-52 | 0.47 | 0.05701 | 0.00167 | 0.62888 | 0.01876 | 0.07998 | 0.00121 | 492 | 39 | 495 | 12 | 496 | 7 | -0.2 |
| Q403-53 | 0.47 | 0.05676 | 0.00162 | 0.60627 | 0.0177 | 0.07745 | 0.00117 | 482 | 38 | 481 | 11 | 481 | 7 | 0 |
| Q403-54 | 0.37 | 0.05639 | 0.00151 | 0.58547 | 0.0161 | 0.07529 | 0.00112 | 468 | 35 | 468 | 10 | 468 | 7 | 0 |
| Q403-55 | 0.44 | 0.05599 | 0.00127 | 0.55434 | 0.01319 | 0.07179 | 0.00105 | 452 | 28 | 448 | 9 | 447 | 6 | 0.2 |
| Q403-56 | 0.56 | 0.06928 | 0.00161 | 1.4616 | 0.03534 | 0.15298 | 0.00229 | 907 | 26 | 915 | 15 | 918 | 13 | -0.3 |
| Q403-57 | 0.52 | 0.05768 | 0.00137 | 0.58718 | 0.01446 | 0.07381 | 0.00109 | 518 | 29 | 469 | 9 | 459 | 7 | 2.2 |
| Q403-58 | 0.5 | 0.05549 | 0.00221 | 0.54558 | 0.02179 | 0.07129 | 0.00113 | 432 | 61 | 442 | 14 | 444 | 7 | -0.5 |
| Q403-59 | 0.43 | 0.05648 | 0.00194 | 0.56374 | 0.01953 | 0.07238 | 0.00114 | 471 | 49 | 454 | 13 | 450 | 7 | 0.9 |
| Q403-60 | 0.48 | 0.05561 | 0.0015 | 0.53042 | 0.01472 | 0.06916 | 0.00104 | 437 | 36 | 432 | 10 | 431 | 6 | 0.2 |
| Q403-61 | 0.34 | 0.05481 | 0.00412 | 0.50259 | 0.0375 | 0.06649 | 0.00125 | 404 | 134 | 413 | 25 | 415 | 8 | -0.5 |
| Q403-62 | 0.39 | 0.0553 | 0.00145 | 0.57794 | 0.01559 | 0.07578 | 0.00113 | 424 | 34 | 463 | 10 | 471 | 7 | -1.7 |
| Q403-63 | 0.61 | 0.05979 | 0.00585 | 0.53118 | 0.05111 | 0.06443 | 0.00116 | 596 | 220 | 433 | 34 | 403 | 7 | 7.4 |
| Q403-64 | 0.47 | 0.0561 | 0.00177 | 0.56241 | 0.01806 | 0.07269 | 0.00111 | 456 | 44 | 453 | 12 | 452 | 7 | 0.2 |

| | | | | | | | | | | | | | | |
|---|---|---|---|---|---|---|---|---|---|---|---|---|---|---|
| Q403-65 | 0.4 | 0.05891 | 0.00269 | 0.61049 | 0.02628 | 0.07516 | 0.00116 | 564 | 102 | 484 | 17 | 467 | 7 | 3.6 |
| Q403-66 | 0.53 | 0.05646 | 0.00147 | 0.58353 | 0.01567 | 0.07494 | 0.00113 | 471 | 34 | 467 | 10 | 466 | 7 | 0.2 |
| Q403-67 | 0.6 | 0.05667 | 0.00152 | 0.60076 | 0.01651 | 0.07686 | 0.00116 | 479 | 35 | 478 | 10 | 477 | 7 | 0.2 |
| Q403-68 | 0.76 | 0.05154 | 0.00298 | 0.30641 | 0.01766 | 0.0431 | 0.00073 | 265 | 101 | 271 | 14 | 272 | 5 | -0.4 |
| Q403-69 | 0.54 | 0.05613 | 0.00189 | 0.58332 | 0.01976 | 0.07536 | 0.0012 | 458 | 47 | 467 | 13 | 468 | 7 | -0.2 |
| Q403-70 | 0.34 | 0.05597 | 0.00177 | 0.53914 | 0.01725 | 0.06985 | 0.0011 | 451 | 43 | 438 | 11 | 435 | 7 | 0.7 |
| ~~Q403-71~~ | ~~0.44~~ | ~~0.04605~~ | ~~0.00753~~ | ~~0.46074~~ | ~~0.075~~ | ~~0.07257~~ | ~~0.00111~~ | | ~~288~~ | ~~385~~ | ~~52~~ | ~~452~~ | ~~7~~ | ~~-14.8~~ |
| Q403-72 | 0.45 | 0.05792 | 0.00143 | 0.60186 | 0.01542 | 0.07535 | 0.00113 | 527 | 31 | 478 | 10 | 468 | 7 | 2.1 |
| Q403-73 | 0.96 | 0.0564 | 0.00129 | 0.59157 | 0.0141 | 0.07605 | 0.00113 | 468 | 28 | 472 | 9 | 473 | 7 | -0.2 |
| Q403-74 | 0.54 | 0.0561 | 0.00154 | 0.56246 | 0.01574 | 0.07269 | 0.00112 | 456 | 35 | 453 | 10 | 452 | 7 | 0.2 |
| Q403-75 | 0.4 | 0.05497 | 0.00224 | 0.50451 | 0.02064 | 0.06655 | 0.00106 | 411 | 63 | 415 | 14 | 415 | 6 | 0 |
| Q403-76 | 0.43 | 0.05694 | 0.00156 | 0.61212 | 0.01723 | 0.07795 | 0.00119 | 489 | 36 | 485 | 11 | 484 | 7 | 0.2 |
| Q403-77 | 0.48 | 0.05518 | 0.00539 | 0.5107 | 0.04951 | 0.06711 | 0.00139 | 420 | 181 | 419 | 33 | 419 | 8 | 0 |
| Q403-78 | 0.42 | 0.05628 | 0.00198 | 0.60597 | 0.0215 | 0.07808 | 0.00122 | 463 | 51 | 481 | 14 | 485 | 7 | -0.8 |
| Q403-79 | 0.43 | 0.05659 | 0.00128 | 0.59582 | 0.01411 | 0.07634 | 0.00113 | 476 | 28 | 475 | 9 | 474 | 7 | 0.2 |
| Q403-80 | 0.38 | 0.05706 | 0.00181 | 0.60111 | 0.0194 | 0.07639 | 0.00118 | 494 | 44 | 478 | 12 | 475 | 7 | 0.6 |
| Q403-81 | 0.51 | 0.05673 | 0.00167 | 0.59647 | 0.0179 | 0.07624 | 0.00119 | 481 | 39 | 475 | 11 | 474 | 7 | 0.2 |
| Q403-82 | 0.43 | 0.05683 | 0.00181 | 0.59412 | 0.01916 | 0.0758 | 0.00118 | 485 | 44 | 473 | 12 | 471 | 7 | 0.4 |
| Q403-83 | 0.7 | 0.05633 | 0.00156 | 0.58063 | 0.01651 | 0.07474 | 0.00114 | 465 | 37 | 465 | 11 | 465 | 7 | 0 |
| Q403-84 | 0.45 | 0.06077 | 0.00161 | 0.60342 | 0.01641 | 0.072 | 0.0011 | 631 | 33 | 479 | 10 | 448 | 7 | 6.9 |
| Q403-85 | 0.63 | 0.05829 | 0.00184 | 0.58412 | 0.01868 | 0.07267 | 0.00114 | 541 | 43 | 467 | 12 | 452 | 7 | 3.3 |
| Q403-86 | 0.49 | 0.05628 | 0.00136 | 0.5859 | 0.01475 | 0.07549 | 0.00113 | 463 | 30 | 468 | 9 | 469 | 7 | -0.2 |
| Q403-87 | 0.44 | 0.05644 | 0.0018 | 0.59256 | 0.01915 | 0.07613 | 0.00118 | 470 | 44 | 473 | 12 | 473 | 7 | 0 |
| Q403-88 | 0.64 | 0.05671 | 0.00225 | 0.59956 | 0.0239 | 0.07666 | 0.00124 | 480 | 59 | 477 | 15 | 476 | 7 | 0.2 |
| Q403-89 | 0.42 | 0.05989 | 0.00184 | 0.63213 | 0.01976 | 0.07653 | 0.00119 | 600 | 41 | 497 | 12 | 475 | 7 | 4.6 |
| Q403-90 | 0.29 | 0.05657 | 0.00138 | 0.59733 | 0.0151 | 0.07657 | 0.00115 | 475 | 30 | 476 | 10 | 476 | 7 | 0 |
| Q403-91 | 0.38 | 0.05572 | 0.00167 | 0.56384 | 0.01726 | 0.07337 | 0.00113 | 441 | 41 | 454 | 11 | 456 | 7 | -0.4 |
| Q403-92 | 0.47 | 0.05701 | 0.00174 | 0.60382 | 0.01871 | 0.0768 | 0.0012 | 492 | 41 | 480 | 12 | 477 | 7 | 0.6 |

| | | | | | | | | | | | | | | |
|---|---|---|---|---|---|---|---|---|---|---|---|---|---|---|
| Q403-93 | 0.47 | 0.05681 | 0.00145 | 0.58483 | 0.01537 | 0.07464 | 0.00113 | 484 | 32 | 468 | 10 | 464 | 7 | 0.9 |
| Q403-94 | 0.43 | 0.05538 | 0.00181 | 0.49459 | 0.01633 | 0.06475 | 0.00102 | 428 | 46 | 408 | 11 | 404 | 6 | 1 |
| Q403-95 | 0.43 | 0.15172 | 0.00306 | 9.71889 | 0.20896 | 0.46448 | 0.00685 | 2365 | 18 | 2408 | 20 | 2459 | 30 | -3.8 |
| Q403-96 | 0.55 | 0.06759 | 0.00328 | 0.85065 | 0.03901 | 0.09128 | 0.00146 | 856 | 103 | 625 | 21 | 563 | 9 | 11 |
| Q403-97 | 0.58 | 0.05964 | 0.00279 | 0.60579 | 0.02674 | 0.07367 | 0.00114 | 590 | 104 | 481 | 17 | 458 | 7 | 5 |
| Q403-98 | 0.89 | 0.0563 | 0.0014 | 0.59385 | 0.01528 | 0.07648 | 0.00115 | 464 | 31 | 473 | 10 | 475 | 7 | -0.4 |
| Q403-99 | 0.59 | 0.0939 | 0.00198 | 3.31967 | 0.07414 | 0.25633 | 0.0038 | 1506 | 21 | 1486 | 17 | 1471 | 19 | 2.4 |
| ~~Q403-100~~ | ~~0.79~~ | ~~0.11625~~ | ~~0.00239~~ | ~~4.15385~~ | ~~0.09093~~ | ~~0.25909~~ | ~~0.00382~~ | ~~1899~~ | ~~20~~ | ~~1665~~ | ~~18~~ | ~~1485~~ | ~~20~~ | ~~27.9~~ |
| **Q1618** | | | | | | | | | | | | | | |
| Q1618-001 | 0.53 | 0.05506 | 0.00111 | 0.51778 | 0.0113 | 0.0682 | 0.001 | 415 | 25 | 424 | 8 | 425 | 6 | -0.2 |
| Q1618-002 | 0.28 | 0.05486 | 0.00372 | 0.4751 | 0.03211 | 0.06279 | 0.00113 | 407 | 119 | 395 | 22 | 393 | 7 | 0.5 |
| Q1618-003 | 0.45 | 0.05527 | 0.00113 | 0.518 | 0.01145 | 0.06796 | 0.001 | 423 | 25 | 424 | 8 | 424 | 6 | 0 |
| Q1618-004 | 0.41 | 0.05509 | 0.00132 | 0.46525 | 0.01175 | 0.06124 | 0.00091 | 416 | 31 | 388 | 8 | 383 | 6 | 1.3 |
| Q1618-005 | 0.24 | 0.05415 | 0.00275 | 0.45398 | 0.0231 | 0.06079 | 0.00103 | 377 | 84 | 380 | 16 | 380 | 6 | 0 |
| Q1618-006 | 0.5 | 0.05397 | 0.00519 | 0.45224 | 0.0432 | 0.06076 | 0.00125 | 370 | 178 | 379 | 30 | 380 | 8 | -0.3 |
| Q1618-007 | 0.5 | 0.05508 | 0.00109 | 0.51566 | 0.01107 | 0.06789 | 0.001 | 415 | 24 | 422 | 7 | 423 | 6 | -0.2 |
| Q1618-008 | 0.39 | 0.05671 | 0.00114 | 0.53093 | 0.01157 | 0.06789 | 0.001 | 480 | 24 | 432 | 8 | 423 | 6 | 2.1 |
| Q1618-009 | 0.26 | 0.05403 | 0.00121 | 0.47919 | 0.01142 | 0.06431 | 0.00096 | 372 | 28 | 398 | 8 | 402 | 6 | -1 |
| Q1618-010 | 0.39 | 0.05501 | 0.00122 | 0.52444 | 0.01238 | 0.06913 | 0.00103 | 413 | 28 | 428 | 8 | 431 | 6 | -0.7 |
| Q1618-011 | 0.43 | 0.05552 | 0.00125 | 0.51725 | 0.01243 | 0.06755 | 0.001 | 433 | 28 | 423 | 8 | 421 | 6 | 0.5 |
| Q1618-012 | 0.49 | 0.05774 | 0.00124 | 0.54041 | 0.01249 | 0.06787 | 0.001 | 520 | 26 | 439 | 8 | 423 | 6 | 3.8 |
| Q1618-013 | 0.37 | 0.06115 | 0.00135 | 0.58499 | 0.01371 | 0.06937 | 0.00104 | 645 | 26 | 468 | 9 | 432 | 6 | 8.3 |
| Q1618-014 | 0.47 | 0.05549 | 0.00122 | 0.53392 | 0.01254 | 0.06977 | 0.00104 | 432 | 27 | 434 | 8 | 435 | 6 | -0.2 |
| Q1618-015 | 0.54 | 0.05526 | 0.00099 | 0.5205 | 0.01037 | 0.0683 | 0.001 | 423 | 21 | 425 | 7 | 426 | 6 | -0.2 |
| Q1618-016 | 0.37 | 0.05507 | 0.00117 | 0.52209 | 0.01184 | 0.06874 | 0.00102 | 415 | 26 | 427 | 8 | 429 | 6 | -0.5 |
| Q1618-017 | 0.39 | 0.05539 | 0.00105 | 0.54117 | 0.01122 | 0.07085 | 0.00104 | 428 | 23 | 439 | 7 | 441 | 6 | -0.5 |
| Q1618-018 | 0.52 | 0.05633 | 0.00103 | 0.52379 | 0.01058 | 0.06743 | 0.00098 | 465 | 22 | 428 | 7 | 421 | 6 | 1.7 |

| | | | | | | | | | | | | | | |
|---|---|---|---|---|---|---|---|---|---|---|---|---|---|---|
| Q1618-019 | 0.3 | 0.05404 | 0.00108 | 0.45158 | 0.00979 | 0.06059 | 0.00089 | 373 | 24 | 378 | 7 | 379 | 5 | -0.3 |
| Q1618-020 | 0.37 | 0.10417 | 0.00145 | 4.12592 | 0.06831 | 0.28719 | 0.00414 | 1700 | 14 | 1659 | 14 | 1627 | 21 | 4.5 |
| Q1618-021 | 0.36 | 0.05543 | 0.00205 | 0.52509 | 0.01772 | 0.0687 | 0.00103 | 430 | 84 | 429 | 12 | 428 | 6 | 0.2 |
| Q1618-022 | 0.36 | 0.0552 | 0.00121 | 0.52596 | 0.01228 | 0.06909 | 0.00102 | 420 | 27 | 429 | 8 | 431 | 6 | -0.5 |
| Q1618-023 | 0.44 | 0.05518 | 0.00255 | 0.53374 | 0.02325 | 0.07015 | 0.00109 | 420 | 106 | 434 | 15 | 437 | 7 | -0.7 |
| Q1618-024 | 0.56 | 0.05365 | 0.00147 | 0.46778 | 0.01324 | 0.06323 | 0.00098 | 356 | 37 | 390 | 9 | 395 | 6 | -1.3 |
| Q1618-025 | 0.42 | 0.05688 | 0.00263 | 0.53023 | 0.02303 | 0.06761 | 0.00106 | 487 | 105 | 432 | 15 | 422 | 6 | 2.4 |
| Q1618-026 | 0.33 | 0.05642 | 0.00109 | 0.53252 | 0.01123 | 0.06844 | 0.00101 | 469 | 23 | 433 | 7 | 427 | 6 | 1.4 |
| Q1618-027 | 0.31 | 0.05389 | 0.00378 | 0.46642 | 0.03268 | 0.06276 | 0.00111 | 366 | 127 | 389 | 23 | 392 | 7 | -0.8 |
| Q1618-028 | 0.45 | 0.05427 | 0.00131 | 0.48401 | 0.01234 | 0.06467 | 0.00097 | 382 | 31 | 401 | 8 | 404 | 6 | -0.7 |
| Q1618-029 | 0.47 | 0.05572 | 0.00126 | 0.53683 | 0.01291 | 0.06987 | 0.00104 | 441 | 28 | 436 | 9 | 435 | 6 | 0.2 |
| Q1618-030 | 0.53 | 0.05641 | 0.00109 | 0.55162 | 0.0116 | 0.07091 | 0.00105 | 469 | 23 | 446 | 8 | 442 | 6 | 0.9 |
| Q1618-031 | 0.4 | 0.05475 | 0.00273 | 0.46932 | 0.02344 | 0.06216 | 0.00106 | 402 | 81 | 391 | 16 | 389 | 6 | 0.5 |
| Q1618-032 | 0.34 | 0.05525 | 0.00199 | 0.47591 | 0.01738 | 0.06246 | 0.001 | 422 | 53 | 395 | 12 | 391 | 6 | 1 |
| Q1618-033 | 0.65 | 0.05529 | 0.00122 | 0.52385 | 0.01231 | 0.0687 | 0.00103 | 424 | 27 | 428 | 8 | 428 | 6 | 0 |
| Q1618-034 | 0.39 | 0.05516 | 0.00144 | 0.50279 | 0.01366 | 0.06609 | 0.001 | 419 | 34 | 414 | 9 | 413 | 6 | 0.2 |
| Q1618-035 | 0.38 | 0.05555 | 0.00126 | 0.53196 | 0.01282 | 0.06944 | 0.00104 | 434 | 28 | 433 | 8 | 433 | 6 | 0 |
| Q1618-036 | 0.47 | 0.05787 | 0.0011 | 0.536 | 0.01117 | 0.06716 | 0.00099 | 525 | 22 | 436 | 7 | 419 | 6 | 4.1 |
| Q1618-037 | 0.4 | 0.05936 | 0.00135 | 0.57584 | 0.01388 | 0.07034 | 0.00106 | 580 | 28 | 462 | 9 | 438 | 6 | 5.5 |
| Q1618-038 | 0.44 | 0.05546 | 0.00108 | 0.52336 | 0.01112 | 0.06842 | 0.00101 | 431 | 23 | 427 | 7 | 427 | 6 | 0 |
| Q1618-039 | 0.35 | 0.05579 | 0.00131 | 0.52303 | 0.01295 | 0.06798 | 0.00102 | 444 | 30 | 427 | 9 | 424 | 6 | 0.7 |
| Q1618-040 | 0.28 | 0.05425 | 0.00273 | 0.46428 | 0.02336 | 0.06206 | 0.00106 | 381 | 82 | 387 | 16 | 388 | 6 | -0.3 |
| Q1618-041 | 0.36 | 0.05679 | 0.00129 | 0.52995 | 0.01281 | 0.06766 | 0.00102 | 483 | 28 | 432 | 9 | 422 | 6 | 2.4 |
| Q1618-042 | 0.42 | 0.05521 | 0.00155 | 0.53125 | 0.01547 | 0.06978 | 0.00108 | 421 | 38 | 433 | 10 | 435 | 7 | -0.5 |
| Q1618-043 | 0.42 | 0.05504 | 0.00126 | 0.52103 | 0.01266 | 0.06864 | 0.00104 | 414 | 29 | 426 | 8 | 428 | 6 | -0.5 |
| Q1618-044 | 0.38 | 0.05566 | 0.00117 | 0.53527 | 0.01213 | 0.06973 | 0.00104 | 439 | 26 | 435 | 8 | 435 | 6 | 0 |
| Q1618-045 | 0.43 | 0.05642 | 0.00122 | 0.53521 | 0.0124 | 0.06879 | 0.00103 | 469 | 26 | 435 | 8 | 429 | 6 | 1.4 |
| Q1618-046 | 0.42 | 0.05566 | 0.00215 | 0.51761 | 0.01837 | 0.06745 | 0.00103 | 439 | 88 | 424 | 12 | 421 | 6 | 0.7 |

| | | | | | | | | | | | | | | |
|---|---|---|---|---|---|---|---|---|---|---|---|---|---|---|
| Q1618-047 | 0.31 | 0.05426 | 0.00194 | 0.47754 | 0.01736 | 0.06382 | 0.00102 | 382 | 53 | 396 | 12 | 399 | 6 | -0.8 |
| Q1618-048 | 0.37 | 0.05646 | 0.00114 | 0.53873 | 0.01181 | 0.06919 | 0.00103 | 471 | 24 | 438 | 8 | 431 | 6 | 1.6 |
| Q1618-049 | 0.45 | 0.05665 | 0.00121 | 0.52428 | 0.01203 | 0.0671 | 0.00101 | 478 | 26 | 428 | 8 | 419 | 6 | 2.1 |
| Q1618-050 | 0.34 | 0.05542 | 0.00099 | 0.53532 | 0.0106 | 0.07004 | 0.00103 | 429 | 21 | 435 | 7 | 436 | 6 | -0.2 |
| Q1618-051 | 0.59 | 0.05436 | 0.00174 | 0.4707 | 0.01539 | 0.06278 | 0.00098 | 386 | 46 | 392 | 11 | 393 | 6 | -0.3 |
| Q1618-052 | 0.38 | 0.05485 | 0.00104 | 0.47165 | 0.00985 | 0.06236 | 0.00092 | 406 | 23 | 392 | 7 | 390 | 6 | 0.5 |
| Q1618-053 | 0.5 | 0.05504 | 0.00317 | 0.54458 | 0.03138 | 0.07175 | 0.00126 | 414 | 97 | 441 | 21 | 447 | 8 | -1.3 |
| Q1618-054 | 0.47 | 0.0552 | 0.00123 | 0.51445 | 0.01219 | 0.06758 | 0.00102 | 420 | 28 | 421 | 8 | 422 | 6 | -0.2 |
| Q1618-055 | 0.41 | 0.05579 | 0.00128 | 0.54406 | 0.01322 | 0.07071 | 0.00107 | 444 | 29 | 441 | 9 | 440 | 6 | 0.2 |
| Q1618-056 | 0.46 | 0.05664 | 0.00131 | 0.52548 | 0.01288 | 0.06728 | 0.00102 | 478 | 29 | 429 | 9 | 420 | 6 | 2.1 |
| Q1618-057 | 0.36 | 0.05672 | 0.00127 | 0.53275 | 0.01273 | 0.06811 | 0.00103 | 481 | 28 | 434 | 8 | 425 | 6 | 2.1 |
| Q1618-058 | 0.99 | 0.05034 | 0.00194 | 0.28626 | 0.01117 | 0.04123 | 0.00067 | 211 | 60 | 256 | 9 | 260 | 4 | -1.5 |
| Q1618-059 | 0.39 | 0.05615 | 0.00139 | 0.51831 | 0.01347 | 0.06694 | 0.00102 | 458 | 32 | 424 | 9 | 418 | 6 | 1.4 |
| Q1618-060 | 0.39 | 0.05502 | 0.00151 | 0.52949 | 0.01504 | 0.06979 | 0.00108 | 413 | 37 | 431 | 10 | 435 | 7 | -0.9 |
| Q1618-061 | 0.51 | 0.07508 | 0.00151 | 1.65137 | 0.03586 | 0.15949 | 0.00242 | 1071 | 21 | 990 | 14 | 954 | 13 | 3.8 |
| Q1618-062 | 0.4 | 0.05484 | 0.00124 | 0.52633 | 0.01265 | 0.06959 | 0.00106 | 406 | 28 | 429 | 8 | 434 | 6 | -1.2 |
| Q1618-063 | 0.58 | 0.0574 | 0.00099 | 0.51625 | 0.01002 | 0.06521 | 0.00096 | 507 | 20 | 423 | 7 | 407 | 6 | 3.9 |
| Q1618-064 | 0.27 | 0.05071 | 0.00153 | 0.24127 | 0.00748 | 0.0345 | 0.00054 | 228 | 43 | 219 | 6 | 219 | 3 | 0 |
| Q1618-065 | 0.5 | 0.05988 | 0.00123 | 0.61118 | 0.0136 | 0.07402 | 0.00111 | 599 | 24 | 484 | 9 | 460 | 7 | 5.2 |
| Q1618-066 | 0.43 | 0.05528 | 0.00135 | 0.52907 | 0.01362 | 0.06941 | 0.00106 | 424 | 31 | 431 | 9 | 433 | 6 | -0.5 |
| Q1618-067 | 0.5 | 0.0552 | 0.00125 | 0.52754 | 0.01268 | 0.0693 | 0.00105 | 420 | 28 | 430 | 8 | 432 | 6 | -0.5 |
| Q1618-068 | 0.52 | 0.05685 | 0.00134 | 0.54634 | 0.0136 | 0.06969 | 0.00107 | 486 | 29 | 443 | 9 | 434 | 6 | 2.1 |
| Q1618-069 | 0.42 | 0.05482 | 0.0014 | 0.52551 | 0.014 | 0.06951 | 0.00108 | 405 | 33 | 429 | 9 | 433 | 7 | -0.9 |
| Q1618-070 | 0.52 | 0.0543 | 0.00224 | 0.47208 | 0.01953 | 0.06304 | 0.00107 | 384 | 62 | 393 | 13 | 394 | 6 | -0.3 |
| Q1618-071 | 0.24 | 0.05514 | 0.00115 | 0.48024 | 0.0108 | 0.06316 | 0.00095 | 418 | 25 | 398 | 7 | 395 | 6 | 0.8 |
| ~~Q1618-072~~ | ~~0.45~~ | ~~0.06145~~ | ~~0.00304~~ | ~~0.53199~~ | ~~0.02618~~ | ~~0.06278~~ | ~~0.00114~~ | ~~655~~ | ~~74~~ | ~~433~~ | ~~17~~ | ~~393~~ | ~~7~~ | ~~10.2~~ |
| Q1618-073 | 0.41 | 0.05771 | 0.00234 | 0.57807 | 0.02159 | 0.07265 | 0.00113 | 519 | 91 | 463 | 14 | 452 | 7 | 2.4 |
| Q1618-074 | 0.42 | 0.05647 | 0.00115 | 0.53756 | 0.01187 | 0.06903 | 0.00104 | 471 | 24 | 437 | 8 | 430 | 6 | 1.6 |

| | | | | | | | | | | | | | | |
|---|---|---|---|---|---|---|---|---|---|---|---|---|---|---|
| Q1618-075 | 0.33 | 0.05587 | 0.0037 | 0.49423 | 0.03258 | 0.06415 | 0.00121 | 447 | 113 | 408 | 22 | 401 | 7 | 1.7 |
| Q1618-076 | 0.47 | 0.05719 | 0.00127 | 0.54396 | 0.01288 | 0.06897 | 0.00105 | 499 | 27 | 441 | 8 | 430 | 6 | 2.6 |
| Q1618-077 | 0.43 | 0.0544 | 0.00121 | 0.47888 | 0.0114 | 0.06383 | 0.00097 | 388 | 28 | 397 | 8 | 399 | 6 | -0.5 |
| Q1618-078 | 0.17 | 0.05743 | 0.0018 | 0.50176 | 0.0138 | 0.06336 | 0.00095 | 508 | 71 | 413 | 9 | 396 | 6 | 4.3 |
| Q1618-079 | 0.46 | 0.05613 | 0.00118 | 0.54091 | 0.01227 | 0.06988 | 0.00106 | 458 | 25 | 439 | 8 | 435 | 6 | 0.9 |
| Q1618-080 | 0.42 | 0.05915 | 0.00146 | 0.58915 | 0.01532 | 0.07222 | 0.00111 | 573 | 31 | 470 | 10 | 450 | 7 | 4.4 |
| Q1618-081 | 0.4 | 0.05553 | 0.00131 | 0.54851 | 0.01365 | 0.07163 | 0.0011 | 434 | 29 | 444 | 9 | 446 | 7 | -0.4 |
| Q1618-082 | 0.39 | 0.05668 | 0.00118 | 0.54437 | 0.01223 | 0.06964 | 0.00106 | 479 | 25 | 441 | 8 | 434 | 6 | 1.6 |
| ~~Q1618-083~~ | ~~0.61~~ | ~~0.06757~~ | ~~0.00133~~ | ~~0.62092~~ | ~~0.01334~~ | ~~0.06663~~ | ~~0.00101~~ | ~~855~~ | ~~22~~ | ~~490~~ | ~~8~~ | ~~416~~ | ~~6~~ | ~~17.8~~ |
| Q1618-084 | 0.26 | 0.05509 | 0.00176 | 0.50412 | 0.0165 | 0.06636 | 0.00106 | 416 | 45 | 414 | 11 | 414 | 6 | 0 |
| Q1618-085 | 0.56 | 0.05632 | 0.00132 | 0.55532 | 0.01377 | 0.07149 | 0.0011 | 465 | 29 | 448 | 9 | 445 | 7 | 0.7 |
| Q1618-086 | 0.75 | 0.13108 | 0.00224 | 6.55349 | 0.12621 | 0.36253 | 0.00547 | 2112 | 16 | 2053 | 17 | 1994 | 26 | 5.9 |
| Q1618-087 | 0.57 | 0.05647 | 0.00114 | 0.56042 | 0.01229 | 0.07197 | 0.00109 | 471 | 24 | 452 | 8 | 448 | 7 | 0.9 |
| Q1618-088 | 0.36 | 0.05569 | 0.00118 | 0.55408 | 0.01266 | 0.07214 | 0.0011 | 440 | 26 | 448 | 8 | 449 | 7 | -0.2 |
| Q1618-089 | 0.46 | 0.05831 | 0.00142 | 0.53819 | 0.01378 | 0.06693 | 0.00104 | 541 | 30 | 437 | 9 | 418 | 6 | 4.5 |
| Q1618-090 | 0.43 | 0.05591 | 0.00106 | 0.50027 | 0.01041 | 0.06488 | 0.00098 | 449 | 22 | 412 | 7 | 405 | 6 | 1.7 |
| Q1618-091 | 0.42 | 0.06017 | 0.00265 | 0.60375 | 0.02484 | 0.07277 | 0.00115 | 610 | 98 | 480 | 16 | 453 | 7 | 6 |
| Q1618-092 | 0.55 | 0.05797 | 0.00128 | 0.55841 | 0.01317 | 0.06985 | 0.00107 | 529 | 27 | 450 | 9 | 435 | 6 | 3.4 |
| Q1618-093 | 0.44 | 0.0595 | 0.00119 | 0.55956 | 0.01221 | 0.06819 | 0.00103 | 585 | 23 | 451 | 8 | 425 | 6 | 6.1 |
| Q1618-094 | 0.94 | 0.05959 | 0.00138 | 0.5074 | 0.0125 | 0.06174 | 0.00095 | 589 | 28 | 417 | 8 | 386 | 6 | 8 |
| Q1618-095 | 0.4 | 0.05605 | 0.00128 | 0.54013 | 0.01308 | 0.06987 | 0.00107 | 454 | 28 | 439 | 9 | 435 | 6 | 0.9 |
| ~~Q1618-096~~ | ~~0.26~~ | ~~0.0696~~ | ~~0.00147~~ | ~~0.99522~~ | ~~0.02255~~ | ~~0.10368~~ | ~~0.0016~~ | ~~917~~ | ~~23~~ | ~~701~~ | ~~11~~ | ~~636~~ | ~~9~~ | ~~10.2~~ |
| Q1618-097 | 0.41 | 0.05743 | 0.00168 | 0.56108 | 0.01693 | 0.07084 | 0.00113 | 508 | 39 | 452 | 11 | 441 | 7 | 2.5 |
| Q1618-098 | 0.38 | 0.05497 | 0.00156 | 0.51793 | 0.01524 | 0.06833 | 0.00108 | 411 | 38 | 424 | 10 | 426 | 7 | -0.5 |
| Q1618-099 | 0.28 | 0.05466 | 0.00252 | 0.46852 | 0.02163 | 0.06215 | 0.00107 | 398 | 72 | 390 | 15 | 389 | 6 | 0.3 |
| ~~Q1618-100~~ | ~~0.86~~ | ~~0.06224~~ | ~~0.00304~~ | ~~0.36116~~ | ~~0.01762~~ | ~~0.04208~~ | ~~0.00074~~ | ~~682~~ | ~~74~~ | ~~313~~ | ~~13~~ | ~~266~~ | ~~5~~ | ~~17.7~~ |

| **Q1643** | | | | | | | | | | | | | | |
|---|---|---|---|---|---|---|---|---|---|---|---|---|---|---|
| Q1643-01 | 0.62 | 0.05536 | 0.00101 | 0.53568 | 0.01016 | 0.07016 | 0.00094 | 427 | 21 | 436 | 7 | 437 | 6 | -0.2 |
| Q1643-02 | 0.27 | 0.05457 | 0.002 | 0.46851 | 0.01704 | 0.06226 | 0.00095 | 395 | 54 | 390 | 12 | 389 | 6 | 0.3 |
| Q1643-03 | 0.56 | 0.05554 | 0.00107 | 0.53391 | 0.01055 | 0.0697 | 0.00095 | 434 | 22 | 434 | 7 | 434 | 6 | 0 |
| Q1643-04 | 0.28 | 0.05411 | 0.00225 | 0.45772 | 0.01885 | 0.06134 | 0.00094 | 376 | 65 | 383 | 13 | 384 | 6 | -0.3 |
| Q1643-05 | 0.33 | 0.0547 | 0.00443 | 0.47124 | 0.03777 | 0.06246 | 0.00118 | 400 | 147 | 392 | 26 | 391 | 7 | 0.3 |
| Q1643-06 | 0.24 | 0.05419 | 0.00103 | 0.46156 | 0.00906 | 0.06176 | 0.00084 | 379 | 22 | 385 | 6 | 386 | 5 | -0.3 |
| Q1643-07 | 0.48 | 0.05454 | 0.00181 | 0.46622 | 0.01538 | 0.06198 | 0.00092 | 393 | 47 | 389 | 11 | 388 | 6 | 0.3 |
| Q1643-08 | 1.11 | 0.05366 | 0.00382 | 0.41893 | 0.0295 | 0.05661 | 0.00104 | 357 | 126 | 355 | 21 | 355 | 6 | 0 |
| Q1643-09 | 0.67 | 0.12614 | 0.00363 | 6.42135 | 0.16066 | 0.3692 | 0.00523 | 2045 | 52 | 2035 | 22 | 2026 | 25 | 0.9 |
| Q1643-10 | 0.37 | 0.05553 | 0.00101 | 0.55505 | 0.01044 | 0.07248 | 0.00098 | 434 | 20 | 448 | 7 | 451 | 6 | -0.7 |
| Q1643-11 | 0.36 | 0.05508 | 0.00104 | 0.49469 | 0.00962 | 0.06513 | 0.00088 | 415 | 21 | 408 | 7 | 407 | 5 | 0.2 |
| ~~Q1643-12~~ | ~~0.72~~ | ~~0.06189~~ | ~~0.00107~~ | ~~0.30894~~ | ~~0.00555~~ | ~~0.0362~~ | ~~0.00048~~ | ~~670~~ | ~~18~~ | ~~273~~ | ~~4~~ | ~~229~~ | ~~3~~ | ~~19.2~~ |
| Q1643-13 | 0.43 | 0.05575 | 0.0011 | 0.53705 | 0.01088 | 0.06985 | 0.00095 | 442 | 23 | 436 | 7 | 435 | 6 | 0.2 |
| ~~Q1643-14~~ | ~~0.83~~ | ~~0.05888~~ | ~~0.00307~~ | ~~0.24903~~ | ~~0.01246~~ | ~~0.03067~~ | ~~0.00045~~ | ~~563~~ | ~~117~~ | ~~226~~ | ~~10~~ | ~~195~~ | ~~3~~ | ~~15.9~~ |
| Q1643-15 | 0.61 | 0.05466 | 0.00216 | 0.46733 | 0.01829 | 0.062 | 0.00095 | 398 | 60 | 389 | 13 | 388 | 6 | 0.3 |
| Q1643-16 | 0.39 | 0.05514 | 0.00193 | 0.46691 | 0.01622 | 0.0614 | 0.00092 | 418 | 51 | 389 | 11 | 384 | 6 | 1.3 |
| Q1643-17 | 0.4 | 0.05486 | 0.00116 | 0.52168 | 0.01123 | 0.06895 | 0.00094 | 407 | 25 | 426 | 7 | 430 | 6 | -0.9 |
| ~~Q1643-18~~ | ~~0.69~~ | ~~0.07204~~ | ~~0.00121~~ | ~~0.51742~~ | ~~0.00907~~ | ~~0.05208~~ | ~~0.0007~~ | ~~987~~ | ~~17~~ | ~~423~~ | ~~6~~ | ~~327~~ | ~~4~~ | ~~29.4~~ |
| Q1643-19 | 0.3 | 0.05451 | 0.00193 | 0.45599 | 0.01602 | 0.06066 | 0.00093 | 392 | 51 | 381 | 11 | 380 | 6 | 0.3 |
| Q1643-20 | 0.43 | 0.05446 | 0.00188 | 0.46196 | 0.01586 | 0.06151 | 0.00093 | 390 | 50 | 386 | 11 | 385 | 6 | 0.3 |
| Q1643-21 | 0.16 | 0.06713 | 0.00112 | 1.16382 | 0.02034 | 0.12572 | 0.00169 | 842 | 17 | 784 | 10 | 763 | 10 | 2.8 |
| ~~Q1643-22~~ | ~~0.78~~ | ~~0.14099~~ | ~~0.00208~~ | ~~6.74915~~ | ~~0.10734~~ | ~~0.34712~~ | ~~0.00455~~ | ~~2239~~ | ~~12~~ | ~~2079~~ | ~~14~~ | ~~1921~~ | ~~22~~ | ~~16.6~~ |
| Q1643-23 | 0.53 | 0.05633 | 0.00095 | 0.54269 | 0.00956 | 0.06986 | 0.00093 | 465 | 18 | 440 | 6 | 435 | 6 | 1.1 |
| Q1643-24 | 0.47 | 0.05584 | 0.00109 | 0.53829 | 0.01084 | 0.0699 | 0.00095 | 446 | 22 | 437 | 7 | 436 | 6 | 0.2 |
| Q1643-25 | 0.52 | 0.05431 | 0.00225 | 0.47335 | 0.01948 | 0.0632 | 0.00098 | 384 | 64 | 394 | 13 | 395 | 6 | -0.3 |
| ~~Q1643-26~~ | ~~0.69~~ | ~~0.09045~~ | ~~0.00323~~ | ~~0.80558~~ | ~~0.02813~~ | ~~0.06458~~ | ~~0.00106~~ | ~~1435~~ | ~~42~~ | ~~600~~ | ~~16~~ | ~~403~~ | ~~6~~ | ~~48.9~~ |
| Q1643-27 | 0.49 | 0.05692 | 0.00108 | 0.5231 | 0.01018 | 0.06664 | 0.00092 | 488 | 21 | 427 | 7 | 416 | 6 | 2.6 |

| | | | | | | | | | | | | | | |
|---|---|---|---|---|---|---|---|---|---|---|---|---|---|---|
| ~~Q1643-28~~ | ~~0.66~~ | ~~0.14936~~ | ~~0.00228~~ | ~~7.57258~~ | ~~0.12334~~ | ~~0.36764~~ | ~~0.00487~~ | ~~2339~~ | ~~13~~ | ~~2182~~ | ~~15~~ | ~~2018~~ | ~~23~~ | ~~15.9~~ |
| Q1643-29 | 0.29 | 0.05957 | 0.00217 | 0.55316 | 0.01846 | 0.06735 | 0.00097 | 588 | 81 | 447 | 12 | 420 | 6 | 6.4 |
| Q1643-30 | 0.13 | 0.07005 | 0.0011 | 1.60903 | 0.02682 | 0.16655 | 0.00221 | 930 | 16 | 974 | 10 | 993 | 12 | -1.9 |
| Q1643-31 | 0.3 | 0.05409 | 0.00245 | 0.46797 | 0.02103 | 0.06274 | 0.001 | 375 | 72 | 390 | 15 | 392 | 6 | -0.5 |
| Q1643-32 | 0.5 | 0.07539 | 0.0013 | 1.80303 | 0.03244 | 0.17342 | 0.00235 | 1079 | 17 | 1047 | 12 | 1031 | 13 | 4.7 |
| Q1643-33 | 0.63 | 0.05548 | 0.00092 | 0.52534 | 0.00918 | 0.06867 | 0.00092 | 432 | 18 | 429 | 6 | 428 | 6 | 0.2 |
| Q1643-34 | 0.34 | 0.05579 | 0.00122 | 0.52298 | 0.01161 | 0.06797 | 0.00095 | 444 | 26 | 427 | 8 | 424 | 6 | 0.7 |
| ~~Q1643-35~~ | ~~0.58~~ | ~~0.15976~~ | ~~0.00425~~ | ~~4.70803~~ | ~~0.10649~~ | ~~0.21373~~ | ~~0.00299~~ | ~~2453~~ | ~~46~~ | ~~1769~~ | ~~19~~ | ~~1249~~ | ~~16~~ | ~~96.4~~ |
| Q1643-36 | 0.71 | 0.05386 | 0.00264 | 0.46115 | 0.02227 | 0.06208 | 0.00105 | 365 | 78 | 385 | 15 | 388 | 6 | -0.8 |
| Q1643-37 | 0.4 | 0.05572 | 0.00114 | 0.52942 | 0.01107 | 0.0689 | 0.00096 | 441 | 24 | 431 | 7 | 430 | 6 | 0.2 |
| Q1643-38 | 0.37 | 0.05404 | 0.00114 | 0.44523 | 0.00954 | 0.05974 | 0.00083 | 373 | 25 | 374 | 7 | 374 | 5 | 0 |
| Q1643-39 | 0.56 | 0.06123 | 0.00185 | 0.59699 | 0.01798 | 0.07069 | 0.00105 | 647 | 39 | 475 | 11 | 440 | 6 | 8 |
| Q1643-40 | 0.62 | 0.05597 | 0.00188 | 0.4593 | 0.01528 | 0.05951 | 0.0009 | 451 | 47 | 384 | 11 | 373 | 5 | 2.9 |
| Q1643-41 | 0.78 | 0.09994 | 0.00169 | 3.69532 | 0.06547 | 0.26811 | 0.00365 | 1623 | 15 | 1570 | 14 | 1531 | 19 | 6 |
| ~~Q1643-42~~ | ~~0.87~~ | ~~0.14845~~ | ~~0.00602~~ | ~~2.87454~~ | ~~0.10803~~ | ~~0.14041~~ | ~~0.00314~~ | ~~2328~~ | ~~35~~ | ~~1375~~ | ~~28~~ | ~~847~~ | ~~18~~ | ~~62.3~~ |
| Q1643-43 | 0.53 | 0.07356 | 0.00135 | 1.89433 | 0.03594 | 0.18674 | 0.00257 | 1029 | 18 | 1079 | 13 | 1104 | 14 | -6.8 |
| Q1643-44 | 0.59 | 0.11397 | 0.00186 | 5.0156 | 0.08645 | 0.31909 | 0.00428 | 1864 | 14 | 1822 | 15 | 1785 | 21 | 4.4 |
| Q1643-45 | 0.44 | 0.05572 | 0.00129 | 0.53599 | 0.0125 | 0.06975 | 0.00099 | 441 | 28 | 436 | 8 | 435 | 6 | 0.2 |
| Q1643-46 | 0.64 | 0.05291 | 0.00155 | 0.29308 | 0.00858 | 0.04017 | 0.00059 | 325 | 40 | 261 | 7 | 254 | 4 | 2.8 |
| ~~Q1643-47~~ | ~~0.89~~ | ~~0.09787~~ | ~~0.00171~~ | ~~3.15917~~ | ~~0.05732~~ | ~~0.23407~~ | ~~0.00322~~ | ~~1584~~ | ~~16~~ | ~~1447~~ | ~~14~~ | ~~1356~~ | ~~17~~ | ~~16.8~~ |
| Q1643-48 | 0.23 | 0.11513 | 0.0019 | 5.17563 | 0.09002 | 0.32596 | 0.00438 | 1882 | 15 | 1849 | 15 | 1819 | 21 | 3.5 |
| Q1643-49 | 0.93 | 0.05149 | 0.00223 | 0.25058 | 0.01077 | 0.03529 | 0.00055 | 263 | 70 | 227 | 9 | 224 | 3 | 1.3 |
| Q1643-50 | 0.42 | 0.05522 | 0.0011 | 0.47592 | 0.00966 | 0.0625 | 0.00087 | 421 | 23 | 395 | 7 | 391 | 5 | 1 |
| Q1643-51 | 0.4 | 0.05753 | 0.00106 | 0.54012 | 0.01032 | 0.06807 | 0.00093 | 512 | 20 | 439 | 7 | 425 | 6 | 3.3 |
| ~~Q1643-52~~ | ~~2.05~~ | ~~0.07391~~ | ~~0.00204~~ | ~~1.19391~~ | ~~0.03216~~ | ~~0.11713~~ | ~~0.00187~~ | ~~1039~~ | ~~30~~ | ~~798~~ | ~~15~~ | ~~714~~ | ~~11~~ | ~~11.8~~ |
| Q1643-53 | 0.47 | 0.05551 | 0.00162 | 0.47716 | 0.01377 | 0.06232 | 0.00094 | 433 | 38 | 396 | 9 | 390 | 6 | 1.5 |
| ~~Q1643-54~~ | ~~1.22~~ | ~~0.06721~~ | ~~0.00212~~ | ~~0.40067~~ | ~~0.01232~~ | ~~0.04323~~ | ~~0.0007~~ | ~~844~~ | ~~38~~ | ~~342~~ | ~~9~~ | ~~273~~ | ~~4~~ | ~~25.3~~ |
| ~~Q1643-55~~ | ~~0.25~~ | ~~0.11608~~ | ~~0.002~~ | ~~4.81397~~ | ~~0.08654~~ | ~~0.3007~~ | ~~0.00409~~ | ~~1897~~ | ~~15~~ | ~~1787~~ | ~~15~~ | ~~1695~~ | ~~20~~ | ~~11.9~~ |

| | | | | | | | | | | | | | | |
|---|---|---|---|---|---|---|---|---|---|---|---|---|---|---|
| Q1643-56 | 0.69 | 0.05595 | 0.00366 | 0.36786 | 0.02382 | 0.04768 | 0.00084 | 450 | 113 | 318 | 18 | 300 | 5 | 6 |
| ~~Q1643-57~~ | ~~0.72~~ | ~~0.06326~~ | ~~0.00204~~ | ~~0.38514~~ | ~~0.01215~~ | ~~0.04414~~ | ~~0.00072~~ | ~~717~~ | ~~40~~ | ~~331~~ | ~~9~~ | ~~278~~ | ~~4~~ | ~~19.1~~ |
| ~~Q1643-58~~ | ~~0.32~~ | ~~0.11306~~ | ~~0.00196~~ | ~~4.54099~~ | ~~0.08214~~ | ~~0.29123~~ | ~~0.00397~~ | ~~1849~~ | ~~15~~ | ~~1739~~ | ~~15~~ | ~~1648~~ | ~~20~~ | ~~12.2~~ |
| ~~Q1643-59~~ | ~~0.91~~ | ~~0.08573~~ | ~~0.00607~~ | ~~0.80488~~ | ~~0.05492~~ | ~~0.06809~~ | ~~0.0013~~ | ~~1332~~ | ~~141~~ | ~~600~~ | ~~31~~ | ~~425~~ | ~~8~~ | ~~41.2~~ |
| Q1643-60 | 0.56 | 0.0566 | 0.00142 | 0.35814 | 0.00895 | 0.04588 | 0.00068 | 476 | 30 | 311 | 7 | 289 | 4 | 7.6 |
| Q1643-61 | 0.46 | 0.07258 | 0.00135 | 1.52049 | 0.02907 | 0.15191 | 0.00211 | 1002 | 19 | 939 | 12 | 912 | 12 | 3 |
| **Q123** | | | | | | | | | | | | | | |
| Q123-01 | 0.44 | 0.06197 | 0.00122 | 0.60628 | 0.01304 | 0.07094 | 0.00107 | 673 | 23 | 481 | 8 | 442 | 6 | 8.8 |
| Q123-02 | 0.84 | 0.06215 | 0.00192 | 0.60284 | 0.01908 | 0.07034 | 0.00113 | 679 | 41 | 479 | 12 | 438 | 7 | 9.4 |
| Q123-03 | 0.4 | 0.05766 | 0.00113 | 0.56194 | 0.01209 | 0.07067 | 0.00105 | 517 | 23 | 453 | 8 | 440 | 6 | 3 |
| Q123-04 | 0.46 | 0.05487 | 0.00121 | 0.5017 | 0.01185 | 0.06629 | 0.00101 | 407 | 27 | 413 | 8 | 414 | 6 | -0.2 |
| Q123-05 | 0.6 | 0.0611 | 0.00211 | 0.63966 | 0.02248 | 0.07591 | 0.00123 | 643 | 48 | 502 | 14 | 472 | 7 | 6.4 |
| ~~Q123-06~~ | ~~0.47~~ | ~~0.07418~~ | ~~0.00418~~ | ~~0.78477~~ | ~~0.04192~~ | ~~0.07673~~ | ~~0.00137~~ | ~~1046~~ | ~~117~~ | ~~588~~ | ~~24~~ | ~~477~~ | ~~8~~ | ~~23.3~~ |
| Q123-07 | 0.6 | 0.05834 | 0.00115 | 0.60131 | 0.01302 | 0.07474 | 0.00112 | 543 | 23 | 478 | 8 | 465 | 7 | 2.8 |
| ~~Q123-08~~ | ~~1.07~~ | ~~0.08804~~ | ~~0.00317~~ | ~~1.54535~~ | ~~0.05592~~ | ~~0.12728~~ | ~~0.00222~~ | ~~1383~~ | ~~43~~ | ~~949~~ | ~~22~~ | ~~772~~ | ~~13~~ | ~~22.9~~ |
| Q123-09 | 0.5 | 0.05831 | 0.00094 | 0.59675 | 0.01111 | 0.0742 | 0.00109 | 541 | 19 | 475 | 7 | 461 | 7 | 3 |
| Q123-10 | 0.57 | 0.05944 | 0.001 | 0.5371 | 0.01032 | 0.06552 | 0.00096 | 583 | 20 | 437 | 7 | 409 | 6 | 6.8 |
| ~~Q123-11~~ | ~~0.42~~ | ~~0.06694~~ | ~~0.00313~~ | ~~0.64582~~ | ~~0.0283~~ | ~~0.06998~~ | ~~0.00115~~ | ~~836~~ | ~~100~~ | ~~506~~ | ~~17~~ | ~~436~~ | ~~7~~ | ~~16.1~~ |
| Q123-12 | 0.45 | 0.05202 | 0.00229 | 0.32689 | 0.0146 | 0.04556 | 0.00073 | 286 | 73 | 287 | 11 | 287 | 5 | 0 |
| Q123-13 | 0.41 | 0.06028 | 0.00111 | 0.61064 | 0.01252 | 0.07346 | 0.00109 | 614 | 21 | 484 | 8 | 457 | 7 | 5.9 |
| ~~Q123-14~~ | ~~0.74~~ | ~~0.08188~~ | ~~0.00493~~ | ~~0.8559~~ | ~~0.04897~~ | ~~0.07581~~ | ~~0.00141~~ | ~~1243~~ | ~~121~~ | ~~628~~ | ~~27~~ | ~~471~~ | ~~8~~ | ~~33.3~~ |
| Q123-15 | 0.51 | 0.0558 | 0.00118 | 0.54678 | 0.01251 | 0.07105 | 0.00106 | 444 | 26 | 443 | 8 | 442 | 6 | 0.2 |
| Q123-16 | 0.48 | 0.05758 | 0.00117 | 0.53519 | 0.01189 | 0.0674 | 0.001 | 514 | 25 | 435 | 8 | 420 | 6 | 3.6 |
| Q123-17 | 0.43 | 0.05583 | 0.0016 | 0.52682 | 0.01569 | 0.06841 | 0.00105 | 446 | 39 | 430 | 10 | 427 | 6 | 0.7 |
| Q123-18 | 0.66 | 0.06155 | 0.0014 | 0.55875 | 0.01353 | 0.06583 | 0.00101 | 659 | 27 | 451 | 9 | 411 | 6 | 9.7 |
| Q123-19 | 0.52 | 0.05959 | 0.00098 | 0.5909 | 0.01114 | 0.0719 | 0.00106 | 589 | 19 | 471 | 7 | 448 | 6 | 5.1 |

| | | | | | | | | | | | | | | |
|---|---|---|---|---|---|---|---|---|---|---|---|---|---|---|
| ~~Q123-20~~ | ~~0.53~~ | ~~0.06319~~ | ~~0.00305~~ | ~~0.61018~~ | ~~0.02767~~ | ~~0.07003~~ | ~~0.00117~~ | ~~715~~ | ~~105~~ | ~~484~~ | ~~17~~ | ~~436~~ | ~~7~~ | ~~11~~ |
| Q123-21 | 0.46 | 0.059 | 0.0016 | 0.54701 | 0.01553 | 0.06723 | 0.00104 | 567 | 36 | 443 | 10 | 419 | 6 | 5.7 |
| Q123-22 | 0.65 | 0.05749 | 0.00091 | 0.57486 | 0.01062 | 0.07251 | 0.00106 | 510 | 19 | 461 | 7 | 451 | 6 | 2.2 |
| Q123-23 | 0.32 | 0.05607 | 0.0022 | 0.57216 | 0.02264 | 0.07399 | 0.00123 | 455 | 58 | 459 | 15 | 460 | 7 | -0.2 |
| ~~Q123-24~~ | ~~0.52~~ | ~~0.06564~~ | ~~0.00119~~ | ~~0.5654~~ | ~~0.01143~~ | ~~0.06246~~ | ~~0.00093~~ | ~~795~~ | ~~20~~ | ~~455~~ | ~~7~~ | ~~391~~ | ~~6~~ | ~~16.4~~ |
| Q123-25 | 0.46 | 0.05644 | 0.00166 | 0.55157 | 0.01682 | 0.07086 | 0.0011 | 470 | 40 | 446 | 11 | 441 | 7 | 1.1 |
| Q123-26 | 0.46 | 0.05527 | 0.00119 | 0.51966 | 0.01206 | 0.06817 | 0.00104 | 423 | 26 | 425 | 8 | 425 | 6 | 0 |
| Q123-27 | 0.6 | 0.0559 | 0.00172 | 0.54729 | 0.01742 | 0.07098 | 0.0011 | 448 | 43 | 443 | 11 | 442 | 7 | 0.2 |
| Q123-28 | 1.51 | 0.06255 | 0.00123 | 0.61369 | 0.01325 | 0.07114 | 0.00107 | 693 | 23 | 486 | 8 | 443 | 6 | 9.7 |
| Q123-29 | 0.55 | 0.05518 | 0.00094 | 0.5076 | 0.00986 | 0.0667 | 0.00098 | 420 | 20 | 417 | 7 | 416 | 6 | 0.2 |
| Q123-30 | 0.46 | 0.05605 | 0.00137 | 0.57948 | 0.01503 | 0.07496 | 0.00114 | 454 | 32 | 464 | 10 | 466 | 7 | -0.4 |
| Q123-31 | 0.74 | 0.055 | 0.00109 | 0.55904 | 0.01211 | 0.07369 | 0.00111 | 412 | 24 | 451 | 8 | 458 | 7 | -1.5 |
| Q123-32 | 0.49 | 0.05697 | 0.00123 | 0.52402 | 0.01221 | 0.06669 | 0.001 | 490 | 27 | 428 | 8 | 416 | 6 | 2.9 |
| Q123-33 | 0.48 | 0.05535 | 0.0013 | 0.50478 | 0.01259 | 0.06613 | 0.00102 | 426 | 30 | 415 | 8 | 413 | 6 | 0.5 |
| Q123-34 | 0.57 | 0.05642 | 0.00116 | 0.59082 | 0.01316 | 0.07593 | 0.00115 | 469 | 25 | 471 | 8 | 472 | 7 | -0.2 |
| Q123-35 | 0.62 | 0.05794 | 0.00157 | 0.49722 | 0.01405 | 0.06223 | 0.00097 | 527 | 35 | 410 | 10 | 389 | 6 | 5.4 |
| Q123-36 | 0.56 | 0.05498 | 0.00099 | 0.49645 | 0.01003 | 0.06547 | 0.00098 | 411 | 21 | 409 | 7 | 409 | 6 | 0 |
| Q123-37 | 0.59 | 0.05698 | 0.00088 | 0.57281 | 0.01038 | 0.07288 | 0.00107 | 491 | 18 | 460 | 7 | 453 | 6 | 1.5 |
| Q123-38 | 0.47 | 0.05523 | 0.00135 | 0.50284 | 0.01298 | 0.06602 | 0.00103 | 422 | 31 | 414 | 9 | 412 | 6 | 0.5 |
| Q123-39 | 0.56 | 0.05499 | 0.00151 | 0.50779 | 0.01437 | 0.06696 | 0.00108 | 412 | 35 | 417 | 10 | 418 | 7 | -0.2 |
| ~~Q123-40~~ | ~~0.51~~ | ~~0.06415~~ | ~~0.00301~~ | ~~0.57586~~ | ~~0.02533~~ | ~~0.0651~~ | ~~0.00105~~ | ~~747~~ | ~~102~~ | ~~462~~ | ~~16~~ | ~~407~~ | ~~6~~ | ~~13.5~~ |
| ~~Q123-41~~ | ~~0.47~~ | ~~0.06044~~ | ~~0.00228~~ | ~~0.37117~~ | ~~0.01417~~ | ~~0.04453~~ | ~~0.00074~~ | ~~619~~ | ~~54~~ | ~~321~~ | ~~10~~ | ~~281~~ | ~~5~~ | ~~14.2~~ |
| Q123-42 | 0.5 | 0.05534 | 0.00166 | 0.51244 | 0.01588 | 0.06714 | 0.00106 | 426 | 41 | 420 | 11 | 419 | 6 | 0.2 |
| Q123-43 | 0.53 | 0.0554 | 0.00103 | 0.54589 | 0.01125 | 0.07144 | 0.00107 | 428 | 22 | 442 | 7 | 445 | 6 | -0.7 |
| ~~Q123-44~~ | ~~0.67~~ | ~~0.06436~~ | ~~0.00155~~ | ~~0.68692~~ | ~~0.01745~~ | ~~0.07738~~ | ~~0.0012~~ | ~~753~~ | ~~29~~ | ~~531~~ | ~~11~~ | ~~480~~ | ~~7~~ | ~~10.6~~ |
| Q123-45 | 0.66 | 0.05597 | 0.00137 | 0.55886 | 0.01447 | 0.07239 | 0.00112 | 451 | 31 | 451 | 9 | 451 | 7 | 0 |
| Q123-46 | 0.7 | 0.05624 | 0.00143 | 0.58575 | 0.01556 | 0.07551 | 0.0012 | 462 | 32 | 468 | 10 | 469 | 7 | -0.2 |
| Q123-47 | 0.71 | 0.05595 | 0.00103 | 0.56972 | 0.01164 | 0.07382 | 0.00111 | 450 | 22 | 458 | 8 | 459 | 7 | -0.2 |

| | | | | | | | | | | | | | | |
|---|---|---|---|---|---|---|---|---|---|---|---|---|---|---|
| Q123-48 | 0.43 | 0.05561 | 0.00133 | 0.51475 | 0.01298 | 0.06711 | 0.00104 | 437 | 30 | 422 | 9 | 419 | 6 | 0.7 |
| Q123-49 | 0.55 | 0.05669 | 0.00158 | 0.51978 | 0.01507 | 0.06648 | 0.00104 | 479 | 37 | 425 | 10 | 415 | 6 | 2.4 |
| Q123-50 | 0.59 | 0.0558 | 0.00169 | 0.5459 | 0.01704 | 0.07093 | 0.00112 | 444 | 42 | 442 | 11 | 442 | 7 | 0 |
| Q123-51 | 0.39 | 0.05206 | 0.00211 | 0.32991 | 0.01351 | 0.04594 | 0.00076 | 288 | 63 | 289 | 10 | 290 | 5 | -0.3 |
| Q123-52 | 0.45 | 0.05206 | 0.00214 | 0.31393 | 0.01306 | 0.04372 | 0.00072 | 288 | 65 | 277 | 10 | 276 | 4 | 0.4 |
| Q123-53 | 0.67 | 0.05641 | 0.00167 | 0.55537 | 0.01694 | 0.07139 | 0.00114 | 469 | 40 | 449 | 11 | 445 | 7 | 0.9 |
| Q123-54 | 0.49 | 0.05504 | 0.00114 | 0.50347 | 0.0113 | 0.06633 | 0.00101 | 414 | 25 | 414 | 8 | 414 | 6 | 0 |
| Q123-55 | 0.72 | 0.05623 | 0.00091 | 0.56892 | 0.01065 | 0.07336 | 0.00109 | 461 | 19 | 457 | 7 | 456 | 7 | 0.2 |
| Q123-56 | 0.54 | 0.05564 | 0.00157 | 0.51886 | 0.01516 | 0.06761 | 0.00108 | 438 | 37 | 424 | 10 | 422 | 7 | 0.5 |
| Q123-57 | 0.71 | 0.05633 | 0.00127 | 0.57265 | 0.01373 | 0.07371 | 0.00115 | 465 | 27 | 460 | 9 | 458 | 7 | 0.4 |
| Q123-58 | 0.39 | 0.05576 | 0.00144 | 0.54737 | 0.01471 | 0.07118 | 0.00114 | 443 | 32 | 443 | 10 | 443 | 7 | 0 |
| Q123-59 | 0.04 | 0.05485 | 0.00127 | 0.50939 | 0.01259 | 0.06734 | 0.00104 | 406 | 29 | 418 | 8 | 420 | 6 | -0.5 |
| Q123-60 | 0.52 | 0.06033 | 0.00152 | 0.55312 | 0.01461 | 0.06647 | 0.00104 | 615 | 31 | 447 | 10 | 415 | 6 | 7.7 |
| Q123-61 | 0.47 | 0.06029 | 0.0014 | 0.5568 | 0.01371 | 0.06697 | 0.00104 | 614 | 28 | 449 | 9 | 418 | 6 | 7.4 |
| Q123-62 | 0.55 | 0.05637 | 0.00103 | 0.58682 | 0.01199 | 0.07548 | 0.00114 | 467 | 22 | 469 | 8 | 469 | 7 | 0 |
| Q123-63 | 0.4 | 0.0551 | 0.00105 | 0.50463 | 0.0106 | 0.0664 | 0.00101 | 416 | 23 | 415 | 7 | 414 | 6 | 0.2 |
| Q123-64 | 0.47 | 0.05564 | 0.00227 | 0.52529 | 0.02151 | 0.06845 | 0.00119 | 438 | 60 | 429 | 14 | 427 | 7 | 0.5 |
| Q123-65 | 0.43 | 0.05676 | 0.00119 | 0.52026 | 0.01184 | 0.06646 | 0.00102 | 482 | 25 | 425 | 8 | 415 | 6 | 2.4 |
| Q123-66 | 0.46 | 0.05535 | 0.00149 | 0.5164 | 0.01437 | 0.06765 | 0.0011 | 426 | 34 | 423 | 10 | 422 | 7 | 0.2 |
| Q123-67 | 0.48 | 0.05574 | 0.00175 | 0.54733 | 0.01747 | 0.07119 | 0.00119 | 442 | 42 | 443 | 11 | 443 | 7 | 0 |
| Q123-68 | 0.76 | 0.05599 | 0.00103 | 0.56247 | 0.01153 | 0.07285 | 0.0011 | 452 | 22 | 453 | 7 | 453 | 7 | 0 |
| Q123-69 | 0.44 | 0.05607 | 0.00182 | 0.55649 | 0.01831 | 0.07197 | 0.00121 | 455 | 44 | 449 | 12 | 448 | 7 | 0.2 |
| Q123-70 | 0.45 | 0.05538 | 0.00148 | 0.51217 | 0.01428 | 0.06706 | 0.00107 | 428 | 35 | 420 | 10 | 418 | 6 | 0.5 |
| Q123-71 | 0.32 | 0.0555 | 0.00148 | 0.52973 | 0.01468 | 0.0692 | 0.00112 | 432 | 34 | 432 | 10 | 431 | 7 | 0.2 |
| Q123-72 | 0.61 | 0.05623 | 0.00103 | 0.57374 | 0.01171 | 0.07398 | 0.00112 | 461 | 21 | 460 | 8 | 460 | 7 | 0 |
| Q123-73 | 0.43 | 0.05413 | 0.00107 | 0.55106 | 0.01196 | 0.07381 | 0.00113 | 376 | 24 | 446 | 8 | 459 | 7 | -2.8 |
| Q123-74 | 0.56 | 0.05528 | 0.00111 | 0.50524 | 0.01114 | 0.06627 | 0.00101 | 424 | 24 | 415 | 8 | 414 | 6 | 0.2 |
| Q123-75 | 0.52 | 0.05519 | 0.00181 | 0.51466 | 0.01732 | 0.06762 | 0.00109 | 420 | 47 | 422 | 12 | 422 | 7 | 0 |

| | | | | | | | | | | | | | | |
|---|---|---|---|---|---|---|---|---|---|---|---|---|---|---|
| Q123-76 | 0.45 | 0.05554 | 0.00198 | 0.50216 | 0.01822 | 0.06555 | 0.00109 | 434 | 51 | 413 | 12 | 409 | 7 | 1 |
| Q123-77 | 0.73 | 0.05883 | 0.00152 | 0.56077 | 0.01524 | 0.06911 | 0.00108 | 561 | 33 | 452 | 10 | 431 | 7 | 4.9 |
| Q123-78 | 0.39 | 0.05883 | 0.00362 | 0.59655 | 0.03615 | 0.07352 | 0.00155 | 561 | 95 | 475 | 23 | 457 | 9 | 3.9 |
| Q123-79 | 0.54 | 0.05607 | 0.00103 | 0.57068 | 0.01172 | 0.0738 | 0.00112 | 455 | 22 | 458 | 8 | 459 | 7 | -0.2 |
| Q123-80 | 0.51 | 0.05532 | 0.00132 | 0.51599 | 0.01298 | 0.06763 | 0.00107 | 425 | 29 | 422 | 9 | 422 | 6 | 0 |
| Q123-81 | 1.02 | 0.05604 | 0.00168 | 0.56856 | 0.0174 | 0.07357 | 0.00123 | 454 | 39 | 457 | 11 | 458 | 7 | -0.2 |
| Q123-82 | 0.77 | 0.059 | 0.00142 | 0.58464 | 0.01485 | 0.07185 | 0.00113 | 567 | 29 | 467 | 10 | 447 | 7 | 4.5 |
| Q123-83 | 0.38 | 0.05173 | 0.00246 | 0.31173 | 0.01489 | 0.04369 | 0.00075 | 273 | 78 | 276 | 12 | 276 | 5 | 0 |
| Q123-84 | 0.48 | 0.05311 | 0.00131 | 0.50028 | 0.013 | 0.0683 | 0.00109 | 333 | 31 | 412 | 9 | 426 | 7 | -3.3 |
| Q123-85 | 0.75 | 0.05584 | 0.00104 | 0.56395 | 0.01168 | 0.07323 | 0.00112 | 446 | 22 | 454 | 8 | 456 | 7 | -0.4 |
| Q123-86 | 0.65 | 0.06184 | 0.00148 | 0.63672 | 0.01615 | 0.07466 | 0.00117 | 669 | 29 | 500 | 10 | 464 | 7 | 7.8 |
| Q123-87 | 0.43 | 0.05562 | 0.00118 | 0.54021 | 0.01235 | 0.07043 | 0.0011 | 437 | 25 | 439 | 8 | 439 | 7 | 0 |
| Q123-88 | 0.54 | 0.05535 | 0.00141 | 0.51469 | 0.01373 | 0.06742 | 0.00108 | 426 | 32 | 422 | 9 | 421 | 7 | 0.2 |
| Q123-89 | 0.52 | 0.05553 | 0.00178 | 0.52559 | 0.01709 | 0.06863 | 0.00116 | 434 | 43 | 429 | 11 | 428 | 7 | 0.2 |
| Q123-90 | 0.54 | 0.05528 | 0.00116 | 0.522 | 0.01185 | 0.06847 | 0.00106 | 424 | 25 | 426 | 8 | 427 | 6 | -0.2 |
| Q123-91 | 0.46 | 0.05516 | 0.00179 | 0.51074 | 0.01691 | 0.06714 | 0.00113 | 419 | 44 | 419 | 11 | 419 | 7 | 0 |
| Q123-92 | 0.64 | 0.05995 | 0.00203 | 0.59561 | 0.0205 | 0.07203 | 0.0012 | 602 | 46 | 474 | 13 | 448 | 7 | 5.8 |
| Q123-93 | 0.43 | 0.06108 | 0.00159 | 0.54998 | 0.01497 | 0.06529 | 0.00105 | 642 | 32 | 445 | 10 | 408 | 6 | 9.1 |
| Q123-94 | 0.62 | 0.05624 | 0.00164 | 0.57746 | 0.01726 | 0.07445 | 0.00124 | 462 | 38 | 463 | 11 | 463 | 7 | 0 |
| Q123-95 | 0.49 | 0.05495 | 0.00139 | 0.5097 | 0.01354 | 0.06725 | 0.00107 | 410 | 32 | 418 | 9 | 420 | 6 | -0.5 |
| Q123-96 | 1.04 | 0.05494 | 0.00113 | 0.50301 | 0.01128 | 0.06638 | 0.00103 | 410 | 25 | 414 | 8 | 414 | 6 | 0 |
| Q123-97 | 0.58 | 0.05675 | 0.00129 | 0.56161 | 0.01363 | 0.07176 | 0.00112 | 482 | 28 | 453 | 9 | 447 | 7 | 1.3 |
| Q123-98 | 0.36 | 0.05489 | 0.00174 | 0.50675 | 0.01639 | 0.06695 | 0.00112 | 408 | 43 | 416 | 11 | 418 | 7 | -0.5 |
| Q123-99 | 0.54 | 0.05611 | 0.00108 | 0.57503 | 0.01226 | 0.07431 | 0.00114 | 457 | 23 | 461 | 8 | 462 | 7 | -0.2 |
| Q123-100 | 0.57 | 0.05758 | 0.00153 | 0.5411 | 0.01501 | 0.06814 | 0.00109 | 514 | 34 | 439 | 10 | 425 | 7 | 3.3 |
| | | | | | | | | | | | | | | |
| **Q7** | | | | | | | | | | | | | | |
| Q7-01 | 0.41 | 0.08179 | 0.00136 | 2.4048 | 0.04076 | 0.2132 | 0.00266 | 1240 | 16 | 1244 | 12 | 1246 | 14 | -0.5 |

| | | | | | | | | | | | | | | |
|---|---|---|---|---|---|---|---|---|---|---|---|---|---|---|
| Q7-02 | 1.17 | 0.07418 | 0.0014 | 1.79255 | 0.03397 | 0.17523 | 0.00226 | 1046 | 19 | 1043 | 12 | 1041 | 12 | 0.5 |
| Q7-03 | 0.41 | 0.05949 | 0.00129 | 0.54995 | 0.01178 | 0.06704 | 0.00089 | 585 | 25 | 445 | 8 | 418 | 5 | 6.5 |
| Q7-04 | 0.77 | 0.05589 | 0.00176 | 0.38503 | 0.01193 | 0.04996 | 0.00069 | 448 | 44 | 331 | 9 | 314 | 4 | 5.4 |
| ~~Q7-05~~ | ~~0.66~~ | ~~0.06237~~ | ~~0.00297~~ | ~~0.33542~~ | ~~0.01571~~ | ~~0.039~~ | ~~0.00062~~ | ~~687~~ | ~~73~~ | ~~294~~ | ~~12~~ | ~~247~~ | ~~4~~ | ~~19~~ |
| Q7-06 | 0.84 | 0.05326 | 0.00141 | 0.24955 | 0.00648 | 0.03398 | 0.00047 | 340 | 34 | 226 | 5 | 215 | 3 | 5.1 |
| Q7-07 | 0.42 | 0.05364 | 0.00224 | 0.418 | 0.01715 | 0.05651 | 0.00084 | 356 | 66 | 355 | 12 | 354 | 5 | 0.3 |
| ~~Q7-08~~ | ~~0.55~~ | ~~0.11641~~ | ~~0.00219~~ | ~~2.7855~~ | ~~0.05186~~ | ~~0.17351~~ | ~~0.00231~~ | ~~1902~~ | ~~16~~ | ~~1352~~ | ~~14~~ | ~~1031~~ | ~~13~~ | ~~84.5~~ |
| Q7-09 | 0.78 | 0.05396 | 0.00217 | 0.2899 | 0.01152 | 0.03896 | 0.00056 | 369 | 63 | 258 | 9 | 246 | 3 | 4.9 |
| Q7-10 | 0.91 | 0.11371 | 0.00215 | 5.03959 | 0.09517 | 0.32138 | 0.00422 | 1860 | 17 | 1826 | 16 | 1796 | 21 | 3.6 |
| Q7-11 | 0.37 | 0.05181 | 0.00207 | 0.27673 | 0.01079 | 0.03873 | 0.0006 | 277 | 61 | 248 | 9 | 245 | 4 | 1.2 |
| Q7-12 | 0.55 | 0.06772 | 0.00116 | 1.146 | 0.01994 | 0.12271 | 0.00153 | 860 | 17 | 775 | 9 | 746 | 9 | 3.9 |
| Q7-13 | 1.16 | 0.11339 | 0.00217 | 4.98294 | 0.09508 | 0.31866 | 0.00421 | 1854 | 17 | 1816 | 16 | 1783 | 21 | 4 |
| Q7-14 | 0.72 | 0.06124 | 0.00152 | 0.6041 | 0.01482 | 0.07153 | 0.00096 | 648 | 30 | 480 | 9 | 445 | 6 | 7.9 |
| Q7-15 | 0.88 | 0.05375 | 0.00112 | 0.28156 | 0.00589 | 0.03798 | 0.00048 | 361 | 25 | 252 | 5 | 240 | 3 | 5 |
| Q7-16 | 0.5 | 0.0535 | 0.0024 | 0.295 | 0.01302 | 0.03999 | 0.0006 | 350 | 72 | 262 | 10 | 253 | 4 | 3.6 |
| Q7-17 | 0.6 | 0.05299 | 0.00117 | 0.28601 | 0.00626 | 0.03914 | 0.00051 | 328 | 27 | 255 | 5 | 248 | 3 | 2.8 |
| Q7-18 | 0.19 | 0.06059 | 0.0015 | 0.60083 | 0.01456 | 0.0719 | 0.00099 | 625 | 29 | 478 | 9 | 448 | 6 | 6.7 |
| ~~Q7-19~~ | ~~0.41~~ | ~~0.07626~~ | ~~0.00132~~ | ~~1.3183~~ | ~~0.02309~~ | ~~0.12536~~ | ~~0.00157~~ | ~~1102~~ | ~~17~~ | ~~854~~ | ~~10~~ | ~~761~~ | ~~9~~ | ~~12.2~~ |
| ~~Q7-20~~ | ~~0.36~~ | ~~0.11112~~ | ~~0.02196~~ | ~~3.25302~~ | ~~0.62753~~ | ~~0.21233~~ | ~~0.00911~~ | ~~1818~~ | ~~395~~ | ~~1470~~ | ~~150~~ | ~~1241~~ | ~~48~~ | ~~46.5~~ |
| Q7-21 | 0.76 | 0.05216 | 0.00144 | 0.25868 | 0.00706 | 0.03596 | 0.00048 | 292 | 38 | 234 | 6 | 228 | 3 | 2.6 |
| Q7-22 | 0.72 | 0.0565 | 0.00134 | 0.4881 | 0.01146 | 0.06264 | 0.00083 | 472 | 29 | 404 | 8 | 392 | 5 | 3.1 |
| Q7-23 | 0.9 | 0.05051 | 0.00358 | 0.27191 | 0.01907 | 0.03904 | 0.00066 | 219 | 129 | 244 | 15 | 247 | 4 | -1.2 |
| Q7-24 | 1.15 | 0.11502 | 0.00202 | 5.20498 | 0.09216 | 0.32815 | 0.00415 | 1880 | 15 | 1853 | 15 | 1829 | 20 | 2.8 |
| Q7-25 | 0.55 | 0.11792 | 0.0021 | 5.84844 | 0.10482 | 0.35965 | 0.00458 | 1925 | 16 | 1954 | 16 | 1981 | 22 | -2.8 |
| Q7-26 | 0.7 | 0.05518 | 0.00156 | 0.30676 | 0.0085 | 0.04031 | 0.00057 | 420 | 37 | 272 | 7 | 255 | 4 | 6.7 |
| ~~Q7-27~~ | ~~0.62~~ | ~~0.0582~~ | ~~0.00536~~ | ~~0.33404~~ | ~~0.03012~~ | ~~0.04163~~ | ~~0.00078~~ | ~~537~~ | ~~209~~ | ~~293~~ | ~~23~~ | ~~263~~ | ~~5~~ | ~~11.4~~ |
| Q7-28 | 0.59 | 0.11744 | 0.00207 | 5.33096 | 0.09479 | 0.32918 | 0.00416 | 1918 | 16 | 1874 | 15 | 1834 | 20 | 4.6 |
| Q7-29 | 0.51 | 0.05864 | 0.00129 | 0.56239 | 0.01228 | 0.06955 | 0.00091 | 554 | 26 | 453 | 8 | 433 | 5 | 4.6 |

| | | | | | | | | | | | | | | |
|---|---|---|---|---|---|---|---|---|---|---|---|---|---|---|
| ~~Q7-30~~ | ~~0.19~~ | ~~0.14519~~ | ~~0.00269~~ | ~~4.50643~~ | ~~0.08317~~ | ~~0.22507~~ | ~~0.00293~~ | ~~2290~~ | ~~16~~ | ~~1732~~ | ~~15~~ | ~~1309~~ | ~~15~~ | ~~74.9~~ |
| Q7-31 | 0.52 | 0.0922 | 0.00173 | 3.08816 | 0.058 | 0.24288 | 0.00312 | 1472 | 18 | 1430 | 14 | 1402 | 16 | 5 |
| ~~Q7-32~~ | ~~0.74~~ | ~~0.06249~~ | ~~0.00129~~ | ~~0.55272~~ | ~~0.01131~~ | ~~0.06414~~ | ~~0.00083~~ | ~~691~~ | ~~23~~ | ~~447~~ | ~~7~~ | ~~401~~ | ~~5~~ | ~~11.5~~ |
| Q7-33 | 0.08 | 0.07106 | 0.00136 | 1.44415 | 0.02771 | 0.14737 | 0.00189 | 959 | 20 | 907 | 12 | 886 | 11 | 2.4 |
| ~~Q7-34~~ | ~~0.39~~ | ~~0.06663~~ | ~~0.00212~~ | ~~0.2436~~ | ~~0.00754~~ | ~~0.02651~~ | ~~0.00039~~ | ~~826~~ | ~~40~~ | ~~221~~ | ~~6~~ | ~~169~~ | ~~2~~ | ~~30.8~~ |
| Q7-35 | 0.86 | 0.05283 | 0.00366 | 0.3076 | 0.02098 | 0.04222 | 0.00075 | 322 | 123 | 272 | 16 | 267 | 5 | 1.9 |
| Q7-36 | 0.47 | 0.11599 | 0.00206 | 5.11064 | 0.09168 | 0.31951 | 0.00401 | 1895 | 16 | 1838 | 15 | 1787 | 20 | 6 |
| Q7-37 | 0.73 | 0.05749 | 0.00186 | 0.52297 | 0.01667 | 0.06597 | 0.00094 | 510 | 45 | 427 | 11 | 412 | 6 | 3.6 |
| Q7-38 | 0.43 | 0.06104 | 0.00173 | 0.57656 | 0.016 | 0.0685 | 0.00097 | 641 | 36 | 462 | 10 | 427 | 6 | 8.2 |
| ~~Q7-39~~ | ~~0.57~~ | ~~0.06766~~ | ~~0.00343~~ | ~~0.2865~~ | ~~0.01389~~ | ~~0.03071~~ | ~~0.00046~~ | ~~858~~ | ~~108~~ | ~~256~~ | ~~11~~ | ~~195~~ | ~~3~~ | ~~31.3~~ |
| Q7-40 | 0.57 | 0.05889 | 0.00124 | 0.53973 | 0.01129 | 0.06646 | 0.00087 | 563 | 24 | 438 | 7 | 415 | 5 | 5.5 |
| Q7-41 | 0.38 | 0.11607 | 0.00212 | 5.05045 | 0.09263 | 0.31553 | 0.00399 | 1897 | 16 | 1828 | 16 | 1768 | 20 | 7.3 |
| ~~Q7-42~~ | ~~0.72~~ | ~~0.06841~~ | ~~0.0013~~ | ~~0.52227~~ | ~~0.00994~~ | ~~0.05536~~ | ~~0.00071~~ | ~~881~~ | ~~20~~ | ~~427~~ | ~~7~~ | ~~347~~ | ~~4~~ | ~~23.1~~ |
| Q7-43 | 0.42 | 0.07408 | 0.00142 | 1.62435 | 0.03117 | 0.159 | 0.00205 | 1044 | 19 | 980 | 12 | 951 | 11 | 3.1 |
| Q7-44 | 0.83 | 0.12584 | 0.00247 | 6.01945 | 0.11743 | 0.34688 | 0.00462 | 2041 | 17 | 1979 | 17 | 1920 | 22 | 6.3 |
| Q7-45 | 0.5 | 0.1404 | 0.0026 | 7.17266 | 0.13333 | 0.37047 | 0.00473 | 2232 | 16 | 2133 | 17 | 2032 | 22 | 9.8 |
| Q7-46 | 0.83 | 0.05721 | 0.00189 | 0.33843 | 0.0108 | 0.0429 | 0.00066 | 500 | 43 | 296 | 8 | 271 | 4 | 9.2 |
| ~~Q7-47~~ | ~~0.99~~ | ~~0.06918~~ | ~~0.00228~~ | ~~0.4422~~ | ~~0.01393~~ | ~~0.04635~~ | ~~0.00075~~ | ~~904~~ | ~~39~~ | ~~372~~ | ~~10~~ | ~~292~~ | ~~5~~ | ~~27.4~~ |
| Q7-48 | 0.51 | 0.05493 | 0.00137 | 0.36773 | 0.00894 | 0.04854 | 0.00067 | 409 | 30 | 318 | 7 | 306 | 4 | 3.9 |
| Q7-49 | 0.97 | 0.05615 | 0.00138 | 0.53333 | 0.01282 | 0.06888 | 0.00095 | 458 | 30 | 434 | 8 | 429 | 6 | 1.2 |
| Q7-50 | 0.74 | 0.16934 | 0.00323 | 11.26515 | 0.21459 | 0.48241 | 0.00628 | 2551 | 16 | 2545 | 18 | 2538 | 27 | 0.5 |
| Q7-51 | 0.33 | 0.05029 | 0.00133 | 0.22764 | 0.00593 | 0.03282 | 0.00048 | 208 | 34 | 208 | 5 | 208 | 3 | 0 |
| Q7-52 | 0.52 | 0.05464 | 0.00129 | 0.47164 | 0.01114 | 0.06258 | 0.00086 | 398 | 29 | 392 | 8 | 391 | 5 | 0.3 |
| Q7-53 | 0.54 | 0.05107 | 0.00137 | 0.25702 | 0.00686 | 0.03649 | 0.00052 | 244 | 36 | 232 | 6 | 231 | 3 | 0.4 |
| Q7-54 | 0.7 | 0.05231 | 0.04373 | 0.31474 | 0.26013 | 0.04362 | 0.00559 | 299 | ### | 278 | 201 | 275 | 35 | 1.1 |
| Q7-55 | 0.63 | 0.05668 | 0.0021 | 0.57588 | 0.02113 | 0.07367 | 0.00109 | 479 | 55 | 462 | 14 | 458 | 7 | 0.9 |
| Q7-56 | 0.47 | 0.05436 | 0.00136 | 0.44507 | 0.01104 | 0.05936 | 0.00085 | 386 | 31 | 374 | 8 | 372 | 5 | 0.5 |
| Q7-57 | 0.6 | 0.06945 | 0.00144 | 1.44375 | 0.03017 | 0.15074 | 0.00207 | 912 | 22 | 907 | 13 | 905 | 12 | 0.2 |

| | | | | | | | | | | | | | | |
|---|---|---|---|---|---|---|---|---|---|---|---|---|---|---|
| Q7-58 | 0.48 | 0.05578 | 0.00092 | 0.47873 | 0.0082 | 0.06223 | 0.0008 | 444 | 18 | 397 | 6 | 389 | 5 | 2.1 |
| Q7-59 | 0.56 | 0.10549 | 0.00157 | 4.44966 | 0.07004 | 0.30585 | 0.00393 | 1723 | 13 | 1722 | 13 | 1720 | 19 | 0.2 |
| Q7-60 | 0.59 | 0.05478 | 0.00119 | 0.49196 | 0.01075 | 0.06512 | 0.00088 | 403 | 26 | 406 | 7 | 407 | 5 | -0.2 |
| Q7-61 | 0.16 | 0.05167 | 0.00095 | 0.28676 | 0.00541 | 0.04024 | 0.00053 | 271 | 21 | 256 | 4 | 254 | 3 | 0.8 |
| Q7-62 | 0.51 | 0.05113 | 0.00096 | 0.24155 | 0.00461 | 0.03426 | 0.00045 | 247 | 22 | 220 | 4 | 217 | 3 | 1.4 |
| Q7-63 | 0.66 | 0.14587 | 0.00244 | 7.79689 | 0.13412 | 0.38757 | 0.00527 | 2298 | 14 | 2208 | 15 | 2112 | 24 | 8.8 |
| Q7-64 | 0.61 | 0.05473 | 0.00112 | 0.50225 | 0.01034 | 0.06654 | 0.0009 | 401 | 24 | 413 | 7 | 415 | 5 | -0.5 |
| Q7-65 | 0.44 | 0.05014 | 0.00181 | 0.22263 | 0.00798 | 0.0322 | 0.00047 | 201 | 56 | 204 | 7 | 204 | 3 | 0 |
| Q7-66 | 0.78 | 0.05082 | 0.0013 | 0.26698 | 0.00682 | 0.03809 | 0.00053 | 233 | 34 | 240 | 5 | 241 | 3 | -0.4 |
| Q7-67 | 0.7 | 0.05156 | 0.00112 | 0.31021 | 0.00677 | 0.04362 | 0.00059 | 266 | 27 | 274 | 5 | 275 | 4 | -0.4 |
| Q7-68 | 0.25 | 0.11411 | 0.00177 | 5.02951 | 0.082 | 0.31961 | 0.00414 | 1866 | 14 | 1824 | 14 | 1788 | 20 | 4.4 |
| Q7-69 | 0.74 | 0.05438 | 0.00122 | 0.46202 | 0.0104 | 0.06161 | 0.00085 | 387 | 27 | 386 | 7 | 385 | 5 | 0.3 |
| Q7-70 | 0.77 | 0.05473 | 0.0012 | 0.44994 | 0.00991 | 0.05961 | 0.00081 | 401 | 26 | 377 | 7 | 373 | 5 | 1.1 |
| Q7-71 | 0.89 | 0.10449 | 0.00222 | 3.91557 | 0.08263 | 0.27173 | 0.00398 | 1705 | 19 | 1617 | 17 | 1550 | 20 | 10 |
| Q7-72 | 0.68 | 0.051 | 0.00127 | 0.27112 | 0.00675 | 0.03855 | 0.00053 | 241 | 33 | 244 | 5 | 244 | 3 | 0 |
| Q7-73 | 0.59 | 0.05357 | 0.00124 | 0.42129 | 0.00975 | 0.05702 | 0.00079 | 353 | 28 | 357 | 7 | 357 | 5 | 0 |
| Q7-74 | 1.65 | 0.05285 | 0.00137 | 0.33367 | 0.00865 | 0.04578 | 0.00064 | 322 | 34 | 292 | 7 | 289 | 4 | 1 |
| Q7-75 | 0.43 | 0.05231 | 0.00181 | 0.34806 | 0.0119 | 0.04825 | 0.00073 | 299 | 50 | 303 | 9 | 304 | 4 | -0.3 |
| Q7-76 | 1.05 | 0.05583 | 0.00199 | 0.51867 | 0.01817 | 0.06737 | 0.00105 | 446 | 50 | 424 | 12 | 420 | 6 | 1 |
| Q7-77 | 0.79 | 0.05091 | 0.00112 | 0.2551 | 0.00563 | 0.03633 | 0.0005 | 237 | 27 | 231 | 5 | 230 | 3 | 0.4 |
| Q7-78 | 0.91 | 0.05348 | 0.00131 | 0.40674 | 0.00992 | 0.05515 | 0.00077 | 349 | 31 | 347 | 7 | 346 | 5 | 0.3 |
| Q7-79 | 0.59 | 0.06538 | 0.00118 | 1.16354 | 0.02155 | 0.12905 | 0.00172 | 787 | 19 | 784 | 10 | 782 | 10 | 0.3 |
| Q7-80 | 0.49 | 0.05507 | 0.00172 | 0.50006 | 0.01543 | 0.06585 | 0.00098 | 415 | 43 | 412 | 10 | 411 | 6 | 0.2 |
| Q7-81 | 0.74 | 0.05453 | 0.00139 | 0.46748 | 0.0118 | 0.06217 | 0.00091 | 393 | 31 | 389 | 8 | 389 | 6 | 0 |
| Q7-82 | 0.39 | 0.05493 | 0.00112 | 0.49515 | 0.01019 | 0.06536 | 0.00089 | 409 | 23 | 408 | 7 | 408 | 5 | 0 |
| Q7-83 | 0.56 | 0.11035 | 0.00227 | 4.66269 | 0.09629 | 0.30638 | 0.00434 | 1805 | 19 | 1761 | 17 | 1723 | 21 | 4.8 |
| Q7-84 | 0.7 | 0.0713 | 0.00136 | 1.51664 | 0.02944 | 0.15423 | 0.00209 | 966 | 19 | 937 | 12 | 925 | 12 | 1.3 |
| Q7-85 | 0.71 | 0.05171 | 0.00175 | 0.30499 | 0.01017 | 0.04277 | 0.00065 | 273 | 49 | 270 | 8 | 270 | 4 | 0 |

| | | | | | | | | | | | | | | |
|---|---|---|---|---|---|---|---|---|---|---|---|---|---|---|
| Q7-86 | 1.06 | 0.19304 | 0.00345 | 13.35691 | 0.24539 | 0.50172 | 0.00669 | 2768 | 14 | 2705 | 17 | 2621 | 29 | 5.6 |
| Q7-87 | 0.3 | 0.09085 | 0.00166 | 2.88216 | 0.05404 | 0.23003 | 0.00309 | 1443 | 17 | 1377 | 14 | 1335 | 16 | 8.1 |
| Q7-88 | 0.57 | 0.05751 | 0.0017 | 0.64261 | 0.01869 | 0.08102 | 0.00122 | 511 | 38 | 504 | 12 | 502 | 7 | 0.4 |
| Q7-89 | 0.1 | 0.05642 | 0.0012 | 0.58128 | 0.01241 | 0.07471 | 0.00104 | 469 | 24 | 465 | 8 | 464 | 6 | 0.2 |
| Q7-90 | 0.51 | 0.05147 | 0.00139 | 0.29664 | 0.00792 | 0.04179 | 0.0006 | 262 | 36 | 264 | 6 | 264 | 4 | 0 |
| Q7-91 | 0.34 | 0.05408 | 0.0012 | 0.41802 | 0.00931 | 0.05605 | 0.00078 | 374 | 26 | 355 | 7 | 352 | 5 | 0.9 |
| ~~Q7-92~~ | ~~0.47~~ | ~~0.13409~~ | ~~0.00391~~ | ~~6.33518~~ | ~~0.16147~~ | ~~0.34265~~ | ~~0.00483~~ | ~~2152~~ | ~~52~~ | ~~2023~~ | ~~22~~ | ~~1899~~ | ~~23~~ | ~~13.3~~ |
| Q7-93 | 0.12 | 0.05502 | 0.00119 | 0.49977 | 0.01091 | 0.06586 | 0.00091 | 413 | 26 | 412 | 7 | 411 | 6 | 0.2 |
| Q7-94 | 0.73 | 0.05632 | 0.00156 | 0.53835 | 0.01478 | 0.06932 | 0.00102 | 465 | 35 | 437 | 10 | 432 | 6 | 1.2 |
| Q7-95 | 0.97 | 0.05565 | 0.00147 | 0.54358 | 0.01429 | 0.07083 | 0.00103 | 438 | 33 | 441 | 9 | 441 | 6 | 0 |
| Q7-96 | 2.25 | 0.05106 | 0.0017 | 0.27224 | 0.00897 | 0.03866 | 0.00058 | 244 | 48 | 244 | 7 | 245 | 4 | -0.4 |
| Q7-97 | 0.82 | 0.05128 | 0.0014 | 0.27948 | 0.00761 | 0.03952 | 0.00057 | 253 | 37 | 250 | 6 | 250 | 4 | 0 |
| Q7-98 | 0.84 | 0.0555 | 0.00211 | 0.51967 | 0.01949 | 0.06789 | 0.00107 | 432 | 55 | 425 | 13 | 423 | 6 | 0.5 |
| Q7-99 | 0.43 | 0.05512 | 0.00129 | 0.5029 | 0.01172 | 0.06616 | 0.00095 | 417 | 28 | 414 | 8 | 413 | 6 | 0.2 |
| Q7-100 | 0.47 | 0.05189 | 0.0023 | 0.32488 | 0.01415 | 0.0454 | 0.00075 | 281 | 69 | 286 | 11 | 286 | 5 | 0 |
| Q7-101 | 0.75 | 0.05032 | 0.00124 | 0.22238 | 0.00547 | 0.03204 | 0.00046 | 210 | 31 | 204 | 5 | 203 | 3 | 0.5 |
| Q7-102 | 0.47 | 0.05607 | 0.0013 | 0.47942 | 0.01106 | 0.062 | 0.00089 | 455 | 27 | 398 | 8 | 388 | 5 | 2.6 |
| Q7-103 | 0.69 | 0.0508 | 0.00145 | 0.25464 | 0.00719 | 0.03634 | 0.00055 | 232 | 38 | 230 | 6 | 230 | 3 | 0 |
| Q7-104 | 0.91 | 0.05069 | 0.00168 | 0.24883 | 0.0081 | 0.0356 | 0.00055 | 227 | 47 | 226 | 7 | 226 | 3 | 0 |
| Q7-105 | 0.7 | 0.0546 | 0.00167 | 0.47109 | 0.01422 | 0.06256 | 0.00095 | 396 | 41 | 392 | 10 | 391 | 6 | 0.3 |
| | | | | | | | | | | | | | | |
| **Z2** | | | | | | | | | | | | | | |
| ~~Z2-01~~ | ~~0.47~~ | ~~0.0631~~ | ~~0.00216~~ | ~~0.5318~~ | ~~0.01684~~ | ~~0.06112~~ | ~~0.00079~~ | ~~712~~ | ~~74~~ | ~~433~~ | ~~11~~ | ~~382~~ | ~~5~~ | ~~13.4~~ |
| ~~Z2-02~~ | ~~1.84~~ | ~~0.07295~~ | ~~0.00139~~ | ~~0.71073~~ | ~~0.01338~~ | ~~0.07065~~ | ~~0.00091~~ | ~~1013~~ | ~~19~~ | ~~545~~ | ~~8~~ | ~~440~~ | ~~5~~ | ~~23.9~~ |
| Z2-03 | 0.7 | 0.06013 | 0.0013 | 0.4835 | 0.0104 | 0.05831 | 0.00076 | 608 | 25 | 400 | 7 | 365 | 5 | 9.6 |
| Z2-04 | 1.23 | 0.06097 | 0.0011 | 0.54274 | 0.00977 | 0.06455 | 0.00081 | 638 | 19 | 440 | 6 | 403 | 5 | 9.2 |
| Z2-05 | 0.69 | 0.07619 | 0.00115 | 1.555 | 0.02398 | 0.148 | 0.00179 | 1100 | 14 | 952 | 10 | 890 | 10 | 7 |

| | | | | | | | | | | | | | | |
|---|---|---|---|---|---|---|---|---|---|---|---|---|---|---|
| Z2-06 | 0.1 | 0.06486 | 0.00097 | 0.85581 | 0.01312 | 0.09568 | 0.00115 | 770 | 15 | 628 | 7 | 589 | 7 | 6.6 |
| ~~Z2-07~~ | ~~1.56~~ | ~~0.11619~~ | ~~0.00963~~ | ~~0.49604~~ | ~~0.03974~~ | ~~0.03096~~ | ~~0.00066~~ | ~~1898~~ | ~~154~~ | ~~409~~ | ~~27~~ | ~~197~~ | ~~4~~ | ~~108~~ |
| ~~Z2-08~~ | ~~0.31~~ | ~~0.06261~~ | ~~0.00119~~ | ~~0.51212~~ | ~~0.00969~~ | ~~0.05932~~ | ~~0.00075~~ | ~~695~~ | ~~20~~ | ~~420~~ | ~~7~~ | ~~371~~ | ~~5~~ | ~~13.2~~ |
| Z2-09 | 1 | 0.05587 | 0.00136 | 0.49089 | 0.01187 | 0.06371 | 0.00082 | 447 | 31 | 406 | 8 | 398 | 5 | 2 |
| Z2-10 | 1.3 | 0.05973 | 0.00101 | 0.54266 | 0.00924 | 0.06589 | 0.00082 | 594 | 18 | 440 | 6 | 411 | 5 | 7.1 |
| Z2-11 | 0.26 | 0.05736 | 0.00096 | 0.53061 | 0.00899 | 0.06709 | 0.00082 | 505 | 18 | 432 | 6 | 419 | 5 | 3.1 |
| Z2-12 | 0.91 | 0.05423 | 0.003 | 0.28435 | 0.01525 | 0.03803 | 0.00053 | 381 | 128 | 254 | 12 | 241 | 3 | 5.4 |
| ~~Z2-13~~ | ~~1.05~~ | ~~0.07702~~ | ~~0.00157~~ | ~~1.79005~~ | ~~0.03621~~ | ~~0.16854~~ | ~~0.00218~~ | ~~1122~~ | ~~21~~ | ~~1042~~ | ~~13~~ | ~~1004~~ | ~~12~~ | ~~11.8~~ |
| Z2-14 | 0.53 | 0.05811 | 0.00104 | 0.50818 | 0.00912 | 0.06342 | 0.00079 | 534 | 19 | 417 | 6 | 396 | 5 | 5.3 |
| ~~Z2-15~~ | ~~0.69~~ | ~~0.05779~~ | ~~0.00136~~ | ~~0.30552~~ | ~~0.00704~~ | ~~0.03834~~ | ~~0.00051~~ | ~~522~~ | ~~28~~ | ~~271~~ | ~~5~~ | ~~243~~ | ~~3~~ | ~~11.5~~ |
| Z2-16 | 0.48 | 0.05492 | 0.0015 | 0.49264 | 0.01333 | 0.06504 | 0.00085 | 409 | 37 | 407 | 9 | 406 | 5 | 0.2 |
| Z2-17 | 0.55 | 0.0588 | 0.0012 | 0.42043 | 0.00853 | 0.05185 | 0.00067 | 560 | 23 | 356 | 6 | 326 | 4 | 9.2 |
| Z2-18 | 0.29 | 0.07133 | 0.00104 | 1.43304 | 0.02156 | 0.14569 | 0.00174 | 967 | 14 | 903 | 9 | 877 | 10 | 3 |
| Z2-19 | 0.58 | 0.05094 | 0.0019 | 0.22834 | 0.00841 | 0.03251 | 0.00046 | 238 | 59 | 209 | 7 | 206 | 3 | 1.5 |
| ~~Z2-20~~ | ~~0.3~~ | ~~0.092~~ | ~~0.00229~~ | ~~1.25256~~ | ~~0.02699~~ | ~~0.09875~~ | ~~0.00124~~ | ~~1467~~ | ~~48~~ | ~~825~~ | ~~12~~ | ~~607~~ | ~~7~~ | ~~35.9~~ |
| Z2-21 | 0.38 | 0.07764 | 0.00219 | 1.96351 | 0.04953 | 0.18343 | 0.00234 | 1138 | 58 | 1103 | 17 | 1086 | 13 | 4.8 |
| ~~Z2-22~~ | ~~0.36~~ | ~~0.0618~~ | ~~0.00107~~ | ~~0.54773~~ | ~~0.00949~~ | ~~0.06426~~ | ~~0.0008~~ | ~~667~~ | ~~18~~ | ~~444~~ | ~~6~~ | ~~401~~ | ~~5~~ | ~~10.7~~ |
| Z2-23 | 0.64 | 0.07764 | 0.00117 | 1.51556 | 0.0234 | 0.14154 | 0.00171 | 1138 | 14 | 937 | 9 | 853 | 10 | 9.8 |
| ~~Z2-24~~ | ~~0.1~~ | ~~0.07338~~ | ~~0.00173~~ | ~~1.05634~~ | ~~0.0213~~ | ~~0.1044~~ | ~~0.00126~~ | ~~1025~~ | ~~49~~ | ~~732~~ | ~~11~~ | ~~640~~ | ~~7~~ | ~~14.4~~ |
| Z2-25 | 0.72 | 0.06057 | 0.00264 | 0.61907 | 0.02571 | 0.07413 | 0.001 | 624 | 96 | 489 | 16 | 461 | 6 | 6.1 |
| Z2-26 | 0.56 | 0.05617 | 0.00141 | 0.494 | 0.01226 | 0.06377 | 0.00084 | 459 | 32 | 408 | 8 | 399 | 5 | 2.3 |
| ~~Z2-27~~ | ~~1.7~~ | ~~0.05869~~ | ~~0.00134~~ | ~~0.29076~~ | ~~0.00652~~ | ~~0.03593~~ | ~~0.00048~~ | ~~556~~ | ~~27~~ | ~~259~~ | ~~5~~ | ~~228~~ | ~~3~~ | ~~13.6~~ |
| Z2-28 | 0.83 | 0.05409 | 0.00137 | 0.24724 | 0.0062 | 0.03314 | 0.00044 | 375 | 33 | 224 | 5 | 210 | 3 | 6.7 |
| Z2-29 | 0.71 | 0.05146 | 0.0025 | 0.27642 | 0.01321 | 0.03895 | 0.0006 | 261 | 81 | 248 | 11 | 246 | 4 | 0.8 |
| Z2-30 | 0.94 | 0.05233 | 0.00195 | 0.32106 | 0.01163 | 0.04449 | 0.00069 | 300 | 54 | 283 | 9 | 281 | 4 | 0.7 |
| Z2-31 | 0.33 | 0.05812 | 0.00167 | 0.55916 | 0.01451 | 0.06978 | 0.00086 | 534 | 64 | 451 | 9 | 435 | 5 | 3.7 |
| ~~Z2-32~~ | ~~1.03~~ | ~~0.06281~~ | ~~0.00109~~ | ~~0.5582~~ | ~~0.00977~~ | ~~0.06444~~ | ~~0.0008~~ | ~~702~~ | ~~18~~ | ~~450~~ | ~~6~~ | ~~403~~ | ~~5~~ | ~~11.7~~ |
| ~~Z2-33~~ | ~~0.65~~ | ~~0.07703~~ | ~~0.00408~~ | ~~1.40296~~ | ~~0.07104~~ | ~~0.13209~~ | ~~0.00206~~ | ~~1122~~ | ~~108~~ | ~~890~~ | ~~30~~ | ~~800~~ | ~~12~~ | ~~11.3~~ |

| | | | | | | | | | | | | | | |
|---|---|---|---|---|---|---|---|---|---|---|---|---|---|---|
| Z2-34 | 0.61 | 0.05249 | 0.00391 | 0.1966 | 0.01427 | 0.02716 | 0.00046 | 307 | 172 | 182 | 12 | 173 | 3 | 5.2 |
| ~~Z2-35~~ | ~~0.47~~ | ~~0.06283~~ | ~~0.00208~~ | ~~0.46217~~ | ~~0.01472~~ | ~~0.05334~~ | ~~0.00084~~ | ~~702~~ | ~~41~~ | ~~386~~ | ~~10~~ | ~~335~~ | ~~5~~ | ~~15.2~~ |
| ~~Z2-36~~ | ~~1.67~~ | ~~0.11609~~ | ~~0.0018~~ | ~~4.2966~~ | ~~0.06755~~ | ~~0.26837~~ | ~~0.00332~~ | ~~1897~~ | ~~13~~ | ~~1693~~ | ~~13~~ | ~~1533~~ | ~~17~~ | ~~23.7~~ |
| Z2-37 | 0.64 | 0.05955 | 0.00271 | 0.47845 | 0.02079 | 0.05828 | 0.0008 | 587 | 101 | 397 | 14 | 365 | 5 | 8.8 |
| Z2-38 | 0.83 | 0.05975 | 0.00099 | 0.53916 | 0.00902 | 0.06543 | 0.0008 | 595 | 17 | 438 | 6 | 409 | 5 | 7.1 |
| Z2-39 | 0.58 | 0.06021 | 0.001 | 0.56946 | 0.00957 | 0.06858 | 0.00084 | 611 | 17 | 458 | 6 | 428 | 5 | 7 |
| Z2-40 | 0.57 | 0.0547 | 0.00101 | 0.26838 | 0.00496 | 0.03557 | 0.00044 | 400 | 21 | 241 | 4 | 225 | 3 | 7.1 |
| ~~Z2-41~~ | ~~0.55~~ | ~~0.05657~~ | ~~0.00229~~ | ~~0.2469~~ | ~~0.00948~~ | ~~0.03165~~ | ~~0.00041~~ | ~~475~~ | ~~92~~ | ~~224~~ | ~~8~~ | ~~201~~ | ~~3~~ | ~~11.4~~ |
| Z2-42 | 1.16 | 0.05523 | 0.0038 | 0.3628 | 0.02464 | 0.04763 | 0.00079 | 422 | 123 | 314 | 18 | 300 | 5 | 4.7 |
| ~~Z2-43~~ | ~~1~~ | ~~0.06956~~ | ~~0.00173~~ | ~~0.55522~~ | ~~0.0136~~ | ~~0.05788~~ | ~~0.00077~~ | ~~915~~ | ~~29~~ | ~~448~~ | ~~9~~ | ~~363~~ | ~~5~~ | ~~23.4~~ |
| Z2-44 | 0.47 | 0.05894 | 0.00288 | 0.4772 | 0.02239 | 0.05872 | 0.0008 | 565 | 109 | 396 | 15 | 368 | 5 | 7.6 |
| Z2-45 | 0.99 | 0.05868 | 0.00464 | 0.48067 | 0.03718 | 0.05941 | 0.00096 | 555 | 178 | 399 | 25 | 372 | 6 | 7.3 |
| Z2-46 | 0.38 | 0.05784 | 0.00106 | 0.46136 | 0.0084 | 0.05784 | 0.00073 | 524 | 20 | 385 | 6 | 362 | 4 | 6.4 |
| Z2-47 | 0.26 | 0.05875 | 0.00175 | 0.55388 | 0.01497 | 0.06838 | 0.00086 | 558 | 67 | 448 | 10 | 426 | 5 | 5.2 |
| ~~Z2-48~~ | ~~0.4~~ | ~~0.06641~~ | ~~0.00126~~ | ~~0.51759~~ | ~~0.00975~~ | ~~0.05652~~ | ~~0.00072~~ | ~~819~~ | ~~20~~ | ~~424~~ | ~~7~~ | ~~354~~ | ~~4~~ | ~~19.8~~ |
| Z2-49 | 0.85 | 0.05528 | 0.00324 | 0.47022 | 0.02667 | 0.06169 | 0.00091 | 424 | 134 | 391 | 18 | 386 | 6 | 1.3 |
| Z2-50 | 0.25 | 0.05821 | 0.00109 | 0.50822 | 0.00941 | 0.06331 | 0.0008 | 538 | 20 | 417 | 6 | 396 | 5 | 5.3 |
| ~~Z2-51~~ | ~~0.83~~ | ~~0.12623~~ | ~~0.00216~~ | ~~5.03778~~ | ~~0.08591~~ | ~~0.28938~~ | ~~0.0037~~ | ~~2046~~ | ~~14~~ | ~~1826~~ | ~~14~~ | ~~1638~~ | ~~18~~ | ~~24.9~~ |
| Z2-52 | 0.62 | 0.05881 | 0.00157 | 0.50063 | 0.0131 | 0.06172 | 0.00085 | 560 | 34 | 412 | 9 | 386 | 5 | 6.7 |
| Z2-53 | 0.33 | 0.05539 | 0.00183 | 0.50484 | 0.01541 | 0.0661 | 0.00085 | 428 | 76 | 415 | 10 | 413 | 5 | 0.5 |
| Z2-54 | 1.29 | 0.05372 | 0.00424 | 0.37282 | 0.0288 | 0.05033 | 0.00079 | 359 | 181 | 322 | 21 | 317 | 5 | 1.6 |
| Z2-55 | 0.5 | 0.05209 | 0.00092 | 0.24761 | 0.00441 | 0.03447 | 0.00042 | 289 | 20 | 225 | 4 | 218 | 3 | 3.2 |
| Z2-56 | 0.93 | 0.05383 | 0.00142 | 0.43446 | 0.0111 | 0.05852 | 0.00083 | 364 | 33 | 366 | 8 | 367 | 5 | -0.3 |
| ~~Z2-57~~ | ~~0.74~~ | ~~0.07738~~ | ~~0.00313~~ | ~~1.10246~~ | ~~0.04198~~ | ~~0.10333~~ | ~~0.00142~~ | ~~1131~~ | ~~83~~ | ~~755~~ | ~~20~~ | ~~634~~ | ~~8~~ | ~~19.1~~ |
| Z2-58 | 0.27 | 0.05636 | 0.00177 | 0.46161 | 0.0133 | 0.0594 | 0.00075 | 467 | 71 | 385 | 9 | 372 | 5 | 3.5 |
| Z2-59 | 0.48 | 0.05375 | 0.00187 | 0.22248 | 0.00753 | 0.03001 | 0.00044 | 361 | 50 | 204 | 6 | 191 | 3 | 6.8 |
| Z2-60 | 0.77 | 0.06096 | 0.00112 | 0.55669 | 0.01019 | 0.06621 | 0.00083 | 638 | 20 | 449 | 7 | 413 | 5 | 8.7 |
| ~~Z2-61~~ | ~~1.48~~ | ~~0.17382~~ | ~~0.00787~~ | ~~1.29639~~ | ~~0.05381~~ | ~~0.05409~~ | ~~0.00098~~ | ~~2595~~ | ~~77~~ | ~~844~~ | ~~24~~ | ~~340~~ | ~~6~~ | ~~148~~ |

| | | | | | | | | | | | | | | |
|---|---|---|---|---|---|---|---|---|---|---|---|---|---|---|
| Z2-62 | 0.39 | 0.05993 | 0.00145 | 0.46751 | 0.01092 | 0.05656 | 0.0008 | 601 | 27 | 389 | 8 | 355 | 5 | 9.6 |
| Z2-63 | 0.88 | 0.05656 | 0.0011 | 0.45638 | 0.0088 | 0.0585 | 0.00074 | 474 | 22 | 382 | 6 | 366 | 5 | 4.4 |
| Z2-64 | 1.18 | 0.05824 | 0.00101 | 0.54853 | 0.00952 | 0.06829 | 0.00084 | 539 | 18 | 444 | 6 | 426 | 5 | 4.2 |
| ~~Z2-65~~ | ~~0.85~~ | ~~0.09502~~ | ~~0.00154~~ | ~~2.58027~~ | ~~0.04217~~ | ~~0.1969~~ | ~~0.00242~~ | ~~1528~~ | ~~15~~ | ~~1295~~ | ~~12~~ | ~~1159~~ | ~~13~~ | ~~31.8~~ |
| ~~Z2-66~~ | ~~0.81~~ | ~~0.09548~~ | ~~0.00536~~ | ~~0.60578~~ | ~~0.03265~~ | ~~0.04602~~ | ~~0.00073~~ | ~~1538~~ | ~~108~~ | ~~481~~ | ~~21~~ | ~~290~~ | ~~4~~ | ~~65.9~~ |
| Z2-67 | 0.74 | 0.0537 | 0.00233 | 0.26979 | 0.01139 | 0.03643 | 0.00059 | 358 | 66 | 243 | 9 | 231 | 4 | 5.2 |
| Z2-68 | 0.78 | 0.05451 | 0.00174 | 0.42703 | 0.01335 | 0.0568 | 0.0008 | 392 | 45 | 361 | 9 | 356 | 5 | 1.4 |
| Z2-69 | 0.98 | 0.04605 | 0.00274 | 0.22565 | 0.013 | 0.03554 | 0.00052 |  | 130 | 207 | 11 | 225 | 3 | -8 |
| Z2-70 | 0.48 | 0.05444 | 0.0026 | 0.32832 | 0.01504 | 0.04374 | 0.0006 | 389 | 110 | 288 | 11 | 276 | 4 | 4.3 |
| Z2-71 | 0.69 | 0.06821 | 0.00132 | 1.18918 | 0.02269 | 0.12641 | 0.00162 | 875 | 20 | 796 | 11 | 767 | 9 | 3.8 |
| ~~Z2-72~~ | ~~0.45~~ | ~~0.05987~~ | ~~0.0022~~ | ~~0.38354~~ | ~~0.01312~~ | ~~0.04646~~ | ~~0.00061~~ | ~~599~~ | ~~81~~ | ~~330~~ | ~~10~~ | ~~293~~ | ~~4~~ | ~~12.6~~ |
| Z2-73 | 0.52 | 0.05826 | 0.00098 | 0.55414 | 0.00933 | 0.06897 | 0.00084 | 540 | 18 | 448 | 6 | 430 | 5 | 4.2 |
| Z2-74 | 0.51 | 0.05488 | 0.00151 | 0.49639 | 0.01347 | 0.06558 | 0.00087 | 407 | 37 | 409 | 9 | 409 | 5 | 0 |
| Z2-75 | 0.28 | 0.05504 | 0.00205 | 0.47439 | 0.01654 | 0.06251 | 0.00083 | 414 | 85 | 394 | 11 | 391 | 5 | 0.8 |
| Z2-76 | 0.85 | 0.05858 | 0.00132 | 0.52281 | 0.01153 | 0.0647 | 0.00086 | 552 | 26 | 427 | 8 | 404 | 5 | 5.7 |
| Z2-77 | 0.4 | 0.05535 | 0.00201 | 0.24824 | 0.00843 | 0.03253 | 0.00042 | 426 | 83 | 225 | 7 | 206 | 3 | 9.2 |
| Z2-78 | 0.59 | 0.06151 | 0.00121 | 0.4858 | 0.00941 | 0.05726 | 0.00073 | 657 | 21 | 402 | 6 | 359 | 4 | 12 |
| Z2-79 | 0.77 | 0.05498 | 0.00168 | 0.48659 | 0.01468 | 0.06417 | 0.00087 | 411 | 43 | 403 | 10 | 401 | 5 | 0.5 |
| Z2-80 | 0.41 | 0.0564 | 0.00115 | 0.5298 | 0.01067 | 0.06811 | 0.00086 | 468 | 23 | 432 | 7 | 425 | 5 | 1.6 |
| ~~Z2-81~~ | ~~0.3~~ | ~~0.06114~~ | ~~0.00128~~ | ~~0.48713~~ | ~~0.00998~~ | ~~0.05777~~ | ~~0.00075~~ | ~~644~~ | ~~23~~ | ~~403~~ | ~~7~~ | ~~362~~ | ~~5~~ | ~~11.3~~ |
| Z2-82 | 0.7 | 0.05732 | 0.00113 | 0.43282 | 0.00845 | 0.05474 | 0.00069 | 504 | 22 | 365 | 6 | 344 | 4 | 6.1 |
| ~~Z2-83~~ | ~~0.34~~ | ~~0.0627~~ | ~~0.00118~~ | ~~0.5095~~ | ~~0.00948~~ | ~~0.05892~~ | ~~0.00074~~ | ~~698~~ | ~~20~~ | ~~418~~ | ~~6~~ | ~~369~~ | ~~5~~ | ~~13.3~~ |
| ~~Z2-84~~ | ~~0.58~~ | ~~0.06572~~ | ~~0.00161~~ | ~~0.59502~~ | ~~0.01427~~ | ~~0.06565~~ | ~~0.00088~~ | ~~797~~ | ~~28~~ | ~~474~~ | ~~9~~ | ~~410~~ | ~~5~~ | ~~15.6~~ |
| Z2-85 | 0.46 | 0.0509 | 0.00201 | 0.29026 | 0.01082 | 0.04136 | 0.00054 | 236 | 93 | 259 | 9 | 261 | 3 | -0.8 |
| Z2-86 | 0.6 | 0.05929 | 0.0011 | 0.54443 | 0.01 | 0.06658 | 0.00084 | 578 | 20 | 441 | 7 | 416 | 5 | 6 |
| ~~Z2-87~~ | ~~0.72~~ | ~~0.08162~~ | ~~0.0014~~ | ~~0.5929~~ | ~~0.01014~~ | ~~0.05267~~ | ~~0.00065~~ | ~~1236~~ | ~~16~~ | ~~473~~ | ~~6~~ | ~~331~~ | ~~4~~ | ~~42.9~~ |
| Z2-88 | 0.49 | 0.06489 | 0.00173 | 1.14144 | 0.02938 | 0.12755 | 0.00183 | 771 | 31 | 773 | 14 | 774 | 10 | -0.1 |
| Z2-89 | 0.45 | 0.05608 | 0.00118 | 0.53205 | 0.01106 | 0.0688 | 0.00089 | 456 | 24 | 433 | 7 | 429 | 5 | 0.9 |

| | | | | | | | | | | | | | | |
|---|---|---|---|---|---|---|---|---|---|---|---|---|---|---|
| ~~Z2-90~~ | ~~0.94~~ | ~~0.05691~~ | ~~0.00348~~ | ~~0.30571~~ | ~~0.01825~~ | ~~0.03895~~ | ~~0.0007~~ | ~~488~~ | ~~100~~ | ~~271~~ | ~~14~~ | ~~246~~ | ~~4~~ | ~~10.2~~ |
| Z2-91 | 0.56 | 0.05196 | 0.00193 | 0.25452 | 0.00923 | 0.03552 | 0.00052 | 284 | 56 | 230 | 7 | 225 | 3 | 2.2 |
| Z2-92 | 0.96 | 0.05703 | 0.00105 | 0.5648 | 0.01034 | 0.07181 | 0.0009 | 493 | 20 | 455 | 7 | 447 | 5 | 1.8 |
| Z2-93 | 0.42 | 0.05648 | 0.00228 | 0.47442 | 0.01812 | 0.06092 | 0.00081 | 471 | 92 | 394 | 12 | 381 | 5 | 3.4 |
| Z2-94 | 0.31 | 0.05538 | 0.00189 | 0.27418 | 0.00867 | 0.03591 | 0.00046 | 428 | 78 | 246 | 7 | 227 | 3 | 8.4 |
| Z2-95 | 0.96 | 0.0528 | 0.00128 | 0.27109 | 0.00641 | 0.03723 | 0.0005 | 320 | 30 | 244 | 5 | 236 | 3 | 3.4 |
| Z2-96 | 0.68 | 0.0589 | 0.00104 | 0.51676 | 0.00905 | 0.06361 | 0.00079 | 563 | 19 | 423 | 6 | 398 | 5 | 6.3 |
| ~~Z2-97~~ | ~~0.81~~ | ~~0.12264~~ | ~~0.00732~~ | ~~0.35643~~ | ~~0.02032~~ | ~~0.02108~~ | ~~0.00037~~ | ~~1995~~ | ~~109~~ | ~~310~~ | ~~15~~ | ~~134~~ | ~~2~~ | ~~131~~ |
| Z2-98 | 0.32 | 0.05966 | 0.00205 | 0.53714 | 0.01703 | 0.06529 | 0.00086 | 591 | 76 | 437 | 11 | 408 | 5 | 7.1 |
| **ADT1** | | | | | | | | | | | | | | |
| ~~ADT1-01~~ | ~~0.75~~ | ~~0.16542~~ | ~~0.0022~~ | ~~9.20263~~ | ~~0.14396~~ | ~~0.40341~~ | ~~0.00558~~ | ~~2512~~ | ~~12~~ | ~~2358~~ | ~~14~~ | ~~2185~~ | ~~26~~ | ~~15~~ |
| ADT1-02 | 0.63 | 0.05071 | 0.00295 | 0.25008 | 0.01451 | 0.03576 | 0.00059 | 228 | 103 | 227 | 12 | 226 | 4 | 0.4 |
| ~~ADT1-03~~ | ~~0.66~~ | ~~0.09694~~ | ~~0.00134~~ | ~~3.29453~~ | ~~0.05305~~ | ~~0.24645~~ | ~~0.00339~~ | ~~1566~~ | ~~14~~ | ~~1480~~ | ~~13~~ | ~~1420~~ | ~~18~~ | ~~10.3~~ |
| ~~ADT1-04~~ | ~~0.26~~ | ~~0.06907~~ | ~~0.00164~~ | ~~0.69357~~ | ~~0.01711~~ | ~~0.07281~~ | ~~0.00106~~ | ~~901~~ | ~~28~~ | ~~535~~ | ~~10~~ | ~~453~~ | ~~6~~ | ~~18.1~~ |
| ADT1-05 | 0.94 | 0.05682 | 0.00169 | 0.43722 | 0.01315 | 0.0558 | 0.00087 | 485 | 39 | 368 | 9 | 350 | 5 | 5.1 |
| ADT1-06 | 0.91 | 0.05596 | 0.00206 | 0.54766 | 0.02031 | 0.07096 | 0.00111 | 451 | 55 | 443 | 13 | 442 | 7 | 0.2 |
| ADT1-07 | 0.84 | 0.05533 | 0.00219 | 0.46519 | 0.01837 | 0.06097 | 0.00101 | 426 | 58 | 388 | 13 | 382 | 6 | 1.6 |
| ADT1-08 | 0.47 | 0.05421 | 0.00333 | 0.44328 | 0.02689 | 0.0593 | 0.00113 | 380 | 102 | 373 | 19 | 371 | 7 | 0.5 |
| ADT1-09 | 0.54 | 0.05483 | 0.00271 | 0.49409 | 0.02441 | 0.06535 | 0.00107 | 405 | 81 | 408 | 17 | 408 | 6 | 0 |
| ADT1-10 | 0.49 | 0.05036 | 0.00127 | 0.24084 | 0.00627 | 0.03468 | 0.0005 | 212 | 34 | 219 | 5 | 220 | 3 | -0.5 |
| ~~ADT1-11~~ | ~~0.54~~ | ~~0.08828~~ | ~~0.00123~~ | ~~2.49673~~ | ~~0.0404~~ | ~~0.20509~~ | ~~0.00282~~ | ~~1389~~ | ~~14~~ | ~~1271~~ | ~~12~~ | ~~1203~~ | ~~15~~ | ~~15.5~~ |
| ADT1-12 | 1.1 | 0.05554 | 0.00098 | 0.51755 | 0.00995 | 0.06757 | 0.00095 | 434 | 20 | 424 | 7 | 421 | 6 | 0.7 |
| ADT1-13 | 0.63 | 0.05026 | 0.00165 | 0.23503 | 0.00783 | 0.03391 | 0.0005 | 207 | 50 | 214 | 6 | 215 | 3 | -0.5 |
| ADT1-14 | 0.53 | 0.05029 | 0.00214 | 0.22738 | 0.00969 | 0.03279 | 0.00052 | 208 | 69 | 208 | 8 | 208 | 3 | 0 |
| ADT1-15 | 0.75 | 0.05062 | 0.00144 | 0.24168 | 0.00706 | 0.03462 | 0.00051 | 224 | 41 | 220 | 6 | 219 | 3 | 0.5 |
| ADT1-16 | 0.45 | 0.05321 | 0.00269 | 0.23815 | 0.01145 | 0.03246 | 0.00051 | 338 | 118 | 217 | 9 | 206 | 3 | 5.3 |

| | | | | | | | | | | | | | | |
|---|---|---|---|---|---|---|---|---|---|---|---|---|---|---|
| ADT1-17 | 0.51 | 0.05453 | 0.00581 | 0.45097 | 0.04762 | 0.05997 | 0.00131 | 393 | 198 | 378 | 33 | 375 | 8 | 0.8 |
| ADT1-18 | 0.57 | 0.05446 | 0.00363 | 0.45725 | 0.03018 | 0.06088 | 0.00114 | 390 | 115 | 382 | 21 | 381 | 7 | 0.3 |
| ADT1-19 | 0.43 | 0.05049 | 0.0013 | 0.23612 | 0.00629 | 0.03391 | 0.00049 | 218 | 36 | 215 | 5 | 215 | 3 | 0 |
| ~~ADT1-20~~ | ~~0.41~~ | ~~0.09609~~ | ~~0.00273~~ | ~~2.78806~~ | ~~0.06819~~ | ~~0.21044~~ | ~~0.00304~~ | ~~1549~~ | ~~55~~ | ~~1352~~ | ~~18~~ | ~~1231~~ | ~~16~~ | ~~25.8~~ |
| ADT1-21 | 0.59 | 0.05525 | 0.00568 | 0.49528 | 0.04993 | 0.06501 | 0.00175 | 422 | 178 | 409 | 34 | 406 | 11 | 0.7 |
| ~~ADT1-22~~ | ~~0.77~~ | ~~0.06546~~ | ~~0.00183~~ | ~~0.53638~~ | ~~0.0152~~ | ~~0.05942~~ | ~~0.00092~~ | ~~789~~ | ~~34~~ | ~~436~~ | ~~10~~ | ~~372~~ | ~~6~~ | ~~17.2~~ |
| ADT1-23 | 0.06 | 0.05924 | 0.00145 | 0.56689 | 0.01158 | 0.06941 | 0.00095 | 576 | 55 | 456 | 8 | 433 | 6 | 5.3 |
| ADT1-24 | 0.58 | 0.05538 | 0.00389 | 0.47971 | 0.03342 | 0.06281 | 0.00116 | 428 | 123 | 398 | 23 | 393 | 7 | 1.3 |
| ADT1-25 | 0.46 | 0.05042 | 0.00214 | 0.23297 | 0.00986 | 0.03351 | 0.00055 | 214 | 67 | 213 | 8 | 212 | 3 | 0.5 |
| ~~ADT1-26~~ | ~~0.38~~ | ~~0.06474~~ | ~~0.00198~~ | ~~0.49115~~ | ~~0.01333~~ | ~~0.05503~~ | ~~0.00077~~ | ~~766~~ | ~~66~~ | ~~406~~ | ~~9~~ | ~~345~~ | ~~5~~ | ~~17.7~~ |
| ADT1-27 | 0.73 | 0.05491 | 0.00176 | 0.49906 | 0.01617 | 0.06591 | 0.00102 | 409 | 45 | 411 | 11 | 411 | 6 | 0 |
| ADT1-28 | 0.41 | 0.05041 | 0.00194 | 0.22744 | 0.00877 | 0.03272 | 0.00052 | 214 | 60 | 208 | 7 | 208 | 3 | 0 |
| ~~ADT1-29~~ | ~~0.79~~ | ~~0.0714~~ | ~~0.00228~~ | ~~0.34692~~ | ~~0.01113~~ | ~~0.03524~~ | ~~0.00056~~ | ~~969~~ | ~~40~~ | ~~302~~ | ~~8~~ | ~~223~~ | ~~3~~ | ~~35.4~~ |
| ADT1-30 | 0.66 | 0.05049 | 0.00121 | 0.2308 | 0.00575 | 0.03315 | 0.00048 | 218 | 32 | 211 | 5 | 210 | 3 | 0.5 |
| ADT1-31 | 0.82 | 0.0519 | 0.00323 | 0.241 | 0.01493 | 0.03367 | 0.00057 | 281 | 111 | 219 | 12 | 213 | 4 | 2.8 |
| ~~ADT1-32~~ | ~~0.52~~ | ~~0.06674~~ | ~~0.00217~~ | ~~0.73803~~ | ~~0.02416~~ | ~~0.08018~~ | ~~0.00126~~ | ~~830~~ | ~~42~~ | ~~561~~ | ~~14~~ | ~~497~~ | ~~8~~ | ~~12.9~~ |
| ADT1-33 | 0.22 | 0.0553 | 0.0014 | 0.49105 | 0.01286 | 0.06439 | 0.00092 | 424 | 34 | 406 | 9 | 402 | 6 | 1 |
| ~~ADT1-34~~ | ~~0.82~~ | ~~0.07423~~ | ~~0.00618~~ | ~~0.34772~~ | ~~0.02804~~ | ~~0.03397~~ | ~~0.00071~~ | ~~1048~~ | ~~174~~ | ~~303~~ | ~~21~~ | ~~215~~ | ~~4~~ | ~~40.9~~ |
| ADT1-35 | 0.4 | 0.05066 | 0.0012 | 0.23914 | 0.0059 | 0.03423 | 0.00049 | 225 | 32 | 218 | 5 | 217 | 3 | 0.5 |
| ADT1-36 | 0.39 | 0.05589 | 0.00232 | 0.50631 | 0.0211 | 0.0657 | 0.00104 | 448 | 64 | 416 | 14 | 410 | 6 | 1.5 |
| ADT1-37 | 0.7 | 0.0553 | 0.00153 | 0.50765 | 0.01432 | 0.06657 | 0.00099 | 424 | 37 | 417 | 10 | 415 | 6 | 0.5 |
| ADT1-38 | 0.61 | 0.05042 | 0.00211 | 0.24083 | 0.0101 | 0.03464 | 0.00054 | 214 | 68 | 219 | 8 | 220 | 3 | -0.5 |
| ~~ADT1-39~~ | ~~0.97~~ | ~~0.09047~~ | ~~0.00493~~ | ~~2.78871~~ | ~~0.14473~~ | ~~0.22356~~ | ~~0.00371~~ | ~~1435~~ | ~~107~~ | ~~1353~~ | ~~39~~ | ~~1301~~ | ~~20~~ | ~~10.3~~ |
| ~~ADT1-40~~ | ~~0.8~~ | ~~0.05818~~ | ~~0.00169~~ | ~~0.26054~~ | ~~0.00771~~ | ~~0.03247~~ | ~~0.00048~~ | ~~537~~ | ~~39~~ | ~~235~~ | ~~6~~ | ~~206~~ | ~~3~~ | ~~14.1~~ |
| ADT1-41 | 0.34 | 0.05714 | 0.00307 | 0.56909 | 0.03039 | 0.07223 | 0.00126 | 497 | 87 | 457 | 20 | 450 | 8 | 1.6 |
| ADT1-42 | 0.77 | 0.08163 | 0.00114 | 2.3245 | 0.03751 | 0.20649 | 0.00282 | 1237 | 14 | 1220 | 11 | 1210 | 15 | 2.2 |
| ADT1-43 | 0.49 | 0.09301 | 0.00142 | 3.12348 | 0.0534 | 0.24352 | 0.00339 | 1488 | 15 | 1438 | 13 | 1405 | 18 | 5.9 |
| ADT1-44 | 0.61 | 0.05504 | 0.00325 | 0.47569 | 0.0279 | 0.06268 | 0.0011 | 414 | 100 | 395 | 19 | 392 | 7 | 0.8 |

| | | | | | | | | | | | | | | |
|---|---|---|---|---|---|---|---|---|---|---|---|---|---|---|
| ADT1-45 | 0.54 | 0.0569 | 0.00098 | 0.45651 | 0.00857 | 0.05818 | 0.00081 | 488 | 20 | 382 | 6 | 365 | 5 | 4.7 |
| ~~ADT1-46~~ | ~~0.72~~ | ~~0.06624~~ | ~~0.00338~~ | ~~0.55613~~ | ~~0.02685~~ | ~~0.06089~~ | ~~0.00099~~ | ~~814~~ | ~~109~~ | ~~449~~ | ~~18~~ | ~~381~~ | ~~6~~ | ~~17.8~~ |
| ~~ADT1-47~~ | ~~0.75~~ | ~~0.09173~~ | ~~0.0056~~ | ~~0.7602~~ | ~~0.04457~~ | ~~0.06011~~ | ~~0.00103~~ | ~~1462~~ | ~~119~~ | ~~574~~ | ~~26~~ | ~~376~~ | ~~6~~ | ~~52.7~~ |
| ~~ADT1-48~~ | ~~0.25~~ | ~~0.09414~~ | ~~0.00131~~ | ~~2.47008~~ | ~~0.03971~~ | ~~0.19026~~ | ~~0.0026~~ | ~~1511~~ | ~~14~~ | ~~1263~~ | ~~12~~ | ~~1123~~ | ~~14~~ | ~~34.6~~ |
| ADT1-49 | 0.57 | 0.05211 | 0.00242 | 0.25039 | 0.01098 | 0.03485 | 0.00053 | 290 | 109 | 227 | 9 | 221 | 3 | 2.7 |
| ADT1-50 | 0.56 | 0.05389 | 0.00203 | 0.25408 | 0.00947 | 0.03419 | 0.00057 | 366 | 54 | 230 | 8 | 217 | 4 | 6 |
| ~~ADT1-51~~ | ~~0.79~~ | ~~0.05736~~ | ~~0.00341~~ | ~~0.25855~~ | ~~0.01481~~ | ~~0.03269~~ | ~~0.00053~~ | ~~505~~ | ~~135~~ | ~~233~~ | ~~12~~ | ~~207~~ | ~~3~~ | ~~12.6~~ |
| ADT1-52 | 0.9 | 0.05562 | 0.00092 | 0.50881 | 0.00923 | 0.06634 | 0.00092 | 437 | 19 | 418 | 6 | 414 | 6 | 1 |
| ADT1-53 | 2.09 | 0.09047 | 0.00129 | 2.92264 | 0.04775 | 0.23428 | 0.00322 | 1435 | 14 | 1388 | 12 | 1357 | 17 | 5.7 |
| ADT1-54 | 0.55 | 0.0926 | 0.0013 | 3.12935 | 0.05048 | 0.24507 | 0.00335 | 1480 | 14 | 1440 | 12 | 1413 | 17 | 4.7 |
| ADT1-55 | 0.09 | 0.05528 | 0.00231 | 0.47796 | 0.01882 | 0.06271 | 0.00089 | 424 | 96 | 397 | 13 | 392 | 5 | 1.3 |
| ADT1-56 | 0.55 | 0.05407 | 0.0028 | 0.25222 | 0.01242 | 0.03383 | 0.00054 | 374 | 120 | 228 | 10 | 214 | 3 | 6.5 |
| ~~ADT1-57~~ | ~~0.67~~ | ~~0.06261~~ | ~~0.00338~~ | ~~0.51567~~ | ~~0.02724~~ | ~~0.05973~~ | ~~0.00118~~ | ~~695~~ | ~~79~~ | ~~422~~ | ~~18~~ | ~~374~~ | ~~7~~ | ~~12.8~~ |
| ~~ADT1-58~~ | ~~0.79~~ | ~~0.06695~~ | ~~0.00169~~ | ~~0.6134~~ | ~~0.01574~~ | ~~0.06644~~ | ~~0.00102~~ | ~~836~~ | ~~29~~ | ~~486~~ | ~~10~~ | ~~415~~ | ~~6~~ | ~~17.1~~ |
| ADT1-59 | 0.88 | 0.05146 | 0.00139 | 0.29422 | 0.00809 | 0.04146 | 0.00063 | 261 | 36 | 262 | 6 | 262 | 4 | 0 |
| ~~ADT1-60~~ | ~~0.95~~ | ~~0.06344~~ | ~~0.00158~~ | ~~0.29742~~ | ~~0.00755~~ | ~~0.034~~ | ~~0.00051~~ | ~~723~~ | ~~29~~ | ~~264~~ | ~~6~~ | ~~216~~ | ~~3~~ | ~~22.2~~ |
| ADT1-61 | 0.76 | 0.06022 | 0.0049 | 0.54041 | 0.04266 | 0.06508 | 0.00129 | 611 | 182 | 439 | 28 | 406 | 8 | 8.1 |
| ~~ADT1-62~~ | ~~0.83~~ | ~~0.07303~~ | ~~0.03043~~ | ~~0.36463~~ | ~~0.1513~~ | ~~0.03621~~ | ~~0.00141~~ | ~~1015~~ | ~~893~~ | ~~316~~ | ~~113~~ | ~~229~~ | ~~9~~ | ~~38~~ |
| ADT1-63 | 0.77 | 0.05324 | 0.00291 | 0.2468 | 0.01291 | 0.03362 | 0.00053 | 339 | 127 | 224 | 11 | 213 | 3 | 5.2 |
| ADT1-64 | 0.61 | 0.05512 | 0.00088 | 0.53033 | 0.00937 | 0.06977 | 0.00096 | 417 | 18 | 432 | 6 | 435 | 6 | -0.7 |
| ~~ADT1-65~~ | ~~0.49~~ | ~~0.06016~~ | ~~0.00319~~ | ~~0.28423~~ | ~~0.0143~~ | ~~0.03426~~ | ~~0.00057~~ | ~~609~~ | ~~118~~ | ~~254~~ | ~~11~~ | ~~217~~ | ~~4~~ | ~~17.1~~ |
| ADT1-66 | 0.28 | 0.06125 | 0.00187 | 0.92278 | 0.02491 | 0.10928 | 0.00155 | 648 | 67 | 664 | 13 | 669 | 9 | -0.7 |
| ADT1-67 | 0.45 | 0.05245 | 0.00165 | 0.23827 | 0.00749 | 0.03294 | 0.00052 | 305 | 43 | 217 | 6 | 209 | 3 | 3.8 |
| ADT1-68 | 0.24 | 0.0558 | 0.00227 | 0.51361 | 0.02062 | 0.06674 | 0.00115 | 444 | 59 | 421 | 14 | 416 | 7 | 1.2 |
| ~~ADT1-69~~ | ~~0.61~~ | ~~0.08948~~ | ~~0.00149~~ | ~~2.4616~~ | ~~0.04476~~ | ~~0.1995~~ | ~~0.00282~~ | ~~1414~~ | ~~16~~ | ~~1261~~ | ~~13~~ | ~~1173~~ | ~~15~~ | ~~20.5~~ |
| ADT1-70 | 0.75 | 0.06253 | 0.00177 | 0.64032 | 0.01824 | 0.07426 | 0.00116 | 692 | 35 | 503 | 11 | 462 | 7 | 8.9 |
| ADT1-71 | 0.74 | 0.05497 | 0.00157 | 0.26368 | 0.00761 | 0.03479 | 0.00054 | 411 | 37 | 238 | 6 | 220 | 3 | 8.2 |
| ADT1-72 | 0.66 | 0.05425 | 0.00144 | 0.2643 | 0.00713 | 0.03533 | 0.00053 | 381 | 34 | 238 | 6 | 224 | 3 | 6.3 |

| | | | | | | | | | | | | | | |
|---|---|---|---|---|---|---|---|---|---|---|---|---|---|---|
| ADT1-73 | 0.9 | 0.09224 | 0.00156 | 3.13441 | 0.05758 | 0.24641 | 0.0035 | 1472 | 16 | 1441 | 14 | 1420 | 18 | 3.7 |
| ADT1-74 | 0.51 | 0.05549 | 0.00124 | 0.46956 | 0.01084 | 0.06136 | 0.00089 | 432 | 27 | 391 | 7 | 384 | 5 | 1.8 |
| ADT1-75 | 0.6 | 0.05624 | 0.00133 | 0.47535 | 0.01154 | 0.0613 | 0.00091 | 462 | 29 | 395 | 8 | 384 | 6 | 2.9 |
| ADT1-76 | 0.38 | 0.07845 | 0.00119 | 1.64091 | 0.02784 | 0.15167 | 0.00209 | 1158 | 15 | 986 | 11 | 910 | 12 | 8.4 |
| ~~ADT1-77~~ | ~~0.57~~ | ~~0.0591~~ | ~~0.00404~~ | ~~0.27748~~ | ~~0.01829~~ | ~~0.03405~~ | ~~0.00062~~ | ~~571~~ | ~~153~~ | ~~249~~ | ~~15~~ | ~~216~~ | ~~4~~ | ~~15.3~~ |
| ADT1-78 | 0.85 | 0.05425 | 0.00133 | 0.43737 | 0.01097 | 0.05846 | 0.00087 | 381 | 31 | 368 | 8 | 366 | 5 | 0.5 |
| ADT1-79 | 0.48 | 0.05603 | 0.00119 | 0.46502 | 0.01033 | 0.06019 | 0.00087 | 454 | 25 | 388 | 7 | 377 | 5 | 2.9 |
| ADT1-80 | 0.69 | 0.05054 | 0.00193 | 0.24427 | 0.00923 | 0.03505 | 0.00058 | 220 | 57 | 222 | 8 | 222 | 4 | 0 |
| ~~ADT1-81~~ | ~~0.91~~ | ~~0.0594~~ | ~~0.00171~~ | ~~0.41556~~ | ~~0.012~~ | ~~0.05073~~ | ~~0.00079~~ | ~~582~~ | ~~36~~ | ~~353~~ | ~~9~~ | ~~319~~ | ~~5~~ | ~~10.7~~ |
| ADT1-82 | 0.53 | 0.04947 | 0.0013 | 0.24025 | 0.00641 | 0.03522 | 0.00053 | 170 | 35 | 219 | 5 | 223 | 3 | -1.8 |
| ADT1-83 | 1.1 | 0.0779 | 0.00152 | 1.99989 | 0.04103 | 0.18617 | 0.0027 | 1144 | 20 | 1115 | 14 | 1101 | 15 | 3.9 |
| ADT1-84 | 0.62 | 0.05124 | 0.00179 | 0.24666 | 0.00859 | 0.03491 | 0.00056 | 252 | 51 | 224 | 7 | 221 | 3 | 1.4 |
| ~~ADT1-85~~ | ~~0.61~~ | ~~0.09216~~ | ~~0.00145~~ | ~~2.41105~~ | ~~0.04204~~ | ~~0.18972~~ | ~~0.00264~~ | ~~1471~~ | ~~15~~ | ~~1246~~ | ~~13~~ | ~~1120~~ | ~~14~~ | ~~31.3~~ |
| ADT1-86 | 0.57 | 0.05114 | 0.00239 | 0.44394 | 0.02049 | 0.06295 | 0.00112 | 247 | 73 | 373 | 14 | 394 | 7 | -5.3 |
| ADT1-87 | 0.55 | 0.05668 | 0.00162 | 0.48327 | 0.01386 | 0.06182 | 0.00096 | 479 | 37 | 400 | 9 | 387 | 6 | 3.4 |
| ADT1-88 | 0.63 | 0.05924 | 0.00436 | 0.483 | 0.03431 | 0.05913 | 0.00112 | 576 | 165 | 400 | 23 | 370 | 7 | 8.1 |
| ADT1-89 | 0.79 | 0.07156 | 0.00366 | 1.49543 | 0.07258 | 0.15156 | 0.00244 | 974 | 107 | 929 | 30 | 910 | 14 | 2.1 |
| ADT1-90 | 1.21 | 0.05631 | 0.0011 | 0.46309 | 0.00957 | 0.05964 | 0.00085 | 465 | 23 | 386 | 7 | 373 | 5 | 3.5 |
| ~~ADT1-91~~ | ~~0.74~~ | ~~0.06798~~ | ~~0.0022~~ | ~~0.3058~~ | ~~0.00981~~ | ~~0.03262~~ | ~~0.00053~~ | ~~868~~ | ~~40~~ | ~~271~~ | ~~8~~ | ~~207~~ | ~~3~~ | ~~30.9~~ |
| ADT1-92 | 0.64 | 0.08236 | 0.00132 | 2.34219 | 0.04146 | 0.20623 | 0.00287 | 1254 | 16 | 1225 | 13 | 1209 | 15 | 3.7 |
| ADT1-93 | 0.46 | 0.05531 | 0.00106 | 0.44585 | 0.00908 | 0.05845 | 0.00083 | 425 | 22 | 374 | 6 | 366 | 5 | 2.2 |
| ~~ADT1-94~~ | ~~0.55~~ | ~~0.15617~~ | ~~0.02305~~ | ~~1.56275~~ | ~~0.22555~~ | ~~0.07258~~ | ~~0.00225~~ | ~~2415~~ | ~~265~~ | ~~956~~ | ~~89~~ | ~~452~~ | ~~13~~ | ~~112~~ |
| ADT1-95 | 0.6 | 0.052 | 0.00149 | 0.2389 | 0.00688 | 0.03331 | 0.00051 | 285 | 38 | 218 | 6 | 211 | 3 | 3.3 |
| ADT1-96 | 0.48 | 0.0522 | 0.00193 | 0.23398 | 0.00859 | 0.0325 | 0.00054 | 294 | 54 | 213 | 7 | 206 | 3 | 3.4 |
| ADT1-97 | 0.52 | 0.04881 | 0.00158 | 0.22963 | 0.00745 | 0.03412 | 0.00054 | 139 | 47 | 210 | 6 | 216 | 3 | -2.8 |
| ADT1-98 | 0.97 | 0.11119 | 0.00192 | 5.01324 | 0.09328 | 0.32694 | 0.00468 | 1819 | 16 | 1822 | 16 | 1824 | 23 | -0.3 |
| ADT1-99 | 0.51 | 0.07749 | 0.00266 | 1.5753 | 0.04893 | 0.14744 | 0.00217 | 1134 | 70 | 961 | 19 | 887 | 12 | 8.3 |
| ADT1-100 | 0.29 | 0.05757 | 0.00102 | 0.4916 | 0.00937 | 0.06192 | 0.00087 | 513 | 20 | 406 | 6 | 387 | 5 | 4.9 |

| | | | | | | | | | | | | | | |
|---|---|---|---|---|---|---|---|---|---|---|---|---|---|---|
| **ADT4** | | | | | | | | | | | | | | |
| ADT4-01 | 0.02 | 0.05511 | 0.00165 | 0.5458 | 0.01451 | 0.07183 | 0.001 | 417 | 69 | 442 | 10 | 447 | 6 | -1.1 |
| ~~ADT4-02~~ | ~~0.7~~ | ~~0.063~~ | ~~0.00178~~ | ~~0.34825~~ | ~~0.01006~~ | ~~0.04008~~ | ~~0.00059~~ | ~~708~~ | ~~37~~ | ~~303~~ | ~~8~~ | ~~253~~ | ~~4~~ | ~~19.8~~ |
| ADT4-03 | 0.39 | 0.04915 | 0.00375 | 0.18866 | 0.01408 | 0.02784 | 0.00045 | 155 | 173 | 175 | 12 | 177 | 3 | -1.1 |
| ADT4-04 | 0.65 | 0.05135 | 0.00202 | 0.29443 | 0.01167 | 0.04157 | 0.00063 | 257 | 63 | 262 | 9 | 263 | 4 | -0.4 |
| ~~ADT4-05~~ | ~~1.2~~ | ~~0.08386~~ | ~~0.00758~~ | ~~0.08575~~ | ~~0.00753~~ | ~~0.00742~~ | ~~0.00016~~ | ~~1289~~ | ~~182~~ | ~~84~~ | ~~7~~ | ~~48~~ | ~~1~~ | ~~75~~ |
| ADT4-06 | 0.61 | 0.11954 | 0.00162 | 5.50456 | 0.08739 | 0.33389 | 0.00461 | 1949 | 13 | 1901 | 14 | 1857 | 22 | 5 |
| ADT4-07 | 0.61 | 0.05858 | 0.00239 | 0.50772 | 0.02079 | 0.06285 | 0.00098 | 552 | 62 | 417 | 14 | 393 | 6 | 6.1 |
| ADT4-08 | 0.51 | 0.05096 | 0.00118 | 0.23776 | 0.00576 | 0.03383 | 0.00048 | 239 | 31 | 217 | 5 | 214 | 3 | 1.4 |
| ~~ADT4-09~~ | ~~0.9~~ | ~~0.0749~~ | ~~0.00702~~ | ~~0.54879~~ | ~~0.05026~~ | ~~0.05314~~ | ~~0.00107~~ | ~~1066~~ | ~~196~~ | ~~444~~ | ~~33~~ | ~~334~~ | ~~7~~ | ~~32.9~~ |
| ~~ADT4-10~~ | ~~0.14~~ | ~~0.05806~~ | ~~0.00125~~ | ~~0.34012~~ | ~~0.00773~~ | ~~0.04248~~ | ~~0.0006~~ | ~~532~~ | ~~26~~ | ~~297~~ | ~~6~~ | ~~268~~ | ~~4~~ | ~~10.8~~ |
| ~~ADT4-11~~ | ~~0.99~~ | ~~0.07011~~ | ~~0.00338~~ | ~~0.5763~~ | ~~0.02631~~ | ~~0.05961~~ | ~~0.00092~~ | ~~932~~ | ~~101~~ | ~~462~~ | ~~17~~ | ~~373~~ | ~~6~~ | ~~23.9~~ |
| ADT4-12 | 0.77 | 0.06167 | 0.00155 | 0.57256 | 0.01491 | 0.06732 | 0.00097 | 663 | 32 | 460 | 10 | 420 | 6 | 9.5 |
| ~~ADT4-13~~ | ~~0.67~~ | ~~0.08384~~ | ~~0.00711~~ | ~~0.78535~~ | ~~0.06463~~ | ~~0.06793~~ | ~~0.00138~~ | ~~1289~~ | ~~171~~ | ~~589~~ | ~~37~~ | ~~424~~ | ~~8~~ | ~~38.9~~ |
| ADT4-14 | 0.58 | 0.05512 | 0.00206 | 0.48972 | 0.01845 | 0.06442 | 0.00097 | 417 | 57 | 405 | 13 | 402 | 6 | 0.7 |
| ADT4-15 | 0.42 | 0.05584 | 0.00214 | 0.44629 | 0.01586 | 0.05796 | 0.00084 | 446 | 87 | 375 | 11 | 363 | 5 | 3.3 |
| ~~ADT4-16~~ | ~~0.41~~ | ~~0.06268~~ | ~~0.00311~~ | ~~0.57326~~ | ~~0.02695~~ | ~~0.06633~~ | ~~0.00105~~ | ~~697~~ | ~~108~~ | ~~460~~ | ~~17~~ | ~~414~~ | ~~6~~ | ~~11.1~~ |
| ADT4-17 | 0.26 | 0.0503 | 0.00128 | 0.23697 | 0.00625 | 0.03416 | 0.0005 | 209 | 35 | 216 | 5 | 217 | 3 | -0.5 |
| ~~ADT4-18~~ | ~~1.67~~ | ~~0.07936~~ | ~~0.00915~~ | ~~0.79859~~ | ~~0.09023~~ | ~~0.07298~~ | ~~0.00169~~ | ~~1181~~ | ~~239~~ | ~~596~~ | ~~51~~ | ~~454~~ | ~~10~~ | ~~31.3~~ |
| ADT4-19 | 0.39 | 0.06192 | 0.00255 | 0.61544 | 0.02367 | 0.07209 | 0.00108 | 671 | 90 | 487 | 15 | 449 | 6 | 8.5 |
| ADT4-20 | 0.21 | 0.07862 | 0.00209 | 1.63589 | 0.03721 | 0.15091 | 0.00209 | 1163 | 54 | 984 | 14 | 906 | 12 | 8.6 |
| ADT4-21 | 0.22 | 0.05565 | 0.00124 | 0.49887 | 0.01163 | 0.065 | 0.00093 | 438 | 28 | 411 | 8 | 406 | 6 | 1.2 |
| ADT4-22 | 0.55 | 0.05526 | 0.00128 | 0.54701 | 0.01318 | 0.07178 | 0.00104 | 423 | 29 | 443 | 9 | 447 | 6 | -0.9 |
| ~~ADT4-23~~ | ~~0.79~~ | ~~0.05697~~ | ~~0.00232~~ | ~~0.2957~~ | ~~0.01212~~ | ~~0.03763~~ | ~~0.00057~~ | ~~490~~ | ~~64~~ | ~~263~~ | ~~9~~ | ~~238~~ | ~~4~~ | ~~10.5~~ |
| ~~ADT4-24~~ | ~~0.88~~ | ~~0.07001~~ | ~~0.00617~~ | ~~0.37455~~ | ~~0.03271~~ | ~~0.03879~~ | ~~0.00077~~ | ~~929~~ | ~~148~~ | ~~323~~ | ~~24~~ | ~~245~~ | ~~5~~ | ~~31.8~~ |
| ~~ADT4-25~~ | ~~0.7~~ | ~~0.0753~~ | ~~0.00212~~ | ~~0.58544~~ | ~~0.01679~~ | ~~0.05637~~ | ~~0.00085~~ | ~~1077~~ | ~~34~~ | ~~468~~ | ~~11~~ | ~~354~~ | ~~5~~ | ~~32.2~~ |

| | | | | | | | | | | | | | | |
|---|---|---|---|---|---|---|---|---|---|---|---|---|---|---|
| ADT4-26 | 0.86 | 0.05643 | 0.001 | 0.50362 | 0.00974 | 0.06471 | 0.0009 | 469 | 21 | 414 | 7 | 404 | 5 | 2.5 |
| ~~ADT4-27~~ | ~~0.81~~ | ~~0.06881~~ | ~~0.00349~~ | ~~0.36356~~ | ~~0.01753~~ | ~~0.03832~~ | ~~0.0006~~ | ~~893~~ | ~~107~~ | ~~315~~ | ~~13~~ | ~~242~~ | ~~4~~ | ~~30.2~~ |
| ADT4-28 | 0.24 | 0.06816 | 0.00195 | 1.21619 | 0.03041 | 0.1294 | 0.00181 | 874 | 61 | 808 | 14 | 784 | 10 | 3.1 |
| ADT4-29 | 0.86 | 0.04605 | 0.00841 | 0.03633 | 0.00658 | 0.00572 | 0.00013 | | 312 | 36 | 6 | 36.8 | 0.8 | -2.2 |
| ~~ADT4-30~~ | ~~0.64~~ | ~~0.06555~~ | ~~0.00358~~ | ~~0.58107~~ | ~~0.03039~~ | ~~0.06429~~ | ~~0.00102~~ | ~~792~~ | ~~118~~ | ~~465~~ | ~~20~~ | ~~402~~ | ~~6~~ | ~~15.7~~ |
| ~~ADT4-31~~ | ~~0.98~~ | ~~0.07807~~ | ~~0.00435~~ | ~~0.37922~~ | ~~0.02016~~ | ~~0.03523~~ | ~~0.00059~~ | ~~1149~~ | ~~114~~ | ~~326~~ | ~~15~~ | ~~223~~ | 4 | ~~46.2~~ |
| ADT4-32 | 0.6 | 0.05323 | 0.00275 | 0.34175 | 0.01687 | 0.04656 | 0.0007 | 339 | 120 | 298 | 13 | 293 | 4 | 1.7 |
| ADT4-33 | 0.18 | 0.05887 | 0.00129 | 0.58111 | 0.01334 | 0.07158 | 0.00102 | 562 | 26 | 465 | 9 | 446 | 6 | 4.3 |
| ~~ADT4-34~~ | ~~0.56~~ | ~~0.07955~~ | ~~0.00139~~ | ~~1.63027~~ | ~~0.031~~ | ~~0.1486~~ | ~~0.00209~~ | ~~1186~~ | ~~18~~ | ~~982~~ | ~~12~~ | ~~893~~ | ~~12~~ | ~~10~~ |
| ~~ADT4-35~~ | ~~0.23~~ | ~~0.07856~~ | ~~0.00228~~ | ~~1.35577~~ | ~~0.03434~~ | ~~0.12516~~ | ~~0.00177~~ | ~~1161~~ | ~~59~~ | ~~870~~ | ~~15~~ | ~~760~~ | ~~10~~ | ~~14.5~~ |
| ~~ADT4-36~~ | ~~0.67~~ | ~~0.07506~~ | ~~0.00188~~ | ~~0.9273~~ | ~~0.02386~~ | ~~0.08958~~ | ~~0.00132~~ | ~~1070~~ | ~~29~~ | ~~666~~ | ~~13~~ | ~~553~~ | ~~8~~ | ~~20.4~~ |
| ~~ADT4-37~~ | ~~0.08~~ | ~~0.08958~~ | ~~0.0034~~ | ~~0.87132~~ | ~~0.03052~~ | ~~0.07054~~ | ~~0.00103~~ | ~~1417~~ | ~~74~~ | ~~636~~ | ~~17~~ | ~~439~~ | ~~6~~ | ~~44.9~~ |
| ~~ADT4-38~~ | ~~0.88~~ | ~~0.07121~~ | ~~0.0019~~ | ~~0.64176~~ | ~~0.01754~~ | ~~0.06534~~ | ~~0.00097~~ | ~~963~~ | ~~32~~ | ~~503~~ | ~~11~~ | ~~408~~ | ~~6~~ | ~~23.3~~ |
| ADT4-39 | 0.71 | 0.05271 | 0.00256 | 0.34695 | 0.01689 | 0.04773 | 0.00074 | 316 | 82 | 302 | 13 | 301 | 5 | 0.3 |
| ~~ADT4-40~~ | ~~0.8~~ | ~~0.09185~~ | ~~0.00177~~ | ~~0.65353~~ | ~~0.01333~~ | ~~0.05159~~ | ~~0.00074~~ | ~~1464~~ | ~~19~~ | ~~511~~ | ~~8~~ | ~~324~~ | ~~5~~ | ~~57.7~~ |
| ~~ADT4-41~~ | ~~0.66~~ | ~~0.07079~~ | ~~0.0037~~ | ~~0.58076~~ | ~~0.02887~~ | ~~0.0595~~ | ~~0.00097~~ | ~~951~~ | ~~110~~ | ~~465~~ | ~~19~~ | ~~373~~ | ~~6~~ | ~~24.7~~ |
| ADT4-42 | 0.07 | 0.07358 | 0.00159 | 1.59108 | 0.02718 | 0.15683 | 0.00209 | 1030 | 45 | 967 | 11 | 939 | 12 | 3 |
| ~~ADT4-43~~ | ~~0.78~~ | ~~0.05957~~ | ~~0.00304~~ | ~~0.37948~~ | ~~0.01844~~ | ~~0.0462~~ | ~~0.00071~~ | ~~588~~ | ~~114~~ | ~~327~~ | ~~14~~ | ~~291~~ | ~~4~~ | ~~12.4~~ |
| ~~ADT4-44~~ | ~~0.89~~ | ~~0.07688~~ | ~~0.00509~~ | ~~1.22418~~ | ~~0.07812~~ | ~~0.11548~~ | ~~0.00205~~ | ~~1118~~ | ~~136~~ | ~~812~~ | ~~36~~ | ~~705~~ | ~~12~~ | ~~15.2~~ |
| ADT4-45 | 0.22 | 0.05492 | 0.00142 | 0.49641 | 0.01321 | 0.06554 | 0.00095 | 409 | 34 | 409 | 9 | 409 | 6 | 0 |
| ~~ADT4-46~~ | ~~0.77~~ | ~~0.06783~~ | ~~0.00198~~ | ~~0.54956~~ | ~~0.01631~~ | ~~0.05875~~ | ~~0.00088~~ | ~~863~~ | ~~37~~ | ~~445~~ | ~~11~~ | ~~368~~ | ~~5~~ | ~~20.9~~ |
| ~~ADT4-47~~ | ~~0.45~~ | ~~0.06202~~ | ~~0.00249~~ | ~~0.56821~~ | ~~0.02123~~ | ~~0.06645~~ | ~~0.00098~~ | ~~675~~ | ~~88~~ | ~~457~~ | ~~14~~ | ~~415~~ | ~~6~~ | ~~10.1~~ |
| ~~ADT4-48~~ | ~~0.6~~ | ~~0.06797~~ | ~~0.00121~~ | ~~0.57474~~ | ~~0.01113~~ | ~~0.06131~~ | ~~0.00085~~ | ~~868~~ | ~~19~~ | ~~461~~ | ~~7~~ | ~~384~~ | ~~5~~ | ~~20.1~~ |
| ADT4-49 | 0.67 | 0.05673 | 0.00118 | 0.4329 | 0.00948 | 0.05534 | 0.00079 | 481 | 25 | 365 | 7 | 347 | 5 | 5.2 |
| ~~ADT4-50~~ | ~~0.56~~ | ~~0.10729~~ | ~~0.00342~~ | ~~3.21002~~ | ~~0.09077~~ | ~~0.21699~~ | ~~0.00319~~ | ~~1754~~ | ~~60~~ | ~~1460~~ | ~~22~~ | ~~1266~~ | ~~17~~ | ~~38.5~~ |
| ~~ADT4-51~~ | ~~0.89~~ | ~~0.0766~~ | ~~0.0068~~ | ~~0.3294~~ | ~~0.0285~~ | ~~0.03119~~ | ~~0.00063~~ | ~~1111~~ | ~~184~~ | ~~289~~ | ~~22~~ | ~~198~~ | ~~4~~ | ~~46~~ |
| ADT4-52 | 0.23 | 0.05736 | 0.00123 | 0.51859 | 0.01168 | 0.06555 | 0.00093 | 505 | 26 | 424 | 8 | 409 | 6 | 3.7 |
| ~~ADT4-53~~ | ~~1.18~~ | ~~0.0715~~ | ~~0.00453~~ | ~~0.65007~~ | ~~0.03978~~ | ~~0.06594~~ | ~~0.00109~~ | ~~972~~ | ~~133~~ | ~~509~~ | ~~24~~ | ~~412~~ | ~~7~~ | ~~23.5~~ |

| | | | | | | | | | | | | | | |
|---|---|---|---|---|---|---|---|---|---|---|---|---|---|---|
| ~~ADT4-54~~ | ~~1.08~~ | ~~0.11986~~ | ~~0.00549~~ | ~~4.21702~~ | ~~0.17873~~ | ~~0.25518~~ | ~~0.00443~~ | ~~1954~~ | ~~84~~ | ~~1677~~ | ~~35~~ | ~~1465~~ | ~~23~~ | ~~33.4~~ |
| ~~ADT4-55~~ | ~~0.48~~ | ~~0.06977~~ | ~~0.00161~~ | ~~0.90658~~ | ~~0.02165~~ | ~~0.09422~~ | ~~0.00137~~ | ~~922~~ | ~~26~~ | ~~655~~ | ~~12~~ | ~~580~~ | ~~8~~ | ~~12.9~~ |
| ADT4-56 | 1.12 | 0.05691 | 0.00121 | 0.5546 | 0.01237 | 0.07066 | 0.00101 | 488 | 26 | 448 | 8 | 440 | 6 | 1.8 |
| ADT4-57 | 0.4 | 0.07406 | 0.00272 | 1.62149 | 0.05444 | 0.1588 | 0.00234 | 1043 | 76 | 979 | 21 | 950 | 13 | 3.1 |
| ADT4-58 | 0.43 | 0.05884 | 0.00271 | 0.54051 | 0.02351 | 0.06662 | 0.001 | 561 | 103 | 439 | 15 | 416 | 6 | 5.5 |
| ADT4-59 | 0.36 | 0.05646 | 0.00223 | 0.52067 | 0.01908 | 0.06689 | 0.00097 | 470 | 89 | 426 | 13 | 417 | 6 | 2.2 |
| ~~ADT4-60~~ | ~~0.55~~ | ~~0.10122~~ | ~~0.00727~~ | ~~0.46191~~ | ~~0.03196~~ | ~~0.0331~~ | ~~0.00063~~ | ~~1647~~ | ~~137~~ | ~~386~~ | ~~22~~ | ~~210~~ | ~~4~~ | ~~83.8~~ |
| ~~ADT4-61~~ | ~~0.56~~ | ~~0.06385~~ | ~~0.00155~~ | ~~0.61457~~ | ~~0.01542~~ | ~~0.06979~~ | ~~0.00101~~ | ~~737~~ | ~~29~~ | ~~486~~ | ~~10~~ | ~~435~~ | ~~6~~ | ~~11.7~~ |
| ADT4-62 | 0.57 | 0.06249 | 0.00251 | 0.6155 | 0.02297 | 0.07143 | 0.00105 | 691 | 88 | 487 | 14 | 445 | 6 | 9.4 |
| ADT4-63 | 0.88 | 0.05727 | 0.0017 | 0.5321 | 0.01604 | 0.06737 | 0.001 | 502 | 41 | 433 | 11 | 420 | 6 | 3.1 |
| ADT4-64 | 0.53 | 0.0542 | 0.00178 | 0.23468 | 0.00777 | 0.0314 | 0.00047 | 379 | 48 | 214 | 6 | 199 | 3 | 7.5 |
| ADT4-65 | 1.18 | 0.06518 | 0.00145 | 1.13102 | 0.02612 | 0.12583 | 0.00182 | 780 | 26 | 768 | 12 | 764 | 10 | 0.5 |
| ADT4-66 | 0.78 | 0.05882 | 0.00281 | 0.51949 | 0.02357 | 0.06406 | 0.00096 | 560 | 107 | 425 | 16 | 400 | 6 | 6.3 |
| ADT4-67 | 0.08 | 0.0554 | 0.00144 | 0.26419 | 0.00587 | 0.03459 | 0.00047 | 428 | 59 | 238 | 5 | 219 | 3 | 8.7 |
| ~~ADT4-68~~ | ~~0.46~~ | ~~0.06319~~ | ~~0.00259~~ | ~~0.50904~~ | ~~0.01942~~ | ~~0.05842~~ | ~~0.00087~~ | ~~715~~ | ~~89~~ | ~~418~~ | ~~13~~ | ~~366~~ | ~~5~~ | ~~14.2~~ |
| ~~ADT4-69~~ | ~~0.43~~ | ~~0.10806~~ | ~~0.00178~~ | ~~4.06047~~ | ~~0.07343~~ | ~~0.27247~~ | ~~0.00381~~ | ~~1767~~ | ~~15~~ | ~~1646~~ | ~~15~~ | ~~1553~~ | ~~19~~ | ~~13.8~~ |
| ~~ADT4-70~~ | ~~0.29~~ | ~~0.11401~~ | ~~0.00173~~ | ~~4.05533~~ | ~~0.06919~~ | ~~0.25794~~ | ~~0.00353~~ | ~~1864~~ | ~~14~~ | ~~1645~~ | ~~14~~ | ~~1479~~ | ~~18~~ | ~~26~~ |
| ADT4-71 | 0.4 | 0.08446 | 0.00248 | 2.41585 | 0.06212 | 0.20745 | 0.00295 | 1303 | 58 | 1247 | 18 | 1215 | 16 | 7.2 |
| ~~ADT4-72~~ | ~~0.35~~ | ~~0.09481~~ | ~~0.00198~~ | ~~0.53836~~ | ~~0.01168~~ | ~~0.04117~~ | ~~0.0006~~ | ~~1524~~ | ~~21~~ | ~~437~~ | ~~8~~ | ~~260~~ | ~~4~~ | ~~68.1~~ |
| ADT4-73 | 0.6 | 0.05773 | 0.00181 | 0.46983 | 0.01496 | 0.05901 | 0.00087 | 520 | 44 | 391 | 10 | 370 | 5 | 5.7 |
| ADT4-74 | 0.39 | 0.05977 | 0.00263 | 0.51097 | 0.02109 | 0.062 | 0.00094 | 595 | 98 | 419 | 14 | 388 | 6 | 8 |
| ~~ADT4-75~~ | ~~0.55~~ | ~~0.08347~~ | ~~0.00589~~ | ~~0.46471~~ | ~~0.03176~~ | ~~0.04038~~ | ~~0.00071~~ | ~~1280~~ | ~~142~~ | ~~388~~ | ~~22~~ | ~~255~~ | ~~4~~ | ~~52.2~~ |
| ADT4-76 | 1.18 | 0.09735 | 0.0022 | 2.13521 | 0.04954 | 0.15905 | 0.0024 | 1574 | 22 | 1160 | 16 | 951 | 13 | 22 |
| ADT4-77 | 0.5 | 0.06076 | 0.00115 | 0.54842 | 0.01109 | 0.06545 | 0.00091 | 631 | 22 | 444 | 7 | 409 | 6 | 8.6 |
| ADT4-78 | 0.78 | 0.06662 | 0.00274 | 1.0542 | 0.04319 | 0.11475 | 0.00187 | 826 | 58 | 731 | 21 | 700 | 11 | 4.4 |
| ADT4-79 | 0.52 | 0.05599 | 0.0014 | 0.26324 | 0.00678 | 0.03409 | 0.0005 | 452 | 32 | 237 | 5 | 216 | 3 | 9.7 |
| ADT4-80 | 0.95 | 0.057 | 0.00358 | 0.48274 | 0.02932 | 0.06143 | 0.00097 | 491 | 142 | 400 | 20 | 384 | 6 | 4.2 |
| ~~ADT4-81~~ | ~~0.25~~ | ~~0.14569~~ | ~~0.00394~~ | ~~3.62837~~ | ~~0.08304~~ | ~~0.18062~~ | ~~0.00261~~ | ~~2296~~ | ~~48~~ | ~~1556~~ | ~~18~~ | ~~1070~~ | ~~14~~ | ~~115~~ |

| | | | | | | | | | | | | | | |
|---|---|---|---|---|---|---|---|---|---|---|---|---|---|---|
| ~~ADT4-82~~ | ~~0.82~~ | ~~0.06693~~ | ~~0.00327~~ | ~~0.61965~~ | ~~0.02873~~ | ~~0.06715~~ | ~~0.00103~~ | ~~836~~ | ~~104~~ | ~~490~~ | ~~18~~ | ~~419~~ | ~~6~~ | ~~16.9~~ |
| ADT4-83 | 0.41 | 0.05785 | 0.00125 | 0.54962 | 0.01238 | 0.0689 | 0.00098 | 524 | 26 | 445 | 8 | 430 | 6 | 3.5 |
| ADT4-84 | 0.81 | 0.05649 | 0.00153 | 0.4312 | 0.01186 | 0.05535 | 0.00083 | 472 | 35 | 364 | 8 | 347 | 5 | 4.9 |
| ~~ADT4-85~~ | ~~0.74~~ | ~~0.06314~~ | ~~0.00192~~ | ~~0.50772~~ | ~~0.01555~~ | ~~0.05831~~ | ~~0.00089~~ | ~~713~~ | ~~39~~ | ~~417~~ | ~~10~~ | ~~365~~ | ~~5~~ | ~~14.2~~ |
| ADT4-86 | 0.2 | 0.05144 | 0.00273 | 0.23767 | 0.01206 | 0.03351 | 0.00052 | 261 | 125 | 217 | 10 | 212 | 3 | 2.4 |
| ADT4-87 | 2.45 | 0.07706 | 0.00147 | 1.57142 | 0.03178 | 0.14786 | 0.00209 | 1123 | 20 | 959 | 13 | 889 | 12 | 7.9 |
| ~~ADT4-88~~ | ~~0.67~~ | ~~0.16884~~ | ~~0.00283~~ | ~~8.80975~~ | ~~0.1609~~ | ~~0.37837~~ | ~~0.00529~~ | ~~2546~~ | ~~14~~ | ~~2319~~ | ~~17~~ | ~~2069~~ | ~~25~~ | ~~23.1~~ |
| ~~ADT4-89~~ | ~~0.59~~ | ~~0.10421~~ | ~~0.00182~~ | ~~3.54958~~ | ~~0.06698~~ | ~~0.24698~~ | ~~0.00346~~ | ~~1700~~ | ~~16~~ | ~~1538~~ | ~~15~~ | ~~1423~~ | ~~18~~ | ~~19.5~~ |
| ~~ADT4-90~~ | ~~0.73~~ | ~~0.06481~~ | ~~0.00593~~ | ~~0.33636~~ | ~~0.03011~~ | ~~0.03764~~ | ~~0.00071~~ | ~~768~~ | ~~200~~ | ~~294~~ | ~~23~~ | ~~238~~ | 4 | ~~23.5~~ |
| ADT4-91 | 1.71 | 0.06896 | 0.0014 | 1.28425 | 0.02736 | 0.13503 | 0.00192 | 898 | 22 | 839 | 12 | 816 | 11 | 2.8 |
| ~~ADT4-92~~ | ~~0.46~~ | ~~0.06106~~ | ~~0.00334~~ | ~~0.25471~~ | ~~0.01337~~ | ~~0.03025~~ | ~~0.00047~~ | ~~641~~ | ~~121~~ | ~~230~~ | ~~11~~ | ~~192~~ | ~~3~~ | ~~19.8~~ |
| ADT4-93 | 0.37 | 0.07444 | 0.00145 | 1.67808 | 0.03452 | 0.16347 | 0.00232 | 1053 | 21 | 1000 | 13 | 976 | 13 | 2.5 |
| ~~ADT4-94~~ | ~~0.48~~ | ~~0.0748~~ | ~~0.00138~~ | ~~0.7347~~ | ~~0.01445~~ | ~~0.07122~~ | ~~0.001~~ | ~~1063~~ | ~~19~~ | ~~559~~ | ~~8~~ | ~~444~~ | ~~6~~ | ~~25.9~~ |
| ~~ADT4-95~~ | ~~0.3~~ | ~~0.11803~~ | ~~0.00207~~ | ~~4.87284~~ | ~~0.09216~~ | ~~0.29938~~ | ~~0.0042~~ | ~~1927~~ | ~~16~~ | ~~1798~~ | ~~16~~ | ~~1688~~ | ~~21~~ | ~~14.2~~ |
| ADT4-96 | 0.87 | 0.04605 | 0.00392 | 0.22973 | 0.01918 | 0.03619 | 0.00061 | | 188 | 210 | 16 | 229 | 4 | -8.3 |
| ~~ADT4-97~~ | ~~0.57~~ | ~~0.06382~~ | ~~0.00785~~ | ~~0.56779~~ | ~~0.06892~~ | ~~0.06453~~ | ~~0.00126~~ | ~~736~~ | ~~274~~ | ~~457~~ | ~~45~~ | ~~403~~ | ~~8~~ | ~~13.4~~ |
| ADT4-98 | 1.39 | 0.05564 | 0.00135 | 0.52641 | 0.01319 | 0.0686 | 0.00099 | 438 | 31 | 429 | 9 | 428 | 6 | 0.2 |
| ~~ADT4-99~~ | ~~0.53~~ | ~~0.06602~~ | ~~0.00308~~ | ~~0.62182~~ | ~~0.0274~~ | ~~0.06831~~ | ~~0.00105~~ | ~~807~~ | ~~100~~ | ~~491~~ | ~~17~~ | ~~426~~ | ~~6~~ | ~~15.3~~ |
| ADT4-100 | 0.61 | 0.05881 | 0.00451 | 0.41353 | 0.03097 | 0.051 | 0.00084 | 560 | 173 | 351 | 22 | 321 | 5 | 9.3 |
| | | | | | | | | | | | | | | |
| **ADT6** | | | | | | | | | | | | | | |
| ADT6-01 | 0.49 | 0.05702 | 0.00272 | 0.45444 | 0.02158 | 0.05779 | 0.00095 | 492 | 76 | 380 | 15 | 362 | 6 | 5 |
| ADT6-02 | 0.68 | 0.05432 | 0.00121 | 0.4467 | 0.01044 | 0.05962 | 0.00084 | 384 | 28 | 375 | 7 | 373 | 5 | 0.5 |
| ADT6-03 | 0.46 | 0.05417 | 0.0012 | 0.44636 | 0.01039 | 0.05975 | 0.00084 | 378 | 28 | 375 | 7 | 374 | 5 | 0.3 |
| ADT6-04 | 0.59 | 0.05454 | 0.00137 | 0.45767 | 0.01187 | 0.06085 | 0.00087 | 393 | 33 | 383 | 8 | 381 | 5 | 0.5 |
| ADT6-05 | 0.55 | 0.05516 | 0.00138 | 0.469 | 0.01213 | 0.06165 | 0.00089 | 419 | 33 | 390 | 8 | 386 | 5 | 1 |
| ADT6-06 | 0.39 | 0.05514 | 0.00115 | 0.4628 | 0.01019 | 0.06086 | 0.00086 | 418 | 25 | 386 | 7 | 381 | 5 | 1.3 |

| | | | | | | | | | | | | | | |
|---|---|---|---|---|---|---|---|---|---|---|---|---|---|---|
| ADT6-07 | 0.52 | 0.05086 | 0.0028 | 0.28407 | 0.01502 | 0.04051 | 0.00063 | 234 | 128 | 254 | 12 | 256 | 4 | -0.8 |
| ADT6-08 | 0.81 | 0.05706 | 0.00105 | 0.48335 | 0.00962 | ~~0.06142~~ | 0.00085 | 494 | 22 | 400 | 7 | 384 | 5 | 4.2 |
| ADT6-09 | 0.7 | 0.05669 | 0.00098 | 0.48505 | 0.00915 | 0.06204 | 0.00086 | 479 | 20 | 402 | 6 | 388 | 5 | 3.6 |
| ADT6-10 | 0.74 | 0.05424 | 0.00319 | 0.43779 | 0.02568 | 0.05852 | 0.00098 | 381 | 102 | 369 | 18 | 367 | 6 | 0.5 |
| ~~ADT6-11~~ | ~~0.83~~ | ~~0.06257~~ | ~~0.00315~~ | ~~0.49163~~ | ~~0.02355~~ | ~~0.05699~~ | ~~0.00087~~ | ~~694~~ | ~~110~~ | ~~406~~ | ~~16~~ | ~~357~~ | ~~5~~ | ~~13.7~~ |
| ADT6-12 | 0.63 | 0.05809 | 0.00269 | 0.4573 | 0.02005 | 0.0571 | 0.00085 | 533 | 104 | 382 | 14 | 358 | 5 | 6.7 |
| ADT6-13 | 0.84 | 0.05455 | 0.00125 | 0.45209 | 0.01085 | 0.06009 | 0.00085 | 394 | 29 | 379 | 8 | 376 | 5 | 0.8 |
| ~~ADT6-14~~ | ~~0.75~~ | ~~0.06878~~ | ~~0.00301~~ | ~~0.54537~~ | ~~0.0224~~ | ~~0.05751~~ | ~~0.00086~~ | ~~892~~ | ~~93~~ | ~~442~~ | ~~15~~ | ~~360~~ | ~~5~~ | ~~22.8~~ |
| ~~ADT6-15~~ | ~~1.24~~ | ~~0.10216~~ | ~~0.00488~~ | ~~0.73376~~ | ~~0.03295~~ | ~~0.05209~~ | ~~0.00085~~ | ~~1664~~ | ~~91~~ | ~~559~~ | ~~19~~ | ~~327~~ | ~~5~~ | ~~70.9~~ |
| ADT6-16 | 0.87 | 0.05657 | 0.0012 | 0.5145 | 0.01144 | 0.06595 | 0.00094 | 475 | 26 | 421 | 8 | 412 | 6 | 2.2 |
| ADT6-17 | 0.4 | 0.0582 | 0.00089 | 0.46884 | 0.00803 | 0.05841 | 0.0008 | 537 | 17 | 390 | 6 | 366 | 5 | 6.6 |
| ADT6-18 | 0.58 | 0.05425 | 0.00128 | 0.4538 | 0.01117 | 0.06066 | 0.00086 | 381 | 31 | 380 | 8 | 380 | 5 | 0 |
| ADT6-19 | 0.57 | 0.05433 | 0.00096 | 0.45702 | 0.00879 | 0.06099 | 0.00084 | 385 | 21 | 382 | 6 | 382 | 5 | 0 |
| ADT6-20 | 0.65 | 0.05415 | 0.00113 | 0.44929 | 0.0099 | 0.06017 | 0.00085 | 377 | 26 | 377 | 7 | 377 | 5 | 0 |
| ADT6-21 | 0.7 | 0.05445 | 0.00169 | 0.45751 | 0.01434 | 0.06093 | 0.00092 | 390 | 43 | 383 | 10 | 381 | 6 | 0.5 |
| ADT6-22 | 0.64 | 0.05662 | 0.00131 | 0.48472 | 0.01164 | 0.06208 | 0.00089 | 477 | 29 | 401 | 8 | 388 | 5 | 3.4 |
| ADT6-23 | 0.8 | 0.05404 | 0.00107 | 0.43611 | 0.00918 | 0.05852 | 0.00082 | 373 | 24 | 368 | 6 | 367 | 5 | 0.3 |
| ADT6-24 | 0.65 | 0.05422 | 0.00146 | 0.45858 | 0.01264 | 0.06133 | 0.0009 | 380 | 36 | 383 | 9 | 384 | 5 | -0.3 |
| ADT6-25 | 0.54 | 0.05417 | 0.0017 | 0.45468 | 0.01448 | 0.06087 | 0.00091 | 378 | 45 | 381 | 10 | 381 | 6 | 0 |
| ADT6-26 | 0.72 | 0.05716 | 0.00147 | 0.49437 | 0.01302 | 0.06271 | 0.00092 | 498 | 33 | 408 | 9 | 392 | 6 | 4.1 |
| ~~ADT6-27~~ | ~~0.58~~ | ~~0.07154~~ | ~~0.00302~~ | ~~0.54725~~ | ~~0.02162~~ | ~~0.05548~~ | ~~0.00082~~ | ~~973~~ | ~~88~~ | ~~443~~ | ~~14~~ | ~~348~~ | ~~5~~ | ~~27.3~~ |
| ADT6-28 | 0.73 | 0.05448 | 0.00127 | 0.46019 | 0.01117 | 0.06125 | 0.00088 | 391 | 30 | 384 | 8 | 383 | 5 | 0.3 |
| ~~ADT6-29~~ | ~~0.93~~ | ~~0.05894~~ | ~~0.00105~~ | ~~0.32513~~ | ~~0.00628~~ | ~~0.04~~ | ~~0.00055~~ | ~~565~~ | ~~20~~ | ~~286~~ | ~~5~~ | ~~253~~ | ~~3~~ | ~~13~~ |
| ADT6-30 | 1 | 0.05552 | 0.00106 | 0.48087 | 0.00978 | 0.0628 | 0.00088 | 433 | 22 | 399 | 7 | 393 | 5 | 1.5 |
| ADT6-31 | 0.39 | 0.05626 | 0.00107 | 0.54075 | 0.01095 | 0.0697 | 0.00098 | 463 | 22 | 439 | 7 | 434 | 6 | 1.2 |
| ADT6-32 | 0.53 | 0.05404 | 0.00204 | 0.44666 | 0.01688 | 0.05993 | 0.00093 | 373 | 57 | 375 | 12 | 375 | 6 | 0 |
| ADT6-33 | 0.61 | 0.05465 | 0.00161 | 0.45182 | 0.01362 | 0.05994 | 0.00087 | 398 | 42 | 379 | 10 | 375 | 5 | 1.1 |
| ADT6-34 | 0.55 | 0.05449 | 0.00171 | 0.45274 | 0.01446 | 0.06025 | 0.00088 | 391 | 46 | 379 | 10 | 377 | 5 | 0.5 |

| | | | | | | | | | | | | | | |
|---|---|---|---|---|---|---|---|---|---|---|---|---|---|---|
| ~~ADT6-35~~ | ~~0.52~~ | ~~0.07372~~ | ~~0.00218~~ | ~~0.5135~~ | ~~0.01536~~ | ~~0.05051~~ | ~~0.00077~~ | ~~1034~~ | ~~36~~ | ~~421~~ | ~~10~~ | ~~318~~ | ~~5~~ | ~~32.4~~ |
| ~~ADT6-36~~ | ~~0.64~~ | ~~0.06843~~ | ~~0.00314~~ | ~~0.50357~~ | ~~0.02179~~ | ~~0.05337~~ | ~~0.00082~~ | ~~882~~ | ~~97~~ | ~~414~~ | ~~15~~ | ~~335~~ | ~~5~~ | ~~23.6~~ |
| ADT6-37 | 0.58 | 0.05416 | 0.00154 | 0.44852 | 0.01307 | 0.06005 | 0.00087 | 378 | 40 | 376 | 9 | 376 | 5 | 0 |
| ~~ADT6-38~~ | ~~0.68~~ | ~~0.06168~~ | ~~0.00137~~ | ~~0.50807~~ | ~~0.01178~~ | ~~0.05973~~ | ~~0.00085~~ | ~~663~~ | ~~27~~ | ~~417~~ | ~~8~~ | ~~374~~ | ~~5~~ | ~~11.5~~ |
| ADT6-39 | 0.51 | 0.0542 | 0.00119 | 0.44716 | 0.01031 | 0.05982 | 0.00084 | 379 | 28 | 375 | 7 | 375 | 5 | 0 |
| ADT6-40 | 0.54 | 0.05542 | 0.00236 | 0.4494 | 0.01799 | 0.05881 | 0.00086 | 429 | 97 | 377 | 13 | 368 | 5 | 2.4 |
| ADT6-41 | 0.55 | 0.05438 | 0.00154 | 0.45896 | 0.01324 | 0.0612 | 0.0009 | 387 | 39 | 384 | 9 | 383 | 5 | 0.3 |
| ADT6-42 | 0.56 | 0.05438 | 0.00146 | 0.45787 | 0.01254 | 0.06105 | 0.00089 | 387 | 36 | 383 | 9 | 382 | 5 | 0.3 |
| ADT6-43 | 0.52 | 0.05572 | 0.00164 | 0.48779 | 0.0146 | 0.06348 | 0.00094 | 441 | 41 | 403 | 10 | 397 | 6 | 1.5 |
| ~~ADT6-44~~ | ~~1.33~~ | ~~0.05739~~ | ~~0.00342~~ | ~~0.31963~~ | ~~0.0188~~ | ~~0.04039~~ | ~~0.00075~~ | ~~507~~ | ~~97~~ | ~~282~~ | ~~14~~ | ~~255~~ | ~~5~~ | ~~10.6~~ |
| ADT6-45 | 0.62 | 0.11501 | 0.00182 | 5.42898 | 0.09517 | 0.34228 | 0.00473 | 1880 | 15 | 1889 | 15 | 1898 | 23 | -0.9 |
| ADT6-46 | 0.49 | 0.05659 | 0.0029 | 0.49676 | 0.02531 | 0.06365 | 0.00108 | 476 | 83 | 410 | 17 | 398 | 7 | 3 |
| ADT6-47 | 0.62 | 0.05598 | 0.00119 | 0.50726 | 0.01131 | 0.06571 | 0.00093 | 452 | 26 | 417 | 8 | 410 | 6 | 1.7 |
| ADT6-48 | 0.63 | 0.05435 | 0.00145 | 0.45935 | 0.01255 | 0.06129 | 0.00089 | 386 | 36 | 384 | 9 | 383 | 5 | 0.3 |
| ADT6-49 | 0.41 | 0.05763 | 0.0013 | 0.3915 | 0.00922 | 0.04926 | 0.0007 | 516 | 28 | 335 | 7 | 310 | 4 | 8.1 |
| ADT6-50 | 0.41 | 0.0536 | 0.00102 | 0.45371 | 0.00924 | 0.06138 | 0.00086 | 354 | 23 | 380 | 6 | 384 | 5 | -1 |
| ADT6-51 | 0.82 | 0.05418 | 0.00132 | 0.44617 | 0.01121 | 0.05971 | 0.00086 | 379 | 31 | 375 | 8 | 374 | 5 | 0.3 |
| ADT6-52 | 0.61 | 0.05487 | 0.00109 | 0.47044 | 0.00993 | 0.06217 | 0.00087 | 407 | 24 | 391 | 7 | 389 | 5 | 0.5 |
| ADT6-53 | 0.61 | 0.05384 | 0.0012 | 0.44104 | 0.01024 | 0.0594 | 0.00085 | 364 | 28 | 371 | 7 | 372 | 5 | -0.3 |
| ADT6-54 | 0.6 | 0.05434 | 0.00177 | 0.45615 | 0.01497 | 0.06086 | 0.00092 | 385 | 47 | 382 | 10 | 381 | 6 | 0.3 |
| ~~ADT6-55~~ | ~~1~~ | ~~0.07095~~ | ~~0.00633~~ | ~~0.40894~~ | ~~0.03576~~ | ~~0.04181~~ | ~~0.00074~~ | ~~956~~ | ~~189~~ | ~~348~~ | ~~26~~ | ~~264~~ | ~~5~~ | ~~31.8~~ |
| ADT6-56 | 0.53 | 0.05443 | 0.00187 | 0.45576 | 0.01573 | 0.06072 | 0.00093 | 389 | 50 | 381 | 11 | 380 | 6 | 0.3 |
| ADT6-57 | 0.56 | 0.05432 | 0.00206 | 0.44838 | 0.01708 | 0.05986 | 0.00092 | 384 | 58 | 376 | 12 | 375 | 6 | 0.3 |
| ~~ADT6-58~~ | ~~0.7~~ | ~~0.06431~~ | ~~0.00263~~ | ~~0.39382~~ | ~~0.01609~~ | ~~0.04441~~ | ~~0.0007~~ | ~~752~~ | ~~60~~ | ~~337~~ | ~~12~~ | ~~280~~ | ~~4~~ | ~~20.4~~ |
| ADT6-59 | 0.69 | 0.05438 | 0.00134 | 0.45673 | 0.01161 | 0.0609 | 0.00087 | 387 | 32 | 382 | 8 | 381 | 5 | 0.3 |
| ADT6-60 | 0.54 | 0.05425 | 0.00193 | 0.4472 | 0.01601 | 0.05977 | 0.00091 | 381 | 53 | 375 | 11 | 374 | 6 | 0.3 |
| ADT6-61 | 0.57 | 0.05456 | 0.0014 | 0.46349 | 0.01216 | 0.0616 | 0.0009 | 394 | 33 | 387 | 8 | 385 | 5 | 0.5 |
| ~~ADT6-62~~ | ~~0.89~~ | ~~0.06807~~ | ~~0.00159~~ | ~~0.53275~~ | ~~0.01288~~ | ~~0.05675~~ | ~~0.00082~~ | ~~871~~ | ~~27~~ | ~~434~~ | ~~9~~ | ~~356~~ | ~~5~~ | ~~21.9~~ |

| | | | | | | | | | | | | | | |
|---|---|---|---|---|---|---|---|---|---|---|---|---|---|---|
| ADT6-63 | 0.99 | 0.0541 | 0.00211 | 0.44001 | 0.01713 | 0.05897 | 0.00093 | 375 | 59 | 370 | 12 | 369 | 6 | 0.3 |
| ADT6-64 | 0.82 | 0.05696 | 0.00341 | 0.42964 | 0.02486 | 0.0547 | 0.00085 | 490 | 136 | 363 | 18 | 343 | 5 | 5.8 |
| ADT6-65 | 0.54 | 0.05413 | 0.00159 | 0.44112 | 0.01317 | 0.05909 | 0.00087 | 376 | 41 | 371 | 9 | 370 | 5 | 0.3 |
| ADT6-66 | 0.6 | 0.05435 | 0.00143 | 0.46697 | 0.0126 | 0.06231 | 0.00091 | 386 | 35 | 389 | 9 | 390 | 6 | -0.3 |
| ADT6-67 | 0.61 | 0.05687 | 0.00132 | 0.46437 | 0.01113 | 0.05921 | 0.00085 | 486 | 29 | 387 | 8 | 371 | 5 | 4.3 |
| ADT6-68 | 0.6 | 0.05411 | 0.0016 | 0.44448 | 0.01335 | 0.05956 | 0.00088 | 376 | 41 | 373 | 9 | 373 | 5 | 0 |
| ADT6-69 | 0.7 | 0.05159 | 0.00108 | 0.24943 | 0.0055 | 0.03506 | 0.00049 | 267 | 26 | 226 | 4 | 222 | 3 | 1.8 |
| ADT6-70 | 0.53 | 0.04893 | 0.00481 | 0.24146 | 0.02342 | 0.03579 | 0.00058 | 144 | 220 | 220 | 19 | 227 | 4 | -3.1 |
| ADT6-71 | 0.47 | 0.05416 | 0.00125 | 0.45397 | 0.01087 | 0.06078 | 0.00087 | 378 | 29 | 380 | 8 | 380 | 5 | 0 |
| ADT6-72 | 0.76 | 0.05427 | 0.00148 | 0.46149 | 0.01289 | 0.06166 | 0.0009 | 382 | 37 | 385 | 9 | 386 | 5 | -0.3 |
| ADT6-73 | 0.14 | 0.05575 | 0.001 | 0.53912 | 0.01038 | 0.07012 | 0.00097 | 442 | 21 | 438 | 7 | 437 | 6 | 0.2 |
| ADT6-74 | 0.55 | 0.05435 | 0.00136 | 0.45688 | 0.01175 | 0.06096 | 0.00088 | 386 | 33 | 382 | 8 | 381 | 5 | 0.3 |
| ADT6-75 | 0.74 | 0.06004 | 0.00164 | 0.48589 | 0.01356 | 0.05868 | 0.00086 | 605 | 36 | 402 | 9 | 368 | 5 | 9.2 |
| ADT6-76 | 0.56 | 0.05338 | 0.00282 | 0.43023 | 0.02179 | 0.05846 | 0.00088 | 345 | 123 | 363 | 15 | 366 | 5 | -0.8 |
| ADT6-77 | 0.46 | 0.0557 | 0.00162 | 0.4798 | 0.01412 | 0.06246 | 0.00093 | 440 | 39 | 398 | 10 | 391 | 6 | 1.8 |
| ADT6-78 | 0.71 | 0.0541 | 0.00159 | 0.4413 | 0.01309 | 0.05915 | 0.00089 | 375 | 40 | 371 | 9 | 370 | 5 | 0.3 |
| ADT6-79 | 0.56 | 0.05064 | 0.00115 | 0.24958 | 0.00589 | 0.03574 | 0.00051 | 224 | 29 | 226 | 5 | 226 | 3 | 0 |
| ADT6-80 | 0.81 | 0.05608 | 0.00145 | 0.44802 | 0.01186 | 0.05792 | 0.00084 | 456 | 34 | 376 | 8 | 363 | 5 | 3.6 |
| ~~ADT6-81~~ | ~~0.5~~ | ~~0.04605~~ | ~~0.00573~~ | ~~0.37134~~ | ~~0.04584~~ | ~~0.05849~~ | ~~0.00097~~ | | ~~238~~ | ~~321~~ | ~~34~~ | ~~366~~ | ~~6~~ | ~~-12.3~~ |
| ~~ADT6-82~~ | ~~0.62~~ | ~~0.06172~~ | ~~0.00113~~ | ~~0.49906~~ | ~~0.00979~~ | ~~0.05863~~ | ~~0.00082~~ | ~~664~~ | ~~20~~ | ~~411~~ | ~~7~~ | ~~367~~ | ~~5~~ | ~~12~~ |
| ADT6-83 | 0.61 | 0.05407 | 0.00133 | 0.4512 | 0.01137 | 0.06051 | 0.00088 | 374 | 31 | 378 | 8 | 379 | 5 | -0.3 |
| ADT6-84 | 0.67 | 0.05467 | 0.00144 | 0.45985 | 0.01238 | 0.06099 | 0.00089 | 399 | 35 | 384 | 9 | 382 | 5 | 0.5 |
| ADT6-85 | 0.54 | 0.05666 | 0.00118 | 0.44864 | 0.00976 | 0.05742 | 0.00081 | 478 | 25 | 376 | 7 | 360 | 5 | 4.4 |
| ADT6-86 | 0.55 | 0.0565 | 0.0012 | 0.57806 | 0.01283 | 0.07419 | 0.00105 | 472 | 26 | 463 | 8 | 461 | 6 | 0.4 |
| ~~ADT6-87~~ | ~~0.71~~ | ~~0.07467~~ | ~~0.00408~~ | ~~0.55184~~ | ~~0.02879~~ | ~~0.0536~~ | ~~0.00086~~ | ~~1060~~ | ~~113~~ | ~~446~~ | ~~19~~ | ~~337~~ | ~~5~~ | ~~32.3~~ |
| ADT6-88 | 0.59 | 0.05702 | 0.00141 | 0.47602 | 0.0121 | 0.06053 | 0.00088 | 492 | 31 | 395 | 8 | 379 | 5 | 4.2 |
| ADT6-89 | 0.74 | 0.05413 | 0.00171 | 0.41402 | 0.01324 | 0.05546 | 0.00083 | 376 | 45 | 352 | 10 | 348 | 5 | 1.1 |
| ADT6-90 | 0.47 | 0.05408 | 0.00155 | 0.4493 | 0.01308 | 0.06024 | 0.00089 | 374 | 39 | 377 | 9 | 377 | 5 | 0 |

| | | | | | | | | | | | | | | |
|---|---|---|---|---|---|---|---|---|---|---|---|---|---|---|
| ADT6-91 | 0.75 | 0.05443 | 0.00153 | 0.44522 | 0.01273 | 0.05932 | 0.00087 | 389 | 38 | 374 | 9 | 371 | 5 | 0.8 |
| ADT6-92 | 0.96 | 0.05827 | 0.00135 | 0.48892 | 0.01168 | 0.06084 | 0.00088 | 540 | 28 | 404 | 8 | 381 | 5 | 6 |
| ADT6-93 | 0.36 | 0.05408 | 0.00131 | 0.44257 | 0.01107 | 0.05934 | 0.00085 | 374 | 31 | 372 | 8 | 372 | 5 | 0 |
| ADT6-94 | 0.54 | 0.05421 | 0.00191 | 0.43926 | 0.01551 | 0.05876 | 0.0009 | 380 | 52 | 370 | 11 | 368 | 5 | 0.5 |
| ~~ADT6-95~~ | ~~0.58~~ | ~~0.06196~~ | ~~0.00164~~ | ~~0.44187~~ | ~~0.01187~~ | ~~0.05171~~ | ~~0.00077~~ | ~~673~~ | ~~33~~ | ~~372~~ | ~~8~~ | ~~325~~ | ~~5~~ | ~~14.5~~ |
| ADT6-96 | 0.66 | 0.05432 | 0.00206 | 0.46275 | 0.01764 | 0.06177 | 0.00094 | 384 | 58 | 386 | 12 | 386 | 6 | 0 |
| ADT6-97 | 0.83 | 0.05469 | 0.00118 | 0.43841 | 0.00987 | 0.05812 | 0.00083 | 400 | 26 | 369 | 7 | 364 | 5 | 1.4 |
| ~~ADT6-98~~ | ~~0.47~~ | ~~0.16614~~ | ~~0.00323~~ | ~~0.88079~~ | ~~0.01792~~ | ~~0.03844~~ | ~~0.00055~~ | ~~2519~~ | ~~17~~ | ~~641~~ | ~~10~~ | ~~243~~ | ~~3~~ | ~~164~~ |
| ADT6-99 | 0.88 | 0.14146 | 0.00285 | 7.64916 | 0.1611 | 0.39209 | 0.0057 | 2245 | 18 | 2191 | 19 | 2133 | 26 | 5.3 |
| ADT6-100 | 0.68 | 0.05455 | 0.00144 | 0.45723 | 0.01233 | 0.06078 | 0.00089 | 394 | 35 | 382 | 9 | 380 | 5 | 0.5 |
| **ADT3** | | | | | | | | | | | | | | |
| ADT3-01 | 0.53 | 0.05966 | 0.00198 | 0.47722 | 0.01573 | 0.058 | 0.0009 | 591 | 45 | 396 | 11 | 363 | 5 | 9.1 |
| ADT3-02 | 0.64 | 0.05487 | 0.00183 | 0.4417 | 0.01464 | 0.05836 | 0.00089 | 407 | 47 | 371 | 10 | 366 | 5 | 1.4 |
| ADT3-03 | 0.85 | 0.05315 | 0.00158 | 0.42007 | 0.01246 | 0.05731 | 0.00086 | 335 | 40 | 356 | 9 | 359 | 5 | -0.8 |
| ADT3-04 | 0.52 | 0.05558 | 0.00138 | 0.43433 | 0.01083 | 0.05666 | 0.00083 | 436 | 30 | 366 | 8 | 355 | 5 | 3.1 |
| ADT3-05 | 0.59 | 0.05409 | 0.00161 | 0.42137 | 0.01251 | 0.05648 | 0.00085 | 375 | 40 | 357 | 9 | 354 | 5 | 0.8 |
| ADT3-06 | 0.55 | 0.05498 | 0.0029 | 0.43721 | 0.02208 | 0.05767 | 0.00089 | 411 | 121 | 368 | 16 | 361 | 5 | 1.9 |
| ADT3-07 | 0.48 | 0.05363 | 0.00168 | 0.42039 | 0.01312 | 0.05683 | 0.00086 | 356 | 43 | 356 | 9 | 356 | 5 | 0 |
| ADT3-08 | 0.93 | 0.05637 | 0.00153 | 0.42075 | 0.01145 | 0.05411 | 0.00081 | 467 | 34 | 357 | 8 | 340 | 5 | 5 |
| ADT3-09 | 0.49 | 0.05347 | 0.00145 | 0.41171 | 0.01115 | 0.05582 | 0.00083 | 349 | 35 | 350 | 8 | 350 | 5 | 0 |
| ADT3-10 | 0.46 | 0.05331 | 0.00273 | 0.42006 | 0.02126 | 0.05713 | 0.00096 | 342 | 84 | 356 | 15 | 358 | 6 | -0.6 |
| ADT3-11 | 0.56 | 0.05394 | 0.00166 | 0.40571 | 0.01243 | 0.05453 | 0.00082 | 369 | 42 | 346 | 9 | 342 | 5 | 1.2 |
| ADT3-12 | 0.69 | 0.05829 | 0.0016 | 0.45174 | 0.01239 | 0.05619 | 0.00084 | 541 | 34 | 378 | 9 | 352 | 5 | 7.4 |
| ADT3-13 | 0.59 | 0.05414 | 0.0019 | 0.4242 | 0.01477 | 0.05681 | 0.00089 | 377 | 50 | 359 | 11 | 356 | 5 | 0.8 |
| ADT3-14 | 0.4 | 0.05305 | 0.00167 | 0.40489 | 0.01265 | 0.05533 | 0.00085 | 331 | 43 | 345 | 9 | 347 | 5 | -0.6 |
| ADT3-15 | 0.59 | 0.05349 | 0.00196 | 0.41649 | 0.01513 | 0.05645 | 0.00088 | 350 | 54 | 354 | 11 | 354 | 5 | 0 |
| ADT3-16 | 0.62 | 0.0535 | 0.00198 | 0.41405 | 0.01515 | 0.05611 | 0.00088 | 350 | 54 | 352 | 11 | 352 | 5 | 0 |

| | | | | | | | | | | | | | | |
|---|---|---|---|---|---|---|---|---|---|---|---|---|---|---|
| ADT3-17 | 0.54 | 0.05386 | 0.00161 | 0.41392 | 0.01228 | 0.05571 | 0.00084 | 365 | 40 | 352 | 9 | 349 | 5 | 0.9 |
| ADT3-18 | 1.11 | 0.05502 | 0.00149 | 0.41832 | 0.01126 | 0.05512 | 0.00082 | 413 | 34 | 355 | 8 | 346 | 5 | 2.6 |
| ADT3-19 | 0.65 | 0.05523 | 0.00135 | 0.44855 | 0.01144 | 0.05888 | 0.00087 | 422 | 32 | 376 | 8 | 369 | 5 | 1.9 |
| ADT3-20 | 0.7 | 0.05437 | 0.00132 | 0.42948 | 0.01091 | 0.05726 | 0.00084 | 386 | 32 | 363 | 8 | 359 | 5 | 1.1 |
| ADT3-21 | 0.78 | 0.05286 | 0.00192 | 0.26027 | 0.00957 | 0.03569 | 0.00055 | 323 | 55 | 235 | 8 | 226 | 3 | 4 |
| ADT3-22 | 0.59 | 0.0564 | 0.00165 | 0.46925 | 0.01415 | 0.06032 | 0.00089 | 468 | 41 | 391 | 10 | 378 | 5 | 3.4 |
| ADT3-23 | 0.78 | 0.05463 | 0.00124 | 0.44914 | 0.01077 | 0.0596 | 0.00086 | 397 | 29 | 377 | 8 | 373 | 5 | 1.1 |
| ADT3-24 | 0.61 | 0.05427 | 0.00161 | 0.43645 | 0.0133 | 0.0583 | 0.00087 | 382 | 42 | 368 | 9 | 365 | 5 | 0.8 |
| ADT3-25 | 0.69 | 0.05666 | 0.00154 | 0.46527 | 0.01313 | 0.05953 | 0.00088 | 478 | 37 | 388 | 9 | 373 | 5 | 4 |
| ADT3-26 | 0.62 | 0.05639 | 0.00194 | 0.45885 | 0.01601 | 0.05899 | 0.00091 | 468 | 50 | 383 | 11 | 369 | 6 | 3.8 |
| ADT3-27 | 0.52 | 0.05565 | 0.00145 | 0.44186 | 0.01199 | 0.05756 | 0.00085 | 438 | 35 | 372 | 8 | 361 | 5 | 3 |
| ADT3-28 | 0.55 | 0.05492 | 0.00202 | 0.43634 | 0.01627 | 0.05759 | 0.00088 | 409 | 56 | 368 | 12 | 361 | 5 | 1.9 |
| ADT3-29 | 0.55 | 0.05413 | 0.00162 | 0.44058 | 0.01349 | 0.05901 | 0.00089 | 376 | 42 | 371 | 10 | 370 | 5 | 0.3 |
| ADT3-30 | 0.49 | 0.05501 | 0.00176 | 0.43676 | 0.01426 | 0.05756 | 0.00087 | 413 | 46 | 368 | 10 | 361 | 5 | 1.9 |
| ADT3-31 | 0.68 | 0.05601 | 0.0016 | 0.44645 | 0.01311 | 0.05778 | 0.00087 | 453 | 39 | 375 | 9 | 362 | 5 | 3.6 |
| ADT3-32 | 0.63 | 0.05452 | 0.00161 | 0.44331 | 0.01344 | 0.05895 | 0.00088 | 393 | 42 | 373 | 9 | 369 | 5 | 1.1 |
| ADT3-33 | 0.73 | 0.0602 | 0.00274 | 0.50575 | 0.02175 | 0.06093 | 0.00092 | 611 | 101 | 416 | 15 | 381 | 6 | 9.2 |
| ADT3-34 | 0.67 | 0.05606 | 0.0031 | 0.44958 | 0.02384 | 0.05816 | 0.00092 | 455 | 126 | 377 | 17 | 364 | 6 | 3.6 |
| ADT3-35 | 0.46 | 0.05399 | 0.00282 | 0.44269 | 0.02312 | 0.05945 | 0.00097 | 371 | 88 | 372 | 16 | 372 | 6 | 0 |
| ADT3-36 | 0.51 | 0.05456 | 0.00158 | 0.44762 | 0.01327 | 0.05948 | 0.00089 | 394 | 40 | 376 | 9 | 372 | 5 | 1.1 |
| ADT3-37 | 0.75 | 0.0543 | 0.00204 | 0.45033 | 0.01711 | 0.06013 | 0.00093 | 384 | 57 | 378 | 12 | 376 | 6 | 0.5 |
| ADT3-38 | 0.59 | 0.05543 | 0.00118 | 0.44497 | 0.01005 | 0.0582 | 0.00084 | 430 | 26 | 374 | 7 | 365 | 5 | 2.5 |
| ADT3-39 | 0.59 | 0.05666 | 0.00255 | 0.45987 | 0.01948 | 0.05887 | 0.00089 | 478 | 102 | 384 | 14 | 369 | 5 | 4.1 |
| ADT3-40 | 0.8 | 0.05426 | 0.00439 | 0.44773 | 0.03599 | 0.05982 | 0.00113 | 382 | 148 | 376 | 25 | 375 | 7 | 0.3 |
| ADT3-41 | 0.76 | 0.05405 | 0.00168 | 0.44233 | 0.01404 | 0.05934 | 0.00089 | 373 | 45 | 372 | 10 | 372 | 5 | 0 |
| ADT3-42 | 0.66 | 0.05727 | 0.00116 | 0.46263 | 0.01007 | 0.05857 | 0.00084 | 502 | 24 | 386 | 7 | 367 | 5 | 5.2 |
| ADT3-43 | 0.74 | 0.05422 | 0.00199 | 0.45728 | 0.01701 | 0.06115 | 0.00094 | 380 | 56 | 382 | 12 | 383 | 6 | -0.3 |
| ADT3-44 | 0.74 | 0.05417 | 0.00162 | 0.43166 | 0.01318 | 0.05778 | 0.00087 | 378 | 42 | 364 | 9 | 362 | 5 | 0.6 |

| | | | | | | | | | | | | | | |
|---|---|---|---|---|---|---|---|---|---|---|---|---|---|---|
| ADT3-45 | 0.64 | 0.05799 | 0.00131 | 0.46038 | 0.01098 | 0.05756 | 0.00084 | 529 | 28 | 385 | 8 | 361 | 5 | 6.6 |
| ADT3-46 | 0.8 | 0.06005 | 0.00315 | 0.47655 | 0.02389 | 0.05756 | 0.0009 | 605 | 117 | 396 | 16 | 361 | 5 | 9.7 |
| ADT3-47 | 0.6 | 0.05484 | 0.00129 | 0.45302 | 0.01115 | 0.0599 | 0.00087 | 406 | 30 | 379 | 8 | 375 | 5 | 1.1 |
| ADT3-48 | 0.58 | 0.05515 | 0.00164 | 0.44912 | 0.01368 | 0.05905 | 0.00088 | 418 | 42 | 377 | 10 | 370 | 5 | 1.9 |
| ADT3-49 | 0.68 | 0.05595 | 0.00107 | 0.45729 | 0.00946 | 0.05926 | 0.00084 | 450 | 23 | 382 | 7 | 371 | 5 | 3 |
| ADT3-50 | 0.57 | 0.05409 | 0.00259 | 0.42945 | 0.0206 | 0.05757 | 0.00092 | 375 | 79 | 363 | 15 | 361 | 6 | 0.6 |
| ADT3-51 | 0.66 | 0.05619 | 0.00142 | 0.4536 | 0.01185 | 0.05854 | 0.00086 | 460 | 33 | 380 | 8 | 367 | 5 | 3.5 |
| ADT3-52 | 0.61 | 0.05619 | 0.00288 | 0.44019 | 0.02151 | 0.05681 | 0.00089 | 460 | 117 | 370 | 15 | 356 | 5 | 3.9 |
| ADT3-53 | 0.61 | 0.054 | 0.00142 | 0.43883 | 0.01187 | 0.05893 | 0.00088 | 371 | 35 | 369 | 8 | 369 | 5 | 0 |
| ADT3-54 | 0.77 | 0.05568 | 0.00143 | 0.44585 | 0.01185 | 0.05806 | 0.00086 | 440 | 34 | 374 | 8 | 364 | 5 | 2.7 |
| ADT3-55 | 0.5 | 0.05388 | 0.00187 | 0.42948 | 0.01511 | 0.0578 | 0.00088 | 366 | 52 | 363 | 11 | 362 | 5 | 0.3 |
| ADT3-56 | 0.63 | 0.05387 | 0.00172 | 0.43607 | 0.01411 | 0.0587 | 0.0009 | 366 | 45 | 367 | 10 | 368 | 5 | -0.3 |
| ADT3-57 | 0.51 | 0.05487 | 0.00174 | 0.43452 | 0.01401 | 0.05743 | 0.00086 | 407 | 45 | 366 | 10 | 360 | 5 | 1.7 |
| ADT3-58 | 0.46 | 0.05464 | 0.00148 | 0.43174 | 0.01199 | 0.0573 | 0.00085 | 398 | 36 | 364 | 9 | 359 | 5 | 1.4 |
| ADT3-59 | 0.58 | 0.05442 | 0.00264 | 0.43312 | 0.02101 | 0.05771 | 0.00093 | 388 | 80 | 365 | 15 | 362 | 6 | 0.8 |
| ADT3-60 | 0.64 | 0.05402 | 0.00214 | 0.43319 | 0.01732 | 0.05815 | 0.0009 | 372 | 62 | 365 | 12 | 364 | 5 | 0.3 |
| ~~ADT3-61~~ | ~~0.93~~ | ~~0.07136~~ | ~~0.00169~~ | ~~0.56468~~ | ~~0.01391~~ | ~~0.05738~~ | ~~0.00084~~ | ~~968~~ | ~~27~~ | ~~455~~ | ~~9~~ | ~~360~~ | ~~5~~ | ~~26.4~~ |
| ADT3-62 | 0.69 | 0.05473 | 0.00162 | 0.44004 | 0.01327 | 0.0583 | 0.00087 | 401 | 41 | 370 | 9 | 365 | 5 | 1.4 |
| ADT3-63 | 0.71 | 0.05478 | 0.00141 | 0.4306 | 0.01145 | 0.057 | 0.00083 | 403 | 34 | 364 | 8 | 357 | 5 | 2 |
| ADT3-64 | 0.41 | 0.05454 | 0.00274 | 0.45273 | 0.02274 | 0.06019 | 0.001 | 393 | 83 | 379 | 16 | 377 | 6 | 0.5 |
| ADT3-65 | 0.63 | 0.05715 | 0.00347 | 0.46496 | 0.0272 | 0.05901 | 0.00096 | 497 | 138 | 388 | 19 | 370 | 6 | 4.9 |
| ADT3-66 | 0.53 | 0.05529 | 0.00156 | 0.43647 | 0.01261 | 0.05725 | 0.00085 | 424 | 38 | 368 | 9 | 359 | 5 | 2.5 |
| ADT3-67 | 0.58 | 0.05355 | 0.00218 | 0.43687 | 0.01787 | 0.05916 | 0.00093 | 352 | 64 | 368 | 13 | 371 | 6 | -0.8 |
| ADT3-68 | 0.52 | 0.05401 | 0.00187 | 0.43998 | 0.01544 | 0.05908 | 0.0009 | 371 | 52 | 370 | 11 | 370 | 5 | 0 |
| ADT3-69 | 0.58 | 0.0582 | 0.0034 | 0.46993 | 0.02639 | 0.05856 | 0.00094 | 537 | 131 | 391 | 18 | 367 | 6 | 6.5 |
| ADT3-70 | 0.53 | 0.05352 | 0.00157 | 0.42342 | 0.01269 | 0.05738 | 0.00085 | 351 | 41 | 358 | 9 | 360 | 5 | -0.6 |
| ADT3-71 | 0.55 | 0.05693 | 0.00163 | 0.45674 | 0.0134 | 0.05818 | 0.00087 | 489 | 39 | 382 | 9 | 365 | 5 | 4.7 |
| ADT3-72 | 1 | 0.05434 | 0.00168 | 0.44147 | 0.01383 | 0.05891 | 0.00089 | 385 | 43 | 371 | 10 | 369 | 5 | 0.5 |

| | | | | | | | | | | | | | | |
|---|---|---|---|---|---|---|---|---|---|---|---|---|---|---|
| ADT3-73 | 0.57 | 0.0542 | 0.00153 | 0.42995 | 0.01242 | 0.05753 | 0.00085 | 379 | 39 | 363 | 9 | 361 | 5 | 0.6 |
| ADT3-74 | 0.53 | 0.05385 | 0.00152 | 0.43273 | 0.0125 | 0.05827 | 0.00086 | 365 | 39 | 365 | 9 | 365 | 5 | 0 |
| ADT3-75 | 0.49 | 0.05358 | 0.00164 | 0.41613 | 0.01294 | 0.05632 | 0.00084 | 353 | 44 | 353 | 9 | 353 | 5 | 0 |
| ADT3-76 | 0.69 | 0.05354 | 0.00208 | 0.42863 | 0.01676 | 0.05805 | 0.0009 | 352 | 60 | 362 | 12 | 364 | 5 | -0.5 |
| ADT3-77 | 0.65 | 0.05391 | 0.00192 | 0.4311 | 0.01546 | 0.058 | 0.00089 | 367 | 53 | 364 | 11 | 363 | 5 | 0.3 |
| ADT3-78 | 0.58 | 0.05442 | 0.00204 | 0.43406 | 0.01638 | 0.05785 | 0.0009 | 388 | 57 | 366 | 12 | 363 | 5 | 0.8 |
| ADT3-79 | 0.42 | 0.05436 | 0.00264 | 0.43518 | 0.02116 | 0.05805 | 0.00093 | 386 | 80 | 367 | 15 | 364 | 6 | 0.8 |
| ADT3-80 | 0.78 | 0.05424 | 0.00143 | 0.43171 | 0.01171 | 0.05772 | 0.00084 | 381 | 35 | 364 | 8 | 362 | 5 | 0.6 |
| ADT3-81 | 0.67 | 0.05428 | 0.00137 | 0.45304 | 0.01182 | 0.06053 | 0.00088 | 383 | 33 | 379 | 8 | 379 | 5 | 0 |
| ADT3-82 | 0.63 | 0.05682 | 0.00352 | 0.4494 | 0.02688 | 0.05736 | 0.00094 | 484 | 141 | 377 | 19 | 360 | 6 | 4.7 |
| ADT3-83 | 0.47 | 0.05429 | 0.00153 | 0.42158 | 0.01217 | 0.05631 | 0.00083 | 383 | 39 | 357 | 9 | 353 | 5 | 1.1 |
| ADT3-84 | 0.46 | 0.05435 | 0.0022 | 0.4383 | 0.01783 | 0.05848 | 0.00091 | 386 | 63 | 369 | 13 | 366 | 6 | 0.8 |
| ADT3-85 | 0.69 | 0.05396 | 0.00151 | 0.42298 | 0.01207 | 0.05684 | 0.00084 | 369 | 38 | 358 | 9 | 356 | 5 | 0.6 |
| ADT3-86 | 0.8 | 0.05967 | 0.00152 | 0.47611 | 0.01246 | 0.05787 | 0.00085 | 592 | 32 | 395 | 9 | 363 | 5 | 8.8 |
| ADT3-87 | 0.71 | 0.05447 | 0.00157 | 0.42666 | 0.01256 | 0.05681 | 0.00085 | 391 | 40 | 361 | 9 | 356 | 5 | 1.4 |
| ~~ADT3-88~~ | ~~0.77~~ | ~~0.0633~~ | ~~0.00165~~ | ~~0.4933~~ | ~~0.01322~~ | ~~0.05652~~ | ~~0.00083~~ | ~~718~~ | ~~33~~ | ~~407~~ | ~~9~~ | ~~354~~ | ~~5~~ | ~~15~~ |
| ADT3-89 | 0.7 | 0.05764 | 0.00128 | 0.46353 | 0.01077 | 0.05832 | 0.00084 | 516 | 27 | 387 | 7 | 365 | 5 | 6 |
| ADT3-90 | 0.6 | 0.05354 | 0.00257 | 0.42792 | 0.02047 | 0.05797 | 0.00096 | 352 | 78 | 362 | 15 | 363 | 6 | -0.3 |
| ADT3-91 | 0.57 | 0.05458 | 0.00162 | 0.44309 | 0.01332 | 0.05887 | 0.00088 | 395 | 41 | 372 | 9 | 369 | 5 | 0.8 |
| ADT3-92 | 0.44 | 0.0559 | 0.00142 | 0.44013 | 0.01148 | 0.0571 | 0.00083 | 448 | 33 | 370 | 8 | 358 | 5 | 3.4 |
| ADT3-93 | 0.63 | 0.0541 | 0.00172 | 0.43879 | 0.01409 | 0.05882 | 0.00089 | 375 | 45 | 369 | 10 | 368 | 5 | 0.3 |
| ADT3-94 | 0.46 | 0.05426 | 0.00266 | 0.44291 | 0.0216 | 0.0592 | 0.00098 | 382 | 80 | 372 | 15 | 371 | 6 | 0.3 |
| ADT3-95 | 0.55 | 0.05433 | 0.00198 | 0.42445 | 0.01554 | 0.05666 | 0.00087 | 385 | 55 | 359 | 11 | 355 | 5 | 1.1 |
| ADT3-96 | 0.5 | 0.05466 | 0.00124 | 0.43842 | 0.01036 | 0.05817 | 0.00084 | 398 | 28 | 369 | 7 | 364 | 5 | 1.4 |
| ADT3-97 | 0.39 | 0.06004 | 0.00276 | 0.51241 | 0.02354 | 0.06189 | 0.00098 | 605 | 72 | 420 | 16 | 387 | 6 | 8.5 |
| ADT3-98 | 0.53 | 0.05649 | 0.00164 | 0.45032 | 0.0133 | 0.05781 | 0.00086 | 472 | 39 | 378 | 9 | 362 | 5 | 4.4 |
| ADT3-99 | 0.6 | 0.05368 | 0.00213 | 0.42533 | 0.0169 | 0.05746 | 0.0009 | 358 | 61 | 360 | 12 | 360 | 5 | 0 |
| ADT3-100 | 0.62 | 0.05539 | 0.00183 | 0.45804 | 0.01526 | 0.05997 | 0.00092 | 428 | 47 | 383 | 11 | 375 | 6 | 2.1 |

## Appendix to Chapter 3.1

SUPPLEMENTAL ITEM 1: Description of zircon separation and LA-ICP-MS U–Pb dating of zircon

Detrital heavy minerals were separated following standard procedures (e.g. Liu et al., 2013). A quantity of zircon grains (generally more than 200) were randomly selected, enclosed in epoxy resin and polished to yield a smooth flat internal surface (slice). After being photographed under reflected and transmitted light, the samples were prepared for cathodoluminescence (CL) imaging in order to choose potential internal target sites for U-Pb dating (e.g. Liu et al., 2013; Yang et al., 2013). CL imaging was carried out using a Quanta 200 FEG Scanning Electron Microscope at the SEEC lab, in the School of Earth and Space Science at Peking University. The U-Pb dating was performed on an Agilent 7500a ICP-MS connected to a 193 nm Excimer laser ablation system of American New Wave UP 193 SS at the China University of Geosciences, Beijing, following the method described by Yang et al. (2013). The operating parameters were as follows: Ar plasma gas flow rate was 1.13 l/min, radio frequency (RF) power was 1350 W and elemental integral time was 10 ms for Si and Zr and 50 ms for other elements. Helium with a flow rate of 0.89 l/min was used as the carrier gas to enhance the transport efficiency of the ablated material. The spot diameter was 36 μm with an analytical laser frequency of 10 Hz. Each analysis consisted of 5 s pre-denudation and 45 s signal acquisition. The Glitter 4.4.1 software was used to calculate the U/Pb isotope ratios and element contents. Age calculations, plotting of relative probability and concordia diagrams were made using ISOPLOT (version 3.0) (Ludwig, 2003). Standard zircon TEMORA 1 was used as an external standard for correction of isotopic ratios to

calculate the U/Pb ages, while zircons Qinghu and 91500 were the monitoring standards. For elemental concentration analysis, NIST 610 was the external standard, and 29Si was the internal standard (Wiedenbeck et al., 1995; Black et al., 2003). Meanwhile, NIST 612 and NIST 614 were used as monitoring standards. The common Pb correction was performed following the method described by Andersen (2002). A detailed description of the technical procedure is given in Liu et al. (2013). For ICP-MS analyses, those ages with a discordance degree >10% were excluded from analysis (e.g. Gehrels et al., 2003; Yang et al., 2013).

REFERENCES CITED

Andersen, T., 2002, Correction of common lead in U–Pb analyses that do not report $^{204}$Pb: Chemical Geology, v. 192, p. 59-79.

Black, L. P., Kamo, S. L., Allen, C. M., Aleinikoff, J. N., Davis, D. W., Korsch, R. J., and Foudoulis, C., 2003, TEMORA 1: a new zircon standard for Phanerozoic U–Pb geochronology: Chemical Geology, v. 200, no. 1–2, p. 155-170, doi: 10.1016/S0009-2541(03)00165-7.

Gehrels, G. E., Yin, A., and Wang, X. F., 2003, Detrital-zircon geochronology of the northeastern Tibetan plateau: Geological Society of America Bulletin, v. 115, no. 7, p. 881-896, doi: 10.1130/0016-7606(2003)115<0881:DGOTNT>2.0.CO;2.

Liu, D. D., Jolivet, M., Yang, W., Zhang, Z. Y., Feng, C., Zhu, B., and Guo, Z. J., 2013a, Latest Palaeozoic-Early Mesozoic basin-range interactions in South Tian Shan (Northwest China) and their tectonic significance: Constraints from detrital zircon U-Pb ages: Tectonophysics v. 599, 197-213, 10.1016/j.tecto.2013.04.018.

Ludwig, K.R., 2003, User's Manual for Isoplot/Ex, Version 3.00: A Geochronological Toolkit for Microsoft Excel: Berkeley Geochronology Center Special Publication 4, 77 p.

Wiedenbeck, M., Alle, P., Corfu, F., Griffin, W., Meier, M., Oberli, F., Quadt, A. v., Roddick, J., and Spiegel, W., 1995, Three natural zircon standards for U‐Th‐Pb, Lu‐Hf, trace element and REE analyses: Geostandards Newsletter, v. 19, no. 1, p. 1-23, doi: 10.1111/j.1751-908X.1995.tb00147.x.

Yang, W., Jolivet, M., Dupont‐Nivet, G., Guo, Z., Zhang, Z., and Wu, C., 2013, Source to sink relations between the Tian Shan and Junggar Basin (northwest China) from Late Palaeozoic to Quaternary: evidence from detrital U‐Pb zircon geochronology: Basin Research, v. 25, no. 2, p. 219-240, doi: 10.1111/j.1365-2117.2012.00558.x.

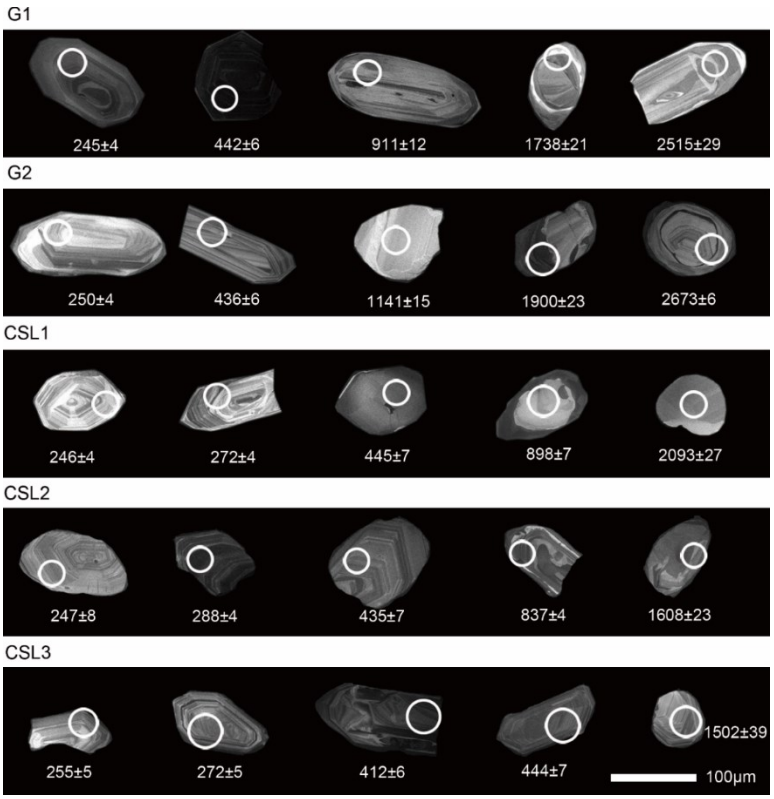


Figure DR1. Representative CL images of zircons from the five sandstone samples. The white circles show the locations of the U-Pb analysis. Numbers are U-Pb ages in Ma.

Table DR1. LA-ICP-MS U-Pb data of detrital zircons from the five sandstone samples.

| Analysis number | Th/U | Isotopic ratios and errors | | | | | | Ages and errors (Ma) | | | | | | Disc.% |
|---|---|---|---|---|---|---|---|---|---|---|---|---|---|---|
| | | $^{207}Pb/^{206}Pb$ | 1σ | $^{207}Pb/^{235}U$ | 1σ | $^{206}Pb/^{238}U$ | 1σ | $^{207}Pb/^{206}Pb$ | 1σ | $^{207}Pb/^{235}U$ | 1σ | $^{206}Pb/^{238}U$ | 1σ | |
| **G1** | | | | | | | | | | | | | | |
| G1-01 | 0.63 | 0.0515 | 0.0033 | 0.24542 | 0.0158 | 0.03455 | 0.0007 | 263 | 113 | 223 | 13 | 219 | 4 | 1.8 |
| G1-02 | 0.83 | 0.05187 | 0.0011 | 0.29852 | 0.0066 | 0.04173 | 0.0006 | 280 | 26 | 265 | 5 | 264 | 4 | 0.4 |
| G1-03 | 1.02 | 0.10533 | 0.0019 | 4.38056 | 0.0838 | 0.30157 | 0.0044 | 1720 | 17 | 1709 | 16 | 1699 | 22 | 1.2 |
| G1-04 | 0.56 | 0.05157 | 0.0017 | 0.30509 | 0.0099 | 0.0429 | 0.0007 | 266 | 47 | 270 | 8 | 271 | 4 | -0.4 |
| G1-05 | 1.29 | 0.05069 | 0.0018 | 0.24618 | 0.009 | 0.03522 | 0.0005 | 227 | 56 | 223 | 7 | 223 | 3 | 0 |
| G1-06 | 0.83 | 0.0557 | 0.0019 | 0.54558 | 0.0186 | 0.07103 | 0.0011 | 440 | 48 | 442 | 12 | 442 | 7 | 0 |
| G1-07 | 0.53 | 0.05508 | 0.0025 | 0.49104 | 0.0212 | 0.06465 | 0.001 | 416 | 105 | 406 | 14 | 404 | 6 | 0.5 |
| G1-08 | 0.58 | 0.05718 | 0.002 | 0.63047 | 0.0218 | 0.07996 | 0.0013 | 498 | 48 | 496 | 14 | 496 | 8 | 0 |
| G1-09 | 0.38 | 0.05482 | 0.0011 | 0.49534 | 0.0104 | 0.06552 | 0.0009 | 405 | 24 | 409 | 7 | 409 | 6 | 0 |
| G1-10 | 0.18 | 0.1137 | 0.0026 | 4.85082 | 0.0883 | 0.30941 | 0.0043 | 1859 | 42 | 1794 | 15 | 1738 | 21 | 7 |
| G1-11 | 0.92 | 0.05097 | 0.0016 | 0.26092 | 0.0081 | 0.03712 | 0.0006 | 239 | 44 | 235 | 7 | 235 | 3 | 0 |
| G1-12 | 0.34 | 0.05153 | 0.0012 | 0.29683 | 0.0072 | 0.04177 | 0.0006 | 265 | 31 | 264 | 6 | 264 | 4 | 0 |
| G1-13 | 0.9 | 0.05569 | 0.0014 | 0.53408 | 0.0141 | 0.06954 | 0.001 | 440 | 34 | 435 | 9 | 433 | 6 | 0.5 |
| G1-14 | 0.47 | 0.14373 | 0.0021 | 8.10866 | 0.1333 | 0.4091 | 0.0057 | 2273 | 13 | 2243 | 15 | 2211 | 26 | 2.8 |
| G1-15 | 0.45 | 0.16304 | 0.0023 | 9.76594 | 0.1598 | 0.43437 | 0.006 | 2487 | 12 | 2413 | 15 | 2325 | 27 | 7 |
| G1-16 | 1.08 | 0.10442 | 0.0018 | 4.38305 | 0.081 | 0.30438 | 0.0044 | 1704 | 16 | 1709 | 15 | 1713 | 22 | -0.5 |
| G1-17 | 0.35 | 0.16566 | 0.0024 | 10.891 | 0.1808 | 0.47673 | 0.0066 | 2514 | 13 | 2514 | 15 | 2513 | 29 | 0 |
| G1-18 | 0.52 | 0.08408 | 0.0013 | 2.38023 | 0.0417 | 0.20527 | 0.0029 | 1294 | 16 | 1237 | 13 | 1204 | 15 | 7.5 |
| G1-19 | 0.16 | 0.17233 | 0.0026 | 11.3413 | 0.1917 | 0.47722 | 0.0067 | 2580 | 13 | 2552 | 16 | 2515 | 29 | 2.6 |
| G1-20 | 0.81 | 0.05116 | 0.0017 | 0.27949 | 0.0095 | 0.03961 | 0.0006 | 248 | 51 | 250 | 8 | 250 | 4 | 0 |
| G1-21 | 0.44 | 0.05066 | 0.0027 | 0.25517 | 0.0138 | 0.03652 | 0.0006 | 225 | 95 | 231 | 11 | 231 | 4 | 0 |
| G1-22 | 0.52 | 0.11444 | 0.0017 | 5.28953 | 0.0881 | 0.33516 | 0.0046 | 1871 | 14 | 1867 | 14 | 1863 | 22 | 0.4 |

| | | | | | | | | | | | | | | |
|---|---|---|---|---|---|---|---|---|---|---|---|---|---|---|
| G1-23 | 0.57 | 0.05122 | 0.002 | 0.27755 | 0.011 | 0.0393 | 0.0006 | 251 | 62 | 249 | 9 | 248 | 4 | 0.4 |
| G1-24 | 0.54 | 0.05526 | 0.0012 | 0.50941 | 0.0116 | 0.06684 | 0.001 | 423 | 27 | 418 | 8 | 417 | 6 | 0.2 |
| G1-25 | 1.14 | 0.0547 | 0.0043 | 0.49384 | 0.038 | 0.06547 | 0.0014 | 400 | 136 | 408 | 26 | 409 | 8 | -0.2 |
| ~~G1-26~~ | 0.68 | ~~0.14597~~ | ~~0.0042~~ | ~~6.33588~~ | ~~0.1552~~ | ~~0.3148~~ | ~~0.0047~~ | ~~2299~~ | ~~50~~ | ~~2023~~ | ~~21~~ | ~~1764~~ | ~~23~~ | 30.3 |
| G1-27 | 0.8 | 0.05102 | 0.0028 | 0.27828 | 0.015 | 0.03955 | 0.0007 | 242 | 92 | 249 | 12 | 250 | 4 | -0.4 |
| G1-28 | 0.19 | 0.07063 | 0.0012 | 1.54431 | 0.0295 | 0.15856 | 0.0022 | 947 | 19 | 948 | 12 | 949 | 12 | -0.1 |
| G1-29 | 0.65 | 0.05084 | 0.0017 | 0.24375 | 0.0084 | 0.03476 | 0.0005 | 234 | 52 | 221 | 7 | 220 | 3 | 0.5 |
| G1-30 | 0.45 | 0.05584 | 0.0013 | 0.5427 | 0.0128 | 0.07047 | 0.001 | 446 | 28 | 440 | 8 | 439 | 6 | 0.2 |
| ~~G1-31~~ | 0.9 | ~~0.15784~~ | ~~0.0024~~ | ~~8.87929~~ | ~~0.1531~~ | ~~0.40793~~ | ~~0.0058~~ | ~~2433~~ | ~~13~~ | ~~2326~~ | ~~16~~ | ~~2205~~ | ~~26~~ | 10.3 |
| G1-32 | 0.85 | 0.05119 | 0.0018 | 0.27434 | 0.0099 | 0.03886 | 0.0006 | 249 | 54 | 246 | 8 | 246 | 4 | 0 |
| G1-33 | 1 | 0.11312 | 0.0017 | 4.99015 | 0.0862 | 0.31988 | 0.0045 | 1850 | 14 | 1818 | 15 | 1789 | 22 | 3.4 |
| G1-34 | 0.51 | 0.10895 | 0.0017 | 4.68899 | 0.0823 | 0.3121 | 0.0044 | 1782 | 15 | 1765 | 15 | 1751 | 22 | 1.8 |
| G1-35 | 0.35 | 0.05151 | 0.0016 | 0.29349 | 0.0091 | 0.04132 | 0.0007 | 264 | 43 | 261 | 7 | 261 | 4 | 0 |
| G1-36 | 0.71 | 0.05039 | 0.0031 | 0.2389 | 0.0145 | 0.03438 | 0.0007 | 213 | 105 | 218 | 12 | 218 | 4 | 0 |
| G1-37 | 1.13 | 0.05252 | 0.0016 | 0.34415 | 0.0107 | 0.04752 | 0.0007 | 308 | 43 | 300 | 8 | 299 | 4 | 0.3 |
| G1-38 | 0.45 | 0.08533 | 0.0015 | 2.8191 | 0.0532 | 0.23957 | 0.0034 | 1323 | 17 | 1361 | 14 | 1384 | 18 | -4.4 |
| G1-39 | 0.93 | 0.10591 | 0.0019 | 4.22105 | 0.0831 | 0.28902 | 0.0042 | 1730 | 17 | 1678 | 16 | 1637 | 21 | 5.7 |
| G1-40 | 0.85 | 0.10884 | 0.0021 | 4.72962 | 0.0975 | 0.31511 | 0.0047 | 1780 | 18 | 1773 | 17 | 1766 | 23 | 0.8 |
| G1-41 | 0.42 | 0.05491 | 0.001 | 0.50591 | 0.0102 | 0.06681 | 0.001 | 409 | 22 | 416 | 7 | 417 | 6 | -0.2 |
| G1-42 | 0.68 | 0.11445 | 0.0018 | 5.28829 | 0.0917 | 0.33507 | 0.0047 | 1871 | 14 | 1867 | 15 | 1863 | 23 | 0.4 |
| G1-43 | 0.92 | 0.05653 | 0.001 | 0.59129 | 0.0118 | 0.07585 | 0.0011 | 473 | 21 | 472 | 8 | 471 | 6 | 0.2 |
| G1-44 | 0.39 | 0.05515 | 0.0016 | 0.50229 | 0.0148 | 0.06605 | 0.001 | 418 | 39 | 413 | 10 | 412 | 6 | 0.2 |
| G1-45 | 0.53 | 0.14585 | 0.0022 | 8.00285 | 0.1384 | 0.39788 | 0.0056 | 2298 | 14 | 2231 | 16 | 2159 | 26 | 6.4 |
| ~~G1-46~~ | 0.23 | ~~0.16008~~ | ~~0.0024~~ | ~~7.31502~~ | ~~0.1265~~ | ~~0.33136~~ | ~~0.0046~~ | ~~2457~~ | ~~13~~ | ~~2151~~ | ~~15~~ | ~~1845~~ | ~~22~~ | 33.2 |
| G1-47 | 0.6 | 0.05206 | 0.0025 | 0.30914 | 0.0148 | 0.04306 | 0.0007 | 288 | 80 | 274 | 11 | 272 | 4 | 0.7 |
| G1-48 | 0.41 | 0.05107 | 0.0014 | 0.277 | 0.0076 | 0.03933 | 0.0006 | 244 | 36 | 248 | 6 | 249 | 4 | -0.4 |
| G1-49 | 0.43 | 0.08344 | 0.0016 | 2.53296 | 0.0522 | 0.22014 | 0.0032 | 1280 | 20 | 1282 | 15 | 1283 | 17 | -0.2 |
| G1-50 | 0.5 | 0.06668 | 0.0012 | 1.24406 | 0.0245 | 0.1353 | 0.0019 | 828 | 20 | 821 | 11 | 818 | 11 | 0.4 |

| | | | | | | | | | | | | | | |
|---|---|---|---|---|---|---|---|---|---|---|---|---|---|---|
| G1-51 | 0.33 | 0.09204 | 0.0015 | 3.04097 | 0.0549 | 0.23957 | 0.0034 | 1468 | 16 | 1418 | 14 | 1384 | 18 | 6.1 |
| G1-52 | 0.66 | 0.05189 | 0.0031 | 0.32212 | 0.0193 | 0.04501 | 0.0008 | 281 | 104 | 284 | 15 | 284 | 5 | 0 |
| G1-53 | 0.62 | 0.05075 | 0.0021 | 0.25792 | 0.0109 | 0.03685 | 0.0006 | 229 | 68 | 233 | 9 | 233 | 4 | 0 |
| G1-54 | 0.8 | 0.05077 | 0.0014 | 0.26328 | 0.0073 | 0.0376 | 0.0006 | 230 | 37 | 237 | 6 | 238 | 3 | -0.4 |
| G1-55 | 0.59 | 0.05153 | 0.0013 | 0.2961 | 0.0079 | 0.04167 | 0.0006 | 265 | 34 | 263 | 6 | 263 | 4 | 0 |
| G1-56 | 1.41 | 0.05368 | 0.0012 | 0.37075 | 0.0089 | 0.05008 | 0.0007 | 358 | 29 | 320 | 7 | 315 | 4 | 1.6 |
| G1-57 | 0.33 | 0.06898 | 0.0021 | 1.42189 | 0.0384 | 0.14951 | 0.0022 | 898 | 65 | 898 | 16 | 898 | 12 | 0 |
| G1-58 | 0.64 | 0.05093 | 0.0012 | 0.25904 | 0.0064 | 0.03688 | 0.0005 | 238 | 31 | 234 | 5 | 233 | 3 | 0.4 |
| G1-59 | 0.17 | 0.11423 | 0.0018 | 5.10596 | 0.0912 | 0.32414 | 0.0046 | 1868 | 15 | 1837 | 15 | 1810 | 22 | 3.2 |
| G1-60 | 0.71 | 0.05077 | 0.0015 | 0.26541 | 0.0079 | 0.03791 | 0.0006 | 230 | 42 | 239 | 6 | 240 | 3 | -0.4 |
| ~~G1-61~~ | 0.96 | ~~0.06652~~ | ~~0.0053~~ | ~~0.81213~~ | ~~0.0633~~ | ~~0.08855~~ | ~~0.0016~~ | ~~823~~ | ~~173~~ | ~~604~~ | ~~35~~ | ~~547~~ | ~~10~~ | 10.4 |
| G1-62 | 0.37 | 0.0575 | 0.0011 | 0.63345 | 0.0129 | 0.07989 | 0.0011 | 511 | 22 | 498 | 8 | 495 | 7 | 0.6 |
| G1-63 | 1.26 | 0.15045 | 0.0025 | 8.58319 | 0.159 | 0.41369 | 0.0059 | 2351 | 15 | 2295 | 17 | 2232 | 27 | 5.3 |
| G1-64 | 0.65 | 0.05543 | 0.0014 | 0.49439 | 0.0127 | 0.06467 | 0.001 | 430 | 32 | 408 | 9 | 404 | 6 | 1 |
| G1-65 | 0.4 | 0.05612 | 0.0011 | 0.5488 | 0.0118 | 0.07092 | 0.001 | 457 | 24 | 444 | 8 | 442 | 6 | 0.5 |
| G1-66 | 0.21 | 0.07078 | 0.0012 | 1.48119 | 0.0277 | 0.15175 | 0.0022 | 951 | 18 | 923 | 11 | 911 | 12 | 1.3 |
| G1-67 | 0.84 | 0.11869 | 0.0023 | 5.38012 | 0.1092 | 0.32871 | 0.0049 | 1937 | 17 | 1882 | 17 | 1832 | 24 | 5.7 |
| G1-68 | 0.14 | 0.07213 | 0.0013 | 1.60154 | 0.0315 | 0.161 | 0.0023 | 990 | 19 | 971 | 12 | 962 | 13 | 0.9 |
| ~~G1-69~~ | 0.78 | ~~0.06946~~ | ~~0.0036~~ | ~~0.37967~~ | ~~0.0199~~ | ~~0.03964~~ | ~~0.0007~~ | ~~912~~ | ~~80~~ | ~~327~~ | ~~15~~ | ~~251~~ | ~~4~~ | 30.3 |
| G1-70 | 0.51 | 0.05114 | 0.0014 | 0.27216 | 0.0076 | 0.03859 | 0.0006 | 247 | 37 | 244 | 6 | 244 | 4 | 0 |
| G1-71 | 0.56 | 0.05472 | 0.002 | 0.49634 | 0.018 | 0.06578 | 0.0011 | 401 | 52 | 409 | 12 | 411 | 7 | -0.5 |
| G1-72 | 0.13 | 0.05626 | 0.0012 | 0.52365 | 0.0114 | 0.06749 | 0.001 | 463 | 25 | 428 | 8 | 421 | 6 | 1.7 |
| G1-73 | 0.79 | 0.1766 | 0.003 | 11.6643 | 0.2187 | 0.47896 | 0.0069 | 2621 | 15 | 2578 | 18 | 2523 | 30 | 3.9 |
| G1-74 | 0.47 | 0.05452 | 0.0021 | 0.47244 | 0.0179 | 0.06283 | 0.0011 | 393 | 55 | 393 | 12 | 393 | 6 | 0 |
| G1-75 | 0.79 | 0.05071 | 0.0103 | 0.24626 | 0.0496 | 0.03521 | 0.0011 | 228 | 340 | 224 | 40 | 223 | 7 | 0.4 |
| G1-76 | 0.54 | 0.05112 | 0.0014 | 0.27337 | 0.0078 | 0.03878 | 0.0006 | 246 | 38 | 245 | 6 | 245 | 4 | 0 |
| G1-77 | 0.73 | 0.05537 | 0.0013 | 0.50816 | 0.0123 | 0.06655 | 0.001 | 427 | 29 | 417 | 8 | 415 | 6 | 0.5 |
| G1-78 | 0.47 | 0.05527 | 0.0034 | 0.4982 | 0.0305 | 0.06537 | 0.0011 | 423 | 105 | 410 | 21 | 408 | 7 | 0.5 |

| | | | | | | | | | | | | | | |
|---|---|---|---|---|---|---|---|---|---|---|---|---|---|---|
| G1-79 | 0.35 | 0.05087 | 0.0017 | 0.25931 | 0.0086 | 0.03697 | 0.0006 | 235 | 48 | 234 | 7 | 234 | 4 | 0 |
| G1-80 | 0.84 | 0.05531 | 0.0015 | 0.51813 | 0.0145 | 0.06793 | 0.001 | 425 | 36 | 424 | 10 | 424 | 6 | 0 |
| G1-81 | 0.6 | 0.07042 | 0.0016 | 1.48552 | 0.0343 | 0.15298 | 0.0023 | 941 | 24 | 924 | 14 | 918 | 13 | 0.7 |
| G1-82 | 1.51 | 0.05108 | 0.0015 | 0.26725 | 0.0081 | 0.03794 | 0.0006 | 244 | 42 | 240 | 6 | 240 | 4 | 0 |
| G1-83 | 0.74 | 0.07602 | 0.002 | 1.85895 | 0.0499 | 0.17731 | 0.0028 | 1096 | 30 | 1067 | 18 | 1052 | 15 | 4.2 |
| ~~G1-84~~ | 0.58 | ~~0.07162~~ | ~~0.0015~~ | ~~1.08971~~ | ~~0.024~~ | ~~0.11033~~ | ~~0.0016~~ | ~~975~~ | ~~23~~ | ~~748~~ | ~~12~~ | ~~675~~ | ~~9~~ | 10.8 |
| ~~G1-85~~ | 1.19 | ~~0.0734~~ | ~~0.0023~~ | ~~0.32264~~ | ~~0.0103~~ | ~~0.03187~~ | ~~0.0005~~ | ~~1025~~ | ~~39~~ | ~~284~~ | ~~8~~ | ~~202~~ | ~~3~~ | 40.6 |
| G1-86 | 0.46 | 0.15437 | 0.0027 | 9.35623 | 0.1809 | 0.4395 | 0.0063 | 2395 | 16 | 2374 | 18 | 2348 | 28 | 2 |
| G1-87 | 0.65 | 0.05088 | 0.0036 | 0.25225 | 0.0178 | 0.03595 | 0.0007 | 235 | 127 | 228 | 14 | 228 | 4 | 0 |
| G1-88 | 0.66 | 0.05795 | 0.0015 | 0.67309 | 0.0184 | 0.08422 | 0.0013 | 528 | 34 | 523 | 11 | 521 | 8 | 0.4 |
| G1-89 | 0.41 | 0.11923 | 0.0022 | 5.46625 | 0.1079 | 0.33244 | 0.0048 | 1945 | 17 | 1895 | 17 | 1850 | 23 | 5.1 |
| G1-90 | 0.63 | 0.05086 | 0.0022 | 0.25954 | 0.011 | 0.037 | 0.0006 | 234 | 68 | 234 | 9 | 234 | 4 | 0 |
| G1-91 | 0.45 | 0.10806 | 0.0024 | 4.68482 | 0.1086 | 0.31437 | 0.0049 | 1767 | 21 | 1765 | 19 | 1762 | 24 | 0.3 |
| G1-92 | 0.4 | 0.05481 | 0.0013 | 0.4883 | 0.0123 | 0.06461 | 0.001 | 404 | 31 | 404 | 8 | 404 | 6 | 0 |
| G1-93 | 0.26 | 0.05167 | 0.0014 | 0.31416 | 0.0086 | 0.04409 | 0.0007 | 271 | 36 | 277 | 7 | 278 | 4 | -0.4 |
| G1-94 | 0.54 | 0.05132 | 0.004 | 0.27236 | 0.0209 | 0.03849 | 0.0006 | 255 | 180 | 245 | 17 | 243 | 4 | 0.8 |
| G1-95 | 0.33 | 0.0555 | 0.0013 | 0.5231 | 0.013 | 0.06835 | 0.001 | 432 | 30 | 427 | 9 | 426 | 6 | 0.2 |
| ~~G1-96~~ | 0.62 | ~~0.06956~~ | ~~0.0039~~ | ~~0.28522~~ | ~~0.0153~~ | ~~0.02974~~ | ~~0.0005~~ | ~~915~~ | ~~119~~ | ~~255~~ | ~~12~~ | ~~189~~ | ~~3~~ | 34.9 |
| G1-97 | 0.35 | 0.05547 | 0.0013 | 0.52505 | 0.0125 | 0.06864 | 0.001 | 431 | 28 | 429 | 8 | 428 | 6 | 0.2 |
| ~~G1-98~~ | 0.44 | ~~0.07538~~ | ~~0.003~~ | ~~1.09414~~ | ~~0.0398~~ | ~~0.10528~~ | ~~0.0016~~ | ~~1079~~ | ~~81~~ | ~~751~~ | ~~19~~ | ~~645~~ | ~~9~~ | 16.4 |
| ~~G1-99~~ | 0.71 | ~~0.09205~~ | ~~0.0018~~ | ~~2.61051~~ | ~~0.0534~~ | ~~0.20566~~ | ~~0.003~~ | ~~1468~~ | ~~19~~ | ~~1304~~ | ~~15~~ | ~~1206~~ | ~~16~~ | 21.7 |
| ~~G1-100~~ | 0.2 | ~~0.06036~~ | ~~0.0016~~ | ~~0.4407~~ | ~~0.0118~~ | ~~0.05295~~ | ~~0.0008~~ | ~~617~~ | ~~32~~ | ~~371~~ | ~~8~~ | ~~333~~ | ~~5~~ | 11.4 |
| **G2** | | | | | | | | | | | | | | |
| G2-01 | 0.84 | 0.05626 | 0.0014 | 0.5906 | 0.0155 | 0.07612 | 0.0012 | 463 | 32 | 471 | 10 | 473 | 7 | -0.4 |
| G2-02 | 0.53 | 0.05598 | 0.0017 | 0.57068 | 0.0179 | 0.07392 | 0.0012 | 452 | 41 | 458 | 12 | 460 | 7 | -0.4 |
| G2-03 | 0.42 | 0.09234 | 0.0024 | 3.23511 | 0.0882 | 0.25406 | 0.0041 | 1474 | 28 | 1466 | 21 | 1459 | 21 | 1 |
| ~~G2-04~~ | ~~0.78~~ | ~~0.08027~~ | ~~0.0024~~ | ~~0.81933~~ | ~~0.0246~~ | ~~0.07402~~ | ~~0.0012~~ | ~~1204~~ | ~~34~~ | ~~608~~ | ~~14~~ | ~~460~~ | ~~7~~ | ~~32.2~~ |
| G2-05 | 0.6 | 0.05589 | 0.0017 | 0.56596 | 0.0174 | 0.07343 | 0.0012 | 448 | 40 | 455 | 11 | 457 | 7 | -0.4 |

| | | | | | | | | | | | | | | |
|---|---|---|---|---|---|---|---|---|---|---|---|---|---|---|
| G2-06 | 1.26 | 0.12134 | 0.002 | 5.88373 | 0.1081 | 0.35162 | 0.005 | 1976 | 15 | 1959 | 16 | 1942 | 24 | 1.8 |
| G2-07 | 0.38 | 0.17154 | 0.0027 | 11.0958 | 0.1987 | 0.46906 | 0.0065 | 2573 | 14 | 2531 | 17 | 2479 | 29 | 3.8 |
| G2-08 | 0.55 | 0.1031 | 0.0019 | 4.13918 | 0.0816 | 0.29112 | 0.0042 | 1681 | 17 | 1662 | 16 | 1647 | 21 | 2.1 |
| G2-09 | 0.68 | 0.18964 | 0.0032 | 13.5033 | 0.2492 | 0.51634 | 0.0074 | 2739 | 14 | 2716 | 17 | 2684 | 31 | 2 |
| G2-10 | 0.16 | 0.12279 | 0.0021 | 6.02188 | 0.1127 | 0.35564 | 0.0051 | 1997 | 16 | 1979 | 16 | 1961 | 24 | 1.8 |
| G2-11 | 0.31 | 0.11343 | 0.0019 | 5.23371 | 0.0951 | 0.33459 | 0.0047 | 1855 | 15 | 1858 | 15 | 1861 | 23 | -0.3 |
| G2-12 | 0.52 | 0.056 | 0.0017 | 0.56248 | 0.0177 | 0.07284 | 0.0011 | 452 | 42 | 453 | 11 | 453 | 7 | 0 |
| G2-13 | 0.55 | 0.17143 | 0.0028 | 11.1497 | 0.2028 | 0.47165 | 0.0066 | 2572 | 14 | 2536 | 17 | 2491 | 29 | 3.3 |
| G2-14 | 0.75 | 0.0909 | 0.002 | 2.92728 | 0.0669 | 0.23354 | 0.0035 | 1445 | 22 | 1389 | 17 | 1353 | 18 | 6.8 |
| G2-15 | 0.3 | 0.05808 | 0.0034 | 0.68658 | 0.0403 | 0.08572 | 0.0016 | 533 | 96 | 531 | 24 | 530 | 9 | 0.2 |
| G2-16 | 0.51 | 0.13659 | 0.0023 | 7.40382 | 0.1397 | 0.39307 | 0.0056 | 2184 | 15 | 2161 | 17 | 2137 | 26 | 2.2 |
| G2-17 | 0.66 | 0.18589 | 0.0032 | 12.9027 | 0.2447 | 0.50333 | 0.0073 | 2706 | 15 | 2673 | 18 | 2628 | 31 | 3 |
| G2-18 | 0.37 | 0.17399 | 0.0029 | 11.5864 | 0.2137 | 0.48289 | 0.0068 | 2596 | 14 | 2572 | 17 | 2540 | 30 | 2.2 |
| G2-19 | 0.46 | 0.05651 | 0.002 | 0.54624 | 0.0193 | 0.0701 | 0.0011 | 472 | 51 | 443 | 13 | 437 | 7 | 1.4 |
| G2-20 | 0.71 | 0.05565 | 0.0012 | 0.53938 | 0.0122 | 0.07028 | 0.001 | 438 | 26 | 438 | 8 | 438 | 6 | 0 |
| G2-21 | 0.45 | 0.08983 | 0.0016 | 3.19892 | 0.0622 | 0.25825 | 0.0037 | 1422 | 18 | 1457 | 15 | 1481 | 19 | -4 |
| G2-22 | 0.49 | 0.16659 | 0.0028 | 10.883 | 0.2013 | 0.47373 | 0.0067 | 2524 | 15 | 2513 | 17 | 2500 | 29 | 1 |
| G2-23 | 1.05 | 0.11376 | 0.0019 | 5.01273 | 0.0945 | 0.31954 | 0.0045 | 1860 | 16 | 1821 | 16 | 1787 | 22 | 4.1 |
| G2-24 | 0.73 | 0.05594 | 0.0016 | 0.55434 | 0.0159 | 0.07186 | 0.0011 | 450 | 37 | 448 | 10 | 447 | 7 | 0.2 |
| G2-25 | 1.56 | 0.05652 | 0.0012 | 0.57131 | 0.0127 | 0.07329 | 0.0011 | 473 | 25 | 459 | 8 | 456 | 6 | 0.7 |
| G2-26 | 0.42 | 0.07846 | 0.0019 | 2.0931 | 0.0526 | 0.19346 | 0.0029 | 1159 | 27 | 1147 | 17 | 1140 | 16 | 1.7 |
| G2-27 | 0.16 | 0.07979 | 0.0017 | 2.12992 | 0.0471 | 0.19358 | 0.0028 | 1192 | 22 | 1159 | 15 | 1141 | 15 | 4.5 |
| G2-28 | 0.58 | 0.10339 | 0.0018 | 4.10674 | 0.0791 | 0.28803 | 0.0041 | 1686 | 17 | 1656 | 16 | 1632 | 21 | 3.3 |
| G2-29 | 0.61 | 0.0562 | 0.0011 | 0.53945 | 0.0117 | 0.06961 | 0.001 | 460 | 24 | 438 | 8 | 434 | 6 | 0.9 |
| G2-30 | 0.69 | 0.0563 | 0.0011 | 0.55476 | 0.0117 | 0.07145 | 0.001 | 464 | 23 | 448 | 8 | 445 | 6 | 0.7 |
| G2-31 | 0.61 | 0.05661 | 0.0012 | 0.55822 | 0.0129 | 0.0715 | 0.0011 | 476 | 27 | 450 | 8 | 445 | 6 | 1.1 |
| G2-32 | ~~0.68~~ | 0.0563 | 0.0011 | 0.57298 | 0.0117 | 0.0738 | 0.0011 | ~~464~~ | ~~22~~ | ~~460~~ | ~~8~~ | ~~459~~ | ~~6~~ | ~~0.2~~ |
| G2-33 | 0.96 | 0.10738 | 0.0021 | 4.23401 | 0.0887 | 0.28592 | 0.0042 | 1755 | 19 | 1681 | 17 | 1621 | 21 | 8.3 |

| | | | | | | | | | | | | | | |
|---|---|---|---|---|---|---|---|---|---|---|---|---|---|---|
| G2-34 | 0.32 | 0.05543 | 0.0018 | 0.5344 | 0.0179 | 0.06991 | 0.0011 | 430 | 47 | 435 | 12 | 436 | 7 | -0.2 |
| G2-35 | 0.32 | 0.16319 | 0.0041 | 10.3325 | 0.2134 | 0.45921 | 0.0066 | 2489 | 43 | 2465 | 19 | 2436 | 29 | 2.2 |
| G2-36 | 0.10 | 0.07019 | 0.0013 | 1.4545 | 0.0291 | 0.15026 | 0.0022 | 934 | 20 | 912 | 12 | 902 | 12 | 1.1 |
| G2-37 | 0.75 | 0.05645 | 0.0014 | 0.54389 | 0.0143 | 0.06986 | 0.001 | 470 | 33 | 441 | 9 | 435 | 6 | 1.4 |
| G2-38 | 0.62 | 0.05555 | 0.0012 | 0.5357 | 0.0125 | 0.06994 | 0.001 | 434 | 27 | 436 | 8 | 436 | 6 | 0 |
| G2-39 | 0.12 | 0.12994 | 0.0022 | 6.44196 | 0.1223 | 0.3595 | 0.0051 | 2097 | 16 | 2038 | 17 | 1980 | 24 | 5.9 |
| G2-40 | 0.63 | 0.07344 | 0.0016 | 1.84264 | 0.0423 | 0.18194 | 0.0027 | 1026 | 24 | 1061 | 15 | 1078 | 15 | -4.8 |
| G2-41 | 0.51 | 0.1519 | 0.0044 | 8.66058 | 0.2119 | 0.4135 | 0.0062 | 2367 | 50 | 2303 | 22 | 2231 | 28 | 6.1 |
| G2-42 | 0.41 | 0.0693 | 0.0014 | 1.38754 | 0.03 | 0.1452 | 0.0021 | 908 | 22 | 884 | 13 | 874 | 12 | 1.1 |
| G2-43 | 0.62 | 0.05625 | 0.0015 | 0.56316 | 0.0154 | 0.0726 | 0.0011 | 462 | 34 | 454 | 10 | 452 | 7 | 0.4 |
| G2-44 | 0.39 | 0.16562 | 0.0029 | 10.7561 | 0.2086 | 0.47095 | 0.0068 | 2514 | 15 | 2502 | 18 | 2488 | 30 | 1 |
| G2-45 | 0.51 | 0.13215 | 0.0027 | 7.28326 | 0.1575 | 0.39967 | 0.006 | 2127 | 19 | 2147 | 19 | 2168 | 28 | -1.9 |
| G2-46 | 0.48 | 0.0934 | 0.0019 | 3.19514 | 0.069 | 0.24807 | 0.0037 | 1496 | 20 | 1456 | 17 | 1429 | 19 | 4.7 |
| G2-47 | 0.35 | 0.05563 | 0.0012 | 0.54634 | 0.0127 | 0.07122 | 0.001 | 438 | 27 | 443 | 8 | 444 | 6 | -0.2 |
| G2-48 | 0.32 | 0.09267 | 0.0017 | 3.2087 | 0.0637 | 0.25108 | 0.0036 | 1481 | 18 | 1459 | 15 | 1444 | 19 | 2.6 |
| G2-49 | 0.30 | 0.17529 | 0.0031 | 11.8677 | 0.2316 | 0.49094 | 0.007 | 2609 | 16 | 2594 | 18 | 2575 | 30 | 1.3 |
| G2-50 | 0.48 | 0.05621 | 0.0015 | 0.55819 | 0.0152 | 0.07201 | 0.0011 | 461 | 34 | 450 | 10 | 448 | 7 | 0.4 |
| G2-51 | 0.51 | 0.0562 | 0.0011 | 0.57713 | 0.0119 | 0.07447 | 0.0011 | 460 | 23 | 463 | 8 | 463 | 6 | 0 |
| G2-52 | 0.42 | 0.14868 | 0.0028 | 8.7967 | 0.1787 | 0.42902 | 0.0063 | 2331 | 17 | 2317 | 19 | 2301 | 28 | 1.3 |
| G2-53 | 0.43 | 0.10283 | 0.0019 | 4.10471 | 0.0826 | 0.28947 | 0.0042 | 1676 | 18 | 1655 | 16 | 1639 | 21 | 2.3 |
| G2-54 | 1.98 | 0.05612 | 0.0011 | 0.50006 | 0.0107 | 0.06461 | 0.0009 | 457 | 24 | 412 | 7 | 404 | 6 | 2 |
| G2-55 | 0.76 | 0.0562 | 0.0012 | 0.55998 | 0.0123 | 0.07226 | 0.0011 | 460 | 25 | 452 | 8 | 450 | 6 | 0.4 |
| G2-56 | 1.23 | 0.1122 | 0.0021 | 5.21027 | 0.1075 | 0.33673 | 0.0049 | 1835 | 18 | 1854 | 18 | 1871 | 24 | -1.9 |
| G2-57 | 0.92 | 0.10884 | 0.0021 | 4.67533 | 0.0968 | 0.31149 | 0.0046 | 1780 | 18 | 1763 | 17 | 1748 | 22 | 1.8 |
| G2-58 | 0.15 | 0.12871 | 0.0023 | 6.52646 | 0.1294 | 0.36771 | 0.0053 | 2080 | 17 | 2049 | 17 | 2019 | 25 | 3 |
| G2-59 | 0.64 | 0.1979 | 0.0043 | 14.7199 | 0.3323 | 0.53937 | 0.0086 | 2809 | 18 | 2797 | 21 | 2781 | 36 | 1 |
| G2-60 | 0.52 | 0.18485 | 0.0034 | 13.3539 | 0.2689 | 0.52386 | 0.0076 | 2697 | 16 | 2705 | 19 | 2716 | 32 | -0.7 |
| G2-61 | 0.67 | 0.05609 | 0.0014 | 0.56348 | 0.0145 | 0.07285 | 0.0011 | 456 | 31 | 454 | 9 | 453 | 7 | 0.2 |

| | | | | | | | | | | | | | | |
|---|---|---|---|---|---|---|---|---|---|---|---|---|---|---|
| G2-62 | 0.81 | 0.0564 | 0.0015 | 0.57914 | 0.0155 | 0.07446 | 0.0011 | 468 | 34 | 464 | 10 | 463 | 7 | 0.2 |
| G2-63 | 0.71 | 0.05767 | 0.0022 | 0.63205 | 0.0242 | 0.07947 | 0.0013 | 517 | 55 | 497 | 15 | 493 | 8 | 0.8 |
| G2-64 | 0.11 | 0.11911 | 0.003 | 5.62975 | 0.1159 | 0.34279 | 0.0049 | 1943 | 46 | 1921 | 18 | 1900 | 23 | 2.3 |
| G2-65 | 0.58 | 0.05656 | 0.0014 | 0.55247 | 0.0141 | 0.07083 | 0.0011 | 474 | 31 | 447 | 9 | 441 | 6 | 1.4 |
| G2-66 | 0.60 | 0.05609 | 0.0015 | 0.56505 | 0.0156 | 0.07306 | 0.0011 | 456 | 35 | 455 | 10 | 455 | 7 | 0 |
| G2-67 | 0.61 | 0.05591 | 0.0013 | 0.55606 | 0.0135 | 0.07212 | 0.0011 | 449 | 29 | 449 | 9 | 449 | 6 | 0 |
| G2-68 | 0.98 | 0.05105 | 0.0029 | 0.27784 | 0.0158 | 0.03947 | 0.0007 | 243 | 100 | 249 | 13 | 250 | 4 | -0.4 |
| G2-69 | 1.06 | 0.05627 | 0.0012 | 0.55705 | 0.0122 | 0.07179 | 0.0011 | 463 | 25 | 450 | 8 | 447 | 6 | 0.7 |
| G2-70 | 0.43 | 0.0912 | 0.002 | 3.19857 | 0.0742 | 0.25432 | 0.0038 | 1451 | 23 | 1457 | 18 | 1461 | 20 | -0.7 |
| G2-71 | 0.73 | 0.05625 | 0.0014 | 0.57203 | 0.0143 | 0.07374 | 0.0011 | 462 | 30 | 459 | 9 | 459 | 7 | 0 |
| G2-72 | 1.43 | 0.15581 | 0.003 | 9.27764 | 0.1955 | 0.43178 | 0.0064 | 2411 | 18 | 2366 | 19 | 2314 | 29 | 4.2 |
| G2-73 | 0.56 | 0.05602 | 0.0013 | 0.56793 | 0.014 | 0.07351 | 0.0011 | 453 | 30 | 457 | 9 | 457 | 7 | 0 |
| G2-74 | 0.46 | 0.05575 | 0.0013 | 0.53869 | 0.0133 | 0.07007 | 0.001 | 442 | 30 | 438 | 9 | 437 | 6 | 0.2 |
| G2-75 | 0.24 | 0.16565 | 0.0032 | 10.773 | 0.2257 | 0.4716 | 0.0069 | 2514 | 17 | 2504 | 19 | 2491 | 30 | 0.9 |
| G2-76 | 0.09 | 0.07688 | 0.0018 | 2.00678 | 0.0488 | 0.18928 | 0.0029 | 1118 | 26 | 1118 | 16 | 1117 | 16 | 0.1 |
| G2-77 | 0.34 | 0.05566 | 0.0013 | 0.53129 | 0.0132 | 0.06921 | 0.001 | 439 | 30 | 433 | 9 | 431 | 6 | 0.5 |
| G2-78 | 0.39 | 0.05601 | 0.0017 | 0.55315 | 0.0173 | 0.07161 | 0.0011 | 453 | 42 | 447 | 11 | 446 | 7 | 0.2 |
| G2-79 | 0.46 | 0.05721 | 0.0013 | 0.62606 | 0.0154 | 0.07935 | 0.0012 | 500 | 29 | 494 | 10 | 492 | 7 | 0.4 |
| G2-80 | 0.45 | 0.05632 | 0.0014 | 0.5674 | 0.015 | 0.07305 | 0.0011 | 465 | 33 | 456 | 10 | 455 | 7 | 0.2 |
| G2-81 | 0.22 | 0.08855 | 0.0018 | 2.91119 | 0.0633 | 0.2384 | 0.0035 | 1394 | 21 | 1385 | 16 | 1378 | 18 | 1.2 |
| G2-82 | 0.61 | 0.05974 | 0.0015 | 0.63635 | 0.0169 | 0.07724 | 0.0012 | 594 | 32 | 500 | 10 | 480 | 7 | 4.2 |
| G2-83 | 0.66 | 0.05522 | 0.0014 | 0.55545 | 0.0147 | 0.07295 | 0.0011 | 421 | 33 | 449 | 10 | 454 | 7 | -1.1 |
| G2-84 | 0.32 | 0.05593 | 0.0014 | 0.54168 | 0.0137 | 0.07023 | 0.0011 | 450 | 31 | 440 | 9 | 438 | 6 | 0.5 |
| G2-85 | 0.67 | 0.05585 | 0.0014 | 0.56389 | 0.0151 | 0.07321 | 0.0011 | 446 | 33 | 454 | 10 | 455 | 7 | -0.2 |
| G2-86 | 0.43 | 0.0555 | 0.0013 | 0.55145 | 0.0139 | 0.07206 | 0.0011 | 432 | 30 | 446 | 9 | 449 | 7 | -0.7 |
| G2-87 | 0.37 | 0.12253 | 0.0024 | 6.13432 | 0.1314 | 0.36302 | 0.0053 | 1993 | 19 | 1995 | 19 | 1996 | 25 | -0.2 |
| G2-88 | 0.32 | 0.05547 | 0.0014 | 0.53321 | 0.0143 | 0.06971 | 0.0011 | 431 | 33 | 434 | 9 | 434 | 6 | 0 |
| G2-89 | 0.31 | 0.08161 | 0.0018 | 2.38432 | 0.0552 | 0.21186 | 0.0032 | 1236 | 23 | 1238 | 17 | 1239 | 17 | -0.2 |

| | | | | | | | | | | | | | | |
|---|---|---|---|---|---|---|---|---|---|---|---|---|---|---|
| G2-90 | 0.55 | 0.08392 | 0.0034 | 2.61628 | 0.0964 | 0.22612 | 0.0035 | 1291 | 80 | 1305 | 27 | 1314 | 19 | -1.8 |
| G2-91 | 0.55 | 0.0556 | 0.0015 | 0.54394 | 0.0153 | 0.07094 | 0.0011 | 436 | 36 | 441 | 10 | 442 | 7 | -0.2 |
| G2-92 | 1.02 | 0.05739 | 0.0015 | 0.58373 | 0.0157 | 0.07375 | 0.0011 | 507 | 33 | 467 | 10 | 459 | 7 | 1.7 |
| G2-93 | 0.54 | 0.05596 | 0.0016 | 0.55635 | 0.0158 | 0.0721 | 0.0011 | 451 | 37 | 449 | 10 | 449 | 7 | 0 |
| G2-94 | 0.72 | 0.06365 | 0.0019 | 0.66556 | 0.0203 | 0.07582 | 0.0012 | 730 | 38 | 518 | 12 | 471 | 7 | 10 |
| G2-95 | 0.12 | 0.12968 | 0.0034 | 6.5453 | 0.1452 | 0.36607 | 0.0053 | 2094 | 48 | 2052 | 20 | 2011 | 25 | 4.1 |
| G2-96 | 0.79 | 0.1017 | 0.0023 | 4.11779 | 0.0993 | 0.29362 | 0.0045 | 1655 | 23 | 1658 | 20 | 1660 | 22 | -0.3 |
| G2-97 | 0.70 | 0.0625 | 0.0024 | 0.983 | 0.0371 | 0.11406 | 0.002 | 691 | 51 | 695 | 19 | 696 | 11 | -0.1 |
| G2-98 | 0.41 | 0.08038 | 0.0033 | 2.25637 | 0.0838 | 0.2036 | 0.0033 | 1206 | 82 | 1199 | 26 | 1195 | 18 | 0.9 |
| G2-99 | 0.40 | 0.05614 | 0.0013 | 0.5606 | 0.0138 | 0.07241 | 0.0011 | 458 | 29 | 452 | 9 | 451 | 7 | 0.2 |
| G2-100 | 0.68 | 0.10211 | 0.0026 | 4.18777 | 0.1114 | 0.2974 | 0.0047 | 1663 | 27 | 1672 | 22 | 1678 | 23 | -0.9 |
| **CSL1** | | | | | | | | | | | | | | |
| CSL1-01 | 0.47 | 0.05531 | 0.001 | 0.52714 | 0.0105 | 0.06911 | 0.001 | 425 | 21 | 430 | 7 | 431 | 6 | -0.2 |
| CSL1-02 | 0.67 | 0.05537 | 0.0013 | 0.50288 | 0.0121 | 0.06585 | 0.001 | 427 | 29 | 414 | 8 | 411 | 6 | 0.7 |
| CSL1-03 | 0.68 | 0.09502 | 0.0013 | 3.41491 | 0.0555 | 0.2606 | 0.0036 | 1528 | 14 | 1508 | 13 | 1493 | 19 | 2.3 |
| CSL1-04 | 0.86 | 0.10431 | 0.0017 | 4.63072 | 0.0821 | 0.32192 | 0.0046 | 1702 | 15 | 1755 | 15 | 1799 | 22 | -5.4 |
| CSL1-05 | 0.60 | 0.05116 | 0.002 | 0.28751 | 0.0114 | 0.04075 | 0.0007 | 248 | 62 | 257 | 9 | 257 | 4 | 0 |
| CSL1-06 | 0.58 | 0.07112 | 0.0021 | 1.46546 | 0.0446 | 0.14941 | 0.0023 | 961 | 37 | 916 | 18 | 898 | 13 | 2 |
| CSL1-07 | 0.76 | 0.05566 | 0.0012 | 0.54107 | 0.0123 | 0.07049 | 0.001 | 439 | 26 | 439 | 8 | 439 | 6 | 0 |
| CSL1-08 | 0.58 | 0.0565 | 0.0009 | 0.57685 | 0.0105 | 0.07404 | 0.001 | 472 | 19 | 462 | 7 | 460 | 6 | 0.4 |
| CSL1-09 | 1.00 | 0.12957 | 0.0025 | 6.85303 | 0.1402 | 0.38354 | 0.0058 | 2092 | 17 | 2093 | 18 | 2093 | 27 | 0 |
| CSL1-10 | 0.57 | 0.06345 | 0.001 | 0.6445 | 0.0114 | 0.07366 | 0.001 | 723 | 17 | 505 | 7 | 458 | 6 | 10.3 |
| CSL1-11 | 0.36 | 0.06618 | 0.0022 | 1.27842 | 0.0378 | 0.14009 | 0.002 | 812 | 70 | 836 | 17 | 845 | 12 | -1.1 |
| CSL1-12 | 0.35 | 0.05634 | 0.0011 | 0.56859 | 0.0119 | 0.07318 | 0.001 | 466 | 23 | 457 | 8 | 455 | 6 | 0.4 |
| CSL1-13 | 0.88 | 0.11323 | 0.0016 | 5.17647 | 0.0856 | 0.33151 | 0.0047 | 1852 | 13 | 1849 | 14 | 1846 | 23 | 0.3 |
| ~~CSL1-14~~ | ~~0.33~~ | ~~0.05156~~ | ~~0.0027~~ | ~~0.29478~~ | ~~0.0154~~ | ~~0.04146~~ | ~~0.0007~~ | ~~266~~ | ~~90~~ | ~~262~~ | ~~12~~ | ~~262~~ | ~~4~~ | ~~0~~ |
| CSL1-15 | 0.60 | 0.05696 | 0.001 | 0.58621 | 0.011 | 0.07463 | 0.0011 | 490 | 20 | 468 | 7 | 464 | 6 | 0.9 |
| CSL1-16 | 0.61 | 0.05613 | 0.0011 | 0.55694 | 0.0115 | 0.07195 | 0.001 | 458 | 23 | 450 | 8 | 448 | 6 | 0.4 |

| | | | | | | | | | | | | | | |
|---|---|---|---|---|---|---|---|---|---|---|---|---|---|---|
| CSL1-17 | 0.13 | 0.05635 | 0.0016 | 0.58034 | 0.0172 | 0.07468 | 0.0011 | 466 | 39 | 465 | 11 | 464 | 7 | 0.2 |
| CSL1-18 | 0.35 | 0.07033 | 0.0011 | 1.42101 | 0.0254 | 0.14652 | 0.0021 | 938 | 17 | 898 | 11 | 881 | 12 | 1.9 |
| CSL1-19 | 0.47 | 0.05431 | 0.0023 | 0.45465 | 0.0192 | 0.06071 | 0.001 | 384 | 66 | 381 | 13 | 380 | 6 | 0.3 |
| CSL1-20 | 0.14 | 0.06725 | 0.007 | 0.36566 | 0.0372 | 0.03944 | 0.0007 | 845 | 224 | 316 | 28 | 249 | 4 | 26.9 |
| CSL1-21 | 0.43 | 0.11071 | 0.003 | 3.66399 | 0.0826 | 0.24002 | 0.0034 | 1811 | 50 | 1564 | 18 | 1387 | 18 | 30.6 |
| CSL1-22 | 0.45 | 0.05634 | 0.001 | 0.5627 | 0.0111 | 0.07242 | 0.001 | 466 | 21 | 453 | 7 | 451 | 6 | 0.4 |
| CSL1-23 | 0.39 | 0.14714 | 0.0021 | 7.90503 | 0.132 | 0.38959 | 0.0055 | 2313 | 13 | 2220 | 15 | 2121 | 26 | 9.1 |
| CSL1-24 | 0.62 | 0.05744 | 0.0013 | 0.64583 | 0.0157 | 0.08153 | 0.0012 | 508 | 29 | 506 | 10 | 505 | 7 | 0.2 |
| CSL1-25 | 0.78 | 0.05586 | 0.0013 | 0.5575 | 0.0137 | 0.07238 | 0.0011 | 447 | 30 | 450 | 9 | 450 | 6 | 0 |
| CSL1-26 | 1.87 | 0.05557 | 0.0015 | 0.54011 | 0.0151 | 0.07048 | 0.0011 | 435 | 36 | 438 | 10 | 439 | 7 | -0.2 |
| CSL1-27 | 0.10 | 0.14872 | 0.0035 | 1.60787 | 0.0297 | 0.07841 | 0.0011 | 2331 | 41 | 973 | 12 | 487 | 7 | 99.8 |
| CSL1-28 | 0.22 | 0.10589 | 0.0015 | 4.35369 | 0.0729 | 0.29816 | 0.0042 | 1730 | 14 | 1704 | 14 | 1682 | 21 | 2.9 |
| CSL1-29 | 0.48 | 0.09789 | 0.0017 | 3.58208 | 0.0696 | 0.26536 | 0.0039 | 1584 | 17 | 1546 | 15 | 1517 | 20 | 4.4 |
| CSL1-30 | 0.28 | 0.07024 | 0.0011 | 1.11378 | 0.0197 | 0.11498 | 0.0016 | 935 | 17 | 760 | 9 | 702 | 9 | 8.3 |
| CSL1-31 | 0.19 | 0.06896 | 0.001 | 1.31719 | 0.0225 | 0.13851 | 0.0019 | 898 | 16 | 853 | 10 | 836 | 11 | 2 |
| CSL1-32 | 0.89 | 0.05729 | 0.0014 | 0.56089 | 0.0148 | 0.07099 | 0.001 | 503 | 33 | 452 | 10 | 442 | 6 | 2.3 |
| CSL1-33 | 0.73 | 0.05153 | 0.0014 | 0.2996 | 0.0085 | 0.04216 | 0.0006 | 265 | 39 | 266 | 7 | 266 | 4 | 0 |
| CSL1-34 | 1.24 | 0.05119 | 0.0024 | 0.2841 | 0.0131 | 0.04024 | 0.0007 | 249 | 75 | 254 | 10 | 254 | 4 | 0 |
| CSL1-35 | 2.05 | 0.05139 | 0.0016 | 0.26846 | 0.0087 | 0.03788 | 0.0006 | 258 | 46 | 241 | 7 | 240 | 4 | 0.4 |
| CSL1-36 | 0.95 | 0.0549 | 0.0018 | 0.50002 | 0.0164 | 0.06604 | 0.001 | 408 | 46 | 412 | 11 | 412 | 6 | 0 |
| ~~CSL1-37~~ | ~~0.55~~ | ~~0.05143~~ | ~~0.0014~~ | ~~0.29579~~ | ~~0.0082~~ | ~~0.04171~~ | ~~0.0006~~ | ~~260~~ | ~~37~~ | ~~263~~ | ~~6~~ | ~~263~~ | ~~4~~ | ~~0~~ |
| ~~CSL1-38~~ | ~~0.25~~ | ~~0.0525~~ | ~~0.0012~~ | ~~0.36486~~ | ~~0.0088~~ | ~~0.05039~~ | ~~0.0007~~ | ~~307~~ | ~~29~~ | ~~316~~ | ~~7~~ | ~~317~~ | ~~5~~ | ~~-0.3~~ |
| CSL1-39 | 0.31 | 0.08718 | 0.0015 | 2.79585 | 0.0538 | 0.23255 | 0.0034 | 1364 | 17 | 1354 | 14 | 1348 | 18 | 1.2 |
| CSL1-40 | 1.02 | 0.05606 | 0.001 | 0.58253 | 0.0113 | 0.07535 | 0.0011 | 455 | 21 | 466 | 7 | 468 | 6 | -0.4 |
| CSL1-41 | 0.55 | 0.05636 | 0.001 | 0.56719 | 0.0114 | 0.07297 | 0.0011 | 467 | 21 | 456 | 7 | 454 | 6 | 0.4 |
| CSL1-42 | 0.87 | 0.05575 | 0.0024 | 0.5671 | 0.0248 | 0.07376 | 0.0012 | 442 | 68 | 456 | 16 | 459 | 7 | -0.7 |
| CSL1-43 | 0.54 | 0.1501 | 0.0023 | 8.94687 | 0.1586 | 0.43224 | 0.0062 | 2347 | 14 | 2333 | 16 | 2316 | 28 | 1.3 |
| ~~CSL1-44~~ | ~~0.67~~ | ~~0.06305~~ | ~~0.0015~~ | ~~1.08482~~ | ~~0.0267~~ | ~~0.12478~~ | ~~0.0019~~ | ~~710~~ | ~~28~~ | ~~746~~ | ~~13~~ | ~~758~~ | ~~11~~ | ~~-1.6~~ |

| | | | | | | | | | | | | | | |
|---|---|---|---|---|---|---|---|---|---|---|---|---|---|---|
| CSL1-45 | 0.30 | 0.06881 | 0.0012 | 1.44568 | 0.0273 | 0.15236 | 0.0022 | 893 | 18 | 908 | 11 | 914 | 12 | -0.7 |
| CSL1-46 | 1.55 | 0.0518 | 0.0017 | 0.29859 | 0.01 | 0.0418 | 0.0007 | 277 | 48 | 265 | 8 | 264 | 4 | 0.4 |
| CSL1-47 | 0.69 | 0.05673 | 0.0012 | 0.55456 | 0.0124 | 0.07089 | 0.001 | 481 | 25 | 448 | 8 | 442 | 6 | 1.4 |
| CSL1-48 | 1.18 | 0.05485 | 0.0014 | 0.49614 | 0.0133 | 0.06559 | 0.001 | 406 | 34 | 409 | 9 | 410 | 6 | -0.2 |
| CSL1-49 | 0.37 | 0.05652 | 0.001 | 0.59282 | 0.0113 | 0.07605 | 0.0011 | 473 | 20 | 473 | 7 | 473 | 7 | 0 |
| CSL1-50 | 0.65 | 0.05587 | 0.001 | 0.5562 | 0.0113 | 0.07219 | 0.0011 | 447 | 22 | 449 | 7 | 449 | 6 | 0 |
| CSL1-51 | 0.78 | 0.07849 | 0.0166 | 0.72336 | 0.1521 | 0.06684 | 0.0017 | 1159 | 463 | 553 | 90 | 417 | 11 | 32.6 |
| CSL1-52 | 0.82 | 0.05097 | 0.0015 | 0.2729 | 0.0082 | 0.03883 | 0.0006 | 239 | 41 | 245 | 7 | 246 | 4 | -0.4 |
| CSL1-53 | 0.29 | 0.05724 | 0.0019 | 0.54847 | 0.0162 | 0.06949 | 0.001 | 501 | 74 | 444 | 11 | 433 | 6 | 2.5 |
| CSL1-54 | 0.57 | 0.06015 | 0.0011 | 0.58844 | 0.0117 | 0.07095 | 0.001 | 609 | 21 | 470 | 7 | 442 | 6 | 6.3 |
| CSL1-55 | 1.03 | 0.0564 | 0.0019 | 0.55552 | 0.0193 | 0.07142 | 0.0011 | 468 | 49 | 449 | 13 | 445 | 7 | 0.9 |
| CSL1-56 | 0.70 | 0.05115 | 0.0017 | 0.27639 | 0.0091 | 0.03918 | 0.0006 | 248 | 48 | 248 | 7 | 248 | 4 | 0 |
| CSL1-57 | 0.49 | 0.05165 | 0.0013 | 0.3068 | 0.0081 | 0.04307 | 0.0007 | 270 | 34 | 272 | 6 | 272 | 4 | 0 |
| CSL1-58 | 0.16 | 0.05837 | 0.0079 | 0.45477 | 0.061 | 0.05651 | 0.0011 | 544 | 309 | 381 | 43 | 354 | 7 | 7.6 |
| CSL1-59 | 0.97 | 0.05544 | 0.0017 | 0.52333 | 0.0165 | 0.06846 | 0.0011 | 430 | 42 | 427 | 11 | 427 | 7 | 0 |
| CSL1-60 | 0.48 | 0.05625 | 0.0011 | 0.5426 | 0.0117 | 0.06995 | 0.001 | 462 | 24 | 440 | 8 | 436 | 6 | 0.9 |
| CSL1-61 | 0.57 | 0.05204 | 0.0019 | 0.3066 | 0.0113 | 0.04272 | 0.0007 | 287 | 56 | 272 | 9 | 270 | 4 | 0.7 |
| CSL1-62 | 0.79 | 0.05572 | 0.0013 | 0.5486 | 0.013 | 0.0714 | 0.0011 | 441 | 28 | 444 | 9 | 445 | 6 | -0.2 |
| CSL1-63 | 0.81 | 0.05616 | 0.0011 | 0.57212 | 0.0119 | 0.07387 | 0.0011 | 459 | 23 | 459 | 8 | 459 | 6 | 0 |
| CSL1-64 | 0.38 | 0.05112 | 0.0021 | 0.27008 | 0.0112 | 0.03831 | 0.0006 | 246 | 64 | 243 | 9 | 242 | 4 | 0.4 |
| CSL1-65 | 1.06 | 0.05103 | 0.0055 | 0.27967 | 0.0301 | 0.03974 | 0.0008 | 242 | 204 | 250 | 24 | 251 | 5 | -0.4 |
| CSL1-66 | 0.40 | 0.05653 | 0.0014 | 0.58485 | 0.015 | 0.07503 | 0.0011 | 473 | 31 | 468 | 10 | 466 | 7 | 0.4 |
| CSL1-67 | 0.54 | 0.05402 | 0.0018 | 0.44134 | 0.015 | 0.05925 | 0.0009 | 372 | 48 | 371 | 11 | 371 | 6 | 0 |
| CSL1-68 | 0.68 | 0.05157 | 0.0026 | 0.30688 | 0.0152 | 0.04315 | 0.0007 | 266 | 83 | 272 | 12 | 272 | 4 | 0 |
| CSL1-69 | 0.38 | 0.07633 | 0.0014 | 1.92678 | 0.0381 | 0.18306 | 0.0027 | 1104 | 19 | 1090 | 13 | 1084 | 14 | 1.8 |
| CSL1-70 | 0.75 | 0.05612 | 0.0012 | 0.60723 | 0.014 | 0.07847 | 0.0012 | 457 | 26 | 482 | 9 | 487 | 7 | -1 |
| CSL1-71 | 0.63 | 0.05189 | 0.0021 | 0.33062 | 0.0136 | 0.04621 | 0.0008 | 281 | 64 | 290 | 10 | 291 | 5 | -0.3 |
| CSL1-72 | 0.53 | 0.05698 | 0.0013 | 0.55174 | 0.0129 | 0.07022 | 0.0011 | 491 | 27 | 446 | 8 | 437 | 6 | 2.1 |

| | | | | | | | | | | | | | | |
|---|---|---|---|---|---|---|---|---|---|---|---|---|---|---|
| CSL1-73 | 0.45 | 0.05581 | 0.0013 | 0.55599 | 0.0138 | 0.07224 | 0.0011 | 445 | 29 | 449 | 9 | 450 | 7 | -0.2 |
| CSL1-74 | 1.09 | 0.05706 | 0.0015 | 0.5736 | 0.0152 | 0.0729 | 0.0011 | 494 | 33 | 460 | 10 | 454 | 7 | 1.3 |
| CSL1-75 | 0.39 | 0.05669 | 0.0012 | 0.6019 | 0.0132 | 0.07699 | 0.0011 | 479 | 24 | 478 | 8 | 478 | 7 | 0 |
| CSL1-76 | 0.37 | 0.09919 | 0.0018 | 4.01267 | 0.0793 | 0.29335 | 0.0043 | 1609 | 18 | 1637 | 16 | 1658 | 21 | -3 |
| CSL1-77 | 0.88 | 0.05832 | 0.0011 | 0.58506 | 0.0121 | 0.07274 | 0.0011 | 542 | 22 | 468 | 8 | 453 | 6 | 3.3 |
| CSL1-78 | 0.13 | 0.05774 | 0.0012 | 0.60346 | 0.0133 | 0.07578 | 0.0011 | 520 | 24 | 479 | 8 | 471 | 7 | 1.7 |
| CSL1-79 | 0.26 | 0.05549 | 0.0012 | 0.52664 | 0.0117 | 0.06882 | 0.001 | 432 | 25 | 430 | 8 | 429 | 6 | 0.2 |
| CSL1-80 | 1.41 | 0.05712 | 0.0015 | 0.57355 | 0.0152 | 0.07281 | 0.0011 | 496 | 32 | 460 | 10 | 453 | 7 | 1.5 |
| CSL1-81 | 1.44 | 0.05073 | 0.0075 | 0.25196 | 0.037 | 0.03602 | 0.001 | 229 | 274 | 228 | 30 | 228 | 6 | 0 |
| CSL1-82 | 0.20 | 0.05578 | 0.0019 | 0.5735 | 0.0173 | 0.07457 | 0.0011 | 444 | 77 | 460 | 11 | 464 | 7 | -0.9 |
| CSL1-83 | 0.82 | 0.0553 | 0.0037 | 0.50891 | 0.034 | 0.06673 | 0.0014 | 424 | 113 | 418 | 23 | 416 | 8 | 0.5 |
| CSL1-84 | 0.57 | 0.07057 | 0.0014 | 1.46625 | 0.031 | 0.15067 | 0.0022 | 945 | 21 | 917 | 13 | 905 | 12 | 1.3 |
| CSL1-85 | 0.82 | 0.05635 | 0.0014 | 0.57064 | 0.015 | 0.07344 | 0.0011 | 466 | 32 | 458 | 10 | 457 | 7 | 0.2 |
| CSL1-86 | 0.90 | 0.05553 | 0.0011 | 0.53494 | 0.0111 | 0.06986 | 0.001 | 434 | 23 | 435 | 7 | 435 | 6 | 0 |
| CSL1-87 | 0.13 | 0.11647 | 0.0021 | 5.48676 | 0.1099 | 0.34161 | 0.005 | 1903 | 17 | 1899 | 17 | 1894 | 24 | 0.5 |
| CSL1-88 | 1.14 | 0.05973 | 0.0012 | 0.60338 | 0.0128 | 0.07325 | 0.0011 | 594 | 23 | 479 | 8 | 456 | 6 | 5 |
| CSL1-89 | 0.48 | 0.05715 | 0.0018 | 0.62184 | 0.0198 | 0.07891 | 0.0013 | 497 | 42 | 491 | 12 | 490 | 8 | 0.2 |
| CSL1-90 | 0.37 | 0.07555 | 0.0178 | 0.41927 | 0.0984 | 0.04025 | 0.0011 | 1083 | 521 | 356 | 70 | 254 | 7 | 40.2 |
| CSL1-91 | 0.33 | 0.05692 | 0.0017 | 0.6071 | 0.0187 | 0.07734 | 0.0012 | 488 | 40 | 482 | 12 | 480 | 7 | 0.4 |
| CSL1-92 | 0.73 | 0.05623 | 0.0016 | 0.57019 | 0.0168 | 0.07353 | 0.0012 | 461 | 38 | 458 | 11 | 457 | 7 | 0.2 |
| CSL1-93 | 0.82 | 0.05137 | 0.003 | 0.29007 | 0.0168 | 0.04095 | 0.0008 | 257 | 99 | 259 | 13 | 259 | 5 | 0 |
| CSL1-94 | 0.54 | 0.07355 | 0.0038 | 1.58273 | 0.0774 | 0.15608 | 0.0026 | 1029 | 107 | 963 | 30 | 935 | 15 | 3 |
| CSL1-95 | 0.57 | 0.06932 | 0.0014 | 1.42772 | 0.0313 | 0.14935 | 0.0022 | 908 | 23 | 901 | 13 | 897 | 13 | 0.4 |
| CSL1-96 | 1.10 | 0.05167 | 0.0041 | 0.31241 | 0.0248 | 0.04384 | 0.0008 | 271 | 146 | 276 | 19 | 277 | 5 | -0.4 |
| CSL1-97 | 0.78 | 0.05601 | 0.0019 | 0.54947 | 0.0193 | 0.07114 | 0.0012 | 453 | 49 | 445 | 13 | 443 | 7 | 0.5 |
| CSL1-98 | 0.15 | 0.07128 | 0.0015 | 1.49786 | 0.0347 | 0.15238 | 0.0023 | 965 | 24 | 930 | 14 | 914 | 13 | 1.8 |
| CSL1-99 | 0.76 | 0.19485 | 0.0041 | 15.3616 | 0.3482 | 0.5717 | 0.0091 | 2784 | 18 | 2838 | 22 | 2915 | 37 | -4.5 |
| CSL1-100 | 0.24 | 0.09631 | 0.0019 | 3.58594 | 0.0775 | 0.27 | 0.004 | 1554 | 20 | 1546 | 17 | 1541 | 20 | 0.8 |

| | | | | | | | | | | | | | | |
|---|---|---|---|---|---|---|---|---|---|---|---|---|---|---|
| **CSL2** | | | | | | | | | | | | | | |
| CSL2-01 | 0.65 | 0.05592 | 0.0013 | 0.55508 | 0.0131 | 0.07198 | 0.0011 | 449 | 28 | 448 | 9 | 448 | 6 | 0 |
| CSL2-02 | 0.60 | 0.05196 | 0.0048 | 0.31859 | 0.0295 | 0.04446 | 0.0008 | 284 | 177 | 281 | 23 | 280 | 5 | 0.4 |
| CSL2-03 | 0.33 | 0.06987 | 0.0015 | 1.41254 | 0.0317 | 0.1466 | 0.0022 | 925 | 24 | 894 | 13 | 882 | 12 | 1.4 |
| CSL2-04 | 0.97 | 0.14565 | 0.0028 | 8.45586 | 0.1738 | 0.42098 | 0.0061 | 2295 | 17 | 2281 | 19 | 2265 | 28 | 1.3 |
| CSL2-05 | 0.64 | 0.05547 | 0.0016 | 0.53346 | 0.0154 | 0.06974 | 0.0011 | 431 | 37 | 434 | 10 | 435 | 7 | -0.2 |
| CSL2-06 | 0.59 | 0.0556 | 0.0017 | 0.51871 | 0.0161 | 0.06766 | 0.0011 | 436 | 42 | 424 | 11 | 422 | 6 | 0.5 |
| CSL2-07 | 0.66 | 0.0558 | 0.0016 | 0.55406 | 0.0163 | 0.072 | 0.0011 | 444 | 38 | 448 | 11 | 448 | 7 | 0 |
| CSL2-08 | 0.39 | 0.05514 | 0.0014 | 0.50757 | 0.0136 | 0.06675 | 0.001 | 418 | 34 | 417 | 9 | 417 | 6 | 0 |
| CSL2-09 | 0.06 | 0.06424 | 0.0014 | 1.04703 | 0.0234 | 0.11819 | 0.0017 | 750 | 24 | 727 | 12 | 720 | 10 | 1 |
| CSL2-10 | 0.79 | 0.05199 | 0.0022 | 0.33322 | 0.0142 | 0.04648 | 0.0008 | 285 | 67 | 292 | 11 | 293 | 5 | -0.3 |
| CSL2-11 | 0.28 | 0.08981 | 0.0019 | 3.05629 | 0.0679 | 0.24678 | 0.0037 | 1421 | 21 | 1422 | 17 | 1422 | 19 | -0.1 |
| CSL2-12 | 0.48 | 0.05103 | 0.0022 | 0.27902 | 0.0117 | 0.03964 | 0.0007 | 242 | 66 | 250 | 9 | 251 | 4 | -0.4 |
| CSL2-13 | 0.16 | 0.06883 | 0.0014 | 1.30188 | 0.0288 | 0.13716 | 0.002 | 894 | 23 | 847 | 13 | 829 | 11 | 2.2 |
| CSL2-14 | 1.01 | 0.05692 | 0.0017 | 0.61357 | 0.0183 | 0.07817 | 0.0012 | 488 | 39 | 486 | 12 | 485 | 7 | 0.2 |
| CSL2-15 | 0.55 | 0.05492 | 0.0019 | 0.48597 | 0.0167 | 0.06416 | 0.001 | 409 | 49 | 402 | 11 | 401 | 6 | 0.2 |
| CSL2-16 | 0.59 | 0.05102 | 0.0018 | 0.27512 | 0.01 | 0.0391 | 0.0006 | 242 | 54 | 247 | 8 | 247 | 4 | 0 |
| CSL2-17 | 0.46 | 0.05548 | 0.0016 | 0.52256 | 0.0151 | 0.0683 | 0.0011 | 432 | 38 | 427 | 10 | 426 | 6 | 0.2 |
| CSL2-18 | 0.58 | 0.07085 | 0.0018 | 1.54562 | 0.04 | 0.1582 | 0.0024 | 953 | 29 | 949 | 16 | 947 | 14 | 0.2 |
| CSL2-19 | 0.69 | 0.08495 | 0.0019 | 2.39368 | 0.0549 | 0.20431 | 0.0031 | 1314 | 23 | 1241 | 16 | 1198 | 16 | 9.7 |
| CSL2-20 | 0.45 | 0.05099 | 0.0013 | 0.2736 | 0.007 | 0.03891 | 0.0006 | 240 | 32 | 246 | 6 | 246 | 4 | 0 |
| CSL2-21 | 0.65 | 0.101 | 0.0041 | 3.94432 | 0.1449 | 0.28322 | 0.0046 | 1643 | 76 | 1623 | 30 | 1608 | 23 | 2.2 |
| CSL2-22 | 1.12 | 0.05141 | 0.0015 | 0.2866 | 0.0086 | 0.04043 | 0.0006 | 259 | 41 | 256 | 7 | 255 | 4 | 0.4 |
| CSL2-23 | 1 | 0.06996 | 0.0017 | 1.46857 | 0.0372 | 0.15222 | 0.0023 | 927 | 28 | 918 | 15 | 913 | 13 | 0.5 |
| CSL2-24 | 0.65 | 0.05234 | 0.0029 | 0.35254 | 0.0197 | 0.04884 | 0.0008 | 300 | 96 | 307 | 15 | 307 | 5 | 0 |
| CSL2-25 | 0.78 | 0.05304 | 0.0023 | 0.38058 | 0.0162 | 0.05203 | 0.0009 | 331 | 67 | 327 | 12 | 327 | 5 | 0 |
| CSL2-26 | 0.35 | 0.05579 | 0.0014 | 0.55287 | 0.0138 | 0.07186 | 0.0011 | 444 | 30 | 447 | 9 | 447 | 7 | 0 |
| CSL2-27 | 0.87 | 0.05112 | 0.0042 | 0.27564 | 0.0223 | 0.0391 | 0.0007 | 246 | 150 | 247 | 18 | 247 | 4 | 0 |

| | | | | | | | | | | | | | | |
|---|---|---|---|---|---|---|---|---|---|---|---|---|---|---|
| CSL2-28 | 0.29 | 0.05265 | 0.0023 | 0.35913 | 0.0159 | 0.04947 | 0.0008 | 314 | 70 | 312 | 12 | 311 | 5 | 0.3 |
| CSL2-29 | 0.12 | 0.06985 | 0.0016 | 1.47996 | 0.0346 | 0.15364 | 0.0023 | 924 | 25 | 922 | 14 | 921 | 13 | 0.1 |
| ~~CSL2-30~~ | ~~0.76~~ | ~~0.05454~~ | ~~0.0016~~ | ~~0.47763~~ | ~~0.0138~~ | ~~0.06351~~ | ~~0.001~~ | ~~393~~ | ~~37~~ | ~~396~~ | ~~9~~ | ~~397~~ | ~~6~~ | ~~-0.3~~ |
| CSL2-31 | 0.92 | 0.05582 | 0.002 | 0.55234 | 0.0196 | 0.07175 | 0.0012 | 445 | 49 | 447 | 13 | 447 | 7 | 0 |
| ~~CSL2-32~~ | ~~1.05~~ | ~~0.0557~~ | ~~0.0022~~ | ~~0.53667~~ | ~~0.0208~~ | ~~0.06987~~ | ~~0.0011~~ | ~~440~~ | ~~57~~ | ~~436~~ | ~~14~~ | ~~435~~ | ~~7~~ | ~~0.2~~ |
| CSL2-33 | 0.69 | 0.05503 | 0.0014 | 0.49893 | 0.0132 | 0.06574 | 0.001 | 413 | 33 | 411 | 9 | 410 | 6 | 0.2 |
| CSL2-34 | 1.46 | 0.06558 | 0.002 | 1.17825 | 0.0369 | 0.13027 | 0.0021 | 793 | 39 | 790 | 17 | 789 | 12 | 0.1 |
| CSL2-35 | 0.26 | 0.073 | 0.002 | 1.72455 | 0.0483 | 0.17129 | 0.0027 | 1014 | 32 | 1018 | 18 | 1019 | 15 | -0.5 |
| CSL2-36 | 0.4 | 0.05162 | 0.0019 | 0.30651 | 0.0112 | 0.04305 | 0.0007 | 269 | 55 | 271 | 9 | 272 | 4 | -0.4 |
| CSL2-37 | 0.46 | 0.05144 | 0.0014 | 0.29729 | 0.0083 | 0.0419 | 0.0007 | 261 | 36 | 264 | 6 | 265 | 4 | -0.4 |
| CSL2-38 | 0.81 | 0.05484 | 0.0019 | 0.45335 | 0.0162 | 0.05995 | 0.001 | 406 | 51 | 380 | 11 | 375 | 6 | 1.3 |
| CSL2-39 | 0.92 | 0.05256 | 0.0022 | 0.35723 | 0.0149 | 0.04928 | 0.0009 | 310 | 64 | 310 | 11 | 310 | 5 | 0 |
| CSL2-40 | 0.47 | 0.05875 | 0.0014 | 0.66081 | 0.0168 | 0.08156 | 0.0012 | 558 | 30 | 515 | 10 | 505 | 7 | 2 |
| CSL2-41 | 0.5 | 0.05216 | 0.0043 | 0.33844 | 0.0278 | 0.04705 | 0.0009 | 292 | 151 | 296 | 21 | 296 | 6 | 0 |
| CSL2-42 | 0.55 | 0.0554 | 0.0019 | 0.53112 | 0.0184 | 0.06951 | 0.0011 | 428 | 49 | 433 | 12 | 433 | 7 | 0 |
| CSL2-43 | 0.99 | 0.11369 | 0.0026 | 5.02233 | 0.1187 | 0.32032 | 0.0049 | 1859 | 22 | 1823 | 20 | 1791 | 24 | 3.8 |
| CSL2-44 | 0.58 | 0.12028 | 0.0028 | 5.54722 | 0.1347 | 0.33441 | 0.0052 | 1960 | 23 | 1908 | 21 | 1860 | 25 | 5.4 |
| CSL2-45 | 0.65 | 0.05147 | 0.0036 | 0.30196 | 0.0211 | 0.04254 | 0.0008 | 262 | 124 | 268 | 16 | 269 | 5 | -0.4 |
| CSL2-46 | 0.29 | 0.05619 | 0.0015 | 0.5648 | 0.0157 | 0.07289 | 0.0011 | 460 | 35 | 455 | 10 | 454 | 7 | 0.2 |
| CSL2-47 | 0.61 | 0.10511 | 0.0025 | 4.46385 | 0.1114 | 0.30794 | 0.0048 | 1716 | 24 | 1724 | 21 | 1731 | 23 | -0.9 |
| ~~CSL2-48~~ | ~~0.33~~ | ~~0.05663~~ | ~~0.0016~~ | ~~0.62028~~ | ~~0.0178~~ | ~~0.07942~~ | ~~0.0012~~ | ~~477~~ | ~~37~~ | ~~490~~ | ~~11~~ | ~~493~~ | ~~7~~ | ~~-0.6~~ |
| CSL2-49 | 0.15 | 0.06584 | 0.0017 | 1.25947 | 0.0331 | 0.13871 | 0.0022 | 801 | 30 | 828 | 15 | 837 | 12 | -1.1 |
| CSL2-50 | 0.54 | 0.05527 | 0.0016 | 0.52329 | 0.015 | 0.06866 | 0.0011 | 423 | 37 | 427 | 10 | 428 | 7 | -0.2 |
| CSL2-51 | 0.56 | 0.05571 | 0.0016 | 0.54285 | 0.0156 | 0.07066 | 0.001 | 441 | 38 | 440 | 10 | 440 | 6 | 0 |
| CSL2-52 | 0.36 | 0.07689 | 0.0018 | 1.91983 | 0.0458 | 0.18105 | 0.0027 | 1118 | 25 | 1088 | 16 | 1073 | 14 | 4.2 |
| CSL2-53 | 1.55 | 0.05134 | 0.0019 | 0.2804 | 0.0102 | 0.03961 | 0.0006 | 256 | 56 | 251 | 8 | 250 | 4 | 0.4 |
| CSL2-54 | 0.42 | 0.05499 | 0.0034 | 0.51347 | 0.0312 | 0.06771 | 0.0011 | 412 | 106 | 421 | 21 | 422 | 7 | -0.2 |
| CSL2-55 | 0.4 | 0.06929 | 0.003 | 1.09812 | 0.0447 | 0.11494 | 0.0018 | 907 | 92 | 752 | 22 | 701 | 10 | 7.3 |

| | | | | | | | | | | | | | | |
|---|---|---|---|---|---|---|---|---|---|---|---|---|---|---|
| CSL2-56 | 0.45 | 0.05169 | 0.0023 | 0.30701 | 0.0135 | 0.04307 | 0.0007 | 272 | 71 | 272 | 11 | 272 | 4 | 0 |
| CSL2-57 | 0.68 | 0.12532 | 0.0021 | 5.9464 | 0.108 | 0.34409 | 0.0048 | 2033 | 15 | 1968 | 16 | 1906 | 23 | 6.7 |
| CSL2-58 | 0.03 | 0.05845 | 0.0013 | 0.67258 | 0.0153 | 0.08344 | 0.0012 | 547 | 26 | 522 | 9 | 517 | 7 | 1 |
| CSL2-59 | 0.99 | 0.0569 | 0.0014 | 0.61328 | 0.0157 | 0.07816 | 0.0012 | 488 | 31 | 486 | 10 | 485 | 7 | 0.2 |
| CSL2-60 | 0.27 | 0.07618 | 0.0014 | 1.8584 | 0.0359 | 0.17691 | 0.0025 | 1100 | 18 | 1066 | 13 | 1050 | 14 | 4.8 |
| CSL2-61 | 0.34 | 0.05756 | 0.0011 | 0.65646 | 0.0138 | 0.0827 | 0.0012 | 513 | 23 | 512 | 8 | 512 | 7 | 0 |
| CSL2-62 | 0.49 | 0.08566 | 0.0016 | 2.66194 | 0.0522 | 0.22535 | 0.0032 | 1331 | 18 | 1318 | 14 | 1310 | 17 | 1.6 |
| CSL2-63 | 0.18 | 0.08677 | 0.0015 | 2.73884 | 0.0506 | 0.22889 | 0.0032 | 1355 | 17 | 1339 | 14 | 1329 | 17 | 2 |
| ~~CSL2-64~~ | ~~0.61~~ | ~~0.05258~~ | ~~0.0016~~ | ~~0.35858~~ | ~~0.011~~ | ~~0.04945~~ | ~~0.0007~~ | ~~311~~ | ~~43~~ | ~~311~~ | ~~8~~ | ~~311~~ | ~~5~~ | ~~0~~ |
| CSL2-65 | 1.46 | 0.07206 | 0.0017 | 1.66622 | 0.0414 | 0.16767 | 0.0025 | 988 | 27 | 996 | 16 | 999 | 14 | -0.3 |
| CSL2-66 | 0.62 | 0.0559 | 0.0015 | 0.54445 | 0.0147 | 0.07062 | 0.001 | 448 | 35 | 441 | 10 | 440 | 6 | 0.2 |
| CSL2-67 | 0.81 | 0.07618 | 0.0016 | 1.76413 | 0.038 | 0.16792 | 0.0024 | 1100 | 22 | 1032 | 14 | 1001 | 13 | 9.9 |
| CSL2-68 | 0.69 | 0.05617 | 0.0011 | 0.52498 | 0.0108 | 0.06777 | 0.001 | 459 | 23 | 428 | 7 | 423 | 6 | 1.2 |
| CSL2-69 | 0.26 | 0.05344 | 0.0011 | 0.37238 | 0.0083 | 0.05053 | 0.0007 | 348 | 26 | 321 | 6 | 318 | 4 | 0.9 |
| CSL2-70 | 0.57 | 0.07438 | 0.0031 | 1.78768 | 0.0701 | 0.1743 | 0.0027 | 1052 | 87 | 1041 | 26 | 1036 | 15 | 1.5 |
| CSL2-71 | 0.16 | 0.06603 | 0.0018 | 1.10355 | 0.0261 | 0.1212 | 0.0017 | 807 | 59 | 755 | 13 | 737 | 10 | 2.4 |
| CSL2-72 | 0.52 | 0.05245 | 0.0013 | 0.35161 | 0.0088 | 0.04861 | 0.0007 | 305 | 31 | 306 | 7 | 306 | 4 | 0 |
| CSL2-73 | 0.68 | 0.06615 | 0.0015 | 1.23256 | 0.0298 | 0.13512 | 0.002 | 811 | 27 | 816 | 14 | 817 | 11 | -0.1 |
| CSL2-74 | 0.62 | 0.0471 | 0.0068 | 0.29254 | 0.042 | 0.04505 | 0.0009 | 54 | 269 | 261 | 33 | 284 | 5 | -8.1 |
| CSL2-75 | 0.44 | 0.05578 | 0.0012 | 0.54872 | 0.0123 | 0.07134 | 0.001 | 444 | 26 | 444 | 8 | 444 | 6 | 0 |
| ~~CSL2-76~~ | ~~0.96~~ | ~~0.0528~~ | ~~0.002~~ | ~~0.36765~~ | ~~0.0137~~ | ~~0.0505~~ | ~~0.0008~~ | ~~320~~ | ~~55~~ | ~~318~~ | ~~10~~ | ~~318~~ | ~~5~~ | ~~0~~ |
| CSL2-77 | 0.51 | 0.05584 | 0.0015 | 0.56255 | 0.0155 | 0.07305 | 0.0011 | 446 | 34 | 453 | 10 | 455 | 7 | -0.4 |
| CSL2-78 | 1 | 0.05608 | 0.0015 | 0.55762 | 0.0155 | 0.07211 | 0.0011 | 456 | 35 | 450 | 10 | 449 | 7 | 0.2 |
| CSL2-79 | 0.46 | 0.05602 | 0.0015 | 0.35311 | 0.0097 | 0.04571 | 0.0007 | 453 | 34 | 307 | 7 | 288 | 4 | 6.6 |
| CSL2-80 | 0.81 | 0.05682 | 0.0017 | 0.54034 | 0.0161 | 0.06896 | 0.0011 | 485 | 38 | 439 | 11 | 430 | 7 | 2.1 |
| CSL2-81 | 0.4 | 0.06906 | 0.0017 | 1.51337 | 0.0388 | 0.15891 | 0.0025 | 901 | 29 | 936 | 16 | 951 | 14 | -1.6 |
| CSL2-82 | 0.4 | 0.05752 | 0.0016 | 0.66337 | 0.0189 | 0.08363 | 0.0013 | 512 | 36 | 517 | 12 | 518 | 8 | -0.2 |
| CSL2-83 | 0.43 | 0.05743 | 0.0016 | 0.60143 | 0.0168 | 0.07594 | 0.0012 | 508 | 35 | 478 | 11 | 472 | 7 | 1.3 |

| | | | | | | | | | | | | | | |
|---|---|---|---|---|---|---|---|---|---|---|---|---|---|---|
| CSL2-84 | 0.3 | 0.07185 | 0.0017 | 1.5712 | 0.0395 | 0.15859 | 0.0024 | 982 | 27 | 959 | 16 | 949 | 14 | 1.1 |
| CSL2-85 | 0.13 | 0.06888 | 0.0017 | 1.46715 | 0.0384 | 0.15446 | 0.0024 | 895 | 30 | 917 | 16 | 926 | 13 | -1 |
| CSL2-86 | 0.65 | 0.05642 | 0.0023 | 0.58027 | 0.0236 | 0.07458 | 0.0013 | 469 | 60 | 465 | 15 | 464 | 8 | 0.2 |
| CSL2-87 | 0.21 | 0.0733 | 0.0018 | 1.65061 | 0.0427 | 0.1633 | 0.0025 | 1022 | 28 | 990 | 16 | 975 | 14 | 1.5 |
| CSL2-88 | 0.83 | 0.05144 | 0.0022 | 0.29488 | 0.0127 | 0.04157 | 0.0007 | 261 | 67 | 262 | 10 | 263 | 4 | -0.4 |
| CSL2-89 | 0.7 | 0.19207 | 0.0049 | 13.5337 | 0.3581 | 0.51097 | 0.0084 | 2760 | 23 | 2718 | 25 | 2661 | 36 | 3.7 |
| CSL2-90 | 0.53 | 0.05422 | 0.0023 | 0.45612 | 0.0197 | 0.061 | 0.001 | 380 | 66 | 382 | 14 | 382 | 6 | 0 |
| ~~CSL2-91~~ | ~~0.53~~ | ~~0.05545~~ | ~~0.0026~~ | ~~0.51916~~ | ~~0.0246~~ | ~~0.06789~~ | ~~0.0012~~ | ~~430~~ | ~~75~~ | ~~425~~ | ~~16~~ | ~~423~~ | ~~7~~ | ~~0.5~~ |
| CSL2-92 | 0.52 | 0.09124 | 0.0024 | 3.09334 | 0.0834 | 0.24585 | 0.0039 | 1452 | 28 | 1431 | 21 | 1417 | 20 | 2.5 |
| CSL2-93 | 0.39 | 0.07239 | 0.002 | 1.62315 | 0.0467 | 0.16259 | 0.0026 | 997 | 33 | 979 | 18 | 971 | 14 | 0.8 |
| CSL2-94 | 0.21 | 0.05552 | 0.0015 | 0.54068 | 0.0151 | 0.07062 | 0.0011 | 433 | 35 | 439 | 10 | 440 | 7 | -0.2 |
| CSL2-95 | 0.57 | 0.09055 | 0.004 | 3.13844 | 0.1278 | 0.25139 | 0.0041 | 1437 | 86 | 1442 | 31 | 1446 | 21 | -0.6 |
| CSL2-96 | 0.25 | 0.06849 | 0.002 | 1.24203 | 0.0373 | 0.1315 | 0.0021 | 883 | 36 | 820 | 17 | 796 | 12 | 3 |
| CSL2-97 | 0.54 | 0.0567 | 0.0016 | 0.6166 | 0.0182 | 0.07887 | 0.0013 | 480 | 38 | 488 | 11 | 489 | 8 | -0.2 |
| CSL2-98 | 0.23 | 0.05594 | 0.0014 | 0.54958 | 0.0148 | 0.07124 | 0.0011 | 450 | 33 | 445 | 10 | 444 | 7 | 0.2 |
| CSL2-99 | 0.87 | 0.05145 | 0.0024 | 0.29205 | 0.0135 | 0.04117 | 0.0008 | 261 | 72 | 260 | 11 | 260 | 5 | 0 |
| CSL2-100 | 0.35 | 0.05713 | 0.0021 | 0.6434 | 0.0236 | 0.08167 | 0.0014 | 497 | 51 | 504 | 15 | 506 | 8 | -0.4 |
| **CSL3** | | | | | | | | | | | | | | |
| CSL3-01 | ~~0.13~~ | ~~0.05517~~ | ~~0.0013~~ | ~~0.50171~~ | ~~0.012~~ | ~~0.06594~~ | ~~0.001~~ | ~~419~~ | ~~28~~ | ~~413~~ | ~~8~~ | ~~412~~ | ~~6~~ | ~~0.2~~ |
| CSL3-02 | 0.58 | 0.05553 | 0.0017 | 0.54093 | 0.0172 | 0.07063 | 0.0011 | 434 | 43 | 439 | 11 | 440 | 7 | -0.2 |
| CSL3-03 | 0.97 | 0.05158 | 0.0023 | 0.31051 | 0.0139 | 0.04365 | 0.0008 | 267 | 71 | 275 | 11 | 275 | 5 | 0 |
| CSL3-04 | 0.45 | 0.07636 | 0.0015 | 1.82299 | 0.0383 | 0.17311 | 0.0026 | 1105 | 20 | 1054 | 14 | 1029 | 14 | 7.4 |
| CSL3-05 | 0.51 | 0.05168 | 0.0015 | 0.30315 | 0.009 | 0.04254 | 0.0007 | 271 | 40 | 269 | 7 | 269 | 4 | 0 |
| CSL3-06 | ~~0.66~~ | ~~0.08359~~ | ~~0.0017~~ | ~~2.38147~~ | ~~0.0506~~ | ~~0.20659~~ | ~~0.0031~~ | ~~1283~~ | ~~20~~ | ~~1237~~ | ~~15~~ | ~~1211~~ | ~~16~~ | ~~5.9~~ |
| CSL3-07 | ~~0.64~~ | ~~0.05664~~ | ~~0.002~~ | ~~0.58377~~ | ~~0.0206~~ | ~~0.07473~~ | ~~0.0012~~ | ~~478~~ | ~~49~~ | ~~467~~ | ~~13~~ | ~~465~~ | ~~7~~ | ~~0.4~~ |
| CSL3-08 | 0.61 | 0.05592 | 0.0013 | 0.55642 | 0.0139 | 0.07215 | 0.0011 | 449 | 29 | 449 | 9 | 449 | 7 | 0 |
| CSL3-09 | 0.51 | 0.05039 | 0.0014 | 0.24655 | 0.0072 | 0.03547 | 0.0006 | 213 | 39 | 224 | 6 | 225 | 3 | -0.4 |
| CSL3-10 | 0.94 | 0.0989 | 0.0018 | 3.90235 | 0.0772 | 0.28609 | 0.0043 | 1603 | 17 | 1614 | 16 | 1622 | 21 | -1.2 |

| | | | | | | | | | | | | | | |
|---|---|---|---|---|---|---|---|---|---|---|---|---|---|---|
| CSL3-11 | 0.46 | 0.05608 | 0.0015 | 0.55141 | 0.0155 | 0.07129 | 0.0011 | 456 | 36 | 446 | 10 | 444 | 7 | 0.5 |
| CSL3-12 | 0.73 | 0.05159 | 0.0033 | 0.30602 | 0.0194 | 0.04301 | 0.0008 | 267 | 112 | 271 | 15 | 271 | 5 | 0 |
| CSL3-13 | 0.77 | 0.0521 | 0.0036 | 0.29028 | 0.0197 | 0.0404 | 0.0007 | 290 | 122 | 259 | 16 | 255 | 5 | 1.6 |
| CSL3-14 | 0.58 | 0.05159 | 0.0016 | 0.29206 | 0.0094 | 0.04105 | 0.0006 | 267 | 45 | 260 | 7 | 259 | 4 | 0.4 |
| CSL3-15 | 0.5 | 0.05646 | 0.0011 | 0.5388 | 0.0115 | 0.0692 | 0.001 | 471 | 23 | 438 | 8 | 431 | 6 | 1.6 |
| CSL3-16 | ~~0.93~~ | ~~0.05133~~ | ~~0.0017~~ | ~~0.2997~~ | ~~0.01~~ | ~~0.04233~~ | ~~0.0007~~ | ~~256~~ | ~~49~~ | ~~266~~ | ~~8~~ | ~~267~~ | ~~4~~ | ~~-0.4~~ |
| CSL3-17 | 0.59 | 0.056 | 0.0011 | 0.55924 | 0.012 | 0.07241 | 0.0011 | 452 | 24 | 451 | 8 | 451 | 6 | 0 |
| CSL3-18 | 0.33 | 0.05569 | 0.0012 | 0.54468 | 0.0122 | 0.07092 | 0.0011 | 440 | 25 | 442 | 8 | 442 | 6 | 0 |
| CSL3-19 | 0.89 | 0.05161 | 0.0018 | 0.30471 | 0.0107 | 0.04281 | 0.0007 | 268 | 51 | 270 | 8 | 270 | 4 | 0 |
| CSL3-20 | 0.73 | 0.05081 | 0.0017 | 0.25666 | 0.0086 | 0.03663 | 0.0006 | 232 | 47 | 232 | 7 | 232 | 4 | 0 |
| CSL3-21 | 0.42 | 0.05556 | 0.0017 | 0.54721 | 0.0165 | 0.07142 | 0.0011 | 435 | 39 | 443 | 11 | 445 | 7 | -0.4 |
| CSL3-22 | ~~0.53~~ | ~~0.0553~~ | ~~0.0015~~ | ~~0.52915~~ | ~~0.015~~ | ~~0.06938~~ | ~~0.0011~~ | ~~424~~ | ~~36~~ | ~~431~~ | ~~10~~ | ~~432~~ | ~~7~~ | ~~-0.2~~ |
| CSL3-23 | 0.67 | 0.05749 | 0.0047 | 0.34096 | 0.0271 | 0.04302 | 0.0008 | 510 | 185 | 298 | 21 | 272 | 5 | 9.6 |
| CSL3-24 | 0.66 | 0.05469 | 0.0012 | 0.48332 | 0.011 | 0.06408 | 0.001 | 400 | 26 | 400 | 7 | 400 | 6 | 0 |
| CSL3-25 | 0.51 | 0.05182 | 0.0025 | 0.31577 | 0.0152 | 0.04418 | 0.0008 | 277 | 78 | 279 | 12 | 279 | 5 | 0 |
| CSL3-26 | 0.54 | 0.05517 | 0.0017 | 0.51708 | 0.0157 | 0.06796 | 0.0011 | 419 | 40 | 423 | 10 | 424 | 7 | -0.2 |
| CSL3-27 | 0.39 | 0.05633 | 0.0012 | 0.55078 | 0.012 | 0.07089 | 0.0011 | 465 | 24 | 446 | 8 | 442 | 6 | 0.9 |
| CSL3-28 | 0.4 | 0.05498 | 0.0011 | 0.49057 | 0.0108 | 0.0647 | 0.001 | 411 | 25 | 405 | 7 | 404 | 6 | 0.2 |
| CSL3-29 | 0.78 | 0.05534 | 0.0012 | 0.54647 | 0.0123 | 0.0716 | 0.0011 | 426 | 25 | 443 | 8 | 446 | 6 | -0.7 |
| CSL3-30 | 0.47 | 0.0516 | 0.0013 | 0.29915 | 0.0077 | 0.04204 | 0.0006 | 268 | 32 | 266 | 6 | 265 | 4 | 0.4 |
| CSL3-31 | 0.3 | 0.05561 | 0.0019 | 0.53045 | 0.0179 | 0.06916 | 0.0011 | 437 | 46 | 432 | 12 | 431 | 7 | 0.2 |
| CSL3-32 | 0.58 | 0.0508 | 0.0018 | 0.25068 | 0.0092 | 0.03578 | 0.0006 | 232 | 55 | 227 | 7 | 227 | 4 | 0 |
| CSL3-33 | 0.63 | 0.05162 | 0.0017 | 0.29987 | 0.0098 | 0.04212 | 0.0007 | 269 | 46 | 266 | 8 | 266 | 4 | 0 |
| CSL3-34 | 0.5 | 0.05041 | 0.0012 | 0.25617 | 0.0063 | 0.03685 | 0.0006 | 214 | 31 | 232 | 5 | 233 | 3 | -0.4 |
| CSL3-35 | 0.54 | 0.05477 | 0.0012 | 0.48707 | 0.0113 | 0.06448 | 0.001 | 403 | 27 | 403 | 8 | 403 | 6 | 0 |
| CSL3-36 | 0.25 | 0.05507 | 0.0014 | 0.52684 | 0.0133 | 0.06937 | 0.0011 | 415 | 30 | 430 | 9 | 432 | 6 | -0.5 |
| CSL3-37 | 0.47 | 0.05509 | 0.0014 | 0.55457 | 0.014 | 0.07299 | 0.0011 | 416 | 30 | 448 | 9 | 454 | 7 | -1.3 |
| CSL3-38 | 0.57 | 0.11151 | 0.002 | 4.87149 | 0.0944 | 0.31675 | 0.0046 | 1824 | 17 | 1797 | 16 | 1774 | 23 | 2.8 |

| | | | | | | | | | | | | | | |
|---|---|---|---|---|---|---|---|---|---|---|---|---|---|---|
| CSL3-39 | 0.94 | 0.05119 | 0.0019 | 0.28993 | 0.0108 | 0.04107 | 0.0007 | 249 | 56 | 259 | 8 | 259 | 4 | 0 |
| CSL3-40 | 0.55 | 0.05135 | 0.0031 | 0.29487 | 0.0176 | 0.04163 | 0.0007 | 257 | 105 | 262 | 14 | 263 | 5 | -0.4 |
| CSL3-41 | 0.4 | 0.16483 | 0.0031 | 10.6646 | 0.2173 | 0.46913 | 0.0071 | 2506 | 16 | 2494 | 19 | 2480 | 31 | 1 |
| CSL3-42 | 1.12 | 0.05156 | 0.0022 | 0.30229 | 0.013 | 0.04251 | 0.0007 | 266 | 66 | 268 | 10 | 268 | 5 | 0 |
| CSL3-43 | 0.61 | 0.05584 | 0.0013 | 0.55993 | 0.0133 | 0.07271 | 0.0011 | 446 | 28 | 451 | 9 | 452 | 7 | -0.2 |
| CSL3-44 | 0.9 | 0.05148 | 0.0014 | 0.29588 | 0.0082 | 0.04168 | 0.0006 | 262 | 37 | 263 | 6 | 263 | 4 | 0 |
| CSL3-45 | 0.32 | 0.05744 | 0.0016 | 0.61627 | 0.0176 | 0.0778 | 0.0012 | 508 | 37 | 488 | 11 | 483 | 7 | 1 |
| CSL3-46 | 1.12 | 0.05248 | 0.0026 | 0.34374 | 0.0167 | 0.04749 | 0.0008 | 306 | 80 | 300 | 13 | 299 | 5 | 0.3 |
| CSL3-47 | 0.53 | 0.05116 | 0.0025 | 0.2908 | 0.0143 | 0.04121 | 0.0007 | 248 | 82 | 259 | 11 | 260 | 4 | -0.4 |
| CSL3-48 | 0.47 | 0.05069 | 0.0024 | 0.24289 | 0.0116 | 0.03475 | 0.0006 | 227 | 78 | 221 | 9 | 220 | 4 | 0.5 |
| CSL3-49 | 0.59 | 0.05574 | 0.0019 | 0.5371 | 0.0187 | 0.06987 | 0.0011 | 442 | 49 | 437 | 12 | 435 | 7 | 0.5 |
| CSL3-50 | 0.9 | 0.05127 | 0.0019 | 0.29027 | 0.011 | 0.04105 | 0.0007 | 253 | 58 | 259 | 9 | 259 | 4 | 0 |
| CSL3-51 | 0.45 | 0.0556 | 0.0011 | 0.53934 | 0.0114 | 0.07034 | 0.001 | 436 | 23 | 438 | 8 | 438 | 6 | 0 |
| CSL3-52 | 0.81 | 0.05158 | 0.0018 | 0.30681 | 0.0105 | 0.04313 | 0.0007 | 267 | 50 | 272 | 8 | 272 | 4 | 0 |
| CSL3-53 | 0.59 | 0.05148 | 0.0017 | 0.29343 | 0.0097 | 0.04133 | 0.0007 | 262 | 47 | 261 | 8 | 261 | 4 | 0 |
| CSL3-54 | 0.54 | 0.05613 | 0.0013 | 0.32317 | 0.008 | 0.04175 | 0.0006 | 458 | 29 | 284 | 6 | 264 | 4 | 7.6 |
| CSL3-55 | 0.38 | 0.0565 | 0.0012 | 0.56451 | 0.0129 | 0.07245 | 0.0011 | 472 | 26 | 454 | 8 | 451 | 6 | 0.7 |
| CSL3-56 | 1.03 | 0.05527 | 0.0033 | 0.4838 | 0.0282 | 0.06346 | 0.0012 | 423 | 98 | 401 | 19 | 397 | 7 | 1 |
| CSL3-57 | 0.58 | 0.05179 | 0.0018 | 0.30555 | 0.0104 | 0.04278 | 0.0007 | 276 | 50 | 271 | 8 | 270 | 4 | 0.4 |
| CSL3-58 | 0.62 | 0.05151 | 0.0016 | 0.29928 | 0.0093 | 0.04213 | 0.0007 | 264 | 42 | 266 | 7 | 266 | 4 | 0 |
| CSL3-59 | 0.67 | 0.10164 | 0.0021 | 3.86428 | 0.0828 | 0.27568 | 0.0041 | 1654 | 20 | 1606 | 17 | 1570 | 21 | 5.4 |
| CSL3-60 | 0.45 | 0.05783 | 0.0021 | 0.646 | 0.023 | 0.08099 | 0.0013 | 523 | 50 | 506 | 14 | 502 | 8 | 0.8 |
| CSL3-61 | 0.49 | 0.05665 | 0.0017 | 0.32486 | 0.0096 | 0.04158 | 0.0006 | 478 | 39 | 286 | 7 | 263 | 4 | 8.7 |
| CSL3-62 | 0.48 | 0.05564 | 0.0015 | 0.53916 | 0.0148 | 0.07026 | 0.0011 | 438 | 34 | 438 | 10 | 438 | 7 | 0 |
| CSL3-63 | 0.52 | 0.05567 | 0.0017 | 0.52766 | 0.0164 | 0.06873 | 0.0011 | 439 | 41 | 430 | 11 | 428 | 7 | 0.5 |
| CSL3-64 | 1.45 | 0.05803 | 0.0024 | 0.70382 | 0.0295 | 0.08795 | 0.0015 | 531 | 62 | 541 | 18 | 543 | 9 | -0.4 |
| CSL3-65 | 0.53 | 0.09522 | 0.0036 | 3.43202 | 0.1182 | 0.26142 | 0.0042 | 1532 | 73 | 1512 | 27 | 1497 | 21 | 2.3 |
| CSL3-66 | 0.65 | 0.05436 | 0.0017 | 0.45752 | 0.0146 | 0.06103 | 0.001 | 386 | 44 | 383 | 10 | 382 | 6 | 0.3 |

| | | | | | | | | | | | | | | |
|---|---|---|---|---|---|---|---|---|---|---|---|---|---|---|
| CSL3-67 | 0.51 | 0.05542 | 0.0015 | 0.52583 | 0.0141 | 0.0688 | 0.0011 | 429 | 33 | 429 | 9 | 429 | 6 | 0 |
| CSL3-68 | 0.92 | 0.05146 | 0.0024 | 0.29693 | 0.0137 | 0.04184 | 0.0007 | 261 | 75 | 264 | 11 | 264 | 4 | 0 |
| CSL3-69 | ~~0.94~~ | 0.05152 | 0.0021 | 0.29733 | 0.0123 | 0.04185 | 0.0007 | 264 | 65 | 264 | 10 | 264 | 4 | 0 |
| CSL3-70 | 1.04 | 0.05177 | 0.002 | 0.31234 | 0.0119 | 0.04374 | 0.0008 | 275 | 56 | 276 | 9 | 276 | 5 | 0 |
| CSL3-71 | 0.56 | 0.05331 | 0.0019 | 0.30094 | 0.0106 | 0.04093 | 0.0007 | 342 | 51 | 267 | 8 | 259 | 4 | 3.1 |
| CSL3-72 | 0.5 | 0.05166 | 0.0027 | 0.29172 | 0.0153 | 0.04094 | 0.0007 | 270 | 87 | 260 | 12 | 259 | 5 | 0.4 |
| CSL3-73 | 0.28 | 0.05525 | 0.0013 | 0.53166 | 0.0129 | 0.06978 | 0.0011 | 422 | 29 | 433 | 9 | 435 | 6 | -0.5 |
| CSL3-74 | 0.57 | 0.05173 | 0.0018 | 0.30412 | 0.0105 | 0.04263 | 0.0007 | 273 | 50 | 270 | 8 | 269 | 4 | 0.4 |
| ~~CSL3-75~~ | 1.34 | 0.08126 | 0.0025 | 0.43458 | 0.0132 | 0.03878 | 0.0007 | 1228 | 34 | 366 | 9 | 245 | 4 | 49.4 |
| CSL3-76 | 3.82 | 0.05124 | 0.0023 | 0.28649 | 0.0127 | 0.04054 | 0.0007 | 252 | 69 | 256 | 10 | 256 | 4 | 0 |
| CSL3-77 | 0.71 | 0.05171 | 0.0019 | 0.30653 | 0.011 | 0.04299 | 0.0007 | 273 | 53 | 271 | 9 | 271 | 4 | 0 |
| ~~CSL3-78~~ | ~~0.51~~ | 0.06587 | 0.0017 | 0.61079 | 0.0157 | 0.06724 | 0.001 | 802 | 29 | 484 | 10 | 420 | 6 | 15.2 |
| CSL3-79 | 0.45 | ~~0.05575~~ | ~~0.0014~~ | ~~0.5408~~ | ~~0.0139~~ | ~~0.07034~~ | ~~0.0011~~ | ~~442~~ | ~~31~~ | ~~439~~ | ~~9~~ | ~~438~~ | ~~7~~ | ~~0.2~~ |
| CSL3-80 | 1 | 0.0859 | 0.0026 | 2.77293 | 0.0832 | 0.23408 | 0.0038 | 1336 | 33 | 1348 | 22 | 1356 | 20 | -1.5 |
| CSL3-81 | 0.6 | 0.05147 | 0.0024 | 0.30168 | 0.0141 | 0.0425 | 0.0007 | 262 | 76 | 268 | 11 | 268 | 5 | 0 |
| CSL3-82 | 0.74 | 0.05152 | 0.007 | 0.28864 | 0.0388 | 0.04063 | 0.0009 | 264 | 259 | 257 | 31 | 257 | 6 | 0 |
| CSL3-83 | 0.54 | 0.0553 | 0.0014 | 0.52934 | 0.0134 | 0.06941 | 0.0011 | 424 | 30 | 431 | 9 | 433 | 6 | -0.5 |
| CSL3-84 | 0.6 | 0.05135 | 0.0019 | 0.29861 | 0.0108 | 0.04217 | 0.0007 | 257 | 53 | 265 | 8 | 266 | 4 | -0.4 |
| CSL3-85 | 0.75 | 0.05119 | 0.0016 | 0.2579 | 0.008 | 0.03653 | 0.0006 | 249 | 42 | 233 | 6 | 231 | 4 | 0.9 |
| CSL3-86 | 0.66 | 0.05156 | 0.0018 | 0.3026 | 0.0104 | 0.04256 | 0.0007 | 266 | 49 | 268 | 8 | 269 | 4 | -0.4 |
| CSL3-87 | 0.66 | 0.05536 | 0.0014 | 0.52022 | 0.0137 | 0.06814 | 0.0011 | 427 | 32 | 425 | 9 | 425 | 6 | 0 |
| CSL3-88 | 0.86 | 0.05155 | 0.0022 | 0.29682 | 0.0128 | 0.04175 | 0.0007 | 266 | 66 | 264 | 10 | 264 | 5 | 0 |
| CSL3-89 | 0.64 | 0.05191 | 0.0017 | 0.31777 | 0.0101 | 0.04439 | 0.0007 | 281 | 44 | 280 | 8 | 280 | 4 | 0 |
| CSL3-90 | 0.77 | 0.05526 | 0.0018 | 0.50689 | 0.0168 | 0.06651 | 0.0011 | 423 | 46 | 416 | 11 | 415 | 6 | 0.2 |
| ~~CSL3-91~~ | 0.42 | 0.08731 | 0.0022 | 1.70999 | 0.0445 | 0.14202 | 0.0022 | 1367 | 27 | 1012 | 17 | 856 | 13 | 18.2 |
| CSL3-92 | 0.43 | 0.05546 | 0.0015 | 0.5249 | 0.0141 | 0.06864 | 0.0011 | 431 | 33 | 428 | 9 | 428 | 6 | 0 |
| CSL3-93 | ~~0.5~~ | 0.07675 | 0.002 | 1.96941 | 0.0515 | 0.18607 | 0.0029 | 1115 | 28 | 1105 | 18 | 1100 | 16 | 1.4 |
| CSL3-94 | 0.47 | 0.05145 | 0.0016 | 0.29321 | 0.0093 | 0.04132 | 0.0007 | 261 | 43 | 261 | 7 | 261 | 4 | 0 |

| | | | | | | | | | | | | | | |
|---|---|---|---|---|---|---|---|---|---|---|---|---|---|---|
| CSL3-95 | 0.43 | 0.05591 | 0.002 | 0.55431 | 0.0195 | 0.0719 | 0.0012 | 449 | 50 | 448 | 13 | 448 | 7 | 0 |
| CSL3-96 | 0.62 | 0.0517 | 0.0019 | 0.31532 | 0.0114 | 0.04423 | 0.0007 | 272 | 53 | 278 | 9 | 279 | 4 | -0.4 |
| CSL3-97 | ~~0.52~~ | 0.06833 | 0.0019 | 1.33206 | 0.0363 | 0.14138 | 0.0022 | 879 | 31 | 860 | 16 | 852 | 13 | 0.9 |
| CSL3-98 | 1.25 | 0.0515 | 0.0018 | 0.29382 | 0.0105 | 0.04138 | 0.0007 | 263 | 52 | 262 | 8 | 261 | 4 | 0.4 |
| CSL3-99 | 0.68 | 0.05173 | 0.0044 | 0.3006 | 0.0253 | 0.04214 | 0.0008 | 273 | 155 | 267 | 20 | 266 | 5 | 0.4 |
| CSL3-100 | 0.59 | 0.10151 | 0.0025 | 3.96501 | 0.0998 | 0.28327 | 0.0044 | 1652 | 25 | 1627 | 20 | 1608 | 22 | 2.7 |

Table DR2. Zircon U-Pb ages from plutons of the Eastern Kunlun Range, Altyn Tagh Range and Qilian Shan.

| Altyn Tagh Range | | | Qilian Shan | | | East Kunlun Range | | |
|---|---|---|---|---|---|---|---|---|
| Author | Year | Age(Ma) | Author | Year | Age(Ma) | Author | Year | Age(Ma) |
| | 2005 | 413 | Yue et al., | 2005 | 1728 | She Hongquan et al., | 2007 | 215 |
| | | 482 | | | 482 | Li Shijin et al., | 2008 | 224 |
| | | 1870 | | | 424 | Wang Song et al., | 2009 | 237 |
| | | 1877 | | | 472 | Li Dongsheng et al., | 2009 | 206 |
| Yue et al., | | 479 | | | 480 | | | 223 |
| | 2003 | 270 | | | 423 | Feng Chengyou et al., | 2009 | 237 |
| | | 272 | | | 406 | Huang Limei et al., | 2012 | 459 |
| | | 270 | | | 425 | Guo Lei et al., | 2010 | 256 |
| Gehrels et al., | | 440 | | | 366 | Gao Yongbao et al., | 2012 | 228 |
| | 2003 | 922 | | | 248 | | | 234 |
| | | 389 | | | 434 | Liu Chengdong et al., | 2003 | 242 |
| | | 2720 | | | 441 | Liu Yunhua et al., | 2006 | 204 |
| | | 442 | | | 473 | Wu Xiangke et al., | 2011 | 218 |
| | | 290 | | | 430 | Feng Chengyou et al., | 2011 | 219 |
| | | 404 | Gehrels et al., | 2003 | 461 | | | 235 |
| Cowgill et al., | | 457 | Cowgill et al., | 2003 | 459 | Chen Danling et al., | 2011 | 212 |

| | | | | | | | | |
|---|---|---|---|---|---|---|---|---|
| | | 518 | | | 922 | Ren Erfeng et al., | 2012 | 403 |
| | | 475 | | | 928 | | | 394 |
| | | 969 | | | 442 | Feng Chengyou et al., | 2010 | 227 |
| | | 444 | | | 422 | | | 220 |
| | | 2396 | Lu Songnian et al., | 2008 | 2366 | Gao Yongbao et al., | 2011 | 430 |
| | 2008 | 2582 | | | 2412 | | | 431 |
| | | 2604 | | | 1939 | Feng Chengyou et al., | 2009 | 417 |
| | | 2830 | | | 2348 | | | 468 |
| | | 3574 | | | 1852 | Chen Junlu et al., | 2004 | 405 |
| | | 3665 | | | 1763 | | | 2380 |
| | | 2396 | | | 844 | | | 816 |
| | | 1978 | | | 740 | | | 401 |
| | | 2670 | | | 1050 | Cui Meihui et al., | 2011 | 480 |
| | | 2830 | | | 1020 | Wang Bingzhang et al., | 2009 | 271 |
| | | 1986 | | | 1020 | | | 284 |
| | | 2374 | | | 1020 | | | 251 |
| | | 2351 | | | 987 | Mo xuanxue et al., | 2005 | 212 |
| | | 2358 | | | 928 | Qinghai Geology | 2008 | 214 |
| | | 2366 | | | 917 | investigation institute | | 225 |
| | | 2412 | | | 917 | Xiao Aifang et al., | 2005 | 405 |
| | | 2426 | | | 878 | Wang Xiangli et al., | 2010 | 1090 |
| | | 1900 | | | 953 | | | 312 |
| Lu Songnian et al., | | 930 | | | 875 | Gao Yongbao et al., | 2010 | 430 |
| | 2005 | 474 | | | 878 | | | 430 |
| Wu Cailai et al., | | 446 | | | 864 | | | 430 |

| | | | | | | | | |
|---|---|---|---|---|---|---|---|---|
| | | 435 | | | 855 | Qinghai Geology | 2003 | 410 |
| | | 431 | | | 844 | investigation institute | | 419 |
| Yang Jingsui et al., | 2008 | 479 | | | 821 | Ma Yongshou et al., | 2010 | 550 |
| Yang Wenqiang et al., | 2012 | 453 | | | 1776 | | | 2046 |
| Hao Jie et al., | 2006 | 467 | | | 740 | Wu Shaofeng et al., | 2012 | 429 |
| Sun Jiming et al., | 2012 | 497 | | | 1793 | Tan Shengxiang et al., | 2004 | 831 |
| | 2013 | 923 | | | 1800 | Cao Shitai et al., | 2011 | 429 |
| | | 910 | Wang Chao et al., | 2013 | 976 | | | 430 |
| | | 927 | | | 952 | Wang Binzhang | 2012 | 440 |
| | | 924 | | | 941 | | | 450 |
| | | 906 | | | 935 | Feng Chengyou et al., | 2010 | 219 |
| | | 916 | | | 953 | Xi Rengang et al., | 2011 | 231 |
| | | 938 | | | 915 | Guo Tongzhen et al., | 2011 | 389 |
| | | 907 | | | 907 | Qinghai Geology | 2010 | 224 |
| Wang Chao et al., | | | | | | investigation institute | | |
| Xiu Qunye et al., | 2007 | 449 | | | 932 | Feng Chengyou et al., | 2012 | 227 |
| | 2012 | 446 | | | 918 | | | 220 |
| | | 477 | | | 930 | Chang Youying et al., | 2009 | 223 |
| | | 477 | Liu Liang et al., | 2013 | 783 | | | 214 |
| | | 514 | | | 748 | | | 225 |
| | | 417 | | | 847 | Liu Xiaokang et al., | 2011 | 419 |
| | | 488 | | | 847 | Chen Bo et al., | 2012 | 410 |
| | | 479 | | | 457 | Gao Xiaofeng et al., | 2011 | 443 |
| | | 506 | | | 446 | Luo Zhaohua et al., | 2002 | 212 |
| Han Dengbin et al., | | 431 | | | 909 | Mo xuanxue et al., | 2007 | 471 |

| | | | | | | | |
|---|---|---|---|---|---|---|---|
| | | 443 | | | 1005 | | 485 |
| | | 417 | | | 891 | Mo xuanxue et al., 2005 | 387 |
| | | 431 | | | 890 | | 386 |
| | | 440 | | | 516 | | 408 |
| | 2007 | 435 | Shi Rendeng et al., | 2004 | 550 | | 408 |
| | | 433 | Meng Fancong et al., | 2010 | 505 | | 401 |
| | | 435 | Zeng Jianyuan et al., | 2007 | 497 | Chen Hongwei et al., 2006 | 403 |
| Wu Cailai et al., | | 431 | Wu Cailai et al., | 2010 | 501 | | 394 |
| | 2012 | 750 | | | 512 | Lu Songnian et al., 2002 | 522 |
| | | 763 | | | 508 | | 2468 |
| Liu Han et al., | | 754 | | | 477 | | 1955 |
| Liu Liang et al., | 1999 | 524 | | | 463 | Yang Jinsui et al., 1996 | 518 |
| | 2006 | 776 | | | 424 | Feng Jianyun et al., 2010 | 509 |
| Zeng Jianyuan et al., | | 774 | | | 435 | Wang Binzhang 2012 | 509 |
| | 2009 | 757 | | | 429 | | 434 |
| | | 438 | Song Zhongbao et al., | 2004 | 482 | | 435 |
| Lu Songnian et al., | | 425 | Song Zhongbao et al., | 2007 | 458 | | 419 |
| | 2009 | 2679 | Huang Chuanjian et al., | 1995 | 486 | | 421 |
| | | 856 | Wu Cailai et al., | 2007 | 477 | | 413 |
| | | 1312 | | | 463 | | 409 |
| | | 1209 | Wang Yusheng et al., | 2001 | 940 | | 1782 |
| | | 871 | | | 1030 | | 2642 |
| | | 1311 | | | 1020 | | 881 |
| | | 450 | Wang Yusheng et al., | 2000 | 930 | | 923 |
| Wu Yuezhong et al., | | 465 | | | 930 | | 427 |

| | | | | | | | | |
|---|---|---|---|---|---|---|---|---|
| | | 445 | | | 750 | | | 451 |
| | | 452 | Guo Jinjing et al., | 1999 | 920 | | | 189 |
| | | 448 | | | 910 | | | 290 |
| | | 327 | Mei Hualin et al., | 1998 | 2670 | | | 397 |
| | | 313 | Mei Hualin et al., | 1999 | 880 | | | 683 |
| | | 397 | Xu Wanchun et al., | 2007 | 891 | | | 373 |
| Xiao Peixi et al., | 2003 | 495 | Wang Christina Yan et al., | 2005 | 445 | | | 394 |
| Song Zhongbao et al., | 2004 | 482 | Xu Wangchun et al., | 2007 | 776 | | | 373 |
| | 2011 | 462 | | | 774 | | | 369 |
| Liu Han et al., | | 437 | Li Xianhua et al., | 2004 | 827 | | | 370 |
| Zhang Zhicheng et al., | 2008 | 521 | Ayers et al., | 2002 | 1921 | | | 397 |
| Kang Lei et al., | 2011 | 500 | Mattinson et al., | 2006 | 433 | | | 395 |
| Gherels et al., | 1999 | 480 | Xia Xiaohong et al., | 2009 | 490 | | | 370 |
| Chen Xuanhua et al., | 2003 | 443 | He Shiping et al., | 2007 | 443 | | | 357 |
| | 2013 | 450 | | | 1782 | | | 284 |
| Dong Shunli et al., | | 465 | | | 385 | | | 241 |
| | 2012 | 478 | | | 471 | | | 250 |
| Zhang Zhanwu et al., | | 470 | Li Shuguang et al., | 2004 | 447 | | | 217 |
| Dong Zengchan et al., | 2011 | 445 | Zhang Zhaowei et al., | 2012 | 441 | | | 224 |
| Liu Han et al., | 2012 | 2007 | Wei Fanghui et al., | 2012 | 441 | Ma Shengchao et al., | 2012 | 219 |
| | 2012 | 467 | Zhang Zhaowei et al., | 2012 | 443 | | | 235 |
| | | 462 | Mao Jingwen et al., | 2000 | 460 | Cui Meihui et al., | 2012 | 480 |
| | | 470 | Xiong Ziliang et al., | 2012 | 424 | Zhang Dequan et al., | 2001 | 438 |
| Ma Zhongping et al., | | 464 | | | 402 | Cheng Nengsong et al., | 2008 | 517 |
| Yang Qi et al., | 2004 | 443 | Su Jianping et al., | 2004 | 444 | | | 516 |

| | | | | | | | | |
|---|---|---|---|---|---|---|---|---|
| | | 485 | Yu Jiyuan et al., | 2012 | 455 | | | 559 |
| Liu Liang et al., | 2007 | 750 | Wu Cailai et al., | 2006 | 476 | | | 482 |
| | 2005 | 846 | | | 463 | | | 516 |
| Zhangjianxin | | 844 | Wang Yinchuan et al., | 2012 | 1765 | | | 549 |
| zhangjianxin | 2004 | 842 | Wu Cailai et al., | 2004 | 383 | Yang Jingsui et al., | 1995 | 518 |
| | 2009 | 1800 | Chen Junlu et al., | 2006 | 440 | Lu Songnian et al., | 2002 | 522 |
| Liuliang | | 821 | Wang Hongliang et al., | 2007 | 1192 | Yang Jingsui et al., | 1996 | 579 |
| | 2005 | 482 | Qi Ruirong et al., | 2012 | 463 | Li Huaikun et al., | 2006 | 506 |
| Qixuexiang | | 404 | Huang Zengbao et al., | 2010 | 414 | Guangxi Geology | 2003 | 1209 |
| | 2013 | 754 | Xiang Zengqun et al., | 2007 | 504 | investigation institute | | 871 |
| | | 752 | Yang Jinsui et al., | 2008 | 479 | | | 550 |
| | | 647 | Xiao Lin et al., | 1997 | 2152 | | | 408 |
| | | 730 | Yong Yong et al., | 2008 | 454 | | | 397 |
| | | 857 | | | 846 | | | 320 |
| | | 719 | | | 756 | | | 381 |
| | | 867 | | | 853 | | | 271 |
| | | 563 | Xu Xueyi et al., | 2008 | 723 | Qinghai Geology | 2004 | 831 |
| Liuliang | | | | | | investigation institute | | |
| Wu Cailai et al., | 2001 | 446 | Zeng Jianyuan et al., | 2006 | 776 | Yang Jinsui et al., | 2005 | 417 |
| | 2003 | 2926 | | | 774 | | | 421 |
| | | 1728 | Chen Junlu et al., | 2008 | 445 | | | 250 |
| Chen Xuanhua et al., | | 405 | Xia Xiaohong et al., | 2010 | 490 | | | 308 |
| Wu Suoping et al., | 2007 | 385 | He Yanhong et al., | 2005 | 447 | Bian Qiantao et al., | 1999 | 402 |
| Li Weidong et al., | 2012 | 462 | Guo Jinjing et al., | 1999 | 917 | Cheng Nengsong et al., | 2000 | 447 |
| Cao Yuting et al., | 2013 | 579 | Pei Xianzhi et al., | 2007 | 440 | Gao Xiaofeng et al., | 2010 | 458 |

| | | | | | | | | |
|---|---|---|---|---|---|---|---|---|
| | 2010 | 410 | | | 450 | Shanxi Geology investigation institute | 2003 | 432 |
| Liu Feng et al., | | | | | | | | |
| | 2013 | 457 | He Yanhong et al., | 2005 | 1900 | Feng Jianyun et al., | 2010 | 509 |
| | | 419 | | | 2350 | Zhang Yafeng et al., | 2010 | 515 |
| | | 411 | | | 2500 | Sun Yu et al., | 2009 | 255 |
| | | 503 | Wu Cailai et al., | 2008 | 465 | Liu Chengdong et al., | 2004 | 239 |
| | | 420 | | | 470 | | | 242 |
| | | 419 | | | 444 | Liu Chengdong et al., | 2000 | 236 |
| | | 411 | | | 372 | | | 235 |
| | | 420 | | | 271 | Long Xiaoping et al., | 2006 | 411 |
| Liu Han et al., | | 405 | | | 260 | | | 396 |
| | 2003 | 418 | Li Jianfeng et al., | 2010 | 415 | Zhang Jianxin et al., | 2003 | 402 |
| | | 413 | | | 435 | Liu Zhanqing et al., | 2011 | 516 |
| Chen Xuanhua et al., | | 413 | Dong Guoan et al., | 2007 | 930 | | | 332 |
| | | | | | 918 | | | 441 |
| | | | | | 790 | Li Wangye et al., | 2007 | 493 |
| | | | Wu Cailai et al., | 2007 | 446 | Lu Lu et al., | 2010 | 423 |
| | | | | | 409 | Zhang Yaoling et al., | 2010 | 406 |
| | | | | | 403 | Sun Yu et al., | 2009 | 254 |
| | | | | | 375 | China University of Geosciences (Wuhan) | 2003 | 205 |
| | | | | | 372 | Ren Junhu et al., | 2009 | 436 |
| | | | Wu Peng et al., | 2012 | 499 | | | 413 |
| | | | Yu Jiyuan et al., | 2012 | 910 | | | 403 |
| | | | Xue Ning et al., | 2009 | 829 | Xiong Fuhao et al., | 2011 | 249 |

| | | |
|---|---|---|
| | | 842 |
| Su Jianping et al., | 2004 | 751 |
| Lu Xinxiang et al., | 2007 | 440 |
| Xia Xiaohong et al., | 2012 | 501 |
| | | 495 |
| Dang Jinhua et al., | 2011 | 345 |
| Liu Bin et al., | 2012 | 407 |
| | | 406 |
| Liu et al., | 2004 | 242 |
| | | 239 |
| Cheng Nengsong et al., | 2002 | 448 |
| | | 427 |
| | | 920 |
| Zhang Jianxin et al., | 2003 | 460 |
| Cheng Nengsong et al., | 1999 | 500 |
| Li Huaikun et al., | 2006 | 500 |
| China University of Geosciences (Wuhan) | 2003 | 438 |
| Zhu Yunhai et al., | 2005 | 419 |
| | | 401 |
| Li Fudong et al., | 1993 | 222 |
| | | 206 |
| | | 223 |
| Zhan fayu et al., | 2007 | 230 |
| | | 222 |
| | | 215 |
| | | 228 |
| | | 219 |
| Zhang Hongfei et al., | 2006 | 218 |
| Bian Qiantao et al., | 2007 | 402 |
| Lu Lu et al., | 2010 | 409 |

| | | | |
|---|---|---|---|
| | | | 391 |
| | Robbinson et al., | 2003 | 74 |
| | Li wei et al., | 2013 | 485 |
| | Li wei et al., | 2013 | 439 |
| | Li wei et al., | 2013 | 424 |
| | Li wei et al., | 2013 | 262 |
| | Li wei et al., | 2013 | 462 |
| | Li wei et al., | 2013 | 428 |
| | Li wei et al., | 2013 | 446 |

## Appendix to Chapter 3.2

Appendix S1 U-Pb analysis of detrital zircons from the 11 sandstone samples.

| Analysis number | Th/U | Isotopic ratios and errors | | | | | | | | Ages and errors (Ma) | | | | Disc. % |
|---|---|---|---|---|---|---|---|---|---|---|---|---|---|---|
| | | $^{207}Pb/^{206}Pb$ | 1σ | $^{207}Pb/^{235}U$ | 1σ | $^{206}Pb/^{238}U$ | 1σ | $^{207}Pb/^{206}Pb$ | 1σ | $^{207}Pb/^{235}U$ | 1 σ | $^{206}Pb/^{238}U$ | 1 σ | |
| Eboliang Section | | | | | | | | | | | | | | |
| **E122** | | | | | | | | | | | | | | |
| E122-01 | 0.52 | 0.0554 | 0.00116 | 0.49806 | 0.01086 | 0.0652 | 0.00089 | 428 | 26 | 410 | 7 | 407 | 5 | 0.74 |
| ~~E122-02~~ | ~~0.09~~ | ~~0.10225~~ | ~~0.0017~~ | ~~3.17139~~ | ~~0.05659~~ | ~~0.2249~~ | ~~0.00305~~ | ~~1665~~ | ~~15~~ | ~~1450~~ | ~~14~~ | ~~1308~~ | ~~16~~ | ~~27.29~~ |
| E122-03 | 0.12 | 0.05628 | 0.00709 | 0.31113 | 0.03871 | 0.04009 | 0.0008 | 464 | 287 | 275 | 30 | 253 | 5 | 8.70 |
| E122-04 | 0.16 | 0.05481 | 0.00117 | 0.4915 | 0.01088 | 0.06503 | 0.00089 | 404 | 26 | 406 | 7 | 406 | 5 | 0.00 |

| | | | | | | | | | | | | | | |
|---|---|---|---|---|---|---|---|---|---|---|---|---|---|---|
| E122-05 | 0.18 | 0.05521 | 0.00114 | 0.5273 | 0.01134 | 0.06926 | 0.00096 | 421 | 25 | 430 | 8 | 432 | 6 | -0.46 |
| E122-06 | 0.18 | 0.05579 | 0.0015 | 0.52337 | 0.01427 | 0.06803 | 0.00097 | 444 | 36 | 427 | 10 | 424 | 6 | 0.71 |
| E122-07 | 0.19 | 0.0672 | 0.00118 | 1.27243 | 0.02387 | 0.1373 | 0.00184 | 844 | 19 | 833 | 11 | 829 | 10 | 0.48 |
| E122-08 | 0.19 | 0.05133 | 0.00316 | 0.28735 | 0.01749 | 0.04059 | 0.00073 | 256 | 107 | 256 | 14 | 256 | 5 | 0.00 |
| E122-09 | 0.19 | 0.05678 | 0.00466 | 0.31603 | 0.02584 | 0.04036 | 0.00069 | 483 | 152 | 279 | 20 | 255 | 4 | 9.41 |
| E122-10 | 0.24 | 0.0513 | 0.00162 | 0.29954 | 0.00953 | 0.04234 | 0.00062 | 254 | 46 | 266 | 7 | 267 | 4 | -0.37 |
| E122-11 | 0.25 | 0.05551 | 0.00121 | 0.49239 | 0.01108 | 0.06432 | 0.00088 | 433 | 27 | 407 | 8 | 402 | 5 | 1.24 |
| E122-12 | 0.25 | 0.05504 | 0.00127 | 0.49814 | 0.01182 | 0.06563 | 0.00091 | 414 | 29 | 410 | 8 | 410 | 6 | 0.00 |
| E122-13 | 0.27 | 0.05629 | 0.00146 | 0.55426 | 0.01466 | 0.0714 | 0.00101 | 464 | 34 | 448 | 10 | 445 | 6 | 0.67 |
| ~~E122-14~~ | ~~0.28~~ | ~~0.07471~~ | ~~0.00135~~ | ~~1.18126~~ | ~~0.02263~~ | ~~0.11465~~ | ~~0.00156~~ | ~~1061~~ | ~~19~~ | ~~792~~ | ~~11~~ | ~~700~~ | ~~9~~ | ~~13.14~~ |
| E122-15 | 0.29 | 0.05495 | 0.00212 | 0.50292 | 0.01937 | 0.06637 | 0.00103 | 410 | 58 | 414 | 13 | 414 | 6 | 0.00 |
| E122-16 | 0.29 | 0.05454 | 0.00109 | 0.44195 | 0.00919 | 0.05876 | 0.0008 | 393 | 24 | 372 | 6 | 368 | 5 | 1.09 |
| ~~E122-17~~ | ~~0.30~~ | ~~0.08134~~ | ~~0.00178~~ | ~~1.97992~~ | ~~0.04471~~ | ~~0.1765~~ | ~~0.00248~~ | ~~1230~~ | ~~23~~ | ~~1109~~ | ~~15~~ | ~~1048~~ | ~~14~~ | ~~17.37~~ |
| E122-18 | 0.31 | 0.09088 | 0.00153 | 2.84816 | 0.05136 | 0.22725 | 0.00308 | 1444 | 16 | 1368 | 14 | 1320 | 16 | 9.39 |
| E122-19 | 0.32 | 0.0553 | 0.0016 | 0.50138 | 0.0147 | 0.06575 | 0.00094 | 424 | 40 | 413 | 10 | 410 | 6 | 0.73 |
| E122-20 | 0.33 | 0.06351 | 0.00113 | 1.01438 | 0.01925 | 0.11582 | 0.00157 | 725 | 20 | 711 | 10 | 706 | 9 | 0.71 |
| E122-21 | 0.34 | 0.0513 | 0.00253 | 0.28041 | 0.01376 | 0.03964 | 0.00062 | 254 | 84 | 251 | 11 | 251 | 4 | 0.00 |
| ~~E122-22~~ | ~~0.35~~ | ~~0.09845~~ | ~~0.00489~~ | ~~0.56439~~ | ~~0.02652~~ | ~~0.04158~~ | ~~0.00067~~ | ~~1595~~ | ~~95~~ | ~~454~~ | ~~17~~ | ~~263~~ | ~~4~~ | ~~72.62~~ |
| E122-23 | 0.35 | 0.05372 | 0.00244 | 0.40019 | 0.01802 | 0.05401 | 0.00088 | 359 | 72 | 342 | 13 | 339 | 5 | 0.88 |
| ~~E122-24~~ | ~~0.38~~ | ~~0.09506~~ | ~~0.00745~~ | ~~0.46102~~ | ~~0.03503~~ | ~~0.03517~~ | ~~0.00068~~ | ~~1529~~ | ~~152~~ | ~~385~~ | ~~24~~ | ~~223~~ | ~~4~~ | ~~72.65~~ |
| E122-25 | 0.39 | 0.05507 | 0.00122 | 0.51675 | 0.01183 | 0.06804 | 0.00095 | 415 | 27 | 423 | 8 | 424 | 6 | -0.24 |
| E122-26 | 0.41 | 0.05507 | 0.00176 | 0.52356 | 0.01692 | 0.06894 | 0.00099 | 415 | 47 | 428 | 11 | 430 | 6 | -0.47 |
| E122-27 | 0.41 | 0.11964 | 0.00289 | 5.55451 | 0.13611 | 0.33665 | 0.00504 | 1951 | 23 | 1909 | 21 | 1871 | 24 | 4.28 |
| E122-28 | 0.42 | 0.05454 | 0.00104 | 0.45579 | 0.00913 | 0.0606 | 0.00083 | 393 | 22 | 381 | 6 | 379 | 5 | 0.53 |
| ~~E122-29~~ | ~~0.43~~ | ~~0.16137~~ | ~~0.00292~~ | ~~8.3304~~ | ~~0.15825~~ | ~~0.37434~~ | ~~0.0053~~ | ~~2470~~ | ~~15~~ | ~~2268~~ | ~~17~~ | ~~2050~~ | ~~25~~ | ~~20.49~~ |
| E122-30 | 0.43 | 0.05508 | 0.00147 | 0.50454 | 0.0137 | 0.06643 | 0.00095 | 415 | 36 | 415 | 9 | 415 | 6 | 0.00 |
| E122-31 | 0.44 | 0.05561 | 0.0017 | 0.54981 | 0.0169 | 0.07169 | 0.00104 | 437 | 43 | 445 | 11 | 446 | 6 | -0.22 |
| E122-32 | 0.45 | 0.05523 | 0.00123 | 0.50988 | 0.01169 | 0.06694 | 0.00093 | 422 | 28 | 418 | 8 | 418 | 6 | 0.00 |

| | | | | | | | | | | | | | | |
|---|---|---|---|---|---|---|---|---|---|---|---|---|---|---|
| E122-33 | 0.45 | 0.05518 | 0.00151 | 0.5081 | 0.01407 | 0.06677 | 0.00098 | 420 | 36 | 417 | 9 | 417 | 6 | 0.00 |
| ~~E122-34~~ | ~~0.45~~ | ~~0.0697~~ | ~~0.00222~~ | ~~0.8972~~ | ~~0.02559~~ | ~~0.09336~~ | ~~0.00131~~ | ~~919~~ | ~~67~~ | ~~650~~ | ~~14~~ | ~~575~~ | ~~8~~ | ~~13.04~~ |
| E122-35 | 0.45 | 0.05097 | 0.00256 | 0.27525 | 0.01381 | 0.03916 | 0.00061 | 239 | 87 | 247 | 11 | 248 | 4 | -0.40 |
| E122-36 | 0.47 | 0.10084 | 0.00221 | 3.94729 | 0.08912 | 0.28383 | 0.00409 | 1640 | 22 | 1623 | 18 | 1611 | 21 | 1.80 |
| E122-37 | 0.48 | 0.05502 | 0.00133 | 0.51592 | 0.01277 | 0.068 | 0.00096 | 413 | 31 | 422 | 9 | 424 | 6 | -0.47 |
| E122-38 | 0.49 | 0.05141 | 0.00198 | 0.28248 | 0.0108 | 0.03985 | 0.00062 | 259 | 59 | 253 | 9 | 252 | 4 | 0.40 |
| ~~E122-39~~ | ~~0.50~~ | ~~0.06467~~ | ~~0.00209~~ | ~~0.568~~ | ~~0.01841~~ | ~~0.06369~~ | ~~0.00094~~ | ~~764~~ | ~~44~~ | ~~457~~ | ~~12~~ | ~~398~~ | ~~6~~ | ~~14.82~~ |
| E122-40 | 0.50 | 0.05297 | 0.00156 | 0.3766 | 0.01117 | 0.05156 | 0.00075 | 328 | 41 | 325 | 8 | 324 | 5 | 0.31 |
| E122-41 | 0.51 | 0.05126 | 0.00194 | 0.2897 | 0.01089 | 0.04098 | 0.00064 | 253 | 58 | 258 | 9 | 259 | 4 | -0.39 |
| E122-42 | 0.51 | 0.05618 | 0.00154 | 0.57044 | 0.01584 | 0.07362 | 0.00107 | 459 | 36 | 458 | 10 | 458 | 6 | 0.00 |
| E122-43 | 0.51 | 0.05501 | 0.00152 | 0.50342 | 0.01404 | 0.06636 | 0.00098 | 413 | 36 | 414 | 9 | 414 | 6 | 0.00 |
| E122-44 | 0.52 | 0.05507 | 0.00129 | 0.51751 | 0.01242 | 0.06814 | 0.00097 | 415 | 29 | 423 | 8 | 425 | 6 | -0.47 |
| E122-45 | 0.52 | 0.0556 | 0.00173 | 0.52994 | 0.01657 | 0.06912 | 0.00104 | 436 | 43 | 432 | 11 | 431 | 6 | 0.23 |
| E122-46 | 0.53 | 0.05334 | 0.00145 | 0.37283 | 0.01026 | 0.05069 | 0.00074 | 343 | 36 | 322 | 8 | 319 | 5 | 0.94 |
| E122-47 | 0.54 | 0.05533 | 0.00128 | 0.52147 | 0.01242 | 0.06833 | 0.00097 | 426 | 29 | 426 | 8 | 426 | 6 | 0.00 |
| ~~E122-48~~ | ~~0.55~~ | ~~0.13115~~ | ~~0.00775~~ | ~~0.68322~~ | ~~0.03829~~ | ~~0.03778~~ | ~~0.00071~~ | ~~2113~~ | ~~106~~ | ~~529~~ | ~~23~~ | ~~239~~ | 4 | ~~121.34~~ |
| E122-49 | 0.57 | 0.055 | 0.00242 | 0.51077 | 0.02238 | 0.06734 | 0.00108 | 412 | 69 | 419 | 15 | 420 | 7 | -0.24 |
| E122-50 | 0.57 | 0.05541 | 0.00138 | 0.5364 | 0.01363 | 0.07019 | 0.00101 | 429 | 32 | 436 | 9 | 437 | 6 | -0.23 |
| E122-51 | 0.57 | 0.05666 | 0.00166 | 0.55631 | 0.01635 | 0.0712 | 0.00106 | 478 | 39 | 449 | 11 | 443 | 6 | 1.35 |
| E122-52 | 0.58 | 0.05523 | 0.002 | 0.52011 | 0.01886 | 0.06829 | 0.00102 | 422 | 54 | 425 | 13 | 426 | 6 | -0.23 |
| E122-53 | 0.58 | 0.05501 | 0.00157 | 0.50499 | 0.01456 | 0.06657 | 0.00097 | 413 | 39 | 415 | 10 | 415 | 6 | 0.00 |
| E122-54 | 0.58 | 0.07188 | 0.00161 | 1.64689 | 0.03795 | 0.16613 | 0.00238 | 983 | 25 | 988 | 15 | 991 | 13 | -0.30 |
| E122-55 | 0.59 | 0.04605 | 0.00345 | 0.2773 | 0.02022 | 0.04368 | 0.00074 | | 166 | 249 | 16 | 276 | 5 | -9.78 |
| E122-56 | 0.59 | 0.0591 | 0.00166 | 0.53659 | 0.01514 | 0.06583 | 0.00098 | 571 | 36 | 436 | 10 | 411 | 6 | 6.08 |
| ~~E122-57~~ | ~~0.60~~ | ~~0.06445~~ | ~~0.00268~~ | ~~0.39721~~ | ~~0.01639~~ | ~~0.04469~~ | ~~0.00072~~ | ~~756~~ | ~~60~~ | ~~340~~ | ~~12~~ | ~~282~~ | ~~4~~ | ~~20.57~~ |
| E122-58 | 0.61 | 0.05561 | 0.00152 | 0.52775 | 0.01456 | 0.06882 | 0.001 | 437 | 36 | 430 | 10 | 429 | 6 | 0.23 |
| ~~E122-59~~ | ~~0.62~~ | ~~0.09041~~ | ~~0.00283~~ | ~~2.28277~~ | ~~0.06365~~ | ~~0.18312~~ | ~~0.00262~~ | ~~1434~~ | ~~61~~ | ~~1207~~ | ~~20~~ | ~~1084~~ | ~~14~~ | ~~32.29~~ |

| | | | | | | | | | | | | | | |
|---|---|---|---|---|---|---|---|---|---|---|---|---|---|---|
| E122-60 | 0.62 | 0.05407 | 0.00151 | 0.44631 | 0.01261 | 0.05985 | 0.00088 | 374 | 38 | 375 | 9 | 375 | 5 | 0.00 |
| E122-61 | 0.63 | 0.05343 | 0.00786 | 0.43342 | 0.06326 | 0.05882 | 0.00141 | 347 | 282 | 366 | 45 | 368 | 9 | -0.54 |
| E122-62 | 0.65 | 0.05118 | 0.00209 | 0.27503 | 0.01117 | 0.03897 | 0.00063 | 249 | 64 | 247 | 9 | 246 | 4 | 0.41 |
| ~~E122-63~~ | ~~0.65~~ | ~~0.0837~~ | ~~0.00219~~ | ~~2.01817~~ | ~~0.05349~~ | ~~0.17484~~ | ~~0.00258~~ | ~~1286~~ | ~~29~~ | ~~1122~~ | ~~18~~ | ~~1039~~ | ~~14~~ | ~~23.77~~ |
| E122-64 | 0.66 | 0.09948 | 0.00219 | 3.725 | 0.08429 | 0.27151 | 0.00392 | 1614 | 22 | 1577 | 18 | 1548 | 20 | 4.26 |
| E122-65 | 0.67 | 0.05106 | 0.00209 | 0.28513 | 0.01163 | 0.04049 | 0.00064 | 244 | 65 | 255 | 9 | 256 | 4 | -0.39 |
| E122-66 | 0.68 | 0.05556 | 0.0018 | 0.54149 | 0.01764 | 0.07067 | 0.00106 | 435 | 46 | 439 | 12 | 440 | 6 | -0.23 |
| E122-67 | 0.68 | 0.05635 | 0.0014 | 0.58911 | 0.01491 | 0.07581 | 0.0011 | 466 | 31 | 470 | 10 | 471 | 7 | -0.21 |
| ~~E122-68~~ | ~~0.68~~ | ~~0.07969~~ | ~~0.00195~~ | ~~1.58734~~ | ~~0.03961~~ | ~~0.14444~~ | ~~0.00211~~ | ~~1189~~ | ~~27~~ | ~~965~~ | ~~16~~ | ~~870~~ | ~~12~~ | ~~10.92~~ |
| E122-69 | 0.70 | 0.05562 | 0.00187 | 0.52307 | 0.01753 | 0.06819 | 0.00105 | 437 | 47 | 427 | 12 | 425 | 6 | 0.47 |
| E122-70 | 0.70 | 0.05524 | 0.00295 | 0.51502 | 0.02697 | 0.06761 | 0.00128 | 422 | 83 | 422 | 18 | 422 | 8 | 0.00 |
| E122-71 | 0.70 | 0.05647 | 0.00143 | 0.58703 | 0.01512 | 0.07538 | 0.0011 | 471 | 32 | 469 | 10 | 468 | 7 | 0.21 |
| E122-72 | 0.70 | 0.05211 | 0.00238 | 0.33275 | 0.01515 | 0.04631 | 0.00074 | 290 | 75 | 292 | 12 | 292 | 5 | 0.00 |
| E122-73 | 0.74 | 0.05485 | 0.00231 | 0.48992 | 0.02046 | 0.06477 | 0.00104 | 406 | 65 | 405 | 14 | 405 | 6 | 0.00 |
| E122-74 | 0.76 | 0.06537 | 0.00168 | 1.10357 | 0.02876 | 0.12242 | 0.00181 | 786 | 31 | 755 | 14 | 744 | 10 | 1.48 |
| E122-75 | 0.77 | 0.05685 | 0.00226 | 0.29848 | 0.01178 | 0.03807 | 0.00061 | 486 | 59 | 265 | 9 | 241 | 4 | 9.96 |
| ~~E122-76~~ | ~~0.80~~ | ~~0.0975~~ | ~~0.00224~~ | ~~2.60489~~ | ~~0.06112~~ | ~~0.19372~~ | ~~0.00282~~ | ~~1577~~ | ~~23~~ | ~~1302~~ | ~~17~~ | ~~1141~~ | ~~15~~ | ~~38.21~~ |
| E122-77 | 0.81 | 0.06175 | 0.00236 | 0.77124 | 0.02943 | 0.09057 | 0.00143 | 665 | 55 | 580 | 17 | 559 | 8 | 3.76 |
| E122-78 | 0.83 | 0.05534 | 0.00141 | 0.52063 | 0.01342 | 0.06822 | 0.00101 | 426 | 32 | 426 | 9 | 425 | 6 | 0.24 |
| ~~E122-79~~ | ~~0.84~~ | ~~0.07033~~ | ~~0.00162~~ | ~~0.89965~~ | ~~0.02117~~ | ~~0.09276~~ | ~~0.00134~~ | ~~938~~ | ~~26~~ | ~~652~~ | ~~11~~ | ~~572~~ | ~~8~~ | ~~13.99~~ |
| E122-80 | 0.84 | 0.05573 | 0.00147 | 0.48095 | 0.01284 | 0.06258 | 0.00093 | 442 | 34 | 399 | 9 | 391 | 6 | 2.05 |
| E122-81 | 0.84 | 0.05449 | 0.00135 | 0.49646 | 0.01249 | 0.06607 | 0.00097 | 391 | 31 | 409 | 8 | 412 | 6 | -0.73 |
| E122-82 | 0.86 | 0.0556 | 0.0017 | 0.52104 | 0.01595 | 0.06795 | 0.00103 | 436 | 41 | 426 | 11 | 424 | 6 | 0.47 |
| E122-83 | 0.89 | 0.07142 | 0.0018 | 1.49145 | 0.03811 | 0.15142 | 0.00225 | 969 | 29 | 927 | 16 | 909 | 13 | 1.98 |
| E122-84 | 0.90 | 0.0546 | 0.00145 | 0.407 | 0.01088 | 0.05405 | 0.00081 | 396 | 34 | 347 | 8 | 339 | 5 | 2.36 |
| E122-85 | 0.93 | 0.05119 | 0.00257 | 0.29461 | 0.01465 | 0.04173 | 0.0007 | 249 | 83 | 262 | 11 | 264 | 4 | -0.76 |
| E122-86 | 0.94 | 0.0557 | 0.00189 | 0.54539 | 0.01853 | 0.071 | 0.00109 | 440 | 48 | 442 | 12 | 442 | 7 | 0.00 |
| E122-87 | 0.94 | 0.0552 | 0.00166 | 0.523 | 0.01579 | 0.0687 | 0.00103 | 420 | 41 | 427 | 11 | 428 | 6 | -0.23 |

| | | | | | | | | | | | | | | |
|---|---|---|---|---|---|---|---|---|---|---|---|---|---|---|
| ~~E122-88~~ | ~~0.96~~ | ~~0.09752~~ | ~~0.00238~~ | ~~3.23386~~ | ~~0.0803~~ | ~~0.24046~~ | ~~0.00357~~ | ~~1577~~ | ~~25~~ | ~~1465~~ | ~~19~~ | ~~1389~~ | ~~19~~ | ~~13.53~~ |
| E122-89 | 1.01 | 0.05121 | 0.00142 | 0.28193 | 0.00787 | 0.03992 | 0.00061 | 250 | 37 | 252 | 6 | 252 | 4 | 0.00 |
| E122-90 | 1.02 | 0.06166 | 0.00154 | 0.59592 | 0.01513 | 0.07008 | 0.00103 | 662 | 30 | 475 | 10 | 437 | 6 | 8.70 |
| E122-91 | 1.06 | 0.05508 | 0.00184 | 0.51205 | 0.01705 | 0.06741 | 0.00106 | 415 | 46 | 420 | 11 | 421 | 6 | -0.24 |
| E122-92 | 1.10 | 0.05699 | 0.00202 | 0.62179 | 0.02192 | 0.07912 | 0.00125 | 491 | 50 | 491 | 14 | 491 | 7 | 0.00 |
| E122-93 | 1.11 | 0.05629 | 0.00314 | 0.34594 | 0.01915 | 0.04457 | 0.00075 | 464 | 93 | 302 | 14 | 281 | 5 | 7.47 |
| E122-94 | 1.12 | 0.05637 | 0.00215 | 0.60428 | 0.02298 | 0.07773 | 0.00123 | 467 | 56 | 480 | 15 | 483 | 7 | -0.62 |
| E122-95 | 1.17 | 0.0533 | 0.00164 | 0.41201 | 0.01269 | 0.05605 | 0.00086 | 342 | 42 | 350 | 9 | 352 | 5 | -0.57 |
| E122-96 | 1.24 | 0.05529 | 0.00226 | 0.51791 | 0.02096 | 0.06792 | 0.00113 | 424 | 61 | 424 | 14 | 424 | 7 | 0.00 |
| E122-97 | 1.27 | 0.05657 | 0.00382 | 0.61391 | 0.04095 | 0.07868 | 0.00151 | 475 | 114 | 486 | 26 | 488 | 9 | -0.41 |
| E122-98 | 1.32 | 0.05663 | 0.00182 | 0.55621 | 0.01781 | 0.07123 | 0.00112 | 477 | 43 | 449 | 12 | 444 | 7 | 1.13 |
| E122-99 | 1.36 | 0.06638 | 0.00331 | 0.89959 | 0.04256 | 0.09828 | 0.00152 | 819 | 107 | 652 | 23 | 604 | 9 | 7.95 |
| E122-100 | 1.50 | 0.07139 | 0.00189 | 1.53676 | 0.04099 | 0.15608 | 0.00235 | 969 | 31 | 945 | 16 | 935 | 13 | 1.07 |
| E122-101 | 1.58 | 0.05153 | 0.00188 | 0.2918 | 0.01062 | 0.04106 | 0.00065 | 265 | 54 | 260 | 8 | 259 | 4 | 0.39 |
| ~~E122-102~~ | ~~1.74~~ | ~~0.11687~~ | ~~0.00301~~ | ~~3.01009~~ | ~~0.07827~~ | ~~0.18676~~ | ~~0.00283~~ | ~~1909~~ | ~~26~~ | ~~1410~~ | ~~20~~ | ~~1104~~ | ~~15~~ | ~~72.92~~ |
| ~~E122-103~~ | ~~1.79~~ | ~~0.05947~~ | ~~0.01845~~ | ~~0.20007~~ | ~~0.06186~~ | ~~0.0244~~ | ~~0.00064~~ | ~~584~~ | ~~602~~ | ~~185~~ | ~~52~~ | ~~155~~ | ~~4~~ | ~~19.35~~ |
| E122-104 | 1.80 | 0.05372 | 0.00165 | 0.42462 | 0.01306 | 0.05732 | 0.00089 | 359 | 42 | 359 | 9 | 359 | 5 | 0.00 |
| E122-105 | 2.51 | 0.0705 | 0.00188 | 1.43784 | 0.03868 | 0.14788 | 0.00224 | 943 | 31 | 905 | 16 | 889 | 13 | 1.80 |
| | | | | | | | | | | | | | | |
| **E123** | | | | | | | | | | | | | | |
| E123-01 | 0.83 | 0.05097 | 0.00166 | 0.27264 | 0.00884 | 0.03879 | 0.0006 | 239 | 46 | 245 | 7 | 245 | 4 | 0.00 |
| E123-02 | 0.70 | 0.05628 | 0.002 | 0.58143 | 0.02066 | 0.07492 | 0.00113 | 463 | 52 | 465 | 13 | 466 | 7 | -0.21 |
| E123-03 | 0.36 | 0.05547 | 0.00175 | 0.53115 | 0.01682 | 0.06944 | 0.00103 | 431 | 44 | 433 | 11 | 433 | 6 | 0.00 |
| E123-04 | 0.66 | 0.05529 | 0.00125 | 0.51648 | 0.01201 | 0.06774 | 0.00095 | 424 | 28 | 423 | 8 | 423 | 6 | 0.00 |
| E123-05 | 1.03 | 0.0513 | 0.00208 | 0.28237 | 0.0114 | 0.03992 | 0.00062 | 254 | 64 | 253 | 9 | 252 | 4 | 0.40 |
| E123-06 | 0.12 | 0.0703 | 0.00142 | 1.47643 | 0.03105 | 0.1523 | 0.0021 | 937 | 22 | 921 | 13 | 914 | 12 | 0.77 |
| E123-07 | 0.78 | 0.05064 | 0.00159 | 0.24322 | 0.00765 | 0.03483 | 0.00052 | 224 | 45 | 221 | 6 | 221 | 3 | 0.00 |
| E123-08 | 0.63 | 0.05531 | 0.00153 | 0.52283 | 0.01466 | 0.06854 | 0.00098 | 425 | 37 | 427 | 10 | 427 | 6 | 0.00 |

| | | | | | | | | | | | | | | |
|---|---|---|---|---|---|---|---|---|---|---|---|---|---|---|
| E123-09 | 0.62 | 0.05533 | 0.00148 | 0.52074 | 0.01408 | 0.06825 | 0.00099 | 426 | 35 | 426 | 9 | 426 | 6 | 0.00 |
| E123-10 | 0.62 | 0.05152 | 0.00304 | 0.29557 | 0.01726 | 0.0416 | 0.00074 | 264 | 101 | 263 | 14 | 263 | 5 | 0.00 |
| E123-11 | 0.71 | 0.05576 | 0.00268 | 0.54452 | 0.02594 | 0.07082 | 0.00116 | 443 | 77 | 441 | 17 | 441 | 7 | 0.00 |
| E123-12 | 0.52 | 0.07203 | 0.00162 | 1.52594 | 0.03533 | 0.15363 | 0.00216 | 987 | 25 | 941 | 14 | 921 | 12 | 2.17 |
| E123-13 | 0.55 | 0.05139 | 0.00238 | 0.28751 | 0.0132 | 0.04057 | 0.00066 | 258 | 75 | 257 | 10 | 256 | 4 | 0.39 |
| E123-14 | 0.13 | 0.07048 | 0.00142 | 1.4688 | 0.03084 | 0.15113 | 0.00208 | 942 | 22 | 918 | 13 | 907 | 12 | 1.21 |
| E123-15 | 0.64 | 0.05518 | 0.00135 | 0.51406 | 0.01287 | 0.06756 | 0.00096 | 420 | 31 | 421 | 9 | 421 | 6 | 0.00 |
| E123-16 | 0.59 | 0.06948 | 0.00156 | 1.45273 | 0.03344 | 0.15162 | 0.00215 | 913 | 25 | 911 | 14 | 910 | 12 | 0.11 |
| E123-17 | 0.76 | 0.05089 | 0.00226 | 0.26417 | 0.01166 | 0.03764 | 0.0006 | 236 | 72 | 238 | 9 | 238 | 4 | 0.00 |
| E123-18 | 0.12 | 0.06917 | 0.00141 | 1.42494 | 0.03016 | 0.14938 | 0.00207 | 904 | 22 | 899 | 13 | 897 | 12 | 0.22 |
| E123-19 | 0.77 | 0.05102 | 0.00172 | 0.26664 | 0.00902 | 0.0379 | 0.00057 | 242 | 50 | 240 | 7 | 240 | 4 | 0.00 |
| E123-20 | 0.35 | 0.05391 | 0.00194 | 0.45125 | 0.01497 | 0.06071 | 0.00085 | 367 | 83 | 378 | 10 | 380 | 5 | -0.53 |
| E123-21 | 0.10 | 0.07142 | 0.00142 | 1.45737 | 0.03036 | 0.14798 | 0.00203 | 969 | 22 | 913 | 13 | 890 | 11 | 2.58 |
| E123-22 | 0.54 | 0.05527 | 0.00153 | 0.51887 | 0.01453 | 0.06807 | 0.00098 | 423 | 37 | 424 | 10 | 425 | 6 | -0.24 |
| E123-23 | 0.14 | 0.07088 | 0.00142 | 1.46728 | 0.03071 | 0.15011 | 0.00207 | 954 | 22 | 917 | 13 | 902 | 12 | 1.66 |
| E123-24 | 0.12 | 0.0692 | 0.00141 | 1.46157 | 0.03099 | 0.15316 | 0.00212 | 905 | 22 | 915 | 13 | 919 | 12 | -0.44 |
| E123-25 | 0.80 | 0.05104 | 0.00168 | 0.27668 | 0.00915 | 0.03931 | 0.00058 | 243 | 49 | 248 | 7 | 249 | 4 | -0.40 |
| E123-26 | 0.65 | 0.05108 | 0.00205 | 0.27479 | 0.01101 | 0.03901 | 0.0006 | 244 | 64 | 247 | 9 | 247 | 4 | 0.00 |
| E123-27 | 0.69 | 0.05714 | 0.0013 | 0.58866 | 0.01374 | 0.0747 | 0.00105 | 497 | 28 | 470 | 9 | 464 | 6 | 1.29 |
| E123-28 | 0.63 | 0.05523 | 0.00144 | 0.5166 | 0.01363 | 0.06783 | 0.00098 | 422 | 34 | 423 | 9 | 423 | 6 | 0.00 |
| E123-29 | 0.84 | 0.0561 | 0.00148 | 0.51941 | 0.01389 | 0.06714 | 0.00096 | 456 | 35 | 425 | 9 | 419 | 6 | 1.43 |
| ~~E123-30~~ | ~~0.59~~ | ~~0.06137~~ | ~~0.00201~~ | ~~0.32562~~ | ~~0.01071~~ | ~~0.03847~~ | ~~0.00057~~ | ~~652~~ | ~~45~~ | ~~286~~ | ~~8~~ | ~~243~~ | 4 | ~~17.70~~ |
| E123-31 | 0.45 | 0.05632 | 0.00152 | 0.58867 | 0.01611 | 0.07579 | 0.00109 | 465 | 36 | 470 | 10 | 471 | 7 | -0.21 |
| E123-32 | 0.59 | 0.05144 | 0.00318 | 0.28371 | 0.01738 | 0.04 | 0.00068 | 261 | 109 | 254 | 14 | 253 | 4 | 0.40 |
| E123-33 | 0.78 | 0.05086 | 0.00182 | 0.26311 | 0.00941 | 0.03751 | 0.00057 | 234 | 54 | 237 | 8 | 237 | 4 | 0.00 |
| E123-34 | 0.18 | 0.05564 | 0.00125 | 0.49308 | 0.01142 | 0.06426 | 0.0009 | 438 | 28 | 407 | 8 | 401 | 5 | 1.50 |
| E123-35 | 0.60 | 0.05502 | 0.0015 | 0.50697 | 0.01403 | 0.06681 | 0.00095 | 413 | 37 | 416 | 9 | 417 | 6 | -0.24 |
| E123-36 | 0.64 | 0.05579 | 0.00159 | 0.52287 | 0.01508 | 0.06797 | 0.00098 | 444 | 39 | 427 | 10 | 424 | 6 | 0.71 |

| | | | | | | | | | | | | | | |
|---|---|---|---|---|---|---|---|---|---|---|---|---|---|---|
| E123-37 | 0.63 | 0.05135 | 0.00338 | 0.28958 | 0.01893 | 0.04089 | 0.0007 | 257 | 119 | 258 | 15 | 258 | 4 | 0.00 |
| E123-38 | 0.73 | 0.06904 | 0.00146 | 1.43813 | 0.03158 | 0.15104 | 0.0021 | 900 | 24 | 905 | 13 | 907 | 12 | -0.22 |
| E123-39 | 0.53 | 0.05526 | 0.00169 | 0.51676 | 0.01598 | 0.06781 | 0.00098 | 423 | 43 | 423 | 11 | 423 | 6 | 0.00 |
| E123-40 | 0.56 | 0.05576 | 0.00161 | 0.54797 | 0.01593 | 0.07126 | 0.00104 | 443 | 39 | 444 | 10 | 444 | 6 | 0.00 |
| E123-41 | 0.51 | 0.05489 | 0.00152 | 0.50169 | 0.01413 | 0.06627 | 0.00095 | 408 | 38 | 413 | 10 | 414 | 6 | -0.24 |
| ~~E123-42~~ | ~~0.27~~ | ~~0.0871~~ | ~~0.00191~~ | ~~1.26754~~ | ~~0.02858~~ | ~~0.10553~~ | ~~0.00148~~ | ~~1363~~ | ~~23~~ | ~~831~~ | ~~13~~ | ~~647~~ | ~~9~~ | ~~28.44~~ |
| E123-43 | 1.28 | 0.0508 | 0.00198 | 0.25868 | 0.01003 | 0.03693 | 0.00058 | 232 | 60 | 234 | 8 | 234 | 4 | 0.00 |
| E123-44 | 0.56 | 0.05571 | 0.00229 | 0.52089 | 0.02129 | 0.0678 | 0.00109 | 441 | 62 | 426 | 14 | 423 | 7 | 0.71 |
| ~~E123-45~~ | ~~0.72~~ | ~~0.07834~~ | ~~0.00199~~ | ~~1.87648~~ | ~~0.04827~~ | ~~0.1737~~ | ~~0.00256~~ | ~~1156~~ | ~~28~~ | ~~1073~~ | ~~17~~ | ~~1032~~ | ~~14~~ | ~~12.02~~ |
| E123-46 | 0.22 | 0.06928 | 0.00159 | 1.5055 | 0.03533 | 0.15759 | 0.00223 | 907 | 26 | 933 | 14 | 943 | 12 | -1.06 |
| E123-47 | 0.24 | 0.07269 | 0.00251 | 1.815 | 0.06263 | 0.18106 | 0.00279 | 1005 | 45 | 1051 | 23 | 1073 | 15 | -6.34 |
| E123-48 | 0.82 | 0.05511 | 0.00153 | 0.48839 | 0.01374 | 0.06427 | 0.00093 | 417 | 37 | 404 | 9 | 402 | 6 | 0.50 |
| E123-49 | 0.39 | 0.06985 | 0.00143 | 1.4017 | 0.02987 | 0.14552 | 0.00201 | 924 | 23 | 890 | 13 | 876 | 11 | 1.60 |
| ~~E123-50~~ | ~~0.73~~ | ~~0.06627~~ | ~~0.00237~~ | ~~0.35375~~ | ~~0.01263~~ | ~~0.03871~~ | ~~0.00059~~ | ~~815~~ | ~~49~~ | ~~308~~ | ~~9~~ | ~~245~~ | ~~4~~ | ~~25.71~~ |
| E123-51 | 1.40 | 0.05264 | 0.00211 | 0.37941 | 0.0152 | 0.05226 | 0.00079 | 313 | 63 | 327 | 11 | 328 | 5 | -0.30 |
| E123-52 | 1.11 | 0.05088 | 0.00486 | 0.26747 | 0.02536 | 0.03812 | 0.00072 | 235 | 179 | 241 | 20 | 241 | 4 | 0.00 |
| E123-53 | 0.45 | 0.07113 | 0.00157 | 1.49981 | 0.03415 | 0.15289 | 0.00214 | 961 | 25 | 930 | 14 | 917 | 12 | 1.42 |
| E123-54 | 0.50 | 0.05521 | 0.00163 | 0.52659 | 0.01561 | 0.06917 | 0.00102 | 421 | 40 | 430 | 10 | 431 | 6 | -0.23 |
| E123-55 | 0.59 | 0.05122 | 0.00205 | 0.28835 | 0.01144 | 0.04082 | 0.00065 | 251 | 62 | 257 | 9 | 258 | 4 | -0.39 |
| E123-56 | 0.63 | 0.05541 | 0.00159 | 0.52393 | 0.01514 | 0.06856 | 0.00099 | 429 | 39 | 428 | 10 | 427 | 6 | 0.23 |
| E123-57 | 0.79 | 0.05366 | 0.00248 | 0.28451 | 0.01309 | 0.03845 | 0.0006 | 357 | 76 | 254 | 10 | 243 | 4 | 4.53 |
| E123-59 | 0.10 | 0.06964 | 0.00191 | 1.3939 | 0.03297 | 0.14517 | 0.002 | 918 | 58 | 886 | 14 | 874 | 11 | 1.37 |
| E123-60 | 0.71 | 0.0963 | 0.00223 | 3.29517 | 0.07781 | 0.24812 | 0.00358 | 1554 | 24 | 1480 | 18 | 1429 | 18 | 8.75 |
| E123-61 | 0.51 | 0.0556 | 0.00176 | 0.53196 | 0.01692 | 0.06937 | 0.00102 | 436 | 45 | 433 | 11 | 432 | 6 | 0.23 |
| E123-62 | 0.24 | 0.07365 | 0.0018 | 1.52621 | 0.03787 | 0.15026 | 0.00217 | 1032 | 28 | 941 | 15 | 902 | 12 | 4.32 |
| E123-63 | 1.08 | 0.05214 | 0.00858 | 0.34281 | 0.05605 | 0.04768 | 0.00115 | 292 | 304 | 299 | 42 | 300 | 7 | -0.33 |
| E123-64 | 0.40 | 0.05588 | 0.00222 | 0.57166 | 0.02265 | 0.07418 | 0.00114 | 448 | 61 | 459 | 15 | 461 | 7 | -0.43 |
| E123-65 | 0.70 | 0.05069 | 0.00141 | 0.25851 | 0.00728 | 0.03698 | 0.00053 | 227 | 39 | 233 | 6 | 234 | 3 | -0.43 |

| | | | | | | | | | | | | | | |
|---|---|---|---|---|---|---|---|---|---|---|---|---|---|---|
| E123-66 | 0.54 | 0.05556 | 0.00169 | 0.52553 | 0.01606 | 0.06859 | 0.00101 | 435 | 42 | 429 | 11 | 428 | 6 | 0.23 |
| E123-67 | 0.85 | 0.05074 | 0.00286 | 0.26611 | 0.01483 | 0.03803 | 0.00066 | 229 | 97 | 240 | 12 | 241 | 4 | -0.41 |
| ~~E123-68~~ | ~~0.20~~ | ~~0.09592~~ | ~~0.00204~~ | ~~2.57881~~ | ~~0.05687~~ | ~~0.19496~~ | ~~0.00271~~ | ~~1546~~ | ~~22~~ | ~~1295~~ | ~~16~~ | ~~1148~~ | ~~15~~ | ~~34.67~~ |
| E123-69 | 0.13 | 0.07016 | 0.00162 | 1.44615 | 0.03424 | 0.14945 | 0.00211 | 933 | 26 | 908 | 14 | 898 | 12 | 1.11 |
| E123-70 | 0.78 | 0.05119 | 0.00296 | 0.27501 | 0.01585 | 0.03896 | 0.00062 | 249 | 104 | 247 | 13 | 246 | 4 | 0.41 |
| E123-71 | 0.80 | 0.05555 | 0.00145 | 0.5316 | 0.0141 | 0.06939 | 0.001 | 434 | 34 | 433 | 9 | 432 | 6 | 0.23 |
| E123-72 | 0.65 | 0.0558 | 0.0021 | 0.54425 | 0.02039 | 0.07073 | 0.0011 | 444 | 56 | 441 | 13 | 441 | 7 | 0.00 |
| E123-73 | 0.75 | 0.06901 | 0.0019 | 1.44684 | 0.04016 | 0.15202 | 0.00225 | 899 | 33 | 909 | 17 | 912 | 13 | -0.33 |
| E123-74 | 0.86 | 0.05131 | 0.00263 | 0.27103 | 0.01368 | 0.0383 | 0.00068 | 255 | 83 | 244 | 11 | 242 | 4 | 0.83 |
| E123-75 | 0.57 | 0.05151 | 0.00294 | 0.2841 | 0.01604 | 0.03999 | 0.0007 | 264 | 97 | 254 | 13 | 253 | 4 | 0.40 |
| E123-76 | 0.80 | 0.05116 | 0.00229 | 0.27836 | 0.01232 | 0.03945 | 0.00065 | 248 | 71 | 249 | 10 | 249 | 4 | 0.00 |
| E123-77 | 0.15 | 0.07006 | 0.00172 | 1.46182 | 0.03654 | 0.15129 | 0.00218 | 930 | 28 | 915 | 15 | 908 | 12 | 0.77 |
| E123-78 | 0.80 | 0.05085 | 0.00563 | 0.26438 | 0.02904 | 0.0377 | 0.00076 | 234 | 210 | 238 | 23 | 239 | 5 | -0.42 |
| E123-79 | 0.60 | 0.05109 | 0.00275 | 0.27516 | 0.01471 | 0.03905 | 0.00063 | 245 | 93 | 247 | 12 | 247 | 4 | 0.00 |
| E123-80 | 0.09 | 0.06919 | 0.00193 | 1.34945 | 0.03279 | 0.14146 | 0.00196 | 904 | 59 | 867 | 14 | 853 | 11 | 1.64 |
| E123-81 | 0.77 | 0.05391 | 0.00344 | 0.44454 | 0.02802 | 0.05979 | 0.0011 | 367 | 109 | 373 | 20 | 374 | 7 | -0.27 |
| E123-82 | 0.55 | 0.05545 | 0.0019 | 0.52855 | 0.01806 | 0.06912 | 0.00106 | 430 | 49 | 431 | 12 | 431 | 6 | 0.00 |
| E123-83 | 0.92 | 0.05107 | 0.00315 | 0.27385 | 0.01675 | 0.03889 | 0.00067 | 244 | 109 | 246 | 13 | 246 | 4 | 0.00 |
| E123-84 | 0.69 | 0.05182 | 0.00209 | 0.31246 | 0.01255 | 0.04372 | 0.00068 | 277 | 63 | 276 | 10 | 276 | 4 | 0.00 |
| E123-85 | 0.57 | 0.05476 | 0.00145 | 0.48306 | 0.01291 | 0.06397 | 0.00093 | 402 | 34 | 400 | 9 | 400 | 6 | 0.00 |
| E123-86 | 0.79 | 0.05449 | 0.00189 | 0.47864 | 0.01653 | 0.06369 | 0.00099 | 391 | 50 | 397 | 11 | 398 | 6 | -0.25 |
| E123-87 | 0.82 | 0.05824 | 0.00187 | 0.533 | 0.01706 | 0.06636 | 0.00101 | 539 | 44 | 434 | 11 | 414 | 6 | 4.83 |
| ~~E123-88~~ | ~~0.57~~ | ~~0.06186~~ | ~~0.00182~~ | ~~0.54314~~ | ~~0.01609~~ | ~~0.06367~~ | ~~0.00093~~ | ~~669~~ | ~~39~~ | ~~440~~ | ~~11~~ | ~~398~~ | ~~6~~ | ~~10.55~~ |
| E123-89 | 1.55 | 0.05089 | 0.00813 | 0.26653 | 0.04218 | 0.03798 | 0.001 | 236 | 288 | 240 | 34 | 240 | 6 | 0.00 |
| E123-90 | 0.60 | 0.05511 | 0.00147 | 0.46725 | 0.01263 | 0.06148 | 0.00089 | 417 | 35 | 389 | 9 | 385 | 5 | 1.04 |
| E123-91 | 0.49 | 0.05527 | 0.0016 | 0.52338 | 0.01525 | 0.06866 | 0.00102 | 423 | 39 | 427 | 10 | 428 | 6 | -0.23 |
| E123-92 | 0.61 | 0.05121 | 0.00245 | 0.27861 | 0.01316 | 0.03945 | 0.00066 | 250 | 78 | 250 | 10 | 249 | 4 | 0.40 |
| E123-93 | 0.72 | 0.05127 | 0.00317 | 0.27865 | 0.01706 | 0.03941 | 0.00067 | 253 | 109 | 250 | 14 | 249 | 4 | 0.40 |

| | | | | | | | | | | | | | | |
|---|---|---|---|---|---|---|---|---|---|---|---|---|---|---|
| E123-94 | 1.57 | 0.05124 | 0.00241 | 0.25985 | 0.01218 | 0.03677 | 0.00058 | 252 | 79 | 235 | 10 | 233 | 4 | 0.86 |
| E123-95 | 0.47 | 0.05628 | 0.00146 | 0.55503 | 0.01462 | 0.07151 | 0.00104 | 463 | 33 | 448 | 10 | 445 | 6 | 0.67 |
| E123-96 | 0.59 | 0.05669 | 0.00179 | 0.51996 | 0.01642 | 0.06651 | 0.00101 | 479 | 43 | 425 | 11 | 415 | 6 | 2.41 |
| E123-97 | 0.10 | 0.05522 | 0.00154 | 0.50066 | 0.01404 | 0.06574 | 0.00096 | 421 | 37 | 412 | 9 | 410 | 6 | 0.49 |
| E123-98 | 0.54 | 0.05563 | 0.00156 | 0.53956 | 0.01517 | 0.07033 | 0.00104 | 438 | 37 | 438 | 10 | 438 | 6 | 0.00 |
| E123-99 | 0.76 | 0.07141 | 0.00179 | 1.4484 | 0.03683 | 0.14708 | 0.00212 | 969 | 29 | 909 | 15 | 885 | 12 | 2.71 |
| E123-100 | 0.42 | 0.05525 | 0.00182 | 0.51855 | 0.01704 | 0.06806 | 0.00103 | 422 | 46 | 424 | 11 | 424 | 6 | 0.00 |
| **EBLE** | | | | | | | | | | | | | | |
| ~~EBLE-01~~ | ~~0.16~~ | ~~0.15424~~ | ~~0.00377~~ | ~~6.23369~~ | ~~0.12741~~ | ~~0.29312~~ | ~~0.00394~~ | ~~2393~~ | ~~43~~ | ~~2009~~ | ~~18~~ | ~~1657~~ | ~~20~~ | ~~44.42~~ |
| EBLE-02 | 0.66 | 0.05655 | 0.00138 | 0.59554 | 0.0145 | 0.07637 | 0.0011 | 474 | 29 | 474 | 9 | 474 | 7 | 0.00 |
| EBLE-03 | 0.61 | 0.05611 | 0.00175 | 0.56966 | 0.01766 | 0.07362 | 0.0011 | 457 | 43 | 458 | 11 | 458 | 7 | 0.00 |
| EBLE-04 | 1.22 | 0.05142 | 0.00172 | 0.28997 | 0.00954 | 0.0409 | 0.00063 | 260 | 47 | 259 | 8 | 258 | 4 | 0.39 |
| EBLE-05 | 1.02 | 0.05459 | 0.00158 | 0.43733 | 0.01253 | 0.05809 | 0.00086 | 395 | 38 | 368 | 9 | 364 | 5 | 1.10 |
| EBLE-06 | 0.77 | 0.05152 | 0.0023 | 0.29882 | 0.01315 | 0.04206 | 0.00068 | 264 | 71 | 265 | 10 | 266 | 4 | -0.38 |
| EBLE-07 | 0.79 | 0.05199 | 0.00161 | 0.25137 | 0.00774 | 0.03506 | 0.00052 | 285 | 44 | 228 | 6 | 222 | 3 | 2.70 |
| EBLE-08 | 0.49 | 0.05613 | 0.00215 | 0.56663 | 0.02137 | 0.07321 | 0.00117 | 458 | 55 | 456 | 14 | 455 | 7 | 0.22 |
| EBLE-09 | 1.04 | 0.05748 | 0.00203 | 0.64321 | 0.0223 | 0.08115 | 0.00129 | 510 | 48 | 504 | 14 | 503 | 8 | 0.20 |
| EBLE-10 | 0.93 | 0.09888 | 0.00226 | 3.84768 | 0.08806 | 0.28217 | 0.00411 | 1603 | 22 | 1603 | 18 | 1602 | 21 | 0.06 |
| EBLE-11 | 0.76 | 0.06946 | 0.00365 | 1.08281 | 0.05569 | 0.11304 | 0.0021 | 912 | 75 | 745 | 27 | 690 | 12 | 7.97 |
| ~~EBLE-12~~ | ~~0.52~~ | ~~0.07558~~ | ~~0.00217~~ | ~~0.89493~~ | ~~0.02522~~ | ~~0.08587~~ | ~~0.00134~~ | ~~1084~~ | ~~32~~ | ~~649~~ | ~~14~~ | ~~531~~ | ~~8~~ | ~~22.22~~ |
| EBLE-13 | 0.87 | 0.05153 | 0.00162 | 0.29376 | 0.00911 | 0.04134 | 0.00062 | 265 | 44 | 262 | 7 | 261 | 4 | 0.38 |
| EBLE-14 | 1.66 | 0.05151 | 0.00129 | 0.29378 | 0.00736 | 0.04136 | 0.00059 | 264 | 32 | 262 | 6 | 261 | 4 | 0.38 |
| EBLE-15 | 0.54 | 0.05543 | 0.0021 | 0.52765 | 0.01952 | 0.06904 | 0.00116 | 430 | 53 | 430 | 13 | 430 | 7 | 0.00 |
| EBLE-16 | 0.45 | 0.05461 | 0.00469 | 0.47171 | 0.04012 | 0.06264 | 0.00119 | 396 | 158 | 392 | 28 | 392 | 7 | 0.00 |
| EBLE-17 | 1.21 | 0.05733 | 0.00714 | 0.42361 | 0.05209 | 0.05358 | 0.00131 | 504 | 231 | 359 | 37 | 336 | 8 | 6.85 |
| EBLE-18 | 0.66 | 0.05117 | 0.00271 | 0.28811 | 0.01506 | 0.04083 | 0.00068 | 248 | 90 | 257 | 12 | 258 | 4 | -0.39 |
| EBLE-19 | 0.49 | 0.05496 | 0.0029 | 0.49362 | 0.02561 | 0.06513 | 0.00112 | 411 | 85 | 407 | 17 | 407 | 7 | 0.00 |

| | | | | | | | | | | | | | | |
|---|---|---|---|---|---|---|---|---|---|---|---|---|---|---|
| EBLE-20 | 0.02 | 0.05981 | 0.00154 | 0.80069 | 0.02047 | 0.09709 | 0.00142 | 597 | 31 | 597 | 12 | 597 | 8 | 0.00 |
| EBLE-21 | 0.58 | 0.05153 | 0.00491 | 0.28883 | 0.02718 | 0.04065 | 0.00085 | 265 | 174 | 258 | 21 | 257 | 5 | 0.39 |
| EBLE-22 | 0.33 | 0.05575 | 0.00278 | 0.53508 | 0.02617 | 0.0696 | 0.0012 | 442 | 78 | 435 | 17 | 434 | 7 | 0.23 |
| EBLE-23 | 0.51 | 0.05534 | 0.00185 | 0.5201 | 0.01712 | 0.06815 | 0.00106 | 426 | 46 | 425 | 11 | 425 | 6 | 0.00 |
| EBLE-24 | 0.37 | 0.05564 | 0.00149 | 0.53907 | 0.01427 | 0.07026 | 0.00104 | 438 | 33 | 438 | 9 | 438 | 6 | 0.00 |
| EBLE-25 | 0.06 | 0.05711 | 0.00274 | 0.65143 | 0.02948 | 0.08273 | 0.00131 | 496 | 108 | 509 | 18 | 512 | 8 | -0.59 |
| EBLE-26 | 0.08 | 0.05879 | 0.00178 | 0.72548 | 0.02162 | 0.08949 | 0.00136 | 559 | 39 | 554 | 13 | 553 | 8 | 0.18 |
| EBLE-27 | 0.91 | 0.06884 | 0.002 | 1.40042 | 0.03985 | 0.14753 | 0.00231 | 894 | 34 | 889 | 17 | 887 | 13 | 0.23 |
| EBLE-28 | 0.09 | 0.05935 | 0.00154 | 0.76731 | 0.01976 | 0.09376 | 0.00138 | 580 | 31 | 578 | 11 | 578 | 8 | 0.00 |
| EBLE-29 | 1.06 | 0.16123 | 0.00359 | 10.09879 | 0.22524 | 0.45426 | 0.00645 | 2469 | 20 | 2444 | 21 | 2414 | 29 | 2.28 |
| EBLE-30 | 0.25 | 0.06857 | 0.00176 | 1.14444 | 0.02908 | 0.12104 | 0.00178 | 886 | 29 | 775 | 14 | 737 | 10 | 5.16 |
| EBLE-31 | 0.33 | 0.05068 | 0.00193 | 0.24711 | 0.00925 | 0.03536 | 0.00057 | 226 | 57 | 224 | 8 | 224 | 4 | 0.00 |
| EBLE-32 | 0.20 | 0.0704 | 0.0019 | 1.50219 | 0.03982 | 0.15474 | 0.00238 | 940 | 30 | 931 | 16 | 927 | 13 | 0.43 |
| EBLE-33 | 0.59 | 0.05571 | 0.00196 | 0.53588 | 0.01831 | 0.06975 | 0.00115 | 441 | 47 | 436 | 12 | 435 | 7 | 0.23 |
| EBLE-34 | 0.66 | 0.05761 | 0.00389 | 0.52862 | 0.03517 | 0.06655 | 0.00125 | 515 | 113 | 431 | 23 | 415 | 8 | 3.86 |
| EBLE-35 | 0.56 | 0.05597 | 0.00159 | 0.5553 | 0.01561 | 0.07195 | 0.00107 | 451 | 37 | 448 | 10 | 448 | 6 | 0.00 |
| EBLE-36 | 0.29 | 0.05655 | 0.00164 | 0.58635 | 0.01679 | 0.0752 | 0.00113 | 474 | 37 | 469 | 11 | 467 | 7 | 0.43 |
| EBLE-37 | 0.59 | 0.05242 | 0.00148 | 0.34686 | 0.00966 | 0.04799 | 0.00072 | 304 | 37 | 302 | 7 | 302 | 4 | 0.00 |
| EBLE-38 | 0.25 | 0.05605 | 0.00167 | 0.5598 | 0.01637 | 0.07244 | 0.00112 | 454 | 38 | 451 | 11 | 451 | 7 | 0.00 |
| EBLE-39 | 0.75 | 0.05518 | 0.00263 | 0.54808 | 0.02545 | 0.07204 | 0.00129 | 420 | 72 | 444 | 17 | 448 | 8 | -0.89 |
| EBLE-40 | 1.01 | 0.05719 | 0.00249 | 0.62889 | 0.02686 | 0.07975 | 0.00134 | 499 | 64 | 495 | 17 | 495 | 8 | 0.00 |
| EBLE-41 | 0.80 | 0.09172 | 0.00218 | 3.4319 | 0.08107 | 0.27136 | 0.00392 | 1462 | 24 | 1512 | 19 | 1548 | 20 | -5.56 |
| EBLE-42 | 0.16 | 0.05536 | 0.00184 | 0.55179 | 0.01799 | 0.07229 | 0.00114 | 427 | 45 | 446 | 12 | 450 | 7 | -0.89 |
| EBLE-43 | 0.93 | 0.05243 | 0.00272 | 0.34913 | 0.0177 | 0.04829 | 0.00088 | 304 | 82 | 304 | 13 | 304 | 5 | 0.00 |
| EBLE-44 | 0.15 | 0.06883 | 0.00181 | 1.49285 | 0.03855 | 0.15729 | 0.00236 | 894 | 29 | 927 | 16 | 942 | 13 | -1.59 |
| EBLE-45 | 0.40 | 0.05634 | 0.00157 | 0.51194 | 0.01402 | 0.06589 | 0.00099 | 466 | 35 | 420 | 9 | 411 | 6 | 2.19 |
| EBLE-46 | 0.90 | 0.05714 | 0.00166 | 0.63091 | 0.0179 | 0.08008 | 0.00124 | 497 | 36 | 497 | 11 | 497 | 7 | 0.00 |
| EBLE-47 | 0.55 | 0.07175 | 0.00218 | 1.20748 | 0.03585 | 0.12204 | 0.00189 | 979 | 36 | 804 | 16 | 742 | 11 | 8.36 |

| | | | | | | | | | | | | | | |
|---|---|---|---|---|---|---|---|---|---|---|---|---|---|---|
| EBLE-48 | 0.86 | 0.07153 | 0.0021 | 1.64366 | 0.04696 | 0.16664 | 0.00263 | 973 | 33 | 987 | 18 | 994 | 15 | -0.70 |
| EBLE-49 | 1.38 | 0.05141 | 0.00321 | 0.28512 | 0.01746 | 0.04022 | 0.00076 | 259 | 106 | 255 | 14 | 254 | 5 | 0.39 |
| EBLE-50 | 1.13 | 0.05663 | 0.00214 | 0.59569 | 0.02185 | 0.07628 | 0.00129 | 477 | 51 | 474 | 14 | 474 | 8 | 0.00 |
| EBLE-51 | 0.66 | 0.08232 | 0.00462 | 2.46304 | 0.13194 | 0.21699 | 0.00362 | 1253 | 113 | 1261 | 39 | 1266 | 19 | -1.03 |
| EBLE-52 | 0.43 | 0.05582 | 0.00159 | 0.5423 | 0.01515 | 0.07045 | 0.00106 | 445 | 36 | 440 | 10 | 439 | 6 | 0.23 |
| ~~EBLE-53~~ | ~~0.75~~ | ~~0.06064~~ | ~~0.00425~~ | ~~0.47741~~ | ~~0.03255~~ | ~~0.0571~~ | ~~0.00091~~ | ~~627~~ | ~~156~~ | ~~396~~ | ~~22~~ | ~~358~~ | ~~6~~ | ~~10.61~~ |
| EBLE-54 | 0.46 | 0.05474 | 0.00181 | 0.48047 | 0.01552 | 0.06365 | 0.001 | 402 | 44 | 398 | 11 | 398 | 6 | 0.00 |
| EBLE-55 | 0.47 | 0.05152 | 0.00175 | 0.29305 | 0.00975 | 0.04125 | 0.00065 | 264 | 48 | 261 | 8 | 261 | 4 | 0.00 |
| EBLE-56 | 0.46 | 0.05205 | 0.00171 | 0.3259 | 0.01042 | 0.04541 | 0.00073 | 288 | 44 | 286 | 8 | 286 | 5 | 0.00 |
| EBLE-57 | 0.25 | 0.05948 | 0.00207 | 0.76845 | 0.02605 | 0.09369 | 0.0015 | 585 | 46 | 579 | 15 | 577 | 9 | 0.35 |
| EBLE-58 | 0.21 | 0.0564 | 0.00178 | 0.5748 | 0.01765 | 0.0739 | 0.00117 | 468 | 40 | 461 | 11 | 460 | 7 | 0.22 |
| EBLE-59 | 0.54 | 0.05466 | 0.00317 | 0.4748 | 0.02692 | 0.063 | 0.00118 | 398 | 93 | 394 | 19 | 394 | 7 | 0.00 |
| EBLE-60 | 0.40 | 0.1006 | 0.00257 | 4.30114 | 0.10791 | 0.31004 | 0.00459 | 1635 | 26 | 1694 | 21 | 1741 | 23 | -6.09 |
| EBLE-61 | 0.71 | 0.05422 | 0.00395 | 0.45022 | 0.03222 | 0.06021 | 0.00118 | 380 | 126 | 377 | 23 | 377 | 7 | 0.00 |
| EBLE-62 | 0.45 | 0.05419 | 0.00215 | 0.45406 | 0.01751 | 0.06076 | 0.00102 | 379 | 57 | 380 | 12 | 380 | 6 | 0.00 |
| EBLE-63 | 0.34 | 0.05627 | 0.00172 | 0.57623 | 0.01721 | 0.07426 | 0.00115 | 463 | 39 | 462 | 11 | 462 | 7 | 0.00 |
| EBLE-64 | 0.49 | 0.0545 | 0.00308 | 0.46071 | 0.02561 | 0.06131 | 0.00108 | 392 | 93 | 385 | 18 | 384 | 7 | 0.26 |
| EBLE-65 | 0.90 | 0.06721 | 0.00208 | 1.32604 | 0.03986 | 0.14308 | 0.00226 | 844 | 37 | 857 | 17 | 862 | 13 | -0.58 |
| EBLE-66 | 0.57 | 0.05119 | 0.00229 | 0.27419 | 0.01193 | 0.03884 | 0.00068 | 249 | 68 | 246 | 10 | 246 | 4 | 0.00 |
| EBLE-67 | 0.42 | 0.07787 | 0.00209 | 2.0848 | 0.05468 | 0.19415 | 0.00294 | 1144 | 29 | 1144 | 18 | 1144 | 16 | 0.00 |
| EBLE-68 | 0.71 | 0.05457 | 0.00166 | 0.46962 | 0.01395 | 0.06241 | 0.00097 | 395 | 39 | 391 | 10 | 390 | 6 | 0.26 |
| EBLE-69 | 1.09 | 0.07142 | 0.00235 | 1.6305 | 0.05191 | 0.16555 | 0.00272 | 969 | 39 | 982 | 20 | 988 | 15 | -0.61 |
| EBLE-70 | 0.49 | 0.05319 | 0.00247 | 0.39244 | 0.01775 | 0.0535 | 0.00094 | 337 | 71 | 336 | 13 | 336 | 6 | 0.00 |
| EBLE-71 | 0.92 | 0.05476 | 0.00177 | 0.49783 | 0.01564 | 0.06592 | 0.00104 | 402 | 42 | 410 | 11 | 412 | 6 | -0.49 |
| EBLE-72 | 0.63 | 0.05453 | 0.00245 | 0.47014 | 0.02048 | 0.06253 | 0.00111 | 393 | 66 | 391 | 14 | 391 | 7 | 0.00 |
| EBLE-73 | 0.41 | 0.05055 | 0.00206 | 0.24042 | 0.00952 | 0.03449 | 0.00058 | 220 | 60 | 219 | 8 | 219 | 4 | 0.00 |
| EBLE-74 | 0.72 | 0.05641 | 0.00244 | 0.58364 | 0.02447 | 0.07503 | 0.00133 | 469 | 61 | 467 | 16 | 466 | 8 | 0.21 |
| EBLE-75 | 0.96 | 0.05903 | 0.00204 | 0.74616 | 0.02504 | 0.09166 | 0.00148 | 568 | 45 | 566 | 15 | 565 | 9 | 0.18 |

| | | | | | | | | | | | | | | |
|---|---|---|---|---|---|---|---|---|---|---|---|---|---|---|
| EBLE-76 | 0.92 | 0.05124 | 0.0041 | 0.2815 | 0.02202 | 0.03984 | 0.00087 | 252 | 138 | 252 | 17 | 252 | 5 | 0.00 |
| EBLE-77 | 1.29 | 0.08695 | 0.00284 | 2.78739 | 0.08802 | 0.23248 | 0.00387 | 1359 | 36 | 1352 | 24 | 1347 | 20 | 0.89 |
| ~~EBLE-78~~ | ~~0.17~~ | ~~0.08563~~ | ~~0.00264~~ | ~~2.3541~~ | ~~0.07017~~ | ~~0.19936~~ | ~~0.0032~~ | ~~1330~~ | ~~33~~ | ~~1229~~ | ~~21~~ | ~~1172~~ | ~~17~~ | ~~13.48~~ |
| EBLE-79 | 0.79 | 0.05622 | 0.00189 | 0.57563 | 0.01869 | 0.07425 | 0.00121 | 461 | 43 | 462 | 12 | 462 | 7 | 0.00 |
| EBLE-80 | 1.10 | 0.0929 | 0.00258 | 3.31686 | 0.08948 | 0.25889 | 0.00396 | 1486 | 29 | 1485 | 21 | 1484 | 20 | 0.13 |
| EBLE-81 | 0.88 | 0.06238 | 0.00196 | 1.12047 | 0.03413 | 0.13026 | 0.00209 | 687 | 38 | 763 | 16 | 789 | 12 | -3.30 |
| EBLE-82 | 0.59 | 0.05037 | 0.00179 | 0.22709 | 0.00781 | 0.03269 | 0.00054 | 212 | 49 | 208 | 6 | 207 | 3 | 0.48 |
| EBLE-83 | 0.86 | 0.05536 | 0.00194 | 0.53636 | 0.01822 | 0.07025 | 0.00116 | 427 | 47 | 436 | 12 | 438 | 7 | -0.46 |
| EBLE-85 | 0.20 | 0.07019 | 0.0023 | 1.44418 | 0.04575 | 0.14919 | 0.00244 | 934 | 39 | 907 | 19 | 896 | 14 | 1.23 |
| EBLE-86 | 0.74 | 0.05601 | 0.002 | 0.57207 | 0.01978 | 0.07406 | 0.00122 | 453 | 48 | 459 | 13 | 461 | 7 | -0.43 |
| EBLE-87 | 4.04 | 0.16052 | 0.00503 | 10.55132 | 0.31749 | 0.47663 | 0.00828 | 2461 | 28 | 2484 | 28 | 2513 | 36 | -2.07 |
| EBLE-88 | 0.15 | 0.11569 | 0.00339 | 5.62295 | 0.15916 | 0.35242 | 0.0056 | 1891 | 29 | 1920 | 24 | 1946 | 27 | -2.83 |
| EBLE-89 | 0.31 | 0.05062 | 0.00198 | 0.24858 | 0.00943 | 0.03561 | 0.0006 | 224 | 57 | 225 | 8 | 226 | 4 | -0.44 |
| EBLE-90 | 1.05 | 0.05095 | 0.0028 | 0.26785 | 0.01433 | 0.03812 | 0.00071 | 239 | 89 | 241 | 11 | 241 | 4 | 0.00 |
| EBLE-91 | 0.23 | 0.05802 | 0.00215 | 0.68511 | 0.02452 | 0.08561 | 0.00145 | 531 | 49 | 530 | 15 | 530 | 9 | 0.00 |
| EBLE-92 | 0.48 | 0.0601 | 0.00202 | 0.5798 | 0.01879 | 0.06995 | 0.00113 | 607 | 42 | 464 | 12 | 436 | 7 | 6.42 |
| EBLE-93 | 0.16 | 0.05607 | 0.00173 | 0.56103 | 0.01673 | 0.07255 | 0.00115 | 455 | 39 | 452 | 11 | 452 | 7 | 0.00 |
| EBLE-94 | 0.92 | 0.05141 | 0.00264 | 0.2757 | 0.01378 | 0.03889 | 0.00071 | 259 | 81 | 247 | 11 | 246 | 4 | 0.41 |
| EBLE-95 | 0.64 | 0.056 | 0.00206 | 0.55528 | 0.01964 | 0.0719 | 0.00124 | 452 | 48 | 448 | 13 | 448 | 7 | 0.00 |
| EBLE-96 | 0.69 | 0.05548 | 0.00221 | 0.52408 | 0.02015 | 0.06849 | 0.00117 | 432 | 55 | 428 | 13 | 427 | 7 | 0.23 |
| EBLE-97 | 0.54 | 0.05561 | 0.00202 | 0.53078 | 0.0186 | 0.0692 | 0.00114 | 437 | 49 | 432 | 12 | 431 | 7 | 0.23 |
| EBLE-98 | 0.94 | 0.0472 | 0.00177 | 0.05785 | 0.0021 | 0.00889 | 0.00015 | 59 | 51 | 57 | 2 | 57.1 | 1 | -0.18 |
| EBLE-99 | 0.69 | 0.05505 | 0.00195 | 0.56694 | 0.01932 | 0.07466 | 0.00124 | 414 | 47 | 456 | 13 | 464 | 7 | -1.72 |
| EBLE-100 | 0.94 | 0.05112 | 0.00241 | 0.27577 | 0.01251 | 0.03911 | 0.00074 | 246 | 70 | 247 | 10 | 247 | 5 | 0.00 |
| | | | | | | | | | | | | | | |
| **E2-2** | | | | | | | | | | | | | | |
| E22-01 | 0.89 | 0.05566 | 0.00119 | 0.52896 | 0.01161 | 0.06891 | 0.00091 | 439 | 26 | 431 | 8 | 430 | 5 | 0.23 |
| ~~E22-02~~ | ~~1.02~~ | ~~0.10325~~ | ~~0.00154~~ | ~~3.29917~~ | ~~0.05315~~ | ~~0.2317~~ | ~~0.003~~ | ~~1683~~ | ~~14~~ | ~~1481~~ | ~~13~~ | ~~1343~~ | ~~16~~ | ~~25.32~~ |

| | | | | | | | | | | | | | | |
|---|---|---|---|---|---|---|---|---|---|---|---|---|---|---|
| ~~E22-03~~ | ~~0.33~~ | ~~0.16039~~ | ~~0.00204~~ | ~~7.82901~~ | ~~0.11221~~ | ~~0.35395~~ | ~~0.00445~~ | ~~2460~~ | ~~11~~ | ~~2212~~ | ~~13~~ | ~~1953~~ | ~~21~~ | ~~25.96~~ |
| ~~E22-04~~ | ~~1.52~~ | ~~0.0795~~ | ~~0.01369~~ | ~~0.51848~~ | ~~0.0883~~ | ~~0.04729~~ | ~~0.00141~~ | ~~1185~~ | ~~303~~ | ~~424~~ | ~~59~~ | ~~298~~ | ~~9~~ | ~~42.28~~ |
| E22-05 | 0.56 | 0.11572 | 0.00157 | 5.23075 | 0.07844 | 0.32777 | 0.00417 | 1891 | 12 | 1858 | 13 | 1828 | 20 | 3.45 |
| E22-06 | 3.28 | 0.05132 | 0.00344 | 0.28455 | 0.01894 | 0.0402 | 0.00065 | 255 | 123 | 254 | 15 | 254 | 4 | 0.00 |
| E22-07 | 0.87 | 0.05879 | 0.00103 | 0.69497 | 0.01284 | 0.08571 | 0.0011 | 559 | 20 | 536 | 8 | 530 | 7 | 1.13 |
| ~~E22-08~~ | ~~0.50~~ | ~~0.05792~~ | ~~0.00147~~ | ~~0.23948~~ | ~~0.00617~~ | ~~0.02998~~ | ~~0.00041~~ | ~~527~~ | ~~33~~ | ~~218~~ | ~~5~~ | ~~190~~ | ~~3~~ | ~~14.74~~ |
| E22-09 | 0.65 | 0.05131 | 0.00104 | 0.26443 | 0.00555 | 0.03737 | 0.00049 | 255 | 25 | 238 | 4 | 237 | 3 | 0.42 |
| E22-10 | 1.36 | 0.05347 | 0.00102 | 0.37303 | 0.00741 | 0.05058 | 0.00066 | 349 | 23 | 322 | 5 | 318 | 4 | 1.26 |
| E22-11 | 0.57 | 0.05268 | 0.00253 | 0.35708 | 0.01705 | 0.04915 | 0.00075 | 315 | 81 | 310 | 13 | 309 | 5 | 0.32 |
| E22-12 | 0.22 | 0.05542 | 0.00097 | 0.50153 | 0.00929 | 0.06562 | 0.00085 | 429 | 20 | 413 | 6 | 410 | 5 | 0.73 |
| E22-13 | 0.80 | 0.05137 | 0.00348 | 0.26788 | 0.01795 | 0.03781 | 0.00067 | 257 | 121 | 241 | 14 | 239 | 4 | 0.84 |
| E22-14 | 0.89 | 0.18641 | 0.00243 | 12.81803 | 0.18745 | 0.4986 | 0.0063 | 2711 | 11 | 2666 | 14 | 2608 | 27 | 3.95 |
| E22-15 | 0.34 | 0.07112 | 0.00101 | 1.57562 | 0.02455 | 0.16065 | 0.00204 | 961 | 14 | 961 | 10 | 960 | 11 | 0.10 |
| ~~E22-16~~ | ~~0.48~~ | ~~0.10491~~ | ~~0.00142~~ | ~~2.84101~~ | ~~0.04255~~ | ~~0.19636~~ | ~~0.00248~~ | ~~1713~~ | ~~12~~ | ~~1366~~ | ~~11~~ | ~~1156~~ | ~~13~~ | ~~48.18~~ |
| E22-17 | 0.87 | 0.05116 | 0.00165 | 0.26799 | 0.00867 | 0.03798 | 0.00053 | 248 | 49 | 241 | 7 | 240 | 3 | 0.42 |
| E22-18 | 0.74 | 0.08918 | 0.00124 | 2.71598 | 0.04156 | 0.22084 | 0.00279 | 1408 | 13 | 1333 | 11 | 1286 | 15 | 9.49 |
| E22-19 | 0.88 | 0.0527 | 0.00658 | 0.34792 | 0.04317 | 0.04787 | 0.00097 | 316 | 243 | 303 | 33 | 301 | 6 | 0.66 |
| E22-20 | 0.57 | 0.05644 | 0.00096 | 0.53814 | 0.00969 | 0.06914 | 0.00089 | 470 | 19 | 437 | 6 | 431 | 5 | 1.39 |
| ~~E22-21~~ | ~~0.55~~ | ~~0.06243~~ | ~~0.00247~~ | ~~0.57045~~ | ~~0.02262~~ | ~~0.06626~~ | ~~0.00095~~ | ~~689~~ | ~~60~~ | ~~458~~ | ~~15~~ | ~~414~~ | ~~6~~ | ~~10.63~~ |
| E22-22 | 0.35 | 0.0705 | 0.00175 | 1.37737 | 0.0346 | 0.14167 | 0.00196 | 943 | 29 | 879 | 15 | 854 | 11 | 2.93 |
| E22-23 | 0.63 | 0.05618 | 0.00124 | 0.52173 | 0.01189 | 0.06733 | 0.00089 | 459 | 28 | 426 | 8 | 420 | 5 | 1.43 |
| E22-24 | 0.39 | 0.05512 | 0.00144 | 0.50051 | 0.01327 | 0.06585 | 0.00088 | 417 | 36 | 412 | 9 | 411 | 5 | 0.24 |
| E22-25 | 0.78 | 0.053 | 0.00134 | 0.37332 | 0.00963 | 0.05107 | 0.00068 | 329 | 35 | 322 | 7 | 321 | 4 | 0.31 |
| E22-26 | 1.28 | 0.05112 | 0.00231 | 0.27186 | 0.01227 | 0.03856 | 0.00056 | 246 | 77 | 244 | 10 | 244 | 3 | 0.00 |
| E22-27 | 0.84 | 0.05031 | 0.0016 | 0.23245 | 0.00741 | 0.0335 | 0.00047 | 209 | 48 | 212 | 6 | 212 | 3 | 0.00 |
| E22-28 | 0.69 | 0.05473 | 0.00168 | 0.49692 | 0.01536 | 0.06583 | 0.00091 | 401 | 45 | 410 | 10 | 411 | 6 | -0.24 |
| E22-29 | 0.80 | 0.05177 | 0.00292 | 0.29264 | 0.01648 | 0.04099 | 0.0006 | 275 | 102 | 261 | 13 | 259 | 4 | 0.77 |
| E22-30 | 0.34 | 0.08355 | 0.00216 | 2.29683 | 0.06024 | 0.19932 | 0.00278 | 1282 | 30 | 1211 | 19 | 1172 | 15 | 9.39 |

| | | | | | | | | | | | | | | |
|---|---|---|---|---|---|---|---|---|---|---|---|---|---|---|
| ~~E22-31~~ | ~~0.27~~ | ~~0.09608~~ | ~~0.00238~~ | ~~2.60666~~ | ~~0.05482~~ | ~~0.19677~~ | ~~0.00256~~ | ~~1549~~ | ~~48~~ | ~~1303~~ | ~~15~~ | ~~1158~~ | ~~14~~ | ~~33.77~~ |
| ~~E22-32~~ | ~~0.30~~ | ~~0.09227~~ | ~~0.00134~~ | ~~2.09444~~ | ~~0.03324~~ | ~~0.16458~~ | ~~0.00209~~ | ~~1473~~ | ~~14~~ | ~~1147~~ | ~~11~~ | ~~982~~ | ~~12~~ | ~~16.80~~ |
| E22-33 | 1.20 | 0.0497 | 0.00562 | 0.28883 | 0.0322 | 0.04215 | 0.00078 | 181 | 251 | 258 | 25 | 266 | 5 | -3.01 |
| E22-34 | 0.13 | 0.12283 | 0.00176 | 5.56008 | 0.08732 | 0.32822 | 0.00417 | 1998 | 13 | 1910 | 14 | 1830 | 20 | 9.18 |
| E22-35 | 0.78 | 0.05697 | 0.00116 | 0.62408 | 0.0132 | 0.07944 | 0.00104 | 490 | 25 | 492 | 8 | 493 | 6 | -0.20 |
| E22-36 | 0.86 | 0.05336 | 0.00204 | 0.29991 | 0.01143 | 0.04075 | 0.0006 | 344 | 59 | 266 | 9 | 257 | 4 | 3.50 |
| E22-37 | 0.72 | 0.05705 | 0.00135 | 0.42163 | 0.01022 | 0.05359 | 0.00071 | 493 | 31 | 357 | 7 | 337 | 4 | 5.93 |
| E22-38 | 1.02 | 0.05229 | 0.00312 | 0.31085 | 0.01842 | 0.04311 | 0.00068 | 298 | 107 | 275 | 14 | 272 | 4 | 1.10 |
| ~~E22-39~~ | ~~1.66~~ | ~~0.08419~~ | ~~0.00168~~ | ~~1.6013~~ | ~~0.03302~~ | ~~0.13791~~ | ~~0.00184~~ | ~~1297~~ | ~~21~~ | ~~971~~ | ~~13~~ | ~~833~~ | ~~10~~ | ~~16.57~~ |
| E22-40 | 0.82 | 0.0597 | 0.00188 | 0.54264 | 0.01715 | 0.0659 | 0.00092 | 593 | 44 | 440 | 11 | 411 | 6 | 7.06 |
| E22-41 | 0.57 | 0.05148 | 0.0012 | 0.27932 | 0.00665 | 0.03934 | 0.00053 | 262 | 31 | 250 | 5 | 249 | 3 | 0.40 |
| E22-42 | 2.57 | 0.11623 | 0.00203 | 5.21804 | 0.09583 | 0.3255 | 0.00433 | 1899 | 16 | 1856 | 16 | 1817 | 21 | 4.51 |
| ~~E22-43~~ | ~~0.68~~ | ~~0.08309~~ | ~~0.00288~~ | ~~1.55524~~ | ~~0.04938~~ | ~~0.13575~~ | ~~0.00188~~ | ~~1271~~ | ~~69~~ | ~~953~~ | ~~20~~ | ~~821~~ | ~~11~~ | ~~16.08~~ |
| E22-44 | 0.18 | 0.07517 | 0.00123 | 1.8158 | 0.03168 | 0.17515 | 0.00226 | 1073 | 17 | 1051 | 11 | 1040 | 12 | 3.17 |
| ~~E22-45~~ | ~~1.22~~ | ~~0.05786~~ | ~~0.0027~~ | ~~0.30007~~ | ~~0.01392~~ | ~~0.0376~~ | ~~0.00056~~ | ~~524~~ | ~~75~~ | ~~266~~ | ~~11~~ | ~~238~~ | ~~3~~ | ~~11.76~~ |
| E22-46 | 0.24 | 0.05655 | 0.0014 | 0.59007 | 0.01487 | 0.07566 | 0.00102 | 474 | 32 | 471 | 9 | 470 | 6 | 0.21 |
| E22-47 | 0.89 | 0.05585 | 0.00151 | 0.53315 | 0.01457 | 0.06922 | 0.00096 | 446 | 36 | 434 | 10 | 431 | 6 | 0.70 |
| E22-48 | 0.77 | 0.05204 | 0.0014 | 0.31321 | 0.00857 | 0.04364 | 0.00059 | 287 | 38 | 277 | 7 | 275 | 4 | 0.73 |
| E22-49 | 0.56 | 0.05226 | 0.0015 | 0.35633 | 0.01033 | 0.04944 | 0.00068 | 297 | 41 | 309 | 8 | 311 | 4 | -0.64 |
| E22-50 | 1.07 | 0.06562 | 0.00438 | 1.14162 | 0.07546 | 0.12614 | 0.00221 | 794 | 110 | 773 | 36 | 766 | 13 | 0.91 |
| E22-51 | 0.48 | 0.05196 | 0.00147 | 0.29366 | 0.00838 | 0.04098 | 0.00056 | 284 | 40 | 261 | 7 | 259 | 3 | 0.77 |
| ~~E22-52~~ | ~~0.65~~ | ~~0.08509~~ | ~~0.00276~~ | ~~0.56702~~ | ~~0.01834~~ | ~~0.04832~~ | ~~0.0007~~ | ~~1318~~ | ~~40~~ | ~~456~~ | ~~12~~ | ~~304~~ | ~~4~~ | ~~50.00~~ |
| E22-53 | 0.35 | 0.1145 | 0.00182 | 4.88675 | 0.08337 | 0.30946 | 0.00399 | 1872 | 14 | 1800 | 14 | 1738 | 20 | 7.71 |
| E22-54 | 0.45 | 0.05761 | 0.00127 | 0.65053 | 0.01476 | 0.08187 | 0.00108 | 515 | 28 | 509 | 9 | 507 | 6 | 0.39 |
| ~~E22-55~~ | ~~1.05~~ | ~~0.17136~~ | ~~0.00283~~ | ~~10.31985~~ | ~~0.18069~~ | ~~0.43667~~ | ~~0.00575~~ | ~~2571~~ | ~~14~~ | ~~2464~~ | ~~16~~ | ~~2336~~ | ~~26~~ | ~~10.06~~ |
| E22-56 | 0.28 | 0.0947 | 0.00151 | 3.27258 | 0.05587 | 0.25057 | 0.00322 | 1522 | 15 | 1475 | 13 | 1441 | 17 | 5.62 |
| E22-57 | 0.56 | 0.05515 | 0.00343 | 0.51281 | 0.03169 | 0.06742 | 0.00107 | 418 | 110 | 420 | 21 | 421 | 6 | -0.24 |
| ~~E22-58~~ | ~~0.81~~ | ~~0.07723~~ | ~~0.00131~~ | ~~0.97307~~ | ~~0.0175~~ | ~~0.09136~~ | ~~0.00118~~ | ~~1127~~ | ~~17~~ | ~~690~~ | ~~9~~ | ~~564~~ | ~~7~~ | ~~22.34~~ |

| | | | | | | | | | | | | | | |
|---|---|---|---|---|---|---|---|---|---|---|---|---|---|---|
| E22-59 | 0.21 | 0.06601 | 0.00148 | 1.11053 | 0.02543 | 0.12199 | 0.00166 | 807 | 26 | 758 | 12 | 742 | 10 | 2.16 |
| E22-60 | 0.62 | 0.07577 | 0.00142 | 2.03301 | 0.03971 | 0.19455 | 0.00257 | 1089 | 20 | 1127 | 13 | 1146 | 14 | -4.97 |
| E22-61 | 0.36 | 0.05066 | 0.00166 | 0.23824 | 0.00784 | 0.0341 | 0.00048 | 225 | 50 | 217 | 6 | 216 | 3 | 0.46 |
| E22-62 | 0.55 | 0.05684 | 0.00125 | 0.58231 | 0.01316 | 0.07429 | 0.00099 | 485 | 27 | 466 | 8 | 462 | 6 | 0.87 |
| E22-63 | 1.01 | 0.05346 | 0.0015 | 0.36609 | 0.01034 | 0.04965 | 0.00069 | 348 | 39 | 317 | 8 | 312 | 4 | 1.60 |
| E22-64 | 0.95 | 0.05985 | 0.002 | 0.55753 | 0.01867 | 0.06754 | 0.00095 | 598 | 48 | 450 | 12 | 421 | 6 | 6.89 |
| E22-65 | 0.45 | 0.12825 | 0.00223 | 6.44501 | 0.11805 | 0.36438 | 0.0048 | 2074 | 16 | 2038 | 16 | 2003 | 23 | 3.54 |
| ~~E22-66~~ | ~~0.76~~ | ~~0.06626~~ | ~~0.00207~~ | ~~0.29214~~ | ~~0.00911~~ | ~~0.03197~~ | ~~0.00046~~ | ~~815~~ | ~~41~~ | ~~260~~ | ~~7~~ | ~~203~~ | ~~3~~ | ~~28.08~~ |
| ~~E22-67~~ | ~~0.63~~ | ~~0.11456~~ | ~~0.0023~~ | ~~4.77476~~ | ~~0.09853~~ | ~~0.30221~~ | ~~0.00416~~ | ~~1873~~ | ~~19~~ | ~~1780~~ | ~~17~~ | ~~1702~~ | ~~21~~ | ~~10.05~~ |
| E22-68 | 0.70 | 0.14652 | 0.00287 | 8.01644 | 0.162 | 0.3967 | 0.00544 | 2306 | 17 | 2233 | 18 | 2154 | 25 | 7.06 |
| E22-69 | 0.61 | 0.0519 | 0.0014 | 0.31906 | 0.0087 | 0.04457 | 0.00061 | 281 | 38 | 281 | 7 | 281 | 4 | 0.00 |
| E22-70 | 0.55 | 0.08278 | 0.00151 | 2.31807 | 0.04415 | 0.20305 | 0.00267 | 1264 | 18 | 1218 | 14 | 1192 | 14 | 6.04 |
| E22-71 | 1.18 | 0.05174 | 0.00821 | 0.31185 | 0.04916 | 0.0437 | 0.001 | 274 | 294 | 276 | 38 | 276 | 6 | 0.00 |
| E22-72 | 0.44 | 0.0688 | 0.00141 | 1.27643 | 0.02708 | 0.13453 | 0.00179 | 893 | 23 | 835 | 12 | 814 | 10 | 2.58 |
| E22-73 | 0.81 | 0.05587 | 0.00169 | 0.51072 | 0.01551 | 0.06628 | 0.00092 | 447 | 43 | 419 | 10 | 414 | 6 | 1.21 |
| E22-74 | 1.70 | 0.11633 | 0.00226 | 5.15504 | 0.1035 | 0.32132 | 0.00434 | 1901 | 18 | 1845 | 17 | 1796 | 21 | 5.85 |
| ~~E22-75~~ | ~~0.69~~ | ~~0.1172~~ | ~~0.00207~~ | ~~4.66314~~ | ~~0.08648~~ | ~~0.28848~~ | ~~0.00377~~ | ~~1914~~ | ~~16~~ | ~~1761~~ | ~~16~~ | ~~1634~~ | ~~19~~ | ~~17.14~~ |
| E22-76 | 0.72 | 0.05476 | 0.00119 | 0.48828 | 0.01093 | 0.06465 | 0.00086 | 402 | 27 | 404 | 7 | 404 | 5 | 0.00 |
| E22-77 | 0.24 | 0.07076 | 0.00153 | 1.42787 | 0.0316 | 0.14631 | 0.00197 | 950 | 24 | 901 | 13 | 880 | 11 | 2.39 |
| E22-78 | 0.27 | 0.1172 | 0.0021 | 5.13918 | 0.0967 | 0.31793 | 0.00416 | 1914 | 17 | 1843 | 16 | 1780 | 20 | 7.53 |
| E22-79 | 0.82 | 0.05952 | 0.00118 | 0.48898 | 0.01005 | 0.05956 | 0.00079 | 586 | 23 | 404 | 7 | 373 | 5 | 8.31 |
| E22-80 | 0.47 | 0.14732 | 0.00271 | 8.69286 | 0.1668 | 0.42784 | 0.00568 | 2315 | 16 | 2306 | 17 | 2296 | 26 | 0.83 |
| E22-81 | 0.83 | 0.05921 | 0.00241 | 0.55329 | 0.02248 | 0.06776 | 0.001 | 575 | 63 | 447 | 15 | 423 | 6 | 5.67 |
| E22-82 | 0.92 | 0.17139 | 0.00307 | 11.32017 | 0.21268 | 0.4789 | 0.00626 | 2571 | 15 | 2550 | 18 | 2522 | 27 | 1.94 |
| ~~E22-83~~ | ~~0.60~~ | ~~0.12296~~ | ~~0.00221~~ | ~~4.62564~~ | ~~0.08716~~ | ~~0.27276~~ | ~~0.00355~~ | ~~2000~~ | ~~17~~ | ~~1754~~ | ~~16~~ | ~~1555~~ | ~~18~~ | ~~28.62~~ |
| E22-84 | 0.91 | 0.05358 | 0.00264 | 0.42537 | 0.0209 | 0.05757 | 0.00084 | 353 | 85 | 360 | 15 | 361 | 5 | -0.28 |
| ~~E22-85~~ | ~~0.41~~ | ~~0.1495~~ | ~~0.00271~~ | ~~6.94671~~ | ~~0.132~~ | ~~0.33691~~ | ~~0.00441~~ | ~~2340~~ | ~~16~~ | ~~2105~~ | ~~17~~ | ~~1872~~ | ~~21~~ | ~~25.00~~ |
| E22-86 | 0.63 | 0.05703 | 0.00145 | 0.555 | 0.0142 | 0.07056 | 0.00098 | 493 | 33 | 448 | 9 | 440 | 6 | 1.82 |

| | | | | | | | | | | | | | | |
|---|---|---|---|---|---|---|---|---|---|---|---|---|---|---|
| E22-87 | 1.26 | 0.06583 | 0.00196 | 1.11102 | 0.03303 | 0.12237 | 0.00176 | 801 | 38 | 759 | 16 | 744 | 10 | 2.02 |
| ~~E22-88~~ | ~~0.39~~ | ~~0.0607~~ | ~~0.00166~~ | ~~0.48816~~ | ~~0.01341~~ | ~~0.05831~~ | ~~0.00081~~ | ~~629~~ | ~~36~~ | ~~404~~ | ~~9~~ | ~~365~~ | ~~5~~ | ~~10.68~~ |
| E22-89 | 0.38 | 0.07755 | 0.00157 | 1.86711 | 0.03895 | 0.17457 | 0.00234 | 1135 | 22 | 1070 | 14 | 1037 | 13 | 9.45 |
| E22-90 | 0.70 | 0.05223 | 0.00195 | 0.27744 | 0.01029 | 0.03851 | 0.00057 | 295 | 58 | 249 | 8 | 244 | 4 | 2.05 |
| E22-91 | 1.03 | 0.05111 | 0.00294 | 0.28054 | 0.01606 | 0.0398 | 0.00062 | 246 | 103 | 251 | 13 | 252 | 4 | -0.40 |
| E22-92 | 0.59 | 0.05116 | 0.0063 | 0.2757 | 0.03371 | 0.03908 | 0.00081 | 248 | 238 | 247 | 27 | 247 | 5 | 0.00 |
| E22-93 | 0.77 | 0.05478 | 0.00241 | 0.49398 | 0.02162 | 0.06539 | 0.00098 | 403 | 71 | 408 | 15 | 408 | 6 | 0.00 |
| E22-94 | 0.26 | 0.07047 | 0.00222 | 1.45284 | 0.04135 | 0.14952 | 0.00204 | 942 | 66 | 911 | 17 | 898 | 11 | 1.45 |
| E22-95 | 0.51 | 0.05916 | 0.00146 | 0.64416 | 0.01615 | 0.07894 | 0.00108 | 573 | 31 | 505 | 10 | 490 | 6 | 3.06 |
| ~~E22-96~~ | ~~1.43~~ | ~~0.05563~~ | ~~0.00146~~ | ~~0.24113~~ | ~~0.0064~~ | ~~0.03143~~ | ~~0.00043~~ | ~~438~~ | ~~35~~ | ~~219~~ | ~~5~~ | ~~199~~ | ~~3~~ | ~~10.05~~ |
| E22-97 | 0.47 | 0.07585 | 0.00178 | 1.77315 | 0.04228 | 0.16949 | 0.00234 | 1091 | 26 | 1036 | 15 | 1009 | 13 | 8.13 |
| E22-98 | 0.23 | 0.11971 | 0.00236 | 5.55536 | 0.11326 | 0.33648 | 0.00448 | 1952 | 19 | 1909 | 18 | 1870 | 22 | 4.39 |
| E22-99 | 0.83 | 0.05282 | 0.00259 | 0.35776 | 0.0174 | 0.04911 | 0.00076 | 321 | 82 | 311 | 13 | 309 | 5 | 0.65 |
| E22-100 | 0.47 | 0.05185 | 0.00203 | 0.31347 | 0.01222 | 0.04384 | 0.00065 | 279 | 62 | 277 | 9 | 277 | 4 | 0.00 |
| E22-101 | 0.21 | 0.18104 | 0.00359 | 12.30849 | 0.2523 | 0.49297 | 0.00658 | 2662 | 17 | 2628 | 19 | 2584 | 28 | 3.02 |
| E22-102 | 0.31 | 0.06139 | 0.00131 | 0.55013 | 0.01206 | 0.06498 | 0.00087 | 653 | 25 | 445 | 8 | 406 | 5 | 9.61 |
| E22-103 | 0.36 | 0.07292 | 0.00155 | 1.39473 | 0.03042 | 0.13869 | 0.00187 | 1012 | 23 | 887 | 13 | 837 | 11 | 5.97 |
| E22-104 | 0.82 | 0.05127 | 0.00196 | 0.27486 | 0.01049 | 0.03887 | 0.00057 | 253 | 61 | 247 | 8 | 246 | 4 | 0.41 |
| E22-105 | 0.44 | 0.17388 | 0.00347 | 10.90171 | 0.22485 | 0.45459 | 0.00604 | 2595 | 18 | 2515 | 19 | 2416 | 27 | 7.41 |
| **EBLN** | | | | | | | | | | | | | | |
| EBLN-01 | 1.35 | 0.05144 | 0.00237 | 0.28787 | 0.01318 | 0.04058 | 0.00067 | 261 | 75 | 257 | 10 | 256 | 4 | 0.39 |
| EBLN-02 | 0.86 | 0.05112 | 0.00295 | 0.28109 | 0.01612 | 0.03987 | 0.00068 | 246 | 101 | 252 | 13 | 252 | 4 | 0.00 |
| EBLN-03 | 0.08 | 0.05586 | 0.0011 | 0.54894 | 0.01138 | 0.07126 | 0.00101 | 447 | 23 | 444 | 7 | 444 | 6 | 0.00 |
| EBLN-04 | 0.91 | 0.05586 | 0.00168 | 0.51618 | 0.01569 | 0.06701 | 0.00101 | 447 | 41 | 423 | 11 | 418 | 6 | 1.20 |
| EBLN-05 | 0.45 | 0.05481 | 0.00265 | 0.48829 | 0.02344 | 0.0646 | 0.00109 | 404 | 77 | 404 | 16 | 404 | 7 | 0.00 |
| EBLN-06 | 0.66 | 0.05204 | 0.00158 | 0.32566 | 0.00994 | 0.04538 | 0.00069 | 287 | 42 | 286 | 8 | 286 | 4 | 0.00 |
| EBLN-07 | 0.68 | 0.05605 | 0.00124 | 0.5642 | 0.01293 | 0.07299 | 0.00106 | 454 | 27 | 454 | 8 | 454 | 6 | 0.00 |

| | | | | | | | | | | | | | | |
|---|---|---|---|---|---|---|---|---|---|---|---|---|---|---|
| EBLN-08 | 0.44 | 0.05472 | 0.00235 | 0.48563 | 0.02075 | 0.06435 | 0.00104 | 401 | 67 | 402 | 14 | 402 | 6 | 0.00 |
| EBLN-09 | 0.48 | 0.05161 | 0.0027 | 0.29671 | 0.0153 | 0.04169 | 0.00076 | 268 | 85 | 264 | 12 | 263 | 5 | 0.38 |
| EBLN-10 | 0.35 | 0.06323 | 0.00165 | 0.67688 | 0.01796 | 0.07763 | 0.00116 | 716 | 32 | 525 | 11 | 482 | 7 | 8.92 |
| EBLN-11 | 0.81 | 0.05487 | 0.00124 | 0.51794 | 0.01209 | 0.06845 | 0.001 | 407 | 28 | 424 | 8 | 427 | 6 | -0.70 |
| EBLN-12 | 1.08 | 0.05571 | 0.00133 | 0.54648 | 0.01337 | 0.07114 | 0.00104 | 441 | 30 | 443 | 9 | 443 | 6 | 0.00 |
| EBLN-13 | 0.21 | 0.05156 | 0.00296 | 0.29386 | 0.01652 | 0.04133 | 0.00081 | 266 | 93 | 262 | 13 | 261 | 5 | 0.38 |
| EBLN-14 | 0.48 | 0.05547 | 0.00151 | 0.5278 | 0.01453 | 0.069 | 0.00104 | 431 | 35 | 430 | 10 | 430 | 6 | 0.00 |
| EBLN-15 | 1.34 | 0.05147 | 0.0024 | 0.29241 | 0.0134 | 0.0412 | 0.00074 | 262 | 72 | 260 | 11 | 260 | 5 | 0.00 |
| EBLN-16 | 0.79 | 0.0517 | 0.0018 | 0.31526 | 0.01093 | 0.04422 | 0.0007 | 272 | 51 | 278 | 8 | 279 | 4 | -0.36 |
| EBLN-17 | 0.43 | 0.05089 | 0.00333 | 0.271 | 0.0175 | 0.03862 | 0.00074 | 236 | 113 | 243 | 14 | 244 | 5 | -0.41 |
| EBLN-18 | 0.51 | 0.05118 | 0.00361 | 0.28333 | 0.01979 | 0.04014 | 0.00074 | 249 | 125 | 253 | 16 | 254 | 5 | -0.39 |
| EBLN-19 | 0.64 | 0.05169 | 0.00328 | 0.31258 | 0.01959 | 0.04385 | 0.00083 | 272 | 109 | 276 | 15 | 277 | 5 | -0.36 |
| EBLN-20 | 0.54 | 0.05511 | 0.00184 | 0.50601 | 0.01687 | 0.06658 | 0.00106 | 417 | 46 | 416 | 11 | 416 | 6 | 0.00 |
| EBLN-21 | 0.66 | 0.05586 | 0.00162 | 0.55548 | 0.01618 | 0.07211 | 0.00112 | 447 | 38 | 449 | 11 | 449 | 7 | 0.00 |
| EBLN-22 | 0.44 | 0.0514 | 0.00267 | 0.29288 | 0.01501 | 0.04132 | 0.00075 | 259 | 84 | 261 | 12 | 261 | 5 | 0.00 |
| EBLN-23 | 0.63 | 0.05564 | 0.00141 | 0.54149 | 0.01395 | 0.07057 | 0.00105 | 438 | 32 | 439 | 9 | 440 | 6 | -0.23 |
| EBLN-24 | 0.59 | 0.05573 | 0.00158 | 0.54205 | 0.0155 | 0.07053 | 0.00107 | 442 | 37 | 440 | 10 | 439 | 6 | 0.23 |
| EBLN-25 | 0.87 | 0.05591 | 0.00207 | 0.55139 | 0.02031 | 0.07152 | 0.00115 | 449 | 53 | 446 | 13 | 445 | 7 | 0.22 |
| EBLN-26 | 0.45 | 0.05126 | 0.00218 | 0.27782 | 0.01171 | 0.03931 | 0.00065 | 253 | 66 | 249 | 9 | 249 | 4 | 0.00 |
| EBLN-27 | 0.69 | 0.05555 | 0.00121 | 0.56249 | 0.01271 | 0.07343 | 0.00106 | 434 | 26 | 453 | 8 | 457 | 6 | -0.88 |
| EBLN-28 | 0.93 | 0.05222 | 0.00184 | 0.31887 | 0.01117 | 0.04428 | 0.00071 | 295 | 51 | 281 | 9 | 279 | 4 | 0.72 |
| EBLN-29 | 0.54 | 0.05517 | 0.00177 | 0.51239 | 0.01651 | 0.06734 | 0.00103 | 419 | 45 | 420 | 11 | 420 | 6 | 0.00 |
| EBLN-30 | 0.73 | 0.05578 | 0.00135 | 0.54356 | 0.01346 | 0.07066 | 0.00105 | 444 | 30 | 441 | 9 | 440 | 6 | 0.23 |
| EBLN-31 | 0.75 | 0.05151 | 0.00209 | 0.29439 | 0.0119 | 0.04144 | 0.00067 | 264 | 63 | 262 | 9 | 262 | 4 | 0.00 |
| EBLN-32 | 0.61 | 0.05179 | 0.00189 | 0.31338 | 0.01133 | 0.04387 | 0.00073 | 276 | 52 | 277 | 9 | 277 | 5 | 0.00 |
| EBLN-33 | 0.22 | 0.07893 | 0.00168 | 1.98443 | 0.04375 | 0.18233 | 0.00266 | 1170 | 22 | 1110 | 15 | 1080 | 15 | 8.33 |
| EBLN-34 | 0.60 | 0.05096 | 0.00279 | 0.26475 | 0.01421 | 0.03767 | 0.00072 | 239 | 88 | 238 | 11 | 238 | 4 | 0.00 |
| EBLN-35 | 0.15 | 0.05659 | 0.00126 | 0.59577 | 0.01372 | 0.07634 | 0.00111 | 476 | 27 | 475 | 9 | 474 | 7 | 0.21 |

| | | | | | | | | | | | | | | |
|---|---|---|---|---|---|---|---|---|---|---|---|---|---|---|
| EBLN-36 | 0.01 | 0.05521 | 0.0012 | 0.56046 | 0.01265 | 0.07361 | 0.00106 | 421 | 26 | 452 | 8 | 458 | 6 | -1.31 |
| EBLN-37 | 0.43 | 0.05544 | 0.00229 | 0.51852 | 0.02112 | 0.06783 | 0.00116 | 430 | 60 | 424 | 14 | 423 | 7 | 0.24 |
| EBLN-38 | 0.64 | 0.05175 | 0.00191 | 0.30859 | 0.01131 | 0.04324 | 0.0007 | 274 | 54 | 273 | 9 | 273 | 4 | 0.00 |
| EBLN-39 | 0.14 | 0.05579 | 0.00138 | 0.56681 | 0.01432 | 0.07367 | 0.0011 | 444 | 31 | 456 | 9 | 458 | 7 | -0.44 |
| EBLN-40 | 0.93 | 0.05193 | 0.00216 | 0.31905 | 0.01324 | 0.04456 | 0.00072 | 282 | 65 | 281 | 10 | 281 | 4 | 0.00 |
| EBLN-41 | 1.00 | 0.05095 | 0.00261 | 0.26465 | 0.01345 | 0.03767 | 0.00063 | 239 | 86 | 238 | 11 | 238 | 4 | 0.00 |
| EBLN-42 | 0.58 | 0.05176 | 0.00381 | 0.31273 | 0.02269 | 0.04382 | 0.00088 | 275 | 129 | 276 | 18 | 276 | 5 | 0.00 |
| EBLN-43 | 0.52 | 0.05529 | 0.00159 | 0.51913 | 0.015 | 0.06809 | 0.00106 | 424 | 37 | 425 | 10 | 425 | 6 | 0.00 |
| EBLN-44 | 0.51 | 0.06866 | 0.0017 | 1.36188 | 0.0343 | 0.14384 | 0.00215 | 889 | 28 | 873 | 15 | 866 | 12 | 0.81 |
| EBLN-45 | 0.70 | 0.05592 | 0.002 | 0.48676 | 0.01728 | 0.06312 | 0.00103 | 449 | 50 | 403 | 12 | 395 | 6 | 2.03 |
| EBLN-46 | 0.40 | 0.07454 | 0.00166 | 1.83209 | 0.04207 | 0.17823 | 0.00262 | 1056 | 24 | 1057 | 15 | 1057 | 14 | -0.09 |
| EBLN-47 | 0.73 | 0.05553 | 0.00195 | 0.54243 | 0.01887 | 0.07083 | 0.00116 | 434 | 49 | 440 | 12 | 441 | 7 | -0.23 |
| EBLN-48 | 0.69 | 0.0515 | 0.00255 | 0.29336 | 0.01436 | 0.04131 | 0.00073 | 263 | 80 | 261 | 11 | 261 | 5 | 0.00 |
| EBLN-49 | 0.64 | 0.05191 | 0.00381 | 0.32092 | 0.02315 | 0.04483 | 0.00093 | 281 | 127 | 283 | 18 | 283 | 6 | 0.00 |
| EBLN-50 | 0.48 | 0.05539 | 0.00135 | 0.52848 | 0.01317 | 0.06918 | 0.00103 | 428 | 30 | 431 | 9 | 431 | 6 | 0.00 |
| EBLN-51 | 0.43 | 0.05394 | 0.0023 | 0.4411 | 0.01868 | 0.05927 | 0.00091 | 369 | 68 | 371 | 13 | 371 | 6 | 0.00 |
| EBLN-52 | 0.72 | 0.05492 | 0.00316 | 0.48739 | 0.02783 | 0.06432 | 0.00106 | 409 | 98 | 403 | 19 | 402 | 6 | 0.25 |
| EBLN-53 | 0.75 | 0.05547 | 0.00216 | 0.53313 | 0.02071 | 0.06966 | 0.00103 | 431 | 60 | 434 | 14 | 434 | 6 | 0.00 |
| EBLN-54 | 0.65 | 0.05441 | 0.00223 | 0.46704 | 0.01906 | 0.06221 | 0.00096 | 388 | 64 | 389 | 13 | 389 | 6 | 0.00 |
| EBLN-55 | 0.55 | 0.05165 | 0.00954 | 0.31528 | 0.05772 | 0.04425 | 0.00129 | 270 | 325 | 278 | 45 | 279 | 8 | -0.36 |
| EBLN-56 | 0.63 | 0.05527 | 0.00201 | 0.51427 | 0.01862 | 0.06745 | 0.00102 | 423 | 54 | 421 | 12 | 421 | 6 | 0.00 |
| EBLN-57 | 0.65 | 0.05174 | 0.00309 | 0.31854 | 0.01881 | 0.04462 | 0.00078 | 274 | 103 | 281 | 14 | 281 | 5 | 0.00 |
| EBLN-58 | 0.68 | 0.05133 | 0.00506 | 0.28224 | 0.02759 | 0.03986 | 0.0008 | 256 | 183 | 252 | 22 | 252 | 5 | 0.00 |
| EBLN-59 | 0.37 | 0.05619 | 0.00247 | 0.56948 | 0.02483 | 0.07347 | 0.00117 | 460 | 68 | 458 | 16 | 457 | 7 | 0.22 |
| EBLN-60 | 0.86 | 0.05158 | 0.0032 | 0.30106 | 0.01853 | 0.04231 | 0.00071 | 267 | 110 | 267 | 14 | 267 | 4 | 0.00 |
| EBLN-61 | 0.15 | 0.07201 | 0.00202 | 1.59043 | 0.04508 | 0.1601 | 0.00229 | 986 | 35 | 966 | 18 | 957 | 13 | 0.94 |
| EBLN-62 | 1.14 | 0.10737 | 0.00335 | 4.6069 | 0.14259 | 0.31101 | 0.00492 | 1755 | 34 | 1751 | 26 | 1746 | 24 | 0.52 |
| EBLN-63 | 0.24 | 0.05183 | 0.0033 | 0.2948 | 0.01862 | 0.04123 | 0.00068 | 278 | 114 | 262 | 15 | 260 | 4 | 0.77 |

| | | | | | | | | | | | | | | |
|---|---|---|---|---|---|---|---|---|---|---|---|---|---|---|
| EBLN-64 | 0.08 | 0.05601 | 0.0014 | 0.56846 | 0.01449 | 0.07357 | 0.00101 | 453 | 33 | 457 | 9 | 458 | 6 | -0.22 |
| EBLN-65 | 0.79 | 0.05156 | 0.00986 | 0.29819 | 0.05662 | 0.04193 | 0.00112 | 266 | 338 | 265 | 44 | 265 | 7 | 0.00 |
| EBLN-66 | 1.28 | 0.05108 | 0.00323 | 0.26458 | 0.01666 | 0.03755 | 0.0006 | 244 | 115 | 238 | 13 | 238 | 4 | 0.00 |
| EBLN-67 | 0.71 | 0.05132 | 0.00431 | 0.29114 | 0.02422 | 0.04112 | 0.00077 | 255 | 154 | 259 | 19 | 260 | 5 | -0.38 |
| EBLN-68 | 0.45 | 0.05229 | 0.00634 | 0.3421 | 0.04113 | 0.04743 | 0.00102 | 298 | 232 | 299 | 31 | 299 | 6 | 0.00 |
| EBLN-69 | 0.67 | 0.05554 | 0.00174 | 0.52777 | 0.01655 | 0.06889 | 0.00101 | 434 | 44 | 430 | 11 | 429 | 6 | 0.23 |
| EBLN-70 | 0.57 | 0.05533 | 0.00237 | 0.522 | 0.02211 | 0.0684 | 0.00109 | 426 | 66 | 426 | 15 | 427 | 7 | -0.23 |
| EBLN-71 | 0.45 | 0.05538 | 0.00144 | 0.52335 | 0.01367 | 0.0685 | 0.00098 | 428 | 33 | 427 | 9 | 427 | 6 | 0.00 |
| EBLN-72 | 0.36 | 0.05232 | 0.00411 | 0.34094 | 0.02647 | 0.04725 | 0.00089 | 299 | 143 | 298 | 20 | 298 | 5 | 0.00 |
| EBLN-73 | 0.41 | 0.05507 | 0.00543 | 0.50325 | 0.04907 | 0.06625 | 0.00138 | 415 | 182 | 414 | 33 | 414 | 8 | 0.00 |
| EBLN-74 | 0.63 | 0.0516 | 0.00544 | 0.29688 | 0.03094 | 0.04171 | 0.0009 | 268 | 195 | 264 | 24 | 263 | 6 | 0.38 |
| EBLN-75 | 0.87 | 0.05128 | 0.00357 | 0.27974 | 0.01926 | 0.03954 | 0.0007 | 253 | 125 | 250 | 15 | 250 | 4 | 0.00 |
| EBLN-76 | 0.29 | 0.05661 | 0.00185 | 0.5933 | 0.01934 | 0.07599 | 0.00111 | 476 | 46 | 473 | 12 | 472 | 7 | 0.21 |
| EBLN-77 | 0.51 | 0.05577 | 0.00145 | 0.54215 | 0.01421 | 0.07048 | 0.001 | 443 | 34 | 440 | 9 | 439 | 6 | 0.23 |
| EBLN-78 | 0.64 | 0.08575 | 0.00184 | 2.71854 | 0.05948 | 0.22985 | 0.00321 | 1333 | 22 | 1334 | 16 | 1334 | 17 | -0.07 |
| EBLN-79 | 0.54 | 0.05171 | 0.00807 | 0.29944 | 0.04636 | 0.04198 | 0.00104 | 273 | 290 | 266 | 36 | 265 | 6 | 0.38 |
| EBLN-80 | 0.75 | 0.05137 | 0.00324 | 0.28477 | 0.01769 | 0.04019 | 0.00072 | 257 | 110 | 254 | 14 | 254 | 4 | 0.00 |
| EBLN-81 | 0.52 | 0.05487 | 0.00302 | 0.4951 | 0.0268 | 0.06541 | 0.00118 | 407 | 89 | 408 | 18 | 408 | 7 | 0.00 |
| EBLN-82 | 0.86 | 0.05073 | 0.00465 | 0.25487 | 0.02307 | 0.03643 | 0.00074 | 229 | 167 | 231 | 19 | 231 | 5 | 0.00 |
| EBLN-83 | 0.48 | 0.05146 | 0.0034 | 0.28276 | 0.0184 | 0.03984 | 0.00074 | 261 | 115 | 253 | 15 | 252 | 5 | 0.40 |
| EBLN-84 | 0.47 | 0.05358 | 0.00302 | 0.4213 | 0.02347 | 0.05701 | 0.00096 | 353 | 95 | 357 | 17 | 357 | 6 | 0.00 |
| EBLN-85 | 0.58 | 0.05162 | 0.00459 | 0.29869 | 0.02625 | 0.04195 | 0.00083 | 269 | 163 | 265 | 21 | 265 | 5 | 0.00 |
| EBLN-86 | 0.76 | 0.05081 | 0.0168 | 0.27349 | 0.08988 | 0.03903 | 0.00157 | 232 | 512 | 245 | 72 | 247 | 10 | -0.81 |
| EBLN-87 | 1.46 | 0.0511 | 0.01761 | 0.26198 | 0.08962 | 0.03717 | 0.00166 | 245 | 530 | 236 | 72 | 235 | 10 | 0.43 |
| EBLN-88 | 0.54 | 0.05173 | 0.00678 | 0.30156 | 0.03914 | 0.04226 | 0.00098 | 273 | 251 | 268 | 31 | 267 | 6 | 0.37 |
| EBLN-89 | 0.67 | 0.05185 | 0.00395 | 0.31374 | 0.02359 | 0.04387 | 0.00083 | 279 | 137 | 277 | 18 | 277 | 5 | 0.00 |
| EBLN-90 | 0.52 | 0.05584 | 0.00208 | 0.5526 | 0.02021 | 0.07175 | 0.00115 | 446 | 53 | 447 | 13 | 447 | 7 | 0.00 |
| EBLN-91 | 0.25 | 0.05178 | 0.01638 | 0.30507 | 0.09576 | 0.04272 | 0.00178 | 276 | 497 | 270 | 75 | 270 | 11 | 0.00 |

| | | | | | | | | | | | | | | |
|---|---|---|---|---|---|---|---|---|---|---|---|---|---|---|
| EBLN-92 | 0.44 | 0.05516 | 0.00157 | 0.50094 | 0.01433 | 0.06584 | 0.00094 | 419 | 39 | 412 | 10 | 411 | 6 | 0.24 |
| EBLN-93 | 0.72 | 0.05538 | 0.00311 | 0.50947 | 0.0283 | 0.0667 | 0.00112 | 428 | 94 | 418 | 19 | 416 | 7 | 0.48 |
| EBLN-94 | 0.52 | 0.05529 | 0.00129 | 0.51686 | 0.01219 | 0.06778 | 0.00095 | 424 | 29 | 423 | 8 | 423 | 6 | 0.00 |
| EBLN-95 | 0.45 | 0.05584 | 0.00159 | 0.55045 | 0.01558 | 0.07148 | 0.00106 | 446 | 37 | 445 | 10 | 445 | 6 | 0.00 |
| EBLN-96 | 0.65 | 0.05588 | 0.00156 | 0.55064 | 0.01528 | 0.07145 | 0.00107 | 448 | 36 | 445 | 10 | 445 | 6 | 0.00 |
| EBLN-97 | 0.01 | 0.05131 | 0.0016 | 0.28145 | 0.00872 | 0.03977 | 0.00059 | 255 | 44 | 252 | 7 | 251 | 4 | 0.40 |
| EBLN-98 | 1.06 | 0.05124 | 0.00417 | 0.27894 | 0.02246 | 0.03948 | 0.00073 | 252 | 149 | 250 | 18 | 250 | 5 | 0.00 |
| EBLN-99 | 0.35 | 0.05605 | 0.00122 | 0.55821 | 0.01234 | 0.07221 | 0.001 | 454 | 26 | 450 | 8 | 449 | 6 | 0.22 |
| EBLN-100 | 0.35 | 0.05571 | 0.00159 | 0.53992 | 0.01529 | 0.07028 | 0.00104 | 441 | 37 | 438 | 10 | 438 | 6 | 0.00 |
| **E-E1** | | | | | | | | | | | | | | |
| EE1-01 | 0.44 | 0.0569 | 0.00146 | 0.61574 | 0.01599 | 0.07847 | 0.00109 | 488 | 33 | 487 | 10 | 487 | 7 | 0.00 |
| EE1-02 | 1.01 | 0.05245 | 0.00817 | 0.29482 | 0.0456 | 0.04077 | 0.00077 | 305 | 325 | 262 | 36 | 258 | 5 | 1.55 |
| EE1-03 | 0.31 | 0.05581 | 0.00136 | 0.5447 | 0.01343 | 0.07077 | 0.00099 | 445 | 31 | 442 | 9 | 441 | 6 | 0.23 |
| ~~EE1-04~~ | ~~0.11~~ | ~~0.06787~~ | ~~0.00136~~ | ~~0.72157~~ | ~~0.01495~~ | ~~0.07709~~ | ~~0.00104~~ | ~~865~~ | ~~22~~ | ~~552~~ | ~~9~~ | ~~479~~ | ~~6~~ | ~~15.24~~ |
| EE1-05 | 0.41 | 0.05637 | 0.00121 | 0.55323 | 0.01222 | 0.07115 | 0.00096 | 467 | 26 | 447 | 8 | 443 | 6 | 0.90 |
| EE1-06 | 1.26 | 0.05479 | 0.00241 | 0.48706 | 0.02138 | 0.06446 | 0.00096 | 404 | 71 | 403 | 15 | 403 | 6 | 0.00 |
| EE1-07 | 0.57 | 0.05906 | 0.00112 | 0.54782 | 0.01085 | 0.06725 | 0.00089 | 569 | 22 | 444 | 7 | 420 | 5 | 5.71 |
| EE1-08 | 0.68 | 0.05179 | 0.00543 | 0.31219 | 0.03251 | 0.04371 | 0.00084 | 276 | 200 | 276 | 25 | 276 | 5 | 0.00 |
| EE1-09 | 1.09 | 0.0535 | 0.00413 | 0.28259 | 0.02129 | 0.03831 | 0.00063 | 350 | 177 | 253 | 17 | 242 | 4 | 4.55 |
| EE1-10 | 1.23 | 0.05936 | 0.0047 | 0.56417 | 0.0436 | 0.06894 | 0.00116 | 580 | 178 | 454 | 28 | 430 | 7 | 5.58 |
| EE1-11 | 0.68 | 0.05511 | 0.00114 | 0.50726 | 0.01078 | 0.06674 | 0.00089 | 417 | 25 | 417 | 7 | 416 | 5 | 0.24 |
| EE1-12 | 0.23 | 0.07607 | 0.00215 | 1.80375 | 0.04495 | 0.17198 | 0.00231 | 1097 | 58 | 1047 | 16 | 1023 | 13 | 7.23 |
| EE1-13 | 1.02 | 0.05525 | 0.0034 | 0.51547 | 0.03151 | 0.06765 | 0.00108 | 422 | 108 | 422 | 21 | 422 | 7 | 0.00 |
| EE1-14 | 1.11 | 0.05141 | 0.00287 | 0.28311 | 0.01537 | 0.03993 | 0.00078 | 259 | 89 | 253 | 12 | 252 | 5 | 0.40 |
| EE1-15 | 0.75 | 0.0524 | 0.00168 | 0.35442 | 0.01137 | 0.04904 | 0.00071 | 303 | 47 | 308 | 9 | 309 | 4 | -0.32 |
| EE1-16 | 0.82 | 0.05518 | 0.00107 | 0.51245 | 0.0103 | 0.06734 | 0.00089 | 420 | 23 | 420 | 7 | 420 | 5 | 0.00 |

| | | | | | | | | | | | | | | |
|---|---|---|---|---|---|---|---|---|---|---|---|---|---|---|
| EE1-17 | 1.02 | 0.05126 | 0.00434 | 0.2787 | 0.02335 | 0.03943 | 0.00077 | 253 | 154 | 250 | 19 | 249 | 5 | 0.40 |
| EE1-18 | 1.18 | 0.05112 | 0.00229 | 0.27054 | 0.0121 | 0.03837 | 0.00057 | 246 | 75 | 243 | 10 | 243 | 4 | 0.00 |
| EE1-19 | 0.98 | 0.05547 | 0.00216 | 0.5242 | 0.02043 | 0.06852 | 0.00099 | 431 | 61 | 428 | 14 | 427 | 6 | 0.23 |
| EE1-20 | 0.54 | 0.07945 | 0.0034 | 2.29407 | 0.09207 | 0.20941 | 0.00312 | 1183 | 87 | 1210 | 28 | 1226 | 17 | -3.51 |
| EE1-21 | 1.52 | 0.05137 | 0.00422 | 0.28247 | 0.02307 | 0.03987 | 0.00067 | 257 | 155 | 253 | 18 | 252 | 4 | 0.40 |
| EE1-22 | 1.24 | 0.05108 | 0.00235 | 0.27636 | 0.0126 | 0.03923 | 0.00061 | 244 | 76 | 248 | 10 | 248 | 4 | 0.00 |
| EE1-23 | 0.60 | 0.14649 | 0.00265 | 7.8407 | 0.14796 | 0.3881 | 0.00525 | 2305 | 16 | 2213 | 17 | 2114 | 24 | 9.04 |
| EE1-24 | 0.38 | 0.05638 | 0.00153 | 0.56821 | 0.01554 | 0.07307 | 0.00102 | 467 | 36 | 457 | 10 | 455 | 6 | 0.44 |
| ~~EE1-25~~ | ~~1.16~~ | ~~0.07506~~ | ~~0.00705~~ | ~~0.41524~~ | ~~0.03825~~ | ~~0.04013~~ | ~~0.00073~~ | ~~1070~~ | ~~196~~ | ~~353~~ | ~~27~~ | ~~254~~ | ~~5~~ | ~~38.98~~ |
| ~~EE1-26~~ | ~~0.42~~ | ~~0.08003~~ | ~~0.00166~~ | ~~1.36764~~ | ~~0.0292~~ | ~~0.12391~~ | ~~0.00168~~ | ~~1198~~ | ~~22~~ | ~~875~~ | ~~13~~ | ~~753~~ | ~~10~~ | ~~16.20~~ |
| EE1-27 | 0.58 | 0.05135 | 0.0017 | 0.28336 | 0.00939 | 0.04001 | 0.00057 | 257 | 50 | 253 | 7 | 253 | 4 | 0.00 |
| EE1-28 | 0.73 | 0.05931 | 0.0091 | 0.58311 | 0.08838 | 0.07131 | 0.00167 | 578 | 344 | 466 | 57 | 444 | 10 | 4.95 |
| EE1-29 | 0.68 | 0.06167 | 0.00146 | 0.57812 | 0.01383 | 0.06797 | 0.00094 | 663 | 28 | 463 | 9 | 424 | 6 | 9.20 |
| ~~EE1-30~~ | ~~0.86~~ | ~~0.06249~~ | ~~0.00411~~ | ~~0.35218~~ | ~~0.02299~~ | ~~0.04087~~ | ~~0.00067~~ | ~~691~~ | ~~112~~ | ~~306~~ | ~~17~~ | ~~258~~ | ~~4~~ | ~~18.60~~ |
| EE1-31 | 0.63 | 0.05118 | 0.00212 | 0.27812 | 0.01144 | 0.0394 | 0.00061 | 249 | 66 | 249 | 9 | 249 | 4 | 0.00 |
| EE1-32 | 0.04 | 0.05645 | 0.00116 | 0.58872 | 0.01245 | 0.07563 | 0.00101 | 470 | 25 | 470 | 8 | 470 | 6 | 0.00 |
| EE1-33 | 0.69 | 0.05806 | 0.00718 | 0.52513 | 0.06423 | 0.0656 | 0.00116 | 532 | 280 | 429 | 43 | 410 | 7 | 4.63 |
| EE1-34 | 0.84 | 0.05145 | 0.00474 | 0.29393 | 0.02681 | 0.04142 | 0.00082 | 261 | 170 | 262 | 21 | 262 | 5 | 0.00 |
| ~~EE1-35~~ | ~~0.85~~ | ~~0.08146~~ | ~~0.00992~~ | ~~0.46531~~ | ~~0.05578~~ | ~~0.04143~~ | ~~0.0009~~ | ~~1232~~ | ~~251~~ | ~~388~~ | ~~39~~ | ~~262~~ | ~~6~~ | ~~48.09~~ |
| EE1-36 | 0.54 | 0.11479 | 0.00245 | 4.88045 | 0.10658 | 0.30829 | 0.00432 | 1877 | 20 | 1799 | 18 | 1732 | 21 | 8.37 |
| EE1-37 | 0.62 | 0.05502 | 0.0053 | 0.2982 | 0.02828 | 0.03931 | 0.00064 | 413 | 220 | 265 | 22 | 249 | 4 | 6.43 |
| EE1-38 | 0.54 | 0.05504 | 0.00127 | 0.5093 | 0.01192 | 0.0671 | 0.00092 | 414 | 29 | 418 | 8 | 419 | 6 | -0.24 |
| ~~EE1-39~~ | ~~0.47~~ | ~~0.07022~~ | ~~0.00447~~ | ~~0.70124~~ | ~~0.04329~~ | ~~0.07243~~ | ~~0.0011~~ | ~~935~~ | ~~134~~ | ~~540~~ | ~~26~~ | ~~451~~ | ~~7~~ | ~~19.73~~ |
| EE1-40 | 0.77 | 0.05622 | 0.00369 | 0.28454 | 0.01822 | 0.0367 | 0.00075 | 461 | 106 | 254 | 14 | 232 | 5 | 9.48 |
| EE1-41 | 0.99 | 0.05359 | 0.00716 | 0.41991 | 0.0556 | 0.05681 | 0.0013 | 354 | 257 | 356 | 40 | 356 | 8 | 0.00 |
| EE1-42 | 0.49 | 0.05467 | 0.00264 | 0.44252 | 0.02129 | 0.05869 | 0.00088 | 399 | 81 | 372 | 15 | 368 | 5 | 1.09 |
| EE1-43 | 0.75 | 0.05134 | 0.00231 | 0.29386 | 0.01315 | 0.0415 | 0.00064 | 256 | 74 | 262 | 10 | 262 | 4 | 0.00 |
| ~~EE1-44~~ | ~~1.09~~ | ~~0.08277~~ | ~~0.00568~~ | ~~0.84326~~ | ~~0.05609~~ | ~~0.07389~~ | ~~0.00124~~ | ~~1264~~ | ~~138~~ | ~~621~~ | ~~31~~ | ~~460~~ | ~~7~~ | ~~35.00~~ |

| | | | | | | | | | | | | | | |
|---|---|---|---|---|---|---|---|---|---|---|---|---|---|---|
| ~~EE1-45~~ | ~~0.19~~ | ~~0.09751~~ | ~~0.0026~~ | ~~2.51088~~ | ~~0.05782~~ | ~~0.18675~~ | ~~0.0025~~ | ~~1577~~ | ~~51~~ | ~~1275~~ | ~~17~~ | ~~1104~~ | ~~14~~ | ~~42.84~~ |
| EE1-46 | 0.14 | 0.05643 | 0.00225 | 0.54484 | 0.02164 | 0.07001 | 0.00106 | 469 | 61 | 442 | 14 | 436 | 6 | 1.38 |
| EE1-47 | 0.43 | 0.07492 | 0.00281 | 1.78188 | 0.06204 | 0.1725 | 0.00242 | 1066 | 77 | 1039 | 23 | 1026 | 13 | 3.90 |
| EE1-48 | 1.02 | 0.05158 | 0.00213 | 0.28841 | 0.01184 | 0.04054 | 0.00062 | 267 | 66 | 257 | 9 | 256 | 4 | 0.39 |
| EE1-49 | 0.13 | 0.05618 | 0.00128 | 0.56809 | 0.01315 | 0.07332 | 0.001 | 459 | 28 | 457 | 9 | 456 | 6 | 0.22 |
| EE1-50 | 0.23 | 0.05543 | 0.00155 | 0.51614 | 0.01454 | 0.06751 | 0.00094 | 430 | 38 | 423 | 10 | 421 | 6 | 0.48 |
| ~~EE1-51~~ | ~~0.32~~ | ~~0.05883~~ | ~~0.00629~~ | ~~0.32639~~ | ~~0.0344~~ | ~~0.04024~~ | ~~0.00073~~ | ~~561~~ | ~~242~~ | ~~287~~ | ~~26~~ | ~~254~~ | ~~5~~ | ~~12.99~~ |
| EE1-52 | 0.70 | 0.10871 | 0.0022 | 4.30469 | 0.08942 | 0.28713 | 0.00393 | 1778 | 19 | 1694 | 17 | 1627 | 20 | 9.28 |
| EE1-53 | 0.86 | 0.05165 | 0.00169 | 0.28655 | 0.0094 | 0.04023 | 0.00058 | 270 | 49 | 256 | 7 | 254 | 4 | 0.79 |
| EE1-54 | 0.53 | 0.05504 | 0.0023 | 0.4542 | 0.01887 | 0.05984 | 0.00091 | 414 | 66 | 380 | 13 | 375 | 6 | 1.33 |
| EE1-55 | 0.65 | 0.05619 | 0.00174 | 0.53329 | 0.01646 | 0.06882 | 0.001 | 460 | 43 | 434 | 11 | 429 | 6 | 1.17 |
| ~~EE1-56~~ | ~~1.05~~ | ~~0.08~~ | ~~0.01759~~ | ~~0.43808~~ | ~~0.09563~~ | ~~0.03972~~ | ~~0.00105~~ | ~~1197~~ | ~~481~~ | ~~369~~ | ~~68~~ | ~~251~~ | ~~6~~ | ~~47.01~~ |
| ~~EE1-57~~ | ~~0.48~~ | ~~0.06557~~ | ~~0.00565~~ | ~~0.64505~~ | ~~0.05439~~ | ~~0.07135~~ | ~~0.00126~~ | ~~793~~ | ~~187~~ | ~~505~~ | ~~34~~ | ~~444~~ | ~~8~~ | ~~13.74~~ |
| ~~EE1-58~~ | ~~0.26~~ | ~~0.07072~~ | ~~0.00216~~ | ~~0.98416~~ | ~~0.02695~~ | ~~0.10093~~ | ~~0.00137~~ | ~~949~~ | ~~64~~ | ~~696~~ | ~~14~~ | ~~620~~ | ~~8~~ | ~~12.26~~ |
| EE1-59 | 1.12 | 0.05129 | 0.00259 | 0.28048 | 0.01405 | 0.03966 | 0.00062 | 254 | 86 | 251 | 11 | 251 | 4 | 0.00 |
| EE1-60 | 0.66 | 0.05141 | 0.00622 | 0.29192 | 0.03514 | 0.04117 | 0.0008 | 259 | 236 | 260 | 28 | 260 | 5 | 0.00 |
| EE1-61 | 0.47 | 0.05554 | 0.00255 | 0.53329 | 0.02328 | 0.06964 | 0.00099 | 434 | 105 | 434 | 15 | 434 | 6 | 0.00 |
| EE1-62 | 0.65 | 0.05525 | 0.00117 | 0.51939 | 0.01125 | 0.06816 | 0.00092 | 422 | 26 | 425 | 8 | 425 | 6 | 0.00 |
| EE1-63 | 0.58 | 0.05206 | 0.00209 | 0.32769 | 0.01305 | 0.04564 | 0.00071 | 288 | 62 | 288 | 10 | 288 | 4 | 0.00 |
| EE1-64 | 1.15 | 0.05194 | 0.00396 | 0.32109 | 0.02432 | 0.04483 | 0.00076 | 283 | 141 | 283 | 19 | 283 | 5 | 0.00 |
| EE1-65 | 0.38 | 0.05554 | 0.00133 | 0.51703 | 0.01251 | 0.06751 | 0.00093 | 434 | 30 | 423 | 8 | 421 | 6 | 0.48 |
| EE1-66 | 0.25 | 0.0515 | 0.00213 | 0.29397 | 0.01206 | 0.04139 | 0.00063 | 263 | 66 | 262 | 9 | 261 | 4 | 0.38 |
| EE1-67 | 1.06 | 0.05537 | 0.00321 | 0.51409 | 0.02961 | 0.06732 | 0.00108 | 427 | 100 | 421 | 20 | 420 | 7 | 0.24 |
| EE1-68 | 0.80 | 0.05128 | 0.0025 | 0.28186 | 0.01366 | 0.03986 | 0.00062 | 253 | 83 | 252 | 11 | 252 | 4 | 0.00 |
| EE1-69 | 0.57 | 0.05417 | 0.00156 | 0.44323 | 0.01279 | 0.05933 | 0.00085 | 378 | 39 | 373 | 9 | 372 | 5 | 0.27 |
| EE1-70 | 0.73 | 0.05592 | 0.00245 | 0.51688 | 0.02215 | 0.06703 | 0.00115 | 449 | 65 | 423 | 15 | 418 | 7 | 1.20 |
| ~~EE1-71~~ | ~~0.83~~ | ~~0.05739~~ | ~~0.00376~~ | ~~0.31222~~ | ~~0.01989~~ | ~~0.03945~~ | ~~0.00061~~ | ~~507~~ | ~~148~~ | ~~276~~ | ~~15~~ | ~~249~~ | 4 | ~~10.84~~ |
| ~~EE1-72~~ | ~~0.41~~ | ~~0.06321~~ | ~~0.01992~~ | ~~0.36456~~ | ~~0.11446~~ | ~~0.04183~~ | ~~0.00114~~ | ~~715~~ | ~~631~~ | ~~316~~ | ~~85~~ | ~~264~~ | ~~7~~ | ~~19.70~~ |

| | | | | | | | | | | | | | | |
|---|---|---|---|---|---|---|---|---|---|---|---|---|---|---|
| EE1-73 | 0.84 | 0.05273 | 0.01311 | 0.27028 | 0.06696 | 0.03718 | 0.0008 | 317 | 457 | 243 | 54 | 235 | 5 | 3.40 |
| EE1-74 | 0.65 | 0.05616 | 0.00223 | 0.56783 | 0.02206 | 0.07331 | 0.00122 | 459 | 57 | 457 | 14 | 456 | 7 | 0.22 |
| EE1-75 | 1.02 | 0.05115 | 0.00198 | 0.27746 | 0.01067 | 0.03934 | 0.00059 | 248 | 61 | 249 | 8 | 249 | 4 | 0.00 |
| ~~EE1-76~~ | ~~0.65~~ | ~~0.05807~~ | ~~0.01015~~ | ~~0.3196~~ | ~~0.0554~~ | ~~0.03992~~ | ~~0.00091~~ | ~~532~~ | ~~376~~ | ~~282~~ | ~~43~~ | ~~252~~ | ~~6~~ | ~~11.90~~ |
| EE1-77 | 0.05 | 0.0547 | 0.00123 | 0.49529 | 0.01134 | 0.06566 | 0.0009 | 400 | 28 | 409 | 8 | 410 | 5 | -0.24 |
| EE1-78 | 0.52 | 0.05129 | 0.00158 | 0.28952 | 0.00887 | 0.04093 | 0.0006 | 254 | 44 | 258 | 7 | 259 | 4 | -0.39 |
| EE1-79 | 0.59 | 0.05681 | 0.00156 | 0.5871 | 0.01613 | 0.07493 | 0.00107 | 484 | 36 | 469 | 10 | 466 | 6 | 0.64 |
| EE1-80 | 0.96 | 0.05577 | 0.00444 | 0.52901 | 0.04152 | 0.06879 | 0.00139 | 443 | 139 | 431 | 28 | 429 | 8 | 0.47 |
| EE1-81 | 0.39 | 0.05134 | 0.002 | 0.29126 | 0.01128 | 0.04113 | 0.00062 | 256 | 61 | 260 | 9 | 260 | 4 | 0.00 |
| EE1-82 | 0.90 | 0.05259 | 0.00274 | 0.32594 | 0.01672 | 0.04494 | 0.00078 | 311 | 85 | 286 | 13 | 283 | 5 | 1.06 |
| ~~EE1-83~~ | ~~1.18~~ | ~~0.06156~~ | ~~0.01089~~ | ~~0.36438~~ | ~~0.06395~~ | ~~0.04293~~ | ~~0.00093~~ | ~~659~~ | ~~394~~ | ~~315~~ | ~~48~~ | ~~271~~ | ~~6~~ | ~~16.24~~ |
| EE1-84 | 0.55 | 0.05476 | 0.00138 | 0.48863 | 0.01245 | 0.06471 | 0.0009 | 402 | 33 | 404 | 8 | 404 | 5 | 0.00 |
| EE1-85 | 0.67 | 0.051 | 0.00369 | 0.27791 | 0.01993 | 0.03951 | 0.00069 | 241 | 131 | 249 | 16 | 250 | 4 | -0.40 |
| EE1-86 | 0.50 | 0.05775 | 0.00291 | 0.52297 | 0.02528 | 0.06568 | 0.00095 | 520 | 114 | 427 | 17 | 410 | 6 | 4.15 |
| ~~EE1-87~~ | ~~1.09~~ | ~~0.07289~~ | ~~0.01318~~ | ~~0.3872~~ | ~~0.0694~~ | ~~0.03853~~ | ~~0.00091~~ | ~~1011~~ | ~~398~~ | ~~332~~ | ~~51~~ | ~~244~~ | ~~6~~ | ~~36.07~~ |
| EE1-88 | 0.78 | 0.05162 | 0.00266 | 0.28127 | 0.01435 | 0.03951 | 0.00064 | 269 | 87 | 252 | 11 | 250 | 4 | 0.80 |
| ~~EE1-89~~ | ~~0.16~~ | ~~0.09003~~ | ~~0.00204~~ | ~~0.60252~~ | ~~0.0138~~ | ~~0.04853~~ | ~~0.00067~~ | ~~1426~~ | ~~24~~ | ~~479~~ | ~~9~~ | ~~305~~ | ~~4~~ | ~~57.05~~ |
| EE1-90 | 0.84 | 0.05113 | 0.00286 | 0.28041 | 0.01553 | 0.03977 | 0.00066 | 247 | 97 | 251 | 12 | 251 | 4 | 0.00 |
| EE1-91 | 0.61 | 0.05497 | 0.00232 | 0.49612 | 0.02061 | 0.06545 | 0.00106 | 411 | 64 | 409 | 14 | 409 | 6 | 0.00 |
| EE1-92 | 1.15 | 0.05161 | 0.00419 | 0.27288 | 0.02172 | 0.03835 | 0.0006 | 268 | 186 | 245 | 17 | 243 | 4 | 0.82 |
| EE1-93 | 0.75 | 0.05119 | 0.0018 | 0.27705 | 0.00964 | 0.03924 | 0.00059 | 249 | 52 | 248 | 8 | 248 | 4 | 0.00 |
| EE1-94 | 0.51 | 0.05566 | 0.00317 | 0.56632 | 0.03204 | 0.07378 | 0.00117 | 439 | 98 | 456 | 21 | 459 | 7 | -0.65 |
| EE1-95 | 0.66 | 0.1259 | 0.00434 | 5.99185 | 0.18689 | 0.34517 | 0.00507 | 2041 | 62 | 1975 | 27 | 1912 | 24 | 6.75 |
| EE1-96 | 0.45 | 0.05531 | 0.00206 | 0.49841 | 0.01844 | 0.06534 | 0.001 | 425 | 55 | 411 | 12 | 408 | 6 | 0.74 |
| EE1-97 | 1.37 | 0.05508 | 0.00189 | 0.49653 | 0.01691 | 0.06537 | 0.00098 | 415 | 49 | 409 | 11 | 408 | 6 | 0.25 |
| EE1-98 | 0.70 | 0.05547 | 0.00398 | 0.53677 | 0.03806 | 0.07016 | 0.0013 | 431 | 126 | 436 | 25 | 437 | 8 | -0.23 |
| EE1-99 | 0.03 | 0.08212 | 0.00203 | 2.19029 | 0.04584 | 0.19344 | 0.00256 | 1248 | 50 | 1178 | 15 | 1140 | 14 | 9.47 |
| EE1-100 | 0.72 | 0.05552 | 0.00158 | 0.53572 | 0.01514 | 0.06997 | 0.00102 | 433 | 37 | 436 | 10 | 436 | 6 | 0.00 |

| | | | | | | | | | | | | | | |
|---|---|---|---|---|---|---|---|---|---|---|---|---|---|---|
| EE1-101 | 0.50 | 0.05877 | 0.00415 | 0.54693 | 0.03765 | 0.0675 | 0.00104 | 559 | 159 | 443 | 25 | 421 | 6 | 5.23 |
| EE1-102 | 0.26 | 0.0571 | 0.00155 | 0.58653 | 0.01597 | 0.07449 | 0.00106 | 495 | 35 | 469 | 10 | 463 | 6 | 1.30 |
| EE1-103 | 0.52 | 0.05116 | 0.00198 | 0.27015 | 0.01033 | 0.03829 | 0.0006 | 248 | 59 | 243 | 8 | 242 | 4 | 0.41 |
| EE1-104 | 0.77 | 0.05139 | 0.0022 | 0.28962 | 0.01219 | 0.04087 | 0.00067 | 258 | 66 | 258 | 10 | 258 | 4 | 0.00 |
| EE1-105 | 0.07 | 0.06049 | 0.00173 | 0.71953 | 0.01808 | 0.08628 | 0.00117 | 621 | 63 | 550 | 11 | 533 | 7 | 3.19 |
| **E-D1** | | | | | | | | | | | | | | |
| ED1-01 | 0.39 | 0.05475 | 0.00123 | 0.50946 | 0.01176 | 0.06747 | 0.00093 | 402 | 28 | 418 | 8 | 421 | 6 | -0.71 |
| ED1-02 | 0.84 | 0.05114 | 0.00216 | 0.27443 | 0.01154 | 0.03891 | 0.0006 | 247 | 68 | 246 | 9 | 246 | 4 | 0.00 |
| ED1-03 | 0.26 | 0.05491 | 0.00163 | 0.49656 | 0.01493 | 0.06557 | 0.00092 | 409 | 42 | 409 | 10 | 409 | 6 | 0.00 |
| ED1-04 | 0.35 | 0.05672 | 0.00097 | 0.49287 | 0.00899 | 0.06301 | 0.00084 | 481 | 19 | 407 | 6 | 394 | 5 | 3.30 |
| ED1-05 | 1.17 | 0.05113 | 0.00408 | 0.27318 | 0.02174 | 0.03874 | 0.00063 | 247 | 151 | 245 | 17 | 245 | 4 | 0.00 |
| ED1-06 | 1.08 | 0.05119 | 0.00175 | 0.26778 | 0.00915 | 0.03793 | 0.00057 | 249 | 51 | 241 | 7 | 240 | 4 | 0.42 |
| ED1-07 | 0.65 | 0.05475 | 0.00403 | 0.48362 | 0.03534 | 0.06405 | 0.0011 | 402 | 134 | 401 | 24 | 400 | 7 | 0.25 |
| ED1-08 | 0.67 | 0.05386 | 0.00152 | 0.41917 | 0.01197 | 0.05643 | 0.0008 | 365 | 39 | 355 | 9 | 354 | 5 | 0.28 |
| ED1-09 | 0.77 | 0.0514 | 0.00244 | 0.27544 | 0.01298 | 0.03886 | 0.00061 | 259 | 79 | 247 | 10 | 246 | 4 | 0.41 |
| ED1-10 | 0.31 | 0.05474 | 0.00112 | 0.4878 | 0.01043 | 0.06462 | 0.00086 | 402 | 25 | 403 | 7 | 404 | 5 | -0.25 |
| ED1-11 | 0.12 | 0.05682 | 0.00165 | 0.53504 | 0.01381 | 0.06829 | 0.00091 | 485 | 66 | 435 | 9 | 426 | 6 | 2.11 |
| ED1-12 | 0.46 | 0.05124 | 0.00196 | 0.28278 | 0.01087 | 0.04002 | 0.00058 | 252 | 62 | 253 | 9 | 253 | 4 | 0.00 |
| ED1-13 | 0.77 | 0.05533 | 0.00137 | 0.48903 | 0.01239 | 0.06408 | 0.00089 | 426 | 32 | 404 | 8 | 400 | 5 | 1.00 |
| ED1-14 | 0.25 | 0.05528 | 0.00174 | 0.49229 | 0.01564 | 0.06458 | 0.00092 | 424 | 46 | 406 | 11 | 403 | 6 | 0.74 |
| ED1-15 | 0.91 | 0.0556 | 0.00121 | 0.51409 | 0.01157 | 0.06705 | 0.00091 | 436 | 27 | 421 | 8 | 418 | 5 | 0.72 |
| ED1-16 | 0.37 | 0.0563 | 0.00187 | 0.48413 | 0.01463 | 0.06236 | 0.00085 | 464 | 75 | 401 | 10 | 390 | 5 | 2.82 |
| ED1-17 | 0.65 | 0.05565 | 0.0027 | 0.54884 | 0.02641 | 0.07152 | 0.00115 | 438 | 78 | 444 | 17 | 445 | 7 | -0.22 |
| ED1-18 | 0.52 | 0.05091 | 0.00196 | 0.26564 | 0.01024 | 0.03784 | 0.00057 | 237 | 61 | 239 | 8 | 239 | 4 | 0.00 |
| ED1-19 | 0.29 | 0.05519 | 0.0014 | 0.49735 | 0.01285 | 0.06535 | 0.00092 | 420 | 33 | 410 | 9 | 408 | 6 | 0.49 |
| ED1-20 | 1.07 | 0.05507 | 0.01022 | 0.48515 | 0.08916 | 0.06388 | 0.00193 | 415 | 342 | 402 | 61 | 399 | 12 | 0.75 |
| ED1-21 | 1.27 | 0.05159 | 0.0055 | 0.27447 | 0.02913 | 0.03858 | 0.00071 | 267 | 206 | 246 | 23 | 244 | 4 | 0.82 |

| | | | | | | | | | | | | | | |
|---|---|---|---|---|---|---|---|---|---|---|---|---|---|---|
| ED1-22 | 0.73 | 0.05109 | 0.00327 | 0.27369 | 0.01744 | 0.03884 | 0.00062 | 245 | 117 | 246 | 14 | 246 | 4 | 0.00 |
| ~~ED1-23~~ | ~~0.26~~ | ~~0.08291~~ | ~~0.00244~~ | ~~1.82484~~ | ~~0.04733~~ | ~~0.15962~~ | ~~0.00221~~ | ~~1267~~ | ~~59~~ | ~~1054~~ | ~~17~~ | ~~955~~ | ~~12~~ | ~~10.37~~ |
| ED1-24 | 0.74 | 0.05094 | 0.00287 | 0.26982 | 0.01513 | 0.03841 | 0.00062 | 238 | 100 | 243 | 12 | 243 | 4 | 0.00 |
| ED1-25 | 0.38 | 0.05472 | 0.00172 | 0.48447 | 0.01532 | 0.0642 | 0.00093 | 401 | 45 | 401 | 10 | 401 | 6 | 0.00 |
| ED1-26 | 0.10 | 0.06348 | 0.00173 | 0.67007 | 0.01593 | 0.07656 | 0.00103 | 724 | 59 | 521 | 10 | 476 | 6 | 9.45 |
| ED1-27 | 0.40 | 0.05565 | 0.0018 | 0.5103 | 0.0166 | 0.06649 | 0.00095 | 438 | 47 | 419 | 11 | 415 | 6 | 0.96 |
| ED1-28 | 0.67 | 0.05477 | 0.00176 | 0.49528 | 0.01602 | 0.06557 | 0.00095 | 403 | 47 | 409 | 11 | 409 | 6 | 0.00 |
| ED1-29 | 0.48 | 0.07029 | 0.00136 | 1.42365 | 0.02887 | 0.14688 | 0.002 | 937 | 21 | 899 | 12 | 883 | 11 | 1.81 |
| ED1-30 | 0.70 | 0.05147 | 0.00354 | 0.27145 | 0.01855 | 0.03824 | 0.00066 | 262 | 125 | 244 | 15 | 242 | 4 | 0.83 |
| ED1-31 | 1.17 | 0.05499 | 0.00784 | 0.51041 | 0.07226 | 0.06731 | 0.00156 | 412 | 277 | 419 | 49 | 420 | 9 | -0.24 |
| ED1-32 | 0.30 | 0.0551 | 0.00112 | 0.52068 | 0.01101 | 0.06853 | 0.00093 | 416 | 24 | 426 | 7 | 427 | 6 | -0.23 |
| ED1-33 | 0.40 | 0.0648 | 0.00123 | 0.9182 | 0.01831 | 0.10275 | 0.00138 | 768 | 21 | 661 | 10 | 631 | 8 | 4.75 |
| ED1-34 | 0.91 | 0.05561 | 0.0022 | 0.51228 | 0.02018 | 0.0668 | 0.00102 | 437 | 60 | 420 | 14 | 417 | 6 | 0.72 |
| ED1-35 | 0.52 | 0.05125 | 0.00153 | 0.28183 | 0.00853 | 0.03988 | 0.00056 | 252 | 44 | 252 | 7 | 252 | 3 | 0.00 |
| ED1-36 | 0.59 | 0.05544 | 0.00174 | 0.49712 | 0.0157 | 0.06502 | 0.00095 | 430 | 44 | 410 | 11 | 406 | 6 | 0.99 |
| ED1-37 | 0.76 | 0.05106 | 0.00219 | 0.28396 | 0.01205 | 0.04033 | 0.00064 | 244 | 68 | 254 | 10 | 255 | 4 | -0.39 |
| ED1-38 | 0.75 | 0.0515 | 0.00342 | 0.29532 | 0.01946 | 0.04158 | 0.00071 | 263 | 120 | 263 | 15 | 263 | 4 | 0.00 |
| ED1-39 | 0.55 | 0.0514 | 0.00199 | 0.2845 | 0.01098 | 0.04013 | 0.0006 | 259 | 61 | 254 | 9 | 254 | 4 | 0.00 |
| ED1-40 | 0.67 | 0.05713 | 0.00144 | 0.56479 | 0.01434 | 0.07168 | 0.00104 | 497 | 31 | 455 | 9 | 446 | 6 | 2.02 |
| ED1-41 | 1.33 | 0.0543 | 0.00249 | 0.2769 | 0.01259 | 0.03697 | 0.0006 | 384 | 73 | 248 | 10 | 234 | 4 | 5.98 |
| ED1-42 | 0.53 | 0.05422 | 0.00124 | 0.47802 | 0.01123 | 0.06392 | 0.00088 | 380 | 29 | 397 | 8 | 399 | 5 | -0.50 |
| ED1-43 | 0.93 | 0.05531 | 0.0048 | 0.50151 | 0.04316 | 0.06575 | 0.00125 | 425 | 160 | 413 | 29 | 410 | 8 | 0.73 |
| ED1-44 | 0.68 | 0.05105 | 0.00317 | 0.28278 | 0.01746 | 0.04016 | 0.00066 | 243 | 112 | 253 | 14 | 254 | 4 | -0.39 |
| ED1-45 | 0.75 | 0.05493 | 0.00119 | 0.4977 | 0.01114 | 0.0657 | 0.0009 | 409 | 27 | 410 | 8 | 410 | 5 | 0.00 |
| ED1-46 | 0.61 | 0.0513 | 0.00227 | 0.2873 | 0.01271 | 0.04061 | 0.00062 | 254 | 73 | 256 | 10 | 257 | 4 | -0.39 |
| ED1-47 | 0.65 | 0.05094 | 0.00328 | 0.26622 | 0.01695 | 0.0379 | 0.00069 | 238 | 113 | 240 | 14 | 240 | 4 | 0.00 |
| ED1-48 | 0.65 | 0.05477 | 0.00142 | 0.48674 | 0.01277 | 0.06444 | 0.00091 | 403 | 34 | 403 | 9 | 403 | 6 | 0.00 |
| ED1-49 | 0.17 | 0.0551 | 0.0012 | 0.48003 | 0.01082 | 0.06317 | 0.00086 | 416 | 27 | 398 | 7 | 395 | 5 | 0.76 |

| | | | | | | | | | | | | | | |
|---|---|---|---|---|---|---|---|---|---|---|---|---|---|---|
| ED1-50 | 0.46 | 0.0551 | 0.00123 | 0.51407 | 0.0118 | 0.06765 | 0.00093 | 416 | 28 | 421 | 8 | 422 | 6 | -0.24 |
| ED1-51 | 0.67 | 0.05091 | 0.00417 | 0.26407 | 0.02153 | 0.03761 | 0.00064 | 237 | 154 | 238 | 17 | 238 | 4 | 0.00 |
| ED1-52 | 1.10 | 0.05468 | 0.006 | 0.46719 | 0.05088 | 0.06196 | 0.0013 | 399 | 207 | 389 | 35 | 388 | 8 | 0.26 |
| ED1-53 | 1.34 | 0.05118 | 0.00959 | 0.28735 | 0.05341 | 0.04071 | 0.00114 | 249 | 327 | 256 | 42 | 257 | 7 | -0.39 |
| ED1-54 | 0.99 | 0.05114 | 0.00143 | 0.26845 | 0.00761 | 0.03807 | 0.00054 | 247 | 39 | 241 | 6 | 241 | 3 | 0.00 |
| ED1-55 | 0.34 | 0.05791 | 0.00175 | 0.52191 | 0.01594 | 0.06535 | 0.00093 | 526 | 42 | 426 | 11 | 408 | 6 | 4.41 |
| ED1-56 | 0.37 | 0.05141 | 0.00363 | 0.2876 | 0.02004 | 0.04056 | 0.00076 | 259 | 125 | 257 | 16 | 256 | 5 | 0.39 |
| ED1-57 | 0.49 | 0.055 | 0.0016 | 0.50152 | 0.01479 | 0.06612 | 0.00093 | 412 | 41 | 413 | 10 | 413 | 6 | 0.00 |
| ED1-58 | 0.81 | 0.05112 | 0.00345 | 0.26872 | 0.01802 | 0.03811 | 0.00063 | 246 | 123 | 242 | 14 | 241 | 4 | 0.41 |
| ED1-59 | 0.84 | 0.08684 | 0.00231 | 2.5669 | 0.06896 | 0.21432 | 0.00319 | 1357 | 29 | 1291 | 20 | 1252 | 17 | 8.39 |
| ED1-60 | 0.63 | 0.05157 | 0.00218 | 0.26441 | 0.01121 | 0.03718 | 0.00055 | 266 | 70 | 238 | 9 | 235 | 3 | 1.28 |
| ED1-61 | 2.43 | 0.04605 | 0.00451 | 0.2355 | 0.02272 | 0.03709 | 0.00061 | | 205 | 215 | 19 | 235 | 4 | -8.51 |
| ED1-62 | 0.41 | 0.05112 | 0.00256 | 0.26577 | 0.01319 | 0.0377 | 0.00062 | 246 | 84 | 239 | 11 | 239 | 4 | 0.00 |
| ED1-63 | 0.72 | 0.05099 | 0.00306 | 0.27765 | 0.01646 | 0.03948 | 0.0007 | 240 | 104 | 249 | 13 | 250 | 4 | -0.40 |
| ED1-64 | 0.85 | 0.05118 | 0.00601 | 0.27246 | 0.03178 | 0.0386 | 0.0008 | 249 | 225 | 245 | 25 | 244 | 5 | 0.41 |
| ED1-65 | 1.03 | 0.05477 | 0.00495 | 0.49421 | 0.04423 | 0.06543 | 0.00132 | 403 | 166 | 408 | 30 | 409 | 8 | -0.24 |
| ED1-66 | 0.46 | 0.05097 | 0.0021 | 0.2622 | 0.01079 | 0.0373 | 0.00056 | 239 | 67 | 236 | 9 | 236 | 3 | 0.00 |
| ED1-67 | 0.57 | 0.05555 | 0.0042 | 0.52225 | 0.03902 | 0.06818 | 0.00133 | 434 | 132 | 427 | 26 | 425 | 8 | 0.47 |
| ED1-68 | 0.61 | 0.05541 | 0.00189 | 0.52565 | 0.01797 | 0.06879 | 0.00103 | 429 | 50 | 429 | 12 | 429 | 6 | 0.00 |
| ED1-69 | 0.84 | 0.05112 | 0.00469 | 0.27753 | 0.02535 | 0.03937 | 0.0007 | 246 | 173 | 249 | 20 | 249 | 4 | 0.00 |
| ED1-70 | 0.41 | 0.05534 | 0.00151 | 0.51461 | 0.01425 | 0.06742 | 0.00097 | 426 | 37 | 422 | 10 | 421 | 6 | 0.24 |
| ED1-71 | 0.41 | 0.05603 | 0.00166 | 0.52498 | 0.01558 | 0.06794 | 0.00101 | 454 | 40 | 428 | 10 | 424 | 6 | 0.94 |
| ED1-72 | 0.59 | 0.05099 | 0.00221 | 0.26692 | 0.01151 | 0.03796 | 0.00059 | 240 | 71 | 240 | 9 | 240 | 4 | 0.00 |
| ED1-73 | 0.49 | 0.05516 | 0.00131 | 0.50699 | 0.0123 | 0.06665 | 0.00093 | 419 | 30 | 416 | 8 | 416 | 6 | 0.00 |
| ED1-74 | 0.33 | 0.05098 | 0.0015 | 0.2661 | 0.00791 | 0.03785 | 0.00055 | 240 | 42 | 240 | 6 | 239 | 3 | 0.42 |
| ED1-75 | 0.78 | 0.05144 | 0.00285 | 0.27297 | 0.01497 | 0.03847 | 0.00065 | 261 | 95 | 245 | 12 | 243 | 4 | 0.82 |
| ED1-76 | 1.28 | 0.05085 | 0.00496 | 0.27255 | 0.02641 | 0.03887 | 0.00075 | 234 | 183 | 245 | 21 | 246 | 5 | -0.41 |
| ED1-77 | 0.50 | 0.05123 | 0.00278 | 0.28354 | 0.01525 | 0.04013 | 0.00067 | 251 | 93 | 253 | 12 | 254 | 4 | -0.39 |

| | | | | | | | | | | | | | | |
|---|---|---|---|---|---|---|---|---|---|---|---|---|---|---|
| ED1-78 | 0.28 | 0.06976 | 0.00154 | 1.36816 | 0.03111 | 0.14222 | 0.00198 | 921 | 25 | 875 | 13 | 857 | 11 | 2.10 |
| ~~ED1-79~~ | ~~0.55~~ | ~~0.06234~~ | ~~0.00213~~ | ~~0.55365~~ | ~~0.01897~~ | ~~0.06439~~ | ~~0.00095~~ | ~~686~~ | ~~48~~ | ~~447~~ | ~~12~~ | ~~402~~ | ~~6~~ | ~~11.19~~ |
| ED1-80 | 0.65 | 0.05106 | 0.0036 | 0.27021 | 0.0188 | 0.03837 | 0.00071 | 244 | 125 | 243 | 15 | 243 | 4 | 0.00 |
| ED1-81 | 0.51 | 0.05495 | 0.00153 | 0.49226 | 0.01391 | 0.06495 | 0.00093 | 410 | 38 | 406 | 9 | 406 | 6 | 0.00 |
| ~~ED1-82~~ | ~~0.12~~ | ~~0.07406~~ | ~~0.00163~~ | ~~0.89628~~ | ~~0.0203~~ | ~~0.08775~~ | ~~0.00122~~ | ~~1043~~ | ~~24~~ | ~~650~~ | ~~11~~ | ~~542~~ | ~~7~~ | ~~19.93~~ |
| ED1-83 | 1.69 | 0.05145 | 0.00154 | 0.27783 | 0.0084 | 0.03915 | 0.00056 | 261 | 43 | 249 | 7 | 248 | 3 | 0.40 |
| ED1-84 | 0.94 | 0.05112 | 0.00421 | 0.27862 | 0.02281 | 0.03952 | 0.0007 | 246 | 153 | 250 | 18 | 250 | 4 | 0.00 |
| ~~ED1-85~~ | ~~0.87~~ | ~~0.11326~~ | ~~0.00264~~ | ~~2.35281~~ | ~~0.05587~~ | ~~0.15063~~ | ~~0.00217~~ | ~~1852~~ | ~~23~~ | ~~1228~~ | ~~17~~ | ~~904~~ | ~~12~~ | ~~35.84~~ |
| ED1-86 | 1.02 | 0.05131 | 0.00197 | 0.27634 | 0.01055 | 0.03905 | 0.0006 | 255 | 59 | 248 | 8 | 247 | 4 | 0.40 |
| ED1-87 | 0.88 | 0.05102 | 0.0041 | 0.26961 | 0.02151 | 0.03832 | 0.00068 | 242 | 149 | 242 | 17 | 242 | 4 | 0.00 |
| ED1-88 | 0.39 | 0.05422 | 0.00718 | 0.46994 | 0.06186 | 0.06284 | 0.00134 | 380 | 258 | 391 | 43 | 393 | 8 | -0.51 |
| ED1-89 | 0.77 | 0.05102 | 0.00198 | 0.26847 | 0.01038 | 0.03815 | 0.00058 | 242 | 61 | 241 | 8 | 241 | 4 | 0.00 |
| ~~ED1-90~~ | ~~1.07~~ | ~~0.08609~~ | ~~0.00352~~ | ~~0.49617~~ | ~~0.02002~~ | ~~0.04179~~ | ~~0.00069~~ | ~~1340~~ | ~~52~~ | ~~409~~ | ~~14~~ | ~~264~~ | ~~4~~ | ~~54.92~~ |
| ED1-91 | 1.09 | 0.05124 | 0.00245 | 0.27192 | 0.0129 | 0.03848 | 0.00062 | 252 | 79 | 244 | 10 | 243 | 4 | 0.41 |
| ED1-92 | 0.61 | 0.05485 | 0.00173 | 0.49103 | 0.01564 | 0.06491 | 0.00094 | 406 | 45 | 406 | 11 | 405 | 6 | 0.25 |
| ED1-93 | 0.64 | 0.05465 | 0.01365 | 0.48843 | 0.12138 | 0.0648 | 0.00197 | 398 | 430 | 404 | 83 | 405 | 12 | -0.25 |
| ED1-94 | 1.12 | 0.05088 | 0.00511 | 0.27698 | 0.02721 | 0.03947 | 0.00102 | 235 | 173 | 248 | 22 | 250 | 6 | -0.80 |
| ED1-95 | 0.71 | 0.05158 | 0.00346 | 0.2786 | 0.01851 | 0.03917 | 0.00069 | 267 | 120 | 250 | 15 | 248 | 4 | 0.81 |
| ED1-96 | 0.39 | 0.05088 | 0.00279 | 0.28755 | 0.01562 | 0.04098 | 0.00069 | 235 | 94 | 257 | 12 | 259 | 4 | -0.77 |
| ED1-97 | 0.41 | 0.0562 | 0.00168 | 0.5221 | 0.01573 | 0.06736 | 0.00099 | 460 | 41 | 427 | 10 | 420 | 6 | 1.67 |
| ~~ED1-98~~ | ~~0.50~~ | ~~0.07315~~ | ~~0.00322~~ | ~~0.53757~~ | ~~0.02337~~ | ~~0.05328~~ | ~~0.00089~~ | ~~1018~~ | ~~61~~ | ~~437~~ | ~~15~~ | ~~335~~ | ~~5~~ | ~~30.45~~ |
| ED1-99 | 0.31 | 0.05145 | 0.00155 | 0.27687 | 0.0084 | 0.03902 | 0.00057 | 261 | 43 | 248 | 7 | 247 | 4 | 0.40 |
| ED1-100 | 1.02 | 0.05624 | 0.00302 | 0.31235 | 0.01661 | 0.04027 | 0.00069 | 462 | 87 | 276 | 13 | 255 | 4 | 8.24 |
| | | | | | | | | | | | | | | |
| **EB1** | | | | | | | | | | | | | | |
| EB1-01 | 1.06 | 0.05102 | 0.00149 | 0.27416 | 0.00816 | 0.03897 | 0.00059 | 242 | 41 | 246 | 7 | 246 | 4 | 0.00 |
| EB1-02 | 0.89 | 0.05633 | 0.00163 | 0.53744 | 0.01598 | 0.06919 | 0.00103 | 465 | 40 | 437 | 11 | 431 | 6 | 1.39 |
| EB1-03 | 0.83 | 0.05428 | 0.00549 | 0.46 | 0.04603 | 0.06145 | 0.00135 | 383 | 186 | 384 | 32 | 384 | 8 | 0.00 |

| | | | | | | | | | | | | | | |
|---|---|---|---|---|---|---|---|---|---|---|---|---|---|---|
| EB1-04 | 0.51 | 0.05536 | 0.00589 | 0.51156 | 0.05386 | 0.06701 | 0.0015 | 427 | 196 | 419 | 36 | 418 | 9 | 0.24 |
| EB1-05 | 0.35 | 0.05547 | 0.00139 | 0.53677 | 0.01389 | 0.07016 | 0.00104 | 431 | 32 | 436 | 9 | 437 | 6 | -0.23 |
| EB1-06 | 0.87 | 0.05544 | 0.00185 | 0.51585 | 0.01736 | 0.06747 | 0.00107 | 430 | 47 | 422 | 12 | 421 | 6 | 0.24 |
| EB1-07 | 0.65 | 0.05142 | 0.0023 | 0.28967 | 0.01289 | 0.04085 | 0.00069 | 260 | 71 | 258 | 10 | 258 | 4 | 0.00 |
| EB1-08 | 1.09 | 0.05106 | 0.00216 | 0.27844 | 0.01177 | 0.03954 | 0.00065 | 244 | 67 | 249 | 9 | 250 | 4 | -0.40 |
| EB1-09 | 0.96 | 0.05123 | 0.00192 | 0.28524 | 0.01076 | 0.04037 | 0.00064 | 251 | 58 | 255 | 9 | 255 | 4 | 0.00 |
| EB1-10 | 0.98 | 0.05443 | 0.0014 | 0.42485 | 0.01127 | 0.0566 | 0.00083 | 389 | 34 | 360 | 8 | 355 | 5 | 1.41 |
| EB1-11 | 0.60 | 0.05135 | 0.0014 | 0.27505 | 0.00772 | 0.03884 | 0.00057 | 257 | 38 | 247 | 6 | 246 | 4 | 0.41 |
| EB1-12 | 0.96 | 0.05581 | 0.00312 | 0.51746 | 0.02884 | 0.06723 | 0.00113 | 445 | 94 | 423 | 19 | 419 | 7 | 0.95 |
| EB1-13 | 0.35 | 0.05132 | 0.00225 | 0.29056 | 0.01273 | 0.04105 | 0.00068 | 255 | 70 | 259 | 10 | 259 | 4 | 0.00 |
| EB1-14 | 1.15 | 0.05161 | 0.00221 | 0.29376 | 0.01264 | 0.04128 | 0.00065 | 268 | 70 | 262 | 10 | 261 | 4 | 0.38 |
| EB1-15 | 0.81 | 0.05524 | 0.00353 | 0.50834 | 0.03231 | 0.06672 | 0.00116 | 422 | 111 | 417 | 22 | 416 | 7 | 0.24 |
| EB1-16 | 0.53 | 0.07648 | 0.00182 | 1.87134 | 0.04623 | 0.17741 | 0.00264 | 1108 | 27 | 1071 | 16 | 1053 | 14 | 5.22 |
| EB1-17 | 0.85 | 0.05641 | 0.00593 | 0.57698 | 0.06003 | 0.07416 | 0.00166 | 469 | 193 | 463 | 39 | 461 | 10 | 0.43 |
| EB1-18 | 0.08 | 0.0553 | 0.00105 | 0.4187 | 0.00858 | 0.0549 | 0.00077 | 424 | 23 | 355 | 6 | 345 | 5 | 2.90 |
| EB1-19 | 0.63 | 0.05128 | 0.00226 | 0.28075 | 0.01236 | 0.0397 | 0.00065 | 253 | 71 | 251 | 10 | 251 | 4 | 0.00 |
| EB1-20 | 1.04 | 0.05163 | 0.0022 | 0.30553 | 0.01301 | 0.04291 | 0.00069 | 269 | 68 | 271 | 10 | 271 | 4 | 0.00 |
| EB1-21 | 1.20 | 0.05392 | 0.00126 | 0.41156 | 0.01004 | 0.05534 | 0.0008 | 368 | 30 | 350 | 7 | 347 | 5 | 0.86 |
| EB1-22 | 0.09 | 0.05545 | 0.00122 | 0.50554 | 0.01165 | 0.0661 | 0.00095 | 430 | 27 | 415 | 8 | 413 | 6 | 0.48 |
| EB1-23 | 1.20 | 0.05114 | 0.00378 | 0.27516 | 0.02015 | 0.03901 | 0.00074 | 247 | 132 | 247 | 16 | 247 | 5 | 0.00 |
| EB1-24 | 0.75 | 0.05347 | 0.00171 | 0.29884 | 0.00973 | 0.04052 | 0.0006 | 349 | 47 | 265 | 8 | 256 | 4 | 3.52 |
| EB1-25 | 0.33 | 0.05546 | 0.00147 | 0.53106 | 0.01441 | 0.06944 | 0.00104 | 431 | 35 | 433 | 10 | 433 | 6 | 0.00 |
| EB1-26 | 0.59 | 0.0551 | 0.00144 | 0.50762 | 0.0136 | 0.0668 | 0.001 | 416 | 34 | 417 | 9 | 417 | 6 | 0.00 |
| EB1-27 | 0.44 | 0.05156 | 0.00363 | 0.30116 | 0.02112 | 0.04235 | 0.00074 | 266 | 128 | 267 | 16 | 267 | 5 | 0.00 |
| EB1-28 | 0.33 | 0.05557 | 0.00172 | 0.52186 | 0.01633 | 0.0681 | 0.00104 | 435 | 43 | 426 | 11 | 425 | 6 | 0.24 |
| EB1-29 | 0.42 | 0.05499 | 0.00118 | 0.50021 | 0.0113 | 0.06596 | 0.00095 | 412 | 26 | 412 | 8 | 412 | 6 | 0.00 |
| EB1-30 | 0.24 | 0.0515 | 0.00148 | 0.29673 | 0.00869 | 0.04178 | 0.00063 | 263 | 40 | 264 | 7 | 264 | 4 | 0.00 |
| EB1-31 | 0.72 | 0.05153 | 0.00191 | 0.29471 | 0.01091 | 0.04147 | 0.00066 | 265 | 56 | 262 | 9 | 262 | 4 | 0.00 |

| | | | | | | | | | | | | | | |
|---|---|---|---|---|---|---|---|---|---|---|---|---|---|---|
| EB1-32 | 0.40 | 0.05529 | 0.00165 | 0.51374 | 0.01562 | 0.06737 | 0.001 | 424 | 42 | 421 | 10 | 420 | 6 | 0.24 |
| EB1-33 | 2.19 | 0.05173 | 0.00207 | 0.3143 | 0.01262 | 0.04405 | 0.00069 | 273 | 63 | 278 | 10 | 278 | 4 | 0.00 |
| EB1-34 | 1.47 | 0.05124 | 0.00157 | 0.28583 | 0.00886 | 0.04045 | 0.00061 | 252 | 44 | 255 | 7 | 256 | 4 | -0.39 |
| EB1-35 | 0.52 | 0.0556 | 0.00129 | 0.49882 | 0.01206 | 0.06505 | 0.00094 | 436 | 29 | 411 | 8 | 406 | 6 | 1.23 |
| EB1-36 | 0.74 | 0.0515 | 0.00196 | 0.29334 | 0.01126 | 0.0413 | 0.00063 | 263 | 60 | 261 | 9 | 261 | 4 | 0.00 |
| EB1-37 | 1.14 | 0.05132 | 0.00266 | 0.27903 | 0.01438 | 0.03942 | 0.00067 | 255 | 87 | 250 | 11 | 249 | 4 | 0.40 |
| EB1-38 | 0.32 | 0.05643 | 0.00131 | 0.54546 | 0.01315 | 0.07009 | 0.00102 | 469 | 29 | 442 | 9 | 437 | 6 | 1.14 |
| EB1-39 | 0.40 | 0.05381 | 0.00299 | 0.43111 | 0.02385 | 0.05809 | 0.00098 | 363 | 94 | 364 | 17 | 364 | 6 | 0.00 |
| EB1-40 | 0.71 | 0.05553 | 0.00149 | 0.5338 | 0.01467 | 0.0697 | 0.00103 | 434 | 35 | 434 | 10 | 434 | 6 | 0.00 |
| ~~EB1-41~~ | ~~0.98~~ | ~~0.05818~~ | ~~0.00316~~ | ~~0.33051~~ | ~~0.01788~~ | ~~0.04119~~ | ~~0.00068~~ | ~~537~~ | ~~89~~ | ~~290~~ | ~~14~~ | ~~260~~ | ~~4~~ | ~~11.54~~ |
| EB1-42 | 0.62 | 0.05511 | 0.00133 | 0.50901 | 0.01267 | 0.06697 | 0.00097 | 417 | 31 | 418 | 9 | 418 | 6 | 0.00 |
| EB1-43 | 0.33 | 0.05119 | 0.00141 | 0.28865 | 0.00811 | 0.04089 | 0.0006 | 249 | 38 | 257 | 6 | 258 | 4 | -0.39 |
| EB1-44 | 0.47 | 0.05399 | 0.00154 | 0.30365 | 0.00883 | 0.04078 | 0.0006 | 371 | 39 | 269 | 7 | 258 | 4 | 4.26 |
| ~~EB1-45~~ | ~~0.42~~ | ~~0.09304~~ | ~~0.00362~~ | ~~1.68923~~ | ~~0.06055~~ | ~~0.13167~~ | ~~0.00198~~ | ~~1489~~ | ~~75~~ | ~~1004~~ | ~~23~~ | ~~797~~ | ~~11~~ | ~~25.97~~ |
| EB1-46 | 0.92 | 0.05124 | 0.00243 | 0.28245 | 0.01331 | 0.03997 | 0.00066 | 252 | 78 | 253 | 11 | 253 | 4 | 0.00 |
| EB1-47 | 1.02 | 0.05543 | 0.0011 | 0.48486 | 0.01023 | 0.06342 | 0.00089 | 430 | 24 | 401 | 7 | 396 | 5 | 1.26 |
| EB1-48 | 0.68 | 0.06068 | 0.00226 | 0.57806 | 0.02158 | 0.06908 | 0.00107 | 628 | 54 | 463 | 14 | 431 | 6 | 7.42 |
| ~~EB1-49~~ | ~~0.10~~ | ~~0.07772~~ | ~~0.00206~~ | ~~1.15~~ | ~~0.02596~~ | ~~0.10732~~ | ~~0.00149~~ | ~~1140~~ | ~~54~~ | ~~777~~ | ~~12~~ | ~~657~~ | ~~9~~ | ~~18.26~~ |
| EB1-50 | 0.51 | 0.05626 | 0.00135 | 0.50747 | 0.01259 | 0.0654 | 0.00095 | 463 | 30 | 417 | 8 | 408 | 6 | 2.21 |
| EB1-51 | 0.41 | 0.05452 | 0.00138 | 0.47452 | 0.0123 | 0.06311 | 0.00089 | 393 | 33 | 394 | 8 | 395 | 5 | -0.25 |
| EB1-51 | 0.72 | 0.05596 | 0.00123 | 0.56379 | 0.01293 | 0.07305 | 0.00105 | 451 | 27 | 454 | 8 | 455 | 6 | -0.22 |
| EB1-52 | 0.70 | 0.05094 | 0.00238 | 0.26478 | 0.01221 | 0.0377 | 0.00064 | 238 | 75 | 239 | 10 | 239 | 4 | 0.00 |
| EB1-52 | 0.44 | 0.05577 | 0.00126 | 0.51319 | 0.01204 | 0.06672 | 0.00095 | 443 | 28 | 421 | 8 | 416 | 6 | 1.20 |
| EB1-53 | 0.74 | 0.05485 | 0.00369 | 0.49237 | 0.03294 | 0.0651 | 0.00109 | 406 | 120 | 407 | 22 | 407 | 7 | 0.00 |
| EB1-53 | 0.88 | 0.05528 | 0.00519 | 0.53557 | 0.04981 | 0.07025 | 0.00145 | 424 | 172 | 435 | 33 | 438 | 9 | -0.68 |
| EB1-54 | 0.62 | 0.05535 | 0.00199 | 0.50825 | 0.01839 | 0.06659 | 0.00098 | 426 | 54 | 417 | 12 | 416 | 6 | 0.24 |
| EB1-55 | 0.30 | 0.05497 | 0.00142 | 0.50122 | 0.01312 | 0.06612 | 0.00095 | 411 | 34 | 413 | 9 | 413 | 6 | 0.00 |
| EB1-56 | 1.65 | 0.05083 | 0.00448 | 0.25675 | 0.02248 | 0.03663 | 0.00068 | 233 | 163 | 232 | 18 | 232 | 4 | 0.00 |

| | | | | | | | | | | | | | | |
|---|---|---|---|---|---|---|---|---|---|---|---|---|---|---|
| EB1-57 | 0.99 | 0.05444 | 0.00602 | 0.47493 | 0.05209 | 0.06326 | 0.00131 | 389 | 210 | 395 | 36 | 395 | 8 | 0.00 |
| EB1-58 | 0.64 | 0.05156 | 0.00282 | 0.28445 | 0.01548 | 0.04 | 0.00065 | 266 | 95 | 254 | 12 | 253 | 4 | 0.40 |
| EB1-59 | 1.31 | 0.05107 | 0.00135 | 0.26992 | 0.00726 | 0.03833 | 0.00055 | 244 | 36 | 243 | 6 | 242 | 3 | 0.41 |
| EB1-60 | 0.90 | 0.05102 | 0.003 | 0.26326 | 0.01541 | 0.03742 | 0.00061 | 242 | 105 | 237 | 12 | 237 | 4 | 0.00 |
| EB1-61 | 0.56 | 0.05088 | 0.00129 | 0.25839 | 0.00671 | 0.03683 | 0.00052 | 235 | 35 | 233 | 5 | 233 | 3 | 0.00 |
| EB1-62 | 0.35 | 0.05528 | 0.00144 | 0.51227 | 0.01352 | 0.0672 | 0.00096 | 424 | 34 | 420 | 9 | 419 | 6 | 0.24 |
| EB1-63 | 0.18 | 0.05089 | 0.00171 | 0.26111 | 0.00878 | 0.0372 | 0.00056 | 236 | 50 | 236 | 7 | 235 | 3 | 0.43 |
| EB1-64 | 0.81 | 0.05112 | 0.00348 | 0.27155 | 0.01831 | 0.03852 | 0.00069 | 246 | 121 | 244 | 15 | 244 | 4 | 0.00 |
| EB1-65 | 0.57 | 0.05148 | 0.00255 | 0.29586 | 0.01451 | 0.04167 | 0.0007 | 262 | 82 | 263 | 11 | 263 | 4 | 0.00 |
| EB1-66 | 0.58 | 0.05135 | 0.00363 | 0.26867 | 0.01889 | 0.03794 | 0.00065 | 257 | 129 | 242 | 15 | 240 | 4 | 0.83 |
| EB1-67 | 0.59 | 0.05131 | 0.00184 | 0.28135 | 0.00999 | 0.03976 | 0.00063 | 255 | 53 | 252 | 8 | 251 | 4 | 0.40 |
| EB1-68 | 0.36 | 0.0571 | 0.00157 | 0.47403 | 0.01312 | 0.0602 | 0.00088 | 495 | 36 | 394 | 9 | 377 | 5 | 4.51 |
| EB1-69 | 0.23 | 0.05554 | 0.00182 | 0.52263 | 0.01708 | 0.06823 | 0.00105 | 434 | 46 | 427 | 11 | 425 | 6 | 0.47 |
| EB1-70 | 0.53 | 0.05569 | 0.00175 | 0.5146 | 0.01612 | 0.06701 | 0.00102 | 440 | 43 | 422 | 11 | 418 | 6 | 0.96 |
| EB1-71 | 0.38 | 0.05511 | 0.00185 | 0.51166 | 0.01709 | 0.06732 | 0.00104 | 417 | 47 | 420 | 11 | 420 | 6 | 0.00 |
| EB1-72 | 0.47 | 0.05517 | 0.00181 | 0.51003 | 0.01667 | 0.06704 | 0.00103 | 419 | 46 | 418 | 11 | 418 | 6 | 0.00 |
| EB1-73 | 1.40 | 0.05102 | 0.00335 | 0.2662 | 0.01727 | 0.03783 | 0.00069 | 242 | 115 | 240 | 14 | 239 | 4 | 0.42 |
| EB1-74 | 0.33 | 0.06749 | 0.00273 | 1.24492 | 0.04672 | 0.13379 | 0.00201 | 853 | 86 | 821 | 21 | 809 | 11 | 1.48 |
| EB1-75 | 0.47 | 0.05507 | 0.00387 | 0.31138 | 0.02163 | 0.041 | 0.00077 | 415 | 122 | 275 | 17 | 259 | 5 | 6.18 |
| EB1-76 | 0.62 | 0.05628 | 0.00143 | 0.52246 | 0.01349 | 0.06731 | 0.00096 | 463 | 33 | 427 | 9 | 420 | 6 | 1.67 |
| EB1-77 | 0.95 | 0.05513 | 0.0039 | 0.51014 | 0.03587 | 0.06709 | 0.00115 | 417 | 127 | 419 | 24 | 419 | 7 | 0.00 |
| EB1-78 | 0.51 | 0.05625 | 0.00215 | 0.56564 | 0.02165 | 0.07292 | 0.00111 | 462 | 58 | 455 | 14 | 454 | 7 | 0.22 |
| EB1-79 | 1.32 | 0.05096 | 0.00418 | 0.27512 | 0.02224 | 0.03914 | 0.00082 | 239 | 145 | 247 | 18 | 248 | 5 | -0.40 |
| EB1-80 | 0.47 | 0.05541 | 0.00201 | 0.51439 | 0.01863 | 0.06731 | 0.00102 | 429 | 54 | 421 | 12 | 420 | 6 | 0.24 |
| EB1-81 | 0.80 | 0.05088 | 0.00229 | 0.2709 | 0.01212 | 0.0386 | 0.0006 | 235 | 74 | 243 | 10 | 244 | 4 | -0.41 |
| EB1-82 | 1.27 | 0.05106 | 0.00329 | 0.26441 | 0.01687 | 0.03755 | 0.00067 | 244 | 114 | 238 | 14 | 238 | 4 | 0.00 |
| EB1-83 | 0.66 | 0.0516 | 0.00218 | 0.30781 | 0.0129 | 0.04325 | 0.0007 | 268 | 66 | 272 | 10 | 273 | 4 | -0.37 |
| EB1-84 | 0.40 | 0.05544 | 0.00186 | 0.51043 | 0.01714 | 0.06675 | 0.00102 | 430 | 48 | 419 | 12 | 417 | 6 | 0.48 |

| | | | | | | | | | | | | | | |
|---|---|---|---|---|---|---|---|---|---|---|---|---|---|---|
| EB1-85 | 1.12 | 0.05151 | 0.00281 | 0.29128 | 0.01563 | 0.041 | 0.00073 | 264 | 90 | 260 | 12 | 259 | 5 | 0.39 |
| EB1-86 | 0.18 | 0.06044 | 0.00202 | 0.86545 | 0.02619 | 0.10386 | 0.00147 | 619 | 74 | 633 | 14 | 637 | 9 | -0.63 |
| EB1-87 | 0.68 | 0.05627 | 0.00162 | 0.5448 | 0.01574 | 0.07019 | 0.00104 | 463 | 38 | 442 | 10 | 437 | 6 | 1.14 |
| EB1-88 | 0.89 | 0.05542 | 0.00177 | 0.49601 | 0.01592 | 0.06489 | 0.00096 | 429 | 45 | 409 | 11 | 405 | 6 | 0.99 |
| EB1-89 | 0.75 | 0.05552 | 0.00263 | 0.50851 | 0.02389 | 0.06641 | 0.0011 | 433 | 75 | 417 | 16 | 414 | 7 | 0.72 |
| EB1-90 | 0.67 | 0.05087 | 0.00263 | 0.27148 | 0.01391 | 0.0387 | 0.00065 | 235 | 87 | 244 | 11 | 245 | 4 | -0.41 |
| EB1-91 | 0.57 | 0.06092 | 0.0017 | 0.55548 | 0.01567 | 0.06612 | 0.00097 | 636 | 36 | 449 | 10 | 413 | 6 | 8.72 |
| EB1-92 | 0.82 | 0.05096 | 0.00184 | 0.27481 | 0.00992 | 0.0391 | 0.00059 | 239 | 55 | 247 | 8 | 247 | 4 | 0.00 |
| EB1-93 | 1.11 | 0.05148 | 0.0041 | 0.28826 | 0.02275 | 0.0406 | 0.00076 | 262 | 145 | 257 | 18 | 257 | 5 | 0.00 |
| EB1-94 | 0.14 | 0.05858 | 0.00141 | 0.50696 | 0.01252 | 0.06275 | 0.00089 | 552 | 30 | 416 | 8 | 392 | 5 | 6.12 |
| EB1-95 | 0.82 | 0.05504 | 0.00422 | 0.51057 | 0.03891 | 0.06727 | 0.00118 | 414 | 140 | 419 | 26 | 420 | 7 | -0.24 |
| EB1-96 | 1.12 | 0.05133 | 0.00377 | 0.28244 | 0.02067 | ~~0.0399~~ | 0.00064 | 256 | 137 | 253 | 16 | 252 | 4 | 0.40 |
| EB1-97 | 0.55 | 0.05161 | 0.00291 | 0.29801 | 0.01676 | 0.04187 | 0.00065 | 268 | 101 | 265 | 13 | 264 | 4 | 0.38 |
| EB1-98 | 0.31 | 0.05114 | 0.0011 | 0.27954 | 0.00621 | 0.03963 | 0.00053 | 247 | 28 | 250 | 5 | 251 | 3 | -0.40 |
| EB1-99 | 0.62 | 0.05163 | 0.00364 | 0.28309 | 0.01984 | 0.03976 | 0.00066 | 269 | 130 | 253 | 16 | 251 | 4 | 0.80 |
| EB1-100 | 0.58 | 0.05581 | 0.0025 | 0.53246 | 0.02375 | 0.06918 | 0.00109 | 445 | 71 | 433 | 16 | 431 | 7 | 0.46 |
| | | | | | | | | | | | | | | |
| Huatugou Section **S23** | | | | | | | | | | | | | | |
| S23-01 | 0.90 | 0.05982 | 0.00111 | 0.58324 | 0.01128 | 0.07069 | 0.00092 | 597 | 21 | 467 | 7 | 440 | 6 | 6.14 |
| ~~S23-02~~ | ~~0.40~~ | ~~0.28214~~ | ~~0.00383~~ | ~~16.27658~~ | ~~0.24462~~ | ~~0.41832~~ | ~~0.00527~~ | ~~3375~~ | ~~11~~ | ~~2893~~ | ~~14~~ | ~~2253~~ | ~~24~~ | ~~49.80~~ |
| S23-03 | 0.57 | 0.07536 | 0.00113 | 1.66574 | 0.02707 | 0.16027 | 0.00204 | 1078 | 15 | 996 | 10 | 958 | 11 | 3.97 |
| S23-04 | 1.04 | 0.05776 | 0.00136 | 0.64895 | 0.01562 | 0.08147 | 0.00109 | 521 | 30 | 508 | 10 | 505 | 6 | 0.59 |
| S23-05 | 0.42 | 0.05107 | 0.00193 | 0.27371 | 0.01037 | 0.03887 | 0.00054 | 244 | 62 | 246 | 8 | 246 | 3 | 0.00 |
| ~~S23-06~~ | ~~0.72~~ | ~~0.07544~~ | ~~0.00256~~ | ~~1.24423~~ | ~~0.04222~~ | ~~0.11959~~ | ~~0.00173~~ | ~~1080~~ | ~~45~~ | ~~821~~ | ~~19~~ | ~~728~~ | ~~10~~ | ~~12.77~~ |
| ~~S23-07~~ | ~~0.25~~ | ~~0.09551~~ | ~~0.00251~~ | ~~0.96832~~ | ~~0.02199~~ | ~~0.07353~~ | ~~0.00097~~ | ~~1538~~ | ~~51~~ | ~~688~~ | ~~11~~ | ~~457~~ | ~~6~~ | ~~50.55~~ |
| S23-08 | 0.52 | 0.07119 | 0.00114 | 1.31571 | 0.02256 | 0.13401 | 0.00172 | 963 | 17 | 853 | 10 | 811 | 10 | 5.18 |

| | | | | | | | | | | | | | | |
|---|---|---|---|---|---|---|---|---|---|---|---|---|---|---|
| ~~S23-09~~ | ~~0.77~~ | ~~0.09241~~ | ~~0.00136~~ | ~~2.15715~~ | ~~0.03452~~ | ~~0.16927~~ | ~~0.00215~~ | ~~1476~~ | ~~14~~ | ~~1167~~ | ~~11~~ | ~~1008~~ | ~~12~~ | ~~46.43~~ |
| S23-10 | 0.91 | 0.05709 | 0.0023 | 0.4597 | 0.0185 | 0.05839 | 0.00083 | 495 | 63 | 384 | 13 | 366 | 5 | 4.92 |
| ~~S23-11~~ | ~~0.62~~ | ~~0.06271~~ | ~~0.00102~~ | ~~0.49215~~ | ~~0.00856~~ | ~~0.05691~~ | ~~0.00073~~ | ~~698~~ | ~~18~~ | ~~406~~ | ~~6~~ | ~~357~~ | ~~4~~ | ~~13.73~~ |
| ~~S23-12~~ | ~~1.37~~ | ~~0.09164~~ | ~~0.003~~ | ~~0.82553~~ | ~~0.02674~~ | ~~0.06532~~ | ~~0.00098~~ | ~~1460~~ | ~~39~~ | ~~611~~ | ~~15~~ | ~~408~~ | ~~6~~ | ~~49.75~~ |
| ~~S23-13~~ | ~~0.71~~ | ~~0.05959~~ | ~~0.00215~~ | ~~0.29976~~ | ~~0.01082~~ | ~~0.03648~~ | ~~0.00052~~ | ~~589~~ | ~~53~~ | ~~266~~ | ~~8~~ | ~~231~~ | ~~3~~ | ~~15.15~~ |
| S23-14 | 0.80 | 0.05617 | 0.00191 | 0.50875 | 0.01741 | 0.06567 | 0.0009 | 459 | 51 | 418 | 12 | 410 | 5 | 1.95 |
| S23-15 | 1.50 | 0.05563 | 0.00162 | 0.50568 | 0.01483 | 0.06591 | 0.00091 | 438 | 41 | 416 | 10 | 411 | 6 | 1.22 |
| S23-16 | 0.18 | 0.11457 | 0.00163 | 4.9073 | 0.07669 | 0.31059 | 0.00392 | 1873 | 13 | 1804 | 13 | 1744 | 19 | 7.40 |
| S23-17 | 0.29 | 0.05358 | 0.0018 | 0.39153 | 0.01319 | 0.05299 | 0.00076 | 353 | 50 | 335 | 10 | 333 | 5 | 0.60 |
| ~~S23-18~~ | ~~1.03~~ | ~~0.06568~~ | ~~0.00384~~ | ~~0.31858~~ | ~~0.01848~~ | ~~0.03517~~ | ~~0.00057~~ | ~~796~~ | ~~95~~ | ~~281~~ | ~~14~~ | ~~223~~ | ~~4~~ | ~~26.01~~ |
| S23-19 | 0.90 | 0.05108 | 0.00224 | 0.26581 | 0.01165 | 0.03773 | 0.00053 | 244 | 75 | 239 | 9 | 239 | 3 | 0.00 |
| S23-20 | 0.69 | 0.052 | 0.00155 | 0.29968 | 0.00902 | 0.04179 | 0.00056 | 285 | 44 | 266 | 7 | 264 | 3 | 0.76 |
| S23-21 | 0.52 | 0.05879 | 0.00153 | 0.59425 | 0.01576 | 0.0733 | 0.00098 | 559 | 35 | 474 | 10 | 456 | 6 | 3.95 |
| S23-22 | 0.54 | 0.05744 | 0.00115 | 0.63505 | 0.01318 | 0.08017 | 0.00105 | 508 | 24 | 499 | 8 | 497 | 6 | 0.40 |
| S23-23 | 0.92 | 0.05922 | 0.00149 | 0.5921 | 0.01512 | 0.07249 | 0.001 | 575 | 32 | 472 | 10 | 451 | 6 | 4.66 |
| ~~S23-24~~ | ~~0.59~~ | ~~0.11824~~ | ~~0.00178~~ | ~~3.46697~~ | ~~0.05646~~ | ~~0.21261~~ | ~~0.00271~~ | ~~1930~~ | ~~13~~ | ~~1520~~ | ~~13~~ | ~~1243~~ | ~~14~~ | ~~55.27~~ |
| S23-25 | 0.84 | 0.05272 | 0.00118 | 0.26428 | 0.00607 | 0.03635 | 0.00048 | 317 | 29 | 238 | 5 | 230 | 3 | 3.48 |
| S23-26 | 0.50 | 0.05183 | 0.00193 | 0.28998 | 0.01082 | 0.04057 | 0.00057 | 278 | 60 | 259 | 9 | 256 | 4 | 1.17 |
| S23-27 | 0.39 | 0.06869 | 0.00142 | 1.31071 | 0.02794 | 0.13838 | 0.00185 | 889 | 23 | 850 | 12 | 835 | 10 | 1.80 |
| ~~S23-28~~ | ~~0.50~~ | ~~0.13723~~ | ~~0.00207~~ | ~~6.6602~~ | ~~0.10875~~ | ~~0.35192~~ | ~~0.0045~~ | ~~2193~~ | ~~13~~ | ~~2067~~ | ~~14~~ | ~~1944~~ | ~~21~~ | ~~12.81~~ |
| S23-29 | 0.19 | 0.05802 | 0.00148 | 0.64309 | 0.01655 | 0.08037 | 0.00111 | 531 | 33 | 504 | 10 | 498 | 7 | 1.20 |
| S23-30 | 0.68 | 0.05659 | 0.0015 | 0.54797 | 0.01469 | 0.07022 | 0.00097 | 476 | 35 | 444 | 10 | 437 | 6 | 1.60 |
| S23-31 | 0.27 | 0.05706 | 0.00122 | 0.42005 | 0.00924 | 0.05339 | 0.00071 | 494 | 26 | 356 | 7 | 335 | 4 | 6.27 |
| S23-32 | 0.52 | 0.05283 | 0.00296 | 0.38118 | 0.0213 | 0.05232 | 0.00079 | 322 | 100 | 328 | 16 | 329 | 5 | -0.30 |
| ~~S23-33~~ | ~~0.58~~ | ~~0.09534~~ | ~~0.00174~~ | ~~2.65888~~ | ~~0.05058~~ | ~~0.20223~~ | ~~0.0027~~ | ~~1535~~ | ~~18~~ | ~~1317~~ | ~~14~~ | ~~1187~~ | ~~14~~ | ~~29.32~~ |
| S23-34 | 0.28 | 0.05849 | 0.00155 | 0.65082 | 0.01745 | 0.08069 | 0.00111 | 548 | 35 | 509 | 11 | 500 | 7 | 1.80 |
| ~~S23-35~~ | ~~0.84~~ | ~~0.06678~~ | ~~0.00152~~ | ~~0.58491~~ | ~~0.01363~~ | ~~0.06352~~ | ~~0.00086~~ | ~~831~~ | ~~27~~ | ~~468~~ | ~~9~~ | ~~397~~ | ~~5~~ | ~~17.88~~ |
| ~~S23-36~~ | ~~0.90~~ | ~~0.07486~~ | ~~0.00211~~ | ~~1.10063~~ | ~~0.03122~~ | ~~0.10662~~ | ~~0.00151~~ | ~~1065~~ | ~~35~~ | ~~754~~ | ~~15~~ | ~~653~~ | ~~9~~ | ~~15.47~~ |

| | | | | | | | | | | | | | | |
|---|---|---|---|---|---|---|---|---|---|---|---|---|---|---|
| S23-37 | 0.30 | 0.05444 | 0.00253 | 0.44363 | 0.02052 | 0.05909 | 0.00089 | 389 | 77 | 373 | 14 | 370 | 5 | 0.81 |
| ~~S23-38~~ | ~~1.84~~ | ~~0.0865~~ | ~~0.01437~~ | ~~0.49774~~ | ~~0.08151~~ | ~~0.04173~~ | ~~0.00116~~ | ~~1349~~ | ~~345~~ | ~~410~~ | ~~55~~ | ~~264~~ | ~~7~~ | ~~55.30~~ |
| ~~S23-39~~ | ~~0.30~~ | ~~0.11819~~ | ~~0.00197~~ | ~~4.88162~~ | ~~0.08646~~ | ~~0.29951~~ | ~~0.00391~~ | ~~1929~~ | ~~15~~ | ~~1799~~ | ~~15~~ | ~~1689~~ | ~~19~~ | ~~14.21~~ |
| ~~S23-40~~ | ~~0.55~~ | ~~0.06573~~ | ~~0.00153~~ | ~~0.69384~~ | ~~0.01643~~ | ~~0.07655~~ | ~~0.00104~~ | ~~798~~ | ~~28~~ | ~~535~~ | ~~10~~ | ~~475~~ | ~~6~~ | ~~12.63~~ |
| ~~S23-41~~ | ~~0.78~~ | ~~0.06953~~ | ~~0.0014~~ | ~~0.63775~~ | ~~0.01329~~ | ~~0.06651~~ | ~~0.00088~~ | ~~915~~ | ~~22~~ | ~~501~~ | ~~8~~ | ~~415~~ | ~~5~~ | ~~20.72~~ |
| ~~S23-42~~ | ~~0.37~~ | ~~0.06436~~ | ~~0.00132~~ | ~~0.67922~~ | ~~0.01442~~ | ~~0.07653~~ | ~~0.00102~~ | ~~753~~ | ~~24~~ | ~~526~~ | ~~9~~ | ~~475~~ | ~~6~~ | ~~10.74~~ |
| ~~S23-43~~ | ~~0.26~~ | ~~0.116~~ | ~~0.00192~~ | ~~4.40414~~ | ~~0.07773~~ | ~~0.27532~~ | ~~0.00358~~ | ~~1895~~ | ~~15~~ | ~~1713~~ | ~~15~~ | ~~1568~~ | ~~18~~ | ~~20.85~~ |
| ~~S23-44~~ | ~~1.66~~ | ~~0.12684~~ | ~~0.00272~~ | ~~4.02296~~ | ~~0.08773~~ | ~~0.22998~~ | ~~0.00325~~ | ~~2055~~ | ~~20~~ | ~~1639~~ | ~~18~~ | ~~1334~~ | ~~17~~ | ~~54.05~~ |
| ~~S23-45~~ | ~~0.52~~ | ~~0.07301~~ | ~~0.00199~~ | ~~0.70317~~ | ~~0.01905~~ | ~~0.06984~~ | ~~0.00103~~ | ~~1014~~ | ~~32~~ | ~~541~~ | ~~11~~ | ~~435~~ | ~~6~~ | ~~24.37~~ |
| S23-46 | 0.72 | 0.05709 | 0.00111 | 0.53841 | 0.01085 | 0.06839 | 0.0009 | 495 | 23 | 437 | 7 | 426 | 5 | 2.58 |
| S23-47 | 0.34 | 0.056 | 0.00133 | 0.31324 | 0.00756 | 0.04056 | 0.00055 | 452 | 30 | 277 | 6 | 256 | 3 | 8.20 |
| S23-48 | 0.51 | 0.07226 | 0.00124 | 1.41492 | 0.0258 | 0.14199 | 0.00184 | 993 | 18 | 895 | 11 | 856 | 10 | 4.56 |
| ~~S23-49~~ | ~~0.77~~ | ~~0.11574~~ | ~~0.00216~~ | ~~3.24577~~ | ~~0.06313~~ | ~~0.20336~~ | ~~0.00272~~ | ~~1891~~ | ~~17~~ | ~~1468~~ | ~~15~~ | ~~1193~~ | ~~15~~ | ~~58.51~~ |
| S23-50 | 0.48 | 0.05651 | 0.00138 | 0.52018 | 0.01287 | 0.06675 | 0.00091 | 472 | 31 | 425 | 9 | 417 | 5 | 1.92 |
| S23-51 | 1.15 | 0.05521 | 0.00441 | 0.33102 | 0.02623 | 0.04348 | 0.00077 | 421 | 147 | 290 | 20 | 274 | 5 | 5.84 |
| ~~S23-52~~ | ~~0.38~~ | ~~0.10268~~ | ~~0.0028~~ | ~~3.5135~~ | ~~0.08335~~ | ~~0.24818~~ | ~~0.00332~~ | ~~1673~~ | ~~52~~ | ~~1530~~ | ~~19~~ | ~~1429~~ | ~~17~~ | ~~17.07~~ |
| S23-53 | 0.14 | 0.05745 | 0.00119 | 0.58464 | 0.01255 | 0.0738 | 0.00098 | 509 | 25 | 467 | 8 | 459 | 6 | 1.74 |
| ~~S23-54~~ | ~~0.46~~ | ~~0.0621~~ | ~~0.00229~~ | ~~0.33745~~ | ~~0.01232~~ | ~~0.0394~~ | ~~0.0006~~ | ~~678~~ | ~~52~~ | ~~295~~ | ~~9~~ | ~~249~~ | ~~4~~ | ~~18.47~~ |
| S23-55 | 1.02 | 0.05203 | 0.00199 | 0.32044 | 0.01222 | 0.04466 | 0.00066 | 287 | 60 | 282 | 9 | 282 | 4 | 0.00 |
| ~~S23-56~~ | ~~0.61~~ | ~~0.08221~~ | ~~0.00346~~ | ~~0.43717~~ | ~~0.01719~~ | ~~0.03857~~ | ~~0.00058~~ | ~~1250~~ | ~~84~~ | ~~368~~ | ~~12~~ | ~~244~~ | ~~4~~ | ~~50.82~~ |
| S23-57 | 0.89 | 0.05833 | 0.00129 | 0.49542 | 0.01123 | 0.06159 | 0.00083 | 542 | 27 | 409 | 8 | 385 | 5 | 6.23 |
| ~~S23-58~~ | ~~0.92~~ | ~~0.06049~~ | ~~0.00154~~ | ~~0.43169~~ | ~~0.0112~~ | ~~0.05175~~ | ~~0.0007~~ | ~~621~~ | ~~33~~ | ~~364~~ | ~~8~~ | ~~325~~ | ~~4~~ | ~~12.00~~ |
| S23-59 | 0.42 | 0.05114 | 0.00166 | 0.27261 | 0.00888 | 0.03865 | 0.00054 | 247 | 49 | 245 | 7 | 244 | 3 | 0.41 |
| ~~S23-60~~ | ~~0.21~~ | ~~0.06801~~ | ~~0.00126~~ | ~~0.86006~~ | ~~0.0167~~ | ~~0.0917~~ | ~~0.0012~~ | ~~869~~ | ~~20~~ | ~~630~~ | ~~9~~ | ~~566~~ | ~~7~~ | ~~11.31~~ |
| S23-61 | 0.66 | 0.05647 | 0.00141 | 0.563 | 0.01426 | 0.0723 | 0.00099 | 471 | 32 | 453 | 9 | 450 | 6 | 0.67 |
| ~~S23-62~~ | ~~1.20~~ | ~~0.07977~~ | ~~0.00342~~ | ~~0.26333~~ | ~~0.01112~~ | ~~0.02394~~ | ~~0.00039~~ | ~~1191~~ | ~~58~~ | ~~237~~ | ~~9~~ | ~~153~~ | ~~2~~ | ~~54.90~~ |
| S23-63 | 0.61 | 0.05702 | 0.00151 | 0.44945 | 0.01208 | 0.05715 | 0.00078 | 492 | 36 | 377 | 8 | 358 | 5 | 5.31 |
| ~~S23-64~~ | ~~0.44~~ | ~~0.06968~~ | ~~0.00141~~ | ~~0.83841~~ | ~~0.01763~~ | ~~0.08725~~ | ~~0.00116~~ | ~~919~~ | ~~23~~ | ~~618~~ | ~~10~~ | ~~539~~ | ~~7~~ | ~~14.66~~ |

| | | | | | | | | | | | | | | |
|---|---|---|---|---|---|---|---|---|---|---|---|---|---|---|
| S23-65 | 0.30 | 0.06744 | 0.00206 | 1.05614 | 0.02903 | 0.11359 | 0.00153 | 851 | 65 | 732 | 14 | 694 | 9 | 5.48 |
| ~~S23-66~~ | ~~0.47~~ | ~~0.10688~~ | ~~0.0021~~ | ~~2.18495~~ | ~~0.04437~~ | ~~0.14824~~ | ~~0.00199~~ | ~~1747~~ | ~~19~~ | ~~1176~~ | ~~14~~ | ~~891~~ | ~~11~~ | ~~31.99~~ |
| ~~S23-67~~ | ~~1.39~~ | ~~0.09779~~ | ~~0.00306~~ | ~~0.41085~~ | ~~0.01283~~ | ~~0.03047~~ | ~~0.00044~~ | ~~1582~~ | ~~37~~ | ~~349~~ | ~~9~~ | ~~193~~ | ~~3~~ | ~~80.83~~ |
| ~~S23-68~~ | ~~0.46~~ | ~~0.0626~~ | ~~0.00242~~ | ~~0.30222~~ | ~~0.01161~~ | ~~0.03501~~ | ~~0.00053~~ | ~~695~~ | ~~56~~ | ~~268~~ | ~~9~~ | ~~222~~ | ~~3~~ | ~~20.72~~ |
| S23-69 | 0.93 | 0.05644 | 0.00275 | 0.50189 | 0.02438 | 0.06448 | 0.00095 | 470 | 81 | 413 | 16 | 403 | 6 | 2.48 |
| ~~S23-70~~ | ~~0.95~~ | ~~0.15705~~ | ~~0.00292~~ | ~~7.1459~~ | ~~0.13915~~ | ~~0.32995~~ | ~~0.00437~~ | ~~2424~~ | ~~17~~ | ~~2130~~ | ~~17~~ | ~~1838~~ | ~~21~~ | ~~31.88~~ |
| S23-71 | 0.49 | 0.0585 | 0.00128 | 0.47121 | 0.01061 | 0.05841 | 0.00079 | 549 | 27 | 392 | 7 | 366 | 5 | 7.10 |
| ~~S23-72~~ | ~~0.90~~ | ~~0.07804~~ | ~~0.00353~~ | ~~0.38954~~ | ~~0.01752~~ | ~~0.0362~~ | ~~0.00055~~ | ~~1148~~ | ~~65~~ | ~~334~~ | ~~13~~ | ~~229~~ | ~~3~~ | ~~45.85~~ |
| S23-73 | 0.84 | 0.07472 | 0.00276 | 1.67624 | 0.06171 | 0.16267 | 0.00244 | 1061 | 50 | 1000 | 23 | 972 | 14 | 2.88 |
| S23-74 | 1.09 | 0.07257 | 0.0016 | 1.65798 | 0.03749 | 0.16567 | 0.00225 | 1002 | 25 | 993 | 14 | 988 | 12 | 0.51 |
| S23-75 | 0.48 | 0.05951 | 0.00172 | 0.56859 | 0.01656 | 0.06928 | 0.00097 | 586 | 39 | 457 | 11 | 432 | 6 | 5.79 |
| S23-76 | 0.57 | 0.0531 | 0.00235 | 0.36647 | 0.01618 | 0.05005 | 0.00075 | 333 | 73 | 317 | 12 | 315 | 5 | 0.63 |
| ~~S23-77~~ | ~~0.59~~ | ~~0.11243~~ | ~~0.00748~~ | ~~4.14382~~ | ~~0.27242~~ | ~~0.26727~~ | ~~0.00518~~ | ~~1839~~ | ~~91~~ | ~~1663~~ | ~~54~~ | ~~1527~~ | ~~26~~ | ~~20.43~~ |
| S23-78 | 0.48 | 0.05647 | 0.00139 | 0.52322 | 0.01309 | 0.06718 | 0.00093 | 471 | 32 | 427 | 9 | 419 | 6 | 1.91 |
| S23-79 | 0.93 | 0.0563 | 0.00149 | 0.54066 | 0.01445 | 0.06963 | 0.00097 | 464 | 35 | 439 | 10 | 434 | 6 | 1.15 |
| ~~S23-80~~ | ~~0.83~~ | ~~0.07164~~ | ~~0.00192~~ | ~~0.54993~~ | ~~0.01488~~ | ~~0.05566~~ | ~~0.00078~~ | ~~976~~ | ~~33~~ | ~~445~~ | ~~10~~ | ~~349~~ | ~~5~~ | ~~27.51~~ |
| S23-81 | 1.00 | 0.05454 | 0.00163 | 0.46337 | 0.01387 | 0.06161 | 0.00089 | 393 | 41 | 387 | 10 | 385 | 5 | 0.52 |
| S23-82 | 1.04 | 0.05622 | 0.00172 | 0.26853 | 0.00826 | 0.03464 | 0.00049 | 461 | 43 | 242 | 7 | 220 | 3 | 10.00 |
| ~~S23-83~~ | ~~0.52~~ | ~~0.158~~ | ~~0.00318~~ | ~~6.63991~~ | ~~0.13842~~ | ~~0.30475~~ | ~~0.00412~~ | ~~2434~~ | ~~18~~ | ~~2065~~ | ~~18~~ | ~~1715~~ | ~~20~~ | ~~41.92~~ |
| S23-84 | 0.53 | 0.07549 | 0.00189 | 1.51616 | 0.03833 | 0.14565 | 0.00207 | 1082 | 29 | 937 | 15 | 877 | 12 | 6.84 |
| ~~S23-85~~ | ~~0.62~~ | ~~0.06274~~ | ~~0.00299~~ | ~~0.30336~~ | ~~0.01438~~ | ~~0.03506~~ | ~~0.00053~~ | ~~699~~ | ~~75~~ | ~~269~~ | ~~11~~ | ~~222~~ | ~~3~~ | ~~21.17~~ |
| S23-86 | 0.61 | 0.06149 | 0.00328 | 0.74273 | 0.03806 | 0.08761 | 0.00129 | 656 | 117 | 564 | 22 | 541 | 8 | 4.25 |
| S23-87 | 0.70 | 0.06905 | 0.00145 | 1.08881 | 0.02364 | 0.11435 | 0.00154 | 900 | 24 | 748 | 11 | 698 | 9 | 7.16 |
| S23-88 | 0.78 | 0.05774 | 0.00145 | 0.58246 | 0.01483 | 0.07315 | 0.00102 | 520 | 32 | 466 | 10 | 455 | 6 | 2.42 |
| ~~S23-89~~ | ~~0.23~~ | ~~0.10682~~ | ~~0.00217~~ | ~~2.89306~~ | ~~0.06097~~ | ~~0.1964~~ | ~~0.00263~~ | ~~1746~~ | ~~20~~ | ~~1380~~ | ~~16~~ | ~~1156~~ | ~~14~~ | ~~51.04~~ |
| S23-90 | 0.30 | 0.05557 | 0.00339 | 0.50205 | 0.03035 | 0.06551 | 0.00109 | 435 | 105 | 413 | 21 | 409 | 7 | 0.98 |
| ~~S23-91~~ | ~~0.68~~ | ~~0.0673~~ | ~~0.00218~~ | ~~0.76152~~ | ~~0.02472~~ | ~~0.08205~~ | ~~0.00119~~ | ~~847~~ | ~~43~~ | ~~575~~ | ~~14~~ | ~~508~~ | ~~7~~ | ~~13.19~~ |
| S23-92 | 0.66 | 0.06629 | 0.00335 | 0.85555 | 0.04291 | 0.09359 | 0.0015 | 816 | 78 | 628 | 23 | 577 | 9 | 8.84 |

| | | | | | | | | | | | | | | |
|---|---|---|---|---|---|---|---|---|---|---|---|---|---|---|
| S23-93 | 0.48 | 0.05824 | 0.00152 | 0.51203 | 0.01351 | 0.06375 | 0.00089 | 539 | 34 | 420 | 9 | 398 | 5 | 5.53 |
| S23-94 | 0.64 | 0.07896 | 0.0021 | 2.09477 | 0.05617 | 0.19237 | 0.00275 | 1171 | 31 | 1147 | 18 | 1134 | 15 | 3.26 |
| S23-95 | 0.59 | 0.07104 | 0.00181 | 1.14503 | 0.02961 | 0.11687 | 0.00164 | 959 | 30 | 775 | 14 | 713 | 9 | 8.70 |
| ~~S23-96~~ | ~~0.59~~ | ~~0.07591~~ | ~~0.00219~~ | ~~0.91575~~ | ~~0.0264~~ | ~~0.08748~~ | ~~0.00128~~ | ~~1093~~ | ~~35~~ | ~~660~~ | ~~14~~ | ~~541~~ | ~~8~~ | ~~22.00~~ |
| ~~S23-97~~ | ~~0.90~~ | ~~0.07554~~ | ~~0.00221~~ | ~~1.05384~~ | ~~0.031~~ | ~~0.10117~~ | ~~0.00145~~ | ~~1083~~ | ~~36~~ | ~~731~~ | ~~15~~ | ~~621~~ | ~~8~~ | ~~17.71~~ |
| S23-98 | 1.59 | 0.05432 | 0.00422 | 0.29322 | 0.02264 | 0.03914 | 0.00067 | 384 | 144 | 261 | 18 | 248 | 4 | 5.24 |
| S23-99 | 0.52 | 0.05085 | 0.00132 | 0.20762 | 0.00546 | 0.02961 | 0.00041 | 234 | 36 | 192 | 5 | 188 | 3 | 2.13 |
| ~~S23-100~~ | ~~0.53~~ | ~~0.07504~~ | ~~0.002~~ | ~~1.28609~~ | ~~0.03464~~ | ~~0.12428~~ | ~~0.00176~~ | ~~1070~~ | ~~32~~ | ~~840~~ | ~~15~~ | ~~755~~ | ~~10~~ | ~~11.26~~ |
| ~~S23-101~~ | ~~0.80~~ | ~~0.16182~~ | ~~0.00363~~ | ~~6.39452~~ | ~~0.14657~~ | ~~0.28655~~ | ~~0.004~~ | ~~2475~~ | ~~21~~ | ~~2032~~ | ~~20~~ | ~~1624~~ | ~~20~~ | ~~52.40~~ |
| S23-102 | 0.51 | 0.07223 | 0.00179 | 1.37014 | 0.03447 | 0.13756 | 0.00191 | 992 | 29 | 876 | 15 | 831 | 11 | 5.42 |
| | | | | | | | | | | | | | | |
| **QX1-2** | | | | | | | | | | | | | | |
| QX12-01 | 0.98 | 0.16544 | 0.00258 | 10.87573 | 0.18187 | 0.47671 | 0.00627 | 2512 | 13 | 2513 | 16 | 2513 | 27 | -0.04 |
| QX12-02 | 0.39 | 0.09239 | 0.00183 | 3.2869 | 0.06704 | 0.25799 | 0.00352 | 1475 | 20 | 1478 | 16 | 1480 | 18 | -0.34 |
| QX12-03 | 1.08 | 0.05616 | 0.00121 | 0.57956 | 0.01285 | 0.07484 | 0.001 | 459 | 27 | 464 | 8 | 465 | 6 | -0.22 |
| QX12-04 | 0.64 | 0.05436 | 0.00255 | 0.46272 | 0.02162 | 0.06173 | 0.00093 | 386 | 78 | 386 | 15 | 386 | 6 | 0.00 |
| ~~QX12-05~~ | ~~0.51~~ | ~~0.07223~~ | ~~0.00279~~ | ~~0.79208~~ | ~~0.02839~~ | ~~0.07954~~ | ~~0.00116~~ | ~~992~~ | ~~81~~ | ~~592~~ | ~~16~~ | ~~493~~ | ~~7~~ | ~~20.08~~ |
| QX12-06 | 0.88 | 0.0515 | 0.00298 | 0.30001 | 0.01723 | 0.04225 | 0.00067 | 263 | 103 | 266 | 13 | 267 | 4 | -0.37 |
| QX12-07 | 0.32 | 0.05724 | 0.00099 | 0.66779 | 0.01225 | 0.0846 | 0.0011 | 501 | 20 | 519 | 7 | 524 | 7 | -0.95 |
| QX12-08 | 0.72 | 0.07573 | 0.00175 | 1.86887 | 0.04396 | 0.17896 | 0.00249 | 1088 | 26 | 1070 | 16 | 1061 | 14 | 2.54 |
| QX12-09 | 0.91 | 0.05711 | 0.00123 | 0.57663 | 0.01278 | 0.07323 | 0.00098 | 496 | 26 | 462 | 8 | 456 | 6 | 1.32 |
| QX12-10 | 0.54 | 0.11013 | 0.00171 | 4.83599 | 0.08081 | 0.31845 | 0.00413 | 1802 | 14 | 1791 | 14 | 1782 | 20 | 1.12 |
| QX12-11 | 0.98 | 0.05598 | 0.00226 | 0.56441 | 0.02271 | 0.07311 | 0.00109 | 452 | 63 | 454 | 15 | 455 | 7 | -0.22 |
| QX12-12 | 1.57 | 0.08027 | 0.002 | 2.25843 | 0.05667 | 0.20403 | 0.00291 | 1204 | 28 | 1199 | 18 | 1197 | 16 | 0.58 |
| ~~QX12-13~~ | ~~0.70~~ | ~~0.09105~~ | ~~0.00322~~ | ~~1.99752~~ | ~~0.06479~~ | ~~0.15912~~ | ~~0.00226~~ | ~~1448~~ | ~~69~~ | ~~1115~~ | ~~22~~ | ~~952~~ | ~~13~~ | ~~17.12~~ |
| QX12-14 | 0.64 | 0.05686 | 0.00191 | 0.58285 | 0.01962 | 0.07433 | 0.00107 | 486 | 49 | 466 | 13 | 462 | 6 | 0.87 |
| QX12-15 | 0.75 | 0.05462 | 0.00165 | 0.47799 | 0.01453 | 0.06346 | 0.00088 | 397 | 43 | 397 | 10 | 397 | 5 | 0.00 |
| QX12-16 | 0.15 | 0.05701 | 0.00104 | 0.60077 | 0.01147 | 0.07642 | 0.00099 | 492 | 21 | 478 | 7 | 475 | 6 | 0.63 |

| | | | | | | | | | | | | | | |
|---|---|---|---|---|---|---|---|---|---|---|---|---|---|---|
| QX12-17 | 4.87 | 0.06529 | 0.00131 | 1.17088 | 0.02421 | 0.13004 | 0.00174 | 784 | 22 | 787 | 11 | 788 | 10 | -0.13 |
| QX12-18 | 1.10 | 0.05598 | 0.00196 | 0.57328 | 0.02007 | 0.07426 | 0.00106 | 452 | 52 | 460 | 13 | 462 | 6 | -0.43 |
| QX12-19 | 0.77 | 0.05675 | 0.00182 | 0.59943 | 0.01929 | 0.07659 | 0.00109 | 482 | 46 | 477 | 12 | 476 | 7 | 0.21 |
| QX12-20 | 0.62 | 0.05629 | 0.00233 | 0.58256 | 0.02388 | 0.07505 | 0.00116 | 464 | 63 | 466 | 15 | 467 | 7 | -0.21 |
| QX12-21 | 0.75 | 0.05632 | 0.00178 | 0.58417 | 0.01845 | 0.07522 | 0.00108 | 465 | 45 | 467 | 12 | 468 | 6 | -0.21 |
| ~~QX12-22~~ | ~~0.59~~ | ~~0.13856~~ | ~~0.00218~~ | ~~6.71233~~ | ~~0.11333~~ | ~~0.35129~~ | ~~0.00458~~ | ~~2209~~ | ~~14~~ | ~~2074~~ | ~~15~~ | ~~1941~~ | ~~22~~ | ~~13.81~~ |
| QX12-23 | 0.53 | 0.06129 | 0.00181 | 0.83931 | 0.02497 | 0.0993 | 0.00138 | 649 | 40 | 619 | 14 | 610 | 8 | 1.48 |
| QX12-24 | 0.98 | 0.10752 | 0.00239 | 4.52605 | 0.10229 | 0.30524 | 0.00435 | 1758 | 22 | 1736 | 19 | 1717 | 21 | 2.39 |
| QX12-25 | 0.96 | 0.05172 | 0.00256 | 0.30546 | 0.01506 | 0.04283 | 0.00065 | 273 | 85 | 271 | 12 | 270 | 4 | 0.37 |
| QX12-26 | 0.68 | 0.05663 | 0.00145 | 0.58717 | 0.01529 | 0.07519 | 0.00103 | 477 | 34 | 469 | 10 | 467 | 6 | 0.43 |
| QX12-27 | 0.38 | 0.07005 | 0.00134 | 1.48045 | 0.02944 | 0.15325 | 0.00203 | 930 | 21 | 922 | 12 | 919 | 11 | 0.33 |
| QX12-28 | 0.69 | 0.05622 | 0.00216 | 0.58505 | 0.02247 | 0.07546 | 0.0011 | 461 | 59 | 468 | 14 | 469 | 7 | -0.21 |
| QX12-29 | 0.76 | 0.05653 | 0.00155 | 0.56013 | 0.01543 | 0.07186 | 0.001 | 473 | 37 | 452 | 10 | 447 | 6 | 1.12 |
| QX12-30 | 1.12 | 0.05573 | 0.00095 | 0.54749 | 0.00989 | 0.07123 | 0.00092 | 442 | 19 | 443 | 6 | 444 | 6 | -0.23 |
| QX12-31 | 0.34 | 0.06106 | 0.00139 | 0.89185 | 0.02061 | 0.10591 | 0.00145 | 641 | 27 | 647 | 11 | 649 | 8 | -0.31 |
| QX12-32 | 0.66 | 0.05564 | 0.0016 | 0.54968 | 0.01583 | 0.07164 | 0.00102 | 438 | 39 | 445 | 10 | 446 | 6 | -0.22 |
| QX12-33 | 1.48 | 0.07623 | 0.00268 | 1.90419 | 0.06686 | 0.18113 | 0.00271 | 1101 | 46 | 1083 | 23 | 1073 | 15 | 2.61 |
| QX12-34 | 0.82 | 0.08791 | 0.00201 | 2.87374 | 0.06686 | 0.23704 | 0.00328 | 1381 | 24 | 1375 | 18 | 1371 | 17 | 0.73 |
| QX12-35 | 1.89 | 0.06417 | 0.00214 | 1.06299 | 0.03555 | 0.12011 | 0.00171 | 747 | 47 | 735 | 17 | 731 | 10 | 0.55 |
| QX12-36 | 0.62 | 0.05213 | 0.00594 | 0.32721 | 0.03698 | 0.04552 | 0.00094 | 291 | 217 | 287 | 28 | 287 | 6 | 0.00 |
| QX12-37 | 0.95 | 0.05627 | 0.00398 | 0.55184 | 0.03871 | 0.07111 | 0.0012 | 463 | 126 | 446 | 25 | 443 | 7 | 0.68 |
| QX12-38 | 0.48 | 0.05042 | 0.00312 | 0.23573 | 0.0145 | 0.0339 | 0.00055 | 214 | 111 | 215 | 12 | 215 | 3 | 0.00 |
| QX12-39 | 0.26 | 0.07032 | 0.00126 | 1.42486 | 0.02683 | 0.14693 | 0.00193 | 938 | 19 | 899 | 11 | 884 | 11 | 1.70 |
| QX12-40 | 0.32 | 0.0569 | 0.0015 | 0.56991 | 0.01522 | 0.07263 | 0.001 | 488 | 35 | 458 | 10 | 452 | 6 | 1.33 |
| QX12-41 | 0.65 | 0.06442 | 0.00179 | 1.10746 | 0.03099 | 0.12466 | 0.00176 | 755 | 36 | 757 | 15 | 757 | 10 | 0.00 |
| QX12-42 | 0.66 | 0.05635 | 0.00168 | 0.57562 | 0.01729 | 0.07407 | 0.00104 | 466 | 42 | 462 | 11 | 461 | 6 | 0.22 |
| QX12-43 | 0.47 | 0.09583 | 0.00163 | 3.26367 | 0.05852 | 0.24694 | 0.00324 | 1544 | 16 | 1472 | 14 | 1423 | 17 | 8.50 |
| QX12-44 | 0.14 | 0.06729 | 0.00161 | 1.15268 | 0.02321 | 0.12424 | 0.0016 | 847 | 51 | 779 | 11 | 755 | 9 | 3.18 |

| | | | | | | | | | | | | | | |
|---|---|---|---|---|---|---|---|---|---|---|---|---|---|---|
| QX12-45 | 0.15 | 0.05149 | 0.00154 | 0.29294 | 0.00879 | 0.04125 | 0.00058 | 263 | 43 | 261 | 7 | 261 | 4 | 0.00 |
| QX12-46 | 0.54 | 0.05662 | 0.00131 | 0.60318 | 0.01427 | 0.07724 | 0.00104 | 477 | 29 | 479 | 9 | 480 | 6 | -0.21 |
| QX12-47 | 1.02 | 0.05204 | 0.00308 | 0.32845 | 0.01932 | 0.04576 | 0.00071 | 287 | 106 | 288 | 15 | 288 | 4 | 0.00 |
| QX12-48 | 0.54 | 0.05691 | 0.00135 | 0.57156 | 0.01377 | 0.07283 | 0.00099 | 488 | 30 | 459 | 9 | 453 | 6 | 1.32 |
| QX12-49 | 1.24 | 0.16762 | 0.00408 | 10.90377 | 0.26622 | 0.47166 | 0.00729 | 2534 | 21 | 2515 | 23 | 2491 | 32 | 1.73 |
| QX12-50 | 0.60 | 0.08904 | 0.00154 | 3.04165 | 0.05547 | 0.24769 | 0.00326 | 1405 | 17 | 1418 | 14 | 1427 | 17 | -1.54 |
| QX12-51 | 0.47 | 0.05622 | 0.00135 | 0.58389 | 0.01429 | 0.07531 | 0.00102 | 461 | 31 | 467 | 9 | 468 | 6 | -0.21 |
| QX12-52 | 0.58 | 0.05644 | 0.00146 | 0.57695 | 0.01515 | 0.07412 | 0.00101 | 470 | 34 | 462 | 10 | 461 | 6 | 0.22 |
| QX12-53 | 0.08 | 0.05607 | 0.00135 | 0.52638 | 0.01288 | 0.06806 | 0.00093 | 455 | 31 | 429 | 9 | 424 | 6 | 1.18 |
| QX12-54 | 0.47 | 0.05674 | 0.00139 | 0.61004 | 0.01524 | 0.07795 | 0.00106 | 481 | 32 | 484 | 10 | 484 | 6 | 0.00 |
| QX12-55 | 0.12 | 0.05548 | 0.00162 | 0.52374 | 0.01359 | 0.06847 | 0.0009 | 431 | 66 | 428 | 9 | 427 | 5 | 0.23 |
| QX12-56 | 0.74 | 0.05569 | 0.00123 | 0.53634 | 0.01207 | 0.06983 | 0.00094 | 440 | 27 | 436 | 8 | 435 | 6 | 0.23 |
| QX12-57 | 1.01 | 0.05686 | 0.00208 | 0.583 | 0.02133 | 0.07434 | 0.00107 | 486 | 55 | 466 | 14 | 462 | 6 | 0.87 |
| ~~QX12-58~~ | ~~0.87~~ | ~~0.07349~~ | ~~0.00188~~ | ~~0.6113~~ | ~~0.01576~~ | ~~0.06031~~ | ~~0.00084~~ | ~~1027~~ | ~~30~~ | ~~484~~ | ~~10~~ | ~~378~~ | ~~5~~ | ~~28.04~~ |
| QX12-59 | 0.76 | 0.05608 | 0.00552 | 0.54045 | 0.05285 | 0.06987 | 0.00131 | 456 | 186 | 439 | 35 | 435 | 8 | 0.92 |
| ~~QX12-60~~ | ~~1.18~~ | ~~0.06658~~ | ~~0.00163~~ | ~~0.66821~~ | ~~0.01661~~ | ~~0.07277~~ | ~~0.00099~~ | ~~825~~ | ~~30~~ | ~~520~~ | ~~10~~ | ~~453~~ | ~~6~~ | ~~14.79~~ |
| QX12-61 | 0.63 | 0.05669 | 0.00156 | 0.58424 | 0.01616 | 0.07472 | 0.00104 | 479 | 37 | 467 | 10 | 465 | 6 | 0.43 |
| QX12-62 | 0.83 | 0.10127 | 0.00198 | 4.14488 | 0.08358 | 0.29677 | 0.00404 | 1648 | 19 | 1663 | 16 | 1675 | 20 | -1.61 |
| QX12-63 | 0.52 | 0.05647 | 0.00135 | 0.57567 | 0.014 | 0.07392 | 0.00101 | 471 | 30 | 462 | 9 | 460 | 6 | 0.43 |
| QX12-64 | 1.05 | 0.05986 | 0.00183 | 0.80308 | 0.02449 | 0.09727 | 0.0014 | 599 | 41 | 599 | 14 | 598 | 8 | 0.17 |
| QX12-65 | 0.94 | 0.05612 | 0.00141 | 0.58171 | 0.01485 | 0.07515 | 0.00103 | 457 | 33 | 466 | 10 | 467 | 6 | -0.21 |
| QX12-66 | 0.54 | 0.07914 | 0.00148 | 2.10921 | 0.04105 | 0.19323 | 0.00257 | 1176 | 19 | 1152 | 13 | 1139 | 14 | 3.25 |
| QX12-67 | 0.94 | 0.05612 | 0.0017 | 0.56207 | 0.01714 | 0.07262 | 0.00102 | 457 | 43 | 453 | 11 | 452 | 6 | 0.22 |
| QX12-68 | 0.85 | 0.05589 | 0.00163 | 0.56009 | 0.0164 | 0.07265 | 0.00104 | 448 | 40 | 452 | 11 | 452 | 6 | 0.00 |
| QX12-69 | 0.48 | 0.06966 | 0.00141 | 1.44058 | 0.03009 | 0.14993 | 0.00201 | 918 | 22 | 906 | 13 | 901 | 11 | 0.55 |
| QX12-70 | 0.59 | 0.05641 | 0.00148 | 0.58013 | 0.0154 | 0.07456 | 0.00103 | 469 | 35 | 465 | 10 | 464 | 6 | 0.22 |
| QX12-71 | 0.49 | 0.05523 | 0.00203 | 0.53376 | 0.01952 | 0.07007 | 0.00102 | 422 | 56 | 434 | 13 | 437 | 6 | -0.69 |
| QX12-72 | 1.05 | 0.0517 | 0.00142 | 0.31741 | 0.00882 | 0.04451 | 0.00061 | 272 | 39 | 280 | 7 | 281 | 4 | -0.36 |

| | | | | | | | | | | | | | | |
|---|---|---|---|---|---|---|---|---|---|---|---|---|---|---|
| QX12-73 | 0.61 | 0.05623 | 0.00134 | 0.57607 | 0.01392 | 0.07428 | 0.00102 | 461 | 30 | 462 | 9 | 462 | 6 | 0.00 |
| QX12-74 | 0.38 | 0.0556 | 0.00135 | 0.52692 | 0.01296 | 0.06871 | 0.00094 | 436 | 31 | 430 | 9 | 428 | 6 | 0.47 |
| QX12-75 | 0.53 | 0.05089 | 0.00197 | 0.27132 | 0.01045 | 0.03866 | 0.00056 | 236 | 62 | 244 | 8 | 245 | 3 | -0.41 |
| QX12-76 | 0.17 | 0.05802 | 0.00126 | 0.67936 | 0.01508 | 0.08489 | 0.00115 | 531 | 26 | 526 | 9 | 525 | 7 | 0.19 |
| QX12-77 | 0.69 | 0.05732 | 0.00131 | 0.63599 | 0.01483 | 0.08045 | 0.0011 | 504 | 28 | 500 | 9 | 499 | 7 | 0.20 |
| QX12-78 | 0.88 | 0.08273 | 0.00232 | 2.491 | 0.06993 | 0.2183 | 0.00322 | 1263 | 32 | 1269 | 20 | 1273 | 17 | -0.79 |
| QX12-79 | 0.92 | 0.05659 | 0.00165 | 0.58228 | 0.01696 | 0.0746 | 0.00106 | 476 | 40 | 466 | 11 | 464 | 6 | 0.43 |
| QX12-80 | 0.75 | 0.05643 | 0.00147 | 0.58574 | 0.01539 | 0.07526 | 0.00104 | 469 | 34 | 468 | 10 | 468 | 6 | 0.00 |
| QX12-81 | 0.54 | 0.05622 | 0.00123 | 0.57271 | 0.01281 | 0.07386 | 0.001 | 461 | 27 | 460 | 8 | 459 | 6 | 0.22 |
| QX12-82 | 0.45 | 0.05672 | 0.00121 | 0.59679 | 0.01305 | 0.07628 | 0.00102 | 481 | 26 | 475 | 8 | 474 | 6 | 0.21 |
| QX12-83 | 0.39 | 0.05637 | 0.0013 | 0.55414 | 0.013 | 0.07127 | 0.00097 | 467 | 29 | 448 | 8 | 444 | 6 | 0.90 |
| QX12-84 | 0.13 | 0.07604 | 0.00229 | 1.4311 | 0.03869 | 0.13651 | 0.00183 | 1096 | 62 | 902 | 16 | 825 | 10 | 9.33 |
| QX12-85 | 0.29 | 0.07007 | 0.00141 | 1.47637 | 0.03063 | 0.15276 | 0.00205 | 930 | 22 | 921 | 13 | 916 | 11 | 0.55 |
| QX12-86 | 0.61 | 0.05728 | 0.00125 | 0.57293 | 0.01277 | 0.07252 | 0.00098 | 502 | 26 | 460 | 8 | 451 | 6 | 2.00 |
| QX12-87 | 0.55 | 0.05585 | 0.00152 | 0.56251 | 0.01543 | 0.07302 | 0.00103 | 446 | 36 | 453 | 10 | 454 | 6 | -0.22 |
| QX12-88 | 0.87 | 0.05601 | 0.00138 | 0.56669 | 0.01414 | 0.07336 | 0.00101 | 453 | 32 | 456 | 9 | 456 | 6 | 0.00 |
| QX12-89 | 0.47 | 0.05206 | 0.00154 | 0.32345 | 0.0096 | 0.04504 | 0.00064 | 288 | 42 | 285 | 7 | 284 | 4 | 0.35 |
| QX12-90 | 1.88 | 0.05612 | 0.00161 | 0.57916 | 0.0166 | 0.07481 | 0.00107 | 457 | 39 | 464 | 11 | 465 | 6 | -0.22 |
| QX12-91 | 0.22 | 0.10798 | 0.00198 | 4.61033 | 0.08808 | 0.30954 | 0.00409 | 1766 | 17 | 1751 | 16 | 1738 | 20 | 1.61 |
| QX12-92 | 0.76 | 0.05692 | 0.00145 | 0.5887 | 0.01513 | 0.07499 | 0.00104 | 488 | 33 | 470 | 10 | 466 | 6 | 0.86 |
| QX12-93 | 0.77 | 0.05666 | 0.00184 | 0.58596 | 0.01899 | 0.07497 | 0.0011 | 478 | 46 | 468 | 12 | 466 | 7 | 0.43 |
| QX12-94 | 0.46 | 0.05484 | 0.00131 | 0.49459 | 0.01198 | 0.06538 | 0.0009 | 406 | 30 | 408 | 8 | 408 | 5 | 0.00 |
| QX12-95 | 0.65 | 0.05607 | 0.00132 | 0.56714 | 0.0135 | 0.07333 | 0.00101 | 455 | 29 | 456 | 9 | 456 | 6 | 0.00 |
| QX12-96 | 0.72 | 0.05191 | 0.00207 | 0.3286 | 0.0129 | 0.04589 | 0.00074 | 281 | 60 | 288 | 10 | 289 | 5 | -0.35 |
| QX12-97 | 0.63 | 0.0573 | 0.00178 | 0.59506 | 0.01839 | 0.07529 | 0.00111 | 503 | 42 | 474 | 12 | 468 | 7 | 1.28 |
| QX12-98 | 0.42 | 0.06986 | 0.00135 | 1.48761 | 0.02983 | 0.15437 | 0.00205 | 924 | 21 | 925 | 12 | 925 | 11 | 0.00 |
| QX12-99 | 0.72 | 0.0566 | 0.0017 | 0.53984 | 0.01609 | 0.06914 | 0.00102 | 476 | 40 | 438 | 11 | 431 | 6 | 1.62 |
| ~~QX12-100~~ | ~~0.27~~ | ~~0.07158~~ | ~~0.00225~~ | ~~0.89404~~ | ~~0.02533~~ | ~~0.09058~~ | ~~0.00122~~ | ~~974~~ | ~~65~~ | ~~649~~ | ~~14~~ | ~~559~~ | ~~7~~ | ~~16.10~~ |

| | | | | | | | | | | | | | | |
|---|---|---|---|---|---|---|---|---|---|---|---|---|---|---|
| QX12-101 | 0.76 | 0.05309 | 0.00161 | 0.3525 | 0.0106 | 0.04813 | 0.00071 | 333 | 42 | 307 | 8 | 303 | 4 | 1.32 |
| QX12-102 | 4.95 | 0.05688 | 0.00163 | 0.60994 | 0.01753 | 0.07774 | 0.00111 | 487 | 39 | 484 | 11 | 483 | 7 | 0.21 |
| QX12-103 | 2.22 | 0.08821 | 0.00193 | 2.80568 | 0.06258 | 0.2306 | 0.00318 | 1387 | 23 | 1357 | 17 | 1338 | 17 | 3.66 |
| ~~QX12-104~~ | ~~1.18~~ | ~~0.08321~~ | ~~0.00192~~ | ~~0.75961~~ | ~~0.01762~~ | ~~0.06618~~ | ~~0.00093~~ | ~~1274~~ | ~~24~~ | ~~574~~ | ~~10~~ | ~~413~~ | ~~6~~ | ~~38.98~~ |
| QX12-105 | 0.61 | 0.05736 | 0.00144 | 0.62582 | 0.01585 | 0.07909 | 0.00111 | 505 | 32 | 493 | 10 | 491 | 7 | 0.41 |
| | | | | | | | | | | | | | | |
| **QX1-1** | | | | | | | | | | | | | | |
| QX11-01 | 0.43 | 0.12106 | 0.00237 | 5.75521 | 0.11939 | 0.3447 | 0.00494 | 1972 | 18 | 1940 | 18 | 1909 | 24 | 3.30 |
| QX11-02 | 0.87 | 0.05115 | 0.00162 | 0.26807 | 0.00855 | 0.038 | 0.00058 | 248 | 46 | 241 | 7 | 240 | 4 | 0.42 |
| QX11-03 | 0.20 | 0.06854 | 0.00141 | 1.26705 | 0.02748 | 0.13403 | 0.0019 | 885 | 23 | 831 | 12 | 811 | 11 | 2.47 |
| QX11-04 | 0.27 | 0.0517 | 0.00231 | 0.28611 | 0.01275 | 0.04013 | 0.00064 | 272 | 73 | 255 | 10 | 254 | 4 | 0.39 |
| QX11-05 | 0.53 | 0.05456 | 0.00146 | 0.31714 | 0.00867 | 0.04215 | 0.00062 | 394 | 36 | 280 | 7 | 266 | 4 | 5.26 |
| QX11-06 | 0.70 | 0.16508 | 0.00317 | 10.88889 | 0.22156 | 0.47827 | 0.00682 | 2508 | 17 | 2514 | 19 | 2520 | 30 | -0.48 |
| QX11-07 | 0.61 | 0.05147 | 0.0015 | 0.29769 | 0.00881 | 0.04194 | 0.00062 | 262 | 41 | 265 | 7 | 265 | 4 | 0.00 |
| ~~QX11-08~~ | ~~0.84~~ | ~~0.07476~~ | ~~0.00215~~ | ~~0.59077~~ | ~~0.01721~~ | ~~0.05729~~ | ~~0.00087~~ | ~~1062~~ | ~~35~~ | ~~471~~ | ~~11~~ | ~~359~~ | ~~5~~ | ~~31.20~~ |
| QX11-09 | 0.46 | 0.05057 | 0.00171 | 0.24406 | 0.00826 | 0.035 | 0.00055 | 221 | 49 | 222 | 7 | 222 | 3 | 0.00 |
| QX11-10 | 0.73 | 0.10903 | 0.00416 | 4.71724 | 0.16453 | 0.31378 | 0.00487 | 1783 | 71 | 1770 | 29 | 1759 | 24 | 1.36 |
| QX11-11 | 0.36 | 0.05758 | 0.00136 | 0.65895 | 0.01598 | 0.08298 | 0.00121 | 514 | 29 | 514 | 10 | 514 | 7 | 0.00 |
| ~~QX11-12~~ | ~~0.53~~ | ~~0.0843~~ | ~~0.00312~~ | ~~2.18569~~ | ~~0.07398~~ | ~~0.18805~~ | ~~0.0028~~ | ~~1299~~ | ~~74~~ | ~~1176~~ | ~~24~~ | ~~1111~~ | ~~15~~ | ~~16.92~~ |
| QX11-13 | 0.51 | 0.0816 | 0.00193 | 2.34736 | 0.05678 | 0.20858 | 0.0031 | 1236 | 25 | 1227 | 17 | 1221 | 17 | 1.23 |
| QX11-14 | 0.63 | 0.05556 | 0.00212 | 0.53579 | 0.02046 | 0.06993 | 0.00109 | 435 | 57 | 436 | 14 | 436 | 7 | 0.00 |
| QX11-15 | 0.49 | 0.05208 | 0.00207 | 0.33304 | 0.01317 | 0.04637 | 0.00074 | 289 | 61 | 292 | 10 | 292 | 5 | 0.00 |
| QX11-16 | 0.63 | 0.05379 | 0.0022 | 0.41682 | 0.01707 | 0.05619 | 0.00087 | 362 | 64 | 354 | 12 | 352 | 5 | 0.57 |
| QX11-17 | 0.84 | 0.05169 | 0.00245 | 0.31615 | 0.01489 | 0.04435 | 0.00074 | 272 | 77 | 279 | 11 | 280 | 5 | -0.36 |
| QX11-18 | 0.54 | 0.05174 | 0.00317 | 0.30696 | 0.01865 | 0.04302 | 0.00075 | 274 | 107 | 272 | 14 | 272 | 5 | 0.00 |
| QX11-19 | 0.24 | 0.06966 | 0.00165 | 1.44573 | 0.03512 | 0.15048 | 0.00219 | 918 | 27 | 908 | 15 | 904 | 12 | 0.44 |
| QX11-20 | 0.45 | 0.05336 | 0.00205 | 0.38208 | 0.01472 | 0.05192 | 0.00079 | 344 | 60 | 329 | 11 | 326 | 5 | 0.92 |
| QX11-21 | 0.90 | 0.05721 | 0.00163 | 0.64131 | 0.01857 | 0.08128 | 0.00119 | 500 | 38 | 503 | 11 | 504 | 7 | -0.20 |

| | | | | | | | | | | | | | | |
|---|---|---|---|---|---|---|---|---|---|---|---|---|---|---|
| QX11-22 | 0.00 | 0.05593 | 0.00198 | 0.55102 | 0.0196 | 0.07143 | 0.00109 | 450 | 52 | 446 | 13 | 445 | 7 | 0.22 |
| QX11-23 | 0.46 | 0.07281 | 0.00175 | 1.55307 | 0.03813 | 0.15467 | 0.00227 | 1009 | 27 | 952 | 15 | 927 | 13 | 2.70 |
| QX11-24 | 0.53 | 0.05551 | 0.00219 | 0.52815 | 0.02079 | 0.06899 | 0.0011 | 433 | 59 | 431 | 14 | 430 | 7 | 0.23 |
| QX11-25 | 1.06 | 0.05813 | 0.00293 | 0.68403 | 0.03417 | 0.08533 | 0.00146 | 535 | 79 | 529 | 21 | 528 | 9 | 0.19 |
| QX11-26 | 0.40 | 0.07511 | 0.00192 | 1.87304 | 0.0485 | 0.18082 | 0.00273 | 1071 | 29 | 1072 | 17 | 1071 | 15 | 0.00 |
| QX11-27 | 0.74 | 0.05671 | 0.00177 | 0.58088 | 0.01813 | 0.07427 | 0.00115 | 480 | 42 | 465 | 12 | 462 | 7 | 0.65 |
| ~~QX11-28~~ | ~~0.31~~ | ~~0.12816~~ | ~~0.00375~~ | ~~4.5386~~ | ~~0.11543~~ | ~~0.25684~~ | ~~0.00373~~ | ~~2073~~ | ~~53~~ | ~~1738~~ | ~~21~~ | ~~1474~~ | ~~19~~ | ~~40.64~~ |
| QX11-29 | 0.48 | 0.05913 | 0.00692 | 0.75485 | 0.08755 | 0.09256 | 0.00209 | 572 | 217 | 571 | 51 | 571 | 12 | 0.00 |
| QX11-30 | 0.78 | 0.0556 | 0.00132 | 0.53901 | 0.01311 | 0.07029 | 0.00102 | 436 | 29 | 438 | 9 | 438 | 6 | 0.00 |
| QX11-31 | 0.50 | 0.05708 | 0.00178 | 0.62736 | 0.0196 | 0.0797 | 0.00122 | 495 | 42 | 494 | 12 | 494 | 7 | 0.00 |
| QX11-32 | 0.61 | 0.05456 | 0.00123 | 0.46464 | 0.01077 | 0.06175 | 0.00088 | 394 | 28 | 387 | 7 | 386 | 5 | 0.26 |
| QX11-33 | 0.38 | 0.06058 | 0.0013 | 0.57402 | 0.01279 | 0.0687 | 0.00097 | 624 | 25 | 461 | 8 | 428 | 6 | 7.71 |
| QX11-34 | 1.11 | 0.05577 | 0.00152 | 0.55238 | 0.01523 | 0.07181 | 0.00106 | 443 | 36 | 447 | 10 | 447 | 6 | 0.00 |
| QX11-35 | 0.55 | 0.05466 | 0.00197 | 0.45791 | 0.0165 | 0.06074 | 0.00094 | 398 | 53 | 383 | 11 | 380 | 6 | 0.79 |
| QX11-36 | 0.36 | 0.05234 | 0.00252 | 0.38486 | 0.01755 | 0.05333 | 0.00081 | 300 | 112 | 331 | 13 | 335 | 5 | -1.19 |
| QX11-37 | 0.42 | 0.05505 | 0.0015 | 0.50172 | 0.01379 | 0.06608 | 0.00097 | 414 | 36 | 413 | 9 | 412 | 6 | 0.24 |
| QX11-38 | 0.48 | 0.07132 | 0.00169 | 1.51879 | 0.03682 | 0.15441 | 0.00223 | 967 | 27 | 938 | 15 | 926 | 12 | 1.30 |
| QX11-39 | 0.21 | 0.0546 | 0.00175 | 0.44958 | 0.01442 | 0.05971 | 0.0009 | 396 | 45 | 377 | 10 | 374 | 5 | 0.80 |
| QX11-40 | 1.25 | 0.0556 | 0.00151 | 0.54291 | 0.01487 | 0.07081 | 0.00105 | 436 | 35 | 440 | 10 | 441 | 6 | -0.23 |
| QX11-41 | 0.94 | 0.05658 | 0.00279 | 0.5946 | 0.02916 | 0.07621 | 0.00124 | 475 | 80 | 474 | 19 | 473 | 7 | 0.21 |
| QX11-42 | 0.83 | 0.05516 | 0.00219 | 0.50986 | 0.02012 | 0.06702 | 0.00106 | 419 | 60 | 418 | 14 | 418 | 6 | 0.00 |
| QX11-43 | 0.58 | 0.05564 | 0.0016 | 0.54424 | 0.01576 | 0.07093 | 0.00105 | 438 | 39 | 441 | 10 | 442 | 6 | -0.23 |
| QX11-44 | 0.39 | 0.05623 | 0.00137 | 0.50123 | 0.01245 | 0.06464 | 0.00092 | 461 | 31 | 413 | 8 | 404 | 6 | 2.23 |
| QX11-45 | 0.32 | 0.05513 | 0.00199 | 0.50622 | 0.01829 | 0.06658 | 0.00102 | 417 | 53 | 416 | 12 | 416 | 6 | 0.00 |
| QX11-46 | 0.43 | 0.0554 | 0.00143 | 0.50109 | 0.01313 | 0.06559 | 0.00095 | 428 | 33 | 412 | 9 | 410 | 6 | 0.49 |
| QX11-47 | 0.63 | 0.05211 | 0.00363 | 0.33315 | 0.02294 | 0.04636 | 0.00086 | 290 | 123 | 292 | 17 | 292 | 5 | 0.00 |
| QX11-48 | 0.66 | 0.11523 | 0.00256 | 5.24332 | 0.11947 | 0.32995 | 0.00476 | 1883 | 21 | 1860 | 19 | 1838 | 23 | 2.45 |
| QX11-49 | 0.14 | 0.25577 | 0.0054 | 22.09347 | 0.48131 | 0.62634 | 0.00891 | 3221 | 18 | 3188 | 21 | 3135 | 35 | 2.74 |

| | | | | | | | | | | | | | | |
|---|---|---|---|---|---|---|---|---|---|---|---|---|---|---|
| QX11-50 | 0.68 | 0.09747 | 0.00241 | 3.60613 | 0.09039 | 0.26828 | 0.00395 | 1576 | 26 | 1551 | 20 | 1532 | 20 | 2.87 |
| QX11-51 | 0.53 | 0.05478 | 0.00145 | 0.48321 | 0.01292 | 0.06396 | 0.00093 | 403 | 34 | 400 | 9 | 400 | 6 | 0.00 |
| QX11-52 | 0.29 | 0.0563 | 0.00276 | 0.50126 | 0.02345 | 0.06457 | 0.00096 | 464 | 112 | 413 | 16 | 403 | 6 | 2.48 |
| QX11-53 | 0.97 | 0.05624 | 0.00147 | 0.55803 | 0.01469 | 0.07195 | 0.00105 | 462 | 33 | 450 | 10 | 448 | 6 | 0.45 |
| QX11-54 | 0.89 | 0.05493 | 0.00209 | 0.49639 | 0.0188 | 0.06553 | 0.00102 | 409 | 57 | 409 | 13 | 409 | 6 | 0.00 |
| QX11-55 | 0.96 | 0.05484 | 0.00267 | 0.49216 | 0.02373 | 0.06507 | 0.00107 | 406 | 78 | 406 | 16 | 406 | 6 | 0.00 |
| QX11-56 | 0.49 | 0.05148 | 0.00205 | 0.30348 | 0.01208 | 0.04275 | 0.00065 | 262 | 63 | 269 | 9 | 270 | 4 | -0.37 |
| QX11-57 | 1.00 | 0.05963 | 0.00164 | 0.56532 | 0.01564 | 0.06875 | 0.00101 | 590 | 35 | 455 | 10 | 429 | 6 | 6.06 |
| QX11-58 | 0.45 | 0.05091 | 0.00241 | 0.21292 | 0.00955 | 0.03033 | 0.00045 | 237 | 111 | 196 | 8 | 193 | 3 | 1.55 |
| QX11-59 | 0.36 | 0.05575 | 0.0017 | 0.52278 | 0.01593 | 0.068 | 0.00101 | 442 | 42 | 427 | 11 | 424 | 6 | 0.71 |
| QX11-60 | 0.48 | 0.1137 | 0.00253 | 4.86928 | 0.11044 | 0.31053 | 0.00441 | 1859 | 22 | 1797 | 19 | 1743 | 22 | 6.66 |
| QX11-61 | 0.75 | 0.05539 | 0.00188 | 0.51466 | 0.01749 | 0.06738 | 0.00101 | 428 | 49 | 422 | 12 | 420 | 6 | 0.48 |
| QX11-62 | 0.80 | 0.05497 | 0.00185 | 0.50338 | 0.01683 | 0.0664 | 0.00103 | 411 | 47 | 414 | 11 | 414 | 6 | 0.00 |
| QX11-63 | 0.18 | 0.124 | 0.00275 | 6.1883 | 0.14022 | 0.36188 | 0.00513 | 2015 | 21 | 2003 | 20 | 1991 | 24 | 1.21 |
| QX11-64 | 0.19 | 0.05848 | 0.00209 | 0.65378 | 0.02321 | 0.08107 | 0.00124 | 548 | 51 | 511 | 14 | 503 | 7 | 1.59 |
| QX11-65 | 0.08 | 0.06092 | 0.0017 | 0.63955 | 0.01546 | 0.07613 | 0.00106 | 637 | 61 | 502 | 10 | 473 | 6 | 6.13 |
| ~~QX11-66~~ | ~~1.79~~ | ~~0.07212~~ | ~~0.00273~~ | ~~0.60598~~ | ~~0.0227~~ | ~~0.06093~~ | ~~0.00097~~ | ~~989~~ | ~~50~~ | ~~481~~ | ~~14~~ | ~~381~~ | ~~6~~ | ~~26.25~~ |
| ~~QX11-67~~ | ~~0.23~~ | ~~0.06097~~ | ~~0.00147~~ | ~~0.48682~~ | ~~0.01187~~ | ~~0.0579~~ | ~~0.00083~~ | ~~638~~ | ~~29~~ | ~~403~~ | ~~8~~ | ~~363~~ | ~~5~~ | ~~11.02~~ |
| QX11-68 | 0.24 | 0.06963 | 0.00163 | 1.40082 | 0.03323 | 0.14587 | 0.00208 | 917 | 26 | 889 | 14 | 878 | 12 | 1.25 |
| QX11-69 | 0.44 | 0.05686 | 0.0017 | 0.60669 | 0.0181 | 0.07737 | 0.00115 | 486 | 40 | 481 | 11 | 480 | 7 | 0.21 |
| ~~QX11-70~~ | ~~0.55~~ | ~~0.0789~~ | ~~0.00247~~ | ~~1.94063~~ | ~~0.06048~~ | ~~0.17836~~ | ~~0.00274~~ | ~~1170~~ | ~~38~~ | ~~1095~~ | ~~21~~ | ~~1058~~ | ~~15~~ | ~~10.59~~ |
| QX11-71 | 0.47 | 0.06788 | 0.00173 | 1.24972 | 0.03206 | 0.13351 | 0.00194 | 865 | 30 | 823 | 14 | 808 | 11 | 1.86 |
| QX11-72 | 0.49 | 0.1089 | 0.00285 | 4.6494 | 0.12144 | 0.30958 | 0.00466 | 1781 | 26 | 1758 | 22 | 1739 | 23 | 2.42 |
| QX11-73 | 0.96 | 0.0559 | 0.00352 | 0.55795 | 0.03473 | 0.07237 | 0.00126 | 448 | 108 | 450 | 23 | 450 | 8 | 0.00 |
| QX11-74 | 0.66 | 0.0559 | 0.00154 | 0.54079 | 0.0149 | 0.07016 | 0.00103 | 448 | 36 | 439 | 10 | 437 | 6 | 0.46 |
| QX11-75 | 0.74 | 0.0552 | 0.00182 | 0.51267 | 0.01673 | 0.06735 | 0.00104 | 420 | 45 | 420 | 11 | 420 | 6 | 0.00 |
| QX11-76 | 0.90 | 0.06666 | 0.00274 | 1.15326 | 0.04693 | 0.12546 | 0.00202 | 827 | 58 | 779 | 22 | 762 | 12 | 2.23 |
| QX11-77 | 0.46 | 0.05595 | 0.00159 | 0.56792 | 0.0161 | 0.0736 | 0.00109 | 450 | 37 | 457 | 10 | 458 | 7 | -0.22 |

| | | | | | | | | | | | | | | |
|---|---|---|---|---|---|---|---|---|---|---|---|---|---|---|
| QX11-78 | 0.44 | 0.05752 | 0.00983 | 0.65239 | 0.11068 | 0.08224 | 0.00213 | 512 | 330 | 510 | 68 | 509 | 13 | 0.20 |
| QX11-79 | 0.76 | 0.07296 | 0.00186 | 1.56337 | 0.03982 | 0.15539 | 0.00225 | 1013 | 29 | 956 | 16 | 931 | 13 | 2.69 |
| QX11-80 | 0.18 | 0.05745 | 0.00165 | 0.65301 | 0.01862 | 0.08242 | 0.00123 | 509 | 37 | 510 | 11 | 511 | 7 | -0.20 |
| QX11-81 | 1.20 | 0.05536 | 0.00199 | 0.52338 | 0.01863 | 0.06856 | 0.00104 | 427 | 52 | 427 | 12 | 427 | 6 | 0.00 |
| QX11-82 | 0.72 | 0.0553 | 0.00181 | 0.52169 | 0.01687 | 0.06841 | 0.00104 | 424 | 45 | 426 | 11 | 427 | 6 | -0.23 |
| QX11-83 | 0.74 | 0.05537 | 0.00239 | 0.50967 | 0.02186 | 0.06674 | 0.00104 | 427 | 68 | 418 | 15 | 416 | 6 | 0.48 |
| QX11-84 | 0.39 | 0.05491 | 0.00162 | 0.48263 | 0.01417 | 0.06374 | 0.00094 | 409 | 40 | 400 | 10 | 398 | 6 | 0.50 |
| QX11-85 | 1.53 | 0.07638 | 0.00312 | 1.89066 | 0.07597 | 0.17949 | 0.00302 | 1105 | 53 | 1078 | 27 | 1064 | 17 | 3.85 |
| QX11-86 | 0.68 | 0.05392 | 0.00254 | 0.43298 | 0.02019 | 0.05823 | 0.00092 | 368 | 76 | 365 | 14 | 365 | 6 | 0.00 |
| QX11-87 | 1.07 | 0.05562 | 0.00162 | 0.5298 | 0.01531 | 0.06908 | 0.00102 | 437 | 38 | 432 | 10 | 431 | 6 | 0.23 |
| QX11-88 | 0.40 | 0.05325 | 0.00438 | 0.39734 | 0.03238 | 0.05411 | 0.001 | 339 | 152 | 340 | 24 | 340 | 6 | 0.00 |
| QX11-89 | 0.72 | 0.05577 | 0.00154 | 0.55348 | 0.01521 | 0.07196 | 0.00106 | 443 | 36 | 447 | 10 | 448 | 6 | -0.22 |
| QX11-90 | 0.88 | 0.05616 | 0.00179 | 0.56209 | 0.01769 | 0.07257 | 0.0011 | 459 | 43 | 453 | 11 | 452 | 7 | 0.22 |
| ~~QX11-91~~ | ~~0.96~~ | ~~0.06482~~ | ~~0.00231~~ | ~~0.56111~~ | ~~0.01975~~ | ~~0.06278~~ | ~~0.00097~~ | ~~768~~ | ~~48~~ | ~~452~~ | ~~13~~ | ~~393~~ | ~~6~~ | ~~15.01~~ |
| QX11-92 | 0.26 | 0.07055 | 0.00185 | 1.45582 | 0.03787 | 0.14965 | 0.00218 | 944 | 30 | 912 | 16 | 899 | 12 | 1.45 |
| QX11-93 | 0.70 | 0.05418 | 0.00227 | 0.4544 | 0.01872 | 0.06082 | 0.00098 | 379 | 64 | 380 | 13 | 381 | 6 | -0.26 |
| QX11-94 | 0.63 | 0.09011 | 0.00232 | 2.98386 | 0.07625 | 0.24014 | 0.00351 | 1428 | 27 | 1404 | 19 | 1387 | 18 | 2.96 |
| QX11-95 | 0.41 | 0.05438 | 0.00151 | 0.42693 | 0.01176 | 0.05693 | 0.00084 | 387 | 36 | 361 | 8 | 357 | 5 | 1.12 |
| QX11-96 | 0.84 | 0.16262 | 0.00426 | 10.49347 | 0.27218 | 0.46793 | 0.0071 | 2483 | 24 | 2479 | 24 | 2474 | 31 | 0.36 |
| QX11-97 | 0.53 | 0.05443 | 0.00244 | 0.45236 | 0.01994 | 0.06027 | 0.00099 | 389 | 69 | 379 | 14 | 377 | 6 | 0.53 |
| QX11-98 | 0.57 | 0.05411 | 0.00205 | 0.44568 | 0.01662 | 0.05973 | 0.00094 | 376 | 56 | 374 | 12 | 374 | 6 | 0.00 |
| QX11-99 | 0.46 | 0.05498 | 0.00179 | 0.50368 | 0.01619 | 0.06644 | 0.00101 | 411 | 45 | 414 | 11 | 415 | 6 | -0.24 |
| QX11-100 | 0.31 | 0.05312 | 0.00186 | 0.38975 | 0.01343 | 0.05321 | 0.00082 | 334 | 50 | 334 | 10 | 334 | 5 | 0.00 |

## Appendix to Chapter 4

Detailed parameter constraints

1. Northeastward migration of the Qaidam Basin along the Altyn Tagh Fault.

Guo et al. (1998) first reported that geochemical fingerprints (e.g. carbon isotopic composition) in the Jurassic oil-bearing sandstone of the Tula Basin were similar to that of the geochemical fingerprints in the Jurassic oil-bearing sandstone oil in the Qaidam Basin. Based on sedimentology along the western Qaidam Basin and low temperature thermochronology studies, Wang et al. (2006) suggested that the Qaidam Basin should derive from the Tula area and be largely northwards transported. By correlating stratigraphic contacts and lithologies with the U-Pb age spectra of Mesozoic samples within sections along the western Qaidam Basin and Tula Basin, Cheng (2015a) also revealed hundreds of kilometers of northeastward migration of the Qaidam Basin along the Altyn Tagh Fault (ATF) since its Eocene initiation.

2. 360 ± 40 km offset along the Altyn Tagh Fault

By matching Late Paleozoic magmatic belts in the western and eastern Kunlun Shan, ranges of 300 to 550 km of displacement have been estimated (Tapponnier et al., 1986; Peltzer and Tapponnier, 1988; Cowgill et al., 2003). By correlating the geological features with the magmatic histories in the Altyn Tagh Range, Qilian Shan and Nan Shan, Gehrels et al. (2003) suggest a 370 to 400 km offsets along the ATF. By reconstructing the crustal shortening of the Qilian Shan region, Yin and Harrison (2000) inferred 360 ± 50 km of displacement along the fault. Based on integrated analysis of the geologic features along the north margin of the Tibetan Plateau, Molnar and Tapponnier (1975) proposed ~400 km of offset along the ATF. In addition, a 400 ± 60 km offset has also been suggested based on the reconstruction of a Jurassic facies boundary across the ATF (Ritts and Biffi, 2000). Collectively, previous estimations of the offset along the ATF generally vary from 300~400 km. Alternatively, based on a detailed analysis of the stratigraphy and geochronology of three key lithologic sections along the ATF, we recently identify two key piercing points which suggest 360 ± 40 km offset along the ATF (Cheng et al., 2015a). Taking into account

all these estimations we define the Cenozoic offset along the ATF to be 360 ± 40 km (Fig. 3A).

2. Simultaneous deformation along the Altyn Tagh Fault and within the Qilian Shan since their Eocene initiation

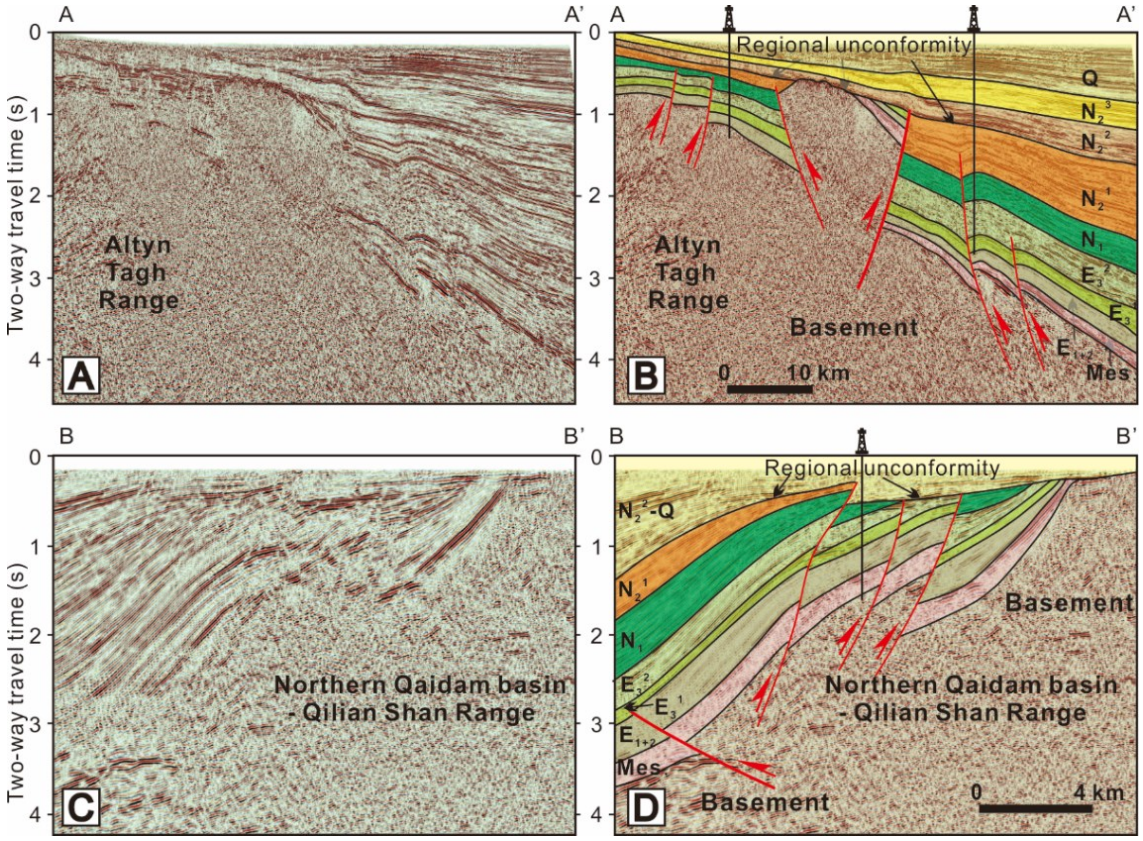


Fig. S1 Seismic profiles in the western Qaidam Basin. (A) Interpreted and (B) non-interpreted seismic profile AA'. (C) Interpreted and (D) non-interpreted seismic profile BB'. See Fig. 1B for location. Note the offset of the Paleogene strata in seismic profiles AA' and BB' indicates the long-term deformation along the ATF and within the Qilian Shan, respectively, since Eocene initiation. $Q_1$ (Pleistocene strata); $N_2^3$ (Late Miocene to Pliocene strata); $N_2^2$ (Middle Miocene strata); $N_2^1$ (Early Miocene strata); $N_1$ (Oligocene strata); $E_3^2$ (Late Eocene strata); $E_3^1$ (Middle Eocene strata); $E_{1+2}$ (Paleocene to Early Eocene strata); Mes. (Mesozoic strata).

Proposed Cenozoic initiation of the ATF generally varies from Eocene to Miocene. Based on magnetostratigraphy and sedimentological analysis, Yin et al (2002) suggested that the ATF has been active since ca. 49 Ma (Yin et al., 2002). Thermochronological data from the Altyn Tagh Range in conjunction with sedimentological evidence suggests that left-

lateral strike-slip faulting occurred from late Eocene to early Oligocene time (Chen et al., 2001; Jolivet et al., 2001; Meng et al., 2001; Yue et al., 2001; Ritts et al., 2004). By identifying Eocene deformed strata in the western segment of ATF, we recently suggested an Eocene initiation of the left-lateral strike-slip motion along the ATF (Cheng et al., 2015a). In addition, on the seismic profile AA' (trending perpendicular to the strike of the ATF), several basement-involved thrust faults offset the Mesozoic strata and die out in the Eocene and Oligocene strata, which probably indicates the Eocene initiation of the ATF (Fig. S1-B).

With regards to the initiation of the NE-SW crustal shortening in the Qilian Shan, recent finding that the Paleocene to early Eocene initiation of the Cenozoic deformation in the Qilian Shan, shortly after the India-Asia collision, indicating initiation of crustal thickening since then (Jolivet et al. 2001; Yin et al., 2008a; Clark et al., 2010; Duvall et al., 2011; Zhuang et al., 2011; Yuan et al., 2013), challenges the post-Pliocene initial deformation in the northern Tibetan Plateau (Bovet et al., 2009) inferred from northward progressive plateau growth hypothesis (Métivier et al., 1998; Tapponnier et al., 2001). In addition, on the seismic profile BB'' (trending perpendicular to the strike of the Qilian Shan), several basement-involved thrust faults offset the Mesozoic strata and die out in the Eocene and Oligocene strata, which probably indicates the Eocene initiation of the NE-SW crustal shortening (Fig. S1-D).

More importantly, all the faults on the seismic profile AA' and BB' is characterized by long-term activity since Eocene initiation, indicative of simultaneous deformation along the ATF and within the Qilian Shan since Eocene initiation (Fig. S1). The simultaneous deformation of the ATF and the Qilian Shan since the Eocene calls for the possibility that deformation in these two regions are controlled by the same kinematical mechanism (e.g. Yin and Harrison, 2000; Zhang et al., 2014)

4. No integral rotation of Qaidam block since the Eocene.

Based on paleomagnetic data which was obtained from the middle to late Eocene strata and the early to middle Miocene strata from the entire Qaidam Basin, Dupont-Nivet et al. (2002) and Yu et al. (2014) demonstrated that the relatively rigid Qaidam block has been transported northeastward along the ATF during the Cenozoic (Wang et al., 2006), without

obvious basin-scale vertical axis rotation with respect to the Eurasia Plate since the early Eocene.

5. Relative rigid Qaidam block

Effective elastic thickness calculation indicate that the mechanical strength of the Qaidam crust is exceptionally strong compared to that of the Qilian Shan, or even to the rest of the Tibetan Plateau (Braitenberg et al., 2003). In addition, Global anisotropic and isotropic 2D modelling of the Tibetan Plateau crust also reveal the relative Qaidam block comparing with the surrounding mountains, such as Qilian Shan (Le Pape et al., 2009).

Although fold and faults are well developed in the Qaidam Basin, the balanced cross-section within the Qaidam Basin suggest only less than 20 km (10%) NE-SW crustal shortening within the basin (Zhou et al., 2006). Yin et al. (2008b) conducted the balanced cross-section restoration within the Qaidam Basin and give an average of ~35% NE-SW crustal shortening within the basin, but the interpreted deep faults in his model are suspicious duo to the poor quality of the 2D seismic profiles. Based on newly acquired high-quality 3D seismic profile, Cheng et al. (2014, 2015b) suggested that the southwestern Qaidam Basin is governed by a series of strike-slip faults rather than south- or north-directed thrusts which rejects large amounts of NE-SW crustal shortening the southwestern Qaidam Basin. Moreover, based on basin-scale paleomagnetic sampling, Yu et al. (2014) also suggest that the crustal shortening of the Qaidam block have been minimal since Eocene.

We thus consider that post-Early Eocene crustal shortening as well as vertical axis rotation of the Qaidam Block have been minimal. The amount of northeastward migration of that block along the ATF (Wang et al., 2006) must thus have been largely transferred into the Qilian Shan where it can be vertically partitioned into crustal shortening and eastward extrusion (Fig. 2). In other words, the amount of crustal shortening and lateral movement in the Qilian Shan would be largely equivalent to the amount of contemporaneous northeastward migration of the Qaidam Block along the ATF.

6. Mass balance or Volume balance

As shown by Yakovlev and Clark (2014), neglecting the density contrast between the upper and lower crust hardly changes the resulting estimates of the modern orogenic mass.

The occurrence of lower crustal flow in the northeastern Tibetan Plateau has recently been rejected (Lease et al., 2012). From this conclusion and the lack of Cenozoic magmatism in the Qaidam Basin and Qilian Shan (Yin and Harrison, 2000), we consider the Cenozoic crust-mantle interaction and transition as sufficiently week to be neglected in our model. We thus simplified the mass balance to volume balance, and use the term “mass” and “volume” interchangeably.

7. Definition of the “Extrusion” in this study

Due to the northeastward migration of the relative rigid Qaidam block along the ATF, hundreds of kilometers of offset were totally absorbed within the Qilian Shan, which led to the N20E-directed crustal shortening as well as the N110E-directed elongated of the Qilian Shan crust. We thus define the N110E-directed elongation of the Qilian Shan crust as the “eastward extrusion”.

8. The Altyn Tagh Fault terminates within the Qilian Shan.

In this study, we define the ATF terminates within the Qilian Shan rather than bypassing the northern margin of Qilian Shan. In recent years, based on the remote sensing image interpretation, field geological mapping, sedimentology studies, seismic profile interpretation, most researchers suggest that the ATF ends in the Qilian Shan region (e.g. Burchfiel et al., 1989; Meyer et al., 1998; Wittlinger et al., 1998; Tapponnier et al., 2001; Yin and Harrison, 2000; Jolivet et al., 2001; Yin et al., 2002; Cowgill et al., 2003; Dupont-Nivet et al., 2004; Wang et al., 2006; Cheng et al., 2015a). On the contrary, Yue and Liou (1999) and Darby et al. (2005) asserted that the ATF extend beyond the Qilian Shan region and could link to the faults in the Alxa block, the East Mongolia, or even related to the subduction of the subduction in the Sea of Okhotsk. However, their estimation are generally petrotectonic assembles and those strike-slip faults within the Alxa block are far away from the ATF, which would likely to be individual strike-slip fault system. More importantly, based on recent magnetotelluric survey in the northern Tibetan Plateau, the northward expanding of the Altyn Tagh Fault (bypassing the Qilian Shan and expanding to the Alxa block) is completely rejected (Xiao et al., 2015). (Profiles are located in the foreland of the Qilian Shan Ranges and are oriented perpendicular to the inferred fault zone that could be

the continuation of Altyn Tagh Fault). Please check details in the paper of Xiao et al. (2015) JGR, Eastern termination of the Altyn Tagh Fault, western China: Constraints from a magnetotelluric survey Journal of Geophysical Research: Solid Earth.

9. Initial crustal thickness within the Qilian Shan

The initial crustal thickness within the Qilian Shan is poorly constrained. The thick Jurassic and Cretaceous clastic packages and synorogenic conglomerates enable Wang and Coward (1993) to suggest flexural loading of crust around the Qilian Shan during the Jurassic to Cretaceous. Based on comprehensive analysis of geological data in the northern Tibetan Plateau, Meyer et al. (1998) suggested ~47.5 ± 5 km initial crustal thickness of the northern Tibetan Plateau. By conducting low temperature thermochronological study integrated with balance cross-section restoration, Lease et al. (2012) recently estimated a 45 ± 5 km initial crustal thickness. In order to account for this uncertainty we calculated solutions for multiple values of $H_0$ (35, 40, 45, 50 and 55 km; with a probable value around 45 km).

References

Bovet, P.M., Ritts, B.D., Gehrels, G., et al., 2009. Evidence of Miocene crustal shortening in the north Qilian Shan from Cenozoic stratigraphy of the western Hexi Corridor, Gansu Province, China. *American Journal of Science*, **309**, 290-329.

Braitenberg, C., Wang, Y., Fang, J. and Hsu, H., 2003. Spatial variations of flexure parameters over the Tibet–Quinghai plateau. *Earth and Planetary Science Letters*, **205**, 211-224.

Burchfiel, B.C., Quidong, D., Molnar, P., et al., 1989. Intracrustal detachment within zones of continental deformation. *Geology*, **17**, 748-752.

Cheng, F., Jolivet, M., Fu, S., et al., 2014. Northward growth of the Qimen Tagh Range: A new model accounting for the Late Neogene strike-slip deformation of the SW Qaidam Basin. *Tectonophysics*, **632**, 32-47.

Chen, Z.L., Zhang, Y.Q., Wang, X.F. and Chen, X.H., 2001. Fission Track Dating of Apatite Constrains on the Cenozoic Uplift of the Altyn Tagh Mountain. *Acta Geoscientia Sinica*, **22**, 413-418 (in Chinese with English abstract).

Cheng, F., Guo, Z., Jenkins, H.S., et al., 2015a. Initial rupture and displacement on the Altyn

Tagh fault, northern Tibetan Plateau: Constraints based on residual Mesozoic to Cenozoic strata in the western Qaidam Basin. *Geosphere*, **11**, 921-942.

Cheng, X., Fu, S., Wang, H., et al., 2015b. Geometry and kinematics of the Arlar strike-slip fault, SW Qaidam basin, China: New insights from 3-D seismic data. *Journal of Asian Earth Sciences*, **98**, 198-208.

Clark, M.K., Farley, K.A., Zheng, D., et al., 2010. Early Cenozoic faulting of the northern Tibetan Plateau margin from apatite (U–Th)/He ages. *Earth and Planetary Science Letters*, **296**, 78-88.

Cowgill, E., Yin, A., Harrison, T.M. and Xiao-Feng, W., 2003. Reconstruction of the Altyn Tagh fault based on U-Pb geochronology: Role of back thrusts, mantle sutures, and heterogeneous crustal strength in forming the Tibetan Plateau. Journal of *Geophysical Research*, **108**, 2346.

Darby, B.J., Ritts, B.D., Yue, Y. and Meng, Q., 2005. Did the Altyn Tagh fault extend beyond the Tibetan Plateau? *Earth and Planetary Science Letters*, **240**, 425-435.

Dupont-Nivet, G., Butler, R.F., Yin, A. and Chen, X., 2002. Paleomagnetism indicates no Neogene rotation of the Qaidam Basin in northern Tibet during Indo-Asian collision. *Geology*, **30**, 263-266.

Dupont-Nivet, G., Robinson, D., Butler, R.F., et al., 2004. Concentration of crustal displacement along a weak Altyn Tagh fault: Evidence from paleomagnetism of the northern Tibetan Plateau. *Tectonics*, **23**, TC1020.

Duvall, A.R., Clark, M.K., van der Pluijm, B.A. and Li, C., 2011. Direct dating of Eocene reverse faulting in northeastern Tibet using Ar-dating of fault clays and low-temperature thermochronometry. *Earth and Planetary Science Letters*, **304**, 520-526.

Duvall, A.R., Clark, M.K., Kirby, E., et al., 2013. Low-temperature thermochronometry along the Kunlun and Haiyuan Faults, NE Tibetan Plateau: Evidence for kinematic change during late-stage orogenesis. *Tectonics*, **32**, 1190-1211.

Gehrels, G.E., Yin, A. and Wang, X.F., 2003. Magmatic history of the northeastern Tibetan Plateau. *Journal of Geophysical Research*, **108**, 2423.

Guo, Z.J., Zhang, Z.C. and Zeng, F.G., 1998. Discovery of mega-thick oil sandstone and

asphalt in the Jurassic System in the Tula Basin and its significance. *Chinese Science Bulletin*, **43**, 1898-1901.

Jolivet, M., Brunel, M., Seward, D., et al., 2001. Mesozoic and Cenozoic tectonics of the northern edge of the Tibetan plateau: fission-track constraints. *Tectonophysics*, **343**, 111-134.

Lease, R.O., Burbank, D.W., Zhang, H., et al., 2012. Cenozoic shortening budget for the northeastern edge of the Tibetan Plateau: Is lower crustal flow necessary? *Tectonics*, **31**, TC3011.

Le Pape, F., Jones, A.G., Vozar, J. and Wenbo, W., 2012. Penetration of crustal melt beyond the Kunlun Fault into northern Tibet. *Nature Geoscience*, **5**, 330-335.

Meng, Q.R., Hu, J.M. and Yang, F.Z., 2001. Timing and magnitude of displacement on the Altyn Tagh fault: constraints from stratigraphic correlation of adjoining Tarim and Qaidam basins, NW China. *Terra Nova*, **13**, 86-91.

Métivier, F., Gaudemer, Y., Tapponnier, P. and Meyer, B., 1998. Northeastward growth of the Tibet plateau deduced from balanced reconstruction of two depositional areas: The Qaidam and Hexi Corridor basins, China. *Tectonics*, **17**, 823-842.

Meyer, B., Tapponnier, P., Bourjot, L., et al., 1998. Crustal thickening in Gansu-Qinghai, lithospheric mantle subduction, and oblique, strike-slip controlled growth of the Tibet plateau. *Geophysical Journal International*, **135**, 1-47.

Molnar, P. and Tapponnier, P., 1975. Cenozoic tectonics of Asia: Effects of a continental collision. *Science*, **189**, 419-426.

Peltzer, G. and Tapponnier, P., 1988. Formation and evolution of strike-slip faults, rifts, and basins during the India-Asia collision: An experimental approach. *Journal of Geophysical Research: Solid Earth (1978–2012)*, **93**, 15085-15117.

Ritts, B.D. and Biffi, U., 2000. Magnitude of post-Middle Jurassic (Bajocian) displacement on the central Altyn Tagh fault system, northwest China. *Geological Society of America Bulletin*, **112**, 61-74.

Ritts, B.D., Yue, Y. and Graham, S.A., 2004. Oligocene-Miocene Tectonics and Sedimentation along the Altyn Tagh Fault, Northern Tibetan Plateau: Analysis of the Xorkol, Subei, and Aksay Basins. *The Journal of geology*, **112**, 207-229.

Searle, M., Elliott, J., Phillips, R. and Chung, S.-L., 2011. Crustal–lithospheric structure and continental extrusion of Tibet. *Journal of the Geological Society*, **168**, 633-672.

Tapponnier, P., Peltzer, G. and Armijo, R., 1986. On the mechanics of the collision between India and Asia. *Geological Society, London, Special Publications*, **19**, 113-157.

Tapponnier, P., Xu, Z.Q., Roger, F., et al., 2001. Oblique stepwise rise and growth of the Tibet Plateau. *Science*, **294**, 1671-1677.

Wang, Q. and Coward, M., 1993. The Jiuxi basin, Hexi corridor, NW China: Foreland structural features and hydrocarbon potential. *Journal of Petroleum Geology*, **16**, 169-182.

Wang, E., Xu, F.Y., Zhou, J.X., et al., 2006. Eastward migration of the Qaidam basin and its implications for Cenozoic evolution of the Altyn Tagh fault and associated river systems. *Geological Society of America Bulletin*, **118**, 349-365.

Wittlinger, G., Tapponnier, P., Poupinet, G., et al., 1998. Tomographic evidence for localized lithospheric shear along the Altyn Tagh fault. *Science*, **282**, 74-76.

Wu, L., Xiao, A.C., Yang, S.F., et al., 2012. Two-stage evolution of the Altyn Tagh Fault during the Cenozoic: new insight from provenance analysis of a geological section in NW Qaidam Basin, NW China. *Terra Nova*, **24**, 387-395.

Xiao, Q., Shao G., Liu-Zeng J., et al., 2015. Eastern termination of the Altyn Tagh Fault, western China: Constraints from a magnetotelluric survey, *J. Geophys. Res. Solid Earth*, **120**, doi: 10.1002/2014JB011363.

Yakovlev, P.V. and Clark, M.K., 2014. Conservation and redistribution of crust during the Indo-Asian collision .*Tectonics*, **33**, 1016-1027.

Yin, A. and Harrison, T.M., 2000. Geologic evolution of the Himalayan-Tibetan orogen. *Annual Review of Earth and Planetary Sciences*, **28**, 211-280.

Yin, A., Rumelhart, P., Butler, R., et al., 2002. Tectonic history of the Altyn Tagh fault system in northern Tibet inferred from Cenozoic sedimentation. *Geological Society of America Bulletin*, **114**, 1257-1295.

Yin, A., Dang, Y.Q., Wang, L.C., et al., 2008a. Cenozoic tectonic evolution of Qaidam basin and its surrounding regions (Part 1): The southern Qilian Shan-Nan Shan thrust belt and northern Qaidam basin. *Geological Society of America Bulletin*, **120**, 813-846.

Yin, A., Dang, Y.Q., Zhang, M., et al., 2008b. Cenozoic tectonic evolution of the Qaidam basin and its surrounding regions (Part 3): Structural geology, sedimentation, and regional tectonic reconstruction. *Geological Society of America Bulletin*, **120**, 847-876.

Yu, X.J., Fu, S.T., Guan, S.W., et al., 2014. Paleomagnetism of Eocene and Miocene sediments from the Qaidam basin: Implication for no integral rotation since the Eocene and a rigid Qaidam block. *Geochemistry, Geophysics, Geosystems*, **15**, 2109-2127.

Yue, Y.J. and Liou, J.G., 1999. Two-stage evolution model for the Altyn Tagh fault, China. *Geology*, **27**, 227-230.

Yue, Y.J., Ritts, B.D. and Graham, S.A., 2001. Initiation and long-term slip history of the Altyn Tagh Fault. *International Geology Review*, **43**, 1087-1093.

Yuan, D.Y., Ge, W.P., Chen, Z.W., et al., 2013. The growth of northeastern Tibet and its relevance to large-scale continental geodynamics: A review of recent studies. *Tectonics*, **32**, 2013TC003348.

Yue, Y.J., Graham, S.A., Ritts, B.D. and Wooden, J.L., 2005. Detrital zircon provenance evidence for large-scale extrusion along the Altyn Tagh fault. *Tectonophysics*, **406**, 165-178.

Zhang, H.P., Zhang, P.Z., Zheng, D.W., et al., 2014. Transforming the Miocene Altyn Tagh fault slip into shortening of the north-western Qilian Shan: insights from the drainage basin geometry. *Terra Nova*, **26**, 216-221.

Zhou, J.X., Xu, F.Y., Wang, T.C., et al., 2006. Cenozoic deformation history of the Qaidam Basin, NW China: Results from cross-section restoration and implications for Qinghai–Tibet Plateau tectonics. *Earth and Planetary Science Letters*, **243**, 195-210.

Zhuang, G., Hourigan, J.K., Ritts, B.D. and Kent-Corson, M.L., 2011. Cenozoic multiple-phase tectonic evolution of the northern Tibetan Plateau: Constraints from sedimentary records from Qaidam basin, Hexi Corridor, and Subei basin, northwest China. *American Journal of Science*, **311**, 116-152.

# List of Figures and Tables

**Figures to Chapter 1**

Eastern Kunlun left-slip transpressional system caused the uplift of the Eastern Kunlun Range, which has partitioned the PaleoQaidam basin into the Hoh Xil basin to the south and the Qaidam basin to the north.

Figure 7. Simplified tectonic map of northern Tibet showing major tectonic terranes, sutures, and faults (modified from Yin et al., 2002). Cenozoic stratigraphic sections (locations shown by turquoise blue squares) were measured by this study at Aertashi, Puska, Jianglisai, and Xishuigou in the southern Tarim Basin. Other relevant stratigraphic sections are Mangnai, Lenghu, Lulehe, Xorkoli, and Jiuxi (Hexi Corridor). Map symbols: N-Q—Neogene–Quaternary sediments, Ts—Tert iary sedimentary rocks, THS—Tethyan Himalayan sequences (Proterozoic to Upper Cretaceous passive-continental-margin strata of northern India), GHC—Greater High Himalayan Crystalline Complex, LHS—Lesser Himalayan metasedimentary series. Major plutonic rocks: Czgr—Cenozoic granites, K-Tgr—plutonic rocks belongi ng to the Gangdese batholith, Ladakh batholith, and Kohistan arc, gr(Q)—plutonic rocks in the Qiangtang terrane (mostly Jurassic–Cretaceous), gr(SP)—plutonic roc ks in the Songpan–Ganzi–Hoh Xil terrane (mostly Late Triassic), gr(KQ)—Ordovician–Silurian and Permian–Triassic plutonic rocks in the Kunlun and Qilian terranes. Major sutures: IYS—Indus-Yalu suture, BNS—Bangong-Nujiang suture, JS—Jinsha suture, AKMS—Ayimaqin-Kunlun-Mutztagh suture, KS—Kudi suture, MCT—Main Centra l thrust, MKT—Main Karakoram thrust, STDS—South Tibet detachment system.

Figure 8. Digital topographic map of northern Tibet showing major tectonic terranes, sutures, and faults within the Qilian Shan.

**Figures to Chapter 2.1**

Figure 1. Digital topographic map of the western Qaidam Basin and surrounding area. Topography from SRTM data.

Figure 2. Geological map of the Qimen Tagh Range and SW Qaidam Basin. See Fig. 1 for

Range. The picture, taken from ~10 km south of the Atantihan River checkpoint, shows the strong relief between the Adatan Valley and the mountains bordered by a series of triangular facets and fault scarps belonging to the MQF. The foothill domain is represented by Cenozoic strata which are deformed and pushed into gentle folds. See the location in Fig. 9. (b) Uplifted Pleistocene series covered by Holocene tillites (left) and general stratigraphic column (right). See the photographs' location in Fig. 9.

Figure 9. Geological sketch of the Qimen Tagh Range showing the distribution of the Cenozoic series. Modified after the Kulangmiqiti J46C003001 1:250,000 geological map (IGSQP, 2004) and the Ayakekumu J45C003004 1:250,000 geological map (IGSSP, 2003). See the location in Fig. 2.

Figure 10. Isopach map of the Upper Xiaganchaigou Formation ($E_3^2$xg). Three major faults (the Kunbei fault, the Arlar fault and the Hongliuquan fault) are also marked on the isopach map based on seismic data. These data were acquired by the Qinghai Oilfield Company (China) who compiled information from thousands of drill holes and a dense network of seismic profiles in recent years. Note the offset of the 400 isopach line controlled by the faults and indicating the left-lateral strike-slip faulting of these faults.

Figure 11. Seismic profile C-C'in the SW Qaidam Basin. See the location in Figs. 2 and 10. Note that the thickness of the Paleocene to Eocene strata shows a sharp difference between both sides of the Arlar fault. The growth strata associated to the positiveflower structure started to develop during the initial deposition of the Early Miocene unit ($N_2^1$xy), which suggests that the strike-slip movement on the Arlar fault initiated during the deposition of this unit.

Figure 12. Seismic section D-D'in the SW Qaidam Basin. See Figs. 2 and 10 for location. Note that the strata below the Shangyoushashan Fm. ($N_2^1$xy) keep a constant thickness in the section, while the strata above it are thinning northward. The thickness of the Paleocene to Eocene strata shows a sharp difference between both sides of the Arlar fault. Meanwhile, Early

Miocene growth strata above the Arlar and Hongliuquan faults indicate the onset of left-lateral strike-slip faulting during the Early Miocene.

Figure 13. Seismic profile E-E' in the SW Qaidam Basin. See the location in Figs. 2 and 10. Note that the thickness of the Paleocene to Eocene strata shows a sharp difference between both sides of the Kunbei fault. Meanwhile, Early Miocene growth strata again indicate an onset of left-lateral strike-slip faulting during the Early Miocene.

Figure 14. Tectonic evolution of the Qimen Tagh Range and the SW Qaidam Basin since the Early Neogene. See the text for discussion

**Figures and tables to Chapter 2.2**

Figure 1. Digital topographic map of the Tibetan Plateau modified after Taylor and Yin (2009). Active fault kinematics and suture zones are based on Yin et al. (2007), Taylor and Yin (2009), and Cheng et al. (2014). Note that the Hoh Xil Basin has been diced up by the Neogene uplift phase. The yellow stars refer to the location of sampling sites. IYS—Indus Yalu suture zone; AMS—Anyimagen-Kunlun-Muztagh suture zone; JS—Jinsha suture zone; BNS—Bangong Nujiang suture zone.

Figure 2. Geological map of the southwestern Qaidam Basin and surrounding area, modified after the 1:250,000 geologic map (SIGS, 2003; QIGS, 2004). See Figure 1 for location. Active fault kinematics are based on Cheng et al. (2014), SIGS (2003), and QIGS (2004).

Figure 3. Original (A) and interpreted (B) NE-SW–oriented seismic profile 1 in SW Qaidam Basin. See the location in Figure 2. Note that stratigraphic overlaps between the Paleocene to early Eocene ($E_{1+2}$) and middle to late Eocene ($E_3$) strata, the middle to late Eocene ($E_3$) and Oligocene ($N_1$) strata, and the Oligocene ($N_1$) and early Miocene ($N_2^1$) strata, indicating the gradually enlarging basin from Paleocene to middle Miocene. The growth strata within the middle to late Miocene ($N_2^2$) strata, late Miocene to Pliocene ($N_2^3$) strata, and Pleistocene ($Q_1$) strata demonstrate the shrinking of the basin since the Miocene.

**Figures and tables to Chapter 3.1**

Uninterpreted and (B) interpreted seismic profiles in the SW–NE direction; (C) uninterpreted and (D) interpreted seismic profiles in NW–SE direction. Note that the growth strata since the Xiayoushashan Formation ($N_2^1$xy) indicate the intense tectonic movement of the Altyn Tagh fault during middle Miocene time.

Figure 11. Proposed accelerated motion model for the Cenozoic Altyn Tagh fault (ATF). Note the piercing points along the Altyn Tagh fault. (A) Before early Eocene time, the Caishiling section was originally located where the Tula section is situated today. During early Eocene time (ca. 49 Ma), the left-lateral strike-slip faulting along the Altyn Tagh fault initiated, transporting the Qaidam Basin northeastward. Since then, the Tula unit remained stationary and was separated from the Qaidam Basin (B) during middle Miocene time (ca. 15 Ma), when the Caishiling section migrated northeastward to where the Anxi section is situated today. During this period, an intense left-lateral strike-slip faulting along the Altyn Tagh fault occurred and deformed the pre-Miocene strata in the Anxi section. Since then, the Anxi unit was left and separated from the Qaidam Basin (C) during continuous left-lateral strike-slip faulting along the Altyn Tagh fault that transported the Caishiling section to its present position. Consequently, ~360 km total Cenozoic offset is constrained along the Altyn Tagh fault, which is divided into ~170 km of offset between early Eocene and middle Miocene time and ~190 km of offset from the late Miocene until present.

Table 1. Summary of the major characteristics and corresponding statistical data for each of the samples.

**Figures and tables to Chapter 3.2**

Figure 1. (A) SRTM based digital topographic map of the Tibetan plateau. (B) Digital elevation model (DEM) and major tectonic elements of the Altyn Tagh Range, the Qaidam basin and the surrounding regions. The location of Fig. 2 is identified by the solid box. The DEM map was generated from the 90 m SRTM data. Note that the yellow solid line refers to the location of seismic profile AA'. (C) Interpreted and (D) non-interpreted seismic profile AA'. Note that the succession of Cenozoic depo-centers is marked along the long axis of the

basin. These depo-centers gradually migrated eastward since the Eocene.

Figure 2. Simplified geological map of the northwestern Qaidam basin and eastern segment of the Altyn Tagh Range, adapted from the Geologic Map of the Tibetan plateau and adjacent areas compiled by the Chengdu Institute of Geology and Mineral Resources and Chinese Geological Survey (map scale, 1:1,500,000).

Figure 3. Generalized stratigraphic column of the studied Mesozoic to Cenozoic series. Paleocurrent directions in the Huatugou section were obtained from Meng and Fang, (2008), Wu et al. (2012b) and Zhuang, et al. (2011). Paleocurrent directions in the Eboliang section were obtained from Zhuang, et al. (2011), Wu et al. (2012b) and Heermance et al. (2013). Note that sample CSL3 is cited from Cheng et al. (2015a), and samples HTG-E, HTG-N, CSL4, SZG1 and CSL5 are cited from Cheng et al. (2016). Red arrows refer to the general paleocurrent directions.

Figure 4. Typical photomicrographs and field photographs of the various analyzed sediments. (A) Drill core sample of early to middle Jurassic ($J_{1+2}$) lithic sandstone obtained from drill well in the Eboliang section; (B) Thin section image of lithic sandstone from the Paleocene to early Eocene strata ($E_{1+2}$) in the Eboliang section, under crossed polarized light. (C) Horizontally stratified sandstone interbedded with mudstones of the Xiaganchaigou Formation ($E_3^1$) in the Eboliang section. (D) Thin section image of siltstone from the Oligocene strata ($N_1$), under crossed polarized light, obtained from drill well in the Eboliang section. (E) Thick-bedded sandstone in the early Miocene strata, Xiayoushashan Formation ($N_2^1$), Eboliang section. (F) Thin section image of siltstone from the Pliocene strata ($N_2^3$), in the Eboliang section, under crossed polarized light. (G) Greenish white sandstone intercalated with mudstone in the middle Eocene strata ($E_3^1$), Huatugou section. (H) Greenish white sandstone intercalated with brownish red mudstone in the late Eocene strata ($E_3^1$), Huatugou section. (I) Thin section image of sandstone in the Oligocene strata ($N_1$), Huatugou section, under crossed polarized light.

et al. (2011), Dai et al. (2013), Li et al. (2013), Wang et al. (2013), Long et al. (2014), Song et al (2014), Wang et al.(2014b) , Zhang et al. (2014a), Dong et al. (2014, 2015), Chen et al. (2015) and references therein. The blue arrow refers to the northeastward migration of the Huatugou and Eboliang sections from their origins.

Figure 10. (A) Frequency histograms for restricted early Neoproterzoic ages groups of detrital zircons from the Paleocene to early Eocene Lulehe Fm. ($E_{1+2}$) and the Th/U ratio for those zircon ages. (B) CL images of zircons for all early Neoproterzoic ages zircons from the Paleocene to early Eocene Lulehe Fm. The yellow circles show the location of the U-Pb analysis. Numbers are U-Pb ages in Ma. Note that the ~911 Ma peak age for the Neoproterozoic ages groups coincides with the mean crystallization age of ~910 Ma for the basement rocks in the western segment of the Altyn Tagh Range (Fig. 9A; Wang et al., 2013). The distinctive Th/U ratio and oscillatory zones for those zircons indicate magmatic sources.

Figure 11. Seismic profiles in the southwestern Qaidam basin. See Fig. 2A for location. Note the fold and thrusts in seismic profile BB', indicating the deformation in the northwestern Qaidam basin since the early Miocene. Offset of the Paleogene strata in seismic profiles CC' and DD' indicates the Eocene to Oligocene deformation in the northwestern Qaidam basin which would be associated with deformation along the ATF. Growth strata of the post-Oligocene strata in seismic profiles BB' and CC' indicate intense tectonic movements along the ATF since the Miocene.

Figure 12. Cenozoic kinematic model of the Altyn Tagh Fault and source to sink relation between the western Qaidam basin and the surrounding regions. (A) during the Paleocene to early Eocene, the basement rocks in the Altyn Tagh Range served as the major source for the clastic material deposited in the Eboliang section, while sediments in the Huatugou section were derived from the Eastern Kunlun Range; (B) during the early Eocene to the Oligocene, the Qaidam basin migrated northeastward due to left-lateral strike-slip faulting along the ATF; (3) since the Miocene, intense left-lateral faulting along the ATF continuously offset the

Qaidam basin towards the northeast and triggered post-Oligocene crustal deformation within the Altyn Tagh Range and western Qaidam basin. See text for detailed discussion.

Table 1. Summary of the major characteristics and corresponding U-Pb age data for each sample

**Figures and tables to Chapter 4**

Figure 1. (A) SRTM-based digital topographic map of the Tibetan Plateau and the surrounding region. (B) SRTM-based digital topographic map of the northern Tibetan Plateau. NQSF, Northern Qilian Shan Fault system; NQF, Northern Qaidam Fault; SDF, Saisitengshang-Dakendaban Fault; DF, Danghe-Nanshan Fault; DTF, Daxueshan Yuole-Nanshan Fault; SF, ShuleNanshan Fault; EF, Elashan Fault; RF, Riyueshan Fault; CF, Changma Fault; ZTF, Zhongwei-Tongxing Fault. Solid lines A–A' and B–B' represent the locations of the seismic profiles presented in Appendix S1. Dash-lined right trapezoid represents the studied Qilian Shan region. (C) SRTM-based present-day crustal-thickness map of the northern Tibetan Plateau and the surrounding region, modified from Li et al. (2014). The white solid triangles represent the locations of seismic stations, and numbers refer to the corresponding crustal thickness.

Figure 2. General model for balanced 3D crustal deformation in the Qilian Shan during the Cenozoic. (A) Perspective view of the Qilian Shan region before deformation. (B) Top view of the Qilian Shan region before deformation. (C) Perspective view of the Qilian Shan region after deformation. (D) Top view of the Qilian Shan region after deformation. (E) Sketch of the main active structures in the northern Tibetan plateau, modified from Duvallet al. (2013). To simplify the model, we consider the shape of the Qilian Shan to be an approximately right-angled trapezoid in plan view. The initiation ages are mainly compiled from previous work (e.g. Mocket al., 1999; Yin et al., 2002, 2007, 2008a,b; Jolivet et al., 2003; Lease et al., 2007; Bovet et al., 2009;Clarket al., 2010; Zheng et al., 2010; Craddock et al., 2011; Duvall et al., 2011, 2013; Hough et al., 2011; Yuan et al., 2011).

Figure 3. (A) Offset estimation along the Altyn Tagh Fault. Data were mainly compiled from Ritts and Biffi (2000), Yin et al. (2002), Gehrels et al. (2003), Yue et al. (2005); Searle et al. (2011) and Cheng et al. (2015). The grey rectangle represents the probable offset along the ATF and its probable time of initiation. In this study, we consider an offset of 360 ± 40 km along the ATF since its Eocene initiation based both on newly found piercing points in the western Qaidam Basin (Cheng et al., 2015) and on a summary of previous estimates, which is represented by the yellow circle. (B) Balanced calculation results. The black lines relate the amount of extrusion within the Qilian Shan ($L_e$) to the amount of offset along the ATF ($L_d$), while the blue line relates the amount of N20E directed crustal shortening within the Qilian Shan ($L_s$) to the amount of offset along the ATF ($L_d$). Considering the probable 360 km offset along the ATF (represented by the yellow circle in the figure) and an initial crustal thickness of 45 km in the Qilian Shan, there has been 309 km of eastward extrusion and 250 km of N20E directed crustal shortening in the Qilian Shan range, represented by the red circle and the green circle respectively. The pink region represents the possible range of $L_e$ and $L_s$. In this study, we define the N110E-directed elongation of the Qilian Shan as the eastward extrusion.

Figure 4. (A) Global Positioning System (GPS) velocities relative to stable Eurasia, modified from Zhang et al. (2004). The yellow arrows show the changes in orientation of the displacement vectors, clearly implying ongoing eastward crustal extrusion within the Qilian Shan region. (B) Strike-parallel and strike-perpendicular velocity (N110E) vs. distance. Solid-lined right trapezoid in the Fig. 4A represents the studied Qilian Shan region. GPS data from Gan et al. (2007). Details of the analytical method of geodetic velocities are given in Appendix S2. The sharp decrease in N20E directed GPS velocities from the northern Qaidam Basin to the Hexi Corridor and the large increase in N110E directed GPS velocities from the Altyn Tagh Range to the eastern Qilian Shan imply large amounts of crustal shortening and eastward extrusion within the Qilian Shan region at present.

Figure 5. North-eastward migration model of the Qaidam block, corresponding to crustal

**Figures and tables to Chapter 5**

# List of publications during the PhD. thesis work

***Papers in preparation:***

**Cheng F.**, Jolivet M., Fu S., Zhang C., Zhang, Q., Guo Z., Reconstructing the Cenozoic tectonics in the northern Tibetan plateau: insight from apatite fission track study of deep-drill-core samples from the basement of Qaidam basin. In Prep for Tectonics.

**Cheng F.**, Han B., Jolivet M., Fu S., Zhang C., Guo Z., Tectono-magmatic rejuvenation of the Qaidam craton (northern Tibet): insight from geochronological and geochemical constraints on borehole basement samples. In Prep for EPSL.

***Papers in review and revision:***

16 **Cheng F.,** Jolivet M., Fu S., Zhang C., Zhang, Q., Guo Z., Large-scale displacement along the Altyn Tagh Fault (North Tibet) since its Eocene initiation: insight from detrital zircon U-Pb geochronology and subsurface data: ***Tectonophysics***, accepted with minor revision.

***Published papers:***

15 **Cheng, F.**, Fu, S., Jolivet, M., Zhang, C., and Guo, Z., 2016, Source to sink relation between the Eastern Kunlun Range and the Qaidam Basin, northern Tibetan Plateau, during the Cenozoic: ***Geological Society of America Bulletin***, v. 128, no. 1-2, p. 258-283, doi: 10.1130/B31260.1.

14 **Cheng F.**, Jolivet M., Dupont-Nivet G., Wang L., Yu X., Guo Z., Lateral extrusion along the Altyn Tagh Fault, Qilian Shan (NE Tibet): insight from a 3D crustal budget: ***Terra Nova***, v. 27, no. 6, p. 416-425, doi: 10.1111/ter.12173.

13 Wang L. and **Cheng F.**, 2015. DEM and GIS analysis of the stream gradient index for evaluating effects of active tectonics: Tula basin, north Tibet, China, Geoscience and Remote Sensing Symposium (IGARSS), 2015 IEEE International, Milan, 2015, 4680-4683, doi: 10.1109/IGARSS.2015.7326873.

12 Fu S., Ma D., Guo Z., **Cheng F.**, 2015. Strike-slip superimposed Qaidam basin and control on oil and gas accumulation: ***Petroleum Exploration and Development***, v. 42, no. 6, 712-722, doi: 10.11698/PED.2015.06.03.

11 **Cheng, F.,** Guo Z., Jenkins, H., Fu S., and Cheng X., 2015.Initial Rupture and Displacement on the strike-slip Altyn Tagh Fault, Northern Tibetan Plateau: Constraints based on residual Mesozoic to Cenozoic deposits in the western Qaidam Basin: ***Geosphere***, v. 11, no. 3, 921-942, doi: 10.1130/GES01070.1.

10 Liu, D., **Cheng, F.**, Guo, Z., Jolivet, M., Song, Y., 2015. Lahar facies of the Latest Paleozoic Arbasay Formation: Geomorphological characters and paleoenvironment reconstruction of Northern Tian Shan, NW China. ***Journal of Asian Earth Sciences***, v. 113, Part 1, p. 282-292, doi: 10.1016/j.jseaes.2015.01.024.

9 Cheng, X., Fu, S., Wang, H., Yu, X., **Cheng, F.**, Liu, R., Du, W., Guo, Z., 2015. Geometry and kinematics of the Arlar strike-slip fault, SW Qaidam basin, China: New insights from 3-D seismic data. ***Journal of Asian Earth Sciences*** v. 98, 198-208, doi: 10.1016/j.jseaes.2014.09.039.

8 **Cheng, F.,** Jolivet, M., Fu, S., Zhang, Q., Guan, S., Yu, X., and Guo, Z., 2014, Northward

growth of the Qimen Tagh Range: A new model accounting for the Late Neogene strike-slip deformation of the SW Qaidam Basin: ***Tectonophysics***, v. 632, p. 32-47, doi: 10.1016/j.tecto.2014.05.034.

7 Liu, D., Guo, Z., Jolivet, M., **Cheng, F.**, Song, Y., Zhang, Z., 2014. Petrology and geochemistry of Early Permian volcanic rocks in South Tian Shan, NW China: implications for the tectonic evolution and Phanerozoic continental growth. ***International Journal of Earth Sciences*** 103, 737-756, doi: 10.1007/s00531-013-0994-1.

6 Zhu, B., Guo, Z., Zhang, Z., **Cheng, F.**, 2014. Peperites in the Permian Tarim large igneous province in Northwest China and their constraints on the local eruption environments. ***Science China Earth Sciences*** 57, 2914-2921. doi: 10.1007/s11430-014-4966-5.

5 Yu, X.J., Fu, S.T., Guan, S.W., Huang, B., **Cheng, F.**, Cheng, X., Zhang, T., Guo, Z.J., 2014. Paleomagnetism of Eocene and Miocene sediments from the Qaidam basin: Implication for no integral rotation since the Eocene and a rigid Qaidam block. ***Geochemistry, Geophysics, Geosystems*** 15, 2109-2127., doi: 10.1002/2014GC005230.

4 Yu, X., Huang, B., Guan, S., Fu, S., **Cheng, F.**, Cheng, X., Zhang, T., Guo, Z., 2014. Anisotropy of magnetic susceptibility of Eocene and Miocene sediments in the Qaidam Basin, Northwest China: Implication for Cenozoic tectonic transition and depocenter migration. ***Geochemistry, Geophysics, Geosystems*** 15, 2095-2108, doi: 10.1002/2014GC005231.

3 **Cheng F.,** and Guo Z., 2013. Northward Migration of the Western Segment of Eastern Kunlun Strike-slip Fault: Implications for Late Cenozoic Evolution of the Qimen Tagh Range and Southwestern Qaidam Basin, North Tibet, China. ***Acta Geologica Sinica (English Edition)***, v. 87(supp.), p. 205.

2 Zhang C., **Cheng F.**, Huang G., Huang Y., Xing C., Guan B., Zhang Q., Xu G.,. 2013. Sediment and reservoir characteristics with reservoir evaluation of Lunlehe Formation in Qie16 block of Kunlun oilfield in Qaidam Basin: ***Acta Petrologica Sinica***, v. 29, no. 8, p. 2883-2894 (in Chinese with English abstract).

1 Liu, D., Jolivet, M., Yang, W., Zhang, Z., **Cheng, F.**, Zhu, B., Guo, Z., 2013. Latest Paleozoic–Early Mesozoic basin–range interactions in South Tian Shan (northwest China) and their tectonic significance: Constraints from detrital zircon U–Pb ages. ***Tectonophysics*** 599, 197-213, doi: 10.1016/j.tecto.2013.04.018.